Conference Proceedings, Published Version

Vogt, Norbert; Schuppener, Bernd; Straub, Daniel; Bräu, Gerhard (Hg.)

ISGSR 2011 - Proceedings of the 3rd International Symposium on Geotechnical Safety and Risk

ISGSR 2011

Proceedings of the 3rd International Symposium on Geotechnical Safety and Risk

Munich, Germany
June 2-3, 2011

ISGSR 2011

Editors

Norbert VOGT
Technische Universität München, Germany

Bernd SCHUPPENER
Bundesanstalt für Wasserbau, Germany

Daniel STRAUB
Technische Universität München, Germany

Gerhard BRÄU
Technische Universität München, Germany

Published by: Bundesanstalt für Wasserbau
Federal Waterways Engineering and Research Institute
e-mail:info@baw.de
www.baw.de

BAWProceedings
ISBN 978-3-939230-01-4
ISSN 2700-8444 (online)

Printed in Germany

This book has been printed on FSC (Forest Stewardship Council) certified paper from well managed forests.

FSC
www.fsc.org
MIX
Paper from responsible sources
FSC® C105340

Print CO2 compensated
Id-Nr. 1110224
www.bvdm-online.de

Table of Contents

Preface

The 3rd International Symposium on Geotechnical Risk and Safety (ISGSR), which is held on June 2 and 3, 2011, at the *Oskar-von-Miller-Forum* and the *Technische Universität München* in Munich, Germany, is part of a series of conferences organised by a group of engineers and academics interested in geotechnical reliability, safety and risk. Previous conferences include LSD2000 (November 2000, Melbourne, Australia), IWS Kamakura (April, 2002, Tokyo and Kamakura, Japan), LSD2003 (June, 2003, Cambridge, USA), Georisk 2004 (November, 2004, Bangalore, India), Taipei2006 (November, 2006, Taipei) and the 1st and 2nd International Symposia on Geotechnical Risk and Safety (1st ISGSR, October 2007, Shanghai and 2nd ISGSR, June 2009, in Gifu, Japan). In addition, this group has organized technical sessions in many international and regional conferences from time to time.

The major themes of the symposium are:
- Risk assessment and management through codes and standards;
- Risk and reliability analysis of geotechnical structures;
- Risk assessment and management of natural geotechnical hazards;
- Practical applications and case studies.

The symposium in Munich is organised by
- *geotechnical safety network* GEOSNet;
- *Zentrum Geotechnik, Technische Universität München;*
- *German Federal Waterways Engineering and Research Institute* (BAW).

GEOSNet is a topic-specific international platform to facilitate and promote active interaction on topics related to geotechnical safety and risk among its members, particularly between researchers and practitioners. GEOSNet was formed at the conference in Taipei 2006 in view of the increasing interest and momentum to rationalize the treatment of risks in new design codes using reliability and other methods. As part of this activity, GEOSNet became the organizing body of the series of ISGSR conferences, of which the Munich symposium is the 3rd.

The symposium is supported by the
- Subcommittee *Geotechnical design* of CEN TC 250 *Structural Eurocodes;*
- European Technical Committee ETC 10 Evaluation of Eurocode 7;
- Joint Committee on Structural Safety, JCSS;
- TC 205 *Safety and Serviceability in Geotechnical Design;*
- TC 304 *Engineering Practice of Risk Assessment and Management;*
- German Federal Ministry of Transport, Building and Urban Development and
- Bayerischer Bauindustrieverband.

The symposium takes places under the auspices of the
- *International Society for Soil Mechanic and Geotechnical Engineering* (ISSMGE);
- *German Geotechnical Society* (DGGT).

The organizers greatly appreciate the support of the *Federal Waterways Engineering and Research Institute* (BAW), which financed these proceedings, as well as the support of *Technische Universität München* and *Bauindustrie Bayern*, which provided the conference venues.

As part of the ISGSR conferences, GEOSNet hosts the Wilson Tang Lecture in recognition of the seminal contributions of Professor Wilson Tang, who is one of the founding researchers in geotechnical reliability and risk. The lecture is intended to honour distinguished peers and their achievements in advancing the methods of geotechnical reliability and risk analysis. The Wilson Tang Lecture of this symposium is delivered by Professor Yusuke Honjo of Gifu University, who is one of the eminent researchers in this domain.

Finally, the organizers are grateful to all those who have helped and contributed to the organization of this event. The largest part of the credit for these proceedings goes to the authors and reviewers.

Norbert Vogt
Bernd Schuppener
Daniel Straub
Gerhard Bräu

June 2011, Munich, Germany

Organization

Members of the Organizing Committee

Prof. Dr.-Ing. Norbert Vogt
Dr.-Ing. Bernd Schuppener
Prof. Dr. sc. techn. Daniel Straub
Dipl.-Ing. Gerhard Bräu

Members of the Scientific Committee and Review Panel

Prof. J. Baker, USA
Prof. G.B. Baecher, USA
Dr. D. Becker, Canada
Dr. A. Bond, United Kingdom
Prof. J. Ching, Taiwan
Prof. J. T. Christian, USA
Dr. P. Day, South Africa
Prof. M. H. Faber, Switzerland
Prof. R. Frank, France
Prof. M. A. Hicks, Netherlands
Prof. Y. Honjo, Japan
Dr. S. Lacasse, Norway
Dr. T. Orr, Ireland
Prof. S. Paikowski
Prof. K. K. Phoon, Singapore
Dr. B. Schuppener.Germany
Dr. B. Simpson, United Kingdom
Prof. G. L. Sivakumar Babu, India
Dr. W. Steiner, Switzerland
Prof. D. Straub, Germany
Prof. N. Vogt, Germany
Prof. J. K. Vrijling, Netherlands
Prof. K.-J. Witt, Germany

1 Keynote lectures

ISGSR 2011 - Vogt, Schuppener, Straub & Bräu (eds) - © 2011 Bundesanstalt für Wasserbau ISBN 978-3-939230-01-4

Risk in geotechnical engineering and profession prestige

I. Vaníček
Czech Technical University in Prague, Czech Republic

ABSTRACT: A great deal of attention has been devoted to the risk connected with construction design during the last period. The design principle connected with potential risks was also included in Eurocode 7 – Geotechnical Design. At the same time, we very often speak about the prestige of geotechnical engineering both on the level of engineering professions and in society in general. In most cases, this evaluation is not so good, the prestige of our profession, in agreement with the opinion of most of us, does not correspond to the significance, importance, generally, to the risk with which geotechnical structures are designed, or to the significance which geotechnical engineering entails.

The paper describes some aspects influencing the degree of this risk. It is, first of all, the risk associated with the range and complexity of geotechnical investigation. To what degree this investigation can give precise figures about the geological environment. How great is the potential risk associated with the numerical model which simplifies this geological environment and up to what degree this numerical model, based on different assumptions between changes of stresses and changes of deformations, is really authentic. And, finally, how great is the risk which a new geotechnical structure brings to its environment, first of all in terms of the interaction of this new structure with a nearby older historical structure.

The relationship between the main partners of the building process is also the subject of discussion, whether they all have or do not have the same interest in lowering this risk. Broadly speaking, geotechnical engineers generally deal with a high risk, they take over a high responsibility for this risk and sometimes under increased public pressure (maybe even as a result of a competition) they get to the edge of this risk which in the case of a failure can have a negative impact on the position of our profession, especially on a long-term basis. However, geotechnical engineering has a significant influence on the living standard of population as it reacts to its demands per saltum. At the end, the status of two different professions is compared; the status of geotechnical engineering and medicine, as both work with high risks, and our profession comes out of this comparison as strongly undervalued. Therefore, geotechnical engineers should speak and discuss about this reality on different levels to help to improve the professional prestige. Some recommendations in this direction are summarized in the end.

Keywords: Risk management, site investigation, geological and geotechnical models, profession prestige, foundation –subsoil interaction

1 GEOLOGICAL ENVIRONMENT INVESTIGATION, GEOLOGICAL AND GEOTECHNICAL MODELS

Practically each construction is in a direct interaction with the geological environment, therefore, the correct evaluation of this mutual interaction is the basic presumption of a safe and economic design of such a construction. This interaction is connected with the problem of the structure foundation or with loading of this structure from the geological environment respectively, which are typical challenges of geotechnical engineering.

In addition, specific geotechnical structures also solve the design of these structures. It may be an earth structure, where soil is the fundamental structural material or the structure is constructed in an earth envi-

ronment and the design fully employs the achievements of soil mechanics or it is an underground structure constructed in a rock environment where the achievements of rock mechanics are fully employed.

Optimal interaction design or the design of a geotechnical structure is strongly influenced by a correct evaluation of the geological environment. In principle, two basic steps play an important role there:

- Creation of the **geological model,** which, on the one hand, represents a geometrical model of this environment specifying the thickness and bedding of individual geological layers, their regularity, dislocation by different discontinuities, etc., and, on the other hand, gives them geological specification, however, not only for the area which is directly affected by new construction, but for a much larger area. As ground water is a natural part of the geological environment, the geological model must be supplemented by detailed information about ground water fully employing the achievements of hydrogeology.
- Creation of the **geotechnical model** which specifies the mechanical and physical properties for individual parts of the geological model, including discontinuities. In doing so these properties are obtained either from field investigation methods or from laboratory tests performed on samples obtained during site (ground) investigation.

In the phase of bonding these two models, engineering geology plays a very important role as it is able to evaluate the reaction of the investigated geological environment to different changes as changes in loading, to technology used in the phase of construction etc. The role of engineering geology is very important in this phase and has its unsubstitutable role.

Although the credibility of the geotechnical model is of cardinal importance for further steps, its correctness depends on many factors like:

- Seriousness of the geological environment, its anisotropy, non homogeneity, irregularity of discontinuities; generally speaking, the more problematic this geological environment, the greater the risk connected with the design and performance is;
- Actual state of exploration of this geological environment during earlier steps of site investigation and construction implementation;

  Extend of ground investigation and its credibility. This question is very sensitive; the possibility to investigate the entire rock massif influenced by new constructions is not realistic. In most cases, closer information can be obtained roughly from one millionth of this massif and from this fact it is evident that the risk connected with the interpretation of the obtained results on the whole affected rock massif is really very high.

  Note 1. For planar structures, as foundation slab, there is a certain chance that for small differences the final results can be averaged, however, this possibility is much lower when one dimension prevails, as it is for tunnels, dykes, motorway and railway earth structures etc. In many cases, one bore hole is implemented there in a distance of 100 meters or even more. However, for tunnels, dykes there is another negative factor; they are built in areas where previous investigation was limited and where the variability of subsoil, mostly for dykes along rivers, is very high. Here, it is noteworthy that the interconnection of investigative methods in such a way that they will be able to give data not only for the geological, but also for the geotechnical model is extremely important.

  Note 2. A specificity of earth structures is that the design of these structures utilizes mechanical and physical properties of soils; however, the prescript for implementation generally uses indirect values (mostly moisture content and dry density determined from compaction tests as Proctor test). These indirect values are also used for the structure quality control and, again, only roughly one millionth of compacted soil is controlled.
- Skill of the person responsible for the site investigation interpretation, this skill is connected with a certain feeling for a geological environment, experience, which Terzaghi (1959) denotes as ”capacity for judgment“ and he specifies that ”this capacity can be gained only by years of contact with field conditions“.

2 ABILITY OF THE NUMERICAL MODEL TO DESCRIBE THE GEOTECHNICAL STRUCTURE BEHAVIOUR OR INTERACTION OF SUBSOIL WITH THE NEW STRUCTURE

The combination of seriousness of the geological environment and complexity of the structure significantly influences the manner in which the design and implementation of this structure will be verified. It is not only the difference between different geotechnical structures, but, first of all, the above mentioned combination. The difference between the design of a low earth dam on homogeneous subsoil with low permeability under which there is no built-up area and a large rock-fill dam with a clay core in a steep valley and with non homogeneous subsoil under which there is a highly populated area can be mentioned as an example. A similar difference is between the approach to the foundation design of a single-floor small house and the foundation design for a high rise building where the groundwater level is high and there are existing buildings in the vicinity.

Therefore, it is obvious that the calculation model can and must be different. For a simple geological and geotechnical model and for modest structures the experience gained up to now from previous applications can be used. The present-day approach, which is also recommended by Eurocode 7 Geotechnical Design, strongly distinguishes these combinations and the risk associated with them and defines 3 Geotechnical Categories. The design of very complicated structures and a complicated geological model according to EC 7 falls under the 3rd Geotechnical Category which is connected with the highest risk and in this case it is necessary to utilize all findings, firstly from soil and rock mechanics, and to utilize the numerical model which is able to represent the geotechnical model as precisely as possible.

The finite element method which can relatively easily come out from the previous models offers a great opportunity in this direction. However, FEM can be applied in many versions, which differ both in the precision of the subdivision of the solved environment into individual elements, and in the definition of the function expressing the changes of properties between individual elements, or which differ between different used relations, between changes of stresses and changes of deformations for stress strain problems or for changes of filtration properties for hydraulic problems.

However, it is necessary to mention that only constitutive models expressing the dependence of deformation changes on stress changes can have many different variants from classical linear elastic models up to very complicated models expressing nonlinearity of this dependence. This great variability in this direction is a significant distinction from other structural materials, such as steel, concrete and timber. This difference is intensified by the presence of ground water, as the properties of soil and rock are influenced by water pressure in pores and this water pressure is strongly dependent on the time effect. Therefore, time plays a very important role for the design of geotechnical structures.

In spite of this, the possibilities of numerical models to describe the behaviour of geological environments improve with time; nevertheless, there is always some simplification. But this problem is not only connected with the numerical model, it is also our ability to measure the above mentioned relation between stress changes and strain changes with the help of field or laboratory methods. Therefore, more sophisticated devices are needed for the performance of such tests, more time for their implementation, which also means higher financial inputs. The last question is whether the laboratory tested sample exactly describes the properties which the in-situ obtained sample had.

3 INTERACTION

In principle, two different interactions can be distinguished:

- interaction of new foundations with subsoil or interaction of a new earth structure or underground structure with the surrounding geological environment;
- interaction of a new structure with an older existing neighbouring one.

The first type of interaction is strongly connected with site investigation as this investigation should give as much information as possible about all geological environments which are affected by this interaction. Therefore, it is not possible to propose and perform this investigation without a closer specification of the proposed construction. For a wider spread foundation the area affected by the stress increase in the footing bottom is larger (and deeper) than for a narrower spread foundation. On the other hand, a wider foundation is much easily able to equilibrate small differences in subsoil properties. Therefore, for a pile foundation, mainly for individual piles, small differences in subsoil can play a significant role in terms of settlement. This factor can have an impact on a safe design and performance of pile foundations below bridge piers or for the foundation of individual pylons as are e.g. pylons for wind power plants.

However, technological aspects also play a significant role, especially for underground structures, such as the manner of rock breaking (excavation). The selected technology can differently react to unexpected responses of the rock massif during the process of mining (excavation) and can have a different impact on the change of properties in the vicinity of the excavation perimeter. For example, the question connected with property changes in a good quality near field zone, especially in terms of permeability, is very sensitive for proposed underground nuclear waste repositories. For a rock massif which is not so strong this interaction directly influences the design and construction of lining of tunnels, galleries etc.

The second interaction – with existing objects – has different levels, from a purely technical up to legislative, juridical level. Engineers, firstly geotechnical engineers, know very well that each change in stresses originates changes in deformations. Therefore, when changes of stresses induced under new structures also influence the area under existing older structures, these stress changes induce changes in deformation as well. The problem is especially sensitive when the owner of the older structure agrees with the new structure only under the condition that "the new structure will not have any impact on the older one". It is an obvious contradiction, however, it is very often accepted as this condition can be explained as a new one – the change does not cause "visible" deformations e.g. in the form of micro cracks on the façade of the older structure. Very often all partners agree with this new, but unarticulated condition, and the design and structure construction is adapted to it. Therefore, this form of interaction is very sensitive for older historical structures which are more sensitive to small changes than new modern structures. Therefore, the passportization of an existing older structure before starting a new one is extremely important to be able to distinguish between older existing cracks and new cracks developed in the phase of the new structure construction.

To prevent "visible" changes development modern methods of foundation engineering utilize different approaches how to limit horizontal deformations of vertical walls of excavation pits e.g. with the help of anchors which end under neighbouring structures. With respects to the ownership right the agreement with these anchors is very often connected with a supplemented condition about the deactivation of these anchors when horizontal deformations are limited by inside structural elements like new floors. What the problems of this deactivation can cause was manifested in the case of the towers of the World Trade Centre in New York after their collapse, (Čermák 2003). The excavation of ruins was significantly decelerated as long as the stability of external walls was restored.

4 ACCEPTABLE RISK

The question connected with the risk of faults and accidents of a constructed geotechnical structure is generally very sensitive. The general effort of generations of our predecessors was always and still is to understand to the geological environment as much as possible so that the final numerical calculation model will represent its behaviour most authentically. Subsequent design after that was a little bit on the conservative side. This design used the global factor of safety (stability) to cover most of the risks with which the description of the geological environment, the methods of investigation and calculations were connected. The optimal global factor of safety was selected in such a way that, on the one hand, it was able to cover most of the uncertainties and, on the other one, most design was not so conservative, structures not so much overdesigned, which is naturally connected with higher financial inputs.

The present-day limit state approach applies different partial factors of safety as our ability to describe partial parameters used in the calculation model is different. EC 7 Geotechnical Design gives individual countries a possibility of independently selecting the values of these partial factors according to their previous experience.

In disregard of the above it is very useful to search the frequency of faults and accidents for individual types of structures. The limit state approach was accepted in the Czech Republic roughly 40 years ago and at that time the discussion was also connected with the accepted frequency of accidents. The frequency of roughly 0.01 % was accepted (1 failure from 10 000 cases) for the design of spread foundations and partial factors recommended for this frequency. However, for the last roughly 20 years (as the last code for the spread foundation design was changed in 1987) the author has only been informed about 2 examples where the problem of a structure was connected with the foundation unacceptable behaviour. From this fact we can deduce that partial factors are still on the conservative side.

For larger civil engineering structures the situation is rather different. For large dams the frequency of faults and accidents is much higher than for spread foundations. The study of ICOLD (International Commission on Large Dams) roughly in the seventies devoted great attention to this problem and summarized information about dams constructed after 1900. The frequency of accidents is a little bit over 1%

and the frequency of faults is 3-4 times higher –see also Vaníček, I. and Vaníček, M. (2008). This frequency decreases with time as our knowledge is improving; however, it is still significantly high.

Roughly the same can be stated for tunnels constructed in soils, where even now the frequency is significantly higher. Three faults which have occurred during the construction of the city road Blanka Tunnel in Prague had a very negative impact on the credibility of civil engineering profession in general.

The group of specialists in pile foundations working on the modification of the National Annex to EC 7-1 also started to discuss this fact. The fact that the design of bored piles in the Czech Republic is the most optimistic in Europe is generally known. It means that the specialists in this field are working with a much higher risk than in other countries in Europe. The question is whether to continue this tendency or to recommend such steps to be included in the National Annex which can slightly reduce this potential risk and in such a way prevent possible problems with negative impacts on our profession as mentioned above in relation to tunnels.

Generally, this situation has raised some questions:

- Who should define the risk – only engineers or also governments (politicians) or potentially affected population respectively. With respect to EC 7 there prevails the opinion that only engineers should. However, there is a discrepancy as engineers know that even when respecting all recommended principles and standards (as e.g. EC 7-1) in limited cases (for an acceptable frequency of failures) a failure can occur. The problem is that politicians and the public are of a different opinion, practically always demanding 100 % safety. This fact is obvious for example for anti flood protection systems (dykes). Up to the 100-year flood (for which these dykes are commonly designed) they require 100 % safety, for higher floods they are able to accept a failure as an objective impact. Hence, for structures which are connected with protection against natural hazards politicians (government, local municipality) and even potentially affected population also play an important role. In the Czech Republic after heavy floods in 2002 some local municipalities approved the construction of supplemented measures for higher floods, 200, 500 even 1000-year floods, whereas paradoxically for the protection of towns mobile barriers, whose life time expectancy is only a few decades, are also used.
- How to utilize the politician's interest to our profit. Mainly during natural hazards the probability of a failure is higher and in many cases these natural hazards are connected with lost of human lives and with great material damages. And this is the case where the validity of the limit state approach should be verified. The government (politicians) should not have only an interest to quickly reconstruct the affected area but also with the help of specialists to collect as much as possible information about factors leading to these failures. The subsequent back calculation of these failures can be very important for the verification whether our design methods are correct and safe. With the help of this back analysis of real limit states our design approaches can be improved in the future. However, the government should be prepared for such situations in advance to guarantee that specialists will be on the spot immediately after the structure failure and their competences had been defined in advance.
- What the interrelationship between the main partners of the construction process should be like – namely between the investor, the designer and the contractor. The highest potential risk is connected first of all with the exaggerated importance of the total price. The designer under such an influence can propose a design connected with a higher risk and as the price for the project design often also covers the price for the site investigation, this site investigation is limited as much as possible, but with a lower predicative value. The contractor under the same pressure of the price can select construction technologies connected with a higher risk. The designer together with the contractor (which in principle represent the civil engineering profession) in that way take over the responsibility for this higher risk; from which the investor can get out very easily with the help of signed contract agreements in the framework of the first steps of the bidding process.
- What positive role the contractor can play – the role of the contractor is very sensitive as potential problems connected with repairs, corrections, sanctions for construction delays etc. are first and foremost on their side. Before signing any contract a competent contractor should carry out the evaluation of the risk management process, during which all risks connected with existing uncertainties should be evaluated. The result of this risk management process should be appropriate bidding price or the pressure on the investor to share risk or to improve the geotechnical model with supplemented investigation. The coverage mostly via the insurance company is more likely the manifestation of their own disbelief. In the case of a failure the contractor is financially covered, but their professional credibility is strongly affected.

5 PRESTIGE OF GEOTECHNICAL ENGINEERING PROFESSION

The high position of the geotechnical engineering profession is obvious from the previous chapters as it is the profession dealing with a much higher risk than other structural engineers such as designers of steel, concrete, timber structures. Simultaneously, geotechnical engineers fall under the groups of professions which to the highest extent react to society demands. Providing that the care of good quality drinking water and safe disposal of waste water had an extremely positive impact on the prolongation of the life expectancy of the population in European cities in the second half of the nineteenth century this process is still alive and brings the extension of life expectancy also in the other parts of the world.

At the same time, geotechnical engineering actively reacts not only to classical demands of the construction sector but also to the demands of society with respect to energy, raw materials demands, to natural hazards, protection of the environment in general. From these spheres, mainly the issues connected with the protection of ground water against contamination or the solution of the old ecological burdens present problems which are, on the one hand, very attractive but, on the other one, connected with high potential risks. The problems of contamination spreading and the application of remediation technologies are strongly time depending problems, not so easily controlled and some mistakes can come to light with a significant delay, when their subsequent solution can be very problematic and expensive.

A partial conclusion to this part is simple, geotechnical engineers work with a geological environment which is rather complicated, never investigated in detail. Therefore, the prognosis of the behaviour of such an environment and how this environment will react to changes, primarily caused by loading changes, can be successful only with the help of up to day existing results, with the help of personal experience and intuition.

The fact that society demands only solutions which are able to guarantee 100 % safety is in fact the basic problem. Therefore, the explanation that this way is not the way in the right direction is the main task of the geotechnical engineering profession as this way can lead to uneconomical design and applications, with negative impacts on the whole society.

It is difficult to find some comparison with other branches of human activity, however, with a certain exaggeration, the profession of geotechnical engineering can be compared with medicine. The doctor of medicine also "works" with an extremely complicated environment – with the human body. Nevertheless, already from its basic merits it is a strongly respected branch, as all of us depend on its achievements. The following reality is coming to light when these two professions are compared:

- In medicine nobody speaks about 100 % safety; on the contrary, the probability of success is often mentioned for a certain medical procedure, indirectly the percentage of failures. For geotechnical engineering 100 % safety is expected as mentioned before.
- The range of site investigation for the geological environment is more likely limited than supported; the methods of site investigation are improved by geotechnical engineers themselves. On the contrary, in medicine investigative methods are strongly supported by different financial resources either from all society tools or from the tools of different foundations and individuals (philanthropists). The investigative methods are improved by a wide spectrum of different professionals.
- The monitoring of the observed objects is much more supported in medicine than in geotechnical engineering even if the monitoring can significantly improve our activity in the future.

Not to end this comparison so pessimistically for geotechnical engineering it is suitable to mention the design method also recommended in EC 7-1 Geotechnical Design – it is the observational method. This design method is close to the methods which are applied in medicine and in principle it accepts the fact that our ability to model the geological environment is limited. The design can be modified during the construction phase when the result of the monitored response differs from the most probabilistic value, however, only in the range which was expected in the first phase of design.

6 CONCLUSION

The profession of geotechnical engineering is connected with an extremely high risk which is not fully accepted in society. This high risk is first of all connected with our ability to realistically model the behaviour of a geological environment due to the changes caused by new construction activity. The natural task of geotechnical engineers is to decrease this risk with the help of new design and construction methods utilizing all new findings in this profession, especially the technology of construction process should be able to immediately react on the monitored geological environment responses.

Nevertheless even when all phases – starting from the site investigation up to the post-construction period of monitoring – are performed under up to date standards, still some probability of failure is remaining there, what is in fact with the basic principle of the construction approach.

Therefore, it is also necessary to spread the responsibility for this risk among other partners of construction activity, mostly among investors and politicians. Risk acceptance and sharing will have a positive impact on the prestige of the geotechnical engineering profession. Some recommendations in this field were mentioned in the paper; nevertheless, a short summary is as follows:

- Together with other professions, also working closely with a geological environment, to give publicity to the idea of shared risks, that there is a necessity to accept a certain percentage of failures during the design and performance of structures. Cooperation is needed among colleagues who are members of the learned and professional societies like ISSMGE, IAEG, ISRM, ITA, EFFC, IGS as well societies where the problem of earth structures for transport and water engineering is covered as well;
- To use any possibility to stress the significance of site (ground) investigation – to define minimum demands for site investigation for different geotechnical structures – probably there is still such a possibility to implement it in EC 7-1 (into paragraph 2.1.(8);
- To be very cautious with respect to the risk of uncertainties when classifying the geotechnical structures into three basic geotechnical categories;
- To give priority to the observational method of design;
- During the definition of partial factors of safety (respectively when selecting characteristic values of mechanical physical properties of the ground) to be more likely on the safe side and after some experience (e.g. in cycles of 5 to 10 years) carefully evaluate recommended values and subsequently to refine them. However, it is possible only as a result of well documented failures, what is their probability. Back analysis of well documented examples can help very much. Therefore the idea of creation of experts´ commissions prepared in advance to visit the structures which had failed as soon as possible, should be supported very strongly;
- For the case of the interaction between older and new structures via deformation of the ground to support the fact that this deformation is always higher than zero but should be kept in acceptable limits;
- More care should be devoted to the risk management process, especially for contractors firms;
- To support the idea that the elimination of potential risks mainly via insurance is not the right way.

ACKNOWLEDGEMENTS

The paper was prepared with financial support from a grant of The Czech Ministry of Education MSM 6840770005: Sustainable Construction.

REFERENCES

Čermák,J. (2003) Foundation pit reconstruction after World Trade Towers failure. Invited lecture presented during the European Conference SMGE, Prague.

Terzaghi,K. (1959) Soil Mechanics in Action. Civil Engineering, Vol. 69, February, pp.33-34.

Vaníček,I, Vaníček,M. (2008) Earth Structures in Transport, Water and Environmental Engineering. Springer Science + Media B.V., 637 p.

ISGSR 2011 - Vogt, Schuppener, Straub & Bräu (eds) - © 2011 Bundesanstalt für Wasserbau ISBN 978-3-939230-01-4

Challenges in Geotechnical Reliability Based Design

Y. Honjo
Department of Civil Engineering, Gifu University, Gifu, Japan

ABSTRACT: The author has been proposing a reliability based design (RBD) scheme for practicing geotechnical engineers. The essence of the proposed scheme is the separation of the geotechnical design part from the uncertainty analysis part in geotechnical RBD. In this way, practical engineers are able to perform RBD in a more comfortable way compared to the traditional RBD procedure. Results of RBD on some structures are presented in this paper to highlight the characteristics of the geotechnical RBD. Based on the results, some discussions are made to identify the major issues geotechnical RBD is facing. It is concluded that spatial variability of soil properties is only one of the sources of uncertainty. In many design problems, statistical estimation error, design calculation model error and transformation error associated with estimating soil parameters (*e.g.* friction angle) from the measured quantities (*e.g.* SPT N-values) have higher uncertainty. It is important to recognize these aspects in developing the geotechnical RBD to the next and the higher stage.

Keywords: Reliability base design, Statistical analysis, Random field, Geotechnical design

1 INTRODUCTION

Needs for carrying out reliability analysis (RA) for complex geotechnical design problems are increasing due to the introduction of the limit state design worldwide. On the other hand, in the current practical design of geotechnical structures, many sophisticated calculation methods, *e.g.* commercially available user friendly FEM programs *etc.*, are employed. These methods become more and more user friendly, and can be used with very small efforts for preparing input data and summarizing calculation results.

It takes quite amount of effort for people to combine these programs with RBD. To connect these design tools to RBD tools is not an easy task. Furthermore, to understand and become proficient with these RBD tools need quite amount of time and efforts.

Considering these situations, the author has been proposing a new RBD scheme for geotechnical design. The essence of the issue that makes geotechnical engineers difficult to practice RBD, as I see, is the mixing of geotechnical design tools with RBD tools in the existing RBD procedure. Furthermore, if we mix them together, one tends to lose intuitive understanding to the design problem at hand, which is very important in geotechnical design to make engineering judgements in the course of design.

The RBD scheme we are proposing here attempts to take into account of characteristics of geotechnical design as much as possible. The scheme is for geotechnical engineers who are proficient in various aspects of geotechnical design but not very familiar with RBD tools.

In this presentation, only the overall outline of the scheme is described. The concept of the methodology is more focused, but details are not very well explained. For the details of the methodology, readers are requested to see papers listed in the reference list. I

It is also a purpose of this paper to identify the major sources of uncertainty that are important in geotechnical RBD through four examples. It may be generally recognized that the spatial variability of soil properties is the most important source of uncertainty in geotechnical RBD. However, from the results presented in this paper, it is only one of the sources of uncertainty. In many design problems, statistical estimation error, design calculation model error and transformation error associated with estimating soil

parameters (*e.g.* friction angle) from the measured quantities (*e.g.* SPT N-values) exhibit higher uncertainty.

2 PROPOSED SCHEME FOR GEOTECHNICAL RBD

2.1 *Outline of the Scheme*

The basic concept of the scheme is illustrated in Figure 1. The scheme starts with the basic variables. The basic variables include all variables concerned in design: Various actions, environmental effects, geotechnical parameters, other material properties, configuration and size of structure and supporting ground, boundary conditions are all included in the basic variables.

The scheme proposed here is separated to three parts: (I) geotechnical design, (II) uncertainty analysis of basic variables and (III) reliability assessment.

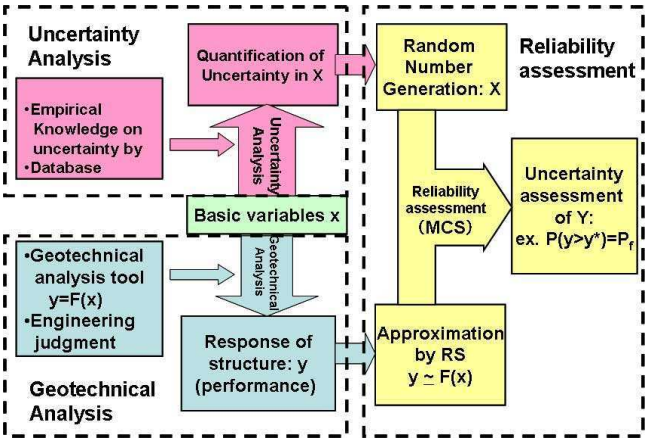

Figure 1. Proposed RBD scheme

Geotechnical design, (I), is almost the same as usual design procedure for geotechnical structures. The response of the structure (safety factor etc.), y, is obtained from the basic variables, x, by the design calculations. In some cases y can be related to x by a relatively simple performance function. In other cases, the response surface (RS) method can be used to relate x to y by a regression analysis (Box & Drepper, 1987).

The uncertainty analysis of basic variables, (II), is the main part of RA. Statistical analysis plays the major role in this analysis. Some basic knowledge on probability theory and statistical analysis are required in this step. Much accumulated knowledge in geotechnical reliability design is employed in carrying out the analyses. The author is recommending use of R language in this step which can make the analysis very easy and efficient. Actually, all the uncertainty analyses and reliability analyses presented in this paper are done by R.

The reliability assessment, (III), is carried out based on the results of the uncertainty analyses and the performance function by simple Monte Carlo simulation (MCS). MCS is recommended due to the following reasons:

(1) MCS is a very straight forward reliability analysis procedure that does not require detailed background knowledge of the probability theory in most cases.

(2) Since the performance function (or the response surface) introduced in the RBD calculation is simple, they do not require much calculation time. Therefore, it is not necessary to introduce any sophisticated reliability analysis methods that save the number of calculations of the performance function.

2.2 *Classification of Uncertainties and Their Treatment*

A classifications of the uncertainties encountered in geotechnical RBD is given in this section together with brief description how they are generally treated in this study. Not all the uncertainties classified here need to be considered in all geotechnical RBD. They need to be chosen according to the needs and the conditions of each design problem. It is assumed in this paper that the uncertainties on actions are separately given.

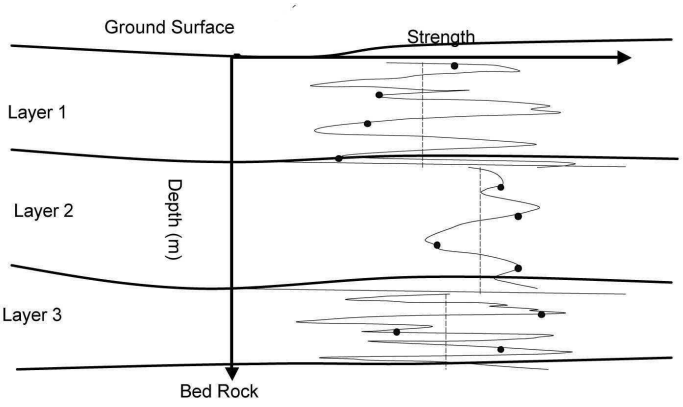

Figure 2. Modelling soil profile by random field

2.2.1 *Measurement error*

It is error involved in measurements in investigations and tests. In the traditional error theory, the measurement error is assumed to independently and identically follow a normal distribution. On the other hand, this error may include biases caused by the equipments and the operators. However, this error is

usually ignored in geotechnical RBD because the influence of it may not be large compared to other uncertainty sources. Furthermore, it is very difficult to separate measurement error from observed spatial variability. Thus, the observed spatial variability may also include the measurement error.

2.2.2 *Spatial variability:*

The spatial variability of geologically identical geotechnical parameters are conveniently (or fictitiously) modelled by the random field (RF) theory in geotechnical RBD. The geotechnical parameters are determined by themselves and already exist at each location. However, because of our ignorance (*i.e.* lack of knowledge or Epistemic uncertainty (Baecher and Christian, 2003)), we model them using RF for our convenience. It is a simplification and an idealization of the problem.

It is a general procedure to model soil profile that belongs to a geologically identical layer by superposition of the trend and the random components (Lumb, 1974; Vanmarcke, 1977; Matsuo, 1984; Phoon and Kulhawy, 1999a *etc.*). The trend component gives a general overall behavior of the soil property, whereas the random component describes discrepancy of each observation from the trend (Figure 2):

$$z(x) = f(x|\beta) + \varepsilon(x|\sigma,\theta) \qquad \varepsilon \sim N(0,\sigma^2,\theta) \tag{1}$$

where

x : spatial coordinate vector (x_1,x_2,x_3), $f(x|\beta)$: a function showing the trend component

β : trend parameter vector, $\varepsilon(x|\sigma,\theta)$: the random component

σ^2 : variance of the random filed, θ : autocorrelation distance vector $\theta = (\theta v, \theta_h)$

θ_v : autocorrelation distance in vertical direction, θ_h : autocorrelation distance in horizontal direction

The random component $\varepsilon(\boldsymbol{x})$ is assumed to consist a stationary (=homogeneous) random filed (RF). The stationarity assumed in this study is that in a weak sense, which implies the RF can be described by the following three statistics:

$$\begin{aligned} &\mu_z(x_1,x_2,x_3) = 0 \\ &{\sigma_z}^2(x_1,x_2,x_3) = \sigma^2 \\ &\rho_z(x_1,x_2,x_3) = \rho(\Delta x_1,\Delta x_2,\Delta x_3) \end{aligned} \tag{2}$$

The first equation states that the mean is a constant, *i.e.* independent of the coordinate $\boldsymbol{x}=(x_1, x_2, x_3)$. In the present context, this mean value is assumed to be 0. The second equation expresses that the variance is also constant. Finally, the third equation states that the autocorrelation function is given not by the absolute coordinate but by the relative distance between the two coordinate positions.

In addition to the above assumptions, the form of autocorrelation function is specified in this study. Due to the deposition process of soil layers, it is generally assumed that autocorrelation structure for the horizontal direction, *i.e.* x_1 and x_2, and for the vertical, *i.e.* x_3, are different. We assume that the autocorrelation function has separable property as suggested by Vanmarcke (1977):

$$\rho_\varepsilon(\sqrt{\Delta x_1^2 + \Delta x_2^2}, \Delta x_3) = \rho_{\varepsilon h}(\sqrt{\Delta x_1^2 + \Delta x_2^2}) \cdot \rho_{\varepsilon v}(\Delta x_3) \tag{3}$$

The exponential type autocorrelation function is assumed in this study

The typical values of these statistics for various types of soil are summarized, for example, in Phoon and Kulhawy (1999a and 1999b).

2.2.3 *Statistical estimation error*

Errors associated with the estimation of parameters of RF are termed the statistical estimation error. It further includes estimation error for parameter values estimated at a certain point in space by, say, Kriging. RF theory is used as a platform to evaluate statistical estimation errors.

In evaluating statistical estimation error, the author believes it very important to distinguish between the two cases below (Honjo and Setiawan,2007; Honjo, 2008).

General Estimation*:* The relative position of investigation location and of a structure to be built <u>is not taken into account</u> in soil parameter estimation. For example, if a large container yard to be designed, the bearing capacity of the ground at an arbitrary location may be evaluated considering general property of ground condition obtained in the whole area.

Local Estimation*:* The relative position of investigation location and of a structure to be built <u>is taken into account</u> in soil parameter estimation. Therefore, there would be considerable reduction in the estimation error if the two locations are very close. A straightforward example of this case is that if one wants to

design a foundation for a house and made a detailed soil investigation at the spot, one need to consider very little uncertainty to ground condition.

The situation described here as General and Local estimation are rather common situations encountered by geotechnical engineers. The engineers surely have treated these conditions in an implicit way, and modified their design. These are a part of so called *engineering judgement* in the traditional geotechnical engineering. The difference here is that we explicitly take into account these situations and try to quantify the uncertainty.

Honjo and Setiawan (2007) has given formulation for these two cases for a particular situation. Honjo (2008) has discussed this problem in connection with actual design. A recent paper by Honjo et al. (2011) gives a general formulation for the general estimation, which is employed in the examples of this paper as well. For the local estimation in this paper, block Kriging is employed (*e.g.* Wachernagel, 1998).

The author believes that a general statistical theory need to be developed for these two situations based on RF theory. It is like the normal population theory gives a general theory for the mathematical statistics. Although any real situation do not exactly satisfy the simplified and idealized assumptions made in the theory, it can contribute quite a lot to give a basic platform for the evaluation of the statistical estimation error in geotechnical parameter estimation and geotechnical RBD.

2.2.4 *Transformation error*

Errors associated with the transformation of measured geotechnical parameters by a soil investigation to geotechnical parameters used in the design calculation are termed transformation error. There are usually both biases and scatters in the transformations.

Readers will see the examples of the transformation errors in the examples of this paper. The most comprehensive reference for this problem is a manual provided by Kulhawy and Mayne (1990), which gives considerable amount of quantitative information on this problem.

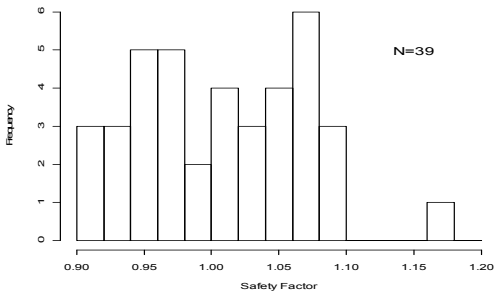

Figure 3. Error in Swedish circular slop analysis (Matsuo and Asaoka, 1976)

2.2.5 *Design calculation model error*

This is error associated with prediction capabilities of simplified and idealized design calculation models on the real phenomena. In geotechnical engineering, the tests and experiments closer to real structure scales (*e.g.* pile load tests, plate loading tests *etc.*) are more commonly performed, and many failure cases are available especially on earth structures such as embankments, cut slopes and excavations. These facts make it easier for us to evaluate the model errors in a quantitative manner in geotechnical design.

For example, the model error of the Swedish circular slip method in stability of embankment on soft cohesive soil is analyzed in detail by Wu and Kraft (1970) and Matsuo and Asaoka (1976). The latter has analyzed failed embankments on soft ground, and concluded that by the cancellations of many factors involved in the stability analysis, the final safety factors calculated follows an uniform distribution that lies between 0.9 and 1.1 (Figure 3). This conclusion is essen-

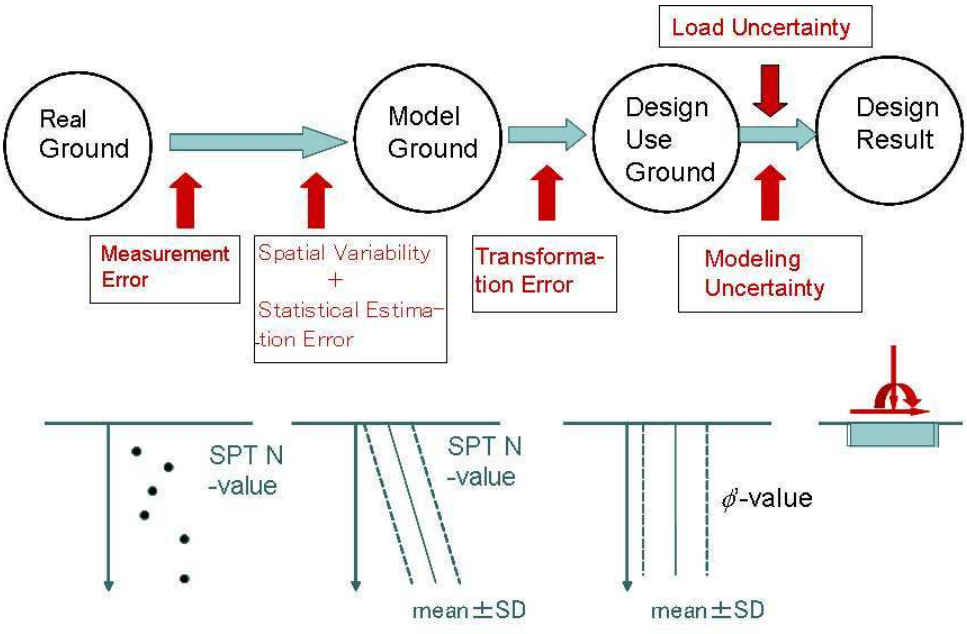

Figure 4. An example of a procedure for geotechnical RBD

tially in accordance with a comprehensive review on this problem by Wu (2009), where he stated that the combined uncertainty for limit equilibrium analysis with circular slip is estimated to be mean 1.0 (i.e. no bias) with COV 0.13-0.24.

By over viewing the uncertainties encountered in geotechnical design, most of uncertainty sources are Epistemic uncertainty (*i.e.* lack of knowledge) rather than Aleatory uncertainty (*i.e.* pure randomness) (Beacher and Christian, 2003). We are like playing cards with the ground where we peep through their cards by some investigations. (In this game, fortunately, the nature does not have any intention to circumvent us.)

An example of sequence of uncertainties entering into geotechnical RBD is illustrated in Figure 4.

2.3 *Local Average and Reliability Assessment*

There is a description on the characteristic value of a geotechnical parameter in Eurocode 7 (CEN,2004) as follows:

> *'The zone of ground governing the behaviour of a geotechnical structure at a limit state is usually much larger than a test sample or the zone of ground affected in an in situ test. Consequently the value of the governing parameter is often the mean of a range of values covering a large surface or volume of the ground. The characteristic value should be a cautious estimate of this mean value' (CEN EN1997-1, 2.4.5.2 (7)).*

The same fact has been pointed out much earlier by Vanmarcke (1977) that it is the local averages (LA) of soil properties that are important in controlling behaviour of geotechnical structures, such as piles, shallow foundations and slopes.

In geotechnical RBD, it is necessary to take the weighted average of geotechnical parameters to obtain the resistance. For example, the shaft resistance of a pile is integration of the soil strength along the pile shaft, resistance moment of a slip surface is integration of soil strength along the slip arc, and settlement of a pad foundation may be controlled by the average stiffness of a certain size of soil mass right under the foundation.

The local average (LA) of the geotechnical parameter for vertical direction over a length L is defined:

$$\overline{Z}_L = \frac{1}{L}\int_0^L Z(x)dx \tag{4}$$

It is apparent that the mean of the LA coincides with the original mean of the RF, μ. Furthermore, the variance reduction of the local average from the original variance of the RF has extensively studied by Vanmarcke (1977 and 1983), where he has derived so called the *variance function*, $\Gamma^2(L)$. If the autocorrelation function is of the exponential type, s_L^2, can be obtained by the variance function as,

$$s_L^2 = E\left[\left\{\frac{1}{\mathrm{L}}\int_0^L Z(x)dx - \mu\right\}^2\right] = \sigma^2\Gamma^2\left(\frac{L}{\theta}\right) = \sigma^2\left(\frac{\theta}{L}\right)^2\left[2\left(\frac{L}{\theta} - 1 + \exp\left(-\tfrac{L}{\theta}\right)\right)\right] \tag{5}$$

Vanmarke has further extended the theory to multidimensional space, and found that if the autocorrelation function is separable, the variance of local average over an area or a volume can be obtained by multiplying the variance functions for each dimension.

In this study, the resistance is calculated based on the local average of a certain soil mass that is controlling the behaviour of a geotechnical structure. Thus the uncertainty of resistance is a reflection of the variance of the local average of the geotechnical parameter.

3 GEOTECHNICAL RELIABILITY BASED DESIGN BY EXAMPLES

The proposed RBD scheme has been applied to several cases. 4 examples are chosen here to illustrate the procedure and highlight the characteristic of the method. Based on the results, some discussions are made to identify the major issues geotechnical RBD are challenged.

The first three examples are problems set by ETC10 for the purpose of a comparative study of the national annexes of Eurocode 7. The problems are relatively straight forward but not excessively simplified to lose the essence of real geotechnical design problems. Due to the limitation of the space, the details of RBD are not described. One should see Honjo et al. (2010, 2011) for the details.

The fourth problem is based on Otake et al. (2011) submitted to this conference. It is a reliability assessment of a 14 km long irrigation channel for liquefaction during expected Tokai-Tonankai earthquake. The difference between the general and the local estimation of the soil parameters on the results are emphasized.

3.1 *Pad foundation on sand (ETC10 EX2-1)*

3.1.1 *Problem description*

The problem is to determine the width of a square pad foundation on a uniform and very dense fine glacial outwash sand layer of 8 (m) thick on the underlying bedrock (Figure 5). It is requested that the settlement should be less than 25 (mm) (SLS) and stability should be secured (ULS). The design working life of the structure is 50 years.

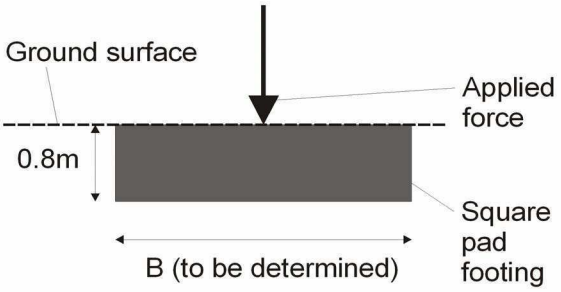

Figure 5. The pad foundation on sand

It is specified that the pad foundation is to be built at embedded depth of 0.8 (m), and vertical permanent and variable loads of the characteristic values 1000 (kN) (excluding the weight of foundation) and 750 (kN) respectively are applied. The unit weight of the concrete is 25 (kN/m^3). No horizontal loading is applied.

There are 4 CPT tests within 15 (m) radius from the point the pad foundation is to be constructed and digitized q_c and f_s values of 0.1 (m) interval are given to 8 (m) depth from the ground surface (Figure 6). The groundwater is 6 (m) below the ground surface. The unit weight of sand is 20 (kN/m^3).

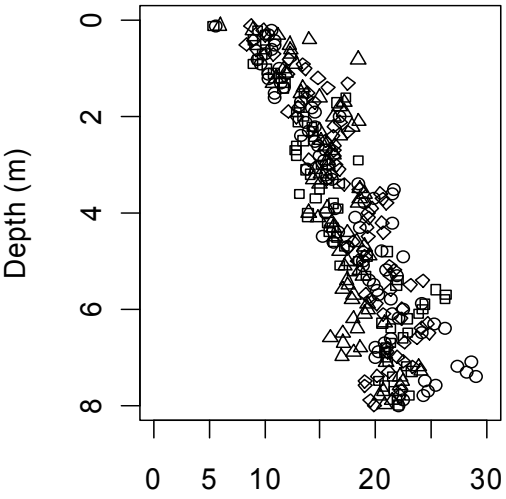

Figure 6. 4 CPT q_c results

3.1.2 *Uncertainty analysis*

There are two limits states to be examined: SLS where the settlement should be less than 25mm, and ULS where the stability should be secured.

For the SLS, the CPT q_c values are used to model the spatial variability of the ground. A linear model is used to describe the trend and the residuals follow a normal distribution. The vertical autocorrelation distance of 0.4 m is estimated. The horizontal autocorrelation distance of 4 m is assumed.

The general estimation is employed and estimation error is evaluated. Also reduction of the variance by taking the local average between the depth of 0.8 to 1.8 m is taken into account. The overall reduction of SD of CPT q_c value is estimated, where SD of 2.28 MPa reduced to 1.66 MPa.

The transformation of CPT q_c values to Yong's modulus is done considering the transformation error. The mean and SD of the error is estimated to be 1.14 and 0.94 respectively. This is considerably large error.

The uncertainty associated with the permanent and the variable loads are taken from Holicky et al. (2007). . These quantities are used in the code calibrations of the structural Eurocodes rather widely. The uncertainties evaluated are listed in Table 1 for SLS.

Table 1. List of basic variables for Ex.2-1 SLS settlement

Basic variables	Notation	mean	SD	Distribution type
Estimation error and local average variance of q_c	I_E is proportional to I_{qc}	qc=10.54+1.66x_3 (MPa)	7.2(MPa) COV=0.13[(1)] at z=1.5(m)	Normal
Transformation error on E' from q_c	δ_E	1.14	0.94	Lognormal
Permanent load	δ_{Gk}	1.0	0.1	Normal[(2)]
Variable load	δ_{Qk}	0.6	0.35x0.6=0.21	Gumbel distribution[(2)]

(Note 1) COV has been obtained by Eq.(3). (Note 2) Based on JCSS (2001) and Holicky et al. (2007).

Table 2. List of basic variables for Ex.2-1 ULS stability

Basic variables	Notation	Mean	SD	Distribution type
Spatial variability	ϕ'_{tc}	42.8 (degree)	0	Deterministic variable
Transformation error from q_c	ϕ'_{tc}	42.8 (degree)	2.8 (degree)	Normal
R_u model error	δ_{Ru}	0.894	0.257	Lognormal
Permanent action	δ_{Gk}	1.0	0.1	Normal
Variable action	δ_{Qk}	0.6	0.35x0.6=0.21	Gumbel distribution

For the ULS, the CPT q_c values are first converted to internal friction angle in a equation proposed by Kulhawy and Mayne (1990). The converted internal friction angle had very small variance, which made the spatial variability of this quantity null. The transformation error in this conversion is given in the same literature.

The model error in the bearing capacity calculation form the internal friction angle is obtained from a recent literature which compares the calculated values with the results of the plate loading test.

The evaluated uncertainties are listed in Table 2 for ULS.

3.1.3 *Geotechnical analysis and performance function*

As for SLS, 3D PLAXIS is used to obtain the relationship between the settlement and the foundation size, B at the mean values of Young's modulus and the loads. It is found that the settlement has a linear relationship with $log(B)$. Since the ground is assumed to be a elastic body, the settlement is doubled if Young's modulus is half or the load is doubled. These relationships are taken into account, and a performance function is obtained:

$$s = \frac{(17.0 - 9.73\log(B))}{I_E \cdot \delta_E}\left(\frac{\gamma \cdot D_f \cdot B^2 + G_k\delta_{Gk} + Q_k\delta_{Qk}}{\gamma \cdot D_f \cdot B^2 + G_k + Q_k}\right) = \frac{(17.0 - 9.73\log(B))}{I_E \cdot \delta_E}\left(\frac{20 \cdot B^2 + 1000\delta_{Gvk} + 750\delta_{Qvk}}{20 \cdot B^2 + 1750}\right) \qquad (6)$$

The performance function for ULS is given as follows:

$$M = Ru(B,\ \phi'_{\mathrm{tc}}) \cdot \delta_{Ru} - G_k \cdot \delta_{Gk} - Q_k \cdot \delta_{Qk} \qquad (7)$$

Where R_u is a classic bearing capacity formula, and M is the safety margin. The definitions of other notations are given in Table 2.

3.1.4 *Reliability assessment and results*

Simple Monte Carlo simulation is employed to carry out the reliability analysis. The uncertainty listed in Table 1 and Eq.(6) are used to evaluate the probability that the settlement exceeds 25 mm for SLS. The same procedure is taken to evaluate the failure probability of the pad foundation based on Table 2 and Eq.(7).

Figure 7 shows the results of MCS on ULS of the pad foundation. The MCS is repeated several times by removing each uncertainty sources to see the impact, which the results are also presented in the figure. The necessary width of the foundation based on the result for both SLS and ULS are presented in Table 4.

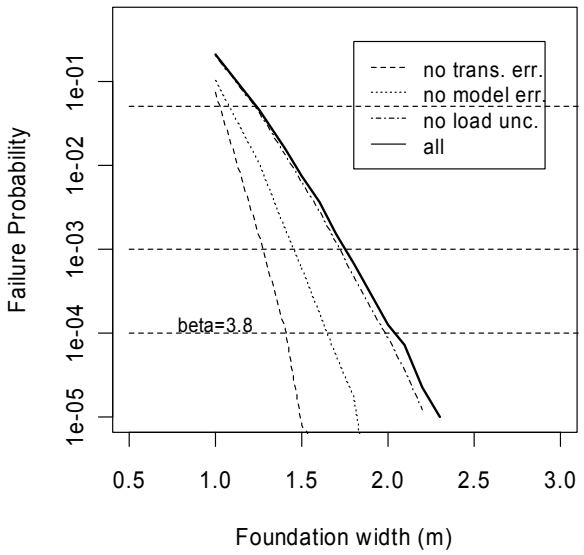

Figure 7. The results of MCS on the stability of the pad foundation.

Table 4. summary of the results for the pad foundation

Limit state	Target β for 50 years design working life. (P_f)	Required width (m)
S.L.S.(s < 25 mm)	1.5 (0.067)	B > 2.4 (m)
U.L.S.(stability)	3.8 (10^{-4})	B > 2.2 (m)

Table 5(a) rate of contribution of each uncertainty source for settlement analysis (B=1.0 m)

Uncertainty sources	All uncertainties Considered	transformation error	spatial variability	load uncertainty
β and β_{-i}	0.595	2.804	0.623	0.590
contribution	100 %	92 %	8 %	0 %

Table 5(b) rate of contribution of each uncertainty source for stability analysis (B=1.0 m)

Uncertainty sources	All uncertainties considered	transformation error	model error	load uncertainty
β and β_{-i}	0.811	1.443	1.261	0.840
contribution	100 %	51 %	44 %	5 %

The influence of each uncertainty source is listed in Table 5(a) and (b). An approximation method to estimate the contribution of each factor is explained in Appendix A. A discussion will be made on these results in the latter section of this paper.

3.2 *Pile foundation in sand (ETC10 EX2-6)*

3.2.1 *Problem description*

The problem is to determine pile length L (m) of a pile foundation of a building. The pile is a bored pile (D = 0.45 m) embedded entirely in a medium dense to dense sand spaced at 2.0 (m) interval (Figure 8). Each pile carries a characteristic vertical permanent load of 300 (kN) and a characteristic vertical variable load of 150 (kN). The soil profile includes Pleistocene fine and medium sand covered by Holocene layers of loose sand, soft clay, and peat (see Table 6).

There is one CPT (q_c measurement only) close to the spot to determine the strength profile of the ground. The water table is about 1.4 (m) below the ground level.

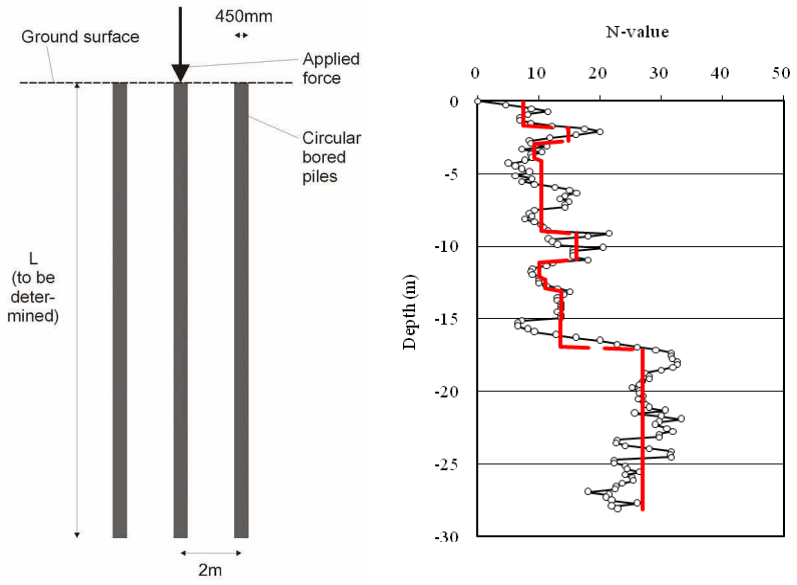

Figure 8. The configuration of the bored pile and soil profile by SPT N-value transformed from CPT q_c value.

3.2.2 *Uncertainty analysis*

The bearing capacity estimation equation for pile the author used is based on SPT N-value. Thus CPT q_c value is converted to SPT N-value by a equation given in Kulhawy and Mayne (1990). This transformation equation has the transformation error of mean 1, COV 1.03 and follows a log normal distribution.

Since there is only one CPT test result, and the layer have quite complex structure, the soil profile is modeled by 10 layers and the mean and the SD of each layer is estimated from the CPT test result.

The model error in the empirical bearing capacity estimation equation used widely in Japan is obtained from a literature which is based on the results of a number of pile loading test results. The model error for estimating shaft resistance and pile tip resistance are given separately as shown in Table 6.

The uncertainties on permanent and variable loads are taken from the same literature used in the previous example, and given in Table 6.

Table 6. Statistical properties of the basic variables

Basic variables		Notations	Mean	SD	Distribution	Note
uncertainty on characteristic value of permanent load		δ_{Gk}	1.0	0.1	Normal	G_k = 300 (kN) (1)
uncertainty of characteristic value of variable load		δ_{Qk}	0.6	0.21	Gumbel	Q_k = 150 (kN) (1)
uncertainty of estimating pile shaft resistance		δ_f	1.07	0.492	Log Normal	Okahara *et.al* (1991)
uncertainty of estimating pile tip resistance		δ_{qd}	1.12	0.706	Log Normal	Okahara *et.al* (1991)
uncertainty of transformation from CPT q_c to N		δ_t	1	1.03	Log Normal	Kulhawy & Mayne (1990)
Layer 1	Clay with sand seams	$N1^{(2)}$	7.51	3.66	Normal	Depth 0.0 - 1.9 (m)
Layer 2	Fine sand	$N2^{(2)}$	14.80	4.58	Normal	Depth 1.9 - 2.9 (m)
Layer 3	Clay with sand seams	$N3^{(2)}$	9.24	1.44	Normal	Depth 2.9 - 4.0 (m)
Layer 4	Fine silty sand	$N4^{(2)}$	10.33	3.22	Normal	Depth 4.0 - 9.0 (m)
Layer 5	Fine silty sand with clay & peat seams	$N5^{(2)}$	16.17	3.31	Normal	Depth 9.0 - 11.0 (m)
Layer 6	Clay with sand seams	$N5^{(2)}$	10.08	1.45	Normal	Depth 11.0 - 12.3 (m)
Layer 7	Clay with peat seams	$N7^{(2)}$	11.14	1.51	Normal	Depth 12.3 - 13.0 (m)
Layer 8	Clay with peat seams	$N8^{(2)}$	13.68	0.54	Normal	Depth 13.0 - 15.0 (m)
Layer 9	Fine sand	$N9^{(2)}$	13.56	7.24	Normal	Depth 15.0 - 17.0 (m)
Layer 10	Fine sand	$N10^{(2)}$	26.98	3.71	Normal	Depth 17.0 (m) below

（Note 1） Based on Holicky, M, J. Markova and H. Gulvanessian (2007). (Note 2) Unit of soil layers are SPT N-values

3.2.3 *Geotechnical analysis and performance function*

The performance function employed in this example is given as follows:

$$M = U\delta_f \sum_{i=1}^{n} \delta_{ti} f_i(\delta_t N_i) L_i + \delta_{qd} q_a(\delta_t N_n) A_p - \delta_{Gk} G_k - \delta_{Qk} Q_k \tag{8}$$

where, U: perimeter of the pile (m), f_i: maximum shaft resistance of each soil layer (kN/m2), L_i: thickness of each soil layer (m), N: standard penetration test (SPT) blow count, q_d: ultimate pile tip resistance intensity per unit area (kN/m2), and other notations are listed in Table 6. The details of f_l and q_d is given in SHB (2002).

3.2.4 *Reliability assessment and results*

Monte Carlo simulation using R language is carried out for different pile length L (m) to obtain the reliability index (or probability of failure). In this analysis, the number of random numbers generated for each case is 500,000 sets. The obtained reliability index for different pile length is shown in Figure 9.

Since the case considered is the ultimate limit sate, the reliability index, β, of more than 3.8 may be required. The pile length of more than 18 (m) is necessary.

In order to investigate the contribution of each uncertainty sources, reliability analyses are carried out by removing each uncertainty source at a time. These results are shown in Figure 9 as well. The rate of contribution of each source is further presented in Table 7. The contributions are estimated based on the approximation method explained in Appendix A. The result of this table will be discussed later.

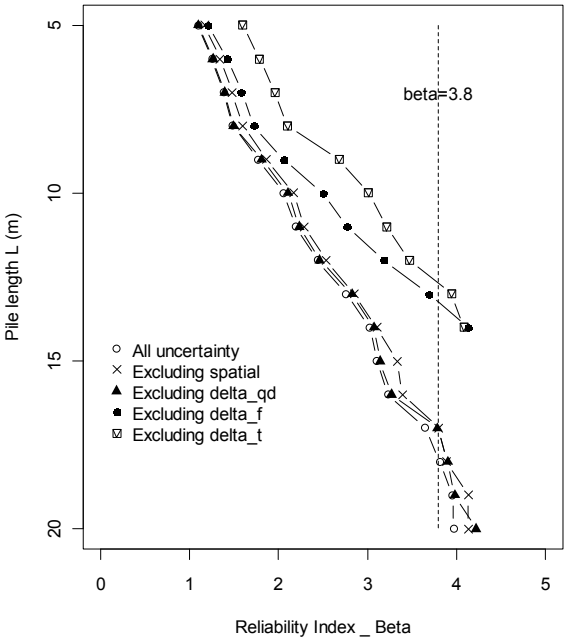

Figure 9. The results of MCS on the stability of the pile foundation.

Table 7. rate of contribution of each uncertainty source for a pile bearing capacity (at L=13 m)

Uncertainty sources	All uncertainty	Spatial variability	Pile tip resistance	Pile shaft resistance	Transformation error
β and β_{-i}	2.75	2.85	2.82	3.69	3.94
contribution	100 %	6 %	5 %	41 %	48 %

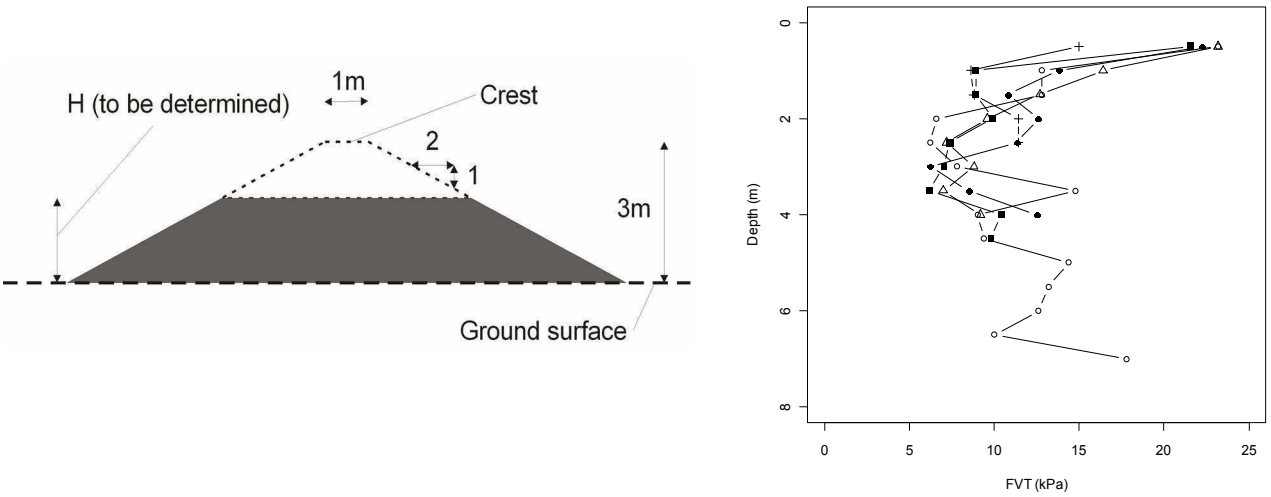

Figure 10. The configuration of an embankment on peat and the results of 5 FVT

3.3 *Embankment on peat ground*

3.3.1 *Problem description*

An embankment is to be designed on a soft peat ground whose final height should be 3 (m) above the ground surface (Figure 10). The problem here is to determine the first stage embankment height. The inclination of the embankment slope is 1:2, whereas the crest width 1 (m). The unit weight, γ, of the embankment soil is 19 (kN/m^3) and the friction angle ϕ'_k=32.5 (degree).

The ground surface is horizontal. The ground consists of a few dm of topsoil and normally consolidated clay (γ=18 (kN/m^3) and γ' = 9 (kN/m^3)) on a 3 to 7 (m) thick peat layer with γ' =2 (kN/m^3) overlaying Pleistocene sand of γ' =11 (kN/m^3) and ϕ'_k =35 (degree). 5 filed vane test (FVT) results are given whose testing interval is 0.5 (m) in the vertical direction and the length varies between 2.5 and 7.0 (m).

Only ultimate limit state needs to considered and no variable loads have to be taken into account.

3.3.2 *Uncertainty analysis*

The five FVT results are plotted in Figure 10. It is observed that s_u at surface layer of about 0.5 (m) is considerably larger than the bottom peat layer indicating different soil layer. It is determined to separate these data, and group them as topsoil. The trend component of the underneath peat layer is obtained as a quadratic curve, and the residual random component fits to a normal distribution with a constant variance of 2.40^2 (kPa^2).

The statistical estimation error for estimating the local average of peat layer is obtained, whose SD is estimated to be 0.528 (kPa), whereas the variance reduction by local averaging for 4 m depth makes SD of spatial variability to be 1.12 (kPa). The resulting SD for the local average of the peat strength is $\sqrt{0.528^2 + 1.12^2} = 1.24$ (kPa).

The uncertainty concerning the thickness of the top soil is introduced, so as the undrained shear strength, s_u. They are all listed in Table 8.

The design calculation model error is obtained based on Matsuo and Asaoka (1976), where an uniform distribution of [-0.1, 0.1] is introduced.

Table 8. Basic variables of embankment on peat

Basic variables	Notations	mean	SD	Distribution
Topsoil s_u	$s_{utopsoil}$	21.04 (kPa)	3.44	Normal
	$(I_{topsoil})$	(1.0)	(0.163)	
Peat s_u	s_{upeat}	14.73-3.51z +0.536z^2 (kPa)	1.20	Normal
	(I_{peat})	(1.0)	(0.13)[(1)]	
Topsoil thickness	D_t	[0.5, 1.0] (m)		Uniform[(2)]
Uncertainty of ϕ'=0 method	δ_{Fs}	[-0.1, 0.1]		Uniform[(3)]
Unit weight of embankment	γ_f	19.0(kN/m^3)	–	Deterministic
Friction of embankment	ϕ_f	32.5 degree	–	Deterministic
Unit weight of topsoil	γ_c'	9.0(kN/m^3)	–	Deterministic
Unit weight of peat	γ_P'	2.0(kN/m^3)	–	Deterministic
Friction of sand	ϕ_s	35 degree	–	Deterministic
Unit weight of sand	γ_s'	11.0(kN/m^3)	–	Deterministic

(Note 1) s_{upeat} (at z=4.0(m)) = 14.73 - 3.5x4.0 + 0.53x4.0^2 = 9.27, COV=1.24/9.27=0.13

(Note 2) It is assumed that the boundary of the topsoil and the peat layer lies somewhere between z = 0.5 to 1.0 (m).

(Note 3) Based on Matsuo & Asaoka (1976).

3.3.3 *Geotechnical analysis and performance function*

A response surface (RS) that relates embankment height, h, s_u of the topsoil layer, s_u of the peat layer, the thickness of the topsoil, D_t, and the safety factor, F_s, is obtained by a regression analysis based on the results of the stability analysis of 75 combinations of these parameters. Swedish circular method is employed for the stability analysis. In order to make the response surface equation simple, s_u of the peat layer and the topsoil layer are normalized at their mean values

$$I_{peat} = s_u/(\text{mean of } s_u \text{ of the peat layer})$$
$$I_{topsoil} = s_u/(\text{mean of } s_u \text{ of the topsoil}) = s_u/21.04 \quad (9)$$

Based on the obtained response surface, a performance function is obtained as follows:

$$Fs = 1.783 - 1.351\ h + 0.213\ h^2 + 1.156\ I_{peat} + 0.272\ I_{topsoil} + 0.091\ D_t + \delta_{Fs} \quad (10)$$

where the notations are given in Table 8.

3.3.4 *Reliability assessment and results*

The performance function obtained in Eq.(10) is employed to evaluate the failure probability of embankment, Prob[$Fs \leq 1.0$], by MCS. The uncertainties considered in the analysis are listed in Table 8.

The MCS results are plotted in Figure 11. It is difficult to determine what level of reliability is required in this structure. If the failure probability of 1 %, which is $\beta = 2.32$ is chosen as a target, the height of the embankment for the fist stage may be 2.1 (m). The safety factor by the Swedish method is about 1.4 if the mean values of soil parameters are used in the stability calculation

The failure probability is evaluated by removing each uncertain source to find out the impact of each source. These results are also presented in Figure 11. The contribution of each source is approximately estimated by the method explained in Appendix A, where the results are listed in Table 9. In this case, the peat soil strength is the dominant source of uncertainty which is followed by the model error.

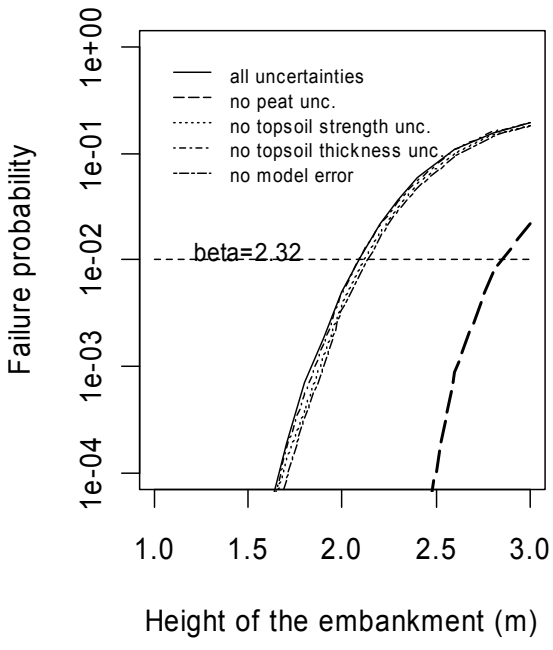

Figure 11. An embankment on peat MCS results

Table 9. The rate of contribution of each uncertainty source for embankment stability (H=2.1 m)

Uncertainty sources	All uncertainty	Peat strength	Top soil strength	Top soil thickness	Model error
β and β_i	2.27	4.58	2.38	2.29	2.44
Contribution	100 %	75 %	9 %	2 %	13 %
Notes		Statistical: 14 % Spatial: 61 %			

3.4 *Liquefaction risk along 12 km long irrigation channel*

3.4.1 *Problem description*

The case described here is based on a paper by Otake et al. (2011) which is one of the papers submitted to this conference. Therefore, only outline of the analysis and the results are given. The parts related to the purposes of this presentation are referred to.

The irrigation channel under study is 25 km long and completed in 1970 (Figure 12). The geology under the channel can be divided into three parts, where 12 km long central part (STA30 – 150) is described in the paper. It is an open channel RC frame structure and 90 % is build in the embankment (Figure 12(a), embankment type), whereas 10% is excavated channel (embedded type) including siphons. The RC frame channel has width of about 10m, height 5m and 10m long.

The channel is located on one of major Alluvial panes in Japan and geology is relatively homogeneous. There is a potentially liquefiable sand layer (As layer) of about 12m thick whose SPT N-value is about 15 and the fine contents (Fc) less than 10%.

The area is in the region where near future occurrence of Tokai-Tonankai earthquake is suspected. Model earthquake motion provided by the central disaster mitigation conference for the earthquake is employed in this study. The downstream part is more susceptible to stronger earthquake motion because it is closer to the epicentre. By the peak ground surface acceleration (PGA), it is 135gal at the most upstream point, 175gal at the middle point and 241gal at the most downstream point. The distinguished characteristics of this earthquake motion are its very long continuous time (about 120 sec) and dominance of the long period components (2 – 4 sec).

The performance requirements of this irrigation channel are *to keep the water level that is sufficient for the natural distribution of water to the surrounding area and to provide sufficient quantity of water to the destinations*. Thus, a limit was set to the absolute settlement of the RC frame for maintaining the water level, and to the relative settlement of the adjacent frames to preserve necessary quantity of water flow. To be more specific, the limit state was set to 60 cm for the absolute settlement based on the free board of the channel, and to 60 cm for the relative settlement due to the frame base thickness.

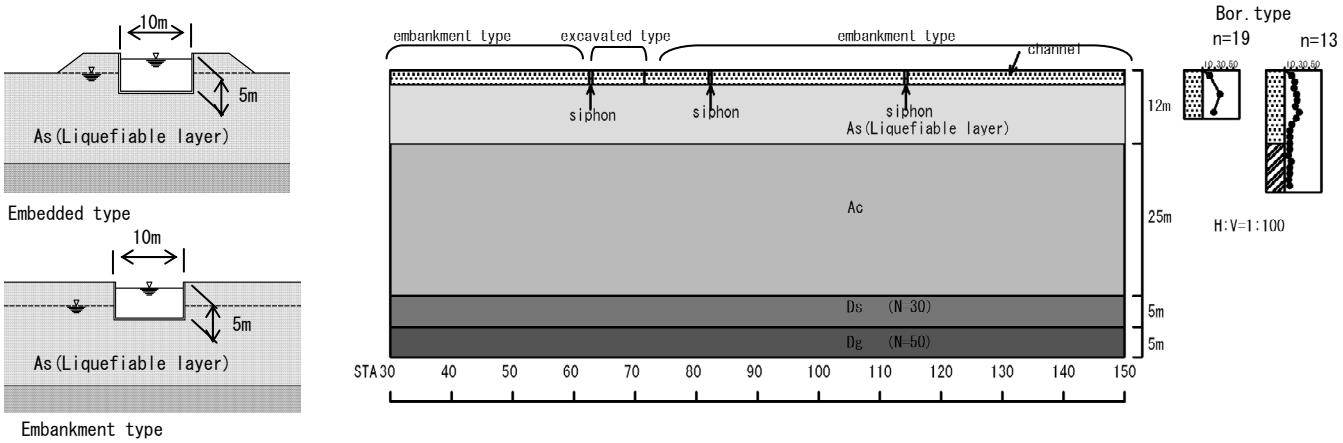

(a) Typical cross section (b) longitudinal section of soil condition

Figure 12. Characteristics of structure and soil condition

3.4.2 *Geotechnical analysis*

It is necessary to select a geotechnical parameter that is appropriate to represent ground characteristic in evaluating potential of liquefaction. S_n value proposed by Goto et al. (1982) is selected in this study to represent the strength of ground for liquefaction. This is weighted integration of adjusted SPT N-value,

N1, over 20m depth. N_1 is defined as $N_1 = 170 \cdot N / (\sigma_v' + 70)$, where σ_v' is the effective overburden stress.

$$S_n = 0.264 \cdot \int_0^{20} e^{-0.04N1(x)-0.24x} dx - 0.885 \quad (11)$$

The characteristic of the sand layer is solely evaluated by N1 value in this index. This is justified in this case because As layer is very homogeneous and the grain size distribution is similar throughout the area, thus S_n is an effective index to evaluate the liquefaction strength of ground at least relatively.

Then, the problem is to evaluate the residual settlement of the irrigation channel for the earthquake with considerably long duration and of long dominant period. The dynamic FEM based on the effective stress analysis, LIQCA2D07, is employed in order to take into account of the mobilization and dissipation of the excess pore pressure. The effectiveness and the limitations of the program was checked by analyzing shaking table test which had modeled the channel.

The settlement of the RC frame is predicted by LIQCA2D07 for various possible conditions. Based on this parametric study, a response surface (RS) is built which is to be used in the reliability assessment.

The settlement induced by the liquefaction is a complex phenomenon which is influenced by many factors. In stead of building a very complex RS, relatively simple RS was introduced in this study. The uncertainty associated to the RS, which is the residual of the regression analysis of the settlement by various factors are also introduced in the reliability assessment.

The vertical displacement is related to S_n and τ by a linear regression line:

$$D = a \cdot S_n + b \cdot \tau + c + \varepsilon \quad (12)$$

where D: vertical displacement(cm) obtained by LIQCA2D07, τ: shear stress(kN/m^2) acting at the centre part of liquefiable sand layer, a,b and c: regression coefficients, and ε: residual error.

Table 10. Input to reliability analysis

Uncertain sources	Notation	mean	SD	Distribution type
S_n-value	Sn	-0.34※1)	0.85※1)	Normal
Earthquake shear stress	τ	[12-17.5]	0	Deterministic
Model error of RS	δ_{RS}	1.0	0.09※2) (0.06) ※2)	Normal
Model error of LIQCA2D07	δ_{FEM}	1.0	0.23	Normal

※1：values by the General estimation. ※2：COV=10.24/110=0.09(embankment type) 2.83/48=0.06(embedded type)

3.4.3 *Uncertainty analysis and performance function*

Uncertainties considered in this study are model uncertainty of LIQCA2D07, spatial variability of soil parameter represented by the spatial variation of S_n, statistical estimation error and error associated to the approximation by RS. These uncertainties are quantitatively analysed by the statistical means. The results of the statistical analysis, which is quantified uncertainty of each uncertainty source, is presented in Table 10.

The performance functions for the embankment type and the embedded type are respectively given as follows:

$$D_{embk} = (-212 \cdot S_n - 18.8 \cdot \tau + 120) \cdot \delta_{RS} \cdot \delta_{FEM} \quad (13)$$

$$D_{embd} = (100 \cdot S_n + 1.97 \cdot \tau + 51) \cdot \delta_{RS} \cdot \delta_{FEM} \quad (14)$$

where D_{emgk} : vertical movement of the embankment type RC frame, and D_{embd} : that of the embedded type.

3.4.4 *Reliability assessment and results*

Figure 11 and Figure 12 shows the mean elevation after shaking of each RC frame (10 m long) for the general estimation and the local estimation of S_n-value respectively. It can be seen, in both cases, the displacement is lager in the downstream because of the stronger earthquake motion. In the downstream part, the mean settlement exceeds the threshold value of 60 (cm). The lager relative displacement occurs at location where the embankment type switches to the embedded type, which implies danger of leakage of water from the channel.

Although the general feature of the vertical displacement is similar for the general and local estimation of S_n, one can see more detailed behavior of each RC frame in the local estimation. For example, there is location where the mean settlement exceed 60 (cm) near STA90 in the local estimation.

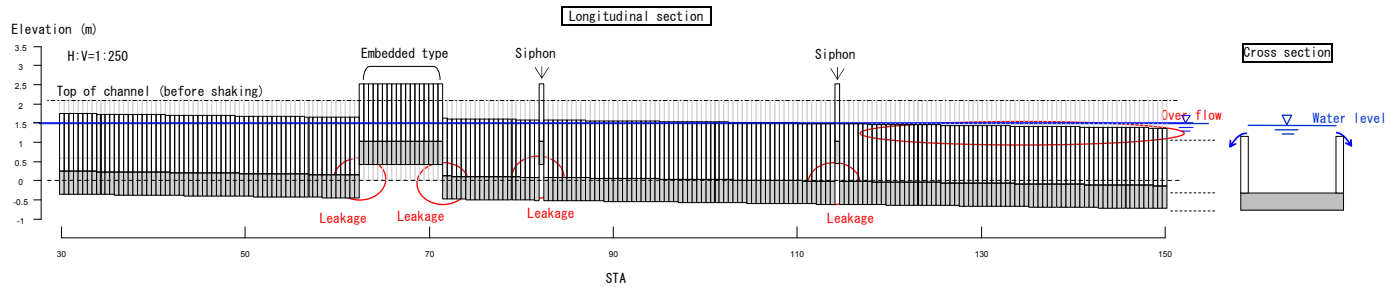

Figure 13. Mean elevation after shaking (general estimation of Sn-value)

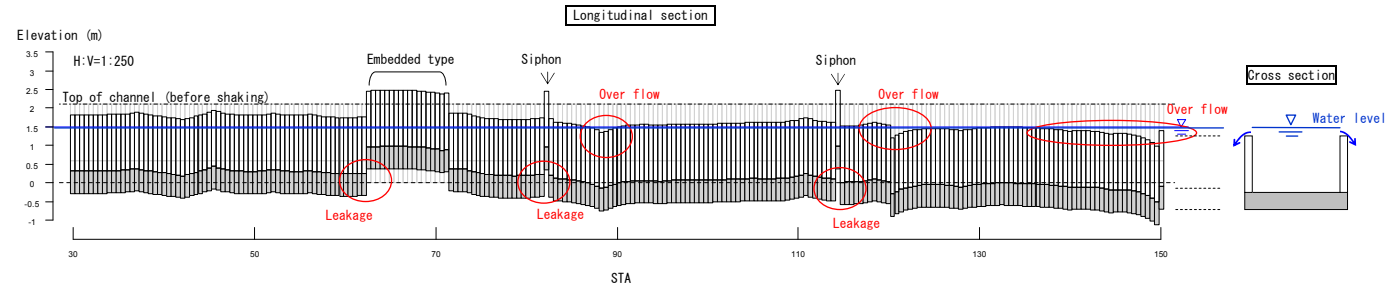

Figure 14. Mean elevation after shaking (local estimation of Sn-value)

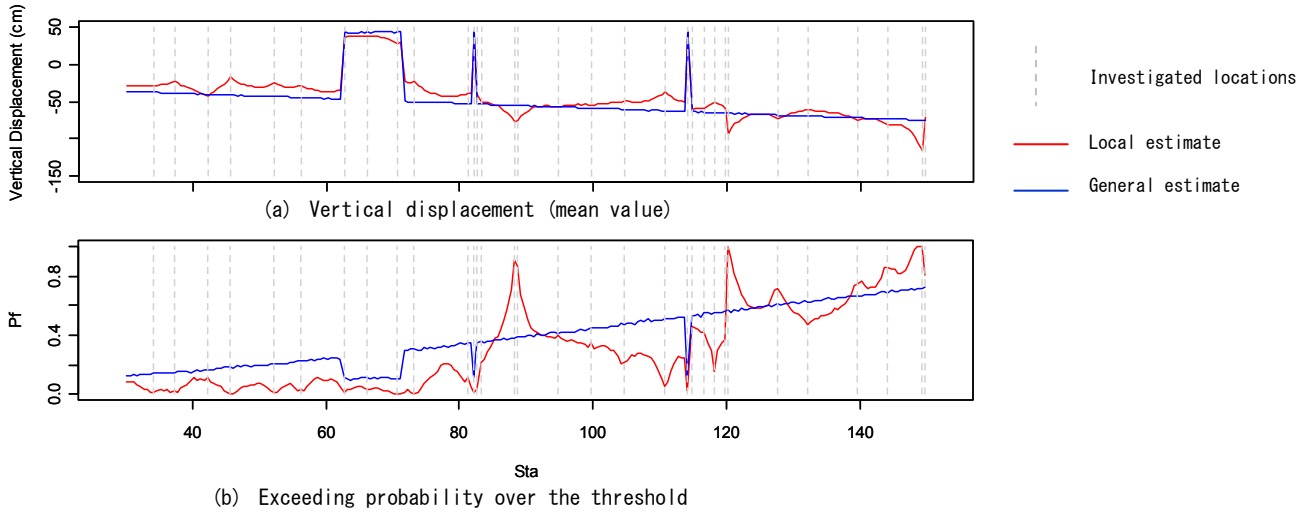

Figure 15. Result of Reliability analysis

Figure 15 presents the mean vertical displacement and the exceeding probability of it over the threshold values (i.e. 60 cm) are presented for the general and local estimation of S_n. The two cases are superposed in these figures for the comparison. The prediction based on the local estimation generally gives smaller exceeding probability, however there are several locations where this relationship is reversed. These probability can be used to determine the optimum enforcement plan of this irrigation channel.

Table 11. Contribution of Uncertainty sources

Uncertainty sources		All uncertainty	Sn-value	Model error	
				FEM	RS
β and β_{-i} (contribution)	Site-r1 (STA63)	1.87 (100%)	1.88 (0%)	8.49 (95%)	1.92 (5%)
	Site-r3 (STA56)	1.58 (100%)	2.32 (54%)	2.05 (41%)	1.63 (6%)
	Site-nr (STA60)	1.02 (100%)	1.42 (48%)	1.33 (41%)	1.08 (11%)

Note) Site-r1:N-values at every 1m, Site-r3: N-values at every 3 m, Site-nr：no investigation at the site

3.5 *Discussions*

It is also one of the purposes of this paper to identify some of the major issues geotechnical RBD is challenged based on the results of the examples. The important sources of uncertainty in geotechnical RBD can be found by carefully discussing the results presented in Tables 5(a), 5(b), 7, 9 and 11. The following observations are possible for RBD of SLS and ULS of the pad foundation, the pile foundation and the embankment on peat:

- It is found from SLS design of the pad foundation that uncertainty is quite large which makes necessary size of the foundation massive (Table 4). This is due to the large uncertainty in transforming CPT q_c to Young's modulus, which can be seen from the results in Table 5(a) that 92% of the uncertainty comes from this transformation error. It is well recognized among geotechnical engineers that estimating stiffness characteristics of ground from the penetration type investigations such as SPT and CPT is not reliable, and the result is ascertaining this fact. Traditionally, therefore, SLS is not checked in the shallow foundation design, and fairly large safety factor, *e.g.* 3, is introduced in ULS design to secure the performance for SLS.
- In stability problem of the foundation, *i.e.* ULS of the pad foundation and the pile foundation, the transformation error and the design calculation model error dominate the uncertainty. In both examples these two uncertainty sources contribute about 40 to 50 % of all uncertainty in the RBD respectively that they are actually controlling the results of the design (Tables 5(b) and 7). The transformation error in the pad foundation design is estimating ϕ' from q_c, whereas in the pile foundation design from q_c to SPT N-value. The model errors of the design calculation equations for the both examples are obtained by comparing the calculated results to the observations (i.e. the results of plate loading tests and pile loading tests). If the author was familiar with the pile capacity calculation formula based on q_c, the transformation error in the pile design may have been considerably reduced. The spatial variability of the soil property in the two examples are small because (1) the variance reduction by the local averaging, and (2) very small fluctuation of ϕ' in the pad foundation example.
- Only in the embankment example, the soil spatial variability is the major source of the uncertainty (Table 9). The spatial variability of the peat and top soil undrained shear strength occupies 70% of the total uncertainty. The statistical estimation error and the design calculation model error contribute 14 and 13 % respectively. This consequence comes partly from the accuracy of the design calculation formula, i.e. Sweetish circular slip method, as presented in Figure 3. The model error in this example is much smaller compared to the former examples.

The soil properties in the first three examples are essentially obtained by the general estimation concept, where we did not take into account the relative location of the soil investigation and the structures. The comparison of the general and the local estimation is specifically made in the irrigation channel example, where the followings are observed:

- By comparing the reliability indices, β, of three locations in Table 11, Site-r1 has the highest β, followed by Site-r3 and then Site-nr. It is actually the reflection of the amount of reliable soil property information at each site. Site-r1 has SPT N-value at each 1 m interval through the sand layer, whereas Site-r3 only in 3 m interval. Site-nr does not have any soil property information at the location and it has to be extrapolated from the nearby investigation results. Note that more information does not necessary means more safety of the structure. There are some locations that the exceeding probability is very high and yet the soil investigation was made (Otake *et al.*, 2011). The more information just implies more precise prediction, and if the soil property is near the average, the location with more information gives higher reliability due to the elimination of statistical estimation error.
- As far as the contribution of each uncertainty source is concerned, the error in estimating S_n and the model error contribute evenly at both Site-nr and Site-r3 (Table 11) to the total uncertainty. The error in estimating S_n includes effects of the spatial variability, the variance reduction by local averaging and the estimation error. (Actually, Kriging and the conditional simulation technique are used in estimating S_n) The model error consists of the FEM model error and the RS model error, where the former is far dominant. At Site-r1, there is no error for S_n estimation, thus the model error overrules the total uncertainty.

The readers may have found by now that the selection of uncertainty sources and their assigned extents may be different from one geotechnical engineer to another based on his knowledge and experiences. If one is more familiar with the local soil property, he/she can narrow down the uncertainty compare to a stranger. Actually, this is one of the essences of geotechnical design and the fact should be reflected in geotechnical RBD as well.

4 CONCLUSIONS

All the examples exhibited in this paper, the description is orders in "*problem description*", *"uncertainty analysis*", "*geotechnical analysis and performance function*" and then "*reliability assessment*". It is expected that readers would comprehend the philosophy of the proposed RBD scheme through these descriptions that the geotechnical analysis part is separated from the uncertainty analysis part. The uncertainty analysis part does require some knowledge in statistical analysis. However, other parts need only small knowledge on probability and statistics. It is anticipated that the readers are able to perceive some engineering judgments introduced in geotechnical analysis part, such as some geotechnical interpretation of the transformation equation from q_c to ϕ' in the pad foundation ULS example, the introduction of top soil layer thickness into embankment stability example, and the introduction of S_n in characterizing the potentially liquefiable layer in the irrigation channel example.

Through these examples, it may be understood that it is not necessarily soil properties spatial variability that controls the major part of uncertainty in many geotechnical design problems. The error in design calculation formulas, transformation of soil investigation results (*e.g.* SPT N-values, FVT, CPT q_c) to actual design parameters (*e.g.* s_u, ϕ', resistance values), and statistical estimation error are more important sources in some cases.

All the statistical and reliability calculations carried out in this paper are done by R language. Due to the restriction of space, it was not possible to explain the superiority of this language in this paper. By using R language, these operations become much user friendly and less time consuming.

ACKNOWLEGEMENT

The author is grateful to the Organizing Committee for the opportunity to make this presentation. The special thanks go to Bernd Schuppener, Norbert Vogt, Kok Kwang Phoon and Gerhard Braeu for various support they have provided in the preparation of this lecture, and to Yu Otake for allowing me to quote a part of the results he have obtained in the irrigation channel liquefaction risk analysis.

APPENDIX A

The estimation method given here is used to estimate the contribution of each uncertain source to the reliability analyses presented in this paper. It is really an approximate method to know these contributions so as to give materials for discussions on geotechnical RA.

The contributions are basically measured by contribution of each variance to the total variance. Suppose the performance function is given by a linear combination of all uncertain sources of resistances and forces. Let $\overline{R}$ be the average of total resistance, $\overline{S}$ that of force. The reliability index, β, can be given as follows:

$$\beta = \frac{\overline{R} - \overline{S}}{\sqrt{\sigma_1^2 + \sigma_2^2 + \cdots + \sigma_n^2}} = \frac{\overline{R} - \overline{S}}{\sqrt{\sigma^2}} \qquad \text{(A-1)}$$

where σ_i^2 : variance of uncertainty source i.

Also, let us define β_{-i} as

$$\beta_{-i} = \frac{\overline{R} - \overline{S}}{\sqrt{\sigma_1^2 + \sigma_2^2 + \cdots + \sigma_{i-1}^2 + \sigma_{i+1}^2 + \cdots + \sigma_n^2}} \qquad \text{(A-2)}$$

Based on Equations (B-1) and (B-2), contribution of σ_i^2 to all uncertainty, σ^2, can be calculated as

$$\frac{\sigma_i^2}{\sigma^2} = \frac{(\overline{R} - \overline{S})^2}{\sigma^2}\left(\frac{1}{\beta^2} - \frac{1}{\beta_{-i}^2}\right) = 1 - \frac{\beta^2}{\beta_{-i}^2} \qquad \text{(A-3)}$$

As stated above, this method is only very rough approximation. The actual performance function is not a linear combination of uncertain sources. Furthermore, some basic variables have biases which changes total mean values of resistance and force. Thus, the interpretation of the results should be done with some care. However, in spite of all these restrictions, the author believes that the information provided by this calculation may give interesting and useful information in the geotechnical reliability analyses.

REFERENCES

Baecher, G. B. and J. T. Christian (2003). Reliability and statistics in geotechnical engineering. New York: John Wiley & Sons.

Box and Draper(1987) : Empirical Model Building with Response Surface , John Wiley.

CEN (2004). *Eurocode 7: Geotechnical design - Part 1: General rules, EN 1997-1:2004 (E), (F) and (G), November 2004*, European Committee for Standardization: Brussels.

ETC 10: Evaluation of Eurocode 7, Design Examples 2, 2009,

Goto, H., H.Kameda and M.Sugito(1982) : Use of N-value profiles for estimation of site dependent earthquake motions,Proceesings of Japan society of civil engineers, No.317,1982.1.

Honjo, Y. and K. Kuroda (1991). A new look at fluctuating geotechnical data for reliability design, Soils and Foundations, Vol.31, N0.1: 110-120.

Honjo, Y. & Setiawan B. (2007), General and local estimation of local average and their application in geotechnical parameter estimations, Georisk, 1(3), 167-176.

Honjo, Y.(2008): General vs. Local Reliability Based Design in Geotechnical Engineering, a keynote lecture at APSSRA'08, Structural Reliability and Its Application (eds. L.S. Katafygiotls, Limin Zhang, W.H. Tang and M. Cheung) pp.41-52.

Honjo, Y., T. Hara and T.C. Kieu Le (2010): Level III reliability based design by response surface: an embankment, Proc. 17th Southeast Asian Geotechnical Conference, Vol.2 pp203-206, Taipei.

Honjo, Y., T. Hara and T.C. Kieu Le (2010): Level III reliability based design by response surface: pad foundation, Proc. 17th Southeast Asian Geotechnical Conference, Vol.2 pp.207-210, Taipei.

Honjo,Y., T.Hara, Y.Otake and T.T.Kieu Le(2011) : Reliability based design of Examples set by ETC10, Geotechnique (submitted).

Holicky, M., Markova, J. & Gulvanessian, H. (2007). Code calibration allowing for reliability differentiation and production quality. Applications of Statistics and Probability in Civil Engineering. Kanda, Takada & Furuat (eds).

Kulhawy, F.H. & Mayne, P.W. (1990). Manual on estimating soil properties for foundation design. Report EL-6800, Electric Power Research Inst., Palo Alto, 306 p.

Jounel, A.G. and Huijbregts, C.J. (1978). Mining Geostatistics: Academic Press.

Lumb, P.(1974): Application of statistics in soil mechanics, 'Soil Mechanics - new horizons', pp.44-111, Newness Butterworths, London, 1974.

Matsuo M. (1984). Theory and practice of reliability based de-sign, Tokyo: Gihodo publishing. (in Japanese).

Matsuo, M & A. Asaoka (1976). A statistical study on conventional “safety factor method”, *Soils and Foundations*, 16(1), 75-90.

Oka, F., Yashima, A., Shibata, T., Kato, M. and Uzuoka, R.(1994), FEM-FDM coupled liquefaction analysis of a porous soil using an elasto-plastic model, *Applied Scientific Research*, Vol.52, pp.209-245

Okahara, M., Takagi, S., Nakatani, S., and Kimura, Y. (1991). A study on bearing capacity of a single pile and design method of cylinder shaped foundations, Technical Memorandum of PWRI, 2919.

Otake, Y., Y. Honjo, T. Hara and S. Moriguchi (2011), Level III reliability based design employing numerical analysis - application of RBD to FEM, *Procs of The Third International Symposium on Geotechnical Risk and Safety* (in press).

Phoon, K.K. and F.H.Kolhawy (1999a). Characterization of geotechnical variability, Canadian Geotechnical J., 36: 612-624.

Phoon, K.K. and F.H Kolhawy (1999b). Evaluation of geotechnical property variability, Canadian Geotechnical J., 36: 625-639.

SHB (2002) Specifications for highway bridges, Japan Road Association..

Vanmarcke, E.H. (1977). Probabilistic modeling of soil profiles, Journal of the. Geotechnical Engineering Division, ASCE, Vol.103, No.GT11, pp.1227-1246.

Vanmarcke, E.H.(1983), Random Field: Analysis and Synthesis, The MIT Press, Cambridge, Massachusetts.

Wachernagel, H. (1998). Multivariate Geostatistics: second completely revied edition: Springer.

Wu, T.H. and Kraft, L.M. (1970). Safety Analysis of Slopes, *Journal of Soil Mechanics and Foundations*, *ASCE,* 96(2), 609-630.

Wu, T.H. (2009), Reliability of geotechnical predictions, *Procs of The Second International Symposium on Geotechnical Risk and Safety*, CRC Press, p3 – 10.

ISGSR 2011 - Vogt, Schuppener, Straub & Bräu (eds) - © 2011 Bundesanstalt für Wasserbau ISBN 978-3-939230-01-4

Safety philosophy of Eurocodes

J.-A. Calgaro
Chairman of CEN/TC250 "Structural Eurocodes"

ABSTRACT: This paper examines how the Eurocodes deal with structural safety and risk management in civil engineering. The questions of responsibility of the designer and/or of the architect are underlying, but are not treated in detail. On one hand, the public aversion to failure and the societal desire of protection are increasing; on the other hand, the organization of the construction industry (research of profits, lower cost of construction processes, strategy of engineering companies, increasing of subcontracting) is a serious source of risks. What can be done in standards to invite engineers to exert their expertise in better conditions? The current format of verification of construction works is the semi-probabilistic format, called limit state design, and based on the partial factor method. Of course, it is possible to adjust the reliability levels by selecting the numerical values of the partial factors at the national levels, but, in reality, such a procedure is rather limited: changes of political nature are needed to reduce risks in civil engineering.

Keywords: Risk, Reliability, Safety, Structural Design, Accidental Actions, Eurocodes.

1 INTRODUCTION

Code of Hammurabi, Babylon, 1760 BC: if a builder builds a house for some one, and does not construct it properly, and the house which he built fall in and kill its owner, then that builder shall be put to death.

The concepts of safety, risk and hazard scenario are defined and mainly commented in two Eurocodes : EN 1990 "Basis of structural design" and EN 1991-1-7 "Eurocode 1 - Actions on structures – Part 1-7 : General actions - Accidental actions". The seismic risk is dealt with in EN 1998 "Eurocode 8 – Design of Structures for Earthquake Resistance" which gives the general performance requirements, the definition of the seismic action, structural analysis methods, and general concepts and rules applicable to civil engineering works.

From a general point of view, safety, risk and uncertainty are key features of most business and government problems and need to be understood to take rational decisions. A risk is an issue, item, event which may occur or not, and which may have a negative impact.

2 GENERAL REQUIREMENTS FOR CONSTRUCTION WORKS

From a general point of view, the main objective of Eurocodes remains the structural resistance to ensure safety of people. Section 2 of EN 1990 gives the general requirements for a structure. Of course, a structure shall be designed to have adequate structural resistance, serviceability, and durability (EN 1990, 2.1(2)P), and in the case of fire, the structural resistance shall be adequate for the required period of time (EN 1990, 2.1(3)P). But, moreover, a structure shall be designed and executed in such a way that it will not be damaged by events such as explosion, impact, and the consequences of human errors, to an extent disproportionate to the original cause (EN 1990, 2.1(4)P).

This last requirement is at the origin of the definition of structural robustness. It derives from Essential Requirement Nr. 1 of Council Directive 89/106/EEC of 21st December 1988 (CPD) on the approximation of laws, regulations and administrative provisions of the Member States relating to construction products (Annex I)[1] and its interpretation is not easy, in particular the "consequences of human errors".

In addition, potential damage shall be avoided or limited by appropriate choice of one or more design principles. Specific requirements are taken into account in case of fire.

In short, the first step of risk management is a good design to limit potential damage in case of undesired events. These events, taken into account through accidental design situations, shall be sufficiently severe and varied so as to encompass all conditions that can reasonably be foreseen to occur during the execution and use of the structure (EN 1990, 3.2(3)P).

In EN 1991-1-7, the global strategy concerning accidental actions distinguishes "identifiable" accidental actions (impact, explosions) and actions "resulting from an unspecified cause" (in clear, unidentified action origins). Of course, the selected design situations shall be sufficiently severe and varied so as to encompass all conditions that can reasonably be foreseen to occur during the execution and use of the structure (EN 1990, 3.2(3)P). Finally, it is the responsibility of the designer to define, for the client, possible reliability levels associated with risk levels (financial, economical, loss of human life, etc.).

3 APPROACH OF STRUCTURAL RELIABILITY IN THE EUROCODES

3.1 Reliability and reliability levels

Reliability is defined in EN 1990 (1.5.2.17) as the ability of a structure or a structural member to fulfil the specified requirements, including the design working life, for which it has been designed. Structural reliability covers in fact four aspects : safety, serviceability, durability and robustness of a structure.

Different levels of reliability may be adopted for structural resistance and for serviceability: they are selected by the designer who takes into account the possible cause and /or mode of attaining a limit state (i.e. an undesired phenomenon), the possible consequences of failure in terms of risk to life, injury, potential economical losses, public aversion to failure, the expense and procedures necessary to reduce the risk of failure.

3.2 How structural safety may be ensured?

The levels of reliability relating to structural resistance and serviceability can be achieved by various methods, or a combination of various methods, listed in EN 1990, like preventative and protective measures, measures relating to design calculations (representative values of actions, choice of partial factors), measures relating to quality management, measures aimed to reduce errors in design and execution of the structure, and gross human errors, other measures relating to the following other design matters: they are the basic requirements ; the degree of robustness (structural integrity) ; durability, including the choice of the design working life ; the extent and quality of preliminary investigations of soils and possible environmental influences ; the accuracy of the mechanical models used ; the detailing, efficient execution, *e.g.* in accordance with execution standards referred to in EN 1991 to EN 1999, adequate inspection and maintenance according to procedures specified in the project documentation.

Concerning design calculations, the first difficulty is that they are intended to establish models of a highly complex reality, following rules which are sufficiently simple to be used by designers. The simplifications do not have absolutely general validity, and any rule must have a clear field of application, and application of standards often necessitates a properly based appraisal (engineering judgment). Another difficulty arises from the fact that no universal measure of safety exists; *even a probability of failure is not invariant at the level of practical applications,* since it varies considerably depending on the information data and assumptions according to which it is calculated. For dealing with problems of structural safety there are three possible approaches : pragmatic (related to the past), dogmatic (related to the future), and progressive (related to the present).

[1] This requirement is kept in the "Construction Product Regulation" (CPR) of the European Parliament and of the Council, adopted on the 20th of January 2011, which will replace the CPD.

3.2.1 - Definition, choice and classification of phenomena to be avoided; limit-states.
It is usually considered that the phenomena to be avoided are modeled through limit-states, generally highly idealized and hence conventional. However the concept of performance criteria is more general (it can directly include the past history of the structure). For some limit-states (exceeding the bearing capacity), the first occurrence should be avoided; for other limit states (e.g. crack opening of a concrete structure), only numerous repetitions can cause damage; but many limit-states are of an intermediate nature (for example upheaval from a support).

Exceeding some limit-states involves immediate collapse (brittle fracture, loss of equilibrium) while other cases involve slow or progressive failure (ductile fracture, cracking). Exceeding limit-states involves consequences which may be more ore less dangerous. The most important of these consequences is the probability - higher or lower - of the loss of human lives. In most cases the risks for the persons are indirectly taken into account by considering the risks for the structure itself.

Taking account of the above distinctions, the limit-states are grouped in categories corresponding to probabilities of the same order of magnitude. One category includes the ultimate limit-states, another includes the serviceability limit-states. Each category should then be sub-divided, e.g. according to whether the limit-state can be reached by the occurrence, on one or more occasions, of certain values of the variable actions, in order to determine the probabilities or permissible frequencies of reaching the corresponding action-effects.

Only certain limit-states can, more or less exactly, be studied by comparing the action-effects applied to a cross-section with resistances. To enlarge the field of application of a numerical value by artificial modification of another factor (compensation) can lead to confusion.

3.2.2 - Nature of the choices of acceptable probabilities of occurrence of phenomena to be avoided.
The choices of degrees of structural safety are not simple technical operations but, between certain limits, the result of arbitrary options of a political nature. It may however be supposed that dimensions close to the lower envelope of those resulting from different national codes should give satisfaction to the competent authorities.

As a consequence of the relative nature of the probability of occurrence of a limit state, the acceptance of a certain value (whether or not stated explicitly) of this probability is linked with the knowledge available at the time of this acceptance; the probability often has to be re-evaluated later on, and the consequences drawn from its acceptance then have to be reconsidered.

3.2.3 - Criteria which may be taken into account when choosing the probabilities of phenomena to be avoided.
a) *Economic criteria*, when used for a simple optimization, have often led, for ultimate limit-states, to safety factors which are too low to be acceptable. This may be explained by the fact that aversion to the risk increases more than proportionally to the magnitude of the risk and the corresponding probability. These criteria do however permit useful analyses and lead, for example, to introduction of the concept of economic barrier (important for ultimate states) and the concept of lifetime of a structure (design working life, important for some serviceability states and for fatigue).

b) *Analogic criteria* are based on knowledge of the risks supported or accepted in circumstances where human life is not connected with the safety of structures. Their relevance is indicative only. In particular, the death rate due to traffic accidents is very much higher than the rate that could be accepted as a result of accidents connected with structural failure.

c) *Psychological criteria* intervene in appraisals by individuals or groups of persons. Appraisals by the widest and the most permanent group constitute the public opinion. This one is subjective, deterministic, variable, emotional, and thus far from rational. For example, it pays more attention to the number of victims in a particular accident than to the total number of victims. Broadly, its demands result from recorded accidents and hence depend on the number of existing structures of different types.

d) *Legal criteria*, at the present time, have remained essentially deterministic, and hence cannot be used for making the choice. Attention is drawn to the fact that the need for clarification of the legal aspects of safety is keenly felt in many countries. Moreover, certain legal practices which automatically link accidents with mistakes and faults, as far as penalties are involved, without drawing certain distinctions, should be reformed.

e) *Ethical criteria* make it possible to take account of the value of human life by determining it indirectly by reference to analogic criteria. But they require in addition that account should be taken of the evolution of probabilities in the course of time in each particular case.

f) *Risks acceptable during execution* should be subjected to a special analysis which should examine certain specific concepts (consequences for the completed construction, nature of the accident at work, safety concerning the contractors execution measures, possibility of influencing the risk, temporary nature of the risk).

3.2.4 - Modification of acceptable probabilities depending on different criteria.
Modifications of this kind (reliability differentiation) should not be confused with modifications of factors intended to maintain the probabilities constant.

In EN 1990 (Informative Annex B), the question of relating different levels of control (or, better, of quality) to different design rules has been introduced. This Annex will be developed and probably become normative in the revised version of EN 1990, in liaison with the classification adopted in EC7.

4 THE SEMI-PROBABILISTIC FORMAT (PARTIAL FACTOR DESIGN)

The basic principles of the semi-probabilistic format for the verification of construction works may be expressed as follows. The verification rules introduce safety:

- by selecting appropriate representative values of the various random variables (actions and resistances),
- through the application of a set of calibrated partial factors,
- through safety margins, more or less apparent, in the various models (models of actions, of effects of actions and of resistances).

In the most common cases, the verification of the safety of construction works is based on the verification of an equation of the following type:

$E_d \leq R_d$

where E_d is the design value of the effect of actions such as internal force, moment or a vector representing several internal forces or moments, R_d is the design value of the corresponding resistance.

The general expressions for E_d and R_d are $E_d = E\{\gamma_{F,i} F_{rep,i} \; ; a_d\}$ and $R_d = R\left\{\eta_i \frac{X_{k,i}}{\gamma_{M,i}}; a_d\right\}$

$F_{rep,i}$ is the relevant representative value of the action Nr. i (characteristic or other value), a_d is the design values of the geometrical data, X_{ki} is the characteristic value of the material or product property Nr. i, η_i is the mean value of the conversion factor taking into account volume and scale effects, effects of moisture and temperature, and any other relevant parameters, $\gamma_{F,i}$ and $\gamma_{M,i}$ are the global partial factors for action effects and resistances.

Their numerical values, which have been partially calibrated by using the structural reliability methods, are, in principle, based on a target value of the reliability index β equal to 3,8, which means a probability of failure of $7{,}2.10^{-5}$ in 50 years. The principles of the reliability theory (limited to the basic case of two random variables : E, effect of actions, and R, resistance) are summarized in figure 1.

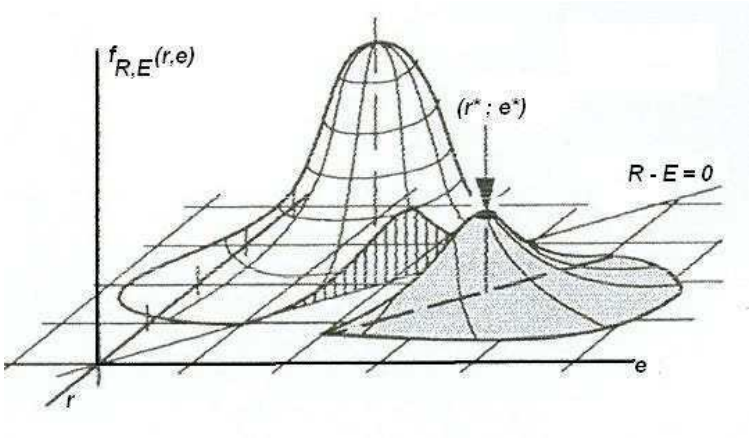

Physical representation of the failure probability and coordinates of the design point

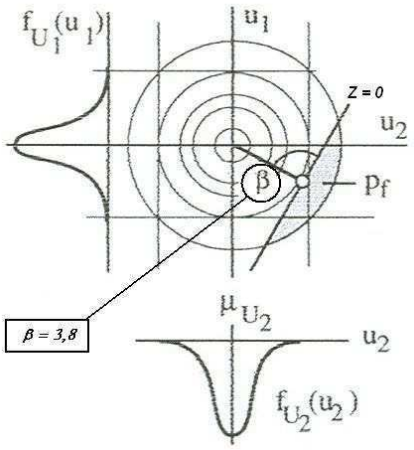

Reliability index in the normalised space

Figure 1. Principles of the reliability theory

Nevertheless, it is obvious that the partial factors cover "small errors". But how can be defined the boundary between "small" and "gross" errors? Is it possible to compare a human error during execution and the misuse of an advanced software?

5 RISKS IN CIVIL ENGINEERING

Structural failures may happen during execution, immediately after execution or during normal use of construction works. Accidents are very frequent during execution. For example, there is probably one failure or collapse per week during construction of bridges in the World. In general, if the number of fatalities is low, information of the public is limited. The causes may be of various origins:

- human error (the most frequent) associated to a lack of supervision of execution,
- errors or underestimations in the design (inappropriate mechanical models, underestimation of actions –direction and magnitude – hazard scenarios not taken into account, construction processes, etc.);
- underestimation of problems due to an insufficient appraisal of scaling effects;
- excessively ambitious projects (architects, engineers, etc.).

Accidents arriving "immediately" after execution, i.e. after a few months or one or two years after the construction works are in use, are often difficult to explain. They may be due to an unforeseen short term behavior of the ground supporting the foundations.

Accidents during normal use of construction works may have many origins : scour effects due to exceptional flood, impacts and explosions, errors in dynamics (footbridges, football stands under crowd loading), errors in stability (in particular in case of structural modification of a building), lack of maintenance, etc.

The following non exhaustive list gives some hazards which may be encountered for construction works in use, or between uses and after use.

a) in use

to people in building

- stairs, floor finishes, glazing

to structure and people

- inadequate maintenance
- change of use

b) in maintenance

to people doing maintenance

- access, confined spaces
- hot materials, toxic materials
- falls from height, fragile roofs

c) in extension refurbishment and repair

- misunderstanding the original structure
- faults in the original structure
- earlier inappropriate modifications

d) in assessment

- incorrect assumptions (materials, structural form, loads)
- inadequate inspection

e) in demolition

- misunderstanding structure
- defects in structure
- inappropriate approach
- premature collapse, flying debris
- high risk elements; cantilevers, flat slabs, prestressed structures, retaining structures.

Of course, at any time, you may encounter risks like abnormal settlement, chemical attack in the ground, overload, misuse, terrorism, explosion, impact, instability, lack of redundancy or other robustness, novel materials and design concepts, corrosion and ageing, progressive/disproportionate collapse, risks to, or from, adjacent buildings, structures and other facilities.

Standards provide guidance to designers. Many of them recall that they must be used by qualified and experienced engineers like in the general assumptions of the Eurocodes. Indeed, the judgements which are common to most designs have been taken by the authors of the code, and the results set down in a manner which can be applied in design. When using a standard, the engineer implicitly accepts those judgements, in many cases without fully understanding the basis for them, or the limits on their application.

In particular, design standards assume that the structures they are applied to are 'normal' structures, and designers are not always able to recognise complexity. Complexity in the field of bridges may be more easily identified than complexity in the field of buildings. Outstanding structures are sometimes designed by architects who consider themselves as artists, and the problems of safety are to be dealt with by engineers, with poor fees !…

Should innovation be limited to avoid risks due to complexity? Of course, no. But for that reason the Eurocodes have introduced the principle, and some rules, of robustness.

Robustness is the ability of a system to resist damage but maintain its important functions. It is not limited to structures or even to physical systems; robustness principles can be applied to management systems. Robustness is somewhat different to other risk management systems in that it does not necessarily eliminate or reduce known risks, although it may do. Its primary value is in reducing the effect of unknown risks.

Strength and robustness are different. A single cantilever beam as a part of the main stability system should not be considered robust, however strong it might be, since its failure would lead to failure of the whole system. Although none of the design load cases could cause it to fail, it might be vulnerable to terrorist attack or a previously undiscovered form of brittle fracture.

EN 1990 proposes a classification of construction works, for the purpose of reliability differentiation, based on "consequences classes" (CC), i.e. by considering the consequences of failure or malfunction of the structure. This classification is described in Table 1 (EN 1990, Table B1).

Table 1. Definition of consequences classes

Consequences Class	Description	Examples of buildings and civil engineering works
CC3	**High** consequence for loss of human life, *or* economic, social or environmental consequences **very great**	Grandstands, public buildings where consequences of failure are high (e.g. a concert hall)
CC2	**Medium** consequence for loss of human life, economic, social or environmental consequences **considerable**	Residential and office buildings, public buildings where consequences of failure are medium (e.g. an office building)
CC1	**Low** consequence for loss of human life, *and* economic, social or environmental consequences **small or negligible**	Agricultural buildings where people do not normally enter (e.g. storage buildings), greenhouses

The criterion for classification of consequences is the importance, in terms of consequences of failure, of the structure or structural member concerned. Reliability classes are associated to these consequence classes. A refined classification for buildings is given in EN 1991-1-7 (Annex A).

For buildings in Consequences Class 3, a systematic risk assessment of the building should be undertaken taking into account both foreseeable and unforeseeable hazards.

6 CONCLUSIONS

Should design standards, and Eurocodes in particular, go beyond what is currently proposed? It is clear that the principles are good, but after, it is a matter of quality in the design, construction and maintenance processes. Lessons from accidents inspire the following additional list of design principles:

- Safety factors are not intended cover gross human errors.
- Foundations of civil engineering works have the same design working life as structures in general.
- Even if all individual parts of a structure are correctly designed, check the stability of the structure as a whole and ensure a minimum robustness.
- Avoid structures the stability of which is ensured by ties anchored in the ground and not protected against corrosion, exceptional or malicious actions.
- Avoid structures which are not damage-tolerant with regard to fatigue.
- Avoid structures with brittle members or sections: in case of rupture there is no pre-warning (the structure should be fault tolerant up to a certain degree).
- Avoid a too slender structure if a refined and pertinent dynamic analysis cannot be performed.
- Take into account structural effects of climatic changes.

Concerning the design process, risks are increasing for the following reasons:

- The societal needs are increasing.
- The cost of the structural part of construction works is decreasing (competition, global economy).
- As a consequence of the previous observation, engineering services are not correctly remunerated, time for design and construction is more and more shortened, the design is ensured by very small (and cheap) design offices without real technical competence, personnel on construction sites are not experienced, the control of quality by specialised companies is underpaid.

Finally, a system where all calculations made in a small design office are checked by the same person is not robust. Due to time constraints, the models may be inappropriate, the designer may have misunderstood the code, an important principle or a rule, or may fail to spot an error due to a particular combination of personal circumstances. Hopefully, for big projects, there is often a panel of experts following seriously the design process and give their opinion in reviews of the proposed approach. In some cases, sensitivity studies may be one way to judge the severity of a risk.

Finally, it is difficult to envisage an extension of the design codes to improve the situation concerning the management of risks in civil engineering : it is not a matter of partial factors or of probabilistic approach ; it is more a matter of education, in particular in engineering schools and universities and of organisation of the construction industry.

REFERENCES

J. Schneider, Introduction to Safety and Reliability of Structures. Structural Engineering Documents Nr.5, IABSE, 1997.

J.-A. Calgaro, H. Gulvanessian “Management of reliability and risk in the Eurocode system”. IABSE International Conference “Safety, Risk and Reliability – Trends in Engineering”, Malta 21-23 mars 2001

J.-A. Calgaro, Maîtrise des Risques et Codes Européens de Conception et de Calcul. Colloque international « Risque, vulnérabilité et fiabilité dans la construction » - Alger, 11 et 12 octobre 2003.

ISO/CD 13824 N180. General Principles on Risk Assessment of Systems Involving Structures.TC98/SC2

Bilal M. Ayyub, Risk Analysis in Engineering and Analysis. Chapman Hall/CRC, Boca Raton (2003).

“Designer's Guide to EN 1990 – Eurocode: Basis of structural design" H. GULVANESSIAN, J.-A. CALGARO, M. HOLICKY – THOMAS TELFORD – 2002

ISGSR 2011 - Vogt, Schuppener, Straub & Bräu (eds) - © 2011 Bundesanstalt für Wasserbau ISBN 978-3-939230-01-4

Life Quality Index for Assessing Risk Acceptance in Geotechnical Engineering

D. Straub
Engineering Risk Analysis Group, TU München, Germany

A. Lentz
COWI A/S, Kongens Lyngby, Denmark

I. Papaioannou
Computation in Engineering, TU München, Germany

R. Rackwitz
TU München, Germany

ABSTRACT: The Life Quality Index (LQI) is a recently developed concept that establishes a relation between the resources invested in improving the safety of an engineering facility and potential fatalities that are avoided by the investment. In this way, the LQI provides a rationale for determining acceptability of decisions involving life safety risks in engineering, including the establishment of target reliabilities. In this contribution, the principle of the LQI is outlined and its relevance for making safety-relevant decisions in geotechnical engineering is highlighted. The methodology is illustrated by an application to the design of a slope, involving a FE-based reliability analysis.

Keywords: Risk acceptance, target reliability

1 INTRODUCTION

In geotechnical engineering, decisions or recommendations on actions must be made, which will affect life-safety risk. Whenever standards and codes do not apply (or when these are to be written), the engineer must answer the question "How safe is safe enough?". On the one hand, the engineer has the responsibility to ensure the safety of people involved in the construction and the use of the facility. On the other hand, he or she has the responsibility to use resources in an economical way. To find the right tradeoff between these two contradicting goals is the responsibility of the engineer. In geotechnical engineering (and general civil engineering), this tradeoff is selected mostly implicitly, i.e. safety-related decisions are made on the basis of past experience and calibration, thus implying an underlying (but unknown) weighting of safety vs. cost. In many instances, this approach leads to good engineering decisions, but in some circumstances it can give rise to inconsistent or even grossly misguided actions. This applies in particular for novel engineering applications or larger projects for which no or little experience is available. A procedure for explicitly defining the right tradeoff is therefore desirable, not least because it enables the documentation and justification of the decisions taken.

The Life Quality Index (LQI) is a recently developed concept for determining acceptability of decisions involving life safety risks in engineering, which provides a rationale for establishing target reliabilities for civil engineering systems (Nathwani et al. 1997, Rackwitz 2002, Lentz 2007). The LQI is a socio-economic utility function that depends on the wealth and life expectancy of a society. Any decision that increases the value of the LQI is deemed acceptable. This increase can be due to an increase in life expectancy (reduction of fatalities) or an increase in societal wealth (reduced use of resources). In this way, the LQI establishes a relation between the resources invested in improving the safety of an engineering facility and potential fatalities and injuries that are avoided by the investment, i.e. it provides a means to quantify the optimal tradeoff between safety and cost.

In this contribution, the principle of the LQI is outlined and its relevance for making safety-relevant decisions in geotechnical engineering is highlighted. The methodology is illustrated by an application to the design of a slope, involving a FE-based reliability analysis.

2 LIFE QUALITY INDEX

There are different ways of assessing whether a safety-related decision should be deemed acceptable or not. One of the most consistent approaches proposes to take a look at the personal utility an individual experiences due to different decisions. Utility, here, is seen as the result of several factors, such as long life in good health, wealth, intact family relations etc. This usage of the concept is common in socio-economics. Unfortunately, many contributors to utility -- or simply to life quality -- cannot be quantified properly. For this reason, income and life expectancy are generally used as representative indicators for life quality as a whole.

Since the 70ies, several economists such as Shepard & Zeckhauser (1984) have made proposals for the formulation of $L = L(e_0,g)$, where e_0 is life expectancy at birth and g denotes average income available for risk reduction measures. In the engineering domain, Nathwani et al. (1997) first formulated the so-called life quality index (LQI). The LQI is essentially a socio-economic utility function, which can be derived in different ways making use of different principles (e.g. Pandey et al. 2006). In its present form (Pandey & Nathwani 2004, Rackwitz 2004), it is written as

$$L = g^q l_d \quad \text{with} \quad q = \frac{1}{\beta}\frac{w^*}{1-w^*} \tag{1}$$

Herein, $\beta \approx 0.7$ quantifies the share of labor in the creation of the GDP. w is the time fraction of life spent at work. The asterisk in w^* signifies that the trade-off between work time and leisure time is at its optimum from the point of view of the average citizen. l_d denotes the average remaining life expectancy of all currently living members of society of various ages a. In fact, age-averaged willingness-to-pay is the correct quantity to use as it must be assumed that a representative cross-section of the population is endangered by the event-type hazard:

$$l_d = E_A[l_d(a)] = \int_0^{a_u} l_d\,(a)h(a,n)\mathrm{d}a \tag{2}$$

The index d stands for discounting: Future income effects require discounting. For mathematical convenience, this effect is integrated in the life expectancy term l_d instead of the utility term g^q. The term $h(a,n)$ denotes the age distribution of a population growing at rate n, while $l_d(a)$ denotes the (discounted) remaining life expectancy of a person aged a:

$$\begin{aligned} l_d(a) &= \int_0^{a_u} S(t|a)\exp\left[-\int_a^t \gamma\,(\tau^*)\mathrm{d}\tau\right]\mathrm{d}t \\ &= \int_0^{a_u} \exp\left[-\int_a^t \mu\,(\tau)\mathrm{d}\tau\right]\exp\left[-\int_a^t \gamma\,(\tau^*)\mathrm{d}\tau\right]\mathrm{d}t \\ &= \int_0^{a_u} \exp\left[-\int_a^t \mu\,(\tau)+\gamma(\tau^*)\mathrm{d}\tau\right]\mathrm{d}t \end{aligned} \tag{3}$$

In the first line, $S(t|a)$ denotes the probability of surviving up to age t for a person aged a today. Survival probabilities are calculated from the age-dependent mortality rate $\mu(a)$. Discounting is performed at some rate $\gamma(\tau^*)$, where $\tau^* = \tau - a$.

If utility is made up of life expectancy l_d and disposable income g, it implies that life expectancy can be exchanged with income at a certain rate without changing overall utility. In fact, it can be observed that people are willing to give a certain amount of their income in order to increase their life expectancy by buying additional safety measures, e.g. when paying extra money for a car with additional safety features. This rate of exchange between income and life expectancy is referred to as willingness-to-pay (WTP). As outlined in Nathwani et al. (1997), this concept can be used for a criterion, by demanding that any safety-related decision shall not lower utility (life quality) L:

$$dL = \frac{\partial L}{\partial g}\mathrm{d}g + \frac{\partial L}{\partial l_d}\mathrm{d}l_d \geq 0 \tag{4}$$

Usually, engineering decisions have a simultaneous effect on safety levels and income. Safety measures lead to a rise in average life expectancy l_d, but their costs lead to a decrease in average available income g. According to the willingness-to-pay (WTP) approach, a decision is judged acceptable if the overall lifetime utility remains equal or rises. It is important to realize that this type of criterion is only suitable for

risk prevention, i.e. saving the life of some member of society who cannot be identified in advance. The criterion is not applicable to identifiable persons already finding themselves in a state of immediate emergency.

Setting $dL = 0$ and inserting Eq. (1) yields

$$-\mathrm{d}g \le \frac{\frac{\partial L}{\partial l_d}}{\frac{\partial L}{\partial g}} \mathrm{d}l_d = \frac{g}{q}\frac{\mathrm{d}l_d}{l_d} = \mathrm{WTP} \qquad (5)$$

Of principle reasons, it is more correct to replace $\mathrm{d}l_d/l_d = E_A[\mathrm{d}l_d(a)]/E_A[l_d(a)]$ by $E_A[\mathrm{d}l_d(a)/l_d(a)]$, see (Lentz 2007). The acceptable domain is then limited by

$$-\mathrm{d}g \le \frac{g}{q} E_A\left[\frac{\mathrm{d}l_d(a)}{l_d(a)}\right] = \mathrm{WTP} \qquad (6)$$

or

$$\frac{\mathrm{d}g}{g} + \frac{1}{q} E_A\left[\frac{\mathrm{d}l_d(a)}{l_d(a)}\right] \ge 0 \qquad (7)$$

Note that safety investments lead to a negative change in income dg, so that $-dg$ adopts a positive value.

Safety-relevant measures cause a change in mortality rate μ, which is defined as the number of deaths divided by the population size. Usually, this calculation is performed for each age group separately, leading to an age-dependent mortality rate $\mu(a)$. Absolute and proportional mortality changes constitute two of the most basic cases. In the first case, an age-independent increment $d\mu(a) = d\mu = \Delta$ is added to background mortality, so that $\mu_\Delta(a) = \mu(a) + \Delta$. In the second case, age-dependent background mortality is multiplied with a constant factor, so that $\mu_\delta(a) = \mu(a) \times (1 + \delta)$. The first case is more typical for accidents (e.g. structural failure), whereas the second case can be observed with the effects of toxic exposure. Other, more complex models exist as well.

For practical purposes, it is convenient to linearize the relationship between (small) changes in mortality $d\mu(a)$ and (small) changes in discounted life expectancy $\mathrm{d}l_d(a)$ (Rackwitz, 2004), so that

$$E_A\left[\frac{\mathrm{d}l_d(a,\Delta)}{l_d(a)}\right] = -J_\Delta \Delta \quad \text{or} \quad E_A\left[\frac{\mathrm{d}l_d(a,\delta)}{l_d(a)}\right] = -J_\delta \delta \qquad (8)$$

Linearization coefficients are in the vicinity of $J_\Delta \approx 13$–17 and $J_\delta \approx 14$–18 for industrialized countries (Lentz 2007). The latter result is multiplied with crude mortality $\mu = \int \mu(a) h(a,n)\, da$. For the absolute risk model, inserting in Eq. (7) leads to

$$-\mathrm{d}g \le -\frac{g}{q} J_\Delta \Delta = -G_\Delta \Delta \qquad (9)$$

It can be shown that $G_\Delta = \frac{g}{q} J_\Delta$ is actually the *WTP for averting one fatality*. In the literature it is known as the 'value of a statistical life' (VSL). However, this terminology appears to be unluckily chosen with respect to ethical considerations. Typical values come close to 2 million PPP US$ for industrialized countries.

Empirical investigations basically confirm this number, e.g. Mrozek & Taylor (2002). However, some cases indicate significantly elevated values. Presumably, this deviation from the analytically derived VSL is due to the psychological phenomenon that people dread events disproportionally, if their perceived control over the situation is small or if a large number of victims are not killed in several small accidents but by one single big accident. Both criteria apply to aircraft passengers – and in fact, civil aviation is known for costly measures against very small residual risks.

3 HUMAN CONSEQUENCE MODELING

The previous section assesses engineering decisions by comparing changes in human mortality with changes in income (caused by project costs). However, the directly controllable result of a safety-related decision is not a change in mortality $\mathrm{d}\mu$, but a change in failure rate $\mathrm{d}r$. Obviously, $\mathrm{d}\mu$ is a function of $\mathrm{d}r$

if the failure is related to some potentially fatal hazard. The present section reviews some basic concepts of how to establish this link.

Most potentially fatal events in civil engineering share some basic properties: They occur at an unpredictable moment and practically all fatalities occur at once. A basic methodology for this type of event-type hazards was introduced in Lentz (2007). According to its basic idea, the expected number of fatalities in case of a failure event F can be written as

$$N_{D|F} = N_{PE}(1 - P_Q)P_{D|F} = N_{PE}k \tag{10}$$

Here, N_{PE} is the number of people endangered. It corresponds to the number of people actually expected to be present at the onset of the event. This is a subset of all people *potentially* present N_{pop}. P_Q is the probability of successful escape and $P_{D|F}$ is the probability of death given no successful escape. The latter probabilities are united in a single factor $k = (1 - P_Q)P_{D|F}$ in order to keep the notation short in long expressions. The strength of the approach lies in the fact that the determination of N_{PE} and P_Q follows the same principles regardless of the specific event-type, such as building collapse after an earthquake, dam failure or tunnel fire. The same statistical information on human behavior and physiology can be used in all cases. Only the last component of Eq. (10), $P_{D|F}$, requires case-specific modeling. All three components of $N_{D|F}$ are made up of several sub-quantities that have been numerically described in Lentz (2007) and elsewhere.

The change in mortality caused by a failure is $N_{D|F}/N_{pop}$, where N_{pop} is the number of people in the entire population (country). By multiplying with the failure rate, the change in mortality is obtained as

$$\Delta = \frac{N_{D|F}}{N_{pop}}\mathrm{d}r = \frac{N_{PE}k}{N_{pop}}\mathrm{d}r \tag{11}$$

For many engineering facilities, the failure rate r is not constant with time, but approximate results can be obtained with a constant (asymptotic) value of r when failed facilities are systematically rebuilt (Rackwitz 2005). In the application presented in this paper, it is assumed that failure events occur as a homogenous Poisson process, and the failure rate therefore is constant.

4 APPLICATION TO TECHNICAL FACILITIES

In design and operation of technical facilities, system parameters $\mathbf{p}$ are selected, which determine the performance of the facility. (In the application example presented later, the parameter is the slope angle of a embankment.) These parameters determine both the life-cycle cost of the facility, which causes a change in societal income dg, as well as the failure rate r, which causes a change in the mortality risk associated with the fatality.

To apply the LQI criterion, both the costs as well as the change in mortality are expressed as annual values. Let $C_a(\mathbf{p})$ be the annualized net present life-cycle cost of the facility and $r(\mathbf{p})$ be the failure rate of the facility, which is here assumed to be constant. Following Rackwitz (2002), we can set the negative change in income of the total population equal to the change in the annualized life-cycle cost of the facility, i.e. $-dg = dC_a(\mathbf{p})/N_{pop}$. (The division with N_{pop} is introduced because g is the per-capita GDP.) Furthermore, the expected change in mortality is given by Eq. (11). Inserting in Eq. (9), it is

$$\frac{\mathrm{d}C_a(\mathbf{p})}{N_{pop}} \leq -\frac{g}{q}J_\Delta \frac{N_{PE}k}{N_{pop}}\mathrm{d}r(\mathbf{p}) \tag{12}$$

N_{pop} cancels out, and rearranging the terms leads to the acceptance criterion:

$$-\frac{\mathrm{d}C_a(\mathbf{p})}{\mathrm{d}r(\mathbf{p})} \geq \frac{g}{q}J_\Delta N_{PE}k = WTP \cdot N_{PE}k \tag{13}$$

Here, $\mathrm{d}C_a(\mathbf{p})/\mathrm{d}r(\mathbf{p})$ is the change in annualized cost with respect to the change in failure rate and will take negative values for reasonable engineering situations (the cost increases with decreasing failure rate).

Eq. (13) is the criterion that engineering decisions **p** must fulfill to comply with societal values as expressed through the LQI. The right hand side depends on the willingness to pay WTP as determined from the LQI principle, as well as the number of people exposed N_{PE} and the probability k that a person exposed is killed during a failure. The left-hand side depends on the effectiveness of measures for reducing the failure rate. When more effective measures (i.e. less costly measures) are available, implicitly a higher level of safety will be required. The application of the principle in Eq. (13) is illustrated in the following for a simple but representative design decision in geotechnical engineering.

5 APPLICATION OF THE LQI PRINCIPLE TO THE ACCEPTABILITY OF SLOPE DESIGN

5.1 *Problem statement*

Consider the embankment shown in Figure 1 to be constructed for a railway line. The height of the embankment h as well as the width at the top is prescribed, but the slope angle α can be selected by the designer. Clearly, an increase in the slope angle will lead to a reduction of cost but also to an increase in the failure rate r. It will be demonstrated how the LQI principle can be used to find the acceptable value of α.

5.2 *Mechanical and probabilistic modeling*

The embankment is modeled in 2D with plain-strain finite elements. The material model used is an elasto-plastic model with a prismatic yield surface according to the Mohr-Coulomb criterion and a non-associated flow rule with zero dilatancy. The elasto-plastic deformations are computed as the converged pseudo time-dependent elasto-viscoplastic solution, applying the viscoplastic strain method (e.g. see Smith and Griffiths 2004).

The considered random variables are those relevant to shear failure, i.e. the strength parameters and specific weights of the soil and fill material, as well as the train loading (Table 1). The correlation coefficient between the strength parameters of the same materials is taken as –0.3. For the stiffness parameters, deterministic values are chosen ($E = 10^5$ kPa, $\nu = 0.3$ for both materials). Random spatial variability of the soil properties is not included in the analysis for simplicity.

Table 1. Random variables

Parameter	Distribution	Mean	COV
Friction angle (Fill) φ_F [°]	Lognormal	21	0.1
Cohesion (Fill) c_F [kPa]	Lognormal	12	0.2
Specific weight (Fill) γ_F [kN/m^3]	Normal	20	0.05
Friction angle (Clay) φ_C [°]	Lognormal	20	0.1
Cohesion (Clay) c_C [kPa]	Lognormal	15	0.2
Specific weight (Clay) γ_C [kN/m^3]	Normal	19	0.05
Train load q [kN/m^2]	Gumbel	50	0.2

Figure 2 shows the deformed mesh at failure for a slope angle $\alpha = 26.6°$, with displacements magnified by a factor of 200.

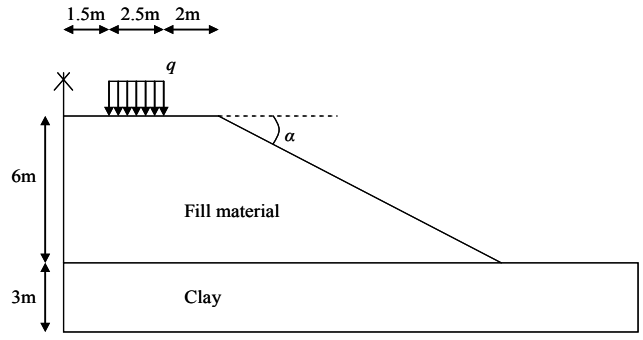

Figure 1. Embankment with train load

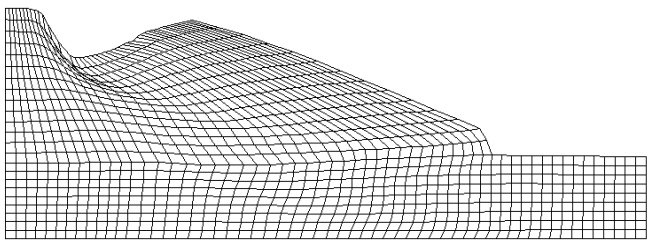

Figure 2. Deformations at failure. Slope angle $\alpha = 26.6°$ (2:1), factor of safety FS = 1.66.

The factor of safety (FS) of the slope is computed applying the shear strength reduction technique (Matsui and San 1992). It is defined as the number by which the original strength parameters must be divided to reach the failure state. According to this approach, the strength parameters are gradually reduced by an increasing factor and an elasto-plastic finite element computation is performed at each step.

5.3 *Reliability analysis*

The limit-state function, with negative values defining the failure event, is expressed as:

$$g(\mathbf{X}) = FS(\mathbf{X}) - 1 \tag{14}$$

where $\mathbf{X}$ is the vector of random variables given in Table 1. A series of reliability analyses are carried out for selected values of the slope angle α by means of the first-order reliability method (FORM), resulting in corresponding values of the reliability index β. For convenience, a 2nd order polynomial function is fitted to the computed values of β:

$$\beta(\alpha) \approx 11.61 - 0.415\alpha + 0.0049\alpha^2 \tag{15}$$

Figure 3 shows the reliability index β as a function of the slope angle, together with the corresponding failure rate r [yr^{-1}], which is related to the reliability index β by $r \approx \Phi(-\beta)$, with $\Phi(.)$ being the standard Normal cumulative distribution function.

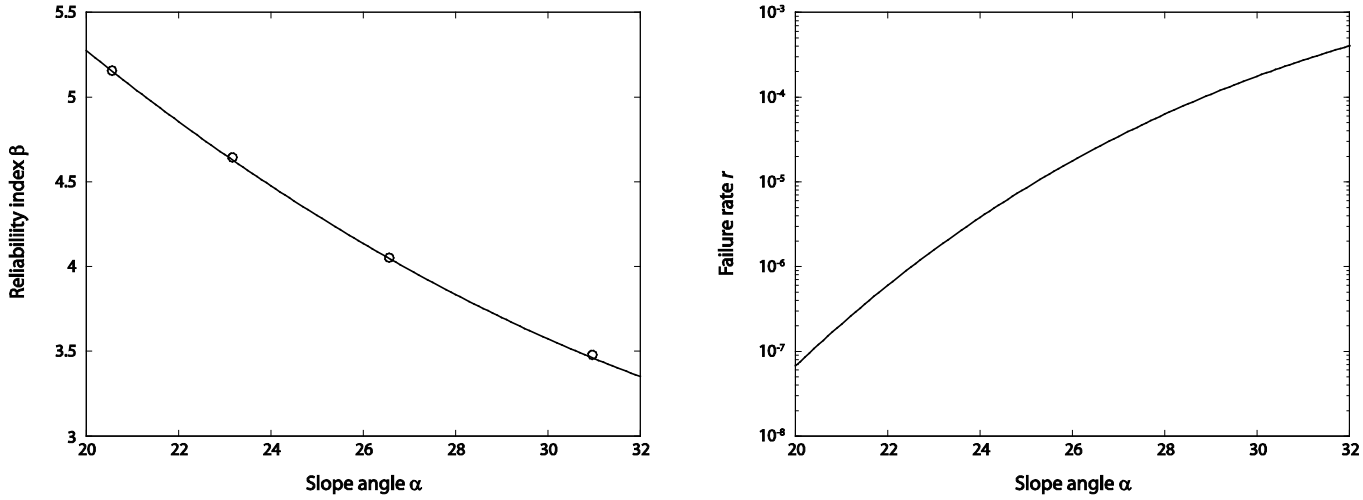

Figure 3. Reliability index β, failure rate r, as a function of slope angle α.

5.4 *Life-cycle cost*

The net present value of the annualized life cycle cost is a function of the slope angle, $C(\alpha)$. Since we are interested only in changes of the cost, $dC(\alpha)$, it is sufficient to consider incremental costs. Simplifying, we can write the construction costs as

$$\begin{aligned} C_c(\alpha) &= c_0 + c_1 \cdot Land\ use(\alpha) + c_2 \cdot Material(\alpha) \\ &= c_0 + c_1 h(\tan\alpha)^{-1} + c_2 \frac{h^2}{2}(\tan\alpha)^{-1} \\ &= c_0 + c \cdot (\tan\alpha)^{-1} \end{aligned} \tag{16}$$

Where the constant is $c = c_1 h + c_2 h^2/2$. For $h = 6$m, a value of $c = 10^5$€ is taken in the following (Note: this value of c is based on assuming that the value of the constant is 10^4€ per meter of embankment and that the embankment can be modeled as a series system whose components have length 10m. The latter asumption depends on the spatial correlation of material properties.)

It is assumed here that the construction costs are the only relevant costs, i.e. that maintenance costs and other costs occurring after construction can be neglected. To compute the annualized life cycle cost, we consider an interest rate of γ of 2%, reflecting a long-term sustainable interest rate (corresponding to economical growth). If the embankment is utilized over a period of t_s years, the costs can be split into constant annuities C_a of

$$C_a(\alpha) = \frac{\gamma C_c(\alpha)}{1 - \exp(-\gamma t_s)} \tag{17}$$

which follows from $C_c(\alpha) = \int_0^{t_s} C_a(\alpha) \exp(-\gamma t)\, \mathrm{d}t$. To avoid selecting an arbirtrary service life time t_s, we consider an infinite time horizon $t_s = \infty$, Rackwitz (2010). In this case, the denominator in Eq. (17) becomes one (it would be 0.86 in the case of $t_s = 100\text{yr}$) and we get

$$\begin{aligned} C_a(\alpha) &= \gamma C_c(\alpha) \\ &= \gamma[c_0 + c \cdot (\tan\alpha)^{-1}] \end{aligned} \tag{18}$$

More sophisticated computations of life cycle costs based on renewal models are presented in Streicher and Rackwitz (2004) and Joanni and Rackwitz (2007). However, the presented calculation is accurate enough for the envisaged application.

5.5 *Consequence model*

Following Section 3, the expected value of the number of people killed given the event of a failure is determined as a function of (a) the number of people present N_{PE} at the onset of the event, which here can be considered as the number of people in a train, (b) the probability of successful escape P_O, which here is equal to the probability that the failure is detected timely and any train can be stopped before approaching the location, (c) the probability of death given no successful escape $P_{D|F}$, which here is the probability of a person being killed given that the train derails due to a slope failure at this location.

With numerical values $N_{PE} = 200$, $P_O = 0.3$, $P_{D|F} = 0.3$, the probability of an exposed person being killed in the case of a failure becomes $k = (1 - 0.3) \cdot 0.3 = 0.21$. The expected value of the number of people killed given the event of a failure is $N_{PE} \cdot k = 42$.

5.6 *Willingness to pay (WTP)*

The WTP is defined in Eq. (13) as $WTP = J_\Delta\, g/q$. All input values depend on socio-economic indicators and must therefore be defined country-specific. Here, values valid for Germany in 2010 are taken and are derived from the data provided in (OECD 2011) following (Lentz 2007). The disposable per-capita income is obtained as $g = 25'300$€, the constant q of Eq. (1) is $q = 0.13$ and the linearization coefficient J_Δ of Eq. (8) is $J_\Delta = 14.4$. It follows that

$$WTP = \frac{25'300\text{€}}{0.13} 14.4 = 2.8 \cdot 10^6\text{€}$$

5.7 *Acceptable slope angle*

The acceptable slope angle is now found by application of Eq. (13). The left-hand side of Eq. (13), which represents the efficiency of mitigating risk by decreasing α, is obtained from Eqs. (15) and (18) as

$$\begin{aligned} \frac{\mathrm{d}C_a(\alpha)}{\mathrm{d}r(\alpha)} &= \frac{\frac{\mathrm{d}C_a(\alpha)}{\mathrm{d}\alpha}}{\frac{\mathrm{d}r(\alpha)}{\mathrm{d}\alpha}} = \frac{\frac{\gamma[c_0 + c \cdot (\tan\alpha)^{-1}]}{\mathrm{d}\alpha}}{\frac{\mathrm{d}\Phi[-(11.61 - 0.415\alpha + 0.0049\alpha^2)]}{\mathrm{d}\alpha}} \\ &= \frac{\gamma c (\sin\alpha)^{-2}}{\varphi[-(11.61 - 0.415\alpha + 0.0049\alpha^2)](-0.415 + 2 \cdot 0.0049\alpha)} \end{aligned}$$

φ is the standard normal probability density function. $\mathrm{d}C_a(\alpha)/\mathrm{d}r(\alpha)$ is plotted in Figure 4. The right hand side of Eq. (13) is readily obtained as $WTP \cdot N_{PE} k = 2.8 \cdot 10^6\text{€} \cdot 42 = 118 \cdot 10^6\text{€}$. Figure 4 illustrates how the acceptable slope angle is determined as $\alpha_{acc} = 23.8°$.

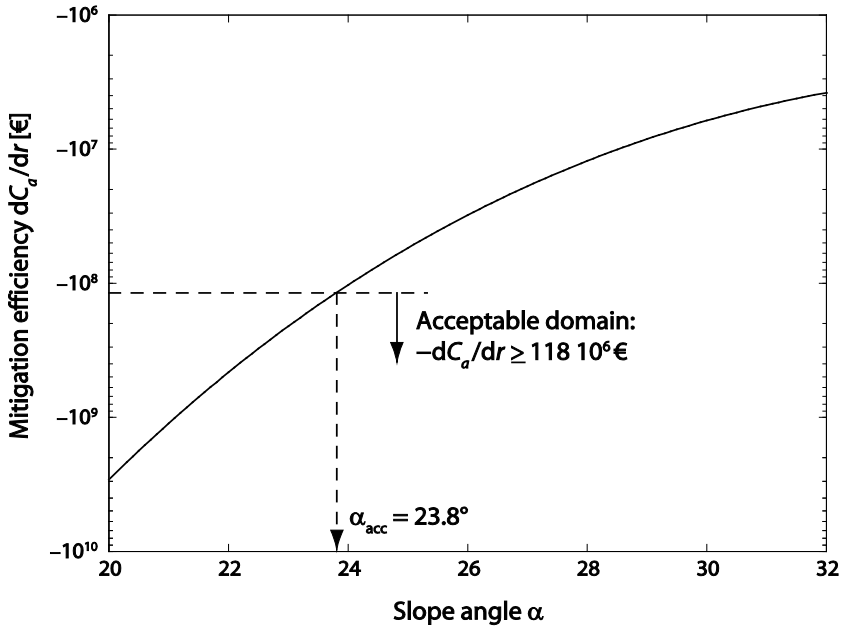

Figure 4. The relative cost of reducing the failure rate, $dC_a(\alpha)/dr(\alpha)$, and the acceptable slope angle derived according to the LQI criterion.

The minimum acceptable slope angle $\alpha_{acc} = 23.8°$ corresponds to a reliability index $\beta = 4.5$, as seen from Figure 3. The corresponding global safety factor is $FS = 1.83$.

6 CONCLUDING REMARKS

The paper summarizes and illustrates the use of the LQI principle for determining the acceptability of geotechnical engineering designs. The central idea is the formulation of an index (LQI) that serves as a proxy for societal utility and is formulated as a function of life expectancy and income (which in turn is a proxy for available resources). By requiring that any engineering decision must not decrease the value of the LQI, a minimum requirement on the resources to be spent for risk-reduction can be deduced.

The presented example serves for illustrational purposes only. No general conclusions must be drawn from this example, since the results are case-specific and are obtained from a simplified probabilistic model. The purpose of the example is purely to demonstrate the steps involved in the application of the LQI principle.

It is pointed out that the LQI is not a tool to be used directly for standard geotechnical projects, where decisions are – and should be – made based on global or partial safety factors concepts. However, the LQI principle can be used to determine the values of the safety factors prescribed by codes and standards. This can be achieved by computing a larger set of examples similar to the one presented in this paper and then calibrate safety factors (e.g., the acceptable slope angle shown in the example above corresponds to a global safety factor of 1.83). Optimally, safety factors are defined as a function of the consequences of a failure; the safety factors should increase with increasing consequences. The LQI principle enables to quantify this dependence. As an example, if the consequences of failure in the above example are reduced by installing a warning system that would increase the probability that trains can stop timely from 0.3 to $P_O = 0.9$, the acceptable slope angle increases to $\alpha_{acc} = 27.3°$ (with corresponding $\beta = 3.9$).

There has been some discussion in the scientific community on the exact formulation of the LQI, in particular on the definition of the factor q in Eq. (1) (see e.g. Ditlevsen 2004). It is noted, however, that the different formulations give results in the same order of magnitude and the dispute is thus of little practical relevance. More relevant is the fact that the LQI in its present form is restricted to considering fatalities. Failures of engineering systems can lead to other types of relevant societal consequences, including environmental damages. The LQI concept has yet to be extended to account for such consequences. A first step in this direction is suggested in Lentz (2007), namely to additionally account for injuries caused by a failure event, by considering only the life spent in good health in the formulation of the LQI concept.

REFERENCES

Ditlevsen O. 2004. Life quality index revisited. *Structural Safety*, **26**(4): 443-451.

Lentz, A. 2007. *Acceptability of civil engineering decisions involving human consequences.* PhD thesis. Munich: Lehrstuhl für Massivbau, Technische Universität München.

Joanni, A. & Rackwitz, R. 2007. Reliability-based optimization of an existing n-unit series system with dependent components and finite renewal times. *Proc. ICASP 10*, Tokio.

Matsui, T. & San, K. C. 1992. Finite element slope stability analysis by shear strength reduction technique. *Soils and Foundations*, **32**(1): 59–70.

Mrozek, J. & Taylor, L. 2002. What determines the value of life? A meta-analysis. *Journal of Policy Analysis and Management* 21(2): 253–270.

Nathwani, J., Lind, N. & Pandey, M. 1997. *Affordable Safety by Choice: The Life Quality Method*. Institute of Risk Research, University of Waterloo, Ontario, Canada.

OECD 2011. *OECD.StatExtracts*. Online database, http://stats.oecd.org, retrieved on Feb. 12, 2011.

Pandey, M. & Nathwani, J. 2004. Life quality index for the estimation of societal willingness-to-pay for safety. *Structural Safety* **26**(2): 181–199.

Pandey, M. D., J. S. Nathwani, & Lind N. C. 2006, The derivation and calibration of the life-quality index (LQI) from economic principles, *Structural Safety,* **28**(4), 341–360.

Rackwitz, R. 2002. Optimization and risk acceptability based on the Life Quality Index, *Structural Safety,* **24**(2-4): 297–331.

Rackwitz, R. 2004. Optimal and acceptable technical facilities involving risks. *Risk Analysis* 24(3): 675–695.

Rackwitz, R. 2005. *The philosophy behind the life quality index and empirical verification*. Updated Memorandum to the Joint Committee on Structural Safety (JCSS).

Rackwitz, R. 2010. Risikoakzeptanz und Lebensqualität. *Bauingenieur*, **85**(1):10–16.

Shepard, D. & Zeckhauser, R. 1984. Survival versus consumption. *Management Science* 30(4): 423–439.

Streicher H., Rackwitz R. 2004. Time-variant reliability-oriented structural optimization and a renewal model for life-cycle costing. *Probabilistic Engineering Mechanics*, **19**(1-2), pp. 171-183.

Smith, I. M. & Griffiths, D. V. 2004. *Programming the Finite Element Method.* 4th ed. Chichester: John Wiley & Sons.

ISGSR 2011 - Vogt, Schuppener, Straub & Bräu (eds) - © 2011 Bundesanstalt für Wasserbau ISBN 978-3-939230-01-4

Developing a LRFD Procedure for Shallow Foundations

K. Lesny
Institute of Geotechnics, Department of Building Sciences, University of Duisburg-Essen, Germany

S. G. Paikowsky
Geotechnical Engineering Research Laboratory, Department of Civil and Environmental Engineering, University of Massachusetts Lowell and Geosciences Testing and Research Inc. (GTR), USA

ABSTRACT: The development of a Load and Resistance Factor Design (LRFD) procedure for the Ultimate Limit State (ULS) design of shallow foundations for highway bridges in the U.S. is presented. Large, high-quality databases of foundations on/in granular soils under varying loading conditions tested to failure are the backbone of this study. A procedural and data management framework had been developed that allowed the evaluation of the LRFD parameters. The study concentrated on the evaluation of model uncertainties associated with the bearing capacity calculation. The model uncertainties were represented by the bias defined as the ratio of measured over calculated bearing capacities using defined soil parameters and design methods. The measured bearing capacities were identified by a unique failure criterion applied to the respective load-displacement curve of the load tests. Investigation of the bearing capacity equation possible via the database identified the bearing capacity parameter N_γ to be the major source of the model uncertainty. A single resistance factor was found insufficient for addressing the bearing capacity equation. As different soil strength and loading conditions result in different levels of uncertainties, different resistance factors were required to be developed in order to maintain a consistent level of reliability under the varying conditions. The resistance factors were established on the basis of probabilistic analyses (FOSM and Monte Carlo simulations) for vertical-centric, vertical-eccentric, inclined-centric and inclined-eccentric loading conditions.

Keywords: Limit State Design, LRFD, shallow foundations, databases, uncertainty evaluation, resistance factors

1 INTRODUCTION

1.1 *Methodology of LRFD and scope of the study*

The intent of LRFD is to separate uncertainties in loading from uncertainties in resistance, and then to use probabilistic procedures to assure a prescribed margin of safety. In the methodology of LRFD the safety is represented by partial factors which are applied separately to the load effects and the resistance. Load effects Q_i are increased by multiplying characteristic or nominal values with load factors γ_i. The resistance is reduced by multiplying the nominal value R_n by a resistance factor $\phi \leq 1{,}0$. The nominal resistance results from a specific, calibrated design method and is not necessary the mean of the resistance. It then has to be ensured that the factored resistance is not smaller than a linear combination of the factored load effects:

$$\phi \cdot R_n \geq \sum_i \gamma_i \cdot Q_i \qquad (1)$$

LRFD represents a Resistance Factor Approach (RFA) where the resistance factor is applied to the resulting resistance calculated with the characteristic values of the strength parameters as well as characteristic values of load components if the geotechnical resistance is defined as a function of the load effects. In opposite to the RFA the Material Factor Approach (MFA) includes the direct application of the partial factors to the characteristic values of the material, i.e. the resistance is calculated using the design values

of the material strength. Eurocode 7 (e.g. DIN EN 1997-1, 2010) generally allows both procedures in three design approaches, the member states specify in their National Annexes which design approaches finally are to be used. The RFA format in Eurocode 7 also differs slightly from the one given in equation (1) as the nominal resistance R_n is divided by a resistance factor $\gamma_R \geq 1.0$.

In the United States design specifications published by AASHTO (American Association of State Highway and Transportation Officials) are traditionally used for all federally aided highway projects and are generally viewed as the national code of highway practice. In the past two decades these specifications were gradually changed from Working Stress Design using global factors of safety (last edition of the 'standard' specifications are AASHTO, 1987) to LRFD within the Limit State Design (LSD) concept. While original changes mostly relied on back analysis (LSD from Working Stress Design (WSD)) and probabilistic approach, the recent development was focused on calibrations utilizing databases. In this context the NCHRP (National Cooperative Highway Research Program) research project 24-31 "LRFD Design Specifications for Shallow Foundations" was initiated with the objective to thoroughly modify Section 10 of the AASHTO LRFD Bridge Design Specifications to implement LRFD for the ULS design of shallow bridge foundations. The results of the NCHRP 24-31 research study were reported by Paikowsky et al. (2010). The major findings relevant to the bearing capacity of shallow foundations on granular soils are presented here.

1.2 *Implementation procedure*

The implementation of LRFD to highway bridge foundations which has been adopted in this research follows a two-step strategy:

Step 1: Assembly and assessment of knowledge and data, including:
- Defining design methods used for the calibration procedures
- Establishing databases of case histories, large and small scale model tests
- Selecting typical bridge foundation structures and case histories
- Defining expected load ranges and their distributions

Step 2: Analysis of data and methods assembled in step 1, including:
- Establishing the uncertainty of the design methods and parameters, investigation of their sources
- Developing resistance factors and their examination in design cases
- Defining final resistance factors and conditions of implementation
- Developing new design specifications

The major task within step 1 and a very important part of the research was the compilation of large, high-quality databases of foundations tested to failure. This was combined with the development of a procedural and data management framework that would enable LRFD parameter evaluation for the ULS of shallow foundations. This study is the first which introduces large-scale reliability-based design calibration of shallow foundations utilizing databases. One database includes 549 cases of field and model tests on shallow foundations in or on granular soils, predominantly subjected to vertical-centric loading, with a sizeable component of foundations subjected to combined loading. A second database provides 122 model tests of foundations on or in rock.

Different design methods for predicting the bearing capacity of shallow foundations in or on soil or rock in the ULS were compiled based on a questionnaire developed and distributed to all state bridge design agencies across the US and Canada as well as an evaluation of existing design methods based on a literature review. As a result, a set of design methods was established as the basis for the probabilistic analyses. Unique failure criteria for foundations on/in soil or rock had been defined, which were consistently used to interpret the failure loads from all load tests in the databases, thus maintaining a consistent failure interpretation for the following probabilistic analyses.

The analysis of the uncertainties associated with bearing capacity predictions was the most important task within step 2. The model uncertainties were expressed inclusively by a bias which is defined as the ratio of measured to calculated bearing resistances.

Based on the results of the uncertainty analyses for the resistances and known load uncertainties, Monte Carlo (MC) simulation as well as a simplified solution derived from First Order Second Moment (FOSM) method, have been used to determine the resistance factors for a predefined reliability index.

2 LOAD DISTRIBUTION AND LOAD FACTORS

The loads and load combinations followed those presented by AASHTO (2007) and demonstrated in examples compiled by Kimmerling (2002). In lack of better data, the uncertainty of the foundation loading has been assumed in this study as that attributed to the design of the structural element. The load factors and uncertainties for vertical live loads and dead loads on the foundation structure have been selected based on Nowak (1999) by Paikowsky et al., 2004, and are summarized in Table 1.

Table 1. Load factors and uncertainties in vertical live load and dead load

Load type	Load factor	Bias	COV
Live Load (LL)	$\gamma_L = 1.75$	1.15	0.20
Dead Load (DL)	$\gamma_L = 1.25$	1.05	0.10

The horizontal dead loads on bridge foundation structures mainly result from earth pressures due to soil and surcharge. The associated sources of uncertainty are, therefore, the variations in the soil unit weight and the soil friction angle. Live loads mainly result from impact, wind, snow, temperature variations, shrinking, creep, etc.

An analysis of the uncertainties related to lateral earth pressures suggested the load factors and uncertainties for horizontal loads as given in Table 2. A lognormal distribution is assumed with these values. The uncertainties of the dead loads are valid for a bias of the soil unit weight of 1.00 and a related COV of 0.10 for natural soil conditions and of 0.08 for engineered backfill.

Table 2. Load factors and uncertainties in horizontal live load and dead load

Load type	Load factor	Bias	COV
Live Load (LL)	$\gamma_{LFL} = 1.00$	1.00	0.15
Dead Load (DL):			
At-rest earth pressure	$\gamma_{EH0} = 1.35$	1.00	0.30
Active earth pressure	$\gamma_{EHa} = 1.50$	1.00	0.30

3 BEARING CAPACITY OF HIGHWAY BRIDGE FOUNDATIONS

3.1 *Bearing capacity formulation utilized for the predicted strength limit state*

The analysis was based on the procedure for the bearing capacity prediction specified in the AASHTO LRFD Bridge Design Specifications (2008). Accordingly, the general bearing capacity formulation by Vesić (1975) was used:

$$q_n = c \cdot N_{cm} + \gamma_1 \cdot D_f \cdot N_{qm} + 0.5 \cdot \gamma_2 \cdot B \cdot N_{\gamma m} \quad (2)$$

in which:

$$N_{cm} = N_c \cdot s_c \cdot d_c \cdot i_c \quad (3a)$$

$$N_{qm} = N_q \cdot s_q \cdot d_q \cdot i_q \quad (3b)$$

$$N_{\gamma m} = N_\gamma \cdot s_\gamma \cdot d_\gamma \cdot i_\gamma \quad (3c)$$

In Eq. (2) and elsewhere, c is the undrained shear strength c_u in a total stress analysis or the effective shear strength c' in an effective stress analysis. Parameters γ_1 and γ_2 are the moist or submerged unit weight of the soil above and below the footing base, respectively, whereas D_f is the embedment depth of the footing. The bearing capacity factors N_c, N_q and N_γ are summarized in Table 3, the shape factors s_c, s_q and s_γ are presented in Table 4. The depth factors d_c, d_q and d_γ, if applicable, as well as the inclination factors i_c, i_q and i_γ are given in Table 5 and Table 6, respectively.

The parameter n in Table 6 is defined as:

$$n = \left[\frac{(2 + L/B)}{(1 + L/B)}\right] \cdot \cos^2\theta + \left[\frac{(2 + B/L)}{(1 + B/L)}\right] \cdot \sin^2\theta \qquad (4)$$

In Eq. (4) the angle θ is the angle between the resultant load and the footing length L (or L') projected in the footing area. Eq. (2) and (4) as well as Tables 4-6 are valid either for the physical footing dimensions B and L in case of centric loading or for the effective footing dimensions $B' = B - 2 \cdot e_B$ and $L' = L - 2 \cdot e_L$ in the case of eccentric loading.

The inclination factors in Table 6 and the effective footing dimensions are calculated with unfactored loads.

Table 3. Bearing capacity factors N_c (Prandtl, 1921), N_q (Reissner, 1924) and N_γ (Vesić, 1975)

Friction angle	N_c [-]	N_q [-]	N_γ [-]
$\phi_f = 0°$:	$2 + \pi$	1.0	0.0
$\phi_f > 0°$:	$(N_q - 1) \cdot \cot\phi_f$	$\exp(\pi \cdot \tan\phi_f) \cdot \tan^2\left(45° + \frac{\phi_f}{2}\right)$	$2 \cdot (N_q + 1) \cdot \tan\phi_f$

Table 4. Shape factors (Vesić, 1975)

Friction angle	s_c [-]	s_q [-]	s_γ [-]
$\phi_f = 0°$:	$1 + 0.2 \cdot \frac{B}{L}$	1.0	1.0
$\phi_f > 0°$:	$1 + \frac{B}{L} \cdot \frac{N_q}{N_c}$	$1 + \frac{B}{L} \cdot \tan\phi_f$	$1 - 0.4 \cdot \frac{B}{L}$

Table 5. Depth factors (Brinch Hansen, 1970)

Friction angle	d_c [-]	d_q [-]	d_γ [-]
$\phi_f = 0°$:	$D_f \le B : 1 + 0.4 \cdot \frac{D_f}{B}$	1.0	1.0
	$D_f > B : 1 + 0.4 \cdot \arctan\left(\frac{D_f}{B}\right)$		
$\phi_f > 0°$:	$d_q - \frac{1 - d_q}{N_q - 1}$	$D_f \le B : 1 + 2 \cdot \tan\phi_f \cdot (1 - \sin\phi_f)^2 \cdot \frac{D_f}{B}$	1.0
		$D_f > B : 1 + 2 \cdot \tan\phi_f \cdot (1 - \sin\phi_f)^2 \cdot \arctan\left(\frac{D_f}{B}\right)$	1.0

Table 6. Inclination factors (Vesić, 1975)

Friction angle	i_c [-]	i_q [-]	i_γ [-]
$\phi_f = 0°$:	$1 - \frac{n \cdot H}{c \cdot B \cdot L \cdot N_c}$	1.0	1.0
$\phi_f > 0°$:	$i_q - \frac{1 - i_q}{N_q - 1}$	$\left[1 - \frac{H}{V + c \cdot B \cdot L \cdot \cot\phi_f}\right]^n$	$\left[1 - \frac{H}{V + c \cdot B \cdot L \cdot \cot\phi_f}\right]^{n+1}$

3.2 *Selection of soil parameters*

Selected correlations were chosen in order to obtain a consistent interpretation of the soil parameters used for the bearing capacity predictions. Where SPT results were available, the soil friction angle has been correlated to the corrected SPT-N value $(N_1)_{60}$ using a procedure proposed by Peck, Hanson and Thornton as mentioned in Kulhawy & Mayne (1990):

$$\phi_f \approx 54 - 27.6034 \cdot \exp\left(-0.014\left(N_1\right)_{60}\right) \quad [°] \quad (5a)$$

$$\left(N_1\right)_{60} = \sqrt{\frac{p_a}{\sigma'_v}} \cdot N_{60} \quad (5b)$$

In Eq. (5b) p_a is the atmospheric pressure, σ'_v the effective vertical stress and N_{60} the corrected SPT blow count.

For load tests conducted on medium to coarse, sharp-edged silica sand at the University of Duisburg-Essen in Germany, a correlation of the soil friction angle to the soil bulk density has been established on the basis of numerous direct shear tests. Eq. 6 is a revision of the original correlation given in Perau (1995) and was used in this study.

$$\phi_f = 3.824 \cdot \gamma - 21.527 \quad [°] \quad (6)$$

where γ is in kN/m^3.

In cases where the unit weight was not specified, but SPT results were available the soil unit weight has been correlated to the SPT blow count according to Eq. (5b) by a procedure suggested in Paikowsky et al. (1995):

$$\gamma = 0.88 \cdot \left(N_1\right)_{60} + 99 \quad [\text{pcf}] \quad \text{for } \gamma \le 146 \text{ pcf} \quad (7)$$

4 DATABASE AND DETERMINATION OF FAILURE LOADS

4.1 *Database for shallow foundations in or on soils*

The UML-GTR ShalFound07 database assembled in the present research study includes 549 load tests for shallow foundations mostly in or on granular soils. The database was constructed in Microsoft ACCESS 2003. The majority of the cases are load tests to failure under vertical centric loading but a sizeable dataset of foundations under combined loading conditions is also included. Tests under vertical centric loading were either field or laboratory tests. Field tests, for which SPT blow counts were available, usually were carried out on larger foundation sizes and were categorized as tests under *natural soil conditions*. The tests under combined loading were mainly small scale laboratory model tests performed in *controlled soil conditions*. For these, the mechanical properties of the tested soils (such as unit weight, density, and shear strength) were determined in advance and were controlled in the tests; such that all the tests from one source could be compared.

The majority of the tests were carried out in Germany, USA, France and Italy. The large number of German tests originated from two sources, tests performed at the DEGEBO in Berlin (Deutsche Forschungsgesellschaft fuer Bodenmechanik) in the 1960-ies and 1970-ies and tests carried out or compiled in various research projects at the University of Duisburg-Essen during the past 25 years. Table 7 presents the content of the database classified by foundation type defined by the width of the foundation, predominant soil type below the footing base and country.

As can be seen in Table 7, there is limited number of large scale foundation tests as typically the serviceability limit is exceeded for these foundations prior to the strength limit state mobilization (i.e. bearing capacity failure). Most tests in the database are plate load tests with a width of less or equal to 1.0 m which include numerous small scale model tests under controlled laboratory conditions as mentioned above.

Table 7. Overview of cases in the UML-GTR ShalFound07 database

Foundation Type	Predominant Soil Type					Total	Country	
	Sand	Gravel	Cohe-sive	Mixed	Others		Germany	Others
Plate load tests, B ≤ 1 m	346	46	--	2	72	**466**	253	213
Small footings, 1 m < B ≤ 3 m	26	2	--	4	1	**33**	--	33
Large footings, 3 m < B ≤ 6 m	30	--	--	1	--	**31**	--	31
Rafts & Mats, B > 6 m	13	--	--	5	1	**19**	1	18
Total	**415**	**48**	**0**	**12**	**74**	**549**	**254**	**295**

Note:
"Mixed" are cases with alternating layers of sand or gravel and clay or silt
"Others" are cases with either unknown soil types or with other granular materials like Loamy Scoria

The existing site conditions in the load tests were classified as shown in Figure 1. The database further includes information on the footings, the subsoil conditions, laboratory test results, field tests, details of the loading as well as the results of the load tests as load-displacement curves.

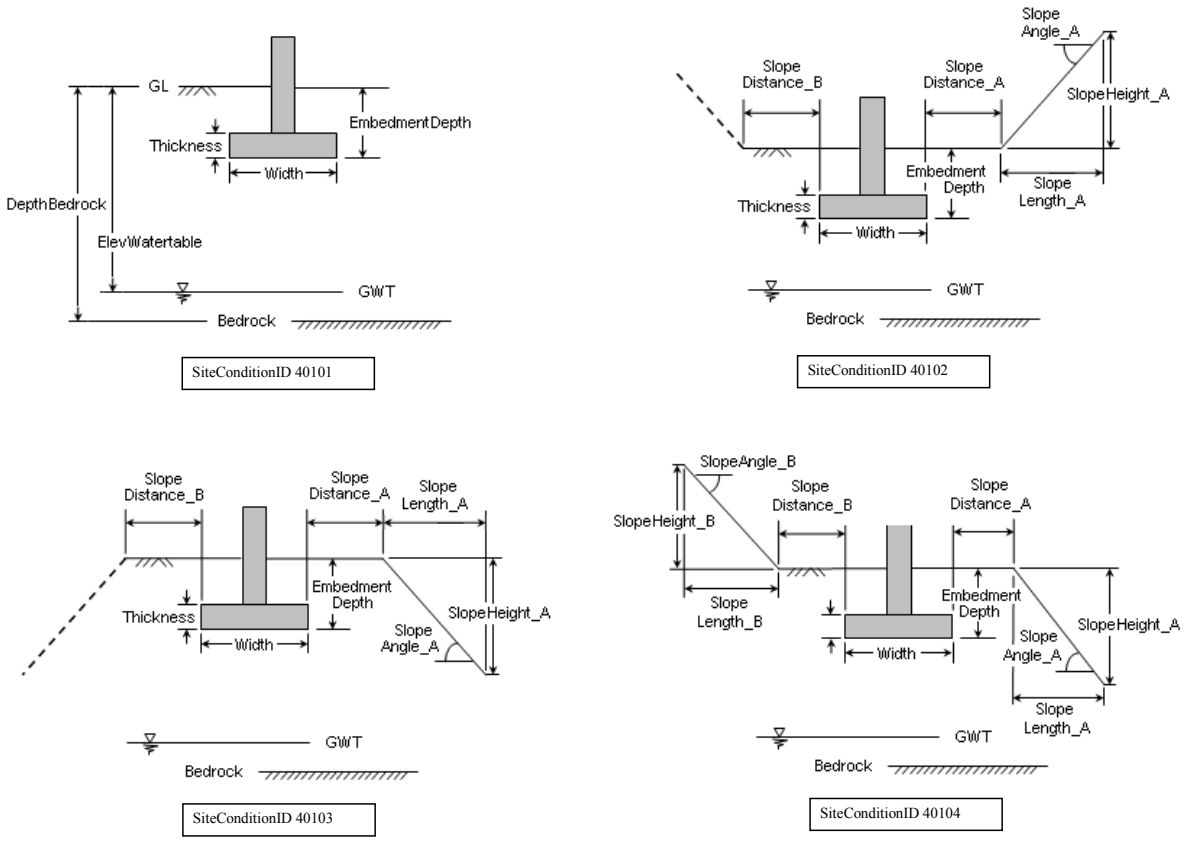

Figure 1. Classification of various site conditions employed in the UML-GTR ShalFound07 database

4.2 *Failure criteria and determination of failure loads from model tests*

In order to evaluate the uncertainties of the bearing capacity model provided by the formulation presented in section 3.1, a consistent procedure is required to identify the measured capacity, i.e. to define the failure loads from the load-displacement test results.

The bearing capacity equation given in Eq. (2) is valid only for a general shear failure and therefore is limited to the foundation's relative depth of D/B ≤ 2. In general shear, the failure pattern is completely developed and reaching the surface beside the foundation (see Figure 2). General shear failure is indicated by a distinctive peak in the load-displacement curve and can therefore be clearly identified. Usually, footings in homogenous, nearly incompressible soils with finite shear strength fail in general shear failure as shown in Figure 2. Out of the cases in the database, especially the plate load tests show this failure pattern, i.e. the small scale model tests conducted under controlled laboratory conditions where the homogeneity of the soil and its density could have been adjusted.

In field tests in inhomogeneous soils, the resultant load-displacement curves do not show a prominent peak indicating a general shear bearing capacity failure. For non-dense soils, the foundation fails in local or punching shear. Depending on the actual mode of failure, a clear peak or at least an asymptote value may not exist at all, so that the failure load needs to be interpreted. Such interpretation requires a load test to be conducted to sufficiently large displacements. Large scale field tests were typically performed to limited displacements where a bearing capacity failure could not be developed or identified. This led to a reduction in the number of load tests available for the reliability analyses.

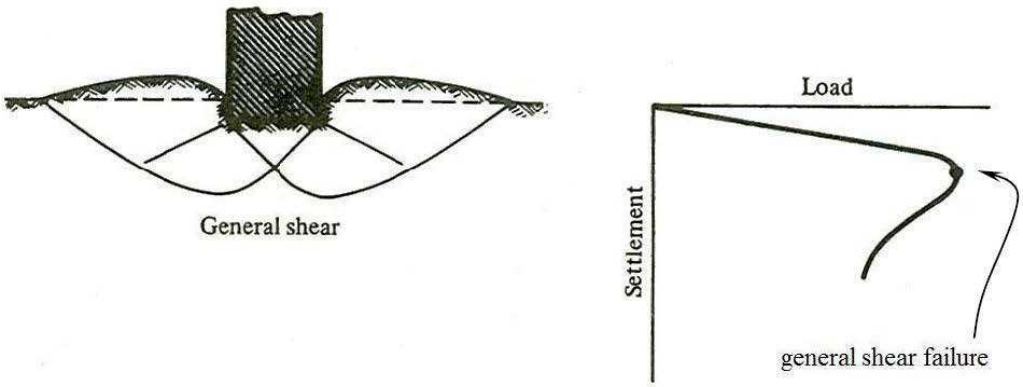

Figure 2. Bearing capacity failure as a general shear failure (Vesić, 1975)

The following criteria for interpreting the failure loads from load-displacement curves have been investigated in this study:

- Minimum slope criterion (Vesić, 1963)
- Limited settlement criterion (Vesić, 1975)
- Interpretation from the log-log plot of the load-displacement curve (De Beer, 1967)
- Two slope criterion (e.g. NAVFAC, 1986)

With the minimum slope criterion (Vesić, 1963) the failure load is defined at the point where the slope of the load-displacement curve first reaches zero or a minimum steady value. For footings in or on soils with high relative density which are more likely to fail in general shear failure the starting point of the minimum slope usually is clearly defined. For footings in or on soils with lower densities the definition of the failure load may sometimes be arbitrary. In this case, a semi-log scale with the load in logarithmic scale may help to identify the failure load.

The limited settlement criterion introduced by Vesić (1975) includes the definition of the failure load at a limited settlement of 10% of the footing width.

If the load-displacement curve is presented in a logarithmic scale with loads and displacements either as normalized or as absolute values, the failure load can be interpreted as the point of break in the load-displacement curve (De Beer, 1967).

The two slope criterion (e.g. NAVFAC, 1986) is a variation of the minimum slope criterion or De Beer's criterion and can be applied by constructing the asymptotes at the initial portion as well as at the end portion of the load-displacement curve which is plotted either in a linear or a logarithmic scale. The load at the intersection point of both asymptotes represents the failure load. A range of failure load may be identified if the location of the end asymptote is not unique.

The application of these failure criteria to the UML-GTR ShalFound07 database was examined for the tests on vertical-centric loading. Out of these tests, 196 cases could have been interpreted using the minimum slope criterion and 119 using De Beer's criterion based on the log-log plot of the load-displacement curves. Most of the footings, especially in small scale model tests on very dense soils, failed before reaching a settlement of 10% of the footing width. This criterion could therefore only be applied to 19 cases.

In order to examine and compare the failure criteria and to establish the uncertainty of the criterion selected for defining the bearing capacity of shallow foundations on soils, a single "representative" value of the relevant measured capacity was assigned to each footing case. This was done by taking an average of the measured capacities interpreted using the minimum slope criterion, the limited settlement criterion of 0.1B (Vesić, 1975), the log-log failure criterion, and the two-slope criterion (shape of curve). The values obtained by each of the failure criteria were then compared case by case to the representative value. The statistics of the ratios of this representative value over the interpreted capacity using the minimum slope criterion and the log-log failure criterion were comparable with the mean of the ratio for the minimum

slope criterion being 0.98 versus that for the limited settlement criterion being 0.99. Due to the simplicity and versatility of its application, the minimum slope criterion was selected as the failure interpretation criterion to be used for all cases of footing, including those with combined loadings. Figure 3 shows the histogram for the ratio of the representative measured capacity to the interpreted capacity using the minimum slope criterion. Figure 3 represents, therefore, the uncertainty associated with the use of the selected criterion, suggesting that the measured capacity interpreted using the minimum slope criterion has a slight overprediction.

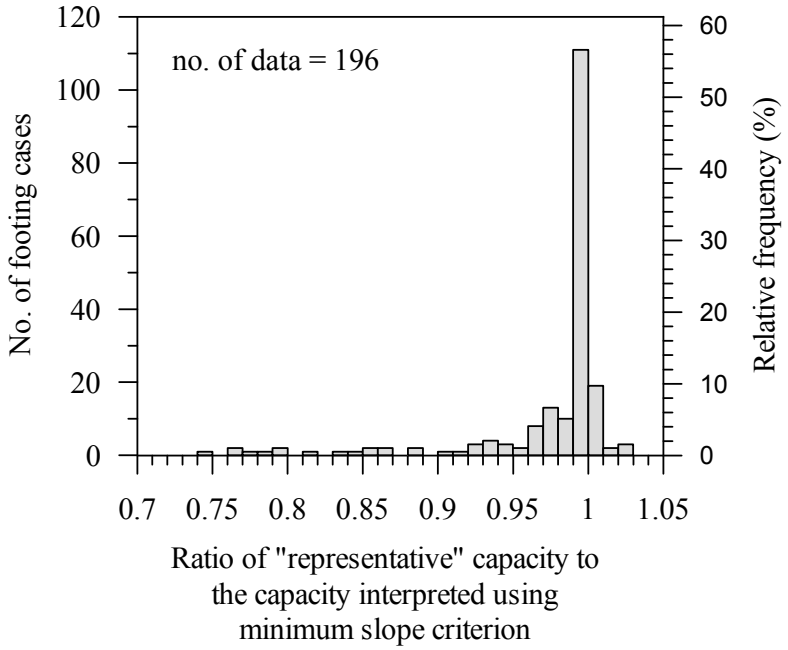

Figure 3. Histogram for the ratio of representative measured capacity to interpreted capacity using the minimum slope criterion for 196 footing cases in granular soils under vertical-centric loading.

5 EVALUATION OF MODEL UNCERTAINTIES

5.1 *Definition of the bias*

The uncertainty of the geotechnical resistance model controls the resistance evaluation of the foundation due to the assumptions and empirical data utilized in its formulation. To evaluate the model uncertainty the bearing capacity model presented in section 2.2 was calibrated as a complete unit while other associated sources of uncertainty were reduced by applying specific procedures, e.g. the soil parameter establishment as previously discussed. This approach, while may be in dispute, was proven effective when applied to the design of deep foundations (see example in Paikowsky et al., 2010) or when examined theoretically against a case study (Teixeira et al., 2011).

The uncertainty associated with the bearing capacity calculation was evaluated on the basis of the test results in the databases by comparing the bearing capacities measured in the load tests with the calculated bearing capacities using the calculation methods defined in section 2.2. The ratio of measured over calculated bearing capacity is defined as the bias λ_R:

$$\lambda_R = \frac{\text{measured bearing capacity}}{\text{calculated bearing capacity}} \qquad (8)$$

This lump-sum procedure includes all sources of uncertainties related to the bearing capacity prediction such as scale effects, variation in soil properties, etc.

The statistics of the bias, especially its mean value and its coefficient of variation (COV), were used to analyze the model uncertainties.

5.2 *Uncertainties in the bearing capacity of footings subjected to vertical-centric loading*

Figure 4 summarizes the results of the statistical analysis for the vertical-centric loading cases. The overall mean bias was 1.59 for all 173 cases which indicates a systematic bearing capacity underprediction. The mean bias for footings in controlled soil conditions was 1.64 and higher, with a COV of 0.267, and therefore significantly different than that for footings in natural soil conditions (mean bias = 1.00, COV = 0.329).

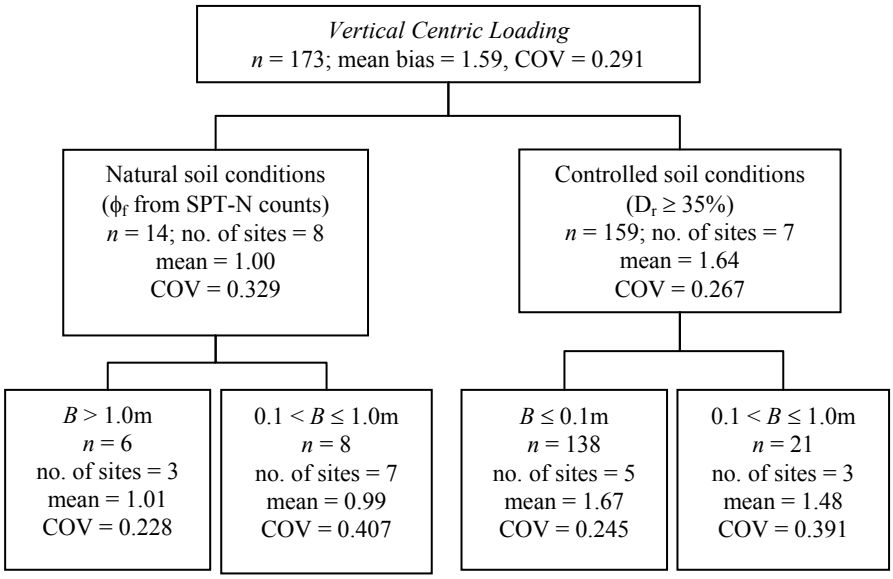

Figure 4. Summary of the bias for vertical-centric loading cases

The higher mean bias in controlled soil conditions is attributed to the conservatism in the theoretical prediction of the bearing capacity formulation as outlined in section 3.1. This conservatism especially results from the bearing capacity factor N_γ proposed by Vesić (1973) (see Table 3).

The uncertainty related to N_γ has been analyzed on the basis of load tests carried out on the surface of granular soils. Under such conditions, the bearing capacity only depends on the weight of the soil as the embedment and cohesion term in Eq. (2) are equal zero.

N_γ can, therefore, be back-calculated from the load tests and the obtained values can be related to the theoretical value proposed by Vesić (1973). With that the bias of the bearing capacity factor N_γ is defined as:

$$\lambda_{N_\gamma} = \frac{N_{\gamma Exp}}{N_{\gamma Vesic}} = \frac{q_u / \left(0.5 \cdot \gamma \cdot B \cdot s_\gamma\right)}{2 \cdot \left(N_q + 1\right) \cdot \tan \phi_f} \qquad (9)$$

Figure 5 presents the bias λ_{N_γ} as a function of the soil friction angle ϕ_f. A clear trend of the bias increasing beyond 1.0 for friction angles $\phi_f \geq 42.5°$ can be observed in Figure 5.

The best fit line of the bias λ_{N_γ} in Figure 5 is expressed as:

$$N_{\gamma Exp} = \exp\left(0.205 \cdot \phi_f - 8.655\right) \cdot N_{\gamma Vesic} \quad \text{for } 42.5° \leq \phi_f \leq 46° \qquad (10)$$

with a coefficient of determination of $R^2 = 0.351$ indicating a large scatter.

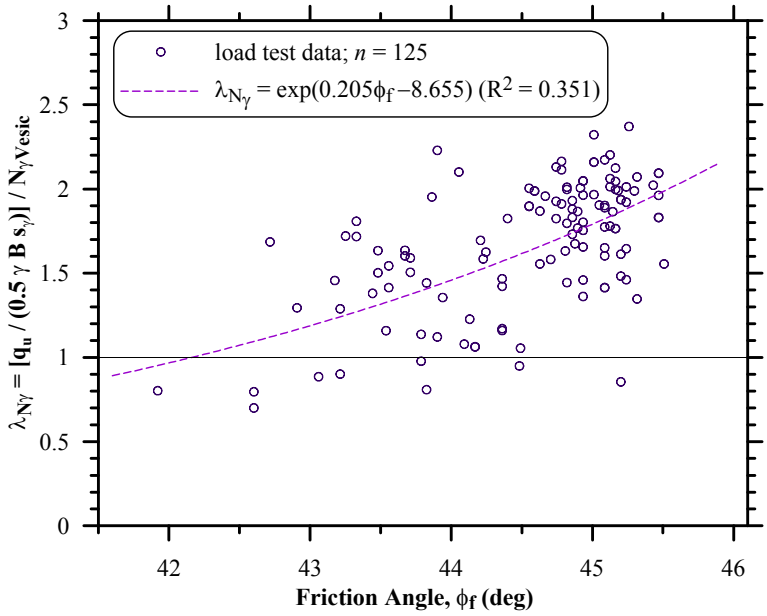

Figure 5. Bias of the bearing capacity factor N_γ as a function of the soil's friction angle ϕ_f

Figure 6 shows the bias of the calculated bearing capacity λ_R and the bias of the bearing capacity factor λ_{N_γ} for the considered range of soil friction angle. The overlapping biases suggest that the bias in the bearing capacity factor N_γ is the dominant factor affecting the uncertainty in the bearing capacity prediction whereas the shape factor has only a negligible influence considering that most foundations were of limited L/B ratio. This has been confirmed by the analysis of footings under vertical-eccentric, inclined-centric and inclined-eccentric loading which revealed a similar trend although the biases did not overlap as cases involving eccentric and/or inclined loading are also sensitive to the loading conditions and their effect on the bearing capacity.

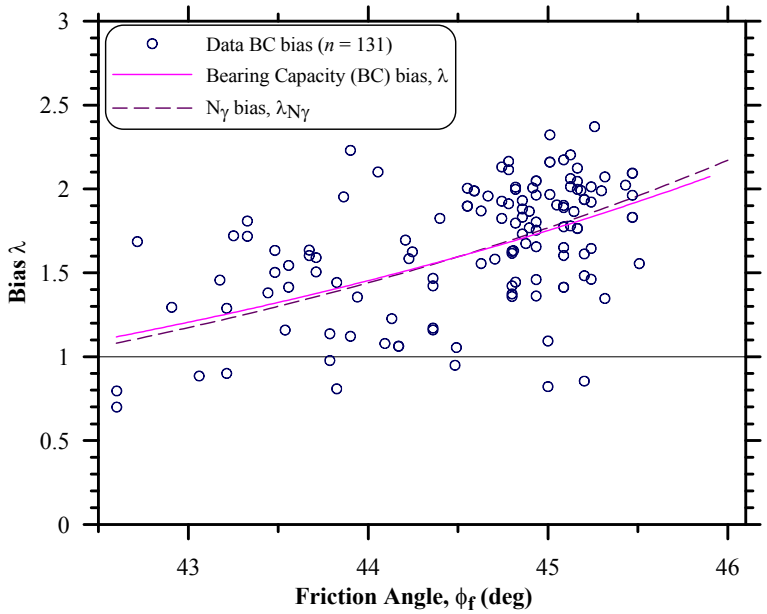

Figure 6. Bias of the bearing capacity prediction compared to the bias of the bearing capacity factor N_γ as a function of the friction angle for footings under vertical-centric loading

5.3 *Uncertainties in the bearing capacity of footings subjected to combined loading*

The uncertainty analysis for footings subjected to combined loading, i.e. vertical-eccentric, inclined-centric and inclined-eccentric loading, was based on results from small scale model tests under controlled laboratory conditions performed by DEGEBO (see e.g. summary in Weiß, 1978), Gottardi (1992), Montrasio (1994) and Perau (1995).

The uncertainty of the bearing capacity prediction for footings subjected to vertical-eccentric loading was based on the results from load tests with a radial load path, i.e. where a constant ratio $e = M/V$ was maintained during the test as the vertical load was applied at a constant eccentricity. A total number of 43 tests were examined. The resulting histogram and PDF of the bias as well as the relationship between measured and calculated bearing capacities are presented in Figure 7.

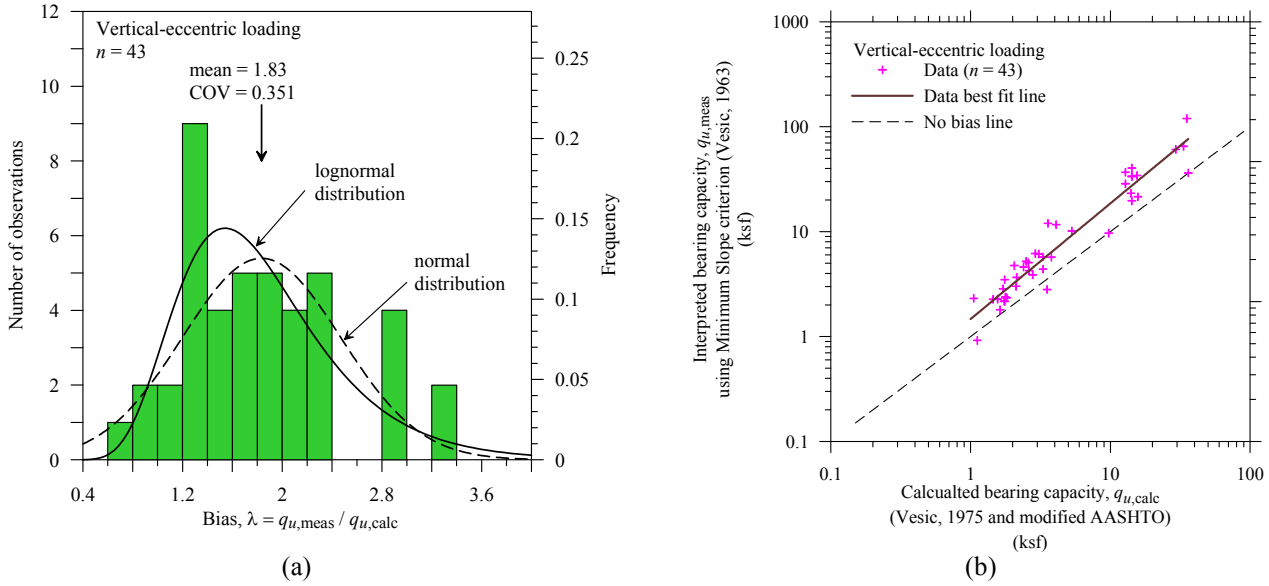

Figure 7. Histogram and probability density function of the bias (a) and relationship between measured and calculated bearing capacity (b) for all footings subjected to vertical-eccentric loading

The analysis shows a mean bias of 1.83 and a COV of 0.351 for all load tests. However, the DEGEBO tests conducted on larger footings ($0.5\ \text{m} \le B \le 1.0\ \text{m}$) lead to a significantly larger bias of 2.22 than the small scale model tests with $0.05\ \text{m} \le B \le 0.5\ \text{m}$ and a mean bias between 1.43 and 1.71 indicating a dependency of the bias on the footing size.

The available tests on foundations subjected to inclined-centric loading were either conducted with a radial load path (DEGEBO; Gottardi, 1992; Montrasio, 1994) or a step-like load path (Gottardi, 1992; Perau, 1995). In the latter, the vertical load was increased to a certain value and then kept constant while the horizontal load was increased to failure. The difference in the applied load path did not have an influence on the bias statistics. As can be seen in Figure 8, a mean bias of 1.43 for all 39 tests was determined with a COV of 0.295. For this load combination, the DEGEBO tests lead to biases of similar magnitude as the small scale model tests.

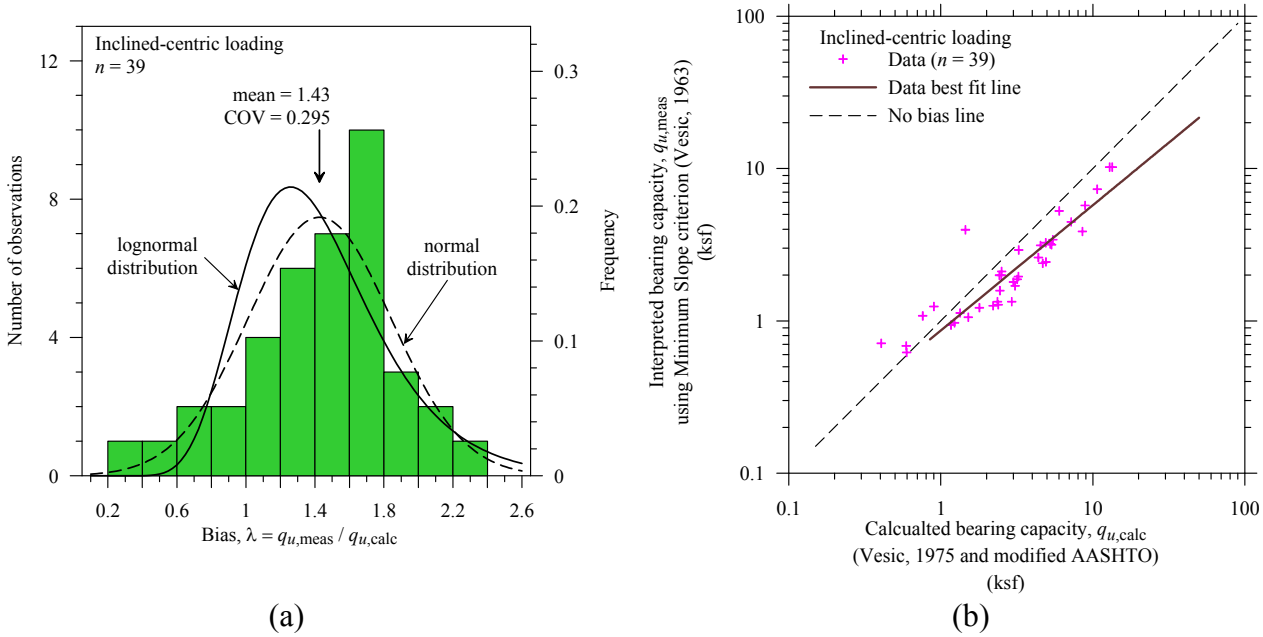

Figure 8. Histogram and probability density function of the bias (a) and relationship between measured and calculated bearing capacity (b) for all footings subjected to inclined-centric loading

Figure 9 shows the histogram and PDF of the bias as well as the relationship between measured and calculated capacity for the 29 tests on foundations subjected to inclined-eccentric loading. These tests were conducted with a radial or a step-like load path. Significant differences in the results due to the different load paths could not be identified in this case as well.

A mean bias of 2.43 with a COV of 0.508 was calculated for all tests. However, detailed examination revealed that the direction of the applied moment or load eccentricity in relation to the direction of the horizontal load affects the measured failure loads.

A resultant moment, which acts in the opposite direction to the horizontal load and causes a negative eccentricity (see Figure 10 top), induces rotations which counteract the horizontal displacements by the horizontal load. The resulting resistance, i.e. the failure load, is higher as compared to inclined-centric loading. A moment which acts in the same direction as the horizontal load and causes a positive eccentricity (see Figure 10 bottom) induces rotations which enforce the horizontal displacements, and hence, the resulting failure load is smaller as compared to inclined-centric loading.

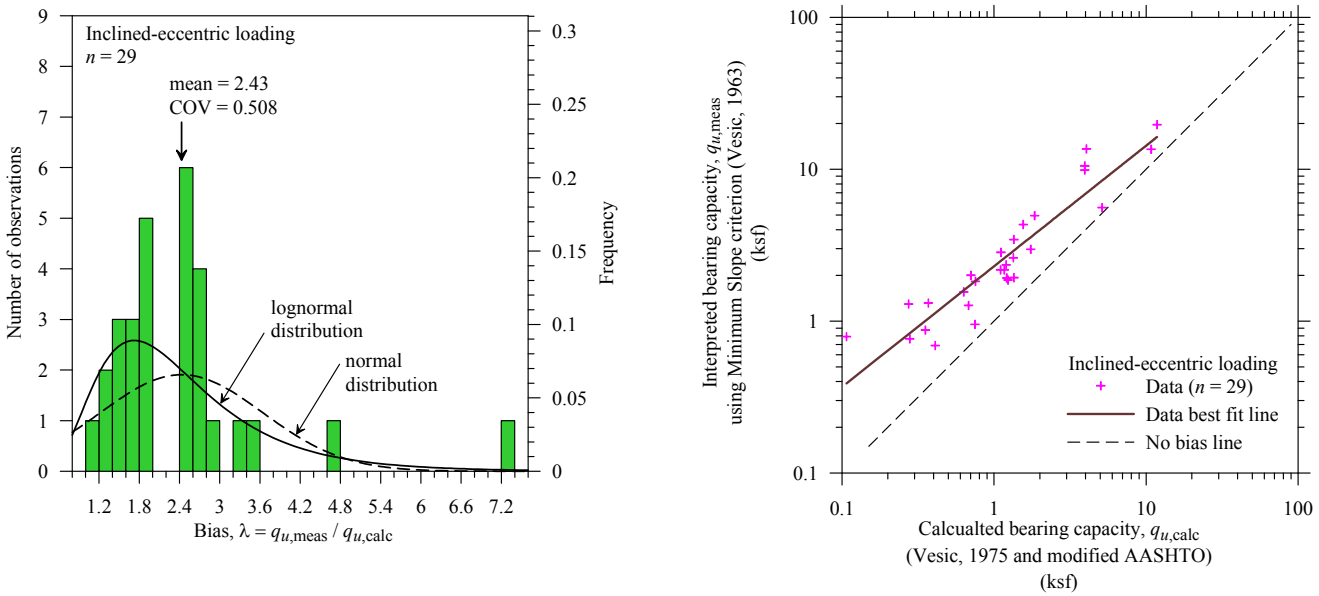

Figure 9. Histogram and probability density function of the bias (a) and relationship between measured and calculated bearing capacity (b) for all footings subjected to inclined-eccentric loading

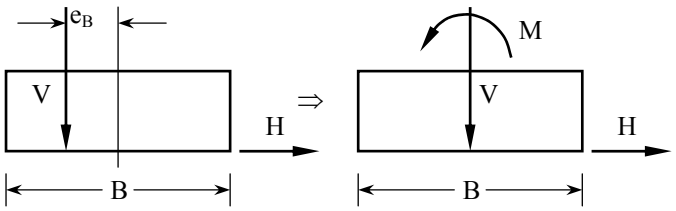

Moment acting in direction opposite to the lateral loading – negative eccentricity

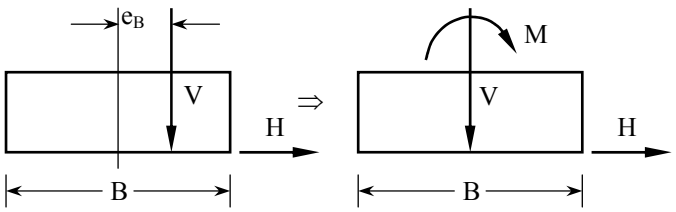

Moment acting in the same direction as the lateral loading – positive eccentricity

Figure 10. Loading directions for the case of inclined-eccentric loadings

Figures 11 and 12 show a significant difference in the bias when the different loading directions are considered. For cases with a negative eccentricity the mean bias is 3.43 compared to a mean bias of 2.16 for the cases with positive eccentricity. The results suggest that the loading direction needs to be considered in the evaluation of the resistance factors. It should, however, be noticed that the effect is less pronounced when the vertical load is relatively high, i.e. the load inclination is relatively small. Lesny (2001) demonstrated that for a vertical load level equal or greater than 0.3 the effect of the loading direction is negligible. The vertical load level is defined as the ratio of the vertical load to the vertical failure load under vertical-centric loading. While the findings clearly demonstrate an important physical effect, the practical ramification of this finding is yet to be investigated.

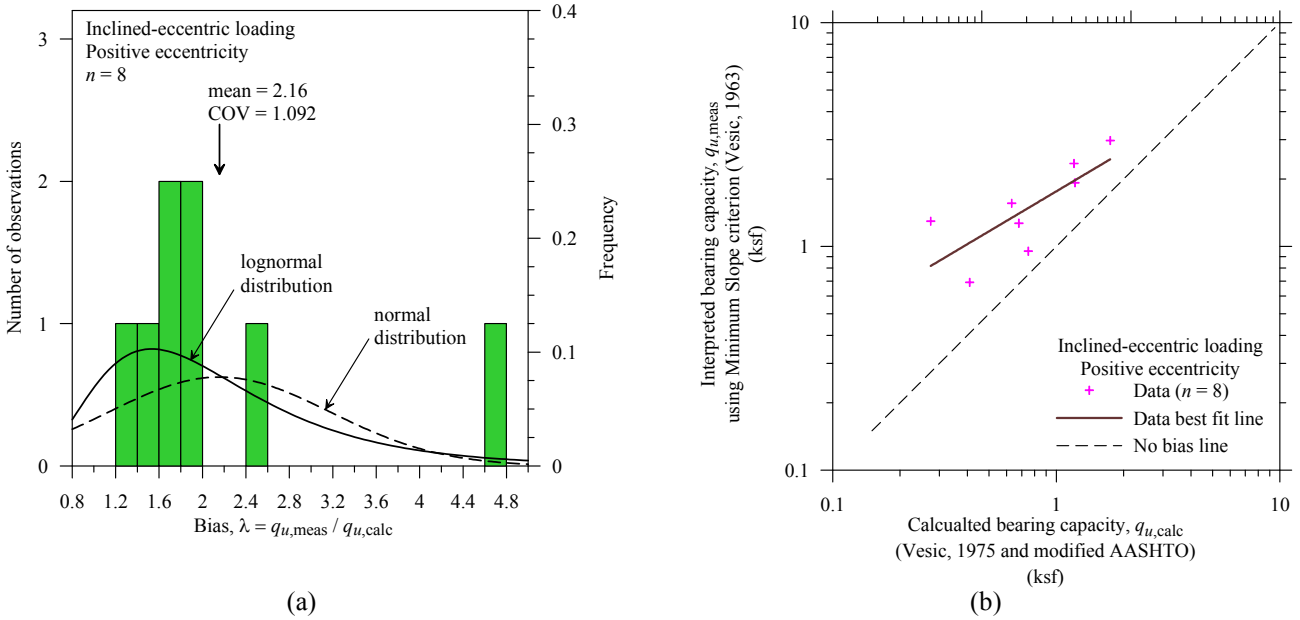

Figure 11. Histogram and probability density function of the bias (a) and relationship between measured and calculated bearing capacity (b) for footings subjected to inclined-eccentric loading with a positive eccentricity

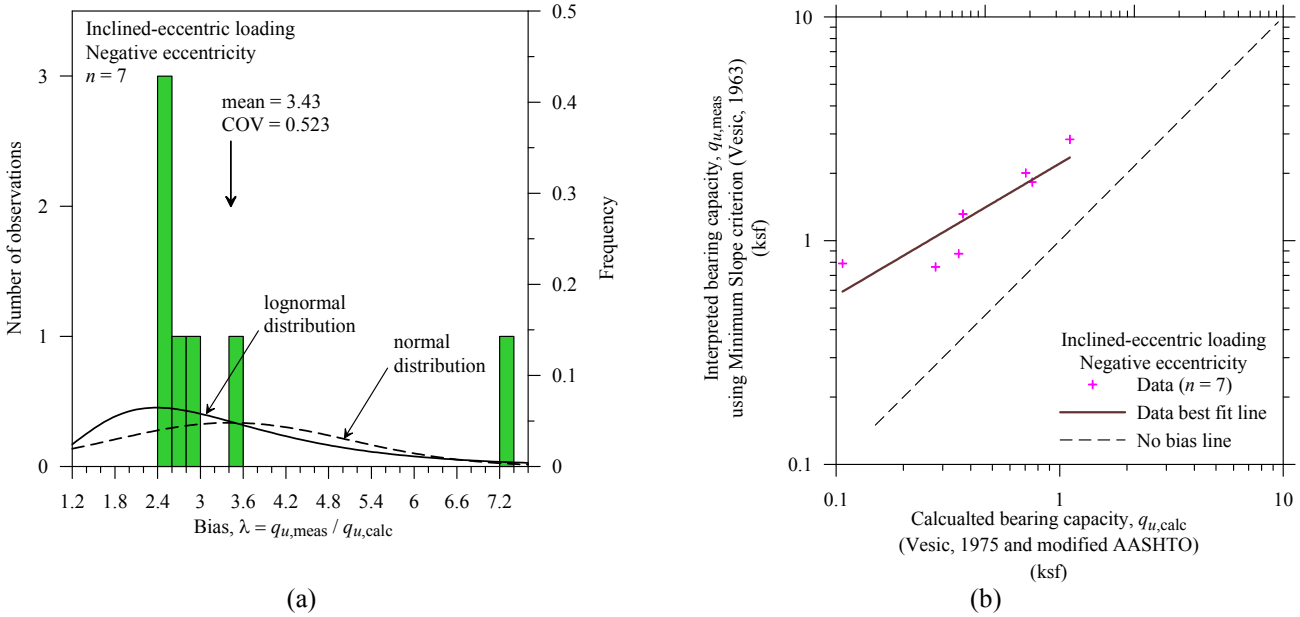

Figure 12. Histogram and probability density function of the bias (a) and relationship between measured and calculated bearing capacity (b) for all footings subjected to inclined-eccentric loading with a negative eccentricity

6 DERIVATION OF RESISTANCE FACTORS

6.1 *Probabilistic analysis procedures*

The partial factors used in the LRFD are derived in this research using so-called Level 2 approaches in which the uncertainties of the design variables are expressed by their mean, standard deviation and/or coefficient of variation. The limit state of the foundation is evaluated by using the First Order Second Moment (FOSM) method as an approximate iterative procedure as well as the more accurate Monte Carlo Simulation (MCS) procedure.

According to the FOSM as originally proposed by Cornell (1969) the mean and the variance of a limit state function $g(\bullet)$ are defined as:

mean: $$m_g \approx g(m_1, m_2, m_3, ..., m_n) \quad (11a)$$

variance: $$\sigma_g^2 \approx \sum_{i=1}^{n} \left(\frac{\partial g}{\partial x_i} \right)^2 \bullet \sigma_i^2 \quad (11b)$$

In Eq. (11) m_i and σ_i are the means and the standard deviations of the basic variables (design parameters) x_i.

The FOSM was later used by Barker et al. (1991) to develop closed form solutions for the calibration of geotechnical resistance factors ϕ that appear in previous AASHTO LRFD specifications:

$$\phi = \frac{\lambda_R \left(\sum \gamma_i \cdot Q_i \right) \cdot \sqrt{\frac{1 + COV_Q^2}{1 + COV_R^2}}}{m_Q \cdot \exp\left\{ \beta \cdot \sqrt{\ln\left[\left(1 + COV_R^2\right) \cdot \left(1 + COV_Q^2\right) \right]} \right\}} \quad (12)$$

In Eq. (12) Q_i are the loads, λ_R is the resistance bias factor defined as the mean ratio of measured resistance over calculated resistance, m_Q is the mean of the loads, COV_R and COV_Q are the coefficients of variation of the resistance and the load, respectively, γ_i are the load factors and β is the target reliability index.

The approach adopted in this research differs from the original Level 2 approach as the load factors and related uncertainties used in the analysis are previously selected (see section 2) and then utilized to determine the resistance factors for a given target reliability index and a given range of loads.

MCS involves the numerical integration of the failure probability defined as:

$$p_f = P(g \le 0) = \frac{1}{N} \cdot \sum_{i=1}^{n} I[g \le 0] \quad (13)$$

In Eq. (13) I is an indicator function which is equal to 1 for $g_i \le 0$, i.e., when the resulting limit state is exceeded (failure), and equal to 0 for $g_i > 0$ when the limit state is not exceeded. N is the number of simulations carried out.

In order to evaluate equation (13) the basic variables and their distributions first need to be defined. Then N random samples for each design variable based on their distributions, i.e. using the statistics of loads and resistances, are generated. The limit state function is evaluated N times taking a set of the design values previously generated and the number N_f is counted for which the indicator function is equal to 1, i.e. failure occurred. The failure probability is finally obtained as the ratio N_f/N.

The resistance factor based on the MCS can be calculated using the fact that to attain a target failure probability p_{fT}, the limit state must be exceeded N_{fT} times. As in the current LRFD concept only one resistance factor needs to be determined for one limit state, while keeping the load factors constant, a suitable choice of the resistance factor shifts the limit state function so that failure occurs N_{fT} times.

It has to be noticed that the results of a MCS is only as good as the determination of the distributions of loads and resistance. This means, the statistical parameters need to be defined as good as possible.

6.2 *Definition of the target reliability index*

Instead of the failure probability, the safety of a system often is expressed by the reliability index β which describes the margin of safety by the number of standard deviations of the probability density function for the limit state g, separating the mean of g from the failure zone beginning at g = 0. The reliability index is related to the failure probability by the error function Φ as given in Eq. (14).

$$p_f = \Phi(-\beta) \tag{14}$$

Accordingly, the target reliability index is the safety margin to be implemented in the design. It can be derived either from the reliability levels implicit in the current WSD codes or by a cost-benefit analysis with an optimum reliability based on minimum costs including costs of economic losses and consequences due to failure. The latter is a difficult process as especially costs related to human injuries or loss of life are hard to determine and therefore not adopted in this research.

Using a target reliability derived from WSD represents the acceptable risks in the current design practice and may therefore be an adequate starting point for a code revision. However, such reliability levels can have considerable variations as various studies have shown (e.g. Phoon and Kulhawy, 2000; Honjo and Amatya, 2005).

It seems to be logical and convenient, therefore, to assign a target reliability index for the foundations equal to that assigned for the superstructure to maintain a comparable reliability level, although the actual reliability level of the combined system of super- and substructure remains unknown. For foundations in/on granular soils a target reliability index of $\beta_T = 3$ has been selected in the probabilistic analyses.

7 RECOMMENDED RESISTANCE FACTORS

7.1 *General*

The aforementioned investigations of the bearing capacity equation vs. shallow foundations load test databases lead to the conclusion that one single resistance factor for the bearing capacity is not sufficient to address the different loading conditions leading to different levels of uncertainties. Consequently, different resistance factors were established based on the probabilistic analyses, each for vertical-centric, vertical-eccentric, inclined-centric and inclined-eccentric loading conditions. These resistance factors are valid only with the calculation methods specified previously for the respective resistances.

7.2 *Vertical-centric loading*

For vertical-centric loading the bias change with the soil's friction angle as described in section 5.2 had to be considered in developing the resistance factors. For this, subsets of the database based on the magnitude of ϕ_f were analyzed for possible outliers to improve the quality of the database and to achieve a better fit of the assumed probability distribution. In the end, only one outlier had been removed, so that 172 cases were available for the resistance factor calibration. Further on, a lognormal distribution of the bias has been defined for the whole range of ϕ_f.

The MCS calculations are based on a mean bias of:

$$\lambda_{BC} = 0.398 \exp(0.0372 \cdot \phi_f) \tag{15}$$

with a COV_λ of 0.25 for controlled soil conditions and 0.35 for natural soil conditions. From the results of the calculations the resistance factors presented in Table 8 finally have been recommended specified for natural soil conditions and controlled soil conditions. The values are valid for soils with a relative density of 35% and greater.

For loose soils with a smaller relative density and friction angles less than 30° it is recommended to consider either ground improvement or ground replacement in the zone of influence beneath the footing or to choose an alternative foundation.

Table 8. Recommended resistance factors for vertical-centric loading

Soil friction angle [°]	Recommended resistance factor ϕ (β_T = 3)	
	natural soil conditions	controlled soil conditions
30 – 34	0.40	0.50
35 – 36	0.45	0.60
37 – 39	0.50	0.70
40 – 44	0.55	0.75
≥ 45	0.65	0.80

7.3 *Vertical-eccentric loading*

Analysis of the cases under vertical-eccentric loading revealed that a clear unique correlation between the bearing capacity bias and the soil's friction angle as in case of vertical-centric loading does not exist (see Figure 13). Derivation of resistance factors depending on the soil friction angle assuming a lognormal distribution of the bias lead to values around 1.0 and are far greater than the values presented in Table 8. This is not consistent as the uncertainties involved with vertical-eccentric loading should not be less than those with vertical-centric loading. Further analysis indicated that the footing size affects the bearing capacity bias, too, but with the available data it was not possible to isolate the effects of the footing size from the effect of the soil friction angle. Thus, it seems to be justified and appropriate to extend the dataset for vertical-eccentric loading by the dataset for vertical-centric loading for deriving the resistance factors because (i) when the source of the lateral load is not permanent, the foundation supports vertical-centric loading in some situations, and (ii) very often the magnitude of the lateral load and with that the eccentricity is not known in the design phase of the bridge foundation.

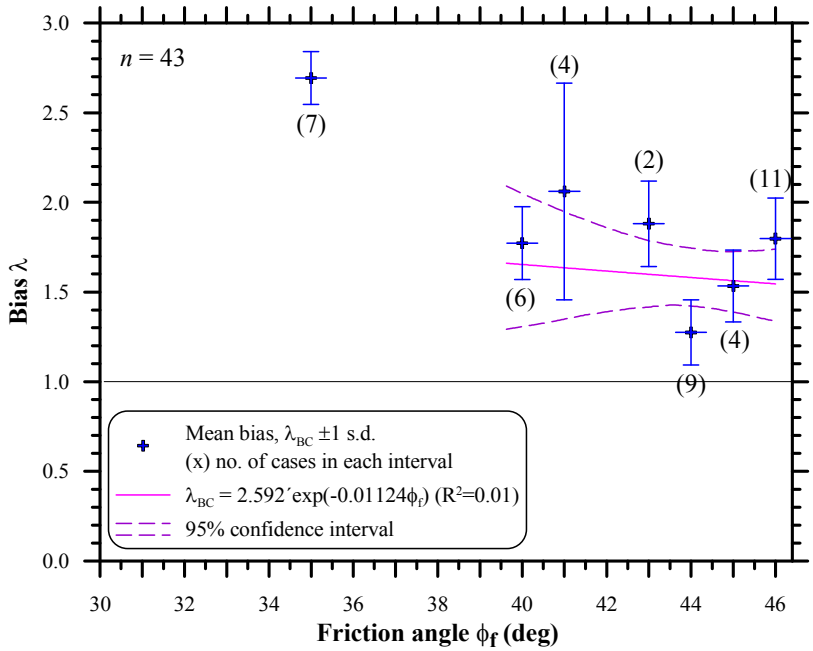

Figure 13. Bias of the bearing capacity prediction versus soil friction angle for footings under vertical-eccentric loading (seven cases for ϕ_f = 35° have been ignored as outliers for obtaining the best fit line)

As a result of the above, the same resistance factors used for vertical-centric loading and presented in Table 8 are recommended for vertical-eccentric loading, too. These are verified by resistance factors obtained on the basis of Figure 13 with a constant mean bias of 1.60 for friction angles between 40° and 46° and a COV for natural and controlled soil conditions of 0.35 and 0.30, respectively:

Natural soil conditions, for all ϕ_f: ϕ = 0.65 (from MCS: ϕ = 0.687)
Controlled soil conditions, for all ϕ_f: ϕ = 0.75 (from MCS: ϕ = 0.796)

7.4 *Inclined-centric loading*

For footings under inclined-centric loading no clear trend of the bias associated to the load inclination and the orientation of the horizontal load or the footing size exists. Thus, the resistance factors again have been obtained based on the variation of the bearing capacity bias on the soil friction angle:

$$\lambda_{BC} = 1.25 + 0.0041 \cdot \phi_f \qquad (16)$$

Eq. (16) has been derived as a best-fit line from an evaluation of the bearing capacity bias versus the soil friction angle. A COV of 0.35 has been adopted for controlled soil conditions and a COV of 0.40 for natural soil conditions. The resistance factors resulting from the MCS calculations needed to be adjusted to guarantee a safe design. Table 9 summarizes the finally recommended resistance factors.

Table 9. Recommended resistance factors for inclined-centric loading

Soil friction angle [°]	Recommended resistance factor ϕ (β_T = 3)	
	natural soil conditions	controlled soil conditions
30 – 34	0.40	0.40
35 – 36	0.40	0.40
37 – 39	0.40	0.45
40 – 44	0.45	0.50
≥ 45	0.50	0.55

7.5 *Inclined-eccentric loading*

Due to the limited available datasets resistance factors for inclined-eccentric loading can only be given as guidance. For a positive loading eccentricity as indicated in Figure 10 (bottom) the probabilistic analysis results in a resistance factor of $\phi = 0.55$ for all eight investigated cases with $44.5° \leq \phi_f \leq 45°$. For a negative loading eccentricity according to Figure 10 (top) the analysis lead to a resistance factor of $\phi = 0.85$ for all seven cases with $44.5° \leq \phi_f \leq 45°$. On this basis the resistance factors presented in Table 10 are recommended.

Table 10. Recommended resistance factors for inclined-eccentric loading

Soil friction angle [°]	Recommended resistance factor ϕ (β_T = 3)			
	natural soil conditions		controlled soil conditions	
	positive	negative	positive	negative
30 – 34	0.35	0.65	0.40	0.70
35 – 36	0.35	0.70	0.40	0.70
37 – 39	0.40	0.70	0.45	0.75
40 – 44	0.40	0.75	0.50	0.80
≥ 45	0.45	0.75	0.50	0.80

8 CONCLUSIONS

The resistance factors recommended in this research are soundly based on the quantified uncertainties of the design methods and follow the parameters that control them. These parameters present a radical change to the existing design specifications for bridge foundations as the bearing capacity of shallow foundations on granular soils is calibrated according to the soil placement (natural vs. controlled conditions) and the magnitude of the angle of internal friction. Further, all possible loading conditions were calibrated, namely vertical-centric, vertical-eccentric, inclined-centric and inclined-eccentric.

The implementation of the developed LRFD procedure is expected to provide a safe design of shallow foundations with a consistent level of reliability for the different design conditions.

The application of these findings in the design of shallow foundations needs, however, to be implemented in the context of a total design including all limit states, especially the serviceability limit state.

ACKNOWLEDGEMENTS

The material presented in this paper is based on a research supported by the National Cooperative Highway Research Program (NCHRP) project 24-31 under a contract with Geosciences Testing and Research Inc. (GTR). NCHRP Report 651 provides a summary of the study. The participants and contributors in this research are greatly acknowledged, specifically Dr. Shailendra Amatya and Mr. Robert Muganga working at the UML Geotechnical Engineering Research Laboratory, Dr. Aloys Kisse working at the University of Duisburg – Essen, and Ms. Mary Canniff of Geosciences Testing and Research. Also are acknowledged Ms. Yu Fu and Mr. Jenia Nemirovsky who participated in the initial establishment of UML-GTR ShalFound07 database working at the Geotechnical Engineering Research Laboratory of the University of Massachusetts Lowell.

REFERENCES

AASHTO 2007. LRFD Bridge Design Specifications Section 10: Foundations, American Association of State Highway & Transportation Officials, Washington, DC.

AASHTO 2008. LRFD Bridge Design Specifications Section 10: Foundations, American Association of State Highway & Transportation Officials, Washington, DC.

Brinch Hansen, J. 1970. A Revised and Extend Formula for Bearing Capacity, Akademiet for de Tekniske Videnskaber, Geoteknisk Institut, Bullentin No.28, Copenhagen, pp.5-11.

De Beer, E.E. 1967 Proefondervindelijke bijdrage tot de studie van het gransdragvermogen van zand onder funderingen op staal; Bepaling von der vormfactor sb, Annales des Travaux Plublics de Belgique, 68, No.6, pp.481-506; 69, No.1, pp.41-88; No.4, pp.321-360; No.5, pp.395-442; No.6, pp.495-522.

DIN EN 1997-1 2009. Entwurf, Berechnung und Bemessung in der Geotechnik – Teil 1: Allgemeine Regeln. , German version of EN 1997-1:2004. Normenausschuss Bauwesen im Deutschen Institut für Normung. Beuth Verlag, Berlin.

Gottardi, G. 1992. Modellazione del comportamento di fondazoni superficiali su sabbia soggette a diverse condizioni di carico, Dottorato di ricerca in ingegneria geotecnica, Instituto di Costruzioni Marittime e di Geotecnica, Universita di Padova

Nowak, A. 1999. NCHRP Report 368: Calibration of LRFD Bridge Design Code. National Cooperative Highway Research Program, TRB, Washington, DC.

Kimmerling, R.E. 2002. Geotechnical Engineering Circular No. 6 Shallow Foundations, FHWA Report no. FHWA-IF-02-054, Washington, DC, 310pp.

Kulhawy, F. and Mayne, P. 1990. Manual on Estimation of Soil Properties for Foundation Design, Report EPRI-EL-6800, Electric Power Research Institute, Palo Alto, CA

Lesny, K. 2001. Entwicklung eines konsistenten Versagensmodells zum Nachweis der Standsicherheit flachgegruendeter Fundamente. Mitteilungen aus dem Fachgebiet Grundbau und Bodenmechanik der Universität Essen, Heft 27, Hrsg.: Prof. Dr.-Ing. W. Richwien, Verlag Glueckauf, Essen, in German.

Montrasio, L. 1994. Un Metodo per il calcolo die cedimenti di fondazioni su sabbia soggette a carichi eccentrici e inclinati, Dottorato di ricerca in Ingegneria Geotecnica, Universita di Milano (in Italian).

NAVFAC. 1986. Foundation and Earth Structures, Design Manual DM7.02, Naval Facilities Engineering Command, Alexandria, Virginia

Paikowsky, S.G. with contributions by Birgission G., McVay M., Nguyen T., Kuo C., Baecher G., Ayyub B., Stenerson K., O'Mally K., Chernauskas L., and O'Neill M. 2004. NCHRP Report 507 Load and Resistance Factor Design (LRFD) for Deep Foundations, National Cooperative Highway Research Program report for Project NCHRP 24-17, TRB, Washington, DC, 2004, pp. 134 (not including Appendices), http://onlinepubs.trb.org/onlinepubs/nchrp/nchrp_rpt_507.pdf

Paikowsky, S.G., Lesny, K., Amatya, S., Kisse, A., Muganga, R. and Canniff, M. 2010. NCHRP Report 651 LRFD Design and Construction of Shallow Foundations for Highway Bridge Structures, National Cooperative Highway Research Program Report for Project NCHRP 24-31, TRB, Washington, DC, June 2010, pp. 139 excluding appendices. http://onlinepubs.trb.org/onlinepubs/nchrp/nchrp_rpt_651.pdf

Paikowsky, S.G., Player, C.M. and Connors, P.J. 1995. A dual interface apparatus for testing unrestricted friction of soil along solid surfaces, Geotechnical Testing Journals, GTJODJ, Vol.18(2), pp.168-193

Perau, E. 1995. Ein systematischer Ansatz zur Berechnung des Grundbruchwiderstands von Fundamenten. Mitteilungen aus dem Fachgebiet Grundbau und Bodenmechanik der Universität Essen, Heft 19, Hrsg.: Prof. Dr.-Ing. W. Richwien, Essen: Glückauf-Verlag

Prandtl, L. 1921. Ueber die Eindringfestigkeit (Haerte) plastischer Baustoffe und die Festigkeit von Schneiden. Zeitschrift für angewandte Mathematik und Mechanik 1, Band 1, pp.15-20.

Reissner, H. 1924. Zum Erddruckproblem, Proc., 1st Int. Congress of Applied Mechanics, Delft, pp.295-311.

Teixeira, A., Gomes Correia, A., Honjo, Y., and Henriques, A. 2011. Reliability analysis of a pile foundation in a residual soil: contribution of the uncertainties involved and partial factors, to be published in the 3rd Intl. Symposium on Geotechnical Safety and Risk (ISGSR2011), 2-3, June, Munich, Germany.

Vesić, A. 1963 Bearing capacity of deep foundations in sand, Highway Research Record, 39, National Academy of Sciences, National Research Council, pp.112-153

Vesić, A. 1975. Bearing Capacity of Shallow Foundations, Foundation Engineering Handbook (eds. H.F. Winterkorn and H.Y. Fang), Van Nostrand Reinhold, New York, pp.121-147.
Weiß, K. 1978. 50 Jahre Deutsche Forschungsgesellschaft für Bodenmechanik (Degebo). Mitteilungen der Deutschen Forschungsgesellschaft für Bodenmechanik (Degebo) an der Technischen Universität Berlin, Heft 33.

ISGSR 2011 - Vogt, Schuppener, Straub & Bräu (eds) - © 2011 Bundesanstalt für Wasserbau ISBN 978-3-939230-01-4

Safety Standards of Flood Defenses

J.K. Vrijling
Delft University of Technology, Delft, The Netherlands

T. Schweckendiek
Delft University of Technology & Deltares, Delft, The Netherlands

W. Kanning
Delft University of Technology, Delft, the Netherlands

ABSTRACT: Current design codes like the Eurocode use safety or reliability classes to assign target reliabilities to different types of structures or structural members according to the potential consequences of failure. That, in essence, is a risk-based criterion. A wide range of structures is designed with such codes, and distinction is made between reliability classes. These reliability classes are not necessarily well suited for flood defense systems, neither are the design rules and partial safety factors, which are calibrated for a wide range of standard applications. For a flood defense system protecting a large area from flooding, on the other hand, it is worthwhile to base the design and safety assessment standards on a risk assessment - a tailor-made solution. The investments can be considerable and the stakes are high, especially for low-lying delta areas, where the consequences of flooding can be devastating. In order to answer the question "How safe is safe enough?" a framework for acceptable risk is required. Subsequently, from acceptable risk we can deduce target reliabilities for the protection system as a whole as well as for its elements. For practical application, these target reliabilities can then be translated into design and assessment rules; for example, using LRFD (load and resistance factor design) to derive partial safety factors.

This paper describes how to define safety standards for flood defenses, in particular dikes, step-by-step. An important aspect in translating high-level requirements into specific (low-level) design rules that apply to specific failure modes for specific flood protection elements is the so-called "length-effect". This is especially relevant for long-linear structures like dikes, where usually the length is much larger than the scale of fluctuation of dominant load or resistance properties. The longer the structure, the higher the chance to encounter either and extreme load or a weak spot (i.e., low resistance) – hence the word "length-effect". The effect is that the probability of failure increases with the length of the dike. The implication for design and assessment rules is that the reliability requirements to a cross section ("zero length") need to be stricter (i.e., higher target reliability) than for the whole reach.

This paper attempts to demonstrate how tailor-made safety standards for large scale flood defense systems can be derived in a risk-based fashion. Since flood defenses differ from smaller scale geotechnical structures in many aspects and given the volume of investments in such large-scale engineering systems, it is very attractive to deviate from the standard design codes. That is not deviating conceptually, but rather deriving safety factors for the specific application to better account for the characteristics and uncertainties involved. The authors strive to show that safety levels and partial safety factors in the presented approach are far from arbitrary. They are part of an overall consistent flood risk framework, a framework that provides a link between geotechnical engineers and other disciplines involved in providing safety from flooding.

Keywords: flood defenses, acceptable risk, uncertainties, probability of failure, length-effect, LRFD

1 INTRODUCTION

Current design codes like Eurocode use safety or reliability classes to assign target reliabilities to different types of structures or structural members according to the potential consequences of failure. That, in essence, is a risk-based criterion. Also the design life plays a role in assigning target reliabilities. Due to

the wide range of structures design with such codes, a differentiation with, for example, three reliability classes makes sense. Because it is not (yet) realistic to design each structure using risk-assessment techniques. For a flood defense system protecting a large area from flooding, on the other hand, it is worthwhile to base the design and safety assessment standards on a risk assessment. The investments can be considerable and the stakes are high, especially for low-lying delta areas, where the consequences of flooding can be devastating. Therefore, tailor-made solutions become much more attractive.
The basic underlying question is "How safe is safe enough?". In order to answer that question a framework for acceptable risk is required. Having established acceptable risk we can deduce a target reliabilities for the protection system as well as for its elements. For practical application, these target reliabilities can then be translated into design and assessment rules; for example, using LRFD (load and resistance factor design) to derive partial safety factors.

This paper describes how to define safety standards for flood defenses, in particular dikes, step-by-step. The first step is to define what is socially acceptable. To this end, often is relied on fatality risk criteria, the risk of individuals of dying due to flooding or the number of expected fatalities. Next, economic considerations play a role, in which the cost of flood protection is weighed against the risk-reduction achieved by improved protection. These criteria allow decision makers to decide on protection standards in form of target reliabilities.

Such target reliabilities are high-level requirements in a sense that they are expressed in terms of the acceptable probability of failure of the flood protection (sub)system under consideration. In order to ensure the protection level of the (sub)system its elements need to be designed with higher target reliabilities. That is because typically flood defenses are linear defenses, in which failure of any element leads to system failure; a dike breach anywhere leads to flooding. From a system reliability point of view, flood defense system are serial systems where the probability of failure is dominated by the weakest links. In fact, the same holds for the different failure mechanisms; any mechanism may cause failure of an element (e.g., dike section).

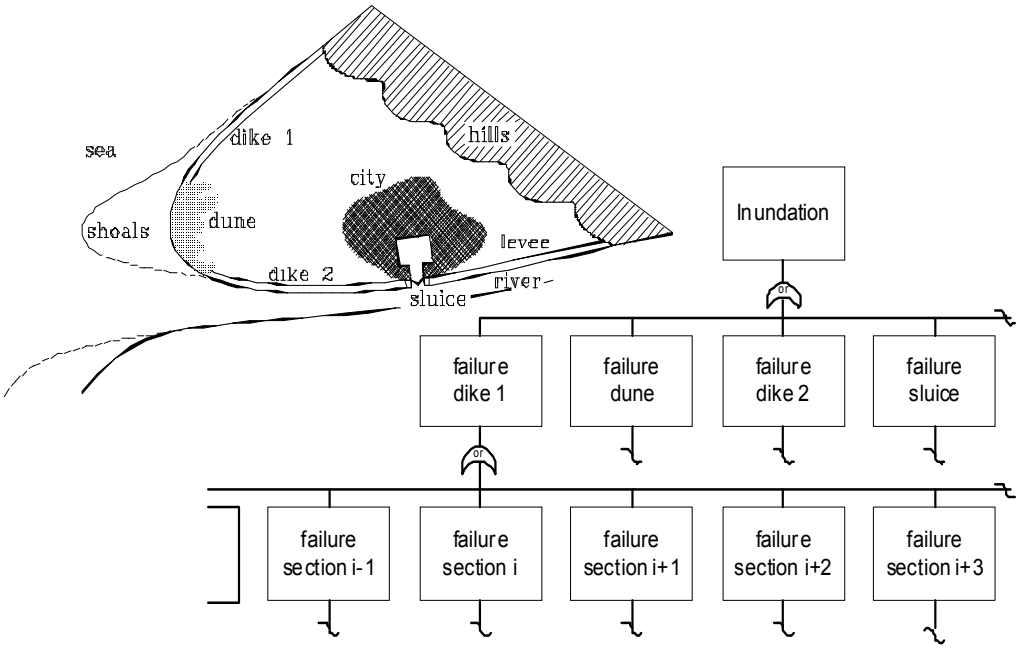

Figure 1. Schematic Overview of a Flood Defense System and its Elements

An important aspect in translating high-level requirements into specific (low-level) design rules that apply to specific failure modes for specific flood protection elements is the so-called "length-effect". This is especially relevant for long-linear structures like dikes, where usually the length is much larger than the scale of fluctuation of dominant load or resistance properties. The longer the structure, the higher the chance to encounter either and extreme load or a weak spot (i.e., low resistance) – hence the word "length-effect". The effect is that the probability of failure increases with the length of the dike. The implication for design and assessment rules is that the reliability requirements to a cross section ("zero length") need to be stricter (i.e., higher target reliability) than for the whole reach.

The organization of this paper follows the top-down structure as described above, from high-level to low level requirements. Section 2 addresses the acceptable risk criteria, followed by an inventory of the failure mechanisms considered in dike design in section 3, enriched by failure observations from New Orleans with Hurricane Katrina (2005). The length-effect is discussed and illustrated in section 4. Section 5 describes the steps from acceptable risk to design rules and partial safety factors. The paper finishes with a discussion in section 6.

2 ACCEPTABLE FLOOD RISK

2.1 *Acceptable Risk Framework*

Protection of individuals and groups against natural and man-made hazards is a task of human civilizations. Historically, most protection efforts were realized after major disasters, the consequences still being very much present in the collective memory. Modern risk-based approaches aim to enable preventive protection by identifying risks, before they manifest themselves as disasters. Risk is defined as the probability of an (unwanted) event times the consequences involved. Expressing them (amongst others) in monetary terms and fatalities is a means to enable weighing investments in prevention against the benefits of risk reduction.

The estimation of the consequences of flooding is a central element in flood risk analysis and management. The totality of flood damage comprises casualties, material and economic damage as well as the loss of or harm to immaterial values like works of art and amenity. However, for practical reasons the notion of risk in a societal context is often reduced to the total number of casualties using a definition as: "the relation between frequency and the number of people suffering from a specified level of harm in a given population from the realization of specified hazards". If the specified level of harm is limited to loss of life, the societal risk may be modeled by the frequency of exceedance curve of the number of deaths, also called the FN-curve (see 2.3).

The consequence part of a risk can also be limited to the material damage expressed in monetary terms. It should be noted however, that the reduction of the consequences either measure may not adequately model the public's perception of the potential loss. The simplification clarifies the reasoning at the cost of accuracy. Nevertheless, for practical tractability, three criteria are defined and used in the following:

1 individual risk
2 group risk
3 economical risk

The first two are belong to the category of “loss of life” criteria, which are often considered as boundary conditions providing minimum protection level. While individual risk refers to the probability of dying of an individual person in a specific location, group risk refers to large numbers of fatalities in one event. Economical risk refers to the direct and indirect economical consequences of a disaster, allowing for a direct comparison of investments in and effects of prevention in monetary terms. Both, group risk and economical risk are considered societal risk criteria, because they are usually applied (i.e., aggregated) on a national scale.

2.2 *Individual Risk*

Individual risk is defined as the probability of an individual residing in a given area to die as a consequence of flooding. This probability includes the nature of the hazard (i.e., probabilities of discharge, water level, wind, waves etc.), the effectiveness of the flood protection system (e.g., probability of a dike breach) and the conditional flood characteristics (e.g., water depth, flow velocity). Jonkman (2007) discusses loss of life related to flooding extensively. Individual risk is typically represented in risk maps; an example is given in Figure 2.

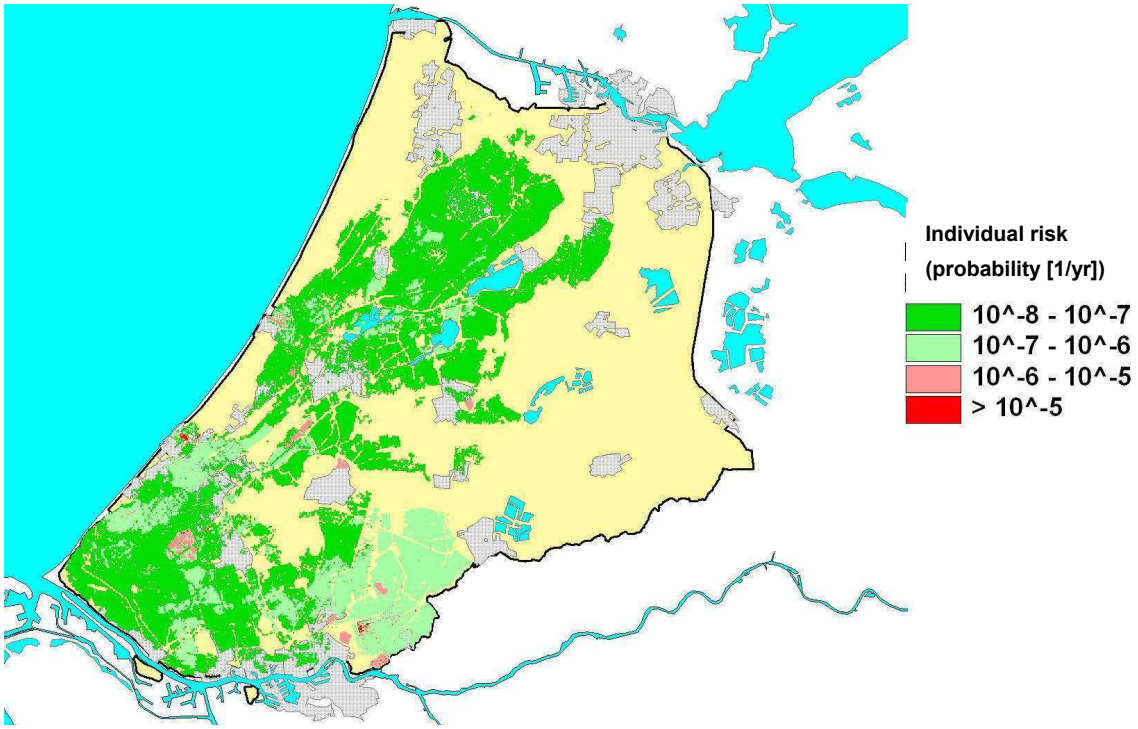

Figure 2. Individual Risk Central Holland, probability of dying to flooding [1/yr] (Jonkman, 2007)

Being able to determine individual risks with flood risk analysis, the question remains what is acceptable. The same question plays a role for many other hazards, especially in external safety (e.g., transport and storage of hazardous goods, chemical plants etc. An indicative figure for acceptable individual risk used in many applications is 10^{-6} per year (e.g. Lerche et. al, 2006).

One method to determine such acceptance limits to using revealed preferences (Vrijling et. al, 1993). That is done by analyzing accident statistics and differentiating between the activities during which persons lost their lives. The fact, that the actual personal risk levels connected to various activities show statistical stability over the years and are approximately equal for the Western countries, indicates a consistent pattern of preferences. The probability of losing one's life in normal daily activities such as driving a car or working in a factory appears to be one or two orders of magnitude lower than the overall probability of dying. Only a purely voluntary activity such as mountaineering entails a higher risk (Figure 3).

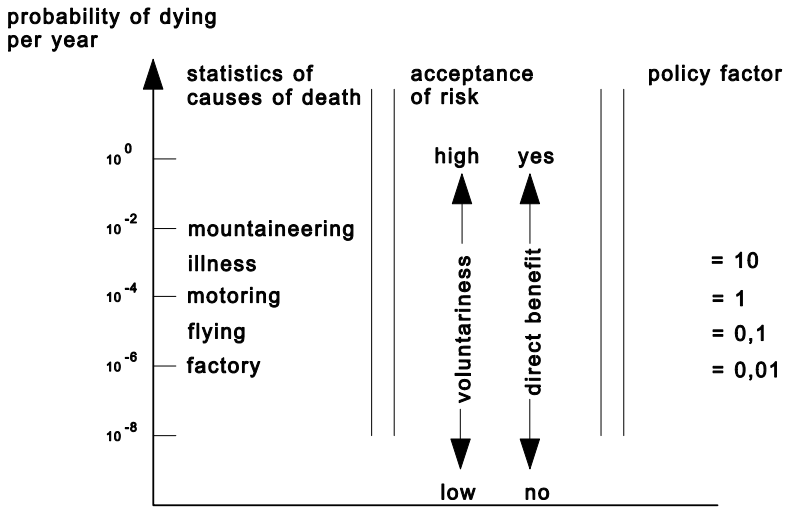

Figure 3. Personal risks in Western countries, deduced from the statistics of causes of death and the number of participants per activity (Vrijling et. al, 1993)

Apart from a slightly decreasing trend of the death risks presented, probably due to technical progress, it seems appropriate to use revealed preferences as a basis for decisions with regard to the personally acceptable probability of an accident (failure) P_{fi} in the following way:

$$P_{fi} = \frac{\beta_i \cdot 10^{-4}}{P_{d|fi}} \qquad (1)$$

where $P_{d|fi}$ denotes the probability of being killed in the event of an accident. In this expression the policy factor β_i varies with the degree of voluntariness with which an activity i is undertaken and with the benefit perceived. It ranges from 100 in the case of complete freedom of choice like mountaineering to 0.01 in case of an imposed risk without any perceived direct benefit (such a large range was already noted in 1969 by Starr). The latter is also applied as individual risk criterion for hazardous installation nears housing areas without any direct benefit to the inhabitants. A proposal for the choice of the value of the policy factor β_i as a function of voluntariness and benefit is given in the table below. For the flood defenses a β_i-value of 1.0 to 0.1 seems appropriate.

Table 1. The value of the policy factor β_i as a function of voluntariness and benefit (Vrijling et. al, 1993)

policy factor β_i	voluntariness	direct benefit	example
100	voluntary	direct benefit	mountaineering
10	voluntary	direct benefit	motor biking
1.0	neutral	direct benefit	car driving
0.1	involuntary	some benefit	factory
0.01	involuntary	no benefit	LPG-station

2.3 *Group Risk*

Another perspective on loss of life besides individual risk is the total number of people that would drown in one flood event. Considering impact on society, single events with large numbers of fatalities (e.g., a place crash with 200 casualties) are less acceptable than large numbers of accidents with small number of fatalities (e.g., 100 car accidents with 2 casualties each). Thus, with group risk the so called risk-averseness (Bernoulli, 1783) enters the assessment.

Since a flood-protected area can inundate due to breaches at various locations and in different scenarios, an FN-curve is an appropriate way to represent this type of risk. As an example the FN-curve of the Brielse polder area in the Netherlands is shown in Figure 4.

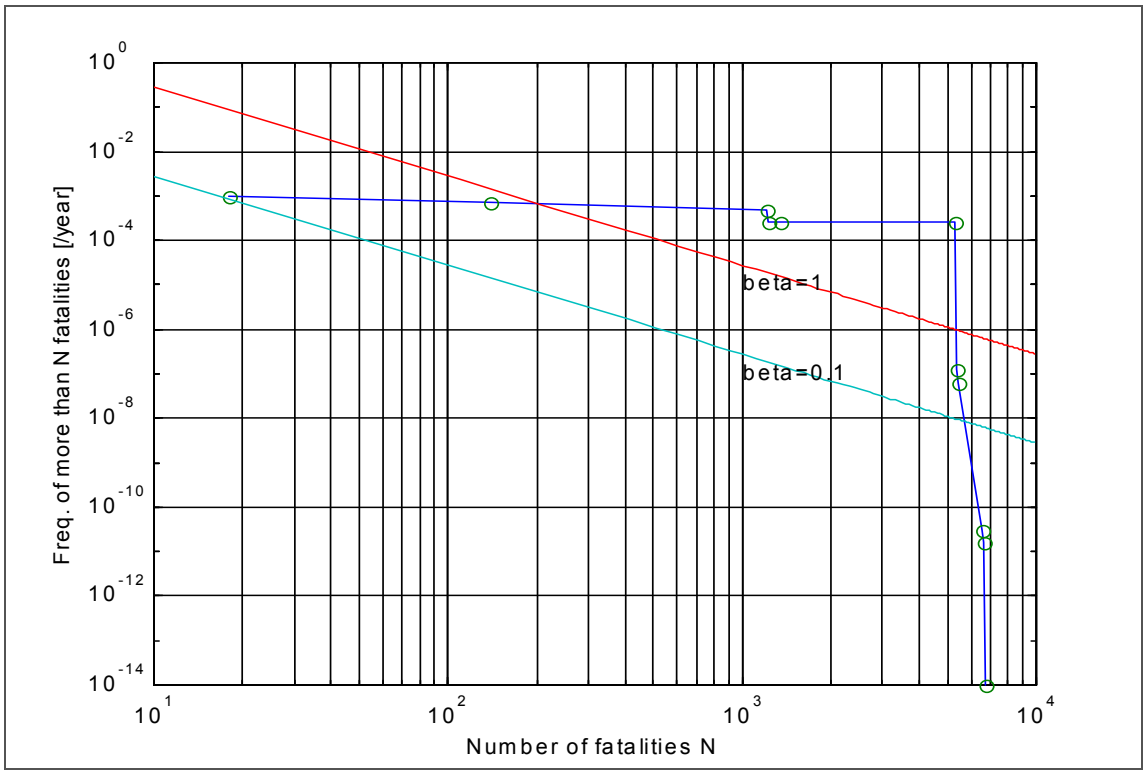

Figure 4. FN-curve for Flooding of the Brielse Polder (NL)

An FN-curve plots the number of expected fatalities per flood scenario over its corresponding occurrence probability. The FN-curve is the description of the current situation or a future scenario and, as for the individual risk, an acceptance criterion is needed. Jonkman (2007) discusses such criteria in detail.

2.4 *Economic Optimization*

While the loss of life-related acceptance criteria discussed above aim to define minimum safety criteria, from an economic point of view an optimal protection standard can be found by balancing the cost of protection against the benefit of risk reduction. In other words, the economically optimal probability of failure $P_{f,opt}$ is the one, for which the (marginal) investment I in a safer flood defense system is equals the (marginal) benefit by the decreasing present value of the risk.

$$\min(Q) = \min(I(P_{f,opt}) + PV(P_{f,opt}\, D)) \qquad (2)$$

where Q is the total cost, PV the present value operator and D the total damage in case of flood defense failure and subsequent flooding.

If (despite ethical objections) the value of a human life is rated at d, the amount of damage is increased by $P_{d|f}\, N_p\, d$, where N_p = number of casualties. A typical value chosen for d is the present value of the net national product per inhabitant. The advantage of taking the possible loss of lives into account in economic terms is that the safety measures are affordable in the context of the national income (see also Vrijling and Van Gelder, 2000).

Omitting the value of human life, the decision problem as formulated by the Delta Committee (van Dantzig, 1953) is given below. The investment $I(h)$ in the protective dike system is given as a function of the crest level h by:

$$I(h) = I_0 + I_1(h - h_0) \qquad (3)$$

where I_0 is the initial cost (i.e., mobilization), I_1 is the marginal cost of raising the dike and h_0 is the current dike crest level. The probability of exceedance of the crest level of the dike is approximated by a shifted exponential distribution:

$$1 - F(h) = e^{-\frac{h-A}{B}} \qquad (4)$$

where in this example the location parameter is A=1.96m and the scale parameter B=0.33m. The risk of inundation in this simplified example is equal to the probability of exceedance of the dike crest times the damage D in case of inundation.

$$Risk = e^{-\frac{(h-A)}{B}} \cdot D \qquad (5)$$

Because the risk is present every year the present value of the risk over an infinite period has is given by its present value.

$$PV(Risk) = e^{-\frac{(h-A)}{B}} \frac{D}{r} \qquad (6)$$

where r is the rate of interest. The total cost is the sum of the investment and the present value of the remaining risk that is accepted.

$$Q(h) = I_0 + I_1(h - h_0) + e^{-\frac{(h-A)}{B}} \frac{D}{r} \qquad (7)$$

Differentiating the total cost with respect to the decision variable h and equating the derivative to 0 gives a rather elegant result.

$$\frac{\partial Q(h)}{\partial h} = I_1 - \frac{1}{B} e^{-\frac{(h-A)}{B}} \frac{D}{r} = 0 \qquad (8)$$

$$P_{f,opt} = e^{-\frac{(h_{opt}-A)}{B}} = \frac{I_1 B r}{D} \qquad (9)$$

The last expression shows that the acceptable probability increases with the marginal cost of dike construction, with the standard deviation of the storm surge level B and the rate of interest. It decreases with the damage that will occur in case of an inundation.

The Delta Committee (van Dantzig, 1953) calculated an economically optimal probability of inundation for Central Holland in 1960 to be 8 10-6 per year (Figure 5).

Some approximate calculations performed by Dutch engineers in 2006 indicated a level of 10^{-3} per year for New Orleans. The city was protected against a hurricane category 3 with a return period of 30 to 100 years. The present system that was resurrected after Katrina has the same safety level.

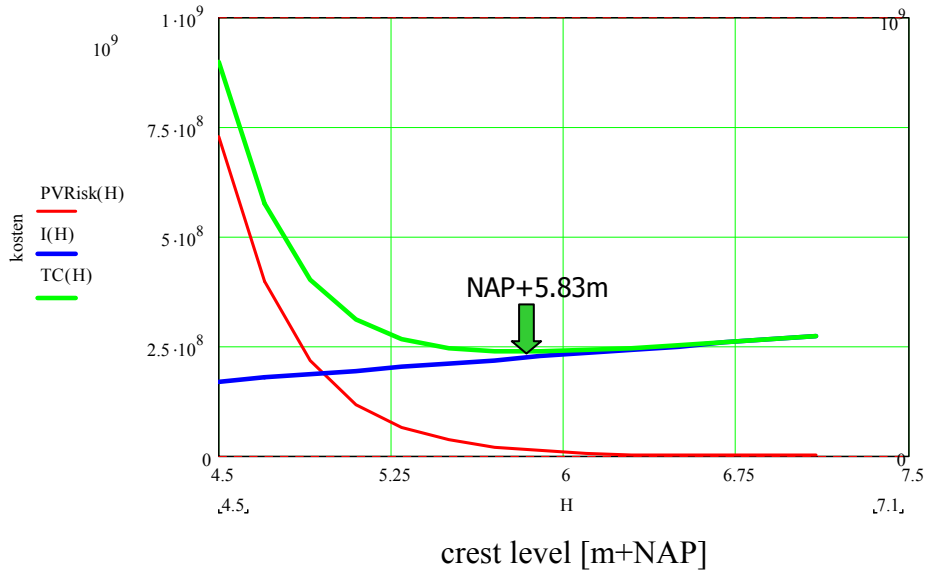

Figure 5. Example Economic Optimization: Optimal Crest Level

The economic criterion presented above should be adopted as a basis for the "technical" input to the political decision process. All information of the risk assessment should be available in the political process. It is emphasized that the decision remains a political one.

Another important remark is that in the historical approach the crest height of the dike was the main resistance parameter, as illustrated here for sake of illustration. Nowadays, such analyses are carried out, analyzing the cost to reach a certain protection level in terms of probability of failure; thus, including all kinds of failure mechanisms in addition to overtopping. The most dominant mechanisms being of geotechnical nature such as instability of the inner slope or piping.

2.5 *Summary*

For large engineering systems like flood defense systems it is worthwhile to determine taylor-made safety standards instead of relying on rather coarse consequence and reliability classes as in the Eurocode or other design codes. In order to establish appropriate target reliabilities, one needs to assess what risk is acceptable. A practical approach to this problem is to look at loss-of-life risk criteria on the one hand and at economical criteria on the other. For loss of life risks, individual risk is typically distinguished from group risk. Both give indications of desirable minimum protection standards. Economically optimal protection, on the contrary, seeks to balance investments and benefits in terms of reduced flood risk monetizing the damage. In principle, the most stringent criterion is to be applied. In other words, the highest target reliability derived from the three criteria should be adopted as target reliability of the flood protection system from a technical point of view.

The following two sections will deal with the failure mechanisms to be taken into account in designing flood defenses and how the target reliability on system level can be translated into practicable design rules for dikes.

3 FAILURE MODES AND LESSONS FROM NEW ORLEANS

While dikes in the field seem straight-forward engineered structures, their behavior can be complicated. This section deals with the physical behavior of flood defenses, especially in terms of failure mechanisms. The geotechnical aspects are very important due to the typically large uncertainties in ground conditions. Both theory and practical observations are discussed.

3.1 *Failure modes of flood defense systems*

Probabilistic design and safety assessment methods have raised the awareness, that the probability of exceedance of the design water level (or the reciprocal: the return period) is not an accurate predictor of the probability of flooding. Traditionally, the crest height is determined by such design water levels and the dike is designed according to design rules. However, other mechanisms, and certainly geotechnical ones like slope failure of piping can result in sudden failure and are poorly accounted for in design frequency approaches. More failure mechanisms than overtopping need to be accounted for, if the reliability target refers to the probability of flooding rather than the probability of a certain load condition (see Figure 6).
As a single dike is only one element, the flood defense whole system should be considered (see Figure 1), which is only as strong as its weakest link; hence, the importance of the geotechnical mechanisms and the subsoil conditions.

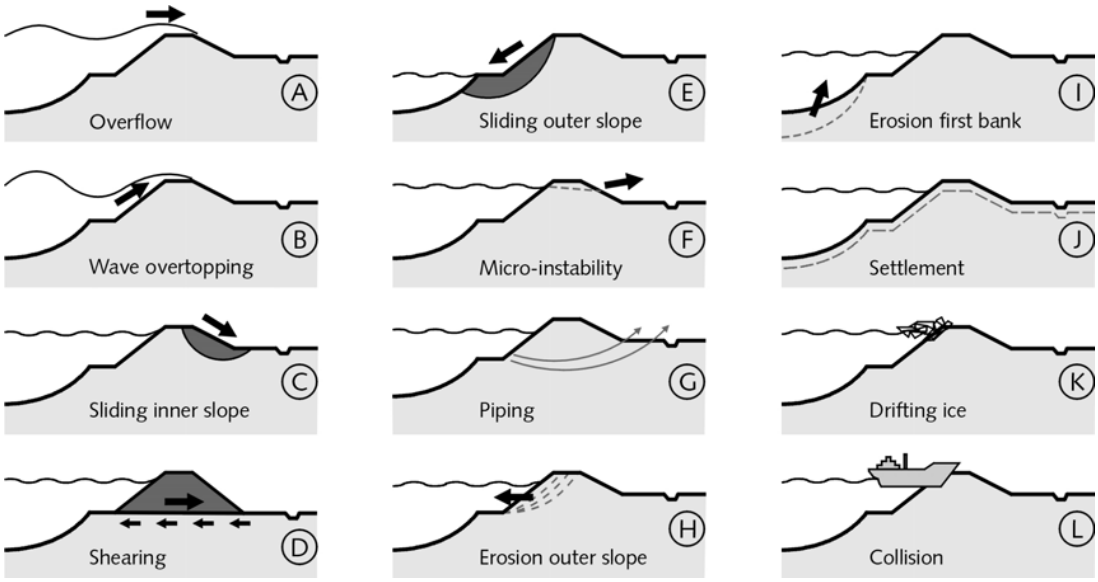

Figure 6. List of most important failure modes of dikes (TAW, 1998)

A similar list of failure mechanisms can be made for dunes and hydraulic structures, where other failure mechanisms should be added to the list, for instance structural failure of sluice doors or the failure to close movable elements.

3.2 *Relative contribution of the failure mechanisms*

The relative contribution of the different failure mechanism to the probability of system failure depends on different factors:

- The nature of the load: River dikes are generally more vulnerable for overflow, whereas sea dike are more vulnerable for overtopping. Piping and stability are time-dependent mechanisms that are more susceptible for long lasting high waters (on rivers).
- The local geology: Areas with a high occurrence of sand layers are more vulnerable for piping than areas consisting of mainly clays. Weak top layers increase the probability of sliding failure.
- The safety level: System designed for events with high safety standards tend to involve high crest levels. While the probability of overtopping may be low, the large potential head difference increases the vulnerability with respect to geotechnical mechanisms like piping.

In terms of observed failures, overtopping used to be dominant in the Netherlands in the past, together with ice-dams. Nowadays, strength related mechanisms are getting more attention and flood defense are explicitly assessed for these mechanisms. Besides, the warming of river due to excess heat from factories and power plants has minimized the risk of ice-dams.

3.3 *Experiences from New Orleans*

Hurricane Katrina caused one of the most catastrophic floods in recent history destroying large parts of the Mexican Gulf and New Orleans in August 2005. Many valuable lessons can be learned from the event

regarding flood defenses. The large amount of breaches exhibited most of the well-known failure mechanism. For a more elaborate description of the breaches it is referred to Kanning et. al (2007). An overview of the breach locations is shown in Figure 7. Generally, the breaches can be distinguished in three groups. The first group (I) is on the east side of the city where the load on the system was much higher than the design resistance. The second group (II) of failure is around the navigation channels where overtopped flood walls failed. The third group of failure (III) occurred around dewatering channels where geotechnical failure caused the centre part of the city to flood. A few interesting breaches are discussed below.

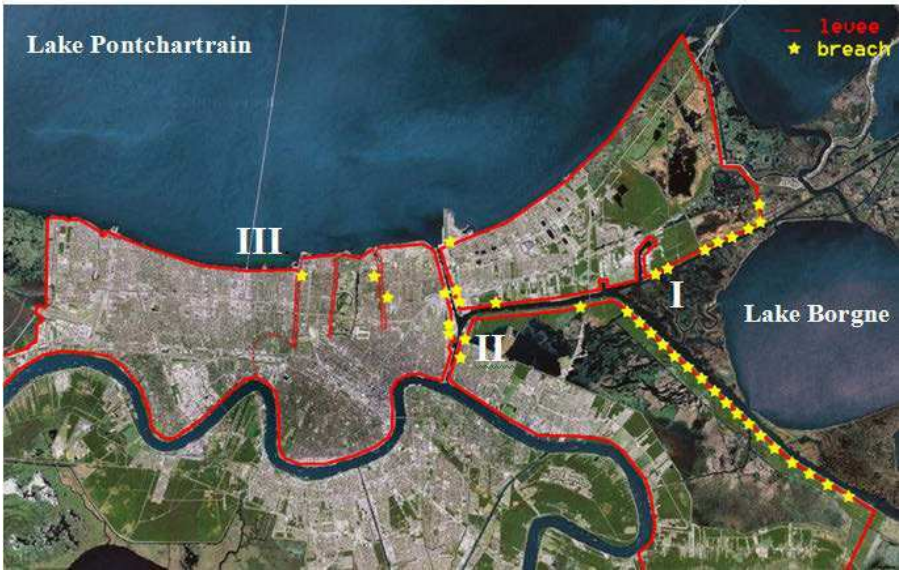

Figure 7. Overview failures in New Orleans

Figure 8 shows the failure of an earthen dike due to overtopping and overflow (area I). The water level in the whole area was much higher than the dikes. The unprotected dike eroded away for over many kilometers. Figure 9 show the geotechnical failure of a levee due to sliding in area III. The water level was below the crest of the floodwall and below design conditions. The subsoil slid horizontally over a weak layer, causing a large breach. Figure 10 shows the failure due to piping of a flood wall, again below the crest and below design conditions. For more information is referred to Kanning et. al (2008). Both failures (both in area III) emphasize the importance of geotechnical sound designs.

Figure 11 shows the failure at transition between a wall and an earthen dike in area II. Both adjacent dike and floodwall survived, only the transition failed. The vulnerability of transition could be observed all over New Orleans. Even small objects as staircases caused increased erosion of the dikes.


Figure 8. Overtopped levee in New Orleans (source: ILIT, 2006)

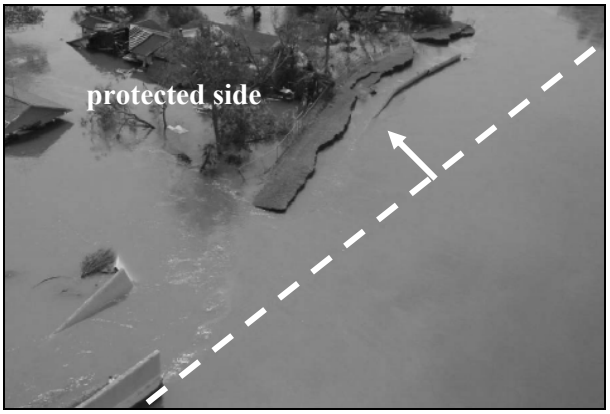

Figure 9. Stability failure in New Orleans due to hurricane Katrina (modified after ILIT, 2006)

Figure 10. Piping failure in New Orleans

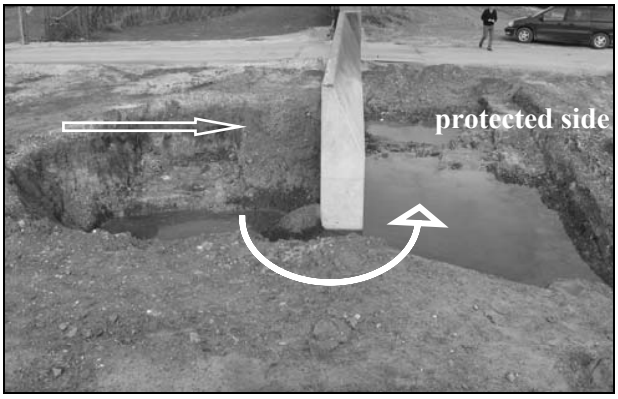

Figure 11. Failure between gate structure and dike

Perhaps more important than the individual failures was the system behavior. Or as stated by IPET (2006): "The System did not perform as a system: the hurricane protection in New Orleans and Southeast Louisiana was a system in name only." For many different reasons (e.g. funding structures, lack of funding etc.) the flood defense system could be regarded as a patchwork of defenses without clear coherence. Examples are missing levee parts, many different levee heights and abrupt changes in heights, the use of different reference datum. All these elements contributed to the total system performance. An interesting additional observation on system level is that most infrastructures (roads, pump pipes) penetrate the defense system (with gates to maintain the flood defense function). In contrast, in the Netherlands for example, infrastructure goes over the dike to reduce the amount of potential vulnerable spots.

3.4 *Summary*

System reliability considerations as well as observations during flood events like Katrina show that dike safety is much more than avoiding overtopping. Other failure mechanisms need to be considered, too. Geotechnical failure mechanisms play a crucial role and can dominate the probability of failure due to the large uncertainties associated with ground conditions. Hence, they need to be properly addressed in design and assessment rules of flood defenses.

4 SPATIAL VARIABILITY AND LENGTH EFFECT

4.1 *What is the Length-Effect?*

Section 2 on acceptable risk has provided a framework to derive an acceptable probability of system failure – the target reliability for the system as a whole. Section 3 has discussed the different mechanisms contributing to the probability of system failure. However, the different failure mechanisms are usually assessed at so-called representative cross sections, dike profiles of zero length. As mentioned, the so-called *length-effect* should not be neglected in deriving safety targets for dike cross sections. It is defined as the increase of the probability of failure with the increasing length of a dike reach. The two main factors determining the magnitude of the length effect are:

- The relative contribution of load and resistance: A high contribution of the resistance to the total variance increases the length effect. This is because for flood defenses, load parameters (e.g., river water level) tend to have much larger scales of fluctuation than resistance parameters (e.g. soil properties) do.
- The spatial variability in the subsoil: the higher the spatial variability in the subsoil (e.g., shorter auto-correlation distances of ground properties), the higher the length effect.

4.2 *Load vs. Resistance Uncertainty*

Usually the probability of failure of a flood defense system is determined by evaluating the following limit station function:

$$Z_i = R_i - S_i \qquad (10)$$

Where R_i is the resistance vector consisting of all relevant dike sections and failure mechanisms contained in index i and S_i is the load vector. Loads usually exhibit large correlation distances (e.g. water levels in rivers). For load-dominated failure mechanisms (e.g. overflow), the probability of failure of a dike reach is close to the probability of failure for a cross section. On the other hand, resistance-dominated mechanisms exhibit significant length-effect, up to a ratio of 100 between the probability for a dike reach and the probability for a cross section. The breaches New Orleans (see section 2) underpin that large variability in ground conditions and resistance properties make the existence of weak spots likely.

4.3 *Heterogeneity in Ground Conditions*

The high resistance uncertainty of flood defenses is mainly caused by the high uncertainty in the subsoil caused by a high spatial variability (heterogeneity) in the subsoil combined with the limited availability of direct measurements. The spatial variability (of heterogeneity) can be subdivided into two classes (see Figure 12):

1. Continuous variability which is associated with continuous fluctuation of properties like layer thickness, hydraulic conductivity or shear strength.
2. Discrete elements like old river beds that are filled with less resistant or highly permeable materials. When undetected, these "anomalies" can represent weak spots.

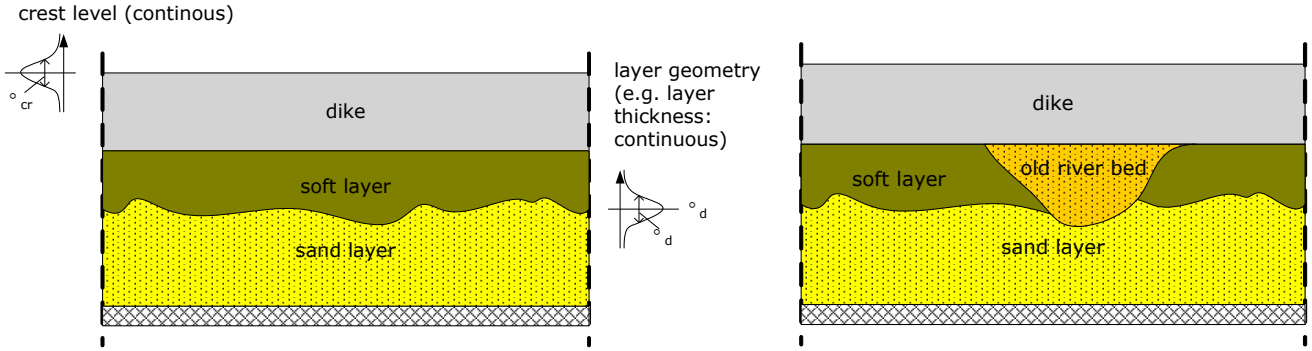

Figure 12. Continuous and discrete variability

4.4 *Modeling Heterogeneity*

Continuous variability can be modeled using random field theory (see e.g. Vanmarcke, 1977). Using this theory, the soil properties are modeled with mean, variance and autocorrelation function. The autocorrelation function describes how the correlation of a property between different locations decays with increasing lag (distance between two points). Vrouwenvelder (2006) uses the following auto-correlation function:

$$\rho(\Delta x) = \rho_x + (1-\rho_x)\cdot e^{-\frac{\Delta x^2}{d^2}} \qquad (11)$$

where $\rho(\Delta x)$ is the correlation between two point separated with distance Δx, ρ_x is the lag-independent correlation and d is the correlation distance of a parameter (see e.g. Vanmarcke, 1977)

Discrete variability is usually modeled using scenarios, see (Schweckendiek & Calle, 2010). Regional geological knowledge and experience can be used to determine (prior) probabilities of weak spots.

4.5 *Mathematical Treatment of the Length-Effect*

Vanmarcke (1977) and Vrouwenvelder (2006) use the outcrossing approach to determine the probability of exceedance of a threshold (here: the limit state Z=0) of length L using the mathematical properties of the autocorrelation function. Assuming full spatial correlation of the loads, for a *single* resistance variable *R,* this yields:

$$P_f = \Phi(-\beta_{\text{section}})\left(1+\alpha_R \frac{\beta_{\text{section}} L}{\sqrt{\pi} d}\right) \qquad (12)$$

Where $P_{f,system}$ is the probability of system failure, $\beta_{section}$ is the reliability index of a cross section, α_R is the importance factor of the resistance R, L is the considered length and d is again the scale of fluctuation Note that a low α_R corresponds to a low length effect, as mentioned in section 4.2

For a *multi-dimensional* problem (several resistance and/or load parameters), the length effect can be incorporated by using the equivalent mechanism length l_{eq} (see Calle, 2010):

$$P_{f,system} = P_{f,\text{section}}\left(1+\frac{L}{l_{eq}}\right) \qquad (13)$$

$$l_{eq} \approx \frac{\sqrt{2\pi}}{\beta_{\text{section}}} \frac{1}{\sqrt{-\rho''(0)}} \qquad (14)$$

$$\rho''(0) = \sum_{i=1}^{N} \frac{2\alpha_i^2 (1-\rho_{x,i})}{d_i^2} \qquad (15)$$

Where the subscript i refers to the different basic random variables. Finally the length effect factor for a mechanism, n_{mech} is given by:

$$n_{mech} = \frac{P_{f,system}}{P_{f,\text{section}}} \qquad (16)$$

The influence of the probability of weak spots (discrete elements) can be incorporated by using conditional probability (Schweckendiek & Calle, 2010):

$$p_f = \sum p_{weak\,spot} \cdot p_{failure|weak\,spot} + \sum p_{f,\text{section i}} \qquad (17)$$

The different failure probabilities of different dike reaches cannot just be summed as they are correlated. For more information about combining correlated dike sections is referred to Vrouwenvelder (2006). It must be noted that these theories are an extension of a two dimensional analysis into the third dimension. Efforts are being done to extend these theories towards full heterogeneous and three dimensional models (e.g. Fenton & Griffiths, 2003 and Hicks, 2005).

4.6 *Example: Piping*

In this example we consider the failure mechanism piping. In Figure 13 the length-effect factor n_{mech} is plotted over the length L of the dike part of the flood defense system. Different combinations of the importance factor α_R and scale of fluctuation (d) are used. The case with $\alpha_R = 0.8$ and $d = 200m$ is representative for piping in typical Dutch ground conditions, see Lopez de la Cruz et. al (2010). It shows the length-effect factor can be larger than 100 in extreme cases. The other combinations of α_R and d illustrate the sensitivity of the length effect.

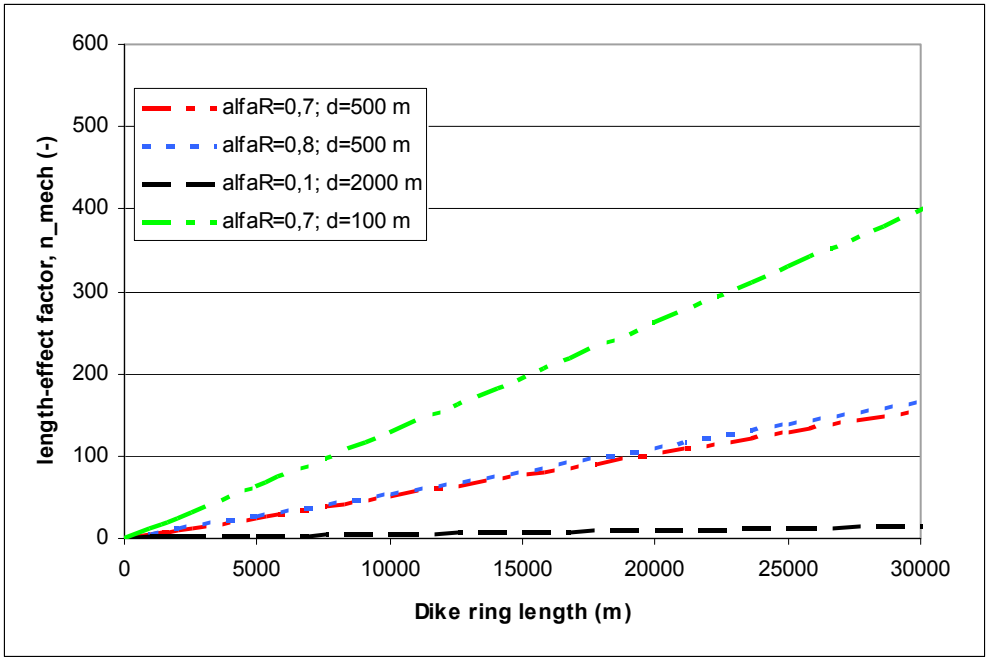

Figure 13. Length-effect factor of piping ring for different examples

5 FROM TARGET RELIABILITY TO PARTIAL SAFETY FACTORS

So far, we treated acceptable risk and made and inventory of what needs to be accounted for in terms of failure mechanisms and length-effect. This section shows how partial safety factors in design and assessment rules can be deduced from high-level requirements like acceptable probabilities of failure on system level.

5.1 *System Definition*

In section 2, the issue of acceptable flood risk was discussed without specifying the geographic extent or system that should be contemplated, when analyzing the likelihood and consequences of flooding. Purely in a theoretical sense, one would choose an independent system, for example a whole river basin, where there is no interaction with flood risk measures outside the chosen boundaries (Schweckendiek et. al, 2008). From a practical point of view, one rather works on a smaller scale. Hydraulic structures and dike sections with a similar flood pattern in case of failure and, therefore, similar consequences can be grouped and defined as the system to work with. N.B. legal aspects frequently impose boundary conditions, too, for example where flood defenses cross national or state boundaries. Regarding the acceptance criteria, the economical optimization only involves the risk contribution of a chosen (sub)system, while the criteria for social acceptability still need to be applied on the scale they were derived for. That means that for the location-specific individual risk one needs to consider the contributions of all sub-systems to the probability of dying in a certain spot. For group risk usually even all contributions on national or state scale need to be considered.

Figure 14. Fictitious Dike Ring in The Netherlands

For sake of illustration, in the remainder of this section, we will consider a fictitious example from the Netherlands. A so-called dike ring (polder surrounded by flood defenses and/or high grounds) exhibits very similar consequences regardless of the location of the failing dike or hydraulic structure. In fact, this is rather realistic for low-lying delta areas.

5.2 *Sub-System Requirements*

This section deals with the requirements in terms of reliability; their derivation from risk is out of the scope of this paper. The highest level requirement is the acceptable probability of failure of the (sub)system: $P_{f,adm,sys}$.

5.3 *Dikes and Hydraulic Structures*

The first step is to distribute the acceptable probability of failure over the structures in the dike ring:

$$P_{f,adm,sys} = P_{f,adm,dike} + \Sigma P_{f,adm,other,i} \qquad (18)$$

where $P_{f,adm,dike}$ is the acceptable probability of failure of any dike section in the system and $P_{f,adm,other,i}$ is the acceptable probability of failure of any other structure in the system. Since the geotechnical aspects are of most interest here, the remainder of this section is restricted to the dikes.
Note that implicitly the assumption was made that the probabilities of failure of the elements are independent. In reality, there is often a positive correlation mainly due to the rather large spatial correlation of the loads. For example, long dike reaches in riverine areas experience very similar loadings, in coastal areas similar wave conditions. This assumption is conservative, which seems reasonable in this standardization procedure.

5.4 *Failure Mechanisms*

The second step is to establish acceptable probabilities of failure per mechanism $P_{f,adm,dike,mech,i}$:

$$P_{f,adm,dike} = \Sigma P_{f,adm,dike,mech,i} = P_{f,adm,dike,over} + P_{f,adm,dike,inst} + P_{f,adm,dike,pip} + \ldots \qquad (19)$$

where $P_{f,adm,dike,over}$ is the acceptable probability of failure due to overtopping, $P_{f,adm,dike,inst}$ due to instability of the inner slope and $P_{f,adm,dike,pip}$ due to piping etc..

In principle, the $P_{f,adm,dike,mech,i}$ can be chosen in an economically optimal way. Mechanisms, for which high reliability target are inexpensive to realize should "occupy" less of the acceptable probability than mechanisms requiring relatively costly safety measures. In the Netherlands, such (historically rather qualitative) considerations suggest a (target) distribution as summarized in Table 2.

Table 2. Distribution of $P_{f,adm,dike}$ over mechanisms

Failure mechanism	$\delta = P_{f,adm,dike,mech,i} \,/\, P_{f,adm,dike}$
Overtopping	90%
Piping	3%
Instability	3%
Other	~1%

Note that in the considerations regarding efficient distributions also interaction between design parameters for different failure mechanisms plays a role. For example, a dike that needs to be high for overtopping and that has a gentle slopes for slope stability automatically has quite some seepage length, which is the main resistance parameter for piping. Also, in deriving new standards, the current conditions of the flood defense system under consideration (i.e., starting point) have an influence on what is optimal.

5.5 *Dike Sections (Accounting for the Length-Effect)*

$P_{f,adm,dike,mech,i}$ is the acceptable probability of failure per mechanism for all the dike sections in the (sub)system. However, designs and safety assessments are usually made for dike sections a few hundred meters or several kilometers long, with rather homogeneous properties (both, loading and resistance). As discussed in section 4, the length-effect plays an important role in this step. The essence is that the longer the dike with respect to the scale of fluctuation, most importantly of the resistance, the higher the probability of failure. For deriving requirements this implies that the acceptable probability of failure per

mechanism for a dike section (or a cross section that is representative for a dike section) $P_{f,adm,ds,mech,i}$ needs to be smaller than for all dikes in the considered reach:

$$P_{f,adm,ds,mech,i} = P_{f,adm,dike,mech} / n_{mech} \qquad (20)$$

The length-effect factor n_{mech} is typically about 2 to 10 for load-dominated mechanisms like overtopping, and can be in the order of magnitude of 100 for resistance dominated mechanisms like piping.

5.6 *Partial Safety Factors*

$P_{f,adm,ds,mech,i}$ is the (low-level) target reliability β_{req}, to which design and safety assessment rules apply and for which partial safety factors are derived.

$$\beta_{req,mech} = -\Phi\,(P_{f,adm,ds,mech,i}) \qquad (21)$$

A common approach is to use level-I reliability theory with standardized importance factors (Table 3). For a lognormal-distributed resistance variable, the partial safety factor is determined by:

$$\gamma_R = \exp\left(-\left(1.65 - \alpha_R \beta\right)\sqrt{\ln\left(1+V_R^2\right)}\right) \qquad (22)$$

where $V_R = \sigma_R / \mu_R$, β is the target reliability index and α_R is the importance factor of the resistance.

Table 3. Standardized Importance Factors for LRFD

Parameter	α
dominant load parameter	0.80
other load parameters	0.28
dominant strength parameter	0.70
other strength parameters	0.32

Figure 15 shows the dependence of the partial resistance factor of the target reliability index, the importance factor and the uncertainty in the (overall) resistance (here expressed in terms of the coefficient of variation V_R) with typical values for a resistance dominated failure mechanism like piping.

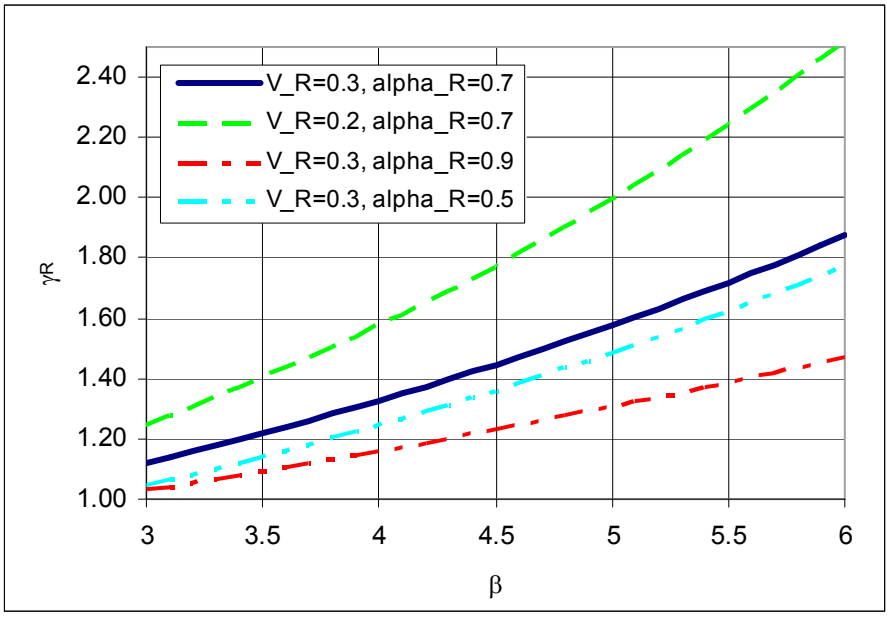

Figure 15. Relation of Partial resistance Factor and Target Reliability Index

Recently, Lopez de la Cruz et. al (2011) reported on a code calibration exercise for the failure mechanism piping in the Netherlands where a slightly different, more detailed approach was adopted. Instead of using standardized importance factors, the authors analyzed the performance for different values of the partial resistance factor in terms of resulting reliability indices. Furthermore, they established a reliability-dependent partial safety factor (see Figure 16) that can be used flexibly depending on the target reliability in a given area or (sub-system).

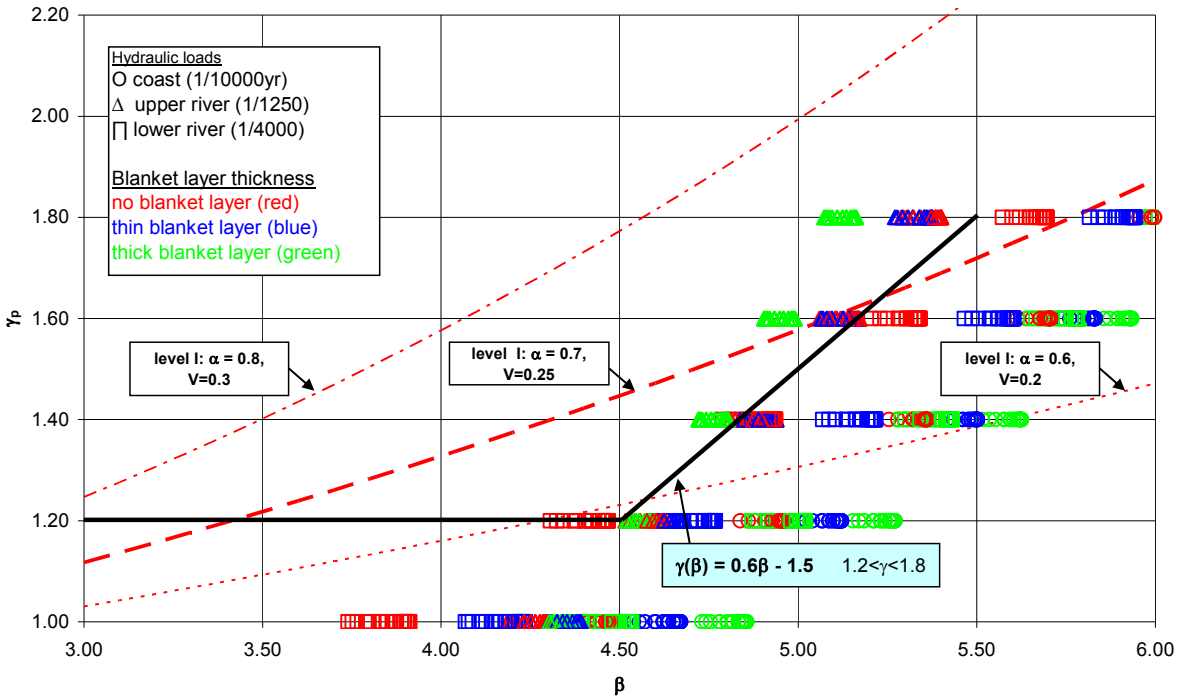

Figure 16. Partial Resistance Factor γ_p vs. Reliability Index β for Piping according to Lopez de la Cruz et. al (2011)

5.7 *Overview / Example*

Figure 17 gives an overview of the steps described above for the different mechanisms, including a realistic numerical example. Note that, so far, only the treatment of resistance uncertainties has been treated. For the definition of design loads often an exceedance probability of the load combination is defined by:

$$F = P(S>S_D) = \Phi(1- \Phi(-\alpha_S \beta_{req})) \qquad (23)$$

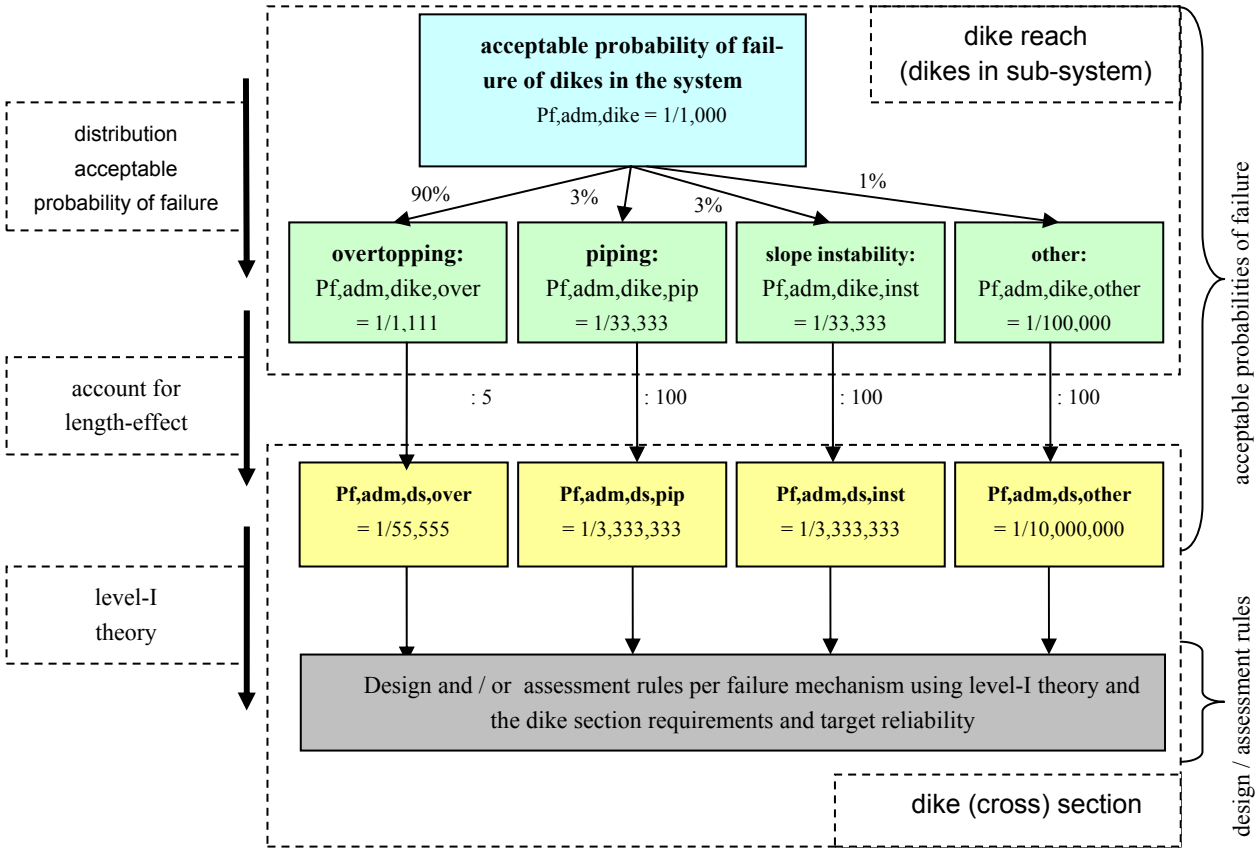

Figure 17. Overview of the Steps from high-level to low-level Requirements with a numerical example

Note that the difference between target the acceptable probability of failure on system and on mechanism level for a cross section can easily be a factor 1000 depending on the way it is dealt with different mechanisms and length effects.

5.8 *Alternative approaches*

The approach described so far is based on pragmatic choices. It is emphasized that there are numerous alternatives to the approach and also within the described framework. On example is to change the order of the distribution of the admissible probability of failure: go from system level to structures and dike sections first, then to the mechanisms. There are advantages and disadvantages that have mainly to do with the envisaged use of the rules in practice.

Furthermore, there are many possibilities for optimization. For example, correlations between mechanisms or structures can be taken into account in deriving the specific requirements from the high-level requirements.

Another obvious opportunity for improvement with large impact potential is the application of reliability analysis or reliability-based design (RBD), which can reduce the implicit conservatism in level-I approaches by better accounting for the uncertainties in specific conditions.

6 DISCUSSION

This paper attempts to demonstrate how tailor-made safety standards for large scale flood defense systems can be derived in a risk-based fashion. Since flood defenses differ from smaller scale geotechnical structures in many aspects and given the volume of investments in such large-scale engineering systems, it is very attractive to deviate from the standard design codes. That is not deviating conceptually, but rather deriving safety factors for the specific application to better account for the characteristics and uncertainties involved. The authors strive to show that safety levels and partial safety factors in the presented approach are far from arbitrary. They are part of an overall consistent flood risk framework, a framework that provides a link between geotechnical engineers and other disciplines involved in providing safety from flooding.

REFERENCES

Bernoulli, D. (1783). *Exposition of a New Theory on the measurement of risk* (original publication: 'Specimen TheoriaeNovae de Mensura Sortis, Comentarii Academiae Imperialis Petropolitanas, Tomus V.' 1738, pp. 175-192), Econometrica (1954), 22: 23-26.

Calle, E.O.F. (2010) *Lengte-effect en kalibratie van een toetsregel*. Deltares memo 15-04-2010.

Dantzig, D. (1956). *Economic Decision Problems for Flood Prevention*. Econometrica, Vol 24 (3), July 1956.

Fenton, G.A. and Griffiths, D.V. (2003). *Bearing capacity prediction of spatially random c - phi soils*. Canadian geotechnical journal , 40(1), pp. 54-65

Hicks, M.A. (2005). *Risk and Variability in Geotechnical Engineering*. Thomas Telford publishing, ISBN: 9780727734860

ILIT (Independent Levee Investigation Team; 2006*) Investigation of the Performance of the New Orleans Flood Protection Systems in Hurricane Katrina on August 29, 2005*, Report No. UCB/CCRM – 06/01

Jonkman S.N. (2007) *Loss of life estimation in flood risk assessment. Theory and applications*. Phd thesis, Delft University of Technology.

Kanning, W., S. van Baars, P.H.A.J.M.van Gelder and J.K Vrijling (2007). *Lessons from New Orleans for the design and maintenance of flood defence systems*. Proc. ESREL 2007

Kanning, W., S. van Baars and Vrijling (2008). *The stability of flood defences on permeable soils – the London Avenue Canal failures in New Orleans*. Proc. 6th International Conference Case Studies in Geotechnical Engineering

Lerche, Ian; Glaesser, Walter (2006), Environmental risk assessment : quantitative measures, anthropogenic influences, human impact., Berlin: Springer, ISBN 3-540-26249-0.

Lopez de la Cruz, J., T. Schweckendiek, C. Mai Van & W. Kanning (2010). S*BW Hervalidatie piping - HP8b Kalibratie van de veiligheidsfactoren*. Deltares report 1202123-002-GEO-0005

Lopez de la Cruz, J., Calle, E.O.F., Schweckendiek, T. (2011). *Calibration of Piping Assessment Models in The Netherlands*. International Symposium of Geotechnical Safety and Risk, ISGSR 2011, Munich, Germany. (in press)

Vanmarcke, E.H. (1977). *PROBABILISTIC MODELING OF SOIL PROFILES*. ASCE-JOURNAL OF THE GEOTECHNICAL ENGINEERING DIVISION, Vol. 103.

Vrijling, J.K. van Gelder, P.H.A.J.M., (2000): *An Analysis of the Valuation of a Human Life*, ESREL 2000 AND SRA - EUROPE ANNUAL CONFERENCE, "FORESIGHT AND PRECAUTION", Volume 1, pp.197-200, Eds. M.P. Cottam, D.W. Harvey, R.P. Pape, & J.Tait, May 14-17 2000 Edinburgh, Scotland, UK.

Vrijling, J.K., W. van Hengel & R.J. Houben (1993). *What is acceptable risk*. Technische Universiteit Delft and Bouwdienst Rijkswaterstaat.
Vrouwenvelder, A.C.W.M. (2006). *Spatial effects in reliability analysis of flood protection systems*. IFED Forum 2006, Lake Louise, Canada.
Schweckendiek, T. & Calle, E.O.F.(2010): *A Factor of Safety for Geotechnical Characterization* . Proc. of the Seventeenth Southeast Asian Geotechnical Conference (17SEAGC) – Geo-Engineering for Natural Hazard Mitigation and Sustainable Development. Vol. II: Plenary and Special Sessions, p. 227-230. Editors: J.C. Chung Li, M.-L. Lin. ISBN 978-957-29749-4-0. Taipei, Taiwan, May 10-13 2010.
Starr, C. (1969): *Social benefit vs. Technological risk*, Science, Vol.165, p.1232-1283.
TAW - Technical Advisory Committee on Water Defences (1998) *Fundamentals on water defences*, TAW, www.tawinfo.nl

ISGSR 2011 - Vogt, Schuppener, Straub & Bräu (eds) - © 2011 Bundesanstalt für Wasserbau ISBN 978-3-939230-01-4

How Reliable Are Reliability-Based Multiple Factor Code Formats?

K. K. Phoon
National University of Singapore, Singapore

J. Ching
National Taiwan University, Taipei, Taiwan

J. R. Chen
National Chi Nan University, Puli, Taiwan

ABSTRACT: The objective of this paper is to investigate the degree of deviation from the target reliability index produced when LRFD/MRFD equations are applied to a database of forty-two actual drilled shafts installed in soil profiles underlying the city of Taipei, which contain clay, sand, gravel and rock layers or some partial combination thereof. In general, for soil profiles with multiple layers, conventional formats containing resistance and load factors are unable to achieve the prescribed target reliability index with the same consistency as that reported for homogeneous soil profiles. For the drilled shaft examples considered in this study, the direct application of quantiles in the RBD equation (uniform quantile – η approach), rather than converting the quantiles to conventional resistance and load factors (uniform quantile – standard approach), appears to deliver the most consistent and most robust performance. There is a practical drawback associated with the application of the uniform quantile – η approach. The engineer is required to perform Monte Carlo simulation to estimate the η quantile of lumped random variables such as the total side resistance. This drawback is not present if the uniform quantile – η approach is applied to appropriate parameters where the probability distribution is known analytically or empirically.

Keywords: drilled shafts, axial compression, LRFD, MRFD, reliability code calibration, FORM design point method, uniform quantile method, calibration domain

1 INTRODUCTION

The objective of reliability-based design (RBD) is to adjust a set of design parameters such that a prescribed target probability of failure is achieved or at least not exceeded. For example, the depth of a drilled shaft is a practical design parameter that can be adjusted readily. In principle, it is possible to adjust the shaft diameter but it is less practical to constantly change the diameter of a rotary auger within a single site. These practical considerations apply to the current working stress design (WSD) method. In fact, from a mechanical calculation perspective, there is no difference between RBD and WSD. The former considers a design to be satisfactory if a target probability of failure, say one in a thousand, is achieved. The latter considers a design to be satisfactory if a target global factor of safety, say three, is achieved. The substantive advantage of using the probability of failure (or an equivalent reliability index) in place of the global factor of safety has been discussed elsewhere (Phoon et al. 2003a).

Using the classical example of a drilled shaft under axial compression, the objective of RBD can be stated formally as follows:

$$\text{Prob}(Q < L) \le p_T \tag{1}$$

in which Q = shaft capacity, L = axial load, and p_T = target probability of failure. EN1990:2002 (British Standards Institute, 2002) prescribes $p_T = 7.2 \times 10^{-5}$ (or reliability index, $\beta = 3.8$) for a reliability class 2 (RC2) structure (ultimate limit state). Note that it is straightforward to convert β to p_T and vice-versa using the following convenient EXCEL functions: p_T = NORMSDIST(-β) and β = NORMSINV(1–p_T). It is worthy to observe in passing that Q and L are typically modeled as independent lognormal variables in a number of geotechnical RBD code calibration exercises. This assumption is largely a matter of computa-

tional convenience because the left hand side of Eq. (1) can be evaluated in closed-form using the following classical lognormal formula:

$$\beta = \frac{\ln\left[\mu_Q / \mu_L \sqrt{(1+\theta_L^2)/(1+\theta_Q^2)}\right]}{\sqrt{\ln\left[(1+\theta_L^2)(1+\theta_Q^2)\right]}} \tag{2}$$

in which μ_Q, μ_L = mean shaft capacity and mean axial load, respectively and θ_Q, θ_L = coefficient of variation of shaft capacity and coefficient of variation of axial load, respectively. This lumped capacity assumption is convenient from a reliability calculation perspective, but it is rarely emphasized that it could be inconvenient from a physics perspective. The shaft capacity is typically related to side resistance and tip resistance. These resistances are related to geotechnical parameters that can be measured in the laboratory or in the field for obvious practical reasons. The statistics of these geotechnical parameters can be estimated directly from the measured data. Based on this physics perspective, the shaft capacity is a function of more basic random variables (geotechnical parameters). This function is generally nonlinear and the statistics of Q can only be estimated using Monte Carlo simulation. More fundamentally, Q is *not* a lognormal random variable even if all basic random variables are lognormally distributed and Eq. (2) is no longer valid. It could be argued that there are insufficient data to decide which approach is more correct. Nevertheless, it is the position of the authors that one should conform with the best physical model available to date, assign the simplest probability models consistent with measured laboratory/field data and known physical bounds, and live with the resulting complexity in reliability calculations. In short, a physics-centered approach is better than a reliability-centered approach.

For geotechnical problems where simple models are adequate, which is indeed the case for shaft capacity, it is relatively simple to evaluate the left hand side of Eq. (2) using Monte Carlo simulation. More complex problems requiring numerical solution models such as FEM can also be analyzed probabilistically using Monte Carlo simulation, but the computational cost is onerous for common PC platforms. Monte Carlo simulation is a completely general technique. The main disadvantage is tedium, because tens of thousands of design checks (i.e. Q < L?) are needed. In contrast, WSD only requires a single check per trial design. There are clever mathematical short-cuts such as the First-Order Reliability Method (FORM) that can reduce tens of thousands of design checks to less than ten design checks at the cost of loss of generality, more complex calculation steps, and occasionally hard-to-detect erroneous solutions. An alternate method called subset simulation (Au & Beck 2001) is gaining popularity, because it is almost as general as Monte Carlo simulation, but requires only about two thousands design checks to achieve a reasonably accurate estimate of the probability of failure. It is accurate to say that very few practitioners are comfortable to perform reliability analysis beyond Monte Carlo simulation which is physically appealing and requires very limited knowledge of probability theory as long as random number generators are available (it is available under "Data Analysis" > "Random Number Generation" in EXCEL). In fact, most practitioners do not find it worthwhile to perform Monte Carlo simulation even when it is available in commercial geotechnical softwares.

Simplified RBD equations in the form of Load and Resistance Factor Design (LRFD), Multiple Resistance Factor Design (MRFD), and partial factor approach (PFA) are popular because practitioners can comply with Eq. (1), albeit approximately, while retaining the simplicity of performing one check per trial design. To the authors' knowledge, this simplified RBD approach is adopted in all geotechnical RBD codes to date. The practical challenge is to calibrate a set of resistance factors or soil partial factors that would produce designs that comply with Eq. (1) approximately over a range of representative design scenarios. Needless to say, one would prefer the smallest possible set of factors (generating a humungous list like a phonebook would be impractical) covering the widest possible design scenarios that would produce the least deviation from the target reliability index. Phoon et al. (2003a) explicitly recognized this challenge and proposed the following RBD calibration approach to balance pragmatism and compliance with Eq. (1):

1. Perform a parametric study on the variation of the reliability level with respect to each deterministic and statistical parameter in the design problem. Examples of deterministic parameters that control the design of foundations include the diameter (width) and depth to diameter (width) ratio. Examples of statistical parameters for foundations loaded under undrained conditions include the mean and coefficient of variation (COV) of the undrained shear strength.

2. Partition the parameter space into several smaller domains. An example of a simple parameter space is shown in Fig. 1. The reason for partitioning is to achieve greater uniformity in reliability over the full range of deterministic and statistical parameters. For those parameters identified in Step (1) as having a significant influence on the reliability level, the size of the partition clearly should be smaller. In addition, partitioning ideally should conform to existing geotechnical conventions.
3. Select a set of representative points from each domain. Note that each point in the parameter space denotes a specific set of parameter values (Fig. 1). Ideally, the set of representative points should capture the full range of variation in the reliability level over the whole domain.
4. Determine an acceptable foundation design for each point and evaluate the reliability levels in the designs. Foundation design is performed using the set of parameter values associated with each point, along with a simplified RBD format and a set of trial resistance factors. The reliability of the resulting foundation design then is evaluated using Monte Carlo simulation, FORM, or other algorithms.
5. Quantify the deviations of the reliability levels from a prescribed target reliability index, β_T. The following simple objective function can be used:

$$H(\lambda_1,\lambda_2,\lambda_3\cdots)=\sum_{i=1}^{n}(\beta_i-\beta_T)^2 \tag{3}$$

in which $H(\cdot)$ = objective function to be minimized, λ_i = partial/resistance factors that are being calibrated, n = number of points in the calibration domain, and β_i = reliability index for the i^{th} point in the domain.
6. Adjust the resistance factors and repeat Steps (4) and (5) until the objective function is minimized. The set of partial/resistance factors that minimizes the objective function (H) is the most desirable because the degree of uniformity in the reliability levels of all the designs in the domain is maximized. The following measure can be used to quantify the degree of uniformity that has been achieved:

$$\Delta\beta=\sqrt{H/n} \tag{4}$$

in which $\Delta\beta$ = average deviation from the target reliability index in the calibration domain.
7. Repeat Steps (3) to (6) for the other domains.

Comparable calibration methods have been adopted elsewhere (e.g., CIRIA 1977, Ellingwood et al. 1980, Moses and Larrabee 1988). The effectiveness of applying these simplified RBD equations to more realistic ground conditions containing multiple strata has not been studied, despite its obvious practical importance. The objective of this paper is to investigate the degree of deviation from the target reliability index produced when LRFD/MRFD equations are applied to a database of forty-two actual drilled shafts installed in the city of Taipei. The effect of the RBD calibration method (design point method, quantile-based method) and number of calibration points are also studied.

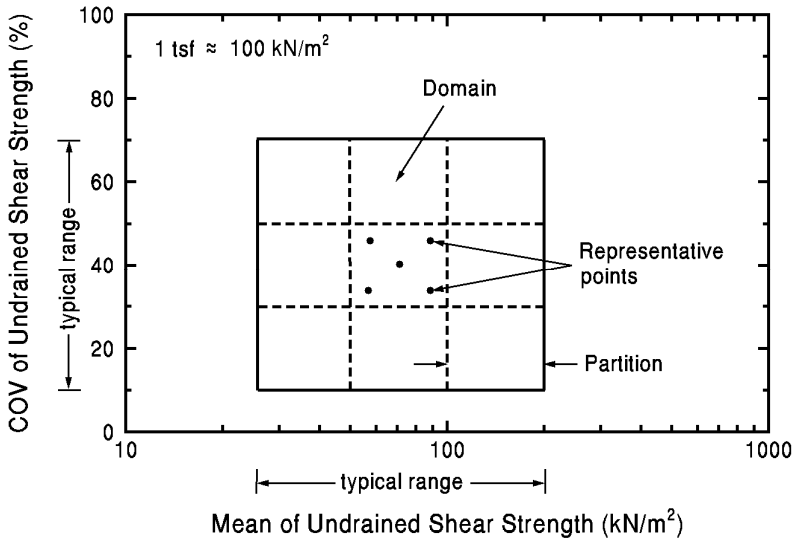

Figure 1. Partitioning of parameter space for calibration of resistance factors.

2 DRILLED SHAFT DATABASE

2.1 *Overview of database*

Table 1 summarizes the basic shaft and geotechnical information for forty-two drilled shafts installed in the city of Taipei. The shaft diameter, B, varies between 0.8 m and 2.5 m with an average of 1.24 m. The shaft length, D, varies between 20.7 m and 76 m with an average of 48.8 m. The D/B ratio varies between 18.8 and 63.3 with an average of 40.3. The compression capacity interpreted using the slope-tangent method varies between 6172 kN an 15372 kN with an average of 10772 kN. More details are reported elsewhere (Ching et al. 2011).

Table 1. Basic shaft and geotechnical information for drilled shafts installed in the city of Taipei.

Shaft No.	Site Location	Diameter B (m)	Depth D (m)	Water Table (m)	D/B	Soil Description	Q_{ST}* (kN)	Q_{L2}* (kN)	Group
CT-02	Xinyi District	1.2	29.2	-	24.3	Silty clay over sandstone	6172	11237	CR
CT-04	Da'an District	2.0	37.5	-	18.8	Interbeded silty clay and silty sand over gravel	-	-	CSG
CT-05	Xinyi District	1.0	53.5	-	53.5	Silty clay over gravel & sandstone	10069	13047	CGR
CT-07	Xinyi District	1.2	59.0	-	49.2	Interbeded silty clay and silty sand over gravel & mudstone	17638	17658	ALL
CT-09	Xinyi District	1.2	47.7	-	39.8	Interbeded silty clay and silty sand over sandstone	15990	17168	CSR
CT-10	Zhongshan District	1.0	55.5	-	55.5	Interbeded silty clay and silty sand over gravel	17040	21680	CS
CT-11	Beitou District	1.0	44.5	-	44.5	Silty clay over sandstone	6293	7456	CSR
CT-13	Taipei County	1.2	43.0	-	35.8	Interbeded silty sand and silty clay over gravel	13337	17291	CSG
CT-14-1	Xinyi District	1.2	76.0	-	63.3	Interbeded silty clay and silty sand over gravel & mudstone	32226	35542	ALL
CT-14-2	Xinyi District	1.5	66.0	-	44.0		36572	42948	ALL
CT-14-3	Xinyi District	1.5	65.0	-	43.3		37769	46499	ALL
CT-14-4	Xinyi District	1.5	56.0	-	37.3		25790	34266	ALL
CT-14-5	Xinyi District	1.2	59.0	-	49.2		26634	34835	ALL
CT-14-6	Xinyi District	2.5	70.3	-	28.1		66414	75213	ALL
CT-15	Shilin District	1.0	29.0	-	29.0	Interbeded silty sand and silty clay over sandstone	6959	7652	CSR
CT-16	Xinyi District	1.5	66.0	-	44.0	Interbeded silty clay and silty sand over gravel & mudstone	15892	36336	ALL
CT-17	Da'an District	1.5	48.0	3.6	32.0	Interbeded silty sand and silty clay over gravel	19483	25280	CSG
CT-18	Zhongzheng District	1.2	29.4	-	24.5	Interbeded silty sand and silty clay over sandstone	13214	16304	CSR
CT-19	Xinyi District	1.2	59.0	-	49.2		28917	36336	CSR
CT-20	Zhongzheng District	1.2	64.4	3.6	53.6		15127	17550	CSR
CT-21	Xinyi District	1.2	52.0	-	43.3	Interbeded silty clay and silty sand over gravel & mudstone	-	-	ALL
CT-22	Xinyi District	1.2	54.0	-	45.0	Interbeded silty clay and silty sand over gravel or mudstone	-	-	CSG
CT-23	Xinyi District	1.0	53.0	4.0	53.0		-	-	CSR
CT-24	Xinyi District	1.2	54.0	3.0	45.0		-	-	CSG
CT-25-1	Da'an District	1.5	45.2	5.5	30.1	Interbeded silty clay and silty sand over sandstone	19465	24280	CSR
CT-27	Xinyi District	1.2	76.0	-	63.3	Interbeded silty clay and silty sand over gravel & mudstone	27263	37327	ALL
CT-30	Zhongshan District	1.0	47.5	-	47.5	Interbeded silty clay and silty sand over sandstone	9609	11644	CSR
CT-31	Beitou District	1.0	46.6	-	46.6		6253	7720	ALL
CT-32	Beitou District	1.0	31.4	-	31.4		5960	5690	CSR
CT-33	Shilin District	1.0	31.4	-	31.4		7173	7917	CSR
CT-34-1	Zhongzheng District	0.9	42.0	-	46.7	Interbeded silty clay and silty sand over gravel	6355	7120	CS

Shaft No.	Site Location	Diameter B (m)	Depth D (m)	Water Table (m)	D/B	Soil Description	Q_{ST}* (kN)	Q_{L2}* (kN)	Group
CT-35-1	Zhongzheng District	1.2	46.4	-	38.6		11903	13381	CSG
CT-36-1	Zhongzheng District	0.9	47.6	-	52.9		6642	7161	CSG
CT-37-1	Taipei County	1.2	34.2	-	28.5		7808	8584	CSG
CT-38-1	Taipei County	1.8	48.5	3.8	26.9		32227	40643	CSG
CT-39-1	Songshan District	1.8	49.5	0.2	27.5	Interbeded silty sand and silty clay over gravel & clay layer	12724	23014	CSG
CT-40-1	Taipei County	0.8	29.1	6.0	36.4	Interbeded silty sand and silty clay over gravel	7624	9584	CS
CT-41	Zhongshan District	1.3	54.9	3.0	42.2		15733	18763	CSG
CT-42	Zhongzheng District	1.2	47.4	-	39.5		14056	17854	CSG
CT-43	Zhongshan District	1.0	46.2	0.2	46.2		11836	15629	CSG
CT-44	Beitou District	1.0	32.0	0.2	32.0	Silty clay over sandstone	6523	7014	CR
CT-45	Shilin District	1.0	20.7	0.2	20.7		15372	20012	CR

*Measured compression capacity from load test: Q_{ST} = capacity interpreted using the slope-tangent method, Q_{L2} = capacity interpreted using the L1-L2 method.

It is useful to observe that common drilled shaft diameters are covered in the database. However, based on D/B ratio, the database covers predominantly long friction shafts. More importantly, all the shafts are installed in non-homogeneous layered soils. Based on the strata that provide the side resistances, the shafts are classified into five groups: (a) Group ALL: the strata include clay, sand, gravel, and rock layers (11 shafts); (b) Group CSR: the strata include clay, sand, and rock layers (11 shafts); (c) Group CSG: the strata include clay, sand, and gravel layers (13 shafts); (d) Group CGR: the strata include clay, gravel, and rock layers (1 shaft); (e) Group CR: the strata include clay and rock layers (3 shafts); and (f) Group CS: the strata include clay and sand layers (3 shafts). It is apparent that this database covers a fairly comprehensive range of layered soil profiles.

2.2 *Axial compression capacity and its associated uncertainties*

The axial compression capacity of a drilled shaft is the sum of side resistances along the shaft and end bearing at the tip minus its own self-weight. For the long friction shafts shown in Table 1, it is adequate to assume that the shaft capacity (Q) is approximately equal to the total side resistance (S). For shafts installed in multiple strata with possible appearance of clay, sand, gravel, and rock layers, the total side resistance is expressed as:

$$S = S_c + S_s + S_g + S_r \tag{5}$$

in which S_c , S_s, S_g, and S_r = side resistances for the clay, sand, gravel, and rock layers, respectively. The side resistance in a given layer, denoted by S_x (the subscript 'x' denotes either 'c', 's', 'g', or 'r', depending on the stratum type of interest), can be computed as:

$$S_x = \pi B \sum_{i=1}^{N} f_{si} t_i \tag{6}$$

in which B = shaft diameter. For calculation purposes, each stratum is discretized into N layers, with f_{si} being the unit side resistance for the i^{th} layer and t_i being the thickness of the i^{th} layer. Note that Eq. (6) assumes that there is only one layer per geomaterial type (clay, sand, gravel, or rock). It is rather common to have interbeds consisting of different geomaterials, particularly clay, sand and gravel, in actual profiles. Eq. (6) can be easily generalized to more complex profiles. The models for unit side resistances in clay, sand, gravel, and rock are summarized in Table 2. They are developed from the α-method for clay and rock and β-method for sand and gravel. The model uncertainties, ε_{Sc}, ε_{Ss}, ε_{Sg}, ε_{Sr}, are described by zero-mean normal random variables with standard deviations given in Table 2. Details on calibration of

these unit side resistance models and estimation of associated model statistics are given by Ching et al. (2011).

In addition, the measured soil parameters are modeled as the actual parameters contaminated with measurement errors:

$$\begin{aligned}
\ln(\sigma'_{vs,m}) &= \ln(\sigma'_{vs}) + e_{\sigma'_{vs}} \\
\ln(\sigma'_{vg,m}) &= \ln(\sigma'_{vg}) + e_{\sigma'_{vg}} \\
\ln(s_{u,m}) &= \ln(s_u) + e_{s_u} \\
\ln(q_{u,m}) &= \ln(q_u) + e_{q_u}
\end{aligned} \tag{7}$$

in which $\sigma'_{vs,m}$, $\sigma'_{vg,m}$, $s_{u,m}$, $q_{u,m}$ = measured values of average vertical effective stress of sand layer, average vertical effective stress of gravel layer, undrained shear strength of clay layer, unconfined compression strength for rock layer, respectively and e_{su}, $e_{\sigma'vs}$, $e_{\sigma'vg}$, e_{qu}. = measurement errors associated with the subscripted soil parameters. These measurement errors are modeled as zero-mean normal random variables with the following standard deviations: 0.20 for e_{su}, 0.10 for $e_{\sigma'vs}$ and $e_{\sigma'vg}$, and 0.47 for e_{qu}.

Table 2. Models for unit side resistances in clay, sand, gravel, and rock.

Geomaterial	Correlation model for unit side resistance (kN/m^2)	Standard deviation of model uncertainty ε
Clay	$f_c = \exp[2.70 + 0.30\ln(s_u) + \varepsilon_{s_c}]$	0.32
Sand	$f_s = \exp[1.08 - 0.66\ln(z) + \ln(\sigma'_v) + \varepsilon_{s_s}]$	0.54
Gravel	$f_g = \exp[2.18 - 0.75\ln(z) + \ln(\sigma'_v) + \varepsilon_{s_g}]$	0.67
Rock	$f_r = \exp[3.03 + 0.41\ln(q_u) + \varepsilon_{s_r}]$	0.72

Note: s_u = undrained shear strength, σ'_v = vertical effective stress, and q_u = unconfined compression strength.

3 RELIABILITY CALIBRATION

3.1 *Performance function*

The performance function, G, is an arbitrary function that is less than zero when its arguments result in a failure state. For drilled shafts considered in this study, it is natural to define the performance function as:

$$G = S_c + S_s + S_g + S_r - L_D - L_L \tag{8}$$

in which L_D = dead load and L_L = live load. It is clear that the ultimate limit state is exceeded when $G < 0$. The basic random variables describing the uncertainties in the side resistances are the unit side resistance model errors shown in Table 2 (ε_{Sc}, ε_{Ss}, ε_{Sg}, ε_{Sr}) and the soil parameter measurement errors (e_{su}, $e_{\sigma'vs}$, $e_{\sigma'vg}$, e_{qu}) mentioned in Section 2.2. If N = 1 in Eq. (6), the side resistance contributed by the clay layer is:

$$S_c = \pi B f_c t_c = \pi B \exp\{2.70 + 0.30[\ln(s_{u,m}) - e_{s_u}] + \varepsilon_{s_c}\} t_c \tag{9}$$

It is clear that S_c is a lognormal random variable in this special, because $\ln(S_c)$ = constant – $0.3e_{su} + \varepsilon_{Sc}$ is a normal variable by hypothesis. For the more general case in which N > 1, S_c is a sum of lognormal random variables and hence, it is *not* a lognormal random variable. The total side resistance $S = S_c + S_s + S_g + S_r$ is *not* a lognormal variable even if S_c, S_s, S_g, S_r are individually lognormal variables for the same reason. The dead load is modeled as a lognormal random variable with mean = μ_{LD} and coefficient of variation = $\theta_{LD} = 0.10$. The live load is also modeled as a lognormal random variable with mean = μ_{LL} and coefficient of variation = $\theta_{LL} = 0.25$. The ratio $\mu_{LL}/\mu_{LD} = 0.5$ unless stated otherwise.

Given that the capacity (S) and the load ($L_D + L_L$) are not lognormal variables, Eq. (2) cannot be applied. The probability of failure, Prob(G < 0), is computed using Monte Carlo simulation in this study.

3.2 *Simplified RBD equations*

Four simplified RBD equations are considered: LRFD, MRFD2, MRFD3, and MRFD4. They are defined in Table 3 below.

Table 3. Simplified RBD equations.

RBD equation	Definition	Comment
LRFD	$\gamma_{total}\left(S_c^* + S_s^* + S_g^* + S_r^*\right) \geq \gamma_D L_D^* + \gamma_L L_L^*$	Calibrate 1 resistance factor: γ_{total}
MRFD2	$\gamma_{csg}\left(S_c^* + S_s^* + S_g^*\right) + \gamma_r S_r^* \geq \gamma_D L_D^* + \gamma_L L_L^*$	Calibrate 2 resistance factors: γ_{csg}, γ_r
MRFD3	$\gamma_{cs}\left(S_c^* + S_s^*\right) + \gamma_g S_g^* + \gamma_r S_r^* \geq \gamma_D L_D^* + \gamma_L L_L^*$	Calibrate 3 resistance factors: γ_{cs}, γ_g, γ_r
MRFD4	$\gamma_c S_c^* + \gamma_s S_s^* + \gamma_g S_g^* + \gamma_r S_r^* \geq \gamma_D L_D^* + \gamma_L L_L^*$	Calibrate 4 resistance factors: γ_{cs}, γ_s, γ_g, γ_r

Note: Asterisk denotes nominal resistances or nominal loads. Nominal resistances, S_c^*, S_s^*, S_g^*, and S_r^*, are computed by assuming the model errors and soil parameter measurement errors are zero. Nominal loads, L_D^* and L_L^*, are computed at their mean values.

3.3 *RBD calibration method 1: FORM design point*

Two RBD calibration methods are considered in this study: (1) FORM design point method and (2) uniform quantile method. The first method is described in this section.

The First-Order Reliability Method (FORM) involves seeking for a design point lying on the performance function G that is closest to the origin in standard normal space. An illustrative example containing two standard normal random variables, U_1 and U_2, is shown in Fig. 2. It is possible to transform a set of non-normal physical random variables to a set of standard normal random variables. The probability of failure estimated using FORM is Prob(G_L < 0) = Φ(-β), in which Φ(·) = standard normal cumulative distribution function evaluated using say NORMSDIST in EXCEL. By definition, the reliability index of a design satisfying the equation below is approximately equal to β (error due to linearization in FORM, $G_L \approx G$):

$$G\left(u_1^d, u_2^d\right) = G\left(x_1^d, x_2^d\right) = 0 \tag{10}$$

in which X_1, X_2 = physical random variables. Examples of physical random variables are given below.

This FORM design point method is described in Ang & Tang (1984). It is rarely emphasized that Eq. (10) forces the performance function to be coupled to the simplified RBD equation. For example, the LRFD format shown in Table 3 can only be calibrated using this design point method by stating the performance function in the following form:

$$G = S - L_D - L_L \tag{11}$$

in which S is the total side resistance. There are three physical random variables: $X_1 = S$, $X_2 = L_D$ and $X_3 = L_L$. Applying Eq. (10), it can be seen that:

$$x_1^d - x_2^d - x_3^d = 0 \tag{12}$$

Eq. (12) can be re-written in the LRFD format as follows:

$$\gamma_{total} x_1^* - \gamma_D x_2^* - \gamma_L x_3^* = 0 \tag{13}$$

in which x_1^*, x_2^*, x_3^* = nominal values of S, L_D, and L_L, respectively. The resistance and load factors are calibrated using: $\gamma_{total} = x_1^d / x_1^*$, $\gamma_D = x_2^d / x_2^*$ and $\gamma_L = x_3^d / x_3^*$.
For MRFD2, the performance function is stated in the following form:

$$G = S_{csg} + S_r - L_D - L_L \tag{14}$$

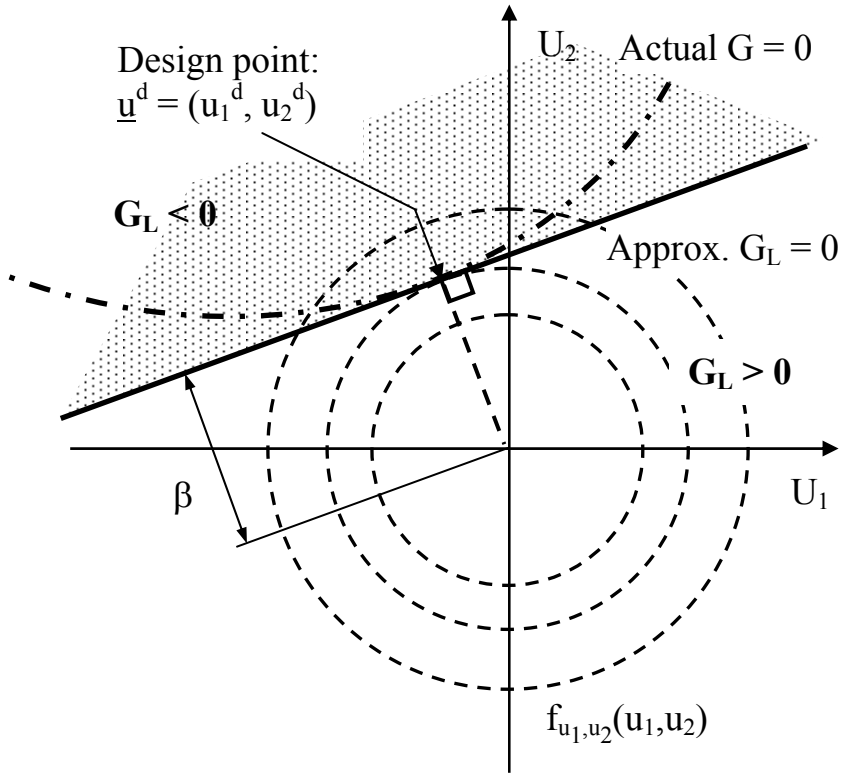

Figure 2. Definition of design point in First-Order Reliability Method (FORM).

in which $S_{csg} = S_c + S_s + S_g$. There are four physical random variables: $X_1 = S_{csg}$, $X_2 = S_r$, $X_3 = L_D$ and $X_4 = L_L$. Applying Eq. (10), it can be seen that:

$$x_1^d - x_2^d - x_3^d - x_4^d = 0 \tag{15}$$

Eq. (15) can be re-written in the MRFD2 format as follows:

$$\gamma_{csg} x_1^* + \gamma_r x_2^* - \gamma_D x_3^* - \gamma_L x_4^* = 0 \tag{16}$$

in which $\gamma_{csg} = x_1^d / x_1^*$, $\gamma_r = x_2^d / x_2^*$, $\gamma_D = x_3^d / x_3^*$ and $\gamma_L = x_4^d / x_4^*$.

Based on the above LRFD and MRFD2 examples, the nature of the coupling is clear. The physical random variables must be defined such that the resistance/load factor can appear as $\gamma_i = x_i^d / x_i^*$. For LRFD/MRFD, it is apparent that this is only possible when the resistances and loads are separable. A simple example where the resistance and the load cannot be separated is the bearing capacity of a shallow foundation subjected to inclined loading. The inclined load factor in the bearing capacity equation is a function of both the vertical and horizontal loads for drained loading (e.g., Annex D, BS EN1997-1:2004). It could be possible to circumvent this problem by assuming that the bearing capacity is correlated to the vertical load. Nonetheless, a second ad-hoc assumption that the non-normal bearing capacity and non-normal vertical load are correlated using a translation procedure is practically necessary at present (Phoon 2006). The adequacy of this ad-hoc assumption as applied to code calibration has not been examinued thus far.

For the drilled shaft example considered in this study, it is possible calibrate LRFD and MRFD formats using the FORM design point method. However, there is an important practical difficulty that is not highlighted in previous studies. Although Eq. (8), Eq. (11) and Eq. (14) are mathematically equivalent, the probability distributions of S and S_{csg} are *not* lognormals as explained in Section 3.1 and cannot be derived analytically even for the relatively simple drilled shaft example in this study where the model and

parametric errors are assumed to be lognormally distributed. However, the probability distributions of S and S_{csg} can be derived *empirically* using Monte Carlo simulation. In general, these empirical probability distributions will not fit classical closed-form probability distributions commonly found in standard texts. The authors found that the FORM algorithm is not stable when the physical random variables such as S and S_{csg} are defined using empirical distributions (known only at discrete sample points and likely to be inaccurate at probability tails where the design point is located). This FORM computational difficulty is currently being studied.

It is possible to take the pragmatic approach of assuming the resistances S and S_{csg} as lognormals, rather than assuming that the model and parametric errors are lognormals as in Section 3.1. Nonetheless, it has been pointed out in Section 1 that it is not judicious to make probabilistic assumptions for the convenience of reliability calculations and in the same vein, certainly not for the convenience of code calibrations. Probability distributions should be fitted to measured laboratory/field data, comply with known physical upper and/or lower bounds, and respect the accumulated knowledge base on correlations between various soil properties. It may not be possible to identify an appropriate probability distribution for a basic soil parameter exactly, because of insufficient data and/or imperfect knowledge. However, a probability distribution that fits known data and state-of-the-art knowledge is "best" at a particular point in time. It can be revised when more data and/or state of knowledge improves – this is true for all aspects of scientific pursuit; not merely probabilistic analysis. In some past critiques of RBD, the inability to identify "correct" probability distributions has been used as a reason for doubting the practical relevance of RBD. While it may be fair to critique undue probabilistic simplifications made to suit computational convenience, it appears unreasonable to demand perfect knowledge of probability distributions (which is merely a mathematical model of reality) and it is against the grain of evolving scientific progress.

In this study, the basic physical random variables characterized in Section 3.1 are assumed to be "correct", because they are based on actual measured data. To apply the FORM design point method to LRFD/MRFD, it is necessary to use *lumped* variables such as S and S_{csg}. To circumvent potential numerical instability of FORM associated with the use of empirical distributions for S and S_{csg}, it is assumed that these lumped variables are lognormally distributed. However, the second-moment statistics (mean and standard deviation) of these lumped variables are correctly estimated using Monte Carlo simulation. Note that this ad-hoc lognormal assumption is only applied to calibrate the various resistance and load factors in the LRFD/MRFD formats. These calibrated formats are validated by evaluating the reliability indices of drilled shafts outside the calibration domain in Section 4. The reliability indices computed during validation in Section 4 are based on the "correct" probability models given in Section 3.1.

Finally, it is of interest to observe that the calibration of resistance and load factors using Eq. (12) and Eq. (13) for LRFD is carried out to conform to the historical practice of producing a simplified RBD design equation with the same "look and feel" as existing working stress design equation. This calibration method is termed "FORM-standard" in this study. It is possible to consider an alternate FORM-based calibration approach using the design point in standard normal space (u_1^d, u_2^d, u_3^d):

$$u_1^d - u_2^d - u_3^d = 0 \tag{17}$$

In this approach, the design point (u_1^d, u_2^d, u_3^d) determined from a single calibration shaft is assumed to apply to all other shafts. The LRFD equation is now written as:

$$x_1\left(u_1^d\right) - x_2\left(u_2^d\right) - x_3\left(u_3^d\right) = 0 \tag{18}$$

in which $x_i(u_i^d)$ = value of i^{th} physical variable for a validation shaft calculated using the value of the i^{th} standard normal variable at the *design point of the calibration shaft*. This calibration method is termed "FORM-u" in this study.

3.4 *RBD calibration method 2: uniform quantile*

The uniform quantile calibration method was proposed by Ching & Phoon (2011). The procedure is illustrated below using the LRFD format. Theoretical details are given in the above cited paper.

The η quantile of the total side resistance, S^η, is defined by:

$$\mathrm{Prob}\left(S < S^\eta\right) = \eta \tag{19}$$

in which η = number between 0 and 1, but typically order of 0.01 for practical problems. S^{η} is also called the 100η% exclusion limit. For example, for a normal random variable, the 5% quantile, $S^{0.05} = \mu_S (1 - 1.645\theta_S)$, in which μ_S and θ_S are the mean and coefficient of variation of S, respectively. This definition is sensible for resistances, because S^{η} is a conservative value less than the mean value. For loads, it is natural to consider the (1-η) quantile. For example, the (1-η) quantile of the live load, $L_L^{1-\eta}$, is defined by:

$$\begin{aligned} \text{Prob}\left(L_L < L_L^{1-\eta}\right) &= 1-\eta \\ \text{Prob}\left(L_L > L_L^{1-\eta}\right) &= \eta \end{aligned} \tag{20}$$

Hence, the probability of L_L *exceeding* $L_L^{1-\eta}$ is η. $L_L^{1-\eta}$ is also called the $1/\eta$ return period load if L_L is defined as the annual maximum load and L_L varies independently from year to year. For a normal random variable, the (100-5)% = 95% quantile, $L_L^{0.95} = \mu_{LL} (1 + 1.645\theta_{LL})$, in which μ_{LL} and θ_{LL} are the mean and coefficient of variation of L_L, respectively. This definition is sensible for loads, because $L_L^{1-\eta}$ or $L_D^{1-\eta}$ is a conservative value greater than the mean value.

For LRFD, the uniform quantile calibration method produces the following simplified RBD equation:

$$S^{\eta} \geq L_D^{1-\eta} + L_L^{1-\eta} \tag{21}$$

Comparing with the LRFD format shown in Table 3, it is clear that $\gamma_{total} = S^{\eta}/S^*$, $\gamma_D = L_D^{1-\eta}/L_D^*$, and $\gamma_L = L_L^{1-\eta}/L_L^*$. The resistance and load factors for the MRFD formats in Table 3 can be calibrated in a similar way. For example, the resistance and load factors for the MRFD2 format can be derived from the following quantile equation:

$$S_{csg}^{\eta} + S_r^{\eta} \geq L_D^{1-\eta} + L_L^{1-\eta} \tag{22}$$

in which S_{csg}^{η}, S_r^{η} = η quantile of S_{csg} and S_r, respectively.

The distinctive feature of the uniform quantile approach is that the *same* quantile, η, is applied to all resistance and load components, regardless of the number of components. In fact, it is also possible to apply the uniform quantile approach to the partial factor format, although this format is not included in the present study. The quantile is simply applied on more basic soil parameters such as the undrained shear strength in this instance. Examples of partial factors calibrated using the uniform quantile approach are given in Ching & Phoon (2011). Ching & Phoon (2011) also demonstrated theoretically that a *single* quantile applied in the manner illustrated by Eq. (21) or Eq. (22) can be found such that the probabilistic RBD objective given in Eq. (1) is achieved. This unique relationship between η and p_T exists for a single set of design parameters. For this relationship to be useful for RBD code calibration, it should be insensitive to changes in the design parameters over a range of practical values. For example, almost the same relationship should apply for undrained shear strength varying from 25 kPa (soft clay) to 200 kPa (very stiff clay). Ching & Phoon (2011) presented four common geotechnical examples to demonstrate the relative stability of this η and p_T relationship empirically. They did not study the effect of changes in soil profiles. This important variation in the design scenario is studied in Section 4. It is worthy to note in passing that the change in soil profile must not result in a change of the failure mechanism (or performance function). For example, the failure mechanism for a shallow foundation resting on a thin layer of dense sand overlying soft clay is not the same as the classical Buisman-Terzaghi mechanism for homogeneous soils. It is obvious that the $\eta - p_T$ relationships are distinctively different for different performance functions.

Note that the probability distributions of S and S_{csg} are not available in analytical forms as mentioned in Section 3.3. They can only be characterized empirically using Monte Carlo simulation. Nonetheless, there is an important computational difference between using empirical distributions in FORM or using empirical distributions to compute quantiles. The former creates potential numerical instabilities while the latter can be carried out in a very robust non-parametric way using ranks. In this study, S^{η}, S_{csg}^{η}, and similar statistics are estimated correctly using Monte Carlo simulation. The ad-hoc lognormal assumption adopted in Section 3.3 is not applied in the uniform quantile approach. Similar to the FORM design point calibration approach, two variations are considered. The first variation is termed "uniform quantile –

standard", which calibrates the usual resistance and load factors that would be applied to drilled shafts outside the calibration domain for validation. The second variation is termed "uniform quantile – η", which applies the calibrated quantile η directly to drilled shafts outside the calibration domain for validation.

It is worth emphasizing here that the uniform quantile approach bears no theoretical resemblance to the application of quantile in characteristic/nominal values. The latter refers to Eq. (19) or Eq. (20). The quantile is prescribed by design codes without reference to the target probability of failure. For example, a quantile between 5% and 10% is typically prescribed for the concrete compressive strength, f_{cu}, in structural design codes. The main purpose of this definition is to produce a suitably conservative compressive strength that varies consistently with the coefficient of variation of f_{cu}. The same quantile is applied to different performance functions, for example moment/shear capacity of a beam or compression capacity of a column. The quantile appearing in Eq. (21) or Eq. (22) is fundamentally different. It is calibrated rather than prescribed to achieve a specific target probability of failure. It decreases in a relatively unique way with the target probability of failure for a given performance function. It is intrinsically related to the performance function. Hence, the quantile for a given soil property, say undrained shear strength, will vary when the property is applied within the context of different performance functions, even for the same target probability of failure.

4 VALIDATION STUDIES

4.1 *FORM-standard versus uniform quantile-standard*

In this section, resistance and load factors are calibrated using the "FORM – standard" approach and the "uniform quantile – standard" approach. These approaches have been presented in Section 3.3 and Section 3.4, respectively. A single drilled shaft from Group ALL is selected for calibration. Note that Group ALL contains drilled shafts installed in soil profiles with clay, sand, gravel, and rock layers. The calibrated resistance and load factors are applied to determine the mean dead load corresponding to each drilled shaft in Table 1 in the following way for LRFD:

$$\mu_{LD} = \frac{\gamma_{total}\mu_S}{\left(\gamma_D + \gamma_L \dfrac{\mu_{LL}}{\mu_{LD}}\right)} = \frac{\gamma_{total}\mu_S}{\left(\gamma_D + 0.5\gamma_L\right)} \tag{23}$$

in which γ_{TOTAL}, γ_D, γ_L = resistance and load factors computed from a *single* shaft in Group ALL using the FORM – standard/uniform quantile – standard approach, μ_S = mean total side resistance for any validation shaft in Table 1, and μ_{LD} = mean dead load required to satisfy the LRFD format corresponding to an assumed mean live load to mean dead load ratio of 0.5. It is easy to generalize Eq. (23) to the MRFD formats shown in Table 3.

It is more common to compute the shaft depth for a given set of loads in actual foundation engineering practice. However, the foundation depths are already given in Table 1. Hence, the mean dead load implied by the LRFD format is computed. This "design" approach is rather unorthodox, but it has no impact on the evaluation of the performance of the LRFD/MRFD formats presented in Table 4 below. In other words, the ability of the LRFD/MRFD formats to achieve a uniform target reliability index of 3 for the validation shafts can be evaluated by computing the foundation depth from a given set of loads or vice-versa. The latter approach has been applied by Phoon et al. (2003b) as well. The effect of varying the coefficients of variation in the basic random variables is studied in Section 4.4. The effect of varying the mean live load to mean dead load ratio is studied in Section 4.5. It is of interest to note that there are only 11 shafts in Group ALL. The rest of the shafts (31 shafts) are installed in soil profiles with 3 or less soil layers. In short, 31/42 = 74% of the validation shafts are installed in soil profiles that are distinctively different from the 4-layer profile in Group ALL.

Once the mean dead load is computed using Eq. (23), the "actual" reliability index of each validation shaft can be estimated using Monte Carlo simulation. Note that the same nonlinear performance function and the same set of basic random variables (model and measurement errors) presented in Section 3.1 are applied to estimate the "actual" reliability indices for all validation shafts, regardless of the code formats under study. It has been emphasized in Section 3.3 that the performance function and basic random variables presented in Section 3.1 constitute our current best understanding of "reality". Hence, the reliability indices estimated using these realistic physical and probabilistic models are described as "actual" in this sense. For brevity, the term "actual" is dropped from hereon, because all reliability indices reported in

Section 4 are "actual". The ad-hoc lognormal assumption occasionally used in the FORM design point method is purely applied at the calibration stage. Once the resistance and load factors are calibrated, it is no longer relevant to the validation studies presented herein.

For each calibration shaft in GROUP ALL, 42 reliability indices can be determined. This calibration/validation exercise is carried out for all the 11 shafts in GROUP ALL, resulting in 42 × 11 = 462 reliability indices. The mean, coefficient of variation, highest value and lowest value of these reliability indices are reported in Table 4 under the column heading "1 shaft". It is worthy to clarify here that Eq. (23) is the same regardless of the RBD calibration approach (FORM – standard or uniform quantile – standard) used. The RBD calibration approach only affects the specific numerical values of the resistance and load factors used in Eq. (23). Note that the reliability index = 4.75 (corresponding to a probability of failure = 10^{-6}) appearing in Table 4 is an *error flag* indicating that the probability of failure is too small and cannot be estimated using the Monte Carlo simulation sample size = 10^6 adopted in this study. This right censorship will affect the mean and coefficient of variation reported in Table 4. In addition, statistical errors associated with Monte Carlo simulation increase with increasing reliability index. For example, probabilities of failure smaller than 10^{-5} are considered unreliable for a sample size = 10^6. Nonetheless, the performance data presented in Table 4 are useful in a qualitative sense to evaluate the performance of LRFD and MRFD formats. The LRFD format calibrated using FORM – standard is commonly adopted in numerous RBD codes in North America. The associated data are shaded in grey, because they provide useful benchmarks to measure the performance of other code formats and other calibration approaches.

Focusing on the column headings "1 shaft" in Table 4, it is apparent that the FORM approach is inferior to the uniform quantile approach. For LRFD, the mean reliability index is larger than 3 because of the ad-hoc lognormal assumption imposed on lumped random variable, S, during RBD calibration. This systematic bias is not present in the uniform quantile calibrated LRFD, because the ad-hoc lognormal assumption is not necessary during RBD calibration. For the FORM approach, the mean reliability index also decreases monotonically in the order LRFD, MRFD2, MRFD3, and MRFD4. It is postulated that this effect is caused by the increasing random dimension in the performance function. This undesirable effect is not present in the uniform quantile approach. The coefficient of variation (c.o.v.) of β is generally higher for the FORM approach as well. It is interesting to observe that the c.o.v. of β reduces more significantly with the size of the calibration domain when the MRFD format is applied.

Table 4. Comparison between FORM – standard and uniform quantile – standard RBD calibration method.

RBD Eq.	FORM – standard			Uniform quantile – standard		
	1 shaft	14 shafts	41 shafts	1 shaft	14 shafts	41 shafts
LRFD						
mean β	3.29	3.38	3.46	2.77	3.03	3.03
c.o.v. β	0.23	0.16	0.16	0.18	0.16	0.15
highest β	4.75	4.75	4.26	3.85	4.01	3.69
Lowest β	1.41	1.80	1.99	1.41	1.62	1.74
MRFD2						
mean β	3.17	3.23	3.25	2.80	3.05	3.01
c.o.v. β	0.25	0.18	0.13	0.20	0.14	0.12
highest β	4.75	4.75	4.01	4.26	4.26	3.54
Lowest β	0.97	0.30	1.90	1.12	1.59	1.72
MRFD3						
mean β	2.49	3.19	3.19	2.50	3.03	3.02
c.o.v. β	0.21	0.21	0.13	0.21	0.15	0.11
highest β	3.62	4.75	4.26	3.63	4.75	3.55
Lowest β	0.92	-0.32	2.06	1.00	1.53	1.86
MRFD4						
mean β	2.41	3.03	3.13	2.63	3.01	3.01
c.o.v. β	0.21	0.21	0.08	0.14	0.09	0.04
highest β	3.28	4.75	3.78	3.45	4.75	3.25
Lowest β	0.70	-0.45	2.19	1.53	2.10	2.72

*Note: Target reliability index = 3; β = 4.75 (corresponding to a probability of failure of 10^{-6}) is just an error flag indicating that the probability of failure is too small and cannot be estimated using the Monte Carlo simulation sample size = 10^6 adopted in this study.

From a practical engineering perspective, the most important index in Table 4 is the lowest reliability index produced by the population of validation shafts. This index describes the departure from the desired target reliability index for the most unconservative design. Both RBD calibration approaches are comparable based on this index. The clear exception is MRFD4, where the uniform quantile approach performs significantly better than the FORM approach. Overall, the degree of reliability control may be deemed unsatisfactory, but this is hardly surprising given that there is only one shaft in the calibration domain and the soil profiles in the validation domain are diverse. It is possible to view the performance under "1 shaft" as worst case, given the rather unreasonable demand of using one shaft to capture the range of diverse shaft and soil conditions.

4.2 *Effect of number of shafts in calibration domain*

It is more realistic to evaluate the performance of the LRFD and MRFD formats using more than one shaft in the calibration domain. Two calibration domains are studied in this section: (1) 14 shafts are selected randomly from the population of 42 shafts for calibration and the resulting resistance and load factors are validated using the remaining 42-14 = 28 shafts and (2) 41 shafts are selected randomly from the population of 42 shafts for calibration and the resulting resistance and load factors are validated using the remaining 42-41= 1 shaft. The former calibration domain ("14 shafts") can be viewed as a practical case, while the latter calibration domain ("41 shafts") is probably a "best case". In contrast, the "1 shaft" example discussed in Section 4.1 is a "worst case".

In general, the resistance and load factors are functions of the shaft and soil conditions. When there is more than one shaft in the calibration domain, it is necessary to deal with the variations in the resistance and load factors arising from *individual* calibration of different shafts. In this study, the resistance and load factors produced by the calibration shafts are predicted via linear regression using the relative side resistance contribution (S_c/S, S_s/S and S_g/S) as explanatory variables. The coefficients of determination of these regression equations are typically higher than 0.9. These regression equations are then applied to estimate the appropriate resistance and load factors for the validation shafts. Note that Phoon et al. (2003b) apply a different strategy of calibrating all the shafts in a group using optimization, rather than calibrating each shaft individually and then applying regression or other methods to reduce the resistance/load factors to a practical form that can be applied to validation shafts.

For each calibration group consisting of 14 shafts, 28 reliability indices can be determined from the validation shafts. This calibration/validation exercise is carried out 20 times by drawing 14 shafts from the population of 42 shafts repeatedly in a random way, resulting in $28 \times 20 = 560$ reliability indices. The mean, coefficient of variation, highest value and lowest value of these reliability indices are reported in Table 4 under the column heading "14 shafts". For each calibration group consisting of 41 shafts, 1 reliability index can be determined from the remaining validation shaft. This calibration/validation exercise can only be carried out 42 times, resulting in $1 \times 42 = 42$ reliability indices. The mean, coefficient of variation, highest value and lowest value of these reliability indices are reported in Table 4 under the column heading "41 shafts".

For the FORM approach, the systematic bias in the mean reliability index cannot be mitigated by increasing the number of shafts in the calibration domain. This is rather obvious as the bias is caused by the ad-hoc lognormal assumption in the case of LRFD and the decreasing mean reliability index from LRFD to MRFD4 is caused by the increasing random dimension. It is also rather obvious that the performance of the LRFD/MRFD formats improves with the number of shafts in the calibration domain. For the uniform quantile approach, the mean, highest β and lowest β converge almost monotonically to the target β with the calibration domain size. This is a desirable result. It provides an assurance that the departures from the target β can be diminished if one is willing to spend efforts to populate the calibration domain. In contrast, the lowest β for the "14 shafts" domain calibrated using FORM can become negative, indicating a probability of failure larger than 50% for the most unconservative validation shaft! This is worse than the lowest β produced by the "1 shaft" calibration domain.

4.3 *FORM – u versus uniform quantile – η*

It has been pointed out that resistance and load factors were developed purely for the practical reason of producing a simplified RBD design equation with the same "look and feel" as existing working stress design equation. For FORM, it is possible to apply the following alternate LRFD approach as given in Eq. (12):

$$\exp\left(\lambda_S + \xi_S u_1^d\right) = \exp\left(\lambda_D + \xi_D u_2^d\right) + \exp\left(\lambda_L + \xi_L u_3^d\right) \tag{24}$$

in which the lognormal parameters (λ_i and ξ_i) are related to the mean (μ_i) and standard deviation (σ_i) of the physical variable as:

$$\lambda_i = \ln(\mu_i) - \frac{1}{2}\xi_i^2$$
$$\xi_i^2 = \ln\left(1 + \frac{\sigma_i^2}{\mu_i^2}\right) \tag{25}$$

The design point in standard space (u_1^d, u_2^d, u_3^d) is determined from a single shaft in Group ALL. The mean dead load for each validation shaft is then computed as:

$$\mu_{LD} = \frac{\mu_S \exp\left(\xi_S u_1^d - 0.5\xi_s^2\right)}{\exp\left(\xi_D u_2^d - 0.5\xi_D^2\right) + \frac{\mu_{LL}}{\mu_{LD}} \exp\left(\xi_L u_3^d - 0.5\xi_L^2\right)} = \frac{\mu_S \exp\left(\xi_S u_1^d - 0.5\xi_s^2\right)}{\exp(\xi_D u_2^d - 0.5\xi_D^2) + 0.5\exp(\xi_L u_3^d - 0.5\xi_L^2)} \tag{26}$$

in which μ_S = mean total side resistance of the *validation* shaft. The design point in standard space (u_1^d, u_2^d, u_3^d) is a vector quantity. At present, there is no simple method of applying the FORM-u calibration approach to more than 1 shaft in the general case. Hence, the results in Table 5 for FORM – u are restricted to the "1 shaft" case.

For the uniform quantile approach, it is possible to apply the following alternate LRFD approach as given in Eq. (21):

$$\exp\left(\lambda_S + \xi_S k_\eta\right) = \exp\left(\lambda_D + \xi_D k_{1-\eta}\right) + \exp\left(\lambda_L + \xi_L k_{1-\eta}\right) \tag{27}$$

in which $k_\eta = \Phi^{-1}(\eta)$ and $k_{1-\eta} = \Phi^{-1}(1-\eta)$. The quantile η can be calibrated from a single shaft. For a calibration domain containing more than one shafts, η can also be predicted via linear regression using the relative side resistance contribution (S_c/S, S_s/S and S_g/S) as explanatory variables. The coefficients of determination of these regression equations are typically higher than 0.9. The mean dead load for each validation shaft is then computed as:

$$\mu_{LD} = \frac{\mu_S \exp\left(\xi_S k_\eta - 0.5\xi_s^2\right)}{\exp\left(\xi_D k_{1-\eta} - 0.5\xi_D^2\right) + \frac{\mu_{LL}}{\mu_{LD}} \exp\left(\xi_L k_{1-\eta} - 0.5\xi_L^2\right)} = \frac{\mu_S \exp\left(\xi_S k_\eta - 0.5\xi_s^2\right)}{\exp(\xi_D k_{1-\eta} - 0.5\xi_D^2) + 0.5\exp(\xi_L k_{1-\eta} - 0.5\xi_L^2)} \tag{28}$$

Eq. (27) and Eq. (28) are presented for conceptual clarity only and for comparison with Eq. (26). In practice, the η quantile of S is estimated directly from Monte Carlo simulation in this study, rather than using the ad-hoc lognormal fit in the above equations.

From the performance data presented in Table 5 below, it is clear that the FORM – u method is slightly better than the FORM – standard method. The margin of improvement is probably not practically significant. On the other hand, the uniform quantile – η is significantly better than the uniform quantile – standard method. It is of practical interest to examine the performance of the "14 shafts" calibration domain. The mean β is almost equal to the target β, the c.o.v is small, and perhaps most importantly, the lowest β is consistently above two. This level of lowest β cannot be achieved consistently even with the best case "41 shafts" calibration domain in Table 4. In Table 5, the performance of the "41 shafts" calibration domain is close to perfect.

There is a practical cost associated with the application of the uniform quantile – η approach that should be highlighted. The engineer is required to perform Monte Carlo simulation to estimate the η quantile of lumped random variables such as S and S_{csg}. The sample size for quantile estimate is typically smaller than that for the probability of failure estimate. For example, if $\eta = 0.05$, a sample size of $10/\eta = 200$ is quite adequate. Hence, the computational cost is not beyond the reach of a PC platform. Nonetheless, the engineer is expected to be comfortable with Monte Carlo simulation. The uniform quantile – standard approach does not require the engineer to perform any Monte Carlo simulation. The code writer

must perform Monte Carlo simulation to produce the resistance and load factors, but once these factors are available, the user only need to calculate a single set of nominal resistances and loads. It is possible to use the uniform quantile – η approach by making an ad-doc lognormal assumption for the lumped resistance, S, as shown in Eq. (28). This obviates the need for the user to carry out Monte Carlo simulation, but the resulting mean β will *not* be unbiased such as that shown in Table 5. The optimum code format associated with the uniform quantile – η approach is possibly the partial factor approach in which the quantile is applied on measured soil parameters, rather than lumped resistance components such as the total side resistance. The quantile for a soil parameter can be estimated directly from a set of measurements without the need to perform Monte Carlo simulation.

Table 5. Comparison between FORM – u and uniform quantile – η RBD calibration method.

RBD Eq.	FORM – u			Uniform quantile – η		
	1 shaft	14 shafts	41 shafts	1 shaft	14 shafts	41 shafts
LRFD						
mean β	3.50	–	–	2.95	3.00	3.00
c.o.v. β	0.12	–	–	0.03	0.03	0.03
highest β	4.75	–	–	3.15	3.18	3.15
Lowest β	2.86	–	–	2.60	2.67	2.68
MRFD2						
mean β	3.01	–	–	2.84	3.02	3.00
c.o.v. β	0.14	–	–	0.14	0.06	0.03
highest β	4.11	–	–	3.67	4.75	3.22
Lowest β	1.04	–	–	2.02	2.65	2.65
MRFD3						
mean β	2.62	–	–	2.59	3.00	3.01
c.o.v. β	0.15	–	–	0.15	0.06	0.05
highest β	3.54	–	–	3.55	4.11	3.32
Lowest β	1.02	–	–	1.68	2.18	2.66
MRFD4						
mean β	2.41	–	–	2.63	3.01	3.01
c.o.v. β	0.21	–	–	0.14	0.06	0.04
highest β	3.31	–	–	3.53	4.75	3.25
Lowest β	0.69	–	–	1.53	2.35	2.74

*Note: Target reliability index = 3; β = 4.75 (corresponding to a probability of failure of 10^{-6}) is just an error flag indicating that the probability of failure is too small and cannot be estimated using the Monte Carlo simulation sample size = 10^6 adopted in this study.

4.4 *"Unexpected" change in the coefficients of variation*

The validation studies conducted in Section 4.1, 4.2, and 4.3 are based on a single set of coefficients of variation for the model errors (ε_{Sc}, ε_{Ss}, ε_{Sg}, ε_{Sr}) and the measurement errors (e_{su}, $e_{\sigma'vs}$, $e_{\sigma'vg}$, e_{qu}). It is of practical interest to evaluate the performance of the code formats calibrated using one set of coefficients of variation when they are applied on validation shafts associated with lower/higher coefficients of variation (c.o.v.s). The c.o.v.s for (ε_{Sc}, ε_{Ss}, ε_{Sg}, ε_{Sr}) and (e_{su}, $e_{\sigma'vs}$, $e_{\sigma'vg}$, e_{qu}) are modified as follows: (1) uniformly reduce all c.ov.s by a factor of 0.5 and (2) uniformly increase all c.o.v.s by a factor of 1.5. The modified c.o.v.s are related to the calculation of side resistances. The c.o.v.s of the dead and live load remain unchanged. The mean live load to mean dead load ratio remains unchanged at 0.5.

It is important to point out that the performance shown in Table 6 (reduce c.o.v.s by 50%) and Table 7 (increase c.o.v.s by 150%) refers to a worst case calibration scenario in which the variations in the c.o.v.s are not included in the calibration shafts. In other words, Table 6 and Table 7 illustrates the performance of LRFD/MRFD formats when they are applied to design scenarios that are "unexpected" and hence, not considered by the code writer. With this observation in mind, it is not surprising that the performance shown in Table 6 and Table 7 are worse than that shown in Table 4 and Table 5. The FORM – standard approach is not robust against unexpected design scenarios, even when the calibration domain contains "41 shafts". It is rather obvious that it is not the total number of calibration shafts that is important per se. In the extreme, one cannot expect the LRFD/MRFD formats to perform adequately if they have been calibrated using say 100 near identical calibration shafts. The outcome is entirely different if

the 100 calibration shafts are carefully selected to cover all expected design scenarios. In some code calibration methods, more commonly encountered design scenarios are assigned more weightage in the calibration domain by using more calibration shafts for instance. For the case of "14 shafts", it is possible to produce bizarre results in which the lowest $\beta = -1.98$ for MRFD3 and lowest $\beta = -1.59$ for MRFD4 when the c.o.v.s are reduced in Table 6. In other words, the designs become even more unconservative, although the underlying uncertainties governing side resistances are smaller!

The uniform quantile – standard approach will produce designs that are safer when c.o.v.s are reduced or designs that are less safe when c.o.v.s are increased. Its behavior is stable in this sense, but it is unable to achieve the prescribed target reliability index under an unexpected change in the c.o.v. that is not considered in the calibration domain. The uniform quantile – η approach is able to accommodate an unexpected change in the c.o.v., particularly when the LRFD/MRFD4 format is adopted. Note the c.o.v. β is lower when LRFD is adopted, but the MRFD4 format produces a mean β closest to the target value.

Table 6. Performance of LRFD/MRFD formats when applied to validation shafts with coefficients of variation of model and measurement errors reduced by **a factor of 0.5**.

RBD Eq.	FORM – standard		Uniform quantile – standard		Uniform quantile – η	
	14 shafts	41 shafts	14 shafts	41 shafts	14 shafts	41 shafts
LRFD						
mean β	4.69	4.69	4.55	4.57	3.39	3.41
c.o.v. β	0.05	0.04	0.09	0.08	0.03	0.03
highest β	4.75	4.75	4.75	4.75	3.62	3.57
Lowest β	3.53	3.71	3.13	3.27	3.06	3.14
MRFD2						
mean β	4.59	4.69	4.60	4.62	3.40	3.19
c.o.v. β	0.12	0.04	0.06	0.06	0.03	0.06
highest β	4.75	4.75	4.75	4.75	3.65	3.58
Lowest β	0.59	3.59	3.13	3.26	3.04	3.00
MRFD3						
mean β	4.40	4.69	4.59	4.64	3.29	3.19
c.o.v. β	0.23	0.04	0.07	0.06	0.05	0.06
highest β	4.75	4.75	4.75	4.75	4.26	3.48
Lowest β	-1.98	3.92	3.00	3.53	2.91	2.72
MRFD4						
mean β	4.49	4.71	4.66	4.69	3.20	3.03
c.o.v. β	0.17	0.03	0.04	0.02	0.11	0.05
highest β	4.75	4.75	4.75	4.75	4.75	3.41
Lowest β	-1.59	4.21	2.57	4.47	1.78	2.68

*Note: Target reliability index = 3; $\beta = 4.75$ (corresponding to a probability of failure of 10^{-6}) is just an error flag indicating that the probability of failure is too small and cannot be estimated using the Monte Carlo simulation sample size = 10^6 adopted in this study.

Table 7. Performance of LRFD/MRFD formats when applied to validation shafts with coefficients of variation of model and measurement errors reduced by a **factor of 1.5**.

RBD Eq.	FORM – standard		Uniform quantile – standard		Uniform quantile – η	
	14 shafts	41 shafts	14 shafts	41 shafts	14 shafts	41 shafts
LRFD						
mean β	2.46	2.39	2.19	2.21	2.77	2.77
c.o.v. β	0.17	0.16	0.17	0.16	0.02	0.02
highest β	3.31	3.08	2.85	2.72	2.87	2.85
Lowest β	1.22	1.34	1.10	1.17	2.52	2.55
MRFD2						
mean β	2.34	2.37	2.17	2.20	2.83	2.81
c.o.v. β	0.16	0.14	0.14	0.13	0.08	0.04
highest β	3.06	2.86	2.75	2.63	4.75	3.38
Lowest β	0.77	1.28	1.05	1.16	2.48	2.52

RBD Eq.	FORM – standard		Uniform quantile – standard		Uniform quantile – η	
	14 shafts	41 shafts	14 shafts	41 shafts	14 shafts	41 shafts
MRFD3						
mean β	2.29	2.32	2.25	2.20	2.87	2.87
c.o.v. β	0.19	0.13	0.17	0.12	0.07	0.05
highest β	3.35	2.77	4.75	2.60	4.11	3.28
Lowest β	-0.54	1.39	1.09	1.24	2.33	2.51
MRFD4						
mean β	2.25	2.28	2.22	2.19	2.98	2.97
c.o.v. β	0.22	0.09	0.12	0.05	0.09	0.05
highest β	4.75	2.73	4.75	2.42	4.75	3.32
Lowest β	-0.15	1.47	1.31	1.97	2.22	2.63

*Note: Target reliability index = 3; β = 4.75 (corresponding to a probability of failure of 10^{-6}) is just an error flag indicating that the probability of failure is too small and cannot be estimated using the Monte Carlo simulation sample size = 10^6 adopted in this study.

4.5 *"Unexpected" change in mean live load to mean dead load ratio, μ_{LL}/μ_{LD}*

The validation studies conducted in Section 4.1, 4.2, and 4.3 are based on a single load ratio, μ_{LL}/μ_{LD} = 0.5. It is of practical interest to evaluate the performance of the code formats calibrated using μ_{LL}/μ_{LD} = 0.5 when they are applied on validation shafts associated with lower/higher load ratios. Two additional load ratios are considered: (1) μ_{LL}/μ_{LD} = 0.1 and (2) μ_{LL}/μ_{LD} = 1.0. The c.o.v.s of all random variables remain unchanged.

Similar to Section 4.4, the performance shown in Table 8 (μ_{LL}/μ_{LD} = 0.1) and Table 9 (μ_{LL}/μ_{LD} = 1.0) refers to a worst case calibration scenario in which variations in the load ratio are "unexpected" and hence, not considered by the code writer. The FORM – standard approach is generally inferior to the uniform quantile – standard approach in terms of robustness against unexpected change in the load ratio. MRFD3 calibrated using FORM – standard and "14 shafts" is the most inferior as it produces a lowest β = -3.43! The uniform quantile – standard approach typically produces a higher c.o.v. β in contrast to the uniform quantile – η approach. – It is of practical interest to note that the negative reliability indices associated with lowest β for some MRFD formats in Table 6 to Table 9 disappear when the calibration domain is enlarged from "14 shafts" to "41 shafts". It is postulated that the MRFD formats require a larger calibration domain than the LRFD format, because it has more degrees of freedom (more resistance factors). It is worthy to reiterate the obvious guideline that the calibration domain should be as large and as representative as possible. It is also judicious to avoid applying LRFD/MRFD formats to design scenarios not covered in the calibration domain.

The performance data shown in Table 6 to Table 9 appear to indicate that the LRFD/MRFD4 format calibrated using the uniform quantile – η approach can produce consistent designs. The MRFD4 format seems to produce the least departures from the target reliability index if the calibration domain is sufficiently large and representative. The LRFD is more stable for a smaller calibration domain, but it is slightly inferior in achieving the target reliability index on the average.

It has been highlighted in Section 4.3 that the uniform quantile – η approach requires the user to perform Monte Carlo simulation to estimate the quantiles of lumped variables. This is practically inconvenient for the user, but given the significantly better performance of the uniform quantile – η approach, it is worth pondering if this approach is a good compromise between conventional multiple factor formats and full probabilistic analysis.

When the uniform quantile – η approach is applied at the level of soil parameters, rather than lumped resistance components, it has been pointed out previously that the user can estimate the required quantiles for design from measured data without performing Monte Carlo simulation in this special case.

Table 8. Performance of LRFD/MRFD formats when applied to validation shafts with mean live load to mean dead load ratio = **0.1**.

RBD Eq.	FORM – standard		Uniform quantile – standard		Uniform quantile – η	
	14 shafts	41 shafts	14 shafts	41 shafts	14 shafts	41 shafts
LRFD						
mean β	3.49	3.43	2.79	2.82	2.84	2.80
c.o.v. β	0.16	0.16	0.16	0.16	0.05	0.02
highest β	4.75	4.75	3.57	3.51	3.85	2.91
Lowest β	1.91	1.95	1.50	1.59	2.51	2.56
MRFD2						
mean β	3.19	3.23	2.89	2.85	2.88	2.84
c.o.v. β	0.18	0.14	0.15	0.13	0.10	0.04
highest β	4.75	4.01	4.75	3.36	4.75	3.17
Lowest β	-0.17	1.85	1.44	1.59	2.46	2.54
MRFD3						
mean β	3.07	3.13	2.89	2.87	2.82	2.87
c.o.v. β	0.30	0.12	0.16	0.12	0.13	0.05
highest β	4.75	3.81	4.75	3.41	4.75	3.17
Lowest β	-3.43	2.01	1.50	1.71	0.72	2.52
MRFD4						
mean β	3.04	3.06	2.94	2.94	2.90	2.89
c.o.v. β	0.22	0.08	0.14	0.14	0.08	0.04
highest β	4.75	3.63	4.75	4.75	4.34	3.12
Lowest β	0.06	2.15	0.56	0.56	2.32	2.63

*Note: Target reliability index = 3; β = 4.75 (corresponding to a probability of failure of 10^{-6}) is just an error flag indicating that the probability of failure is too small and cannot be estimated using the Monte Carlo simulation sample size = 10^6 adopted in this study.

Table 9. Performance of LRFD/MRFD formats when applied to validation shafts with mean live load to mean dead load ratio = **1.0**.

RBD Eq.	FORM – standard		Uniform quantile – standard		Uniform quantile – η	
	14 shafts	41 shafts	14 shafts	41 shafts	14 shafts	41 shafts
LRFD						
mean β	3.41	3.36	3.02	3.07	3.06	3.06
c.o.v. β	0.15	0.14	0.15	0.15	0.03	0.03
highest β	4.75	3.96	3.85	3.75	3.22	3.19
Lowest β	1.86	2.00	1.69	1.82	2.73	2.78
MRFD2						
mean β	3.14	3.21	3.08	3.06	3.03	3.04
c.o.v. β	0.16	0.12	0.13	0.12	0.05	0.04
highest β	4.75	3.84	4.75	3.62	4.26	3.37
Lowest β	0.72	1.93	1.67	1.81	2.70	2.75
MRFD3						
mean β	3.14	3.13	3.01	3.04	3.04	3.02
c.o.v. β	0.22	0.11	0.18	0.11	0.07	0.05
highest β	4.75	3.72	4.75	3.69	4.75	3.35
Lowest β	0.31	2.07	0.55	1.92	2.50	2.69
MRFD4						
mean β	3.07	3.09	3.05	3.01	3.00	3.00
c.o.v. β	0.20	0.08	0.11	0.04	0.06	0.04
highest β	4.75	3.62	4.75	3.31	4.05	3.24
Lowest β	-0.51	2.19	1.15	2.75	2.33	2.76

*Note: Target reliability index = 3; β = 4.75 (corresponding to a probability of failure of 10^{-6}) is just an error flag indicating that the probability of failure is too small and cannot be estimated using the Monte Carlo simulation sample size = 10^6 adopted in this study.

CONCLUSIONS

Simplified RBD equations in the form of LRFD and MRFD formats are increasingly being adopted in geotechnical engineering design codes worldwide. For example, the LRFD format calibrated using the First-Order Reliability Method (FORM) is adopted by AASHTO. The effectiveness of applying these simplified RBD equations to more realistic ground conditions containing multiple strata has not been studied, despite its obvious practical importance. The objective of this paper is to investigate the degree of deviation from the target reliability index produced when LRFD/MRFD equations are applied to a database of forty-two actual drilled shafts installed in soil profiles underlying the city of Taipei, which contain clay, sand, gravel and rock layers or some partial combination thereof.

Two RBD calibration approaches are studied. They are the FORM design point method and the more recently proposed uniform quantile method (Ching & Phoon 2011). The performance of the LRFD/MRFD formats is measured by computing the actual reliability indices produced by validation shafts designed using the code format under evaluation. These reliability indices are summarized using the following statistics: mean, coefficient of variation, highest value, and lowest value. From a practical engineering perspective, the most important statistic is the lowest reliability index produced by the population of validation shafts. This index describes the departure from the desired target reliability index for the most unconservative design.

In general, for soil profiles with multiple layers, conventional formats containing resistance and load factors are unable to achieve the prescribed target reliability index with the same consistency as that reported for homogeneous soil profiles. This is true regardless of the code format (LRFD/MRFD), the RBD calibration approach (FORM or uniform quantile), and the number of values associated with each resistance factor (one value or regression function). For the drilled shaft examples considered in this study, the direct application of quantiles in the RBD equation (uniform quantile – η approach), rather than converting the quantiles to conventional resistance and load factors (uniform quantile – standard approach), appears to deliver the most consistent and most robust performance. Consistency is measured by the ability to achieve the target reliability index on the average with minimum deviation. Robustness is measured by the ability to cater to unexpected design scenarios not covered in the calibration domain.

There is a practical cost associated with the application of the uniform quantile – η approach that should be highlighted. The engineer is required to perform Monte Carlo simulation to estimate the η quantile of lumped random variables such as S and S_{csg}. Some engineers may not be comfortable with Monte Carlo simulation or find it too tedious to perform. The uniform quantile – standard approach does not require the engineer to perform any Monte Carlo simulation. The code writer must perform Monte Carlo simulation to produce the resistance and load factors, but once these factors are available, the user only need to calculate a single set of nominal resistances and loads. This practical cost does not exist if the uniform quantile – η approach is applied to appropriate parameters where the probability distribution is known analytically or empirically. For the former, the MRFD4 format is feasible because the side resistances for each geomaterial type (S_c, S_s, S_g or S_r) happen to be lognormally distributed when the underlying model and measurement errors are normally distributed. For the latter, the partial factor approach in which the quantile is applied on measured soil parameters, rather than lumped resistance components, is feasible. The quantile for a soil parameter can be estimated directly from a set of measurements without the need to perform Monte Carlo simulation.

ACKNOWLEDGMENTS

The lead author would like to thank the Department of Civil Engineering, National Taiwan University for hosting his sabbatical visit.

REFERENCES

Ang, A. H-S. & Tang, W. H. (1984). Probability concepts in engineering planning and design. Vol. 2 (Decision, risk, and reliability), John Wiley & Sons, New York.

Au S. K. & Beck, J. (2001). Estimation of small failure probabilities in high dimensions by subset simulation. Probabilistic Engineering Mechanics, 16(4), 263–77.

British Standards Institute (2002). Eurocode: Basis of structural design. EN 1990:2002, London.

British Standards Institute (2004). Eurocode 7: Geotechnical design – Part 1: General Rules. EN 1997-1:2004, London.

Ching, J.Y. & Phoon, K. K. (2011). A quantile-based approach for calibrating reliability-based partial factors. Structural Safety (in press).
Ching, J. Y., Chen, J. R. & Phoon, K. K. (2011). Multiple resistance factor design for axial compression of drilled shafts. Journal of Geotechnical and Geoenvironmental Engineering, ASCE (under review).
Construction Industry Research & Information Association (1977). Rationalization of safety and serviceability factors in structural codes. Report 63, CIRIA, London.
Ellingwood, B. R., Galambos, T. V., MacGregor, J. G., and Cornell, C. A. (1980). Development of probability-based load criterion for American National Standard A58. Special Publication 577, National Bureau of Standards, Washington.
Moses, F. and Larrabee, R. D. (1988). Calibration of draft RP2A-LRFD for fixed platforms. Proc. 20th Offshore Tech. Conf. (2), Houston, 171-180.
Phoon, K. K., Kulhawy, F. H. & Grigoriu, M. D. (2003a). Development of a reliability-based design framework for transmission line structure foundations. Journal of Geotechnical and Geoenvironmental Engineering, ASCE, 129(9), 798 – 806.
Phoon, K. K., Kulhawy, F. H. & Grigoriu, M. D. (2003b). Multiple resistance factor design (MRFD) for spread foundations. Journal of Geotechnical and Geoenvironmental Engineering, ASCE, 129(9), 807 – 818.
Phoon K. K. (2006). Modeling and simulation of stochastic data", Proc. GeoCongress, ASCE, Atlanta, Feb 26 – Mar 1, 2006.

2 Hazards

ISGSR 2011 - Vogt, Schuppener, Straub & Bräu (eds) - © 2011 Bundesanstalt für Wasserbau ISBN 978-3-939230-01-4

A stochastic approach to rainfall-induced slope failure

P. Arnold
Delft University of Technology, Delft, The Netherlands
University of Manchester, Manchester, United Kingdom

M. A. Hicks
Delft University of Technology, Delft, The Netherlands

ABSTRACT: This paper considers the influence of spatial variability of soil properties on the stability of an unsaturated soil slope during and antecedent to a rainfall event. With water tending to follow a rather tortuous flow path during the infiltration process, slope failures may occur locally due to loss in matric suction with increasing degree of saturation. An elasto-viscoplastic finite element program combined with random field theory is used to analyse the influence of the heterogeneity of the subsoil, as characterised by the point and spatial statistics of the property values. Using a Monte Carlo framework, the results of multiple realisations have been evaluated in terms of reliability as a function of both global factor of safety and time.

Keywords: Heterogeneity, rainfall, reliability, slope stability, unsaturated soil

1 INTRODUCTION

Analysing the stability of soil slopes is one of the oldest tasks in geotechnical engineering. However, even this relatively "simple" task of modelling and analysing the performance of a slope, in a residual soil or as part of a man-made embankment, will become challenging when accounting for the unsaturated state of the soil in interaction with the soil-atmosphere boundary at the ground surface. Changes in moisture content and matric suction as a function of the atmospheric condition directly influence the permeability, stiffness and strength of the subsoil. Thus, in order to address the stability of a soil slope, this boundary needs careful attention. However, the continuing occurrence of slope failures and landslides during or antecedent to rainfall events discloses the need for further investigations.

With the increasing demands of a fast growing world population and developing countries for suitable infrastructures, the design of engineered soil slopes in urban and industrial areas is becoming more required then ever. Since the risk associated with a slope failure may be interpreted as the product of the probability and the consequence, reliability-based methods should be used in order to account for the uncertainties involved within the slope design and construction process. Hence, rather than using the usual "cautious estimate", the risks involved can be individually addressed and quantified.

The degree of uncertainty involved will be influenced by both the *epistemic* (subjective) uncertainty, accounting for the lack of knowledge, e.g. as in sampling, testing and modelling, as well as by the *aleatory* (objective) uncertainty, representing the inherent spatial variability of the subsoil (Helton, 1997). This paper aims to investigate the influence of the second type of uncertainty, that is, due to the subsurface heterogeneity, on the reliability of an unsaturated soil slope subjected to a rainfall event.

Various numerical analyses of rainfall-induced slope failure, in homogeneous unsaturated deposits, have been conducted in recent years, e.g. Cho and Lee (2001), Cai and Ugai (2004), Rahardjo et al. (2007) and Huang and Jia (2009), with reliability-based investigations on unsaturated slope stability being limited to first- and second-order analyses, e.g. Babu and Murthy (2005) and Zhang et al. (2005).

However, even within a moderately heterogeneous soil deposit, failure tends to propagate through the inherent weaker zones. Using random field methodology, the influence of the spatial variability of soil properties on the stability of saturated soil slopes has been investigated for undrained conditions, e.g. by Paice and Griffiths (1997), Hicks and Samy (2002a, 2002b, 2002c, 2004), Griffiths and Fenton (2004) and Hicks and Spencer (2010), for slopes under drained conditions, e.g. Szynakiewicz et al. (2002) and

Griffiths et al. (2009), and for soil slope liqueafaction, e.g. Hicks and Onisiphorou (2005). Random field methodology has also been used by Arnold and Hicks (2010a, 2010b), to analyse the influence of spatial variability of matric suction on unsaturated slope stability under steady state conditions. This paper aims to extend these previous investigations to transient conditions, accounting for the spatial variability of both the soil properties influencing the effective shear strength, as well as those soil properties controlling the infiltration capacity, hydraulic conductivity, water content and thus the local matric suction.

2 METHOD OF ANALYSING RAINFALL-INDUCED SLOPE FAILURE

2.1 *Constitutive model formulation*

In very recent years, several constitutive frameworks have been developed accounting for the direct coupling between the mechanical, hydraulic and thermal behaviour of unsaturated soils. However, the use of sophisticated models is generally accompanied by an increasing number of model parameters, in many cases with a decreasing physical meaning. Due to the scarcety of information on the in-situ variability of soil property data, especially for unsaturated conditions, a rather simple constitutive model formulation has here been applied in order to capture the implications of inherent spatial variability on unsaturated slope failure. For this purpose, the hydraulic model has been implicitly (weakly) coupled with the mechanical model. This means that a change in water content will affect the matric suction and thus the shear strength within the subsoil; however, a change in mechanical properties, such as of the porosity due to a collapse upon wetting and therefore of the hydraulic conductivity, is disregarded in this paper.

Darcy's law is valid for describing flow through an unsaturated soil stratum (Buckingham, 1907), and has been presented in terms of the total head H as the driving potential by Richards (1931). The mass balance equation in mixed form, that is, using the head potential on the driving side and the water content on the residual side, is given by

$$\nabla \cdot K \nabla H + Q = \frac{\partial \theta_w}{\partial t} \tag{1}$$

where K is the hydraulic conductivity, Q is the boundary flux per unit time t, θ_w is the volumetric water content and H is the total head which is the driving potential in moving the water. By assuming a constant gas potential, with the pore-air pressure being equal to the atmospheric condition, and by neglecting the osmotic potential by assuming pure water as the liquid phase, the total head is the sum of the suction head ψ and the elevation head z ($H=\psi+z$). Using the relationships proposed by van Genuchten (1980), in combination with the statistical pore-size distribution relationship by Mualem (1976), θ_w and K can both be computed as functions of the suction head ψ, that is

$$\theta_w = \theta_r + \frac{\theta_s - \theta_r}{\left[1+(\alpha\psi)^n\right]^{1-1/n}} \qquad \text{and} \qquad K = K_s \frac{\left[1-(\alpha\psi)^{n-1}\left[1+(\alpha\psi)^n\right]^{\frac{(1-n)}{n}}\right]^2}{\left[1+(\alpha\psi)^n\right]^{\frac{(n-1)}{2n}}} \tag{2}$$

where θ_s is the volumetric water content at saturation which is equal to the porosity ϕ, θ_r is the residual volumetric water content, α is the inverse of the air-entry suction head ψ_{ae} below which the soil is assumed to behave in a saturated manner, K_s is the saturated hydraulic conductivity and n is the slope of the soil water retention curve about the inflection point.

Bishop's (1959) effective stress concept, combined with a linear elastic, perfectly plastic Mohr-Coulomb type soil model extended to unsaturated conditions, provides the mechanical framework of the model. Hence,

$$\tau_f = c' + (\sigma - u_a)\tan\varphi' + \chi(u_a - u_w)\tan\varphi' \tag{3}$$

where τ_f is the soil shear strength, c' is the effective cohesion, φ' is the effective friction angle, σ is the total stress, u_a and u_w are the pore air and pore water pressure respectively, and (σ-u_a) is the net stress. (u_a-u_w) is the matric suction, which is equal to the suction head times the unit weight of water ($s=-\psi\gamma_w$), and χ is the suction stress parameter, which is a scalar relating to the suction induced effective stress; the product of both, χs, is often referred to as the suction stress. There is an ongoing discussion regarding the definition of χ, since it cannot be measured directly. Of the numerous existing empirical equations,

$$\chi = S_e = \frac{\theta_w - \theta_r}{\theta_s - \theta_r} \tag{4}$$

proposed by Vanapalli et al. (1996) and representing the effective degree of saturation S_e, has been shown to give in most cases an appropriate estimate of the suction stress parameter.

2.2 *Numerical framework*

The constitutive framework has been implemented within a finite element program based on Smith and Griffiths (2004). The suction head values ψ at the nodes are computed by solving Equation 1, using the modified Picard iteration method (Celia et al., 1990) within an implicit Crank-Nicholson time integration scheme. An advantage of this weakly coupled constitutive framework is that the time steps within the seepage and slope stability analyses are independent. At user specified times, the suction head values ψ are used to compute the suction stress χs at the Gaussian integration points of the finite element mesh, for analysing the slope stability. Gravitational loading is applied to the soil slope, in order to generate the in situ stresses. The strength reduction method is utilised to determine the point of failure, which is obtained by gradually reducing the shear strength. The slope stability analysis is thereby performed, whereas the seepage analysis is continuously running in parallel until reaching the next time step specified for a stability analysis.

The net flux applied to the soil-atmosphere boundary is a function of the precipitation, evaporation and run-off. Modelling the evaporation effects is generally quite important when analysing long term and seasonal events, in order to accurately predict the initial conditions prior to a rainfall event, since these have a significant influence on the infiltration capacity of the soil. However, in this investigation a single rainfall event is analysed and the effect of evaporation has not been accounted for. As a function of the moisture content, the infiltration capacity of the surface nodes is calculated interactively. The difference between the precipitation and the net flux is assumed to flow down the slope as run-off and may infiltrate at nodes where the actual infiltration capacity is not utilised by the precipitation. Assuming an efficient drainage system at the right-hand boundary of the domain analysed in this paper, the remaining accumulated run-off is removed at this point from the system.

2.3 *Reliability-based methods*

The local reduction in shear strength accompanying the movement of the wetting front through the subsoil, during and antecedent to a rainfall event, leads to a time dependent factor of safety. Furthermore, the local advancement of this wetting is clearly a function of the spatial variability of the soil properties. As stated by Duncan (2000): “Through regulation or tradition, the same value of safety factor is often applied to conditions that involve widely varying degrees of uncertainty. This is not logical.”

The suction stress, water content and hydraulic conductivity are intrinsically coupled, and are time dependent variables influenced by the changes at the soil-atmosphere boundary. Thus, even the use of a “cautious estimate” of the soil property values within a deterministic analysis may lead to an overestimation of the slope safety. Consequently, the understanding of unsaturated soil mechanics in general and unsaturated slope stability in particular, would benefit from the use of reliability-based design methods.

In order to quantify the uncertainty, approximate first- and second-order probabilistic methods such as the First Order Reliability Method (FORM), Second Order Second Moment (SOSM) method and Point Estimate Method (PEM), as well as the Monte Carlo Method (MCM), are gaining increasing attention in engineering practice. However, by using only the point statistics, usually the mean μ_X as a measure for the central tendency and the variance σ_X^2 as a measure for the variability, of a parameter X_i, the spatial nature of the soil variability is either accounted for in a simplistic manner or possibly not at all. However, since the changes in suction stress are not only a function of time in combination with the applied soil-atmosphere boundary conditions, but also a spatially variable parameter with the water tending to avoid less permeable zones by flowing in a rather torturous manner to follow the path of least resistance, it is important to account for this property within the analysis.

2.4 *Accounting for spatial variability*

The spatial statistics are the scale of fluctuation in the vertical and horizontal directions, $\theta_{X,v}$ and $\theta_{X,h}$ respectively. Vanmarcke (1983) defined the scale of fluctuation as the distance over which X_i is strongly correlated. Thus, the larger the value of θ_X, the more homogeneous the soil deposit.

In this investigation, the heterogeneity within the soil is considered to be moderate. Hence, the aim is to analyse the effect of the spatial variability within what seems to be a homogeneous soil stratum, so that a slope failure will be influenced by local weak zones, rather than by cracks, fractures and layer boundaries implying a strong heterogeneity. Furthermore, the use of the finite element method in analysing unsaturated flow is then straight forward, whereas, in a strongly heterogeneous deposit, more advanced constitutive flow formulations, e.g. double porosity models, would need to be implemented to account for steep hydraulic gradients between, for instance, a crack and the surrounding soil.

In this investigation, fields of random properties are generated using an algorithm based on Local Average Subdivision (Fenton and Vanmarcke, 1990). Based on the spatial statistics, n isotropic standard normal random fields are generated for a square domain through a process of uniform subdivision. Using Cholesky decomposition, the parameters X_i ... X_n are pointwise cross-correlated. A certain degree of anisotropy of the heterogeneity, $\xi_X = \theta_{X,h} / \theta_{X,v}$, may be introduced by squashing and, if required, stretching of the isotropic field, as described by Hicks and Samy (2002b, 2004). The cell values are then transformed to the designated distributions according to μ_X and σ_X^2.

3 EXAMPLE PROBLEM

A 45° slope of height 5m, founded on a firm base at a depth of 10m (Figure 1), has been analysed in 2D assuming plane strain conditions. The problem domain has been discretised using 0.25×0.25m eight-node quadrilateral finite elements for the stability analysis. For the computation of the suction head at any given time, 0.125×0.125m four-node quadrilateral elements have been used. At every user defined time level chosen for analysing the slope stability, the suction stress values are mapped onto the Gaussian integration points of the slope mesh, as shown in Figure 2.

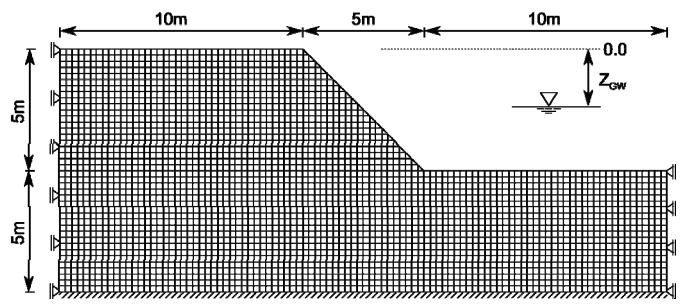

Figure 1. Problem domain, mesh and boundary conditions

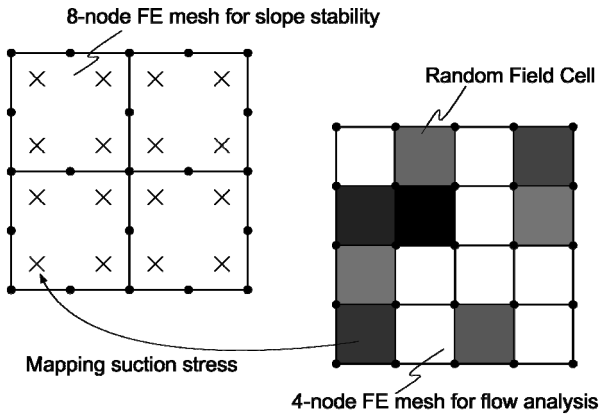

Figure 2. Mapping of the suction stress χs

Although it is generally possible to describe all soil parameters by their point and spatial statistics, in using the implemented constitutive framework for analysing the stability of the unsaturated slope, five predominant parameters have been selected as spatially varying. Specifically, it is assumed that $\tau_f(\boldsymbol{x}) = f(c'(\boldsymbol{x}), \varphi'(\boldsymbol{x}), \phi(\boldsymbol{x}), K_s(\boldsymbol{x}), \alpha(\boldsymbol{x}))$, with the effective shear strength parameters c' and φ' directly influencing the shear strength τ_f, and ϕ, K_s and α indirectly via the suction stress χs. The point statistics and distributions are summarised in Table 1 and are representative of a sandy clayey loam, see e.g. Rawls et al. (1982) and Carsel and Parrish (1988).

It is assumed that c', φ' and ϕ are log-normally distributed, although the low coefficients of variation, $V_X = \sigma_X / \mu_X$, of 0.2, 0.3 and 0.15 respectively suggest that a normal distribution might also be used.

The saturated hydraulic conductivity K_s, as well as the inverse of the air-entry pressure α, are also log-normally distributed, with coefficients of variation of 1.75 and 0.9 respectively.

Table 1. Point statistics and distributions

Material parameter			μ_X	V_X	Distribution
Effective cohesion	c'	[kPa]	10.0	0.2	Log-normal
Effective friction angle	φ'	[°]	25.0	0.3	Log-normal
Porosity	ϕ	[-]	0.4	0.15	Log-normal
Saturated hydraulic conductivity	K_s	[m h^{-1}]	0.0036	1.75	Log-normal
Inverse of the air-entry suction head	α	[m^{-1}]	-1.0	0.9	Log-normal

The "representative" deterministic values assumed for the remaining material parameters are the soil unit weight, $\gamma = 20\text{kN/m}^3$; Young's modulus, $E = 1\times10^5\text{kPa}$; Poisson's ratio, $\nu = 0.3$; dilation angle, $\psi_d = 0°$; slope of the soil-water retention curve, $n = 2.0$; and residual volumetric water content, $\theta_r = 0.08$.

The definition of the covariance structure is one of the key issues in stochastic modelling and is especially difficult for soils; not only the definition of the parameter variance σ_X^2, but mainly the definition of the cross-correlation coefficients $\rho_{Xi,Xj}$ between the parameters is a complex challenge. This is due to the scarcity of data relating to the in situ variability, as well as the difficulty in interpreting the cross-correlative effects on the outcome, e.g. the interpretation of the contributions of c' and φ' to the saturated shear strength.

Based on test results found in literature, a typical correlation matrix $\boldsymbol{R}$ (see Equation 5) has been set up to define the covariance structure for this boundary value problem. Test results mainly show a negative correlation between $\ln(c')$ and $\ln(\varphi')$, here assumed to be -0.5 in the underlying standard normal field; however, this is not always the case, as some results have shown, e.g. Lumb (1970). The strong positive correlation of $\rho_{\ln(\phi),\ln(Ks)} = 0.8$ is reasonable, since the larger the porosity the larger the saturated hydraulic conductivity. Moreover, an increasing porosity is associated with a decreasing air-entry suction head ψ_{ae}, and so a positive correlation for $\rho_{\ln(\phi),\ln(\alpha)} = 0.6$ and implicitly for $\rho_{\ln(Ks),\ln(\alpha)} = 0.5$ is assumed.

Looking at the heterogeneity within a soil layer, for instance, the effective friction angle φ' and the air-entry pressure ψ_{ae} are both more likely to increase in denser zones, that is, with a decreasing porosity ϕ; in contrast, the saturated hydraulic conductivity K_s will tend to decrease. Thus, despite the absence of experimental test data, it seems reasonable to assume some negative correlation between $\ln(\varphi')$ and the inverse of the air-entry pressure $\ln(\alpha)$, as is the case between $\ln(\varphi')$ and $\ln(K_s)$. However, since the correlations between the effective cohesion $\ln(c')$ and $\ln(\phi)$, $\ln(K_s)$ and $\ln(\alpha)$ are not clearly evident from literature, these parameters are assumed to be uncorrelated.

$$\boldsymbol{R} = \begin{bmatrix} 1.0 & -0.5 & 0.0 & 0.0 & 0.0 \\ \rho_{\ln(\varphi'),\ln(c')} & 1.0 & -0.3 & -0.2 & -0.2 \\ \rho_{\ln(\phi),\ln(c')} & \rho_{\ln(\phi),\ln(\varphi')} & 1.0 & 0.8 & 0.6 \\ \rho_{\ln(K_s),\ln(c')} & \rho_{\ln(K_s),\ln(\varphi')} & \rho_{\ln(K_s),\ln(\phi)} & 1.0 & 0.5 \\ \rho_{\ln(\alpha),\ln(c')} & \rho_{\ln(\alpha),\ln(\varphi')} & \rho_{\ln(\alpha),\ln(\phi)} & \rho_{\ln(\alpha),\ln(K_s)} & 1.0 \end{bmatrix} \quad (5)$$

The scale of fluctuation is a function of the geological deposition process and thus it seems reasonable to assume that $\theta_{\ln(c')} = \theta_{\ln(\varphi')} = \theta_{\ln(\phi)} = \theta_{\ln(Ks)} = \theta_{\ln(\alpha)}$ in the underlying standard normal field. A vertical scale of fluctuation of $\theta_{\ln(X),v} = 2\text{m}$ has here been assumed. The influence of the degree of anisotropy of the heterogeneity will be investigated by analysing both isotropic and anisotropic soil property fields, with $\xi_{\ln(X)} = 6$ for the latter.

For the current investigation, the effect of a 48h rainfall event, on the stability of the soil slope shown in Figure 1, is analysed. Using a *Dirichlet-type* boundary condition, a constant suction head of $\psi_{init} = -7.0\text{m}$ is applied to the soil-atmosphere boundary, representing an initially "dry" condition. A constant head of $\psi_{gw} = 0.0\text{m}$ defines the groundwater table, which, in this example, is fixed at the firm base at a depth of $z_{gw} = -10.0\text{m}$. A continuous surface flux of $q_{rain} = 18.0\text{mm h}^{-1}$ is applied as a *Neuman-type* boundray condition for 48h, which is representative of a heavy rainfall event, and this is followed by an antecedent light rainfall event of $q_{ant} = 1.0\text{mm h}^{-1}$, which is representative for a final "wet" condition.

In order to compute the reliability of the soil slope, multiple Monte Carlo simulations are performed in order to obtain a converged solution. The air saturated c'-φ' slope is analysed first: that is, *Case 1*, using only the 2×2 correlation sub-matrix at location North-West in Equation 5.

For a given factor of safety, the reliability of the slope is given by

$$R = 1 - P_f = 1 - \frac{N_f}{N} \tag{6}$$

where P_f is the probability of failure, N is the total number of realisations and N_f is the number of realisations in which the slope fails. Two sets of reliability analyses have been performed for the slope under unsaturated conditions. First, c' and φ' are kept constant at their mean values to analyse only the effect of the spatially variable suction stress on slope stability: that is, *Case 2*, using only the 3×3 correlation submatrix at location South-East in Equation 5. Thereafter, for *Case 3*, a complete analysis with $\tau_f(\boldsymbol{x}) = f(c'(\boldsymbol{x}),\varphi'(\boldsymbol{x}),\phi(\boldsymbol{x}),K_s(\boldsymbol{x}),\alpha(\boldsymbol{x}))$ is performed. Since the factor of safety is variable in time, multiple reliability distributions have been computed in order to quantify reliability R as a function of time t. For this preliminary investigation, 300 Monte Carlo realisations per time step where found to be sufficient to analyse the time dependent structural response in a qualitative manner.

4 DISCUSSION OF RESULTS OF EXAMPLE PROBLEM

Assuming the soil is completely air saturated above the groundwater level, the computed traditional factor of safety based on the mean property values is $FOS_{sat}(\mu) = 1.39$. Figure 3 shows the influence of scale of fluctuation on reliability R versus global factor of safety F for *Case 1*, where F is computed for every Monte Carlo realisation by dividing the traditional factor of safety based on the mean strength values by the factor of safety based on the heterogeneous property field (i.e. $F = FOS_{sat}(\mu) / FOS_{sat}$). It is seen that, for the isotropic and anisotropic fields, most responses are weaker than the deterministic solution based on the property means; that is, with $R < 0.5$ for $F = 1.0$, thereby implying that failure is attracted to the weaker zones. Also, the response distribution becomes wider as the degree of spatial correlation increases, due to each field having a more uniform appearance which leads to a wider range of possible solutions.

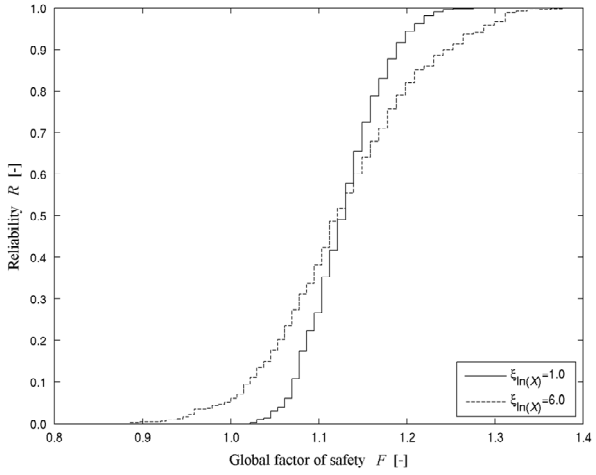

Figure 3: Reliability versus global factor of safety for *Case 1*

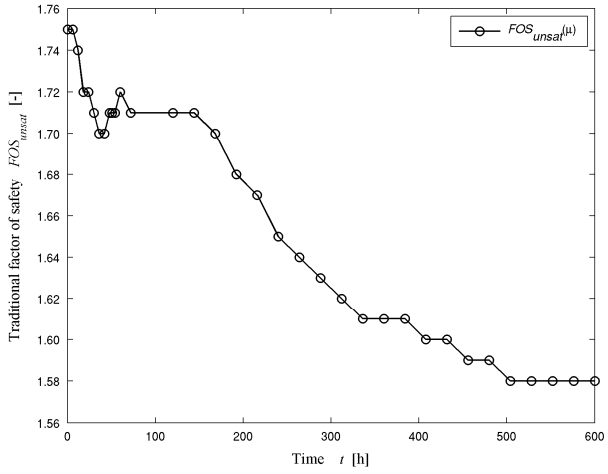

Figure 4. Time dependent factor of safety based only on the mean property values

Based on the deterministic mean property values, Figure 4 shows $FOS_{unsat}(\mu)$ for the soil slope accounting for the unsaturated state as a function of time. At the initial state there is a maximum suction stress of $\chi s \approx 9.71$kPa within the soil, causing the factor of safety to increase from $FOS_{sat}(\mu) = 1.39$ for the air saturated case to $FOS_{unsat}(\mu) = 1.75$. During the 48 hours of heavy rainfall the stability of the slope is only slightly reduced. This is because, firstly, for this sandy clayey loam, the wetting front is moving only slowly through the ground, reaching zones critical for defining the slope failure only antecedent to the rainfall event itself. Secondly, the infiltration capacity reduces quickly as the area close to the surface becomes saturated, leading to run-off and thus to a reduced net influx. Note that, for the current boundary value problem, the matric suction is only temporarily reduced to zero during the heavy rainfall in the local region of the moving wetting front and recovers partly thereafter due to drainage of the soil water. A minimum factor of safety of $FOS_{unsat}(\mu) = 1.58$ for the final wet condition is reached 500h after the start of the heavy rainfall.

For the first 288 hours Figures 5 and 6 summarise, in the form of four contour plots, the reliability $R(t)$ for *Case 2* and *Case 3*. The global factor of safety is now computed by $F(t) = FOS_{unsat}(\mu,t) / FOS_{unsat}(t)$, at every time step specified for the stability analysis. Figure 5 indicates that, for *Case 2*, that is, with only $\chi s(\boldsymbol{x})$ varying and *c'* and φ' fixed to their means, the soil response is stronger relative to the deterministic solution, that is, with $R(t) > 0.5$ for $F(t) = 1.0$. Evaluating the influence of the heterogeneity on the suction stress profile is difficult, since, besides the dependency on the soil properties themselves, χs is largely dependent upon the relative location to the soil-atmosphere boundary and on the elevation above the groundwater level.

Due to the non-linearity of the soil-water retention curve, as well as the positive correlation between $\ln(\phi)$ and $\ln(\alpha)$, the degree of saturation is most likely to be higher in a zone with a lower porosity, that is, for a similar location under the same initially dry steady state conditions. This means that, for a specific suction head value, the effective degree of saturation $S_e = \chi$ (Equation 4) is likely to be higher in a denser zone, thus leading to a higher shear strength than for a soil with mean properties in the same location.

For both the isotropic and anisotropic analyses in *Case 2*, the reliability tends to slightly decrease with time for a certain global factor of safety F, starting from the beginning of the heavy rainfall. This is a consequence of water tending to infiltrate faster through more permeable flow paths, as well as going into storage in the denser zones causing a strength reduction due to the decrease of the initially high suction stresses χs. As for *Case 1*, the variance of the response increases with increasing correlation length.

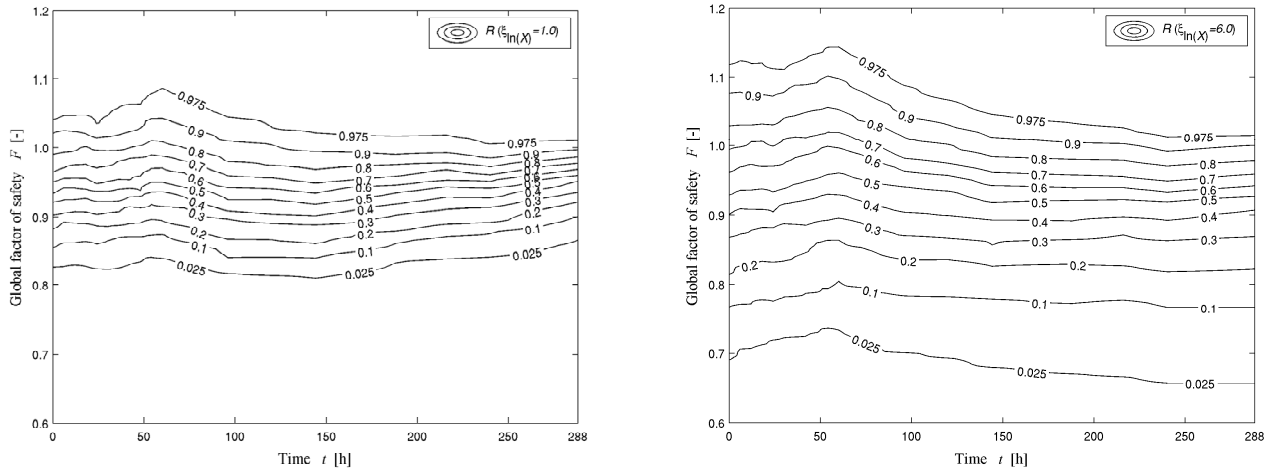

Figure 5. Contour plot of reliability for *Case 2*, for isotropic and anisotropic heterogeneity

From the *Case 3* results in Figure 6, it is evident that, although the soil is gaining some strength due to the spatially variable suction stress (*Case 2*), the response distribution for this example is mainly governed by the spatial variability of the effective shear strength parameters *c'* and φ'. That is, the response based upon the mean properties tends to overestimate the stability of the slope, with R being relatively lower for $\xi_{\ln(X)} = 6$. However the influence of $\chi s(\boldsymbol{x})$ is evident, with R increasing over time for a certain F.

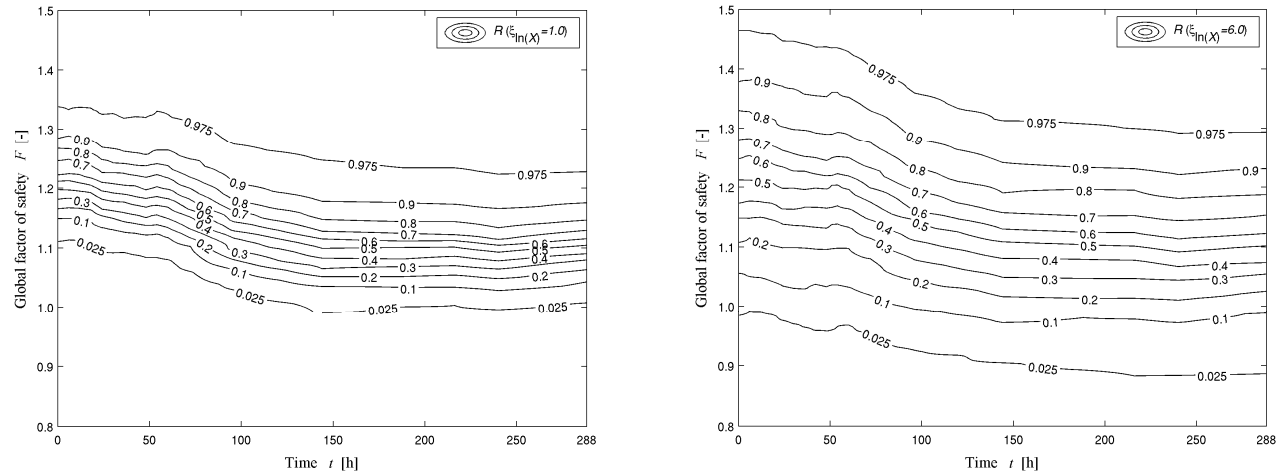

Figure 6. Contour plot of reliability for *Case 3*, for isotropic and anisotropic heterogeneity

5 CONCLUSIONS

The influence of the matric suction on the stability of an unsaturated soil slope has been evaluated accounting for the soil heterogeneity. Based on an example problem it has been shown that, although in this instance the failure is driven by the spatial variability of the effective shear strength parameters, neglecting the influence of the suction stress may lead to an erroneous assessment of the slope reliability.

ACKNOWLEDGEMENTS

This work has been funded by the European Union FP7 Projects IRIS and GEO-INSTALL.

REFERENCES

Arnold, P. and M. A. Hicks (2010a). A stochastic investigation of unsaturated slope stability. In A. Zervos, editor, *Proc.: 18th UK National Conference on Computational Mechanics in Engineering (ACME-UK)*, Southampton, UK, pages 9–12.

Arnold, P. and M. A. Hicks (2010b). Stochastic modelling of unsaturated slope stability. In E. Alonso and A. Gens, editors, *Proc.: Fifth International Conference on Unsaturated Soils (UNSAT)*, Barcelona, Spain, pages 1237–1242.

Babu, S. G. L. and D. S. N. Murthy (2005). Reliability analysis of unsaturated soil slopes. *Journal of Geotechnical and Geoenvironmental Engineering*, 131(11), 1423–1428.

Bishop, A. W. (1959). The principle of effective stress. *Teknisk Ukeblad*, 106(39), 859–863.

Buckingham, E. (1907). Studies on the movement of soil moisture. Technical report, Bulletin 38, USDA, Bureau of Soils, Washington, DC, USA.

Cai, F. and K. Ugai (2004). Numerical analysis of rainfall effects on slope stability. *International Journal of Geomechanics*, 4(2), 69–78.

Carsel, R. F. and R. S. Parrish (1988). Developing joint probability distributions of soil water retention characteristics. *Water Resources Research*, 24(5), 755–769.

Celia, M. A., E. T. Bouloutas, and R. L. Zarba (1990). A general mass-conservative numerical solution for the unsaturated flow equation. *Water Resources Research*, 26(7), 1483–1496.

Cho, S. E. and S. R. Lee (2001). Instability of unsaturated soil slopes due to infiltration. *Computers and Geotechnics*, 28(3), 185–208.

Duncan, J. M. (2000). Factors of safety and reliability in geotechnical engineering. *Journal of Geotechnical and Geoenvironmental Engineering*, 126(4), 307–316.

Fenton, G. A. and E. H. Vanmarcke (1990). Simulation of random fields via local average subdivision. *Journal of Engineering Mechanics, ASCE*, 116(8), 1733–1749.

Griffiths, D. V. and G. A. Fenton (2004). Probabilistic slope stability analysis by finite elements. *Journal of Geotechnical and Geoenvironmental Engineering*, 130(5), 507–518.

Griffiths, D. V., J. Huang, and G. A. Fenton (2009). Influence of spatial variability on slope reliability using 2-D random fields. *Journal of Geotechnical and Geoenvironmental Engineering*, 135(10), 1367–1378.

Helton, J. C. (1997). Uncertainty and sensitivity analysis in the presence of stochastic and subjective uncertainty. *Journal of Statistical Computation and Simulation*, 57(1–4), 3–76.

Hicks, M. A. and C. Onisiphorou (2005). Stochastic evaluation of static liquefaction in a predominantly dilative sand fill. *Géotechnique*, 55(2), 123–133.

Hicks, M. A. and K. Samy (2002a). Influence of anisotropic spatial variability on slope reliability. In G. N. Pande and S. Pietruszczak, editors, *Proc.: 8th International Symposium on Numerical Models in Geomechanics (NUMOG)*, Rome, Italy, pages 535–539.

Hicks, M. A. and K. Samy (2002b). Influence of heterogeneity on undrained clay slope stability. *Quarterly Journal of Engineering Geology and Hydrology*, 35(1), 41–49.

Hicks, M. A. and K. Samy (2002c). Reliability-based characteristic values: A stochastic approach to Eurocode 7. *Ground Engineering*, 35(12), 30–34.

Hicks, M. A. and K. Samy (2004). Stochastic evaluation of heterogeneous slope stability. *Italian Geotechnical Journal*, 38(2), 54–66.

Hicks, M. A. and W. A Spencer (2010). Influence of heterogeneity on the reliability and failure of a long 3D slope. *Computers and Geotechnics*, 37(7–8), 948–955.

Huang, M. and C.-Q. Jia (2009). Strength reduction FEM in stability analysis of soil slopes subjected to transient unsaturated seepage. *Computers and Geotechnics*, 36(1–2), 93–101.

Lumb, P. (1970). Safety factors and the probability distribution of soil strength. *Canadian Geotechnical Journal, 7(3), 225–*242.

Mualem, Y. (1976). A new model for predicting the hydraulic conductivity of unsaturated porous media. *Water Resources Research*, 12(3), 513–522.

Paice, G. M. and D. V. Griffiths (1997). Reliability of an undrained clay slope formed from spatially random soil. In J.-X. Juan, editor, *Proc.: Ninth International Conference on Computer Methods and Advances in Geomechanics (IACMAG)*, Volume 1, Wuhan, China, pages 543–548.

Rahardjo, H., T. H. Ong, R. B. Rezaur and E. C. Leong (2007). Factors controlling instability of homogeneous soil slopes under rainfall. *Journal of Geotechnical and Geoenvironmental Engineering*, 133(12), 1532–1543.

Rawls, W. J., D. L. Brakensiek and K. E. Saxton (1982), Estimating soil water properties. *Transactions of the American Society of Agricultural Engineers*, 25(5), 1316–1320, 1328.

Richards , L. A. (1931). Capillary conduction of liquids through porous mediums. *Journal of Applied Physics*, 1(5), 318–333.

Smith, I. M. and D. V. Griffiths (2004). *Programming the Finite Element Method*. Chichester: John Wiley & Sons.

Szynakiewicz T., D. V. Griffiths and G. A. Fenton (2002). A probabilistic investigation of c', ϕ' slope stability. In C. Muller-Karger et al., editors, *Proc.: 6th International Congress on Numerical Methods in Engineering and Scientific Applications (CIMENICS)*, Caracas, Venezuela, pages 25–36.

van Genuchten, M. T. (1980). A closed-form equation for predicting the hydraulic conductivity of unsaturated soils. *Soil Science Society of America Journal*, 44(5), 892–898.

Vanapalli, S. K., D. G. Fredlund, D. E. Pufahl, and A. W. Clifton (1996). Model for the prediction of shear strength with respect to soil suction. *Canadian Geotechnical Journal*, 33(3), 379–392.

Vanmarcke, E. H. (1983). *Random Fields: Analysis and Synthesis*. Cambridge, Massachusetts: MIT Press.

Zhang, L. L., L. M. Zhang and W. H. Thang (2005). Rainfall-induced slope failure considering variability of soil properties. *Géotechnique*, 55(2), 183–188.

ISGSR 2011 - Vogt, Schuppener, Straub & Bräu (eds) - © 2011 Bundesanstalt für Wasserbau ISBN 978-3-939230-01-4

Influence of foundation embedding on clays shrinkage-swelling hazard consequences

E. Jahangir, O. Deck & F. Masrouri
Laboratoire Environnement Géomécanique & Ouvrages (LAEGO) – INPL, Nancy Université, France

ABSTRACT: Shrinkage-swelling of clayey soils is a natural hazard, which may significantly affect buildings by differential settlements. In this paper we studied the foundation settlement caused by this geohazard for buildings constructed on expansive soils and subjected to a drought period. A soil-structure interaction model was proposed. The hydro-mechanical coupling was taken into account by using the state surface approach. Settlement was evaluated according to foundation depth and a mean building stiffness. The uncertainties related to the choice of the state surface or the environmental factors were considered by using the Monte-Carlo approach. This paper highlights the interest of deeper foundations to reduce the building vulnerability towards this geohazard on expansive soils.

Keywords: Shrinkage-Swelling, Soil Structure Interaction, Foundation depth, Building Stiffness.

1 INTRODUCTION

Shrinkage-swelling of clayey soils is a costly geohazard throughout the world. The study of its impact on buildings for risk management raised many questions, because of the very complex hydro-mechanical behavior of clayey soils and the occurrence of soil-structure interaction phenomena.

The assessment of the ground settlement (or uplift) due to shrinkage (or swelling) under a foundation is a key point to study the building behavior and the associated damages. For clayey unsaturated soils, this ground movement is a consequence of both the variation of suction due to weather conditions (hydraulic part) and the variation of vertical stresses (mechanical part) due to the soil-structure interaction, with a coupling between the hydraulic and mechanical parts. Due to soil spatial variability of hydraulical and mechanical properties, occurrence of shrinkage-swelling hazard of clayey soils leads to differential settlement beneath the foundation which ends up to cracks in facades and structural elements, especially in unreinforced masonry elements.

Vertical stresses transmitted by the building to the ground, change during ground settlement according to the building stiffness. A flexible building could follow the ground settlement with minor changes in the transmitted stresses, while a stiff building can resist and cause a new distribution of the vertical stresses.

The aim of this paper is to study the ground settlements under a foundation during a drying phase, taking into account the hydro-mechanical couplings to investigate the influence of foundation depth.

A simple model of soil-structure interaction was developed. The hydro-mechanical behavior of the soil was modeled by a state surface approach and the building stiffness by its flexural rigidity to take into account the reduction of stresses in the soil during its shrinkage. A Monte Carlo simulation was also applied to consider uncertainties of model's parameters and environmental factors.

2 DESCRIPTION OF THE MODEL

Masonry individual buildings with shallow foundations are most affected by the shrinkage-swelling of clayey soil, as they induce small stresses into the ground and as the maximum suction change occurs near to the surface (ie. near the bottom of foundations).

Generally suction variation is maximum at the extremity of the building, where the soil dries easily, and negligible at its center (figure.1-a). This leads to a differential settlement of the ground and the building between the center and the edges (figure.1-b and c). This differential settlement depends on the building stiffness, the suction variations beneath foundations, the foundation length and the ground hydro-mechanical properties.

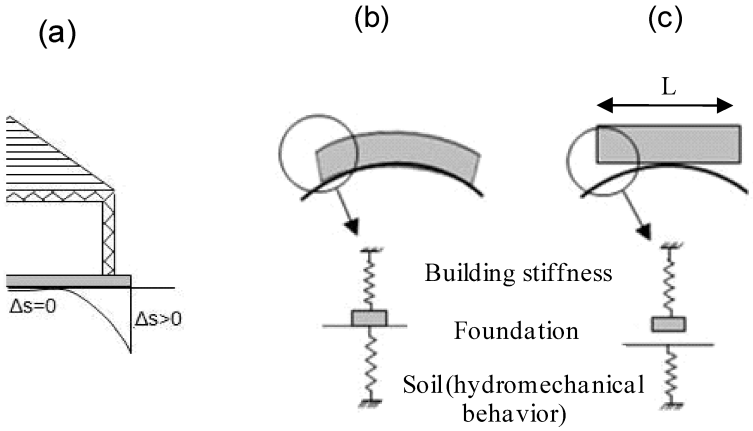

Figure 1. (a) Suction changes at the extremity of building. Soil-foundation interaction and the simplified model for (b) a flexible building, (c) a rigid building.

In this work the soil-foundation interaction at the edge of the building was investigated with a simple model described in figures 1b and 1c. The soil hydro-mechanical behavior was considered with a spring, which is modeled by a state surface (see section 3). The building stiffness is modeled by a spring with a constant stiffness (see section 4). This model is developed to deal with the effect of the foundation depth with respect to the building rigidity on the settlement of a foundation due to a drought period considering all other parameters that may influence the settlement.

In this model the soil was divided into several unit layers with a thickness of h_i = 0.1m, to take into account the suction and the stress variation with depth (Figure 2). The soil shrinkage Δe_i (variation of void ratio) at the middle of each layer is evaluated by the state surface approach taking into account the hydro-mechanical coupling and the soil-structure interaction (section 6). The final settlement of each layer Δh_i is then calculated and the total settlement of the ground surface is obtained with equation 1.

$$\Delta = \sum_{i=1}^{n} \Delta h_i = \sum_{i=1}^{n} h_i \frac{\Delta e_i}{1+e_{0i}} \tag{1}$$

where e_{0i} is the initial void ratio of the layer i, Δe_i the variation of void ratio and h_i the initial thickness of the layer i.

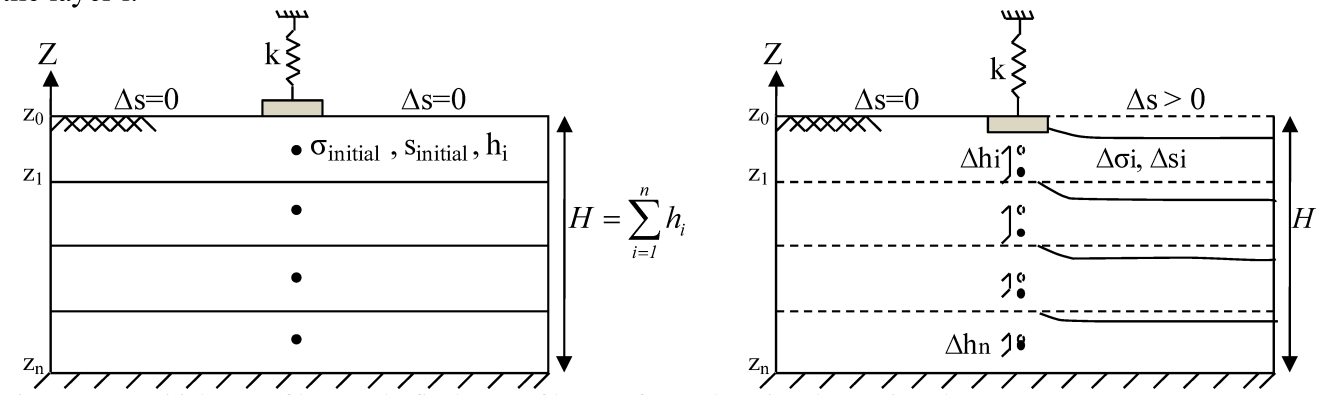

Figure 2. (a) Initial state of layers, (b) final state of layers after undergoing the suction change.

3 MODELING THE HYDRO-MECHANICAL BEHAVIOR OF SWELLING CLAYS

The amplitude of shrinkage-swelling of clayey soils is the sum of two terms: deformation due to the variation of the suction in the soil and deformation due to the changes of vertical stresses applied by the

foundation. In addition, there is a coupling between the hydraulic and mechanical parts. Several authors have highlighted the unsaturated expansive soils hardening; as the increase of the mechanical load decreases the deformations due to the hydraulic variations (Alonso *et al*.2005; Nowamooz 2007; Airo Farulla *et al*.2010).

The influence of hydro-mechanical coupling on the amplitude of settlement under a foundation is modeled with the state surface approach. This concept explains the void ratio e as a function of the net stress $(\sigma\text{-}u_a)$ and the suction $s = (u_a\text{-}u_w)$, where u_a and u_w are respectively the air pressure and the water pressure in the soil and σ is the total stress.

Lloret and Alonso (1985) proposed several analytical functions of state surfaces for different types of slightly plastic soil. Vu (2003) proposed six functions to fit the void ratio constitutive surfaces of an unsaturated expansive soil and tested these functions on swelling clay of Regina (Saskatchewan - Canada). Herein, the function *Unsat-1* was considered because of its reasonable number of parameters (3 parameters) and for its ability to model the experimental results (equation 2).

$$e = a + b\log[1 + (\sigma - u_a) + c(u_a - u_w)] \tag{2}$$

where a is the void ratio at zero net stress and suction. Parameter b controls the total volume change due to suction and stress changes and the parameter c represents the rate of volume change during a variation of suction and may be related to the swelling characteristic of the soil, such as plasticity index (Vu 2003). The fitting parameters a, b, c can be obtained by oedometric or triaxial suction controlled tests.

Three different soils were chosen in this study: the clay of Regina (Vu and Fredlund 2007), the Jossigny silt (Fleureau et al. 2002) and the Boom clay (Alonso et al 1995). Table 1 presents different parameters of the considered state surface *Unsat-1*(equation 1) fitted on the experimental data for the first drying cycle for these three soils. Figure 3 shows the corresponding state surfaces. At the initial state (zero net stress and suction) the Jossigny silt appears to be dense while Regina and Boom clays are loose (parameter a). The Regina clay has a higher parameter c and also a higher value of the plasticity index (40%) than others. Consequently, the Regina clay is more expansive than two other soils and has the highest suction compression index (coefficient of compressibility with respect to suction changes). Among the studied soils, the Boom clay has the lowest coefficient of compressibility with respect to suction change, which means this soil is the less expansive.

Table 1. Numerical values of parameters of the state surface (equation 1), correlation coefficient of the regression, plastic index and dry density of the three investigated soils.

Soil parameters clay	*a*	*b*	*c*	R^2	*Ip(%)*	γ_d *(kN/m³)*
Jossigny silt (Fleureau et *al.* 2002)	1.12	-0.16	0.212	0.893	21	17.4
Regina clay (Vu and Fredlund, 2007)	1.186	-0.092	0.610	0.98	40	15.4
Boom clay (Alonso et al,1995)	1.61	-0.332	0.051	0.94	26.7	14

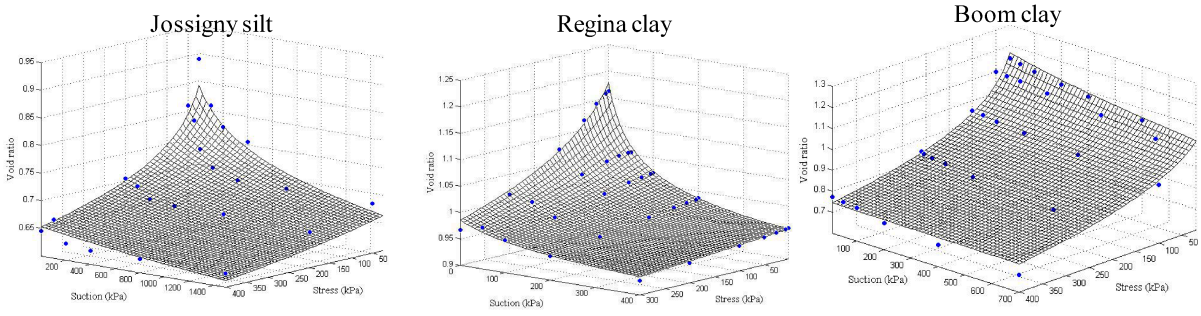

Figure 3. Comparison between experimental data and the fitted state surfaces for three studied soils.

4 MODELING THE BUILDING STIFFNESS AND VERTICAL STRESSES IN THE GROUND

To model the building stiffness, as a first approximation, the building can be considered as a horizontal beam resting on the ground (Figure 1-b and c). Ground shrinkage will lead to a decrease of vertical stresses under the building edges and a transfer of carried loads of the building to other parts of the soil, near the building centre. The final ground settlement Δ under foundations may be calculated by the ap-

proach of the state surface depending on the suction variation of the ground and the building stiffness (Figure 4).

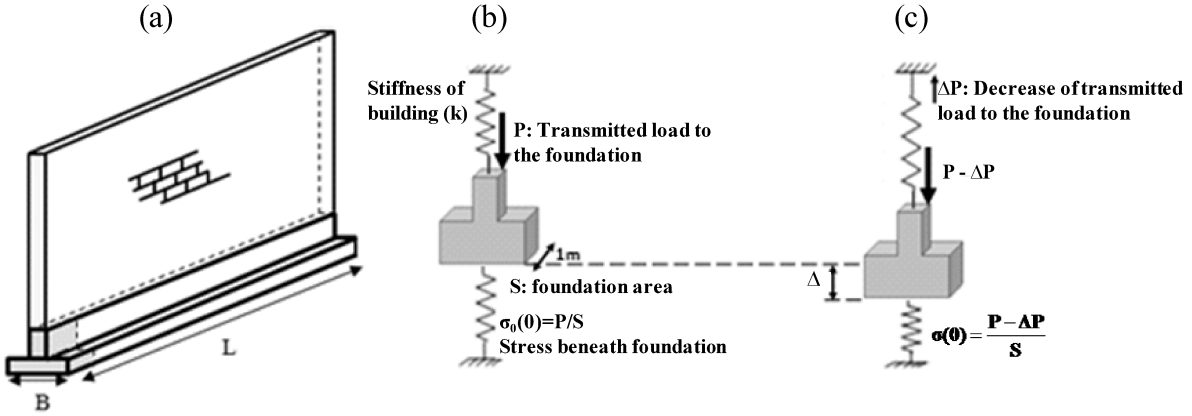

Figure 4. (a) Building flexural rigidity system composed of foundation (strip footing) and wall. Uni-dimensional model to study the soil-structure interaction, (b) initial state, (c) after undergoing the suction change.

The building rigidity system composed of foundation and wall is shown in the figure 4-a. In the proposed uni-dimensional model a length of one meter at the extremity of this rigidity system is isolated (figure 4-b). Then the influence of the structure is modeled by a spring with a characteristic stiffness k to estimate the applied stress variations in soil during its shrinkage (figure 4-c). Estimation of the value of k, which depends on rigidity and geometry of the building, is complex. The stiffness parameter k can be calculated by assuming that the building after undergoing the suction changes, acts as a cantilever beam of a length L/2. The stiffness can then be roughly assessed with EI/L^3, where E is the Young modulus of building, I is the moment of inertia and L the length of building (Frantziskonis and Breysse 2003, Denis 2007). For the calculation of I and E, some authors neglect the masonry wall stiffness compared to the foundation one, while some others take both into account (Bowles, 1997).

Possible values of k may be assessed by considering realistic values of these parameters: E between 5000 and 20 000 MPa (Dimmock and Mair 2008), I between 0.1 m^4 (inertia of the foundation) and 5 m^4 (inertia of both the wall and foundation) and L between 5 and 15m. These result into a range of variation of k between 1MN/m (flexible building) and 5 MN/m (rigid building).

In the first part of calculation a mean building stiffness (2.5 MN/m) was considered to study the effect of foundation embedding towards the occurrence of shrinkage phenomenon. Afterward the uncertainties coming from estimation of building stiffness will be treated in the probabilistic section.

When the foundation follows soil shrinkage (Figure 4-c), the stress in the soil surface can be calculated by equation 3:

$$\Delta P = k \times \Delta$$
$$\sigma(0) = \frac{P - \Delta P}{S} = \frac{P - k \times \Delta}{S} \quad (3)$$

where $\sigma(0)$ is the vertical stress transmitted by the foundation to the ground at zero depth under the foundation, Δ is the settlement due to soil shrinkage, S is the foundation area and P is the building load. For each ground layer under the foundation, vertical stresses are the sum of geostatical and loading stresses. Geostatical stresses $\sigma_{geo}(z)$ are due to the weight of soil and linearly increase with depth (equation 4). Loading stresses $\sigma_{load}(z)$ are due to the building weight and decrease with depth because of the stress diffusion under the foundation. The decrease of stresses in the soil layer with the increase of the depth is calculated with Bousinesq relationship (equation 5).

$$\sigma(z) = \sigma_{load}(z) + \sigma_{geo}(z)$$
$$\sigma_{geo}(z) = \gamma_d \times (z) \quad (4)$$

$$\sigma_{load}(z) = \frac{\sigma(0)LB}{(L+z)(B+z)} = \frac{(\frac{p - k \times \Delta}{S})LB}{(L+z)(B+z)} \quad (5)$$

Where B is the width of the foundation (strip footing), L is the length of the foundation, z is the considered depth under the foundation level and γ_d is the dry density.

5 SUCTION PROFILE

Ground settlement of clayey soils is dependent on the suction profile and increases when the suction increase goes deeper into the ground. Generally the suction change is maximum at the ground surface, where it can reach a few MPa and decreases with depth. The suction profile is dependent on many parameters as: the soil characteristics (nature, structure, particle size, retention curve, permeability etc.), the meteorological parameters (precipitation and evaporation rate) and local conditions as the presence of vegetation etc. To quantify the soil shrinkage and the settlement magnitude, it is necessary to quantify the suction variation and the active depth where the suction change is not negligible under the foundation. In this study a linear suction profile was considered and the uncertainty coming from the suction profile was not taken into account. This problem is explicitly discussed by different authors (Mitchell 1979, McKeen and Johnson 1990,, El-Garhy and Wray 2004, Aubeny and Long 2007, etc). The choice of linear suction profile could be considered as a mean profile by using of equation 6:

$$s(z) = \Delta s(1 - z / z_a) \text{ for } z<z_a \tag{6}$$

where z is the depth; $s(z)$ is the suction value at the depth z; Δs is the magnitude of suction change at the ground surface and z_a is the active depth which is fixed to one meter in this study.

6 RESOLUTION FOR THE CALCULATION OF THE FINAL SETTLEMENT

Calculations of the final equilibrium state and the final settlement of each ground layer may be obtained by combining equations of the state surface (equation 2), of the vertical stresses in each ground layers (equation 5), suction amplitude in each layer (equation 6) and of the layer shrinkage in relation to the change of the void ratio (equation 1). Equation 7 presents the settlement of each layer and the final settlement at the ground surface is the sum of all layer's settlement.

$$\Delta h_i(z) = h_i \times \frac{bLog_{10}(1+\sigma(z)+c\times s(z)) - bLog_{10}(1+\sigma_0(z))}{1+a+bLog_{10}(1+\sigma_0(z))} \tag{7}$$

where $\sigma_0(z)$ is the initial vertical stress at the depth z before any suction variation, calculated with equation 8:

$$\sigma_0(z) = \frac{(P/S)LB}{(z+L)(z+B)} + \sigma_{geo}(z) \tag{8}$$

In this paper the total height H of the clayey soil concerned by the suction variation is divided into 10 sub-layers where the suction value $s(z)$ and the stress state $\sigma(z)$ are determined at the center of each layer.

7 RESULTS

To study the influence of the depth of the foundation over the amplitude of the final settlement, five depths were considered (0 until 0.5m). These shallow depths were taken into account according to a study carried out by Fondasol Company (2009) that showed numerous buildings that have been affected by the drought hazard in France, had the foundation depth lower than 50 cm.

Figure 5-a shows the evolution of the final settlement for the studied soils, for Δs=1MPa and a mean stiffness of 2.5 MN/m. Embedding the foundation in a higher depth avoids its exposition to high suction variations and decreases the final settlement. The more expansive soil (Regina clay) products the higher amplitude of settlement, while the less expansive one (Boom clay) result in smaller settlement. Moreover figure 5-b shows that the influence of the foundation depth is similar for all the studied soils. In other words, the global influence of the foundation depth is not dependant on the ground. For all the studied soils, a 50 cm foundation depth decreases of the final settlement around 70% compared to the case of a zero depth.

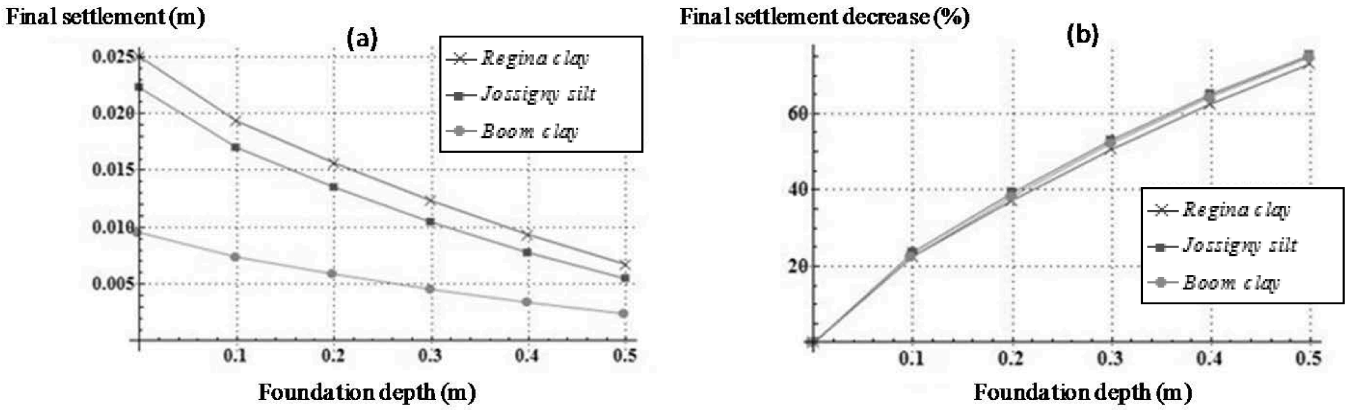

Figure 5. Foundation embedding effect (a) final settlement for the studied soils, (b) percentage of the settlement decrease with depth is similar for all the studied soils.

8 PROBABILISTIC APPROACH

In this section, we consider different uncertainties on the choice of the state surface and its parameters, the building stiffness, environmental factors (as the suction at surface). A Monte-Carlo simulation is then used to assess the variability of the results presented in Fig. 5.

8.1 *Uncertainties due to the choice of the state surface*

Different state surfaces are proposed in the literature (Lloret & Alonso; 1985, Vu & Fredlund; 2007, etc.). Herein four state surfaces were considered (one already used in the previous section) and fitted on experimental data of the three studied soils. Mathematical expressions of the state surfaces and final fitted parameters are shown in table 2. Four calculations were performed considering the different state surfaces of table 2. Results of the final settlement are plotted in Figure 6-a with the standard deviations bar. These results show that the final settlement value can be overestimated or underestimated depending on the chosen state surface. Figure 6-b shows that the mean value of the percentage of settlement decrease is less important for the less expansive soil (Boom clay), with a maximal value of 60% and can rise until 75% for the most expansive soil (Regina clay).

Table 2. Numerical values of parameters for the four considered state surfaces and the three investigated soils.

	Function	Fitting Parameters		
		Jossigny silt	Regina clay	Boom Clay
Fredlund (1979)	$e = a + b\log(\sigma - u_a) + c\log(u_a - u_w)$	a =1.12; b = -0.165; c = -0.035	a =1.186; b = -0.063; c = -0.041	a =1.61; b = -0.301; c = -0.041
Lloret & Alonso (1985)	$e = a + b\log(\sigma - u_a) + c\log(u_a - u_w) + d\log(\sigma - u_a)\log(u_a - u_w)$	a =1.12; b = -0.1767; c = -0.093; d = 0.006	a =1.186; b = -0.091; c = -0.083; d = 0.034	a =1.61; b = -0.300; c = -0.039; d = 0.001
Vu -a(2003)	$e = a + b\log(1 + (\sigma - u_a) + c(u_a - u_w))$	a =1.12; b = -0.180; c = 0.228	a =1.186; b = -0.092; c = 0.610	a =1.61; b = -0.332; c = 0.051
Vu-b (2003)	$e = a + b\log\left[\frac{1 + c(\sigma - u_a) + d(u_a - u_w)}{1 + f(\sigma - u_a) + g(u_a - u_w)}\right]$	a = 1.12; b = -0.246; c = 0.358; d = 0.144; f = 0.001; g = 0.001	a = 1.186; b = -0.2763; c = 0.097; d = 0.015; f = 0.013; g = 6.317×10^{-5}	a = 1.61; b = -0.358; c = 0.632; d = 0.042; f = 2.22×10^{-14}; g = 2.22×10^{-14}

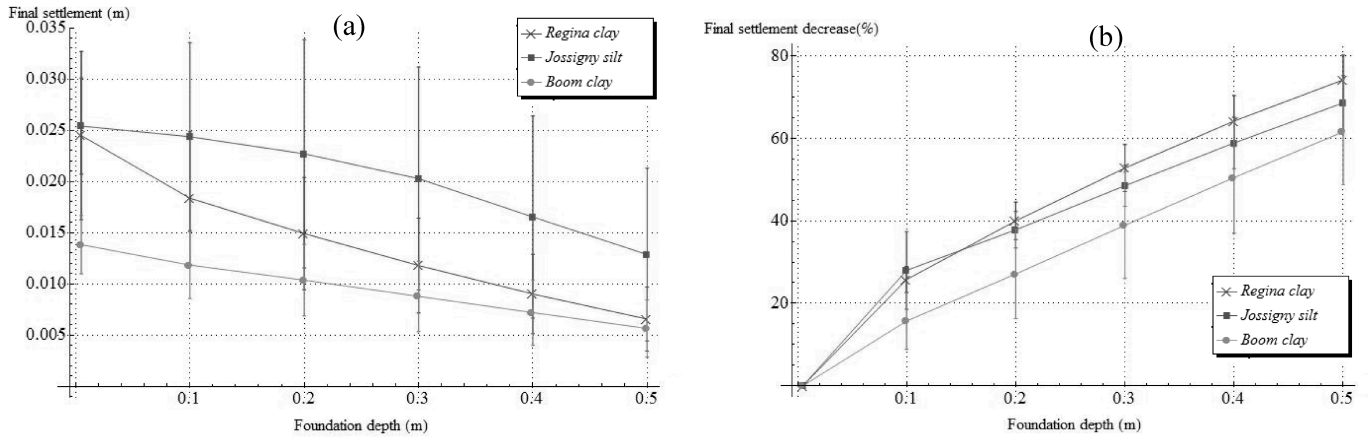

Figure 6. Considering the uncertainty coming from the choice of state surface (a) final settlement for the studied soils, (b) mean value of the percentage of settlement decrease with augmentation of foundation embedding depth.

8.2 *All parameters variability*

In this section the variability of all parameters was considered, including the building stiffness (between 1 and 5MN/m; see section 4), the type of state surface, and the variation of suction at the soil surface. The variation of suction at the ground surface is considered between 0.5 MPa (usual drought period) and 2 MPa (exceptional drought period, Long; 2006). A Monte-Carlo simulation was performed 1000 times for a triangular statistical distribution considering suction changes and building stiffness variations. For each simulation the state surface type was chosen randomly.

Figure 7-a, shows the average value and the standard deviation of final settlement with the foundation depth. The foundation depth appears to have an important effect on the decrease of the settlement amplitude for all studied soils considering all uncertainties of model. For the most expansive soil this effect is more significant.

Figure 7-b illustrates the percentage of settlement decrease, which could rise to 70% for the most expansive soil and to 60% for less expansive ones considering an increase of foundation depth from 0 to 50 cm.

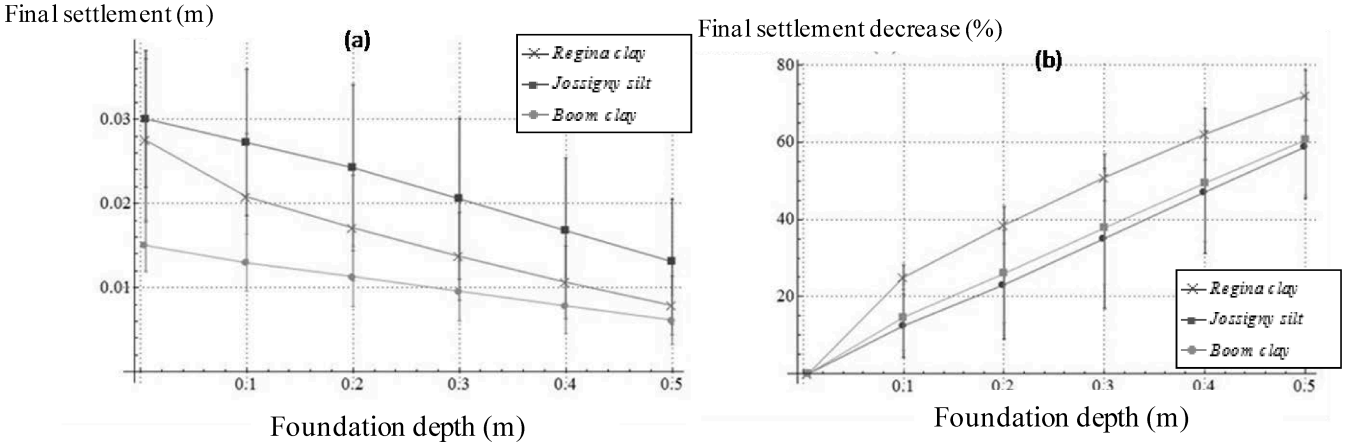

Figure 7. Considering the uncertainty coming from the variability of all the parameters of model, (a) final settlement, (b) Percentage of settlement decrease with augmentation of foundation embedding depth.

9 CONCLUSIONS

A simple method was developed to investigate shrinkage-swelling and soil-structure interaction for clayey soils. This methodology considers the hydro-mechanical coupling of unsaturated clayey soils with the state surface approach, and allows assessing the settlement under foundation due to a drought in relation to the building stiffness, suction vertical profile, suction change intensity and depth of foundation.

Investigation of the influence of foundation depth showed that the increase of the foundation embedding depth, from 0 to 50cm can decrease the amplitude of potential settlement due to drought of about 60 % to 70 % for respectively less expansive and very expansive soils. The results of probabilistic analysis were in agreement with the general effect of foundation embedding depth on the amplitude of settle-

ment due to shrinkage. The model can also be used to estimate the mean value of the final settlement for a group of buildings having the same stiffness and foundation depth, constructed on a site with soil characteristics that displays small variability, and undergoing a drought period.

REFERENCES

Aubeny C. and Long X. (2007). Moisture diffusion in shallow clay masses, Journal of Geotechnical and Geoenvironmental engineering, 133(10), 1241-1248.

Airo Fraulla C., Ferrari A., Romero E. (2010) Volume change behaviour of a compacted scaly clay during cyclic suction changes. Can. Geotech. J. n°47, 668-703.

Alonso, E.E., Lloret, A., Gens, A., Yang, D.Q., 1995. Experimental behaviour of higly expansive double-structure clay- Proc. 1st Int. Conf. on Unsaturated Soils Vol. 1. Balkema, Paris, pp. 11–16.

Alonso E.E., Romero E., Hoffmann C., Garcia-Escudero E. (2005). Expansive bentonite-sand mixtures in cyclic controlled-suction drying and wetting. Engineering Geology, 81, 213-226.

Bowles J.E. (1997). Foundation Analysis and Design, McGraw-Hill Companies, Fifth edition.

Denis A., Elachachi S.M., Niandou H., Chrétien M. (2007). Influence du retrait et de la variabilité naturelle des sols argileux sur le comportement des fondations des maisons individuelles, Revue Française de Géotechnique, n°120-121, 165-174.

Dimmock P.S, Mair R.J. (2008). Effect of building stiffness on tunneling-induced ground movement. Tunnelling and Underground Space Technology, 23, 438-450.

El-Garhy B.M., Wrray W.K., (2004). Method for calculating the edge moisture variation distance. Journal of Geotechnical and Geoenvironmental Engineering, 130, 945-955.

Frantziskonis G., Breysse D. (2003). Influence of soil variability on differential settlements of structures, Computers and Geotechnics 30, 217-230.

Fleureau J.M., Verbrugge J.C., Huegro P.J., Correia A.G., Kheirbek-saoud S. (2002), Aspects of the behaviour of compacted clayey soils on drying and wetting paths, Canadian Geotechnical Journal, Vol 39, 1341-1357.

Fondasol (2009). Projet ARGIC, Tâche 6, Analyse de dossiers d'études géotechniques de pathologie liée à la séchresse et typologie des désordres, Rapport final, Marrlock C., Jaquard C.

Lloret A., Alonso E.E.,(1985). State surfaces for partially saturated soils, In: Proceedings 11th International Conference on Soil Mechanics and Foundation Engineering, vol. 2, San Francisco, 557-562.

Long X. (2006) Prediction of shear strength and vertical movement due to moisture diffusion through expansive soils. Ph.D thesis of TEXAS A&M University

Nowamooz H., (2007). Retrait/gonflement des sols argileux compactés et naturels, Thèse de l'INPL-Nancy.

McKeen R. G., Johnson, L.D (1990). Climate-controlles soil design parameters for mat Foundations. Journal of Geotechnical engineering 116(7): 1073-1094.

Mitchell P.W., (1979). The structural analysis of footing on expansive soil. Research Report No.1, Adelide, South Australia.

Vu H.Q. and Fredlund D.G., (2007) Challenges to modeling heave in expansive soils, Canadian Journal of Geotechnics, n° 43, 1249-1272.

Vu H.Q (2003). Uncoupled and coupled solutions of volume change problems in expansive soils. Thesis University of Saskatchewan.

ISGSR 2011 - Vogt, Schuppener, Straub & Bräu (eds) - © 2011 Bundesanstalt für Wasserbau ISBN 978-3-939230-01-4

Mitigation of liquefaction seismic risk by preloading

F. Lopez-Caballero & A. Modaressi-Farahmand-Razavi
Laboratoire MSS-Mat CNRS UMR 8579, Ecole Centrale Paris, Châtenay-Malabry, France

ABSTRACT: The present paper deals with the use of numerical methods so as to assess the efficiency of an improvement method to reduce the liquefaction potential in a sandy soil profile subjected to shaking. The objective is to reveal the beneficial or unfavorable effects of preloading method on the soil response. This analysis shows the efficiency of the preloading in the mitigation of a liquefiable soil but the intervention at the foundation soil modifies the dynamic characteristics of the signal at surface.

Keywords: Liquefaction, Mitigation Methods, Numerical simulation

1 INTRODUCTION

In practice, in order to mitigate the damage effects of earthquake induced liquefaction in engineering structures, the countermeasure methods such as gravel drains, soil densification or confinement walls among others are used. Such methods are studied by several authors and the principal conclusion of these works is that the efficiency of each solution depends on many parameters (e.g. input signal characteristic, soil properties).

The aim of this work is to assess numerically the efficiency of the soil densification using preloading techniques on the improvement of liquefiable sandy profiles to shaking. Preloading is a temporary loading, usually an embankment, applied at a construction site to improve subsurface soils by densification and increase in lateral stress. For construction sites where sandy layers are predominant, experience has illustrated that about three weeks suffice for soil improvement to take place. The method is frequently used to improve bad soil conditions and make them sustain large static loads (Stamatopoulos and Kotzias, 1985; Petridis et al., 2000).

A finite element modelling is carried out in order to study the influence of the input motion on both the response of the soil profile and the possibility that liquefaction phenomena appear. An elastoplastic multimechanism model is used to represent the soil behaviour. A numerical probabilistic analysis is performed so as to quantify the impact of the uncertainties associated with the input signal and the mitigation method on both the ground motion at the surface and the apparition of liquefaction phenomena. Thus, a liquefaction reliability index profile can be obtained for the profile with or without mitigation for a given seismic hazard.

2 NUMERICAL MODEL

A typical layered soil/rock model is considered. The soil profile is composed principally of clay layers overlaid by 22m of loose sand (i.e. a relative density Dr < 50%). The total thickness of the soil profile is 40m over the bedrock. The numerical model is based on the site measurement of SPT-N_{60} and shear wave velocities (Vs) given in Figure 1 (Lopez-Caballero and Modaressi-Farahmand-Razavi, 2008). The fundamental elastic period of the soil profile is 0.57s. According to the SPT test results and the soil description, it is deduced that the liquefaction phenomena can appear at layers between 4m and 15m depth (SPT-N_{60} between 4 and 10) as from 22m depth the soil is composed principally of overconsolidated clay.

Thus, an elastoplastic model is only used to represent the soil behaviour on the top 29m. In these layers, the shear modulus of the soil increases with depth. For the soil between 29m and 40m, isotropic linear elastic soil behaviour is assumed. The deformable bedrock is placed at 40m depth.

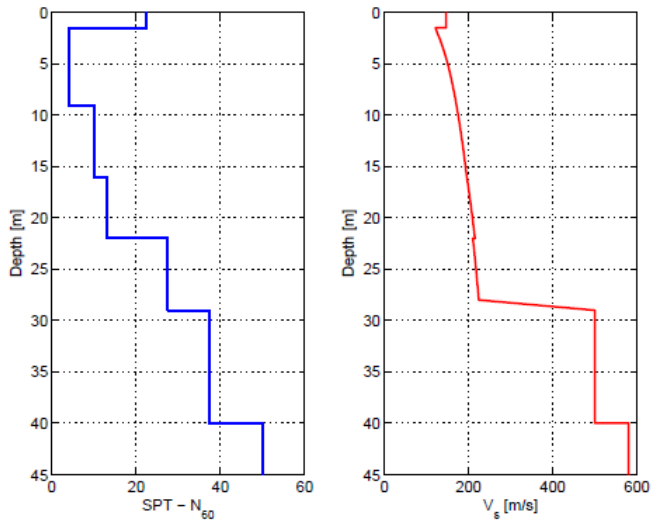

Figure 1. SPT and S velocity profiles of the site and adopted in the numerical analysis.

2D u-p_w coupled finite elements computations with plane-strain assumption are performed. The saturated soil was modelled using quadrilateral isoparametric elements with eight nodes for both solid displacements and fluid pressures. The thickness of the plane-strain elements is 0.5m. An implicit Newmark numerical integration scheme with γ=0.625 and β=0.375 is used in the dynamic analysis (Katona and Zienkiewicz, 1985).

In order to investigate the effect of the preloading method on the response of the soil profile, a comparative dynamical response analysis at the end of shaking for the cases with and without mitigation method is done.

2.1 *Boundary conditions*

In the analysis, only vertically incident shear waves are introduced into the domain and as the response of an infinite semi-space is modelled, equivalent boundaries have been imposed on the nodes of lateral boundaries (i.e. the normal stress on these boundaries remains constant and the displacements of nodes at the same depth in two opposite lateral boundaries are the same in all directions). For the bedrock's boundary condition, paraxial elements simulating“deformable unbounded elastic bedrock” have been used (Modaressi and Benzenati, 1994). The incident waves, defined at the outcropping bedrock are introduced into the base of the model after deconvolution. Thus, the obtained movement at the bedrock is composed of the incident waves and the reflected signal. The bedrock is supposed to be impervious and the water level is placed at the ground surface.

2.2 *Soil model*

The elastoplastic multi-mechanism model developed at Ecole Centrale Paris, known as ECP model (Aubry et al. 1982; Hujeux, 1985) is used to represent the soil behaviour. This model can take into account the soil behaviour in a large range of deformations. The model is written in terms of effective stress. The representation of all irreversible phenomena is made by four coupled elementary plastic mechanisms: three plane-strain deviatoric plastic deformation mechanisms in three orthogonal planes and an isotropic one. The model uses a Coulomb-type failure criterion and the critical state concept. The evolution of hardening is based on the plastic strain (deviatoric and volumetric strain for the deviatoric mechanisms and volumetric strain for the isotropic one). To take into account the cyclic behaviour a kinematical hardening based on the state variables at the last load reversal is used. The soil behaviour is decomposed into pseudo-elastic, hysteretic and mobilized domains. Refer to (Aubry et al. 1982; Hujeux 1985; Lopez-Caballero and Modaressi-Farahmand-Razavi, 2008) among others for further details about the ECP model. For sake of brevity only some models' definitions are given in what follows. Adopting the soil

mechanics sign convention (compression positive), the deviatoric primary yield surface of the *k* plane is given by:

$$f_k = q_k - \sin\phi'_{pp} \cdot p'_k \cdot F_k \cdot r_k \qquad (1)$$

Where, p'_k and q_k are the mean and deviatoric values of stress tensors, ϕ'_{pp} is the friction angle at the critical state, the function F_k permits to control the isotropic hardening associated with the plastic volumetric strain, whereas r_k accounts for the isotropic hardening generated by plastic shearing. They represent progressive friction mobilization in the soil and their product reaches unity at perfect plasticity. Therefore, in order to provide for any state a direct measure of "distance to reach the critical state" (r_k) and based upon our elastoplastic model, it is possible to define an apparent friction angle (ϕ'_{apt}) by:

$$\sin\phi'_{apt} = \frac{q_k}{p'_k \cdot F_k} \qquad (2)$$

$$r_k = \frac{\sin\phi'_{apt}}{\sin\phi'_{pp}} \qquad (3)$$

2.3 *Input earthquake motion*

In order to define appropriate input motions to the non-linear coupled dynamical analysis, a selection of recorded accelerograms is used. The adopted earthquake signals are proposed by (Iervolino and Cornell, 2005; Sorrentino et al. 2008). Thus, 142 unscaled records were chosen from the Pacific Earthquake Engineering Research Center (PEER) database. The events range in magnitude between 5.2 and 7.6 and the recordings are at site-to-source distances from 15 to 50km and dense-to-firm soil conditions (i.e. 360m/s < $V_{s\ 30m}$ < 800m/s).

Concerning the response spectra of input earthquake motions, Figure 2 shows the mean and the response spectra curves with a probability of exceedance (PE) between 2.75 and 97.5%. It can be noted that the mean response spectra is consistent with the response spectra of Type A soil of Eurocode8 scaled to the mean outcropping a_{max} value. The uncertainty on some input earthquake characteristics obtained for the strong ground motions are summarized in Table 1. These earthquake characteristics are maximal outcropping acceleration (a_{max}), Arias intensity (I_{Arias}), predominant period (Tp), mean period (Tm), period of equivalent harmonic wave ($T_{V/A}$=α pgv/pga), spectral intensity (SI), peak ground velocity (pgv), root-mean-square intensity (I_{rms}), Cosenza and Manfredi dimensionless index (I_D) and the significant duration ($t_{5\ 95}$).

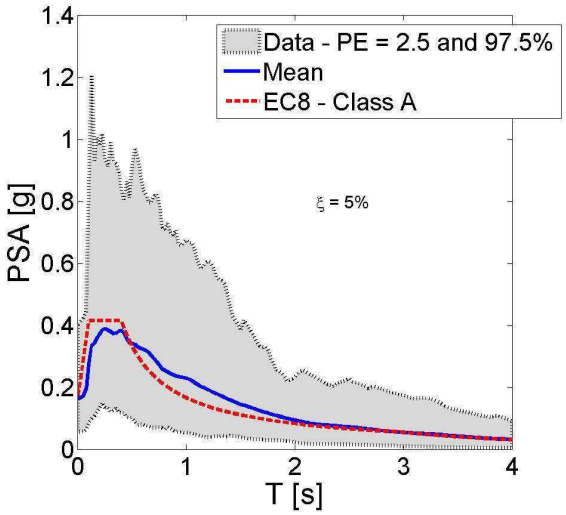

Figure 2. Response spectra of input earthquake motions

Table 1. Uncertain earthquake characteristics for the selected earthquakes

Parameter	Range	Mean	CV [%]
a_{max} [g]	0.04-0.60	0.17	56
Tm [s]	0.28-1.46	0.66	34
Tp [s]	0.10-1.10	0.37	58
$T_{V/A}$ [s]	0.23-1.43	0.58	38
I_{Arias} [m/s]	0.03-5.90	0.59	131
$t_{5\,95}$ [s]	4.40-51.4	19.0	44
I_{rms} [m/s^2]	0.10-1.21	0.26	55
pgv [m/s]	0.03-0.62	0.19	58
I_D [.]	2.97-27.3	10.5	45
SI [m]	0.12-2.52	0.70	57

2.4 *Preloading simulation*

In order to simulate the construction and demolition of the preload embankment, the calculations are performed in two steps. In the first step, since soil behaviour is a function of the effective stress state for nonlinear elastoplastic models, initial in-situ stress state due to gravity loads are computed. After this initialization, the displacements and deformations are eliminated and the initial effective stresses, pore-water pressures and model history variables are stored to be used as initial state of the second step computation. In the second one, a sequential level-by-level construction and demolition of the embankment is performed.

The embankment load is applied as a prescribed normal stress time history at the surface of soil profile. In order to assess the effect of static load applied on the response of the soil profile, two embankment heights were studied, 4 and 8m with a density equal to 2400kg/m^3. The embankment is constructed and demolished in 18.5 days and it stays in place during 3 months before the application of the seismic event. After this period, all over pore pressures are dissipated.

3 LIQUEFACTION ANALYSIS

In order to define the liquefaction reference case, the responses obtained by the model without preloading are analysed. It can be noted from the pore pressure excess (Δp_w) in the soil profile obtained at the end of the signal (i.e. coseismic analyses) for all simulations (Figure 3), that regarding the mean response obtained, the liquefaction phenomenon does not occur (i.e. $\Delta p_w < \sigma'_{vo}$). Otherwise, concerning all simulations, in some cases the apparition of liquefaction is found at layers between 2 and 15m depth. Assuming that the liquefaction appears when the pore pressure ratio ($r_u=\Delta p_w/\sigma'_{vo}$) is greater than 0.8, a liquefaction probability profile could be estimated. The liquefaction probability is estimated as $p_f(z)=N_f(z)/N$, where $N_f(z)$ is the number of simulations when $r_u \geq 0.8$ at depth z and N is the total number of simulations. Using this approach, a profile of Prob[$r_u \geq 0.8$] as a function of depth is presented in Figure 4. According to these results, the maximum liquefaction probability is 32% between 4 and 6m deep.

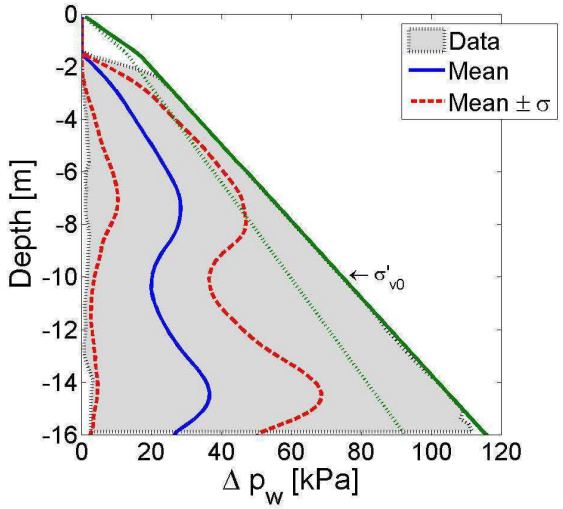

Figure 3. Obtained pore pressure excess in the soil profile

So as to quantify the effect of the liquefaction phenomena, we use the computed Liquefaction Index (Q) for the profile. This parameter is defined by Shinozuka and Ohtomo (1989) as:

$$Q = \frac{1}{H}\int_0^H \frac{\Delta p_w(t,z)}{\sigma'_{vo}(z)}\,dz \qquad (4)$$

where H is the selected depth (in this case, H=10m), $\Delta p_w(t, z)$ is the pore water pressure build-up computed at time t and depth z and $\sigma'_{vo}(z)$ is the initial effective vertical stress at depth z. Figure 5 provides the variation of Q value at the end of shaking with maximum acceleration at the outcropping bedrock ($a_{max\ out}$). Referring again to Figure 5, it can be seen that as expected, the $Q_{H=10m}$ value increases with an increase in $a_{max\ out}$ value. It appears that $a_{max\ out}$ value provides a good correlation with the thickness of the zones where liquefaction takes place (i.e. the liquefaction index).

In order to study the effect of the random shaking on the amplitude of the acceleration obtained at the surface level, Figure 6 shows the variation of peak ground acceleration at the surface (pga) as a function of the maximum acceleration at the outcropping bedrock ($a_{max\ out}$). According to this figure, the amplification of peak ground acceleration on the ground surface relative to bedrock appears before $a_{max\ out}$ value equal to 0.12g.

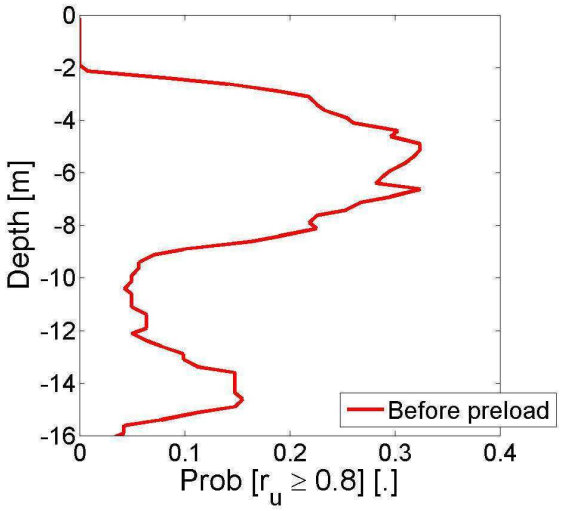

Figure 4. Evolution of liquefaction probability with depth. Case before preloading.

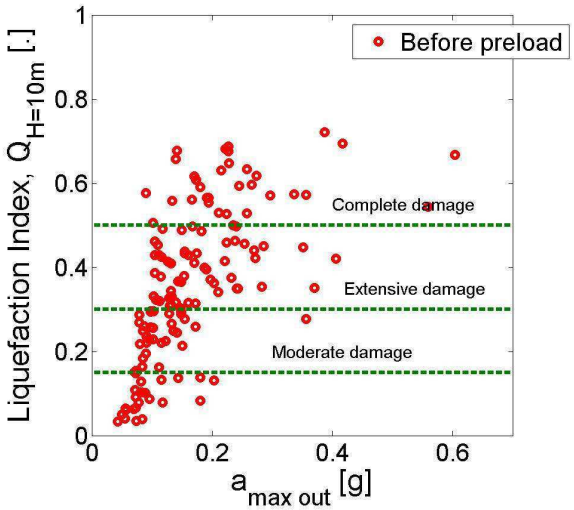

Figure 5. Scatter plot of obtained $Q_{H=10m}$ values as a function of $a_{max\ out}$. Case before preloading.

4 ANALYSIS OF LIQUEFACTION IMPROVEMENT METHOD

In this section, a mitigation method (i.e. preloading) is used in order to improve the ground and to prevent liquefaction apparition. The selected mitigation method reduces the liquefaction potential stiffening the soil and then decreases the settlement. Figure 7 provides a comparison of the mean pore pressure excess

(Δp_w) profile at the end of shaking for the case before preloading and after the two preloading cases (i.e. two embankment heights). A comparison of distribution of Δp_w profiles indicates that, the pore pressure build up decreases strongly when the preloading is used. The comparison between the profile of r_k value (equation 3) before and after the two preloading cases (Figure 8) shows that after the loading and unloading due to mitigation method the "distance to reach the critical state" increases. It produces a soil stiffening effect that allows a reduction of the pore pressure excess.

It is also observed that according to Figure 9, the maximum liquefaction probability decreases from 32% in the reference case to 20%, when the 8m high embankment is considered.

As already mentioned, the remediation method used increases the liquefaction strength and in consequence it will decrease the soil settlement. However, regarding the variation of *pga* values at the surface (Figure 10), it appears that in some cases, it increases because of the soil stiffening effect, hence it could be an unfavorable method from the structural viewpoint.

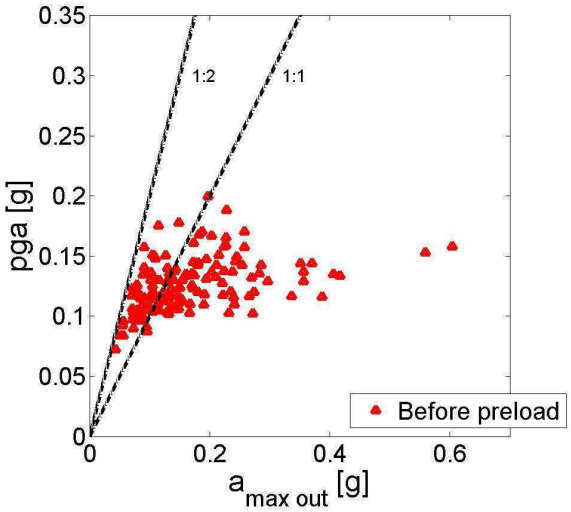

Figure 6. Relationships between maximum outcropping accelerations $a_{max\ out}$ and surface pga obtained for different earthquakes.

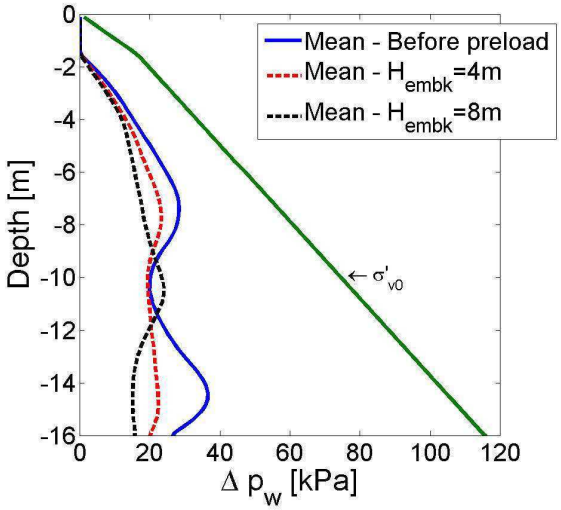

Figure 7. Effect of embankment height on the obtained pore pressure excess in the soil profile.

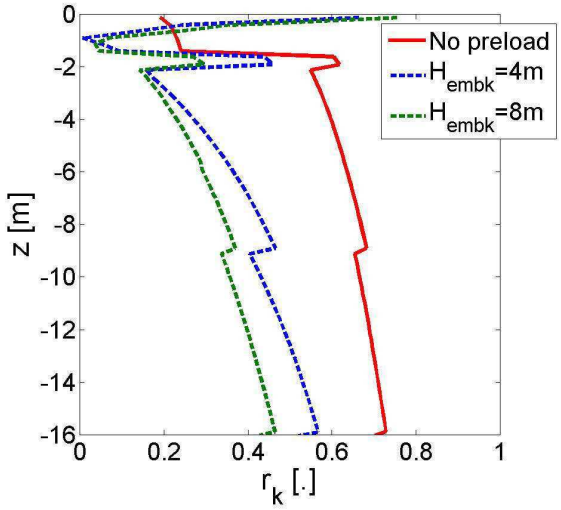

Figure 8. Effect of embankment height on the obtained r_k parameter in the soil profile.

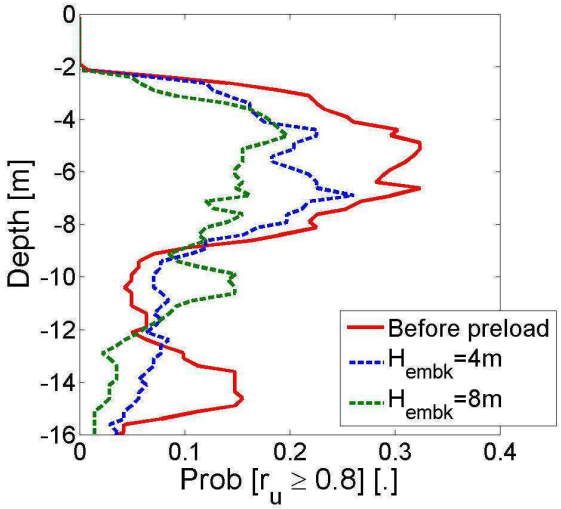

Figure 9. Effect of embankment height on the evolution of liquefaction probability with depth.

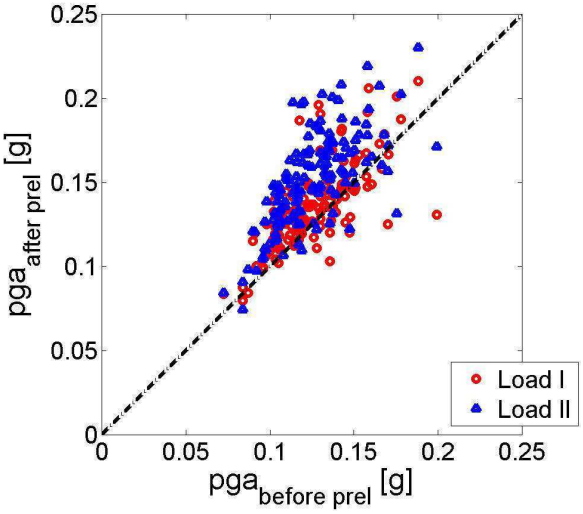

Figure 10. Scatter plot of variation of pga values before and after preloading.

5 VULNERABILITY ANALYSIS

Finally, three damage levels are chosen and showed in Figure 5. They correspond to a moderate liquefaction (Q_{lim} = 0.15), extensive liquefaction (Q_{lim} = 0.3) and complete liquefaction (Q_{lim} = 0.5). Figure 11

presents fitted fragility functions obtained for the second damage level (i.e. extensive damage) with respect to $a_{max\ out}$ for the three studied cases (i.e. before and after preloading). If the fragility curves obtained before and after preloading are compared, it is observed that for all values of $a_{max\ out}$, higher probability to exceed the Q_{lim} value is found before mitigating the soil. A similar behaviour is found for the others Q_{lim} values.

6 CONCLUSIONS

A series of finite element parametric analyses were performed to investigate the effects of the liquefaction countermeasures on the behaviour of soil profile. The main conclusions drawn from this study are as follows.

According to the responses obtained with the model without mitigation, it can be concluded that the choice of the "bedrock" signal remains the most subtle parameter in order to define the liquefiable zones and the characteristics of possible countermeasures. Thus, a parametric analysis is needed in order to study the influence of several signal parameters on the response of the site soil profile.

The analyses showed that the use of the preloading reduces the excess pore pressure generation into the soil profile. As a consequence, for a given seismic hazard the liquefaction probability decreases when the mitigation method is used. However, it increases the amplitude of the surface ground motion which could be a disadvantage on a structural viewpoint.

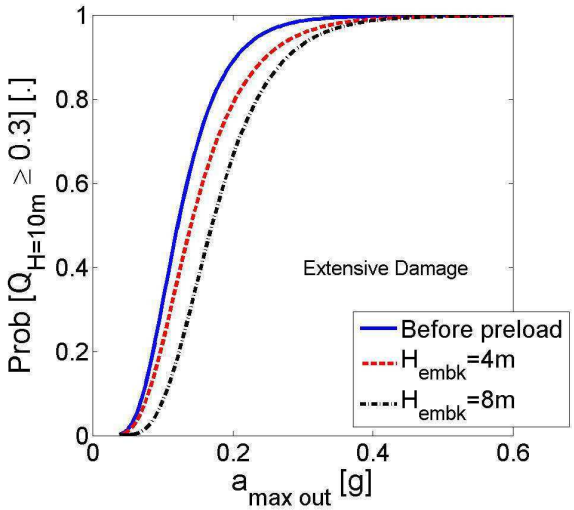

Figure 11. Fragility curves for extensive damage level as a function of $a_{max\ out}$. Effect of mitigation method.

ACKNOWLEDGEMENTS

This study has been done in the framework of the European Community Contract No FP7-SME-2010-1-262161-PREMISERI (PREloading to MItigate SEismic RIsk).

REFERENCES

Aubry, D., Hujeux J.-C.,Lassoudière F., & Meimon Y. 1982. A double memory model with multiple mechanisms for cyclic soil behaviour. In Int. Symp. Num. Mod. Geomech, pp. 3–13. Balkema.

Hujeux, J.-C. 1985. Une loi de comportement pour le chargement cyclique des sols. In Génie Parasismique, pp. 278–302. V. Davidovici, Presses ENPC, France.

Iervolino, I. & Cornell, C. A. 2005. Record selection for nonlinear seismic analysis of structures, Earthquake Spectra 21(3), 685–713.

Katona, M. G. & O. C. Zienkiewicz 1985. A unified set of single step algorithms part 3: the beta-mmethod, a generalization of the newmark scheme. International Journal of NumericalMethods in Engineering 21(7), 1345–1359.

Lopez-Caballero, F. & Modaressi-Farahmand-Razavi A. 2008. Numerical simulation of liquefaction effects on seismic SSI. Soil Dynamics and Earthquake Engineering 28(2), 85–98.

Modaressi, H. & Benzenati I. 1994. Paraxial approximation for poroelastic media. Soil Dynamics and Earthquake Engineering 13(2), 117–129.

Petridis P., Stamatopoulos C. & Stamatopoulos A. (2000). Soil Improvement by preloading of two erratic sites. GeoEng2000, International conference on Geotechnical and Geological Engineering, Melbourne, Australia (on CD, 7 pages).
Shinozuka, M. & Ohtomo K. 1989. Spatial severity of liquefaction. In Proceedings of the second US-Japan workshop in liquefaction, Large Ground Deformation and Their Effects on Lifelines.
Sorrentino, L., Kunnath S., Monti G., & Scalora G. 2008. Seismically induced one-sided rocking response of unreinforced masonry façades. Engineering Structures 30(8), 2140–2153.
Stamatopoulos A. C., & Kotzias P. C. (1985). Soil Improvement by Preloading, John Wiley & Sons, 261 pages, 1985.

ISGSR 2011 - Vogt, Schuppener, Straub & Bräu (eds) - © 2011 Bundesanstalt für Wasserbau ISBN 978-3-939230-01-4

Evaluation of the collapsibility risk of loess based on oedometer test results

A. Mahler, D. Turi & Cs. Vonza
Budapest University of Technology and Economics, Budapest, Hungary

ABSTRACT: 34 oedometer tests were performed on loess specimens to analyze the development of their collapse. The stress range that causes the collapse of soil's structure is determined, and its dependence on moisture content is discussed. 11 out of 34 tests were performed with water flooding. These tests were performed on soil specimens having different initial moisture content, and the effect of the stress level at which the specimen is flooded is analyzed.

Keywords: Loess, Collapsing soil, Unconfined compression test

1 INTRODUCTION

Loess is generally defined as a wind transported, cemented, highly porous material built up mostly by silt particles. The loess is generally homogeneous and exhibits advantageous strength and deformation properties when in dry state. Nevertheless if subjected to water and static or dynamic load the internal forces caused by cementation that provides its strength in the macro porous state gets weaker or disappears. In that case the highly porous soil skeleton collapses and causes significant volume change in the soil mass.

In order to estimate the risk of collapse, we must know the stress level that causes the collapse of the soil's porous structure. This stress rate can be influenced by the grain size distribution (sand and clay content) and the strength of cementation and the porosity, but probably the most important factor is the moisture content. A set of oedometer (unconfined compression) tests was performed to analyze the relation of these soil properties and the stress level that causes the collapse of loess.

2 LABORATORY TESTS

Loess samples were collected from three sites in Hungary. Two sites were located in the city of Dunaújváros and on in Kulcs. The typical grain size distribution curves of the samples are shown in Figure 1. and the characteristic soil properties are summarized in Table 1.

Table 1. Soil properties

	Sand	Silt	Clay	C_u	e	w	S_r
Dunaújváros South	12.93	76.95	10.12	17.08	0.83-0.94	9.89-14.20	0.31-0.41
Dunaújváros East	15.52	75.86	8.62	10.92	0.63-0.91	16.16-17.09	0.63-0.69
Kulcs	22.31	56.87	20.82	>32	0.56-0.72	16.36-19.03	0.78-0.80

The tested soils were of different void ratios; the samples collected from Kulcs and Dunaújváros had a lower void ratio than the "typical" value for loess, but all samples were classified as slightly collapsible according to Knight's criterion (1963).

Altogether 34 oedometer tests were performed on the collected samples, 23 specimens were tested without water flooding and 11 specimens were flooded at different stress levels during the compression test. The aim of the tests was to find the stress that causes the collapse of the soil skeleton.

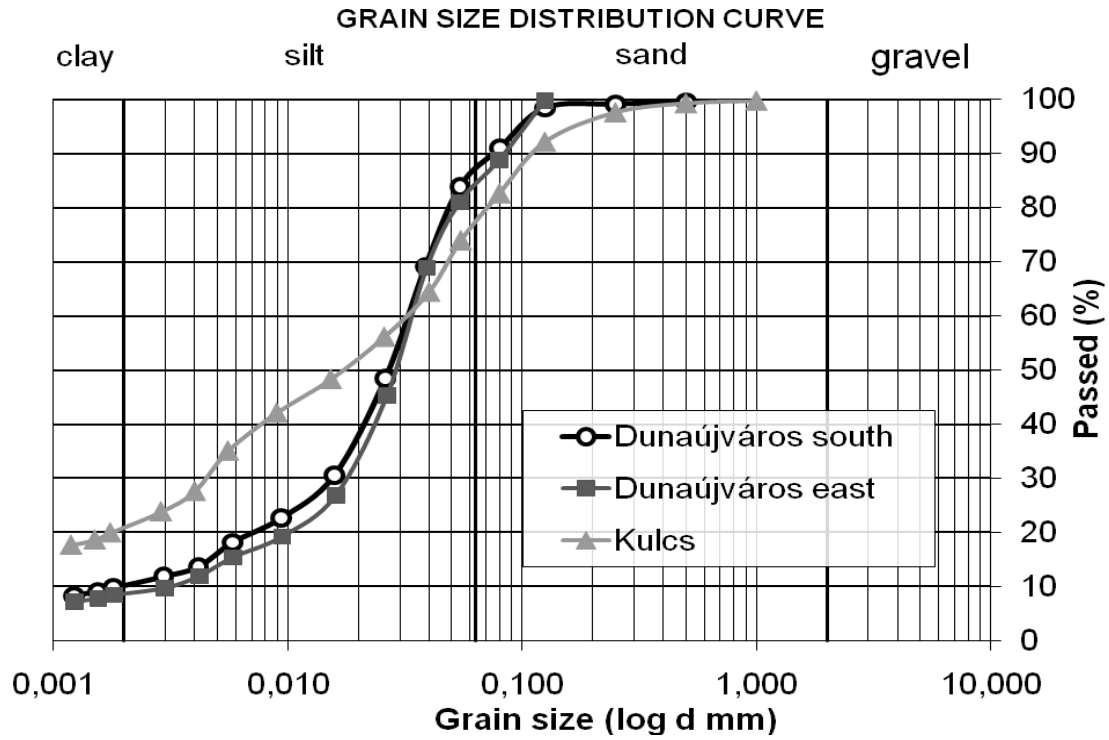

Figure 1. Grain size distribution curves of the tested samples

3 OEDOMETER TEST RESULTS

Figure 2. shows two typical oedometer test results. The compression curves can be divided to three parts: "pre-collapse" zone, "collapse" zone and "post collapse" zone.

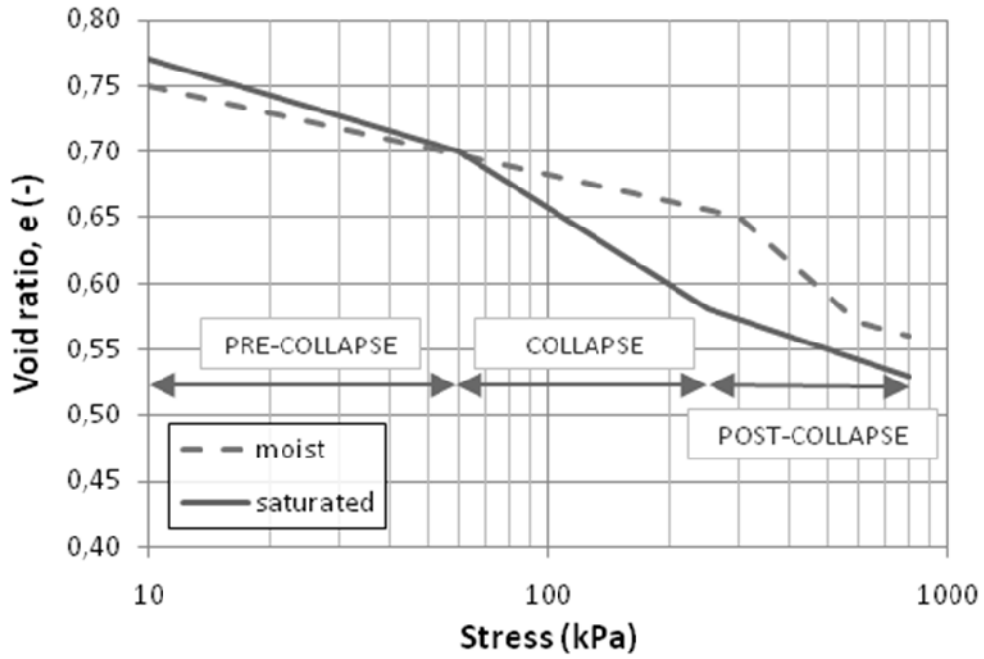

Figure 2. Typical oedometer test results

In the pre-collapse zone the soil behaves as a usual, cemented material, the deformation characteristics are governed mostly by the cemented bonds between the grains.

In the second zone gradual breakage of the bonds can be experienced, so the collapse of the porous structure doesn't occur suddenly at a certain stress rate, but more partial collapse can be observed in a certain stress range (i.e. at more stress level). Because it is irreversible, the collapse is generally consid-

ered as plastic deformation. Alonso et al. (1990) proposed to describe this soil behavior using elasto-plastic soil model. The stress at which the collapse zone starts is therefore called yield stress.

The third zone describes the post collapse behavior of the soil, at this stress range, the cemented bonds are already broken and the soil particles are re-arranged in a more dense state, so the soil behaves as a non-cemented material.

The limits between the three zones are influenced by the different soil properties (as mentioned earlier), but are mostly defined by the moisture content of the loess. Figure 2. illustrates this fact well: in the case of soil with higher moisture content the collapse zone begins and ends at lower stresses than that of soil with lower moisture content. So to estimate the risk of collapse it is essential to analyze the relationship between moisture content and collapse forcing stress level.

4 CORRELATION OF YIELD STRESS AND SOIL PROPERTIES

4.1 *Yield stress against moisture content*

As mentioned previously the collapse does not develop in one step at a certain stress level, but in more steps in a larger stress range. In figure 3. the yield stress is plotted against the moisture content of the soil.

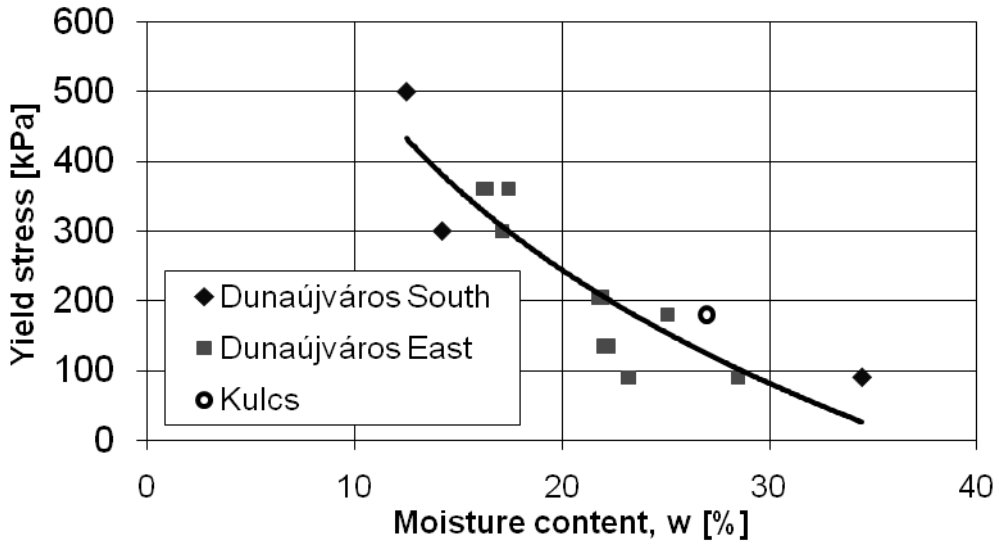

Figure 3. Yield stress against moisture content

In the case of dried soil samples the yield stress was not reached, because applying stress larger than 900 kPa was not possible. So the only fact that can be stated regarding the dried samples is that the yield stress is above 900 kPa.

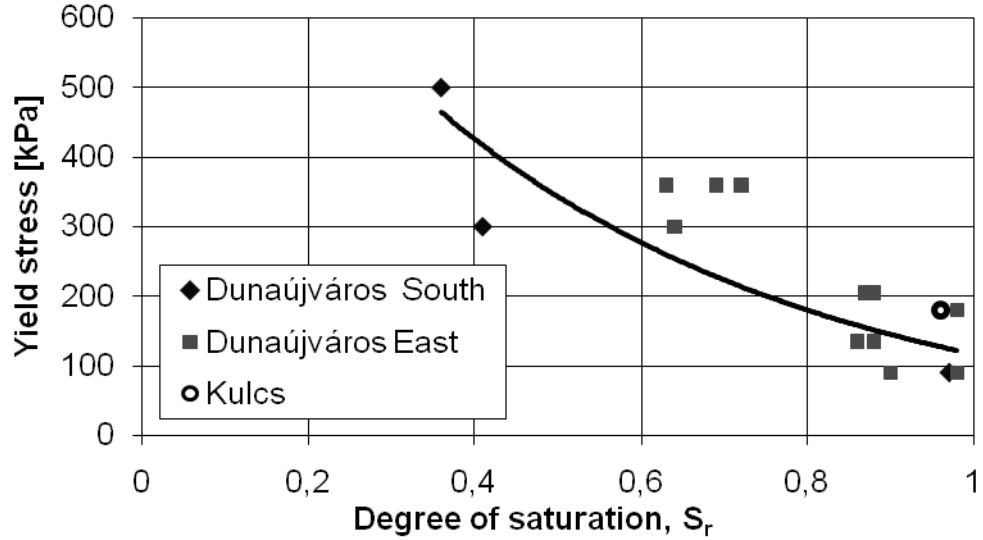

Figure 4. Yield stress against degree of saturation

4.2 *Yield stress against degree of saturation*

Although the correlation coefficient for the moisture content – yield stress relationship was quite good, the yield stress was plotted against the degree of saturation too. This is shown in Figure 4. This figure demonstrates clearly that the same trend can be observed, but the correlation coefficient is definitely worse. Therefore the use of moisture content – yield stress is recommended.

4.3 *Yield stress against void ratio*

The relationship of void ratio and yield stress was also analyzed in this work. These values were plotted against each other, and it is shown in figure 5. It can be observed that there is no significant correlation between void ratio and collapse forcing stress. Thus the importance of the soil's void ratio is marginal from this viewpoint.

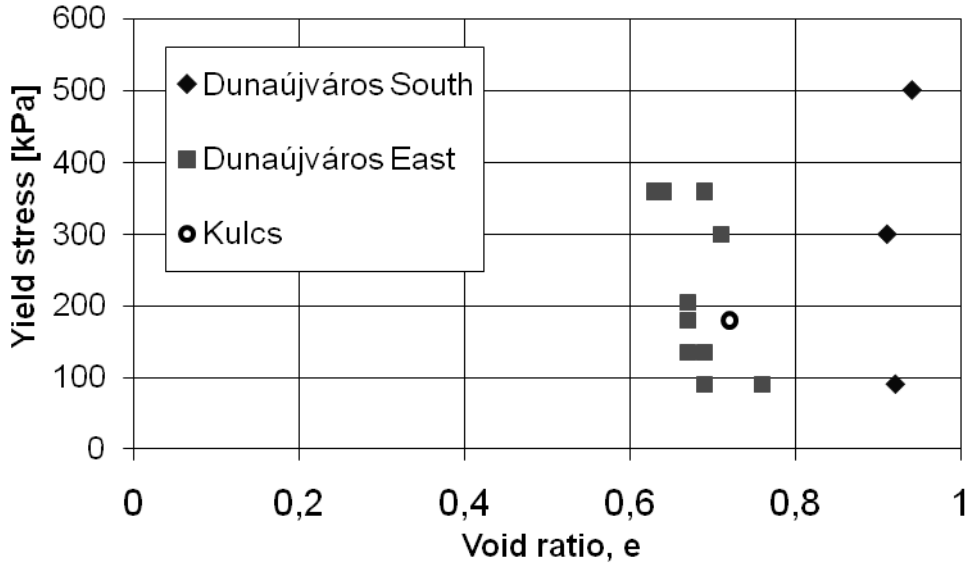

Figure 5. Yield stress against void ratio

5 COLLAPSE CAUSED BY FLOODING

It is well known that the collapse strain is influenced by the initial moisture content of the sample (Delage et al. 2005) and by the stress at which the specimen is flooded.

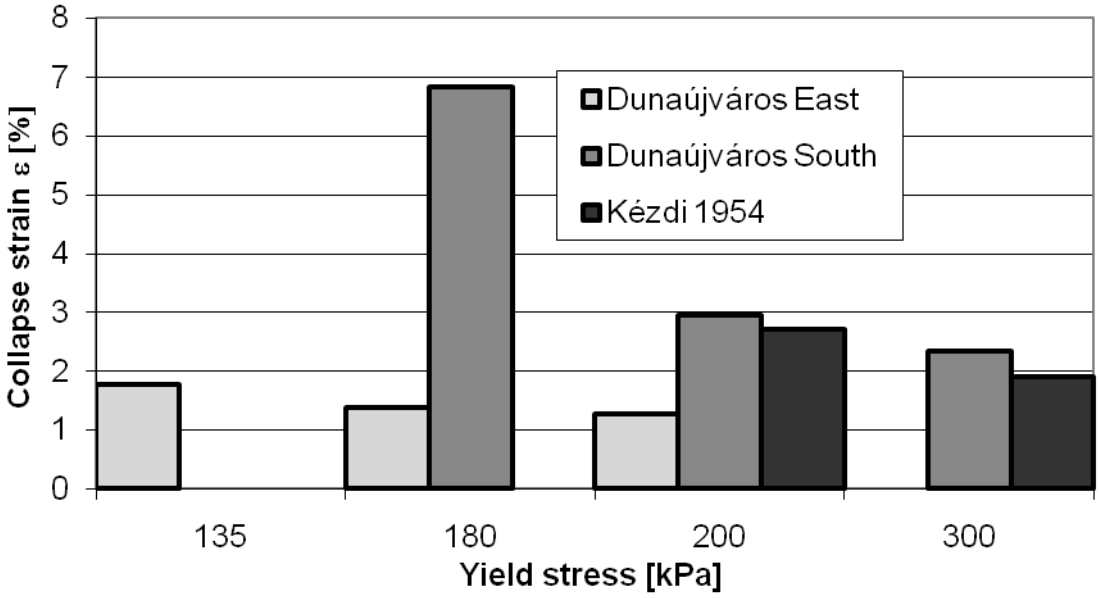

Figure 6. Collapse strain at different stress levels

In the case of the 11 oedometer test the soil specimens were water flooded at different stress levels. The aim of these tests was to analyze the effect of the stress at which the specimen is flooded on the measured collapse strain. Figure 6. shows the measured collapse strains of our tests and earlier tests on samples from Dunaújváros (Kézdi, 1954). A clear tendency can be observed: the higher the stress at which the sample is flooded the lower the collapse strain. Nevertheless it must be mentioned that the soil samples tested had relatively high moisture content, and therefore the yield stress was relatively low. It means that the collapse of the soils having the initial moisture content starts to develop at lower stress rate, so the collapse is already partially developed before the water flooding the samples. The larger the stress the larger part of the collapse is developed, therefore the less collapse occurs during the test (caused by water flooding the specimen).

Presumably in the case of dry soil samples the tendency is the opposite. The yield stress is high, definitely higher than the stress at which the specimen is flooded, so no partial collapse can be expected before the water flooding of the specimen. Therefore the larger the stress the larger the collapse strain.

6 SUMMARY, CONCLUSION

34 oedometer tests were made to analyze the collapse process of loessial soil samples. Based on the test results the following conclusion can be made:

- The compression curve can be divided to three parts: pre-collapse, collapse, and post collapse zone. In the second zone the collapse gradually develops in a specific stress range, which is mainly influenced by the moisture content of the soil.
- A reliable correlation can be found between the yield stress (at the beginning of the collapse zone) and the moisture content, but no such relationship was found for void ratio and yield stress.
- In the case of soil samples having high moisture content, larger stress level at which the specimen is flooded causes smaller collapse strain.

ACKNOWLEDGEMENT

This work is connected to the scientific program of the "Development of quality-oriented and harmonized R+D+I strategy and functional model at BME" project. This project is supported by the New Hungary Development Plan (Project ID: TÁMOP-4.2.1/B-09/1/KMR-2010-0002).

REFERENCES

Delage, P., Ciu, Y.J., Antoine, P. 2005. Geotechnical problems related with loess deposits in Northern France. Proceedings of International Conference on Problematic Soils, Famagusta, N. Cyprus.

Knight, K., 1963. The origin and occurrence of collapsing soils. Proceedings of 3rd Regional African Conference on Soil Mechanics and Foundation Engineering(1), 127-130.

Alonso, E.E., Gens, A., Josa, A. 1990. A constitutive model for partially saturated soils. Géotechnique Vol. 40, No. 3, pp. 405-430.

Kézdi, Á. 1954. Makroporózus talajok vizsgálata roskadás szempontjából. (in English: Investigation of macro porous soils from the viewpoint of collapse) Magyar Tudományos Akadémia Műszaki Tudományok Osztályának Közleményei XII. Kötet 1-4. szám

ISGSR 2011 - Vogt, Schuppener, Straub & Bräu (eds) - © 2011 Bundesanstalt für Wasserbau ISBN 978-3-939230-01-4

Socio-economic vulnerability to natural hazards – proposal for an indicator-based model

U. M. K. Eidsvig
International Centre for Geohazards, NGI, Oslo, Norway

A. McLean
International Centre for Geohazards, NGI, Oslo, Norway
Dalhousie University, Halifax, Nova Scotia, Canada

B. V. Vangelsten
International Centre for Geohazards, NGI, Oslo, Norway

B. Kalsnes
International Centre for Geohazards, NGI, Oslo, Norway

ABSTRACT: The severity of a natural hazard impact on a society depends, among others on the intensity of the hazard and vulnerability factors like the number, and resistance of exposed elements (e.g. persons, buildings and infrastructure). Social conditions strongly influence the vulnerability factors both for direct and indirect impact and therefore have the power to transform the occurrence of a natural hazard into a natural disaster.

This paper presents a model, using an indicator-based methodology, to assess relative socio-economic vulnerability to landslides. The indicators represent the underlying factors which influence a community's ability to deal with, and recover from the damage associated with landslides. The proposed model includes indicators which represent demographic, economic and social characteristics as well as indicators representing the degree of preparedness and recovery capacity. Although this model focuses primarily on the indirect losses, it could easily be extended to include more physical indicators which account for the direct losses. Each indicator is individually ranked from 1 (lowest vulnerability) to 5 (highest vulnerability) and weighted, based on its overall degree of influence. The final vulnerability estimate is formulated as a weighted average of the individual indicator scores. Application of the proposed model is shown for a Norwegian community.

Keywords: Socio-economic vulnerability, indicator-based vulnerability models

1 INTRODUCTION

Vulnerability assessment, with respect to natural hazards, is a complex process that must consider multiple dimensions of vulnerability, including both physical and social factors. Physical vulnerability is a function of the intensity and magnitude of the hazard, the degree of physical protection provided by the natural and built environment, and/or the resistance levels of the exposed elements. However, social factors such as preparedness and institutional and non-institutional abilities for handling natural hazards events are also important elements for a society's vulnerability to natural hazards. Social vulnerability refers to the underlying factors leading to the inability of people, organizations, and societies to withstand impacts from the natural hazards.

Social vulnerability models can be used in combination with physical vulnerability models to estimate both direct losses, i.e. losses that occur during and immediately after the impact, as well as indirect losses, i.e. long-term effects of the event. Direct impact of a landslide typically includes casualties and damages to buildings and infrastructure while indirect losses may include business closures or increased levels of homelessness. The direct losses are mainly assessed using physical vulnerability indicators (e.g. construction material and height of buildings) while indirect losses are mainly assessed with social indicators (e.g. economical resources). The 2010 Haiti earthquake caused enormous direct losses (fatalities and collapsed buildings). One year later, long term effects such as diseases, unemployment and homelessness are still prevailing.

2 BACKGROUND

The proposed model uses an indicator-based methodology to assess socio-economic vulnerability to landslides. A vulnerability indicator is a variable which is an operational representation of a characteristic or quality of a system able to provide information regarding the susceptibility, coping capacity and resilience of a system to an impact of an albeit ill-defined event linked with a hazard of natural origin (Birkmann, 2006).The purpose of the indicators is to set priorities, serve as background for action, raise awareness, analyze trends and empower risk management.

Indicator-based risk models may be divided into two main groups: i) deductive, where measurement of risk is hazard specific and based on disaster impact data or ii) inductive, where measurement of risk is based on underlying factors which influence a community's ability to deal with, and recover from an impact. Such methods are less hazard specific or hazard independent. The model proposed in this paper belongs to the inductive models.

Vulnerability indicators may be expressed at a specific geographical scale (local, regional or global), at a specific organizational level (individual, household, community or national) and for different hazard types. As landslides rarely have socio-economic consequences at global or national levels, the most relevant level for landslides would be community level. With focus on the models applicable to community level, the proposed model is adapted to European conditions based on the work of Steinführer et al. (2009), Tapsell et al.(2005), King and MacGregor (2000), Lahidji (2008) and Cutter et al. (2003).

Steinführer et al. (2009) and Tapsell et al.(2005) describes socio-economic vulnerability for floods for European countries, Lahidji (2008) propose a model for assessing coping capacity developed for Asia, but applicable globally for several hazard types, and Cutter et al. (2003) proposed a social vulnerability index for environmental hazard for use in USA, applicable to community level.

2.1 Choice of indicators

The indicators should be chosen, such that they together represent several aspects of the society's ability to prepare for, deal with, and recover from an impact. Important questions in the indicator selection are:

- What and who is most vulnerable in the society? (e.g. vulnerable groups of people, vulnerable industries, vulnerable buildings)
- Is the population prepared for an emergency? (e.g. emergency response procedures, existence of early warning system, etc.)
- Are there available resources for recovery? (e.g. resources for rebuilding destroyed physical environments, medical facilities)

In the proposed model, the most vulnerable groups considered and assessed were "children and people above 65 years of age", "people with language and cultural barriers" and "rural populations dependent on the land for their primary source of income". Additionally, the "housing type" indicator was considered very important for the assessment of building vulnerability levels.

Preparedness levels were ranked based on the quality of existing hazard evaluations and early warning systems, the stringency of regulation control and the extent of emergency response procedures.

The ability to recover from a landslide was assessed by analyzing insurance and disaster funds and the quality of medical services and finally, the population density was considered, as it is more difficult to evacuate and care for highly dense populations.

2.2 Aggregation of indicators

A weighting system is introduced to account for the relative importance of each indicators on the total vulnerability level. If all the indicators are believed to be of equal significance, equal weighting should be applied. Other techniques to determine weights include expert judgment, analytical hierarchy process, principal component analysis and factor analysis.

The model for aggregation of vulnerability indicators may be quantitative where the vulnerability is a dimensionless number between 0 to 1 representing the degree of loss within a given time- and space-frame, or semi-quantitative where the vulnerability is ranked relatively according to a scale defined within the model. The main groups of models used for the aggregation of indicators are:

- Additive models, produced by e.g. multi-criteria decision approach.
- Multiplicative models, produced by e.g. multiple regression models.
- Definition of vulnerability by decision rules, produced by e.g. use of decision trees.

3 PROPOSED MODEL FOR SOCIO-ECONOMIC VULNERABILITY ASSESSMENT

The proposed model includes indicators which represent demographic, economic and social characteristics as well as indicators representing the degree of preparedness and recovery capacity as outlined in section 2.1. The model describes the vulnerability semi-quantitatively, with additive aggregation of the indicators. Each indicator is individually ranked from 1 (lowest vulnerability) to 5 (highest vulnerability) and weighted, based on its overall degree of influence. The weights are chosen among the values 1, 2 and 3, where weight 1 is assigned to the least influential indicators, 2 to the intermediate influential indicators and 3 to the most influential indicators. In the proposed model, the assignment of weights to the indicators is based on literature review and expert judgment. Table 1 shows the proposed socio-economic vulnerability model with suggested indicators, their corresponding weights and criteria for ranking of the indicators.

When all the indicators are assigned a vulnerability score, the score for each indicator is multiplied with its corresponding weight to give a weighted vulnerability score. The final vulnerability estimate is formulated as a weighted average of the individual indicator scores:

$$\text{Total vulnerability score value} = \sum \text{Weighted vulnerability score} / \sum \text{Weights}$$

Application of the model is shown in section 4.

Table 1. Proposed socio-economic vulnerability model

Indicators	**Weights**	**Criteria for indicator ranking** (1: Low vulnerability, 5: very high vulnerability)
Demographic Indicators		
Age distribution (see note 1)	2	1: Uniform age distribution - less than 20% population is either between 0-5 years of age or over 65.
		2: 20-30% population is either between 0-5 years of age or over 65.
		3: 30-40% population is either between 0-5 years of age or over 65.
		4: 40-50% population is either between 0-5 years of age or over 65.
		5: Over 50% population is either between 0-5 years of age or over 65.
Housing type (see note 2)	3	1: The majority of constructions are of strong resistance, there are some or none of medium resistance and none of weak resistance.
		2: The majority of constructions are of strong resistance, there are some or none of medium resistance and some of weak resistance.
		3: The majority of constructions are of medium resistance, there are some or none of strong resistance and some or none of weak resistance.
		4: The majority of constructions are of weak resistance, there are some or none of medium resistance and some of strong resistance.
		5: The majority of constructions are of weak resistance, there are some or none of medium resistance and none of strong resistance.
Rural population (see note 3)	2	1: Less than 10% population is dependent on the land for primary source of income.
		2: 10-25% population is dependent on the land for primary source of income.
		3: 25-50% population is dependent on the land for primary source of income.
		4: 50-75% population is dependent on the land for primary source of income.
		5: Over 75% population is dependent on the land for primary source of income.
Urban population (see note 3)	1	1: Population density is < 50 people/km^2
		2: Population density is between 50-100 people/km^2
		3: Population density is between 100-250 people/km^2
		4: Population density is between 250-500 people/km^2
		5: Population density is > 500 people/km^2
Economic Indicators		
Personal wealth	2	1 : GDP per capita > 50 thousand USD
		2 : GDP per capita 30 – 50 thousand USD
		3 : GDP per capita 20 – 30 thousand USD
		4: GDP per capita 10 – 20 thousand USD
		5 : GDP per capita < 10 thousand USD

Social Indicators		
Vulnerable groups due to language or cultural barriers	1	1: < 5% of the population is not familiar with majority language and culture
		2: 5-10% of the population is not familiar with majority language and culture
		3: 10-15% of the population is not familiar with majority language and culture
		4: 15-25% of the population is not familiar with majority language and culture
		5: > 25% of the population is not familiar with majority language or culture (indicative of a high percentage of tourists and/or recent immigrants)
Education Level	1	1: > 30% of the eligible population (over 18 years of age) have attended, or are attending, a post-secondary education
		2: 20-30% of the eligible population have attended, or are attending, a post-secondary education
		3: 10-20% of the eligible population have attended, or are attending, a post-secondary education
		4: 5-10% of the eligible population have attended, or are attending, a post-secondary education
		5: <5 % of eligible population have attended, or are attending, a post-secondary education
Preparedness indicators		
Hazard evaluation (Lahidji, R., 2008)	3	1: Detailed hazard maps available
		2: Basic hazard maps available
		3: Hazard mapping research ongoing (with some gaps)
		4: Basic assessment of direct impacts to exposed populations completed
		5: Incomplete assessment of direct impacts to exposed populations
Regulation control (Lahidji, R., 2008) (see note 4)	3	1: Stringent guidelines(which take into account all landslide triggers) in place for all constructions and land-use activities to ensure minimal risk to exposed population
		2: Consistent approach to the regulation of construction and land use on the basis of exposure to landslides
		3: Fairly effective regulations for new developments, however, potential problems with older constructions
		4: Some consideration of risk during construction, but inadequate enforcement of regulations
		5: No consideration of risk in planning and construction
Emergency response (Lahidji, R., 2008)	2 Local government questionnaire	1: Permanent coordination between responders in communities; specialized equipment and well-trained rescue services available throughout the country
		2: Clear definition of roles and responsibilities at local level; proportionate allocation of resources
		3: Existence of an organization of emergency response, with coordination authority; adequate supplies of medical transport, communications and other specialized equipment in all important cities
		4: Professional search and rescue services, evacuation possibilities and central operation centers available in the most landslide-prone areas
		5: Fragmented organization and scattered resources; predominance of voluntary responders
Early warning system (Lahidji, R., 2008)	2 Local government questionnaire	1: Advanced early warning systems used in coordination with emergency response procedures
		2: Adequate early warning system coordinated with media announcements capable of reaching the majority of the population prior to the landslide
		3: Basic early warning systems available to the public
		4: Basic early warning system available to risk managers
		5: No early warning system

Recovery indicators		
Insurance and disaster funds (Lahidji, R., 2008)	2 Local government questionnaire	1: Extensive coverage for private and public buildings, existence of government-sponsored landslide funds
		2: Insurance coverage for the majority of private and public buildings, limited government-funding
		3: Widespread landslide insurance in development phase, but not yet accessible to everyone
		4: Incomplete support for victims of past landslide events
		5: Little or no insurance provided
Quality of medical services (see note 5)	1 Government data	1: > 4 hospital beds per 1000 people
		2: 3 - 4 hospital beds per 1000 people
		3: 2 - 3 hospital beds per 1000 people
		4: 1 - 2 hospital beds per 1000 people
		5: < 1 hospital beds per 1000 people

Note 1: Age distribution:
The population of young children and senior citizens more vulnerable to harm in the event of a landslide is estimated by the percentage of people between 0-5 years of age or over 65. Since the average life expectancy in Europe is approximately 75 years, a uniform age distribution would indicate that 20% of the population is 'vulnerable' – this was used as the basis for the age distribution indicator scale.

Note 2: Housing type:
Strong resistance refers to thick brick or stone wall and reinforced concrete constructions, medium resistance to mixed concrete-timber and thin brick-wall constructions and weak resistance to simple timber and very light constructions (Heinimann, 1999).

Note 3: Rural/urban population:
Rural populations are highly vulnerable due to their lower incomes (on average) and dependence on the surrounding natural resources (e.g., farming, fishing) for sustenance. However, urban regions with very dense populations are more difficult to evacuate during emergencies (Cutter et al., 2003).

Note 4: Regulation control:
This indicator takes into account the quality of infrastructure in the region. If there is a significant amount of control over construction guidelines, the infrastructure is generally well-built and relatively resilient to landslides.

Note 5: Quality of medical services:
This indicator is categorized by the number of hospital beds per 100 000 people. The scale used is based on data provided by the European Commission Eurostat (2008).

4 APPLICATION OF THE MODEL

This section shows the application of the model to the Norwegian city Skien. Skien is a city on the Southern coast of Norway with about 50 000 inhabitants. The area is especially prone to clay landslide because of quick clay deposits. Quick clay is marine clay, where the salt content is reduced through flushing of ground water. When quick clay is either exposed to loads or movement, the clay may turn into a liquid.

The data required to rank the indicators was obtained from census data, interviews (with people knowledgeable of Skien) and/or subjective judgment of the authors.

Table 2 shows the result of the indicator ranking and calculation of the socio-economic vulnerability score for Skien.

Table 2. Calculation of vulnerability score for Skien

Indicator	Indicator score	Indicator weight	Weighted vulnerability score
Age distribution	1	2	2
Housing type	3	3	9
Rural population	2	2	4
Urban population	1	1	1
Personal wealth	1	2	2
Vulnerable groups	1	1	1
Education level	2	1	2
Hazard evaluation	2	3	6
Regulation control	2	3	6
Emergency response	2	2	4
Early warning system	5	2	10
Insurance and disaster funds	1	2	2
Quality of medical services	2	1	2
Total, Σ	Weighted average vulnerability score = 51/25 = 2.04	∑ Weights= 25	∑ Weighted vulnerability score= 51

The vulnerability score for Skien is 2.04, where 1 is the lowest possible vulnerability score and 5 is the highest possible vulnerability score.

5 CONCLUSION AND DISCUSSION

The model proposed in this paper assesses the level of socio-economic vulnerability by ranking the vulnerability on a relative scale. Application of this model enables comparison of socio-economic vulnerability between communities within Europe. This model defines criteria for assigning a score to every indicator, which may be a qualitative, semi-quantitative or quantitative parameter. The ranking approach and unambiguous score criteria make the model easy to use.

This model is still under development and the choice and weighting of indicators will be validated and improved by performing more case studies for European communities. The model may also be extended to include more physical indicators to account for the direct losses.

A logical future step would be to calibrate the model against historical data; comparison of recovery time for communities hit by comparable impacts is one possibility for calibration. This model may also be transferred to, and combined with an existing quantitative vulnerability model (e.g. Li et al. (2010)). Then the absolute estimates of vulnerability in terms of degree of loss within predefined space- and time-frames could be made, which allows direct calibration against disaster loss data.

ACKNOWLEDGEMENT

The work described in this paper was performed as a part of the EC FP7 project SafeLand, and also partly supported by the Research Council of Norway through the International Centre for Geohazards (IGC). The support is gratefully acknowledged.

REFERENCES

Birkmann, J (2006): Indicators and criteria for measuring vulnerability: Theoretical bases and reqirements. In Measuring vulnerability to natural hazards: towards disaster resilient societies, United Nations University Press, 2006.

Cutter, S.L., Boruff, B.J., Shirley, L.W. (2003): Social vulnerability to environmental hazards, Social Science Quarterly 84 (2): 242-261.

European Commission Eurostat (2008): Tables, graphs and maps interface: hospital beds. http://epp.eurostat.ec.europa.eu/tgm/table.do?tab=table&language=en&pcode=tps00046&plugin=0&tableSelection=1&footnotes=yes&labeling=labels

Heinimann, H. R.(2009): Risikoanalyse bei gravitativen Naturgefahren - Fallbeispiele und Daten, Umwelt-Materialen 107/I, Bern, 1999.

IMF (International Monetary Fund) (2010): World economic outlook database-April 2010. http://www.imf.org/external/pubs/ft/weo/2010/01

King, D. and MacGregor, C. (2000): Using social indicators to measure community vulnerability to natural hazards. Australian Journal of Emergency Management 15 (3).

Lahidji, R. (2008): Measuring the capacity to cope with natural disasters. Contribution to the UN OCHA project "Risk assessment and mitigation measures for natural and conflict-related hazards in Asia Pacific" Appendix G in http://www.preventionweb.net/files/10455_OCHANGINaturalconflictrelatedhazard.pdf

Li, Z., Nadim, F., Huang, H., Uzielli, M. and Lacasse, S. (2010): Quantitative vulnerability estimation for scenario-based landslide hazards. Landslides 7 (2): 125-134.

Steinführer, A., De Marchi, B., Kuhlicke, C., Scolobig, A., Tapsell, S. and Tunstall, S (2009): Vulnerability, resilience and social constructions of flood risk in exposed communities. FLOODsite report T11-07-12, http://www.floodsite.net

Tapsell, S. M., Tunstall, S. M., Green, C. and Fernandez, A. (2005): Social indicator set. FLOODsite report T11-07-01 http://www.floodsite.net/html/publications2asp?ALLdocs=on&Submit=View, Enfield: Flood Hazard Research Centre.

ISGSR 2011 - Vogt, Schuppener, Straub & Bräu (eds) - © 2011 Bundesanstalt für Wasserbau ISBN 978-3-939230-01-4

A Guide to Processing Rock-fall Hazard from Field Data

M. Bauer & P. Neumann
Baugeologisches Büro Bauer GmbH, Munich, Germany

ABSTRACT: The assessment of rock-fall hazard in appointed regions of the Bavarian Alps involves the evaluation of occurrence probability and intensity of the potential events. A systematic approach is presented, which allows to establish a regional comparability of the rock-fall hazard determinations. This method is based on simple field-geological data and observations. The rock-fall probability, on the one hand, can be estimated by classifying the rock-fall disposition of the detachment areas and their degree of activity. The rock-fall disposition is the total of geological and geomechanical criteria, that influence the likelihood of rock-fall processes. Furthermore, the role of external influences, like earthquakes and extreme precipitation by heavy rainfalls, and their likelihood as triggering events are discussed. The combination of the above parameters and the quantification procedure for the probability assessment follow mathematical models which are similar to those used in rock mass classifications. On the other hand, the intensity of potential rock-falls, which can be defined by the rock volume and its kinematics, is subdivided into four categories. Finally, the combination of probability and intensity leads to a matrix model, which distinguishes different types of hazards. Without applying complex numerical models, the presented rock-fall matrix model resembles a practical method enabling reasonable and reproducible determinations of rock-fall probability and intensity based on geological field expertise.

Keywords: Rock-fall, slope, discontinuity, activity, matrix

1 INTRODUCTION

Within the broad range of sedimentary processes, the simplest case of mass movement is that of rock fragments falling by gravity off a cliff or down a slope. Rock-falls are rapid depositional phenomena which involve erosion of particles from rock faces, transport in free fall with subsequent bouncing, rolling or sliding and final sedimentation as scree. The term “rock-fall” in this article does not distinguish any volume, but generally refers to phenomena in the range of single falling blocks of few dm^3 to rock volumes of more than 10.000 m^3.

Rock-falls are difficult to predict in their timing and dimension, especially without any extensive instrumentation. In densly populated mountainous regions falling rocks constitute a major hazard that can give rise to casualties, damage and injuries. As a consequence, the assessment of hazards in rock-fall prone areas has become a major research task worldwide (e.g. Budetta 2004, Corominas et al. 2003, Lateltin 1997).

Hazard analysis is a highly complex operation requiring several steps, starting with the regional detection of detachment areas and an exact assessment of run out parameters of falling rocks to determine the endangered areas (e.g. Evans and Hungr 1993, Meißl 1998).

Further steps, which we will discuss in this article, involve the estimation of occurrence probability and intensity of potential rock-fall incidents to assign specific hazard values to the affected areas.

In the present paper, we outline the interplay of the physical principles of rock-fall processes with their preconditions and triggers, on the one hand, and the assessment of probability and intensity on the other. Furthermore, we will propose a semi-quantitative rating method to estimate and describe rock-fall hazard and point out limits and advantages of field-based geological analysis.

During the hazard assessment procedure a variety of parameters have to be examined, quantified and combined with each other as shown in Figs. 1 and 4 and which will be explained in the following chapters.

2 BACKGROUND

In the scope of the project "CatchRisk" of the European Union, regional rock-fall hazard assessment was carried out for the Bavarian Alps. Detachment areas are well documented in the GeoRisk-database of the LfU of Bavaria, modelling of depositional areas was accomplished at the LfU applying a GIS.

Our task was to distinguish these depositional areas in respect to rock-fall hazard. Probability and intensity were processed with a method based on field observations, largely available in the GeoRisk-database. The involved field parameters comprise fundamental rock slope properties, which allow application of the system also independant from the mentioned database and thus in every mountaineous region beyond the Bavarian Alps. The principle concept is presented in Fig. 1. Tab. 1 is an evaluation form sheet providing the total procedure.

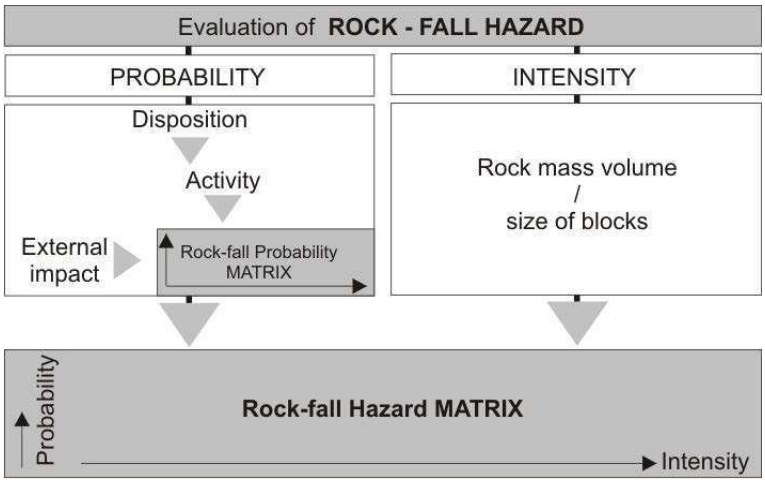

Figure 1. Simplified procedure of rock-fall hazard analysis.

3 ROCK-FALL PROBABILITY

The major task is to find out how close a rock or rock mass is to falling over. Each rock wall poses a hazard and thus a prior probability for falling rocks, otherwise the region would not be considered. These prior probabilities are of a quite general nature and must be updated to enable reasonable and regionally comparable estimations. Different approaches exist (e.g. Einstein 1988). Statistical analysis of past rock-falls is a powerful tool (e.g. Dussauge-Peisser et al. 2002), but depends largely on the quality of historical data sets (archives) or geological indications of previous rock-falls. Frequencies are mostly referred to as annualties or as probabilistic percentage during defined periods of time. Mostly, however, the historical archive is missing and frequencies are only a paraphrase to describe subjective estimations of rock-fall probabilities.

Based on geoscientific know-how, it can be attempted to reproduce and quantify subjective estimations. The basic approach is to include all seizable natural parameters, which not only account for rock-falls but also influence the likelihood. Probability depends on several factors comprising three categories: the rock-fall disposition of the detachment zones (susceptibility), the activity in this region and the external influences acting on the system under consideration (Fig. 1, 4). These must be set in causal relationship, ordered hierarchically and quantified in the following.

3.1 *Disposition for rock-fall processes*

The first step is to make an inventory of the geological, structural, lithological and stratigraphical properties of a slope that influence its susceptibility for failure and thus summarizes all geotechnical preconditions for falls (e.g. loosening, toppling etc.). This inventory is best defined as rock-fall disposition, and comprises static properties (e.g. joint orientation) as well as very slow, quasi-static, processes (e.g. weath-

ering) acting in a rock slope or cliff (rock mechanical characteristics of the detachment zone), as well as large-scale factors, like sagging (regional geomechanical environment).

In principle, geometry and height of detachment areas are critical disposition parameters. However, these must be neglected in probability assessment, since they are already included in the computation of run-out parameters and depositional areas.

The bulk of parameters is related to the structural composition of the rock mass. For regional comparison discontinuities and their properties are described based on international classifications (e.g. ISRM, IAEG).

3.1.1 *Rock-mechanics of the detachment zone*

Specific rock-fall susceptibilities of detachment areas are characterized by the interaction of a set of rock mechanical parameters. These can be summarized as follows:

Orientation of discontinuities: Analyses of discontinuity sets can be highly complex. For rock-fall hazard assessment the critical question arises, whether joints or bedding planes have favourable, random or adverse orientation considering a rock cliff. Adverse joints and also unfavourable cuttings of discontinuities are those that cause block, wedge or toppling failures.

Degree of weathering: Long-term deterioration due to weathering can lead to a reduction of shear strength of discontinuity planes (reduced friction angle and cohesion). The degree of weathering must be quantified, e.g. according to ISRM and IAEG classifications.

Structural configuration: This field comprises the degree of transection of joints, their persistence (length), opening widths (aperture) and the condition of the joint surfaces. The friction along a joint, bedding plane or any other discontinuity is governed by the macro and micro roughness of the surface (degree of undulation and the texture of the surface). Additionally, fault gauge and slickensides are highly significant for surface friction and thus for rock-fall probability estimations.

The spacing of joints, in contrast, is only critical regarding volume of falling masses and their mechanical behaviour. It does not influence probability, since one unfavourable joint is sufficient for failure.

Increasing probability is indicated by high degree of transection of discontinuities, high persistence, open joints and even, smooth surfaces (e.g. slickensides). These parameters presuppose a high mobility of blocks.

Degree of loosening: The above parameters account for the degree of loosening of a slope. Often no detail indications are available for detail structural evaluations and ratings like above. Nevertheless, general observations of symptoms of movements are at hand, like information about open fractures and neck valleys. This point can be seen as parallel estimation of the structural configuration, with minor degree of significance (valuation, see Fig. 4 and chapter 3.4.1).

3.1.2 *Regional geomechanical environment*

The overall geological and morphological situation of a detachment zone and its surrounding mountain slopes (geomechanical environment) has to be considered. The following points must be mentioned:

Type of basement: The type of basement formation influences the state of stress in a rock slope. Dissolvable rocks or clayey, marly beds with highly plastic behaviour must be regarded as unfavourable.

Large-scale, deep-seated deformations: The implications of long-term, large-scale slope deformations on a regional scale (e.g. sagging of mountain slopes, large landslide processes) are difficult to interpret. In principle, these processes imply changes of stress and thus influence stability in the detachment zone.

Mass movements in the foot of slope: Also active creeping or sliding processes in the foot of slope most likely influence the stability of the detachment zone. The effects in detail, however, are not always clear.

The valuation of such processes (regional geomechanical environment) for rock-fall hazard is still in debate. Nevertheless, in Fig. 4 and Tab. 1 we propose a way to include factors.

3.2 *Activity*

Activity is defined as the total of movements occurring within a detachment area and talus slope. The degree of activity results from the general rock-fall disposition and can be identified in the field by evaluating activity indicators (Fig. 3). These indicators give direct proof of recent movements, e.g. fresh impact marks. For probabilistic evaluations of rock-fall processes, activity has to be distinguished as follows.

3.2.1 *Activity in advance of rock-falls (initial activity)*

Activity in advance of rock-falls comprises loosening processes in the detachment area, indicated by e.g. fresh and open joints or strained roots. Proof for or against active movement are critical for probability estimations. The rock-fall disposition mirrors the current condition of the detachment zone, whereas the activity indicators helps to estimate whether the system actually approaches the point of failure or not (Fig. 2).

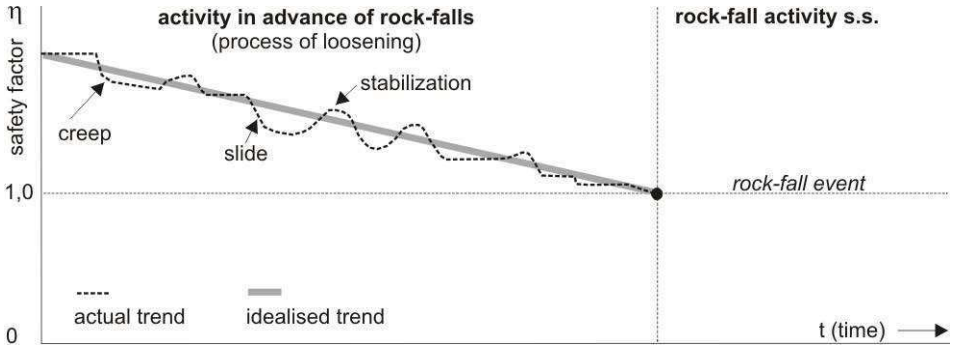

Figure 2. Interpretation of activity of slopes.

3.2.2 *Rock-fall activity s.s.*

Examples of indicators for recent rock-fall activity (activity s.s.) are fresh detachments and scars in the rock slope/cliff or fresh blocks and impact marks in the depositional area. These resemble direct evidence of falls.

The question arises how to valuate the activity in the scope of probability assessment. Fresh marks can indicate subsequent incidences with progressing erosion and the creation of even more unsupported or oversteepened slope conditions, but also hint at a geomechanical stabilization of the system after the event (temporary dormancy). From this point of view it becomes evident, that the initial activity s.l. mentioned above must be emphasized to answer this question. Furthermore, different types of events with distinct probabilities must be taken into account (varying rock-fall intensities with specific likelihoods in one and the same depositional area).

Figure 3. Examples of indicators. Left: Fresh damage of a tree caused by bouncing rock fragments (activity s.s.). Middle and right image: Wide open fractures, partly with stressed vegetation, indicating active loosening and instable conditions in the detachment zone.

3.3 *External impact*

The rock-fall potential must also be considered through assessment of the probability that rocks would fall if large rainfalls or earthquakes occurred. Also other meteorological influence should be regarded if existent, like freeze/thaw cycles, which can dislodge blocks and wedges. In this regional assessment process focus is given to major impacts, for which also reliable probabilistic data are available.

3.3.1 *Significance of earthquakes*

High-intensity short duration forces or vibrations act on rock slopes and their basements. The rock structure can be loosened and blocks and wedges which are at risk can move. Rock-falls can either be prepapered or actually be triggered by these forces. The detail impact of horizontal earthquake acceleration, however, is complicated.

The earthquake zonation provided in German Code DIN 4149 is based on the "Seismic hazard map of the D-A-CH countries". This probabilistic map distinguishes areas of macroseismic intensities with the internationally used recurrence period of 475 years. In DIN 4149, the Bavarian Alps include the warning zone 0, earthquake zone 1 as well as, locally, zone 2, which will be used for probabilistic differentiation.

3.3.2 *Heavy precipitation*

Statistic analyses (e.g. Sandersen et al. 1996) shows, that rock-fall frequencies increase during periods of heavy rainfalls or snow melt. Detail regional distinction of heavy precipitation is provided in the KOSTRA-Atlas of the DWD (Deutscher Wetterdienst; KOordinierte STarkniederschlags – Regionalisierungs – Auswertungen; Bartels et al. 1997). Probabilistic heights of heavy precipitation are supplied for different durations and recurrence intervals, based on 30 year old test series, in an areal pattern of 70km^2. For rock-fall probability estimations, we propose to consider the most intense events with highest durations: 72hrs, 100-years recurrence period.

3.4 *Models for rock-fall probability rating*

In order to assess the exposition to hazards associated with rock-falls we developed a classification scheme designed specifically for detail local evaluations, but also applicable for regional analyses by statistic accumulation.

The following chart shows the simplified way for probability assessment. In Table 1 the detail assessment process is shown.

Rating criteria			Rating	Valuation
Rock-Fall Disposition	Rock mechanics of the Detachment Zone	Orientation of discontinuities	0 — 500 (favourable - unfavourable)	17%
		+ Degree of weathering	0 — 200	7%
		+ Structural Configuration		
		Degree of transection	0 — 200	7%
		Persistence (length)	0 — 200	7%
		Opening width (aperture)	0 — 200	7%
		Condition of surfaces	0 — 200	7%
		or		
		Degree of loosening	0 — 800	28%
	Regional Geomecanical Environment	+ Type of basement	0 — 600	20%
		+ Large-scale, deep-seated deformations	0 — 200	7%
		+ Active movement in the foot of slope	0 — 200	7%
Activity		+ Activity in advance of potential rock falls	0 — 500	14%
= Score		low <800	moderate 800 - 1900	high 1900 - 3000
External Impact		In case probabilistic data available		
		Earthquake zonation	0 — 50	
		Heavy precipitation	0 — 50	
= Impact		weak <30	medium 30 - 60	strong >60

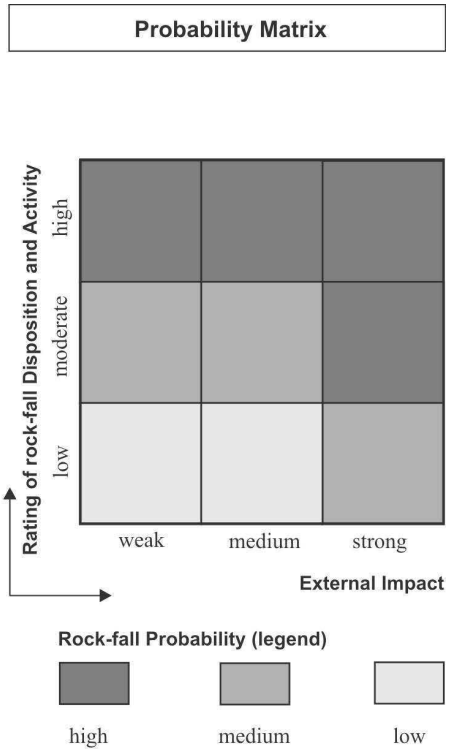

Figure 4. Simplified flow-chart for rock-fall probability rating, with hypothetical rating and valuation indices (see also Fig.1).

3.4.1 *Classification of rock-fall disposition*

Rock-fall disposition, which is the degree of the exposition to the hazard, must be transferred into a stochastic value. Several "rating systems" have been developed in rock mechanics. In our study, we want to present a method, which is mainly based on the ideas of the Rock Mass Rating System of Bienawski (1989) in engineering geology. The principle is presented in Fig. 4. The evaluated properties are rated according to their probabilistic impact and added to a total score. The system is easy to apply and adjustable. The rating procedure is carried out in two steps, assessment of the geological field data (disposition, activity) and assessment of external impact. The second step, however, is only performed when probabilistic data are available.

Rating

The properties mentioned in the fields "Rock mechanics of the detachment zone" and "Regional geomechnaical environment" are referenced with simple numerical scales. Different probabilistic conditions of a property can be expressed with low values indicating advantageous (favourable) conditions and high values indicating disadvantageous (unfavourable) conditions. The rock-fall disposition is finally assessed through the combination of the numerical scores of all evaluated categories.

Some categories require a more subjective evaluation, whereas others can be directly measured and then scored. Also the resulting total score is subject to an artificial probabilistic scale (see Tab. 1), which must be adjusted by personal expertise on the one hand, and experience from regional evaluations on the other.

Valuation of categories (significance)

The valuation of each mentioned property category denotes the degree of importance for probabilistic assessment. Often not all required data are available, especially in comprehensive regional evaluations, and thus cannot be involved in the rating process. In such cases, in general, unfavourable conditions must be assumed in the rating process (highest value). With missing data input the final score looses reliability. The degree of reliability of the result can be provided by including the valuation in addition to the final rating. The total valuation of 100% is decreased by the valuation of the missing category, e.g. 7% for the persistence of joints. Thus the degree of reliability of the result can be easily recognized.

3.4.2 *Classification of activity*

The significance of activity is mentioned in chapter 3.2. Activity in advance of rock-falls gives an important clue to understand the system behavior. A digital distinction between active and non-active detachment zones can be carried out. Active zones have a higher rock-fall probability.

The actual rock-fall activity s.s. helps to verify the assumptions and to differentiate different types of hazards (e.g. frequent falls of single blocks and the hazard of a large rock-fall in on and the same area).

3.4.3 *Classification according to external impact*

Further probabilistic input comes from the evaluation of earthquake zones and high precipitation maps. The mentioned parameters are rated, similar to disposition, giving a total score (see Tab. 1). The total scores of disposition and activity rating on the one hand, and the rating of external impact on the other are combined in a probability matrix and provide the final probability result (Fig. 1 and Tab. 1).

4 ROCK-FALL INTENSITY

Intensity or magnitude describes the energy occurring in a rock-fall event. Different approaches for definition exist in literature including e.g. velocity, energy levels, or the degree of destruction.

In this study, we refer to the block size (single falling blocks) or rock volume (falling rock masses) as a simple measurement which is representative of whichever type of rock-fall event is most likely to occur. This can be determined from geometry and geomechanical inventory of the detachment area or from the maintenance history if available. Other properties, like block shape, fracturing and subsequent defragmentation of rock masses, rock strength and the absorption coefficient of the foot of slope are important, however, mostly hard or impossible to acquire. Thus we confine ourselves to investigate the volume. This measurement is also required for determining remedial measures.

The distinguished categories (see Tab. 1) include, on the one hand, low-magnitude events, which are generally assumed as the classical rock-fall type. They range from single falling blocks to rock mass volumes up to 10000m^3. On the other hand, also high-magnitude events are encompassed in our hazard

analyses, which mostly are referred to as large rock-slides, rock avalanches or even have the dimension of a landslide.

5 DEFINING ROCK-FALL HAZARD BY A MATRIX MODEL

The final result (hazard) of the entire investigations and evaluations can be obtained from the rock-fall hazard matrix (Tab. 1 bottom). The matrix combines three likelihood categories with four intensity categories. Different colours or grey shades of the matrix fields can help differentiate the resulting degrees of intensity, whereas varying styles of hatching reflect probabilities. Thus it is possible to present different rock-fall hazard types in regional hazard maps. Table 1 is a form sheet which summarizes the entire evaluation process discussed in this article.

Table 1. Detail flow chart for rock-fall probability rating, rock-fall hazard matrix.

Occurrence Probability of Rock-fall

→ ***Assessment of Disposition and Activity***

1: Orientation of Discontinuities	**unfavourable**	**fair**	**favourable**
Dip direction of a prominent discontinuity set	adverse or slope-parallel	horizontal	inward or vertical
System of two or more discontinuity sets with similar geomechanical properties	mostly sliding wedges	----------	----------
Probability estimation	high	medium	low
Rating (Valuation 17%)	500	200	0
2: Weathering degree of joints in the detachment area Grades according to ISRM-IAEG	**medium to strong weathering** V4-5	**fresh to slight weathering** V1-3	
Probability estimation	high	low	
Rating (Valuation 7%)	200	0	
3: Structural Configuration of Discontinuities			
Persistence	large discontinuities (area > 100m², extent > 10m)	medium-scale disc. (area 10-100m², extent 1-10m)	small discontinuities (area < 10m², extent < 1m)
Rating (Valuation 7%)	200	100	0
Degree of Transection	no or subordinate mineral bonds	mineral bonds existent	
Rating (Valuation 7%)	200	0	
Opening width / Aperture	open (> 1 cm)	slightly open (0,5 mm bis 1 cm)	closed (< 0,5 mm)
Rating (Valuation 7%)	200	100	0
Condition of surfaces	slickensides	no slickensides	
Rating (Valuation 7%)	200	0	
4 (alternativ for category 3): Degree of Loosening	**high**	**low**	**no indication**
General description	clear indications available: -wide open gaps and fractures -neck valleys etc.	only subordinate indications	no indications given
Probability estimation	high	medium	low
Rating (Valuation 28%)	800	400	0
Total – Rock mechanics of the Detachment Zone [Category 1 + 2+ (3 or 4)]			

5: Type of Basement	**very unfavourable**	**unfavourable**	**favourable**
Type of formation	dissolvable rocks/formations (cavities and/or highly plastic behaviour)	clayey-marly formations (plastic behaviour)	other formations
Probability estimation	high	medium	low
Rating (Valuation 20%)	600	200	0
6: Large-scale, deep-seated deformations (e.g. sagging of mountain slopes, major landslides)	**yes** (detachment area influenced by large-scale slope deformations)	**no** (no large-scale slope deformations)	
Probability estimation	high	low	
Rating (Valuation 7%)	200	0	
7: Active mass movements in the foot of slope	**serious indications for mass movements**	**no or subordinate indications for mass movements**	
Probability estimation	high	low	
Rating (Valuation 7%)	200	0	
Total – Regional Geomechanical Environment [Categories 5 to 7]			

8: Activity			
Initial Activity	active	not active	
Rating (Valuation 14%)	500	0	
Rock-fall activity s.s.	active (in the range of the assessed maximum intensity)	active (in minor volumes compared to maximum assessed intensities)	not active
Probability estimation	**high**	t indicator of **initial activity**	no consideration
Final valuation in hazard matrix	**very likely**	----------	----------
Total – Activity [category 8]			

Total – Disposition and Activity	1) + 2) + [3) or 4)] +5) + 6) + 7) +8) =		
Probability estimation	high	medium	low
Classification	3000 to 1900	1900 to 800	800 to 0

→ ***Assessment of External Impact***

1: Earthquake Zonation	**Zone 2**	**Zone 1**	**Zone 0**
Probability estimation	high	medium	low
Rating	50	20	0
2: Heavy Precipitation	**> 310 mm**	**230 – 310 mm**	**< 230 mm**
Probability estimation	high	medium	low
Rating	50	20	0
Total – External Impact	1) + 2) =		
Probability estimation and classification	high > 60	medium 60 to 30	low < 30
Degree of impact	strong	medium	weak

→ ***Probability Matrix***

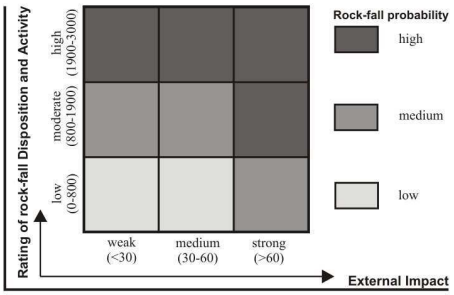

RESULT	**Rock-Fall Probability =**

INTENSITY of potential Rock-falls

→ ***Classification***

Intensity	**High-magnitude Rock-falls**		**Low-magnitude Rock-falls**		
Volume	**Rock avalanche**	**Large Rock-fall**	**Medium Rock-fall**	**Small Rock-fall**	**Single blocks**
Distinction	total rock mass volume > 1 Mio m³	total rock mass volume of up to 1 Mio m³	total rock mass volume of up to 10.000 m³	rock fragments with more than > 200 mm diameter and/or a rock mass total volume of up to 100 m³	one or few single fragments (< 200 mm)

ASSESSMENT of Rock-fall Hazard

→ ***Hazard Matrix***

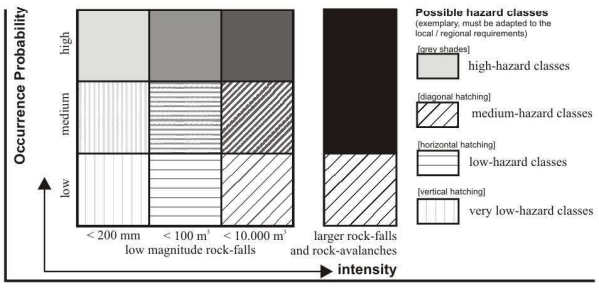

This assessments concept must be seen as a prototype for discussion, testing and development. It distinguishes hazard degrees in a descriptive way, parameters are quantified and combined, the process is also comprehensive and reproducible. Nevertheless, adjustments have to be carried out regarding the graduation/scales of disposition and activity as well as of external impacts. This graduation mainly depends on

regional project requirements. In this article we give proposals in numbers, but these must be verified in future application.

6 ACKNOWLEDGEMENTS

This study was carried out in close collaboration with A. von Poschinger and K. Meyer (LfU Munich). Helpful advice was obtained from the following institutions: Münchner Rück (Munich), Landesamt für Wasserwirtschaft (Munich), Deutscher Wetterdienst (Offenbach), Department of Engineering Geology (TU Munich) and Alp-Infra (Vienna).

REFERENCES

Bartels, H., Malitz, G., Asmus, S., Albrecht, F.M., Dietzer, B., Günther, T. & Ertel, H. 1997. KOSTRA – Starkniederschlagshöhen für Deutschland. Deutscher Wetterdienst, Geschäftsfeld Hydrometeorologie, Offenbach.

Bienawski, Z.T. 1989. Geomechanics Classification (Rock Mass Rating System). In: Bienawski, Z.T. (eds.), Engineering rock mass classifications – A complete manual for engineers, geologists in mining, civil and petroleum engineering, 97-106, John Wiley & Sons.

Budetta, P. 2004. Assessment of rockfall risk along roads. Natural Hazards and Earth System Sciences, 4, 71-81.

Corominas, J., Copons, R., Vilaplana, J.M., Altimir, J. & Amigo, J. 2003. From landslide hazard assessment to management. The Andorran experience. In: Picarelli, L. (eds.), Fast slope movements – prediction and prevention for risk mitigation, 1, 111-118, Associazione Geotecnica Italiana, Bologna, Patron Editore.

Dussauge-Peisser, C., Helmstetter, A., Grasso, J.-R., Hantz, D., Desvarreux, P., Jeannin, M. & Giraud, A. 2002. Probabilistic approach to rock fall hazard assessment: potential of historical data analysis. Natural Hazards and Earth System Sciences, 2, 15-26.

Einstein, H.H. 1988. Landslide risk assessment procedure. Landslides Glissements du Terrain, 2, p. 1075-1090.

Evans, S.G. & Hungr, O. 1993. The assessment of rockfall hazard at the base of talus slopes. Canadian Geotechnical Journal, 30, 620-636.

Lateltin, O. 1997. Empfehlungen – Berücksichtigung der Massenbewegungsgefahren bei raumwirksamen Tätigkeiten, 1-42, Bundesamt für Raumplanung, Bundesamt für Wasserwirtschaft, Bundesamt für Umwelt, Wald und Landschaft, Schweiz.

Meißl, G. 1998. Modellierung der Reichweite von Felsstürzen – Fallbeispiele zur GIS-gestützten Gefahrenbeurteilung aus dem Bayerischen und Tiroler Alpenraum. Innsbrucker Geographische Studien, 28, 1-249.

Sandersen, F., Bakkehoi, S., Hestnes, E. & Lied, K. 1996. The influence of meteorological factors on the initiation of debris flows, rockfalls, rockslides and rockmass stability. Proceedings of the 7th International Symposium on Landslides, 1, 97-114.

ISGSR 2011 - Vogt, Schuppener, Straub & Bräu (eds) - © 2011 Bundesanstalt für Wasserbau ISBN 978-3-939230-01-4

The effectiveness of protection systems toward rockfall risk mitigation

G. Gottardi, L. Govoni, A. Mentani & M. Ranalli
Bologna University

C. Strada
Autonomous Province of Bolzano

ABSTRACT: A comprehensive method for rockfall risk analysis has been recently proposed by the Autonomous Province of Bolzano within the context of European project PARAmount (imProved Accessibility, Reliability and safety of Alpine transport infrastructure related to MOUNTainous hazard in a changing climate). The procedure is especially aimed to a proper planning of effective countermeasures through a rational management of the existent. To such purpose, the process of hazard evaluation has been especially designed to accommodate the presence of protection systems located in the area interested by the analysis. The application of the procedure requires a thorough knowledge of the considered works, which includes passive and active protection systems. With reference to the passive measures, the paper presents a numerical study of falling rock protection barriers at present installed within the Province territory. The investigation addresses the actual effectiveness of these structures toward hazard mitigation. Preliminary analyses and results, concerning a carefully carried out selection of barrier types occurring on the territory are described and commented.

Keywords: hazard, falling rock protection barriers, numerical modelling

1 INTRODUCTION

Rockfall consists of the free falling, bouncing, rolling and sliding of blocks of different sizes detached from a rock slope (Giani, 1992). Typical of mountainous areas the phenomenon is one of the most frequent geological hazard. The related risk can be particularly high in areas extensively crossed by roads and railway arteries and characterized by densely populated towns and tourist infrastructures, such as for instance, the Alpine space. Owing to the ever increasing urban expansion as well as climate changes, the interference between human activities and natural events has considerably grown in these areas. Due to these circumstances, the development of appropriate tools for landslide risk analysis and management has become a crucial issue for the local administrations and agencies in charge of protecting the territory (Fell and Hartford, 1997; Lee and Jones, 2004).

An effective planning of rockfall countermeasures needs to rely on a rational management of the existent. An adequate risk analysis should allow to take in due consideration the presence of the protection systems on the concerned area, either within the rockfall hazard (H) or vulnerability (V) evaluation. A few risk assessment procedures which address the presence of protection structures on the territory are currently available (Oggeri and Tosco 2005, Corominas et al. 2005).

Within the context of the European project PARAmount (imProved Accessibility, Reliability and safety of Alpine transport infrastructure related to MOUNTainous hazard in a changing climate), the Autonomous Province of Bolzano (Italy) has recently developed a tool for rockfall risk analysis. In the procedure, the process of hazard assessment is especially devised to accommodate the presence of existing passive and active countermeasures, yet carefully registered in a complete and constantly updated Province's inventory of protection works.

Among ditches, sheds, earth retaining structures, wire nets, the inventory includes data on falling rock protection barriers, metallic structures designed to intercept and stop the blocks moving along a slope in a rockfall event. Easy to be installed and maintained, these structures are able to stop blocks having a wide

range of kinetic energy values, from only a few up to more than 4500 kJ. For these reasons, over the last three decades, they have been used extensively, especially when urgent conditions required fast solutions and neither a comprehensive planning nor proper design could be completed.

As a result, the behaviour of a significant portion of formerly devised and installed protection barriers is currently uncertain. These circumstances make extremely problematic to complete the procedure of hazard evaluation which at least requires the structure nominal capacity in term of kinetic energy to be known (Figure 1).

This lack of information can be reasonably covered by a suitably designed numerical study addressing the behaviour of these structures in dynamic condition. A numerical investigation as such should be based on detailed information on the geometries, properties and preservation state of the concerned work.

The paper presents preliminary results of an extensive study of the falling rock protection barriers installed within the Autonomous Province of Bolzano and registered in the Province's inventory of the protection works. In particular, a numerical study of selected types of barriers, chosen among the most frequently occurring is presented. The study enables to attain results on the nominal response of a significant portion of falling rock protection barriers of the territory. These data provide the starting point for the investigation of the actual barrier response which also account for the specific on-site arrangement, positioning and state of maintenance.

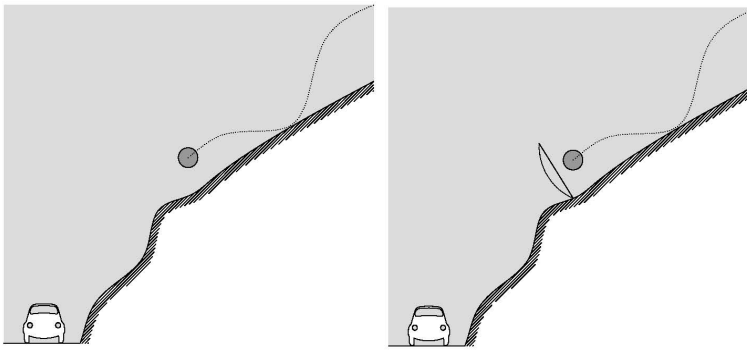

Figure 1. The role of falling rock protection barriers in the process of hazard assessment.

2 HAZARD ASSESSMENT WHITHIN THE AUTONOMOUS PROVINCE OF BOLZANO

Within the Autonomous Province of Bolzano a tool for rockfall risk analysis has been recently developed. In the procedure, the natural slope hazard (H) is modified to account for the possible presence of protection systems (H^*). The procedure to evaluate the modified hazard (H^*) is illustrated in Figure 2.

The relevant parameters which enable to describe a given existing protection system installed along the slope interested by the analysis are: 'design', the 'location' and the 'conditions' of the considered protection work. The 'design' and 'location' parameters describe the system ability to effectively stop the blocks falling along the slope. These parameters are evaluated assuming that the considered protection system is perfect working conditions. These parameters, as illustrated in Figure 2a range from 1 to 5. Value 1 for design (location) represents the optimal condition, that is: the system has been suitably designed (positioned) and is thus able to catch the blocks as predicted by the relevant slope analyses. On the other hand, value 5 represents the worst circumstances.

The 'condition' parameter account for a diminished performance of the protection work owing to its state of maintenance. Values vary from good to problematic (Figure 2b).

Combination of 'design' and 'location' parameters supplies the overall 'utility' of the protection system which decreases from 1 to 5 (Figure 2a).

As depicted in the chart of Figure 2b, the determined 'utility' is combined with the 'condition' parameter providing the 'priority of protection system maintenance'. This parameter describes the actual (i.e. in the real working conditions) system effectiveness. It range from A to E in the sense of decreasing priority. The modified hazard (H^*) is then evaluated according to Figure 2c, by combining the 'hazard of the natural slope' with the 'priority of protection system maintenance'.

According to the procedure, the hazard magnitude can remain unvaried, be reduced or even enhanced owing to the protection system actual effectiveness. A single uncertain parameter (problematic) can itself increase the natural slope hazard (H).

It is therefore apparent that a procedure as such can be successfully applied only if the behaviour of the protection work is thoroughly known.

Suitable numerical analyses can be carried out in order to reduce the uncertainties related to the evaluation of these three parameters, notably the 'design' and 'condition'. A possible procedure is suggested in the following sections, with reference to rockfall protection barriers.

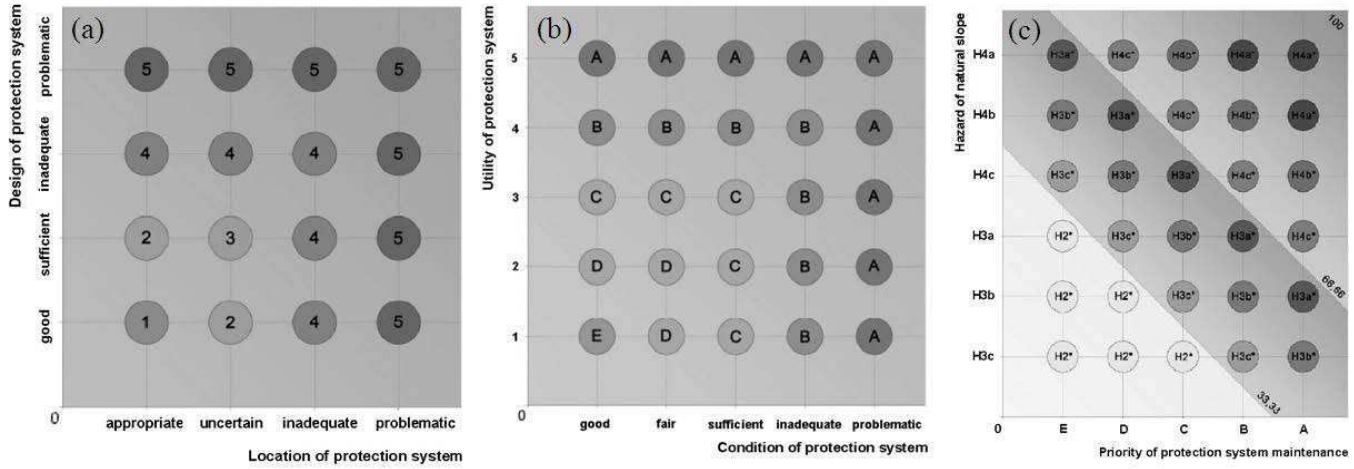

Figure 2. Procedure for the evaluation of the modified hazard *H**: a) chart for the assessment of the protection system 'utility' b) chart for protection system 'maintenance priority' and c) chart for the evaluation of the modified hazard *H**.

3 DEVELOPMENT OF A DATABASE OF FALLING ROCK PROTECTION BARRIERS

A typical falling rock protection barrier is made of a series of identical functional modules installed in sequence to the desired length. Each functional module generally features an interception structure, kept in position by a supporting structure. Connecting components join the barrier elements and transfer the loads to the foundations.

Protection barriers are designed to intercept and stop blocks moving along a slope in a rockfall event. Traditionally the design capacity is related to the maximum energy possessed by a block which the barrier is capable to arrest.

Several models and types barriers are now available, covering a wide range of capacities. Barriers belonging to different capacity classes typically feature diverse structural components. Customarily, all barriers types are grouped in two main categories. Those belonging to low energy classes are named semi-flexible and those of higher energy classes flexible (Peila et al., 2008), but barrier with intermediate characteristics are frequently encountered as depicted in Figure 3.

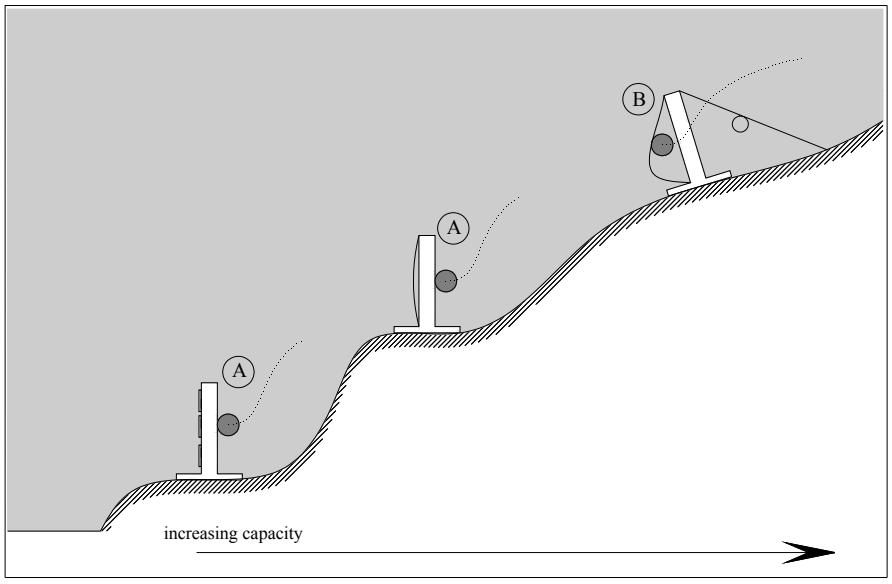

Figure 3. Falling rock protection barrier: scheme of relevant typologies of falling rock protection barriers: A semi-flexible, B flexible.

Although some plastic deformations are likely to occur, semi-flexible barriers mostly deform elastically, under the impact of block having low to medium impact energies. The capacity is thus related to their ability to catch and stop a block without undergoing rupture in the system and system components. Conversely, flexible barriers typically dissipate the high impact energies by developing large plastic deformation: the greater the barrier capacity, the higher its plastic compliance. For these barriers the deformation should be also kept within working levels. As it can be observed in Figure 3, where a photographic example of each barrier category is given, when assembled on site, each barrier becomes a unique item, though retaining the principal features of its capacity class.

Basic information on the barriers of the Autonomous Province of Bolzano, can be now found in VISO, a thorough inventory of the protection works now installed within the province area. With reference the specific hazard event and threatened items, passive systems such as ditches, wire nets, earth dams, sheds, and falling rock protection barriers are registered within the inventory. Data have been mostly acquired by direct inspections carried out over the law few years.

Within the inventory, position, typology and principal dimensions of each protection work are given, along with a relevant photographs and remarks on the state of maintenance.

3.1 *Falling rock protection barrier description and classification*

These data have been recently conveniently integrated, addressing a more precise description of the geometrical and mechanical properties of the structure and principal structural components.

Additional information were mostly acquired from documentation supplied from agencies in charge to protect the relevant road stretches and manufacturer companies. Documents include technical reports, design reports and drawings. These data enable to identify the most frequently occurring barrier types. Within the Province's territory, approximately thirty barrier types were identified: more than twenty among those having the higher energy absorption capacity and less than ten among those belonging to the low and medium energy classes. A thorough description of the typical functional module of the identified barrier type was carried out according to the available documentations. In particular, the interception structure, the supporting structure, the connecting components, including ropes, cables, clamps an energy dissipating device and internal and external restraints were described in details. Also, if available, data of full-scale tests of prototypes, as well as all the design drawings were conveniently analyzed and relevant information were included in the database.

A procedure was then carried out in which the falling rock protection barriers formerly inserted in VISO were grouped according the relevant barrier type.

Figure 4a shows a barrier made of a series of the typical functional module of barrier type ANAS as inventoried in VISO. The schema of the typical functional module is found in Figure 4b, where information are also given on the principal structure components. For this barrier type, no information are available on the nominal behaviour or energy class. Nonetheless, barrier type ANAS can be described as semi-flexible.

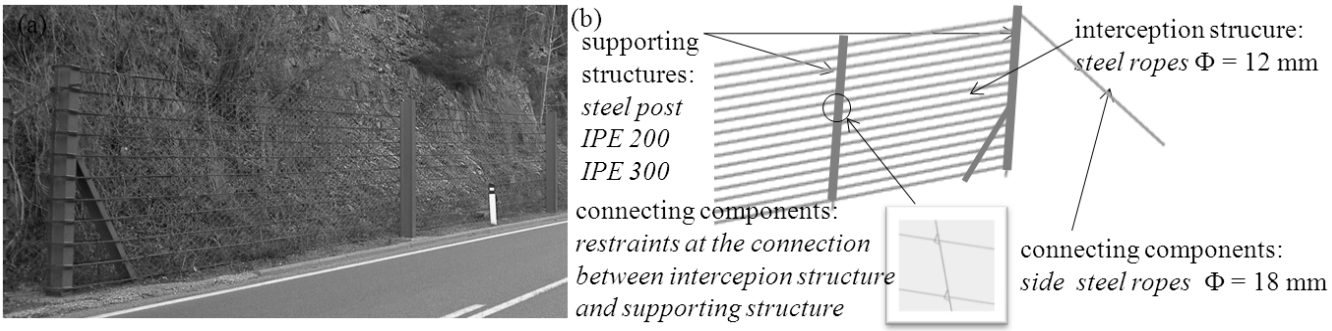

Figure 4. Example of falling rock protection barriers installed in the Autonomous Province of Bolzano: a) barrier ss38_12_1 belonging to type ANAS and b) scheme of the functional module of barrier type ANAS.

Figure 5a shows one of the VISO flexible falling rock protection barrier. The barrier is one of high energy absorption capacity which features a set of the functional modules of barrier type PT_B750 described in the drawing of Figure 5b. For this barrier type a comprehensive technical report documenting the barrier behaviour under impact was available. In the technical report details of results of full scale tests carried

out on PT_B750 prototypes were included assessing the barrier capacity to arrest blocks having energies up to 750 kJ.

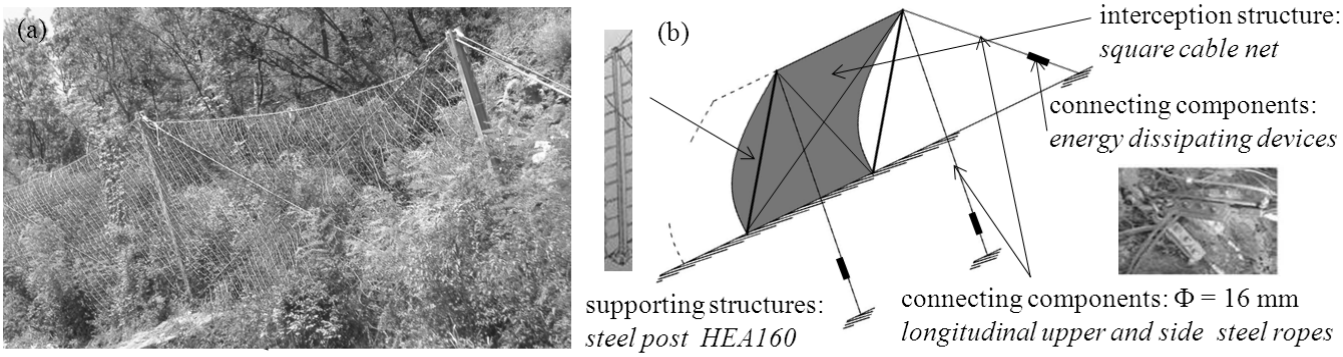

Figure 5. Example of falling rock protection barriers installed in the Autonomous Province of Bolzano: a) barrier 12_5_GR_008/014 belonging to type PT_B750 and b) scheme of the functional module of barrier type PT_B750.

With reference to flexible and semi-flexible systems, Figure 6 provides the number of occurrences of each barrier type divided by the total number of barriers (approximately 700). The name given to the barrier type includes, when available: the manufacture company denomination, the capacity and the date in which the nominal capacity was assessed by full-scale testing and then placed on the market. For instance, barrier type PT_B750, depicted in Figure 6 has a nominal capacity of 750 kJ. The capacity was assessed in 2000 by full scale testing of barrier prototypes. Among all the flexible and semi-flexible barrier types barrier PT_B750 is the most frequently occurring.

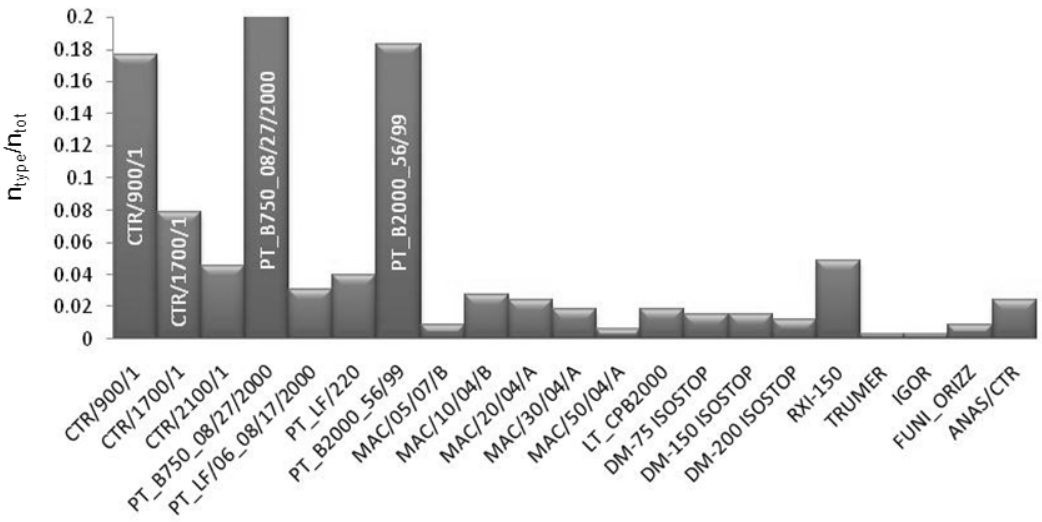

Figure 6. Principal types of flexible falling rock protection barriers within the Autonomous Province of Bolzano.

4 NUMERICAL STUDY OF FALLING ROCK PROTECTION BARRIERS

The data collected in the database provide the starting point for a numerical study of the barriers described in it. To the scope, the commercially available computer program ABAQUS/Explicit v. 6.9 (Hibbit et al. 1997) has been employed as it has been shown it is especially suitable to perform and solve high speed dynamic events (Cazzani et al. 2002, Mentani, 2010).

The preliminary FE study herein presented, addresses the three-dimensional, non linear, dynamic response of the two barrier types described in the previous section. The study is carried out in analogy with a well established full-scale testing procedure (Peila, 1999, Geber, 2001, Gottardi and Govoni, 2010) which is generally used to assess the capacity of a falling rock protection barrier to effectively stop blocks having kinetic energy up the design level. Such procedure has been historically used as a design tool for rockfall fences (Higgins, 2003) and it has lately been applied to flexible barriers in an extensive manner, becoming a mandatory step in the process of CE marking of barrier having energy absorption capacity higher than 100 kJ (EOTA, 2008).

Full-scale impact test are generally carried out at a suitable test site onto samples of falling rock protection barriers consisting of three functional modules (i.e. three spans). At the test site a concrete test block is accelerated to impact, with speed known both in intensity and direction, the centre of the falling rock protection barrier prototype installed at some inclination to a test rock wall.
During the test, relevant quantities, such as the barrier elongation and the forces on the foundations are generally recorded with time. Further information on testing details are comprehensively found in Peila et al. (2006).
Noting that the procedure assesses the barriers response with sole the reference to kinetic energy parameters, although other parameters might significantly affect the barrier response (Cantarelli et al., 2008), the FE study was developed following these instructions.

In the following sections, details on the numerical modelling are illustrated along with briefly commented preliminary results.

4.1 *Details on the numerical modelling: barrier types and testing procedures*

Two barrier types were modeled, which were selected as representative of different capacity classes: the ANAS and the PT_750. Description of these barrier types were provided in Section 3, and relevant pictures were provided in section 3 and Figures 4 and 5.

Following the above described experimental procedure numerical models were made up of three functional modules.
In Figure 7, the three functional modules model of barrier ANAS is shown with nodes numbered from 1 to 10. At node 1 to 6 the barrier was connected to the ground through the two side cables and four posts. All dofs were restrained at these 6 nodes (black dots).
With reference to the barrier structural components illustrated in Figure 4b, steel posts were modeled employing two-nodes beam elements having the relevant, IPE, cross sectional area. One dimensional two-nodes truss elements, with no flexural rigidity and zero compression axial load limit were employed to describe the behaviour of all the steel ropes which form the interception structure as well as the side cables. Sections were assigned according to the actual elements cross sectional area. For all the elements a bilinear, elastic-plastic behaviour was assumed. Particular attention was focused on the modelling of the system connecting elements such as the ropes connections to posts.

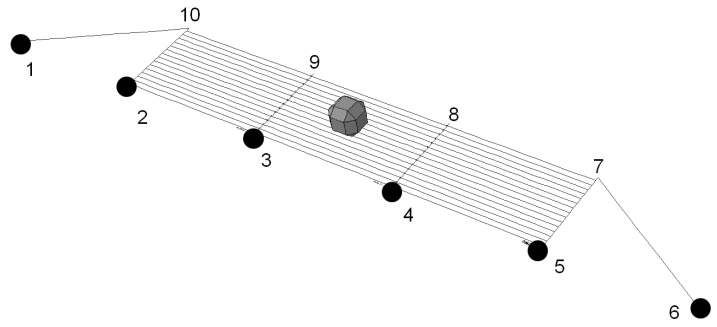

Figure 7. Three functional modules FE model of the ANAS barrier.

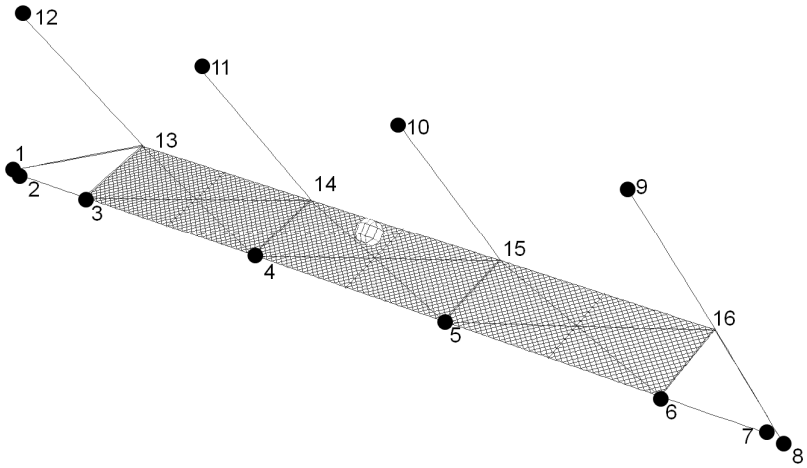

Figure 8. Three functional modules FE model of the PT_750 barrier.

In Figure 8, the three functional modules FE model of barrier PT_750 is shown with nodes numbered from 1 to 16. At node 1 to 12 the barrier was connected to the ground through the side cables, the longitudinal lower ropes, uphill cables and four posts. Connections of the structure to the ground were modeled at these point as cylindrical hinges.
With reference to the barrier structural components illustrated in Figure 4b, two-nodes beam elements were used for the posts. A mesh of one-dimensional two-nodes truss elements was used to model the interception structure. Trusses were also employed for the side and uphill cables. Sections were assigned according to the actual elements cross sectional area. For all the elements a bilinear, elastic-plastic behaviour was assumed.

As mentioned above, no information on the structural behaviour or indication on the energy class were available for barrier type ANAS. The numerical analyses were carried out following widely used full-scale tests procedures at vertical drop test sites (Gerber, 2001, Gottardi and Govoni, 2010). In the procedure a three functional modules barrier prototype, installed normal to a vertical rock wall is impacted vertically by a concrete test block.

In the FE analysis the block was modelled with a three-dimensional deformable body shaped as a polyhedron. By varying the block velocity, the simulation were performed at 25, 50, 75 and 100 kJ, in order to observe the barrier response to increasing values of kinetic energies up to admissible stress values.

Results of full-scale tests on prototypes were, instead, available for the PT_750. Experiments were carried out at an inclined test site (Peila, 1999). Data recorded in the tests were the maximum barrier elongation and the residual height. The FE study was carried out in order to replicate the full-scale tests as close as possible. A model of three functional modules was developed and installed according to the test site geometry as depicted in Figure 8. The barrier model was then subjected to one single launch of a block having kinetic energy higher than 750 kJ.

4.2 *Results*

In Figures 9 to 10 preliminary results of the FE dynamic analyses on the models of barrier types ANAS and PT_750 are provided qualitatively in term of stress and structure deformed shape.

In Figure 9 the data obtained by the numerical simulation carried out at 100 kJ on the ANAS barrier are presented. The Figure depict the barrier at the instant of the test at which the maximum barrier deformation occurred, approximately at 0.15 s since the start of the analysis. The barrier response is depicted by its deformed shape. Maximum non-admissible tensile stress were reached within the truss element involved by the impact (darker gray lines).

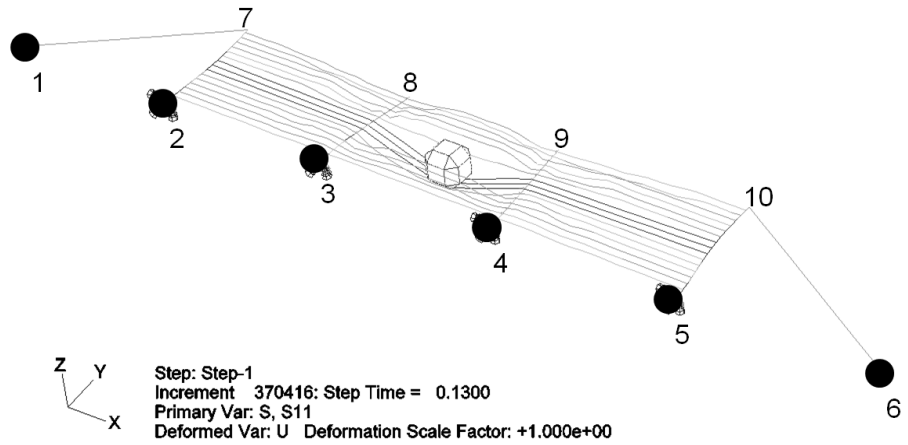

Figure 9. Deformed shape and qualitative stress distribution within the model of the ANAS barrier type at the maximum elongation during 100 kJ analyses. Time = 0.15s.

In Figures 10 the principal results of the analysis carried out on the PT_750 barrier are provided at three different instant at which the maximum elongation has been reached (0.24 s). Frames provide a qualitative assessment of the barrier behaviour during the impact. Results on barrier deformation substantially agree with the experimental, both in terms of maximum displacement (approximately 3m) and time to reach it. Furthermore all stresses were found to be within the admissible limit, assessing the model capacity of describing the barrier behaviour in testing conditions. The model thus enables to provide reliable predictions on other data such as the time histories of the forces at the foundations.

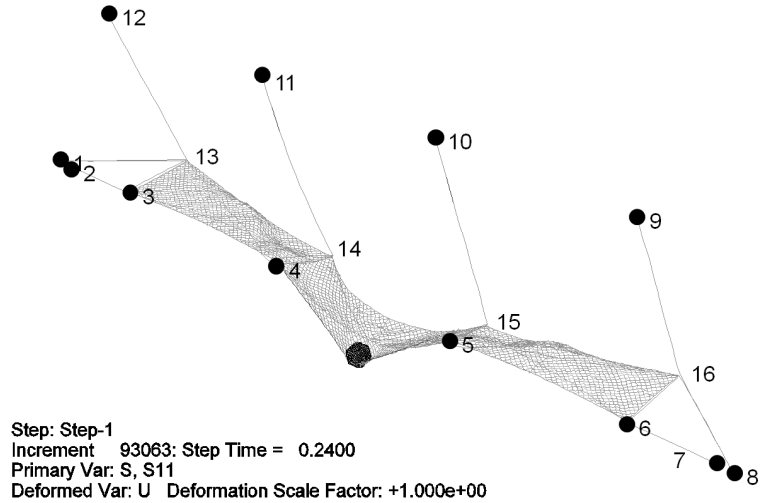

Figure 11. Deformed shape and qualitative stress distribution within the model of the PT_750 barrier type. Time = 0.24s.

5 CONCLUDING REMARKS

The paper has presented the preliminary results of a study on diverse types of falling rock protection barriers installed within the Autonomous Province of Bolzano. The study forms part of the activities of European project PARAmount (imProved Accessibility, Reliability and safety of Alpine transport infrastructure related to MOUNTainous hazard in a changing climate) and particularly addresses a method to evaluate the effects of passive measures against rockfall toward risk mitigation. In the paper the development of a database of the falling rock protection barriers at present installed within the Province is described. The database is aimed to collect the data necessary to a numerical study of the most frequently occurring barrier types. The scope of the numerical study is to produce information on the barrier nominal response in dynamic conditions. Numerical models then provide the data to the description of the nominal behaviour of the protection system during an impact. They can also be used to investigate the actual barrier response if they are suitable modified to accommodate the on-site arrangement, positioning and state of maintenance.

REFERENCES

Cantarelli G., Giani G. P., Gottardi G., Govoni L. (2008) Modelling falling rock protection fences. 1st World Landslide Forum, Tokyo, Novembre 2008.

Cazzani A., Mongiovì L., Frenez T. (2002) Dynamic finite element analysis of interceptive devices for falling rocks. Int. J. Rock Mech. Min. Sci. 39 (3) 303–321.

Corominas J., Copons R., Moya J., Vilaplana J. M., Altimir J., Amigo J. (2005). Quantitative assessment of the residual risk in a rockfall protected area, Landslides, 2 (2005) 343-357

EOTA (2008) Guideline for European technical approval of falling rock protection kits (ETAG 027). February 2008, Brussels.

Fell, R. & Hartford, D. (1997) Landslide risk management. Proc. of the International workshop on landslides risk assessment, Honolulu, 19-21 February 1997, Balkema Rotterdam, pp. 51-110.

Gerber W. (2001) Field testing of falling rock protectionprotection barriers a comparison between inclined ropeway and vertical crane testing. Swiss Agency for the Environment, Forests and Landscape (SAEFL) and the Swiss Federal Research Institute WSL. August 17th 2001. Birmensdorf.

Giani G. P. (1992) Rock slope stability analysis. Balkema, Rotterdam, NL

Gottardi and Govoni (2010) Full scale modelling of rockfall protection barriers, Rock Mech. Rock Engng. 43 (2010), pp. 261-274.

Hibbitt, Karlsson and Soresen Inc. 1997. ABAQUS Theory manual – Version 6.9. Pawtucket, RI.

Higgins J. D. (2003) Recommended procedure for the testing of rock-fall barriers. AASHTO Technical Report, Washington.

Lee, E.M. & Jones, D.K.C. (2004) Landslide risk assessment. Thomas Telford, 2004.

Mentani, A. (2010). Numerical non linear modelling of the response of a rockfall protection barrier to impact loading, Master Thesis, Advisor Prof. G. Gottardi, Bologna 2010 (in Italian)

Peila D., Pelizza S., Sassudelli F. (1998) Evaluation of behaviour of falling rock protection restraining nets by full-scale tests. Rock Mech. Rock Engng. 31 (1998) 1-24.

Oggeri C. and Tosco P. (2005) Identificazione del rischio per fenomeni di caduta massi, GEAM., 2005, Vol. 1, 23-32.

Peila D, Oggeri C, Baratono P (2006) Barriere paramassi a rete, interventi e dimensionamento. GEAM Quaderni di studio e documentazione 25, Torino.

ISGSR 2011 - Vogt, Schuppener, Straub & Bräu (eds) - © 2011 Bundesanstalt für Wasserbau ISBN 978-3-939230-01-4

A GIS-based approach for mapping hazardous areas due to geological slope processes: case study for Jesenice municipality in Slovenia

M. U. Pavlič & B. Praznik
Building and Civil Engineering Institute ZRMK d.o.o., Ljubljana

ABSTRACT: As the human population and the developed areas are increasing, rural areas are getting more and more populated. Development of rural areas creates problems especially in mountainous regions and areas that are highly susceptible to geological slope processes as people often tend to build houses and reside in such areas. Therefore, a need for classification and identification of hazardous zones is present so that precautions can be made in order to lessen the effects of geologically conditioned risks. In order to create a map of hazardous areas, identification of risk present for a specific site has to be made, as different geological processes dominate in specific areas. A case study is presented for a municipality of Jesenice where a steep mountainous region with a large energy potential and precipitation area are one of the main factors of geologically conditioned risks. The purpose of this study was to construct a hazard map classified in several classes according to susceptibility for geological risk and to prepare a set of measures to lessen the damaging effects and allow safe construction of different objects in affected areas. For that, identification of present geological processes in the area was made in order to create a hazard map for each of the prevailing processes. In our work landslides, debris flows and rock fall was identified as a present and prevailing slope processes in the area. According to different types of slope processes we made threat specific maps for each process in order to identify which risk is dominating in specific area. Determination of which process is dominating in specific area was crucial as the protection and countermeasures are completely different for each of the processes. After that we combined individual maps to get a final map of geologically conditioned hazardous areas. Due to a large area of interest Geographical Information System (GIS) based models were used – a different model for each process. Different input data were used for each of the model as the dynamics of each process is different. Data used in models included slope gradient, concavity of slopes, geology, vegetation and precipitation. For modeling rock fall we used a RockyFor3D developed by Luuk K.A. Dorren. Individual models were calibrated and verified on numerous observed locations. Final result of our model produced a hazard map divided in four classes according to degree of risk. For every class a chart was made with a list of conditions that must be met in order to ensure safe building in affected areas and prescribed necessary and relevant geological investigations. Models used in our study turned out to be a good tool for fast rating of geologically induced threats on a regional level, but they can easily be modified for use on a more site specific problems.

Keywords: GIS, landslides, rock fall, debris flow, geotechnics

1 INTRODUCTION

As the human population and the developed areas are increasing, rural areas are getting more and more populated. Development of rural areas creates problems especially in mountainous regions and areas that are highly susceptible to geological slope processes as people often tend to build houses and reside in such areas. Therefore, a need for classification and identification of hazardous zones is present so that precautions can be made in order to lessen the effects of geologically conditioned risks. A case study is presented for a municipality of Jesenice in the northern part of Slovenija, where a steep mountainous re-

gion with a large energy potential, precipitation area and the diversity of lithological units are one of the main factors of geologically conditioned risks.

The purpose of this study was to construct a hazard map classified in several classes according to susceptibility for geological risk and to prepare a set of measures to lessen the damaging effects and allow safe construction of different objects in affected areas. For that, identification of present geological processes was made in order to create a hazard map for each of the prevailing process. During this study several geologically conditioned slope processes were researched and modeled:

- landslides
- debris flows
- rock fall

Based on the type of slope process threat specific maps were constructed for each in order to identify which risk is dominating in specific area. In the last part partial hazard maps as a result of landslides, rock falls and debris flows were combined in order to get a general hazard map of the area.

Different input data were used for each of the model as the dynamics of each process is different. Data used in models included slope gradient, concavity of slopes, geology, vegetation and precipitation.

Final result of our model produced a hazard map divided in four classes according to degree of risk. For every class a chart was made with a list of conditions that must be met in order to ensure safe building in affected areas and prescribed necessary and relevant geological investigations. Models used in our study turned out to be a good tool for fast rating of geologically induced threats on a regional level, but they can easily be modified for use on a more site specific problems.

2 DESCRIPTION

The municipality of Jesenice is situated in the north western part of Slovenia. The city of Jesenice lies in the vales of river Sava, bordered with Karavanke Mountains on the northern part and Julian Alps on the southern part.

Municipality of Jesenice is one of the most versatile areas in Slovenia in geological sense, with the range of geological formations from Paleozoic era to Quaternary sediments. Populated areas in the municipality range in elevations from the main city center at elevation around 700 meters above sea level to remote villages at almost 2000 meters above sea level. Picture below gives the main overview of the municipality.

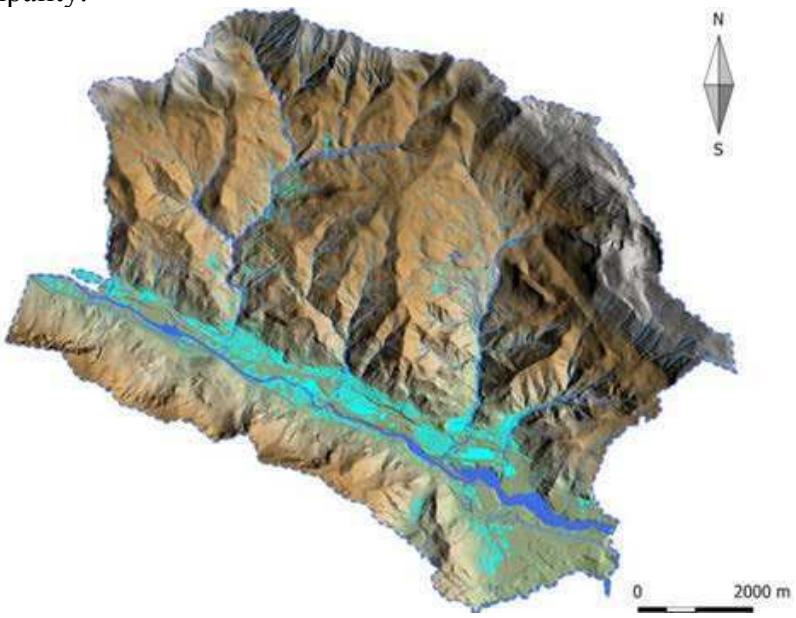

Figure 1. DEM of municipality of Jesenice (populated areas are in cyan color).

Geology and morphology of the terrain play a major role in problems related with catastrophic events. In last years number of catastrophic events is increasing in Slovenia causing major economic damage and loss of human life. Because of that municipality of Jesenice decided to conduct a study, based on which, landscape use will be made.

Landslides, debris flows and rock falls were identified as geologically related slope processes that are most likely to cause damage in the area. A map was created for each of the process in order to identify areas in which each risk is prevailing. The main cause for that was that the measures for increasing safety in given area are highly related to type of hazards. Diagram below shows the concept used in creating a hazard map.

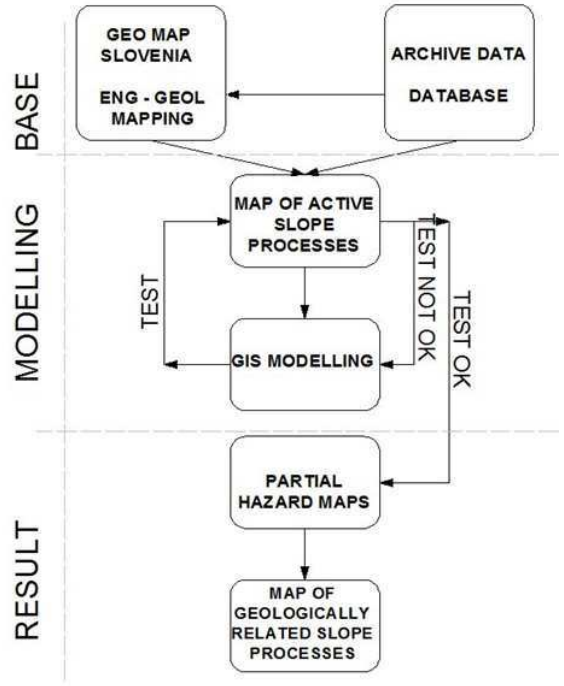

Figure 2. Concept used in creating a hazard map.

In creating of hazard map a base geological map of Slovenia (1:100000) was used as a foundation for engineering - geological mapping. Urban areas and areas with geotechnically worse lithology were mapped in bigger detail that other part of municipality.

GIS system was used as a base tool for spatial analysis and raster creation. Each of the slope process had different input, based on the mechanism that drives the process. Below diagram shows layers used in modeling each process.

	slope process	LANDSLIDE	DEBRIS FLOW	ROCK FALL
FACTORS	TERRAIN	LITHOLOGY SLOPE THICKNESS OF SOIL MORPHOLOGY	LITHOLOGY SLOPE POTENTIAL ELEVATION MORPHOLOGY	LITHOLOGY SLOPE MORPHOLOGY SURFACE ROUGHNESS ROCK DENSITY ROCK SHAPE
	INITIAL	CONCAVE/CONVEX PERCEPITATION	DISTANCE TO SURFACE FLOW ENERGY POTENTIAL OF WATERFLOWS CONCAVE/CONVEX PERCEPITATION	SOURCE POINTS

Figure 3. Factors included in modeling of slope processes.

All factors were normalized to values between 0 and 1 in order to provide equivalence when summing the raster together. This factor is called factor of contribution.

3 METHODOLOGY

Different methodology was used for each slope process. Engineering - geological map was created during mapping of urban and problematic areas. This map was later additionally modified and factor of con-

tribution was dedicated. Factor of contribution was dedicated in accordance to geotechnical characteristics of rocks and sediments that dominate each process. Bellow table shows factors of contribution for given type of lithology used in modeling landslides and debris flows.

Table 1. Factor of contribution for given process

lithology	LANSLIDES	DEBRIS FLOWS
lithified sea sediments	1	0.5
marlstone	0.75	0.67
siltstones and silt	0.75	0.5
claystone	0.75	0.67
deluvial sediments	0.75	0.83
marl limestone	0.5	0.67
alternation of sand stones and siltstones	0.5	0.5
deluvial fans	0.5	0.83
claytones and clay	0.25	0.17
sandstones	0.25	0.5
alluvial sediments and river terraces	0.25	0.33
carbonate rocks	0	0.33
plain alluvial sediment	0	0

Same process was used in most input data raters. Models for landslides and debris flows are in general iteration models, based on trial and error. Data that we collected during geological mapping was saved in a database that was used in model calibration, according to figure 2. Raster was calculated (summed) where different weight was given to each layer until final map coincided with field observations. Bellow landslide risk map is presented.

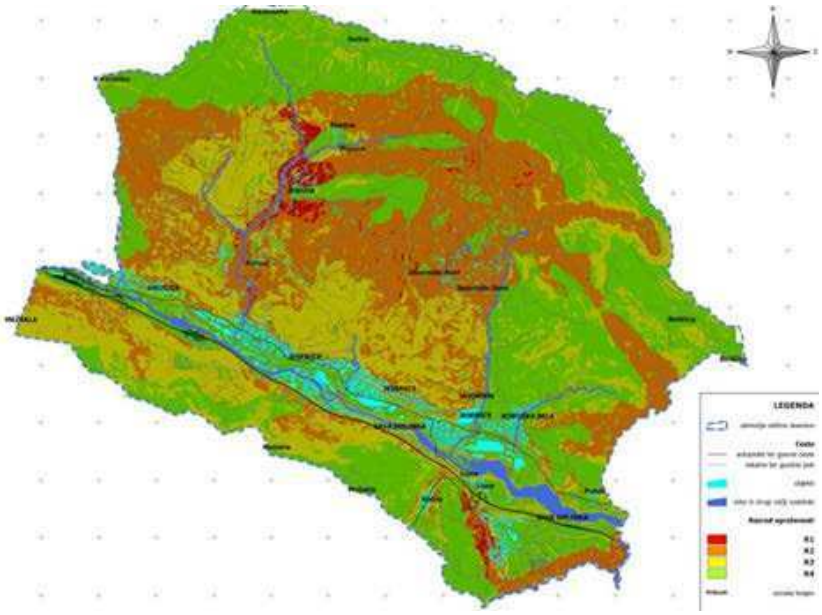

Figure 4. Landslide risk map

End maps were divided in 4 different classes using natural breaks method (“jenks”), where class 1 (red on figures 4 to 7) represents the most highly susceptible map and class 4 (green on figures 4 to 7) represents an area least likely to be hit by disaster.

Model for landslide and debris flows are not numerical model, but analytical. Because of that an additional mapping of run out zones for debris flow was conducted where areas historically stroked with debris flow were estimated. These areas were later accounted in summing the rasters which generated debris flow map. Figure 5 shows debris flow map generated with described methodology.

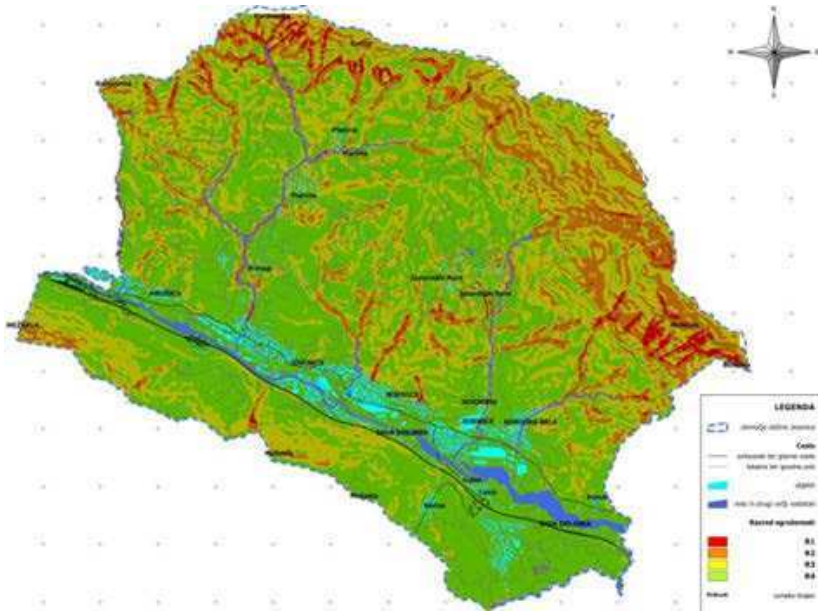

Figure 5. Debris flow map of Jesenice municipality

Methodology for rock fall forecast is different. For rock fall predicting a numerical model was used, developed from Luuk K. A. Dorren. RockyFor3D, a Matlab based model, was used to determine rock fall runout zones and energy created in falling rock. The result analysis was a raster map with quantified energies and trajectories of rocks. First initial zones were determined with the use of spatial analysis and GIS, which served as a base for numerical calculation. Different layers of input data was used, such as:

- lithology type
- rock shape
- falling rock dimensions
- DEM
- density of rock

Hazard map was created and divided in four classes (such as for landslides and debris flows) based on the amount of energy needed to damage certain structure. Bellow table show the logic we used in generating classes of risk from rock fall damage.

Table 2. Classification of rock fall risk classes

risk class	energy [kJ]	description
R4	0 - 200	no risk
R3	0 < E < 200	energy retained reinforced concrete
R2	200 < E < 2000	energy retained by strong containment fence
R1	> 2000	destructive energy

Map of rock fall risk classes is shown below, according to above table.

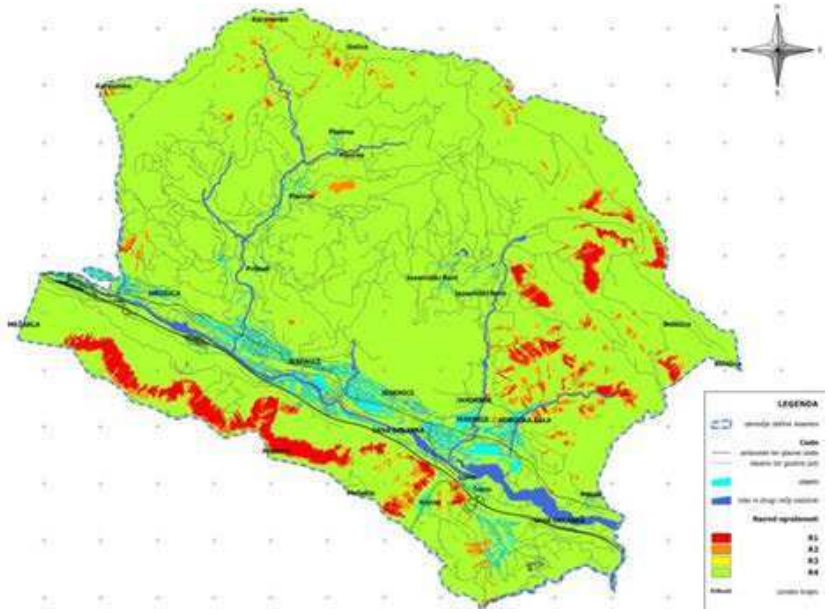

Figure 6. Rock fall risk map.

Final risk map contains all of modeled processes. Maps were joined together, where maximum value of class was determined, according to equation bellow:

Risk class = max([value RockFall], max([value Landslide],[value DF]))

Figure 7 shows final map of geologically conditioned risk as a result of slope processes, combined with the above equation.

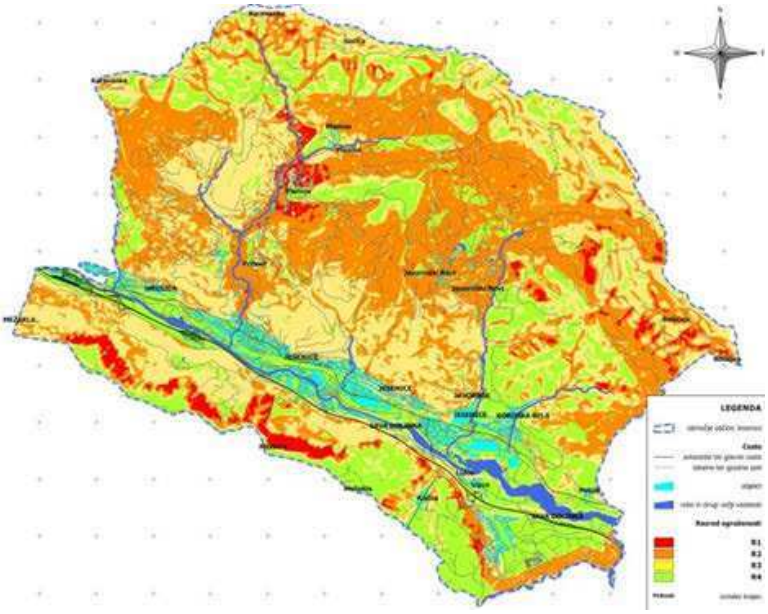

Figure 7. Final map of geologically conditioned risk as a result of slope processes for the municipality of Jesenice.

As a final result, tables were made for risk against each of the modeled slope process, with necessary and proposed geological investigations, that need to be conducted in order to assure safe building and living in endangered areas. Table 3 shows such table, where R1, R2, R3 and R4 represents risk class.

Table 3. Table of necessary site investigation created for landslides risk map. a - j are geological investigations, ranging from geomechanical boring to different types of analysis.

LANDSLIDES	R1	R2	R3	R4
complex objetcs	a,c,d,e,f,g,h,i,j	a,b or c,d,e,g,i,j	a,b,e,i	a,i
less complex objects	a, b or c, e, g, i, j	a,b,i	a, i	a
Non-complex and simple objects	a,i	a	-	-

Tables were made in accordance to current building and spatial laws in Slovenia and European standards for soil and rock investigations (Eurocode standards). Necessary and proposed site investigations are therefore prescribed for a given complexity of objects and the risk class obtained with GIS model.

4 CONCLUSION

GIS based survey made for the municipality of Jesenice showed good results and is serving as a good foundation for further landscape planning. Although the scale of created maps is fairly small (1:25.000) for an exact urban plan, it shows problematic areas which need to be analyzed in greater detail. Main advantage of this study was the wide range of the processes modeled, taking in account landslides, debris flows and rock falls. Mapping or modeling of each of slope processes allowed creation of rules and site investigation for a given risk. As a result of modeling each process independently, tables were created, which are serving municipality officials as a foundation on which they can propose the type of site investigation needed to assure higher safety of objects.

REFERENCES

DORREN, L., K. A., 2010. RockyFor3D revealed - Description of complete 3D rockfall modell, 21p.

KOMAC, M., KUMELJ, Š., RIBIČIČ, M., Model in karta verjetnosti pojavljanja dorbirskih tokov v Sloveniji, 60p.

RIBIČIČ, M., 2004, Metodologija za določanje ogroženih območij in načina razvrščanja zemljišč v razrede ogroženosti zaradi zemeljskih plazov, 46p.

RIBIČIČ, M. et al., 2005. Metodologija ukrapanja ob ogrožajočih plazovih, pp. 39.

MIKOŠ, M., et al., 2007. CRP "Znanje za varnosti in mir 2006 - 2010", ocena ogroženosti zaradi delovanja drobirskih tokov

DI, B. F., CHEN N. S.,CUI P., LI Z. L.,HE Y.C, GAO Y.C., 2009, GIS-based risk analisys of Debris flow: an application in Sichuan, southwest China.

BUSER S. et al, 1977, Osnovna geološka karta Slovenije, list Beljak

Zakon o graditvi objektov, Ur.l. RS, št. 102/2004 (14/2005 popr.), 2004

Uredba o vrstah objektov glede na zahtevnost, Ur.l. RS, št. 27/2008 z dne 15.4.2008

Eurocode 7: Geotechnical design Part 1:General rules

EN ISO 22476:2005 - 2009, Field testing, European comission

ISGSR 2011 - Vogt, Schuppener, Straub & Bräu (eds) - © 2011 Bundesanstalt für Wasserbau ISBN 978-3-939230-01-4

Landslide consequence analysis – mapping expected losses in the Göta river valley

S. Falemo & Y. Andersson-Sköld
Swedish Geotechnical Institute, Göteborg, Sweden

ABSTRACT: Landslide risks are expected to increase with climate change in large parts of Sweden due to increased annual precipitation, more intense precipitation and increased flows combined with dryer summers. In response to this climate threat and on commission of the Ministry of Environment the Swedish Geotechnical Institute has initiated a risk analysis project for the most prominent landslide risk area in Sweden: the Göta river valley. Human life, settlements, industry, contaminated sites, infrastructure of national importance are important elements at risk.

Focusing on the consequences of landslides this paper aims to show the process and structure of this regional consequence analysis by presenting suggestions on how to describe, quantify, value, total and visualize widely different consequences. The consequence analysis is GIS-aided in using existing databases for quantification and estimation of values, in calculating expected monetary losses and within visualization. The goal of the consequence analysis is to produce a map of geographically distributed expected losses, which can be combined with a corresponding map displaying landslide probability.

Keywords: landslide, consequence, economic valuation, GIS, risk analysis

1 INTRODUCTION

1.1 *Sweden facing climate change*

A national inquiry on climate change impacts concludes that Sweden will be heavily impacted by climate change, and that adaptation should start immediately (SOU 2007:60). Expected climate change in Sweden includes; increased precipitation during the autumn, winter and spring; winter precipitation increasingly falling as rain; dryer summers; increase in most intensive rainfall; higher flows and more frequent floods in western Götaland but also occasions with potential less water flows and water levels in some rivers (SOU 2007:60; Bergström et al., 2010).

The risks for floods, landslides and erosion are expected to increase in large parts of the country. Greatly increased risks for these natural hazards justify stronger initiatives for preventive actions (SOU 2007:60). In response to the results of this national inquiry the Swedish Government has commissioned the Swedish Geotechnical Institute to investigate and map the landslide risks in one of the country's most landslide-prominent areas: the Göta river valley (Hultén et al. 2007).

1.2 *The Göta river valley*

In south-west Sweden the Göta river valley, running from Lake Vänern in the north to Göteborg in the south (Figure 1), is the most frequent landslide area in the country, with a number of landslides occurring each year.

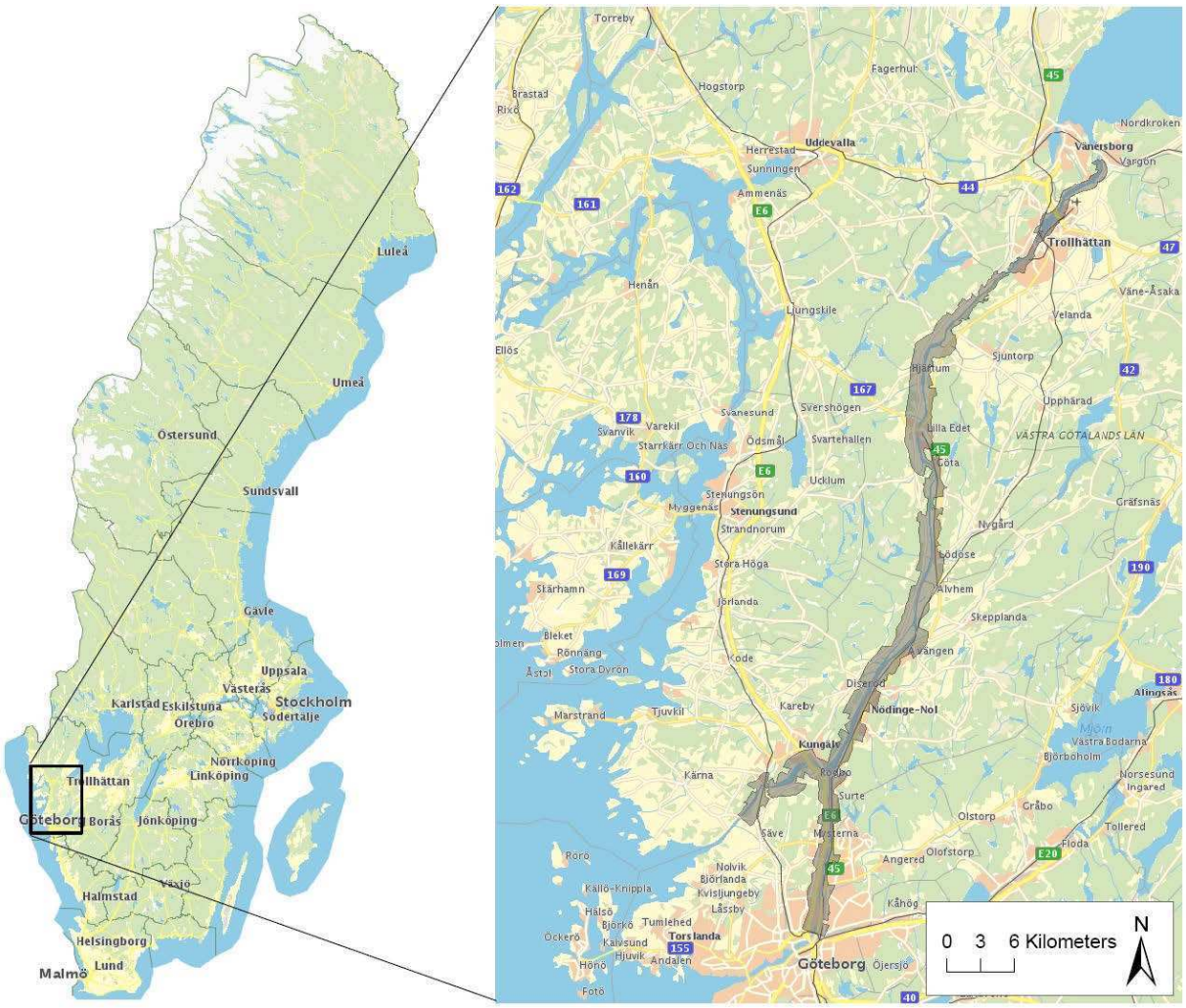

Figure 1. The Göta river valley with the landslide risk study area marked in dark grey. The river passes six municipalities on its way from Lake Vänern to the sea.

In general the landslides are small and shallow and occur as a result of erosion. However a number of large landslides have occurred during the past 100 years, some of them with human casualties and extensive property damages (e.g. Alén et al. 2000; Hultén et al. 2007).

Geologically the prerequisites for landslides formed during and following the latest glaciation period, when deep layers of clay formed in the river valley which was submerged in the sea during this period. Since the material was mainly deposited in a marine environment, quick clay is common in the area. Quick clay is a soil with high water content and weak bindings between the clay particles. Vibrations or a small initial landslide can cause a quick clay layer to collapse and liquefy, resulting in a large rapid landslide with potentially severe consequences (e.g. Andersson-Sköld et al. 2005)

The valley has a long history of anthropogenic activities such as settlements, shipping, harbours and industry and there are numerous areas with contaminated soil. Roads and railroads of national importance stretch along the river bank for several kilometres.

1.3 *The Göta river valley land slide risk analysis*

The ongoing Göta river risk analysis project covering an area of around 300 km^2 (Figure 1) started in 2009 and will be finished by the end of 2011. The results from the risk analysis will be presented in reports, maps and open access GIS presentations. The primary aim with the analysis is to be used as a basis for discussions on prevention and climate adaptation measures and for risk analyses on national level. But it can also serve as the basis for the land use planning of municipalities and government agencies and be used in the surveillance of the safety along the Göta river valley. Results will also help determining which minimum and maximum flows should be allowed in this regulated river.

In addition to extensive geotechnical field investigations and handling complex geotechnical issues this overview risk analysis project involves developing methods for quantitative consequence analysis. The consequence analysis includes identification, quantification, economic valuation and visualisation of consequences for widely different elements at risk. Van Westen et al. (2008) states that GIS has deter-

mined the current state-of-the-art in landslide and hazard risk assessment. In this project GIS is used when gathering and viewing data from existing databases for quantification, when estimating values, calculating expected monetary losses and for visualization purposes.

This paper aims to show the process and structure of this regional, and thereby relatively large-scale, consequence analysis for landslides by presenting suggestions on how to describe, quantify, value and visualise these widely different consequences with the aid of GIS.

2 STRUCTURE OF CONSEQUENCE ANALYSIS

The primary step in the consequence analysis is to identify the elements at risk. Once the elements at risk to be included in the study are settled upon, the proposed method for consequence analysis is divided in six parts, as illustrated in Figure 2.

In the inventory phase, data regarding each element at risk is gathered for the studied area; national registration records for living and working; real property map, electricity grid map etc.

Possible methods for economic valuation of each element at risk are studied and selected in the valuation phase. The expected degree of loss is assessed in the vulnerability phase. For real property it describes the value of damages caused by a landslide. For people it is the probability of death for a person who is in the landslide area at the time of the landslide.

Exposure describes the degree of exposure of each element at risk, e.g. how people divide their time between work, home, school, etc. at different physical addresses. These phases are followed by GIS calculations, and finally the results can be visualized in a number of ways. Here we present the GIS based work procedure for some selected elements at risk in the Göta river valley: human life and properties.

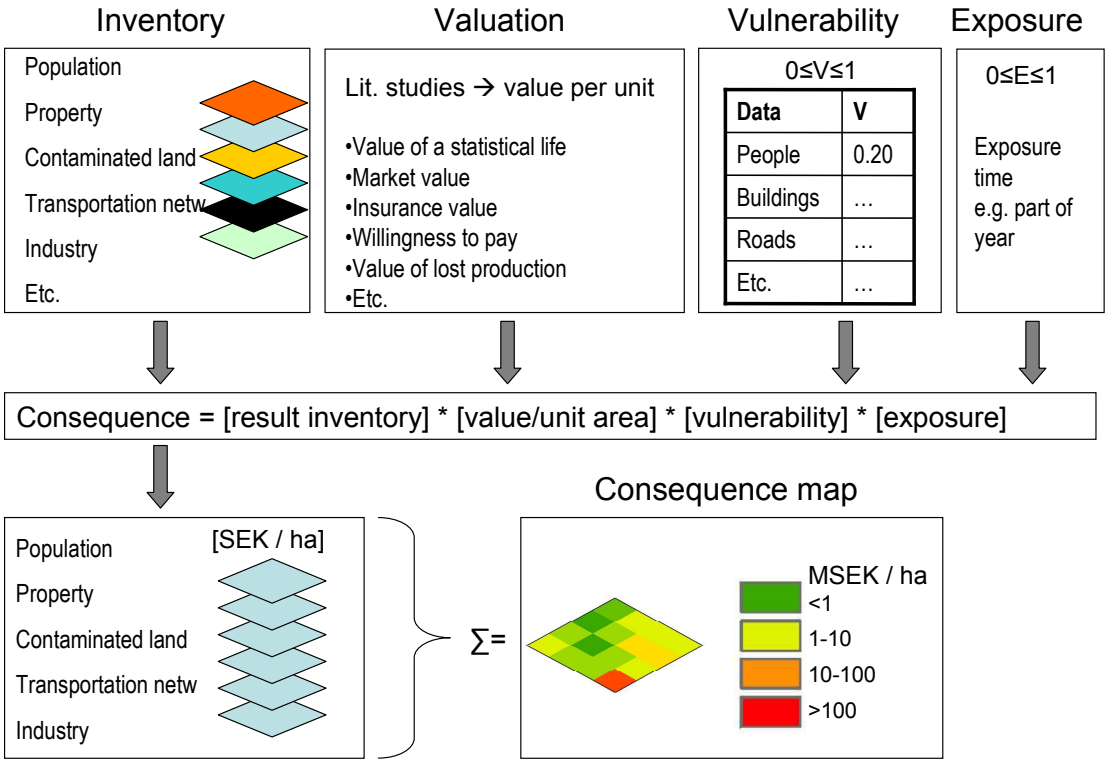

Figure 2. Illustration of the phases in the consequence analysis. The figure is adapted and improved from Falemo et al. (2010).

3 ELEMENTS AT RISK

Previous in use methods for landslide consequence assessment in Sweden were semi-quantitative with consequences scored on a four-grade scale based on type scenarios and included only human life, transportation, buildings and environment (e.g. Alén et al., 2000, Berggren et al., 1991, Hultén et al., 2007). A wider spectrum of consequences, improved transparency, economic valuation and improved visualization possibilities were the main aims when developing the new method.

The consequence categories included in the present investigation are:

- Human life
- Property
- Transportation
  - Road
  - Railroad
  - Shipping
- Environmental risk activities
  - Industrial activities (Seveso, EMIR A, B, C)
  - Contaminated land (MIFO)
- Life lines
  - Energy and telecommunication
  - Water and sewage systems
- Nature and cultural environment
- Business community

The consequence categories have been selected with inspiration from van Westen et al. (2008). This article focuses on human life and property.

4 GIS FOR INVENTORYING

A case study mapping landslide consequences for human life and property in Ale municipality is the basis for the following chapters 4-6 (Falemo & Axelsson 2011). The case study area is 100-1000 m wide and 30 km long.

A GIS format real property map with information on taxation values and property types provided necessary information for valuing land and buildings (Figure 3). Properties without taxation values (e.g. schools, sports halls, care centres) were investigated separately through contacts with the county council and Ale municipality to find information on gross floor area and building use. This information was added to the GIS.

Statistics Sweden provided national registration records in a 100 by 100 squared GIS raster layer, as well as a corresponding raster layer describing the amount of people employed in each square. Each address belongs to one square only, meaning all residents or workers belonging to this address are registered in the same square. In order to avoid unreal hotspots manual adjustments were made for large industries with many employees, distributing them evenly over the area of the industrial buildings.

The numbers of pupils in schools and pre-schools were collected and, in GIS, distributed evenly over the area of the property of each school. This generally works well but in some cases leads to improper scattering of consequences and so the results of this GIS operation must be controlled**.**

5 GIS OPERATIONS FOR QUANTIFYING CONSEQUENCES

5.1 *Quantifying property damage costs*

For properties with taxation values market values are calculated using purchase price / taxation value ratios (Figure 3).

The remaining properties are valued with calculated replacement cost ratios from an insurance company and are based on gross floor area and building use. An alternative is to extend surrounding property value per area unit from a property of the same building type to the property that lacks a basis for valuation. It is assumed that properties within a landslide area has the vulnerability factor 1, i.e. the full market value of the property is lost if it suffers from a landslide.

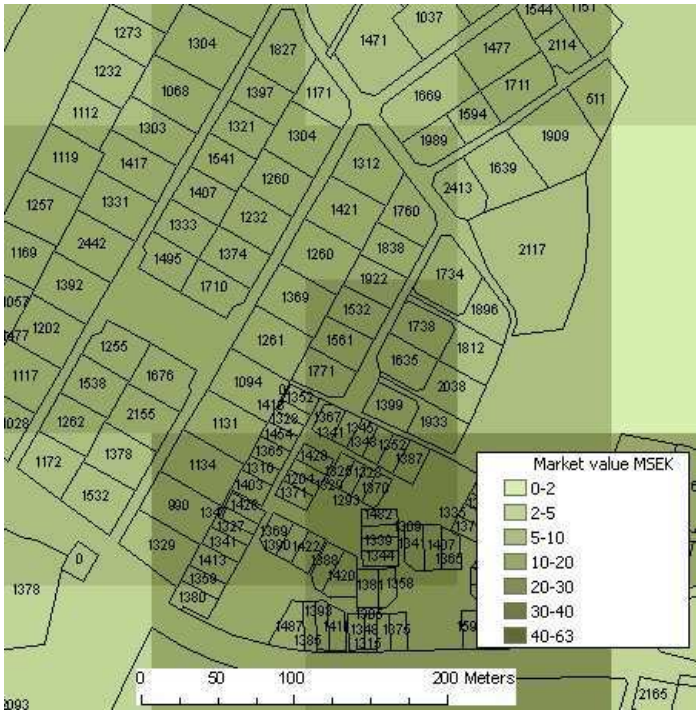

Figure 3. A real property map with taxation values in kSEK (shown in figure) and purchase price / taxation value ratios are the inputs for calculating market values. Market values are shown as raster data with the cell colour showing the value in MSEK of each 100 by 100 m cell. 1 SEK ≈ 0.1 €.

5.2 *Quantifying expected life losses*

Consequences for human life for the pupils are calculated using time-under risk ratios (exposure index describing how large part of the year is spent in the school building), conditional vulnerability (the probability of death for a person who is in the landslide area at the time of the landslide) and the value of a statistical life (VOSL). A more detailed description on calculating consequences for human life and a discussion on applying VOSL in this risk analysis have recently been presented in Falemo et al. (2010).

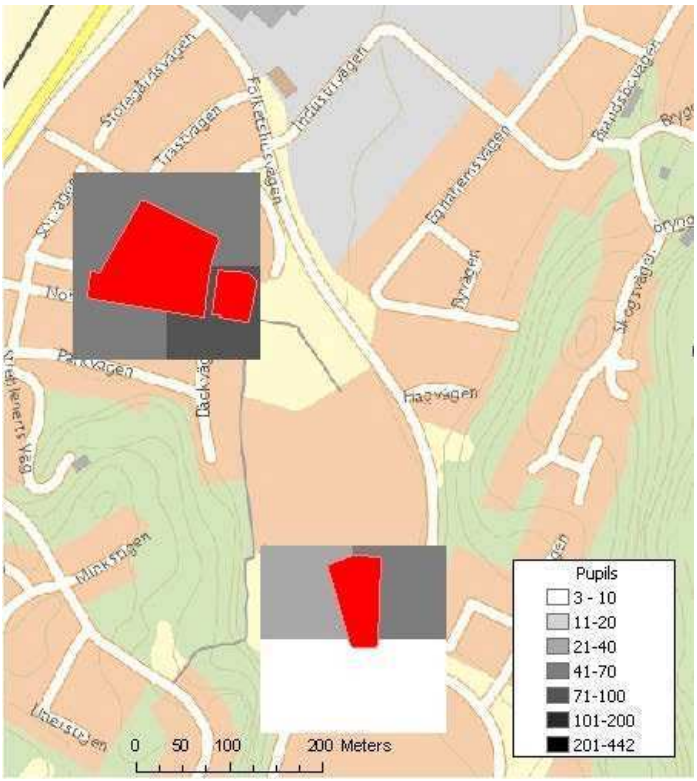

Figure 4. Three schools on separate properties are shown in red. The numbers of pupils of three schools have been distributed evenly over their respective property, and then this information is converted to raster data cells partially covering each school in proportion to the area covered by each cell. The cell colour shows the number of pupils associated with that cell.

Figures 4 and 5 show an example of calculating expected life losses for three schools. In Figure 4 the pupils in these schools have been distributed over the raster data cells partially covering each school in proportion to the area covered by each cell.

The expected life loss for pupils in these schools is obtained by multiplying this raster with exposure factor for pupils and by the vulnerability factor for people. The exposure factor expresses the likelihood of the pupils being in the school when the landslide occurs, so the results show yearly mean values for expected life loss.

Executing these calculations for pupils, employees and residents in the area results in the expected life loss map displayed in Figure 5. Diurnal (day/night) maps is a natural step towards a more detailed consequence analysis, and of course consequences for human life for a certain landslide depend on the time of the slide and what type of buildings are impacted (workplaces, schools or homes).

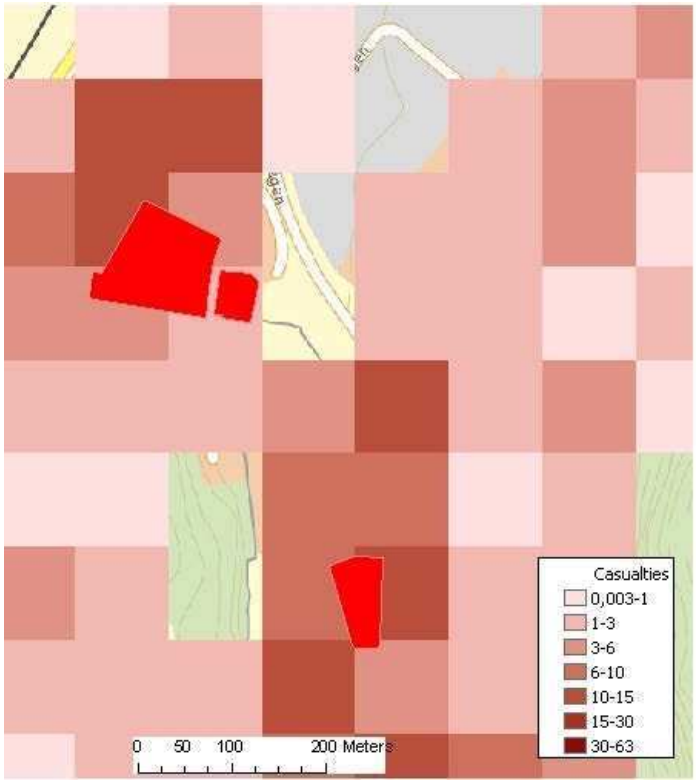

Figure 5. the expected life loss for pupils, employees and residents are shown as raster data. These consequences are calculated as a theoretical mean value of the year in relation to the exposure factors, as described above.

6 GIS FOR VISUALIZATION

There are numerous ways to visualize the results, and by providing a GIS database the results for each element at risk are available separately and as total expected loss measured in SEK/area unit (1 SEK ≈ 0.1 €). Two fictive examples covering the same area are provided here.

One possibility is to present expected economic losses as a raster layer similar to previous examples (Figure 6).

Another possibility is to use iso-cost lines to express the economic loss per meter river (Figure 7).

In the example the expected economic loss for a landslide extending from the river to the first iso-cost line is 1 KSEK per meter river. Maps showing expected life losses are also important output from the analysis.

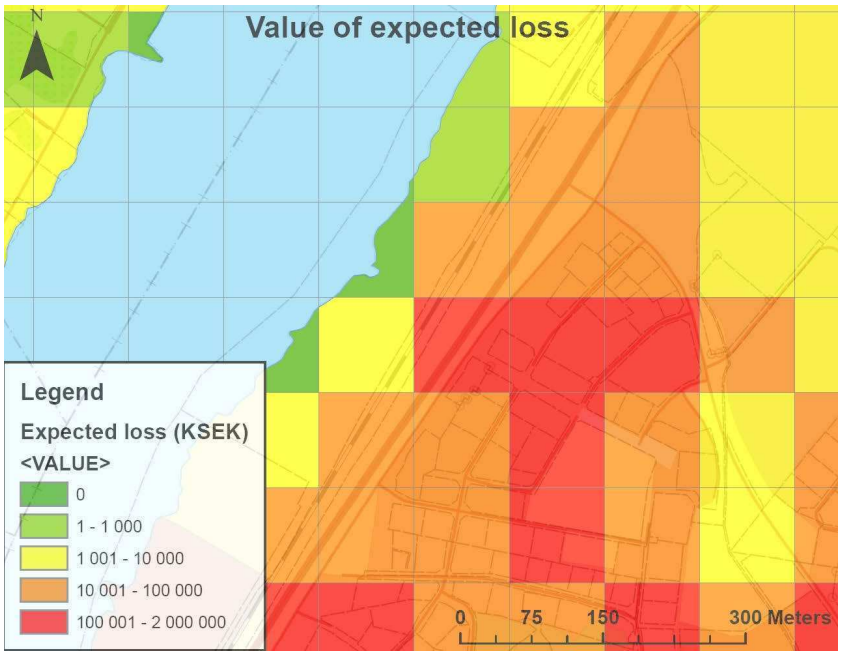

Figure 6. Expected losses visualized as a 100 by 100 meter raster.

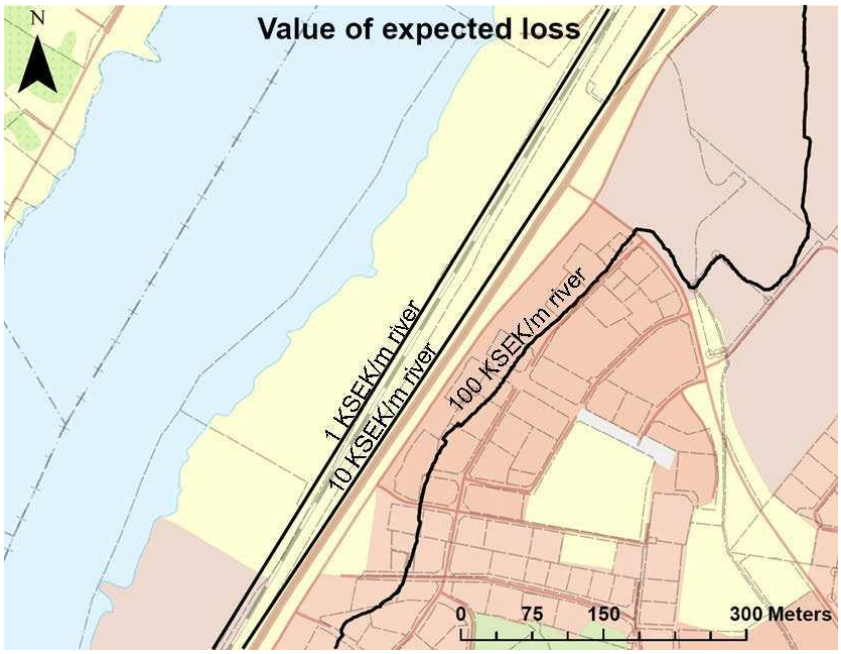

Figure 7. Expected losses expressed as iso-cost lines showing the expected cost of a one meter wide stripe perpendicular to the river extending from the river to each iso-cost line.

7 CONCLUSIONS

The methodology is found to be very useful and to describe consequences of landslides well. It is especially useful for case studies where the potential landslide's borders are known. We believe that the method also can be useful for cost benefit analyses (where and when are invested money most efficient). In such analyses it can be used for example when planning prevention measures for landslides and other natural hazards such as flooding. Using the presented GIS-aided methodology for consequence analysis facilitates updating input data and assures transparency. It is a useful tool when one wants to be able to present total as well as sector-based or category-based consequences, for example industrial activities or human life exposure. This visualization flexibility means that the data and results of the analysis can be useful to a wide spectrum of stakeholders, municipal planners and governmental organizations. It is further a valuable tool offering possibilities for detailing the analysis: seasonal and diurnal (day/night) variations maps etc. When the probability of a natural hazard or accident is known GIS is a strong tool for mapping not only the consequences but also the risks.

8 REFERENCES

Alén, C; Bengtsson, P-E; Berggren, B; Johansson, L; Johansson, Å (2000). *Skredriskanalys i Göta älvdalen – Metodbeskrivning*. (In Swedish). Swedish Geotechnical Institute, Report 58, Linköping.

Andersson-Sköld, Y; Torrance, J K; Lind, B; Odén, K; Stevens, R L; Rankka, K (2005). Quick clay - A case study of chemical perspective in Southwest Sweden, *Engineering Geology*, vol 82, no 2, pp 107-118.

Berggren, B., Fallsvik, J., Hintze, S. and Stille, H., 1991. *Lerslänters stabilitetsförhållanden. Riskvärdering och beslutsteori. Förslag till metod för riskvärdering* (in Swedish), SGI Varia 333.

Bergström, S., Andreasson, J., Losjö, K., Stensen, B., Wern, L. (2010) *Hydrologiska och meteorologiska förhållanden i Göta älvdalen – slutrapport* SMHI, Rapport Nr 2010-81

Falemo, S; Andersson-Sköld, Y; Suer, P; Grahn T (2010). Quantification, economic valuation and visualisation of landslide consequences in the Göta river valley, *International disaster and risk conference, IDRC, 3,* Davos, Switzerland, May 30 - June 3, 2010. Proceedings pp 175-178.

Falemo, S; Axelsson, J (2011). *Göta älv konsekvensbedömning - Bebyggelse och Liv Fallstudie Ale kommun.* (In Swedish). Swedish Geotechnical Institute. In prep.

Hultén, C; Andersson-Sköld, Y; Ottosson, E; Edstam, T; Johansson, Å (2007). Case studies of landslide risk due to climate change in Sweden, *International geotechnical conference on climate change and landslides*, Ventnor, Isle of Wight. Proceedings 2007, pp 149-157.

SOU 2007: 60 Swedish Commission on Climate and Vulnerability (2007). *Sweden facing climate change – threats and opportunities*, 679p, Edita Sverige AB, Stockholm.

Van Westen, C J; Castellanos, E; Kuriakose, S L (2008). Spatial data for landslide susceptibility, hazard, and vulnerability assessment: An overview. *Engineering Geology,* vol 102, pp 112–131.

ISGSR 2011 - Vogt, Schuppener, Straub & Bräu (eds) - © 2011 Bundesanstalt für Wasserbau ISBN 978-3-939230-01-4

A probabilistic approach to risk assessment of slow slope movements

M. Ranalli & G. Gottardi
DISTART, University of Bologna, Italy

Z. Medina-Cetina
Zachry Department of Civil Engineering, Texas A&M University, USA

F. Nadim
International Centre for Geohazards, Oslo, Norway

ABSTRACT: Many regions are getting more and more vulnerable from a hydro-geological point of view. The causes are due to both the fragility of the territory and to the anthropic influence on its continuous modifications. To avoid or reduce the human life and property economic losses, the quantitative prediction of landslide occurrence and the estimation of the amount of consequent slope movements are necessary. In this paper a specific type of landslide, characterized by a viscous behaviour of soil, is discussed. To catch the displacements evolution of this type of landslide, an analytical dynamic-viscous model was set up. In order to develop an advanced analysis and prediction procedure of the behaviour of such creep landslides, a probabilistic approach, based on Bayesian theorem, is presented. The method is validated making use of a well established and highly reliable monitoring database (Alverà landslide), located in Cortina d'Ampezzo (Dolimites, Italy). The model calibration was then probabilistically performed solving the inverse problem. The solution is then characterized by probability density functions of model parameters, including their corresponding correlation structure. Furthermore, this analysis enables to describe statistically the model error, associating a degree of uncertainty to the predictions.

Keywords: Slow slope movements, dynamic-viscous model, probabilistic calibration, risk analysis

1 INTRODUCTION

Landslides represent one of the most common natural hazard in the world. In recent years, landslide risk assessment has gained significant and ever increasing importance. The identification of triggering factors, the investigation of soil properties, the understanding of kinematic mechanism, the prediction of mass movements are then fundamental issues to avoid or reduce the losses of property or people life due to their occurrence. The risk assessment and management process consists in studying all these elements, together with the consequences of landslides trigger and the possible mitigation measures. In particular, the prediction of landslide occurrence and the estimation of the amount of consequent slope movements are the main issues both for estimating the hazard and for designing the mitigation measures and warning systems. To this purpose, probabilistic analyses are powerful tools to combine the several elements of risk management process and take into account the uncertainties inside their definition.

The paper focuses on a particular type of landslide, characterized by shallow and translational movements, which involve fine, essentially clayey material. According to the Varnes classification, they can be identified as extremely or very slow slope movements, with velocities typically of few centimetres per year. The main triggering factor is hydrologic, since the movements show a periodical and seasonal activation, usually strictly connected to ground water level fluctuations. These characteristics can be related to the viscous response of soils.

To catch the displacement evolution of this type of landslides, a well-defined dynamic-viscous model, able to predict the displacements from groundwater level inputs and return a value of mobilised friction angle, was set up. It consists of introducing an additional viscous resisting force into the equation of motion of a block of soil, enabling to model the actual evolution of such slow and seasonal movements (Vulliet and Hutter, 1988; Van Asch and Van Genuchten., 1990; Corominas *et al.*, 2005; Van Asch *et al.*, 2007). Here, a slightly modified version (Ranalli et al., 2010) of the original Gottardi and Butterfield's visco-plastic model (Gottardi and Butterfield, 2001; Butterfield, 2000) is considered.

The relevant and innovative feature of the work is the probabilistic approach used to calibrate the model. Referring on Bayesian theory, the joint probability distribution of model parameters (posterior) is obtained by means of the combination of their prior information (prior) and the performance measure of the predictive model (likelihood). It is thus possible to propagate quantitatively the uncertainty of the geotechnical parameters and the triggering factors into the model parameters (fully probabilistic solution). Starting from the prior and the likelihood, the use of Markov-Chain Monte Carlo method allows to sample the posterior, conditioned on a site specific data (Medina-Cetina, 2006). The so obtained probabilistic solution is then characterized by a full description of each model parameter, given in the form of their probability density functions, including their corresponding correlation structure. Furthermore, this analysis enables to describe statistically the model error, associating a degree of uncertainty to the predictions. Finally, it allows to update the knowledge on the model parameters every time a new information or observation becomes available.

In order to validate the approach, a well established and highly reliable monitoring database (Alverà landslide) located in Cortina d'Ampezzo (Dolimites, Italy), was used (Deganutti e Gasparetto, 1992; Angeli *et al.*, 1996; Gasparetto *et al.*, 1996; Panizza *et al.*, 1996). It is essentially made up of frequent and extensive ground displacement and piezometer records.

The final results aim at improving the now available tools for landslide risk analysis and management in a rational and effective way.

2 THE PROBABILISTIC APPROACH

The Bayes' paradigm is one of the most known probabilistic formulation used to solve the inverse problem (Congdon, 2007). In this process, the solution is inferred by a backward procedure, moving from the observations to the model parameters. So, it is important to use any available prior information on the model parameters and to have a representation of the data uncertainty in an explicit way. To this purpose, the Bayes' theorem is a suitable tool since it combines the prior knowledge about the model parameters with the information coming from a new observation, both defined in terms of probability. The result is an updating of the parameters knowledge, which represents the probabilistic solution to the inverse problem.

The analytical expression of Bayes' paradigm is:

$$\pi\left(\theta|d_{obs}\right)=\frac{f\left(d_{obs}|\theta,g(\theta)\right)\pi(\theta)}{\int f\left(d_{obs}|\theta,g(\theta)\right)\pi(\theta)d\theta} \tag{1}$$

where $g(\theta)$ is a generally non-linear function that relates the set of model parameters θ with the observations d_{obs}, $\pi(\theta)$ is the prior probability density function of parameters, $f(d_{obs}|\theta,g(\theta))$ is the likelihood, which represents a measure of model performance in terms of probability function, and $\pi(\theta|d_{obs})$ is the posterior probability density function of parameters and represents the solution of the inverse problem. The denominator is a normalization constant.

Usually, the Equation (1) can be solved only by means of numerical techniques. The Markov Chain Monte Carlo method allows to sample randomly a large vector of values according to the posterior probability distribution. This process consist in a sequence of random variables $\boldsymbol{X}_0$, $\boldsymbol{X}_1$,…, $\boldsymbol{X}_t$ such that the next state of the chain $\boldsymbol{X}_{t+1}$ depends only on the previous one. The stochastic walk was generated by implementing the Metropolis-Hastings algorithm, since it allows to sample probability distributions which are known except a constant.

3 THE DYNAMIC-VISCOUS MODEL

The viscous behaviour of soil is modelled by considering a linear damping force F_v defined as:

$$F_v = C\dot{x} = \left(\eta/h_m\right)\dot{x} \tag{2}$$

where η is the dynamic viscosity (in kilopascal second) and h_m is the thickness of the shear zone (in meters). Assuming a infinitive slope scheme, which is able to model translational landslides, and referring to Figure 1, the equation of motion of a unit-block soil element, with mass M and thickness D, on an infinite slope inclined at an angle θ is:

$$M\ddot{x} = P - F_{M-C} - F_v \tag{3}$$

where $P = Mgsin(\theta)$ is the driving force, $F_{M\text{-}C} = N'tg(\varphi')$ is the Mohr-Coulomb resisting force, depending, for continuously moving landslides, only on residual friction angle φ'_r.

Introducing a dimensionless variable β, defined as:

$$\beta = \frac{N'}{N} = 1 - \frac{\gamma_w}{\gamma_{sat}} \frac{d}{D} \tag{4}$$

where d is the groundwater level, the Equation (3) becomes:

$$M\ddot{x} + C\dot{x} = N(\tan\theta - \beta \tan\varphi') \tag{5}$$

Also, introducing the initial condition (v_0, β_0), which identifies the step change from static to sliding slope, along with the assumption of acceleration equals to zero, we can estimate the corresponding value of mobilised shear strength angle φ'_0:

$$\tan\varphi'_0 = \frac{1}{\beta_0}\left(\tan\theta - \frac{Cv_0}{N}\right) \tag{6}$$

Combining Equation (5) and (6) and introducing the following dimensionless variables:

$$\begin{aligned} T &= gt/v_0 \\ X &= xg/v_0^2 \\ \dot{X} &= (dX/dT) = \dot{x}/v_0 \\ \ddot{X} &= (d\dot{X}/dT) = \ddot{x}/g \end{aligned} \tag{7}$$

the solution in terms of predicted velocity and displacement is respectively:

$$\begin{aligned} \dot{X} &= \frac{H}{G} + (G - H)\exp(-GT) \\ X &= \frac{H}{G}T + \left(\frac{G-H}{G^2}\right)(1 - \exp(-GT)) \end{aligned} \tag{8}$$

which, translated into the physical space, yields:

$$\begin{aligned} \dot{x}_{pred} &= \dot{X}v_0 \\ x_{pred} &= X\frac{v_0^2}{g} \end{aligned} \tag{9}$$

where the capitol letters are dimensionless variables:

$$\begin{aligned} H &= B + (\beta/\beta_0)G \\ B &= \sin\theta(1 - \beta/\beta_0) \\ G &= Cv_0/Mg \end{aligned} \tag{10}$$

So, the model is characterized by three parameters: v_0, β_0 and C, since γ_{sat}, D and θ are usually known. Once they are defined, it is able to return displacement predictions and an estimation of mobilised friction angle for assigned groundwater levels.

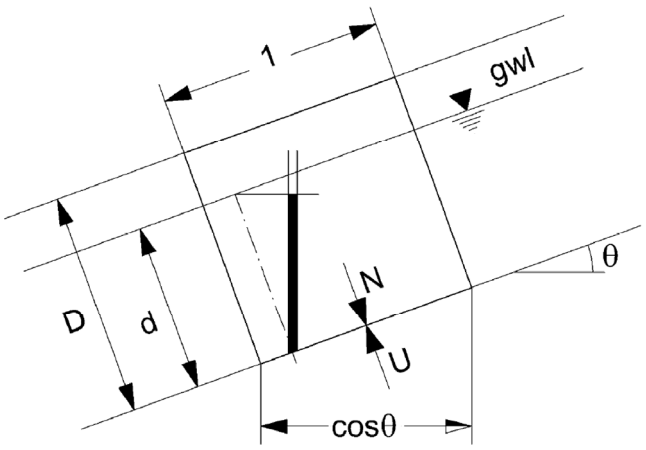

Figure 1. Scheme of infinite slope

4 THE PROBABILISTIC MODEL CALIBRATION

4.1 *Alverà monitoring database*

The Alverà landslide is a well-known and well-studied mudslide, located in the Italian Dolomites, near Cortina d'Ampezzo. It consists of a saturated clayey matrix (20-25 m thick) with irregular, poorly sorted blocks, which moves very slowly on a lower stable unit. A quicker shallow movement is identified within the upper unit, along a 5 m-deep surface. Laboratory tests on the clay fraction of samples recovered at this slip surface indicate the following geotechnical parameters: γ_{sat} = 18.73 kN/m^3, w_L = 0.95, I_p = 0.48 and φ'_r = 15.9° (residual shear strength angle).

An extensive and reliable monitoring system has been installed along the whole body of landslide (Gasparetto et al., 1996; Angeli et al., 1999; Corominas et al., 2000; Ranalli et al., 2010). To model calibration purpose, only the daily records relative to extensometer and piezometer installed in the more active and superficial movement are considered. The measurements are illustrated in the Figure 2.

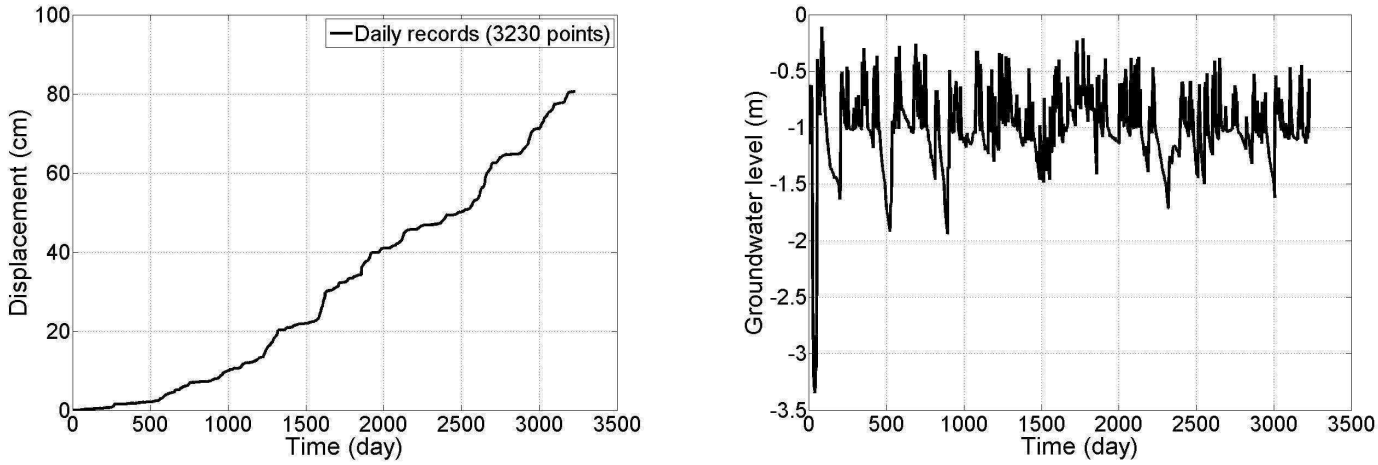

Figure 2. Displacements and groundwater levels records relative to Alverà landslide

4.2 *Results of inverse problem*

The model parameters v_0, β_0 and C are calibrated by means of Equation (1), making use of Alverà landslide database. The almost 9-year monitoring period was divided in four sub-periods, so that four different initial conditions (that is different v_0 and β_0 values) were considered. Instead, the viscous parameter C was taken constant with the time.

As a consequence of this assumption, the number of parameters to be calibrated adds up to nine. In order to apply the Bayes' theorem, a prior for model parameter should be assumed or evaluated. For this purpose, it was defined by an uncertainty identification and propagation analysis, as widely illustrated in Ranalli et al. (2010).

As mentioned above, the integration of Equation (1) was performed through the Markov Chain Monte Carlo method (MCMC), which allows to sample randomly a large vector of values according to the posterior. By way of example, the samplings relative to v_{01} and β_{01} parameters are shown in Figure 3. The solution of probabilistic model calibration consists of marginal probability distribution for each model parameter and their correlation structure. Figure 4 shows the cumulative density functions of v_{01} and β_{01}. Information about their correlation can be obtained by the correlation matrix of parameters or their joint cumulative density function.

Pursuant to probabilistic definition of parameters, it is possible to associate a degree of uncertainty to model predictions. Figure 5 shows the variability of model predictions compared with the observations, highlighting a global good fit. Figure 6 presents instead the trend of residuals with the time, together with the residuals mean and standard deviation. The fluctuation of residuals around the zero value indicates that the model generates unbiased predictions. So, all this statistical information allows to assess the reliability of predictive model.

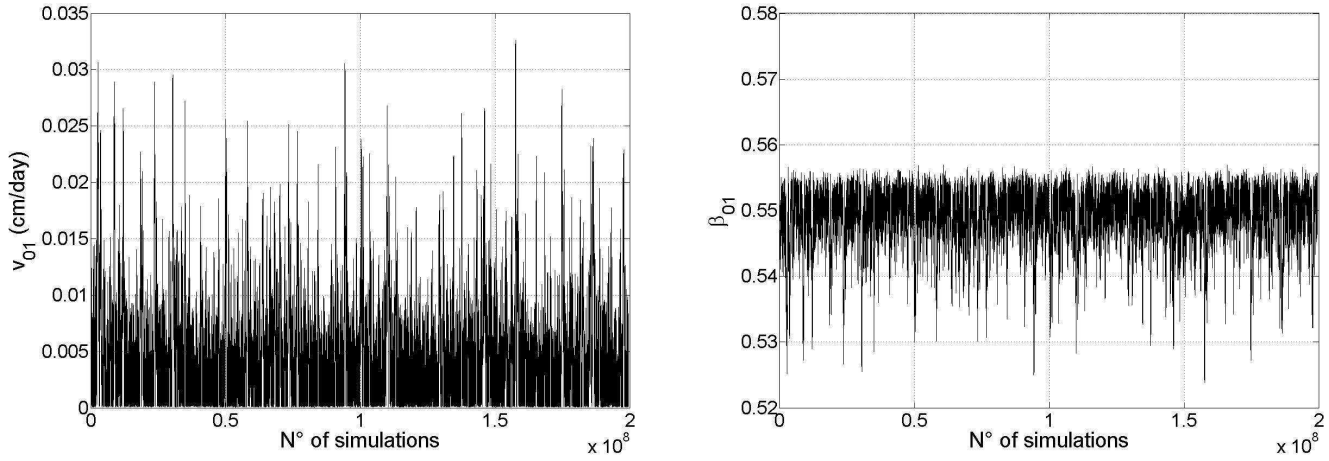

Figure 3. Sampling of v_{01} and β_{01} parameters by MCMC method

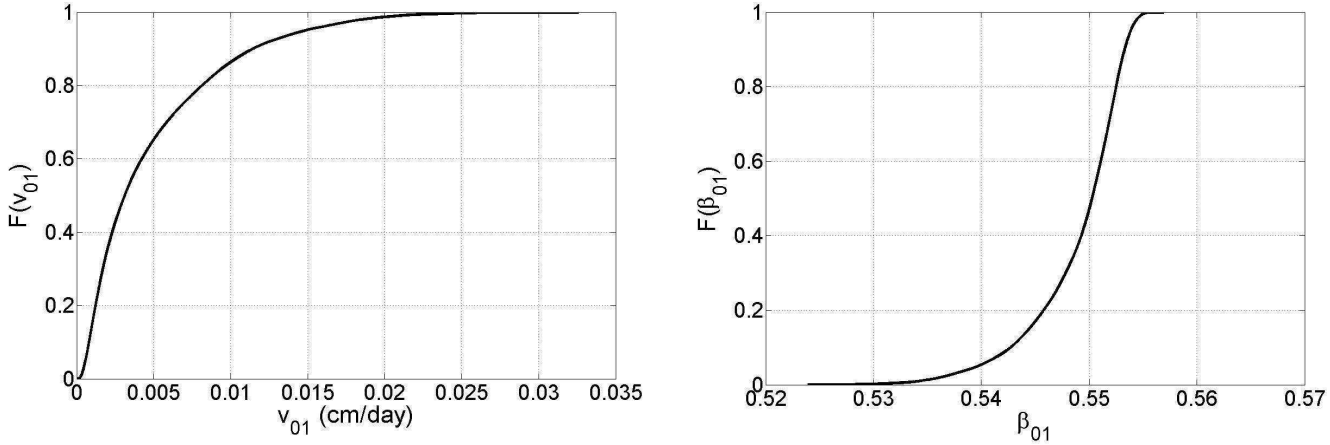

Figure 4. Posterior CDF's of v_{01} and β_{01} parameters; representing the probabilistic solution of model calibration

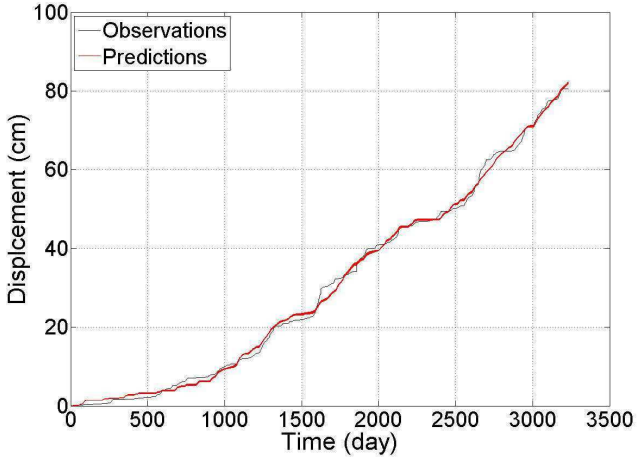

Figure 5. Comparison between model predictions and observations

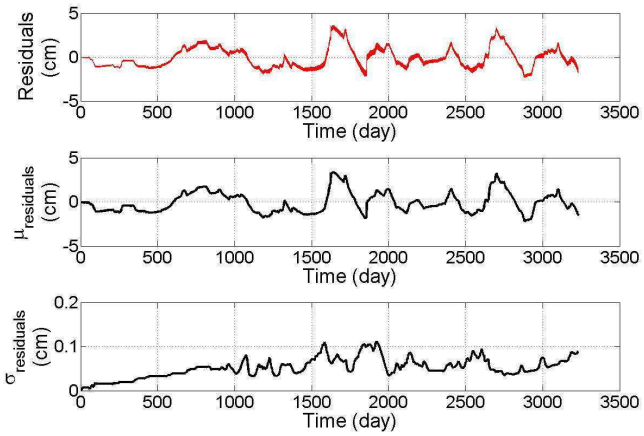

Figure 6. Statistics of model error

5 CONCLUSIONS

The paper concerns with the development of a new methodology for the analysis of slow slope movements, to be included within the landslide risk assessment and management process. In particular, an analytical and dynamic model, able to simulate landslides characterized by soil viscous behaviour, for which periodical movements depend on groundwater fluctuations, was set up.

The proposed methodology consisted in applying the Bayesian probabilistic approach to model calibration. The applicability and the effectiveness of such method was illustrated by using a case study, for which a reliable and extensive monitoring database is available.

The probabilistic solution of model calibration allowed to fully describe the parameters of the model, in terms of their marginal probability distributions and correlation structure. In addition, the error of the model was statistically described, since an uncertainty degree of predictions could be identified. In other words, it was possible to define and quantify the reliability of the model. This aspect is particularly crucial when the model is used as predictive tool into the risk analysis process.

A further advantage of such approach deals with the possibility of updating statistically the information on the parameters. In fact, the probabilistic solution obtained from initial observations can be improved every time new information become available.

REFERENCES

Angeli, M.G., Gasparetto, P., Menotti, R.M., Pasuto, A., Silvano, S. 1996. A visco-plastic model for slope analysis applied to a mudslide in Cortina d'Ampezzo, Italy. Quarterly Journal of Engineering Geology, The Geological Society, 29: 233-240.

Angeli, M.G., Pasuto, A., Silvano, S. 1999. Towards the definition of slope instability behaviour in the Alverà mudslide (Cortina d'Ampezzo, Italy). Geomorphology, Elsevier, 30: 201-211.

Butterfield, R. 2000. A dynamic model of shallow slope motion driven by fluctuating groundwater levels. Proceedings of the 8th International Symposium on Landslides. Thomas Telford, London, Cardiff, UK, Vol 1, pp 203-208.

Congdon, P. 2007. Bayesian statistical modelling. John Wiley & Sons.

Corominas, J., Moya, J., Lloret, A., Gili, J.A., Angeli, M.G., Pasuto, A., Silvano, S. 2000. Measurement of landslide displacements using a wire extensometer. Engineering Geology, Elsevier 55: 149-166.

Corominas, J., Moya, J., Ledesma, A., Lloret, A. & Gili, J.A. 2005. Prediction of ground displacements and velocities from groundwater level changes at the Vallcebre landslide (Eastern Pyrenees, Spain). Landslides, Springer-Verlag, 2: 83-96.

Deganutti, A.M. & Gasparetto, P. 1992. Some aspects of a mudslide in Cortina, Italy. Proceedings of the 6th International Symposium on Landslides. Balkema, Rotterdam, Christchurch, New Zealand, Vol 1, pp 373-378.

Gasparetto, P., Mosselman, M., Van Asch, T.W.J. 1996. The mobility of the Alverà landslide (Cortina d'Ampezzo, Italy). Geomorphology, Elsevier, 15: 327-335.

Gottardi, G. & Butterfield, R. 2001. Modelling ten years of downhill creep data. Proceedings of the 15th International Conference on Soil Mechanics and Geotechnical Engineering. Istanbul, Turkey, 27-31 August 2001. Volumes 1-3.

Medina-Cetina, Z. 2006. Probabilistic calibration of a soil model. Ph.D. Thesis, John Hopkins University, Baltimore, Maryland.

Panizza, M., Pasuto, A., Silvano, S., Soldati, M. 1996. Temporal occurrence and activity of landslides in the area of Cortina d'Ampezzo (Dolomites, Italy). Geomorphology, Elsevier, 15: 311-326.

Ranalli, M, Gottardi, G., Medina-Cetina, Z. & Nadim, F. 2010. Uncertainty quantification in the calibration of a dynamic viscoplastic model of slow slope movements. Landslides, Springer-Verlag, 7: 31-41.

Van Asch, T.W.J. & Van Genuchten P.M.B. 1990. A comparison between theoretical and measured creep profiles of landslides. Geomorphology, Elsevier, 3: 45-55.

Van Asch, T.W.J., Van Beek, L.P.H., Bogaard, T.A. 2007. Problems in predicting the mobility of slow-moving landslides. Engineering Geology, Elsevier, 91: 46-55.

Vulliet. L. & Hutter. K. 1988. Viscous-type sliding laws for landslides. Canadian Geotechnical Journal, 25: 467-477.

3 Risk and Reliability in Geotechnical Engineering

ISGSR 2011 - Vogt, Schuppener, Straub & Bräu (eds) - © 2011 Bundesanstalt für Wasserbau ISBN 978-3-939230-01-4

The Geo-Impuls Programme reducing geotechnical failure in the Netherlands

P. M. C. B. M. Cools, MSc
Manager Geo-Engineering, Secretary Steering Committee Geo-Impuls,
Rijkswaterstaat, Centre for Infrastructure, Ministry of Infrastructure & Environment, the Netherlands

ABSTRACT: Last year in the Netherlands a 5-years development programme, called Geo-Impuls, started with the ambitious goal to half the occurrence of geotechnical failure in our civil engineering projects by 2015. This paper describes the sense of urgency to start this joint industry programme and the way it is organized, together with the geotechnical community of the Netherlands.

Twelve distinct solutions have been distinguished along five themes:

- geo-engineering in contracts
- implementing and sharing of existing knowledge and experience
- quality of design and construction processes
- new knowledge for Geo-Engineering in 2015
- managing expectations

In order to accomplish the goal a '*new working method'* is proposed which will be based on a combination of the following measures:

- apply *geo risk management (GeoRM)* explicitly during all phases of realizing the project
- practise the *geo-principles* in the project
- apply the *tools* developed by the Working Groups in the project

Finally a qualitative approach has been described, how to monitor the goal via three parallel tracks.

Keywords: Risk Management, Infrastructure, Geotechnical Failure, Geo-Impuls

1 INTRODUCTION

The Netherlands are located in a Delta area where the rivers Rhine, Meuse and Scheldt flow into the North Sea. The topsoil consists mainly of peat and clay, saturated with water and the subsoil of sand often lies more than 10 to 20 meters beneath this soft topsoil. Half of the country lies below the sea level and is protected by levees. The area is very densely populated and the demand for new public infrastructure is high.

Under these conditions geo-engineering plays an important role in the process of design and construction of infrastructure, such as roads, levees, bridges, locks and sluices.

Figure 1. Construction of a building pit in the Netherlands

2 SENSE OF URGENCY

Over the years, but also nowadays, huge investments have been and are made in constructing infrastructural works all over the Netherlands, many of which the Dutch are proud of, like the Delta works.

However, every now and then somewhere in the Netherlands geotechnical failure takes place during or after construction of a civil engineering project. In the past century some prominent failures took place, which were unfortunate, but which also greatly advanced geo-engineering (Barends, 2005).

In the past decade, we can mention:

- the collapse of a river dike consisting of peat
- the collapse of a canal dike near a crossing of a water pipe
- the inundation of a tramway tunnel
- collapses of several building pits
- large settlements near a subway
- the collapse of a sheet pile near a highway
- partial collapse of a confined disposal facility (CDF)
- partial uplift of immersed tunnel foundation

The consequences of these failures were sometimes severe. They caused delays in construction time, cost increases of the project, additional costs for the society and, even worse, the loss of life.

Figure 2. Collapse of a river dike consisting of dehydrated peat

Moreover the good reputation was damaged not only of the contractor, the designer and the principal but also of the civil engineering community as a whole, and of geo-engineering specifically. This reputational loss affects for example the willingness of principals to start new projects with geotechnical challenges, for students to choose a study in geo-engineering, and for engineers to apply for vacancies in geo-engineering.

Several studies indicate that failure costs in the construction industry are typically 10 to 30 percent of the total construction costs (Avendano Castillo et al, 2008). Approximately half of these costs are expected to be directly or indirectly soil related, due to unexpected and unfavourable ground conditions (Van Staveren, 2006). The main reason for this is the inherent uncertainty of the properties of the natural soil, which is much larger than those for man-made building materials, such as steel and concrete.

3 GOAL

On initiative of the Ministry of Transport, specifically Rijkswaterstaat, several meetings were held in the first half of 2009 with all relevant stakeholders within the geo-engineering sector in the Netherlands.

All parties recognized the ‘sense of urgency’ mentioned in chapter 2 and their mutual interest “to do something about it”. They agreed to create a clear and SMART goal to deal with this problem, which is:

> “The reduction of geotechnical failure with 50% in 2015”

They also agreed to give an impulse to the field of geo-engineering in the Netherlands, in order to reach this goal and to contribute in money and manpower to start and implement a special programme called "Geo-Impuls".

For this moment, the total budget of this programme amounts up to almost 6.500.000 Euros in money and manpower. The duration of the programme will span a period of five years, from 2010-2015.

Within the Geo-Impuls programme the following organizations and companies have combined forces to reach the ambitious objective:

Clients: Rijkswaterstaat, ProRail, the municipalities Amsterdam, Rotterdam, Utrecht and the Hague, Province of Utrecht.

Contractors: Strukton, BAM, Boskalis, Heijmans, KWS, Van Hattum & Blankevoort, Van Oord, Ballast Nedam, Dura Vermeer, NVAF

Engineers: Arcadis, Witteveen+Bos, DHV, Tauw, Movares, Fugro, Royal Haskoning, Grontmij, CRUX.

Knowledge institutes: Deltares, CURNET (COB, CUR B&I), TUDelft, CROW.

Figure 3. Official start of the Geo-Impuls programme

4 GEO-IMPULS PROGRAMME

During the meetings, which were held in the first half of 2009 with all relevant stakeholders, all kind of causes of geotechnical failure were identified, analyzed, and discussed.

Within this context, geotechnical failure has been defined in a broad sense, as resulting into:

- delays in construction time
- cost increases of the project
- additional costs for the society as a whole
- the loss of life
- damaged reputations

Also, all kind of possible measures to prevent these failures were presented. In the end the measures proposed could be clustered into five themes:

- geo-engineering in contracts
- implementing and sharing of existing knowledge and experience
- quality of design and construction processes
- new knowledge for Geo-Engineering in 2015
- managing expectations

5 TWELVE DISTINCT SOLUTIONS ALONG FIVE THEMES

Eventually, all proposals were ranked by assessing the effect of a proposal in reducing geotechnical failure and by assessing the amount of "energy" present at the stakeholders, to actually participate to a team which would realize that proposal. This process lead to a final choice of 12 specific projects fitting in one of these five themes:

Geo-Engineering in contracts

- Allocation of geo-engineering risks in projects

- Soil investigation before and during tendering: producing a widely supported recommendation for risk-based soil investigations for construction projects
- Process specifications for geo-engineering in contracts: minimum specifications based on explicit geotechnical risks to control building contracts

Implementing and sharing of existing knowledge and experience

- The implementation and transfer of a risk-based approach to acquire an insight in the geotechnical risks of projects at an early stage
- International cooperation; knowledge exchange, focus on the Geo-Impuls programme and geo-technical risk management

Quality of design and construction processes

- Quality in design and construction; how to link up two different "worlds"
- Observational Method; robust en cost-effective projects based on measurements in combination with risk-based scenarios
- Training; how to educate and train practicing geo-engineers as well as students

New knowledge for Geo-Engineering in 2015

- Quality control for elements built on site; how to trace imperfections at an early stage
- Reliable sub-surface model; a better picture of the sub-surface by combining and improving measuring and interpretation techniques
- Long-term measurements; a better understanding of time-dependent geotechnical factors by comparing 'real-time' measurements with predictive models

Managing expectations

- Communication within a project to improve the reputation and positioning of the geotechnical sector

In this programme the development of new knowledge is only a relatively small part of all planned activities. A lot of attention will be paid to the transfer and application of existing knowledge, as well as to education and training. This observation also was made by Van Tol, when he analyzed the causes of failure of 50 building pits (Van Tol et al, 2009). In more than 60% of the cases the failure was due to not (correctly) applying existing knowledge.

6 ORGANIZATION

Starting from the second half of 2009, a sector wide Steering Committee carries the responsibility of the Geo-Impuls programme. Each member from this Committee represents all stakeholders from a specific part of the geo-sector: clients, contractors, dredgers, consultants and knowledge institutes.

Moreover, each member of the Steering Committee volunteered to be 'ambassador' of a specific project, where results of the Working Groups will be applied and tested on their effectiveness.

The daily implementation of the programme has been assigned to a Core Team, being the leaders of the twelve Working Groups as mentioned earlier. Altogether, more than 100 persons are working within the programme. The Programme Bureau is managed by Deltares.

Every year a so-called "Mini-Top Conference" is held, during which the progress of the work is presented to the Directors of all stakeholders.

In order to keep the Steering Committee alert during the execution of the programme for new developments and new insights, the quality of the work is monitored and judged by several independent persons.

The Steering Committee has invited an independent consultant on risk management and also a member of Young Professionals 'de Nieuwbouw' to play this role. Moreover, an International Review Board will be installed (see chapter 8).

7 INTERNATIONAL CO-OPERATION

In the Working Group "International Co-operation" it is proposed to establish contacts with countries who can be compared with the Netherlands regarding density in population, weak soils, and complex infrastructure in delta areas. Such countries are typically dealing with similar geotechnical problems as the Dutch.

The idea is to contact all relevant stakeholders in these countries, such as governmental bodies, contractors, consultants and knowledge institutions who feel connected with the goals of the Geo-Impuls programme and are willing "to combine forces".

Co-operation can be realized by the exchange of knowledge (in both directions), by the creation of liaisons (both personal and organizational) and by brainstorming about similar geotechnical problems and solutions.

Although it is not the main goal, personal contacts during the programme may lead to new alliances between organizations or enterprises of different countries. The meetings may take place in their own country and by video-conferencing.

When several countries have been visited and showed their willingness to co-operate, their representatives are invited to participate in an "International Review Board" which will meet every year in the Netherlands.

Figure 4. Visit of the geo-centrifuge at PARI, Japan

The "financial formula" of these projects will be the usual arrangements regarding Memoranda of Understanding (MOU's). Both countries will be responsible for their own expenses, regarding e.g. the costs of travelling and hotels. No money will be transferred from one country to the other and vice versa. Extra funding from other research programs is of course possible but will be spent in the country where the budget has been allocated.

8 INTERNATIONAL REVIEW BOARD

The International Review Board will consist of representatives of stakeholders from different countries, including the Netherlands, with expertise in the entire field of geo-engineering and risk management.

The Board will meet yearly in the Netherlands at the same time when all Working Groups of the Geo-Impuls programme present their results to the Steering Committee. The Board is invited to discuss with the managers and engineers and show their views on these results. In this way, the Working Groups will be provided with valuable international feedback, information, and ideas about their actual and future approach. This exchange of knowledge may benefit all parties involved.

The Board will advice the Steering Committee on the general approach of the programme and of the quality of the results of the project teams. Their review may lead to recommendations, upon which the Steering Committee will lean strongly and which can modify the programme.

The full installation of the Board will take place in a number of steps in time, starting with Japan and the USA and may be seen as a kind of "growth-model".

9 ELEVEN GEO-PRINCIPLES

In time, the Working Groups will produce a large number of intermediate and end results, like reports, software, data, instruments and guidelines. However, we believe that the production of only *'tools'* will not be sufficient to reach our ultimate goal. We feel strongly that also a change in '*attitude and behaviour'* of all parties involved will be essential.

Usually, it is assumed that behavioural change is achieved by formulating rules, with which all parties have to comply. However, this rule-based approach may lead to a complex system of describing and en-

forcing a large number of rather fixed rules. Such a system lacks flexibility and adaptiveness, which is required because no civil engineering project is exactly the same. Moreover, obligations to apply fixed rules result often in resistance of experienced professionals, rather than in a change of their attitude and behaviour.

That is why we have chosen for a more innovative principle-based approach, which aligns with developments in the organization sciences. We gratefully use the principles already formulated by the ISO-31000 RM Guideline. When applied to geotechnical engineering, these principles state that sound engineers should:

1. Create and protect value
2. Participate in all project phases
3. Participate in decision making
4. Address uncertainty explicitly
5. Work systematic, structured, and timely
6. Apply the best available information
7. Work tailored within the context and objectives of the project
8. Take human and cultural factors into account
9. Work transparent and inclusive
10. Be dynamic, iterative and responsive to change
11. Facilitate continuous improvement of the project organization

The next challenge will be to formulate and translate these by definition abstract principles into concrete geotechnical guidelines for the entire geotechnical community. We anticipate that it will be useful to elaborate on each geo-principle on different levels.

The geotechnical professional will have a different interpretation of each principle than the project organisation or the geo-sector as a whole (CUR Bouw & Infra, 2010). On each level (so-called micro-, meso- and macro-level) the question will be "What can and will I contribute to this principle, in order to contribute to a successful project?"

10 GEO RISK MANAGEMENT

As described earlier, the development and application of tools is important, as well as creating the right attitude and behaviour of all persons involved. However, equally important will be to practise a risk-based approach in all phases of realizing the project (Van Staveren, 2006).

In the Netherlands, RISMAN is a well known risk management approach. Specifically for the geotechnical sector, this method has been further elaborated into the GeoQ concept. Though risk analysis plays an important part in this approach, managing and controlling the risks is the ultimate goal and needs even more attention (Van Staveren, 2009).

The six generic steps of this approach are: (1) setting project objectives and gathering project information, (2) identifying risks, (3) classifying risks, (4) remediating risks, (5) evaluating risks, (6) mobilizing all relevant risk information to the next project phase by a risk register.

When applying geotechnical risk management (GeoRM), multiple tools and instruments are available such as Risk checklists, Electronic Board Room risk classification sessions, Risk allocation practices, Observational Method, Risk based soil investigation and Geo Risk Scans. At Rijkswaterstaat, in recent years we applied Geo Risk Scans in a number of large projects with great success (Van Staveren et al, 2009).

We believe that GeoRM will fit seamlessly in our projects, combining the expertise of geo-engineering and risk management with daily project management.

11 THE NEW WORKING METHOD

In order to accomplish our goal we believe that a sort of '*new working method'* is needed. This new working method will be based on a combination of the earlier mentioned views:

- apply *geo risk management (GeoRM)* explicitly during all phases of realizing the project
- practise the *geo-principles* in the project
- apply the *tools* developed by the Working Groups in the project

Furthermore, it is essential that this new working method will be accepted and adopted in our geotechnical community, by individual professionals and managers, as well as in projects and in organizations. Otherwise, the gained reduction in geotechnical failures will not be durable in time. Possible ways of this type of assurance are:

- knowledge application in new projects
- documenting knowledge in manuals and guidelines
- knowledge transfer by education and training
- clients applying risk based contracts and inspections
- contractors demanding a risk based approach of their subcontractors

12 MONITORING THE GOAL

The goal of the Geo-Impuls Programme "halving geotechnical failure in 2015" proves to be very attractive because of its simplicity, focus, ambition and understandability. Monitoring this goal and making it SMART, however, is far from simple. And yet, it is one of the most frequently asked questions by sponsors, public, and press.

After ample discussion, the Steering Committee has decided not to choose for a quantitative approach. Reason for this is the fact that the information, necessary to perform this calculation, simply is not available, or incomplete, or only can be obtained with great efforts. The chosen qualitative approach will be further elaborated via three parallel tracks:

- *Actual* analysis of geotechnical incidents as published in the trade press, between 2010 and 2015.
- Analysis of the *perception* of geotechnical incidents by geotechnical professionals and the public, by means of surveys in 2011, 2013 and 2015.
- All knowledge and tools of the Geo-Impuls will be implemented in five selected projects. Between 2010 and 2015 the *effects* of this implementation (absence or presence of geotechnical failure) will be monitored.

All tracks will start with a zero measurement, followed by progress measurements. M.Sc. students of the Construction and Engineering Department of the University Twente are now further developing this qualitative approach.

By combining all of these results, obtained by monitoring these three tracks, we believe that we really can demonstrate the effectiveness of the Geo-Impuls Programme, as well as our contribution to society, by substantially reducing the occurrence of geotechnical failures.

REFERENCES

Avendano Castillo, J.E., Al-Jibouri, S.H. and Halman, J.I.M. 2008. Conceptual model for failure costs management in construction. Proc of the 5th Intl Conference on Innovation in Architecture, Engineering and Construction (ACE), Antalya, Turkey, July 23-25.

Barends, F.B.J. 2005. Associating with advancing insight: Terzaghi Oration 2005. In: Proc. 16th Intl Conference on Soil Mechanics and Geotechnical Engineering, 12-16 September, Osaka, Japan, 217-48, Millpress, Rotterdam.

CUR Bouw & Infra 2010. Leren van Geotechnisch Falen: Publicatie 227. Stichting CURNET, Gouda (in dutch).

Van Staveren, M.Th. 2006. Uncertainty and Ground Conditions: A Risk Management Approach. Elsevier Publishers, Oxford.

Van Staveren, M.Th. 2009. Risk, Innovation & Change: Design Propositions for Implementing Risk Management in Organizations. Lambert Academic Publishing, Keulen.

Van Staveren, M.Th., Bles, T.J., Litjens, P.P.T. & Cools, P.M.C.B.M. 2009. Geo Risk Scan – a successful geo management tool. Proc. 17th Intl. Conference on Soil Mechanics and Geotechnical Engineering, Alexandria, Egypt, 2657- 2660.

Van Tol, A.F., Korff, M., & Van Staveren, M. Th. 2009. The education of geotechnical engineers should incorporate risk management. Proc. 17th Intl. Conference on Soil Mechanics and Geotechnical Engineering, Alexandria, Egypt, 2741-2744.

ISGSR 2011 - Vogt, Schuppener, Straub & Bräu (eds) - © 2011 Bundesanstalt für Wasserbau ISBN 978-3-939230-01-4

Shallow Foundation Design through Probabilistic and Deterministic Methods

C. Pereira & L. Caldeira
LNEC, Lisbon, Portugal

ABSTRACT: The design of a shallow foundation with eccentric loading is presented for the ultimate limit state of the bearing resistance, according to the formulation presented in annex D of NP EN 1997-1:2010. Probabilistic and deterministic methods were used. Concerning probabilistic methods, the approximate probabilistic methods, advanced first-order second-moment method (*AFOSM*) and first-order second-moment method (*FOSM*), were applied. For the deterministic calculation, the partial safety factors method recommended by the Eurocode and applied in most practical cases, was implemented. It was assumed that problem variables, such as loads (permanent and variable vertical loads) and soil parameters, follow normal distribution functions. However, the horizontal variable load and the depth of foundation were described by the Gumbel and the rectangular distribution functions, respectively. The results obtained by approximate probabilistic methods were validated by Monte Carlo simulations. Comparisons were made between the results of the three design methods used.

Keywords: Shallow foundation; Hasofer-Lind method; Bearing resistance; Partial safety factor; Probabilistic methods.

1 INTRODUCTION

The traditional approach used in structural analysis and design is deterministic. In these methods, the characteristic values of the random variables are usually considered. However, the respectively random variable uncertainties are indirectly taken into account via partial safety factors calibrated semi-probabilistically, which is essentially, according to Massih and Soubra (2008), in part, a "factor of ignorance", but also, to take into account design situation and parameters not considered in the analysis. As an alternative to the previous method, one can use probabilistic approaches, that are a more rational way of structural analysis and design, which enables to consider directly the inherent uncertainty of each variable in the problem under consideration.

The Eurocode design philosophy (NP EN 1990:2009) prescribes the partial safety factors method as the principal design method. However, the possibility of applying probability methods is also given.

The design of the width B of a square shallow foundation, subjected to an eccentric load, arising from the application of deterministic and probabilistic methods, is herein presented and compared for the ultimate limit state verification of the bearing resistance. As stated into Eurocode 7 (NP EN 1997-1:2010), *EC7*, the geotechnical structures design can be done by analytical, numerical, semi-empirical and prescriptive methods. The design methodology implemented in this paper belongs to the analytical group and follows the formulation presented in annex D of *EC7*. Therefore, in drained conditions and in a homogenous sandy soil with a near horizontal surface, the soil bearing resistance can be obtained by Eq. (1), formulated by the theory of plasticity and based on experimental results. In Eq. (1), N_q and N_γ are the soil bearing capacity factors, s_q and s_γ foundation shape factors, i_q and i_γ coefficients due to load inclination, q' the effective stress at the depth of foundation, γ' the effective soil unit weight, B' the effective width of the shallow foundation and R/A' is the ultimate vertical stress, with $A'=B\cdot B'$. The expressions of the previous variables can be found in annex D of *EC7*. Figure 1 represents a sketch of the problem under study.

$$\frac{R}{A'} = q' N_q s_q i_q + \frac{1}{2}\gamma' B' N_\gamma s_\gamma i_\gamma \qquad (1)$$

In the next section, the random variables considered in the problem are introduced and characterized. The calculation of the width, B, of a square shallow foundation is done in the following for the ultimate limit state of the bearing resistance, through an approximate probabilistic method, developed by Hasofer-Lind (1974). The results obtained are then compared with Monte Carlo simulations. To conclude about the non-linearity of the problem and the applicability of the probabilistic simplified approaches, the same problem was solved using the mean value first-order second-moment (*MVFOSM*). Finally, the shallow foundation was designed based on *EC7*, with the partial safety factors method and some conclusions are drawn.

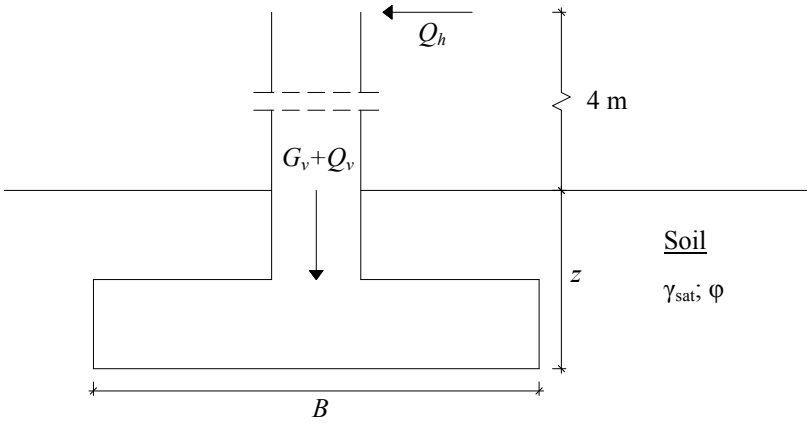

Figure 1. Sketch of the problem.

2 RANDOM VARIABLES

In the probabilistic design, the uncertainties of the loads in time, the soil properties in space and the depth of foundation were directly considered. In Table 1, the random variables considered in the problem are characterized.

Table 1. Random variables properties.

Random variable	Distribution function	μ	CV
Permanent vertical load	Normal	3000	0.10
Variable vertical load	Normal	1000	0.50
Variable horizontal load	Gumbel	250	0.25
Saturated soil weight	Normal	20	0.05
Soil friction angle	Normal	32	0.07
Depth of foundation	Rectangular between z = 1.5 and z = 2.5 m		

The uncertainty quantification of the actions was done according to the Joint Committee on Structural Safety recommendations, JCSS (2001). As a result, a normal distribution was selected to represent the permanent and variable vertical loads with a coefficient of variation, CV, of 10 and 50 %, respectively. JSCC considers the live load constituted by three parts: the overall mean load intensity for a particular user category, a zero mean normal distributed variable and a zero mean random field with a characteristic skewness to the right. For simplicity, only the first and second parts were considered, assuming a constant spatial distribution. Taking into account that the horizontal variable load was due to the wind action, the Gumbel distribution, with a CV of 25 %, was considered for the type of uncertainty involved in this kind of natural phenomenon.

There are numerous studies that characterize and quantify the uncertainties of the physical and mechanical properties of soils. Based on studies of other researchers, Chalermyanont and Benson (2005) reported that a normal distribution is suitable to describe the unit weight and internal friction angle of soils. According to Phoon and Kulhawy (1999), the unit weight and the angle of internal friction typically have values of CV between 3 and 10 % and between 5 and 11 %, respectively, conveniently weighted

along the mobilized soil mass. In the present communication *CV* values equal to 5% and 7% were considered for the unit weight and the internal friction angle, respectively.

Table 2 represents the correlation matrix assumed between the random variables, after some reflection about the physical behaviour of the variables.

Table 2. Random variables correlation matrix.

Random variable	Saturated soil weight	Soil friction angle
Saturated soil weight	1.0	0.5
Soil friction angle	0.5	1.0

3 PROBABILISTIC METHODS

According to the *EC0*, the structural safety verification, for one particular reliability level, is done through the limit state concept. A limit state is the limit beyond which the structure does not satisfy the relevant design criteria. So, for each structural system, the relevant limit state must not be exceeded during the lifetime of the structure, for any design situation with probability of occurrence.

Reliability is the probability of a structure properly performing the functions for which it was designed over a given time. The structural reliability is normally evaluated using two measures, related by

$$\beta = \Phi^{-1}\left(P_f\right) \tag{2}$$

where β is the reliability index and P_f is the failure probability. Φ^{-1} represents the inverse of the cumulative distribution of a standard normal variable. For current structures, with an expected lifetime of 50 yr, the *EC0* sets a minimum reliability index of 3.8 for the ultimate limit states design, which corresponds to a $P_f = 7.2\times10^{-5}$, concerning RC2 class and CC2 (medium consequence for loss of human lives and considerable economic, social or environmental consequences). It was assumed in this paper that the shallow foundation is a current structure.

In general, the failure probability can be determined using: accurate analytical integration, numerical integration methods, approximate analytical methods (like *FORM* methods) and simulation methods. The *FORM* methods include the first-order second-moments methods, *FOSM*, and the advanced first-order second-moment methods, *AFOSM*.

3.1 *Hasofer-Lind method*

In its original form, the Hasofer-Lind method, which belongs to *AFOSM*, is applicable to problems with uncorrelated normal random variables. The corresponding reliability index is defined as the minimum distance from the origin of the reduced coordinate system to the performance function, $g(X')$ and can be expressed as

$$\beta_{HL} = \sqrt{(x'^*)^T (x'^*)} \tag{3}$$

where (x'^*) is the point of the performance function closest to the origin in reduced coordinates, named calculation or design point. In this definition, the original coordinate system $X = (x_1, x_2, ..., x_n)$ is transformed into a reduced coordinate system $X' = (x'_1, x'_2, ..., x'_n)$ according to Eq. (4). Thus, the annulment of the performance function is made in the reduced coordinate system, $g(X') = 0$.

For nonlinear performance functions, the minimum distance calculation is an optimization problem, defined by β_{HL} minimization, with the constraint condition $g(x) = g(x') = 0$. This calculation procedure was implemented in the program Mathcad 14. According to Low and Tang (1997), it is possible to consider the correlation between random variables in the value of the reliability index by Eq. (5), where ρ^{-1} is the inverse matrix of correlation coefficients.

$$X'_i = \frac{X_i - \mu_{X_i}}{\sigma_{X_i}} \tag{4}$$

$$\beta_{HL} = \sqrt{(x'^*)^T \rho^{-1} (x'^*)} \tag{5}$$

For random variables with non-normal distributions, the Rackwitz and Fiessler (1976) method was used to transform the variables distribution into an equivalent normal distribution. The estimation of the equivalent normal distribution parameters, $\mu_{X_i}^N$ and $\sigma_{X_i}^N$, is performed by imposing equality of the cumulative distribution functions, *F*, and probability density functions, *f*, at the design point,

$X'^* = (x'^*_1, x'^*_2, ..., x'^*_n)$ of the non-normal variables and the equivalent normal variables. The parameters of equivalent distributions were determined by

$$\sigma_{X_i}^N = \frac{\phi\left\{\Phi^{-1}\left[F_{X_i}\left(x_i^*\right)\right]\right\}}{f_{X_i}\left(x_i^*\right)} \quad (6) \qquad \mu_{X_i}^N = x_i^* - \Phi^{-1}\left[F_{X_i}\left(x_i^*\right)\right]\sigma_{X_i}^N \quad (7)$$

The ultimate limit state verifications of bearing resistance took into account four load combinations, presented in Table 3. As the problem contains two variable actions, the *EC0* states that, for each combination, one of these actions shall be selected as principal action and the other, named accompanying action, shall be affected by the coefficient, to take into account the reduced probability of the action variables simultaneously reach extreme values. In the probabilistic approach, the *EC0* defines the ψ_0 value for normal distribution according Eq. (8), where V is the *CV* of the accompanying action for the reference period, T_1 the greatest basic period of combined variable actions and T the reference period (50 yr). It was considered that the basic period for the vertical and horizontal variable actions is 7 yr (typical for imposed loads on building floors) and 1 yr (associated to climate actions), respectively. It was found that $T_1 = 7$ yr.

Table 3. Load combinations.

I	$G_v + \gamma_0 Q_v + Q_h$
II	$G_v + Q_v + \gamma_0 Q_h$
III	$G_v + Q_h$
IV	$G_v + Q_v$ (load without eccentricity)

$$\psi_0 = \frac{1 + \left(0.28\beta - 0.7\,ln\left(T/T_1\right)\right)V}{1 + 0.7\beta V} \quad (8)$$

Table 4 presents the values of B for each of the four action combinations, with the respective design points. It was determined $B = 4.56$ m. In this example, the design was determined by the actions combinations I and III.

Table 4. Width B obtained by the Hasofer-Lind method, with the respective design points.

Load combinations	B (m)	ψ_0	γ_{sat}^* (kN/m^3)	φ^* (º)	z^* (m)	G_v^* (kN)	Q_v^* (kN)	Q_h^* (kN)
I	**4.56**	0.36	17.63	25.14	1.70	3059.29	383.66	387.56
II	4.42	0.55	17.39	24.47	1.68	3151.18	1419.82	146.67
III	**4.56**	-	18.25	26.84	1.78	2906.23	-	522.47
IV	4.12	-	17.42	24.53	1.67	3178.60	1495.34	-

3.2 *Monte Carlo simulations*

The validation of the results obtained by the previous method was performed by conducting Monte Carlo simulations. Using the program Risk, the best fit distributions of the results of four Monte Carlo simulations were determined. A simulation was run for each load combination, and the corresponding failure probability and reliability index were evaluated. Each simulation contained the generation of 100 000 sets of random numbers. The adjustment of the distribution function to the Monte Carlo simulation results was made applying chi-square method.

Table 5. Results from the Monte Carlo simulations and validation of the results obtained by Hasofer-Lind method.

Load combinations	B (m)	Best distribution fit	Distribution parameters	P_f	β_{MC}	β_{MC}/β_{HL}
I	4.56	LogNomal	μ = 985.15 σ = 385.7 Shift = -231.35	1.32×10^{-4}	3.65	0.96
II	4.42	LogNormal	μ = 1097.3 σ = 437.97 Shift = -227.84	4.88×10^{-5}	3.90	1.03
III	4.56	LogNormal	μ = 956.47 σ = 375.57 Shift = -218.09	9.97×10^{-5}	3.72	0.98
IV	4.12	LogNormal	μ = 1220.9 σ = 485.29 Shift = -245.39	3.20×10^{-5}	4.00	**1.05**

Table 5 represents the values obtained by Monte Carlo simulations and Figure 2 presents graphically the same results. The results obtained by the Hasofer-Lind method have small deviations compared to those obtained by Monte Carlo simulations. In this case, a maximum deviation of 5 % was found in the reliability index, for the load combination IV. Based on these results, the calculation of width *B*, by the Hasofer-Lind method, is considered as valid.

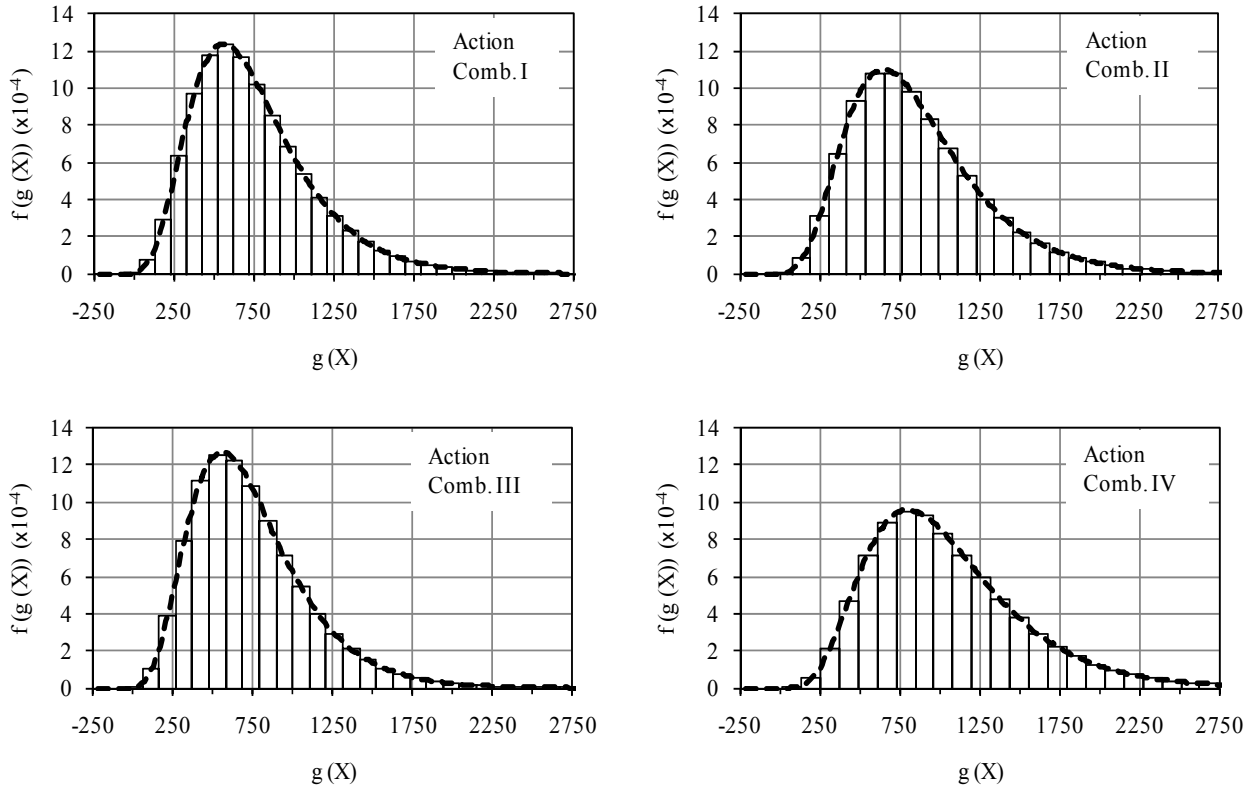

Figure 2. Monte Carlo simulation results.

3.3 *FOSM*

In this section, the *FOSM* was used to solve the same problem. *FOSM* is also known as the mean value first-order second-moment method, *MVFOSM*. In this method, the information of the random variables distribution is ignored. The performance function is linearized by the first-order approximation of a Taylor series development, evaluated at the mean values of the random variables, using the statistical moments up to the second order (mean values and variances). It comprises a higher degree of approximation than the Hasofer-Lind method.

Limiting the Taylor series expansion of the performance function to linear terms produces the expressions represented by Eq. (9) and Eq. (10), as first order approximation of the mean value and the variance, respectively.

$$\mu = g\left(\mu_{X_1}, \mu_{X_2}, ..., \mu_{X_n}\right) \tag{9}$$

$$\sigma = \sqrt{\sum_{i=1}^{n}\sum_{j=1}^{n}\frac{\partial g}{\partial X_i}\frac{\partial g}{\partial X_j}Cov\left(X_i, X_j\right)} \tag{10}$$

where

$$Cov\left(X_i, X_j\right) = \rho_{i,j}\sigma_i\sigma_j \tag{11}$$

In situations of lack of an explicit performance function, such as the results from numerical models, the determination of σ_z can be performed by the central difference approximation for the calculation of the first derivative (finite difference method). According to this method, the expressions represented in Eq. (12) to Eq. (15) are considered.

$$\frac{\partial g}{\partial X_i} \cong \frac{Y_i^+ - Y_i^-}{2\sigma_{X_i}} \tag{12}$$

$$Y_i^+ = g\left[\mu_{X_1}, \mu_{X_2}, ..., \left(\mu_{X_i} + \sigma_{X_i}\right), ..., \mu_{X_n}\right] \tag{13}$$

$$Y_i^- = g\left[\mu_{X_1}, \mu_{X_2}, ..., \left(\mu_{X_i} - \sigma_{X_i}\right), ..., \mu_{X_n}\right] \tag{14}$$

$$\sigma \cong \sqrt{\sum_{i=1}^{n}\left(\frac{Y_i^+ - Y_i^-}{2\sigma_{X_i}}\right)^2 {\sigma_{X_i}}^2} = \sqrt{\sum_{i=1}^{n}\left(\frac{Y_i^+ - Y_i^-}{2}\right)^2} \tag{15}$$

Table 6 represents the reliability index, $\beta = \mu_z / \sigma_z$, and its failure probability, obtained by *FOSM* for the load combinations used in 3.1. The results of the exact derivative and central difference approximation are presented.

Table 6. Reliability index and failure probability determined by *FOSM*.

Action combinations	B (m)	Exact derivative					Central difference approximation				
		ψ_0	μ	σ	β_{FOSM}	$P_{f,FOSM}$	ψ_0	μ	σ	$\beta_{FOSM,a}$	$P_{f,FOSM,a}$
I	4.56	0.349	737.2	362.1	2.036	2.09×10^{-2}	0.348	737.2	367.9	2.004	2.26×10^{-2}
II	4.42	0.590	812.7	398.4	2.040	2.07×10^{-2}	0.589	812.5	405.0	2.006	2.24×10^{-2}
III	4.56	-	727.6	353.6	2.058	1.98×10^{-2}	-	727.6	359.2	2.026	2.14×10^{-2}
IV	4.12	-	894.2	433.8	2.062	1.96×10^{-2}	-	894.2	441.1	2.027	2.13×10^{-2}

The difference between the results of the variance of the performance function, obtained by exact derivative or by central difference approximation, is very small, despite of the very sharp shape and non-linearity nature of the performance function. The reliability indexes obtained are quite similar in both cases. Thus, in the inability to determine the exact partial derivatives of different variables, the central difference approximation allows, in a simple manner, the determination of similar results to the derivation of the exact function of performance.

However, the results obtained by *FOSM* differ greatly from the results obtained by the Hasofer-Lind method, which have been confirmed by Monte Carlo simulations. The *FOSM* is only accurate in special situations, such as when all variables are normal and statistically independent and the performance function is almost a linear combination of these variables, which is not the present case. The absence of the distribution functions of the variables information and the use of a linearized performance function around its mean point can lead to significant errors. In this case, as shown in Figure 3, a reliability index of 3.8 could not be achieved with this method for any load combinations, despite of the width value considered. In this case, this approximate method does not produce acceptable results.

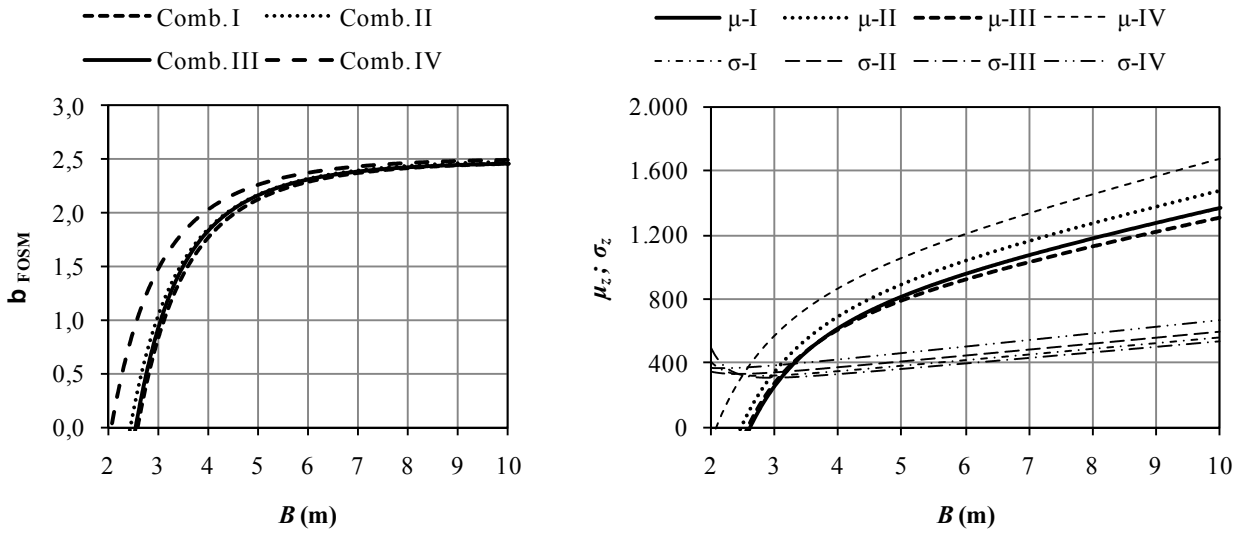

Figure 3. Reliability index, mean value and variance evolution with B for *FOSM*.

4 PARTIAL SAFETY FACTORS METHOD

According to the recommended in *EC7*, the design of the width *B* of a shallow foundation was made by the three approaches presented in Table 7, considering the partial safety factors presented in Table 8 and the characteristic values shown in Table 9, obtained from the distribution functions presented in 2.

This communication presents the comparison between the three Eurocode design approaches, even knowing that each European country adopted only one design approach.

Table 7. Eurocode design approaches.

Design approaches		Combinations
DA1	C1	A1 "+" M1 "+" R1
	C2	A2 "+" M2 "+" R1
DA2		A1 "+" M1 "+" R2
DA3		(A1 or A2) "+" M1 "+" R1

Table 8. Partial safety factors recommended by Eurocode.

Actions				Soil parameters		
Permanent	A1	fav	1	tan(φ)	M1	1
		un-fav	1.35		M2	1.25
	A2	fav	1	γ_{sat}	M1	1
		un-fav	1		M2	1
Variable	A1	fav	0	Resistance		
		un-fav	1.5	R1		1
	A2	fav	0	R2		1.4
		un-fav	1.3	R3		1

Table 9. Characteristic values obtained from the distribution functions of the random variables (*EC7*).

Random variables	Mean values	Characteristic values		Percentile (%)	Random variables	Mean values	Characteristic values		Percentile (%)
G_v (kN)	3000	3493.5	$G_{v,k,sup}$	95	γ_{sat} (kN/m^3)	20	21.65	$\gamma_{sat,k,sup}$	95
		2506.5	$G_{v,k,inf}$	5			18.36	$\gamma_{sat,k,inf}$	5
Q_v (kN)	1000	2026.9	$Q_{v,k,desf}$	98	φ (º)	32	35.7	$\varphi_{k,sup}$	95
		0	$Q_{v,k,fav}$	-			28.3	$\varphi_{k,inf}$	5
Q_h (kN)	250	412	$Q_{h,k,desf}$	98	z (m)	2	2.45	$z_{k,inf}$	95
		0	$Q_{h,k,fav}$	-			1.55	$z_{k,sup}$	5

Table 10 presents the results of width *B* for each design approach considered in Table 7. The corresponding design values of the six variables are also indicated. As can be seen in this example, for the DA1-C1 and DA2 approaches the horizontal load is most relevant while, in the other two approaches, the vertical loads increase their importance in comparison with the horizontal load effects.

In this case, the width *B* would be determined by the approach DA3, obtaining $B = 6.05$ m. This value is 33 % higher than the value obtained by the method of Hasofer-Lind. In the four approaches, the deterministic method gave always higher values of *B* than the probabilistic methods. Assuming, that the Eurocodes take into account the uncertainties considered in the probabilistic methods, this means that, for the variability assumed, the partial safety factors present in *EC7* were calibrated for lower failure probabilities. Table 10 represents the reliability indexes determined in accordance with the Hasofer-Lind method for the dimensions obtained by the partial safety factors method. As can be seen, all the values are higher than the limit imposed by *EC0* (3.8).

Table 10. Width B designed by the partial safety factors method, recommended by the *EC7*.

Calculation approaches		B_{EC7} (m)	$G_{v,d}$ (kN)	$Q_{v,d}$ (kN)	Q_h (kN)	γ_{sat} (kN/m^3)	φ (º)	z (m)	B_{EC7}/B_{HL}	β_{HL}
DA1	C1	4.93	2506.5	0	618.0	18.36	28.32	1.55	1.08	**4.23**
	C2	5.62	3493.5	1843.7*	535.6	18.36	23.32	1.55	1.23	**4.88**
DA2		5.41	2506.5	0	618.0	18.36	28.32	1.55	1.19	**4.70**
DA3		**6.05**	4716.2	2128.2*	618.0	18.36	23.32	1.55	1.33	**5.21**

* value affected by ψ_0

The Eurocodes partial safety factors were calibrated semi-probabilistically, taking into account the past relevant geotechnical experience, in order to not cause any design disruption. For comparison, Table 11 presents the partial safety factors determined from the results obtained in 2.1 with the probabilistic method. The results are very different from those proposed by *EC7*. In general, the partial factors are smaller than those recommended in the regulation. For the material properties, the values of the partial safety factors are close to those recommended by *EC7*. The values for the foundation level are near the unit, comparing with a characteristic value. This means that the consideration of the mean value for geometric variables with significant variance, recommended by *EC0*, is not the best option. At last, the loading partial safety factors are, in some cases, very different than the values suggested by the *EC0*.

However, in these analyses, the experience of historical cases was overlooked, which have in consideration another type of uncertainties, namely, spatial variability, construction activities and calculation model accuracy.

Table 11. Determination of the partial safety factors from the results obtained by the Hasofer-Lind method.

Action combinations	γ_γ	γ_φ	γ_z	G_v^* (kN)	Q_v^* (kN)	Q_h^* (kN)
I	1.041	1.147	0.912($z_{k,sup}$)	0.876($G_{v,k,sup}$)	0.526($Q_{v,k,desf}$)	0.941($Q_{h,k,desf}$)
II	1.056	1.183	0.923($z_{k,sup}$)	0.902($G_{v,k,sup}$)	0.700($Q_{v,k,desf}$)	0.647($Q_{h,k,desf}$)
III	1.006	1.064	0.871($z_{k,sup}$)	0.832($G_{v,k,sup}$)	-	1.268($Q_{h,k,desf}$)
IV	1.054	1.180	0.928($z_{k,sup}$)	0.910($G_{v,k,sup}$)	0.738($Q_{v,k,desf}$)	-

5 CONCLUSIONS

This paper presents the design of the width B of a square shallow foundation subjected to eccentric loading, through deterministic and probabilistic methods for the ultimate limit state of the bearing resistance. Width B was obtained by the Hasofer-Lind method. Those results were validated by Monte Carlo simulations and compared with other design methods, namely probabilistic and deterministic methods.

The *MVFOSM* utilization does not give adequate results, achieving undervalued levels of safety. This method should not be used in problems with high nonlinear solutions.

The results show that the level of safety determined by Hasofer-Lind method is smaller in comparison with the partial safety factors method. In that way, there are two possibilities to explain the differences: the partial safety factors method is overly conservative or the Hasofer-Lind method does not consider all the uncertainties of the problem.

The Eurocodes partial safety factors were calibrated semi-probabilistically by performing probabilistic calculations, being adjusted accordingly to the experience gained over time. What is shown by the results is that the direct utilization of probabilistic methods does not take into consideration important uncertainties related to construction activities and soil variability. So, without consideration of these types of uncertainties, these probabilistic methods should be applied carefully, due to the fact that can produce unsafe designs compared with the level of safety considered over time.

As future development of the present work, the different sources of uncertainties, namely, spatial variability, construction activities and calculation model precision, shall be incorporated in the probabilistic methods for designing shallow foundations, in order to incorporate the calibration of the partial safety factors or to establish the probabilistic methods as an alternative design methodology.

REFERENCES

Chalermyanont, T., and Benson, C. H. (2005). Reliability-based design for external stability of mechanically stabilized earth walls. *International Journal of Geomechanics*, 5(3), 196-205.

Hasofer, A. M., and Lind, N. C. (1974). Exact and invariant second moment code format. *J. Engrg. Mech. Div.*, 100(1), 111-121.

JCSS (2001). Probabilistic model code. Part II – Load models. *JCSS Internet Publication*

Low, B. K., and Tang, W. H. (1997). Efficient reliability evaluation using spreadsheet. *J. Engrg. Mech.*, 123(7), 749-752.

Massih, D. S. Y. A., and Soubra, A. H. (2008). Reliability-based analysis of strip footings using response surface methodology. *International Journal of Geomechanics*, 8(2), 134-143.

NP EN 1990 (2009). Eurocode – Basis of structural design. *IPQ*, December.

NP EN 1997-1 (2010). Eurocode 7 – Geotechnical design. Part 1: General rules. *IPQ*, March.

Phoon, K.-K., and Kulhawy, F. H. (1999). Characterization of geotechnical variability. *Can. Geotech. J.*, 36, 612-624.

Rackwitz, R., and Fiessler, B. (1976). Structural reliability under combined random load sequences. *Computers and structures*, 9(5), 489-494.

ISGSR 2011 - Vogt, Schuppener, Straub & Bräu (eds) - © 2011 Bundesanstalt für Wasserbau ISBN 978-3-939230-01-4

Risks of Tailings Dams Failure

J.-F. Vanden Berghe and J.-C. Ballard
Fugro GeoConsulting, Brussels, Belgium

M. Pirson and U. Reh
Solvay Chemicals GmbH, Bernburg, Germany

ABSTRACT: Tailings dams are geotechnical structures that are increased in height with time. Several factors typical of tailings dams cause a higher risk of failure compared with other earth structures. The factors that influence the risk of tailings dam failure are discussed in this paper. Important factors include a high water level in the tailings dam slope, lack of monitoring, inappropriate site investigation and lack of understanding of the mechanical behavior of tailings material. An approach to mitigate and/or control these risks is then proposed based on appropriate site characterization, design analysis adapted to the tailings characteristics and a sufficient monitoring system that is rigorously used.

Keywords: dam, tailings dam, slope failure, site investigation, monitoring

1 INTRODUCTION

Tailings dams are common in several chemical and mining industries. This type of geotechnical structure is increased in height with time and can reach heights of more than 30 meters. The main characteristics of tailings dams are the length of construction, which may be spread over 40 to 50 years or more, and the repeated application of new maximum loading conditions. As a result, tailings dams cannot be physically tested under maximum loading conditions and the risk of slope failure increases with time.

Broadly, 2 to 5 out of the 3,500 tailings dams in the world experience major failure each year (Lemphers, 2010). Two examples of recent tailings dam failure are shown on Fig. 1. In both failures, spectacular quantities of tailings material escaped from the breach that opened in the dam with severe consequences.

Tailings dams are more than 10 times more likely to fail than other conventional water retaining dams (Lemphers, 2010). Operating a tailings dam involves risks that need to be identified, quantified and mitigated. The main risks of slope failure are discussed in this paper and a methodology to mitigate these is proposed based on the authors' experience.

Kolontárt Devecseri tailings dam, Hungary (2010)

(b) Bernburg tailings dam, Germany (2007) (Ballard, 2008 and Vanden Berghe, 2009).

Figure 1. Two examples of recent tailings dam failure

2 TAILINGS DAM CONSTRUCTION AND OPERATION

A tailings dam is generally a pond where the by-products from the mining or chemical industry are disposed. In most cases, the tailings material is delivered hydraulically from the periphery of the dam (Figure 2). The tailings sludge then flows towards the center of the pond where a water outlet evacuates the overflow of decanted water (European Commission, 2009). The level of this outlet is adjusted so that a pool is created, to permit deposition of fine particles. As a result, a high water level is maintained in the pond. Therefore, water flow is induced through the dam body and the foundation soil. An efficient drainage system that prevents the water table from approaching the dam slope is generally essential (ICOLD, 1996). A network of drainage pipes connected to a main collector is often installed at the bottom of the pond to drain the tailings leachate.

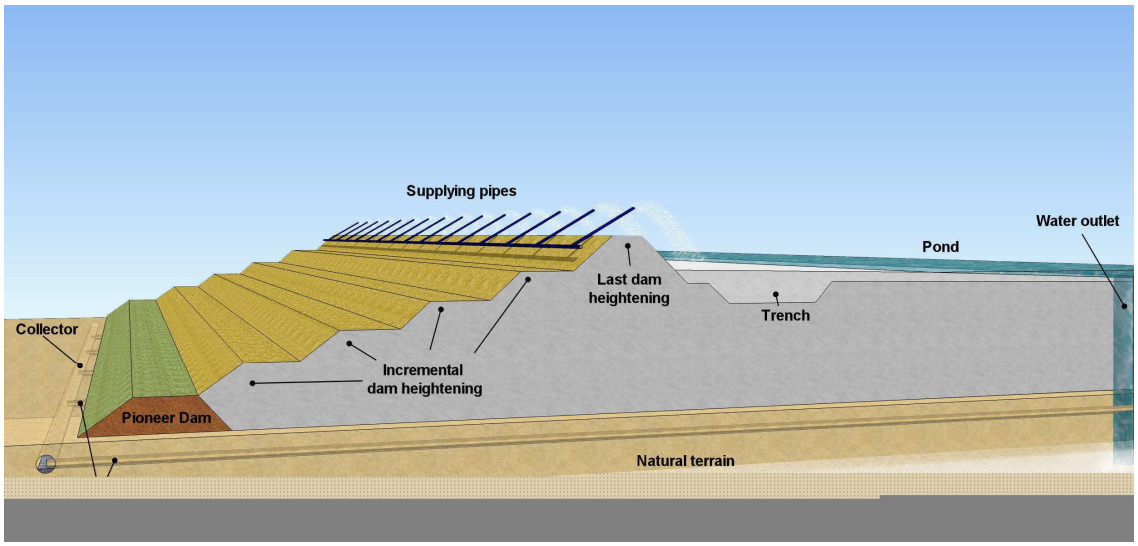

Figure 2. Example of tailings dam profile

The process begins with the construction of a starter dam (pioneer dam on Figure 2), which is only a few meters high. When this initial volume is filled, the starter dam is heightened. There are 3 broad types of methods for raising a tailings dam (ICOLD, 1996):

- Upstream method (Figure 3-a): this method consists of building each new levee on the tailings material that has consolidated. The new levee could either use the tailings material itself or an imported material. This approach is the most cost-effective as it maximizes the storage volume and minimizes the volume of imported material. However, it is also the less robust, especially in case of earthquakes, as the tailings material itself ensures the stability.
- Downstream method (3-b): this method consists of raising the dam by enlarging the retaining structure. The levees are built with imported material, generally selected for its good drainage and shearing properties. In this case the tailings material does not contribute to the dam stability. This approach is the most robust but also the most expensive in terms of imported material. The storage volume is also reduced.
- Centerline method (3-c): this method consists of building the new heightening with imported product placed on top of the existing dam. This approach is an intermediate one between the upstream and downstream methods.

It is also frequent to find combinations of these different techniques. The most common combination is to build the lowest part of the dam downstream or centerline and the last raisings using the upstream method.

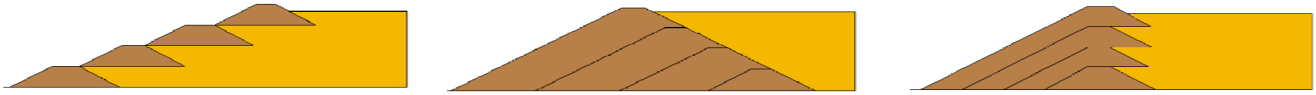

(a) Upstream (b) Downstream (c) Centreline

Figure 3. Broad types of methods for raising tailings dams

By nature, tailings dams are active industrial structures that grow slowly with time. Production is sometimes interrupted to let the pond consolidate. Due to this process, deformation and movements occur. Sometimes, even cracks may appear. This is normal and does not necessarily compromise the stability.

3 TAILINGS DAM OPERATION: A RISKY WORK?

Tailings dams are subjected to many hazards that influence directly their stability. These hazards need to be properly identified and assessed. This section lists and discusses the main hazards potentially influencing the dam stability. The list is based on the authors' experience and is not meant to be exhaustive. Each identified hazard is located in a risk matrix provided on Figure 4.

- Water retaining dams and embankments are generally built in short periods and are tested under maximum load at the end of construction before starting production. Tailings dams are raised very slowly. As a result, they experience each day new maximum loads for which they were never tested. Therefore, the risk of slope failure increases with time as the dam is raised.
- The duration of the tailings dam construction is very long and can be spread over more than 40 years. People who started the construction and all their knowledge and experience may not be available at the end of the tailings dam production. The original design and dam history is sometimes not properly documented.
- Design is performed step by step, generally without considering the final height.
- Some tailings dam operators tend to underestimate (geotechnical) risks associated with tailings dams and not to consider them as part of the industrial process with specific risks that need to be controlled.
- Tailings materials are not natural soils and may behave differently. They have a different chemical content and experience a different depositional process. As a result, they may develop special properties potentially affecting the performance of the dam. For instance, they may have anisotropic shear strength and permeability properties (Vanden Berghe et al, 2009). An in-depth understanding of the fundamental behaviour of the material and a correct modelling of the key aspects is therefore essential (Chang, 2011).
- Water level in the dams is generally very high as the product is disposed in a liquid phase. The water flow through the dam represents generally the most critical and most uncertain destabilising load. During the design of the dam, the seepage modelling will impact significantly the risk assessment. Operating procedures are also very important to minimize the amount of free water at the crest of the dam.
- The drainage system is an essential part of the design to prevent any pore pressure build-up close the dam slope. The system efficiency may reduce with time for several reasons and needs to be controlled.
- The chemical content of the tailings material is not neutral. Several chemical reactions could occur after deposition with the air, the natural water or the foundation soil. This may lead to unexpected behavior of the dam. For instance, undesired chemical reactions may alter the efficiency of the drainage system (Ballard et al, 2008).
- A good monitoring system is very important during operation. An inadequate system will not highlight the potential problems and could lead to the dam failure without warning.
- Tailings dams could be subjected to geohazards such as, for example, earthquakes, fault movements, hydro-geological hazards, etc. If not properly addressed because not identified or poorly characterised, these hazards could have severe consequences on the dam stability. In case of earthquake, the risk of liquefaction or cyclic degradation of the tailings material is a central question.

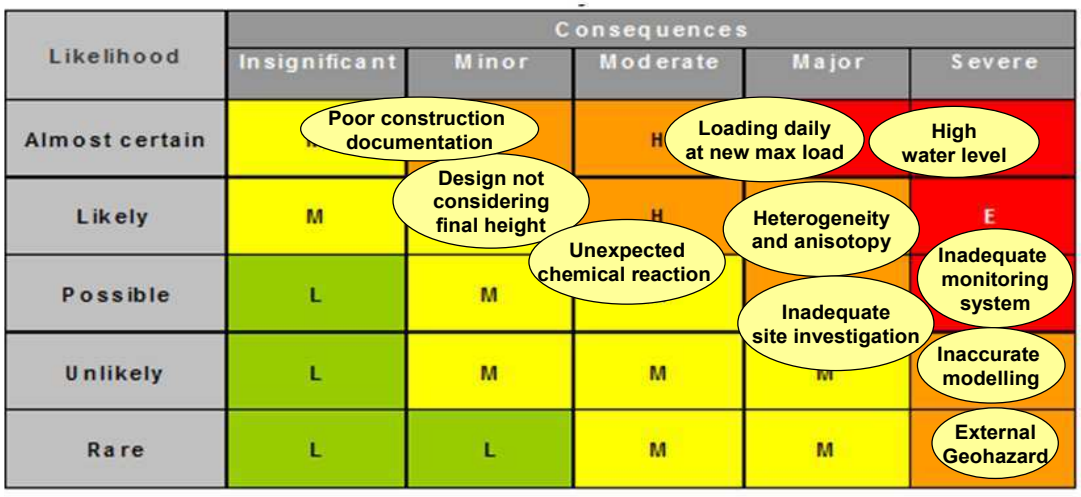

Figure 4. Main risks affecting directly the dam stability

4 MITIGATION OF FAILURE RISKS

This section proposes a methodology based on the author's experience on how mitigate the risks of tailings dam failure based on data collection and analysis, proper design and monitoring.

4.1 *Data collection/analysis*

The determination of the most critical slope failure mechanism is a fundamental step in the risk analysis and the determination of mitigation measures.

Each risk analysis should start with a preliminary desktop analysis based on available data. The objective is to evaluate the quality and reliability of the available data with regard to the determination of the most critical slope failure mechanisms. Parametric analyses are useful to identify the governing parameters. At this stage, the natural geo-hazards should also be identified. The most critical one is earthquakes. Depending on available information, a Probabilistic Seismic Hazard Assessment (PSHA) may be required. This analysis will determine, based on an analysis of the past earthquakes, the probability of occurrence of an earthquake of given intensity at the tailings dam location. It will also provide the induced surface accelerations based on the local geology. Other geological risks such as fault (active or not) or karstic dissolutions should be addressed as they can also influence directly or indirectly the dam integrity.

Based on the outcomes of the preliminary desktop analysis and geo-hazard review, an optimized site investigation program should be set up. The objective will be to know with a sufficient level of accuracy the governing parameters. The program will as a minimum include the determination of (1) the geotechnical parameters of the tailings material and the foundation soil, which will be directly used in the stability analysis and (2) the intrinsic properties of the tailings material. The second set of data is critical in tailings dam design in order to verify that the tailings material behaves like a soil and that standard soil models can be used for the dam design. In most cases, the behaviour of the tailings material is similar to a natural soil but it may present some specific particularities that need to be taken into account (e.g. anisotropy, high permeability, chemical reactivity, etc.). Special attention should be paid to the chemical interaction of the tailings leachate with foundation soil and dam material (Ballard, 2008 & Chang, 2011).

The type of tests should be chosen carefully taking into account the particular nature of the tailing material. The main geotechnical tests are discussed in the following sections.

4.1.1 *Boreholes*

Boreholes will provide valuable information on the stratigraphy. Samples should be taken for laboratory testing. Since tailings deposits are generally very soft, special attention should be paid to the sampling technique and handling. High quality samplers should be used to minimize disturbance. Ladd et al (2003) provides recommendations for drilling, sampling and handling procedures for very soft soils. Borehole should reach the foundation soil such that it can also be properly characterised. Chemical reactions of the tailings leachate with the foundation soil may induce a modification of its properties with time. Therefore, re-evaluating those as the dam height increases is important.

4.1.2 *In situ testing*

Given the generally soft behavior of the tailings material, a combination of Cone Penetration Test (CPT) and in-situ vane tests is generally very efficient. CPT will provide detailed information on the stratigraphy and the variation of resistance with depth while in-situ vane tests will measure the tailings undrained shear strength at specific locations. These tests have the advantage of being reasonably quick and both types of tests can be performed with the same truck. Unfortunately, CPT and vane tests will not provide precise information on the drained shear resistance of the soil/tailings and its potential anisotropy.

More specific in-situ tests are sometimes required to test larger volume of tailings material. The tailings material presents sometimes a blocky, fissured or highly layered structure (Alonso, 2006). In this type of structured material, the macroscopic behavior may differ from the behavior observed in small element tests. Large scale shear box tests, pumping tests and vertical loading tests are useful tests to determine the in-situ drained shear resistance, the mass permeability and the in-situ stiffness, respectively (Ballard, 2008).

4.1.3 *Laboratory testing*

Two types of laboratory testing are generally required: characterisation tests and shear strength tests. The characterisation tests include unit weight, water content, particle size distribution, Atterberg limits, chemical content and micro structure analysis. Even if all the results from these tests are not directly used

for the stability analyses, they are essential for drawing parallels with natural soil and identify special features. The drained and undrained shear strength of the tailings material, the foundation soil and the dam body can be determined using classical direct shear tests, direct simple shear tests and triaxial tests. Since the in-situ testing generally gives a more reliable measurement of the undrained shear strength, laboratory testing should focus on the measurement of the effective stress parameters.

Due to the depositional process by sedimentation, tailings material may exhibit an anisotropic behaviour with a lower shear resistance along horizontal planes. In this case, direct and simple shear tests are preferred to triaxial tests. A design based only on triaxial test results may be unconservative (Ballard, 2008).

As already discussed above, tailings materials are generally very soft and samples should be prepared carefully and tests executed with special caution. Recommendations for sample preparation in very soft soil are provided in Ladd et al (2003). The sample should be extruded from the sampling tube directly in the testing devices with a minimum of manipulation. X-ray of the sample tubes should also be performed to visualize the sample quality and determine the best part of the sample for testing.

4.2 *Design*

Design is the backbone of the entire risk management system of tailings dams. It allows the quantification of the risk level and is the links between the different elements that enter into the analysis. From Author's experience, three aspects are particular to tailings dams and need to be carefully addressed.

4.2.1 *Selection of adequate safety factors*

Given the consequences of a tailings dam failure and the uncertainties related to the fact that the material is not a natural soil, higher safety factors should be adopted for tailings dams than for standard earth slopes (Duncan, 2005). The adopted safety factors should comply with codes of practice but should also incorporate the limitations of these codes regarding the particular case of tailings dam stability. For example, the most recent codes proposing a partial safety factor approach do not request explicitly the application of a partial factor on the pore water pressure although it is often the main (and the most unpredictable) destabilising load for a tailings dam.

It is proposed to design the dam for a global safety factor in drained condition of at least 1.5 and authorise lower value only if a very efficient and proved monitoring and management system is in place. The safety factor should never be lower than the applicable standard. For the Eurocode and the DIN Standard, the equivalent minimum global safety factor is 1.25 in drained condition. A comparison of the safety factors used in Europe (EU commission, 2009) indicates similar values.

4.2.2 *Calculation method compatible with failure mode*

The traditional Bishop approach (Bishop, 1955) assuming a circular slip surface to compute the slope safety factor may not be appropriate in all cases. For instance, in the case of anisotropic shear strength properties, as sometimes observed in tailings dams due the depositional process, the most critical failure mechanism is not a circular one. Commercial software programs are available to check the factor of safety for non-circular mechanisms.

4.2.3 *Drained vs undrained analysis*

The raising of a tailings dam is generally completed sufficiently slowly to allow pore water pressure dissipation to occur. Therefore, the calculations should focus mainly on effective stress analyses (c', ϕ'). However, undrained failure in fine-grained sediments can be triggered by a quick external loading such as an earthquake. In this case, the main question to answer is whether or not the tailings material is susceptible to liquefaction or cyclic degradation.

4.3 *Monitoring*

Monitoring comes naturally from the risk analysis discussed above. Stability analyses of the dam determine the most critical failure modes and the governing parameters. Depending on how confident we are about these parameters, the monitoring provides a continuous control and defines action plan in case of detection of risk increase.

4.3.1 *Monitoring strategy*

Any monitoring needs to be based on a monitoring strategy: what do we want to monitor and why? The quality of the monitoring strategy will determine the quality of the entire monitoring system.

The main risk that could compromise the tailings dam stability in drained condition is generally the water level that is too close to the slope surface. If the water level exceeds a certain limit, the dam is likely to fail. This risk increases as the dam height increases and the water level is difficult to predict in advance. The other parameters influencing directly the slope safety factor are the shear strength and the unit weight of the tailings, the dam body and the foundation soil. If the site investigation program is properly defined, these parameters should be known with a sufficient level of confidence.

In many cases, slope failures are preceded by a series of anomalies that if detected and well interpreted could foresee the incident. These anomalies are generally the apparition of tension cracks and accelerating displacements. These could be monitored by a regular visual inspection of the dam and by measuring the dam displacements. The difficult task will be to differentiate critical situations from normal ones.

A monitoring plan has no value without alarms levels and action plans. For each monitoring location, different levels of alarm should be defined. With each alarm level, a clear and simple action plan should be defined. For example, alarms levels on the measured water level could be linked to the associated safety factor (SF) as illustrated in the table below.

Table 1. Example of alarm levels and corresponding actions for water level monitoring

SF range	Alarm level	Corresponding action
SF > 1.5	No alarm	➔ Continue production
1.5 > SF > 1.25	Alarm 1	➔ Change/adjust deposition location ➔ Increase measurement frequency ➔ Measure closely dam displacements
SF < 1.25	Alarm 2	➔ Stop production in this pond ➔ Measure closely dam displacements ➔ Reassess stability based on actual measurements

To summarise, a monitoring strategy should include:

- Stability analysis with a discussion on the key parameters.
- A list of the most critical failure modes and the parameters to monitor.
- A monitoring plan with the measurement locations, the monitoring equipments, the measurement frequencies, the data treatment and transfer.
- Alarm levels and associated action plans.
- Follow up plan including reporting and back-analysis to maintain the vigilance and increase the knowledge level.

The monitoring strategy should also be well documented with a good report control system such that the monitoring system can be maintained in the long-term, including after the decommissioning of the pond.

4.3.2 *Monitoring operations*

As discussed above, monitoring of tailings dam is generally based on:

- Visual inspections
- Observations of water level
- Measurements of slope displacements (at the surface as well as at depth with inclinometers)

4.3.2.1 *Visual inspection*

The visual inspection should be conducted by an experienced operator on a regular basis. The inspection frequency varies from site to site based on dam height, production type and dam structure. The inspection should mainly focus on cracks, sources of liquid and abnormal behaviours but any other anomaly should also be reported. Generally, the main difficulty of the visual inspection is with the treatment of the observations. It is generally difficult to define simple and clear alarm levels. The operator reporting the anomaly has generally not the background to assess the gravity and the associated risks. Therefore, it is crucial to set up an excellent reporting system that guarantees that the information is communicated to the person that can assess the risks and take the required actions.

4.3.2.2 *Measurement of the water level*

Monitoring the water level aims at controlling one of the most critical trigger of drained slope failure. Therefore, it plays an important role in the management of the pond and the planning of the production. Two types of equipment are generally used: standpipes and piezometers. Standpipes have the advantage

of averaging the water level on a large volume. It can also be easily controlled and inspected. The measurement is normally performed manually but the standpipes can easily be equipped with automatic pressure transducers.
Control and inspection of the equipment on a regular basis is very important. Standpipe can be tested regularly by infiltration/pumping tests. This should guarantee that the water/tailings fluid can freely flow towards the pipe. Inspection is especially important for the equipments installed in the tailings material as the risk of chemical reactions of the tailings fluid, the drainage system of the standpipe and the air in the standpipe is relatively high. These reactions can sometimes clog the perforated section of the standpipe. Water level monitoring is, unlike the other mentioned monitoring operations, a real risk prevention measure. Alarm level is reached commonly before any deformation or damage occurs

4.3.2.3 *Measurement of the displacements*
The objective of monitoring the displacement is to follow the dam reaction to the continuous loading. Deformations are normal and the difficulty of the monitoring is to distinguish a normal deformation from a critical one. There are 2 types of measurement methods: the surface displacement measurement by topographical survey and the measurement of the dam body displacement with inclinometers.

(1) Surface displacement

Surface displacements can be measured manually by a surveyor equipped with a GPS type of system. There exist also continuous measurement tools of the dam surface such as the InSAR technique. InSAR is based on an interferometric technique that provides data on object displacement by comparing phase information, captured at different times, of reflected waves from the object. Data acquisition could be based on satellite images or ground-based installations that follow the displacement of reflectors installed on the dam. Accuracy is in the order of millimeter. The main difficulty for this type of monitoring is to determine alarm levels and the acceptable displacements. In practice, it is not possible to define acceptable total displacements. The alarm level should be based on the displacement rate. An acceleration of the displacement may indicate an imminent risk of failure. Mitigation measures and a rapid action plan should be prepared and tested for such occurrences.

(2) Inclinometer

Inclinometer is the preferred equipment to detect slope displacements. It has the advantage of measuring the distribution of displacement with depth. Simple data processing allows deducing the cumulative shear strain at any depth (Figure 5). The maximum shear resistance for most of the soils and tailings materials is mobilised for a shear strain of the order of 10%. The measured cumulative shear strain should therefore be compared with this value to give an idea of the failure risk. The main limitation of this method is that the installation of the inclinometer can be performed only when the dam has reached a certain height. Therefore, the measured zero shear strain (measured when the inclinometer is installed) is not the actual zero as the dam has already deformed. For this reason, it is strongly recommended to install the inclinometer as soon as it is permitted by the dam height. Considering the uncertainty on the zero value and the required safety factor, it is proposed to define an alarm level for a cumulative shear strain of the order of 1 to 2%. A second alarm level should also be defined on the displacement rate. Any acceleration in the displacement should be analysed carefully. Inclinometer can be measured manually on a regular basis or in case of incident. They could also be equipped with permanent measurement devices that can be continuously monitored.

4.3.2.4 *Data transmission and treatment*
The quality of the monitoring system will strongly depend on how the measured data are treated and transferred. An easy and efficient way is to centralise the measurements in one unique system that could be accessible via a web portal interface (Figure 5). Predefined alarm levels can also be implemented and compared with actual data in real-time. The web interface permits also a quick reaction in case of incident as all the different parties involved in the process have an immediate access to the data.

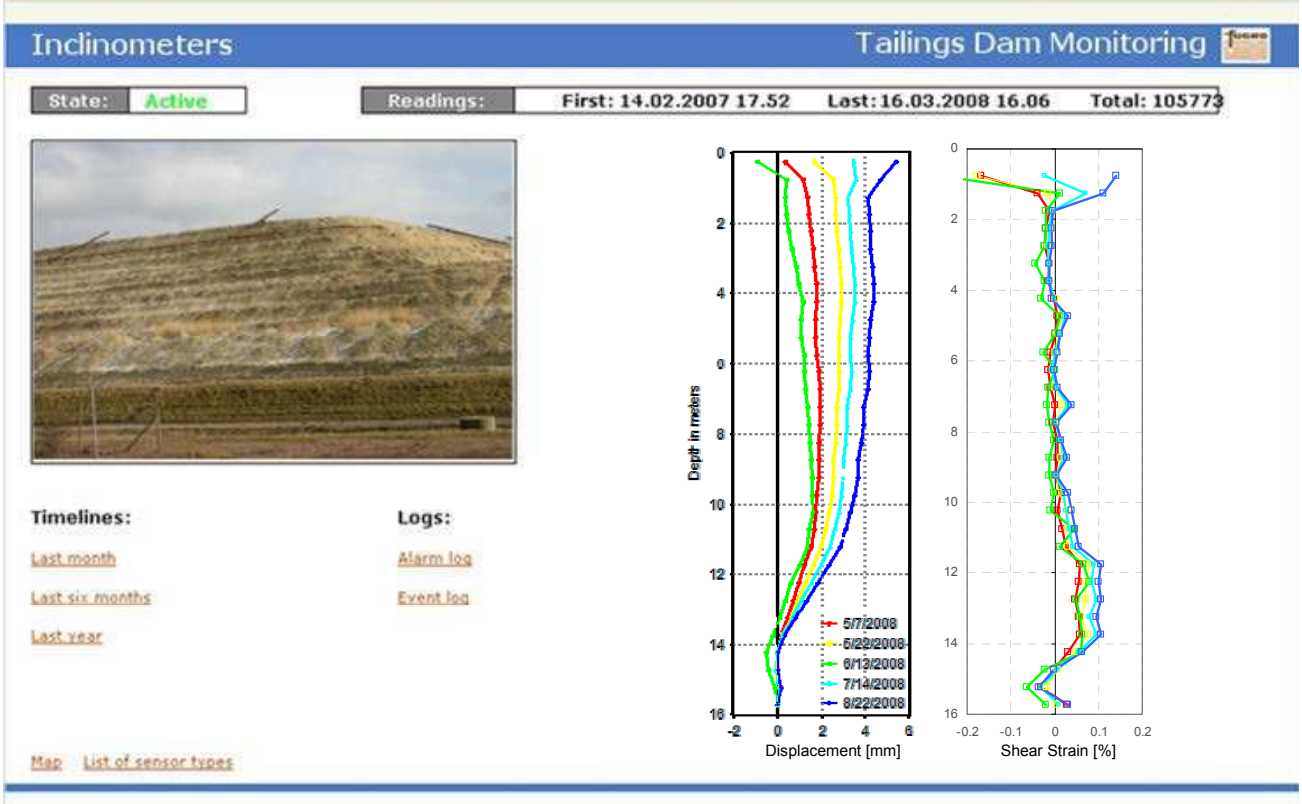

Figure 5. Example of Web portal interface with inclinometer measurement data

5 CONCLUSIONS

Tailings dams are industrial structures having their own particularities. They are life structures that are continuously loaded to the maximum load. Some displacements are thus normal. Often, tailings material is highly heterogeneous and may present anisotropic properties.

There are many factors that could influence the dam stability and the risk of failure. An approach based on a good data collection, appropriate design and efficient monitoring system was proposed. The monitoring is a key tool in this process and should be based on a clear and simple monitoring strategy that defines the risks to be monitored, the alarm levels and the associated actions. The monitoring needs to be reliable in the long term and the instruments regularly inspected and controlled. On a regular basis, monitoring data need to be back-analyzed in order to check the design assumptions and to define the future heightening strategy.

REFERENCES

Alonso E. E. & Gens A. (2006), « Aznalcollar dam failure. Part 1 : Field observations and material properties », Géotechnique 56, No. 3, 165–183.

Ballard J.-C., Vanden Berghe J.-F., Jewell R. and Pirson M (2008). Some lessons from a recent tailings dam failure. Proceeding of the Fourth International Conference on Forensic Engineering, 2008, Institution of Civil Engineers, London, UK.

Bishop A.W. (1955). The use of slip circle in the stability analysis of slopes. Geotechnique, Vol.5, No.1, pp.7-17.

Chang N., Heyman G. and Clayton C., The effect of fabric on the behaviour of gold tailings, Géotechnique 61, N°3, 187-197, 2011.

Duncan J.M. and Wright S.G. (2005). Soil strength and slope stability, John Wiley & Sons Inc.

European Commission (2009). Reference document on best available techniques for management of tailings and waste-rock in mining activity, January 2009, 557 pages.

ICOLD (1996), A guide to tailings dams and impoundments – Design, construction, use and rehabilitation. International Commission on Large Dams.

Ladd C, DeGroot D, (2003). Recommended practice for soft ground site characterization: Arthur Casagrande lecture. Proceedings of 12th Panamerican Conference on Soil Mechanics and Geotechnical Engineering, June 2003, Massachusetts Institute of Technology, Cambridge, USA.

Lemphers N. (2010), Could the Hungarian tailings dam tragedy happen in Alberta?, www.pembina.org - Oct. 12, 2010

Vanden Berghe J-F, Ballard J-C, Jewell R, Pirson M. and Uwe R. (2009). Importance of shear stress anisotropy and bottom drainage on tailings dam stability: a case history. Proceedings of the 17th ICSMGE, October 2009, Alexandria, Egypt.

ISGSR 2011 - Vogt, Schuppener, Straub & Bräu (eds) - © 2011 Bundesanstalt für Wasserbau ISBN 978-3-939230-01-4

Reducing Geo-risks for Offshore Developments

P. T. Power, M. Clare, D. Rushton and M. Rattley
Fugro GeoConsulting Ltd., Wallingford, U.K.

ABSTRACT: This paper describes the systematic and holistic approach to geo-risk reduction that has been developed and applied to numerous deep water oil and gas projects and is now being used for shallow water wind farm developments. Key elements of the approach are:

- Regional Desk Studies to establish the geological context and develop preliminary Ground Models and Risk Management Strategies.
- The use of high and ultra high resolution geophysics to accurately define stratigraphy and geological structure.
- New geotechnical investigation techniques to quantify the physical characteristics of the geological strata.
- Advanced geological and geotechnical laboratory testing of soil samples and long piston cores.
- Analysis of geological/geotechnical processes that will influence areas or structures.
- The use of GIS as a geohazard assessment and screening tool.
- Advanced numerical modelling of soil/structure interaction.

Illustrative examples include projects offshore Angola, the West Nile Delta and the North Sea.

Keywords: Offshore, Geotechnical, Risk Reduction, Geohazard, Ground Model, GIS.

1 INTRODUCTION

Over the last ten years a more systematic and holistic approach to assessing shallow geological and geotechnical risks for offshore oil and gas developments has evolved. This approach is now being used to address similar issues for the offshore renewable energy market – and in particular offshore wind farm developments.

This paper will describe how this approach has evolved, giving some examples of its application off Egypt's West Nile Delta and offshore Angola. It will also explain how data acquisition techniques have developed to better quantify the natural environment and its physical characteristics and thus reduce uncertainties and the associated risks. The role of forensic core logging in Geohazard assessment and advanced laboratory testing of soil samples will be covered as will the use of Geographic Information Systems (GIS) for data management and presentation but also as a risk screening and engineering tool.

Finally, the latest application of the systematic approach to the UK's Round 3 Windfarm licence areas will be described.

But first it is worthwhile to consider the history of geological and geotechnical site investigations and risk assessment in the offshore environments in order to put current developments into context.

Offshore geotechnics was effectively born in the post World War II years; firstly in the Gulf of Mexico and in Lake Maracaibo, Venezuela, when attempts were first made to drill wells and install production platforms in very shallow water close to shore. The industry then spread into deeper water across the continental shelves of many parts of the world, arriving in the North Sea in the 1960's, with a subsequent boom triggered by the oil crisis in 1973. However, throughout this period the primary risk was related to geotechnical variability in one vertical axis and its impact on the bearing capacity and installability of

deep piles. This risk was effectively managed by performing one or more geotechnical boreholes incorporating downhole sampling techniques. The development of large concrete gravity base structures as production facilities did require an accurate evaluation of small scale shallow soil variability across a typical footprint of 100m diameter. This was primarily to ensure that radial steel skirts could be evenly penetrated and differential settlements avoided. This was usually achieved by means of a close grid of seabed Cone Penetration Tests (CPTs) to depths of around 10m to 30m below the seabed. At the same time downhole CPT tools were also developed. The use of seismic sub bottom profiling and seabed imaging with sonar techniques tended to play a minor role in this context being primarily used to identify and avoid major foundation constraints, such as near surface bedrock or deep buried channels infilled with highly variable and/or less consolidated sediments .

The picture started to change in the 1980s when Gulf of Mexico oil & gas exploration moved off the continental shelf and into deeper waters down the continental slope, i.e. moving from water depths of a few hundreds of metres to depths in excess of 1,000 metres. This was associated with field developments that were not just based around a single fixed production platform but comprising more dispersed facilities including floating production systems anchored to the seabed and linked to other subsea wellhead and development structures. It was also discovered (Campbell et al. 1986) that these deepwater environments were more topographically dramatic and populated with multiple forms of high risk geohazards (geological features or processes with potentially detrimental impacts on development facilities and/or human activity). Campbell (1984) was also laying the groundwork for the systematic approach to site evaluation. During this period the value of re-interpreted 3D exploration seismic data, as a preliminary site assessment tool, started to be appreciated and applied to deepwater geohazardous projects.

Deepwater exploitation expanded around the world in areas such as South America, particularly Brazil, and West Africa. In the 1990's the UK joined the deepwater club with exploration and development on the Atlantic margins West of Shetlands (Power, 1997). Figure 1 compares the typical site area that needs to be evaluated for a shallow water, platform-based oil field development with that of a deepwater Floating Production, Storage and Offloading (FPSO) system. The combination of large dispersed development areas and multiple geohazards also encouraged a more risk-based approach to site evaluation in deepwater (Clayton & Power, 2002).

It is this approach that has been adopted and dramatically enhanced by BP and described by JeanJean et al. (2005) and Evans (2011). The latter describes the work of their UK based Geohazard Assessment Teams (GATs), the process they have developed, and how they have been applied to multiple deepwater field developments offshore Angola and the West Nile Delta (WND). Some of the challenges encountered in these areas and how risks are dealt with are described below.

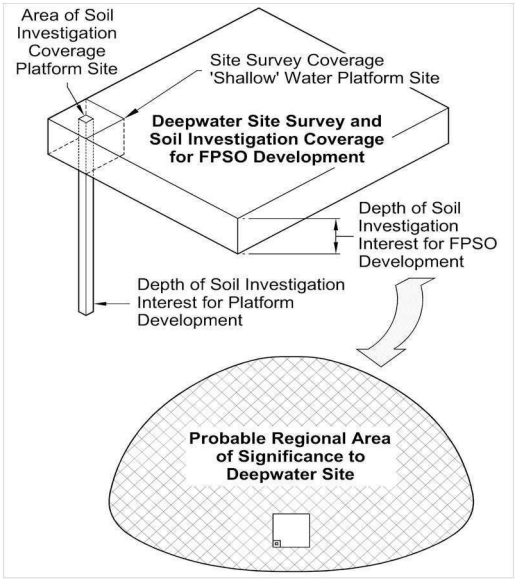

Figure 1. Comparative Survey Coverage Shallow vs Deepwater (Power 1997)

The sequence of steps described by Evans involves an initial desk study for the development area incorporating all available public domain data and any site-specific seismic data that may have been collected for exploration purposes. The desk study is then used as the basis for a geotechnical and geohazards risk assessment that takes into account potential development scenarios and infrastructure.

This approach is also used to start the process of creating a ground model and design preliminary geophysical surveys and geotechnical investigations. The data collected are then fed into the ground model and the wider risk management strategy including a more quantified assessment of probabilities and consequences of encountering the potential hazards indentified. More detailed programmes of data acquisition are defined and the tools required to quantify them are identified. In some cases the necessary tools have not existed and have therefore had to be invented. The quantification process also requires new laboratory testing techniques and analytical models to be developed. Examples of some inventions and developments are given below.

The aim is to evolve the conceptual ground model, developed at the desk study phase, to a geological model, by utilising subsequent geophysical survey data. It is then transformed into a geotechnical model

based upon detailed site investigation data and finally translated into an engineering ground model in which soil- structure interaction can be accurately quantified (see Figure 2).

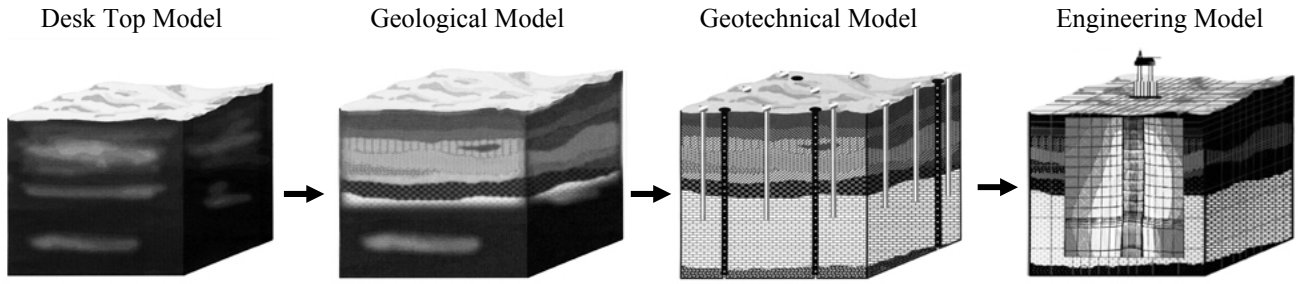

Figure 2. Evolution of the Advanced Ground Model from desk study to engineering design

2 OFFSHORE ANGOLA

Figure 3 illustrates the sort of natural hazards being encountered in deepwater offshore Angola and other parts of West Africa and why the described approach is needed to avoid, manage or mitigate the associated risks to offshore hydrocarbon developments.

Hill et al. (2011) describe in some detail the occurrence of such features. Pockmarks for example, which are conical seabed depressions formed by fluid expulsion which may be hundreds of metres in diameter and tens of metres in depth (Figure 4). The hazards they represent are multiple but can include the expulsion of corrosive fluids and slope instability. Sediment compression and movement due to the mechanism of salt diapirism (the uplift of deeper salt stratum due to their lower density) can result in anomalously hard layers and slope instability. The migration of deep hydrocarbons to the surface has, amongst other manifestations, resulted in atypical conditions such as carbonate-rich claystones or hard asphaltic mounds or lenses.

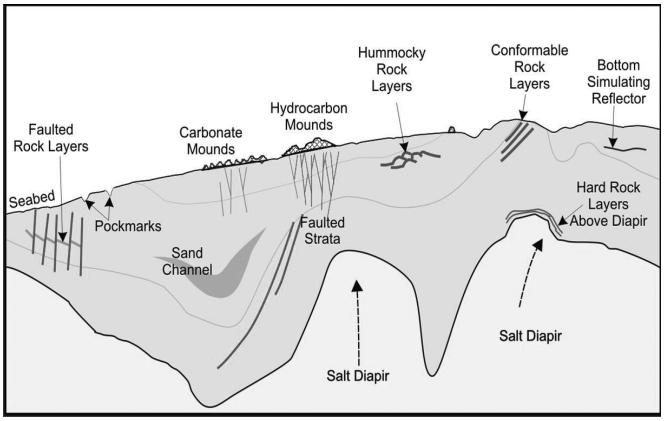

Figure 3. Surface & subsurface hazards offshore Angola

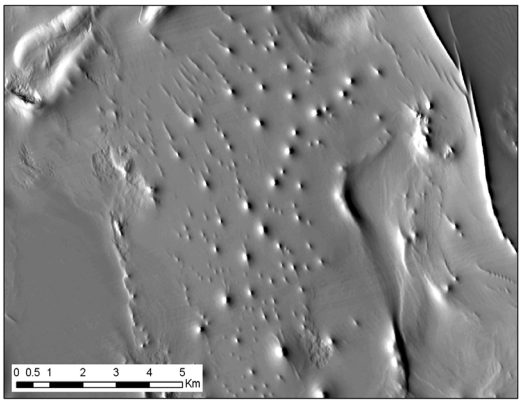

Figure 4. Typical pockmark field (Hill et al 2011)

Cauquil (2009) also describes the approach that Total are proposing for analysing and managing the risks posed by naturally occurring gas hydrates in deepwater offshore areas including West Africa. The methodology is based upon field data, interpretation and knowledge which can be adapted for other non-recurrent geological processes for which probabilistic analysis is not possible due to the absence of historical records at a specific location. The proposed Risk Management approach is illustrated in Figure 5 below.

All of these features can have a profound impact on field layout and engineering design resulting in significant financial costs. The fracture of pipelines or well casings can also have a devastating environmental consequence if they involve significant oil spillage.

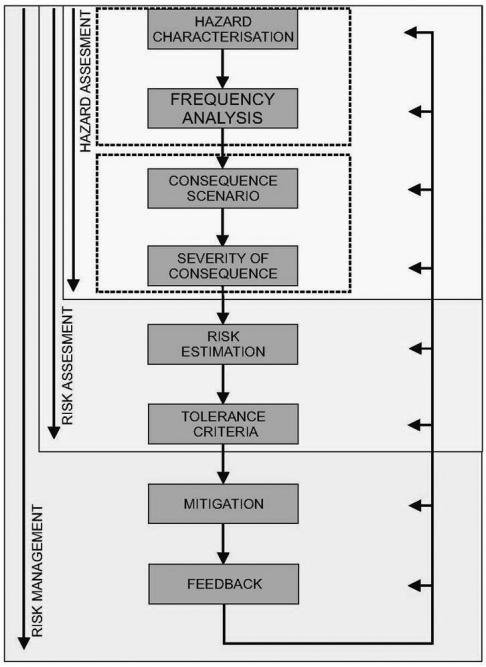

Figure 5. Risk Management Flow chart (Cauquil 2009)

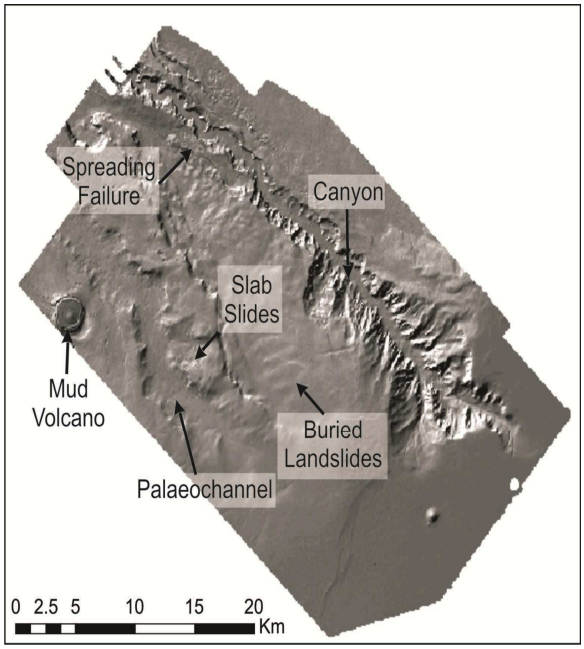

Figure 6. West Nile Delta seabed features (Moore et al..2007)

3 WEST NILE DELTA

The deep waters off Egypt's West Nile Delta also represent a new hydrocarbon province that incorporates significant natural hazards that require a co-ordinated and systematic geo-risk management approach.

Moore et al. (2007) and Evans et al. (2007) describe in detail, the approach that BP has taken to address the challenges posed by hazards such as:

- Seabed slope failures of all scales from a few hundred cubic metres in volume to many cubic kilometres.
- Mud volcanoes.
- Pockmarks and fluid expulsion features.
- Deep channels and scour features on the seabed.
- Variable soil conditions including biogenic hard grounds within soft clay strata.
- Deep seated faults and their surface expression.
- Seismic activity.

Figure 6 illustrates some of the seabed surface features, clearly defined by Autonomous Underwater Vehicle survey data.

4 COMPLEMENTARY DATA ACQUISITION, LABORATORY & ANALYTICAL TECHNIQUES

- *Geophysics /AUV/ downhole logging*

High and ultra high resolution reflection seismics are essential tools in modeling subsurface geological structure and imaging surface features to a sufficiently accurate level to define avoidance strategies or design mitigation measures. The most recent development has been in the use of Autonomous Underwater Vehicles (AUVs) to provide ultra high resolution surface imaging and near surface sub-bottom profiling (Bingham, et al. 2002). In addition downhole geophysical logging tools have also been refined to give a much higher density and resolution of data to further populate the ground model with more accurate information (Digby, 2002).

- *New Geotechnical tools and techniques*

New geotechnical tools developed to help improve the quantification of the physical characteristics of the ground include the downhole piezoprobe (Whittle et al. 2001) that can provide in-situ measurements of equilibrium pore pressures essential in assessing slope stability risks. Downhole sampling devices for recovering naturally occurring gas hydrates at their in-situ confining pressures in order to prevent disassociation during the recovery process are now being regularly used in the investigation of Hydrates not only

as a hazard but also as an alternative energy source (Amman et al. 1998). The uncertainties and risks to seabed pipelines in very deepwater represented by extremely soft soils has been addressed through the development of the Fugro SMARTPIPE® to investigate in-situ soil-pipe interaction (Evans 2011). Laboratory testing techniques are also being developed to provide design input parameters which more reliably represent soil behaviour not conventionally accounted for in geotechnical design (Rattley et al. 2010). In addition, increased attention has been paid to very small strain soil behaviour and measurements of dynamic soil response are also being made as part of advanced laboratory testing programmes. Such measurements allow better definition of soil stiffness and degradation parameters for input into soil structure interaction and seismic response studies such as those carried out as part of the West Nile Delta site response analysis. Only when these techniques are applied consistently enough can accurate design parameters be generated to feed into advanced 3D Finite Element analyses that allow us to model soil structure interaction with an increased confidence.

- *Geohazard (Forensic) Core Logging*

Crucial to the assessment of hazard, and ultimately risk, of processes such as mass movements is an understanding of the frequency and magnitude of events. Ultra high resolution geophysical data, such as Chirp, deployed from an AUV, provide a useful platform from which to interpret sub-surface features; however experience has shown that these data should not be used in isolation for geohazard assessment. Thomas et al. (2011) suggest that reliance solely upon geophysical data may often overestimate magnitudes of events such as landslides, debris flows and turbidity currents. In one example from the West Nile Delta, multiple stacked mass movement deposits appeared as one large seismic unit on AUV Chirp profiles; however the individual event deposits were below the limits of resolution on seismic records and could not be differentiated (Figure 7). The application of detailed sedimentological logging highlighted the individual deposits, thus increasing the interpreted frequency of events, but decreasing the magnitude and hence the perceived risk to the sub sea development. This example, coupled with many others in the authors' experience identifies the critical place of detailed sedimentological logging as part of a comprehensive geohazard assessment.

Thomas et al. (2011) suggest that multiple data acquisition techniques essential, promoting that as well as obtaining standard geotechnical samples there is a need for long core samples to be taken specifically for the purposes of detailed geohazard core logging. Where cores have been sub-sampled for geotechnical testing, often significant sections of the stratigraphic record are removed, thereby allowing for whole event deposits to be missed, adding uncertainty to derivations of event frequencies and magnitudes. Specialist geohazard core logging of long piston cores identifies key sedimentological features, thus facilitating the interpretation of depositional and post-depositional processes. The use of geochronological tests, including biostratigraphic and radiometric analyses, assist in providing a temporal framework from which to determine a frequency of events such as mass movements. It is essential to ensure interpretations from the geohazard core logging are used to target the testing on sediments with a known depositional process to ensure the success of the geochronological testing program.

As stated by Thomas et al. (2011), it is only through the integration of the complete event stratigraphy with the geophysical data and geomorphological interpretation can the magnitude, spatial extent and distribution of the mass movement deposits in the area be fully understood. Outputs from this integration can be used to inform and focus risk assessments and guide mitigation studies.

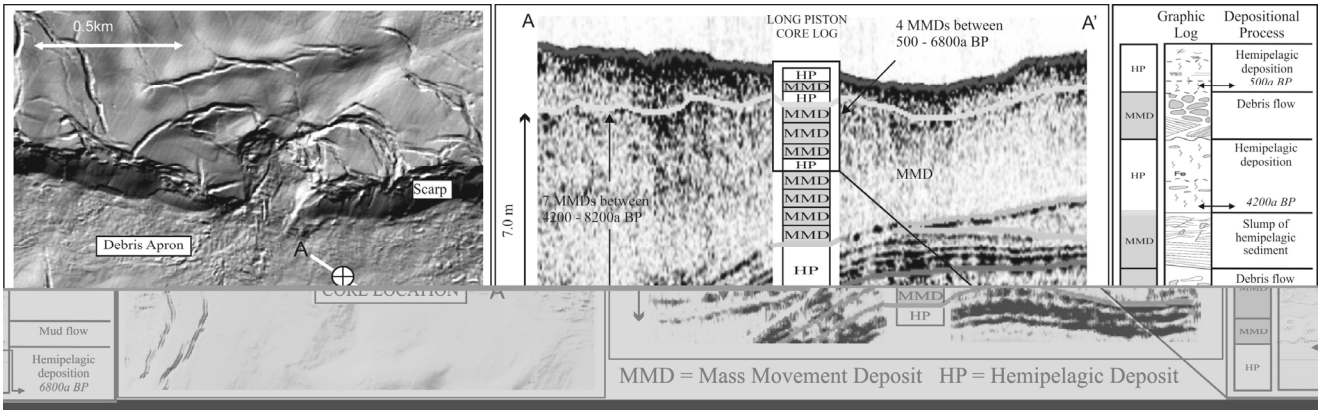

Figure 7. Example of multiple mass movement deposits identified from detailed sedimentological logging where only one MTD (mass movement deposit) was previously interpreted from AUV Chirp data (Thomas et al. 2011)

- *GIS*

GIS is now routinely used as a platform on which to manage, view and interrogate spatially-referenced data acquired during the development of offshore sites. Within a GIS, spatial analysis techniques can be used to apply deterministic methods for identifying and mapping areas susceptible to shallow submarine mass movements. This allows spatially widespread, rapid, repeatable and cost-effective evaluation of shallow submarine slope risk. A deterministic approach of this nature has the advantage of providing a quantitative output, useful in subsequent project risk assessment. The emphasis is placed on GIS modelling of the full three-dimensional variation of geotechnical input parameters, which allows a sophisticated ground model, including output from regional engineering geological and geohazard studies, to be harnessed and exploited. This approach has been applied on deepwater oil and gas projects having development areas of over 1,000 square kilometres (Mackenzie et al. 2010).

5 APPLICATION OF THE ADVANCED GROUND MODEL APPROACH TO UK ROUND 3 WINDFARM SITES

The application of a ground model has been successfully demonstrated by various authors including Evans (2011) and Hill et al. (2011) to assist in the characterisation of soil conditions across large-scale deepwater developments. Key to its effective development is the integration of multiple disciplines as outlined by Campbell et al. (1982). The model developed in this manner evolves from a solely predictive base to an engineering tool based upon calibration with site-specific data (Campbell, 1984). A ground model provides an ideal mechanism to assess sites that feature multiple locations, cover a large area, have more potential for variability, require unconventional engineering considerations, or have a short lead in time requiring highly efficient integration and interpretation of multiple datasets. UK Round 3 windfarm sites provide a good example of all of these considerations, often featuring up to 140 structures, within large offshore sites, that are affected by dynamic and transient lateral and vertical loads that may require innovative foundation solutions. Water depths range between approximately 10m and 50m.

Certain aspects of the Round 3 windfarm sites differ significantly from the deepwater domain. Deepwater Angola is dominated by hemipelagic deposition, while the West Nile Delta development has been shaped to a large extent by large scale landslide events and turbidity current inflows. In contrast, the UK continental shelf has largely been modified by the effects of a series of glaciations over the last few hundred thousand years having featured diverse environments including fluvial, glacial, glaciomarine and subaerial exposure conditions. The combination of different processes that have been operational at a single site over the Quaternary timescale may result in a greater variability compared to even the largest deepwater development.

While direct process analogues may not be immediately transferable to shallower, glacially influenced UK sites from deepwater geohazard-focused developments, the same ground model approach provides a mechanism to identify and understand the depositional and post-depositional processes and their resultant geotechnical character. Fookes (1997) provides several onshore examples, demonstrating the application of a ground model to a variety of settings including glacial, periglacial and fluvial.

A thorough synthesis of geomorphological, geological, geophysical and geotechnical observations within a 3D conceptual block diagram provides a powerful communication tool to explain and portray the diversity of expected or proven ground conditions.

Crucially, the understanding of ground conditions and their spatial variation allows for an optimisation of foundation design as the project moves from concept appraisal, through design, and into the installation phase. The ground model illustrates the spatial variation and serves to highlight any areas of potential risk to foundations, such as is shown in Figure 8.

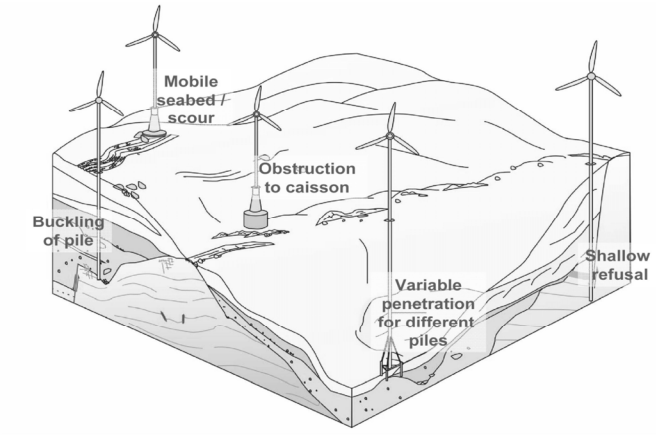

Figure 8. Identification of foundation constraints for offshore wind turbines through use of a conceptual ground model.

6 SUMMARY/ CONCLUSIONS

The reduction of shallow geological and geotechnical risks for offshore developments has advanced significantly over the last 10 years through the application of a systematic and holistic approach. Originally developed for deepwater sites, prone to multiple geohazards, it has now evolved and is being applied to shallow water wind farm sites covering large areas and encompassing significant geological variability.

To be most effective, the approach needs to incorporate the following elements and sequence:

- Initial desk study, based upon all available existing data and incorporating a conceptual geological model, a preliminary risk assessment and recommendations for further data acquisition.
- Geophysical and geotechnical surveys and investigations incorporating specialist tools to ensure that appropriate data of the highest quality and resolution is acquired.
- The application of advanced geological and geotechnical logging and laboratory testing techniques to maximise the value derived from the samples and cores recovered.
- The use of these data and GIS technology to progress the ground model from a geological model to a geotechnical model and finally to an advanced engineering ground model that facilitates quantified risk assessment and the mitigation or management of risk through the optimised design, siting and installation of wells and seabed structures.

7 ACKNOWLEDGEMENTS

The authors would like to thank BP and Total for their support and encouragement and for giving permission to reproduce some of the illustrations used in this paper.

REFERENCES

Amman, H., Baraza, J., Marx, C., Perissoratis, C., Roberts, J., Skinner, A., Valdy, P. and Zuidberg, H. (1998) HYACE, the Gas Hydrate Autoclave Coring Equipment System, in EU-MAST: Project Outlines of all Projects. Published at the occasion of the third European Conference on Marine Research and Technology, Lisbon.

Bingham, D., Drake, T., Hill, A., Lott, R. (2002). The Application of Autonomous Underwater Vehicle (AUV) Technology in the Oil Industry – Vision and Experience, TS4.4 Hydrographic Surveying II, Fig XXII, International Congress, Washington DC, USA.

Campbell, K.J. (1984) Predicting offshore soil conditions. Proceedings of the Annual Offshore Technology Conference, Houston, Texas, OTC Paper Number 4692.

Campbell, K.J., Hooper, J.R. and Prior, D.B. (1986) Engineering Implications of Deepwater Geologic and Soil Conditions, Texas – Louisiana Slope. Offshore Technology Conference Proceedings, Houston, 5-8 May.

Campbell, K.J Dobson, B.M., Ehlers, C.J. (1982) Geotechnical and Engineering Geological Investigations of Deepwater Sits. Proceedings of the Annual Offshore Technology Conference, Houston, Texas. OTC Paper Number 4169.

Clayton, C.R.I. and Power, P.T. (2002) Managing geotechnical risk in deepwater. Proceedings of the International Conference for Offshore Site Investigations, Society for Underwater Technology, 425-439.

Cauquil, E. (2009) Risk Matrix for Non-Recurrent Geological Processes: Application to the Gas Hydrate Hazard. Proceedings of the Annual Offshore Technology Conference, Houston, Texas. OTC Paper Number 20014.

Digby, A (2002) The use of downhole geotechnical logging in the investigation of deep water geohazards. Proceedings of the Offshore Site Investigation and Geotechnics Conference, SUT, London, 26-28 November.

Evans, T.G., Usher, N., Moore, R. (2007) Management of Geotechnical and Geohazard Risks in the West Nile Delta. Proceedings of 6th International Conference, Offshore Site Investigation and Geotechnics, SUT, London.

Evans, T.G. (2011) A systematic approach to offshore engineering for multiple-project developments in geohazardous areas. Proceedings of the Second International Symposium on Frontiers in Offshore Geotechnics, Perth, Australia, November 2010.

Fookes, P.G. (1997) Geology for Engineers: the Geological Model, Prediction and Performance. The Quarterly Journal of Engineering Geology, Vol 30, Part 4, The First Glossop Lecture, 293-424. November 1997.

Hill, A.J., Fiske, M., Fish, P.R., Thomas, S. (2011) Deepwater Angola: Geohazard Mitigation. Proceedings of 2nd International Symposium on Frontiers in Offshore Geotechnics, Perth, Australia, November, 2010.

Jeanjean, P., Liedtke, E., Clukey, E.C., Hampson, K., Evans, T. (2005) An Operator's perspective on offshore risk assessment and geotechnical design in geohazards-prone areas'. First International Symposium on Frontiers in Offshore Geotechnics: ISFOG – Gourvenec & Cassidy (eds).

Mackenzie, B., Hooper, J.R., Rushton, D.R. (2010) Spatial analysis of Shallow Slope Instability Incorporating an Engineering Geological Model, Submarine Mass Movements and Their Consequences, Advances in Natural and Technological Hazards Research, Vol 28, Springer 2010, pp365-376.

Moore, R., Usher, N., Evans, T. (2007). Integrated Multidisciplinary Seismic Geomorphology Assessment of West Nile Delta Geohazards, Proceedings of 6th International Conference, Offshore Site Investigation and Geotechnics, SUT, London.

Power, P.T., Owen, R.J., Stephens, R.V. (1997) Integrated Site and Route Assessments in Deepwater. Proceedings of the International Conference on Deepwater Technologies (DWT), I.B.C., London.
Rattley, M.J., Hill, A.J., Thomas, S., Sampurno, B. (2010). Strain rate dependent simple shear behaviour of deepwater sediments in offshore Angola. Proceedings of the Second International Symposium on Frontiers in Offshore Geotechnics, Perth, Australia, November, 2010. pp377-382.
Thomas, S., Hooper, J and Clare, M. (2010). Constraining Geohazards to the Past – Impact Assessment of Submarine Mass Movements on Seabed Developments. Advances in Natural and Technological Hazards Research, Volume 28.
Thomas, S., Bell, L., Ticehurst, K., Dimmock, P.S. (2011) An investigation of past mass movement events in the West Nile Delta. Proceedings of the Second International Symposium on Frontiers in Offshore Geotechnics, Perth, Australia, November 2010.
Whittle, A.J., Sutabudr, T., Germaine, J.T., Varney, A. (2001) Prediction and Measurement of Pore Pressure Dissipation for a Tapered Piezoprobe. Offshore Technology Conference Proceedings, Houston, 30 April-3 May.

ISGSR 2011 - Vogt, Schuppener, Straub & Bräu (eds) - © 2011 Bundesanstalt für Wasserbau ISBN 978-3-939230-01-4

Probabilistic Analysis of Bearing Capacity of Strip Footings

M. A. Shahin & E. M. Cheung
Department of Civil Engineering, Curtin University, Perth, Australia

ABSTRACT: Predicting bearing capacity of shallow foundations is a common practice in geotechnical engineering and an accurate estimation of its value is essential for a safe and reliable design. Traditional deterministic methods of estimating bearing capacity of shallow foundations do not explicitly consider the uncertainty associated with the factors affecting bearing capacity and rather employ a factor of safety that implicitly accounts for such uncertainty. This factor of safety is in reality "factor of ignorance" as it relies only on past experience and does not reflect the inherent uncertainty in relation to bearing capacity parameters, leading to unreliable bearing capacity predictions. In this paper, a more rational approach for estimating bearing capacity of strip footings subjected to vertical loads is proposed. The approach is based on probabilistic analyses using the Monte Carlo simulation and accounts for the uncertainty associated with two shear strength parameters, i.e. soil cohesion and soil friction angle. The probabilistic solutions negate the need for assuming a factor of safety and provide a more reliable indication of what the actual bearing capacity might be.

Keywords: Probabilistic analysis, Bearing Capacity, Strip footings, Shallow foundations.

1 INTRODUCTION

Bearing capacity and settlement are the two main components of design of shallow foundations; however, bearing capacity usually governs the design process. If bearing capacity is over-estimated, soil will fail, leading to serious consequences and fatalities. If, on the other hand, bearing capacity is under-estimated, undue costs are usually incurred. Consequently, an accurate prediction of bearing capacity is important for a safe and reliable design of shallow foundations. Traditional design methods of bearing capacity of shallow foundations are deterministic in the sense that they do not explicitly account for the inherent uncertainty associated with the factors affecting bearing capacity. Uncertainty associated with bearing capacity can be classified into the following three categories: (*i*) natural spatial variability; (*ii*) model uncertainty; and (*iii*) parameter uncertainty. Natural spatial variability is due the variation of soil properties from one point to another in space, which is caused by the variations in the mineral composition and characteristics of soil strata during soil formation. Model uncertainty is due to the inability of a selected mathematical model to mimic a real phenomenon (Frey 1998). Parameter uncertainty is due to inaccuracy in assessing the soil properties because of the limited number of soil sampling and testing data. It is also due to the inadequacy of interpreting the subsurface geology due to the measurements errors, data handling and transcription errors, inconsistency of data and inadequate representation of data sampling due to time and space limitations (Baecher and Christian 2003). Parameter uncertainty can also be due to the discrepancies between the in-situ implementation of structure and what appears in construction drawings.

In traditional deterministic methods, uncertainties associated with predicting bearing capacity of shallow foundations are implicitly dealt with by employing a fixed global safety factor that may lead to inappropriate bearing capacity predictions. In this paper, an alternative probabilistic approach that provides a more rational estimation of the bearing capacity of strip footings subjected to vertical loads is presented. The approach uses the Monte Carlo simulation to account for parameter uncertainty associated with the soil properties. Other types of uncertainties (i.e. natural soil variability and model uncertainty) are beyond

the scope of this paper and are not considered. The current probabilistic approach provides the likely distribution of predicted bearing capacity, which enables the designer to make informed decisions regarding the level of risk associated with the design. To facilitate the use of the probabilistic approach, a computer algorithm using Excel software is developed and can be readily used by practicing engineers.

2 DETERMINISTIC BEARING CAPACITY OF STRIP FOOTINGS

In order to obtain probabilistic solutions for bearing capacity of shallow foundations, a deterministic model shall first be selected. In this work, the commonly used model proposed by Terzaghi (1943) is selected in which the deterministic ultimate bearing capacity of strip footings can be obtained as follows:

$$q_u = cN_c + qN_q + 0.5\gamma BN_\gamma \quad (1)$$

where q_u is the ultimate bearing capacity, c is the soil cohesion, γ is the soil unit weight, B is the footing breadth, q is the overburden pressure (i.e. the soil unit weight × depth of foundation, D) and N_c, N_q and N_γ are the bearing capacity factors. The bearing capacity factors rely solely on the soil friction angle, ϕ, and are estimated as follows (Terzaghi 1943):

$$N_q = \frac{[e^{(0.75\pi - \phi/2)\tan\phi}]^2}{2\cos^2(45^\circ + \phi/2)} \quad (2)$$

$$N_c = (N_q - 1)\cot\phi \quad (3)$$

$$N_\gamma = \frac{1}{2}\left(\frac{k_{p\gamma}}{\cos^2\phi} - 1\right)\tan\phi \quad (4)$$

where $\pi = 3.14$ and $k_{p\gamma}$ is the passive earth pressure coefficient that relies on ϕ. From values of $k_{p\gamma}$ corresponding to ϕ given by Terzaghi (1943), the following matching empirical equations for $k_{p\gamma}$ can be proposed:

$$k_{p\gamma} = 10.49e^{0.0363\phi} \quad (R^2 = 0.98, \text{ for } \phi = 0.0\text{–}15^o) \quad (5)$$

$$k_{p\gamma} = 5.82e^{0.074\phi} \quad (R^2 = 0.99, \text{ for } \phi = 15^o\text{–}35^o) \quad (6)$$

$$k_{p\gamma} = 0.364e^{0.1516\phi} \quad (R^2 = 0.98, \text{ for } \phi = 35^o\text{–}50^o) \quad (7)$$

3 PROBABILISTIC BEARING CAPACITY OF STRIP FOOTINGS

In the present work, the probabilistic analysis for bearing capacity of strip footings is conducted by utilizing the Monte Carlo simulation and considering parameter uncertainty associated with the input variables in Equation (1). Detailed description of the Monte Carlo simulation can be found in many publications (e.g. Hammersley and Handscomb 1964; Rubinstein 1981). Among the five input variables of Equation (1), the soil cohesion, c, and soil friction angle, ϕ, are likely to include significant parameter uncertainty and thus are assumed to be random variables. The soil unit weight, γ, is assumed to be constant in the present work as it contributes to parameter uncertainty of a lesser degree, as demonstrated by Lee et al. (1983). In addition, the footing breadth, B, and depth of foundation, D, are likely to provide marginal parameter uncertainty and are thus assumed to be deterministic for practical purposes. It should be noted that model uncertainty is not considered in the present work and thus Equation (1) is assumed to be a perfect predictor (i.e. has no model uncertainty). For an individual case of bearing capacity prediction, the

procedure used to obtain probabilistic solutions that account for the parameter uncertainty of c and ϕ is as follows:

1. For each of the bearing capacity input variables (i.e. c, ϕ, γ, B and D), a random value is generated in relation to parameter uncertainty of the input mean value, coefficient of variation (COV), known or assumed probability distribution function (PDF) and any correlation exists between that input variable and the other available input variables;
2. Using the generated input values from Step (1) and assuming that Equation (1) is a perfect predictor, a deterministic value of bearing capacity is obtained;
3. Steps 1 and 2 are repeated hundreds or thousands of times, as part of the Monte Carlo simulation, until certain acceptable convergence is met; and
4. Finally, all the bearing capacities obtained are collated and used to determine the cumulative distribution function (CDF) or to plot the cumulative probability distribution curve from which predictions associated with target reliability levels of 90% and 95% (the reliability levels that are usually needed for design) can be estimated.

In order to illustrate the probabilistic procedure set out above, the following case study is investigated. A strip footing of breadth B = 2.0 m is founded at a depth D = 1.5 m below the ground surface, and the soil is clayey sand with unit weight γ = 18 kN/m^3. The statistical values for c and ϕ are selected as follows: μ_c (mean of cohesion) = 5 kPa, μ_ϕ (mean of friction angle) = 30^o, COV$_c$ (coefficient of variation of soil cohesion) = 27%, COV$_\phi$ (coefficient of variation of soil friction angle) = 10% and $\rho_{c,\phi}$ (correlation coefficient between c and ϕ) = –0.6. The probability distribution functions for both c and ϕ are assumed to follow a lognormal distribution, as has been used in several geotechnical engineering applications. It should be noted that the above statistical values are within the practical ranges that are cited in the literature. For example, the mean of ϕ is typically between 20^o and 40^o (Abdel Massih et al. 2008), with COV ranging from 5% to 15% for sands and 12% to 56% for clays (Lee et al. 1983; Phoon and Kulhawy 1999). The COV for c varies between 10% to 70% (Cherubini 2000) with a recommended value of 30% (Lee et al. 1983). The COV between c and ϕ ranges between –0.24 and –0.7 (Lumb 1970; Wolff 1985; Yuceman et al. 1973) with a recommended value of –0.6 can be used in practice (Cherubini 2000).

The abovementioned statistical data are used to generate sample values of c and ϕ (Step 1) and the corresponding deterministic bearing capacity is calculated using Equation (1) of Terzaghi's model (Step 2). As mentioned previously, Terzaghi's model is assumed to be a perfect predictor with no model uncertainty and uncertainty associated with the natural variability of soil is not considered. Consequently, parameter uncertainty associated with the shear strength properties c and ϕ is the only source of uncertainty considered in this work. Steps 1 and 2 are repeated many times until a convergence criterion is achieved (Step 3). To determine whether convergence has been achieved, the statistics describing the distribution of the predicted bearing capacities are calculated at fixed numbers of simulations and compared with the same statistics at previous simulations. Convergence is deemed to have occurred if the change in the statistics describing the distribution of predicted bearing capacity is 1.5% or less. The predicted bearing capacities obtained from the many simulations conducted are used to plot the cumulative probability distribution curve from which bearing capacity predictions that assure target reliability levels are obtained (Step 4). It should be noted that the probabilistic simulation described in Steps 1 to 4 are conducted with the aid of the PC-based software @Risk (Palisade 2000) and the results are shown in Figure 1, which also includes the predicted deterministic value of bearing capacity. For the case study above, the predicted deterministic bearing capacity is obtained using Equation (1) and is found to be equal to 1067kPa. For target reliability levels of 90% and 95%, the corresponding bearing capacities are estimated from the cumulative probability function (or from Figure 1) to be equal to 730 kPa and 658 kPa, respectively. These values give equivalent factors of safety of 1067/730 = 1.5 and 1067/658 = 1.6, respectively. These results indicate that, for the case study above, the factor of safety of 3 that is usually used in the deterministic analysis is conservative. The results also demonstrate that the uncertainty associated with c and ϕ can considerably affect the bearing capacity of strip footings and thus should not be neglected.

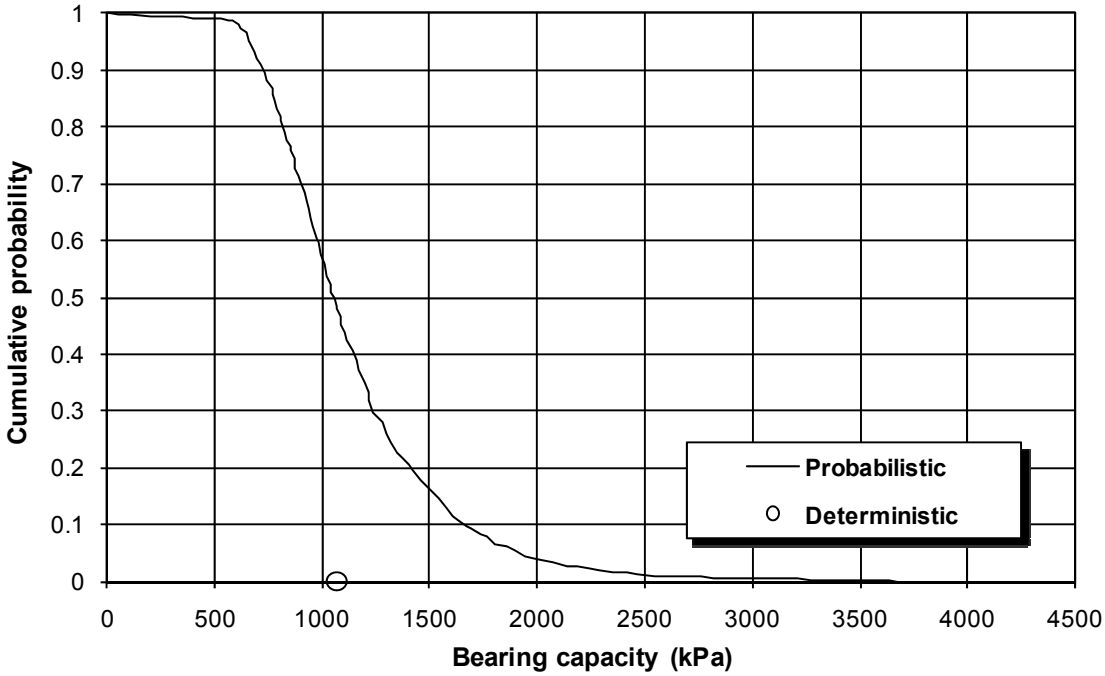

Figure 1. Cumulative probability distribution incorporating parameter uncertainty of c and ϕ for the case study considered

4 DEVELOPMENT OF PROBABILISTIC BEARING CAPACITY GENERIC SOLUTIONS

The probabilistic simulation applied to the case study described in Section 3 is used to develop a generic set of probabilistic solutions for routine use in practice, from which predicted bearing capacity corresponding to 90% and 95% reliability levels can be readily obtained. The solutions are based on the practical recommended parameter uncertainty of COV_c = 30% and COV_ϕ = 20%, and a coefficient of correlation between c and ϕ of –0.6 with lognormal distribution for both c and ϕ. The procedure that is used to develop the solutions is as follows:

1. A combination of input values for c, ϕ, γ, B and D are selected so as to be within the ranges that can be expected in practical applications, as given in Table 1;
2. The probabilistic approach, outlined previously, which incorporates parameter uncertainty for c and ϕ is applied and the corresponding CDF is obtained;
3. From the CFD, bearing capacities corresponding to 90% and 95% reliability levels are determined; and
4. Another combination of values of c, ϕ, γ, B and D are selected from Table 1 and Steps 2 to 3 are repeated until all possible combinations of values of c, ϕ, γ, B and D given in Table 1 are chosen and their probabilistic simulations are conducted. The results are used to develop probabilistic design solutions corresponding to 90% and 95% reliability levels.

Table 1 Values of the input variables used for development of the probabilistic design solutions

Input variable	Values	Number of values
Cohesion, c (kPa)	0, 20, 40, 60, 80, 100	6
Friction angle, ϕ (degrees)	0, 10, 20, 30, 40	5
Soil unit weight, γ (kN/m^3)	16, 18, 20	3
Footing breadth, B (m)	0.5, 1, 2, 3	4
Depth of foundation, D (m)	0, 1.5, 3	3

To facilitate the use of the obtained probabilistic solutions by practicing engineers, a computer code using Excel software is developed and can be readily used. Figure 2 shows the main menu of the developed Excel software with an illustrative example that will be explained below. By considering the number of values given in Table 1 for c, ϕ, γ, B and D, it can be derived that the number of probabilistic simulations conducted in order to develop the probabilistic design solutions are: $6 \times 5 \times 3 \times 4 \times 3 = 1080$. In order to illustrate the use of the design solutions using the developed Excel computer codes, the following numerical example is examined. A copy of Excel software program is available by the authors upon request.

PROBABILISTIC BEARING CAPACITY CALCULATOR COV_c = 30%, COV_ϕ = 20%		
INPUTS (CTRL+Q to Reset)		
Soil Properties		
Cohesion, c (kPa)	**20**	
Soil friction angle, ϕ (degrees)	**35**	
Unit Weight of Soil, γ (kN/m^3)	**20**	
Footing Properties		
Width of Footing, B (m)	**1.5**	
Depth of Foundation, D (m)	**3**	
Factor of Safety for Deterministic Design	**3**	
OUTPUTS		
Probabilistic Bearing Capacity, q_u (kPa)		
95% Confidence (kPa)	**1515**	
90% Confidence (kPa)	**1787**	
Deterministic Bearing Capacity, q_u (kPa)		
Ultimate Bearing Capacity (kPa)	**4211**	
Allowable Bearing Capacity (kPa)	**1404**	
Equivalent Safety Factor		
95% Confidence	**2.8**	
90% Confidence	**2.4**	

Figure 2. Main menu of Excel software: Example

Example: A strip footing of breadth B = 1.5 m is to be constructed at a depth D = 3 m below the ground surface in a soil that has the following properties: c = 20 kPa, $\phi = 35^o$ and γ = 20 kN/m^3. It is required to find the bearing capacity corresponding to reliability level of 90%, and also estimate the equivalent FOS.

Solution: For a reliability level of 90%, the Excel spreadsheet program shown in Figure 2 is used to obtain the bearing capacity corresponding to γ = 20 kN/m^3, leading to a bearing capacity of 1787 kPa. The deterministic bearing capacity is obtained to be equal to 4211 kPa, and for this case, the equivalent FOS = 4211/1787 = 2.4.

5 SUMMARY AND CONCLUSIONS

Probabilistic approach that utilizes the Monte Carlo technique was used to obtain probabilistic bearing capacity of strip footings from the commonly used deterministic Terzaghi's model. The proposed probabilistic approach accounts for parameter uncertainty of soil cohesion and friction angle, and enables bearing capacity to be quantified in the form of a cumulative probability distribution function that provides bearing capacity predictions corresponding to certain reliability levels. The approach was applied to a case study for illustration. A series of probabilistic solutions that incorporate parameter uncertainty of coefficient of variation of 30% and 20% for soil cohesion and friction angle, respectively, were carried out and computer code using Excel was developed to facilitate the use of the proposed approach for routine use by practitioners. A numerical example was given to illustrate the use of charts. The results indicate that the suggested factor of safety of 3 that usually used by available deterministic models is conservative. This indicates the importance of adopting probabilistic analyses in favor of the factor of safety. It was also shown that the developed probabilistic method can be used to predict bearing capacity of strip footings for reliability levels of 90% and 95%. The charts are believed to be a useful tool that can be readily used by practitioners for design of strip footings.

REFERENCES

Abdel Massih, D. Y., Soubra, A., and Low, B. K. (2008). "Reliability-based analysis and design of strip footings against bearing capacity failure." *Journal of Geotechnical and Geoenvironmental Engineering*, 134(7), 917-928.

Baecher, G. B., and Christian, J. T. (2003). *Reliability and statistics in geotechnical engineering*, John Wiley & Sons, West Sussex, England.

Cherubini, C. (2000). "Reliability evaluation of shallow foundation bearing capacity on *c*', ϕ' soils." *Canadian Geotechnical Journal*, 37(1), 264-269.

Frey, C. (1998). "Quantitative analysis of variability and uncertainty in energy and environmental systems." Uncertainty modelling and analysis in civil engineering, B. M. Ayyub, ed., CRC Press, Boca Raton, 381-423.

Hammersley, J. M., and Handscomb, D. C. (1964). *Monte Carlo methods*, Wiley Press, New York.

Lee, I. K., White, W., and Ingles, O. G. (1983). *Geotechnical Engineering*, Pitman Publishing Inc., Boston.

Lumb, P. (1970). "Safety factors and the probability distribution of soil strength." *Canadian Geotechnical Journal*, 7(3), 225-242.

Palisade. (2000). *@Risk: Risk analysis and simulation version 4.0*, Palisade Corp., New York.

Phoon, K. K., and Kulhawy, F. H. (1999). "Characterisation of geotechnical variability." *Canadian Geotechnical Journal*, 36(4), 612-624.

Rubinstein, R. Y. (1981). *Simulation and the Monte Carlo method*, Wiley Press, New York.

Terzaghi, K. (1943). *Theoretical soil mechanics*, John Wiley & Sons, New York.

Wolff, T. H. (1985). "Analysis and design of embankment dam slopes: A probabilistic approach," PhD Thesis, Purdue University, Lafayette, Indiana.

Yuceman, M. S., Tang, M. S., and Ang, A. H. (1973). "A probabilistic study of safety and design of earth slopes." *Civil Engineering Studies, Structural research Series 402*, University of Illinois, Urbana.

ISGSR 2011 - Vogt, Schuppener, Straub & Bräu (eds) - © 2011 Bundesanstalt für Wasserbau ISBN 978-3-939230-01-4

Assessment of reliability and inherent risk levels of geogrid reinforced soil structures

F. Bussert
Tensar International Ltd., Blackburn, United Kingdom

ABSTRACT: Geogrid reinforced soil structures are planned and constructed in increasing amounts due to their various benefits. Little amounts of failures or deformations beyond serviceability limit state are reported. Multiple factors can influence the behavior of reinforced walls and elements that cause risk and reduce reliability have to be assessed. All aspects contributing to reinforced walls as roles and responsibilities, site investigation, applicability of the structure, design methods, materials as well as construction are evaluated and their reliability and risk levels regarding structural behavior investigated. Identification of roles and responsibilities will be assessed as part of the risk assessment under the light of outsourcing and subcontracting. Apart from these influences the construction process will be looked at and conclusions drawn.

Keywords: construction, design, reinforced soil, site investigation

1 INTRODUCTION

The use of geogrid reinforced structures for temporary and permanent slope and wall stabilization is an economical and ecological alternative to traditional structural solutions as gravity or cantilever walls. Especially the economic advantages, multiple structural options and the reliable nature of the constructed walls lead to a significant increase in the use of geogrid reinforced structures over the last decades. Technically the benefits of high load carrying capacity, applicability over soft and variable ground conditions and insensitivity to differential settlement combined with small deformation characteristics increased the reputation of these structures.

These advantages raised the confidence in geogrid reinforced structures and in turn lead to a considerable increase in constructed wall heights for all structural types in recent years. Construction of slopes in excess of 20m height or walls with heights up to 60m have been completed successfully in recent years and pushed the applicability to new levels (figure 1).

Figure 1. **Tensar***tech* GreenSlope at Greater Bargoed (2010), **Tensar***tech* TW1 Wall at Dubai-Fujairah Freeway (2010)

1.1 *Design requirements*

In most European countries the calculation methods are separated into two parts: the ultimate limit state (ULS) or complete structural failure and the serviceability limit state (SLS) where excessive deformations prevent the structure from being used for the intended purpose or where due to excessive deformation collapse is suspected. The proof of limit states of reinforced soil structures is based on the principles set out by the British Standard BS8006-1 (2010).

Deformations can be the result of deformations within subsoil, retained or reinforced fill. Calculation of the reinforced soil deformation is usually approximated by deriving theoretical geogrid strains from the calculated tension force. Dependent on the expected design life, the geogrid strains are derived from the isochrones curves. It has been shown numerous times that the anticipated strains by this method overestimate the measured deformations by far.

1.2 *Occasional observed structural behavior*

Numerous publications in the past indicate that geogrid reinforced soil structures fulfill all requirements set. Recently achieved heights (exceeding 60m) indicate that reinforced soil is regarded as a value solution providing multiple advantages when compared with traditional structures. However, publications (e.g. Bachus, 2010) describe several structures that showed partial collapse or excessive deformations. The structures had to be reconstructed resulting in negative reputation and doubts on the reliability of reinforced soil structures. The reliability and the risk towards failure of reinforced soil structures will be assessed for individual parameters that could contribute to failures:

- Design responsibilities
- Design methods
- Soil investigation
- Construction materials (geogrids, soils)
- Construction

In the following paragraphs every aspect will be analyzed individually and the reliability towards failure rated. Afterwards conclusions are drawn and an approach presented how risk can be minimized further.

2 DESIGN RESPONSIBILITIES

Within a project multiple parties are involved carrying out different parts of the design resulting in different responsibilities to individuals which may sometimes not be straightforward to identify. By submitting feasibility studies, initial designs or full design submissions for a structure different party in a project can assume that certain issues are dealt with by others. The knowledge on how responsibilities is therefore sometimes not fully understood and there is little knowledge on how this can contribute to failures taking place. A large set of exclusions stated by a party involved may appear as if responsibilities are distributed to other parties involved, their validity however is often not fully understood and may be beyond a specific scope.

Within the introduced “Construction (Design & Management) Regulations 2007” the responsibilities of individuals in each project is clearly identified and requirements on actions and activities drawn. The regulations were written with the intention to focus on effective planning and consecutively manage risk and ensure everyone knows its responsibilities which improves health and safety within the construction industry. As for reinforced structures several people/ companies are involved within the design and construction each individual has several tasks which need to be fulfilled in order to comply with the regulation.

2.1 *Designer*

The Designer takes over a crucial part in this process as several demands are placed on him. He has to be competent for the work or has to be guided by a competent person and need to work with other engineers involved in the project in order to manage risk. He has the duty to verify the competence for other designners involved to ensure consistency. As the CDM coordinator collects all relevant information he has to ensure that the CDM coordinator is aware of potential risks. Where soil parameters might be crucial he has to liaise with the geotechnical engineer in order to verify that the made assumptions are relevant or has to verify the soil properties in case any doubts or inconsistencies occur.

When the input parameters are sufficiently determined the designer is required to work according to the latest standards considering all relevant information. If he comes across any uncertainties it is a "duty to warn" to make the CDM coordinator/ contractor or other designers involved aware and ensures that the risk is eliminated wherever possible.

2.2 *Client*

The client himself (e.g. a public body) under whose instructions a reinforced structure is build has to make sure that all people and companies involved in the job have sufficient competence and resources to allow the design or construction of the reinforced structure. As the client may not have sufficient information to take over this work by himself he can appoint a CDM coordinator who takes over his responsibilities. He further has to ensure that a suitable management system is in place as well as sufficient time and resources for all stages. This often becomes crucial for reinforced structures. As they are often regarded as an economical alternative to traditional methods they are brought into the design process quite late which leaves only little time to prepare designs or calculations. Reasonable design time should be ensured at all times in order to prevent failures happening.

2.3 *Contractor*

Last but not lease the duties of the contractor are multisided as on one hand he has to collect the required information and provide a stable and durable structure minimizing the risk of his employees. In order to safeguard a reliable construction the principal contractor has to check the competence of all appointees and verify that all workers had training and sufficient site induction. He has to liaise with the CDM coordinator for all ongoing designs which is usually the case for reinforced soil structures.

Finally the contractor has to check that the client is aware of his duties and that a CDM coordinator has been appointed and the HSE has been notified before the work. This is an elementary point as most reinforced soil structures are done before the "real" construction work starts and may be regarded as initial work procedures which are only shortly looked at. It is his duty to inform the principal contractor when any problems or issues arise with designs or the constructability of the whole structure or parts of them.

As the regulations are quite clear in their responsibilities and they encourage all parties to communicate on possible issues and the responsibilities taken over. This should therefore not be an issue for significant risk.

3 DESIGN METHOD

In line with current practice, the design methods for reinforced soil structures are based on limit states principles. The partial factors included are based on previous experience and statistical variations. They have been calibrated to maintain consistency with current practice (BS8006-1:2010). However, in contrast to some design methods (e.g. EBGEO, 2010) which are based on EC7 (BS EN 1997-1:2004), BS8006-1:2010 specifically excludes the use of BS EN 1997-1:2004 as it "is not for use in the design and execution of reinforced soil". This leads to a hybrid approach currently used in the design: proof of external stability, without intersection of a single layer of reinforcement, according to BS EN 1997-1:2004 while stability of any slip circle that intersects reinforcement is calculated according to BS8006-1:2010. This approach was chosen as the mechanical principle and the load transfer within a reinforced soil structure is not fully understood and cannot be given a specific factor of safety. As the determination of reinforcement length is made by ensuring global stability the different approaches to be used might be a source for confusion.

3.1 *External stability*

External stability describes a global failure of an assumed rigid block (the reinforced soil). Global stability ensures a sufficient grid length and prevents sliding, overturning, bearing capacity failure or slope failure. An adequate safety factor against structural sliding along the base is calculated using the sliding interaction coefficient based on the lower value of reinforced fill or subsoil. Due to geogrid nature this is usually calculated using a sliding coefficient of 0.7 * φ. The weight of the reinforced soil block and the

soil-geogrid friction provides the resisting force while the driving force is represented from the retained soil and loads applied behind the structure. Overturning is derived using similar action and reaction forces. A sufficient factor of safety is achieved when the resulting force is within the middle third of the structure. For the assessment of a sufficient factor of safety against bearing capacity failure the traditional methods are used, the base of the assumed rigid block represents the foundation width. Well established design methods (e.g. DIN 4017) are used for the assessment with their safe approach being proven since many years. Similarly global stability is calculated by Bishop's method of slices being acknowledged as a safe measure for calculation. Presence of any toe or top slope has to be assessed carefully and considered as these may have a significant effect on the required geogrid length to ensure external stability.

These calculation principles represent a well proven approach demonstrated numerous times. With reliable soil data available and a proper site investigation carried out sufficient information on the subsoil conditions and soil properties can be derived. They provide only little possibilities for errors.

3.2 *Internal stability*

According to BS8006-1:2010 equilibrium between an assumed monolithic body (active zone) and the available geogrid tension forces to tie this body into the passive (resisting) zone has to be guaranteed. As the most critical wedge is unknown, every possible wedge has to be analysed. At the same time more complex geometries, due to the presence of two-part-wedges are analysed and the highest required tension force derived from this analysis (see figure 2). The layout of the available geogrid strength present in different structural heights is derived to optimise the design.

As only a limited amount of geogrid strengths are available, the next higher grade in tensile strength is used in design when the given strength of the present geogrid is not sufficient. To avoid mistakes in construction each geogrid strength is used for several layers which form a consistent block in which the total available tension force is usually significant larger than required tension force. Overstressing of individual layers (if occurring at all) is therefore counterbalanced by numerous other grid layers.

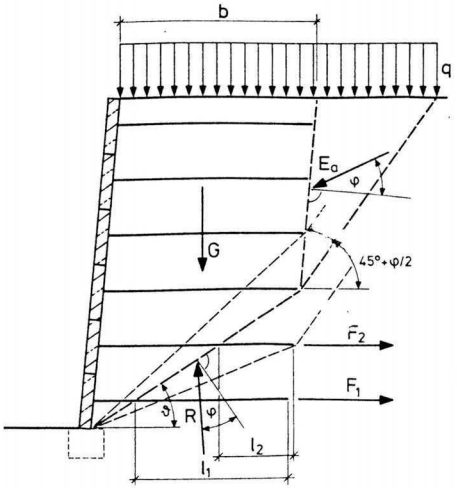

Figure 2. Assumed wedges for the calculation of internal stability

The geogrid anchorage length in the passive body needs to be sufficient to avoid that the geogrids are pulled out of the passive zone. The geogrid strength needs to be sufficient to withstand the activated tensile forces at the end of the design life. The design against pullout is based on conservative assumptions derived from laboratory pull-out tests. These parameters are on the safe side and can due to several implications not become a source for failure: the actual pull-out capacity is underestimated, pull-out can only take part in the upper ~1.5m of a structure, pull-out is not a separate mechanism (to be considered in association with geogrid tensile failure) and pull-out assumes a stress transfer in the reinforced soil that is not yet verified in-situ.

The design methods cannot be considered a source of failure when the appropriate design codes are fulfilled and the stability is analyzed using appropriate material factors for soil and geogrids.

4 SITE INVESTIGATION

A proper site investigation is the basis for every structures. Reliable analysis of required foundation dimensions or the load bearing capacity of the in-soil behavior is essential to avoid structural failure or ex-

cessive deformations. It has to be ensured that the site investigation covers all requirements for the planned construction (early involvement of geotechnical engineer in the planning process), a sufficient quality of the site investigation (reasonable amount of borehole logs, in-situ or soil tests to derive design parameters) is ensured and that the geotechnical engineer is incorporated in the whole planning process and an independent site supervision takes place.

It is inevitable that within the selective choice of boreholes a large risk is present as the conclusions drawn may not be representative for the whole site. It is therefore a risk assessment of the impact of assumed soil parameters from a site investigation. On the other hand the assumptions made should not be too conservative to make structures uneconomical.

4.1 *Foundation soil properties*

For the calculation of external stability the foundation soil properties have to be sufficiently known to calculate external stability. While the reinforced soil properties and the backfill material are usually well known as they are imported or site won (visible and assessed before installation), the foundation soils cannot be verified which indicates the importance of the site investigation report. Possible shear planes due to soil inhomogeneities or a varying groundwater head that affect bearing capacity have to be investigated. Information on sloping ground is to be provided as it may reduce bearing capacity significantly. In case insufficient data is available parameters are assumed for feasibility studies, but additional investigation or independent advice is required before construction takes place in order to avoid failures.

4.2 *Backfill soil properties*

In contrast to the foundation soil parameters the backfill soil properties are likely to be specified more appropriate. As for construction of a reinforced structure excavation behind the structure has to take pace in order to derive a safe working place, the excavated material (normally used as backfill) is visible and can be tested if required. In case the parameters vary significantly a redesign of the required geogrid length is possible or a different backfill material having the parameters assumed in design can be used. Due to the information that can be gained on the backfill soil, the inherent risk is small compared to the foundation soil properties. Additionally the backfill soil properties have due to the calculation method less influence on stability and deformation characteristics of reinforced soil

4.3 *Reinforced soil properties*

Reinforced soil properties are usually well controlled during the construction process as the source of the material is known or the material properties assessed easily. For structures with a face angle >70degree granular material is a requirement given by the relevant design codes. Structural fill avoids long term settlement when sufficient compaction is achieved. This is easily tested by the relevant methods. A well compacted structural fill ensures due to its controlled properties that no long-term deformations occur which could result in deformations that exceed allowable limits.

For structures with a face angle <70degree however, all soil material can be used. Special care is required when these soils are used to avoid long term influences as excessive settlement and associated deformation behavior. Additionally it has to be ensured that a sufficient pore pressure ration is considered in design when cohesive soils are used and compacted in situ. Due to the nature of the soil being compacted in given lift heights the properties can be controlled sufficiently well in order to consider them in the design so that usually theses parameter should not result in major structural deficiencies.

4.4 *Boundary conditions*

All boundary conditions or special circumstances should be considered carefully. Toe or top slopes should be pointed out as well as unusual water conditions. Considerations of water levels or water within the structure should be properly assessed. Reinforced soil structures are usually insensitive to water flow but if inappropriate measures are undertaken they have been reported in the past as being mostly influenced by neglected water conditions (Jaecklin, 2006).

5 CONSTRUCTION MATERIALS

As geogrids and soil within a reinforced structure form a composite with unknown parameters it has to be ensured that the individual properties of the composite are capable of carrying the addressed load in the design. Each individual construction element will be looked at and their assessment described to verify the possibility of each individual element

5.1 *Geogrid*

Geogrids are, like most construction material, continuously assessed and their properties checked as part of internal quality control. Additionally they have to be tested in specific intervals to ensure their reliability. As geogrids are polymer materials their properties change through the design life as part of their rheological behavior. Therefore two types of tests are regularly conducted: short term ultimate tensile tests and long term creep tests (figure 3).
Ultimate tensile tests (BS EN ISO 10319) are short routine test to verify that the stated material properties of the specified material are present and that the material has sufficient short term tensile properties. They are conducted at a strain rate of 20% and have the advantage that the results are available within the test time.

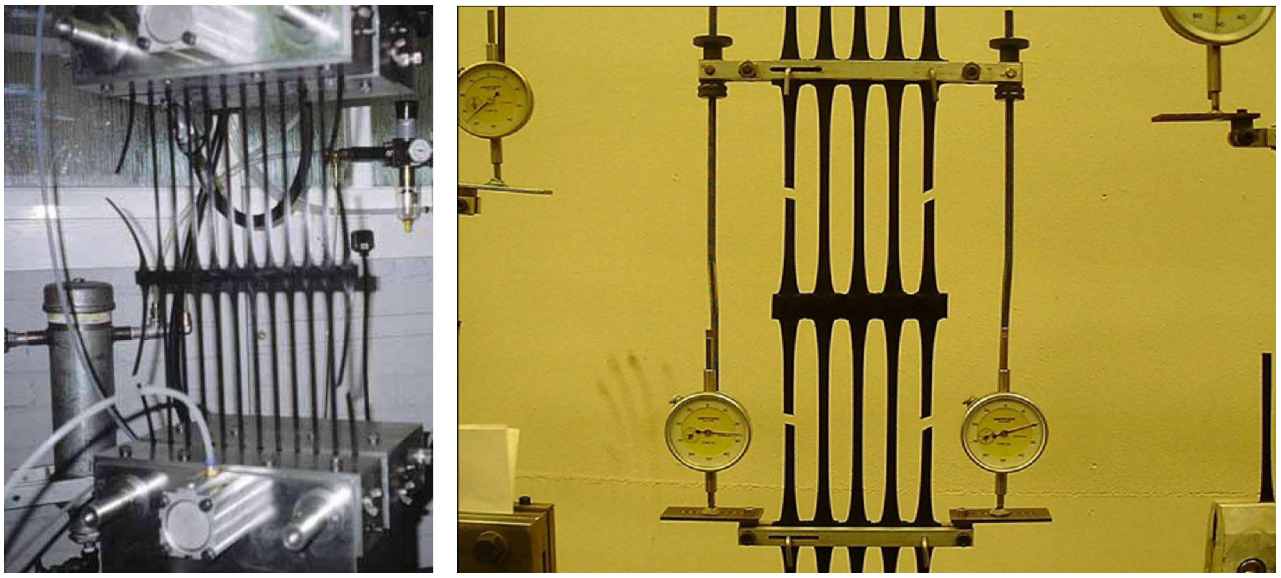

Figure 3. Ultimate tensile test (left) and tests arrangement for creep tests

For a specific project it would result in large time requirements to conduct individual creep tests as their assessment can take up to several months. Their assessment is regulated by BS EN ISO 13431 (1999). The grid is loaded with sustained loads at certain percentages of the short term tensile load under different temperatures (usually 10, 20, 30, 40 and 50 degree) and the load-strain relationship constantly measured. From the time to geogrid rupture under different temperatures the design strength can be derived. While the short term strength has importance for the quality control the designers are interested in the long term design strength as they represent the loads relevant to the design. Usually the long term strength is assessed by external standardization authorities as the BBA (Technical Assessment for Construction). They verify that the materials have the stated long terms strength properties which ensure the designer that the specified loads are verified. IT is the manufacturers' responsibility to ensure the stated material properties. Due to this and the regular assessment of the certificates the risk within the geogrids for a structural failure are extremely small.

5.2 *Facing*

In addition to the geogrid assessment a BBA certificate for whole systems ensures that the connection of geogrid and chosen facing is durable and capable of transferring the specified loads. A failure of the connection is indicated in figure 4. A durable connection of facing and a geogrid is achieved when maximum available geogrid tension force can be transferred by the connection. This can be achieved by a moulded polymer connector that hooks around the transverse bars of the geogrid and is then locked in to place be-

tween the blocks. The high efficiency connection is an important feature. One of the limiting factors on the design strength of the geogrid is the connection efficiency at the face, which may be as low as 25% in systems using a frictional connection only. This is of particular concern where the vertical confining stresses are low, such as in walls up to 8 metres high.

An approved system e.g. according to BBA ensures that a system is indicated as fit for purpose and therefore reduces the clients exposure to risk. It is therefore in the interest of designer, contractor and client to choose proven structural solutions to minimize risk of failures.

5.3 *Soil*

Soil property assessment in contrast to the geogrid strength assessment is a bit more complex due to the natural variation of soil properties and the influence of compaction, shape and particle size distribution on the properties. For structures usually a well graded granular fill is whose parameters can be assumed in reasonable variations. Safe side assumptions are undertaken to account for material variability. However, as the material properties of the placed and compacted materials are visible and well known they represent only a small source of error. The interaction with the geogrids and the confinement of the soil particles within the geogrid apertures has a positive effect on the soil as the soil dilatancy is restricted which increases the soil shear strength. The usual infill material of a reinforced structure can due to the positive effects also not be regarded as a source of failures.

Figure 4. Facing failure, connection ensuring 95% of tensile strength

6 CONSTRUCTION

The construction process is due to the variability and the varying boundary conditions a constant risk for failures. To minimise the risk of structural failures or excessive deformations simple to construct systems have been developed which are assembled on site. With initial installation guidance the risk of installation for e.g. a modular block walls is minimised. The compaction energy used on site and the appropriateness for the soil need to be specified in advance and may require additional tests. As the geogrid manufacturer cannot take any responsibilities for this usual reference to a minimum compaction standard are made. This has to be reached in order to minimise settlements occurring due to insufficient compaction.

Once the formation level is prepared the in-situ concrete strip footing for the facing is cast to line and level. As a precaution the footing is designed wider than the blocks to assist with the load spreading over usual weak foundation. The HDPE geogrids are simply cut from the delivered roll to the length dictated by the design. The vertical spacing between layers for this project is usually 450mm (every 3 courses of blockwork). Once connected to the face it is important to take out any slack present in the geogrid and connection. If left in, this slack would in time manifest itself as a post constructional forward movement of the face. When using conventional granular fill materials this is not a problem as the geogrid may be tensioned lightly using a steel beam and bar mechanism. The dense granular fill provides the perfect reaction to this tensioning effort.

It is in the interest of the manufacturer to reduce inherent risk within structural system solutions. Only easy to install, virtually risk free structures which are durable enough to withstand the applied used will be reused. During the developing process constant communication with construction sites are undertaken to limit all negative influencing factors. The installation is therefore also not the main contributor to failures or significant deformations.

7 CONCLUSIONS

Several parameters that may influence the integrity of a reinforced structure where described and their inherent risk analyzed from practical points. Responsibilities within a project, the design methods and the construction materials are identified, well proven and based on simplifying conservative mechanisms or continuously verified and may therefore not be regarded crucial towards failure.

The site conditions however can be crucial and, as mentioned, need to be assessed carefully. Failure in the site investigation inevitably leads to high risk when the subsoil does not have the assumed strength properties. On the other hand the simplicity of construction is in itself a source for possible failure.

As the construction is rather easy to do it is considered as "I can do that by myself" without consultation of a geotechnical engineer or appropriate design. In fact, as indicated by Bacchus, 2010, most failures were reported for mid-height structures build on private ground where no appropriate risk assessment was carried out and structures build without reasonable soil investigation. Every construction outside of state-of-the-art principles comprises risks that are beyond eventualities of a project. When these principles are violated failures are inevitable and occur with every construction material. Due to the conservatism present within the calculation and the construction materials geogrid reinforced structures can virtually be installed by everyone. With a less conservative approach it may even be possible that structures constructed to state-of-the-art principles are constructed safely while more private structures indicate failure.

Geogrid reinforced structures are a safe means to withstand high applied loads, construction over soft and variable ground and have been proven for long term stability and very small deformations, e.g. Bussert, Naciri, 2008. As most structures are planned by order of public authorities or in conjunction with other construction special considerations are undertaken which prevent failures occurring as they need to undergo established principles and are overlooked by dedicated personnel. Failures occurring on private ground neglecting approved principles cannot be prevented but can also not be regarded as standard and are therefore not representative for reinforced soil structures. They indicate poor workmanship outside current standards and state-of-the-art principles.

REFERENCES

BS EN 1997-1:2004: Eurocode 7: Geotechnical design – Part 1: General rules, British Standard Institution

BS EN ISO 10319 1996. Geotextiles. Wide-width tensile test, 15/08/1996, British Standards (BSI)

BS EN ISO 13431 1999. Geotextiles and geotextile related products – Determination of tensile creep and creep rupture behaviour, British Standards (BSI)

BS 8006-1:2010: Code of practice for strengthened/reinforced soils and other fills, British Standard Institution

Bacchus, R.C., Griffin, L.M. 2010. A perspective on mechanically stabilised earth walls – pushing the limits of pulling us down, Proc of the 2010 Earth Retention Conference, Bellevue, Washington

Bussert, F. 2006. Verformungsverhalten geokunststoffbewehrter Erdstützkörper – Einflußgrössen zur Ermittlung der Gebrauchstauglichkeit. Schriftenreihe des Institutes für Geotechnik und Markscheidewesen. Technische Universität Clausthal. Heft 13/2006

Bussert, F., Naciri, O. 2008. Experiences from deformation measurements on geosynthetic reinforced retaining walls, Proc. Of EuroGeo4, Edinburgh

EBGEO – Empfehlungen für den Entwurf und die Berechnung von Erdkörpern mit Bewehrungen aus Geokunststoffen, DGGT, Fassung 01/2010

Jaecklin, F.P. 2006 Innovative design for repairing Gondo mudslide by 20m high geogrid wall, Proc. Of the 8th Int. Conference on Geosynthetics, Yokohama, Japan

ISGSR 2011 - Vogt, Schuppener, Straub & Bräu (eds) - © 2011 Bundesanstalt für Wasserbau ISBN 978-3-939230-01-4

Variability of the grain size distribution of a soil related to suffusion

M. R. Salehi Sadaghiani & K. J. Witt
Bauhaus-Universität Weimar, Germany

ABSTRACT: A purely deterministic approach in geotechnical engineering usually is chosen despite there is enough knowledge about the uncertainties and spatial variability of the soil parameters. The geotechnical design and recommendations are based on some field observations, measurements and calculations with homogenized material and simplified models. These affect the results and important decisions in the design process. With the knowledge of the spatial variation and autocorrelation of the parameters, statistical methods can be applied in geotechnical design as well as in the risk assessment of the earthen structures. The Paper delivers statistical data and methods to handle these, which are investigated systematically in a river dike. The importance of the spatial variation and autocorrelation of the grain size distribution is demonstrated regarding suffusion phenomena.

Keywords: spatial variability, grain size distribution, internal erosion, earth structure

1 INTRODUCTION

Homogeneity has become a very important issue in geotechnical engineering in recent years. This is a fact that homogeneity is an important characteristic of geological and respectively geotechnical systems and affects a wide range of theoretical and practical issues (Saucke et al. 1999; Witt and Brauns 1984). While in the last decades major progress toward a geotechnical theory of homogeneity is being made, the concept is frequently misused because homogeneity nowadays means different things to different specialist. Quantification of homogeneity is done without a clear notation of what is exactly being quantified. A researcher must explicitly answer the question: homogeneity of what? This has not been the common practice.

To overcome these serious problems, we need a quantitative, effective definition of homogeneity. In this paper we extend the discussion of the definition and quantification of geotechnical homogeneity advocated by Witt and Brauns 1984 and Li and Reynolds 1995. We extend the operational definition of homogeneity proposed by Li and Reynolds and suggest an approach for quantifying homogeneity of a granular soil in respect of sensitivity against suffusion which is consistent with this definition and provide one example that illustrates how this scheme can be applied in practice.

The suffusion is primarily a function of the grain size distribution (geometrical criterion) and secondly depends on the hydraulic impact (hydraulic criterion). Due to the natural interactions, the soil placement or soil treatment the composition of the grains in a soil changes, particularly wide graded soils show a significant degree of variation. Though, in current internal stability design for the earthen structure, usually based on grain size ratios, the variance of the soil parameters is not taken explicitly into account. If the variation of the grain size distribution is neglected and the average grain size distribution or just upper and lower band is proved against suffusion, it can be possible that either the average parameters satisfy the suffusion criteria but in some places of the earthen structure suffusion can be occurred.

This effect of parameter variation on the probability of local failure has been investigated and will be discussed in the following. Along with the new approach for the calculation of suffusion failure probability, the degree of parameter variation as well as the limits of homogeneity in respect of grain size distribution (GSD) will be statistically examined, with help of the field inquiries.

For a probabilistic design, it is necessary to have a suitable equation of limit state to consider the appropriate parameters. Consequently, we go over the main points of the suffusion phenomena and the failure conditions.

2 SUFFUSION PHENOMENA AND CURRENT DESIGN PROCEDURE

"Suffusion" is the migration of the soil particles through the soil skeleton. The physical understanding of stability against suffusion is the ability of the voids of soil skeleton (or more precisely, of their pore constrictions) to hold its smaller particles, which are considered as mobile. With this definition, suffusion can be reduced to a filter/base problem, in which the filter is spatially created by the soils structure and the base conform with the mobile parts of the soil grains, the filling. An ideal limit state equation which defines the failure boundary should have the following general form:

$$Z = f(GSD, CSD, g, n, C_h, F_{Seepage}, \sigma_{eff}) \quad (1)$$

where GSD = grain size distribution of mobile particles of the soil, g = the shape of the grains, CSD = the effective pore constriction size distribution of the skeleton, n = porosity, C_h = degree of homogeneity, $F_{seepage}$ = seepage forces within the soil, σ_{eff} = effective stress

For investigating the worse conditions, it is assumed that sufficient hydraulic conditions exist and the effective stresses do not have any effect on the process because the mobile particles are not stressed. The effect of grain shape (g) and degree of homogeneity (C_h) are neglected. It is assumed that the grain shape has no big effect on the local process and the soil is locally homogenous ($C_h = 1$). With these assumptions the ideal limit state equation reduces to:

$$Z = f(GSD, CSD) \quad (2)$$

In this model only the GSD and CSD of the soil dominate the suffusion process. It may appear crude, but this is a rational way of using engineering simplifications as a guide to sophisticated primary models. In other words, the suffusion problem is reduced to a simple problem of geometry.

It is known that the CSD and the porosity are direct function of GSD. The GSD can be obtained by sieve analysis. However, the determination of the CSD is quite difficult. Several theoretical and experimental approaches have been tried to give a relative exact method for the determination of CSD. The different methods can be mentioned:

- Measurement of void characteristics based on saturation-capillary pressure tests (Payatakes 1973)
- Probabilistic model of randomly packed spherical filter particles (Silveira 1975)
- Measurement of distribution of void areas in specially prepared sample sections (Wittmann 1980)
- Mathematical procedure to determine the controlling constriction size (Schuler 1999, Indraratna 2007, Reboul 2008)

Each of these methods shows its limit of applicability, especially for wide and gap graded soils. Till now there is no possibility to measure the CSD in an appropriate way.

The GSD can be obtained by sieve analysis. It is a fact that the GSD-Curve of a soil has an obscure mathematical characteristic so that simple but exact criteria for stability against suffusion can not be formulated. For that reason in current practice we tend to use more simplifications such as substituting the GSD with a characteristic diameter and inserting a factor regarding to its degree of uniformity. The CSD is also replaced with a characteristic diameter of the GSD and the coefficient of uniformity. These Simplifications lead to a so called "Grain Size Criteria", of which the limit state equation can be written in the following general form:

$$Z = f(C_u) \cdot d_{85,F} - d_{15,S} \quad (3)$$

where $d_{85,F}$ = is a diameter such that 85% of the grain's diameter of the filling are smaller than this size, $d_{15,S}$ = is a diameter such that 15% of the grain's diameter of the skeleton are smaller than this size, $f(C_u)$ = is function of uniformity coefficient.

The positive value of Z gives the stage of the safety of this simple system. The function of non-uniformity coefficient f(Cu) has to be determined experimentally, empirically or by means of theoretical considerations. Such design criteria based on experimental investigations or empirical knowledge are still used in practice. One famous example is the Terzaghi criterion (Terzaghi and Peck1948) with f(Cu) = const. = 4~5 , Including some factor of safety and without safety factor C(cu) = 9, which is only valid for uniform base and filter combinations (In this paper it is assumed that the CSD-Curve of Filling and Skeleton are uniform).

$$Z = 9 \cdot d_{85,F} - d_{15,S} \tag{4}$$

The advantage of the method of GSD separation of the soil into two separate filling and skeleton GSD-Curves is that the produced GSDs are not wide graded soils anymore, i.e. after separation the GSD; the coefficient of uniformity will be extremely reduced. However choosing the separation point is an important part of the whole analysing procedure. The separation point gives the information about the skeleton and filling of soil (according to Kenny and Lau et al. 1985, primary fabric and loose particles).

3 LABORATORY METHODS FOR FINDING THE SKELETON AND FILLING OF A SOIL

The main objective of the laboratory tests which was accomplished in the Bauhaus-Universität Weimar is to finding the skeleton or primary fabric of the chosen soil. The local and global transport of mobile particles of a wide-gap-graded soil was measured by suffusion tests. During each test steady flow conditions with different hydraulic gradients at the embankment dams were simulated. The local structural changes of the soil were determined by measuring the changes of the pore water pressures. The measurement of eroded material (effluent) at the outlet was a primary criterion for the determination of stability of the sample. After each test, changes of the grain size distribution in 5 various layers of the soil column were measured. This allowed a conclusion about global and local structural changes of the soil.

The tests described here, were carried out with one soil sample (figure 1) with 500 mm height. The specimen was placed in 100-mm layers and compacted. Each layer was built in the test apparatus with the same specified grain size distribution which in one hand ensured the homogeneity of the soil and in the other hand, it was possible to measure the transported fractions from each layer. A reference layer of glass balls with the diameter of 16 mm were built at the base of the sample. A mesh grid were used below and above of the reference layer. The reference layer was to avoid losing fine particles of the first layer of the sample during the compaction of this layer.

Four different hydraulic gradients (i = 0,1; 0,2; 0,4; 1,0) were applied for each suffusion test to evaluate the suffusion stability. The weight of the entire dry material from effluent (Washout) was the value between 2,92% and 6% of the total weight of the soil specimen. It is obvious that the selected soil is to be classified as a soil in the border of stability against suffusion. These tests emphasized again that the degree of erodibility of a suffusive soil is correlated to the homogeneity of its structure. The results showd that the preferred flow paths and material transport along these paths were the reason of local segregations. By these tests no global washout could be observed. Nevertheless the observation of the soil column during percolation of water showed that there were mobile particles which were not fixed in the skeleton and there were suffusive particles which were transported from the soil column. The mobile fractions were moved in direction of flow and were captured within the structure after passing through a certain path. In the other hand the suffusive particles were moved through the whole column and the skeleton of the soil was not able to capture them. The flow caused a disarrangement of the original structure into sometimes a more stable one or sometimes an unstable one dependent to the direction of the flow. This resulted in a randomly distributed micro stratification however any changes in flow conditions and direction were able to influence a remobilisation of the mobile particles.

The suffusive particles were determined directly from effluent. The biggest suffusive particle was the soil fractions between 0,125 and 0,5 mm. Moreover the mobile particles were determined by balancing the weight of the different fractions of each soil layer with total weight and the mass of washout fractions. The biggest mobile particle within the soil column was the soil fractions between 0,5 and 1 mm, and these results are in good agreement with the values reported by Binner et al. 2010. According to the grain size distribution of the soil, the fractions with diameter of 1 mm correlate with the value of d_{22}. All of accomplished suffusion tests deliverd the same result with consideration of the suffusive and mobile particles. Due to the fact that the soil samples which were used for the tests was a mixture of several samples

from different locations along the dikes, it can be considered that the used grain size distribution is an average grain size distribution and it is assumed that the d_{22} conforms an average value in regarding to point of separation for all of the dike materials (figure 1).

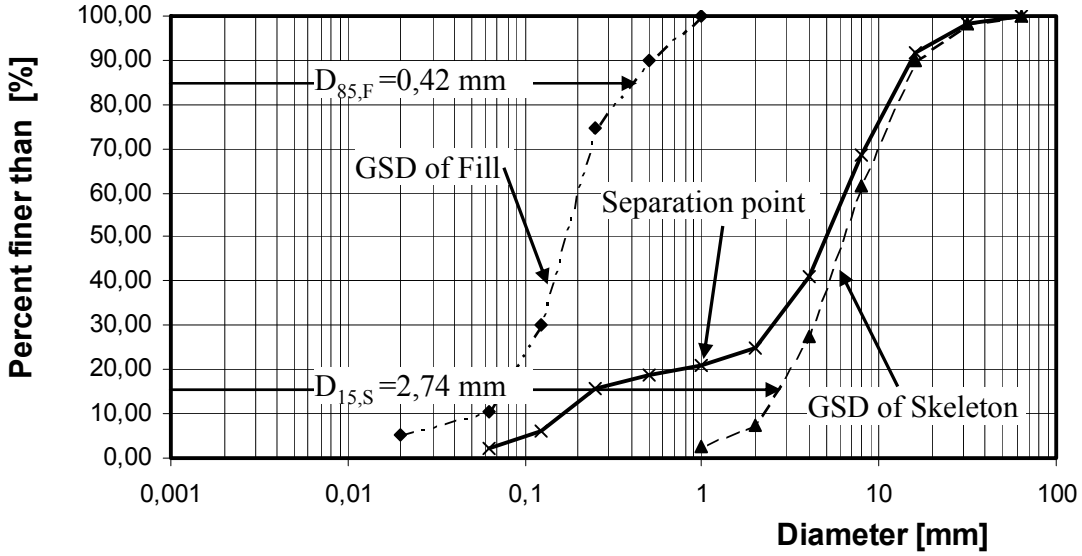

	grain size
$d_{15,S}$	0,15·(100-22)/100 +0,22=0,337=33,7%
$d_{85,F}$	0,85·0,22=0,187=18,7%
d_{22}	1 mm = Separation point

Figure 1. Grain size distribution of the soil specimen used for suffusion tests

Figure 1 shows the separation point which correlates with d_{22} = 1 mm and the other two important grain sizes $d_{85,F}$ which correlates with $d_{18,7}$ and respectively the $D_{15,S}$ correlates with $d_{33,7}$ of the original average grain size distribution. In the following section the descriptive statistical values of these parameters were discussed.

4 HOMOGENEITY AND PARAMETER VARIATION

The homogeneity was defined based on two components (Li and Reynolds 1995): the system property of interest and its complexity or variability. The system property can be anything that is of geotechnical interest, e.g., cohesion, permeability and so on. Complexity refers to qualitative or categorical descriptors of the property. Therefore homogeneity is complexity and/or variability of a system in the space or time. It has to be mentioned that here the time homogeneity is not considered and just the spatial homogeneity is the interest of this paper. It is also obvious that the homogeneity is a function of scale (Witt & Brauns 1985). Li and Reynolds1995 proposed two factors which are called grain and extent, are the primary scaling factors that affect complexity or variability. Grain is the finest resolution of the data (e.g. the volume of the soil sample) and extent is the area encompassed by a study. The observational scale (i.e. grain or extent) is dependent on the sampling scheme used, which in turn is determined by the nature of the phenomenon and the research objective. The observed data and the treatment of the data determine what kind of homogeneity may be measured. From a data analysis viewpoint, data treatment or resampling (e.g. sieve analysing of the soil or hydrometer analyse) may modify grain or extent or both and therefore plays a role in quantification of homogeneity.

As far as the problem of suffusion is concerned, homogeneity is mainly a matter of similarity in regard to the parameter of the soil which has an influence on the vulnerability of the soil against suffusion. A part of a soil in a dike or natural soil may be considered as homogenous, if the variation in gradation from a place to place is within a certain limit which is still to be defined for each case.

In order to get more insight into the actual conditions under practical circumstances, a systematic sampling on Rhein River dikes was performed. The mean GSD band of all samples has been shown in Figure 2. For this material the theoretical sample size (mass) was equal to ca. 15 kg (Witt 1984). In the study area, 158 samples were taken with high resolution within a grid of different distances from 25 cm to 8 m. According to the homogeneity definition, with this kind of sampling the sampling effect is reduced and the evaluation gives a better answer for homogenous distances. On the basis of the 158 samples, the

construction of different groups was performed. For every group, we plotted a histogram and calculated the frequency distribution for the relevant characteristic grain size such as $d_{18,7}$ and $d_{33,7}$.

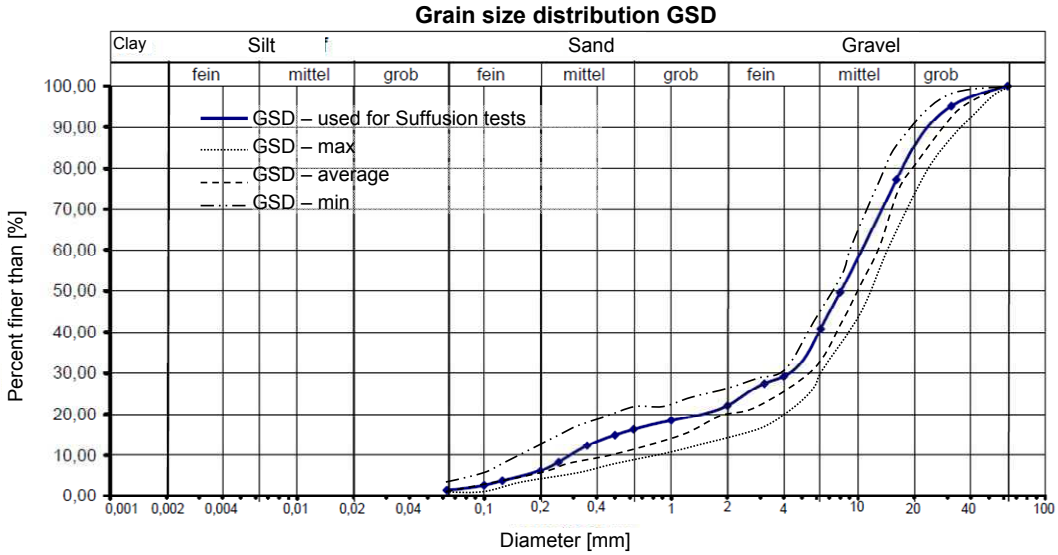

Figure 2. Band of grain size distribution of the soil specimens in the study area

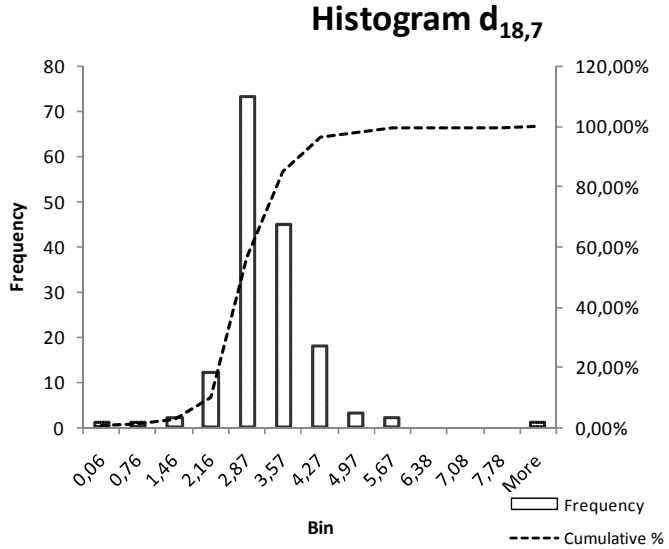

d18,7	
Mean	2,877243
Standard Error	0,068101
Median	2,755915
Mode	#N/A
Standard Deviation	0,856022
Sample Variance	0,732773
Kurtosis	12,02251
Skewness	1,856751
Range	8,423395
Minimum	0,058065
Maximum	8,48146
Sum	454,6045
Count	158
Largest(1)	8,48146
Smallest(1)	0,058065
Confidence Level(95,0%)	0,134513

Figure 3. Histograms and frequency distributions of $d_{18,7}$ for 158 samples

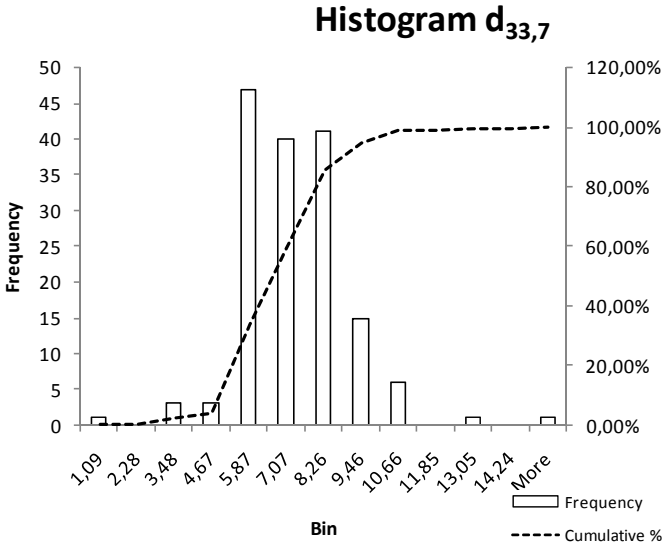

d33,7	
Mean	6,777346308
Standard Error	0,135562796
Median	6,701165
Mode	#N/A
Standard Deviation	1,703997927
Sample Variance	2,903608934
Kurtosis	4,273040781
Skewness	0,779156575
Range	14,35467667
Minimum	1,085866667
Maximum	15,44054333
Sum	1070,820717
Count	158
Largest(1)	15,44054333
Smallest(1)	1,085866667
Confidence Level(95,0%)	0,267762161

Figure 4. Histograms and frequency distributions of $d_{33,7}$ for 158 samples

In figure 3, it is interesting to see that the variability of $d_{18,7}$ is larger than that of $d_{33,7}$. This result is maybe typical for such a soil which was a mixture of the sand and gravel with meadow silt. It could already be seen from the figure 2. which shows grain size distribution band with a smaller upper grain sizes and a broad lower grain sizes of $d_{33,7}$. The normal transformation shows a very good fit of both $d_{18,7}$ and $d_{33,7}$. The corresponding statistical values can be taken from figure 4. The coefficient of variation COV ($d_{18,7}$) is equal to 29,75 % and this value is for COV ($d_{33,7}$) equal to 25,14%. A precise quantitative definition of homogeneity seems difficult. But a coefficient of variation of 15% may be allowable with considering that in the probabilistic, normally distributed random variables with a COV < 10% are regarded as deterministic value. In fact soil with a COV < 15% can be seen as a homogenous material. However the definition of statistically homogenous seems very appropriate for the soil materials.

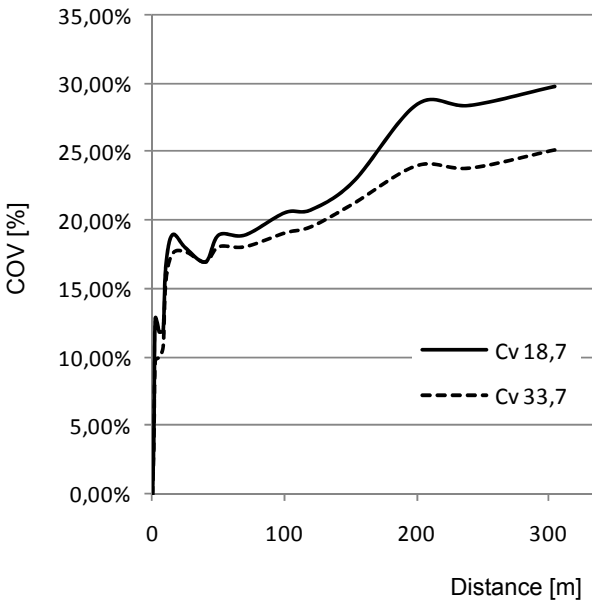

Figure 5. Coefficient of variation in dependence on sample distance

As it is to be expected, the coefficient of variation in figure 5 increases with sample distance. If a distance of 9,3 m for $d_{18,7}$is chosen the diagram gives a result of 15% for coefficient of variation COV .

This clearly shows that in this area the variation of the $d_{18,7}$ is relatively small and in each 9,3 m there is a statistically homogenous distribution of $d_{18,7}$ and respectively for $d_{33,7}$ it will be the homogenous area of 9,8 m.

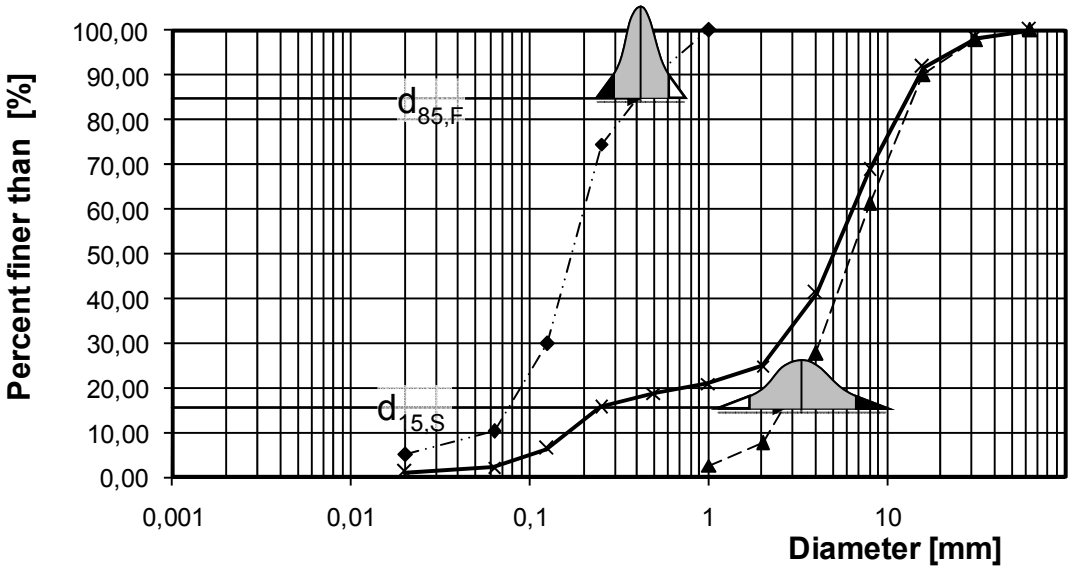

Figure 6. The variation of the $d_{18,7}$ and $d_{33,7}$ of the original grain size distribution

Figure 6 shows the normal distribution of the related grain sizes for the equation 4. Figure 7 gives some other information about mean value and standard deviation of this distribution. The shaded area contains 95% of the area and extends from 3,37 to 10,19 mm for $d_{18,7}$ and the shaded area of the normal distribu-

tion of the $d_{33,7}$ extends from 1,16 to 4,59 mm. For all normal distributions, 95% of the area is within 1.96 standard deviations of the mean. If the upper band of 95 percentile of $d_{33,7}$ and the lower band of the 95 percentile of $d_{18,7}$ are considered, the Z (equation 4) can be calculated as:

$$Z = 9 \cdot 1{,}16 - 10{,}19 = 0{,}25 \approx 0 \tag{4}$$

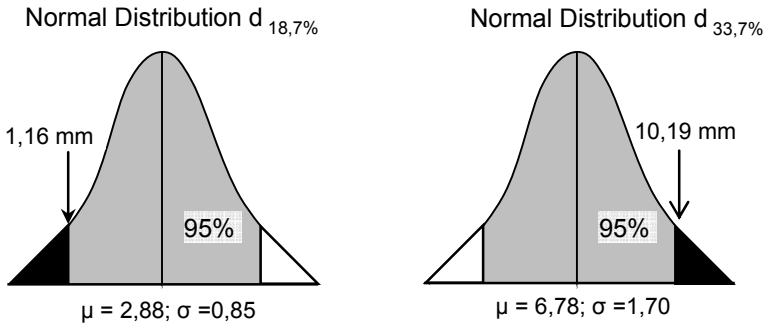

Figure 7. The normal distribution of the grain sizes $d_{18,7}$ and $d_{33,7}$ – 95% of the area is within 1,96 standard deviations of the average value.

This can be interpreted as 5% of the whole samples with mentioned assumptions are suspected to suffusion and the rest of samples seems to be stable (without any safety factor). From this point of view easily the failure probability of the dikes and dams can be evaluated. In the following section some aspect of variation in grain size distribution according to satiability against suffusion are discussed.

5 CONSIDERATION OF GRAIN SIZE VARIATION FOR SUFFUSION CRITERIA

A reliable suffusion criterion has to take into account the random nature of the relevant soil parameters. For getting a reliable criterion, variability of the parameters must be induced into the limit state equation. Here the writers try to induce the variability into the geometrical grain size criterion (eq. 3).

In equation 3, the distribution of Z has to be find with consideration of the relevant parameters (C_u, d_{15} and d_{85}), knowing that the failure is defined by $Z = 0$. If the suffusion has been occurred, the soil probability failure is equal to the probability of the Conditions which Z is less than zero. For simplification, as it was mentioned in section 2, it is assumed that C_u of the separated GSD shows small range of variation so that we can take it as a deterministic function. The random variables in the limit state equation are then: $9 \cdot d_{85}$ (resisting part or R) and d_{15} (active part or S). If we substitute R for $9 \cdot d_{85}$ and S for d_{15}, the equation takes on the well known form used in probabilistic failure considerations:

$$Z = R - S \tag{5}$$

The probability of failure

$$P_f = P(Z < 0) = P(R - S < 0) = P(R / S < 1) \tag{6}$$

Then is (Freundthal et al. 1966)

$$P_f = \int_0^\infty F_R(x) \cdot f_s(x) \cdot dx \tag{7}$$

where F_R = cumulative distribution function of $C_u \cdot d_{85}$, f_s = cumulative distribution function of d_{15}

As shown in section 2 the distribution of both characteristic diameters can be well fitted with normal distribution or log-normal distribution, and in the special case the solution of equation 7 is according to Witt et al. 1993:

$$P_f = P(R/S<1) = \Phi\left(\frac{\ln \frac{\tilde{r}}{\tilde{s}}}{\sqrt{\sigma^2_{\ln R} + \sigma^2_{\ln S}}}\right) = \Phi(-\beta) \quad (8)$$

where $\tilde{r}$ = median value of the R-distribution, $\tilde{s}$ = median value of the S-distribution, $\sigma_{\ln R}$ = Standard deviation of ln R , $\sigma_{\ln S}$ = Standard deviation of ln S, $\Phi(-\beta)$ =Standardized normal distribution function (Gaussioan-distribution function), β = safety index

By substituting the characteristic diameters of the grain size distribution and using the coefficient of variation of their frequency distributions, the probability failure can be defined as.

$$P_f = P(R/S<1) = \Phi\left(\frac{\ln \frac{C_u \cdot \tilde{d}_{85,F}}{\tilde{d}_{15,S}}}{\sqrt{\sigma^2_{\ln d_{15,S}} + \sigma^2_{\ln d_{85,F}}}}\right) = \Phi(-\beta) \quad (9)$$

The equation 9 gives the correlation between the failure probability of the soil against suffusion, the central safety factor $\frac{C_u \cdot \tilde{d}_{85,F}}{\tilde{d}_{15,S}}$ and the standard deviation of $\ln(d_{15,S})$ and $\ln(d_{85,F})$.

The Overall failure probability of an embankment dam, in regard to internal stability, is on the one hand a function of the parameter variation of the materials involved, and on the other, of the spatial arrangement of the constituting elements. In designing of the embankment dam, this fact is taken into account by providing adequate minimum dimensions of a zone depending on the segregation of the material used. Nevertheless the risk related to the parameter variation in embankment materials can not be quantified up to now and design criteria are mainly empirical. Unfortunately there is a big lack of information on homogeneity, autocorrelation of parameters and relevant sample size.

6 DISCUSSION

The challenge in assessing the erosive processes is to determine or to estimate the relevant parameters, i.e. the pore constriction size of wide graded soils under consideration of special uncertainty due to heterogeneity as well as the effective size of mobile particles which are able to block the pores of the soil skeleton to create stable conditions. If these relations cannot be determined with an appropriate accuracy or if there are some soils which are geometrically prone to suffusion and the limit range of the hydraulic impact have to be defined, laboratory tests as described above should be carried out to allow a quantitative assessment of the risk of suffusion.

Minor differences of the particle size composition affect whether a soil is internally stable. It is recommended that for important structures laboratory tests should be carried out on the soils which are tested in the marginal areas of limit state equations or other criteria. The method suggested here is just for the used grain size distribution band and for the other grain size distribution are not be examined by the mentioned method.

For using this approach we need to separate a soil into base-filter grain size. The separation method was described and the experimental way of determining this separation point is a very important topic to discuss. Also the statistical distribution of the parameter has been investigated experimentally by systematic sampling on an embankment dam. It was indicated, that the relevant $d_{15,S}$ and $d_{85,F}$ parameters follow a log normal or normal distribution. The coefficient of variation shows an effect, which are depending on the point of the sampling and its distance. Theoretical considerations lead to a distance for considering of a homogenous area in regard to each parameter.

Considering the relative variation of the separation point, another probability of failure could be achieved with this method. With a systematic sampling of each site with different dike profiles and con-

stitution materials, it is necessary to make some tests to determine the separation point for calculating of failure probability.

7 CONCLUSIONS

This paper deals with the effect of spatial variability of the grain size distribution on internal stability of a gap graded soil. The physical background of suffusion is discussed. The grain size criteria which can be used in practical design are described as simplifications of a more general and more complex function. Such criteria describe both resisting and active parts by a characteristic grain size (d_{15} or d_{85}) and a function considering the uniformity of the soil. This equation is very suitable for a probabilistic approach of a design for reliability against suffusion.

The procedure for predicting and determining the mobile and suffusive particles of sand gravel soils with silty fines based on particle size distribution are proposed. It is shown that the degree of erodibility of a wide-gap-graded soil is close correlated to the homogeneity of its structure and material transport along the preferred paths which often result in local segregation. Even with a very high degree of homogeneity different results were obtained. The observations of the soil column during percolation of water have shown that there are mobile particles which are not fixed in the skeleton and there are suffusive particles which were transported through the soil column.

For using such a criterion we need to separate a soil into base-filter grain size. The separation method was described and the experimental way of determining the separation point was discussed. Also the statistical distribution of the parameter has been investigated experimentally by systematic sampling on an embankment dam. It has been indicated, that the relevant d_{15} and d_{85} parameters follow a normal or log normal distribution. The coefficient of variation shows an effect, which is dependent on the point of the sampling and its distance. Theoretical considerations lead to a distance for considering of a homogenous area in regard to each parameter.

With taking the random nature of the grain size parameters regarding to segregation problem into account the limit state equation allows calculating the failure probability. Thus the relation between the central safety factor, parameter variation and failure probability could be established. The theoretical approaches showed that it can be very dangerous to use the current suffusion criteria, calculating with the average or lower grain size distribution and neglecting the parameter variation, or even underestimate the degree of variation without enough samples.

This contribution has been prepared in order to excite other engineers to investigate dam fills as systematically as possible and publish test data which can form a better basis for the application of the geostatistical methods to quantify the probability of erosion and failure in embankment dams.

8 ACKNOWLEDGMENT

The writers started to investigate the factors affecting internal erosion processes in embankment dams and their foundations as part of a research project funded by German Waterways and Shipping Office Freiburg (WSA). The authors wish to thank the WSA-Freiburg and BAW-Karlsruhe for the financial and technical supports.

REFERENCES

Binner, R., Homberg, U., Prohaska, S., Kalbe, U., Witt, K.J. 2010. Identification of descriptive parameters of the soil pore structure using experiments and CT. Proc. of the fifth international conference on scour and erosion. Geotechnical special publication No. 210, November 7-10, 2010, San Francisco, California, USA, 397-407.

Freudenthal, A.M., Gerrelts, J.M. and Shinozuka, M. 1966. The analysis of structural safety. Journal of the structural Division. ASCE, Vol.92, No. St 1.

Indraratna, B., Raut, A.K., Khabbaz, H. 2007. Constriction-Based retention criterion for granular filter design. Journal of geotechnical and geoenvironmental engineering, ASCE, 266-276, March 2007.

Kenny T. C., Lau D., 1985. Internal stability of granular filters. Canadian geotechnical journal 22, 215-225.

Li H., Reynolds J.F., 1995. On definition and quantification of heterogeneity. Blackwell Publishing on behalf of Nordic Society Oikos, Vol.73, No. 2 (Jun.,1995), 280-284.

Payatakes, C.A., Tien, C. and Turian, R.M. 1973. A new model for granular porous media, Part 1, AICHE Journal, Vol. 19 No. 1.

Reboul, N. 2008. Transport de particules dans les milieux granular. Application à l'érosion interne, L'Ecole Centrale de Lyon, Diss., Nov. 2008.
Saucke, U., Brauns J., Schuler U. 1999. Zur Entmischungsneigung körniger Schüttstoffe. Geotechnik Zeitschrift, V22, Nr.4, 259-268
Schuler, U. 1997. Bemessung von Erdstoff-Filtern unter besonderer Berücksichtigung der Parameterstreuung. Veröffentlichung des Inst. F. Bodenmech. u. Felsmech., Universität Karlsruhe, Heft 143.
Silveira, A. Peixoto Jr. T.L. and Nogueira, J.B. 1975. On void-size distribution of granular materials. Proc. 5th Panam. Conference Soil mechanic Fdn. Engng, Buenos Aires, Vol.3.
Terzaghi, K. and Peck, R.B. 1948. Soil mechanics in engineering practice. John Wiley & Sons Inc., New York.
Wittman, L. 1980. Filtrations- und Transportphänomene in porösen Medien. Veröffentlichung des Inst. F. Bodenmech. u. Felsmech., Universität Karlsruhe, Heft 86.
Witt, K.J., Brauns, J. 1984. The influence of parameter variation on the reliability of the filters. Proc. of the international conference on safety of dams, University of Coimbra.
Witt, K.J. 1993. Reliability study of granular filters. Filters in Geotechnical and hydraulic engineering , Brauns, Heibaum & Schuler. Balkema, Rotherdam, The Niederlands, 35-41.

ISGSR 2011 - Vogt, Schuppener, Straub & Bräu (eds) - © 2011 Bundesanstalt für Wasserbau ISBN 978-3-939230-01-4

Evaluation of Failure Probability of Soil Cushions

M. Zotsenko, Y. Vynnykov & M. Kharchenko
Poltava National Technical University, Poltava, Ukraine

ABSTRACT: Article shows the typical examples of mathematical models realization of probabilistic description of random variables (RV) distribution of geotechnical characteristics and the heterogeneity parameters according to data of laboratory and field tests of compacted soils, mining industrial wastes and their mixtures. It also presents the variability of some technological parameters of soil cushions erection. The statistical parameters of RV distribution of designed and ultimate strengths of compacted soils, as well as settlement of foundations on cushions were determined by analytical methods. By means of numerical simulation of cushion tensely-deformed state (TDS) by method of ultimate elements (MUE) using the elastic plastic model, imitation simulation by Monte Carlo method and experimentally obtained distribution laws of RV of compacted soils characteristics, the statistic parameters and distribution laws of foundations settlements were obtained. Due to statistic analysis of settlements distribution of artificial foundations bases and their relative differential settlements the probability of failure was obtained.

Keywords: compacted soil, soil cushion, angle of internal friction, unit cohesion, modulus of deformation, distribution law, random variables, probabilistic design, method of ultimate elements, foundations settlements, soil design and ultimate strengths, probability of failure.

1 INTRODUCTION

1.1 *Actuality of the problem*

The engineering and geological conditions of building sites often are complicated. For example, for erection of modern building projects, the over flooded territories which are composed of poor-bearing soils are often used. For such circumstances, foundation engineering practice constantly replenishes the positive experience of filled earth massif erection with improved soil physical and mechanical properties. The improvement of soil properties is performed by compaction using modern vibrorollers, heavy tampers, compactors etc.

For utilization of industrial wastes and minimization of cost of soil cushions it is necessary to study the overburden rock and their mixtures as the material of artificial bases. In Poltava region (Ukraine) the large deposits of iron ore were explored. That's why the problems of overburden rock utilization are actual.

Compacted soils are of inherent heterogeneity, the parameters of which are taken the RV of the soil characteristics, anisotropy of mechanical properties etc. These parameters depend on the type and nature of the material properties of artificial bases, technological parameters of its erection and so on. Modern methods of cushions design are deterministic and do not consider the real variation of values of compacted soils properties. These design methods put unreasonable reserves of strength and deformability in their erection. That's why the geotechnical reliability is very actual problem, especially for artificial bases.

1.2 *Analysis of previous investigations*

According to studies of variability of soil properties (B.A. Garagash, 2004, M.N. Goldshtein, 1971, Harrop-Williams, 1985, B. Look, 2009, P. Marijanovij, 2003, A. Rachenmacher, 2005, E. Santos, 2009, Z.G. Ter-Martirosyan, 2010) the curves of RV distribution may have different look depending on their properties. By

M.N. Ermolaev, 1976, M.M. Maslov, V.I. Krutov, A.P. Pshenichkin the distribution curves of soil characteristics coincide with Gaussian normal distribution law. M.N. Goldshtein, 1971, believed that the soil mechanical properties were most characteristic for logarithmically normal distribution. From the study of D.C. Bugrov, 2003, the stochastic properties of the soil are best described by normal and improved Gram-Charlier distribution laws of RV. S. Macij believes that the RV of the angle of internal friction and unit cohesion of soils are better approximated by the normal or logarithmically normal distribution laws. The variation coefficients of natural soils properties are summarized in Table 1.

Table 1. Coefficient of variation v_x for different soil characteristics

Characteristic	Coefficient of variation v_x, %			
	sand	loamy sand	loam	clay
Moisture content w, %	30-50/4.4-49	10-30/6.2-27.7	8-28/3.8-15.0	4-25/12.65
Void ratio e	3-13/1.1-6.7	6-12/2.3-16.5	6-25/3.5-14.2	3-22/19.3
Density ρ, g/cm^3	2-7.5/0.5-3.2	2-4.5/0.5-2.5	2.5-7.5/0.8-3.7	2-6/4.3
The density of particles ρ_s, g/cm^3	-/0-0.3	-/0.2-0.65	-/0.2-0.6	-/0.8
Number of plasticity I_p		25-50/-	5-35/-	7-30/-
Limit of uncoiling W_p, %		6-17/-	5-25/-	7-27/-
Yield limit W_L, %		5-16/-	5-20/-	5-20/-
Shear strength τ, kPa	-/-	9-27/-	6-29/-	-/-
Deformation modulus E, MPa	-/-	-/-	15-35/18.6-65.4	-/-

In the numerator are data by Ermolaev M.M. and Myheyev V.V., 1976 in the denominator – data by Bugrov D.C. and Shilin V.G., 2003

1.3 *Study purposes*

It is necessary to study and determine statistical parameters of strength and deformation characteristics of compacted soils, to investigate factors that influence the distribution of RV, to study patterns that occur in artificial masses during their service for implementation into engineering practice the stochastic models of artificial bases.

Therefore, the purpose of work is taken to carry out the investigations of physical and mechanical properties of compacted soils and to get the statistic data of these characteristics variation; to study experimentally the influence of properties variation of cushion compacted soils on its deformation, to estimate the heterogeneity of compacted soils and to decide on the correct application of distribution laws for RV of soil characteristics of artificial bases; to analyze the cushion TDS by MUE during the use of elastic-plastic model involving the imitation simulation; to estimate the probability of soil cushion failure. Probability of failure criteria adopted safety characteristic $\beta=F_{cep}/\sigma_F>3$ – number of deviations in the range from $F = 0$ to $F = F_{cep}$ (where $\widetilde{F} = \widetilde{p}_u - \widetilde{p}$, σ_F – deviation, p_u – ultimate strength of compacted soil, p – pressure on the base), maximum foundations settlements S_u=10 cm and their relative differential settlements $(\Delta S/L)_u$=0.002 and $(\Delta S/L)_u$=0.004.

2 LABORATORY AND FIELD TESTS OF COMPACTED SOILS

2.1 *Objects of investigation*

Authors carried out scientific and technical support of erection of some artificial bases (Vynnykov Y.L., 2010). On three sites a comprehensive field and laboratory studies of the properties of compacted soils were carried out.

Object № 1 – cushion of thickness $h = 4.0 – 4.4$ m and composed of loess loam. It was erected by surface compaction using heavy tamper and layer-by-layer rolling (50 cm) and loaded lorries weighing 20 tons and doing 8 – 12 passages on one track to the project value of dry density ρ_d=1.65 g/cm^3 (k_s=0.90 – compaction coefficient).

Object № 2 – cushion of thickness $h = 3$ m and diameter $d = 22$ m under oil tanks with capacity of 3000 m^3. Material was loess loamy sand and loam. Cushion was erected by layer-by-layer rolling doing 10 – 12 passages on one track by loaded lorries and carrying out 12 – 14 impacts by a tamper weighing 2 tons, which was thrown down from a height of 5 – 6 m.

Object № 3 – the fill with area of more than 1.9 million m^2 and thickness 4 – 6 m for constructions of electrometallurgical plant. Material was overburden rocks, (fine, silty and medium grained sands, loamy sand and loam). Then the fill was compacted by vibrorollers (weight 14 – 16 tons, frequency 30/1.95 – 40/0.9 hertz/mm) and by pneumatic rollers (weight 22 tons) doing 4 – 8 passages on one track.

2.2 *Methods of testing*

The first stage consisted of sampling soil in foundation pits or, determination of its grain-size composition in the laboratory, indicative characteristics and optimum moisture content for different shock impulses, the maximum dry density of soil and the values of the mechanical characteristics after achieving the project degree of soil compaction. For identification of optimum soils indexes the standard and modification Proctors' tests were used.

The second stage consisted of the control of soil type brought to the site, fixation of the type of compacting mechanism, mode and number of passages on one track and measuring the thickness of layers on hooks before and after compaction. Third stage – sampling soil from each layer of cushion and their laboratory tests (compression, direct shear, penetration).

3 STATISTICAL ANALYSIS OF EXPERIMENTAL DATA

3.1 *Methods of statistical analysis*

The passive single-way analysis of variance plan of experiment for obtaining statistical data of physical and mechanical properties of compacted soil and variability of technological factors making the research program (Augusti G., 1988) was used. Using multi-way analysis of variance the mutual influence of variability of layers thickness, soil grain-size distribution, number of passages on one track and mode of compacting mechanism on variability of compacted soil characteristics was determined.

Mean value (expectation) for discrete and continuous RV is defined by (1):

$$\bar{x} = \sum_{i=1}^{n} P_i x_i \; ; \; \bar{x} = \int_{-\infty}^{+\infty} x \cdot f(x) dx \, , \tag{1}$$

where P_i = probability value x_i; x_i = possible values x; $f(x)$ = density of probability of continuous RV.

Dispersion for discrete and continuous RV is defined by (2):

$$\overset{\cap}{x^2} = \sum_{i=1}^{n} P_i (x_i - \bar{x})^2 \; ; \; \overset{\cap}{x^2} = \int_{-\infty}^{\infty} (x - \bar{x})^2 f(x) dx \, , \tag{2}$$

Deviation (mean root square deviation) σ and variation coefficient v are defined by (3):

$$\sigma = \sqrt{\overset{\cap}{x^2}} \; ; \qquad v = \sigma / x \tag{3}$$

Central moments of k-th degree for discrete and continuous RV are defined by (4):

$$\mu_k(x) = \sum_{i=1}^{n} P_i (x_i - \bar{x})^k \; ; \; \mu_k(x) = \int_{-\infty}^{\infty} (x - \bar{x})^k f(x) dx \, , \tag{4}$$

Asymmetry (skewness) A and excess (kurtosis) E are defined by (5):

$$A = \mu_3 / \sigma^3, \; E = \mu_4 / \sigma^4 - 3, \tag{5}$$

where μ_3, μ_4 = central moment of third and fourth order respectively.

Estimation of approximations of RV of characteristics of compacted soils, overburden rock and their mixtures in cushion is based on these types of distribution laws:

1) normal distribution (Gaussian distribution):

$$p(x) = \frac{1}{\sigma_x \sqrt{2\pi}} \exp\left(- \frac{(x - \bar{x})^2}{2\sigma_x^2} \right), \tag{6}$$

where x = RV; n = number of values.

2) logarithmically normal (log-normal) distribution:

$$p(x) = \frac{1}{\sigma_z \sqrt{2\pi}} \frac{1}{z} \exp\left(- \frac{(\ln x - \bar{z})^2}{2\sigma_z^2} \right), \tag{7}$$

where $\bar{z} = \ln \bar{x}$; $\sigma_z = \sigma_{\ln x}$. Parameters of logarithmically normal law: mean value $\bar{x} = \exp(\bar{z} + \sigma_z^2/2)$; deviation $\sigma_x^2 = (\exp(\bar{z} + \sigma_z^2/2))(\exp(\sigma_z^2) - 1)$; asymmetry $A = (\exp(\sigma_z^2) + 2)\sqrt{(\exp(\sigma_z^2) - 1}$; median $Me = \exp(\bar{z})$; mode $M_0 = \exp(\bar{z} - \sigma_z^2)$.

3) distribution that can describe a Gram-Charlier's range:

$$p(x) = \frac{1}{\sigma_x \sqrt{2\pi}} \exp\left(-\frac{(x - \bar{x})^2}{2\sigma_x^2} \right) \cdot \left(Ex^4 + Ax^3 - 6Ex^2 - 3Ax + 3E + 1 \right), \quad (8)$$

where $A = \mu_3/6\sigma^3$; $E = (\mu_4 - 3\sigma^4)/(24\sigma^4)$.

4) exponential distribution

$$p(x) = 1/\bar{x} \cdot \exp(-x/\bar{x}), \quad (9)$$

5) polinomial-exponential distribution

$$p(x) = \exp\left(C_0 + C_1 x + C_2 x^2 + C_3 x^3 + C_4 x^4 \right), \quad (10)$$

where $C_0 \ldots C_4$ = polynomial coefficients, which are determined by estimation of mean value, deviation, asymmetry, excess and central moments of 1-4-th degree by solving the nonlinear equations.

Strength characteristics of soil (c & φ) are totality of two RV (system of two RV). Geometrically it is interpreted as a random point with coordinates (c; φ) or random vector that is directed from the beginning to the point (c;φ). Distribution function of random vector is the probability of simultaneously realization of two inequalities: $X < x$ and $Y < y$, scilicet, $p(x,y) = P((X < x)(Y < y))$. For such distributions the central moment of k+s-th-degree for discrete and continuous RV is defined by (11):

$$\mu_{k,s}(x,y) = \sum_{i=1}^{n} P_i (x_i - \bar{x})^k \left(y_i - \bar{y} \right)^s ; \quad \mu_{k,s}(x,y) = \int_{-\infty}^{\infty} \left(x - \bar{x} \right)^k \left(y - \bar{y} \right)^s f(x,y) dxdy , \quad (11)$$

Approximation of random distribution function $F(c, \varphi)$ was done on the basis of normal or logarithmically normal law (depending on that, which distribution law will have each of the RV).

$$p(c,\varphi) = \frac{1}{\sigma_c \sigma_\varphi \sqrt{2\pi}} \exp\left(-0{,}5 \left(\frac{(c - \bar{c})^2}{\sigma_c^2} + \frac{(\varphi - \bar{\varphi})^2}{\sigma_\varphi^2} \right) \right);$$

$$p(x) = \frac{1}{\sigma_{\ln c} \sigma_{\ln \varphi} \sqrt{2\pi}} \exp\left(-0{,}5 \left(\frac{(\ln c - \ln \bar{c})^2}{\sigma_{\ln c}^2} + \frac{(\ln \varphi - \ln \bar{\varphi})^2}{\sigma_{\ln \varphi}^2} \right) \right), \quad (12)$$

To check the adequacy of the adopted theoretical distribution law, the Pearson's test χ^2 was used.

3.2 *The volume of experimental sampling*

As a result of field studies, the RV sampling of test characteristics and technological parameters were obtained. Their number was for: humidity w $n = 100$, dry density of soil ρ_d $n = 55$, angle of internal friction φ and unit cohesion c $n = 78$ in horizontal rings and $n = 28$ – in vertical (object № 1); w $n = 155$, ρ_d $n = 140$, unit soil penetration resistance R $n = 104$ (object № 2); humidity w $n = 3000$, dry density of soil ρ_d $n = 3000$, angle of internal friction φ and unit cohesion c $n = 50$, modulus of deformation E $n = 1500$, measurements of passages on one track by compacting mechanism $n = 20$ and layer thickness $n = 100$ (object № 3).

3.3 *Results of statistical analysis*

To describe the experimental distribution of physical characteristics RV of compacted soils it is reasonable to use the normal distribution law and for dry density of soil mixture – polinomo-exponential distribution. Graphical interpretation of these results is shown in Figure 1.

Deformation modulus E of compacted soils and their mixtures it is better to describe by log-normal law. Statistical parameters of these RV depend on the pressure in the oedometer. Research results are

presented in Figure 2. Angle of internal friction φ and unit cohesion c of compacted soils and their mixtures are random vectors and are best described by normal and log-normal distribution laws. Graphical interpretation of research results is shown in Figure 3.

4 PROBABILISTIC DESIGN OF FOUNDATIONS ON SOIL CUSHIONS

4.1 *Grounds of application of the probability design theory for estimation the TDS of foundations artificial bases*

To apply the design scheme as linearly-deforming half-space basis for determining its settlement it is necessary that the average pressure under the foundation should not exceed the soil design strength R. The value of R is a RV due to variability of internal friction angle φ, unit cohesion c and soil unit weight γ, which are included as arguments to the function $R = f(\varphi, c, \gamma)$. The pressure under the foundation p is also RV because loads and actions are random.

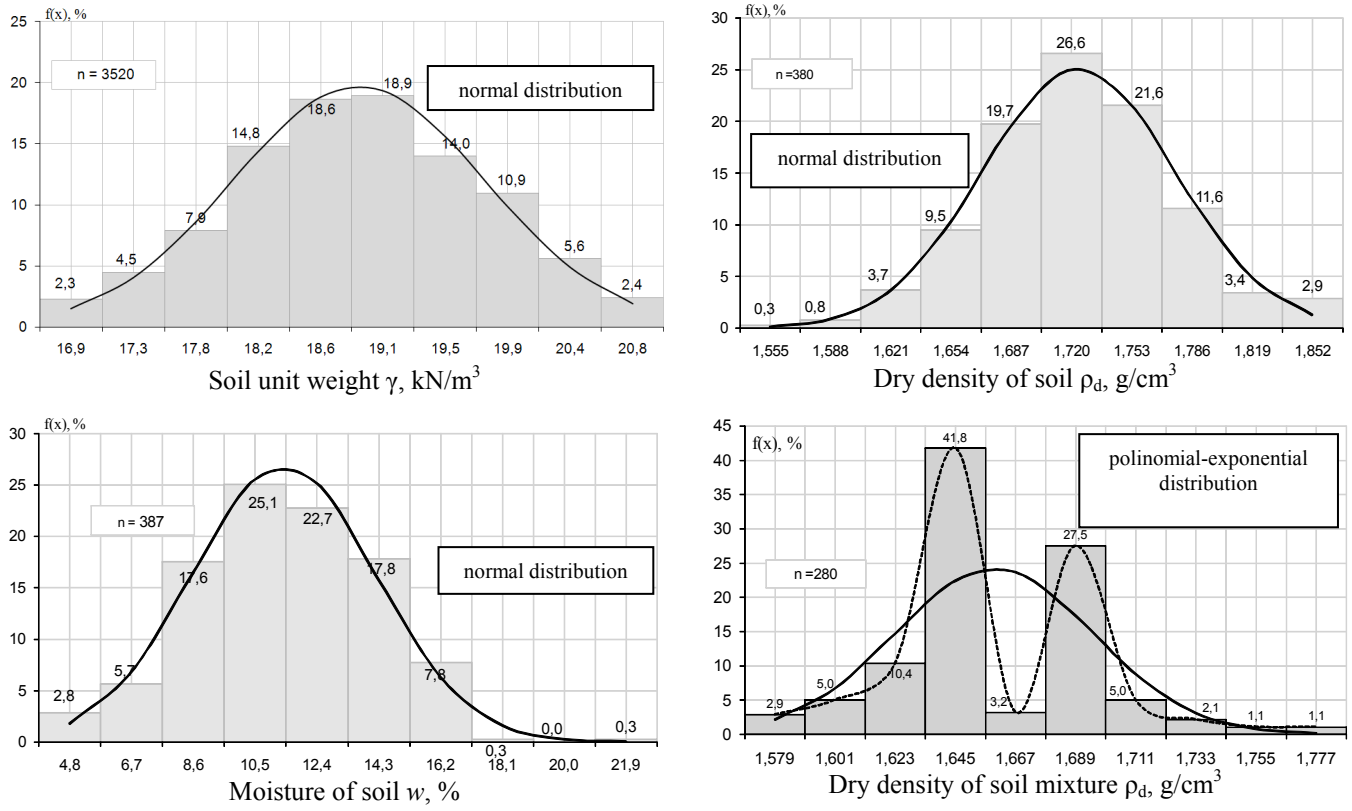

Figure 1. Density distribution diagrams of random variables of soil physical characteristics of cushions: n – number of random variables

Application limit of base model as a linearly-deforming half-space to calculate the settlement of the foundation using function of random arguments $\widetilde{Q} = \widetilde{R} - \widetilde{p}_0$ is presented in Figure 4.

Values of foundation settlement S_L at linear stage of soil deformations are also function of random arguments due to variability main modulus of deformation E, which varies within a layer by the applied law.

The modulus of deformation E depends on the type and condition of the soil, the additional stress in the layer. The additional vertical normal stress in soil σ_{zp}, which depends on distribution of foundation external load (Pichugin S.F., 2009, Rethaty, 1988), and the soil unit weight σ_{zg0} that lies above foundation are influenced by the settlement variability. These parameters are included as arguments to the function $S_L = f(E, \sigma_{zp})$.

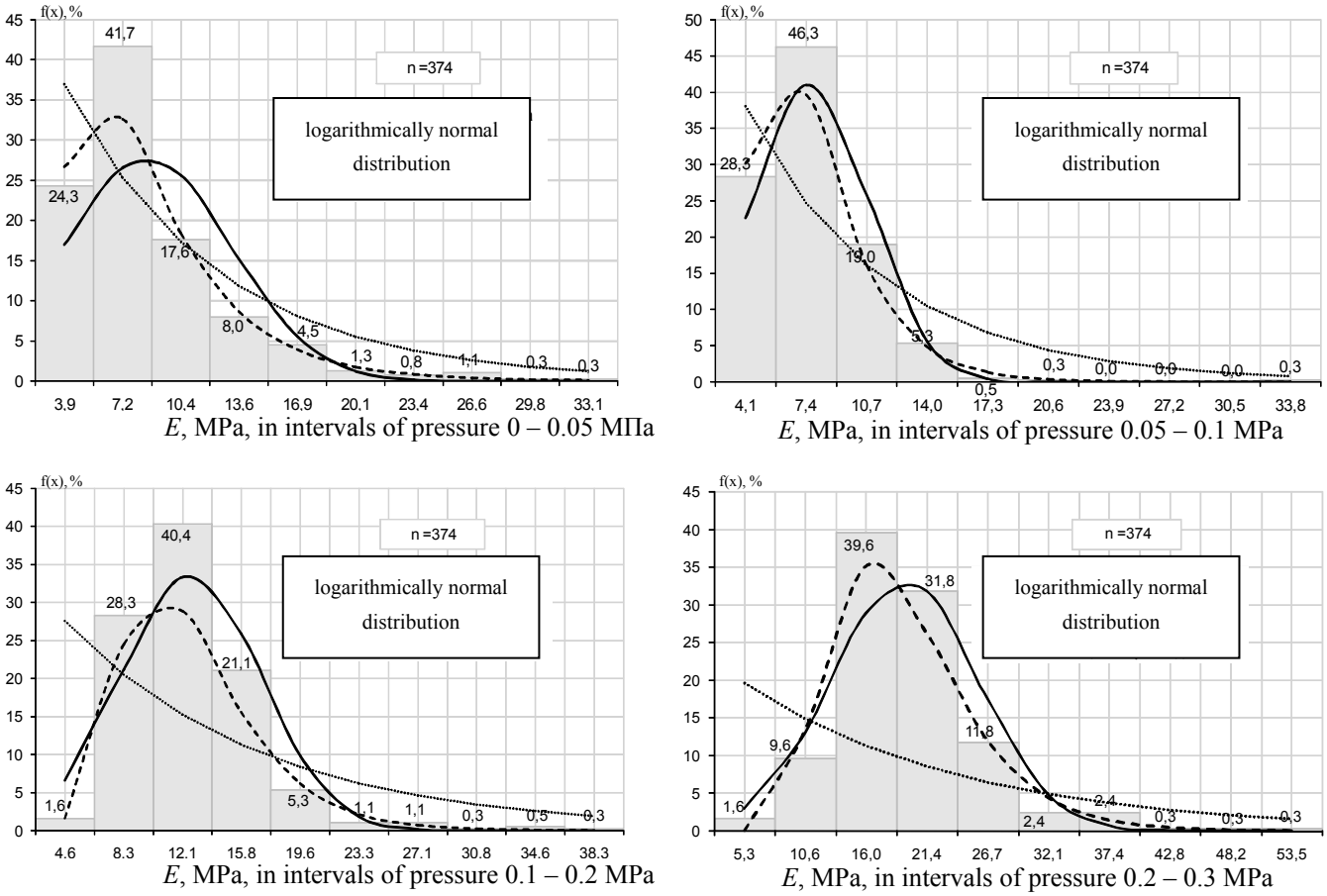

Figure 2. Density distribution of random variables of soil deformability characteristics of cushions: n – number of random variables

Around plastic deformations zones the nonlinear settlement S_{NL} of bases foundations take place. These values are also RV due to variability of foundations settlements by pressure p equal to the soil design strengths R, the soil ultimate strength p_u and vertical stresses of its own weight of soil at the bottom of foundation σ_{zg0}. This is due to the heterogeneity of physical and mechanical soils properties. These parameters are included as arguments to the function $S_{NL} = f(p, R, p_u, \sigma_{zg0})$.

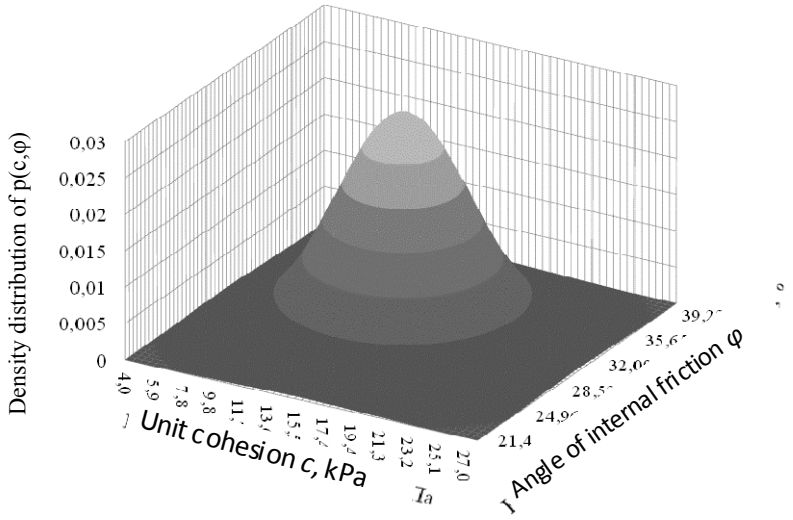

Figure 3. Density distribution of random variables of soil strengths characteristics of cushions

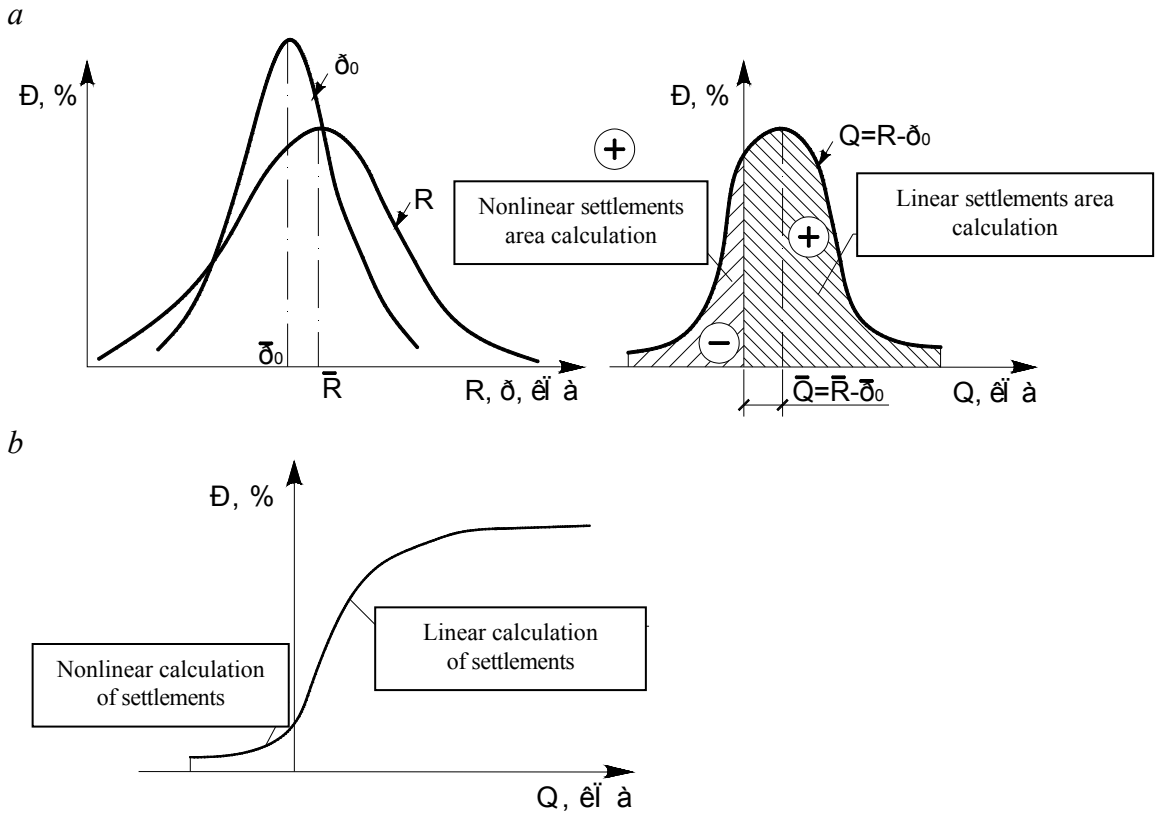

Figure 4. Graphical interpretation of determination of probability of limits of application of base model as a linearly-deforming half-space to calculate the settlement of the foundation: *a* – random variables distribution of soil design strength *R*, pressure under foundation base p_0 and function *Q*; *b* – integral distribution diagrams of random variables of function *Q*

4.2 *Probability design of artificial bases*

The statistical distribution parameters of RV of soil design and ultimate strengths (Table 2) using methods of linearization, Monte-Carlo (Raizer V.D., 1995), A.S. Lychov's, 2008, V.P. Chirkov's, 2006, and experimental data of RV of compacted soils characteristics were obtained. The statistical distribution parameters of RV of foundations settlements on single- and multi-layered soil cushions in linear stage and accounting the limits of variability of bases linear deformation were obtained (Figure 5).

4.3 *Probability design of TDS of soil cushions by numerical simulation method*

The simulation results of TDS of artificial bases by MUE using the elastic-plastic model and Monte-Carlo method with 10^4 iterations (Won J.Y., 2009, Zeigler M., 2006, Staveren M.T., 2009) are shown in Figure 6. Comparative analysis of statistical characteristics of foundations settlements for single- and multi-layered soil cushions by different methods of probability design are presented in Table 3.

Table 2. Statistical parameters of random variables distribution of design and ultimate strengths of compacted soil

Characteristic name	Simulation by		
	approximating polynomial	Monte-Carlo method	O. Lychov's and V. Chyrkov's methods
Mean value, кПа	268.3/1208.5	273.5/1606.3	276.2/1660
Deviation, кПа	59.6/442.3	59.6/550.3	102.8/621.1
Variation coefficient, %	22.2/36.6	21.8/34.4	36.3/37.5

Compacted soil design strength *R* / Compacted soil ultimate strength p_u

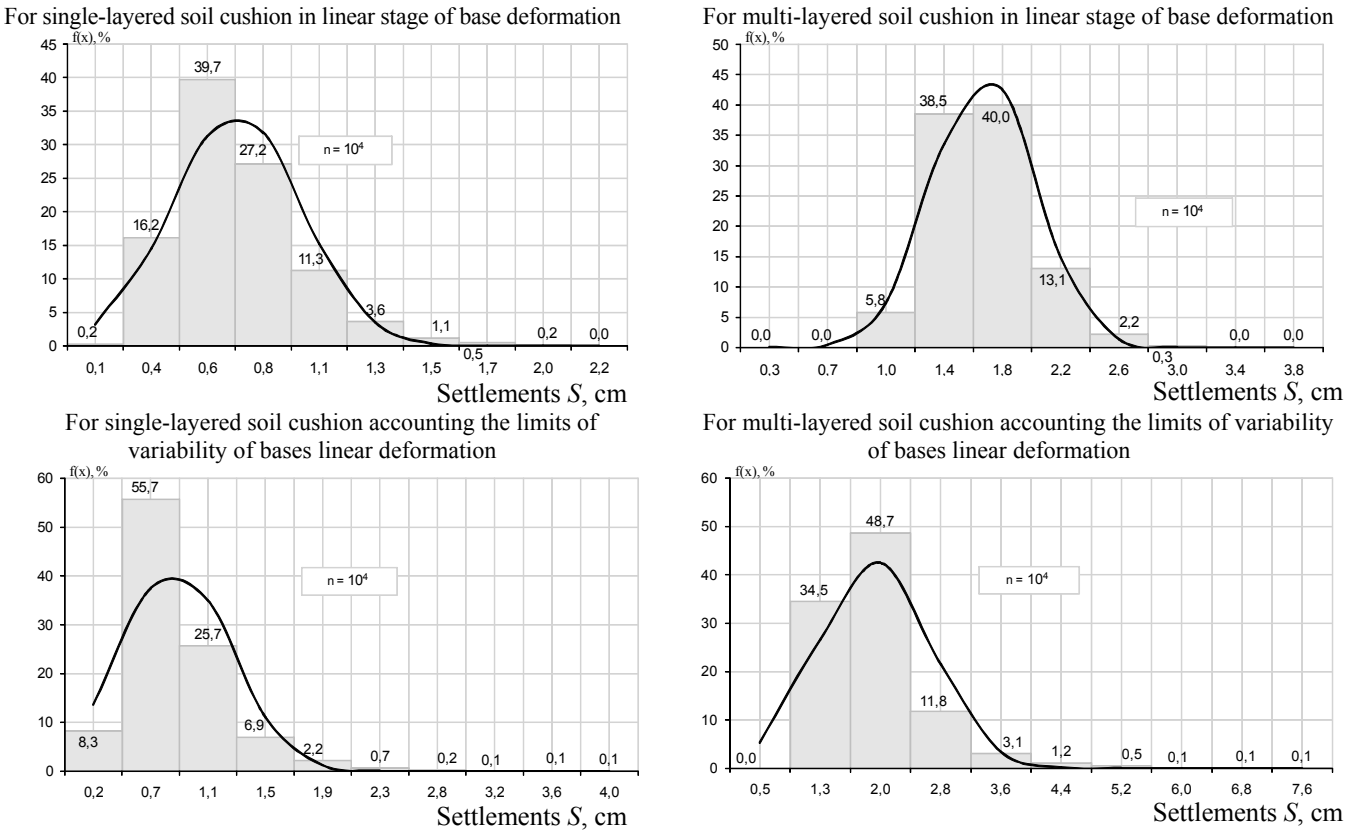

Figure 5. Density distribution of random variables of foundations settlements on cushion according the results of statistical simulation: n – number of random variables

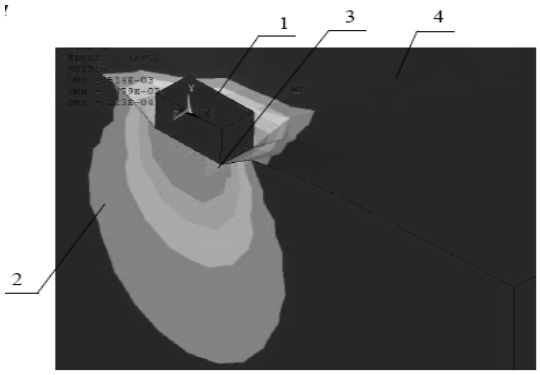

1 – foundation; 2 – distribution of deformations in soil; 3 – zone of plastic deformations; 4 – fragment of compacted soil massif

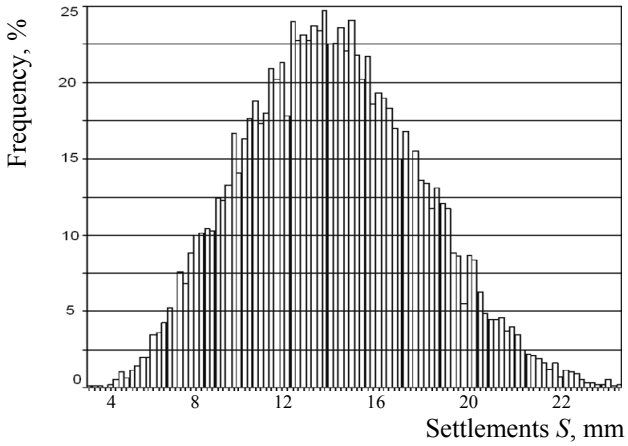

Figure 6. Results of numerical simulation by method of ultimate elements in the probabilistic formulation

Table 3. Comparative analysis of statistical characteristics of foundations settlements for single- and multi-layered soil cushions

Characteristic	Foundation settlements in linear stage of base deformation				Foundation settlements taking into account the limits of variability of bases linear deformation		
	Linearization method		Monte-Carlo method		Single-layered cushion		Multi-layered cushion
	Single-layered cushion	Multi-layered cushion	Single-layered cushion	Multi-layered cushion	Analytical	MUE	Analytical
Mean value, cm	0.67	2.07	0.72	1.7	0.83	1.35	1.98
Deviation, cm	0.22	0.46	0.26	0.33	0.39	0.54	0.69
Variation coefficient, %	33	22	37	19	47	40	35
Probability of failure (excess $S > S_u = 10$ cm)					(S_u-S_{MV} >>5σ)		

CONCLUSIONS

For physical soils properties of cushions the correct application of the normal distribution law, for soil mixtures – polinomial-exponential distribution, for modulus of deformation of soils and soil mixtures – log-normal distribution, for angle of internal friction of soil – normal distribution, for unit cohesion of soil – log-normal distribution has been grounded. By comparison of variation coefficients of characteristics of natural and compacted soils it was proved that in cushion the soil is more homogeneous than in natural state. Variation coefficient of soil dry density is 2 – 4.4 %, moisture – 23 – 36 %, soil unit weight – 4 – 4.6 %, soil modulus of deformation – 33 – 57 %, angle of internal friction of soil – 11 %, unit cohesion of soil – 25 %.

The variation coefficient of design strength of compacted soil is 21.8 – 36.3 %, the ultimate strength – 34.4 – 37.5 %. Therefore the probabilistic approach shows that even without excess pressure under the foundation the design strength of soil is probability as linear so non-linear stages of base deformations. It is due to variability of characteristics of compacted soils and random loads on foundations. The simulation of TDS of artificial bases by MUE using the elastic-plastic model and Monte-Carlo method correctly describes the deformation of cushions. For multi-layered cushion the variation coefficient of settlement v_s is less than single-layered, while mean value of settlement is 2.4 times more. Ratio v_s increases with increasing heterogeneity of layers, particularly by larger compressibility of the upper layers than subsoil and by increasing the ratio of modulus of deformation in them. The way of cushions erection with different degrees of layers compaction reduces the variability of foundations settlements. The failure probability of cushion according to safety characteristics is acceptable $\beta = 4.82 > 3$. According to the criterion of relative differential settlements of foundations on single-layered cushion the failure probability reaches 10 % by ultimate value $(\Delta S/L)_u=0.002$ and 3 % by $(\Delta S/L)_u=0.004$. For multi-layered cushion, these values are only 0.02 % and 0.0006 %.

REFERENCES

Augusti, G., Baratta, A., Casciati, F., 1988. Probabilistic methods in structural Engineering. London, 584 p.

Bugrov, A.K., Shilin, V.G., 2003. Determination of probabilistic characteristics of soil active pressure by Monte Carlo method. Cites Reconstruction and Geotechnical Engineering, P. 92–94.

Chirkov, V.P. 2006. Applied methods of reliability theory in structural analysis. Moscow, 620 p.

Ermolajev, M.N., Miheev, V.V., 1976. Probability of bases and foundations. Leningrad, 152 c.

Garagash, B.A., 2004. Reliability of space controlled systems "structure – foundation" at the different deformation base. Sochi, 908 p.

Goldshtejn, M.N. 1971–1979. Mechanical soil properties. Moscow, V. I, 368 pp., V. II, 375 pp., V. III, 304 p.

Harrop-Williams, K., Ejezie, S. 1985. Stochastic description of undrained soil strengths. Canadian Geotechnical Journal, 422–437.

Look, B., Wijeyakulasuriya, V. 2009. Statistical models for reliability assessment of rock strength. Proc. of the 17th International Conf. on Soil Mechanics and Geotechnical Engineering, Olexandria, Egypt, 60–63.

Lychev, A.S., 2008. Reliability of Building Structures. Moscow, 184 p.

Marijanovij, P., Ivankovic, T., Kovac, I. 2003. Geotechnical parameters as indicator of geotechnical risk. Proc. of the XIIIth European Conf. on Soil Mechanics and Geotechnical Engineering, Prague, P. 699–706.

Mlynarec, Z., Tschuschke, W., Wierzbicki, J. 2005. Statistical criteria of determination of homogenous geotechnical layers. Proc. of the 16th Internat. Conf. on soil Mechanics and Geotechnical Engineering, Rotterdam Mill press Science Publishers, 725–728.

Neher, H.P., Vogler, U., Peschl, G.M. 2003. Deformation of soft tailings – Probabilistic analysis. Proc. of the XIIIth European Conf. on Soil Mechanics and Geotechnical Engineering, Prague, P. 173–179.

Pichugin, S.F., 2009. Reliability of industrial building steel structures. Poltava, 452 p.

Raizer, V.D. 1995. Analysis of structural safety and design code making procedures. Moscow, 352 p.

Rechenmacher, A.L. Medina-Cetina, Z., Ghanem, R.G. 2005. Calibration of heterogeneous, probabilistic soil models. Proc. 16th International Conf. on Soil Mechanics and Geotechnical Engineering, Osaka, P. 851–854.

Rethaty, L. 1988. Probabilistic solutions in geotechnics. – Budapest, 520 p.

Santos, E.C.G., Vilar, O.M., Assis, A.P. 2009. Statistical analysis of geotechnical parameters of recycled construction and demolition waste. Proc. of the 17th International Conf. on Soil Mechanics and Geotechnical Engineering, Olexandria, Egypt, 112–115.

Staveren, M.Th., Bles, T.J.,. Litjens, P.P. 2009. Geo Risk Scan – a successful geo management tool. Proc. of the 17th International Conf. on Soil Mechanics and Geotechnical Engineering, Olexandria, Egypt, 2657–2660.

Ter-Martirosyan, Z.G. 2010. The mechanical properties of heterogeneous soils. Proc. of the International Geotechnical Conf, Moscow, V. 4, p. 1391–1395.

Van Impe, W., Verastegui, R. 2007. Underwater embankments on soft soil: a case history. London, 140 p.

Vynnykov, Y.L., Kharchenko, M.O. 2010. The peculiarities of soil large area cushions erection of overburden rock. Proc. of the International Geotechnical Conf, Moscow, V. 3, p. 1024–1031.

Won, J.Y. 2009. A probabilistic aproach to estimate one-dimensional consolidation settlements. Proc. of the 17th International Conf. on Soil Mechanics and Geotechnical Engineering, Olexandria, Egypt, 2012–2015.

Ziegler, M. 2006. Safety and risks in geotechnical engineering. Active Geotechnical Design in Infrastructure Development: proc. of the XIIIth Danube-European Conf. on Geotechnical Engineering, Ljubljana, P. 89–101.

ISGSR 2011 - Vogt, Schuppener, Straub & Bräu (eds) - © 2011 Bundesanstalt für Wasserbau ISBN 978-3-939230-01-4

Knowledge Based Risk Controlling

J. Zimmermann
Lehrstuhl für Bauprozessmanagement und Immobilienentwicklung, Technische Universität München, Munich, Germany

W. Eber
Lehrstuhl für Bauprozessmanagement und Immobilienentwicklung, Technische Universität München, Munich, Germany

ABSTRACT: Safety, reliability and risk analysis and management are the keywords in engineering these days. Yet while technical solutions are in many respects extended by safety margins of 30 to 70% commercial risks are limited to surcharges of the order of 1% forced by the actual market situation. In this respect a proper and sensible management of risk is the key to handle constructional and mechanical questions as well as operational challenges. The presented approach implies modeling the development of knowledge regarding a specific risk, based on both the physical manifestation and the awareness of risk and a representation of the actual project by some explicit parameters like complexity, connectivity and sensibility. Based on these elements the unknown and unforeseeable consequences of a risk given only by probabilities but in case of occurrence ruling out every schedule can be replaced by well defined measures. We expect such an approach of controllability to provide alternative means to handle risks both on constructional as well as on operative tasks even if statistical methods fail. The remaining risk is well defined while the actual hazard is compensated by measures which generate costs but can be kept within affordable and calculable limits.

Keywords: risk evaluation, strategic planning, system complexity and connectivity, risk management

1 INTRODUCTION

All entrepreneurial activity is characterized by handling risk in a proper way. This concerns technical risk issues in the same way as it concerns commercial risk. In both cases all possible needs to be done to avoid certain situations which cause injury to persons or damage to objects. This includes physical impairment as well as financial distress to individuals and companies. In a somewhat more abstract view to such situations all hazard must be avoided to some degree and therefore their variation is only a matter of scaling. Based on this we propose a general approach to deal with the probability of risks and an adequate description of methods to avoid safety hazard.

2 RISK MANAGEMENT

2.1 *Definition of Risk*

In order to define risk according to Zimmermann, Eber et al (2008) for a specific issue we consider a space of states given by the set of all existing variables where a state is defined as a point. Time is also considered one specific variable t. The development of a system is described as a path through the space of states. If all states and interactions are unambiguously defined the development of a system can be predicted with perfect precision for all times and no risk occurs. Yet as in general the development of some variables $r(t)$ is not completely foreseeable and therefore some deviation $\delta(t) = s(t) - r(t)$ from the expected path $s(t)$ occurs defined as risk. Figure 1 indicates an exemplary corridor of states along the time axis representing possible deviation paths $r(t)$ where for clearness the space of states is reduced to two dimensions as the ordinates.

Without losing generality this concept is applicable for the development of circumstances which affect the process of construction like e.g. the environmental temperature as a failure criterion for appropriate pouring concrete activities as well as the unforeseeable detailed properties of rock to be drilled and thus influencing strategies of securing measures.

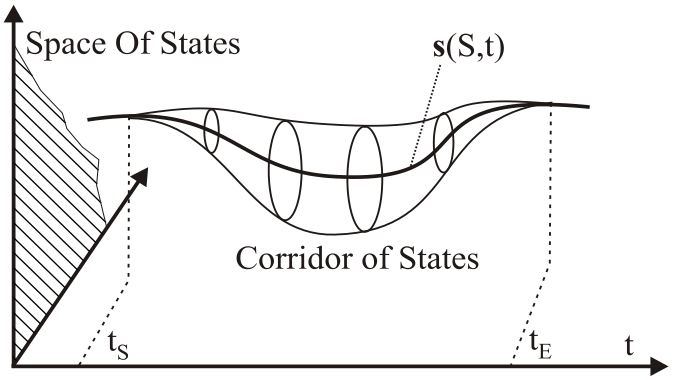

Figure 1. Deviation from an assumed path

Well known models make use of this concept by considering well determined functions of interaction between variables and adding a term representing uncertainty. E.g. the LEN-model represents the interaction of agent and principal regarding their individual interests and the resulting effort on a common project, see e.g. Picot et al (2008), which gives some recommendations about the agreements of the respective contract. In this model the wages are linearly modeled as $s(x) = s_0 + s_1 x$ where the production volume $x = x(a, \vartheta)$ is a function of the effort a and some unknown influencing circumstances ϑ which are only determined by a given distribution. Making use of exponential utility functions for both the participants (Principal: $G(x) = -e^{-\rho(x - s(x))}$ and Agent $H(s,a) = -e^{-r(s - V(a))}$) the resulting constant wages are $s_0 = H_0 - s_1^2 (1 - \sigma^2 \cdot r/2)$ while the optimal output related wage fraction turns out to be $s_1^{opt} = (1 + 2\sigma^2 \cdot r)^{-1}$. In the end the effort of the agent is optimized as $a_{opt} = s_1/2 = (2 + 4\sigma^2 \cdot r)^{-1}$. In such a context, insecurities obviously lead to a perceptible variation of strategies regarding the intended future behaviour in order to minimize risk, represented by the variance σ of the unknown parameter.

2.2 *Classical Risk Management*

Traditionally risk management focuses on the calculation of risk consequences in units of possible damage or injury to persons times the respective probability of the occurrence of risk. The integral of this product over time gives the overall risk of a specific parameter for the total system. In order to identify all possible risks tools like checklists and risk maps are used as completeness of the list of risks considered is essential to any strategic decision about handling the situation. After that, risks are classified into groups by criteria allowing to treat them accordingly, e.g. “insignificant”, “reasonable”, “fatal”, “existence threatening”.

Some of the identified risks can possibly be transferred to other units or organizations; some can be secured by purchasing appropriate insurances. Sometimes modifying technical methods, designs or schedules allow eliminating risks completely or at least minimizing them. After that risks can be sorted to criteria regarding the probability of occurrence or the possible hazard consequences. On this background finally strategic considerations may lead to specific decisions about the remaining risk which is to be borne or ignored.

2.3 *Surcharges due to Risky Issues*

Since the direction of $\delta(t)$ is not determined further, this approach is capable to handle losses as well as gain. In general symmetry should be expected regarding loss and gain, but for some other reasons, which are not to be discussed here, it is known that the loss side weights much more. This is well understood as chances are gladly accepted while negative risks in many cases need to be avoided absolutely. Yet this property results from characteristics of the mental attitude while scheduling and does not affect the concept presented here.

Risks that cannot be transferred to other organizations need to be covered or ignored. Therefore the conventional method to deal with commercial risks is to add surcharges to calculated costs. The technical pendant to such measure is to add safety margins to parameters responsible for stability.

Therefore the question of the amount of safety i.e. volume of surcharges or safety margins becomes crucial in every respect. In many cases an expedient value can be derived from the mean value of the respective risk resulting in the average gain or loss over a sufficiently high number of trials. Yet average processing requires the solution of at some problems:

At first all statistical estimations are based on high numbers of trials which are given only in very few cases. In most situations only probabilities for the occurrence of single events are derived from the frequency of occurrence of a number of investigated projects. Yet probabilities give absolutely no information about the single event, neither for a specific commercial project nor for the absolute stability of a mechanical situation. Therefore as long as only probabilities are given and not absolute limits or at least limits which are violated with definitely ignorable probability, no statement can be made for a single situation.

Secondly it turns out to be difficult to find a sufficient number of experienced situations to form a valid database for statistical investigations. On some aspects, specifically regarding constructional details there are sets of data available e.g. in steel construction. In some other respects most of the situations available for investigation differ too much to be taken representative which is certainly typical for production processes and supposedly for most of the processes dealing with natural resources like geotechnical.

Thirdly in consequence every surcharge based on average situations is invalid for a specific situation. In case of an occurring risk the maximum hazard is pending instead of a mean hazard even if the probability of occurrence was originally low enough to expect only bearable consequences. On the other hand if the considered risk does not turn up every surcharge becomes obsolete and too large. As a consequence such experience is likely to lead to ignoring risks as the evaluation is based on a subjective background. Any parameter calculated correctly in order to fulfill the determined requirements and increased by a surcharge which meets the real average risk is likely to be abolished in the run-up because no contract and no tender will be accepted on this basis. Yet the personal acceptance of risk and risk hazard is commonly very low, safety is on high priority due to good reasons.

Finally decisions are made due to the theory of decisions not on the “basis of risk” if there are no determined values to rely on but on the “basis of insecurity”. In other words risk calculations are done but the final decision considers only well known facts i.e. crucial limits calculated from the possible results. If such processing fails risks tend to be ignored.

3 REDUCING RISK BY ACTIVITIES

3.1 *Understanding Risk Management*

Rarely formulated but widely used and in detail proposed by Zimmermann, Eber et al. (2008) is a very basic understanding of managing risks. The fundamental concept is the replacement of probabilities leading to insecure high efforts by specific activities which reduce the risk definitely to bearable remaining values but require the use of resources and acceptance of additional costs. In contrast to surcharges which will only in average cases cover the risk consequences i.e. are not applicable for unique situations, such activities are affordable constants leaving no unbearable risks.

3.2 *Risk in Construction Management*

Such measures are well known and widely used in construction management as well as in designing constructional details.

Figure 2 visualizes the development of secureness of the construction costs for a infrastructure project. Without making use of any activities no effort is spent on risk management and the expected costs are not obtainable. A first estimation of costs in early phases of a project where only very few valid information is available relies on known parameters like cost per m^2 usable area or net volume. These processes provide some good estimation, accurate enough to enable an investor to decide about terminating or continuing the project. The gain of accuracy is low at this stage but the spent effort is also limited. The resulting distribution of possible cost is symmetrical because the representation of the building by comparable projects includes incompleteness as well as overestimation. During the process of contracting the risk needs to be minimized further. This is done by detailed investigation of activities regarding scheduled methods,

duration and costs which again yields a very narrow distribution of possible costs but also requires additional effort raising the total sum. Further activities alike which we call explicitly "risk management" replace insecure parameters by secure activities accepting their additions costs. E.g. risky activities due to their explicit dependence on open parameters like weather conditions are modified by choosing a different method of production which is not affected by such situations but more expensive or disadvantageous in some other respect, yet acceptable. If done correctly we expect the distribution to become asymmetric due to the actively integrated limitation of insecureness at the top end. After all, the result is expected to match the predictions on the basis of successful risk management.

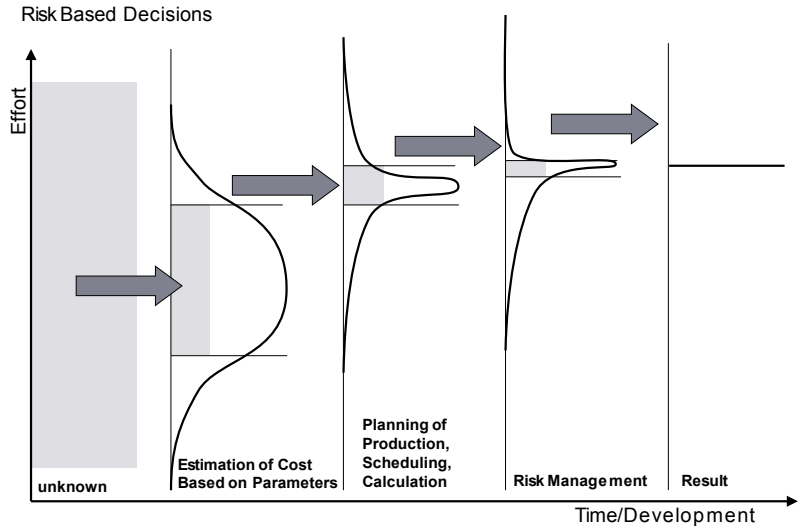

Figure 2. Development of Risk in Steps of Risk Management

3.3 *Risk in Mechanical Engineering*

Regarding constructional details the same procedure is well known: If the stability of a specific system is given only by a distribution of probabilities the respective dimensions are chosen to reduce the remaining risk to an acceptable measure:

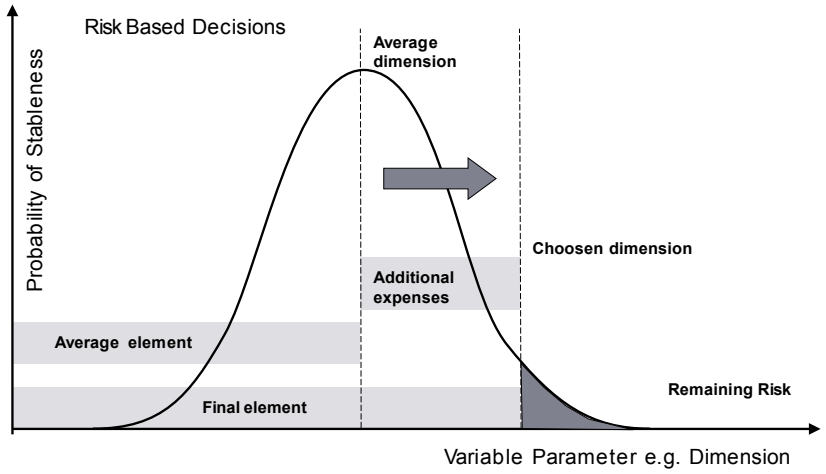

Figure 3. Development of Risk Regarding the Design of a Constructional Element

An element determined by the average stability will fail e.g. with a probability of 50%. Since a construction system usually comprises a set of elements where the failure of a single one or of very few elements already jeopardized the total system such proceeding is in no way acceptable. In this case it is of no great help that the other half of the elements is more stable than assumed due to the statistical distribution. The solution is to increase relevant dimensions, adopt additional expenses in order to reduce the risk of failure to an acceptably low remaining risk in accordance to the overall requirements.

3.4 *Insurance Risk Management*

Processes of insurance business are generally based on the same methods: A single individual is subjected to a particular risk, e.g. health risk or the risk of a car accident. The probability is fairly low but the possible hazard can be tremendous which leads to an unbearable situation. The average risk is taken to be acceptable but any expenses are superfluous if the risk does not occur. Yet if the risk occurs the consequences exceed every acceptable limit. In the view of the concerned individual a measure is required to limit the risk that is the expenses but cover the possible "worst case" consequences.

A large amount of individuals allows for a different point of view. The integral over all risks needs to be covered and is the sum of all risks or equivalently the average risk times the number of individuals. Therefore in this case an average risk is applicable due to the large amount of comparable situations and the existence of a mechanism to couple the individual situations.

Let an insecure value x_i e.g. the expected cost to cover a specific event be described by a distribution of probability $P_i(x)$ and the risk R_i be given by the variance $R_i \sim \sigma_i^2$. For a single individual respectively a single risk issue the squared risk is just $\sigma_i^2 = \int dx_i \left(x_i - x_{m,i}\right)^2 P_i(x_i)$. The cumulated risk of two events of equal distribution is given by the convolution $P_2(x) = \int dx' P_1(x') P_1(x_i - x')$. Continued to higher number j of cumulated situations we find a sequence of convolutions: $P_j(x)$. The solution can be obtained by means of simulation but can be for a basic example shown on the distribution according to A. K. Erlang. The Erlang distribution describes the additive accumulation of a number of elements which are equally given by originally exponential distributions. The resulting distribution is in dependence of the number of elements z and the mean value x_m:

$$P(x) = \frac{z}{x_m (z-1)!} x^{(z-1)} \exp\left(-\frac{zx}{x_m}\right) \qquad (1)$$

The standard deviation is easily derived as $\sigma^2 = x^2 / z$ and develops to zero with the rise of the number of elements. Therefore in order to level down risk to a ratio of only 10% of the mean value at least a number of $z = x^2 / \sigma^2 = (0,1)^2 = 100$ is required. Other distributions show different characteristics but the tendency is equivalent. The fact that mean values cannot be applied on single issues is trivial but this estimation allows to predict a minimum number of elements to be cumulated in order make use of averages. Figure 4 shows the development of risk reduction due to the accumulation of issues.

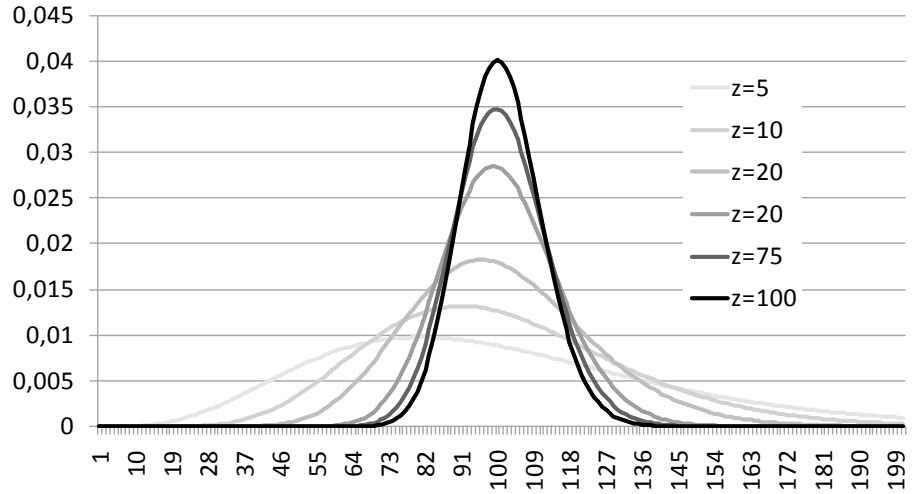

Figure 4. Development of Risk in Accumulating Situations

Thus insuring a risk – if possible – follows the same principle of implementing means to limit the risk taking into account the necessary expenses.

The remaining risk comprises two major elements. At first there is generally a remaining probability of risk consequences to exceed the insured hazard as for example the rare possibility of an extreme springtide. Secondly the risk of something unwanted to happen and causing unlimited hazard is converted to the limited risk of having spent limited effort to means which are probably not required.

4 RISK IN COMPLEX SYSTEMS

Considering risk and risk consequences becomes more difficult if complex systems comprising several parameters underlying different distributions of uncertainty are considered. Within systems not only the number of risky issues causes uncertainty but also their interaction introducing matters of risk propagation.

4.1 *Decomposition of Systems*

Derived from the theory of systems the uncertainty of a complex system can be reduced by decomposing to a number of subsystems. This concept is based on the assumption that on each separation process all interactions between the remaining subsystems are fully understood and can be formulated. Furthermore a system modeled as a graph comprises nodes and edges. Broken down to the finest possible resolution nodes and edges are most simple and contain only one variable or interaction. On this background the "volume" of nodes and edges can be rated equally valued regarding their contribution to the total system. Thus, the number n of separated subsystems implies a number $m = n(n-1)/2$ of fully understood relationships where not existing interactions are also taken as determinedly understood.

If a parameter of the total system can be estimated to an accuracy of ε we expect every subsystem to be estimated to the same degree ε. Yet the arrangement of the separated system comprises n insecure elements and a number of m secured interactions leading to a total insecurity of

$$\varepsilon_n = n \cdot \varepsilon / (n+m) = \frac{2 \cdot \varepsilon}{1+n} \qquad (2)$$

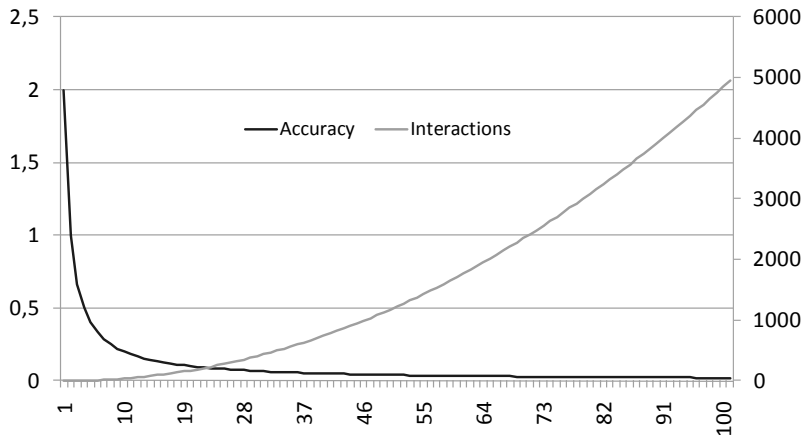

Figure 4. Reduction of Insecureness by the Introduction of Subsystems

The limit of such decomposing is given by the consideration of the validity of perfect knowledge of interactions. Since the number of relationships is increasing to the power of two the problem of identifying and really understanding every single interaction rises as well.

Nevertheless we can derive from such consideration that if the interactions are described well the overall risk decreases to dealing with single risks. Therefore we need to identify the network of interaction and the propagation of risk within the network.

4.2 *Impact of the Structure of Networks*

Networks of interaction can be modeled making use of graphs. Subsystems and their respective interaction are represented by nodes and edges where the presumption of causality of all interrelations requires the graph to be directed.

Any assumed propagation of risks $\delta Q > 0$ would definitively lead to infinite results if the existence of loops was not ruled out. Therefore we assume risk interaction diagrams to be network plans according to the definition of the theory of graphs, comprising one source, one sink and no loops. Such graphs can be sorted by ranks and a maximum number Γ of ranks can be determined. Furthermore the average number of sources for a closing node can be measured as the parameter ς of interoperability while the average number of sinks to a source node is measured as the parameter ξ of impact. Finally we describe the num-

ber of elements per rank through the parameter of parallel operations p. On this background the number of nodes affected can be estimated to $\Omega \simeq \Gamma \cdot p$

With no doubt the complete elimination of loops is not possible. Yet including loops obstructs any approach to analytical investigations. Therefore recursion is taken into account in a different way "spread" all over the otherwise well determined network and modeled as the parameter of recursion β, defined later.

5 RISK INTERACTION

Factors of success are defined as a set of production factors which are directly interfaced to the success of a project, easily to be measured and controlled and give a well established tool to control the progress of a project to success while the actual success cannot be measured and controlled directly and in advance.

The same structure can be made use of by defining factors of risk which can be measured and controlled in advance or during the progress of the project or system. This allows controlling the overall risk as long as the singular risk issues are identified in time and their interaction to the total risk is understood.

Such proceeding requires identifying factors of risk first, then defining their scheduled progression and finally monitoring them continuously. In order not only to observe deviations but to control those methods need to be found which allow acting upon these factors and closing the feedback loop. Only then a system can be kept within the designed corridor of states and occurring risks can be managed in a way that eliminates terms of probability.

5.1 *Composition of Risk in a Network*

In order to model risk issues as a number of ς risk factors the corridor of states requires a definition for each factor. Let every factor F_i contribute f_i to the production or development of a value Q during the process time t. Then we define the rate

$$\frac{\partial Q}{\partial t} = \prod f_i \qquad (3)$$

If all the factors are at the scheduled level the rate of production/development is on schedule and the production/development time as well as the desired quality or result will be on schedule too. Any deviation δf_i contributes to the overall development:

$$\frac{\partial Q}{\partial t} = \prod f_i = \prod (f_i + \delta f_i) = (f_1 + \delta f_1)(f_2 + \delta f_2)(f_3 + \delta f_3)\ldots \approx f_1 f_2 f_3 \ldots + \delta f_1 f_2 f_3 \ldots + \text{higher\_orders}$$

$$\frac{\partial Q}{\partial t} \approx F_0 + \sum \frac{\delta f_i F_0}{f_i} = F_0 \left(1 + \sum \frac{\delta f_i}{f_i}\right) = F_0 \left(1 + \sum \delta f_{R,i}\right) = F_0 (1 + \Delta), \qquad (4)$$

where $F_0 = \prod f_i$ is the scheduled rate and $\delta f_{R,i} = \delta f_i / f_i$ is the relative deviation of the risk factors. Furthermore the cumulated deviation is $\Delta = \sum \delta f_{R,i}$. If the parallel factors can be assumed to be independent of each other Δ is of the order $\sqrt{\zeta}$ otherwise and valid in most cases of the order ζ.

Normalizing the developing process to an average time of a step and to a standard production $F_0 = 1$ the risk propagation per step is estimated to $\delta Q \approx \Delta(\zeta)$ and the cumulated risk of a linear risk chain of length Γ comes to be $\delta Q_\Gamma \approx \Gamma \Delta(\zeta)$

5.2 *Risk Propagation in a Network*

The linear approach to the propagation of a risk is in most cases not applicable due to the complex structure of interacting factors. Yet the number of interactions is in general not as large as the theoretical limit given above and can therefore be reduced if the description of systems structure is known or can be derived. The following concept is taken from an approach estimating consequences of breaking up a system to subsystems. In the considered situation the volume to be dispersed is equivalent to the risk $\delta Q \approx \Delta(\zeta)$ of which we evaluate the consequences.

Let a system of volume $V (= \delta Q \approx \Delta(\zeta))$ influence and therefore be distributed on a number of Ω branches (sub nodes) using a tree structure. The volume of the subnodes is V / Ω if the risk is divided on

the branches otherwise as assumed here fully transmitted. Furthermore let any insecurity induced by a separation be given by the linear equation $T = \eta V + C$ as a fraction η of the respective volume and a constant value c due to the fact of the separation. Then the insecurity of the connecting node is $T_1 = \eta \cdot V + c$ while the insecurity of the new subnodes is $T_2 = \Omega \cdot (V \cdot \eta + c)$.

The affected subnodes are possibly interacting to some degree. This ranges from no interaction at all (i.e. $w = 0$) through the case of each node interacting with two next neighbors ($w = 2$) to systems where each node is actively connected to every other node ($w = \Omega(\Omega - 1)$). The complexity parameter $\alpha \in [0..1]$ allows modeling the variety of situations: $w = \Omega(\Omega^{\alpha} - 1)$. The increase of insecureness due to the additional interactions of the subnodes is accordingly $T_3 = \Omega(\Omega^{\alpha} - 1) \cdot (\eta \cdot V + c)$. The parameter α is understood as the ratio of the dimension of the space of states to the theoretically maximum dimension and for not too small values compatible to the definition of the degree of information according to Shannon (1948).

Finally each interaction of two subnodes is likely to cause the further need of adaption of adjacent nodes. Therefore the degree of transmitting insecureness from one node to another including the case of looped interaction needs to be modeled. The effective number of interactions can be formulated as $W = w \cdot \beta^0 + w \cdot \beta^1 + w \cdot \beta^2 + \ldots$ if the recursion parameter $\beta \in [0..1]$ represents the ratio of propagation. Since this is a geometric series we obtain $W = w \sum \beta^i = w(\beta^{\infty} - 1)/(\beta - 1) = w/(\beta - 1)$ and the additional insecureness is $T_3 = \Omega(\Omega^{\alpha} - 1)(\eta V + c) \sum_{i=0} \beta^i = \Omega(\Omega^{\alpha} - 1)(\eta V + c)/(1 - \beta)$.

5.3 *Development of a risk issue*

All together we model the development of risk as $T = \mu \eta V + \nu c$ where $\mu = \Omega(\Omega^{\alpha} - 1)/(1 - \beta) + \Omega + 1$ and $\nu = \Omega(\Omega^{\alpha} - 1)/(1 - \beta) + \Omega + 1$. The considered volume is given by $V = \delta Q \approx \Delta(\zeta)$. For sufficiently large Ω the linear terms as well as the constant terms are not significant. The factors are reduced to $\mu \simeq \Omega(\Omega^{\alpha} - 1)/(1 - \beta)$ and $\nu \simeq \Omega(\Omega^{\alpha} - 1)/(1 - \beta)$.

Thus the development of a risk issue throughout a complex system is characterized by

$$T \simeq \eta \Omega(\Omega^{\alpha} - 1)\Delta(\zeta)/(1 - \beta) + c \cdot \Omega(\Omega^{\alpha} - 1)/(1 - \beta) \qquad (5)$$

The second term is not dependant of the actual risk and therefore mirrors the generally acquired risk resulting from the fact that structures exist and cause multiple interrelations. This only leads to the nevertheless most important recommendation to keep structures clean and small.

In contrast to this the first term mirrors the development of a specific risk through a given structure. The character of the volume term is dominated by the parameter of complexity, the factor of recursion and the number of subnodes. Since the risk to be transferred is estimated in the chapter before, the ratio η can be assumed to be unity. In particular any development runs with the rise Ω to the power of α.

The parameter of complexity α is spread over all the structure. Therefore it is advisable to define the development by introducing ranks r. Since α is the ratio of existing interactions to possible interactions the expression $\alpha \cdot r/\Gamma$ equals the share of complexity for one step in the sequence of ranks. With this we obtain as a coarse estimation (where the $-\Omega V$ term compensates for the neglected linear term if β is small):

$$T \simeq \Omega(\Omega^{\alpha r/\Gamma} - 1)\Delta(\zeta)/(1 - \beta) \simeq \Omega^{1+\alpha r/\Gamma}\Delta(\zeta)/(1 - \beta) \qquad (6)$$

Thus the factor of risk propagation for the progression of one increment of ranks can be estimated to

$$\omega \simeq \frac{\Omega^{1+\alpha(r+1)/\Gamma}\Delta(\zeta)/(1-\beta)}{\Omega^{1+\alpha r/\Gamma}\Delta(\zeta)/(1-\beta)} = \frac{\Omega^{\alpha(r+1)/\Gamma}}{\Omega^{\alpha r/\Gamma}} = \frac{\Omega^{\alpha r/\Gamma}\Omega^{\alpha/\Gamma}}{\Omega^{\alpha r/\Gamma}} = \Omega^{\alpha/\Gamma} \qquad (7)$$

In considering Ω as the number of affected i.e. subsequent nodes in a structure we assume a node where risk propagation via different paths is counted only once and transferred only as one risk issue. As this is not valid in many cases we need to replace Ω by the number of affected nodes even if they are partly identical which leads to the use of $\widetilde{\Omega} = \xi^{\Gamma}$. Herewith we obtain:

$$T \simeq \xi^{\Gamma+\alpha r}\Delta(\zeta)/(1-\beta) \text{ and } \omega \simeq \xi^{\alpha} \quad (8)$$

Obviously the recursion factor only scales the propagation of risk but does not influence the character of propagation. On very simple models $\alpha = 0$ we obtain constant propagation as expected; i.e. every single risk issue is simply transferred to the final result. Yet as complexity rises to e.g. $\alpha = 0.1$ and structures expand to e.g. only 5 subsequent sink nodes per source we obtain clearly more than a factor of unity for every step of development which leads to exponential rise of effect.

6 CONTROLLING RISK

From the previously derived results we find clearly that there is no way to reduce risk by only reducing probabilities or risk hazard because of the complex structures of risk propagation which increase any value however small it is to unacceptably large consequences. From this we conclude the establishment of methods capable to control a risk during the time t in order to lead Q back to its originally intended value.

Preconditioned the risk to develop like $T \simeq \xi^{\Gamma+\alpha r}\Delta(\zeta)/(1-\beta)$, some recommendations can be derived: Measurement of the respective variables needs to be taken every interval or step r_0 and the deviation needs to be evaluated. Immediately, appropriate activities must be initiated to correct the situation. The power of correction λ following the same characteristics as the deviation itself is closely related to the accepted deviation value, the point of time/step/rank when the activity is started and the point of time (=step/rank) r_0 when the situation is expected to be completely returned to the initial state. Then the development of the deviation during steps r_d is to be compensated during the next γr_d steps. Thus we find: $\xi^{\Gamma+\alpha\gamma r_d}\Delta(\zeta)/(1-\beta) = \lambda\xi^{\Gamma+(\gamma-1)\alpha r_d}\Delta(\zeta)/(1-\beta)$ which solves easily to $\xi^{\alpha\gamma r_d} = \lambda\xi^{(\gamma-1)\alpha r_d}$ and thus a power of correction

$$\lambda = \xi^{\alpha\gamma r_d}/\xi^{(\gamma-1)\alpha r_d} = 1/\xi^{-\alpha r_d} = \xi^{\alpha r_d} \quad (9)$$

which allows to control deviation independent of steps/ranks.

The absolute deviation in this case is determined by the development of the risk issue at $r = r_d$ i.e.: $T \simeq \xi^{\Gamma+\alpha r_d}\Delta(\zeta)/(1-\beta)$, where we find evidence to the recommendation to initiate controlling mechanisms as soon as possible in order to keep the needed force of correction low as well as the deviation from the originally determined corridor of tolerated states.

7 CONCLUSION

In this paper we propose and introduce a fundamental description of dealing with risks, also pointing out possible measures to handle risk consequences even on projects where respective surcharges are limited to only minor values. The approach is based on the fact that the considered universe in a unique construction project in technical as well as in commercial respect is in general much too small to rely on any statistical result. We propose to make use of a well understood development of knowledge regarding the risk, based on both the physical manifestation and the awareness of risk which can be easily modeled as a function of the skills, education and structure of organization of the project team. The second factor of the model is a representation of the actual project by some explicit parameters like complexity, connectivity interoperability and impact which can be extracted from the project description in very early stages of the execution and are independent of scales. Such parameters allow modeling the controllability of the considered risk or as an alternative the risk consequences. Future investigation aims at deriving the parameters of interaction directly from non fictional interaction diagrams and normalizing them to scale free situations.

Based on these elements we propose to replace the unknown and unforeseeable consequences of a risk given only by probabilities but in case of occurrence ruling out every schedule by well defined measures. Such can be developed on the background of the derived controllability and valuated by parameters of efficiency and costs.

We expect such an approach to provide alternative means to handle risks both on constructional as well as on operative tasks even if statistical methods fail. The remaining risk is well defined while the ac-

tual hazard is compensated by measures which generate costs but can be kept within affordable and calculable limits.

REFERENCES

Claude Elwood Shannon: A Mathematical Theory of Communication. In: Bell System Technical Journal. Short Hills N.J. 27.1948, (July, October), S. 379–423, 623–656. ISSN 0005-8580

Arnold Picot/Helmut Dietl/Egon Franck (2008), Organisation - Eine ökonomische Perspektive, 5. überarbeitete Auflage Schäffer-Poeschel, Stuttgart

Grady Booch et al. (2007), Object-Oriented Analysis and Design with Applications, Addison-Wesley, New York

Hermann Haken (1983), Synergetik, Springer Verlag, Berlin, Heidelberg, New York, Tokyo

Fredmund Malik (2003), Systemisches Management, Evolution, Selbstorganisation, Haupt Verlag, Bern, Stuttgart, Wien

Dirk Sackmann (2003), Ablaufplanung mit Petrinetzen, Deutscher Universitäts-Verlag, Wiesbaden

A.-W. Scheer (1997), Wirtschaftsinformatik, Springer Verlag, Berlin

Manfred Schulte-Zurhausen (2002), Organisation, 3.Auflage. Verlag Franz Vahlen, München.

Frederic Vester (2001), Leitmotiv vernetztes Denken, Heyne Verlag, München

Norbert Wiener (1992), Kybernetik, Econ Verlag, Düsseldorf, Wien, New York, Moskau

Wiest, Jerome D. and Levy, Ferdinand K., A Management Guide to PERT/CPM, New Delhi: Prentice-Hall of India Private Limited, 1974

Zimmermann, J., Eber, W., Modelling Processes in Construction Management, 6th International Scientific Conference, Vilnius, Lithuania, ISBN-Nummer: 2029-4441, Business and Management 2010, selected papers, Volume I and II, Vilnius, Lithuania, Mai 2010

Zimmermann, J., Prozessorientierter Nachweis der Kausalität zwischen Ursache und Wirkung bei Bauablaufstörungen, Forschungsarbeit im Auftrag des Bundesamtes für Bauwesen und Raumordnung, ISBN-Nummer: 978-3-939956-12-9, München, November 2009

Zimmermann, J., Günthner, W.A., Eber, W., Haas, B., Lügger, M., Sanladerer, S., Logistik in der Bauwirtschaft - Status quo, Handlungsfelder, Trends und Strategien, ISBN-Nummer: 978-3-9811819-8-2, Bayern Innovativ, München, Oktober 2008

Zimmermann, J., Eber, W., Schieg, M., Nino, E., Risk Evaluation in Construction Management, Conference Business and Management 2008, Selected Papers, Volume I and II, Vilnius/Litauen, Mai 2008

ISGSR 2011 - Vogt, Schuppener, Straub & Bräu (eds) - © 2011 Bundesanstalt für Wasserbau ISBN 978-3-939230-01-4

Managing poorly quantified risks by means of national standards with specific reference to dolomitic ground

P.W. Day
Jones & Wagener Consulting Engineers, Rivonia, South Africa

ABSTRACT: The quantification of risk is fundamental to assessing its acceptability. When drafting codes of practice, the quantified risk is used in assessing the reliability of the structure and ensuring this complies with national norms. Problems arise in complex situations where rational determination of risk is difficult. An example is the development of dolomitic land where sinkholes or other forms of subsidence can result in severe damage to the built environment and loss of life. This paper describes the approach currently being adopted in South Africa for the drafting of national standards for the development of dolomitic land and the regulatory processes involved. It also looks at the steps taken to ensure that the standards are not unduly prescriptive.

Keywords: Dolomite, karst, risk management, standards

1 INTRODUCTION

1.1 *Outline of the Problem*

If engineers are capable of erecting buildings that reach 800m into the sky and suspension bridges with main spans just short of 2km, why should we be prohibited from developing on certain categories of dolomitic land? This is the dilemma faced by standards writers when trying to balance the rights of property owners with protection of the general public.

For many years, the South African authorities have discouraged commercial and residential development on dolomitic land where there is a high risk of subsidence. Only agriculture, recreational areas or essential infrastructure have been permitted in such areas. The inclusion of these restrictions in a draft national standard on the development of dolomitic land provoked a reaction from the geotechnical fraternity who questioned the underlying assumption that the hazards cannot be effectively assessed and addressed.

One also needs to question the logic of such a prohibition in the light of some telling statistics. To date, 38 fatalities are known to have been caused by dolomite subsidence events in South Africa (Department of Public Works, 2003). By contrast, the death toll on South Africa's roads for the 2009 calendar year alone was 13 768 (Road Traffic Management Corporation, 2010).

Despite these observations, one must recognize the difficulties that standards writers face when attempting to prescribe ways of ensuring that dolomitic land is developed in a manner that ensures people live and work in a safe environment. This paper looks at the options being considered and debated in South Africa at present to produce a standard that strikes the right balance.

1.2 *Some Background*

Gauteng is the smallest of South Africa's nine provinces, occupying only 1,4% of the area of the country. However, it houses 22% of the country's population and generates 33% of the national gross domestic product. The population density is sixteen times the national average at 660 persons per square kilometre.

Twenty percent of the province's land area is underlain by dolomite of the Malmani Sub-group. Certain of the formations that make up the 1,4km total thickness of dolomite that occurs in the area, particularly the chert rich formations, are prone to the formation of sinkholes and other forms of subsidence related to the dissolution of the dolomites. Some of the country's most densely populated areas, including parts of Pretoria, Soweto, Tembisa and Katlehong are underlain by dolomite. Against this background, the impact of prohibiting development on dolomitic land, or even on certain categories of such land, is self evident.

The two most common forms of dolomitic instability in South Africa are sinkholes and compaction subsidence (previously referred to as dolines). Sinkholes are formed by progressive collapse of the rubble arch above a void or cavity in the underlying residuum or dolomite rock which eventually daylights at the ground surface (Jennings, 1965, Brink 1979 & Wagener, 1982). The most common triggering mechanism is the ingress of surface water. Lowering of the water table also plays a crucial role as the voids which act as receptacles for collapsed material from above are typically present near the level of the original water table. Lowering of the water table exposes these voids and creates the potential for subterranean erosion of the overlying material giving rise to conditions conducive to sinkhole formation.

Compaction subsidences are also related to lowering of the groundwater table. In this case, compressible residuum from the dissolution of the dolomite, typically highly compressible wad, consolidates due to the increase in effective stress caused by lowering the water table, resulting in broad areas of surface subsidence.

Dewatering by the gold mines on the far West Rand during the 1950s and 1960s resulted in the formation of a number of major sinkholes and compaction subsidences, the worst of which was the catastrophic sinkhole which swallowed the West Driefontein Mine Crushing Plant in December 1962 resulting in the loss of twenty nine lives. Although lowering of the water table is now more strictly controlled in many urban areas, the increased potential for surface water ingress as a result of urban development has resulted in a acceleration in the number of sinkholes recorded during recent years. The Council for Geoscience in South Africa has a database of over 2 000 sinkholes, mainly in the Gauteng area.

2 REGULATORY ENVIRONMENT

Table 1 lists the various authorities who control the development of dolomitic land.

Table 1. Role of various authorities

Authority	Role	Guidelines / Standards issued	Comment
Local Authorities	Ensure health and safety of inhabitants within its jurisdiction, including management of geological risks. Approval of development plans.	Various, including dolomite risk management plans if appropriate.	Hampered by lack of skills and funding. Often ineffective.
Department of Public Works (Central Government)	Responsible for infrastructure development.	Appropriate development of infrastructure on dolomite: Manual for Consultants. September 2010.	DPW also involved in drafting of national standards and working groups on dolomite risk management.
Department of Water Affairs (Central Government)	Controls and regulates the water resources of the country including the abstraction of groundwater.	A guideline for the assessment, planning and management of groundwater resources within dolomitic areas in South Africa. Volumes 1 - 3.	Legislation in place but not adequately monitored or enforced.
National Department of Housing (Central Government)	Responsible for controlling and coordinating housing development.	Generic Specification GFSH-2: Geotechnical site investigations for housing development. September 2002.	Also controls the National Home Builders Registration Council.
National Home Builders Registration Council (NHBRC)	Provides a warranty scheme for new housing development. Sets standards and registers home builders.	Home building Manual, Parts 1, 2 and 3. February 1999.	Requires that all houses built on dolomite to have a dolomite stability report which must be submitted to the Council for Geoscience for confirmation that requirements have been met.

Authority	Role	Guidelines / Standards issued	Comment
Engineering Council of South Africa (ECSA)	Setting standards for registration of engineering professional and of professional conduct.	Rules of Conduct for Registered Persons: Engineering Profession Act (Act No. 46 of 2000).	Regards professional registration as a key measure of competence.
Council for Geoscience	Advises government on the judicious and safe use of land. Confirms dolomite stability reports submitted in terms of NHBRC requirements. Custodian of geological and geotechnical information.	Consultants guide: Approach to sites on dolomitic land. November 2007.	Plays a leading role in drafting national standards on dolomite and a controlling role in the approval of housing developments through NHBRC requirements.
South Africa Bureau of Standards (SABS)	Compiles national standards	SANS 1936, Parts 1 – 4. Development on dolomite land. (Currently being re-drafted). SANS 10400, Application of the National Building Regulations.	Redrafting of SANS 1936 being undertaken by a newly formed sub-committee comprising mainly geologists and geotechnical engineers.

By virtue of stipulations by the authorities in Table 1, some aspects of development on dolomitic land are regulated including abstraction of ground water, and the construction of housing and infrastructure. Although the guidelines issued by the Council for Geoscience specify permissible types of development and development densities for various dolomite hazard classes, the Council has no regulatory authority of its own except when it acts on behalf of the NHBRC or Department of Public Works in confirming the acceptability of dolomite stability assessments. In reality, commercial development is also regulated in that plans have to be approved by the Local Authority who may have their own guidelines in place or refer to the Council for Geoscience. Industrial and mining developments on dolomite are currently not regulated.

In South Africa, National Standards are not mandatory, they are merely statements of good practice. This changes when a standard is incorporated into legislation, for example by virtue of the National Building Regulations and Building Standards Act (Act 103 of 1977). This Act makes allowance for compliance with the Regulations either directly or by virtue of "deemed-to-satisfy" rules laid down in the various parts of SANS 10400. SANS 1936, the proposed national standard for development of dolomite land, will be referenced in deemed-to-satisfy provisions of SANS 10400 once it is finalised. It is not, however, listed as a compulsory standard at present.

3 HAZARD ASSESSMENT AND CLASSIFICATION OF DOLOMITIC LAND

3.1 *Buttrick's scenario of supposition method*

Over the years, a number of methods of assessing the risk of dolomitic instability have been proposed. These included identification of lineations using aerial photo interpretation, steep gravity gradients, local zones of thicker overburden and anomalies on infrared thermal imagery (Day & Wagener, 1984). Many of these were developed for specific geological conditions and were not applicable across the country.

In 1992, Buttrick proposed the use of the "scenario supposition method" which provided a framework for the evaluation of dolomitic stability. This was later developed into a proposal for dolomite land hazard and risk assessment (Buttrick et al, 2001).

Using this method, the stability of an undeveloped parcel of land is viewed in the context of a scenario where either the water table is static or the water table could be drawn down in the future. The method requires a hypothesis on the probable impact of man's activity which could include ground water abstraction or the introduction of surface water into the profile. The applicable scenario provides the framework within which the evaluation procedure can be applied.

The evaluation procedure is based on establishing whether or not the soil profile on the site exhibits inherent conditions that contribute to the formation of sinkholes or subsidences. The method also strives to obtain an indication of the likely maximum size of a sinkhole. Table 2 summarises the factors that are considered in the evaluation process.

In the application of this method, the assumed scenario and the mobilization potential of the blanketing material are the key factors in determining the likelihood of a sinkhole or subsidence occurring. The potential development space is the key factor in assessing the likely size of such features.

Table 2. Factors that influence the development of sinkholes and subsidences

Factor	Brief Explanation
Receptacle development	The formation of a sinkhole requires a receptacle to receive the mobilized material from the overlying profile. Such receptacles may either be disseminated voids or interconnecting openings in the overburden or substantial cavities or caves in the bedrock. Unless there is compelling evidence to the contrary, it is assumed that most dolomitic profiles contain such openings even if not encountered during site exploration.
Mobilising agency	Typically the mobilizing agency is ingress of water or drawdown of the table. It is generally assumed that water ingress will occur to some extent during the life of the development.
Nature and mobilization potential of blanketing layer	The blanketing layer includes all strata that overlie the potential receptacles. The susceptibility of this material to consolidation and subsurface erosion should be assessed considering aspects such as grading, consistency, cohesion, permeability and cementing. The mobilization potential of the materials in this blanketing layer determines the risk that, in the presence of a mobilizing agency, subsidence will occur. Low risk profiles are those with a shallow water table, that include stable horizons (e.g. shales or intrusive sills) or exhibit a general absence of voids. On the other hand, the presence of voids, air/sample loss during drilling, a deep water table and erodible material all indicate a high risk of mobilization.
Potential development space	The potential development space provides an estimate of the potential size of a sinkhole. It is determined primarily by the depth of receptacles and the angle of draw of the various strata overlying these receptacles. Angles of draw may vary from 45° for chert rubble to 90° (vertical sides) for shales or intrusive horizons.
Lateral extent	This factor plays a role particularly in the formation of compaction subsidences where the lateral extent of potentially compressible material is an influencing factor.

3.2 *Proposed classification*

Using the conclusions from the scenario of supposition method, the inherent hazard class for each area of the site is determined based on the likelihood of the inherent hazard (sinkhole or subsidence) occurring in the absence of any special preventative measures and the potential size of the sinkhole. The categories used in the definition of these two parameters are given in Tables 3 and 4 respectively. These parameters may then be used to determine an inherent hazard class as shown in Table 5.

Table 3. Inherent hazard categories

Inherent Hazard	Expected events per hectare per 20 years*	Equivalent return period on one hectare
Low	<0.1	>200 years
Medium	0,1 – 1,0	20 – 200 years
High	>1,0	<20 years
	* In the absence of any special precautions	

Table 4. Sinkhole size categories

Maximum diameter at surface	Size
<2m	Small
2m – 5m	Medium
5m – 15m	Large
>15m	Very large

Table 5. Definition of inherent hazard classes

Inherent Hazard Class	Inherent hazard for given size of sinkhole				Risk of subsidence (doline)	
	Small	Medium	Large	Very large	No dewatering	Dewatered
1	Low	Low	Low	Low	Low	Low
2	Med	Low	Low	Low	Med	-
3	Med	Med	Low	Low	Med	-
4	Med	Med	Med	Med	Med	-
5	High	Low	Low	Low	High	-
6	High	High	Low	Low	High	-
7	High	High	High	Low	High	
8	High	High	High	High	Low-high	Low-high

4 DEVELOPMENT OF A PERFORMANCE BASED STANDARD FOR DOLOMITIC LAND

Watermeyer et al (2008) described a four level performance based regulatory system which has formed the basis for the development of a national standard on the development of dolomite land (SANS1936).

Level 1 is a broad statement of the objective or goal of the regulatory system. The stated objective of SANS 1936 is to provide for the development of dolomite land in a manner that ensures that people live and work in a safe environment, damage to or loss of assets is within limits acceptable to society and the cost effective and sustainable use of land.

Level 2 states the functional requirements in qualitative terms. In SANS1936 this is that land underlain by dolomite shall present an acceptable risk of sinkhole and subsidence formation over time.

Level 3 is the establishment of quantitative performance requirements to give effect to the functional requirement defined in Level 2. Based on the work of Buttrick et al (2001), SANS1936 defines the tolerable hazard as one where the number of events (sinkholes or subsidences) that occur is less than 0,1 events per hectare per 20 years. The code then prescribes the permissible type and density of development and the mitigating measures to be put in place in order to achieve the tolerable hazard level.

Level 4 specifies the method of compliance with the performance requirements. In SANS1936 this is achieved by stipulating that development of dolomite land is to be undertaken under the control of a competent person and by laying down requirements for the investigation of dolomitic land, the design and inspection of precautionary measures and the development of dolomite risk management strategies.

5 PROBLEM AREAS

Although the above framework for the development of a performance based national standard appears reasonably straightforward, there are differences of opinion with regard to the detailed requirements of the draft standard. These differences of opinion have centred on the three key issues discussed below.

5.1 *Prescription of hazard evaluation methods*

The original draft of the code effectively prescribed the use of the scenario supposition method for the assessment of inherent hazard classes. While the method is regarded as a major step forward and can readily be applied for routine evaluation of inherent hazards on dolomitic land, its interpretation remains subjective and its application relies on a number of assumptions. Its entrenchment in the code stifles initiatives in the quest for other rational methods of hazard assessment.

The viability of using alternative approaches was demonstrated during the investigation for the Gautrain, Gauteng's new high speed railway. In this instance, a statistical analysis of the size and distribution of sinkholes in the area was undertaken to arrive at a rational assessment of the hazard.

The working group responsible for drafting the amendments to SANS 1936-2 proposes to keep the scenario supposition approach as a deemed-to-satisfy method of hazard assessment but, in addition, to allow alternative approaches based on rational analysis.

5.2 *Prohibition of development*

In defining the precautionary measures required to reduce the inherent hazard to a tolerable level, four categories of mitigating measures (D1 to D4) were introduced. In the case of the highest category, D4, the early versions of the code stated "no precautionary measures can reduce the dolomite risk to acceptable levels". This statement gave rise to the debate encapsulated in the rhetorical question posed in the introduction to this paper. It effectively stifles the development of designs or construction methods which specifically address and effectively mitigate the particular hazards on the site. The possibility of alternatives to this approach was illustrated by the innovative solutions adopted for the construction of the Gautrain which, of necessity, crosses significant tracks of dolomite land on the southern outskirts of Pretoria including those with some of the highest possible inherent hazard ratings. In this case, teams of local and international engineers came up with appropriate design solutions which included ground reinforcement, compaction grouting, dynamic compaction, preloading, stiffened track slabs and the use of large diameter shafts extending well into competent bedrock at depths of up to 70m for the founding of viaducts.

To address this issue and make allowance for properly engineered solutions, the current working group has proposed five requirements for the D4 dolomite area designation.

These are that:

- investigation, design, specification, supervision and formulation of risk management requirements be undertaken by a competence level 4 geo-professional (see below);
- the design, precautionary measures and risk management plan should specifically address and mitigate the risks present on site;
- the proposals be reviewed by a similarly qualified professional;
- the local authority review the proposals and appoint an independent reviewer if required; and
- that the local authority commit to maintain the necessary dolomite risk management principals.

5.3 *Definition of a competent person*

The definition of competent person in the early versions of the code contained very stringent requirements for experience in specific fields, to the extent that only a handful of persons would qualify. This definition provoked a response from many areas of the engineering and geological community. The Engineering Council of South Africa lodged a formal objection with the Bureau of Standards insisting that the only criteria should be professional registration and possession of the necessary experience.

As a compromise, the definition of competent person was amended to "a person who is qualified by virtue of experience, qualification, training and in-depth conceptual knowledge of development on dolomitic land".

With the proposed removal of the blanket prohibition on the development of certain dolomitic land and the introduction of peer review, the working group felt the need for defining levels of competence for specialised aspects of the work. Fortuitously, the Engineering Council also recognised that certain categories of structural and geotechnical engineering work should be undertaken only by persons with an appropriate level of competence and embarked on the compilation of codes of practice for geotechnical and structural engineering. These codes include definitions of competence levels 1 to 4 which correspond to candidate professionals, registered professionals, experienced professionals and expert professionals. The "gates" that permit from one level to the next are tertiary education, professional registration, experience and recognition by the profession respectively. The proposal is very similar to that proposed by the ICE's Site Investigations Steering Group (1993). As these codes of practice have not yet been published, the working group have proposed that a definition of competent levels similar to that adopted by the Engineering Council be included as a normative annex to the code.

6 CONCLUSION

The use of a performance based standard with clearly stated objectives has provided a solution to the difficulties involved in writing codes intended to deal with poorly quantified risks. Ongoing debate and refinement of the code has resulted in a proposal to remove the restrictive provisions contained in the earlier draft as this will open the door to innovative approaches to dealing with the problem in the future.

REFERENCES

Brink A.B.A. 1979. Engineering Geology of Southern Africa, Vol. 1 – The first 2 000 million years of geological time. Building Publications, Pretoria.

Buttrick D.B., Van Schalkwyk A., Kleywegt R.J. and Watermeyer, R.B. 2001. Proposed method for dolomite land hazard and risk assessment in South Africa. Journal of the South African Institution of Civil Engineering, Volume 43, No 2.

Day P.W. and Wagener F. von M. 1984. Investigation Techniques on Dolomites in South Africa. First Multi-disciplinary Conference on Sinkholes, Orlando, Florida. October 1984, p153-158.

Department of Public Works. 2003. Appropriate development of infrastructure on dolomite: Guidelines for consultants. Pretoria, South Africa.

Jennings J.E. 1966. Building on Dolomites in the Transvaal. The Civil Engineer in South Africa, February 1966.

Road Traffic Management Corporation. 2010. Road traffic report for the calendar year 2009. Pretoria, South Africa.

Site Investigation Steering Group. 1993. Site investigation in construction – Volume 2: Planning, procurement and quality management. Tomas Telford, London.

Wagener F. von M. 1982. Engineering Construction on Dolomite. PhD Thesis, University of Natal, Durban, South Africa.

Watermeyer R.B., Buttrick, D.B., Trollip N,Y,G, Gerber A.A, and Pieterse N. 2008. A performance based approach to the development of dolomitic land. Proc. Problem Soils in South Africa, SAICE Geotechnical Division, 3-4 November 2008. p167-174.

ISGSR 2011 - Vogt, Schuppener, Straub & Bräu (eds) - © 2011 Bundesanstalt für Wasserbau ISBN 978-3-939230-01-4

Risk assessment of uranium mill tailings disposal Boršt, affected by a landslide

T. Beguš & M. Kočevar
Geoinženiring d.o.o., Ljubljana, Slovenia

B. Likar
Rudnik Žirovski vrh, Todraž, Slovenia

ABSTRACT: Risk analysis tools were implemented during closing activities on radioactive mill tailings disposal Boršt, affected by a landslide. The probability of landsliding before and after remediation works was calculated and expressed through relaiability index β. Choosing between three possible variants of redeposition of radioactive waste material was presented by a decision tree. When the closing construction activities were completed, all possible outcomes were determined by event tree diagram based on influence diagram construction. The geological elements that can cause adverse impact on mill tailings were determined and selected by geognostic map. The tools are very useful and outcome is clearly understandable to all the clients in the remediation process.

Keywords: Mill tailings, Landslide, Risk management, Probability of failure, Geognostic map

1 INTRODUCTION

Mining in the only uranium mine in Slovenia, Žirovski vrh, together with research and construction activities lasted for 30 years, from 1960 to 1990. In 1990 the mine was closed due to economic reasons and decomissioning and remediating activities begun. But just before the start of closing activities the landslide, consisting of Carnian clastic rocks and mill tailings material, occurred due to great autumn precipitation in 1990. A problem arised and besides environmental problems the landslide mitigation was of great interest as well. During planning certain risk management activities were implemented in two main steps:

- selecting the most suitable variant for radioactive mill tailings treatment and determining the reliability of calculating the stability of the landslide and
- determination of possible risk scenarios at the disposal site after the closure of the mine.

2 DESCRIPTION OF THE AREA

The mine closing activities included also the treatment of mill tailings disposal situated on hill Boršt, where landslide occurred. A volume of nearly three million cubic meters moved at average velocity of 1,2 mm/dy. Landslide is about 400 m long, 200 m wide and extends 36 meters in average depth (Beguš, 1994). The main remedial measure was the construction of an underground drainage tunnel, from the bottom edge of the landslide in the hinterland, and a construction of vertical drainage wells that diverted groundwater flow outside the landslide (Beguš et al., 1996).

Because of the landslide several alternatives for mill tailings (re)deposition were studied. Three possible variants were established (Figure 1).

- Variant A: Mill tailings stay on the Boršt location. The site must be improved as much as possible with all remediation and environmental protection measures;
- Variant B: Mill tailings and contaminated subsoil will be removed to the underground openings of the abandoned uranium mine;

- Variant C: Mill tailings and contaminated subsoil will be removed with transport into the mine waste disposal site Jazbec.

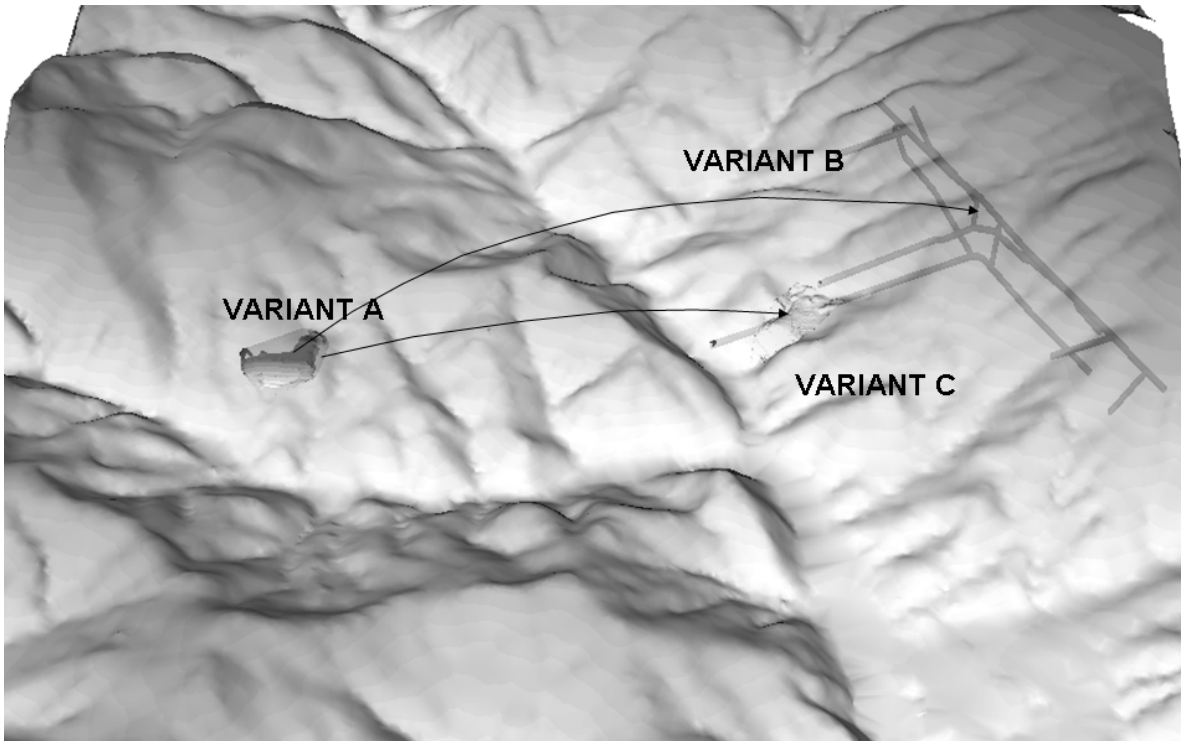

Figure 1. 3D view on the mill talings disposal Boršt, view toward southeast.

Choosing the most appropriate variant was carried out by means of decision-making matrix UMTRA (UMTRAP, 1988, Beguš, 2001). It was necessary to ensure that the level of knowledge for all areas of interes was the same, so we could compare the parameters of the same level. According to the evaluation of parameters the most suitable was variant B (move into the underground mine), but later variant A was accepted.

3 SELECTION OF THE MOST SUITABLE VARIANTS FOR MILL TAILINGS DISPOSAL AND CALCULATION OF RELIABILITY INDEX OF LANDSLIDE

Since sliding is a phenomenon that dictated selection of the site, the evaluation of the stability of disposal site was the most crucial task of the selection. Also the UMTRA matrix recommendations suggest examination of stability of the application by probabilistic approach. The stability of mine tailings disposal Boršt was evaluated with calculation of or reliability index β and calculation in available slope stability software (Rocscience, 2003).

The position of failure plane is well defined by cutted inclinometer boreholes on site. We used two situations: first, the situation in November 1990 when watertable in disposal and in bedrock were merged (Beguš et al., 1996, IBE, 1993) and the second with lowered watertable by drainage facilities, built in 1994. Also the stability of another possible site Jazbec was evaluated. The results are presented in table 1.

Table 1. Calculated factors of safety and probabilities of failure.

Case	Factor of safety – F_{ver}	Probability of failure %	Reliability index β, normal distribution	Reliability index β, lognormal distribution
Boršt in the time of sliding	0,999	50,570	-0,010	-0,058
Boršt after dewatering	1,147	9,570	1,318	1,365
Mine waste disposal Jazbec	1,964	$<10^{-5}$	3,604	4,911

When water levels decreased after dewatering works the probability of failure falls to 9.6%. The results show that the construction of a drainage tunnel in Boršt significantly improved the situation, but reliability index is still below recommended values ($\beta > 3$), so special additional and monitoring measures should be undertaken.

The landslide governs the decision, so we developed a example decision tree for the three variants with included probability of failure. According to this diagram the most favorable is variant A followed by variant B and the last is variant C, although the values are close one to another.

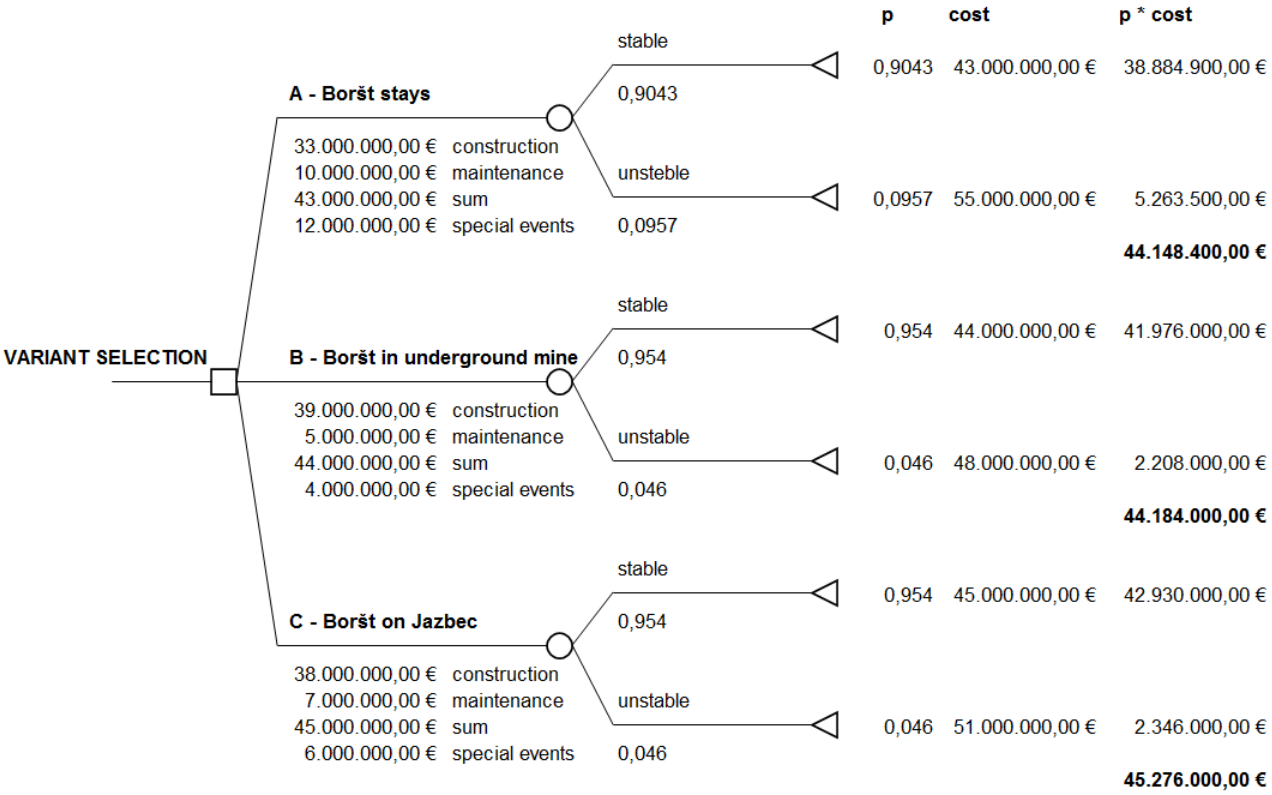

Figure 2. Decision tree for proposed variants of mill tailings material treatment.

4 RISK ANALYSIS AFTER THE MINE CLOSURE - GEOGNOSTICAL MAP

After the closure of the mine it was necessary to look at possible adverse scenarios. These were defined by a careful study of relevant areas of interest (Beguš et al., 2008). Studies were carried out on two levels:

- First level - looking at elements of geology: geological maps, hydrogeological maps, engineering geological map, map of construction, map of all objects etc. The presentation in 3D is a very important part of this level. In this level we were trying to present and process in 3D. Figure 3;
- Second level - evaluation and presentation of knowledge about the problem. We searched for the elements that adversely lead to the potential failure and the product is prepared in a manner that will be clearly understandable for all participants in the process. We called this level geognostic map.

According to Slovene dictionary (SAZU, 1980) geognosy is an archaic word for geology. The term can be refreshed to use as a preparation map about geological factors in a broad sense before risk analysis. In our case we were trying to express the processes about landsliding on Boršt area. The basic brick in geognostic map is geological map of the site. It was made by re-mapping and using all data, generated during research works before and during the construction. Some additional thematic maps representing possible outomes of landslide were made. Afterwards we made a model of the area with main characteristics that could lead to understanding of possible outcomes. For clarification, geognostic map is the synthesis that represents main factors and possible outcomes in a way that could be understandable to wide audience. This product may be the basis for determining the prognosis of possible further developments of phenomena and introduction to risk analysis.

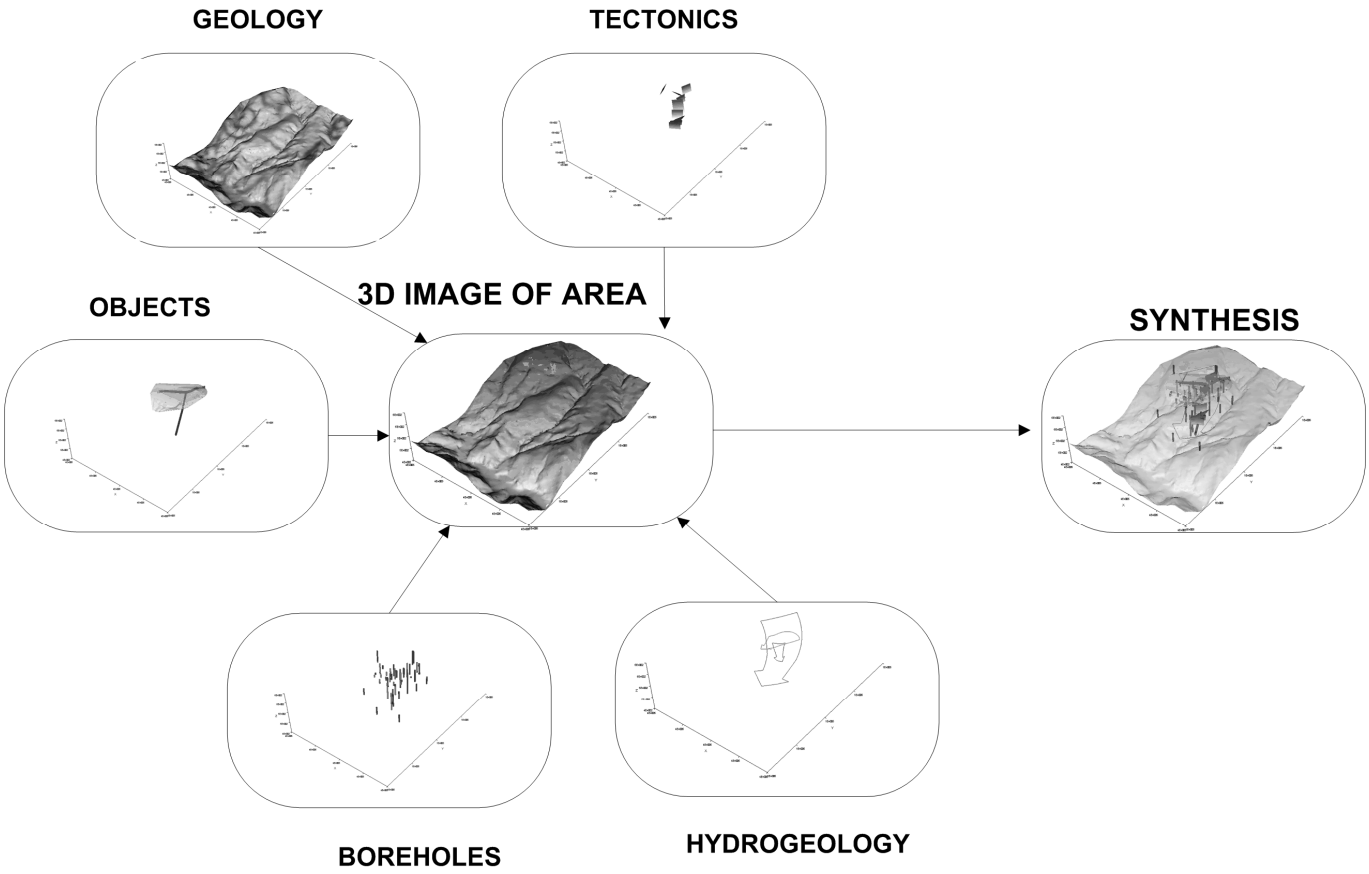

Figure 3. 3D images of disposal Boršt site.

This means that geognostic map searches for images regarding the site and unfavorable factors in the broadest sense and identify possible scenarios of adverse events. In the case of existing mill tailings and landslide we expose following factors:

- geology and tectonics
- hydrogeology and description of water flow,
- engineering geological factors,
- morphology of the terrain,
- movements on the landslide area.

Geognostical map contains a list of knowledge about a phenomena in terms of geological parameters that were determined during process by mapping the terrain, literature review and knowledge of the phenomena. We identify these factors which show clear causal links between parameters leading to landsliding. A graphic presentation of the using the major building blocks in making geognostic map for Boršt disposal site is given in figure 4.

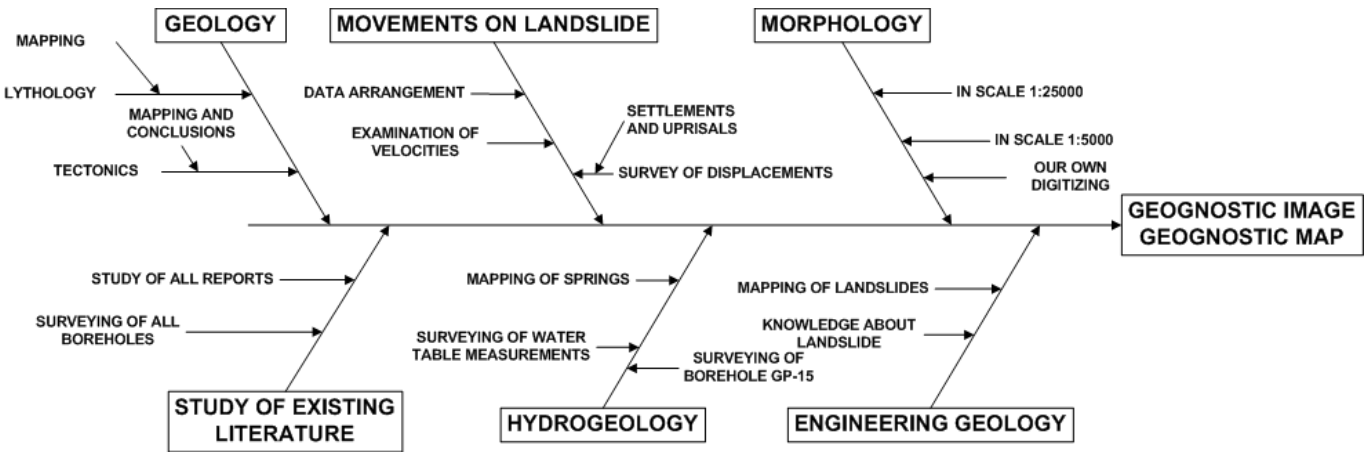

Figure 4. Construction phases in geognostic map construction.

The main factors that are most influental in Boršt area are as follows:

- Geology: geomechanically soft Carnian clastic rocks prevail, the area is interlaced with faults, where fractured zones of open fissures appear;
- Displacement on landslide: landslide is devided to five blocks bonded by faults which are moving separately;
- Morphology: Morphology is strongly dependent on the geology, deep erosional gullies show events in the landslide area in the past;
- Hydrogeology: two levels of ground water exist: in the mill tailins and in the bedrock. The water in cracks and water, that act on sliding surface also plays an important role.

Main parameters, that determine adverse events in broad sense, can be determined from geognostic map. We were especially interested in triggering factors, possible outcomes of landslide reactivation and in mitigation measures.

Based on determined triggering factors the influence diagram was constructed as a basis for event tree development (Baecher and Christian,2003, Hartford and Baecher,2004). Main concern was to determine

- main triggering factors,
- possible consequences of reactivated landslide
- coutermeasures for mitigation of undesirable scenarios.

From the above mentioned demands influence diagrams (Baecher and Christian, 2003, Hartford and Baecher, 2004) were constructed. It is clear that besides proper remediation works carefully selected monitoring is of great importance.

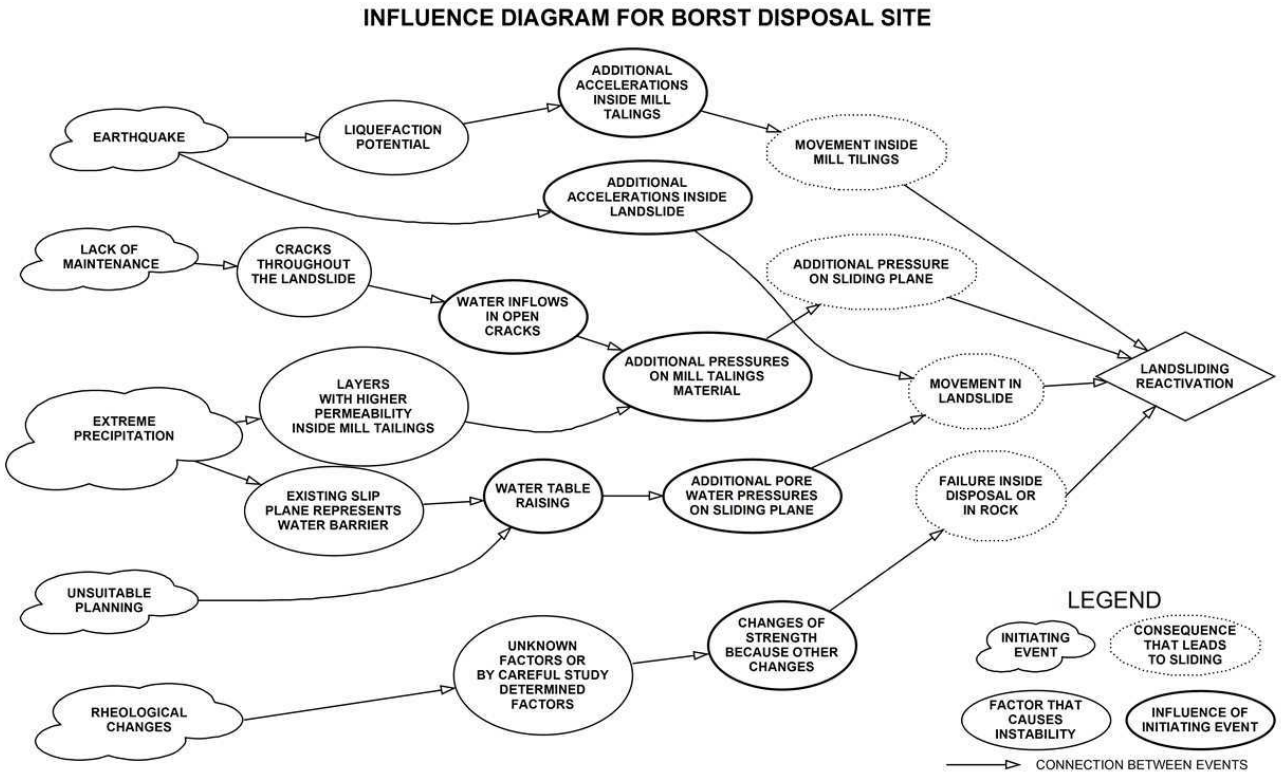

Figure 5. Influence diagram for disposal site Boršt.

5 EVENT TREES

Final issue of implementation of geognostic map and from influence diagram is developing the events into event trees according to triggering factors. The expected triggering factors were earthquake, extreme precipitation, lack of maintenance, unproper design and rheological changes in the landslide body. The presentation in figure 6 is qualitative.

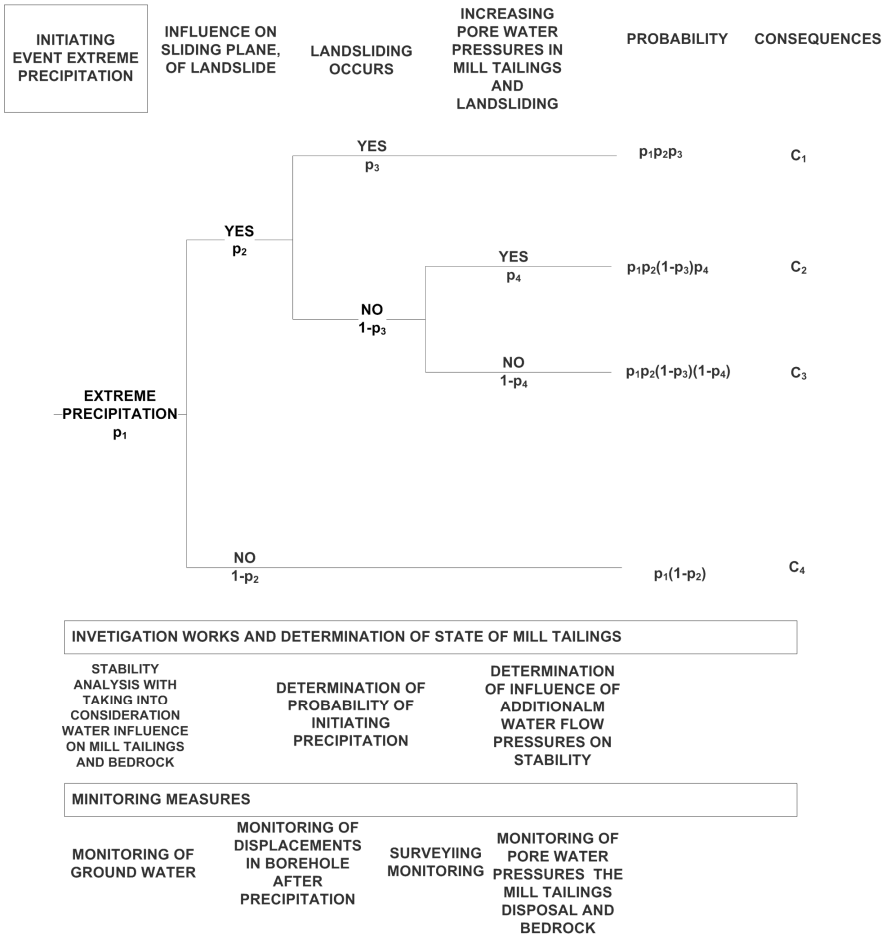

Figure 6: Event tree diagram – an example in occurence of extreme precipitation.

6 CONCLUSION

In large and environmentaly sensitive projects such as radioactive mill tailings disposal, risk analysistools should be included in every phase of operation of the facility. To get an idea about spatial relationships between geological features a three-dimensional picture of elements of risk is of great importance as well as a good knowledge of the areas concerned is basis for proper decision-making. Connection between good knowledge and presentation in a way that provides a knowledge and understanding of the problem is geognostic map - a compilation of data and knowledge, which is processed and presented in an understandable form.

REFERENCES

BAECHER, G. B. in CHRISTIAN, J. T. *Reliability and Statistics in Geotechnical Engineering.* Jonh Wiley & Sons Inc., 2003, 605 pages

BEGUŠ, T. Plaz na jalovišču hidrometalurške jalovine Boršt rudnika urana Žirovski vrh. In *Zbornik prvega slovenskega posvetovanja o zemeljskih plazovih*. Idrija, 1994.

BEGUŠ, T. *Izbira najprimernejše lokacije odlagališča hidrometalurške jalovine v rudniku urana Žirovski vrh: magistrsko delo*. Izdelano na Naravoslovnotehniški fakulteti, Oddelek za geologijo, Ljubljana, 2001, 141 str.

BEGUŠ, T., BUSER, I., ČADEŽ, F. in VIDMAR, S. Landslide stabilization of a mill tailing disposal by a drainage tunnel at the uranium ore mine Žirovski vrh, Slovenia. V *Proc. VII international symposium on landslides,* Editor Senneset, K. A.A. Balkema, Rotterdam, 1996, str. 1651-1656.

BEGUŠ, T., KADUNEC, K. in JAKOPIN, D. *Geognostična karta območja Boršt rudnika Žirovski vrh*. Report Geoinženiring Ljubljana, 2008.

HARTFORD, D. N. D. in BAECHER G. .B. *Risk and uncertainty in dam safety.* CEA Technologies Dam Safety Interest Group, Thomas Telford, 2004, 391 pages.

Rocscience Inc., *SLIDE 2D limit equlilbrium slope stability for soil and rock slope*. User's Guide. Rocscience Inc. 2003.

SAZU. *Slovar slovenskega knjižnega jezika.* Državna založba Slovenije, Ljubljana, 1980.

UMTRAP. *Alternate site selsction process for UMTRA Poject sites*. United States Department of Energy, 1988.

ISGSR 2011 - Vogt, Schuppener, Straub & Bräu (eds) - © 2011 Bundesanstalt für Wasserbau ISBN 978-3-939230-01-4

The evaluation of liquefaction potential of oil-containing sand under cyclic loading

I-H. Ho and V. R. Schaefer
Department of Civil, Construction, and Environmental Engineering, Iowa State University

R. Y.B. Chin
The late professor in National Cheng-Kung University, Taiwan

ABSTRACT: Taiwan is a country lacking crude oil. All crude oil is imported from other countries and is transported to storage tanks. In the process of transporting, spills occur leading to crude oil infiltrating into the soil. The engineering properties of soil may change due to the presence of crude oil. Moreover, the earthquakes are frequent in Taiwan, and the potential risks leading to soil liquefaction are relatively high. The dynamic strength and bearing capacity of oil containing soil will decrease under cyclic loading even when the static loading is unchanged. Hence, earthquake loading of oil storage tank areas pose a potential risk for weakened soils due to the oil in the soil.

In this study, oil containing sand was subjected to loading in a cyclic triaxial test system. The sand was poorly graded and fine grained, typical of that found in southern Taiwan. Tests were conducted on the pure sand, sand with an oil content of 10% by void space, and sand with three contents by weight (1.0%, 1.5% and 2.0%) of carboxymethyl cellulose (CMC) to improve the strength of the oil sand. Three relative density (D_r) were selected: 30%, 45% and 60% and confining stresses of 50, 100 and 150 kPa were used. Through consideration of these variables, the dynamic behavior of oil containing soil was studied and the potential of soil liquefaction and liquefaction resistance were analyzed.

The results indicate that the oil reduces the cyclic strength of the sand by more than 50%. Using the CMC material increases the cyclic soil strength back to that of the oil-free sand. The effect of relative density and confining stress conditions were also studied. The overall results showed that the cyclic strength and liquefaction resistance of oil containing sands can be restored with the addition of small amounts of CMC and is an efficient method to improve ground that contains oil.

Keywords: Oil sands; Cyclic triaxial system; Soil liquefaction; Relative density

1 INTRODUCTION

Taiwan is a county lacking crude oil and all crude oil is imported and placed in storage tanks. The process of filling and emptying the storage tanks presents an opportunity for leakage of the oil from the pipes connected to the storage tanks. This oil finds its way into the underlying soils. In southern Taiwan, the soil beneath the oil tanks is typically a sandy soil. Moreover, the strength of soil will decrease due to the crude oil infiltrates into the soil. Taiwan is located in the Pacific earthquake zone and subject to numerous earthquakes each year.

A study by Yang (2000) showed that adding oil up to 10% by volume increased the static strength of the sand through the addition of a pseudo-cohesion. However, in terms of dynamic strength, when the oil content increases, the cyclic stress ratio (CSR) decreases. The reduction of CSR means the reduction of the liquefaction resistance. The results are different between the static triaxial test and the cyclic triaxial test because the pseudo-cohesion is broken under the cyclic loading and the lower the permeability of oil-containing sand. Due to the reduction of the permeability of soil, the excess pore water pressure will increase rapidly once the dynamic loads are applied. The mechanism of the soil liquefaction is the excess pore water pressure induced by earthquake load cannot dissipate immediately leading to reduction in the effective stress of soil. The soil suddenly loses the shear strength and bearing capacity.

The influential factors of soil liquefaction are summarized as (1) relative density (Seed, 1968; Mulilis, 1975; Wu, 1979), (2) effective stress (Kishida, 1969), (3) grain size distribution, (4) fines content. Hsiao *et.al* (1983) found that adding a stabilizer to a soil with high liquefaction potentialcan increase the resistance under cyclic loading.

In this study a chemical stabilizer in varying amounts is added to the soil and the CRS determined. The results show that the addition of a small of amount of stabilizer, between 1 and 2% by weight, returns the cyclic shear strength back to that of uncontaminated soil.

2 TEST PROCEDURE

In the experimental procedures, several conditions were controlled to model the in-situ conditions. The influencing factors of dynamic strength of oil-sand are mainly (1) confining pressure, (2) relative density, (3) oil content and (4) stabilizer content. According to previous research, when the confining stresses are greater than 200 kPa in the sand, the liquefaction potential of the soil is very low. Accordingly, in the tests, 50, 100 and 150 kPa are selected as the confining pressures. Generally, liquefaction does not occur when the relative density, D_r is greater than 70%. The stabilizer was added in increments of 1, 1.5 and 2% by weight. The crude oil content used was 10% based on the volume of voids in the soil. The sand used for the testing was a local sand called Li-Kang sand. The experimental flow chart is shown in Figure 1. This study adopted the CKC cyclic triaxial test system to test the soil mixed with 10% of oil by volume.

2.1 Soil Sample Preparations

The Li-Kang sand was used and remolded at relative densities 30%, 45% and 60%. The physical indices of Li-Kang sand are specific gravity, G_s=2.71, average particle size, D_{50}=0.42, uniformity coefficient, C_u=2.2, coefficient of gradation, C_c=1.2 and the soil is classified as SP according to Unified Soil Classification System (ASTM 2487-00).

2.2 Soil Stabilizer

The stabilizer used was sodium carboxymethyl cellulose (CMC), which is a white or a slightly yellowish, almost odourless and tasteless hygroscopic powder consisting of very fine particles, fine granules. CMC is a non-toxic white powder, can be absorbed by the water. The solution is cohesive and will form a membrane. The chemical equation is as follows

$$\text{Cell-(OH)}_3+\text{ClCH}_2\text{COONa}+\text{NaOH}\rightarrow\text{Cell-(OH)}_2\text{OCH}_2\text{COONa}+\text{NaCl}+\text{H}_2\text{O} \quad (1)$$

CMC stabilizer is often used in ground improvement, a major component of stabilizing solution which added to the sand layer to increase the stability of the trench. Particularly in salty sand, the salt-resisted CMC is used to improve the ground.

2.3 Definition of Failure

In general, when cyclic triaxial tests are performed, two types of liquefaction failures can be defined in the saturated sand. One definition is based on the effective stress concept, in which soil liquefaction has been defined as occurring when the pore water pressure equals the confining pressure in the chamber during cyclic load. The other definition is based on strain control.

Seed and Lee (1966) performed triaixial tests using Sacramento sand with different relative densities and defined the corresponding axial strain at a certain value as failure. However, Poulos (1985) thought the failure in terms of axial strain was not persuasive, the axial strain can only determine deformation, not failure. Accordingly, the effective stress reducing to zero is adopted as the definition of soil liquefaction in this study.

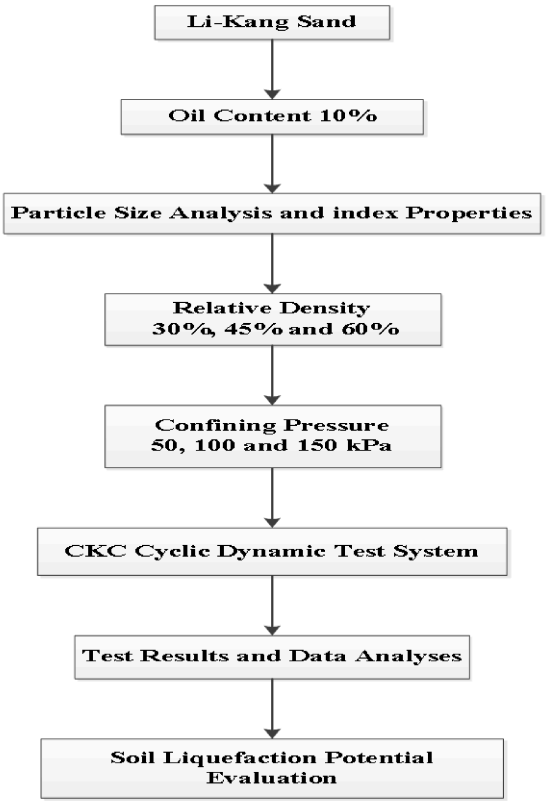

Figure 1. The scheme of testing soil containing crude oil and stabilized with CMC using cyclic triaxial testing system

3 TEST RESULTS AND INTERPRETATION

Three different relative densities were used to remold the samples and three confining pressures were used to test the soils. Six sets of data are given after each test: Number of cycles, cyclic deviator stress, axial strain, confining pressure, effective stress and volume change. Four figures can be formed to illustrate the change of the cyclic strength. According to Yang's (2000) study, the dynamic strength is lowered due to the presence of the soil. The results of the cyclic tests for various combinations of relative densities, confining pressures, and stabilizers are shown in Figure 2 through Figure 4.

4 DISCUSSION

According to Seed et. al (1975), a method was proposed to use the results from cyclic triaxial test to evaluate liquefaction resistance. Based on the earthquake scale M=7.5, the CSR corresponds to number of cycle, N equal to 15 can be used. However, the correction factors of remolded sample are based on wet side compaction, OCR, coefficients of lateral earth pressure and so on. The CSR obtained from the cyclic triaxial test multiply by 0.7 is the CSR leads to soil liquefaction. According to the definition of factor of safety against soil liquefaction, it can be mathematically expressed as the following form

$$FS = \frac{CSR_{(corrected)}}{\left(\tau_{avg}/\sigma_v'\right)} \quad (2)$$

Seed (1975) suggest factor of safety against soil liquefaction should range between 1.25 and 1.5.

The τ_{avg}/σ_v' is based on 0.65 τ_{max}/σ_v' and M equal to 7.5. The number of cycles from cyclic triaxial test is 15. However, if the Richter scale, M is other than 7.5, the cyclic stress ratio (CSR) induced by the earthquake has to be modified. The corresponding number of cycles is also different. The relationships between earthquake magnitude and modification factors are listed in Table 1.

In order to evaluate the liquefaction potential, the scheme shown in Figure 5 is presented to be followed according to different site conditions, earthquake magnitude and the combination of equivalent number of cyclic cycles and modification factor.
Three different relative densities were tested, 30, 45, and 60%. Due to space limitations, only the 45% results are reported herein. Similar trends occurred with the other two relative densities. The results of CSR with respect to the number of cycles are shown in Figure 2, Figure 3 and Figure 4 based on the soil with relative density 45% under different confining pressures.

The results presented in Figure 2 to Figure 4 are the cyclic strength ratios of oil-contaminated soil, pure sand and the stabilized soil with the relative density, D_r=45% under the confining pressures, 50, 100 and 150 kPa, respectively.

Figure 2 indicates the CSR of 10% oil-containing soil is between 0.2 and 0.3. The CSR is about 0.5 to 0.6 for pure sand. If the stabilizer, CMC was added to the soil, and the amount of the stabilizer is between 1.0 and 2.0%. The results show the stabilizer did restore the CSR back to the pure sand level or even slightly higher than the value of pure sand. Figure 3 also presents the similar trend. Figure 4 shows the oil-containing sand with CSR between 0.15 and 0.25. However, the pure sand possesses the CSR between 0.33 and 0.38. Obviously, the stabilizer work more efficiently on the soil confined using lower stresses, such as 50 and 100 kPa. Thus, the results imply this method is suitable for being used in reinforcing the soil close to the surface.

Table 1. The relationship between earthquake magnitude and modification factor

Earthquake Magnitude M	Equivalent Number of Cyclic cycles	Modification factor γ_m*
8.5	26	0.89
7.5	15	1.00
6.75	10	1.13
6.00	5-6	1.32
5.25	2-3	1.50

$$\gamma_m = \frac{\tau_{avg}/\sigma_m \ (M = designed)}{\tau_{avg}/\sigma_m (M = 7.5)}$$

*

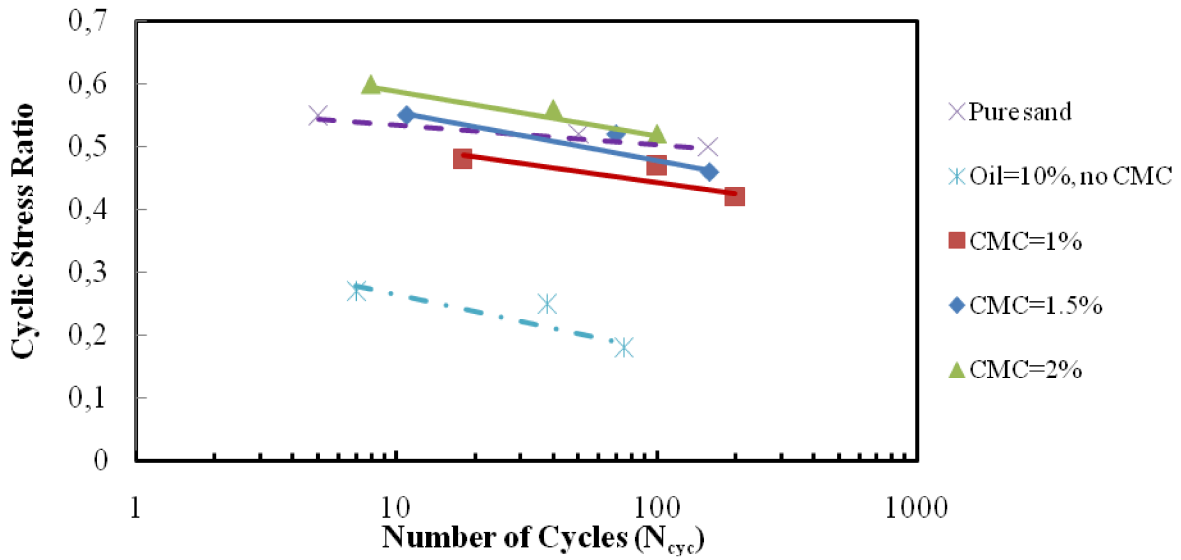

Figure 2. Cyclic stress ratio versus Number of cycles ($\sigma'_3 = 50kPa$, D_r=45%)

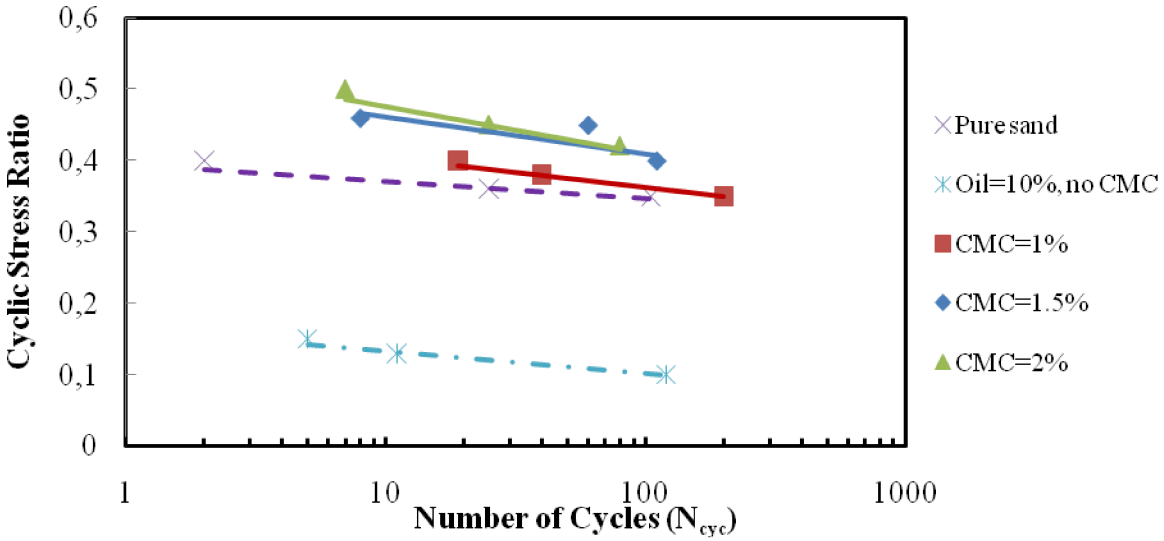

Figure 3. Cyclic stress ratio versus Number of cycles ($\sigma'_3 = 100kPa$, D_r=45%)

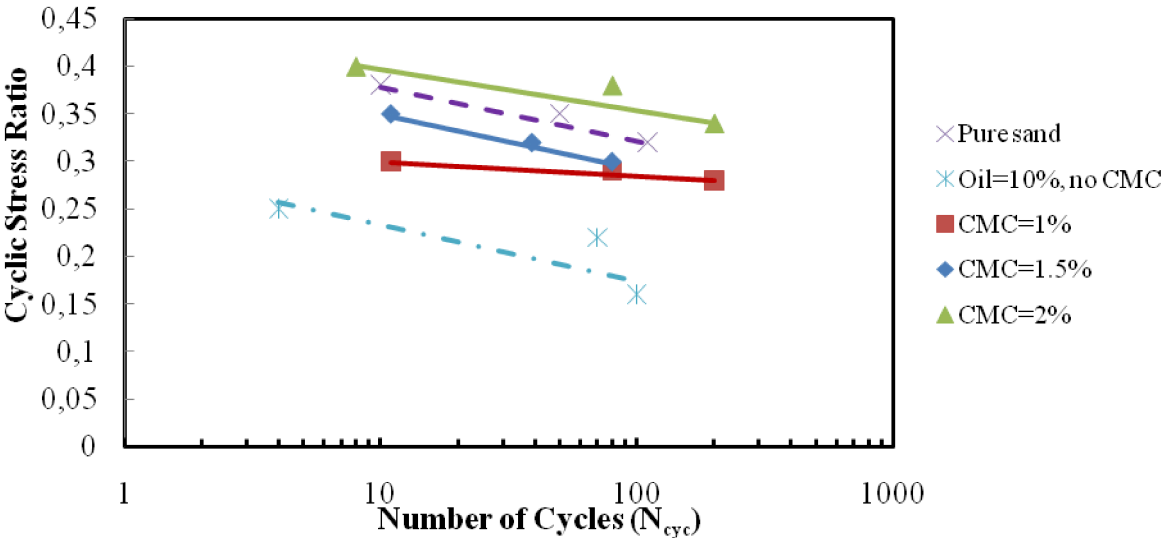

Figure 4. Cyclic stress ratio versus Number of cycles ($\sigma'_3 = 150kPa$, D_r=45%)

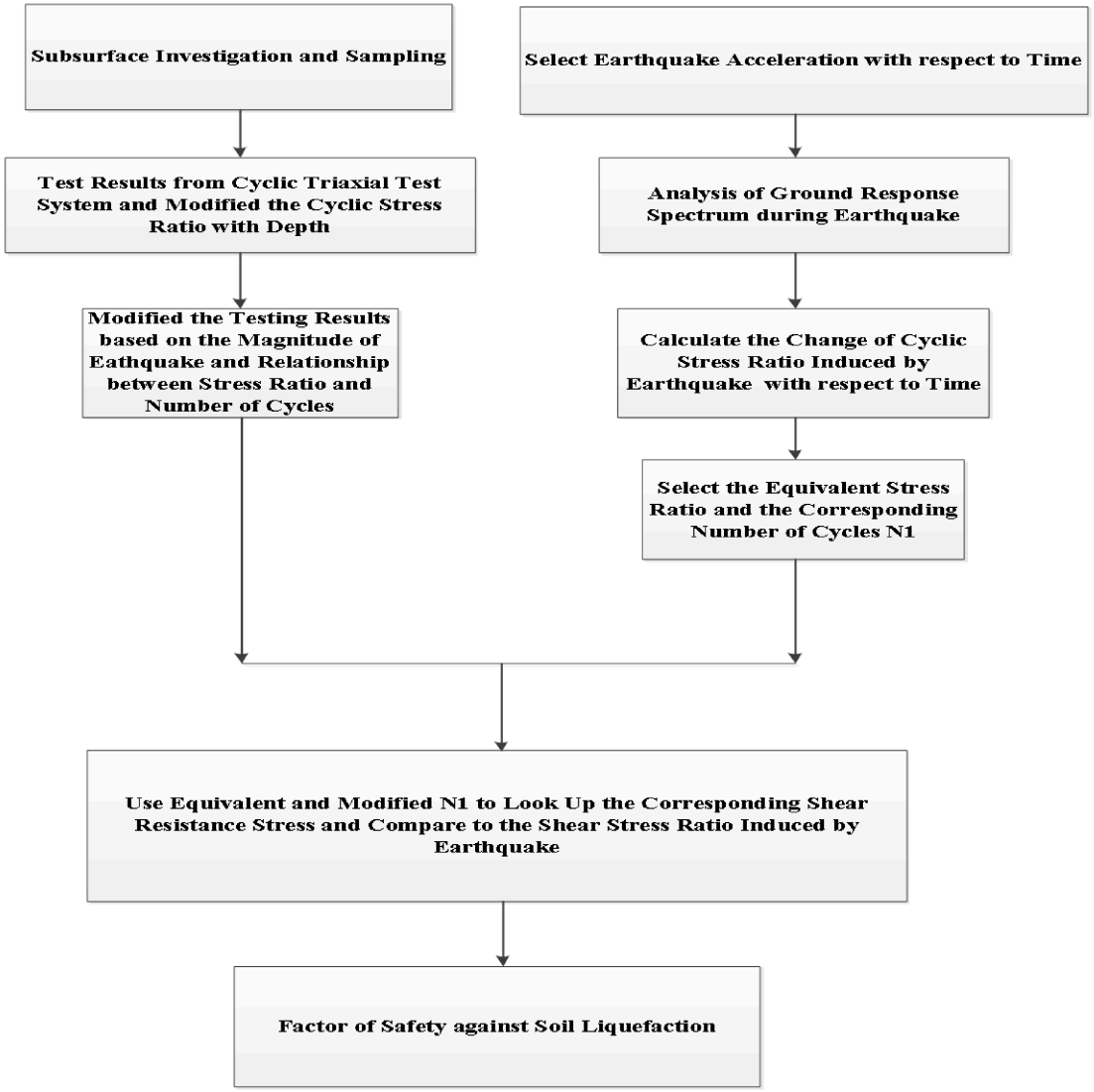

Figure 5. The determination of cyclic stress levels causing liquefaction from laboratory test data

5 SUMMARY AND CONCLUSIONS

The evaluation of liquefaction potential of oil-containing sand is based on the experimental results of cyclic triaxial tests. By making some reasonable assumptions in the tests, several conclusions can be made as follows.

(1) The dynamic strength of oil-containing sand is lowered at 40-60% compared to the pure sand in the same area in terms of CSR if the oil added 10% in the pure sand.
(2) By adding CMC chemical stabilizer into the oil-containing sand, the dynamic strength and the liquefaction resistance will increase even higher than the pure sand if the CMC stabilizer is added more than 1%.
(3) CMC stabilizer was found to increase the liquefaction resistance effectively. Accordingly, the site is not suitable for using some other ground improvement methods can adopt the proposed method to add about 1%-2% of CMC to increase the strength of sandy soil, the bearing capacity and the liquefaction resistance.
(4) In considering to use CMC as the stabilizer to improve the ground, the cost is also the important factor. To make the CMC stabilization as the economical method, the use of CMC stabilizer has to be controlled below 2%. Otherwise, the cost of ground improvement will increase and become uneconomical.

REFERENCES

Chin, Y.P. Robert. 1989. Static and dynamic strength and deformation characteristics of Ottawa and Li-kang sands. Ph.D thesis, The University of Wollongong, Australia.

Hsiao, D.H. 1983. The evaluation of liquefaction potential on cement added to the sand. MS thesis, National Cheng-Kung University, Tainan, Taiwan

Ishibashi, I.M., Sherlif, M.A., and Cheng, W.L. 1982. The effects of soil parameters on pore pressure rise and liquefaction prediction. Soils and Foundations, Vol. 32, No.1, 37-48.

Ishihara, K., and Yoshimine, M. 1992. Evaluation of settlements in sand deposit following liquefaction during earthquakes. Soils and Foundations, Vol. 32, No. 1, 173-188.

Kao, C.S. 2000. The Dynamic behavior of loose sands fines content. MS thesis, National Cheng-Kung University, Tainan, Taiwan.

Kishida, H. 1969. Characteristics of Liquefied Sands during Mino-Owari, Tohnankai, and Fukui Earthquakes. Soils and Foundations, 9(1): 75-92

Lee and Fitton,1969. Factors affecting the cyclic loading strength of soil. Vibration Effects of Earthquakes on Soils and Foundations. ASTM, STP 450, 71-96.

Mulilis, J.P. 1975. The effect of method of sample preparation on the cyclic stress-strain behavior of sands. Report No. EERC 75-18, UC Berkeley Earthquake Engineering Research Center.

Seed, H.B., and Idriss, I.M. 1971. “Simplified procedure for evaluating soil liquefaction potential.” Journal of the Soil Mechanics and Foundation Division, ASCE, Vol. 97, No. SM9, 1249-1273.

Seed., H.B., and Lee, K.L. 1996. “Liquefaction of saturated sands during cyclic loading. ASCE, Vol. 92, No. SM6, 105-134.

Yang, P.H. 2000. The dynamic behavior of loose sands containing the oil. MS thesis, National Cheng-Kung University, Taiwan, Taiwan

ISGSR 2011 - Vogt, Schuppener, Straub & Bräu (eds) - © 2011 Bundesanstalt für Wasserbau ISBN 978-3-939230-01-4

Management of large construction projects and risk minimization by web-based software technology

F. Rackwitz, S. Savidis & J. Rickriem
Berlin University of Technology, Berlin, Germany

ABSTRACT: A web-based software is presented which effectively supports the management of geotechnical construction projects and minimizes risks of execution stages. The software is developed and implemented as client-server application in the model-view-controller (MVC) framework of software architecture and it runs without installation procedure in any web browser. Main parts are a graphical user interface for easy administration and user access, a SQL database for storage of all information and a diagram editor to visualize monitoring results. Software development and implementation concerned also user-friendly handling, security aspects, rapid data access and adaptivity during a running project. The paper describes the basic ideas and main features of the developed software in detail and outlines a practical application.

Keywords: Web-based software, monitoring, information management, risk minimization

1 INTRODUCTION

Planning and execution of geotechnical structures, like tunnels, deep excavations and foundations, are mainly influenced by the fact that they are always prototypes, which makes the essential difference compared to industrial production processes. Geotechnical structures are particularly subjected by the variation of the natural boundary conditions, i.e. the ground and groundwater conditions which are crucial factors for planning and design. In addition to that all other boundary conditions, such as nearby existing buildings, also have to be considered in the design process.

In the stages of concept design and approval planning in most cases only limited data are available, especially concerning the ground conditions. The following stage of implementation or execution planning, where the planning of all details becomes most important, has to be done under enormous pressure of time, i.e. just in time with construction. That kind of procedure can lead to exceptional situations up to disasters, because of limited information or suddenly changing ground conditions. Concepts and methods to prevent geotechnical hazards and to minimize risks are therefore necessary.

Objective of an efficient risk management must be the reduction of the occurrence probability for every possible exceptional situation. This results in the highest possible safety for all involved workers on site as well as the execution of construction in due time and minimization of total construction costs. The key role in project and risk management plays the availability of information and the communication as well as the cooperation between all persons involved in the geotechnical engineering project.

Therefore the management of all information is the core of geotechnical project and risk management systems. The key for an efficient risk management system is therefore a system providing right information at right time and right place. That system must support on the one hand regular construction cycles and on the other hand the dealing with exceptional situations which could occur during execution stages of geotechnical engineering projects. Especially the detailed knowledge of the actual state of each part of the construction as well as the soil-structure interaction is a crucial part. That links to the very important information from monitoring in the frame of the observational method in geotechnical engineering.

The analysis of the above mentioned requirements lead to the idea and development of a web-based software which effectively supports the management of geotechnical construction projects and minimizes risks of execution stages.

2 SOFTWARE DEVELOPMENT

2.1 *Software design framework*

The new software was designed using the Model-View-Controller (MVC) framework. The MVC framework allows especially web-based applications to conveniently separate the software into three main parts: the modeling of the domain (Model), the presentation (View), and the actions (Controller) based on user input (Burbeck 1992).

The model manages the behavior and data of the application domain, responds to requests for information about its state (usually from the view), and responds to instructions to change state (usually from the controller). The view manages the display of information. The controller interprets the inputs from the user, informing the model and/or the view to change as appropriate.

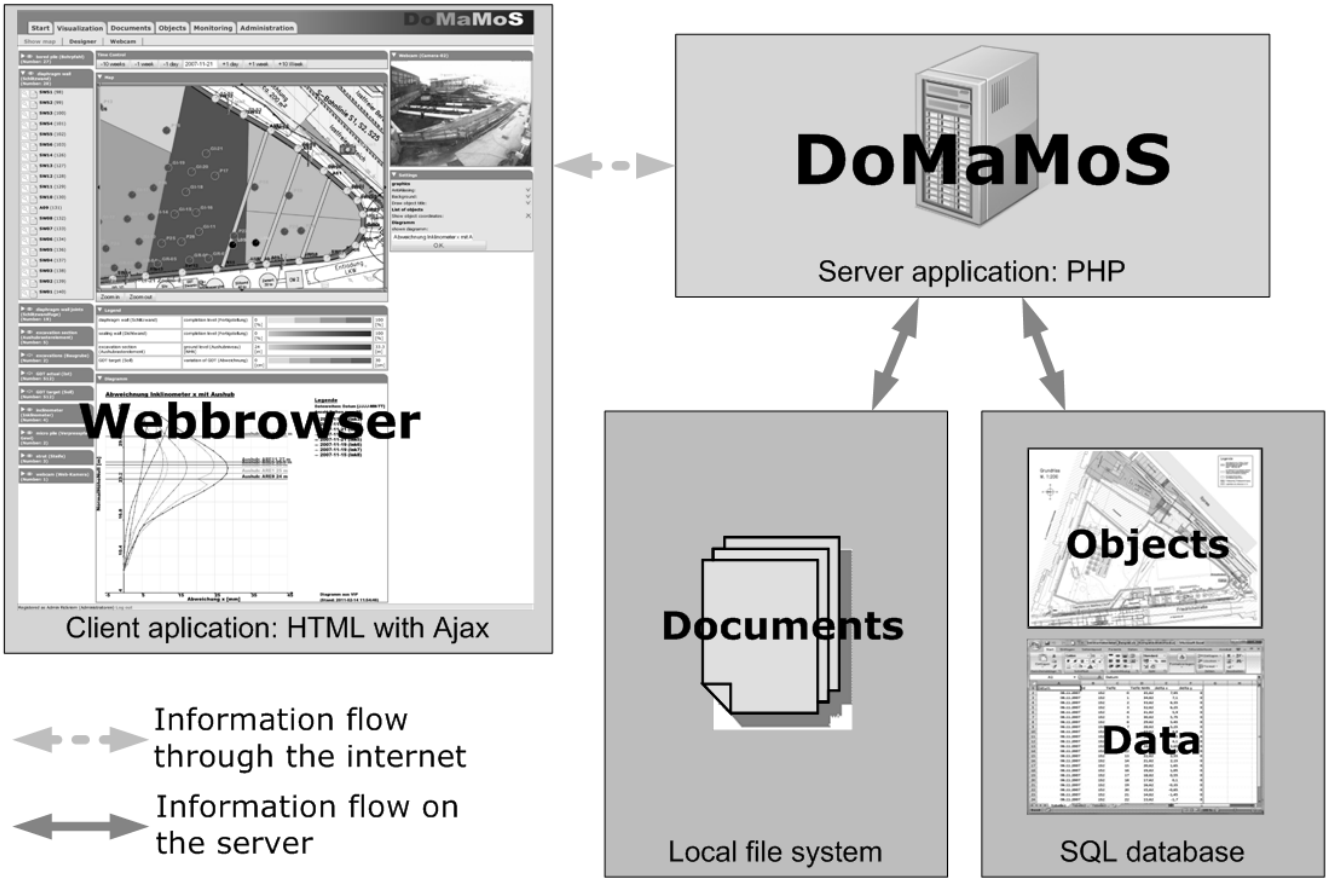

Figure 1. Software design based on the Model-View-Controller (MVC) framework

Figure 1 illustrates the software design in the MVC framework. The SQL database with data and objects as well as the local file system with documents are the model components, the web browser with the client application is the view part and the DoMaMoS server application implemented in PHP is the controller.

At present the SQL database consists of about 40 data tables representing a typical geotechnical project, such as a deep excavation. The number of tables in the database as well as the maximum number of documents in the local file system are not restricted and depend on the practical application and on the available server hardware. Documents are typically unmodifiable PDF files but can be also any other type of file. Results from measurements are directly stored as data in the tables of the database as it is done with the objects, i.e. parts of the construction like diaphragm wall panels, tie backs, jet grouting columns etc., webcams and sensors of the monitoring system.

The user interacts with the project data only by means of the web browser. The layout of the web-browser application is well-arranged but also changeable by the user. It mainly depends on the project specifications and user requirements. Every data request from the user is controlled by the DoMaMoS application. If the user is changing the project view window by changing the view location or by showing or hiding any objects then just an image with small file size is sent back from the controller application.

The data transfer when using the software is therefore rather minimal and allows also the use of smartphones and personal digital assistants (PDA) as clients. A user request for a document is replied by sending the document file back to the user.

It is also shown in Figure 1 that the user interacts by means of the web browser only with the controller, i.e. the server application, without direct access to the data and objects in the database and to the locally filed documents. That software technology and the use of an encrypted hypertext transfer protocol (HTTPS connection) ensure data safety.

2.2 *Data model, data and user rights management*

The well known Entity-Relationship Model (ERM) was used for the design of the database (Chen 1976). ERM uses a special diagrammatic technique, the Entity-Relationship Diagram (ERD) as a tool for database design. The database was implemented by means of *mySQL*, which is an open source database system using the Structured Query Language (SQL). In the database every entity, such as a document, is linked with a document type, an object, a manufacturer and a user by specific relations.

Data as well as user rights management is very important for each real project. The software allows for detailed handling of data and user rights.

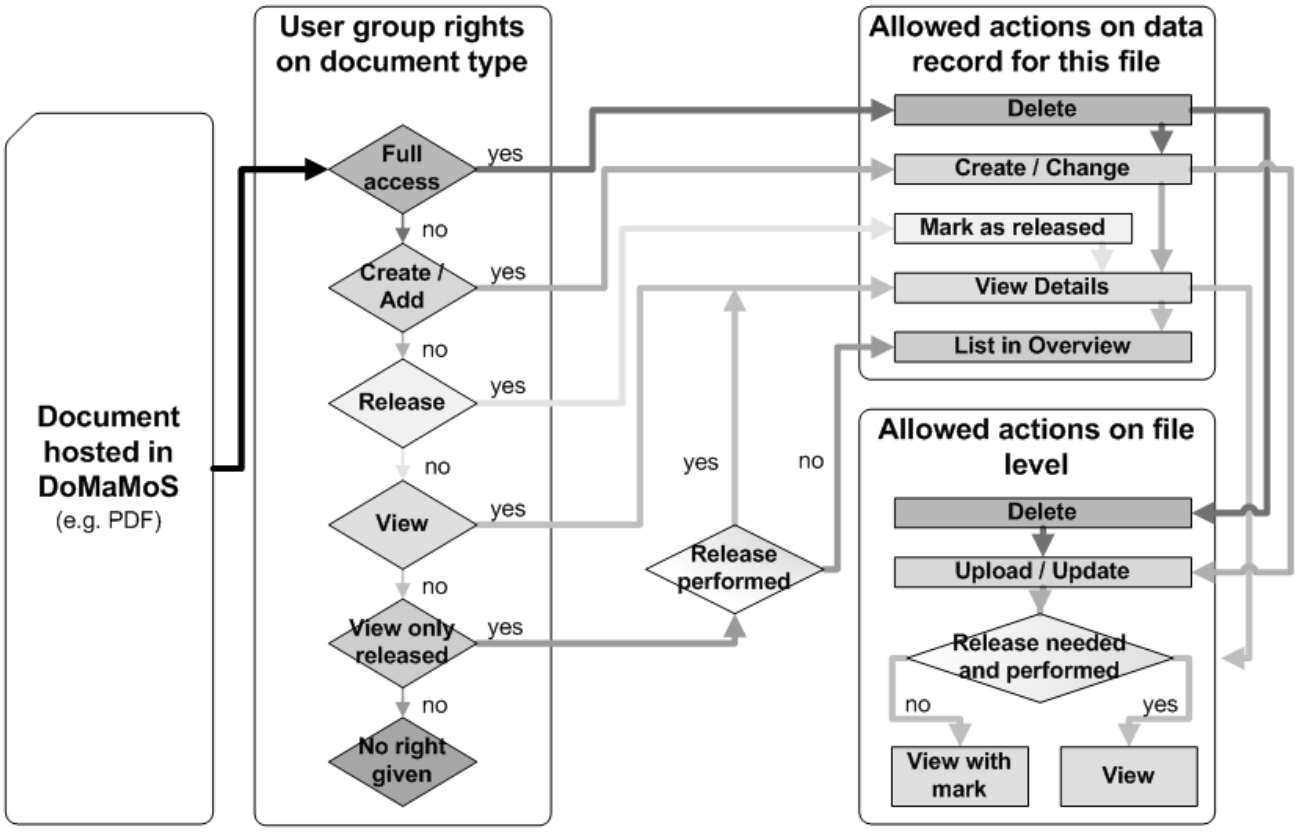

Figure 2. User group rights guideline on documents

Figure 2 illustrates the user group rights guideline on a specific document type. Full access and no access to the documents are the limiting rights, but in between there is any suitable right possible to create. A distinction is made concerning the allowed file actions depending on the given user right. An allowed action on file level regards the file itself on the local file server system whereas an allowed action on the data record regards the database entry for that file.

Each registered user belongs to a user group. Any user request is then checked by DoMaMoS for the given rights on the data, so user without the required rights will not see or get the requested data. The ac-

cess to documents and all other data depends on the rights of the user group in a hierarchical way as shown in Figure 2. E.g. an external geotechnical expert or supervisor may have the right to check and release specific documents or data, which will result in a change of the status of these documents after release. User with the right to see or get only released data cannot see or get the data before the release from the expert. That feature is convenient in any project in geotechnical practice.

3 PRACTICAL APPLICATION

3.1 *Project "Spreedreieck"*

A deep excavation in the city of Berlin was chosen to apply the software platform in a real project. Project "Spreedreieck" was an about 10 m deep excavation with very complicated boundary conditions and a very tight schedule for construction. The excavation was bounded by the railway station building Friedrichstraße in the south, the building Tränenpalast in the west and two railway tunnels in the east and west. The allowable diaphragm wall deformations were strictly limited. A pre-stressed bracing system inside the excavation was installed due to the nearby tunnels and buildings. The deep horizontal sealing base layer was constructed using Gel de Terre (GdT), a newly developed special kind of sodium silicate injection grout material by the company Züblin.

The practical application was successfully done with a previous software version (Mejstrik et al. 2008, Mejstrik & Savidis 2010). That previous software was a pure research prototype version with a number of shortcomings, without client server functionality and no possibility for suitable improvements and extensions.

After the end of the project all data was transferred into the here described completely new developed software. Extensive testing of the new software version was done with these project data and is partially shown in the following subsections.

3.2 *Main web browser view components*

3.2.1 "Start" tab window

The content of the web browser window right after login is shown in Figure 3. It consists of the "Start" tab window showing the recently uploaded and/or changed documents and objects since last login. Date and time of the last login is also recorded. The possibility to change the menu entry language between German and English is convenient especially for international projects. The "News" sub tab window can be used as news service.

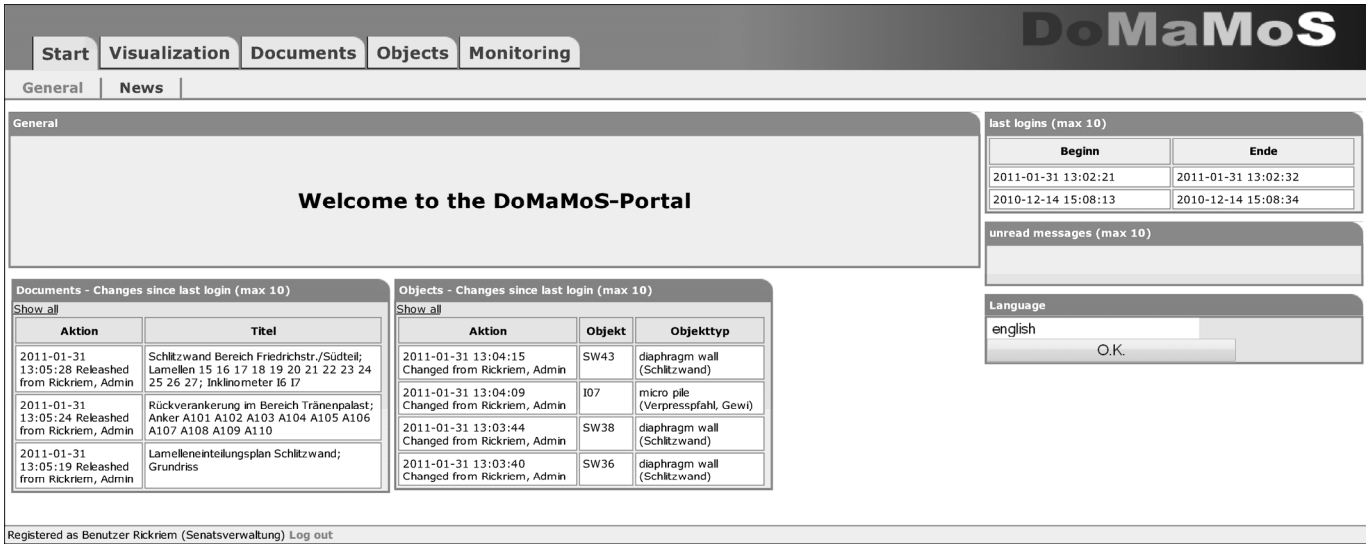

Figure 3. Web browser view after login

3.2.2 "Visualization" tab window

The content of the "Visualization" tab with the "Show map" sub tab window is shown in Figure 4. The "Visualization" tab is the main as well as most convenient interaction point with the user of the platform. It is the core of the graphical user interface. The sub tab "Show map" consists of the main window "Map"

showing a schematic plan view drawing of the construction site with its key information, i.e. construction objects, basic geometries, measurement devices, schedule etc. The diaphragm walls, piles, parts of the bracing system, GdT injection points and the separation of the excavation into two parts can be seen. The main surrounding streets and structures of the construction site are also displayed in the drawing for a quick geographical orientation of the user.

All construction objects are illustrated with their basic geometries, i.e. width, length, diameter, only. Whenever new types of construction objects have to occur in the project, they can be integrated into the model by means of the Project Designer Tool, which can be found with the "Designer" sub tab, but that tool is not shown or described in more detail here.

Two web cams outside the excavation were also installed to report the progress of work in the running project. Pictures were taken and stored automatically into the database. The "Webcam" sub tab gives access to all webcams of the project and all of their taken pictures. The default picture included in the "Show map" sub tab window (Figure 4, top right, "Webcam" window) can be chosen here. Initially the default picture is taken at noon from webcam no. 1.

Below the "Webcam" window there is the "Settings" window enabling the user to set main options directly, e.g. the choice of graphics options.

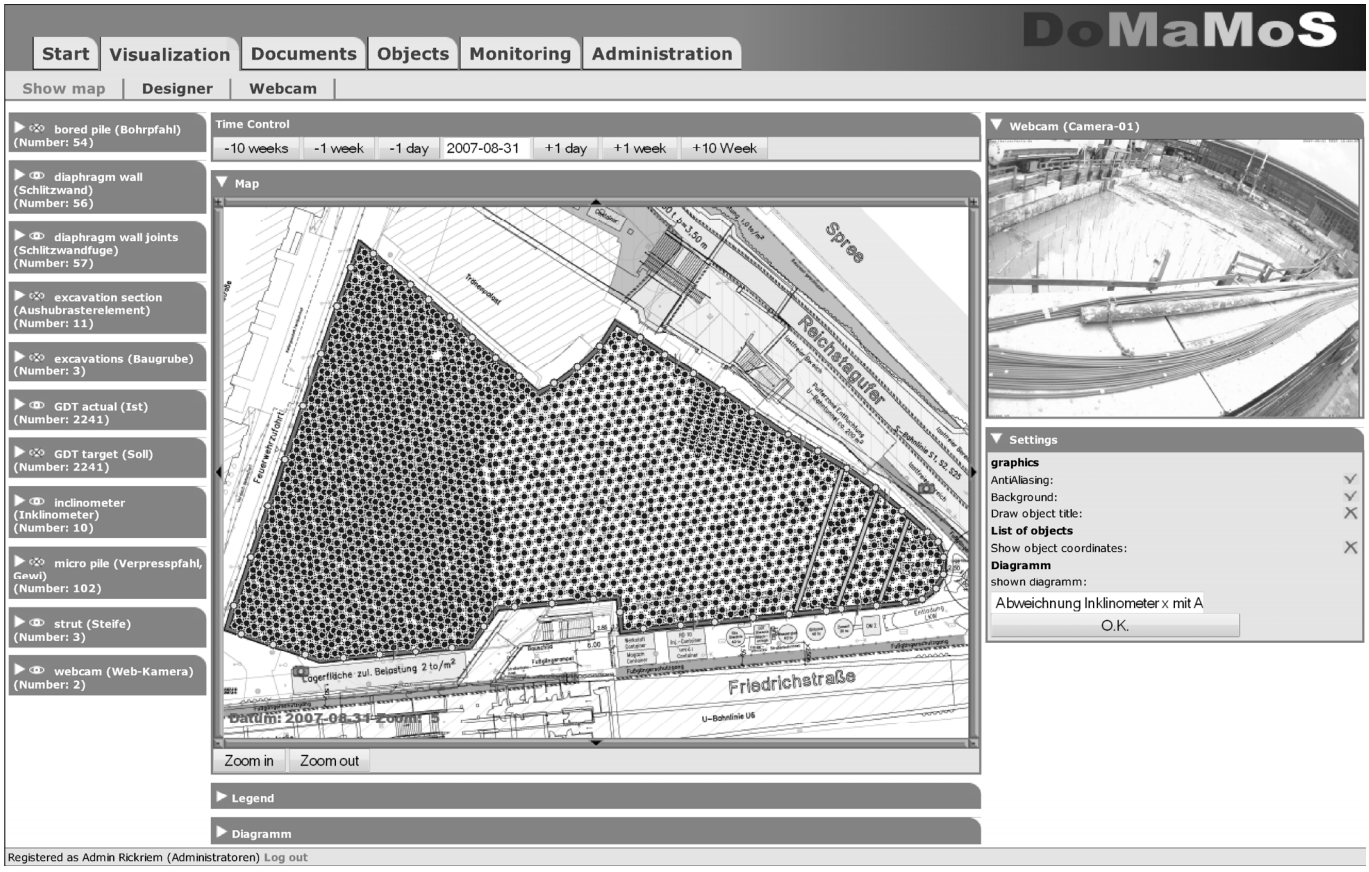

Figure 4. Project windows (most pull down menus reduced) in the web browser view

On the left in Figure 4 there is the object list window, but all pull down menus of the objects are reduced. The window consists of all objects, where the number in brackets is the visible number of objects in the actual main window. Each object type, i.e. bored pile, diaphragm wall panel, diaphragm wall joint, excavation section, excavation, GdT injection point, inclinometer, micro pile, strut and webcam is shown in the object list window.

Above the main project window "Map" there is the "Time control" window visible. It gives the user an easy way to run through the project backwards from the present stage or forward from the past to the present day. The two windows "Legend" and "Diagram" below the "Map" window are reduced in Figure 4.

Figure 5 gives a detailed zoom in view of the northern part of the excavation at a later stage of the project. The legend window is now shown in Figure 5 below the "Map" window. It gives the degree of completion for specific construction objects, such as diaphragm wall panels. Another legend entry represents the ground level inside the excavation pit. For that purpose an irregular grid is drawn overlaid on the excavation plan view. Each grid element is called an excavation section. Different colors mark different depths in the excavation sections.

The “Diagram” window with results from wall inclinometer measurements is shown below the legend window. The user can freely define the layout of the diagram by means of a diagram editor tool, which can be found in the “Monitoring” tab but is not shown here. The diagram in Figure 5 presents not only the horizontal wall displacements but also the corresponding excavation level next to the inclinometer, by a horizontal line. The consistency of all information for the given date in the time control window can be checked by comparison with the webcam picture.

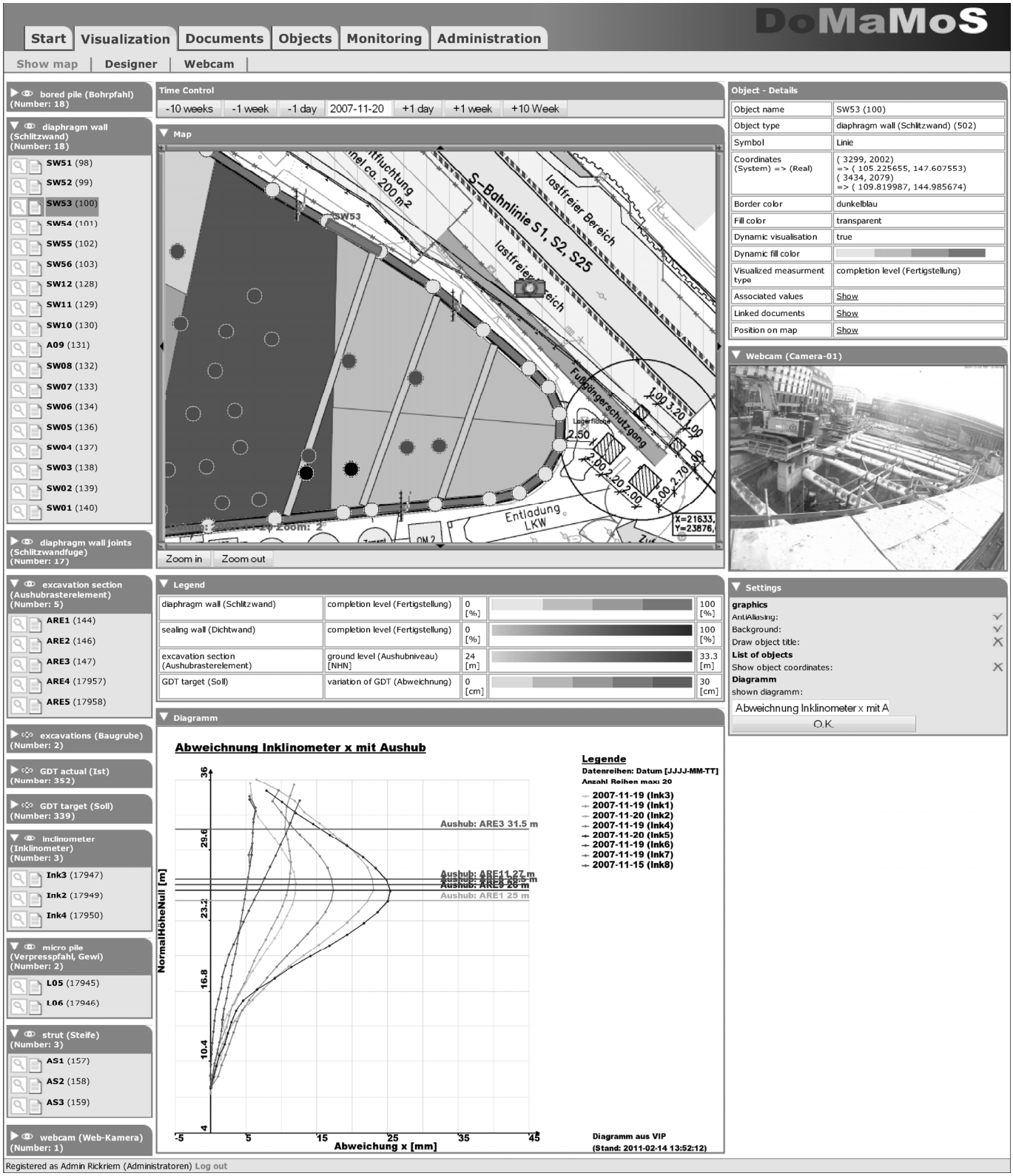

Figure 5. Project windows (most pull down menus open) in the web browser view

The diaphragm wall panel SW 53 is highlighted with dark grey background in the object list window (Figure 5 left) and the details of that panel are given in the “Object - Details” window (Figure 5 right).

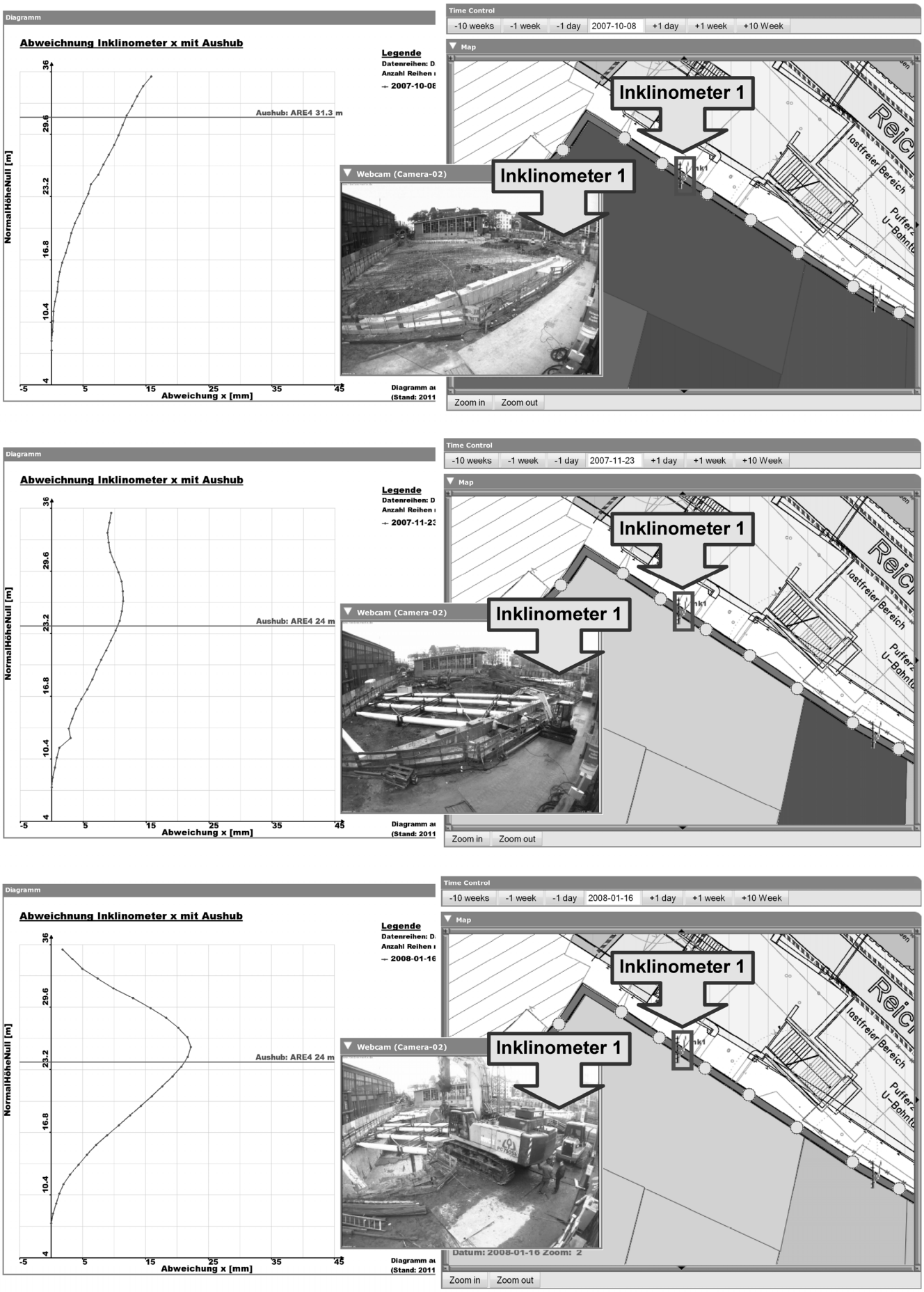

Figure 6. Different completion levels of the excavation

Figure 6 illustrates a partial view of the excavation in the "Map" window with diaphragm wall inclinometer no. 1 at three different days in chronological order from top to bottom, which is seen in the associated "Time Control" windows. The measured wall displacements from the inclinometer are given in the diagram to the right of each "Map" window. The corresponding excavation level next to the inclinometer is drawn by a horizontal line in the diagram. The change of the colors of the excavation sections from top to down in the "Map" windows in Figure 6 is associated with the ongoing excavation works. In the middle is overlaid the picture of webcam no. 2 at noon of each day and also showing the location of the inclinometer. The webcam pictures can be used to check the consistency of all other data.

The presented sequence in Figure 6 gives an outline of the capability of the time control window associated with the visualized project data which can be easily used to check the actual state of the project and to minimize geotechnical risks by efficient management of the available key information.

4 CONCLUSIONS

The purpose of the presented web-based software platform is the support of the daily work of geotechnical engineers. The software is designed to be used for quality management and risk minimization. It can be used independently in time and place by different people working together in the same project. Changing boundary conditions and requirements by clients and contractors require a flexible software architecture, which was recognized during the development stage.

To assess a specific situation on a construction site, only key information is important at first. The controller application and the database map this key information. The web browser user interface presents that key information in an appropriate way which makes it possible for the user to get a quick view of the project's main construction progress and data. All other detailed data can be easily found in the project database.

During practical application of the previous software version it was very well accepted by the construction site management and involved user. After a short time of practice, all participants were able to use the web-based platform in their daily work mainly due to the intuitive usability of the software. The illustration of key information in plain view layout gives a quick overview of the interaction of different types of information in different construction phases. The design of the web-based software in general and the integrated tools have been proved adequate for daily work in a geotechnical project. In a next step the new developed software also has to be tested in practice.

REFERENCES

Burbeck, S. 1992. Applications Programming in Smalltalk-80(TM): How to use Model-View-Controller (MVC). http://st-www.cs.illinois.edu/users/smarch/st-docs/mvc.html

Chen P.P.S. 1976. The Entity-Relationship Model-Toward a Unified View of Data, ACM Transactions on Database Systems, ACM-Press ISSN 0362-5915, Vol.1, No.1: 9–36.

Mejstrik M., Degebrodt P., Rackwitz F. & Savidis S. 2008. Development and Practical Adoption of an Internet-Based Platform for Geotechnical Engineering Projects. Proc. 12th International Conference of the International Association for Computer Methods and Advances in Geomechanics (IACMAG), 1-6 October, 2008, Goa, India, pp. 1943-1951.

Mejstrik M & Savidis S. 2010. A Visual Internet-Based Information Platform for the Improvement of Execution Management in Geotechnical Engineering Projects. Proc. of the 14th World Multi-Conference on Systemics, Cybernetics and Informatics (WMSCI 2010), June 29th - July 2nd, 2010, Orlando (FL), Vol. I: 208-214.

ISGSR 2011 - Vogt, Schuppener, Straub & Bräu (eds) - © 2011 Bundesanstalt für Wasserbau ISBN 978-3-939230-01-4

Optimization of Reinforced Concrete Retaining Walls Using Ant Colony Method

M. Ghazavi
Faculty of Civil Engineering, K. N. T. University of Technology, Tehran, Iran

S. Bazzazian Bonab
Department of Geotechnical Engineering, Islamic Azad University, Arak, Iran

ABSTRACT: Optimization of concrete retaining walls is an important task in geotechnical and structural engineering. Classical optimization search methods are rudimentarily based on direct search methods. Direct search methods belong to a class of optimization methods that do not compute derivatives. However, these algorithms suffer from both trapping in local minima and increasing run time. In order to reduce the possibility of suffering from this problem, the heuristic approaches are more favored among the scientists.

This paper applies a methodology to arrive at optimal design of concrete retaining wall using ant colony optimization (ACO) algorithm that is a general search technique for the solution of difficult combinatorial problems with its theoretical roots based on the foraging behavior of ants. The algorithm is used to find the minimum weight and cost for concrete retaining walls. Coulomb lateral earth pressure theory is used to derive the lateral total thrust on the wall. The results are compared with other available optimization scheme applied by other researchers. The results clearly indicate that ACO yields the solutions for all benchmarks due to its capability to explore and exploit the solution space effectively. As a result, it can be used for optimizing the reinforced concrete retaining walls.

Keywords: Ant Colony, Education, Optimization, Concrete Retaining Wall, Swarm Intelligent.

1 INTRODUCTION

Concrete retaining walls are most widely used structures in civil engineering practice. Such walls are commonly used to support earth, coal, ore piles, and water. Optimization of retaining walls is necessary due to economical consideration. Current optimization structural softwares for retaining wall design often lack the ability to find out optimal design because of their deterministic nature, while those employing stochastic methods are not tailored specifically for retaining walls and massive concrete structures. Classic optimization search methods are rudimentarily based on direct search methods. Direct search methods belong to a class of optimization methods that do not compute derivatives. Examples of direct search method are the Nelder Mead Simplex method, Hooke and Jeeves's pattern search, the box method, and Dennis and Torczon's parallel direct search algorithm employing a multi-sided simplex. However, these algorithms suffer from both trapping in local minima and increasing running time.

In this paper, a methodology is presented to arrive at optimal design of concrete retaining wall using Ant Colony Optimization (ACO) algorithm that is a general search technique for the solution of difficult combinatorial problems with its theoretical roots based on the foraging behavior of ants. ACO is based on the indirect communication of a colony of simple agents, called artificial ants, mediated by artificial pheromone trails. The pheromone trails in ACO serve as distributed numerical information, which the ants use to probabilistically construct solutions to the problem being solved.

Optimum design of retaining walls has been the subject of a number of studies. Saribas and Erbatur presented a detailed study on optimum design of reinforced concrete cantilever retaining walls using cost and weight of walls as objective functions. In their study, they controlled overturning failure, sliding failure, shear and moment capacities of toe slab, heel slab, and stem of wall as constraints [1]. Ceranic and Fryer proposed an optimization algorithm based on Simulated Annealing, which can compute the mini-

mum cost design of reinforced concrete retaining walls [2]. Sivakumar and Munwar introduced a Target Reliability Approach for design optimization of retaining walls [3]. Ahmadi Nedushan and Varaee proposed an optimization algorithm based on Particle Swarm Optimization. They claim that this method require fewer number of function evaluations, while leading to better results in optimization of retaining wall [4].

2 ANT COLONY OPTIMIZATION

From years of study and observation, ethologists have found that ants, although almost completely blind, are able to successfully navigate between their nest and food sources and in the process, discover the shortest path between these points [6]. The ant colony is able to determine the shortest path to food sources using pheromone trails. As an ant moves, it deposits pheromones along its path. A single ant will move essentially at random, however, another ant following behind it will detect the pheromone trail left by the lead ant and will be inclined to follow it. Once an ant selects a path, it lays additional pheromones along the path, reinforcing the increasing pheromone level of the trail and increasing the probability that subsequent ants will follow this path. This type of collective feedback and emerging knowledge in the ant colony is a form of autocatalytic behavior [7].

In the past few years, ant colony optimization (ACO) algorithms have undergone many changes throughout their development, but each different system retains the fundamental ant behavioral mechanisms. The fundamental theory in an ACO algorithm is the simulation of the autocatalytic, positive feedback process exhibited by a colony of ants. This process is modeled by utilizing a virtual substance called ‘‘trail’’ that is analogous to pheromones used by real ants. Each ACO algorithm follows a basic computational structure outlined by the pseudocode in Fig. 1. An ant begins at a randomly selected point and must decide which of the available paths to travel. This decision is based upon the intensity of trail present upon each path leading to the adjacent points. The path with the most trail has a higher probability of being selected. If no trail is present upon a path, there is zero probability that the ant will choose that path. If all paths have an equal amount of trail, then the ant has an equal probability of choosing each path, and its decision is random.

An ant chooses a path using a decision mechanism and travels along it to another point. Some ACO algorithms now apply a local update to the trail (Fig. 1). This process reduces the intensity of trail on the path chosen by the ant. The idea is that when subsequent ants arrive at this point, they will have a slightly smaller probability of choosing the same path as other ants before them. This mechanism is intended to promote exploration among the ants, and helps prevent early stagnation of the search and premature convergence of the solution. The amount of this trail reduction is not great enough to prevent overall solution convergence. The ant continues to choose paths to travel between points, visiting each point, until all points have been visited and it arrives back at its point of origin. When it returns to its starting point, the ant has completed a tour (Fig. 1).

```
Initialize Trail
Do While (Stopping Criteria Not Satisfied)- Cycle Loop
        Do Until ( Each Ant Completes a Tour)- Tour Loop
                Ant Decision Mechanism
                Local Trail Update
        End Do

        Global Trail Update
End Do
```

Figure 1. Ant Colony Optimization algorithm in pseudocode.

The combination of paths an ant chooses to complete a tour is a solution to the problem, and is analyzed to determine how well it solves the problem. The intensity of trail upon each path in the tour is then adjusted through a global update process. The magnitude of the trail adjustment reflects how well the solution produced by an ant’s tour solves the problem. The paths that make up the tours that best solve the problem receive more trail than those paths that make up poor solutions. In this way, when the ant begins the next tour, there is a greater probability that an ant will choose a path that was part of a tour that performed well in the past. When all the ants have completed a tour and all of the tours have been analyzed and the trail levels on the paths have been updated, an ACO cycle is complete [10]. A new cycle now be-

gins and the entire process is repeated. Eventually almost all of the ants will make the same tour on every cycle and converge to a solution. Stopping criteria are typically based on comparing the best solution from the last cycle to the best global solution. If the comparison shows that the algorithm is no longer improving the solution, then the criteria are reached [9].

The first ant algorithm was developed by Dorigo, referred to as ant system (AS) [8]. AS improves on SACO by changing the transition probability, P_{ij}^{k}, to include heuristic information, and by adding a memory capability by the inclusion of a tabu list. In AS, the probability of moving from node i to node j is given as

$$P_{ij}^{k}(t)=\begin{cases}\dfrac{\tau_{ij}^{\alpha}(t)\eta_{ij}^{\beta}(t)}{\sum_{j}\tau_{ij}^{\alpha}(t)\eta_{ij}^{\beta}(t)} & if \quad j\in N_i^k \\ 0 & if \quad j\notin N_i^k\end{cases} \tag{1}$$

where τ_{ij}^{α} represents the *a posteriori* effectiveness of the move from node i to node j, as expressed in the pheromone intensity of the corresponding link, *(i, j)*; η_{ij} represents the *a priori* effectiveness of the move from *i* to *j* (i.e. the attractiveness, or desirability, of the move), computed using some heuristic. The pheromone concentrations, τ_{ij}, indicate how profitable it has been in the past to make a move from *i* to *j*, serving as a memory of previous best moves [8].

3 CONCRETE RETAINING WALL DESIGN

Consider a concrete retaining wall shown in Fig. 2 with a height of H. Expressions for factors of safety against overturning failure, sliding failure, eccentricity failure and bearing failure are given in the following section.

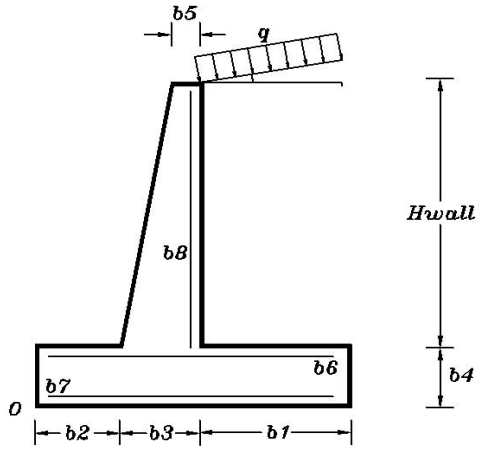

Figure 2. Concrete retaining wall section.

Rankine's earth-pressure theory corresponds to the stress and deformation conditions for the states of plastic equilibrium. The resultant active pressure on a vertical plane of height *H* through a semi-infinite mass of soil whose surface is inclined at an angle β to the horizontal is:

$$P_a=0.5\gamma h^2\left(\cos\beta\frac{\cos\beta-\sqrt{\cos^2\beta-\cos^2\phi}}{\cos\beta+\sqrt{\cos^2\beta-\cos^2\phi}}\right) \tag{2}$$

where ϕ is the backfill friction angle, h is the wall height, b is the backfill surface with horizontal direction, and γ is the backfill unit weight.

It is usually required that the factor of safety against overturning be at least 1.5. However, the stability number for overturning is generally on the order of 1.5 to 2.0 depending on the importance of the wall. This is commonly determined by taking moments about the toe of all forces acting on the wall above the plane of base.

The factor of safety is the ratio of the moment of the forces resisting overturning to the moment of forces tending to cause overturning. Overturning about the toe can be computed by taking a moment summation about that point.

The sum of the moments of forces tending to resist overturning about point *O* (Fig. 2) can be expressed as:

$$\sum M_R = M_c + M_s + M_q + M_v \tag{3}$$

The sum of the moments of forces tending to overturning about point *O* is expressed as:

$$\sum M_0 = P_{ah}\bar{y} \tag{4}$$

where M_c, M_s and M_v are moments about the toe point *O* as shown in Fig. 2 due to weight W_c, W_s and P_{av} respectively. W_c = weight of the concrete; W_s = weight of the soil; P_{av} = vertical component. M_q is related to surcharge load. Various parameters are defined as: ϕ_1 = friction angle of the back fill soil, δ = wall friction angle $2\phi_1/3$, γ_1 = unit weight of the backfill soil (KN/m^3). $\bar{y}$ = moment arm. The factor of safety against overturning failure can be written as:

$$FS_{overturning} = \frac{\sum M_R}{\sum M_O} \tag{5}$$

The overall wall stability requires safety against sliding. The sum of the horizontal resisting forces can be written as:

$$\sum F_r = C_a B' + \sum W \tan\delta + P_D \tag{6}$$

The sum of the horizontal driving forces is given by:

$$\sum F_d = P_{ah} \tag{7}$$

where C_a = adhesion coefficient between base slab and base soil; γ_2 = unit weight of soil below the base slab of retaining wall (KN/m^3); ϕ_2 = friction angle of the soil below the base slab of the retaining wall; $\sum W$ = sum of the vertical forces acting on retaining wall; P_D = any passive earth pressure developed by the soil in front of the wall. The factor of safety against sliding failure can be expressed as:

$$FS_{sliding} = \frac{\sum F_r}{\sum F_d}, \tag{8}$$

The stability number is usually on the order of 1.5 to 2.0, again depending on the importance of the wall.

For stability, the line of action of the resultant force must lie within the middle third of the foundation base. The factor of safety against eccentricity failure is given by:

$$\frac{B}{6} > e \tag{9}$$

where B = base width of the wall and e=eccentricity of the result and force.

In many instances involving the construction of embankments, overpasses or bridge approaches, it is necessary to construct a retaining wall backfilled to a considerable elevation above the existing ground surface. In these circumstances, precaution must be taken to ensure that a base failure beneath the weight of the fill does not occur.

If the subsoil consists of sand or gravel, there is no likelihood of such a failure. However, if the subsoil consists of clays or clayey slit, it is necessary to check their supporting capacity. The stability of the base against a bearing capacity failure is achieved by using a suitable safety factor with the computed ultimate bearing capacity where the safety factor is usually taken as 2 for granular soil and 3.0 for cohesive soil. The allowable soil pressure can be computed using the following bearing capacity equation:

$$q_{ult} = cN_c d_c i_c + \bar{q}N_q d_q i_q + 0.5B\gamma N_\gamma d_\gamma i_\gamma \tag{10}$$

where c=cohesion, d = depth factors; i = inclination factors, B width of the footing, and $\bar{q} = \gamma D$ in which D = depth of the wall base to the ground surface. In the above expression, N_c, N_q and N_γ are bearing capacity factors as functions of ϕ [5].

The maximum intensity of soil pressure at toe can be written as:

$$q_{max} = \frac{\sum W}{B'} \tag{11}$$

The factor of safety against bearing capacity failure can be defined as:

$$FS_q = \frac{q_{ult}}{q_{max}} \tag{12}$$

4 CONCRETE RETAINING WALL OPTIMIZATION

An optimal concrete retaining wall design is one with the minimal weight and cost that still allows the wall to satisfy given constraints. The basic stability requirements for a wall for all conditions of loading are overturning, sliding, and bearing capacity, and rotation and settlement [5].

The wall optimization problem can be expressed as:

$$g = MinW(b_1, b_2, b_3, b_4, b_5, b_6, b_7, b_8) \tag{13}$$

$$h = MinC(b_1, b_2, b_3, b_4, b_5, b_6, b_7, b_8) \tag{14}$$

while considering:

$$FS_q \geq 3 \tag{15}$$

$$FS_{over} \geq (FS_{over})_{all} \tag{16}$$

$$FS_{slid} \geq (FS_{slid})_{all} \tag{17}$$

where g = objective function; W = total weight; h = objective function; C = total price; b_1 = Heel projection; b_2 = Toe projection; b_3 = Stem thickness at bottom; b_4 = Thickness of base slab; b_5 = Stem thickness at top; b_6 = Horizontal steel area of the heel per unit length of the wall; b_7 = Horizontal steel area of the toe per unit length of the wall; b_8 = Vertical steel area of the stem per unit length of the wall; FS_q = factor of safety against bearing capacity failure; FS_{slid} = safety factor against sliding; FS_{over} = safety factor against overturning; $(FS_{slid})_{all}$ and $(FS_{over})_{all}$ = allowable values for FS_{slid} and FS_{over} respectively.

Two weight and cost objective functions have been chosen to optimize the wall from two viewpoints. In cost minimization, the objective function is defined as:

$$h(x) = C_s W_s + C_c V_c \tag{18}$$

where C_s = unit cost of steel; C_c = unit cost of concrete; W_s = weight of steel per unit length of the wall; and V_c = volume of concrete per unit length of the wall.

For weight optimization, the objective function is defined as:

$$g(x) = W_s + 100 V_c \gamma_c \tag{19}$$

where γ_c = unit weight of concrete, and 100 is used for consistency of units.
The ACO algorithm adapted for concrete retaining wall optimization is developed in the Fig. 3.

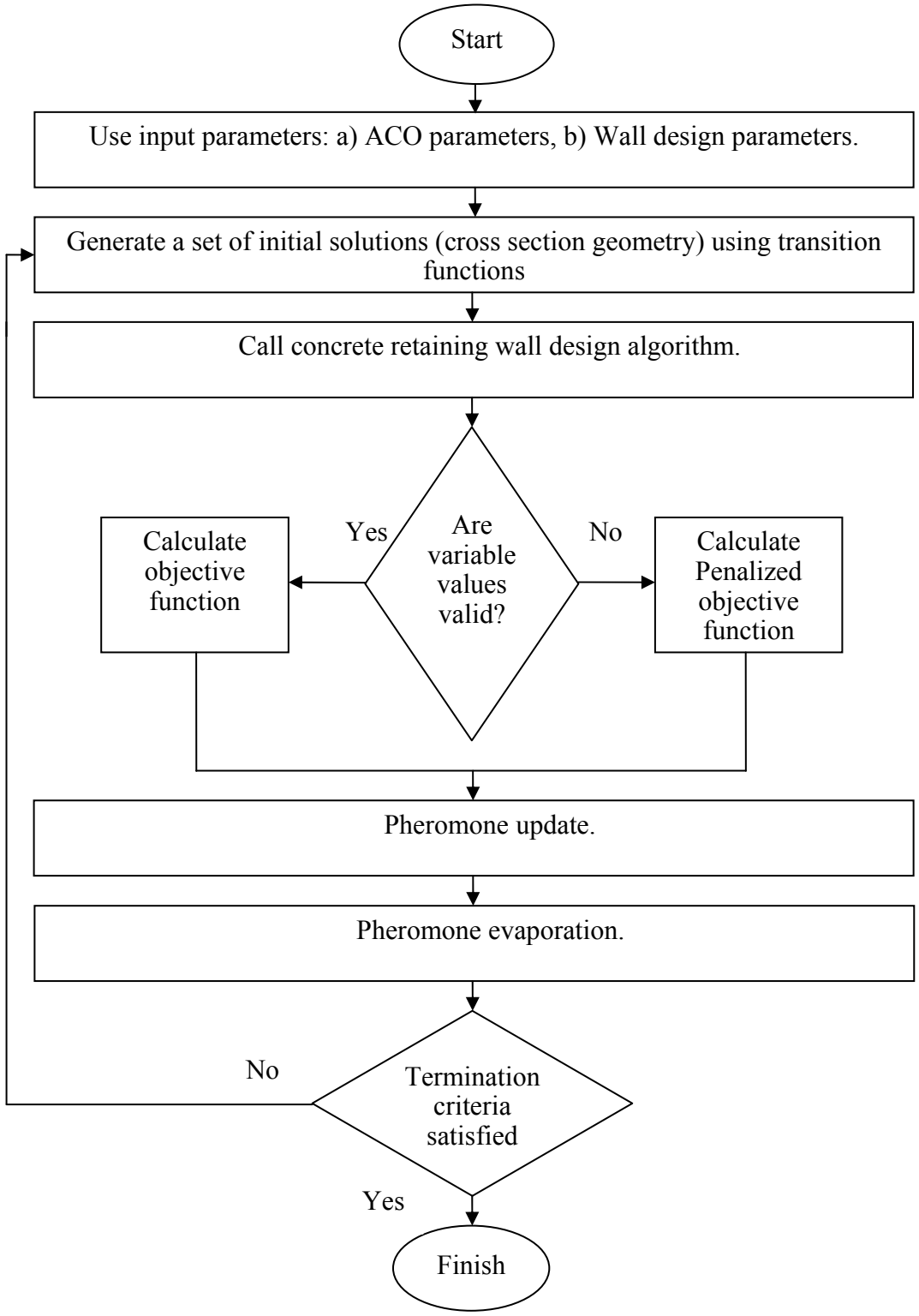

Figure 3. ACO application applied reinforced wall.

5 VERIFICATION

5.1 *Example 1*

To check the performance, robustness, and accuracy of the above algorithm, a retaining wall studied by Saribas and Erbatur [1] is considered. The details of this wall and other necessary input parameters are given in Table 1. It is noted that all the values given in this table are for a unit length of the wall. In the example problem, SI units are used.

Table 1. Input parameters

Input parameters	Unit	Symbol	Value
Height of stem	m	H	4.5
Yield strength of reinforcing steel	Mpa	f_y	400
Compressive strength of concrete	Mpa	f'_c	21
Surcharge load	kPa	q	30
Backfill slope	degree	β	15
Internal friction angle of retained soil	degree	ϕ_1	36
Internal friction angle of base soil	degree	ϕ_2	34
Unit weight of retained soil	kN/m^3	γ_1	17.5
Unit weight of base soil	kN/m^3	γ_2	18.5
Unit weight of concrete	kN/m^3	γ_c	23.5
Cohesion of base soil	kPa	C	100
Depth of soil in front of wall	m	D	0.75
Cost of steel	$/kg	C_s	0.40
Cost of concrete	kg/m^3	C_c	40
Factor of safety for overturning stability	-	N_o	1.5
Factor of safety against sliding	-	N_s	1.5
Factor of safety for bearing capacity	-	SF_q	3.0

The optimum design results are shown in Tables 2 and 3. The optimum values of the design variables are tabulated together with suggested, upper and lower limits for easy interpretation (Table 2).

Table 2. Optimum values of design variables

Design variable	unit	Lower bounds	Upper bounds	Optimum values minimum cost	Optimum values minimum weight
b_1	m	1.059	1.833	1.385	1.385
b_2	m	0.655	1.167	1.143	1.143
b_3	m	0.25	0.50	0.251	0.251
b_4	m	0.40	0.50	0.40	0.40
b_5	m	0.25	0.25	0.25	0.25
b_6	cm^2/m	11.059	67.68	14	14
b_7	cm^2/m	11.059	67.68	14	14
b_8	cm^2/m	5.761	67.68	59	59

Table 3. Optimum values of objective function

Objective function	Unit	Optimum value (Saribas)	Optimum value (AS)
Minimum cost	$/m	189.546	201.185
Minimum weight	kg/m	528.096	554.03

As seen in Table 3, the results obtained from the present optimization analysis (AS) and those reported by Saribas and Erbatur are in close agreement. The deviations between two methods are 6.1% and 4.9% for cost and weight optimizations, respectively.

5.2 *Example 2*

For further validation of the developed optimization method, another example is considered and the results are compared with those given by Saribas and Erbatur [1], Sivakumar and Munwar [3], Bowles [5], and Das [11]. Three walls with heights of 3, 4, and 5 m are considered. Other specifications for the design of these retaining walls are presented in Table 4. To compare the results with Das and Bowles, a value of 0.3 m is assumed for b_5 for all walls.

Tables 5 to 8 compare optimum design results determined from the present method and those given by others as referenced. It is noted that in these tables, some fixed values are considered for b_1, b_2, and b_4. This stems from the fact that Das [11] and Bowles [5] do not optimize these values and they just recommend some experienced-based approximate values which are normally used in practice. As will be seen in these tables, these values can be easily optimized using the method described in this research or other optimization approaches.

Table 4. Input parameters [3]

Input parameters	Unit	Symbol	Value
Height of stem	m	H	3−4−5
Yield strength of reinforcing steel	Mpa	f_y	400
Compressive strength of concrete	Mpa	f'_c	21
Surcharge load	kPa	q	25
Backfill slope	degree	β	10
Internal friction angle of retained soil	degree	ϕ_1	36
Internal friction angle of base soil	degree	ϕ_2	0
Unit weight of retained soil	kN/m^3	γ_1	17.5
Unit weight of base soil	kN/m^3	γ_2	18.5
Unit weight of concrete	kN/m^3	γ_c	23.5
Cohesion of base soil	kPa	C	125
Depth of soil in front of wall	m	D	0.75
Cost of steel	$/kg	C_s	0.40
Cost of concrete	kg/m^3	C_c	40
Factor of safety for overturning stability	-	N_o	1.5
Factor of safety against sliding	-	N_s	1.5
Factor of safety for bearing capacity	-	SF_q	3.0

Table 5. Comparative study for the projection of toe from the base of the stem b_2

Height of stem	3.0	4.0	5.0
Das 0.1H	0.3	0.4	0.5
Bowles 0.233H	0.7	0.933	1.167
Saribas and Erbatur for minimum cost	0.443	0.582	0.727
Saribas and Erbatur for minimum weight	0.436	0.603	0.789
Sivakumar and Munwar	0.72	0.96	1.20
Present study for minimum cost	0.555	0.726	0.939
Present study for minimum weight	0.629	0.842	1.013

Table 6. Comparative study for projection of heel from the base of the stem b_1

Height of stem	3.0	4.0	5.0
Das 0.1H	1.5	2.0	2.5
Bowles 0.233H	1.101	1.468	1.835
Saribas and Erbatur for minimum cost	0.864	1.161	1.411
Saribas and Erbatur for minimum weight	0.873	1.191	1.473
Sivakumar and Munwar	0.6	0.8	1.0
Present study for minimum cost	1.026	1.375	1.687
Present study for minimum weight	0.944	1.255	1.589

Table 7. Comparative study for the thickness of base slab b_4

Height of stem	3.0	4.0	5.0
Das 0.1H	0.3	0.4	0.5
Bowles 0.233H	0.3	0.4	0.5
Saribas and Erbatur for minimum cost	0.273	0.364	0.455
Saribas and Erbatur for minimum weight	0.273	0.364	0.455
Sivakumar and Munwar	0.3	0.4	0.5
Present study for minimum cost	0.271	0.363	0.450
Present study for minimum weight	0.270	0.363	0.451

As seen in Tables 5 to 8, the current optimization method gives reasonable results. It is noted that the values obtained from the present developed optimization from viewpoints of weight and cost of retaining walls are relatively greater than those given by Saribas and Erbatur [1]. This could be attributed to the fact that the results of Saribas and Erbatur [1] do not account for uncertainties that exist in the soil, concrete, steel properties, and geometric properties of the wall [3]. In addition, both methods use different optimization algorithm.

Table 8. Comparative study for the cross sectional area of the retaining wall (m^2)

Height of stem	3.0	4.0	5.0
Das 0.1H	1.440	2.380	3.550
Bowles 0.233H	1.440	2.380	3.550
Saribas and Erbatur for minimum cost	1.340	2.071	3.037
Saribas and Erbatur for minimum weight	1.340	1.962	2.713
Sivakumar and Munwar	1.395	2.080	2.875
Present study for minimum cost	1.407	2.073	2.816
Present study for minimum weight	1.405	2.070	2.811

6 CONCLUSION

The present paper has shown how engineers can learn from ant colony for optimization of reinforced concrete retaining walls. By validation of the predicted results on optimizing the retaining wall that ant colony optimization (ACO) is a successful random search method that educates engineers to find global minimum in difficult combinational problems, which can hardly be attained by classical optimization methods. It has been demonstrated that the presented algorithm is able to find quickly the minimum weight and minimum cost justified geometry and specifications for reinforced concrete retaining walls.

REFERENCES

[1] Saribash, A., & Erbatur, F. 1996. Optimization and Sensitivity of Retaining Structurs. Journal of Geotechnical Engineering, ASCE, Vol. 122, No.8, pp. 649-656.

[2] Ceranic, B., & Fryer, C. 2001. An Application of Simulated Annealing to Optimum Design of Reinforced Concrete Retaining Structures. Journal of Computers and Structures, Vol. 79, pp. 1569-1581.

[3] Sivakumar Babu, G.L., & Munwar, Basha B. 2008. Optimum Design of Cantilever Retaining Walls Using Target Reliability Approach. International Journal of Geomechanics, ASCE, Vol. 8, No. 4, pp. 240-252.

[4] Ahmadi Nedushan, B., & Varaee, H. 2009. Optimal Design of Reinforced Concrete Retaining Walls Using a Swarm Intelligence Technique. The first International Conference on Soft Computing Technology in Civil, Structural and Environmental Engineering, UK.

[5] Bowles, J.E. 1996. Foundation Analysis and Design. The McGraw-Hill Companies, Inc. Fifth edition.

[6] Wahde, M. 2008. Biologically Inspired Optimization Methods: An Introduction. Boston: Wit Pr/Computational Mechanics.

[7] Bonabeau, E., & Dorigo, M., & Theraulaz, G. 1999. Swarm Intelligence: From Natural to Artificial Systems (Santa Fe Institute Studies on the Sciences of Complexity). New York: Oxford University Press, USA.

[8] Engelbrecht, A. 2007. Computational Intelligence: An Introduction. New York. NY: Wiley.

[9] Camp, C., & Bichon, B. 2004. Design of Space Trusses Using Ant Colony Optimization. Journal of Structural Engineering, ASCE ,Vol. 130, No. 5, pp. 741-751.

[10] Dorigo, M., & Maniezzo, V., & Colorni, A. 1996. The Ant System: Optimization by a Colony of Cooperating Agents. IEEE Transactions on Systems, Man, and Cybernetics–Part B, pp. 1-13.

[11] Das, B.M. 1999. Principles of Foundation Engineering. Fourth edition, Publishing Workflow System, Pacific Grove, Calif.

ISGSR 2011 - Vogt, Schuppener, Straub & Bräu (eds) - © 2011 Bundesanstalt für Wasserbau ISBN 978-3-939230-01-4

Sensitivity analysis and design of reinforced concrete cantilever retaining walls using bacterial foraging optimization algorithm

M. Ghazavi
Faculty of Civil Engineering, K. N. T. University of Technology, Tehran, Iran

V. Salavati
Islamic Azad University, Central Tehran branch, Tehran, Iran

ABSTRACT: This paper presents an economic optimization and sensitivity analysis for reinforced concrete cantilever (RCC) retaining walls using the bacterial foraging optimization algorithm (BFOA). For this purpose and to solve the optimization problem, BFOA is inspired by the social foraging behavior of *Escherichia coli*. The results of analyses based on the BFOA method have been compared with other available optimization data extracted from other optimization schemes. The results show that the BFOA method can be successfully applied to find the minimum cost design of RCC retaining walls, overcoming the difficulties associated with the practical and realistic assessment of the structural costs and their complex inter-relationship with the imposed constraints on the solution space. A detailed sensitivity analysis for selected design variables, parameters and related safety factors will be presented.

Keywords: retaining walls, reinforced concrete, bacterial foraging optimization algorithm, sensitivity analysis.

1 INTRODUCTION

Concrete cantilever retaining walls are one soil-structure system used to support earth backfills. The construction of concrete cantilever retaining walls is typically motivated by the need to eliminate slope failure and instability in road construction projects. They are also used to support bridges and similar overpass and underpass elements. Their design must satisfy two major requirements: internal stability, which is ensured by sufficient resistance against bending moments and shear forces, and external stability, which means that, except for small movements necessary to mobilize the earth pressures, the wall must be in equilibrium with respect to external forces.

Current design of concrete retaining walls is highly dependent on the experience of engineers. The structure is defined on a trial-and-error basis. Tentative design must satisfy the limit states prescribed by concrete codes. This process leads to safe designs, but the cost of the RCC walls is, consequently, highly dependent upon the experience of the designer. Structural optimization methods are good alternatives to designs based on experience.

Over the past years a number of optimization algorithms have been used extensively in structural optimization problems, from exact methods, to heuristic search methods widely applied for global optimization. The exact methods usually following iterative techniques of linear programming to find the optimal solution, and heuristic search methods usually used stochastic search algorithms to find the optimal solution. The first category is useful when the number of variables is limited and they require a small number of iterations. The second category involves simple algorithms such as genetic algorithm, particle swarm, ant colony, and so on (Perea et al., 2007). However, they also require a considerable computational effort, since they include a large number of iterations in which the objective function is evaluated and the structural constraints are checked.

Optimum design of retaining walls has been the subject of a number of studies. Saribas and Erbatur (1996) used exact method to solve seven design variable optimization problem. Ceranic et al. (2001) applied simulated annealing (SA) to minimum cost design of retaining walls. Yepes et al. (2008) implemented a parametric study of optimum earth-retaining walls by SA.

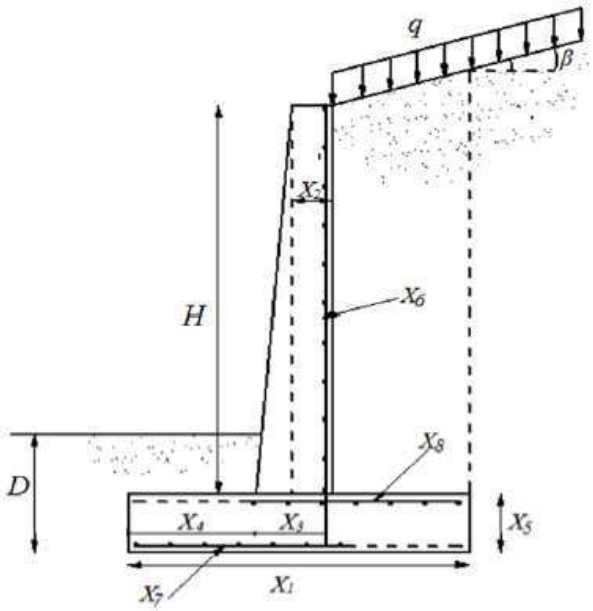

Figure 1. Cross section of the RCC retaining wall.

In this paper, for the first time, authors proposed bacterial foraging optimization algorithm (BFOA) to minimum cost design of RCC retaining walls. BFOA is inspired by the social foraging behavior of *Escherichia coli*. BFOA has already drawn the attention of researchers because of its efficiency in solving real optimization problems arising in several application domains. The formulation of the problem includes 8 design variables: five variables define the geometry of the RCC walls and three variable deal with reinforcement set-up (Figure 1). For structural design details, the recommendations of the Building Code Requirements for Structural Concrete (ACI 318-08) are used. The effectiveness of the approach is illustrated by a common numerical example. As will be shown, BFOA can successfully be applied to minimum cost design of RCC retaining walls with respect to satisfy all geotechnical and structural constraints. To show the robustness of the BFOA, the authors compare the results driven from BFOA with Saribas and Erbatur (1996) for a numerical example. Finally, the solution approach allows to study sensitivity of optimum design.

2 FORMULATION OF THE OPTIMIZATION PROBLEM

The follow potential failure mechanisms considered in design of RCC walls: sliding, overturning, bearing capacity and foundation uplift. Additionally, each element of the wall must individually resist against the forces induced by the weight of backfill material. Thus, the optimization problem deals with the stability of the structure, design requirement, and geometrical constraint.

2.1 *Design variables*

The formulation of the problem includes 8 design variables: five geometrical ones dealing with the thickness of the stem at top and bottom, the thickness of the footing, as well as the toe and the heel lengths; and three variables for reinforcement set-up. Table 1 shows the 8 design variables. Figure 1 indicates the main variables for optimum design.

Table 1. Design variables definition

Symbol	Design variables
X_1	Total base width
X_2	Stem thickness at top
X_3	Stem thickness at bottom
X_4	Toe length
X_5	Thickness of the base slab
X_6	Vertical steel area of the stem
X_7	Horizontal steel area of the toe
X_8	Horizontal steel area of the heel

2.2 *Design parameters*

Parameters are pre-assigned data and they are kept constant in the optimization process. The height of the stem is the main parameter and considered fixed for calculations. Other design parameters include internal friction angle of the retained soil, internal friction angle of the base soil, slope of the retained backfill, backfill density, cohesion of the base soil, surcharge load, and the depth of the soil in front of the wall which are all constant during design process. The soil, structural, and other related design parameters pertinent are presented in Table 2.

Table 2. Input parameters for numerical example

Input parameters for numerical example	Unit	symbol	value
Height of stem	m	H	3
Yield strength of reinforcement steel	MPa	f_y	400
Compressive strength of concrete	MPa	f_c	21
Concrete cover	cm	c_c	7
Diameters of bars	cm	φ_{bar}	1.2
Surcharge load	kPa	q	20
Backfill slope	degree	β	10
Internal friction angle of backfill soil	degree	φ	36
Internal friction angle of base soil	degree	φ_{base}	0
Unit weight of backfill soil	kN/m^3	γ_s	17.5
Unit weight of base soil	kN/m^3	γ_{base}	18.5
Unit weight of concrete	kN/m^3	γ_c	23.5
Cohesion of base soil	kPa	c	125
Depth of soil in front of wall	m	D	0.5
Factor of safety for overturning stability	_	SF_o	1.5
Factor of safety against sliding	_	SF_s	1.5
Factor of safety for bearing capacity	_	SF_b	3
Wide beam shear strength of concrete	MPa	ν	0.65
Maximum steel percentage	_	ρ_{max}	0.016
Minimum steel percentage	_	ρ_{min}	0.00333
Shrinkage reinforcement percent	_	ρ_{st}	0.002

2.3 *Constraints*

To insure the wall stability, 10 constraints are considered. They may be categorized as geotechnical or structural constraints. Geotechnical constraints involve overturning, sliding, ground stresses and no tension condition in foundation soil. Structural constraints involve toe shear, toe moment, heel shear, heel moment, shear at the bottom of the stem and moment at the bottom of the stem. These requirements the failure modes that are expressed as function of the design variables and correspond to 10 behavior constraints, defined as inequalities

$$g_i(x) \le 0 \qquad i=1,\ldots,10 \tag{1}$$

where x is the vector of design variables. The basic expressions for geotechnical constraints are given in Eqs. (2) to (4) as:

$$M_R - SF_o M_o \ge 0 \tag{2}$$

$$\mu N_b - SF_s H_b \ge 0 \tag{3}$$

$$\sigma_{all} - \max|\sigma| \ge 0 \tag{4}$$

Eq. (2) corresponds to overturning stability of the wall, where M_R is the total favorable overturning moment; M_o is the total unfavorable overturning moment and SF_o is the overturning safety factor. Eq. (3) states the limit state of sliding. In Eq. (3), H_b is the total horizontal reaction at the base of the footing; N_b is the total vertical reaction of the base of the footing; μ is the base friction coefficient and SF_s is the sliding safety factor. In Eq. (4), σ is the pressure under the base slab; σ_{all} is the allowable bearing capacity.

The distribution of the ground bearing pressure below the rigid base is assumed to be trapezoidal, that is, the effective eccentricity of the resultant vertical forces must lies within the middle third of the base.

This is the forth geotechnical constraints. Structural constraints such as toe shear, toe moment, heel shear, heel moment, shear at the bottom of the stem and moment at the bottom of the stem, must be satisfied according to Building Code Requirements for Structural Concrete (ACI 318-08). It is worth noting that some side constraints, like maximum or minimum percentage of steel in each section, must be satisfied, too.

2.4 *Cost function*

The problem of structural concrete optimization proposed in this study consists of an economic optimization. It deals with the minimization of the objective function F of Eq. (5), satisfying all the constraints discussed in the previous section.

$$F(x_1, x_2, ..., x_n) = \sum_{i=1}^{r} p_i * m_i(x_1, x_2, ..., x_n) \tag{5}$$

where x_i are design variables, p_i are the unit prices and m_i are the measurements of the seven units in which the construction of the RCC wall is split. The cost function is the value of materials (concrete and steel) and all the entries required to evaluate the entire cost of the wall per linear meter (formwork, excavation, fill, etc.), including, for example, the excavation of the foundation and the lateral fill of the walls.

3 PROPOSED BACTERIAL FORAGING STRATEGY

3.1 *Brief overview*

Bacterial foraging optimization algorithm (BFOA) is a new evolutionary computation technique which has been inspired by the foraging behavior of *Escherichia coli* and proposed by Passino (2002). Bacterial Foraging is an optimization technique based on population search and efficient for global search method. The idea of bacteria foraging principle is based on the fact that natural selection tends to eliminate animals with poor foraging strategies through methods for locating, handling, and ingesting food, and to favor the propagation of genes of those animals that have successful foraging strategies. They are more likely to apply reproductive success to have an optimal solution. After many generations, poor foraging strategies are either eliminated or shaped into good ones. These optimization models could provide a social foraging environment where groups of parameters communicate cooperatively for finding solutions to engineering problems like minimum cost design of structures. The *E. coli* bacteria that are present in our guts have a foraging strategy governed by four processes, namely, chemotaxis, swarming, reproduction, and elimination and dispersal (Passino, 2002). The BFOA parameters required for numerical application are presented in Table 3.

Table 3. BFOA parameters used for numerical example and sensitivity analysis

BFOA parameters	Symbols	value
Dimension of the search space	P	8
Total number of bacteria in the population	S	30
The number of chemotactic steps	N_c	4
The swimming length	N_s	4
The number of reproduction steps	N_{re}	2
The number of elimination-dispersal events	N_{ed}	2
Elimination-dispersal probability	P_{ed}	.2

3.2 *Chemotaxis*

An *E. coli* bacterium can move in two different ways: It can run (swim for a period of time) or it can tumble, and alternate between these two modes of operation in the entire lifetime. In the BFOA, a unit walk with random direction represents a tumble and a unit walk in the same direction indicates a run. In computational chemotaxis, the movement of the *i*th bacterium after one step is represented as:

$$\theta^i(j+1,k,l) = \theta^i(j,k,l) + C(i)\phi(j) \tag{6}$$

where $\theta^i(j,k,l)$ denotes the location of ith bacterium at jth chemotactic, kth reproductive and lth elimination and dispersal step. $C(i)$ is the length of unit walk, which is a constant in basic BFOA and $\phi(j)$ is the direction angle of the jth step. When its activity is run, $\phi(j)$ is same as $\phi(j\text{-}1)$, otherwise, $\phi(j)$ is a random angle directed within a range of $[0,2\pi]$. If the cost at $\theta^i(j+1,k,l)$ is better than the cost at $\theta^i(j,k,l)$ then the bacterium takes another step of size $C(i)$ in that direction otherwise it is allowed to tumble. This process is continued until the number of steps taken is greater than the number of chemotactic loop, N_c.

3.3 *Swarming*

The bacteria in times of stresses release attractants to signal bacteria to swarm together. Each bacterium also releases a repellant to signal others to be at a minimum distance from it. Thus all of them will have a cell to cell attraction via attractant and cell to cell repulsion via repellant. The cell to cell signaling in *E. coli* swarm may be mathematically represented as:

$$j_{cc}\left(\theta, P\left(j,k,l\right)\right) = \sum_{i=1}^{s} j_{cc}\left(\theta, \theta^i\left(j,k,l\right)\right) =$$

$$\sum_{i=1}^{s}\left[-d_a \exp\left(-w_a \sum_{m=1}^{p}\left(\theta_m - \theta_m^i\right)^2\right)\right] + \sum_{i=1}^{s}\left[h_r \exp\left(-w_r \sum_{m=1}^{p}\left(\theta_m - \theta_m^i\right)^2\right)\right] \tag{7}$$

Where $j_{cc}(\theta,P(j,k,l))$ represents the objective function value to be added to the actual objective function, S is the total number of bacteria, p is the number of variables to be optimized and $\theta=[\theta_1,\theta_2,\ldots,\theta_p]^T$ is a point in the p-dimensional search domain. d_a, w_a, h_r and w_r are coefficients to be chosen properly.

3.4 *Reproduction*

The least healthy bacteria eventually die while each of the healthier bacteria (those yielding lower value of the objective function) asexually split into two bacteria, which are then placed in the same location. This keeps the swarm size constant.

3.5 *Elimination and dispersal*

In long term, motile behavior of bacteria involves that all the bacteria may be annihilated at once in the local environment. The life of a population of bacteria changes either gradually by consumption of nutrients or suddenly due to some other influences. Events can kill or disperse all the bacteria in a region. They have the effect of possibly destroying the chemotactic progress, but in contrast, they also assist it, since dispersal may place bacteria near good food sources. Elimination and dispersal helps in reducing the premature solution point or local optima (Ritanjali et al., 2009). The main parameters of BFOA for optimal design of RCC walls are shown in Table 3.

4 NUMERICAL EXAMPLE

The effectiveness of the implemented BFOA algorithm on structural optimization is shown through the use of numerical example based on Saribas and Erbatur (1996). For the sake of comparison, this example was solved again using presented methodology and for the same conditions. Input parameters for analysis and optimal design process are given in Table 2.

It is worth noting that they did not measure the cost of excavation, formwork and backfill. In order to optimum design of this case, the optimal design procedure is coded in MATLAB. This example involves a RCC retaining wall with 3 meter height of the stem. The latter pressure corresponds to the active state and agrees with Rankin's theory. For calculation of ultimate bearing capacity, Hansen method is used. As recommended in Bowles (1982) all design variables have practical minimum and maximum value. Hence these upper and lower bound constraints are presented in Table 4.

Table 4. Lower bounds and upper bounds for design variables

Design variables	Bounds	
	Lower bound	Upper bound
X_1	0.4H(12/11)	(0.7H)/0.9
X_2	0.2	0.5
X_3	0.2	(H/0.9)/10
X_4	[0.4H(12/11)]/3	[(0.7H)/0.9]/3
X_5	[H(12/11)]/12	(H/0.9)/10
X_6	$10000\rho_{min}$ (X_{3l} - 0.01 d)*	$10000\rho_{max}$ (X_{3u}- 0.01 d)*
X_7	$10000\rho_{min}$ (X_{4l} - 0.01 d)*	$10000\rho_{max}$ (X_{4u}- 0.01 d)*
X_8	$10000\rho_{min}$ (X_{4l} - 0.01 d)*	$10000\rho_{max}$ (X_{4u} - 0.01 d)*

*Note: ρ_{min} and ρ_{max} are minimum and maximum steel ratios respectively. X_{il} and X_{iu} are lower bound and upper bound for X_i variable, respectively and $d = \varphi_{bar} / 2 + C_c$.

Table 5 compares the optimization results obtained from the BFOA method and Saribas and Erbatur (1996) for the retaining wall considered. As seen, only X_1 variable had sensible change for both two methods, also the optimum price evaluated using BFOA was 80.53 $/m, which is lower than that evaluated by Saribas and Erbatur (1996). In both of methods the program used lower bounds for X_4, X_5, X_7, X_8 variables.

Table 5. Optimization result for retaining wall

Design variable	Units	Optimum values	
		Saribas and Erbatur	BFOA
X_1	m	1.578	1.507
X_2	m	0.2	0.2
X_3	m	0.258	0.282
X_4	m	0.436	0.436
X_5	m	0.273	0.273
X_6	cm^2	12.574	12.483
X_7	cm^2	6.551	6.551
X_8	cm^2	6.551	6.551
Minimum cost	$/m	82.474	80.53

5 SENSITIVITY ANALYSIS

A sensitivity analysis adds quality to a design and supplies very important information on the work being designed from the view point of cost and reliability. The sensitivity analysis is very useful to (a) the designer, who can know which data values are more influential on the design, (b) to the builder, who can know how changes in prices influence the total cost, and (c) to the code maker, who can know the costs and reliability changes associated with an increase or decrease in the required safety factors or failure probabilities. The basic parameters and prices considered for sensitivity analysis are given in Table 6 and Table 7, respectively. These prices were provided by Yepes et al. (2008). All other requirements for structural design are based on ACI 318-08.

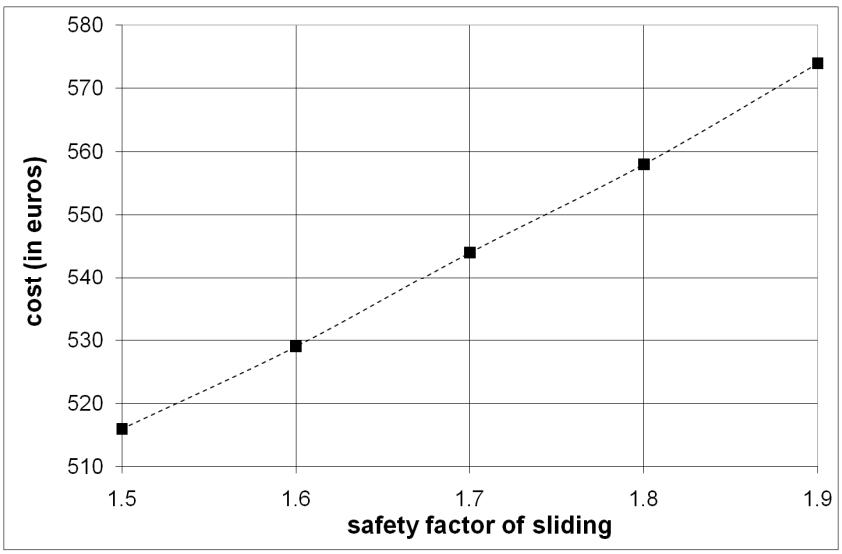

Figure 2. Cost variation against different safety factor of sliding for constant 5 meter height

Table 6. Input parameters for sensitivity analysis

Input parameters for sensitivity analysis	Unit	symbol	value
Yield strength of reinforcement steel	MPa	f_y	400
Compressive strength of concrete	MPa	f_c	21
Concrete cover	cm	c_c	7
Diameters of bars	cm	φ_{bar}	1.6
Surcharge load	kPa	q	20
Backfill slope	degree	β	10
Internal friction angle of backfill soil	degree	φ	36
Internal friction angle of base soil	degree	φ_{base}	20
Unit weight of backfill soil	kN/m^3	γ_s	17.5
Unit weight of base soil	kN/m^3	γ_{base}	18.5
Unit weight of concrete	kN/m^3	γ_c	23.5
Cohesion of base soil	kPa	c	50
Depth of soil in front of wall	m	D	0
Factor of safety for overturning stability	_	SF_o	1.5
Factor of safety against sliding	_	SF_s	1.5
Factor of safety for bearing capacity	_	SF_b	3

Table 7. Basic prices of the cost function of the walls

Units	Cost (euro)
m^3 of earth removal	3.01
m^2 of foundation formwork	18.03
m^2 of stem formwork	18.63
Kg of steel	.56
m^3 of concrete in foundations	50.65
m^{3}of concrete in stem	56.66
m^3 of earth fill-in	4.81

In this study, results concerned with sensitivity of optimum solutions with respect to height, the base friction coefficient, the type of fill as regards its angle of internal friction and safety factor for sliding are presented. In Figure 2 cost variation against safety factor of sliding is depicted. In this case the height of the wall is constant and is equal to 5 meter, the internal friction angle of the backfill soil is equal to 36°, base friction coefficient μ, is equal to .237*(μ=2/3φ_{base}*, where φ_{base} is 20°). A small coefficient for 1.5 causes an average decrease in cost of 11.24% as compared to a coefficient for 1.9.

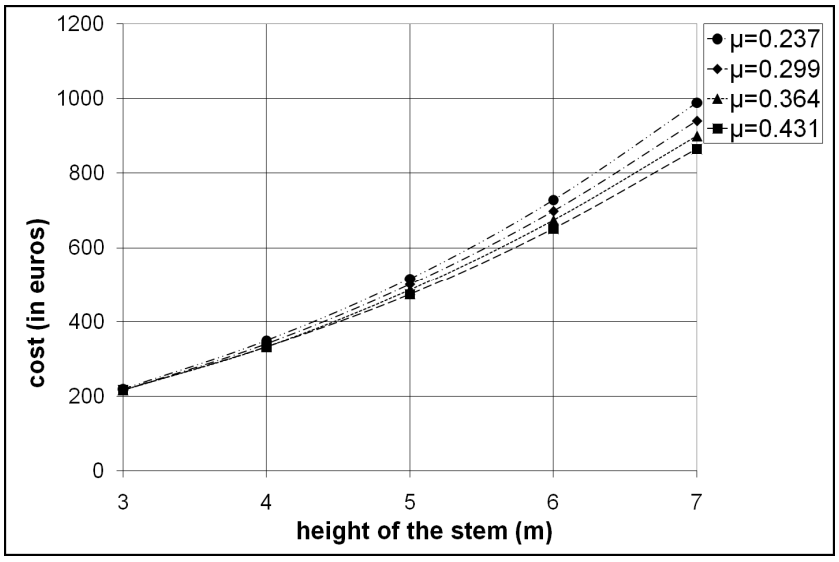

Figure 3. Cost variation for different base friction angle

Figure 3 illustrates the cost variation for different base friction angles. The internal friction angle of the base soil can vary from 20° to 35° with an increment of 5°. The results show that for higher height, optimum cost become more sensitive to internal friction angle of the base soil. For example, for a wall with 7 meter height, choosing μ=0.431, causes cost reduction of 14.33% in comparison with considering μ=0.273.

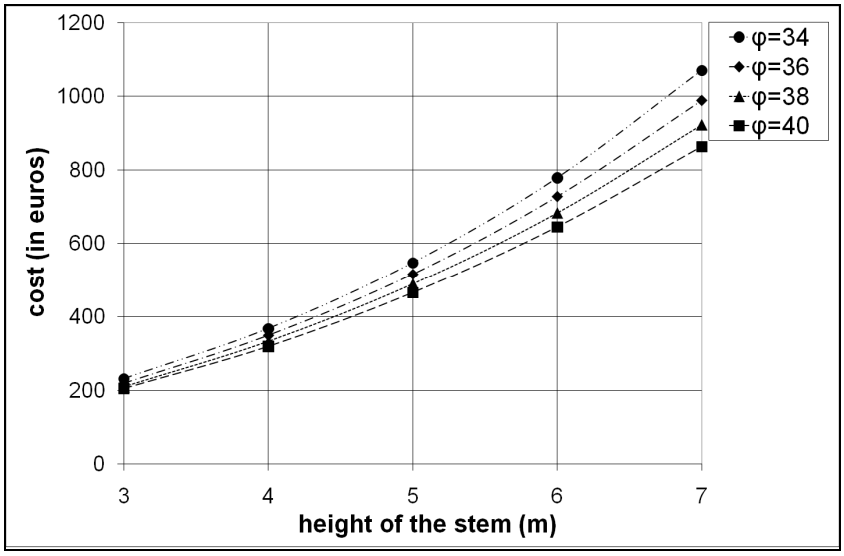

Figure 4. Cost variation for different backfills

Figure 4 shows cost variation against internal friction angle of backfill soil. The internal friction angle of the backfill soil can vary 34° to 40° with 2° increment. Figure 4 explains why it is beneficial to use more compacted soil offering greater internal friction angles.

6 CONCLUSIONS

This paper presents in detail the background and implementation of BFOA suitable for economic optimization and sensitivity analysis of RCC walls. BFOA is inspired by the pattern exhibited by bacterial foraging behavior. The bacterial foraging system primarily consists of four sequential mechanisms namely chemotaxis, swarming, reproduction and elimination-dispersal. The results from the considered numerical example based on using BFOA show the ability of the algorithm to find optimal results. The BFOA results are also comparable to other structural optimization methods and even offer better results. The simplicity of implementation of the BFOA makes it possible to apply for optimization of retaining walls.

REFERENCES

ACI 318-08, 2008. Building Code Requirements for Structural Concrete and Commentary. American Concrete Institute International.

Bowles, J., 1982. Foundation analysis and design. McGraw-Hill, New York.

Ceranic, B., Fryer, B., Baines, R. W . 2001. An application of simulated annealing to the optimum design of reinforced concrete retaining structures. Computers and Structures, 79: 1569-1581.

Majhi, R., Panda, G., Majhi, B., Sahoo, G.2009. Efficient prediction of stock market indices using adaptive bacterial foraging optimization (ABFO) and BFO based techniques. Expert systems with applications, 36: 10097–10104

Passino, K. M. 2002. Biomimicry of bacterial foraging for distributed optimization and control. IEEE Control Syst Mag; 22(3):52–67.

Perea, C., Julian Alcala, J., Yepes, V., Gonzalez-Vidosa, F., Hospitaler, A. 2008. Design of reinforced concrete bridge frames by heuristic optimization . Advances in Engineering Software, 39: 676–688

Saribas, A., Erbatur, F. 1996. Optimization and sensitivity of retaining structures. Journal of Geotechnical Engineering, 122: 649-656.

Yepes, V., Alcala, J., Perea, C., Gonzalez-Vidosa,F. 2008. A parametric study of optimum earth retaining walls by simulated annealing. Engineering Structures, 30(3): 821-830.

ISGSR 2011 - Vogt, Schuppener, Straub & Bräu (eds) - © 2011 Bundesanstalt für Wasserbau ISBN 978-3-939230-01-4

The water level as a time-variant parameter in reliability calculations of river flood embankments

A. Moellmann
Dr. Spang GmbH, Branch Office Stuttgart, Germany

ABSTRACT: Different approaches exist for the determination of the failure probability of a river flood embankment. If the analysis relates to a annual maximum river discharge for a certain river gauge, coming from hydrologic evaluations, four constituents are needed in order to determine the reliability of a river embankment. These four constituents are the limit state equation, the extreme value distribution for the annual maximum river discharge, the exceedance duration line and the relationship between the river water level and the annual maximum river discharge. A fast-converging iteration cycle evaluates the four constituents and leads to the annual failure probability of the embankment. The concept is illustrated by a case study for an embankment at the Elbe river in Eastern Germany.

Keywords: Embankment, failure, hydraulics, statistical analysis, variability

1 INTRODUCTION

When discussing the reliability of river flood embankments, practitioners frequently ask what return period of the river water level is used for the design. Common international standards suggest a design based on specific return periods of the water level. Referring to a reliability analysis based on extreme value distributions, the answer is that all possible return periods are used to determine the annual probability of failure of a river embankment.

The probability of exceedance of the river water level can be described either directly by a probability density function of the annual maximum river water level or indirectly by the annual maximum river discharge. The river water level as the solicitation is therefore a common stochastic parameter differing from other geotechnical stochastic resistance parameters by the unit of its cumulative distribution on the vertical axes which is 1 / year.

2 THE WATER LEVEL AS STOCHASTIC PARAMETER WITH RESPECT TO A RETURN PERIOD

Common design standards suggest to use a single water level with a well-defined return period usually provided by the local authorities in order to design a river embankment. Based on the design standard but taking an uncertainty of the water level into account, van Gelder (2008) suggests a cumulative distribution for the load of a flood defence, i.e. the water level. Also Bachmann et al. (2007) provide a simple, regularly-shaped distribution function for the water level. The mathematical effort to determine the failure probability is quite low.

However, for the determination of the failure probability, the toe of the probability distribution may be of importance as it may largely influence the failure probability. Therefore, the fit of a normal distribution for the frequency of occurrence of a water level at a certain embankment section may not be accurate to model the extremes. In addition to that, the reference period of the failure probability directly corresponds to the return period of the water level which is a constraint for the shift of the annual failure probability to other reference periods.

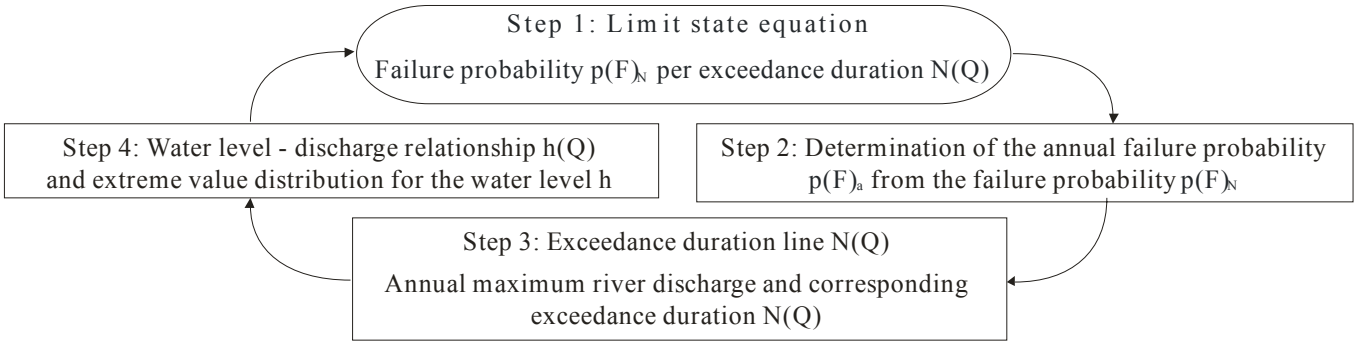

Figure 1. Iteration scheme for the determination of the annual failure probability of an embankment

The iteration scheme shown in Figure 1 is based on an extreme value distribution of the annual maximum river discharge. Four constituents are used in order to determine the reliability of a river embankment which are explained in the following sub-sections. The approach usually leads to an accurate result of the failure probability of an embankment which is shown by the case study in Section 3.

2.1 *Limit state equation*

The determination of the failure probability is based on a limit state equation Z of the following type:

$$Z = R - S \qquad (1)$$

The resistance R against flooding as well as the solicitation S may be a function of any type. In many cases, the solicitation will consist of the water level h which plays a special role among the stochastic parameter as it relates to a return period finally leading to a failure probability with respect to a time unit.

2.2 *Extreme value distribution for the annual maximum river discharge*

There are two ways to formulate the frequency of occurrence of the annual maximum river discharge Q that are appropriate for the iteration scheme used in Figure 1. In the software PC-Ring developed by the Dutch Ministry of Transport, Public Works and Water Management (Steenbergen et al., 2004) for the regular flood risk report in the Netherlands, the relationship is defined as the so-called workline (2).

$$Q(T) = a \cdot \ln T + b \qquad (2)$$

The workline approximates the hydrologic relationship between the annual maximum river discharge Q [in m³/s] and its return period T [in years] for a certain river gauge by a simple logarithmic function. As the approximation may not always be accurate for all return periods, the river characteristics is approximated by three sections with different coefficients a and b. The workline is illustrated in Figure 2 while the return period is plotted in logarithmic scale. A shift of the reference period from the return period T [in years] to the number of exceedance durations T' [in days] can be illustrated by a vertical translation of the workline. In arithmetic terms, the workline can be shifted to the number of exceedance durations T' [in days] for which the discharge will be exceeded. The exceedance duration of a river flood is explained in Section 2.3.

$$T' = \frac{365}{N(Q)} \cdot T \qquad (3)$$

The workline with respect to the number of exceedance durations T' may then be formulated as:

$$Q(T') = a \cdot \ln T' + a \cdot \ln N(Q) - a \cdot \ln 365 + b = a \cdot \ln T' + b' \text{ with } b' = a \cdot \ln N(Q) - a \cdot \ln 365 + b \qquad (4)$$

The second way to formulate the frequency of occurrence of the annual maximum river discharge is an extreme value distribution in which the integral of the distribution from a certain discharge to infinity stands for the probability of exceedance p(Q > Q*) of the discharge Q*. It can be derived that the above-mentioned logarithmic relationship between the return period and the discharge can be transformed into a Gumbel distribution (5) in which the coefficients a and b are adopted from the workline (2):

$$f(Q) = \frac{1}{a} \cdot \mathrm{EXP}[-\frac{1}{a} \cdot (Q - b) - \mathrm{EXP}(-\frac{1}{a} \cdot (Q - b)] \qquad (5)$$

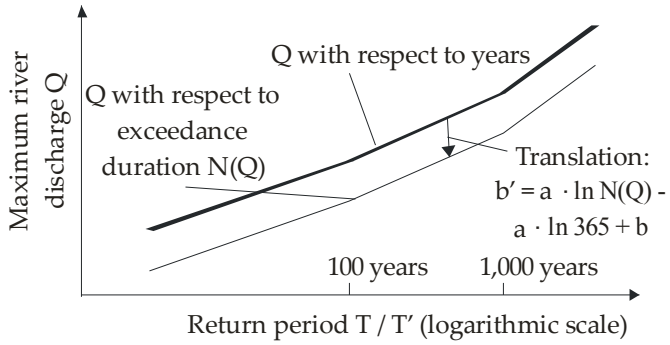

Figure 2. Workline consisting out of three sections as relationship between the annual maximum river discharge Q [in m³/s] and its return period T [in years] and shift of the reference period to the number of exceedance durations T'

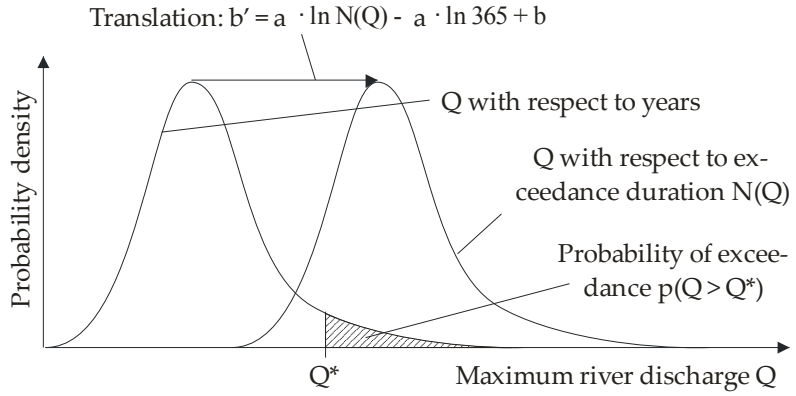

Figure 3. Gumbel distribution as relationship between the annual maximum river discharge Q and its frequency of occurrence p(Q > Q*) and shift of the reference period from the number of years (T) to the number of exceedance durations T'

Similar to the shift of the reference period of the workline (2), the reference period does not change the shape of the extreme value distribution. However, a horizontal translation illustrated in Figure 3 can be noticed for the extreme value distribution which analytically leads to the same transformation from T to T' from equation (3) when b' is used instead of b as mentioned in equation (4).

The return period T can be derived from the probability of exceedance p (Q > Q*) by equation (6):

$$T = -\frac{1}{\ln\left[1 - p(Q > Q^*)\right]} \qquad (6)$$

2.3 *Exceedance duration line*

The exceedance duration line correlates the duration of the flood wave N(Q) with the corresponding river discharge Q. It accounts for the adaptation of the reference period of the frequency of occurrence of the annual maximum river discharge to a shorter period for which flood events can be considered as independent. It originates from the capability of the software PC-Ring to couple high water levels coming from the river discharge with high water levels due to heavy storms which will have a different duration than the river flood.

The determination of the failure probability requires a shift of the reference period to an exceedance duration N(Q) because only for this reference period, flood events coming from heavy rainfall in the catchment area in combination with events coming from a heavy storms can be considered as independent and the extrapolation of the failure probability to one year may be performed taking a correlation of flood events into account.

The iteration scheme illustrated in Figure 1 determines a failure probability per exceedance duration $p(F)_N$. The extrapolation from the exceedance duration N(Q) [in days] to one year is done according to the model by Ferry-Borges and Castanheta (1971). It can be derived that if the water level has a high influence on the failure probability compared to other stochastic parameters, the annual failure probability $p(F)_a$ can be simply extrapolated from the failure probability per exceedance duration $p(F)_N$ as follows:

$$p(F)_a = p(F)_N \frac{365}{N(Q)} \qquad (7)$$

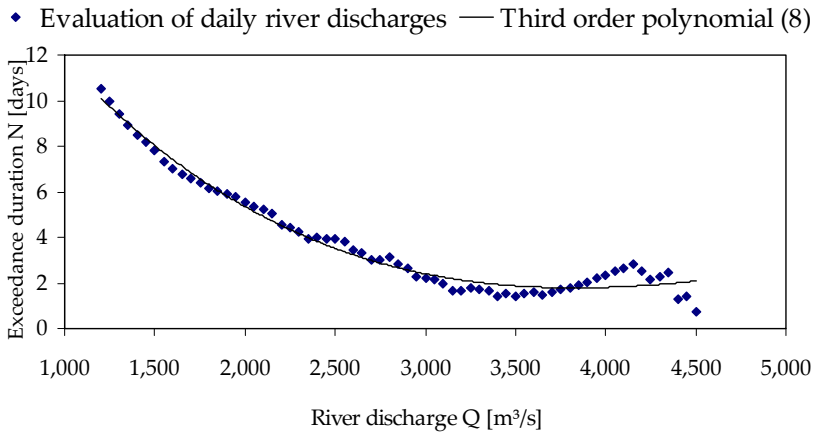

Figure 4. Exceedance duration coming from daily discharge statistics and approximation by a third order polynomial for the river gauge Dresden

If the influence of the water level on the failure probability is not so high, a reduction factor for the annual failure probability considering a correlation of dependent flood events in time must be taken into account.

The relationship of the duration of the flood wave N(Q) [in days] and the corresponding river discharge Q [in m³/s] is evaluated from daily measurements of the river discharge at a certain river gauge and approximated by a third order polynomial in which the coefficients c, d, e and f are fitted:

$$N(Q) = c \cdot Q^3 + d \cdot Q^2 + e \cdot Q + f \qquad (8)$$

2.4 *Relationship between the river discharge and the water level*

In order to evaluate the limit state equation (1) in which the water level h is a stochastic variable, the probability of exceedance of a certain water level is expressed in analytical terms using the extreme value distribution of the annual maximum river discharge. Coming from a hydrodynamic-numerical runoff-model evaluated for various river discharges, the relationship between the river discharge [in m³/s] and the water level [in mNN] at the embankment section can be approximated by a logarithmic function (9) in which the coefficients g and j are fitted. The approximation can be done only for part of the relationship in order to better fit the extremes. The inverse of the logarithmic relationship can be substituted in the extreme value distribution for the annual maximum river discharge (5) leading to a probability density function (10) for the annual maximum water level at the embankment section.

$$h(Q) = g \cdot \ln Q + j \qquad (9)$$

$$f(h) = \frac{1}{a} \cdot \mathrm{EXP}[-\frac{1}{a} \cdot (\mathrm{EXP}\left(\frac{1}{g}(h - j)\right) - b) - \mathrm{EXP}(-\frac{1}{a} \cdot (\mathrm{EXP}\left(\frac{1}{g}(h - j)\right) - b)] \qquad (10)$$

If the probability density function shall be set up not for the annual maximum water level but the water level with respect to the exceedance duration, the parameter b in equation (10) must be replaced by b' according to equation (4).

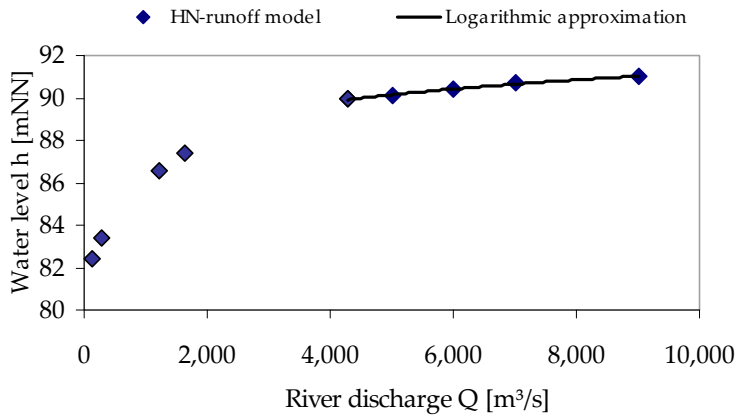

Figure 5. Relationship between the river discharge for the river gauge Dresden and the water level at the embankment section close to Torgau from a hydrodynamic-numerical (HN) runoff model and logarithmic approximation

3 CASE STUDY AT THE ELBE RIVER

3.1 *Hydrologic and hydraulic boundary conditions*

An embankment section at the Elbe river close to Torgau in Eastern Germany is used to illustrate the application of the iteration scheme in Figure 1 to determine the annual failure probability.

The frequency of occurrence of a certain river discharge at the gauge Dresden is given by the workline (2) consisting of three different sections for the corresponding return periods:

$$Q(T) = \begin{cases} 751.24 \cdot \ln T + 895.23 \text{ for} & T < 100 \text{ years} \\ 839.97 \cdot \ln T + 492.26 \text{ for } 100 \text{ years} < T < 1{,}000 \text{ years} \\ 976.34 \cdot \ln T - 458.38 \text{ for} & T > 1{,}000 \text{ years} \end{cases} \quad (11)$$

It can also be formulated as an extreme value distribution according to equation (12) consisting out of three sections which are illustrated in Figure 7:

$$f(Q) = \begin{cases} \frac{1}{751.24} \cdot EXP[-\frac{1}{751.24} \cdot (Q - 895.23) - EXP(-\frac{1}{751.24} \cdot (Q - 895.23))] \text{ for} & Q < 4{,}355 \text{ m}^3/\text{s} \\ \frac{1}{839.97} \cdot EXP[-\frac{1}{839.97} \cdot (Q - 492.26) - EXP(-\frac{1}{839.97} \cdot (Q - 492.26))] \text{ for } 4{,}355 \text{m}^3/\text{s} < Q < 6{,}295 \text{ m}^3/\text{s} \\ \frac{1}{976.34} \cdot EXP[-\frac{1}{976.34} \cdot (Q + 458.38) - EXP(-\frac{1}{976.34} \cdot (Q + 458.38))] \text{ for} & Q > 6{,}295 \text{ m}^3/\text{s} \end{cases} \quad (12)$$

The exceedance duration line for the river gauge in Dresden and the relationship between the river discharge in Dresden and the water level at the considered embankment section are shown in Figures 4 and 5. They can be formulated analytically:

$$N(Q) = -1.682 \cdot 10^{-10} \cdot Q^3 + 2.691 \cdot 10^{-6} \cdot Q^2 - 0.132 \cdot Q + 22.35 \quad (13)$$

$$h(Q) = 1.4882 \cdot \ln Q + 77.475 \quad (14)$$

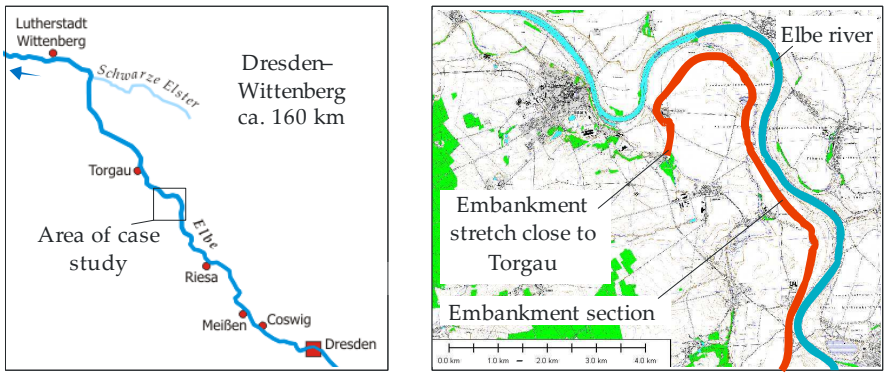

Figure 6. Area of case study at the Elbe river close to Torgau in Eastern Germany

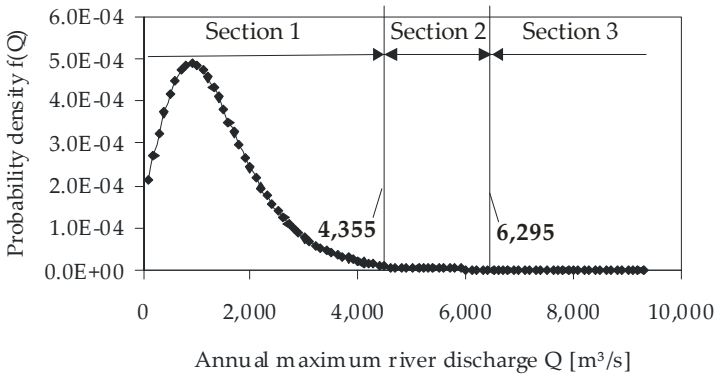

Figure 7. Extreme value distribution for the annual maximum river discharge at the river gauge in Dresden consisting out of three sections

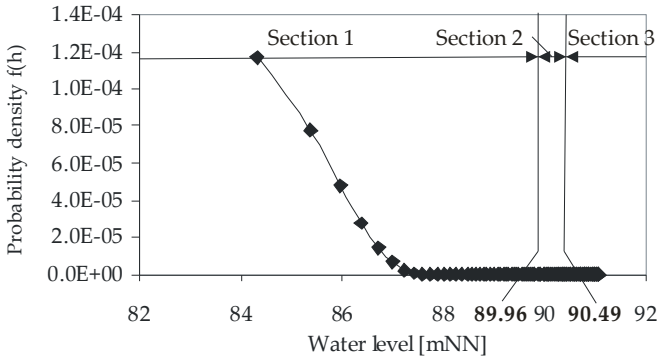

Figure 8. Extreme value distribution for the annual maximum water level at the considered embankment section consisting out of three sections

Using these expressions, a probability density function for the annual maximum water level can be generated which is only expressed in equation (15) for section 1 and which is illustrated in Figure 8:

$$f(Q) = \frac{1}{751.24} \cdot EXP[-\frac{1}{751.24} \cdot (-EXP((h - 77.475)/1.4482) - 895.23) - EXP(-\frac{1}{751.24} \cdot (-EXP((h - 77.475)/1.4482) - 895.23))] \text{ for } h < 89.96 \text{ mNN} \quad (15)$$

3.2 *Validation of the 100-year water level*

The iteration scheme shown in Figure 1 is used to check whether the probability of failure due to overflow of the embankment section close to Torgau is equal to the known return period of the water level when all other uncertainties of the embankment section are neglected. The corresponding limit state equation subtracts the water level h as the only stochastic parameter from the water level of 89.96 mNN with a known return period of 100 years:

$$Z = 89.96 \text{ mNN} - h \quad (16)$$

The iteration starts assuming a exceedance duration of six days. The corresponding translation b' of the extreme value distribution of the water level h can be calculated according to:

$$b' = a \cdot \ln N(Q) - a \cdot \ln 365 + b = \begin{cases} 751.24 \cdot \ln 6 - 751.24 \cdot \ln 365 + 895.23 = -2{,}191 \\ 839.97 \cdot \ln 6 - 839.97 \cdot \ln 365 + 492.26 = -2{,}958 \\ 976.34 \cdot \ln 6 - 976.34 \cdot \ln 365 - 458.38 = -4{,}469 \end{cases} \quad (17)$$

The substitution of the parameters a, b', g and j from the equations (11), (17) and (14) into equation (10) leads to the probability density function of the water level h for the corresponding exceedance duration of 6 days for three sections for different return periods. For the Section 1 of the probability density function in equation (15), the coefficient b = 895.23 must be substituted by the coefficient b' = -2,191.

For the water level as the only one stochastic parameter, the limit state equation can be evaluated without using probabilistic calculation techniques but by simple integration of the probability density function from 89.96 mNN to infinity. The failure probability with respect to the exceedance duration of six days is $1.628 \circ 10^{-4}$ 1 / 6 days. With the water level h being the only stochastic parameter, the failure probability can be simply extrapolated from a reference period of six days to one year by equation (7):

$$p(F)_a = 1.628 \cdot 10^{-4} \cdot \frac{365 \text{ days/a}}{6 \text{ days}} = 9.904 \cdot 10^{-3} / \text{a} \quad (18)$$

Using equation (6), the return period of the water level can be determined:

$$T = -\frac{1}{\ln[1 - 9.904 \cdot 10^{-3}]} = 100.5 \text{ a} \quad (19)$$

The return period can then be written into the section of the workline (11) with the appropriate return period and the exceedance duration can be updated according to equation (13) which leads to the next iteration step.

$$Q(T) = 839.97 \cdot \ln 100.5 + 492.26 = 4{,}364 \text{m}^3/\text{s} \quad \text{for } 100 \text{ years} < T < 1{,}000 \text{ years} \tag{20}$$

$$N(Q) = -1.682 \cdot 10^{-10} \cdot (4{,}364 \text{m}^3/\text{s})^3 + 2.691 \cdot 10^{-6} \cdot (4{,}364 \text{m}^3/\text{s})^2 - 0.132 \cdot (4{,}364 \text{m}^3/\text{s}) + 22.35 = 2.015 \text{days} \tag{21}$$

The results are summarized in Table 1. After two steps, the iteration already converges and yields a return period of 100.5 years which confirms the return period of the water level of 100 years set in the limit state equation. It shall be demonstrated in the next example that the concept to determine the failure probability can also be applied for a reliability analysis for a regular failure mode of an embankment.

Table 1. Results of the validation of the 100-year-water level

Iteration step	N(Q)	$p(F)_{N(Q)}$	$p(F)_a$	T	Q(T)	N(Q)	
1	6 days	$1.628 \cdot 10^{-4}$		$9.904 \cdot 10^{-3}$	100.5 years	4,364 m³/s	2.015 days
2	2.015 days	$5.468 \cdot 10^{-5}$		$9.905 \cdot 10^{-3}$	100.5 years	4,364 m³/s	2.015 days

3.3 *Determination of the annual failure probability for overflow of the embankment*

The iteration scheme in Figure 1 is now applied to a limit state equation for overflow of the embankment which contains more than one stochastic parameter.

$$Z = h_d - h - \Delta h \tag{22}$$

The overflow of an embankment is not only dependent on the return period of the water level h but also on the uncertainty of the crest height h_d of the embankment and on the uncertainty Δh whether the true local water level in front of the embankment section will correspond to the water level at the river chainage in the hydrodynamic-numerical (HN) runoff model. The analysis is done for the same embankment section as in Section 3.2 and therefore the same hydrologic and hydraulic boundary conditions apply. For the crest height and the uncertainty of the local water level, a normal distribution is assumed with mean values and standard deviations shown in Figure 9. A reliability analysis for the embankment section with the software PC-Ring leads to an annual failure probability of $3.25 \cdot 10^{-4}$ 1/a (Moellmann, 2009).

As in Section 3.2, the iteration starts with an assumed exceedance duration of six days for which the translation b' of the extreme value distribution of the water level h can be calculated according to equation (17). As the return period T of the flood is not known, all three sections of the extreme value distribution of the water level need to be evaluated in order to get the annual failure probability p(F)a. In contrast to the simple integration of the probability density function in Section 3.2, the failure probability for overflow must be determined using probabilistic calculation techniques as there are three stochastic parameters. The software Probox (Courage and Steenbergen, 2005) is used to apply the First Order Reliability Method (FORM) (Waarts, 2000). In order to achieve convergence of this iterative calculation technique, the start vector of the stochastic parameters in standard-normalized space needs to be manipulated.

The analysis does not only lead to a failure probability per exceedance duration and a corresponding reliability index β, it also provides sensitivity factors α_i that indicate the sensitivity of the stochastic input parameters on the failure probability. The higher the value, the more the result is affected by the uncertainty of the parameter. In order to update the corresponding river discharge, not the return period T of the flood but the return period of the most probable standard normalized river discharge u_q is used according to equation (6) which corresponds to the probability of exceedance of the river discharge Q*:

$$u_q = -\alpha_q \cdot \beta \tag{23}$$

$$p(Q > Q^*) = \int_{-\infty}^{u_q} \frac{1}{\sqrt{2\pi}} \text{EXP}(-0.5 \cdot t^2) dt \tag{24}$$

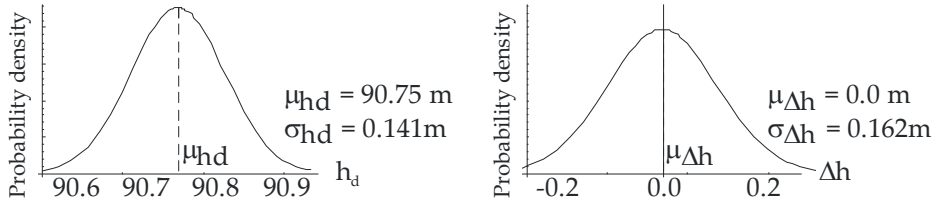

Figure 9. Normal distributions of the stochastic parameters crest height h_d (left) and local water level uncertainty Δh (right)

Table 2. Results of the determination of the annual failure probability for overflow of the embankment

Iteration step	N(Q)	$p(F)_{N(Q)}$	$p(F)_a$	T	α_q	u_q	$p(Q>Q^*)_a$	Q(T)	N(Q)
1	6 days 6701 m³/s	$7.994 \cdot 10^{-6}$ 4.121 days		$4.863 \cdot 10^{-4}$	2056 years		-0.9745	3.214	$6.539 \cdot 10^{-4}$
2	4.121 days 6707 m³/s	$5.496 \cdot 10^{-6}$ 4.122 days		$4.868 \cdot 10^{-4}$	2054 years		-0.9752	3.216	$6.493 \cdot 10^{-4}$
3	4.122 days 6707 m³/s	$5.498 \cdot 10^{-6}$ 4.122 days		$4.868 \cdot 10^{-4}$	2054 years		-0.9752	3.216	$6.493 \cdot 10^{-4}$

The results of the iteration steps are shown in Table 2. As the return period of the flood event is above 1,000 years, section 3 of the extreme value distribution of the water level needs to be evaluated. A convergence of the results can be noticed at least after three iteration steps. Table 3 compares the results of the concept presented in this paper with the results of PC-Ring (Moellmann, 2009). It can be noticed that there is a considerable difference between the results for the applied iteration scheme and the results with PC-Ring. This difference can be mainly explained by the different approximation of the relationship between the river discharge and the water level. In the applied concept, the relationship is approximated by a logarithmic function while it is assumed that a sectionwise linear approximation is used in PC-Ring. The difference becomes quite large as the annual failure probability is low and a slight shift of the probability density function has great influence on the failure probability.

Table 3. Comparison of the results of the applied iteration scheme in Figure 1 with the PC-Ring calculation

Analysis	$p(F)_a$	T	α_{hd}	α_q	$\alpha_{\Delta h}$
Iteration scheme	$4.868 \cdot 10^{-4}$	2054 years	0.1453	-0.9752	-0.1669
PC-Ring	$3.252 \cdot 10^{-4}$	3075 years	0.2264	-0.9522	-0.2028

4 CONCLUSIONS AND LIMITATIONS

It has been shown that it is possible to perform a plausibility check “by hand” of the computer-based calculation of the failure probability for an embankment. A probability density function for the water level with respect to an assumed exceedance duration needs to be set up. The application of the iteration scheme in Figure 1 leads to a convergence of the embankment reliability usually after three iteration steps. For a case study at an embankment at Elbe river in Eastern Germany with given hydrologic and hydraulic boundary conditions, the return period of the 100-year water level was confirmed by fully analytical calculations. The computer-aided determination of the annual failure probability for overflow of the embankment by the software PC-Ring was checked by the application of probabilistic calculation techniques. In contrast to an approach, in which a cumulative distribution for the annual maximum water level is used, the suggested method which sets up a probability density function with respect to the exceedance duration is more flexible and more accurate.

Limitations of the presented concept occur when the sensitivity factor of the annual maximum river discharge becomes smaller than 0.92. The extrapolation from the failure probability with respect to the exceedance duration to the annual failure probability according to equation (7) is not accurate and a correlation in time must be taken into account (Steenbergen and Vrouwenvelder, 2003).

5 REFERENCES

Bachmann, D., Huber, N.P. Köngeter, J. 2007. Multikriterielle Entscheidungsunterstützung zur Erstellung von Hochwasserrisikomanagementplänen. Fünf Jahre nach der Flut, Dresdner Wasserbauliche Mitteilungen 35, 85-94.

Courage, W.M.G., Steenbergen, H.M.G.M. 2005. Probox: variables and expressions, Installation and getting started. TNO-rapport 2005-CI-R0056, April 2005.

Ferry-Borges, J., Castanheta, M. 1971. Structural Safety. National Laboratory of Civil Engineering, Lisbon.

Moellmann, A. 2009. Probabilistische Untersuchung von Hochwasserschutzdeichen mit analytischen Verfahren und der Finite-Elemente-Methode, Mitteilung 64 des Instituts für Geotechnik, Universität Stuttgart.

Steenbergen, H.M.G.M., Vrouwenvelder, A.C.W.M. 2003. Theoriehandleiding PC-Ring. Versie 4.0. Deel B: Statistische modellen. TNO-rapport 2003-CI-R0021, April 2003.

Steenbergen, H.M.G.M., Lassing, B.L., Vrouwenvelder, A.C.W.M. & Waarts, P.H. 2004. Reliability analysis of flood defence systems. Heron 49 (1), 51-73.

van Gelder, P. 2008. Reliability Analysis of Flood Defence Systems, Report T07-09-20, FLOODSite.

Waarts, P.H. 2000. Structural reliability using Finite Element Analysis. TU Delft, Delft University Press, Delft, PhD-Thesis.

ISGSR 2011 - Vogt, Schuppener, Straub & Bräu (eds) - © 2011 Bundesanstalt für Wasserbau ISBN 978-3-939230-01-4

Reliability analysis of a pile foundation in a residual soil: contribution of the uncertainties involved and partial factors

A. Teixeira & A. Gomes Correia
University of Minho – C-TAC, Guimarães, Portugal

Y. Honjo
Gifu University, Gifu, Japan

A. Henriques
University of Porto, Porto, Portugal

ABSTRACT: Reliability evolved from other areas, such as structures, requiring special adaptation when applied to geotechnical engineering. This paper shows one way to treat geotechnical uncertainties in a simple way. A sensitivity analysis, based on a series of calculations of the probability of failure for a single pile foundation is done in order to investigate the influence of each uncertainty source in reliability index. This experimental pile was installed in a residual soil in Portugal and was designed to withstand a vertical axial load. It was found, for this experimental case study, that the most important uncertainty source comes from model error, and not from the soil's spatial variability and uncertainty. Finally, the procedure to evaluate the resistance and load partial safety factors is shown and, for the same pile foundation, the safety factors are calculated and compared to the ones recommended by the Eurocode 7. Both methodologies are based on Monte Carlo simulation technique.

Keywords: bearing capacity, Eurocode, pile foundation, reliability analysis, safety factors

1 INTRODUCTION

All civil engineers are aware of how uncertainties are important for the design. But in some areas, such as in geotechnics, the uncertainties are mostly unknown or really difficult to measure. That is why, unlike in structural design, the traditional way that geotechnical engineers introduce the uncertainties in the design is using high global safety factors (SF), based on past experience. However, this way of treating uncertainties does not give a rational basis to understand their influence on the design. Based on such background, this paper shows one way that geotechnical uncertainties can be treated in a simple way.

The reliability design has traditionally been classified into three levels:

- Level I: semi-probabilistic methods. Deterministic formulas are applied to the representative values (nominal or characteristic) multiplied by partial SF. The characteristic values are calculated based on statistical information, while partial SF are based on level II or III reliability methods.
- Level II: approximate probabilistic methods. The uncertainties are characterized by their mean, variance and covariance only (nonparametric). The probabilistic evaluation of safety is done by approximated numerical techniques, *i.e.* simplified hypothesis like first order reliability method (FORM).
- Level III: full probabilistic methods. Based on techniques that take into account all the variables' probabilistic characteristics, the probability of failure is analytically evaluated, but only when the problem is very simple. In more complex problems one needs to carry out simulations methods, for example, Monte Carlo simulations (MCS).

In this study, the level III methodology used (Honjo et al., 2010) aims to eliminate the possible confusions and difficulties that traditional reliability methodologies, applied in structures, can cause to geotechnical designers in practice. A series of calculations of the probability of failure for a case study were done, in order to investigate the influence of each uncertainty source. SF for the same case study (to be used in level I reliability design) were also evaluated based on design value method formulas and MCS (Kieu Le, 2008 and Honjo et al., 2009). The SF for resistance and load are then compared to the ones recommended by Eurocode 7 (CEN, 2007).

2 CASE STUDY

The case study presented in this paper is a single pile, vertically loaded, from an experimental site in Portugal (Figure 1.a). The pile was bored in residual soil and is 0.6m in diameter and 6m in depth. Different laboratory and *in situ* tests were performed in this experimental site, but only SPT (standard penetration tests) were considered in this paper (Figure 1.b) to evaluate the bearing capacity of the pile.

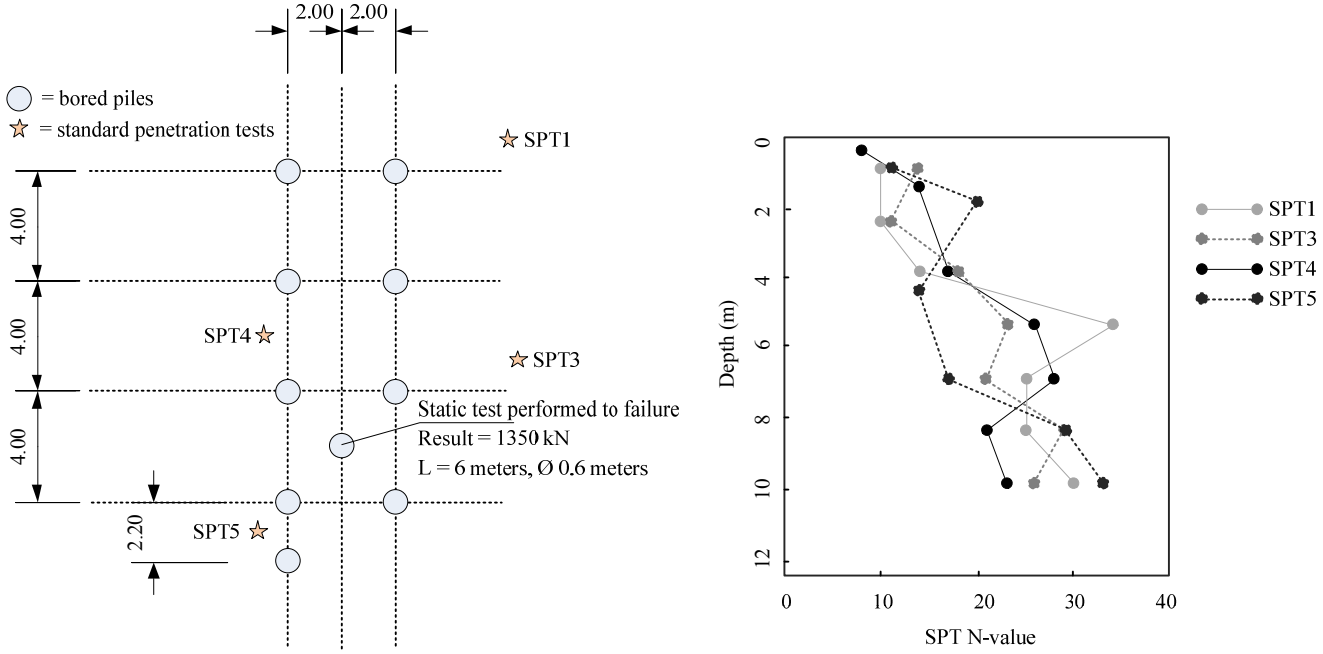

a) plan view b) SPT results

Figure 1. Experimental site - adapted from Fonseca and Santos (2008)

3 RELIABILITY ANALYSIS

3.1 *Methodology*

The methodology used for the reliability analyses has been adapted from previously published work by Honjo et al. (2010) and it is based on Monte Carlo simulations (MCS). This methodology differs from the typical employed in structural analysis. The goal is to remove the uncomfortable feelings that geotechnical engineers may have when using traditional reliability based design tools, like confusion and loss of perception of the results. Therefore, "Geotechnical Design Tools" and "Risk Assessment Tools" are separated as much as possible, allowing a better understanding of the different steps and responses obtained.

For a pile foundation and soil investigation with SPT, the process would be like shown in Figure 2, where the uncertainties are introduced in various stages. This process involves four steps:

1. Spatial variability and statistical estimation error are studied together. In many cases, it is very difficult or impossible to separate them. This step comprehends:
   - the calculation of a trend of *in situ* or laboratory tests (*e.g.* SPT – standard penetration test),
   - and analysis of residual errors, including estimation of autocorrelation distance (Vanmarcke, 1977).
2. Transformation error and modelling uncertainty are evaluated – these values are calculated based on documentation data, see for example Kulhawy and Mayne (1990), Okahara et al. (1991), Uzielli et al. (2006), AASHTO (2007) and Phoon (2008).
3. Resistances (R) and actions (E) are calculated and the performance function defined – Eq. (1):

$$M = g(R,E) = R - E \tag{1}$$

where M = safety margin, g = performance function, R = resistance and E = actions.

It should be noticed that the uncertainties of the actions are also obtained by bibliography and if the performance function is complex and/or requires quite amount of calculation efforts (like finite element method), the response surface method or neural networks can be used to find an approximate simpler function of the basic variables.

4. Finally, *m* MCS are performed in order to assess the probability of failure and reliability index of the problem by Eq. (2).

$$pf = \sum_{1}^{m} I, \quad I = \begin{cases} 0 \; if \;\; M \geq 0 \\ 1 \; if \;\; M < 0 \end{cases} \quad ; \; \beta = -\Phi^{-1}(pf) \tag{2}$$

where pf = probability of failure, m = number of MCS, I = failure indicator, M = safety margin, β = reliability index and Φ = is the normal cumulative density function with mean 0 and variance 1.

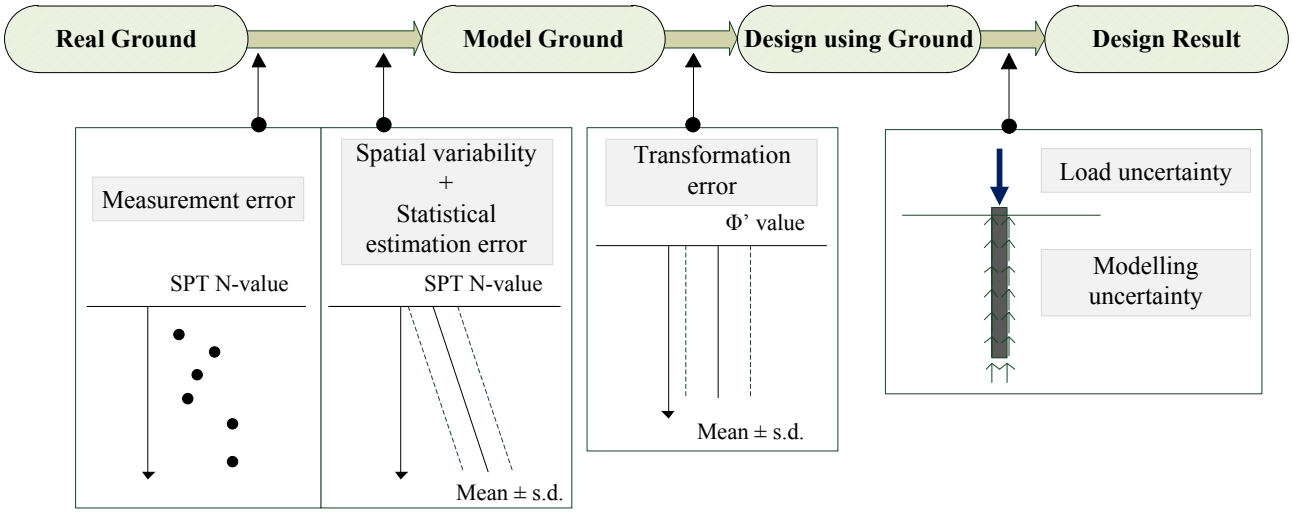

Figure 2. Proposed reliability analysis for a pile foundation

For this case study, where an empirical method was used to predict the bearing capacity of the pile, the performance function is given by Eq. (3).

$$M = \left(R_{tip} + R_{side}\right) - \left(G + Q\right) = \left(\delta_t \times Q_{tip} + \delta_f \times F_{side}\right) - \left(\delta_G \times G_k + \delta_Q \times Q_k\right) \tag{3}$$

where M = safety margin, R_{tip} = tip resistance of the pile, R_{side} = side resistance of the pile, G = permanent load, Q = variable load, δ_t = factor for model error uncertainty (tip resistance), Q_{tip} = predicted tip resistance, δ_f = factor for model error uncertainty (side resistance), F_{side} = predicted side resistance, G_k = permanent characteristic load and Q_k = variable characteristic load. The resistances are predicted by an empirical method, in this case, based on SPT (SHB, 2001 - Japanese method) and the actions were evaluated from the predicted load for a length of 6m and applying partial safety factors from Eurocode 7 (CEN, 2007) according to Eq. (4).

$$R_d \geq E_d \Leftrightarrow \frac{R_{predicted}}{1.15} \geq 1.35 \cdot Load + 1.50 \cdot Load \quad , \; considering \; G_k = Q_k = Load \leq 463\, kN \tag{4}$$

where R_d = design resistance value, E_d = design action value, $R_{predicted}$ = resistance predicted based on empirical method SHB (2001) (result: 1518 kN), *Load* = value of load, [1.15, 1.35, 1.50] = partial safety factors (CEN,2007), G_k = permanent characteristic load and Q_k = variable characteristic load.

3.2 *Characterization and evaluation of uncertainties*

The uncertainties can be characterized as physical uncertainties (inherent uncertain nature of the parameter), modelling uncertainties (theoretical approaches and predictions), statistical uncertainties (finite size and fluctuations in the samples) and human errors (in the execution of multiple tasks). Human errors are a type of uncertainty that is not, in general, included in reliability analysis.

In this case study we have the physical uncertainties of actions (permanent and variable loads) and the inherent soil variability, as well as the modelling uncertainty (or model error) in the evaluation of resistance by an empirical method based on SPT. The Table 1 shows the values of the factors (δ) that take into account those uncertainties. The standard deviation of soil variability (value of N_{SPT}) can be reduced based on autocorrelation (Vanmarcke, 1977). Variables that vary continuously over a space or time are referred to as random fields (autocorrelation between variables). Normally values of a parameter measured at considerable distances are independent, but, if one measures the value of a parameter, the uncertainty in the value at a nearby point becomes less uncertain, because it is highly correlated to the first

point value. That spatial autocorrelation allows the reduction of variances, but it is usually ignored due to difficulties in practical application.

Table 1. Uncertainties evaluation

	Soil variability		Modelling uncertainty		Actions' uncertainties	
	N_{SPT},tip	N_{SPT},side	tip	side	permanent	variable
Mean value	10.26+1.91z		1.12	1.07	1.0	0.6
Standard deviation	4.6*	4.6**	0.706	0.492	0.10	0.21
Distribution	Normal		Lognormal	Lognormal	Normal	Gumbel
Reference			Okahara et al. (1991)		Holicky et al. (2007)	

* reduced taking into account the influence zone on the pile tip (3×Diameter) as averaging over the thickness.
** reduced taking into account the length of the pile as averaging over the thickness.

3.3 *Evaluation of the reliability index and its sensitivity to uncertainties*

After quantifying the uncertainties, one can evaluate its impact on the performance of the structure. MCS (m=100,000) were done in order to evaluate the pile reliability, analysing different lengths [4, 5, 5.5, 6, 6.5, 7, 8, 9, 10] meters and different combinations of the uncertainties. The calculation of the probability of failure (pf) and reliability index (β) was repeated, considering only the uncertainties presented in Table 2 for each combination. The results are shown in Tables 3 and 4.

Table 2. Combinations of uncertainties studied

	Soil variability		Modelling uncertainty		Actions' uncertainties	
Combination	N_{SPT},tip	N_{SPT},side	tip	side	permanent	variable
1.1	√	√	√	√	√	
1.2	√*	√*	√	√	√	
2	√	√	-	-	√	
3	-	-	√	√	√	
4	√	-	√	-	√	
5	-	√	-	√	√	

√ means that the uncertainty was considered
* ignoring the reduction of variance based on autocorrelation (Vanmarcke, 1977).

Table 3. Results of probability of failure for different lengths and combinations

	Probability of failure								
Combination	4 m	5 m	5.5 m	6 m	6.5 m	7 m	8 m	9 m	10 m
1.1	0.31812	0.11033	0.05949	0.03036	0.01484	0.00758	0.00202	0.00094	0.00027
1.2	0.32912	0.12205	0.06791	0.03816	0.01948	0.01056	0.00323	0.00143	0.0005
2	0.09621	0.00317	0.00045	0.00007	0	0	0	0	0
3	0.29972	0.09474	0.04962	0.0243	0.01185	0.00541	0.00184	0.00064	0.00025
4	0.25511	0.02251	0.00422	0.00089	0.00019	0.00005	0	0	0
5	0.29029	0.04341	0.01137	0.00233	0.00047	0.00014	0.00002	0	0

Table 4. Results of reliability index for different lengths and combinations

	Reliability index								
Combination	4 m	5 m	5.5 m	6 m	6.5 m	7 m	8 m	9 m	10 m
1.1	0.47	1.22	1.56	1.88	2.17	2.43	2.88	3.11	3.46
1.2	0.44	1.16	1.49	1.77	2.06	2.31	2.72	2.98	3.29
2	1.3	2.73	3.32	3.81					
3	0.53	1.31	1.65	1.97	2.26	2.55	2.9	3.22	3.48
4	0.66	2	2.63	3.12	3.55	3.89			
5	0.55	1.71	2.28	2.83	3.31	3.63	4.11		

The value obtained for the actual pile length (Table 4 – length of 6m, β=1.88) is lower than the recommended by Eurocode for reliability class 2. The recommended values for the reliability index by Eurocode 0 (CEN, 2002) with a design of working life of 50 years for RC2 is 3.8. This can be justified by the fact that it is an experimental pile, so the consequences of failure are very low or even by the fact that the load predicted (1518 kN) is higher than the one actually used for the design of the pile, although it is not too far from the static load test (1350 kN). If the design of a pile is based on this type of soil, actions and this type of uncertainties, the length of the pile necessary to reach a reliability of 3.8 would have to be more than 10m. When comparing the results of reliability index considering all uncertainties with and without reduction of the variance (Tables 3 and 4 – combinations 1.1 and 1.2), it can be seen that the results are approximately the same. If one does not reduce the variance based on spatial autocorrelation, it

is obviously a conservative action (although technically incorrect) as can be seen in the Tables 3 and 4 ($pf_{1.1} < pf_{1.2}$).

Taking into account the sensitivity analysis, the uncertainty that has more influence in the reliability for this case study is the modelling error (combination 2). The model uncertainty is much more important in the reliability of the pile. When removing the uncertainties of the soil variability, it can be seen that the results are almost the same as the ones obtained when considering all uncertainties (combinations 3 and 1.1). The results also show that the contribution of the side and tip uncertainties (combinations 4 and 5) are approximately the same, the side resistance is dominant (F_{side}/Q_{tip} around 2) but the uncertainties on the tip are higher.

4 PARTIAL SAFETY FACTORS

4.1 *Methodology*

In the geotechnical field, the design resistance of piles is very uncertain and the Eurocode 7 (CEN, 2007) establishes that the major uncertainty is not the strength of the *in situ* ground but the way the construction would interact with it. Therefore, the partial safety factor (SF) is essentially a factor of the resistance model, rather than on the strength of material. In such cases, it is appropriate to use resistance factor method rather than material strength method. The factors should be applied to the overall resistance given by a pile than the material strength of the ground.

The method used here, based on the work of Kieu Le (2008), attempts to combine design value method (DVM) and Monte Carlo simulations (MCS) to calculate load and resistance factors, that is believed to include the advantages of both methods, *i.e.* conceptual transparency, robustness, and flexibility of the calculation. DVM, based on FORM (first order reliability method), is one of the powerful methods to evaluate the partial SF (*e.g.* Thoft-Christensen and Baker, 1982; Honjo et al., 2009). However, if the performance function becomes complex, the application of the DVM using FORM for determination of load and resistance SF becomes very time-consuming or even impossible. The need to use other techniques to calculate load and resistance factors, based on the idea of DVM has been taken into consideration and its combination with MCS was the solution (Kieu Le, 2008).

Thus, the steps to evaluate the load and resistance factors are given as follows:

1. Gather probabilistic information and statistical parameters of the variables involved (Table 1).
2. Carry out MCS and evaluate resistances (R), actions (E) and R/E ratio.
3. Approximate a probability distribution to R and E results (here, normal and lognormal distributions are chosen, but other distributions can be also considered) (Figure 3).
4. Consider the linear function in Eq. (1) and R and E as two independent variables.
5. Select the points close to the limit state line, *i.e.* zone that satisfy the condition $R/E = 1 \pm 0.02$, and evaluate the likelihood of each point ($f_R(R)$ and $f_E(E)$, where f is the probability density function)
6. Compute approximate design point by two ways:
   a. maximum likelihood – $\max[f_R(R) \times f_E(E)]$
   b. normalizing the space by Eq. (5), then calculate the distance to the origin of each point, and the design point is the one with the shortest distance to the origin of the graph (Figure 4).
7. Calculate sensitivity factors (α_R and α_E) using:
   a. DVM formulas for normal fit or lognormal fit by Eq. (6),
   b. normalized space for normal fit or lognormal fit by Eq. (7).
8. And finally calculate the load and resistance factors ($\gamma_R < 1$and $\gamma_S > 1$) by normal fit or lognormal fit – Eq. (8). Both factors are multiplied by the characteristic values (different from Eurocodes approach, where the design resistance is the characteristic resistance divided by the partial SF).

One of the advantages is that DVM implicitly assumes that sensitivity factors calculated in the current design may not be too different from the sensitivity factors of design that satisfies the target reliability index. Therefore, redesign of the structure is not required when the reliability index obtain is different from the target one.

$$Z = \frac{X - \mu_X}{\sigma_X} \tag{5}$$

$$\alpha_{1,R} = -\frac{\sigma_R}{\sqrt{\sigma_R{}^2 + \sigma_E{}^2}};\ \alpha_{1,E} = \frac{\sigma_E}{\sqrt{\sigma_R{}^2 + \sigma_E{}^2}};\ \alpha_{1,\ln(R)} = -\frac{V_R}{\sqrt{V_R{}^2 + V_E{}^2}};\ \alpha_{1,\ln(E)} = \frac{V_E}{\sqrt{V_R{}^2 + V_E{}^2}} \tag{6}$$

$$\begin{cases} \alpha_{2,R} = -\cos(angle) = -\dfrac{Z_R}{\sqrt{Z_R{}^2 + Z_E{}^2}} \\ \alpha_{2,E} = \sin(angle) = \dfrac{Z_E}{\sqrt{Z_R{}^2 + Z_E{}^2}} \end{cases} ; \begin{cases} \alpha_{2,\ln(R)} = -\dfrac{Z_{\ln(R)}}{\sqrt{Z_{\ln(R)}{}^2 + Z_{\ln(E)}{}^2}} \\ \alpha_{2,\ln(E)} = -\dfrac{Z_{\ln(E)}}{\sqrt{Z_{\ln(R)}{}^2 + Z_{\ln(E)}{}^2}} \end{cases} \quad (7)$$

$$\begin{cases} \gamma_R = \dfrac{\mu_R}{R_k} \cdot (1.0 + \beta_T \cdot \alpha_R \cdot V_R) \\ \gamma_E = \dfrac{\mu_E}{E_k} \cdot (1.0 + \beta_T \cdot \alpha_E \cdot V_E) \end{cases} ; \begin{cases} \gamma_{\ln(R)} = \dfrac{1}{\sqrt{1 + V_R{}^2}} \cdot \dfrac{\mu_R}{R_k} \cdot e^{(\beta_T \cdot \alpha_R \cdot V_R)} \\ \gamma_{\ln(E)} = \dfrac{1}{\sqrt{1 + V_E{}^2}} \cdot \dfrac{\mu_E}{E_k} \cdot e^{(\beta_T \cdot \alpha_E \cdot V_E)} \end{cases} \quad (8)$$

where Z = normalized variable ~N(0,1), X = normal random variable ~N(μ_X,σ^2_X), μ = mean value, σ = standard deviation, R = resistances, E = actions, α = sensitivity factor, V = coefficient of variation (σ/μ), *angle* = see Figure 4, R_k = resistance characteristic value, E_k = actions characteristic value, β_T = target reliability index.

4.2 *Evaluation of partial safety factors and comparison with Eurocode*

To evaluate the load and resistance partial SF, the same uncertainties shown in Table 1 were adopted for the single pile of the studied experimental site (bored in residual soil, 6m length and 0.6m of diameter). The MCS were carried out (m=1,000,000) and the histograms were obtained for the resistances (R) and actions (E), see Figure 3. The resistances distribution showed, as expected, that it has a higher dispersion than actions, and the lognormal distribution was the one that had the best fitting for both R and E. The probability of failure (pf = 0.03040 – Figure 4) corresponds to a reliability index of 1.875, that when compared with the one m=100,000 in previous calculations, has the same reliability index (Table 4 – length of 6m, β=1.88).

The characteristic values were assumed as the mean value for the resistance (1671.9 kN) and for the actions (loads) the mean value and the high fractile of 95% (E_{mean}=740.6 kN and $E_{95\%}$=924.8 kN). After the evaluation of all the necessary parameters shown in Table 5, the partial coefficients were calculated based on lognormal fit. The results can be consulted in Table 6.

Analysing the results based on lognormal formulas, the low values of the resistance factor, between 0.20 and 0.53, may result from the high number of points with a very high resistance, a thick tail (as one can see in Figure 3). Also, for load factors, that should be higher than 1, the values obtained are slightly lower than 1 (0.82 to 0.97) when the characteristic value adopted was the 95% fractile, according to the usual procedure. Only when using the mean value for the characteristic value of load, the load partial factors were between 1.03 and 1.21 that, although low, are higher than 1.

The values recommended by the Eurocode 7 (Annex A of CEN, 2007 – resistance factor between 0.67 and 1.00 and load factors between 1.00 and 1.50) are higher than the ones calculated here, the reason could be the fact that the reliability index (1.88) for this case study is far from the target one (3.8).

Table 5. Estimation and sensitivity factors based on lognormal distribution for R and E

	R (kN)	E (kN)
Mean values	1671.9	740.6
Standard deviation	659.4	107.6
Design point:		
- Max likelihood	787.8	772.4
- min(β)=1.37	782.8	767.6
	(Z_{lnR} = -1.82)	(Z_{lnE} =0.31)
Sensitivity factors (1*)	-0.9383	0.3457
Sensitivity factors (2**)	-0.9845	0.1755

* calculation method: DVM Eq. (6)
** calculation method: normalized space Eq. (7)

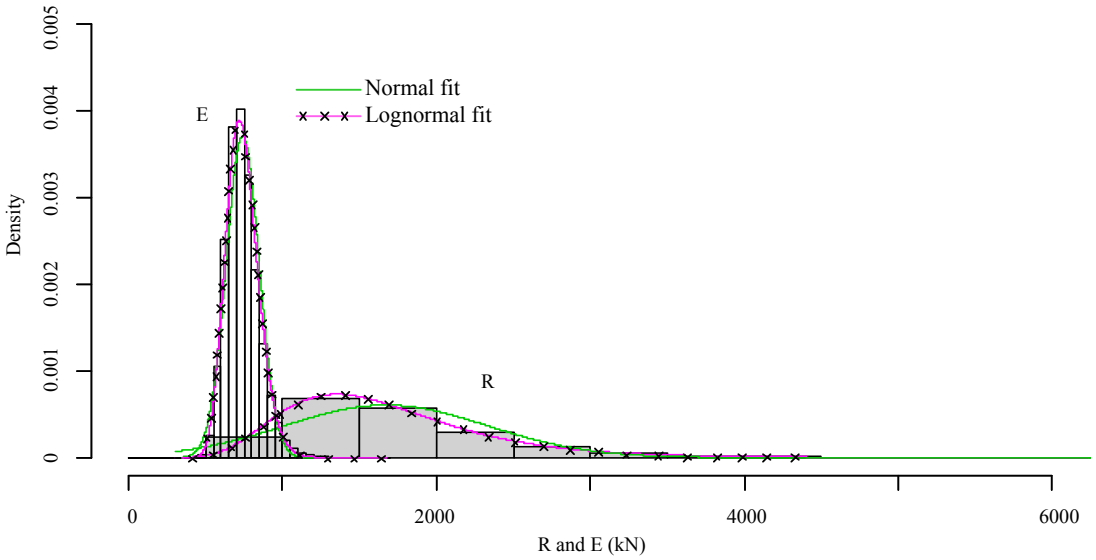

Figure 3. Distribution shape of resistance (R) and actions (E)

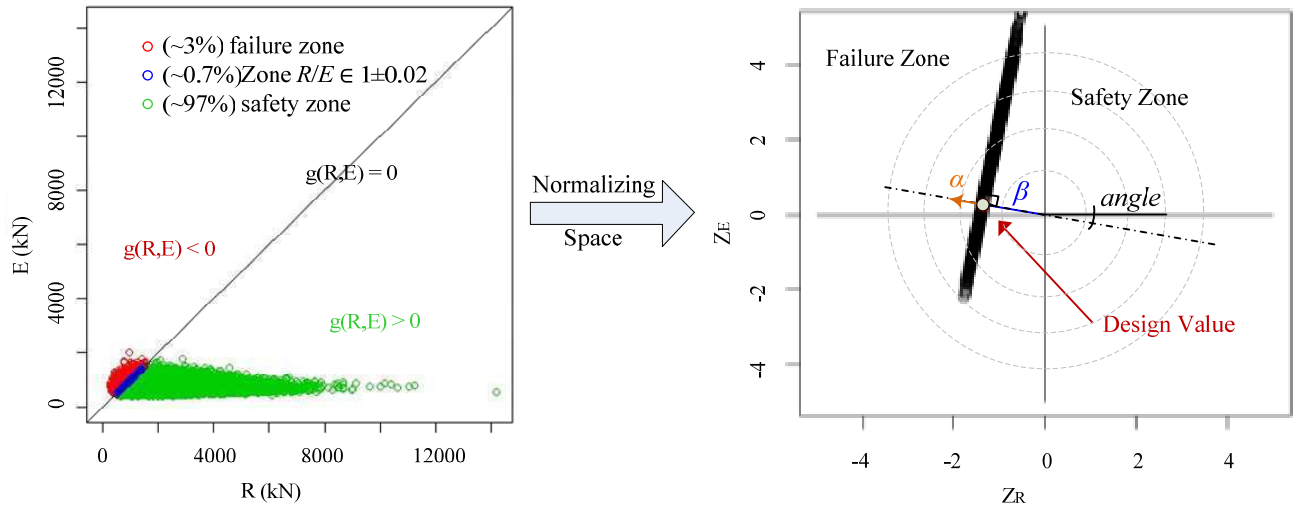

Figure 4. Graphical representation of m simulations and normalization of the space to evaluate the reliability index

Table 6. Partial factors for case study

	$\beta = 1.5$		$\beta = 2.0$		$\beta = 3.0$		$\beta = 4.0$	
	α_1	α_2	α_1	α_2	α_1	α_2	α_1	α_2
γ_R*	0.53	0.52	0.44	0.43	0.31	0.29	0.21	0.20
γ_E*	1.07	1.03	1.09	1.04	1.15	1.07	1.21	1.10
γ_E**	0.85	0.82	0.88	0.83	0.90	0.86	0.97	0.88

* R_k = mean, E_k = mean
** R_k = mean, E_k = high fractile 95%

5 CONCLUSIONS

In this paper, the reliability analysis of a pile foundation was performed based on the methodology proposed by Honjo et al. (2010). The uncertainties involved (actions, soil variability and model error) were evaluated and discussed for a specific case study. The soil variability and statistical error were evaluated by SPT. The proposed method is a user friendly reliability based design tool for geotechnical structures, for those who are not familiar with it. Monte Carlo simulations (100,000) were carried out for a pile installed in residual soil in an experimental site (Fonseca and Santos, 2008). Applying reliability analysis, the length that would give the proper security to the pile was calculated.

The results of this study showed that a length of approximately 10m (diameter 0.6m) was needed to obtain the reliability index required by the Eurocode (EC0 – RC2, β=3.8) and that the value obtained for the actual length of the pile installed (6m), β of 1.88, is lower than the recommended. This value can be

justified by the fact that this is an experimental pile or the fact that the actions used for this problem were evaluated based on the prediction form SPT, and it might be different from the actually used to design the pile.

Also, for the studied case, it was concluded that it is not the soil's spatial variability that controls the major part of the uncertainty in geotechnical design of single pile foundations, that modelling uncertainty is the most important factor in reliability. It is believed that this happens for many other types of geotechnical problems, because the error in design equations, transformation of soil investigation results (*e.g.* SPT N values) to actual design parameters (*e.g.* cohesion, friction angle or even load capacity) is the most important factor in geotechnical reliability analysis (Hansen et al., 1995).

Finally, partial factors were evaluated by design value method formulas and Monte Carlo simulations, that is believed to include the advantages of both methods (Kieu Le, 2008). The lognormal distribution is the one that fits better the resistances and actions results for this case study, and analysing the outcomes: (1) the low values obtained for the resistance factor (0.20 to 0.53) may result from the high number of points with a very high resistance (thick tail of the distribution) and (2) the values obtained for the load factors, that should be higher than 1, resulted in between 0.82 and 0.97 for $E_k=E_{95\%}$ and 1.03 and 1.21 for $E_k=E_{mean}$. Both are very different form the recommendations of Eurocode 7, the reason could be the fact that the reliability index (1.88) for this case study is far from the target one (3.8) due to the value of load used (predicted by empirical SHB method) that might be very different from the actual load used in design.

ACKNOWLEDGEMENTS

The authors wish to thank the Portuguese Foundation for Science and Technology (FCT) for the financial support (grant SFRH/BD/45689/2008) and also to Doctor Kieu Le Thuy Chung for the precious contributions.

REFERENCES

AASHTO. (2007). LFRD Bridge Design Specifications, 4th edition. Washington D.C.: American Association of State Highway and Transportation Officials.

Aoki, N., and Velloso, D. A. (1975). An approximate method to estimate the bearing capacity of piles. V Congresso Panamericano de Mecanica de Suelos y Cimentaciones - PASSMFE. 5, pp. 367-374. Buenos Aires: Sociedade Argentina de Mecánica de Suelos e Ingenieria de Fundaciones.

CEN (European Committee for Standardization). (2002). Eurocode: Basis of Structural Design. EN 1990.

CEN (European Committee for Standardization). (2007). Eurocode 7: Geotechnical Design. EN 1997.

Fonseca, A. V., and Santos, J. A. (2008). International Prediction Event. Behaviour of CFA, Driven and Bored. ISC'2 Experimental Site. Faculdade de Engenharia da Universidade do Porto, IST, Universidade Técnica de Lisboa.

Hansen, P. F., Madsen, H. O., and Tjelta, T. I. (1995). Reliability analysis of a pile design. Marine Structures, 8(2), 171-198.

Holicky, M., Markova, J., and Gulvanessian, H. (2007). Code calibration allowing for reliability differentiation and production quality. Application of Statistics and Probability in Civil Engineering: Proceedings of the 10th International Conference. Kanda, Takada and Furuat.

Honjo, Y., Hara, T., and Kieu Le, T. C. (2010). Level III reliability based design by response surfaces: an embankment. The 17th Southeast Asian Geotechnical Conference, (pp. 203-206). Taipei, Taiwan.

Honjo, Y., Hara, T., Suzuki, M., Shirato, M., Le Kieu, T. C., and Kikuchi, Y. (2009). Code calibration in reliability based design level I verification format for geotechnical structures. 2nd International Symposium on Geotechnical Safety and Risk (IS-Gifu 2009) (pp. 435-452). Japan: Honjo et al. (eds).

Kieu Le, T. C. (2008). Study on Determination of Partial Factors for Geotechnical Design. Doctoral Thesis, Gifu University, Department of Civil Engineering, Gifu, Japan.

Kulhawy, F. H., and Mayne, P. W. (1990). Manual on Estimating Soil Properties for Foundation Design. Report for Electric Power Research Institute, by Cornell University.

Okahara, M., Takagi, S., Nakatani, S., and Kimura, Y. (1991). A Study on Bearing Capacity of a Single Pile and Design Method of Cylinder Shaped Foundations. Technical Memorandum of PWRL.

Phoon, K.-K. (2008). Reliability-Based Design in Geotechnical Engineering: Computations and Applications. (K.-K. Phoon, Ed.) Routledge.

SHB. (2001). Specifications for Highway Bridges. Japan Road Association.

Shioi, Y., and Fukui, J. (1982). Application of N-value to design of foundation in Japan. Proceeding of the Second European Symposium on Penetration Testing, 1, pp. 159-16. Amsterdam.

Thoft-Christensen, P., and Baker, M. J. (1982). Structural Reliability Theory and Its Applications. Berlin, New York: Springer-Verlag.

Uzielli, M., Lacasse, S., Nadim, F., and Phoon, K. K. (2006). Soil variability analysis for geotechnical practice. Proceedings of the 2nd International Workshop on Characterization and Engineering Properties of Natural Soils. Singapore: The Netherlands: Taylor & Francis.

Vanmarcke, E. H. (1977). Probabilistic modeling of soil profiles. Journal of the Geotechnical Engineering Division ASCE, 103(GT11), 1227-1246.

ISGSR 2011 - Vogt, Schuppener, Straub & Bräu (eds) - © 2011 Bundesanstalt für Wasserbau ISBN 978-3-939230-01-4

Realistic Estimates of the Uncertainties and the Reliability Indices for Shallow Foundation Design Considering Seismic Loading

S. O. Akbas & E. Tekin
Gazi University, Ankara, Turkey

ABSTRACT: The Turkish Earthquake Code "Specification for Structures to be Built in Disaster Areas" was strictly followed to design the shallow foundations of a typical reinforced concrete building. Then, the uncertainties in the force and resistance components that are involved in the design of these shallow foundations are evaluated. The uncertainty in the seismic loading was taken into account, since it is believed to be one of the major influencing factors. Typical reliability index values that are realized in the current practice are determined. The results are compared to target reliability indices for superstructures that are usually employed in practice.

Keywords: Shallow Foundation; Footing; Earthquake; Bearing Capacity

1 INTRODUCTION

In many parts of the world, the design codes for foundation design are being transformed from the allowable stress design (ASD) to the load and resistance factor design (LRFD) or to a partial factor approach. Examples of major efforts in such code transformations include but are not limited to AASHTO's LRFD Bridge Design Specifications (Withiam et al. 2001) in the US, National Building Code of Canada (NRC 1995; Becker 1996) in Canada, and Eurocodes (CEN 1993, 1994) in EU countries.

It is a well-established fact that, no significant improvement of the current practice can be achieved by the implementation of a partial factor approach or LRFD primarily through the redistribution of the original global factor of safety in the ASD into separate load and resistance factors or soil parameter partial factors without a probabilistic framework. Phoon et al. (2003) highlighted the need to consider geotechnical LRFD as a simplified reliability-based design (RBD) procedure, rather than an exercise in rearranging the global factor of safety.

The major components of a geotechnical LRFD code calibration, which utilizes reliability analysis as an indispensible basis, are described in Report TR-105000 (Phoon et al. 1995). One of the most important steps of this process is the determination of the range of reliability levels in existing designs. This information is required to adjust the resistance factors in the RBD equations until a consistent and realistic target reliability level that is in agreement with existing practice is achieved within each calibration domain.

This study aims at estimating the reliability levels that are inherent within the shallow foundation designs performed using the current Turkish Earthquake Code (TEC) (2007). For this purpose, a typical reinforced concrete building is chosen and its footings are dimensioned using ASD, at four different seismic zones, in strict conformity with TEC (2007). After an evaluation of the uncertainties in the load and resistance terms involved, these deterministic designs are then evaluated through reliability analyses to estimate the inherent safety levels. The uncertainty of the earthquake force is taken into account because, in Turkey, structural and geotechnical design is significantly affected by seismic considerations, since about 95% of the country's area lies within seismic hazard zones. A critical analysis of the results is performed by comparing them with target reliability indices for superstructures and foundations that are usually employed in practice.

2 DETERMINISTIC DESIGN OF FOOTINGS

2.1 *Estimation of the Equivalent Earthquake Load*

A typical eight-storey reinforced concrete building on shallow footings constructed on a sand deposit, with a total height (H_N) of 24 m. and plan dimensions of 20 m. by 20 m. situated in the first degree earthquake hazard zone according to Earthquake Zoning Map of Turkey is considered. The plan view of the structure is shown in Figure 1. Note that for the first degree hazard zone, the expected acceleration value acting on a normal structure with fifty years of economical life, which will not be exceeded with 90% probability, is 0.4g. The storey height, the slab thickness, and the roof slope of the building are 3 m. 150 mm., and 30^o respectively. The structural system consists of 25 identical columns with dimensions of 300 mm x 600 mm, and beams of 250 x 500 mm.

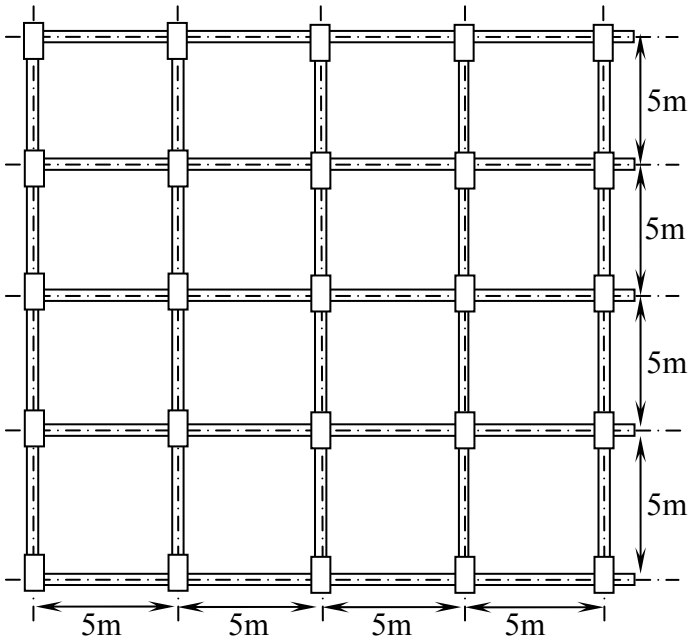

Figure 1. The plan view of the building

Two requirements should be met in order to be able to utilize the equivalent earthquake load concept for a given structure, according to regulatory TEC (2007. First, the height of the building should be less than 25 m. Secondly, the structure should not exhibit A1 type torsional irregularity. The torsional irregularity factor is defined for any of the two orthogonal earthquake directions as the ratio of the maximum storey drift at any storey to the average storey drift in the same direction. For A1 type torsional irregularity, this value must exceed 1.2. The building considered in this study does not have torsional irregularity due to its regular shape and structural system.

The total equivalent earthquake load (base shear), V_t, acting on the entire building in the considered earthquake direction can be determined as follows:

$$V_t = \frac{W \times A(T_1)}{R_a(T_1)} \geq 0.10 \times A_0 \times I \times W \qquad (1)$$

in which, W = total building weight, T_1 = the first natural vibration period, A(T) = spectral acceleration coefficient, $R_a(T_1)$ = seismic load reduction factor, A_0 = effective ground acceleration coefficient, and I = building importance factor. The total building weight to be used in Equation 1 can be determined by Equation 2:

$$W = \sum_{i=1}^{N} w_i \qquad (2)$$

Storey weights, w_i, in Equation 2 can be determined using Equation 3:

$$w_i = g_i + nq_i \qquad (3)$$

in which g_i , q_i= total dead and live loads at the i^{th} storey of the building, respectively, and n = live load participation factor. In this study, for the considered building, n is obtained to be 0.3 according to the pur-

pose of occupancy, and g_i and q_i are taken as 5.5 kPa and 2.1 kPa, respectively, according to the code of practice TS498 "Design Loads for Buildings" (1997). Table 1 summarizes the calculation of the storey weights of the building. The total building weight, which is calculated as the sum of the five storey's weights is equal to 43570 kN.

Table 1. Calculation of the storey weights

Structural Element	Weight (kN)	Structural Element	Weight (kN)
Slabs	2452	Walls	2328
Columns	389	Roof	2200
Beams	600	**Storey Weight**	**5769**

The spectral acceleration coefficient corresponding to 5% damped elastic design acceleration spectrum normalized by the acceleration of gravity, g, is given by Equation 4, which is considered as the basis for the determination of seismic loads:

$$A(T) = A_0 \times I \times S(T) \qquad (4)$$

A_0 and I, which were defined previously, are taken as 0.4 and 1.4, respectively, considering the seismic zone and purpose of occupancy or type of building. The spectrum coefficient, S(T), in Equation 4, is determined by Equation 5, as a function of local site (geotechnical) conditions and the building's natural vibration period, T (Figure 2):

$$S(T) = 1 + 1.5T / T_A \quad (0 \le T \le T_A) \qquad (5a)$$

$$S(T) = 2.5 \quad (T_A \le T \le T_B) \qquad (5b)$$

$$S(T) = 2.5(T_B / T)^{0.8} \quad (T > T_B) \qquad (5c)$$

Spectrums characteristic periods, T_A and T_B, which appear in Equation 5 are specified as 0.10 and 0.3, respectively, based on "Z1" local site class. The acceleration spectrum of the building is shown in Figure 2.

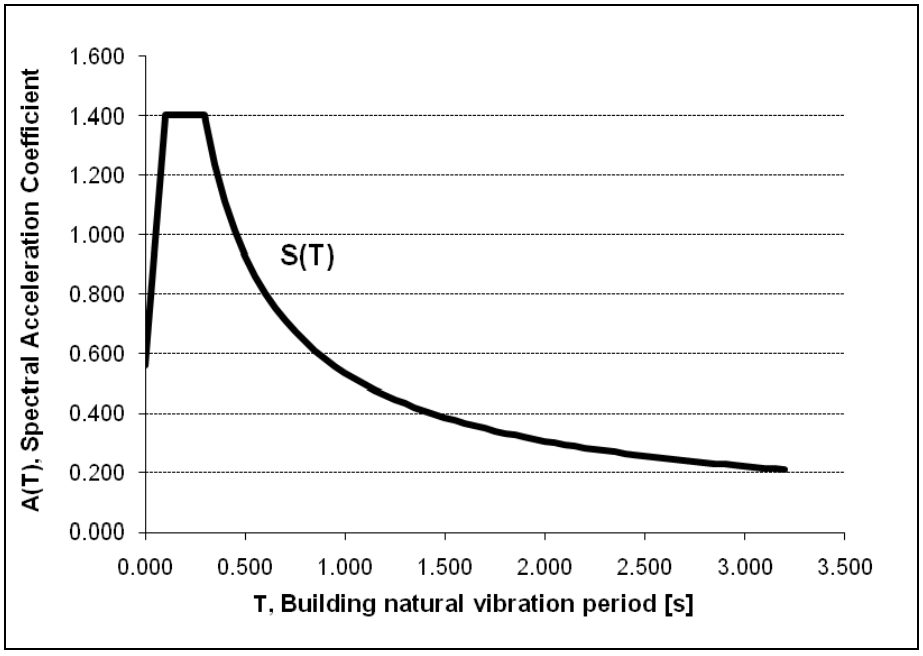

Figure 2. The acceleration spectrum of the building

The first natural vibration period (T_1) of the building is calculated by the approximate method given in Equation 6, which is applicable for buildings with $H_N \le 25$ m. in the first and second degree earthquake hazard zones:

$$T_1 = C_t H_N^{3/4} \qquad (6)$$

in which C_t = coefficient for the approximate calculation of the first natural vibration period in the equivalent seismic load method. It is equal to 0.07 for buildings with structural systems that are composed only of reinforced concrete frames. Thus, according to Equation 6, $T_1 = 0.76$ seconds.

The elastic seismic loads that are determined in terms of spectral acceleration coefficient should be divided by the seismic load reduction factor defined below, to account for the specific nonlinear behavior of the structural system during an earthquake. The seismic load reduction factor, $R_a(T)$, is determined by Equation 7, as a function of the structural behavior factor, R, and the natural vibration period, T:

$$R_a(T) = 1.5 + (R - 1.5)T / T_A \quad (0 \le T \le T_A) \qquad (7a)$$

$$R_a(T) = R \quad (T \ge T_A) \qquad (7b)$$

From Figure 2, $A(T_1) = 0.666$ for $T_1 = 0.76$ sec. Since $T_1 = 0.76 > T_B = 0.3$, Equation 5c can be utilized to obtain $S(T) = 1.19$. The structural behavior factor is specified as 7 for systems of high ductility level and for buildings in which seismic loads are jointly resisted by frames and solid and / or coupled structural walls. This value is also equal to the seismic load reduction factor, as given by Equation 7b. Using these values, the total equivalent earthquake load (base shear), V_t, acting on the entire building is calculated as 4147 kN for the considered building. This process is repeated for the same building, assuming that it is located at seismic hazard zones 2, 3, and 4, and the corresponding local site classes Z2, Z3, and Z4. The resulting equivalent earthquake loads are given in Table 2.

Note that, for footings located in the central zone of the building, the dead load, the live load, and the total axial load are calculated as 1649 kN, 167 kN, and 1816 kN, respectively, regardless of the seismic hazard zone.

Table 2. Equivalent earthquake loads for footings at different seismic hazard zones

Seismic Zone	A_0 (g)	Local Site Class	T_A (sec)	T_B (sec)	Total Earthquake Force (kN)	Design Earthquake Force per Footing (kN)
1	0.4	Z1	0.10	0.30	4147	165
2	0.3	Z2	0.15	0.40	3915	156
3	0.2	Z3	0.15	0.60	3610	144
4	0.1	Z4	0.20	0.90	2178	87

2.2 *Evaluation of Bearing Capacity of Footings*

For a surface footing on cohesionless soil, which is a drained loading problem, the bearing capacity, or tip/base capacity in compression, (Q_{ult}) is given by the following equation:

$$Q_{ult} = 0.5B\bar{\gamma}N_\gamma\zeta_{\gamma s}\zeta_{\gamma d}\zeta_{\gamma r}\zeta_{\gamma t}\zeta_{\gamma g}\zeta_{\gamma i}A_f \qquad (8)$$

in which A_f = footing area, B = footing width, $\bar{\gamma}$ = effective soil unit weight, N_γ = bearing capacity factor, and ζ_{xy} = modifiers described below. The predictive model given in Equation 8 has evolved over many years and is the result of research by many authors. It is based primarily on the authoritative and persuasive summary work by Vesić (1975) and Hansen (1970), with minor improvements by Kulhawy et al. (1983). Key details are given by Vesić (1975).

The bearing capacity factor, N_γ is given by:

$$N_\gamma \approx 2(N_q + 1)\tan\bar{\phi} \qquad (9)$$

in which $\bar{\phi}$ = effective stress friction angle. N_q is calculated as follows:

$$N_q \approx \exp(\pi\tan\bar{\phi})\tan^2(45 + \bar{\phi}/2) \qquad (10)$$

The subscripts of the ζ modifiers indicate the applicable term (N_γ or N_q) and modification (r for soil rigidity, s for foundation shape, d for foundation depth, i for load inclination, t for tilt of foundation base, and g for ground surface inclination). For the considered building foundation, the $\zeta_{\gamma g}$, $\zeta_{\gamma t}$, and $\zeta_{\gamma d}$ factors are equal to 1.0 because the footings are assumed to be on the surface of level ground and with a horizontal base without any load eccentricity. For a square footing on a horizontal soil surface, under a vertical concentric load and horizontal load, the relevant modifiers are calculated as follows:

$$\zeta_{\gamma s} = 1\text{-}0.4(B/L) = 0.6 \qquad (11)$$

$$\zeta_{\gamma i} = (1\text{-}T/N)^{2.5} \quad (12)$$

$$\zeta_{\gamma r} = \exp\{[(-3.8)\tan\bar{\phi}]+[(3.07\sin\bar{\phi})(\log 2I_{rr})/(1+\sin\bar{\phi})]\} \quad (13)$$

in which L = footing length, and T and N are the horizontal and axial loads, respectively. I_{rr} is the reduced rigidity index, which plays an important role in determining the mode of failure and is given by (Vesić 1975):

$$I_{rr} = I_r/(1+I_r\Delta) \quad (14)$$

in which I_r = rigidity index and Δ = volumetric strain. The rigidity index is defined as follows for drained loading (Kulhawy et al. 1983):

$$I_r = G/(\bar{q}\tan\bar{\phi}) \quad (15)$$

in which G = shear modulus of soil and $\bar{q}$ = average vertical effective stress evaluated at a depth of B/2 below the foundation. The shear modulus can be obtained through the elastic modulus (E) and Poisson's ratio (ν).The volumetric strain Δ can be estimated as follows (Trautmann and Kulhawy 1987):

$$\Delta \approx 0.005\,[(45^o - \bar{\phi})/20^o]\bar{q}/p_a \quad (16)$$

in which p_a = atmospheric stress in consistent units, and $\bar{\phi}$ can range between the limits of 20^o and 45^o. Once the value of I_{rr} is determined from Equations 14 through 16, it is compared to the critical rigidity index (I_{rc}) to determine the mode of failure. The critical rigidity index is defined as:

$$I_{rc} = 0.5\exp[2.85\cot(45^o\text{-}\bar{\phi}/2)] \quad (17)$$

If $I_{rr} > I_{rc}$, the soil behaves as a rigid-plastic material, and the soil fails in general shear mode, for which $\zeta_{\gamma r} = 1$. When Irr < Irc, local or punching shear failure would occur because of lower relative soil stiffness, and therefore $\zeta_{\gamma r}$ would be modified using Equation 13. Detailed information about this predictive model can be found elsewhere (e.g., Vesić 1975, Kulhawy et al. 1983).

Using the total axial loads calculated previously as well as horizontal earthquake forces presented in Table 2, shallow foundations of the reinforced concrete building located at different seismic hazard zones are deterministically dimensioned following the bearing capacity prediction method that is explained above. For each case, the modulus E, is calculated using the correlations between E, the effective stress friction angle, and the SPT N values for cohesionless soils given in Kulhawy and Mayne (1990). For simplification, only bearing capacity is taken into account, without considering settlements. Note that, an allowable stress methodology, which can be illustrated by Equation 18, is used to determine the dimensions of the square footings:

$$Q_{ult} / FS = Total\ vertical\ load / B^2 \quad (18)$$

in which FS = factor of safety, which does not have a predetermined value in the current foundation design practice. Thus, typical values of 2.0, 2.5, and 3.0 are considered for the current study. The estimated dimensions of the footings can be seen in Table 3.

3 RELIABILITY ANALYSIS

It is clear that the performance of the footings that were designed using the deterministic allowable stress method in the previous section can not be ascertained with absolute certainty due to variations in the load and resistance parameters. The variability in the various load components are characterized as given in Table 4. On the capacity side, the main uncertain parameters are the effective stress friction angle, the soil modulus, and to a lesser extent, the soil unit weight. $\bar{\phi}$ can be modeled as a log-normal random variable (Spry et al. 1988). Based on the statistical analyses by Phoon et al. (1995), the COV of $\bar{\phi}$ is assumed to lie between 5 and 15%. The results of the same study are also used to decide on the type of distribution and COV of E. Note that the uncertainty in the modulus comes into effect only when local or punching shear failure occurs. The type of distribution, the mean and the coefficient of variation (COV) of all of the considered random variables for the footing design problem are given in Table 5. Note that the footing width and the soil unit weight are considered to be deterministic.

Table 3. Design of footings and resulting reliability indices

Seismic Zone	Vertical Force	Earthquake Force	$\bar{\phi}$	FS=2.0		FS = 2.5		FS=3.0	
	(kN)	(kN)	COV (%)	B(m)	β	B(m)	β	B(m)	β
1	1816	165	5.0	3.1	3.58	3.3	4.42	3.5	5.22
1	1816	165	7.5	3.1	2.55	3.3	3.18	3.5	3.79
1	1816	165	10.0	3.1	1.96	3.3	2.44	3.5	2.93
1	1816	165	12.5	3.1	1.57	3.3	1.97	3.5	2.36
1	1816	165	15.0	3.1	1.30	3.3	1.64	3.5	1.97
2	1816	156	5.0	3.1	3.60	3.3	4.44	3.5	5.26
2	1816	156	7.5	3.1	2.57	3.3	3.19	3.5	3.80
2	1816	156	10.0	3.1	1.96	3.3	2.45	3.5	2.94
2	1816	156	12.5	3.1	1.58	3.3	1.98	3.5	2.37
2	1816	156	15.0	3.1	1.30	3.3	1.64	3.5	1.98
3	1816	144	5.0	3.0	3.19	3.2	4.05	3.5	5.30
3	1816	144	7.5	3.0	2.27	3.2	2.90	3.5	3.82
3	1816	144	10.0	3.0	1.73	3.2	2.22	3.5	2.95
3	1816	144	12.5	3.0	1.38	3.2	1.79	3.5	2.38
3	1816	144	15.0	3.0	1.14	3.2	1.48	3.5	1.99
4	1816	87	5.0	2.9	2.86	3.1	3.74	3.4	5.03
4	1816	87	7.5	2.9	2.01	3.1	2.66	3.4	3.60
4	1816	87	10.0	2.9	1.53	3.1	2.03	3.4	2.77
4	1816	87	12.5	2.9	1.22	3.1	1.63	3.4	2.23
4	1816	87	15.0	2.9	1.00	3.1	1.35	3.4	1.86

Table 4. Characterization of variability in various load components

Load Component	Distribution Type	Bias Factor	COV (%)	Reference
Dead Load	Gaussian	1.05	8-15	Nowak (1994); Ellingwood & Tekie (1999)
Live Load	Log-normal	1.00	25	Ellingwood & Tekie (1999)
Earthquake Load	Extreme Type I	0.30	70	Ellingwood et. al (1980); Nowak (1994)

Table 5. Random variables for the footing design problem

Load Component	Distribution Type	Mean	COV (%)
$\bar{\phi}$	Log-normal	32	5-15
E	Log-normal	10 MPa	40
Dead Load	Normal	1649 kN	10
Live Load	Log-normal	167 kN	25
Earthquake Load	Extreme Type I	163* kN	70

* For seismic hazard zone 1.

Once the underlying random variables have been defined, the probability of failure, or the reliability index (β) can be obtained using the First-Order Reliability Method (FORM) for each of the footings deterministically designed previously. The performance function is defined as the difference between the bearing capacity obtained using Equations 8 through 17 and the applied load. The reliability indices are estimated using constrained nonlinear optimization within MATLAB environment for each case. The results are shown in Table 3.

For a FS = 3, the resulting reliability indices range between 1.86 and 5.30, depending mainly on the COV of the friction angle. The effect of the seismic zone on the reliability index is minor, surprisingly with lower values obtained for the least active 4th seismic hazard zone. Normally, a reliability index value in the range of 3.0–4.0 is accepted for good performance of the system (Baecher and Christian 2003; USACE 1997). Thus, for FS =3, acceptable performance can be obtained up to about 10% COV of $\bar{\phi}$ for all seismic hazard zones except zone 4. For FS = 2.5, which is a frequently used design value in practice, it can be seen that good or acceptable performance can be obtained only for COV values of $\bar{\phi}$ smaller than about 7.5%. Thus, the use of a FS smaller than 3 is warranted only for very high quality subsurface investigation and / or extremely homogeneous geomaterial. For the case of a smaller FS, such as 2, as given in Table 3, it is not possible to achieve the required reliability level unless the COV of $\bar{\phi}$ is smaller than about 5%.

4 CONCLUDING REMARKS

Allowable stress method was used to design the footings of typical reinforced concrete buildings situated at four different seismic hazard zones, strictly following the Turkish Earthquake Code "Specification for Structures to be Built in Disaster Areas". Then, to estimate the inherent reliability in these deterministic designs, the uncertainties in the force and resistance components were evaluated and corresponding reliability index values were determined by FORM analyses.

The results indicate that, the resulting reliability index values are very sensitive to the variability of the effective stress friction angle, which is expressed in terms of COV. Therefore, it can be stated that the quality of the site investigation as well as the inherent soil variability have a significant effect on the realized safety levels. The effect of seismic hazard zone on the β values is minor, especially for higher values of FS, however, this effect becomes more obvious with decreasing FS. Interestingly, for a given FS, the lowest β values generally correspond to designs located at seismic hazard zone 4.

The obtained β values have a very large range, even for a given FS and seismic hazard zone, such that for almost all cases, performance of the designed footing changes between good-very safe to poor-unacceptable, as a function of the COV of ϕ. This indicates the inadequacy of the allowable stress method, i.e., the utilization of FS concept, in obtaining uniform levels of safety and reliability.

REFERENCES

Baecher, G.B. and Christian, J.T., 2003. Reliability and statistics in geotechnical engineering. Chichester,NJ: John Wiley Publications.

Becker, D E., 1996. Limit states design for foundations. Part II. Development for National Building Code of Canada. Can. Geotech. J. 33(6): 984-1007.

CEN/TC250. 1993. Basis of design and actions on structures - Part 1, basis of design. Eurocode 1, ENV-1991-1, European Committee for Standardization (CEN).

CEN/TC250, 1994. Geotechnical design - Part 1, General rules, Eurocode 7, ENV-1997-1, European Committee for Standardization (CEN).

Ellingwood, B., Galambos, T. V., MacGregor, J. G., and Cornell, C. A., 1980. Development of a probability based load criterion for American National Standard A58-Building code requirements for minimum design loads in buildings and other structures. National Bureau of Standards, Washington, D.C.

Ellingwood, B. R. and Tekie, P. B., 1999. Wind load statistics for probability-based structural design. J. Struct. Eng., 125(4), 453-463.

Hansen, J.,1970. "A revised and extended formula for bearing capacity". Danish Geotechnical Institute Bulletin No.28, pp 5-11.

Kulhawy, F.H. and Mayne, P.W., 1990. Manual on Estimating Soil Properties for Foundation Design, Report No. EL-6800, Electric Power Research Institute, Palo Alto, CA, 306 p.

Kulhawy, F. H., Trautmann, C. H., Beech, J. F., O'Rourke, T. D., McGuire, W., Wood, W. A., and Capano, C., 1983. "Transmission line structure foundations for uplift-compression loading." Rep. No. EL-2870, Electric Power Research Institute, Palo Alto, Calif.

National Research Council of Canada 1995. National Building Code of Canada (NBCC), 11th Ed., Ottawa.

Nowak, A. S., 1994. Load model for bridge design code. Can. J. Civ. Eng., 21, 36-49.

Phoon, K. K., Kulhawy, F. H. and Grigoriu, M. D. 1995. Reliability-based design of foundations for transmission line structures. Report TR-105000, Electric Power Research Institute, Palo Alto.

Phoon, K. K., Liu, S. L. and Chow, Y. K. 2003. Estimation of model uncertainties for reliability-based design of cantilever walls in sand. In. Proc. Int. Workshop on Limit State Design in Geotech. Engrg. Practice (LSD2003), Massachusetts Institute of Technology, Cambridge (CDROM).

Spry, M. J., Kulhawy, F. H. and Grigoriu, M. D., 1988. Reliability-based foundation design for transmission line structures: Geotechnical site characterization strategy. Rpt. EL-5507(1), Electric Power Research Institute, Palo Alto.

Trautmann, C. H. and Kulhawy, F. H., 1987. CUFAD: A Computer program for compression and uplift foundation analysis and design, Report EL-4540-CCM (16), Electric Power Reseaarch Institute, Palo Alto, 148 p.

TS 498, 1997. Design loads for buildings, Bases for Design of Structures - Actions Due To The Self - Weight of Structures, Non - Structural Elements and Stored Materials - Density, Turkish Standards Institution, Ankara.

Turkish Earthquake Code (TEC), 2007. Ministry of Public Works and Settlement, Specification Structures To Be Built In Disaster Areas, Part III Earthquake Disaster Prevention, Government of Republic of Turkey, Turkey.

USACE, 1997. Risk-based analysis in Geotechnical Engineering for Support of Planning Studies, Engineering and Design. US Army Corps of Engineers, Department of Army, Washington, DC, p. 20314-100.

Vesić, A. S., 1975. Bearing Capacity of Shallow Foundations, Foundation Engineering Handbook, 1st ed. p. 121-147, Winterkom, Hans F. and Fang, Hsai-Yang, eds., Van Nostrand Reinhold, New York.

Withiam, J. L., Voytko, E. P., Barker, R. M., Duncan, J. M., Kelly, B. C., Musser, S. C., and Elias, V. 2001. Load and Resistance Factor Design (LRFD) for Highway Bridge Substructures. Publication No FHWA HI-98-032, NHI Course No. 13068, Federal Highway Administration, Washington D.C.

ISGSR 2011 - Vogt, Schuppener, Straub & Bräu (eds) - © 2011 Bundesanstalt für Wasserbau ISBN 978-3-939230-01-4

A comparison of Random Set and Point Estimate Methods in Finite Element Analysis of Tunnel Excavation

H.F. Schweiger & A. Nasekhian
Graz University of Technology, Graz, Austria

T. Marcher
ILF Consulting Engineers, Rum/Innsbruck, Austria

ABSTRACT: When performing classical reliability analysis in practical geotechnical engineering subjective assumptions about the probability density function of parameters are often made because in many cases the results of geotechnical investigations are set valued rather than being precise and point valued. Alternatively, imprecise probability theories can be employed and Random Set Theory could be considered as a possible attractive candidate. To demonstrate the applicability and efficiency of Random Set Theory in combination with finite element analysis (RS-FEM) in geotechnical practice, a case study has been chosen, namely a tunnel excavation located in the south of Germany. It is shown that RS-FEM is an efficient tool to determine most likely bounds of the performance of a geotechnical structure being complementary to the observational method. Comparison between calculation and field measurements prove the applicability of the presented approach. In addition, the same problem has been analysed using a point estimate method. It is shown, that under certain assumptions, similar conclusions with respect to the expected behaviour of the tunnel can be obtained.

Keywords: finite element method, random set theory, tunnel, point estimate method

1 INTRODUCTION

Uncertainties in determination of the in situ soil profile and material parameters for individual soil or rock layers are one of the problems geotechnical engineers have to face. In this context it is important to realise that different sources of uncertainty exist, material parameters varying in a known range may be one of them but simply the lack of knowledge may be the more pronounced one. A rigorous mathematical treatment of all aspects of uncertainties is not straightforward and thus is commonly replaced in practice by engineering judgment. Recent theoretical developments and advances made in computational modelling allow for a more formal consideration of uncertainties supporting engineering judgment. It can be expected that theories and models taking uncertainty into account in the design of geotechnical structures, which could form a basis for comprehensive risk analyses, will be more appreciated in near future.

The random set theory developed by several authors (e.g. Dempster (1967), Kendall (1974), Shafer (1976), Dubois & Prade (1991)) has provided an appropriate mathematical model to cope with uncertainty overcoming some of the drawbacks of "classical" probability theory. Tonon et al. (1996, 2000a,b) demonstrated the application of Random Set Theory in rock mechanics and reliability analysis of a tunnel lining. Peschl (2004), Schweiger & Peschl (2007) have extended Random Set Theory to be combined with the finite element method, called Random-Set-Finite-Element-Method (RS-FEM). They illustrated the applicability of the developed framework to practical geotechnical problems and showed that RS-FEM is an efficient tool for reliability analysis in geotechnics in early design phases being highly complementary to the so-called observational method. For further details about basic concepts of RST and RS-FEM procedure the reader is referred to the work of e.g. Tonon & Mammino (1996), Schweiger & Peschl (2007) and therefore only a brief summary of the basic steps to be performed is given in the following for continuity. Finally a comparison with the point estimate method is presented.

2 RANDOM SET FINITE ELEMENT PROCEDURE

An advantage of the RS-FEM is that there is no need to modify the available Finite Element Codes, and any commercial FE software can be used for performing the required "deterministic" calculations. The steps that have to be followed in a RS-FEM procedure are summarized below and graphically illustrated in Figure 1.

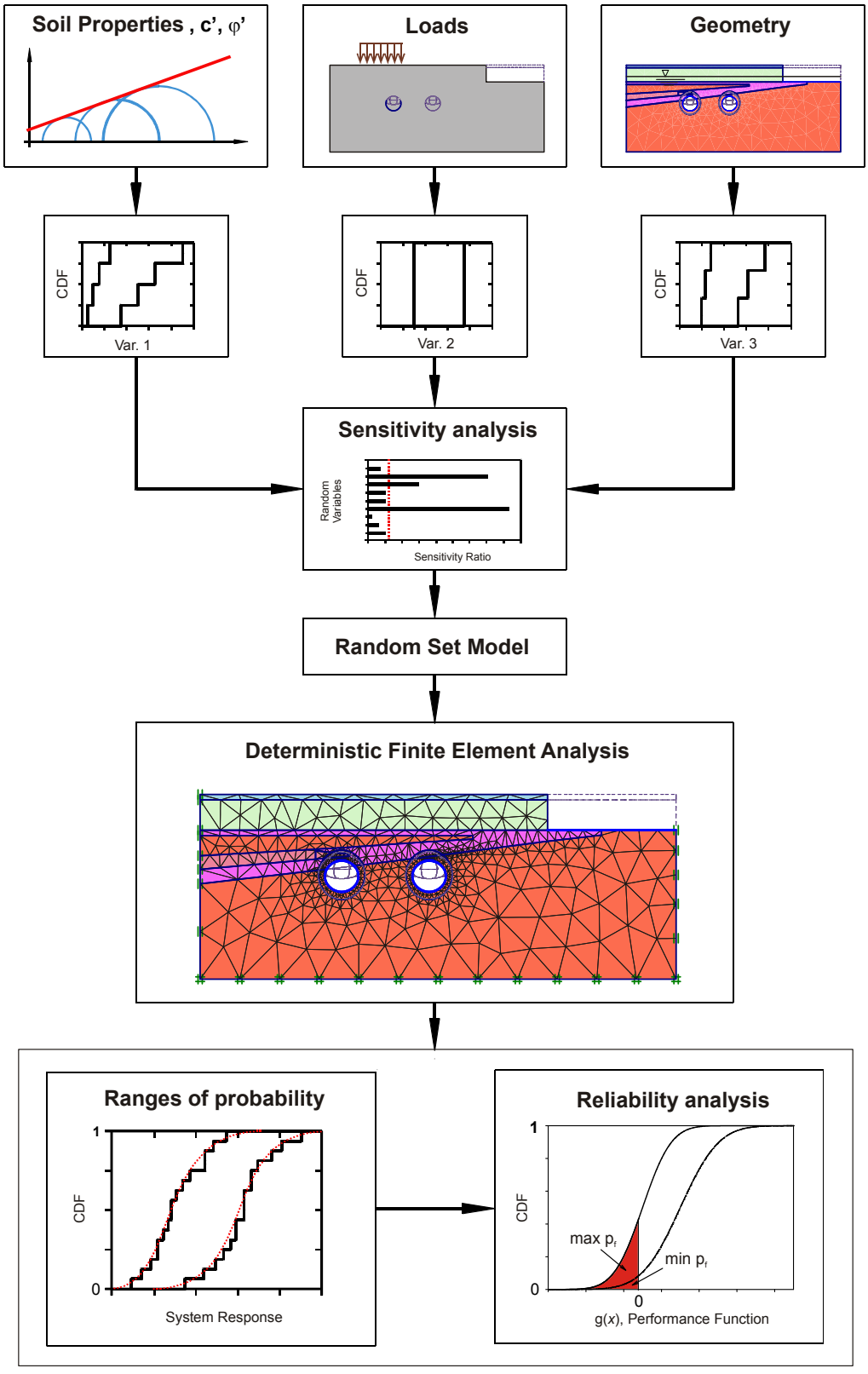

Figure 1. RS-FEM procedure (modified from Peschl, 2004)

Basic steps in setting up a Random Set Finite Element Model:

1. Definition of the geometry or geometries, in case a geometric feature is one of the basic variables, of the problem, preparation of the respective master file(s) and the FE model, selection of an appropriate constitutive model for soil/rock and support elements.
2. Selection of input parameters that should be considered as basic variables in the random set analysis providing the expected ranges from different sources of information (random sets).
3. Modification of the selected random sets, which show spatial variability considering the length of the possible failure mechanism in the model. This step requires the determination of spatial correlation length as well as an estimation of the length of the possible failure surface.
4. The computational effort of RS-FEM increases proportional to 2^n (n is the number of basic random variables). Thus employing a sensitivity scheme to identify the variables that have negligible effect on desired results even if there is a wide uncertainty on them is essential in order to reduce the computational effort.
5. Computation of the calculation matrix, which includes the defined parameter combinations, the preparation of deterministic FE input files and the relevant probability share of the individual calculation considering dependencies (correlation coefficients) between the basic random variables involved (see Peschl 2004).
6. Finite element calculations and determination of results such as stresses, strains, displacements and internal forces in support elements in terms of bounds of discrete cumulative probability functions, which may be compared to measured data once they become available. Subsequently fitting the resulted CDF's using best-fit methods, in order to achieve a continuous distribution function. For this step, commercial software such as the package @RISK® (Palisade, 2008) can be employed.
7. Definition of suitable performance functions. This definition is of paramount importance and is a crucial step in the analysis. For example a function can be defined over the critical deformations such as tunnel crown displacement to control the required clearance of the tunnel and/or maximum stresses carried by shotcrete lining. The performance function can be evaluated with results from the finite element calculations (bounds on continuous distribution functions of the evaluated system parameters), in order to obtain a range for the probability of failure or unsatisfactory performance. This is not considered in this paper, see e.g. Schweiger & Peschl (2005).

3 APPLICATION TO TUNNEL EXCAVATION

A tunnel application was chosen to demonstrate the applicability of the RS-FEM for these types of problems. The 460 m long tunnel located in Germany with a typical horse-shoe shaped section and dimension of 15x12.3 m width and height respectively, is constructed according to the principles of the New Austrian Tunnelling Method (NATM), and is divided into three main excavation stages top-heading, bench and invert. The overburden along the tunnel axis starts from 7.5 m in the portal region to a maximum of 25 m. A section with the overburden of 25 m was selected to apply the RS-FEM. The relevant 2D model geometry and finite element mesh including some model specifications are depicted in Figure 2. Approximately 900 15-noded triangular elements were employed in the model. The finite element software Plaxis has been used for all calculations (Brinkgreve et al. 2008) and the Mohr-Coulomb failure criterion is chosen as constitutive model in order to be able to compare results with conventional design analysis, which is however not topic of this paper.

The Mohr-Coulomb parameters are derived from a Hoek-Brown classification which is based on test results performed on rock samples described in the site investigation report. The choice of the method for determining equivalent cohesion and friction angle is largely a matter of experience (Merifield et al. 2006) and there are two options to derive equivalent cohesion and friction angle from HB parameters. First, by fitting the MC failure line to the HB failure curve tangentially at a specific minor principal stress or normal stress or secondly a regression method can be applied over a dominant stress range of the problem to obtain average values of MC strength parameters. The latter has been adopted here and more details on the parameter determination can be found in Nasekhian (2011). The resulting parameter sets are summarized in Table 1 and a graphical representation of the random sets is provided in Figure 3. E_{rm} is the elastic modulus of the rock mass, φ and c are the usual strength parameters. R_f-values in Table 1 are pre-relaxation factors in order to account for 3D-effects in a 2D analysis. It should be noted that extreme values of R_f for top heading, bench and invert are used simultaneously.

Table 1. Random Set parameters

Variable	E_{rm}	φ	c	$R_{f,\ top\ heading}$	$R_{f,\ bench}$	$R_{f,\ invert}$
Unit	[MPa]	[°]	[kPa]	[-]	[-]	[-]
Set 1	1300-2300	22-32	450-750	0.4-0.6	0.3-0.5	0.2-0.4
Set 2	1900-3400	24-34	1000-1600	0.3-0.5	0.2-0.4	0.1-0.3

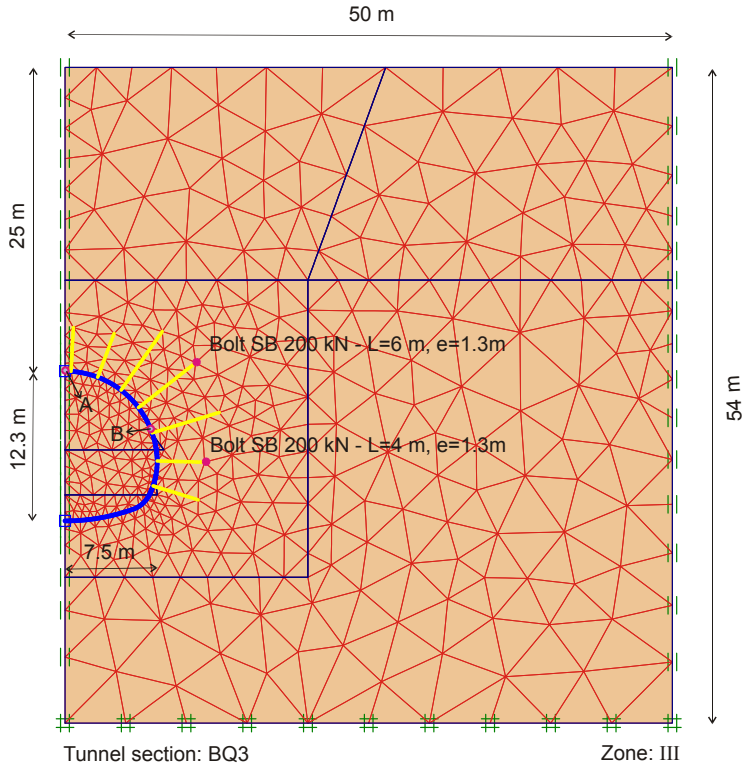

Figure 2. Finite element mesh used in RS-FEM analysis

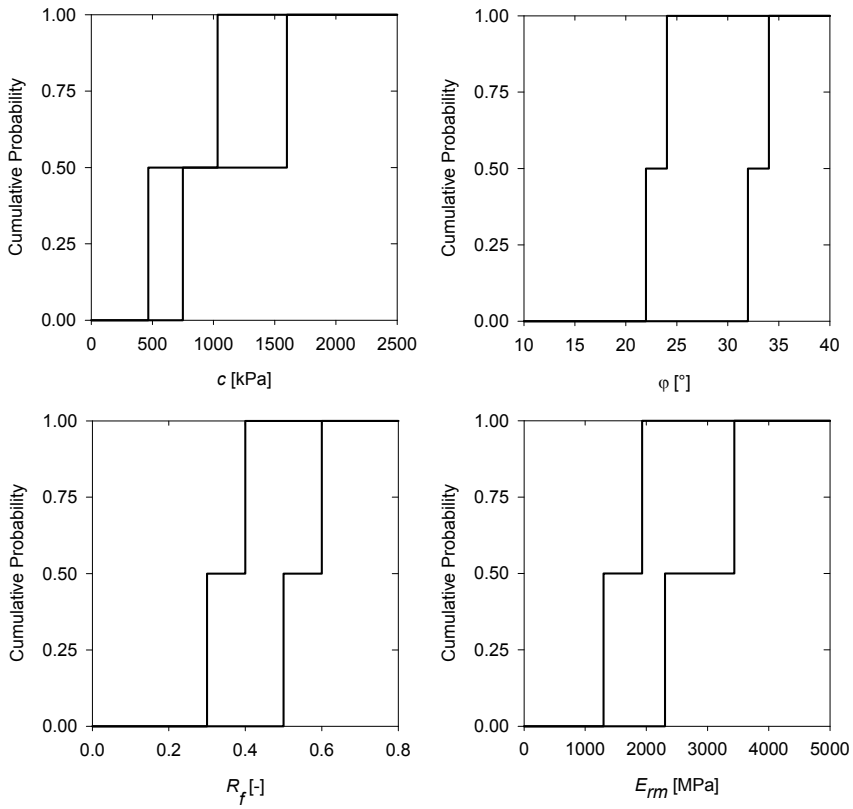

Figure 3. Random sets: cohesion c, friction angle φ, R_f-value for top heading, elastic modulus of rock mass E_{rm}

4 RESULTS FROM RANDOM SET ANALYSIS

Some selected results of the system response are depicted in terms of discrete cumulative probability distributions in Figures 4 and 5. Points A and B denote points where measurements during construction have been obtained, A being at the tunnel crown and B at the tunnel sidewall respectively (see Figure 2). The measured values have been added in Figure 4. Since two observations were available within the considered "homogeneous" section, measurements can be presented in terms of discrete cumulative probabilities too, comprising of two steps. Figure 5 shows calculated maximal normal forces and bending moments in the lining, again in form of discrete cumulative probability distributions. It follows that measured values for crown displacements (Figure 4a) fall well inside the predicted range, but for point B measurements are slightly outside. However, considering the very small displacements this could possibly be attributed to uncertainties or inaccuracies in the measurements. Generally speaking, measurements have to be within the calculated bounds if the range assumed for the input parameters covers the true range of material behaviour and the chosen geotechnical and numerical model is appropriate. Leaving aside the one measurement which is outside the bounds it can be observed that an analysis in terms of worst case parameters would lead to very conservative results (upper bounds of displacements in Figure 4). However, the best case would be too optimistic. From other case histories (see e.g. Schweiger & Peschl 2005) it seems that measurements of displacements would tend to fall in the "lower third" of the predicted range.

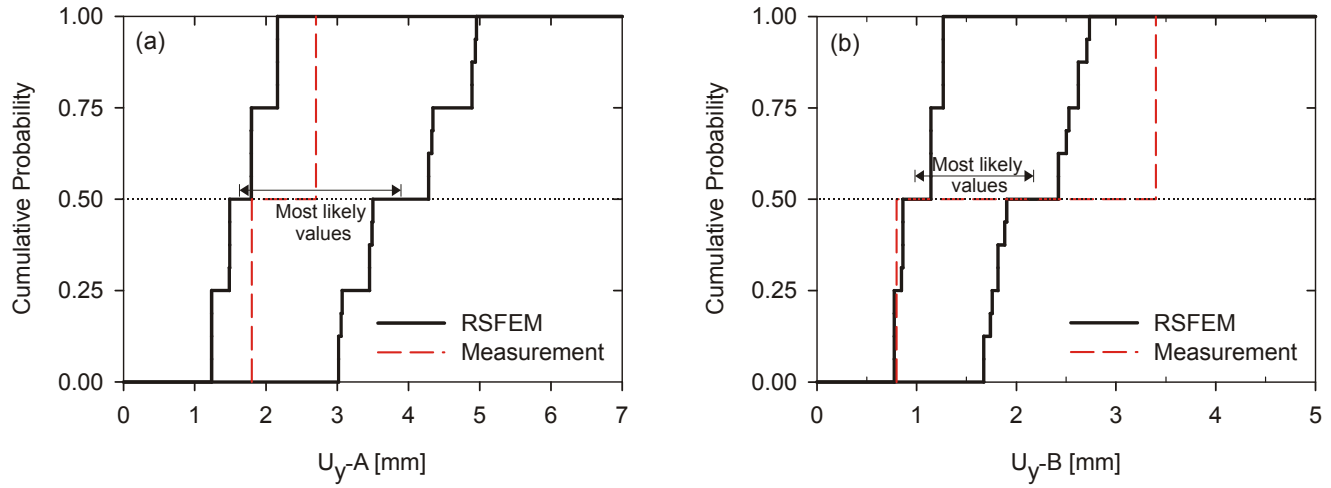

Figure 4. RS-FEM results: a) vertical displacement crown (point A), b) vertical displacement side wall (point B)

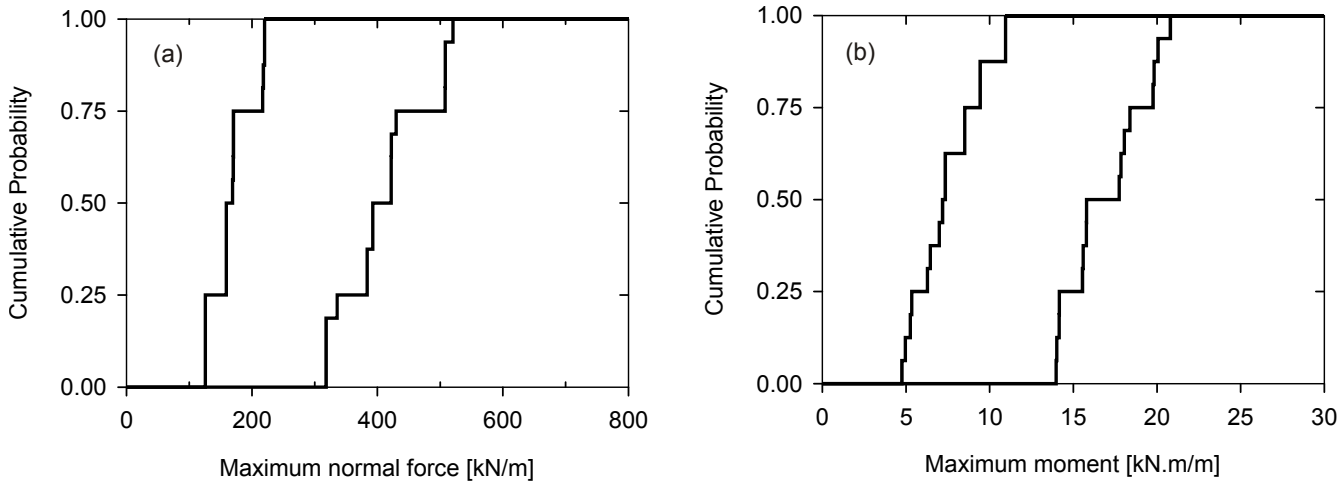

Figure 5. RS-FEM results: a) maximum normal force in lining, b) maximum bending moment in lining

5 COMPARISON WITH POINT ESTIMATE METHOD

In this section the results of two uncertainty models, namely the Point Estimate Method (PEM) and the Random Set Method, having different theoretical background, are compared with the measurements of the tunnel problem presented earlier. PEM has been first introduced by Rosenblueth (1975), but further developments have been published by a number of authors thereafter.

In the Point Estimate Method the continuous density distribution function $f_x(x)$ is replaced by specially defined discrete probabilities which are supposed to model the same low-order moments of $f_x(x)$. The determination of these moments is done by adding up the weighted discrete realisations. In Figure 6 this relationship is shown in a simplified way by the two realisations at x+ and x- represented with the corresponding weights w+ and w-. In the work presented here the approach suggested by Zhou and Nowak (1988) has been applied, employing a $2n^2+1$ (n is the number of basic variables) integration rule, which is considered as an optimum compromise between accuracy and computational effort (Thurner 2000). The method is extensively covered in the literature, e.g. Rosenblueth (1975), Lind (1983), Harr (1989), Hong (1998), Zhou and Nowak (1988) and therefore not described in further detail here.

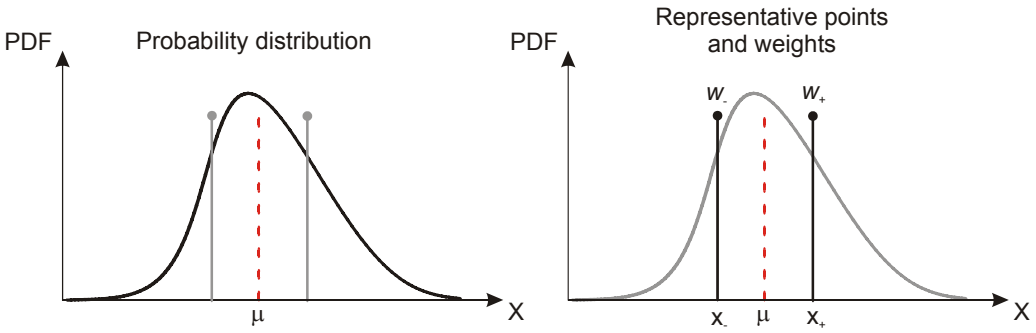

Figure 6. Simplified graphical representation of Point Estimate Method (after Thurner 2000)

In order to compare results from RS-FEM and PEM analyses a probability distribution function which reflects approximately the input data of the RS-FEM analysis is required. Due to the significant differences in the underlying concepts of the two approaches there is no rigorous way of doing this and some assumptions have to be made. The approach utilized here is as follows (for more details see Nasekhian 2011).

First a uniform distribution is constructed whose left and right extreme values are medians of left and right random set bounds respectively. Then, typical distributions are fitted and depending on the shape of the random bounds and the variable, one can select an appropriate distribution for further analysis. For instance, if the approach is applied to the friction angle using Triangular, Normal and Lognormal distributions as depicted in Figure 7 a considerable discrepancy between the different distribution types occurs; therefore, engineering judgment is necessary.

Although the random set exhibits some kind of symmetry on the right and left bounds, the selection of Lognormal looks more reasonable since it covers the whole range of random set values and it is also a commonly used distribution for friction angle always yielding positive values. In a similar way the distributions for the other random variables of the problem have been defined, they are summarized in Table 2.

Table 2. Basic random variables for PEM analysis

Variable	E_{rm}	φ	c	R_f
Unit	[MPa]	[°]	[kPa]	[-]
Distribution type	Lognorm.	Lognorm.	Normal	Normal
Mean	2256	28	950	0.45
Standard dev.	631	5	205	0.09
COV %	28	17.8	21.6	20

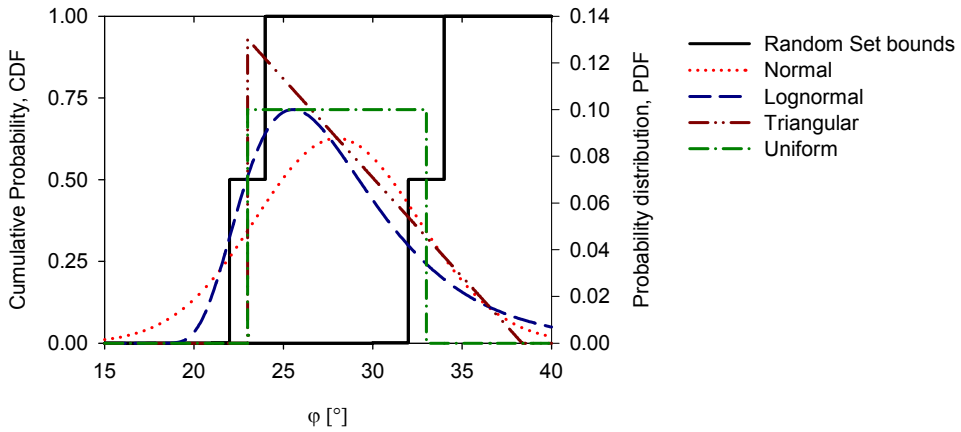

Figure 7. Comparison of assumed distribution for friction angle equivalent to the random set

A comparison of the results from PEM and RS-FEM analyses for crown settlements and maximum normal forces in the shotcrete lining is provided in Figure 8. It follows that displacements and normal forces show a good agreement with the RS-FEM results in the sense that PEM's results are supposed to present the 'true' distribution of the system response and should not exceed the random set bounds. In Figure 8a measured values and in addition intervals $\{-1.8\sigma < x < +1.8\sigma\}$ and $\{-3.0\sigma < x < +3.0\sigma\}$ obtained from PEM results are also shown. PEM only approximates the statistical moments of the system response and therefore a subjective probability distribution function should be selected for individual target values. On the other hand, it follows from probability theory (Pukelsheim 1994) that the interval $\pm 1.8\sigma$ represents the 86% confidence interval irrespective of the distribution of the target variable. Additionally, the range of results obtained from RS-FEM presenting the most likely behaviour is identified here where the cumulative probability of the lower and upper bounds is 0.5. It follows from this Figure that consistent conclusions can be drawn from both analysis in the sense that the "most likely" behaviour can be extracted from both approaches despite their differences in the underlying theories.

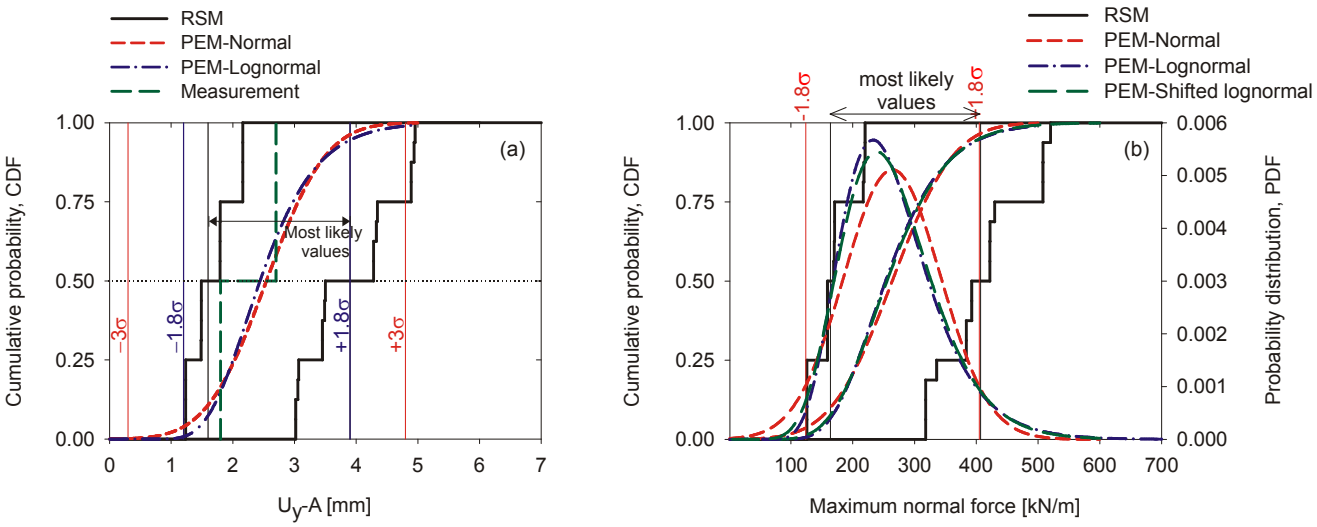

Figure 8. Comparison of results a) vertical displacement crown (point A), b) normal force in lining

6 SUMMARY AND CONCLUSIONS

A tunnel project was used to demonstrate the applicability of the RS-FEM framework in geomechanics where engineers have to face not only imprecise data but also lack of information. RS-FEM proved its capability of capturing uncertainty in a complex geotechnical application producing bounds of the expected system behaviour which compares reasonably well with measurements obtained during construction. The RE-FEM can account for epistemic and aleatory uncertainty and requires less computational effort as compared to fully probabilistic methods such as the Monte-Carlo simulation.

In this paper a comparison of RS-FEM and a point estimate method has been attempted and it could be concluded that despite the fundamentally different underlying theories comparable conclusions with respect to the expected system behaviour could be drawn for this particular problem.

REFERENCES

Brinkgreve, R.B.J. & Broere, W. 2008. PLAXIS, Finite element code for soil and rock analyses, Users Manual, Version 9, Rotterdam: Balkema.

Dempster, A. P. 1967. Upper and lower probabilities induced by a multivalued mapping. Annals of Mathematical Statistics 38, 325-339.

Dubois, D. & Prade, H. 1991. Random sets and fuzzy interval analysis. Fuzzy Sets and Systems, 42, 87-101.

Harr, M.E. 1989. Probabilistic estimates for multivariate analyses. Applied Mathematical Modelling, Vol. 13, No. 5, 313-318.

Hong, H.P. 1998. An efficient point estimate method for probabilistic analysis. Reliability Engineering and System Safety, Vol. 59, No. 3, 261-267.

Kendall, D.G. 1974. Foundations of a theory of random sets. In stochastic Geometry (eds) E.F. Harding & D.G. Kendall. New York: Wiley.

Lind, N.C. 1983. Modelling uncertainty in discrete dynamical systems. Applied Mathematical Modelling; Vol. 7, No. 3, 146-152.

Merifield, R.S., Lyamin, A.V. & Sloan, S.W. 2006. Limit analysis solutions for the bearing capacity of rock masses using the generalised Hoek–Brown yield criterion. Int. J. Rock Mech. Min. Sci., Vol. 43, 920-937.

Nasekhian, A. 2011. Application of Non-probabilistic and Probabilistic Concepts in Finite Element Analysis of Tunnelling. Institute for Soil Mechanics and Foundation Engineering, Graz University of Technology, Dissertation.

Palisade Corp. 2008. @RISK, Risk Analysis and Simulation, Version 5.0, Manual. Newfield USA: Palisade Corporation.

Peschl, G.M. 2004. Reliability analyses in geotechnics with the random set finite element method. Institute for Soil Mechanics and Foundation Engineering, Graz University of Technology, Dissertation.

Pukelsheim, F. 1994. The Three Sigma Rule. The American Statistician, Vol. 48, No. 2 , 88-91.

Rosenblueth, E. 1975. Point estimates for probability moments. Proc. Nat. Acad. Sci. USA, Vol. 72, No. 10, 3812-3814.

Schweiger, H.F. & Peschl, G.M. 2005. Reliability analysis in geotechnics with the random set finite element method. Computers and Geotechnics 32, 422–435.

Schweiger, H.F. & Peschl, G.M. 2007. Basic Concepts and Applications of Random Sets in Geotechnical Engineering. Book Series CISM International Centre for Mechanical Sciences, (eds.) D.V. Griffiths & G.A. Fenton Vol 491, 113-126.

Shafer, G. 1976. A Mathematical Theory of Evidence. Princeton: Princeton University Press.

Thurner, R. 2000. Probabilistische Untersuchungen in der Geotechnik mittels Deterministischer Finite Elemente-Methode. Institute for Soil Mechanics and Foundation Engineering, Graz University of Technology, Dissertation.

Tonon, F. & Mammino, A. 1996. A random set approach to the uncertainties in rock engineering and tunnel lining design. Proc. ISRM International Symposium on Prediction and Performance in Rock Mechanics and Rock Engineering (EUROCK '96), Vol. 2, Barla (ed.). Torino, Italy, Rotterdam, A.A. Balkema, 861-868.

Tonon, F., Bernardini, A. & Mammino, A. 2000(a). Determination of parameters range in rock engineering by means of Random Ret Theory. Reliability Engineering & System Safety, Vol. 70, No. 3, 241-261.

Tonon, F., Bernardini, A. & Mammino, A. 2000(b). Reliability analysis of rock mass response by means of Random Set Theory. Reliability Engineering & System Safety, Vol. 70, No. 3, 263-282.

Zhou, J. & Nowak, A.S. 1988. Integration formulas to evaluate functions of random variables. Structural safety, Vol. 5, No. 4, 267-284.

ISGSR 2011 - Vogt, Schuppener, Straub & Bräu (eds) - © 2011 Bundesanstalt für Wasserbau ISBN 978-3-939230-01-4

Fuzzy Sets concept for optimization underground gas storage

B. Žlender & P. Jelušič
University of Maribor, Faculty of Civil Engineering, Maribor, Slovenia

D. Boumezerane
University of Béjaïa, Civil Engineering Department, Béjaïa, Algeria

ABSTRACT: The paper deals with the underground gas storage (UGS), designed from one or more lined rock caverns (LRC). The LRC is a pressure tank containing stored gas under a high pressure. The gas pressure is transmitted through the cavern wall to the surrounding rock. The design, construction and safe operation of the LRC is influenced by many factors, like: structure and geometry, geomechanical properties of the rock mass, loading (internal gas pressure, external rock pressure), drainage system, entrance tunnels, the construction process, risks and the influence on the environment. This paper presents the Fuzzy Sets concept to improve performance of UGS with LRC's. For this purpose, it is necessary to carry out a number of steps. First is the determination of the geological model of UGS region. Geomechanical rock mass parameters are determined from geological conditions of a selected suitable UGS location and a special FE model is generated. The rock mass strength stability and safety of the system are then analyzed for various combinations between different design parameters like: number of caverns, distance between them, inner gas pressures, cavern depths, cavern diameters and cavern wall thickness. A Fuzzy Inference System (FIS) optimizing cavern is carried out. The approach is illustrated in the case of UGS Senovo, which is in the planning stage. The FIS allows optimizing, regarding to risk conditions, the most suitable solution depending on the site and on the financial possibilities available. Several rules were built and fired for all the intervening parameters and the final result is obtained after defuzzification.

Keywords: Underground gas storage (UGS), Lined rock cavern (LRC), Fuzzy Sets, Fuzzy Inference System (FIS)

1 INTRODUCTION

The underground gas storage (UGS) contains one or more lined rock caverns (LRC). The LRC is a pressure tank containing stored gas under a high pressure. The gas pressure is transmitted through the cavern wall to the surrounding rock. The design, construction and safe operation of the LRC is influenced by many factors, like: LRC structure and geometry, geomechanical properties of the rock mass, loading (internal gas pressure, external rock pressure), drainage system, entrance tunnels, the construction process, risks and the influence on the environment.

In order to achieve the optimal design of UGS with LRC the geomechanical model, the cost optimization model and Fuzzy inference system are involved.

Fuzzy Inference System (FIS) is carried out to improve performance of UGS with LRC's. FIS is one of the tools used to model a multi-input, multi-output system.

Primary objectives to improve performance of UGS with LRC's are:
- Minimization of the total construction and operational costs per unit of gas,
- Safety on all risks which may occurs during the construction and operation,
- Calculation of the inner gas pressure, the cavern depth, the cavern inner diameter, thickness of the cavern concrete wall and the height of the cavern tube through the optimization.

2 UGS WITH LRC

The design of the LRC structure is similar to the already constructed UGS in Skellen [1]. Cavern wall, which transmits the gas pressure on the surrounding rock, is composed of several elements [2]. The task of steel lining is sealing and bridging small cracks of the concrete. Sliding layer enables the corrosion protection for the steel and reduces the friction between steel and concrete wall. Concrete wall uniformly transmits the internal pressure to the rock and consequently uniformly distributes the deformations. The reinforcement in concrete prevents tangential deformations. The task of drainage system is collect and drainage the water. Layer of special low strength permeable shotcrete is placed closest to the rock surface. The purpose of the shotcrete is to protect the drainage system. Rock provides the LRC capacity.

The LRC concept involves large caverns with a diameter of 35 to 40 m and high from 60 to 100 m, with cylindrical wall and sphere upper and lower part. They are located at depths from 100 to 250 m and are surrounded by 2 m or more thick concrete wall and coating with a thin steel sheet (15 mm).

The evaluation of rock mass properties is a partly subjective process because there always exist a different interpretation of the investigated results (deviation). Many methods were developed in the past for the determination/interpretation the rock mass properties. In this work the generalized Hoek-Brown failure criterion [3] is proposed to be applied and the Mohr-Coulomb strength parameters are determined.

The external pressure acts on the wall of the cavern (during the construction and operation). The high of the pressure (2 MPa to 5 MPa) depends on the depth of the cavern. The internal pressure is beginning to occur in service. It is expected that the pressure cyclically increases and decreases during periods of gas supply and discharge between the minimal (3 MPa) and maximal (calculated) value. The internal pressure therefore causes static and cyclic loads. The minimum lifetime of the LRC is limited to be higher than 500 cycles.

Cavern is constructed at a depth of 100 to 300 m, which means that the hydrostatic pressure reaches 1 to 3 MPa. Drainage system is installed on the outer side of the cavern wall. It drainages the water and enables the monitoring, collection and removing of the gas in the case of gas leakage.

The system of tunnels is designed to transport material and allow the access for machinery during the construction of the underground chambers. The tunnels also provide a cost-effective mining of caverns. Cross-section of tunnels amounts about 25 m^2 in the flat areas and 40 m^2 in curved areas.

The LRC is linked with the ground surface by the vertical shaft. The shaft is made from a steel pipe for filling and emptying the gas storage [4]. The construction of the LRC starts with the erection of access tunnels. The mining of caverns is then performed downwards from the top. A drainage system is put on the cavern surface and a free-standing steel lining is assembled. The last phase presents the construction of the cavern wall by filling the space between excavated cavern surface and steel lining with concrete. When self compacted concrete is used, no concrete vibration is needed.

The LRC concept of UGS should provide a safe and environmentally friendly mode for gas storage. Since the gas should never been in contact with the surrounding rock mass, the gas storage is designed as a closed system.

3 GEOMECHANICAL ANALYSIS

3.1 *Geomechanical model*

The geomechanical model is done based on geological data, UGS design data, geomechanical parameters and FEM analyses results.

3.2 *Determination of the rock mass parameters*

The research included a geological mapping of surface, structural drilling of five deep boreholes, geotechnical field measurements and laboratory testing of samples from boreholes in order to determine their geomechanical parameters. Rock mass parameters were determined on the basis of the generalized Hoek-Brown failure criterion [5]. By using the generalized Hoek-Brown failure criterion, all needed parameters were obtained by geological measurements in the field, laboratory testing and calculations, see Table 1. In the beginning determined were strength parameters like the unconfined compressive strength of intact rock σ_{ci} [MPa], the geological strength index GSI [-], the intact rock parameter mi [-] and the disturbance factor D [-] as well as the intact rock deformation modulus E_i [MPa].

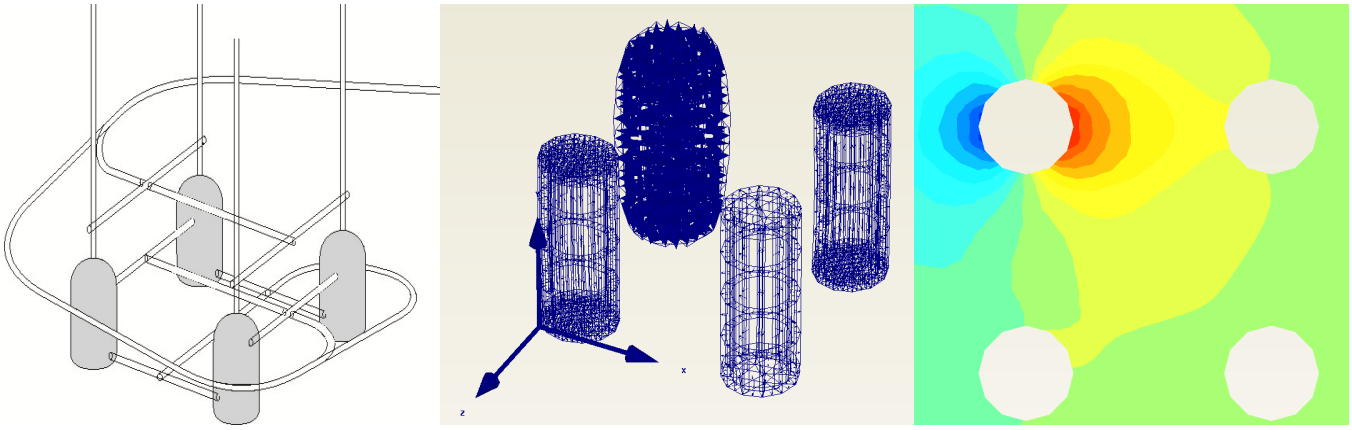

Figure 1. 3D UGS model in Plaxis FEM program

3.3 *Risk conditions*

The risk during construction and in the operation of the system should be analyzed. Geological conditions, hydro geological conditions and geomechanical rock mass properties around LRC significantly impact on all of the risks. The risks which occur during the construction are similar to ones at the construction of tunnels: large scale failure of the rock cover, large deformations of the cavern wall, irruption of the water and impact on water resources in the surrounding area. For the designing and optimization the risks during the operation are decisive. Hence the following risks have to be considered:

- Risk 1: Failure of the rock mass (rock strength is exceeded),
- Risk 2: Uplift of the rock cover,
- Risk 3: Failure of the rock between two caverns,
- Risk 4: Large deformation or destruction of the steel lining,
- Risk 5: Unequally deformation of the LRC structure because of the rock heterogeneity,
- Risk 6: Drainage system does not work.

Using FEM calculation it is insure that rock strength is not exceeded (Risk 1). The last two risks (Risks 5 and 6) are prevented with the correct construction of the LRC in a homogeneous rock mass and with the properly construction and operation of the drainage. Three conditions have to be defined in a form of three geomechanical inequality constraints for the (Risks 2-4):

- Condition 1: Uplift of the rock cover is prevented (Risk 2),
- Condition 2: Failure of the rock between two caverns is prevented (Risk 3),
- Condition 3: Strains of the steel lining need to be limited under the acceptable value (Risk 4).

Condition 1 is satisfied when the calculated safety factor against the rock cover uplift SF_{up} is greater than a defined minimal value $SF_{up,min}$, see Eq. (1).

$$SF_{up} \geq SF_{up,\min} \tag{1}$$

The calculated safety factor against the rock failure between two caverns SF_{hor} must be greater than a defined minimal value $SF_{hor,min}$, see Eq. (2).

$$SF_{hor} \geq SF_{hor,\min} \tag{2}$$

Strains of steel lining ε are limited to be smaller than a defined maximal strain ε_{max}, see Eq. (3).

$$\varepsilon \leq \varepsilon_{\max} \tag{3}$$

The risks increase with the increasing of the gas pressure in the caverns and diameter of the cavern and decrease with the increasing the depth of the LRC and the thickness of the concrete wall. The gas pressure is cyclically increases and decreases, which affects on the fatigue of materials.

3.4 *Geomechanical analyses*

A series of FEM analyses was carried out to satisfy conditions (1), (2) and (3). The FE mesh, consisted from triangle prismatic finite elements, was defined for the rock mass area of 280x280x300 m3 (x-y-z, with z the axis in depth). The FEM computer program Plaxis Version 3D [6] was used.

3.5 *Results*

Analysis with different combinations of parameters can be carried out. In the event that we have six different parameters and three values of each parameter then we have 729 different combinations. Each combination has its own effect on the strain, safety factors against the rock cover uplift SF_{up} and the rock failure between two caverns SF_{hor}. Safety factors SF_{up}, SF_{hor} and strains ε are obtained from a series of FEM analyses for all the mentioned combinations of parameters.

4 COST ANALYSIS

The cost model consist cost data, design data, dimension dependence quantities, and construction cost [7].

4.1 *Cost data*

The geomechanical input data are presented in 3.1.1. Economic data for the optimization include fixed costs per cavern: upper ground works C_{up} and underground works C_{under} and prices per unit like the price of the tunnel excavation $PR_{exc,tun}$ [€/m^3], the price of the tunnel protection $PR_{prot,tun}$ [€/m^3], the price of the cavern excavation $PR_{exc,cav}$ [€/m^3], the price of the cavern protection $PR_{prot,cav}$ [€/m^2], the price of the cavern drainage PR_{drain} [€/m^2], the price of the cavern wall concrete PR_{wall} [€/m^3], the price for the wall reinforcement PR_{reinf} [€/t] and the price of the steel lining PR_{steel} [€/m^2].

4.2 *Design data*

The value $L^{sf}_{exc,tun}$ [m] is the length of tunnel excavation. The length L_0 varies from the case to case and is dependent on the number of LRC's inside the UGS and the cavern depth. $V^{sf}_{exc,cav}$ [m^3] is the cavern excavation volume. $A^{sf}_{exc,cav}$ [m^2] is the cavern excavation area. Term $\left(V^{sf}_{exc,cav} - V^{sf}_{cav}\right)$ denotes the volume of used concrete and V^{sf}_{cav} stands for the inner volume of the cavern. A^{sf}_{cav} is the spread area of the steel lining (inner cavern area). The volume of concrete and the weight of reinforcement are estimated.

4.3 *Construction cost*

The construction cost comprises the investment and operational costs of the UGS system. The total construction cost per cavern [€/$_{cav}$] and total construction cost per unit of gas [€/m^{3}gas] include sum of fixed costs and variable (depending) costs (4): Fixed costs are sum of upper ground works C_{up} and underground works C_{under}. Variable costs are sum of cost for the tunnel excavation $C_{exc,tun}$, the tunnel protection $C_{prot,tun}$, the cavern excavation $C_{exc,cav}$, the cavern protection $C_{prot,cav}$, the cavern drainage C_{drain}, the cavern wall C_{wall} and the cost of the steel lining C_{steel}. Total construction and operational cost per unit depends of number of cycles (No_{cycles} [-]) of gas supply and discharge (6).

$$COST/cav = \left(C_{up} + C_{under}\right)/N_{0,cav} + C_{exc,tun} + C_{prot,tun} + C_{exc,cav} + C_{prot,cav} + C_{drain} + C_{wall} + C_{reinf} + C_{steel} \tag{4}$$

$$\begin{aligned} COST/cav = {} & FC_{up} + FC_{under} + PR_{exc,tun} \cdot L_{exc,tun} + PR_{prot,tun} \cdot L_{exc,tun} + PR_{exc,cav} \cdot V_{exc,cav} + PR_{prot,cav} \cdot A_{exc,cav} \\ & + PR_{drain} \cdot A_{exc,cav} + PR_{wall} \cdot \left(V_{exc,cav} - V_{cav}\right) + PR_{reinf} \cdot \left(V_{exc,cav} - V_{cav}\right) \cdot \rho \cdot r_{perc} + PR_{steel} \cdot A_{cav} \end{aligned} \tag{5}$$

$$COST/m^3 gas = \frac{COST/cav}{V_{gas} \cdot N_{0,cycles}} \tag{6}$$

5 FUZZY INFERENCE SYSTEMS

The article aims to investigate the influence of various parameters on safety factors SF_{up}, SF_{hor} and strain. Because of the enormous number of possible combinations of parameters it is necessary to carry out a lot of geotechnical analysis, which is demanding work. It is also difficult to determine geomechanical parameters from geological data. The main purpose is to obtain optimal parameter values. Nonlinear programming is a powerful tool by which we get the optimal parameters, but requires complex analytical equations to determine the interdependence of parameters.

Fuzzy logic is an effective paradigm to handle imprecision, which significantly reduces a number of geotechnical analyses. It can be used to take fuzzy or imprecise observations for inputs and yet arrive at crisp and precise values for outputs. Also, the Fuzzy Inference System (FIS) is a simple and commonsensical way to build systems without using complex analytical equations. Fuzzy sets [8] are widely used in engineering and especially in geological and geotechnical fields. A fuzzy set is defined as constituted by elements belonging with a degree of membership μ (x) to the set. The membership function varies between 0 and 1. Fig. 2a) shows the concept of FIS.

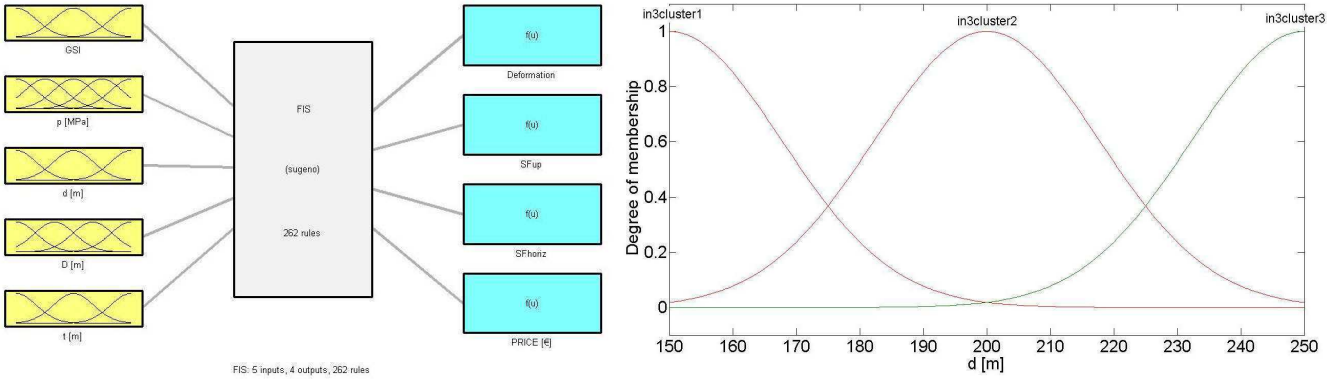

Figure 2. a) Concept of fuzzy inference system; b) Example of fuzzy sets INPUT parameter

5.1 *Fuzzy Inference System*

The fuzzy inference system for UGS is based on, INPUT Parameter, OUTPUT Parameters, Fuzzy rules and Defuzzification of the result (decision).

5.1.1 *Input and Output parameters*

The number of rows represents the number of combinations calculated with geomechanical and cost model. A row constitutes a set of observed values of the 7 input variables (No_{cav}[-], l_{cav} [m], GSI [-], p [MPa], d [m], D [m], t[m]) and the corresponding row, in output represents the calculated values (ε [‰], SF_{up}, SF_{hor}, Price [€]) for the input variables. To identify natural groupings in data from a large data set we use clustering technique, which allow us concise representation of relationships embedded in the data. Each input and output has as many membership functions as the number of clusters that has been identified with clustering. Sugeno-type FIS structure assigns default values and names for inputs, outputs and membership functions [9]. An example of input and output fuzzy sets is presented on Fig.2b.

5.1.2 *Fuzzy rules*

Sugeno-type FIS structure map a cluster in the input space to a cluster in the output space. If the inputs to the FIS, strongly belong to their respective membership functions then the output must strongly belong to its membership function. The (1) at the end of the rule is to indicate that the rule has a weight or an importance of "1". Weights can take any value between 0 and 1. Rules with lesser weights will count for less in the final output. An example of these rules is:

IF (GSI is in1cluster1) AND (p is in2cluster1) AND (d is in3cluster1) AND (D is in4cluster1) AND (t is in5cluster1) THEN (ε is out1cluster1)(SF_{up} is out2cluster1)(SF_{hor} is out3cluster1)(PRICE is out4cluster1) (1)

5.1.3 *Defuzzification*

The output of the FIS, has linear membership functions representing the clusters identified by clustering. The coefficients of the linear membership functions though are not taken directly from the cluster centers.

Instead, they are estimated from the dataset using least squares estimation technique. All membership functions in this case will be of the form $a \cdot No_{cav} + b \cdot l_{cav} + c \cdot GSI + d \cdot p + e \cdot d + f \cdot D + g \cdot t + h$, where a, b, c, d, e, f, g and h represent the coefficients of the linear membership function.

6 APPLICATION

Below is an example of analysis of UGS with LRC planned to place Senovo [10]. The research included a geological mapping, geotechnical field measurements (pressiometer, geophysical measurements, and hydro-geological measurements) and laboratory testing. Data obtained from geological mapping and geological inventory of the core wells, confirming act and limestone Dolomites in the eastern area of mine Senovo [11]. The UGS is planned to be constructed from 4 equal lined rock caverns in order to store 5.56 x 4 = 22.24 millions m^3 of natural gas. The concrete C 30/37 and structural steel S 235 are used for the construction of tunnels, cavern walls and steel lining. Steel S 400 was used for the reinforcement. Steel lining is 12 mm thick. The optimization/calculation of the UGS system comprises: determination of the rock mass parameters, geomechanical analyses, cost analysis and Fuzzy Inference System.

6.1 *Rock mass parameters*

The research included a geological mapping of surface, structural drilling of five deep boreholes, geotechnical field measurements and laboratory testing of samples from boreholes in order to determine their geomechanical parameters. Data obtained from geological mapping and geological inventory of the boreholes, confirming presence of limestone and dolomite in the eastern area of mine Senovo are presented in reference [11]. Rock mass parameters were determined on the basis of the generalized Hoek-Brown failure criterion [12]. By using the generalized Hoek-Brown failure criterion, all needed parameters were obtained by geological measurements in the field, laboratory testing and calculations, see Table 1. In the beginning determined were strength parameters like the unconfined compressive strength of intact rock σ_{ci} [MPa], the geological strength index GSI [-], the intact rock parameter mi [-] and the disturbance factor D [-] as well as the intact rock deformation modulus E_i [MPa].

Table 1. Hoek-Brown parameters, Mohr-Coulomb fit and rock mass parameters

Hoek-Brown Classification	Minimum	Average	Maximum
σci [MPa]	55	60	65
GSI [-]	41	46	51
mi [-]	(9+/-3)	(9+/-3)	(9+/-3)
D [-]	0.200	0.183	0.167
Ei [MPa]	40	55	60
Hoek-Brown criterion			
mb [-]	0.866	1.056	1.333
s [-]	0.0090	0.0016	0.0031
a [-]	0.511	0.508	0.505
Mohr-Coulomb fit			
c [kPa]	700	870	1000
φ [°]	37.5	39	41
Rock mass parameters			
σt [MPa]	0.057	0.092	0.15
σc [GPa]	1.5	2.3	3.5
σcm [GPa]	6.6	8.2	10.1
Erm [GPa]	5.0	10.0	15

6.2 *Geomechanical and cost analyses*

Safety factors against the rock cover uplift SF_{up} and the rock failure between two caverns SF_{hor} were calculated for 180 various combinations between 3 different rock mass parameters GSI (41, 46, 51), 5 different inner gas pressures p (10, 15, 20, 25 and 30 MPa), 3 different cavern depths h (150, 200 and 250 m) and 4 different cavern inner diameters D (15, 20, 25 and 30 m), see Table 2.

The strains of steel lining ε were in addition calculated for 3 different thickness of the concrete wall t (2, 4 and 6 m) having thus together 180x3=540 calculations. These calculations were performed by a series of FEM analyses for the treated UGS of Senovo. These calculations were used for non-linear pro-

gramming and expressed with analytical equations. Non-linear programming serves us for comparing with fuzzy results.

Fuzzy allow us to reduce number of calculations and still give us satisfied results. In this example we reduced number of calculations to 54.

Table 2. Obtained safety factors SF_{up}, SF_{hor} and strains ε from FEM analyses

	Input					Geomechnical output			Cost output
No.	GSI [-]	p [MPa]	d [m]	D [m]	t [m]	SF_{up} [-]	SF_{hor} [-]	ε [‰]	Cost/cav [€]
1	41	10	150	15	2	8,14	5,93	2,98	46936615,09
2	41	15	150	15	2	5,42	4,00	6,85	39465455,06
etc.									
54	51	30	250	30	6	3,5	2,16	3,60	41465145,30

6.3 *Risk conditions*

Risk conditions (4)-(6) for the considered UGS system of Senovo were finally evaluated as follows and put into the Fuzzy sets optimization model. Safety factors $SF_{up,min}$ and $SF_{hor,min}$ were defined to be 2.0. The limit strain ε_{max} was taken 3.5 ‰ for 1000 planed cycles of loadings.

6.4 *Fuzzy Inference System*

The Fuzzy Inference System of the UGS system in Senovo was performed. When executing the fuzzy system some conditions are imposed on deformations in the rock mass and structure with the limitations due to financial possibilities. The system permits to evaluate prices for different combinations of input parameters. The decision to take is illustrated in Figs. 3, 4, 5 and 6. Fig.3a shows the influence of gas-pressure and rock mass parameters on strains for given l_{cav} = 75 m, D = 25 m and t = 2 m. Comparison of Figs.3a and 3b describes the impact of depth (150 m and 200 m) of cavern on strains. Comparison between Figs. 4a and 4b represent the impact of depth of cavern on the safety factor against the rock cover uplift while Figs. 5a and 5b, shows the same thing in terms of safety factor against the rock failure between two caverns.

When all conditions are satisfied we can evaluate price (see Fig.6a and Fig.6b). Other surfaces could be plotted; they serve as a decision support system for the engineer. The system allows analyzing the situation and taking the required decision regarding the feasibility of the LRC.

7 CONCLUSION

The Fuzzy concept for UGS with LRC is presented. For this purpose it is necessary to carry out a number of steps. First is determination the geological model of UGS region. Next is transferring the geological model into the geomechanical model. In this work the system of Hoek and Brown based on the GSI is applied. The equivalent Mohr-Coulomb strength parameters were determined. Geomechanical analysis for risk during construction and later during operation of UGS, using FEM was carried out.

FEM analyses consists a set of calculations for different data (variables) such as: mechanical properties of the soil and the LRC, the depth and the spaces between the LRC, LRC geometry and dimensions, gas pressure, etc. A Fuzzy Inference System is carried out. Uncertainties and vague information are well handled using fuzzy sets.

For lower pressures big caverns are needed with small thickness of concrete, on the other hand if the pressure is “high” this will imply “smaller” caverns with “important” concrete thickness. The prices are very sensitive in each case. The decision to take is facilitated using the fuzzy inference system proposed; we plotted some curves (surfaces) which permit visualizing the parameters on the decision to take.

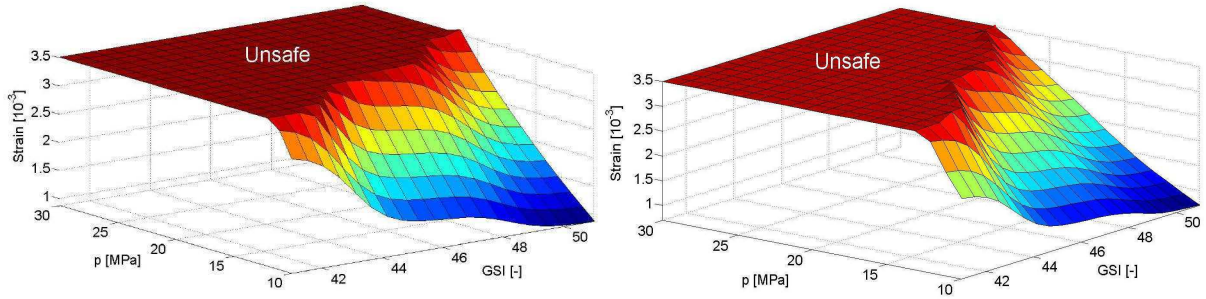

Figure 3. Strain a) d =150 m; b) d = 200m

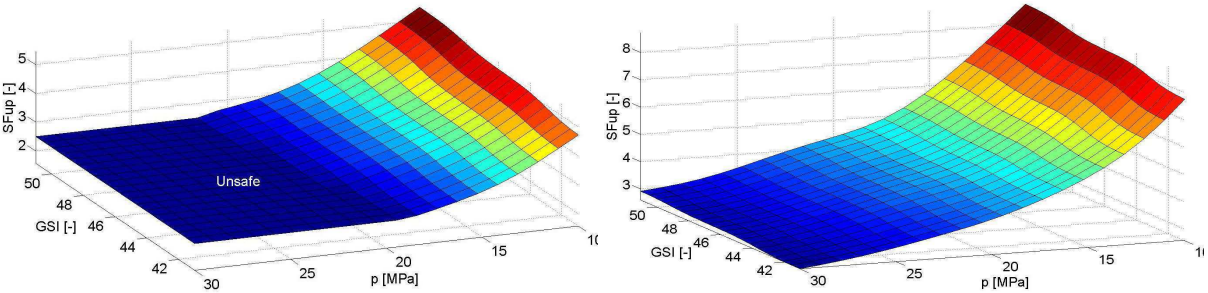

Figure 4. SF_{up} safety a) d =150 m; b) d = 200m

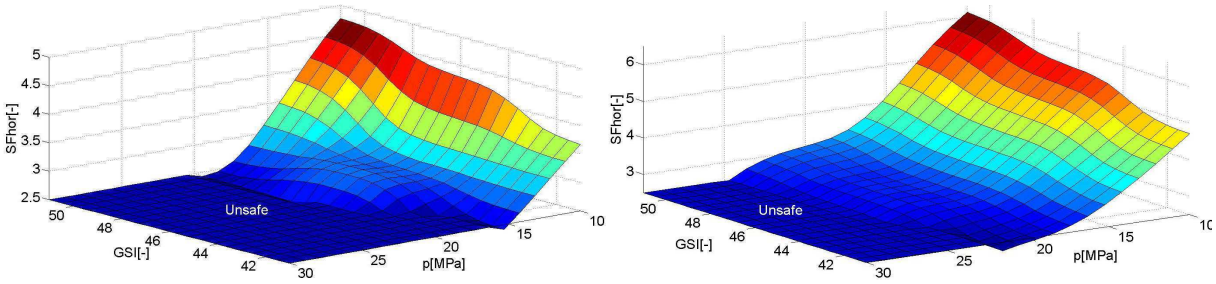

Figure 5. SF_{hor} safety a) d =150 m; b) d = 200m

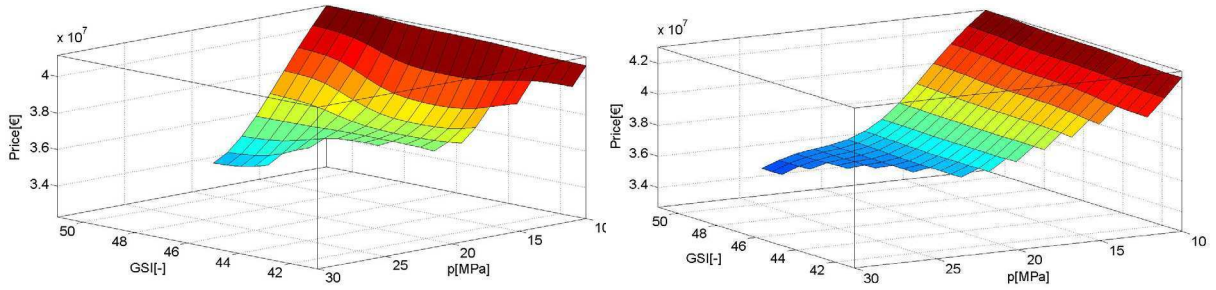

Figure 6. Price in safety area a) d =150 m; b) d = 200m

REFERENCES

[1] Johansson, J. 2003. High Pressure Storage of Gas in Lined Rock Caverns – Cavern Wall Design Principles. Licentiate Thesis. Div. of Soil and Rock Mech., Royal Institute of Technology, Stockholm.

[2] Brandshaug T., Christianson M., Damjanac B.2001. Technical Review of the Lined Rock Cavern (LRC) Concept and Design Methodology: Mechanical Response of Rock Mass, Technical Report, U.S. Department of Energy National Energy Technology Laboratory Morgantown, West Virginia.

[3] Hoek, E., Brown, E.T. 1997. Practical Estimates of Rock Mass Strength. International Journal of Rock Mechanics and Mining Sciences, Vol.34, No.8, 1165-1186.

[4] Hanafy, E.A. 1980. Advancing face simulation of tunnel excavation and lining. Placement. In: Underground Rock Engineering, 13th Canadian Rock Mechanics Symposium, pp. 119–125.

[5] Hoek, E. 1999. Putting numbers to geology – an engineers viewpoint. Felsbau, Vol.17, No.3, 139-151.

[6] PLAXIS 3D Foundation, version 2. In. 2008. Brimkgreve RBJ, Broere W, editors. AA Balkema, Rotterdam, Netherland.
[7] Kravanja, S., Žlender B. 2010. Optimal design of underground gas storage. V: WILDE, Willy Patrick (ur.), BREBBIA, Carlos Alberto (ur.), MANDER, Ülo (ur.). Fifth International Conference on High Performance Structures and Materials, Tallinn, 2010. High performance structures and materials V, (WIT transactions on the built environment, v. 112). Southampton: WIT, 389-399
[8] Zadeh, L. 1965. Fuzzy sets, Information and Control, Vol. 8(3), pp. 338-353.
[9] Sugeno, M. 1985. Industrial applications of fuzzy control, Elsevier Science Pub. Co.
[10] Noren, C. 2006. Underground Storage of Natural Gas in Lined Rock Cavern in Brestanica Area, NCC, Stockholm.
[11] Vukelič Ž., Sternad Ž., Vukadin V., Čadež F., Hude M., Pečovnik, I. 2006. High Pressure Storage of Gas in Area of Coal Mine Senovo, RMZ - Materials and Geoenvironment, Vol. 53, No. 3, pp. 303-313.
[12] Hoek E. practical Rock Engineering. Rocscience, New 2007 edition.

ISGSR 2011 - Vogt, Schuppener, Straub & Bräu (eds) - © 2011 Bundesanstalt für Wasserbau ISBN 978-3-939230-01-4

Level III Reliability Based Design employing Numerical Analysis - Application of RBD to FEM -

Y. Otake , Y. Honjo, T. Hara & S. Moriguchi
Department of Civil Engineerings, Gifu University, Gifu, Japan

ABSTRACT: A reliability based design scheme employing a response surface is applied to 25km long irrigation channel reliability assessment of vertical displacement by liquefaction. The problem includes very complex uncertainties such as statistical estimation error due to limited investigation, and model error involved in sophisticated FEM analysis. This scheme worked well to combine a sophisticated geotechnical analysis tool to the reliability analysis.

Keywords: Reliability based design(RBD), FEM analysis, liquefaction, irrigation channel

1 INTRODUCTION

Reliability based design (RBD) methods are attracting great interest of geotechnical engineers due to the introduction of Level I RBD in design codes development worldwide, e.g. the structural Eurocodes. On the other hand, the numerical methods, e.g. FEM analyses, based on rapid growth of computational capability and development of user friendly software, are frequently used in practical design of geotechnical structures. By these sophisticated methods, more accurate evaluation of performances of the structures are believed to become possible. However, methodologies for matching the RBD and these sophisticated numerical tools that takes into account the characteristics of geotechnical design are not sufficiently developed.

The authors are proposing a design scheme that separates the geotechnical analyses and the reliability analyses in the first stage, which are recombined in the final reliability assessment stage so as to realize level III RBD, i.e. the full probability RBD, that is more convenient for the practicing geotechnical engineers. In this paper, the scheme is applied to the liquefaction risk assessment of an existing 25 km long irrigation channel that includes many complex geotechnical factors. The liquefaction is evaluated by one of the state of the art FEM programs. The purpose is to demonstrate the effectiveness of the scheme proposed for a complex geotechnical reliability design problem. The way to handle the uncertainties involved in the design is described in detail.

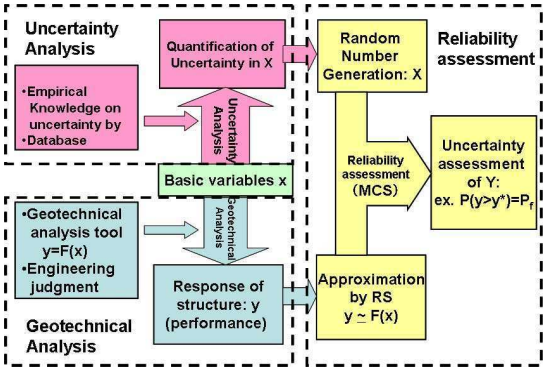

Figure 1. Proposed design scheme by response surface

2 A SCHEME FOR GEOTECHNICAL RBD

The scheme proposed here is illustrated in Figure 1. It is separated to the three parts: (I) geotechnical design, (II) uncertainty analysis of basic variables and (III) reliability assessment.

Geotechnical design, (I), is almost the same as usual design procedure for geotechnical structures. The response of the structure (bearing capacity, displacement at a certain point etc.), y, is obtained from the basic variables, x, by the design calculations.

In some cases y can be related to x by a simple performance function. In other cases, the response surface (RS) method can be used to relate x to y by a regression analysis (Box & Drepper, 1987).

The uncertainty analysis of basic variables, (II), is the main part of the scheme. Statistical analyses play the major role in this analysis. The reliability assessment, (III), is carried out by the results of the uncertainty analyses and the response surface by simple Monte Carlo simulation (MCS). The probability of failure, i.e. probability of the structure to exceed the limit state, is evaluated.

The expected benefits of the proposed scheme are considered to be as follows:

(1) The scheme tries to separate the geotechnical design part and the uncertainty analysis part as much as possible in order for practicing geotechnical engineers to carry out RBD easier, and also make the best use of the numerical analysis tools in the design.

(2) It would be understood by carrying out this scheme that estimating a response surface itself gives quite amount of useful design information. A RS gives impact of each basic variable to the performance of the structure near the limit state. The building of a RS requires mostly the good geotechnical design skill.

(3) The reliability assessment is done by simple MCS, which is easy to understand intuitively. It does not require much knowledge of the probability theory.

3 OUTLINE OF THE FACILITY AND THE VARIFICATION METHOD

3.1 *Outline of the Irrigation Channel*

3.1.1 *The characteristics of the irrigation channel*

The irrigation channel under study is 25 km long and completed in 1970 (Figure 2). The geology under the channel can be divided into three parts, where 12 km long central part (STA30 – 150) is described in the paper. It is an open channel RC frame structure and 90 % is build in the embankment (Figure 2(a), embankment type), whereas 10 % is excavated channel (embedded type) including siphons. The RC frame channel has width of about 10 m, height 5 m and 10 m long, i.e. each 10 m is an independent structure.

The embankment type is made of the RC frame channel and roads for maintenance on both sides of it 3m wide and 4m high embankment. The embedded type is embedded RC frame into the plane ground. At the crossings to the major roads, siphons are build using RC box type structure.

3.1.2 *Ground characteristics*

The channel is located on one of major Alluvial panes in Japan and geology is relatively homogeneous. There is a potentially liquefiable sand layer (As layer) of about 12 m thick whose SPT N-value is about 15 and the fine contents (Fc) less than 10%.

The soil investigation to measure SPT N-value had been carried out at the time of the construction at 32 locations about 450 m interval. However, 19 locations of them are only to 7 m deep with measurement interval of 3m. The quantity of the investigation is far less compared to current practice. Besides these investigations, the dynamic triaxial tests to evaluate liquefaction resistance (R_{L20}) were carried out in more recent years for 2 samples taken at STA.50 and 145. R_{L20} were about 0.25 at STA.50 and 0.21 at STA.145. Note that length of each station is 10 m.

Under the liquefiable sand layer (As), there is a soft clay layer (Ac) of 25 m thick and SPT N-value of about 2, then relatively dense sand layer (Ds), which is underlaid by the bedrock of SPT N-value over 50.

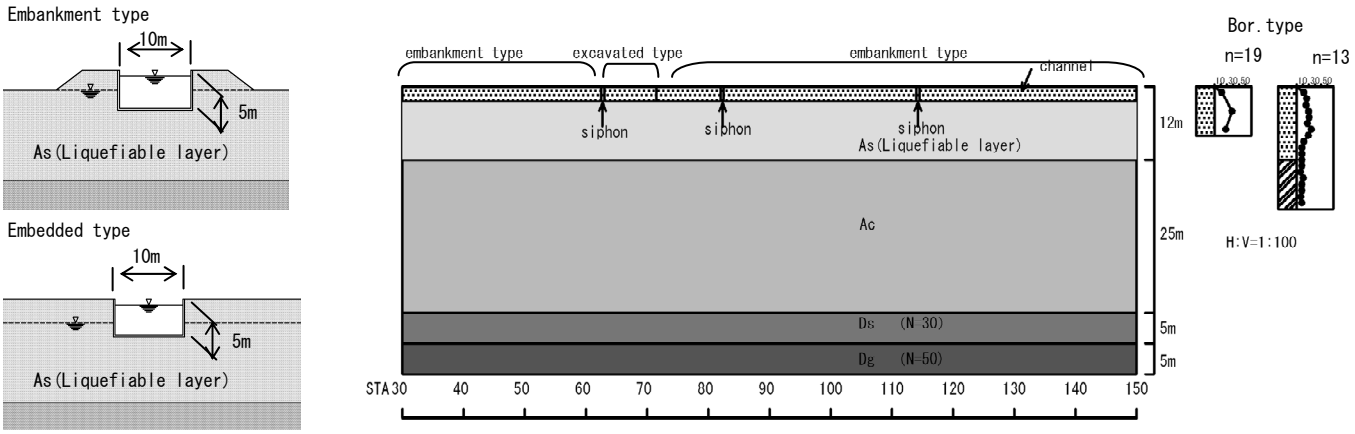

(a) Typical cross section (b) longitudinal section of soil condition

Figure 2. Characteristics of structure and soil condition

3.1.3 *Seismic characteristics of the site*

The area is in the region where near future occurrence of Tokai-Tonankai earthquake is suspected. Model earthquake motion provided by the central disaster mitigation conference (2006) for the earthquake is employed in this study.

The nearer to the epicentre, the stronger the earthquake motion. Therefore, the downstream part is more susceptible to stronger earthquake motion. By the peak ground surface acceleration (PGA), it is 135gal at the most upstream point, 175gal at the middle point and 241gal at the most downstream point. The distinguished characteristics of this earthquake motion are its very long continuous time (about 120 sec) and dominance of the long period components (2 – 4 sec). As far as the continuous time and the spectral characteristics are concerned, there is no difference for the upstream and the downstream.

3.2 *The Limit State and Evaluation of the Performance*

3.2.1 *The limit states*

The performance requirements of this irrigation channel are *to keep the water level that is sufficient for the natural distribution of water to the surrounding area and to provide sufficient quantity of water to the destinations.* Since part of the water is used for urban water supply, it is necessary to keep the water level even right after the earthquake. Thus, to keep this water level after the earthquake is set as the performance requirement of the channel. To be more specific, a limit was set to the absolute settlement of the RC frame for maintaining the water level, and to the relative settlement of the adjacent frames to preserve necessary quantity of water flow. The limit state was set to 60 cm for the absolute settlement based on the free board of the channel, and to 60 cm for the relative settlement due to the frame base thickness.

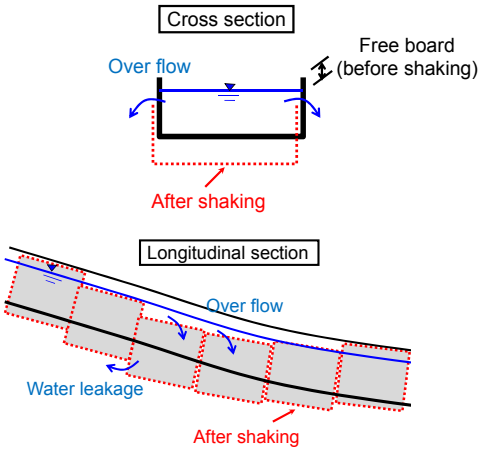

Figure 3. Limit state of this channel

3.2.2 *Method to evaluate the seismic performance*

The problem is to evaluate the residual settlement of the irrigation channel for the earthquake with considerably long duration and of long dominant period. The dynamic FEM based on the effective stress analysis, LIQCA2D07 (Oka et al. 1994), is employed in order to take into account of the mobilization and dissipation of the excess pore pressure. The effectiveness of the program was checked by analyzing shaking table test which had modeled the channel.

LIQCA2D07 has been used to analyze the liquefaction of ground induced by earthquakes, and has been employed in the actual design for several occasions already. If the modelling and soil parameter values are set appropriately, much accurate prediction of the performance is possible. However, there are quite many soil parameters some of which need to be set based on the dynamic triaxial test results. This process requires certain skill, experiance and engineering judgement, whose result may not be the same from one

engineer to another. The detail procedure to determine the model parameters can be seen in Otsushi et al. (2010).

3.3 *Procedure of the design and uncertainty*

The design procedure and the uncertainties to be considered are presented in Figure 4. The settlement of the RC frame is predicted by LIQCA2D07 for various possible conditions. Based on this parametric study, a response surface (RS) is built which is to be used in the reliability assessment.

Uncertainties considered in this study are model uncertainty of LIQCA2D07, spatial variability of soil parameter (i.e. SPT N-value), statistical estimation error and error associated to the approximation by RS. These uncertainties are quantitatively analysed by the statistical means and incorporated to the reliability assessment by MCS.

The settlement induced by the liquefaction is a complex phenomenon which is influenced by many factors. In stead of building a very complex RS, relatively simple RS was introduced in this study. The uncertainty associated to the RS, which is the residual of the regression analysis of the settlement by various factors are also introduced in the reliability assessment.

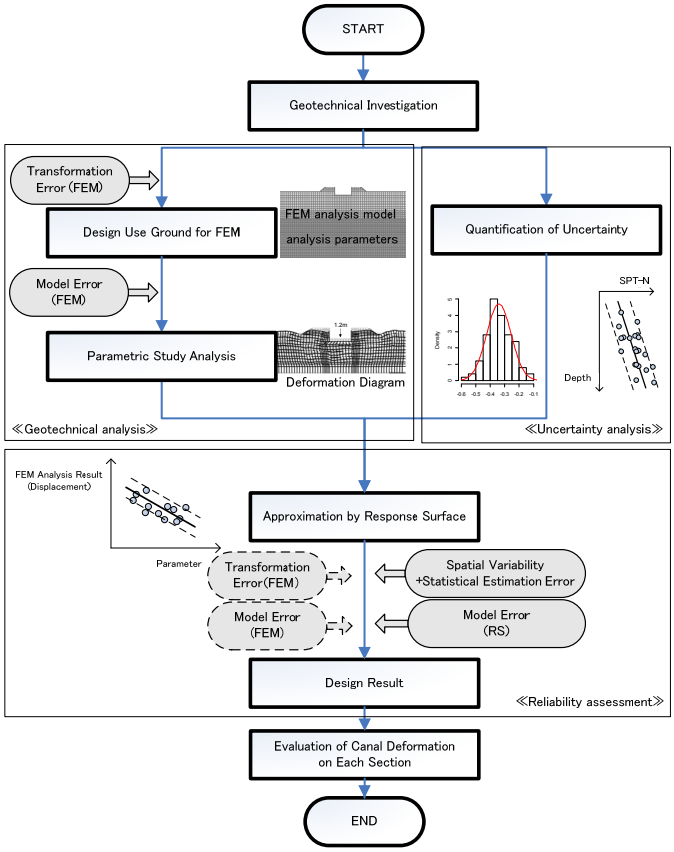

Figure 4. Procedure of the design and uncertainty

4 ANALYSIS OF UNCERTAINTIES

4.1 *Spatial Variability and Statistical Estimation Error*

4.1.1 *Basic variables for the response surface*

It is necessary to select a geotechnical parameter that is appropriate to represent ground characteristic in evaluating potential of liquefaction. Sn value proposed by Goto et al. (1982) is selected in this study to represent the strength of ground for liquefaction. This is weighted integration of adjusted SPT N-value, N1, over 20m depth. N1 is defined as $N1 = 170 \cdot N / (\sigma_v' + 70)$, where σ_v' is the effective overburden stress.

$$S_n = 0.264 \cdot \int_0^{20} e^{-0.04N1(x)-0.24x} dx - 0.885 \qquad (2)$$

The characteristic of the sand layer is solely evaluated by N1 value in this index. This is justified in this case because as layer is very homogeneous and the grain size distribution is similar throughout the area, thus S_n is an effective index to evaluate the liquefaction strength of ground at least relatively. Furthermore, the liquefaction is not a phenomenon at a single point but for certain volume of soil mass. Therefore, it make sense to evaluate the ground property by some weighted averaging value over the depth like S_n.

The irrigation channel is a very long continuous structure. The statistical estimation error of the ground should be different at the location where the soil investigation has been made and at other locations. This difference will be evaluated by distinguishing *the general estimation* and *the local estimation* problems: the relative location of investigation and construction is not taken into account in the former, whereas they are taken into account in the latter.

4.1.2 *The general estimation of S_n*

In the general estimation, the uncertainties of 12m thick As sand layer is treated in a unified way for 12km stretch. The trend of N1-value is modelled by a quadratic line as illustrated in Table 1. The residuals are also plotted against depth in Figure 5(a).

Table 1. Result of regression analysis on N1-value

Models	Trend	SD	AIC	R^2
Linear	9.76+Z	7.38	1615	0.13
Quadratic	$0.86+5.31Z-0.38Z^2$	6.68	1569	0.29
Cubic	$1.17+5.06Z-0.33Z^2-0.0027Z^3$	6.69	1571	0.29

The fitness of the residuals to a normal distribution is checked by Q-Q plot presented in Figure 5(b). It is observed that the residuals are homogeneous over the depth and fit to a normal distribution. The vertical autocorrelation function is estimated by the moment method and the autocorrelation distance of an exponential autocorrelation function is estimated to be 0.80 m (Figure 5(c)).

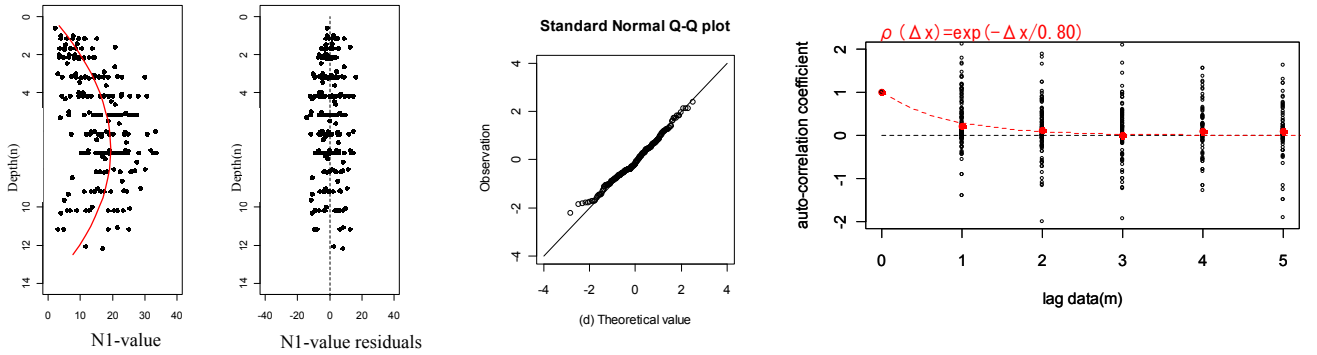

(a) the trend of N1-value and residuals (b) the residulas Q-Qplot (c) vertical autocorrelation of residuals

Figure 5 Special variability modeling

The statistical estimation of the mean value (i.e. the trend) is estimated by the general estimation variance function proposed by Honjo and Setiawan(2007) as

- For the vertical direction : Λ_G (12,0.8)=0.367
- For the horizontal direction: Each investigation point is assumed to be independent since there are more than 400 – 500 m apart. Λ_G (13,0)= 1/n = 1/13.

Therefore, the estimation error of the trend component is calculated as $6.68\times0.367\times(1/13)=0.189$.

Based on these results, uncertainty of S_n is evaluated by MCS, of which the results are presented in Figure 6. The mean value is -0.34 and SD 0.085. Also it is judged that it fits to a normal distribution (Figure 6).

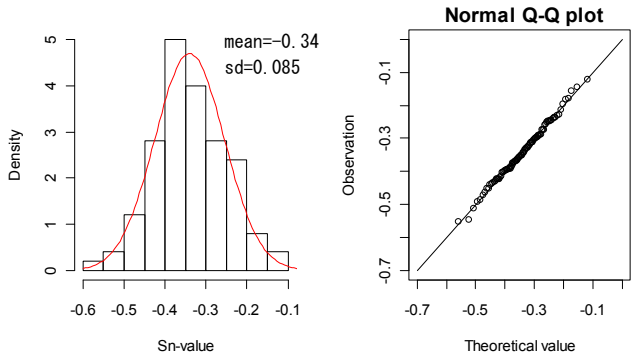

Figure 6. Histogram of S_n-value and Q-Qplot

4.1.3 *The local estimation of S_n*

The estimation error of S_n is obtained by considering the investigation location and the estimation location. The method employed is Kriging and the conditional simulation based on it. The estimation is done in 2 steps as follows:

Step 1: estimation of S_n at the investigation locations

There are two types of SPT investigations for this irrigation channel: N-value is measured at each 1 m interval in some locations (Sites-r1), whereas it is measured at each 3 m in other locations (Sites –r3). By definition, S_n is calculated based on SPT N-value measured at 1 m interval. Thus, S_n become a fixed value for Sites-r1. However, interpolation estimation error must be evaluated for Sites-r3. The conditional

simulation is employed to evaluate uncertainty of S_n at Sites-r3: 1000 sets of N-values of 1m interval samples that pass through the measured values and yet have the same statistical characteristics as estimated above are generated to evaluate the uncertainty of S_n.

Step 2: the conditional simulation of S_n over 12km stretch of the irrigation channel

Sn values evaluated in Step 1 is used to estimate the correlation of Sn for the horizontal direction. Then conditional simulation is used to generate S_n over 12km stretch of the irrigation channel. In this conditional simulation, the estimation error of S_n at Sites-r3 is also taken into account.

An exponential type autocorrelation function is fitted to describe the correlation of S_n for the horizontal direction by the moment estimation method, whose results are smoothed for 50m as presented in Figure 7(a). The autocorrelation distance is estimated to be about 150m. The uncertainty involved in estimated S_n is illustrated in Figure 7(b) by showing mean and mean +/- SD. The mean and SD obtained in the general estimation is also presented in the same figure.

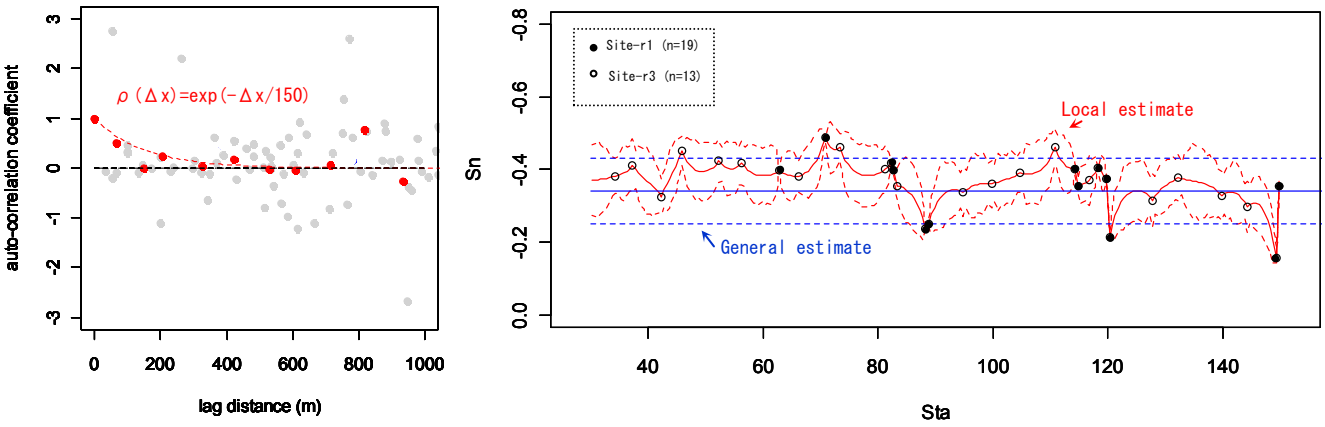

(a) auto-correlation of S_n-value (b) Estimated mean and estimated Error of S_n-value

Figure 7. S_n-value special variability and estimated error

4.2 *Model Error of FEM*

The model error involved in estimating displacement of RC frame channel structure by LIQCA2D07 is evaluated here. The evaluation is done by correcting blind tests results for model tests on similar structures, i.e. embankments and embedded structures. The blind tests are type A prediction where predictions for the displacement is done without knowing the model test results. 17 blind test results are collected from the literature(JICE2002,Uzuok et al.(2003) and Yoshizawa at al.(2009)) and the ratio between "the predicted values" and "the true values" are obtained (Figure 8). The results lie between 0.4 and 1.6, where the mean 1.0 and SD 0.23. A Q-Q plot for a normal distribution is also presented to show that the results fit to a normal distribution.

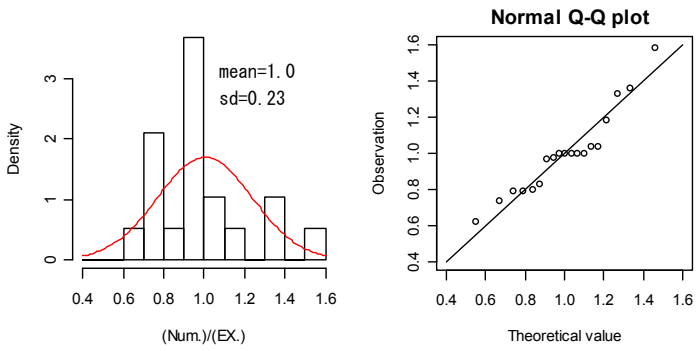

Figure 8. Model error of FEM

4.3 *Response Surface (RS) and Its Model Error*

The vertical displacement (settlement for the embankment type and uplift for the embedded type) is related to S_n and shear stress at the center part of liquefiable layer(τ) based on the 22 results of LIQCA2D07.

In order to evaluate the shear stress distribution along the depth, one dimensional linear equivalent response analysis by SHAKE (Schnable P.B. et al.,1972) is performed especially to take into account of the effect of the underneath soft clay layer.

The vertical displacement is related to S_n and τ by a linear regression line:

$$D = a \cdot S_n + b \cdot \tau + c + \varepsilon \qquad (4)$$

Where D: vertical displacement (cm) obtained by LIQCA2D07, τ: shear stress(kN/m^2) acting at the center part of liquefiable sand layer, a,b and c: regression coefficients, and ε: residual error.

Figure 9 presents fit of the model to the data, which exhibits reasonably good fit. The residuals are plotted on normal Q-Q plot. They follow a normal distribution well with mean 0.0 and SD 10.24 (cm) for the settlement and mean 0.0 and SD 2.83 (cm) for the uplift.

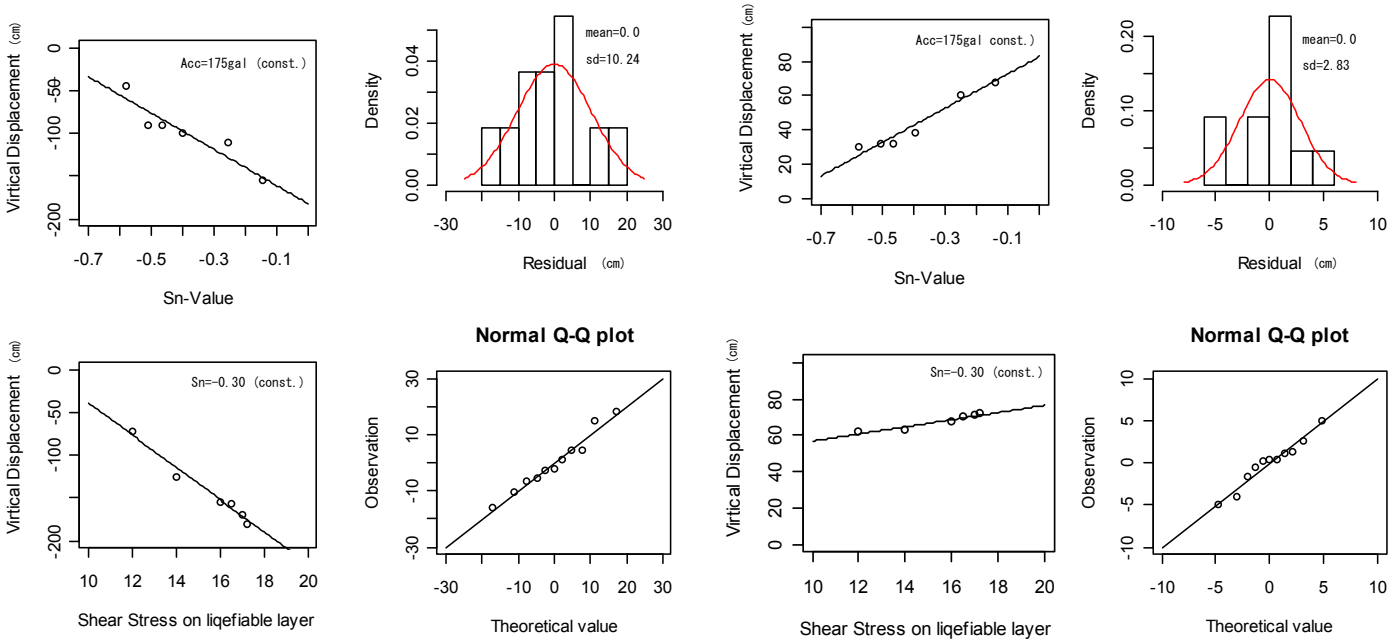

(a) Embankment Type Channel (b) Embedded Type Channel

Figure 9. Result of regression analysis

5 RELIABILITY ASSESSMENT

Finally, exceeding probability of the vertical displacement over the threshold value is evaluated by MCS based on obtained RS and the quantified uncertainty of various sources. The uncertainty considered are listed in Table-2.

The performance functions for the embankment type and the embedded type are respectively given as follows:

$$D_{embk} = (-212 \cdot S_n - 18.8 \cdot \tau + 120) \cdot \delta_{RS} \cdot \delta_{FEM} \qquad (5)$$

$$D_{embd} = (100 \cdot S_n + 1.97 \cdot \tau + 51) \cdot \delta_{RS} \cdot \delta_{FEM} \qquad (6)$$

Table 2. Input to reliability analysis

Uncertain sources	Notation	mean	SD	Distribution type
S_n-value	Sn	-0.34※1)	0.85※1)	Normal
Earthquake shear stress	τ	[12-17.5]	0	Deterministic
Model error of RS	δ_{RS}	1.0	0.09※2) (0.06) ※2)	Normal
Model error of LIQCA2D07	δ_{FEM}	1.0	0.23	Normal

※1：values by the General estimation

※2：COV=10.24/110=0.09(embankment type) 2.83/48=0.06(embedded type)

The results are presented in Figure 10, 11 and 12. Figure 10 and 11 show the mean elevation after shaking of each RC frame (10 m long) for the general estimation and the local estimation of S_n-value respectively. It can be seen, in both cases, the displacement is larger in the downstream because of the stronger earthquake motion. In the downstream part, the mean settlement exceeds the threshold value of 60 (cm). The larger relative displacement occurs at location where the embankment type switches to the embedded type, which implies danger of leakage of water from the channel.

Although the general feature of the vertical displacement is similar for the general and local estimation of S_n, one can see more detailed behavior of each RC frame in the local estimation. For example, there is location where the mean settlement exceed 60 (cm) near STA90 in the local estimation.

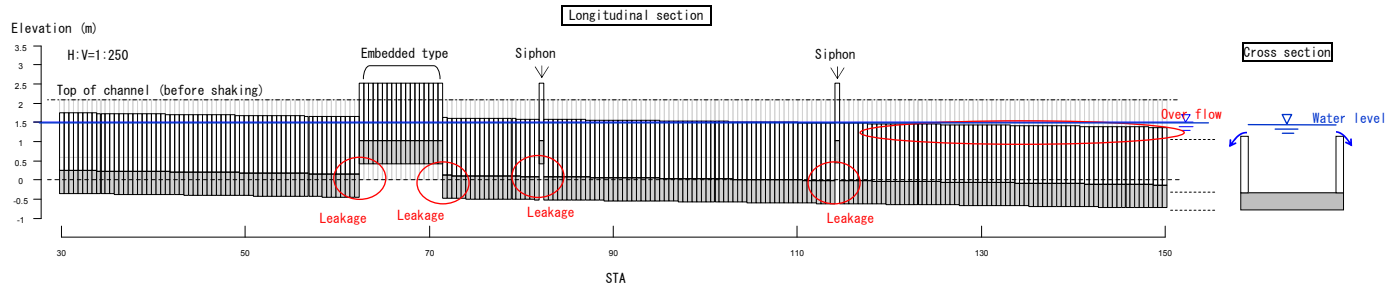

Figure 10. Mean elevation after shaking (general estimation of S_n-value)

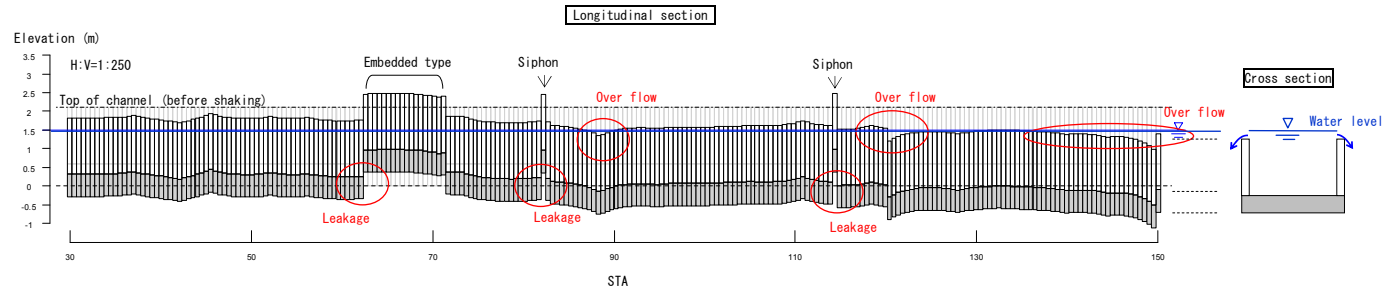

Figure 11. Mean elevation after shaking (local estimation of S_n-value)

Figure 12 presents the mean vertical displacement and the exceeding probability of it over the threshold values (i.e. 60 cm) are presented for the general and local estimation of S_n. The two cases are superposed in these figures for the comparison. The prediction based on the local estimation generally gives smaller exceeding probability, however there are several locations where this relationship is reversed. These probability can be used to determine the optimum enforcement plan of this irrigation channel.

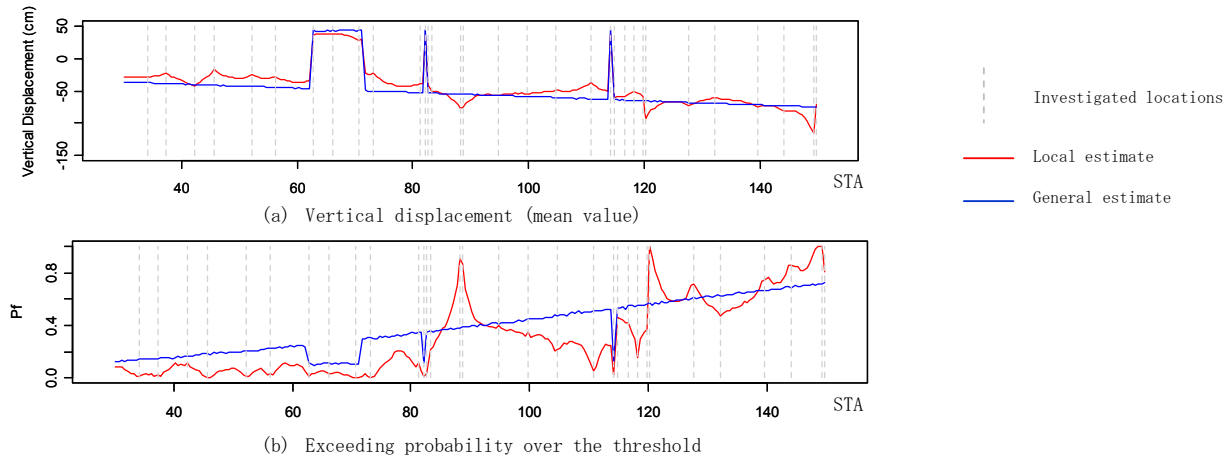

Figure 12. Result of Reliability analysis

6 CONCLUSION

The results of the analysis are believed to provide useful information to designer and the owner of the structure, some of which can be listed as follows:

- The long stretching structure like this irrigation channel, quite amount of time and cost is necessary to conduct an enforcement construction. The information provided here is very useful in making plan for this enforcement construction and determine sequence of the construction.
- The contribution of each uncertain source to the final result can be calculated by an approximate means proposed by Honjo et al.(2011), which the result is shown in Table-3. It should be pointed out that the owner has an alternative to obtain more information on the soil property by adding soil investigation. The result of the local estimation gives very variable information concerning this aspect.
- The response surface obtained itself useful information for the designer. Furthermore, it can be used when additional information on ground property is given to reevaluate the reliability.

Table 3. Contribution of Uncertainty sources

Uncertainty sources		All uncertainty	S_n-value	Model error	
				FEM	RS
β and β_{-i} (contribution)	Site-r1 (STA63)	1.87 (100%)	1.88 (0%)	8.49 (95%)	1.92 (5%)
	Site-r3 (STA56)	1.58 (100%)	2.32 (54%)	2.05 (41%)	1.63 (6%)
	Site-nr (STA60)	1.02 (100%)	1.42 (48%)	1.33 (41%)	1.08 (11%)

Note) Site-nr：no investigation at the site

REFERENCES

Box and Draper (1987)：Empirical Model Building with Response Surface , John Wiley

Oka, F., Yashima, A., Shibata, T., Kato, M. and Uzuoka, R. (1994), FEM-FDM coupled liquefaction analysis of a porous soil using an elasto-plastic model, Applied Scientific Research, Vol.52, pp.209-245

K.Otsushi, Y.Otake, T.Kato, T.Hra, and A.Yashima(2010)：Analytical study on a liquefaction countermeasure for flume channel by sheet-pile with drain, Japanese Geotechnical Journal vol5, No4

H.Goto, H.Kameda, M.Sugito(1982)：Use of N-value profiles for estimation of site dependent earthquake motions, Proceedings of Japan society of civil engineers, No.317,1982.1

Y. Honjo and B. Setiawan (2007)：General and local estimation of local average and their application in geotechnical parameter estimations, Georisk, 1(3),167-176

Schnable P.B., Lyamer J. and Seed.H.B.(1972)：SHAKE A computer program for earthquake response analysis of horizontally layered sites, Report No. EERC72-12, University of California, Berkeley

Y.Honjo, T.Hara, Y.Otake and T.T.Kieu Le (2011)：Reliability based design of Examples set by ETC10,Geotechnique (submitted)

Japan Institute of Construction Engineering(JICE) (2002)：Analytical method for earthquake-induced deformation of a river dike ,JICE report 102001

M.Yoshizawa ,H.Sakai and R.Uzuoka (2009)：Applicability of effective stress analysis to seismic assessment for river dike during a long-time-duration-earthquake

R.Uzuoka , A.Tateishi (2003)：2-dimensional effective stress analysis on uplift of buried pipe in liquefied ground,48th- Symposium of geotechnical engineering.

ISGSR 2011 - Vogt, Schuppener, Straub & Bräu (eds) - © 2011 Bundesanstalt für Wasserbau ISBN 978-3-939230-01-4

Level III Reliability Based Design employing Numerical Analysis - Application of RBD to DEM -

S. Moriguchi, Y. Honjo, T. Hara & Y. Otake
Department of Civil Engineerings, Gifu University, Gifu, Japan

ABSTRACT: This study presents an example of reliability based design using Discrete Element Method. Rockfall retaining wall is employed as target structure. A series of rockfall simulations were carried out using DEM to obtain a response surface of the energy. Then the uncertainty of basic variables is quantified to conduct Monte Carlo Simulation. Finally, a relation between the exceedance provability and the energy was obtained.

Keywords: Reliability based design(RBD), DEM analysis, Rockfall

1 INTRODUCTION

In recent years, numerical analysis is beginning to be used in design of structures and ground. Discrete Element Method (DEM) is well known as one of the strong numerical tools. The method can express collision between solids such as rockfall problem. Because shape of rockfall and complex geometry can be expressed directly, the method can predict complex movement of rockfall. However, simulated results are highly sensitive to numerical parameters, and the results have large variation. Therefore, a framework in which quantitative results can be obtained from DEM analysis is required.

This study aims to show a framework of reliability based design (RBD) using DEM. Rockfall retaining wall is employed as a target structure. Based on results of this study, advantages of proposed framework are discussed.

2 A FRAMEWORK OF RELIABILITY DESIGN USING NUMERICAL ANALYSIS

Authors have proposed a framework of level III reliability based design (RBD) using numerical analysis (Honjo et al., 2010). Based on the framework, process of RBD of rockfall retaining wall using DEM is shown in this study.

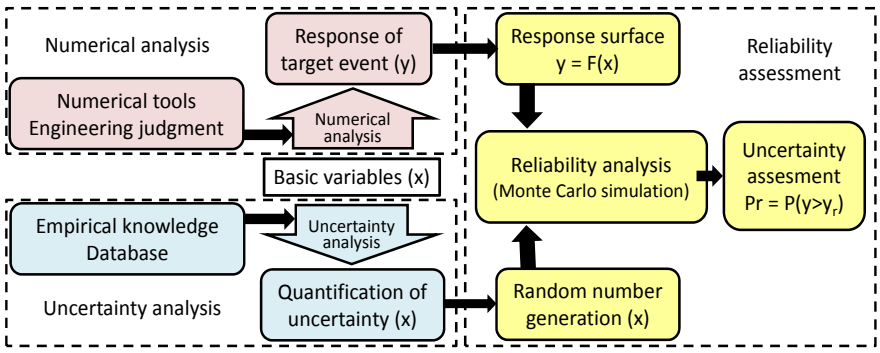

Figure 1. RBD framework using numerical analysis

The framework is separated into three parts: numerical analysis (I), the uncertainty analysis of basic variables (II) and the reliability analysis (III). In the numerical analysis (I), some cases are carried out under the different combination of basic variables (x), and the response of target event (y) is investigated. The energy of rockfall is focused on because that is quite important for design of the retaining wall. Thus, the energy (y) is calculated under the different combination of the parameters, such as the coefficient of restitution, friction angle and shape of rockfall.

The uncertainty analysis (II) is a process in which the uncertainty of basic variables is quantified. Database and empirical knowledge are used to obtain statistical information of basic variables, such as the mean value, the standard deviation and the distribution function. In the reliability assessment process (III), the response surface (RS) of target event is estimated from the results of numerical analysis. Then a simple Monte Carlo Simulation (MCS) is carried out using the RS and results of the uncertainty analysis. Finally, exceedance probability of occurrence of target event is quantified under the given conditions.

The advantages of the proposed framework are as follows,

- It is possible to respond immediately to development of numerical methods because the numerical analysis and the uncertainty analysis are separated.
- The relation between responses of target structures and basic variables provide useful information to designer.
- Designer can understand obtained results intuitively because MCS is used in the reliability assessment process.
- Numerical results are used just for estimating RS. Because MCS is carried out using RS, time and effort spent in the numerical analysis can be minimized.

3 FLOW OF PROPOSED RBM AND UNCERTAINTIES

Figure 2 shows proposed RBM of rockfall retaining wall. The uncertainties that should be considered are also described in the figure.

Like traditional design procedure, the field investigation is carried out. Some investigation items of rockfall such as position, size, shape and rock type is checked. The measuring error arises in this procedure.

After the field investigation, a numerical model and values of parameters are determined. The transformation error of parameters and the model error of DEM arise in this procedure. Then, a parametric study is carried out under the different combination of parameters. The energy of rockfall is obtained from each simulation cases.

In the uncertainty analysis, the uncertainties are quantified. The measuring error is not taken into consideration in this study. The transformation error and the statistical estimation error are treated as variation of numerical parameters. The statistical estimation error is derived from spatial variation of strength and rock type. The variations of the parameters are estimated from literatures in this study. The model error is derived from the numerical modeling. In DEM analysis, rock body is assumed to be rigid body. Thus, it is impossible to reproduce actual phenomena perfectly. The model error includes such uncertainty. In this study, statistical values of the model error are assumed.

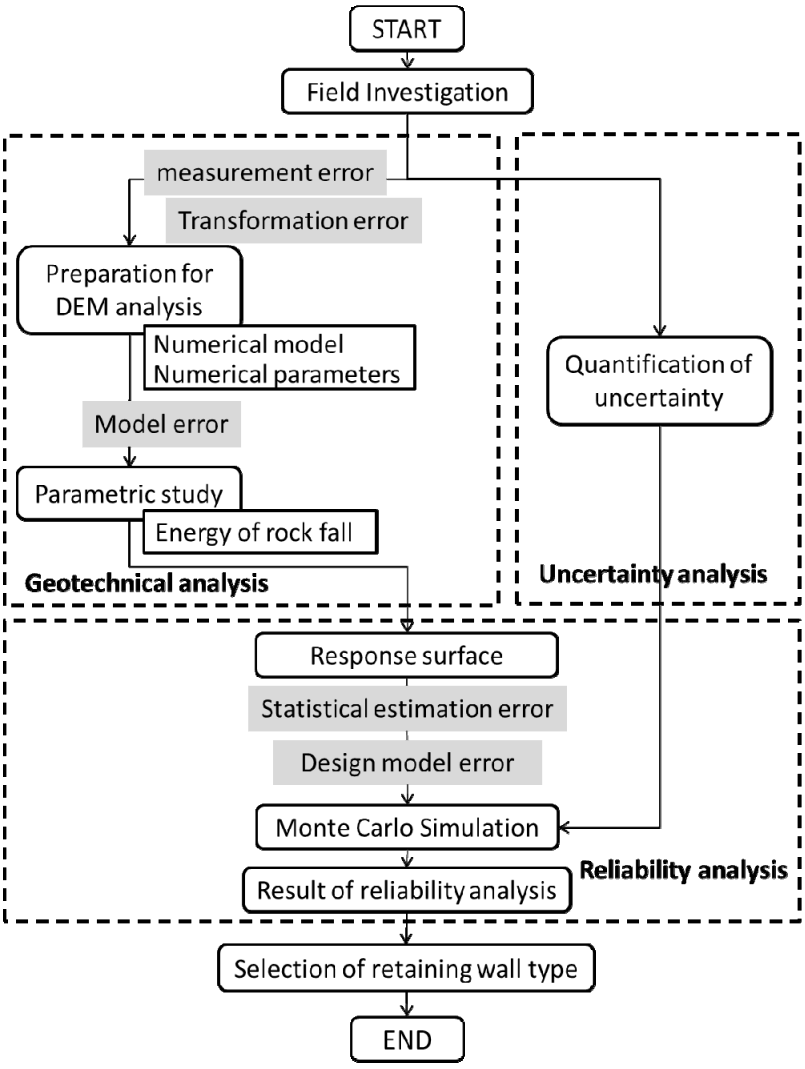

Figure 2. Proposed design scheme by response surface

In the reliability analysis, the RS is estimated. If there is large variation in the numerical results, the design model error should be considered. The error is treated as variation of the RS.

4 NUMERICAL ANALYSIS

4.1 *Numerical method and analysis condition*

2 dimensional DEM was adapted to rockfall simulation. In DEM analysis, as shown in Figure 3, an interparticle model is used to describe collision force. Interparticle force is calculated and movements of each particle are solved based on the equation of motion. Complex shape can be also express by connecting particles. Therefore, shape of rockfall and slope can be modeled directly.

Figure 4 shows schematic view of a numerical model used in this study. In a normal situation, although position and size of rock body and surface configuration of slope should be modeled based on the field investigation, virtual rock body and slope are used in this study. In the initial condition, the rock body is placed at the top of the slope and falls due to the gravity at the start of the simulation. The mass of the rock body is 400 kg. Although a retaining wall is drawn in Figure 4, it doesn't exist in the simulation. The velocity and the rotation rate of rockfall are checked when the rockfall pass thought in front of the retaining wall. The energy of rockfall is calculated from the velocity and the rotation rate.

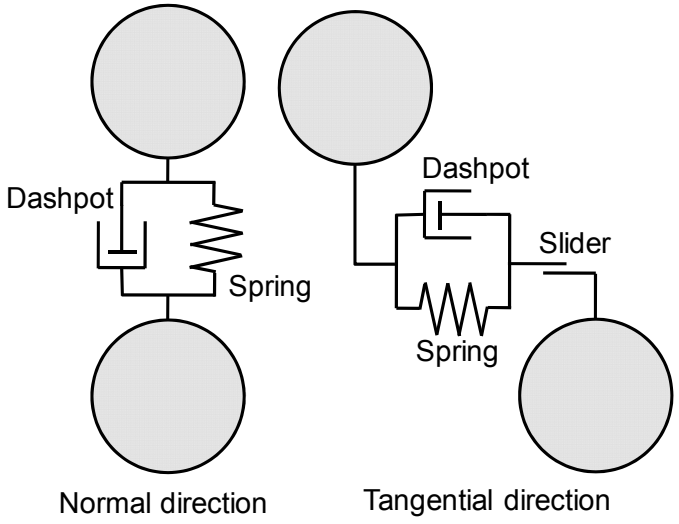

Figure 3. Interparticle force model of DEM

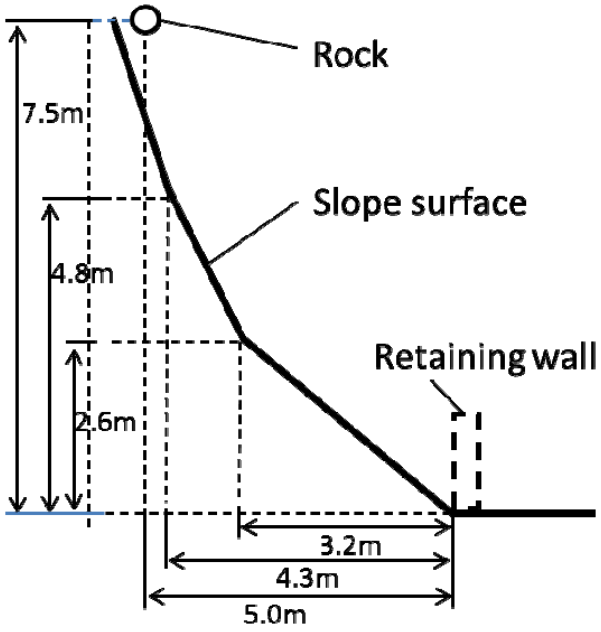

Figure 4. Numerical model

4.2 *Numerical parameters*

The interparticle model of DEM has the spring, the dashpot and the slider. Although many parameters should be determined, the key parameters are the coefficient of restitution and the friction angle. Therefore, these parameters were used as basic variable. In this simulation, shape of rock body is also unknown. Therefore the aspect ratio of the rock body is introduced as basic variable to investigate effect of the shape. The aspect ratio was changed under the constant volume of rock body as shown in Figure 5. We used 5 kinds of the coefficient of restitution (0.4-0.6), 5 kinds of the friction angle (20-40 degrees) and 8 kinds of the aspect ratio (1.083-1.940). A total of 200 cases were carried out under the different combination of the parameters.

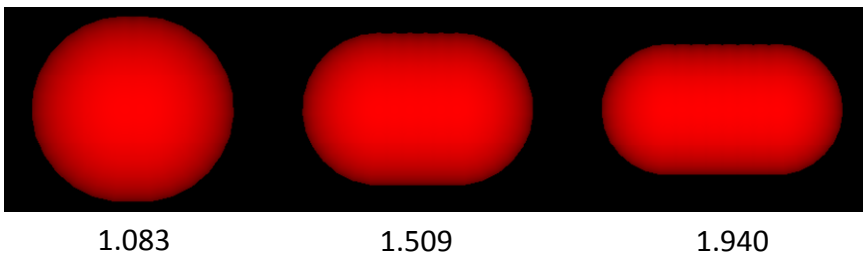

Figure 5. Shape of rock body on different aspect ratios

5 RESPONSE SURFACE

5.1 *Single regression analysis*

As explained previously, results obtained in DEM analysis are analyzed to assume RS. Firstly, we carried out single regression analysis to know correlation between the energy and each parameter. In figures 6, 7 and 8, the energy is plotted against each parameter. As shown in the figures, there is large variation in each result. In particular, strong correlation is not seen in the relation between the energy and the coefficient of restitution.

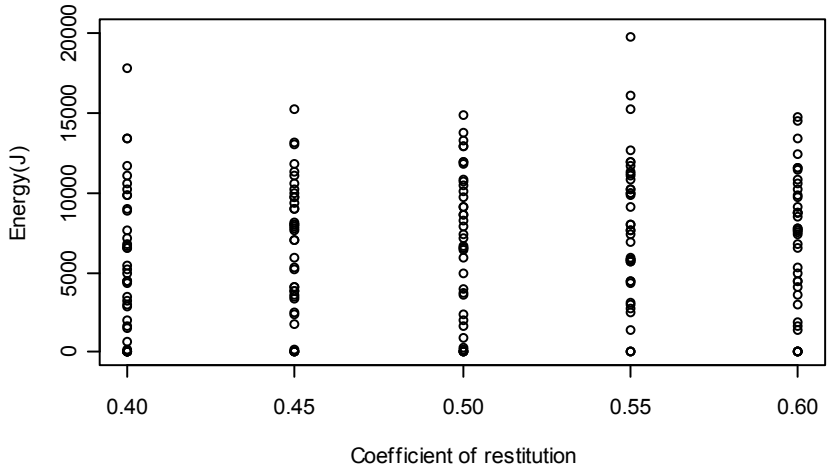

Figure 6. Relation between the energy and the coefficient of restitution

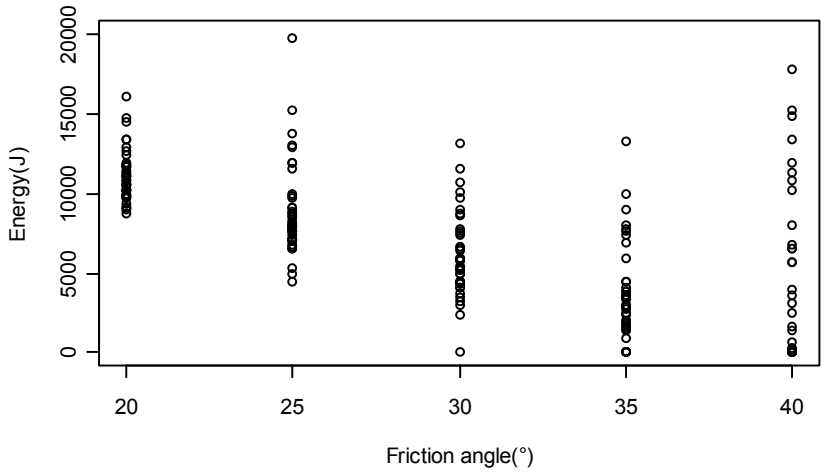

Figure 7. Relation between the energy and the friction angle

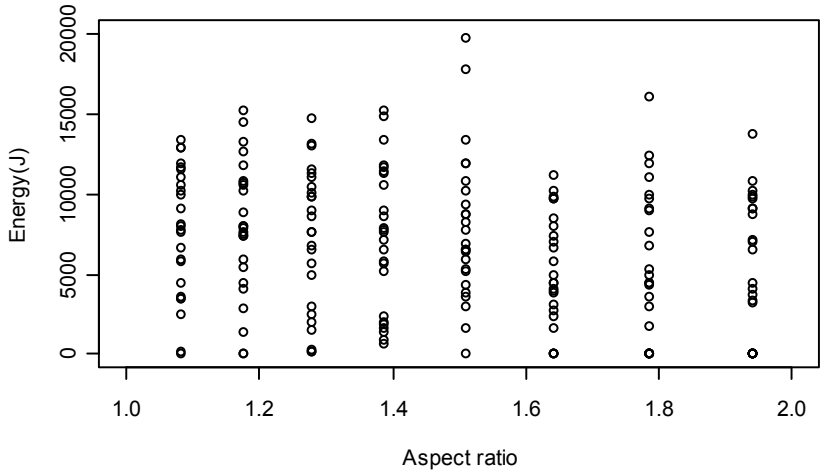

Figure 8. Relation between the energy and the aspect ratio

5.2 *Multiple regression analysis*

Based on results of the single regression analysis, RS was assumed as a function of the friction angle and the aspect ratio. Table 1 shows equations assumed in this analysis. The standard deviation, the residual and AIC value (Akamine, 1973) are also described in the table. Based on the results, No.6 was selected and following RS was obtained.

$$E = 22685\,Asp - 7759\log(F)\,Asp + 11864 \tag{1}$$

where, *E, Asp* and *F* are the energy, the aspect ratio and the friction angle, respectively. Figure 9 shows the obtained RS. As explained previously, the model error of DEM is one of the errors that should be taken into consideration. Furthermore, the design model error should be considered because there is large variation in numerical results. By considering the these errors, the RS is updated as follows,

$$E = \left(22685\,Asp - 7759\log(F)\,Asp + 11864\right)\cdot \delta_{DEM} \cdot \delta_{RS} \tag{2}$$

where δ_{DEM} is the coefficient of the model error and δ_{RS} is the coefficient of the design model error. The design model error was treated as the model error of the RS.

Table 1. Functions used in multiple regression analysis

No.	Function	SD	R^2	AIC
1	$E = a\cdot Asp + b\cdot F + c$	3298	0.443	3811
2	$E = a\cdot Asp^2 + b\cdot F^2 + c$	3298	0.444	3811
3	$E = a\cdot Asp + b\cdot F + c\cdot Asp\cdot F + d$	3263	0.458	3806
4	$E = a\cdot Asp + b\cdot \log(F) + c$	3255	0.458	3806
5	$E = a\cdot Asp + b\cdot \log(F) + c\cdot \log(F)\cdot Asp + d$	3220	0.472	3801
6	$E = a\cdot Asp + b\cdot Asp\cdot \log(F) + c$	3212	0.472	3800

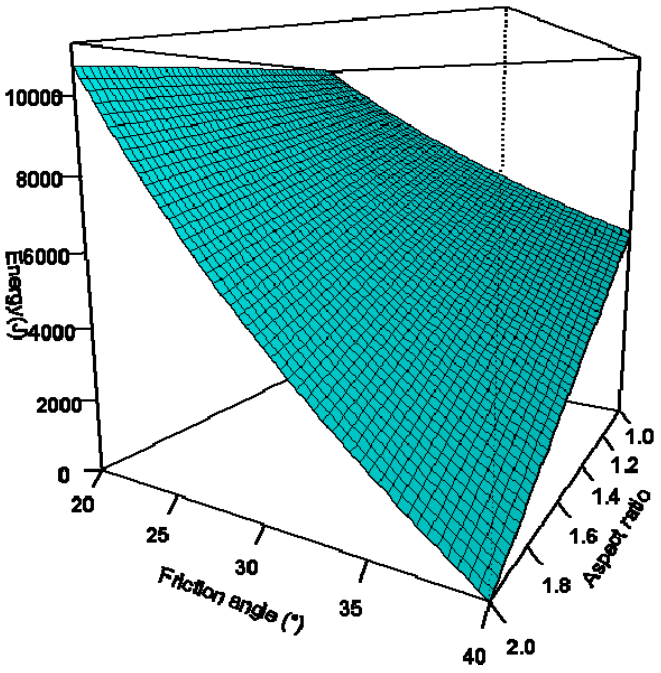

Figure 9. Response surface

6 UNCERTAINTY ANALYSIS

In the RS of energy, 4 kinds of basic variables are included, such as the friction angle, the aspect ratio and the model errors of DEM and RS. In the uncertainty analysis, variations of these basic variables are quantified. The mean value, the standard deviation and the type of distribution function are estimated based on results of the field investigation, database and empirical knowledge. In this study, however, the statistical values were assumed from common values of each basic variable, because virtual rockfall and slope are used in this study. Table 2 shows the statistical values of each basic variable. The variation of the model error of RS is calculated from results of numerical analysis.

Table 2. Statistical values of basic variables

Basic variable	Mean	SD	Distribution type
Friction angle (degree)	30	7	Normal
Aspect ratio	1.5	0.5	Normal
Model error (RS)	0.0	0.55	Normal
Model error (DEM)	1.0	0.2	Normal

7 RELIABILITY ANALYSIS

MCS was carried out using RS and quantified uncertainties of the basic variables. Figure 10 shows a histogram of calculated energy. Figure 11 shows the relation between the energy and the exceedance probability. Generally, type of rockfall retaining wall is selected based on the energy of rockfall. Therefore, the exceedance probability is very useful information for design of rockfall retaining wall. In addition, the energy of rockfall is calculated with consideration for the results of DEM analysis.

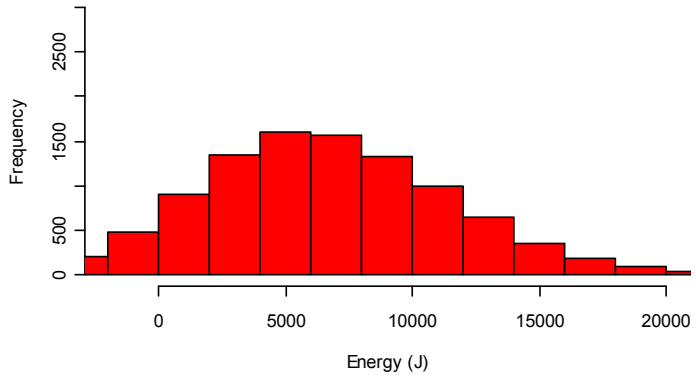

Figure 10. Histogram of energy obtained from MCS

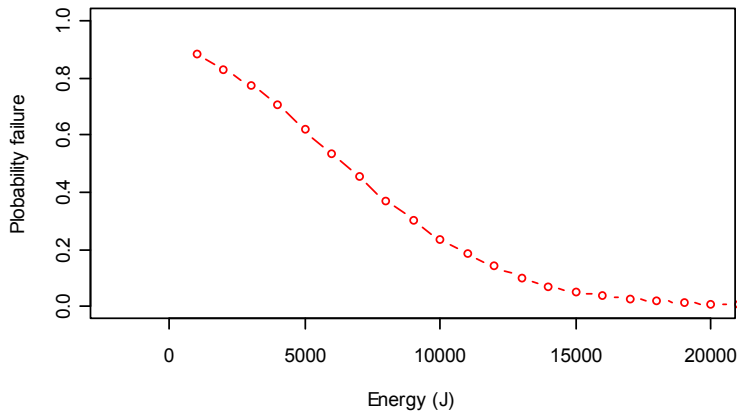

Figure 11. Relation between the energy and the exceedance probability

8 EFFECT OF NUMBER OF CALCULATION CASES

It is well know that calculation cost is one of the disadvantages of DEM. In particular, when we use 3 dimensional DEM, it requires an immense amount of time. However, there is a possibility to reduce effort and time of numerical analysis by using proposed method. Although 200 cases of rockfall simulation were carried out in this study to get relation between the energy of rockfall and numerical parameters, smaller number of calculation cases might be enough. Therefore effect of number of calculation cases is investigated. The number of calculation cases was decreased to 45 cases by reducing number of kinds of the aspect ratio. Base on the results of 45 cases, RS was assumed and the relation between the energy and the exceedance probability was calculated. Figure 12 shows obtained exceedance probability. Blue line is result obtained from 45 calculation cases and red line indicates the results obtained from 200 calculation cases. As shown in the figure, there is not big difference between the results. This indicates that 45 calculation cases are enough for the problem considered in this study.

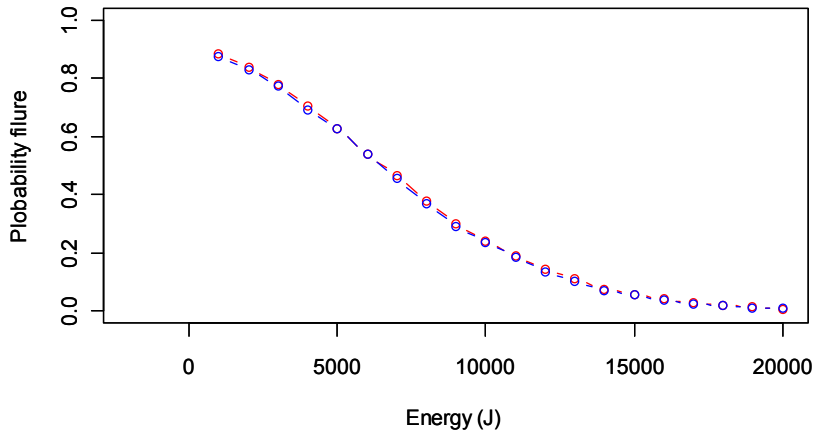

Figure 12. Response surface

9 CONCLUSION

The framework of RBD based on DEM was shown in this study. The rockfall retaining wall was selected as target structure and the exceedance probability was calculated at each value of the energy. By combining RBD and DEM, variation of results of DEM can be quantified and the exceedance provability of rockfall energy can be obtained from the results of MCS. It can be summarized the proposed framework is quiet useful for the design of rockfall retaining wall. In addition, the proposed framework can reduce effort and time of numerical analysis.

This study presents just procedures of the proposed framework. In order to figure out an effectiveness of the proposed framework, more validations are required, such as reproduction of reported real rockfall. In addition, fundamental studies such as qualification of the model error of DEM are required.

REFERENCES

Akaike, H. (1973) : Information theory and an extention of the maximum likelihood principle, 2nd International Symposium on Information Theory, Petrov, B. N., and Csaki, F. (eds.), Akadimiai Kiado, Budapest, 267-281.

Cundall P. A. and Strack O. D. L (1979): A discreat numerical model for granular material, *Geotechnique*, 29, 47-65.

Honjo Y., Hara T. & Kieu Le T.C.(2010): Level III Reliability Based Design of Examples set by ETC10, *Proceedings of 2nd International Workshop on Evaluation of Eurocode 7*.

ISGSR 2011 - Vogt, Schuppener, Straub & Bräu (eds) - © 2011 Bundesanstalt für Wasserbau ISBN 978-3-939230-01-4

Reliability analysis of shallow foundations subjected to varied inclined loads

J. Xue
School of applied Sciences and Engineering, Monash University, Churchill, Australia

D. Nag
School of applied Sciences and Engineering, Monash University, Churchill, Australia

ABSTRACT: Monte Carlo simulation was used to study the effect of inclination factor on the reliability of shallow foundations. The variation of inclination factor was inspected by considering the variation of horizontal and vertical loads. Meyerhof's bearing capacity equation was employed to formulate the performance function of bearing capacity of shallow foundations. A shallow foundation on cohesionless soils under various loading conditions was simulated. Friction angle of soil, horizontal and vertical loads were considered as non-correlated normally distributed variables in the study. The results showed that, probability of failure of the shallow foundation was less influenced by the variation of vertical load than that of friction angle and horizontal load. Reliability indexes of the foundation were derived with the probability of failure (P_f) using different methods. It was found that, when the limit equilibrium function is not normally distributed, for a given value of P_f, the value of reliability index varies with the method employed.

Keywords: reliability, shallow foundation, inclination factor, Meyerhof's bearing capacity equation, Monte Carlo simulation

1 INTRODUCTION

Shallow foundations are designed to bear loads from upper structures, including vertical and horizontal loads, which are combinations of dead and live loads. Live loads vary much more during the life of a foundation comparing to dead load. Live load can be vertically, such as machinery load, human weight and earthquake load, and horizontally, such as wind and earthquake load. Dead load can also be inclined such as load on shallow foundations of bridge abutments. The combination of live and dead loads, or horizontal and vertical loads, result in the variation of magnitude and direction of loading imposed on a foundation. To account for the variation of loading, a reliability analysis based on probabilistic theory is required.

Research has been done to study the influence of variation of soil properties on bearing capacity of shallow foundations "Cherubini (2000); Honjo *et al.* (2000); Phoon *et al.* (2003); Alawneh *et al.* (2006) ". Though load is one of the most variable parameters in shallow foundation design, not much discussion about the effect of variation of inclined load on the bearing capacity of foundations was available in publications. "Honjo *et al.* (2000)" used First Order Reliability Analysis (FORM) to study the variation of inclination factor on the reliability of shallow foundations with a modified Terzaghi equation. Load and resistance factor design (LRFD) method was introduced into shallow and deep foundation design "Paikowsky *et al.* (2004); Paikowsky *et al.* (2010) ". Partial factors were used to consider the variation of loads in Eurocode 7 "ENV(1997-1) (1997) ". For variable actions, a factor of 1.5 is applied for unfavorable / disturbance actions. Orr (2000) discussed the selection of partial factors and suggested that engineers should be careful in selecting these factors in terms of favorable or unfavorable actions. In many cases of shallow foundation design, either horizontal or vertical loads can be unfavorable. Applying same partial factors to these two actions might not be proper, as the variations of the two actions are not the same in many cases. Foye *et al.* (2006) stated that, the load and resistant factors used in current practice can not cover the wide range of problems in shallow foundation design. "Paikowsky *et al.*

(2010)" recommended to reduce the resistence factor of friction anlge of soils to 0.5 after the investigation of a large number of of shallow foundations for bridge abutment under inclined eccentric loads. The authors also suggested different loading factors for horizontal and vertical loads.

In bearing capacity analysis of shallow foundations, the ratio of the horizontal and vertical loading is described with an inclination factor. Different combination of horizontal and vertical loads will result in a variation of the magnitude of inclined load and the inclination factor, which in turn the bearing capacity. In this paper, the reliability of shallow footings is analysed considering the variation of the inclination factor and soil strength. A sensitive analysis was carried out to find out the variation of horizontal and vertical loads on the reliability of shallow foundations.

2 VARIATION OF SOIL AND LOADING PARAMETERS

2.1 *Variation of soil and loading parameters*

To carry out a reliability analysis, a thorough study of the related uncertainties is essential. In regarding to the bearing capacity of shallow foundations, there are many uncertainties involved, e.g. variation of soil properties with time and space, variation of magnitude and direction of loading, uncertainties in the bearing capacity equations or performance functions, distribution and correlation of the uncertainties. This research concentrates on the variation of soil strength and loads on the bearing capacity of shallow foundation.

Among soil properties, unit weight, cohesion, and friction angle are the most frequently studied variables regarding to the reliability analysis of bearing capacity of shallow foundations. As these three parameters are most directly used to evaluate bearing capacity of shallow foundations in many available methods. The variation of a parameter is described with the coefficient of variation (COV) of its distribution. Research found that, unit weight varies in a relatively limited range with COV between 1-10%. COV values for friction angle are in a range of 5%-20 for sands and 7-56% for clays. The most highly varied and hardest to estimated parameter is the COV of shear strength of clays, especially that of undrained shear strength. For saturated clays, an increase of 1% of water content in saturated clay may cause a reduction of 20% of the soil's undrained shear strength "Muni (2000) ". In unsaturated soils, due to the appearance of suction, a decrease of water content will result in the increase of apparent cohesion in soils "Fredlund *et al.* (1978) ". Typical values of COV of soil properties taken from some publications are listed in Table 1.

Table 1. Coefficient of Variation of Soil Properties

Parameter		COV (%)	References
Unit weight (γ)		1-10	Lee *et al.* (1983)
		5-10	Lumb (1974)
		3-7	Duncan (2000)
		2	Christian *et al.* (1994)
Friction angle (ϕ')	Sands	5-15	Lee *et al.* (1983)
	Clay	12-56	Lee *et al.* (1983)
	Clay and sand	5-15	Phoon & Kulhawy (1999 a, b)
Cohesion (c_u)	Sandy soil	25-30	Lee *et al.* (1983)
	Clays	20-50	Lumb (1974); Lee *et al.* (1983)
Undrained strength (S_u)	unconfined	20-55	Phoon & Kulhawy (1999 a, b)
	UU test	10-35	Phoon & Kulhawy (1999 a, b)
	CU test	20-55	Phoon & Kulhawy (1999 a, b)
	Field vane shear	10-40	Phoon & Kulhawy (1999 a, b)
		10-20	Duncan (2000)
		20-32	Christian *et al.* (1994)
	S_u/σ_{vo}'	5-15	Duncan (2000)

A shallow foundation is designed to resist against loading from upper structures. The variation of loading needs to be considered in the reliability analysis of shallow foundations. The variation of loads can be narrow or wide, depending on the nature of the loads. COV of dead load, such as self weight of structures, normally varies within a range of 10%. While for variation of live loads, COV value can reach up to more than 100% for earth quake loads. Typical COVs for different types of loads are shown in Table 2. The table shows that, in a non-earthquake zone, wind load varies the most. Assuming that dead load, live load and snow load act vertically on a shallow foundation, the variation of vertical loads on a shallow

foundation should be within a range of 25% considering the combination of above loading. The value varies from case to case.

Table 2. COV values for loads "EllingwoodGalambos (1982) "

Load	COV
Dead load	0.1
Live load (50-year maximum)	0.25
Snow load (50-year maximum)	0.26
Wind load (50-year maximum)	0.37
Earthquake load (50-year maximum, Western and Eastern USA)	1.38

3 PERFORMANCE FUNCTION

The performance function of shallow foundations can be obtained using a bearing capacity formula. One of the most commonly used equations for bearing capacity analysis is the Terzaghi equation:

$$q_u = cN_c + \gamma z(N_q - 1) + 0.5\gamma' BN_\gamma \qquad (1)$$

where, q_u is the bearing capacity, c is cohesion of soil, γ is the unit weight of soil above ground water, z is the embedment depth, B is the width of the foundation, γ' is the effective unit weight of soil, N_c, N_q and N_γ are the bearing capacity parameters. This equation was used by "Alawneh *et al.* (2006)" to analyse the reliability of shallow foundations by introducing a depth factor. The above equation has a limitation of not accounting for inclined load. "Honjo *et al.* (2000)" used a modified Terzaghi equation to calculate the bearing capacity of shallow foundations on cohesionless soils under inclined load:

$$q_u = 0.5 i_\gamma s_\gamma \gamma' BN_\gamma \qquad (2)$$

where i_γ is the inclination factor and s_γ is a shape factor of foundation.

To consider the effect of inclined load, Meyerhof's bearing capacity equation was used to establish the performance function proposed by "Meyerhof (1951, 1953, 1963) ":

$$q_u = cN_c s_c i_c d_c + \gamma z N_q s_q i_q d_q + 0.5\gamma B N_\gamma s_\gamma i_\gamma d_\gamma \qquad (3)$$

where: s_c, s_q, s_γ are shape factors, i_c, i_q, i_γ are inclination factors, d_c, d_q, d_γ are depth factors. The foundations discussed in this paper are well above ground water table unless specified. The following expressions are used for the coefficients in equation 3:

$N_c = (N_q - 1)\cot(\phi)$ "Meyerhof (1963) "

$N_q = \tan^2(45° + \phi/2)e^{\pi \tan\phi}$ "Meyerhof (1963) "

$N_\gamma = 2(N_q + 1)\tan(\phi)$ "Vesic (1973) "

$s_c = 1 + BN_q / LN_c$ $s_q = 1 + (B/L)\tan\phi$ $s_\gamma = 1 - 0.4B/L$ " De Beer (1970) "

$d_c = 1 + 0.4z/B$ (for z<B)
$= 1 + 0.4\arctan(z/B)$ (for z ≥ B) " Hansen (1970) "

$d_q = 1 + 2\tan\phi(1-\sin\phi)^2 z/B$ (for z<B) " Hansen (1970) "
$= 1 + 2\tan\phi(1-\sin\phi)^2 \arctan(z/B)$ (for z ≥ B)

$d_\gamma = 1$ " Hansen (1970) "

$i_c = i_q = 1 - (\alpha/90)^2$ $i_\gamma = (1 - \alpha/\phi)^2$ "Meyerhof (1953) "

where ϕ is the friction angle of soil, L is the length of the foundation, α is the inclination angle of the load. Assuming load F is composed of a horizontal force F_x and vertical force F_y, then

$$F = \sqrt{F_x^2 + F_y^2} \qquad (4)$$

The factor of safety (FOS) of the foundation can be expressed as:

$$FOS = \frac{q_u - \gamma z}{F / LB} \quad (5)$$

At limit state, set *FOS=1*, the performance function (*LSF*) can be expressed as:

$$LSF = (q_u - \gamma z)LB - F \quad (6)$$

and the inclination angle can be expressed as:

$$\alpha = \arctan(F_x / F_y) \quad (7)$$

4 PROBABILISTIC ANALYSIS

4.1 *General*

In this section the reliability of a few shallow foundations on cohesionless soils was studied using Monte Carlo simulation. The simulation was performed in a Matlab language environment. The distribution of performance function of a shallow foundation was plotted to look into the reliability index and probability of failure. The influence of COV values of the variables on probability of failure was studied.

4.2 *Random variables*

To carry out a reliability analysis, the first thing is to identify the random variables to be considered in the problem. In equations 4 and 5, the basic random variables are soil properties and external actions. For a shallow foundation, the width, length and embedment depth of the foundation can be treated as deterministic values. For soil properties, unit weight, cohesion and friction angle are normally considered as random variables. For forces, as expressed in equations 3, 4, 6, 7, and Table 2, inclination angle (α) and total force F are correlated random variables. When consider random variable, it is always better to use independent variables. So for external forces, horizontal and vertical forces (F_x, F_y) can be used as random variables instead of F and α.

In order to simplify the problem, bearing capacity of shallow foundation on cohehionless soils is analyzed. As indicated in Table 1, unit weight of soil is less varied compare to friction angle. Considering that the aim of this paper is to study the influence of inclination factor on the reliability of bearing capacity of shallow foundations, the random variables considered in the following problems are friction angle (ϕ), horizontal force (F_x) and vertical force (F_y). For simplification, these variables are considered as normally distributed.

4.3 *Probability of failure and reliability index*

A rectangular foundation, 2 m × 4 m was founded at a depth of 1 meter below ground surface. The soil is saturated clay (γ*=20 kN/m*^{3}) with drained strength *c'=0*, ϕ*'=25°*. The mean values of loadings on the foundation were: F_x*=80 kN*, F_y *=400 kN*. While calculated with these mean values, the factor of safety (FOS) of the foundation is 3.971. It is worthwhile to note that, in engineering design, FOS is normally calculated using the characteristic values instead of mean values of the parameters.

To carry out a reliability analysis, the COV values considered for ϕ', F_x and F_y were 0.1, 0.1 and 0.1. Ten thousand normally distributed random variables were created for each parameter to find out the probability of failure of the foundation with Monte Carlo simulation. The probability of failure was determined by:

$$P_f = \text{(number of cases LSF<0) / (total number of cases studied)} \quad (8)$$

Several simulations were run for this case considering that the size of random numbers created is not huge. The result showed that, the probability of failure (P_f) of the foundation was ranging between 0.04% and 0.06%, which is about 4 to 6 failure out 10,000 cases analyzed. The difference between the numbers is due to the limitation of the Monte Carlo simulation in producing consistence results when the size of random numbers used in the simulation is not large enough. By increasing the number of random variable to 100,000, a probability of failure of 0.046% can be obtained. It can be seen that, a size of 10,000 used in the Monte Carlo simulation gave reasonably close estimation. For probability of failure at 0.04%, a

histogram of performance function was plotted in Figure 1. The figure shows that, the performance function is not normally distributed. This is due to the highly nonlinear expression of the performance function.

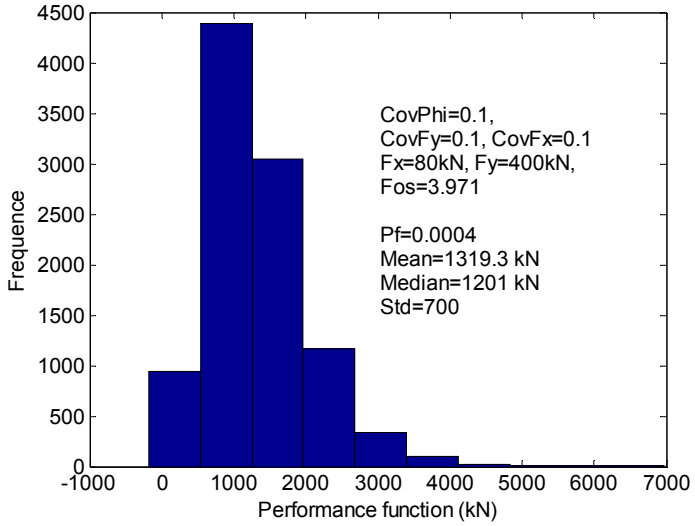

Figure 1. Histogram of performance function

Reliability index (β) is more familiar for engineers to evaluate the reliability of a structure. As shown in Figure 1, the performance function is more likely a shifted lognormal distribution. Using the equation proposed by Rosenbleuth and Esteva in 1972 to calculate reliability index of lognormal distribution "Paikowsky *et al.* (2004) ":

$$\beta = \ln(P_f / 460)/(-4.3) \qquad (9)$$

a reliability index of $\beta=3.245$ can be obtained with $P_f=0.0004$. By assuming normal distribution, the reliability index was 3.353.
The equation proposed by Cornell (1969) gave a reliability index of 1.885:

$$\beta = \frac{\mu(LES)}{\sigma(LES)} \qquad (10)$$

in which $\mu(LES)$ and $\sigma(LES)$ are the mean and standard deviation of performance function. The mean value and standard deviation of performance function were found at 1319.3 kN and 700 kN respectively by statistical analysis of the results.

The results showed that, Cornell's method gave smallest number of reliability index. This makes sense considering that the histogram of the performance function is right skewed. On the other hand, the performance function is highly nonlinear, so the reliability index calculated with equation (10) might not reflect the reliability of the foundation is this case. It has been noticed that the method is highly influenced by the form of the performance function "USACE (1997) ". This result tells that when performance function is not normally distributed, one should be careful in selecting the methods to obtain reliability index from probability of failure or vice versa.

Since reliability index is not consistent when using different methods, probability of failure is used in the following sections for further studies.

4.4 *Variation of probability of failure with COVs*

To study the variation of probability of failure with COVs of the parameters, a set of Monte Carlo simulations were carried out. The above foundation was reanalyzed with varied COV values for the parameters. Eight COVs for each parameter were used. The COVs range from 0.025 to 0.2 with 0.025 intervals. The size of random number was 10,000. In total, 8^3 Monte Carlo simulations were performed. The results were shown in Figure 2. In the figure, each curve represented the variation of P_f with COV(Phi), (COV of ϕ) for certain values of COV(F_x) and COV(F_y), (COV of F_x and F_y). For example, the upmost curve is the probability of failure curve for (COV(F_x), COV(F_y)) at (0.2, 0.2) with COV(Phi) varying. The figure showed that, under such external forces, the probability of failure of the foundation is

very sensitive to the COV of friction angle, COV(Phi). The probability of failure of the foundation increase dramatically when COV(Phi) exceeds the value of 0.1. With COV(Phi) increase from 0.1 to 0.2, the probability of failure increase dramatically from less than 0.5% to more than 4%. The figure also showed that, with the variation of the COVs of external forces, the probability of failure can vary up to a range of 200% or more for the same value of COV(Phi). The next section will discuss about the variation of probability of failure with COV(F_x) and COV(F_y) while COV(Phi) value is set.

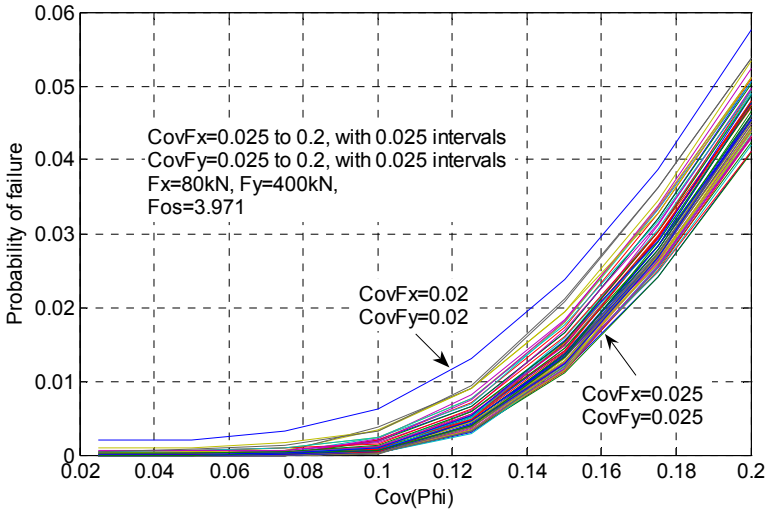

Figure 2. Variation of probability of failure with COVs

5 SENSITIVITY OF PROBABILY OF FAILURE TO INCLINED LOAD

As discussed above, COV values of external loads influence the reliability of shallow foundations. This section was to find out which one influences more on probability of failure: COV of horizontal load, *COV(F_x)* or COV of vertical load, *COV(F_y)*.

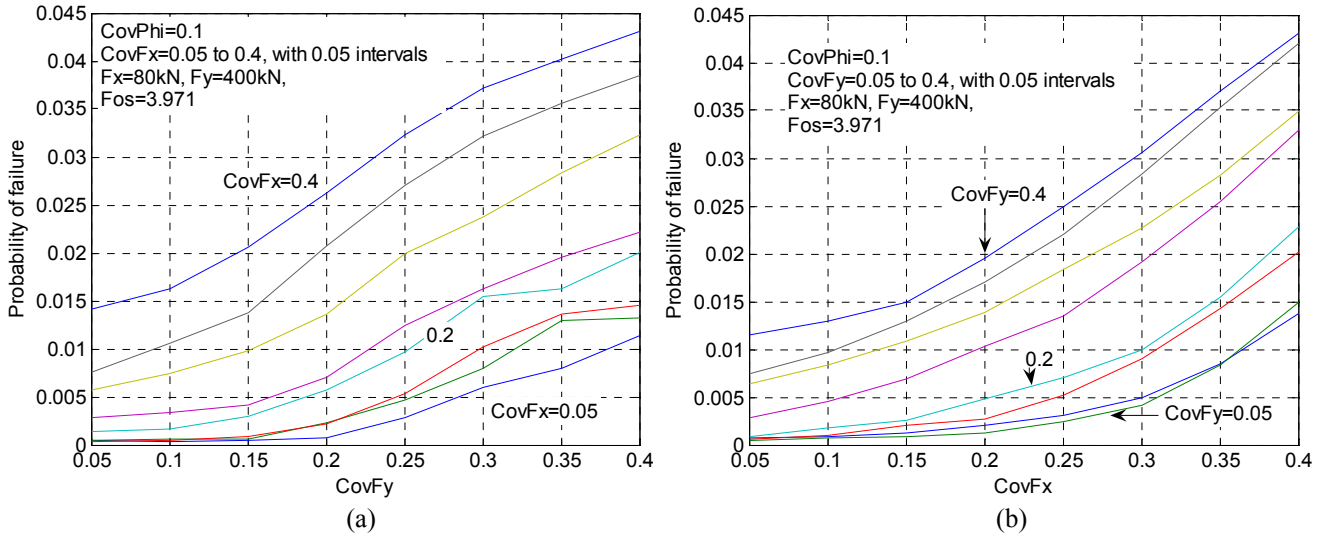

Figure 3. Probability of failure and COV of external forces.

Setting COV(Phi) at 0.1, by varying *COV(F_x)* and *COV(F_y)* from 0.05 to 0.4 with 0.05 intervals, the following plots can be obtained. From the figures, we can see that, P_f values were more sensitive to the variation of *COV(F_x)*, as plots in Figure 3 (a) are more scattered than in (b), especially at higher values of *COV(F_x)*, e.g. *COV(F_x)>0.2*, which is mostly the case for wind load as shown in Table 2. In Figure 3 (b), at lower values of *COV(F_y)*, e.g. less than 0.2, the curves are more condensed. This suggested that with lower variation of vertical load, the probability of failure of a shallow foundation is more influenced by the variation of horizontal load. In Figure 3 (a), take *COV(F_y)=0.15* for example, the probability of failure

of the foundation increased from 0.0025 (β=2.807) to 0.021 (β=2.034) with the increase of $COV(F_x)$ from 0.2 to 0.4, noting that the reliability indexes were obtained from a normal distribution table.

6 CONCLUSION

Monte Carlo simulation was used to investigate the influence of the variation of inclined load on the reliability of shallow foundations. The performance function was built with a Meyerhof's equation. The simulation was performed in a Matlab language environment. A full analysis cost less than 1 minute to run on a HP Elitebook personal laptop for a simulation with $8^3 \times 10{,}000$ times of calculation on the performance function.

The results showed that, the reliability indexes exhibited huge difference using different methods when limit state function is not normally distributed. The authors recommended that, engineers should be careful in using the reliability index, especially when performance function is highly nonlinear and random variables are not normal distribution.

For foundations on cohesionless soils, the probability of failure of shallow foundation is most sensitive to the variation of friction angle of soils based on the simulations. In respect to loads, the variation of horizontal load has more influence on the probability of failure. In the choice of loading factors to carry out a LRFD, attention should be paid in choosing the loading factors, especially in cases when horizontal load is dominant and varies more. With the choice of loading factors, different factors should be considered for horizontal and vertical forces as recommended by "Paikowsky *et al.* (2010)".

REFERENCES

Alawneh, A. S., Nusier, O. K. & Al-Mufty, A. A. 2006. Reliability based assessment of shallow foundations using mathcad. Geotechnical and Geological Engineering 24: 637-660.

Cherubini, C. 2000. Reliability evaluation of shallow foundation bearing capacity on c', ϕ' soils. Canadian Geotechnical Journal 37: 264-269.

Christian, J. T., Ladd, C. C. & Baecher, G. B. 1994. Reliability applied to slope stability analysis. Journal of Geotechnical Engineering (ASCE) 120(12): 2180-2207.

Cornell, C. A. 1969. A probability-based structural code. Journal of the American Concrete Institute (66): 974-985.

De Beer, E. E. 1970. Experimental determination of the shape factor and the bearing capacity factors for sand. Geotechnique. 20(4): 387-411.

Duncan, J. M. 2000. Factors of safety and reliability in geotechnical engineering. Journal of Geotechnical and Geoenvironmental Engineering (ASCE) 126(4): 307-316.

Ellingwood, B. & Galambos, T. V. 1982. Probability-based criteria for structural design. Structural Safety 1(1): 15-26.

ENV(1997-1) 1997. Eurocode 7: Geotechnical design - Part 1: General rules. Brussels, European Committee for Standard (CEN).

Foye, K. C., Salgado, S. & Scott, B. 2006. Risistance factors for use in shallow foundation LRFD. Journal of Geotechnical and Geoenvironmental Engineering (ASCE) 132(9): 1208-1218.

Fredlund, D. G., Morgenstern, N. R. & Widger, R. A. 1978. The shear strength of unsaturated soils. Canadian Geotechnical Journal 15(3): 313-321.

Hansen, J. B. 1970. A revised and extended formula for bearing capacity. Danish Geotechnical Institute Bulletin, 28, 5-11.

Honjo, Y., Suzuki, M. & Matsuo, M. 2000. Reliability analysis of shallow foundation in reference to design codes development. Computers and Geotechnics 26: 331-346.

Lee, I. K., White, W. & Ingles, O. G. 1983. Geotechnical Engineering. Boston, Pitman.

Lumb, P., Ed. 1974. Application of Statistics in Soil Mechanics. Soil Mechanics, New Horizons. London, Butterworths.

Meyerhof, G. G. 1951. The ultimate bearing capacity of foundations. Geotechnique. 1(4): 301-332.

Meyerhof, G. G. 1953. The bearing capacity of foundations under eccentric and inclined loads. Proc., 3rd Int. Conf. of Soil Mechanics and Foundation Engineering. Balkema Publishers, Rotterdam, the Netherlands. Vol. 1: 440–445.

Meyerhof, G. G. 1963. Some recent reserach on the bearing capacity of foundations. Canada Geotechnical Journal 1(1): 16-23.

Orr, T. L. L. 2000. Slection of characteristic values and partial factors in geotechnical designs to Eurocode 7. Computer and Geotechnics 26: 263-279.

Paikowsky, S. G., Birgisson, B., Mcvay, M. & Nguyen, T. et al. 2004. Load and resistance factor design (LRFD) for deep foundations. NCHRP Report 507, Washington, D.C., Transportation Research Board.

Paikowsky, S. G., Lesny, K., Kisse, A., Amatya, S. & Muganga, R. et al. 2010. LRFD Design and Construction of Shallow Foundations for Highway Bridge Structures. NCHRP Report 651, Washington, D.C, Transport Research Board.

Phoon, K. K. & Kulhawy, F. H. 1999 (a). Characterization of geotechnical variability. Canadian Geotechnical Journal 36: 612-624.

Phoon, K. K. & Kulhawy, F. H. 1999 (b). Evaluation of geotechnical property variability. Canadian Geotechnical Journal 36: 625-639.

Phoon, K. K., Kulhawy, F. H. & Grigoriu, M. D. 2003. Multiple resistance factor design for shallow transmission line structure foundations. Journal of Geotechnical and Geoenvironment Engineering. ASCE 129(9): 807-818.
USACE 1997. ETL 1110-2-547 Introduction to probability and reliability methods for use in geotechnical engineering, U.S. Army Corps Engineers Document.
Vesic, A. S. 1973. Analysis of ultimate loads of shallow foundations. Journal of Soil Mechanics and Foundations Division. ASCE 99: 45-73.

ISGSR 2011 - Vogt, Schuppener, Straub & Bräu (eds) - © 2011 Bundesanstalt für Wasserbau ISBN 978-3-939230-01-4

A Consistent Failure Model for Probabilistic Analysis of Shallow Foundations

A. Kisse
CDM Consult GmbH, Bochum, Germany

ABSTRACT: In today's codes of practice, e. g. Eurocode 7 different ultimate limit states are distinguished. To overcome these problems an alternative design approach has been established on the basis of a unique failure condition. This failure condition describes the ultimate limit state of shallow foundations over the whole loading range without distinguishing different failure modes. The failure condition spreads out a failure surface which represents the outer border of the permissible loading. Hence the distance of the actual loading from the failure surface describes the safety of the system. This safety can be determined easily using reliability analysis. Here, the Hasofer-Lind second moment reliability index $ß_{HL}$ will be evaluated. The reliability based design of the foundation for a vertical breakwater based on this model is presented. The influences of individual load combinations on the safety of the system taking into account scatter and correlations of the parameters are examined.

Keywords: Safety, Serviceability Limit State, Shallow foundation, Ultimate Limit State, Hasofer-Lind

1 INTRODUCTION

A thorough understanding of the structure-soil-interaction is the basis for a safe and economical design. In today's codes of practice, e. g. Eurocode 7 (2005) prescribe the limit state design (LSD). Within this design concept several ultimate limit states (ULS) and serviceability limit states (SLS) are investigated. Application of the LSD to shallow foundations includes the separate analysis of different failure modes, e. g. bearing resistance failure or sliding, which describe the complex behaviour of the foundation. This procedure has apparent disadvantages particularly in the design of foundations under complex loading such as coastal structures.

For foundations under complex loading different failure modes have to be examined for different load combinations within the LSD procedure. For example, the design of vertical caisson breakwaters on a feasibility level includes the investigation of loading under still-water level (SWL), wave crest and wave trough (Fig. 1). The limit states of uplift, rotation failure, sliding and bearing resistance failure in the rubble mound or in the subsoil are to be checked. Rotation failure, however, is often substituted by limiting the eccentricity of the resultant vertical loading to b/3 of the foundation width.
In contrast to this, with the failure condition of the Single Surface Hardening Model (Kisse, 2008) the isolated limit states are integrated in a consistent formulation, so that the distinction between different limit states is no longer necessary.

This concept allows for a clear definition of safety and provides a distinct basis for the application of probabilistic methods. The new generation of geotechnical design codes offers such methods. Since it make possible to regard e.g. the inherent uncertainty of the natural boundary conditions.

In this paper such a probabilistic design on basis of the very practicable Hasofer-Lind index $ß_{HL}$ is presented.

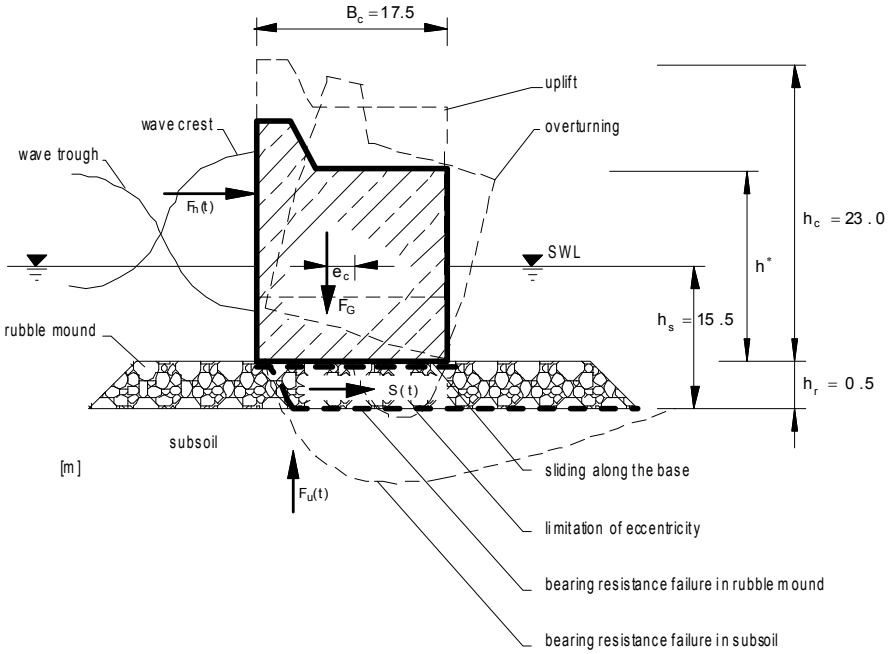

Figure 1. Failure modes for vertical caisson breakwaters (Lesny et al., 2000)

2 CONCEPT OF LIMIT STATES

Basis for the determination of the failure probability is the confrontation of effects S(X) and resistances R(X) in a limit state equation g(X):

$$g(X) = R(X) - S(X) \qquad (1)$$

In which X is a vector of random variables describing the geometry of the foundation, the loads that are applied, the strength of materials etc. The probability of failure p_f is the probability p of ($R \leq S$) or in general

$$p_f = p(g(X) \leq 0) = \int_{g(X) \leq 0} f_X(X)\,dX \qquad (2)$$

where $f_x(X)$ is the joint probability density function of the basic variables.

In general it is not possible to solve the integral analytically. Cornell (1969) introduced a method in which the difference of R - S is considered. So for a normal distribution of the value z it is possible to write

$$\mu_z = \mu_R - \mu_S, \quad \sigma_z = \sqrt{\sigma_R{}^2 + \sigma_S{}^2} \qquad (3)$$

This supplies the definition of the reliability index ß

$$\beta_z = \mu_z / \sigma_z \qquad (4)$$

The failure probability is calculated then to

$$p_f = p(g(X) < 0) = \Phi(-\beta_z) \qquad (5)$$

2.1 *Limit state equation*

The limit state equation g(X) divides the space in a safe region ($g(X) > 0$) and a failure region ($g(X) \leq 0$). As mentioned before, for a vertical breakwater under complex loading a lot of limit states have to be checked. Desirably for the probability analysis it is to have a unique equation to describe the limit states, because with that we could consider the safety of the whole system at once not only for a single failure mode.

Kisse (2008) adopted such a failure condition proposed by Lesny et al. (2002) to calculate the failure of the system within the SSH-Model. Here the footing is loaded by a vertical load F_1, horizontal load components F_2 and F_3, a torsional moment M1 and bending moment components M_2 and M_3 (Fig. 2). The load components are summarized in the load vector:

$$\vec{Q}^T = \left[F_1\, F_2\, F_3\, M_1\, M_2\, M_3\right] \qquad (6)$$

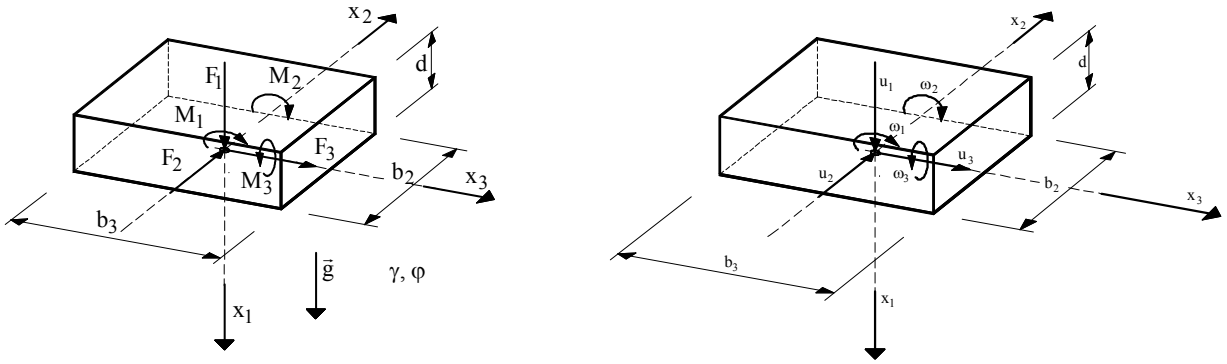

Figure 2. a) Geometry and loading, b) Corresponding displacements and rotations.

For the basic case of a footing on non-cohesive soil without embedment the geometry of the footing described by the side ratio b_2/b_3, weight γ, shear strength φ' of the soil and a quantity μ_S describing the roughness of the footing base have to be considered as well (Fig. 2).
With these input parameters the failure condition is defined by the following expression (Kisse, 2008):

$$g\left(\vec{Q}, F_{10}\right) = \frac{F_1}{F_{10}} \cdot \left(1 - \frac{F_1}{F_{10}}\right)^{\alpha} - \left(\sqrt{\frac{F_2^2 + F_3^2}{\left(a_1 \cdot F_{10}\right)^2} + \frac{M_1^2}{\left(a_2 \cdot \left(b_2 + b_3\right) \cdot F_{10}\right)^2} + \frac{M_2^2}{\left(a_3 \cdot b_3 \cdot F_{10}\right)^2} + \frac{M_3^2}{\left(a_3 \cdot b_2 \cdot F_{10}\right)^2}}\right) = 0 \quad (7)$$

In Eq. (7) all load components are referred to F_{10} which is the bearing resistance of a footing under vertical centric loading. This quantity is calculated using traditional bearing capacity formulae. The advantage of this formulation is that the complex mutual interaction of the load components is described directly without using reduction factors or the concept of the effective width. Other influences on the bearing capacity are included in F_{10}.

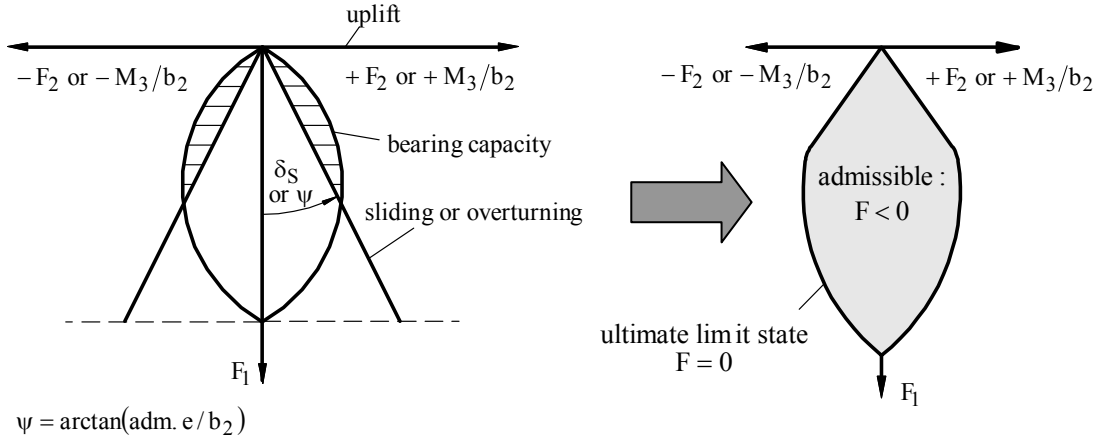

Figure 3. Isolated limit states (left) and resulting consistent failure condition (right).

In an interaction diagram (Fig. 3) the failure condition spans a failure surface, which is the outer boundary of the admissible loading. The parameters $a_{1,2,3}$ govern the inclination of this failure surface for small vertical loading where the limit states sliding and overturning have previously been relevant. These limit states are integrated by defining the parameters $a_{1,2,3}$ and α acc. to Eq. (8) (Lesny, 2001).

$$a_1 = \pi/2 \cdot \mu_S \cdot \tan\varphi' \cdot e^{-\pi/3 \cdot \tan\varphi'},\ a_2 = 0.098,\ a_3 = 0.42,\ \alpha = 1.3 \quad (8)$$

The limit state uplift is already included in Eq. (7), because only positive vertical loads are admissible. The parameters have been derived from an analysis of numerous small scale model tests (Lesny 2001, Lesny and Richwien, 2002).

2.2 *Hasofer-Lind index*

As shown before the failure condition of the model spreads out a failure surface which represents the outer border of the permissible loading. Hence the distance of the actual loading from the failure surface describes the safety of the system (in anticipation of the next chapter see Fig. 5).

This safety can be determined easily using reliability analysis. Here, the widely used Hasofer-Lind second moment reliability index $ß_{HL}$ will be evaluated (Hasofer and Lind, 1974). The classical approach for computing the index is based on the transformation of the limit state surface into the space of standard normal varieties

$$X'_i = \left(X_i - \mu_{X_i}\right) \Big/ \sigma_{X_i} \qquad (9)$$

where μ_{Xi} and σ_{Xi} are the mean and standard deviation of variable X_i. The limit state equation g(X) is also transformed to the standard space (Fig. 4). The reliability index $ß_{HL}$ is defined as the distance from origin to the nearest point D of the limit state surface. This point D is called the design point.

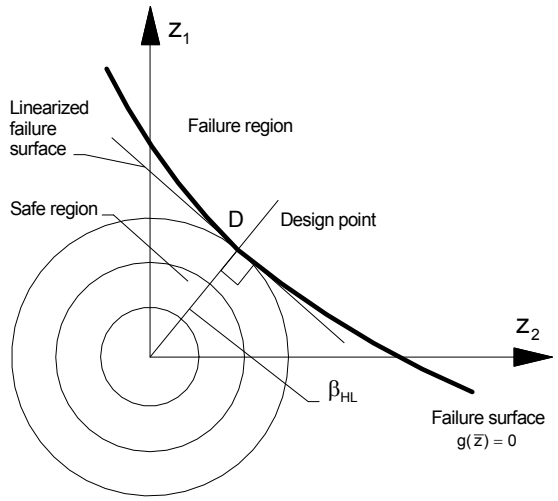

Figure 4. Illustration of reliability index ß in the plane (Burcharth, 1997)

For practical applications the methods proposed by Low and Phoon (2002) and Low (2005) are especially suitable for the determination of the index $ß_{HL}$. With this formulation it is possible to indicate the safety of the system not only for the mean values but also in dependence of correlations of the parameters. The matrix form of the Hasofer-Lind reliability index is (Low, 2005):

$$\beta_{HL} = \min_{X \in F} \sqrt{\left(\frac{x_i - \mu_i}{\sigma_i}\right)^T \cdot R^{-1} \cdot \left(\frac{x_i - \mu_i}{\sigma_i}\right)} \qquad (10)$$

where X is a vector representing the set of random variables X_i, μ_i are the mean values, R is the correlation matrix, σ_i is the standard deviation and F the failure domain.

3 NUMERICAL ANALYSIS

In the following the application of the new system law is shown using the example of a vertical breakwater which is placed on a thin rubble mound on sandy subsoil (Fig. 1). The geometry and soil conditions are taken from De Groot et al. (1996) and Lesny et al. (2000). The loads are calculated within the EU-MAST III PROVERBS project (Probabilistic design tools for vertical breakwaters, Oumeraci et al., 2001).

For the design the loading under still-water level (SWL), wave crest and wave trough are considered. For the case of simplification it is assumed that all wave loads followed a normal distribution. One refers

to that with the method after Eq. (10) other distributions for the wave loads can also be considered. The extreme loads are listed in table 1.

Table 1. Extreme loads for vertical breakwaters after De Groot et al. (1996) and Oumeraci et al. (2001).

Still water level LC 1					
			F_1 [kN/m]	F_3 [kN/m]	M_2 [kNm/m]
			4375	0	5180
Wave trough LC 2					
case	H_{max} [m]	T_0 [sec]	F_1 [kN/m]	F_3 [kN/m]	M_2 [kNm/m]
A1	5	8.5	4183	581	706
A2	6.5	10	4061	918	-1697
A3	8	11	3943	1257	-4149
A4	10	12	3787	1725	-7520
Wave crest LC 3					
case	H_{max} [m]	T_0 [sec]	F_1 [kN/m]	F_3 [kN/m]	M_2 [kNm/m]
A1	5	8.5	4780	-645	7513
A2	6.5	10	4983	-836	8558
A3	8	11	5163	-986	9474
A4	10	12	5395	-1148	10550

3.1 *Ultimate Limit State and Failure Surface*

In Fig. 5 the failure surfaces after Eq. (7) in the F_1-F_3-plane F_1-M_2/b_3-plane for different friction angles are presented. It can be recognized that with increasing friction angle of the subsoil the failure curve expands and, hence, greater bending moments and horizontal loads can be applied.

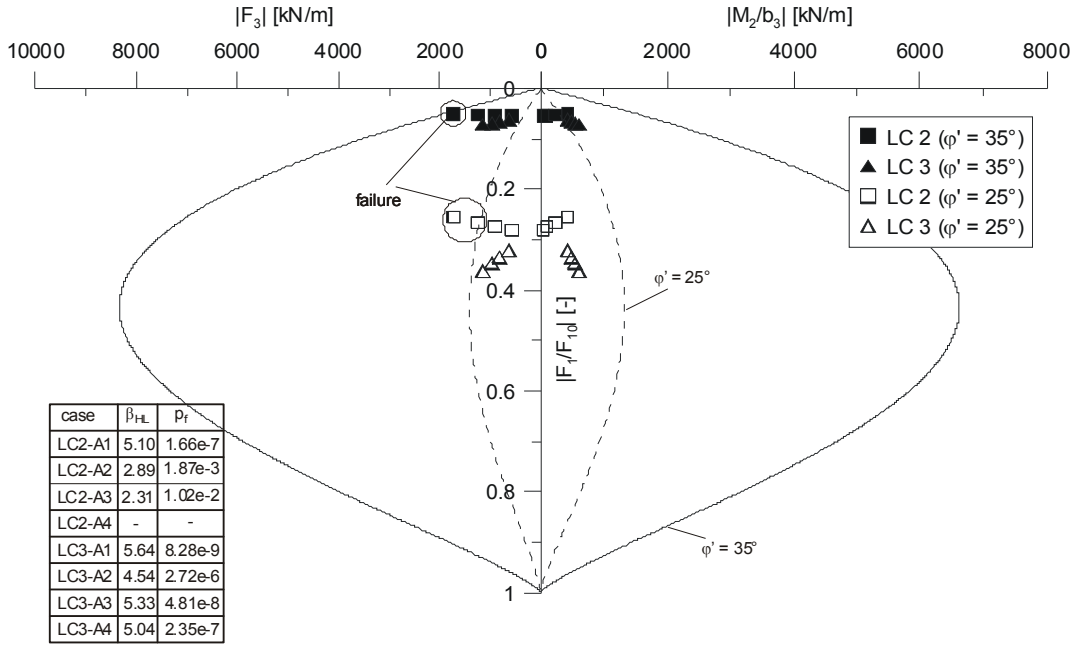

case	β_{HL}	p_f
LC2-A1	5.10	1.66e-7
LC2-A2	2.89	1.87e-3
LC2-A3	2.31	1.02e-2
LC2-A4	-	-
LC3-A1	5.64	8.28e-9
LC3-A2	4.54	2.72e-6
LC3-A3	5.33	4.81e-8
LC3-A4	5.04	2.35e-7

Figure 5. Intersection of failure curves and load points for two different friction angle φ'

Here the surfaces are plotted together with the loads applied the breakwater after table 1. It can be seen that for a friction angle of φ' = 35° all cases lie inside the failure surface (filled out points). For the other case of a friction angle of φ' = 25° some load points lie outside and some insight the failure surface. For the points (= load combinations) outside the body failure occurs. So the interaction diagram displays directly the interaction of the load components within the ULS.

3.2 *Reliability index*

With the load combinations in table 1 and the limit state surface formulated after Eq. (7) a reliability design for the foundation of a vertical caisson breakwater will be performed. For the following calculations

the Microsoft Excel software and its built-in optimization program Solver is used. The computations followed the spreadsheet formulations of Low and Phoon (2002) and Low (2005).
Beside the curves also the calculated values of the reliability index $ß_{HL}$ for a friction angle of φ' = 35° are specified in Fig. 6 (left side). Here the loads are uncorrelated and the coefficient of variation

$$COV = \sigma_{X_i} / \mu_{X_i} \qquad (11)$$

is taken as 20% for all load components. If we adopt a safety factor of 3.0 for the vertical breakwater under the observed loading conditions (for φ' = 35°), only for the cases LC 2-A2 and LC-A3 the ULS is not fulfilled and the foundation is not safe. The load point for LC-A4 lies on the failure surface and so failure occurs.

In general, the index $ß_{HL}$ and so the safety of the system depend on the correlation factor. Therefore the influence of the correlation of the different load components to each other was separately examined for the load case LC2-A2 (Fig. 6). The results for a correlation between F_1-F_3 and F_1-F_3-M_2 differs not, so only one curve can be seen. The reliability index $ß_{HL}$ is not affected by the correlation of F_1-M_2. This is due to the fact, that the dominate failure mode for this load case is sliding.

If the load components are correlated the ellipses are tilted. For positive correlation factors they are positivity tilted and for negative values they are negativity tilted. So in one case the distance from the point of view could be smaller than in the other case.

For the correlation F_1-F_3 and F_1-F_3-M_2 the reliability index $ß_{HL}$ is greater for positive correlations values as for negative ones. The reason for this is that the load point is located in the upper section of the interaction diagram (Fig. 5). Here the surface is curved to the right in the F_1-F_3-plane. If the vertical load component decreases the horizontal load component increases for a negative correlation and so the ellipsoid is negativity tilted. That mean, that the distance between the ellipse and the failure surface become smaller as for a positive correlation.

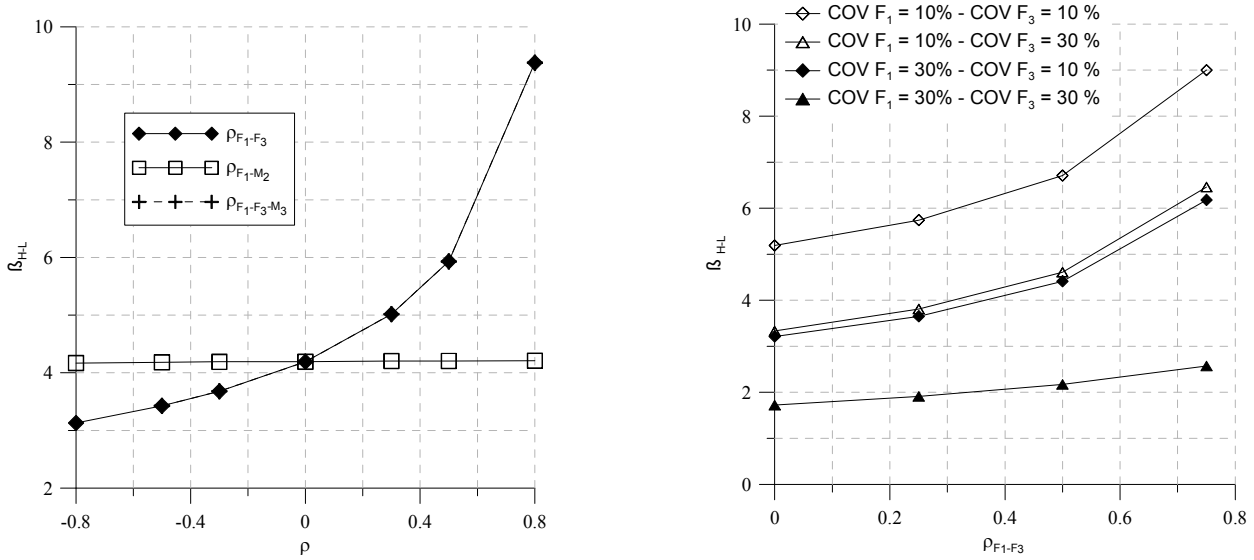

Figure 6. Effect of the correlation (left) and of the variability (right) of the applied loads and on the reliability index

To study the effect of the variability of the applied loads on the failure probability, Fig. 6 (right side) shows the reliability index versus the coefficient of variation of F_1 and F_3 and the correlation of these two loads. The results show that the failure probability is highly influenced by the coefficient of variation of the loads, the greater the scatter in F_3 the higher the failure probability of the foundation. Beyond that the COV affects also the dependence of the correlation. For a small coefficient of variation the influence of the correlation is more pronounced.

This means that the accurate determination of the distribution of this parameter is very important in obtaining reliable probabilistic results.

4 SERVICEABILITY

For the SLS it has to prove that the estimated displacements and rotations u_e are not greater than limiting tolerable displacements and rotations u_{tol}.

$$u_e \leq u_{tol} \qquad (12)$$

Due to the presence of uncertainties the estimated and tolerable displacements and rotations are in fact random variables. So it seems to be preferable to use a reliability based approach to design for SLS.

A performance function g(X) for the reliability-based serviceability limit can be formulated in the following way (Zhang and Ng, 2005):

$$g(X) = u_{tol} - u_e \qquad (13)$$

Here g(X) > 0 defines a satisfactory performance region and g(X) ≤ 0 defines an unsatisfactory performance region like that one for the ULS. If the probability distributions of the displacements and rotations are known the reliability index $ß_{HL}$ can be calculated.

With the Single Surface Hardening Model after Kisse (2008) it is possible to determine the tolerable displacements and rotations over the whole loading range up to the ultimate limit state. So with the performance functions after Eq. (7) and (12) it could be possible to calculate the system failure probability.

4.1 *Displacement rule*

The displacements and rotations of the foundation due to arbitrary loading inside the failure surface are described by the displacement rule. The displacements u_i and rotations ω_i (Fig. 2) are summarized in a displacement vector (Kisse, 2008):

$$\vec{u}^T = \left[u_1\, u_2\, u_3\, \omega_1\, \omega_2\, \omega_3\right] \qquad (14)$$

Due to the complex interaction of load components, displacements and rotations the displacement rule is formulated using the well-known strain hardening plasticity theory with isotropic hardening. Hence, displacements and rotations are calculated according to Eq. (15), assuming that all deformations are plastic.

$$\mathrm{d}\vec{\mathrm{u}} = \frac{1}{\mathrm{H}} \cdot \left(\frac{\partial \mathrm{F}}{\partial \vec{\mathrm{Q}}}\right)^{\mathrm{T}} \cdot \frac{\partial \mathrm{G}}{\partial \vec{\mathrm{Q}}} \cdot \mathrm{d}\vec{\mathrm{Q}} \qquad (15)$$

The components of the displacement rule are a yield surface described by the yield condition F which is derived from the failure condition Eq. (7) with the parameter $a_{1,2,3}$ and α of Eq. (8):

$$F\left(\vec{Q}, F_a\right) = \frac{{F_2}^2 + {F_3}^2}{\left(a_1 \cdot F_a\right)^2} + \frac{{M_1}^2}{\left(a_2 \cdot \left(b_2 + b_3\right) \cdot F_a\right)^2} + \frac{{M_2}^2}{\left(a_3 \cdot b_3 \cdot F_a\right)^2} + \frac{{M_3}^2}{\left(a_3 \cdot b_2 \cdot F_a\right)^2} - \left[\frac{F_1}{F_a} \cdot \left(1 - \frac{F_1}{F_a}\right)^{\alpha}\right]^2 = 0 \qquad (16)$$

a plastic potential G (in the same form) and a hardening function H:

$$H = -\frac{\partial F\left(\vec{Q}, F_a\right)}{\partial F_a} \cdot \frac{\partial F_a}{\partial \vec{u}} \cdot \frac{\partial G\left(\vec{Q}, F_b\right)}{\partial \vec{Q}} \qquad (17)$$

The yield surface acc. to Eq. (16) expands due to isotropic hardening until the failure surface defined by Eq. (7) is reached (Fig. 7). Hence, the parameters of the plastic potential G have to be determined as functions of a_i and α, respectively. The expansion of the yield surface depends mainly on the vertical displacement which itself depends on the degree of mobilization of the maximum resistance F_{10}. With that, it is sufficient enough to define the hardening parameter F_a in Eq. (16) as a function of these two quantities according to:

$$\mathrm{F_a} = \left(\mathrm{F_{10}} + \mathrm{k_f} \cdot \mathrm{u_1}\right) \cdot \left\{1 - \exp\left(\frac{-\mathrm{k_0} \cdot \mathrm{u_1}}{\mathrm{F_{10}} + \mathrm{k_f} \cdot \mathrm{u_1}}\right)\right\} \qquad (18)$$

Many hardening laws (e. g. Nova et al., 1991) require small scale model tests under centric vertical loading to determine the hardening parameter. Since this is not convenient for practical applications, the initial and final stiffness of the corresponding load-displacement curve, k_0 and k_f respectively, may be determined using a method proposed by Mayne and Poulos (2001) in which the soil stiffness can be determined by any standard procedure.

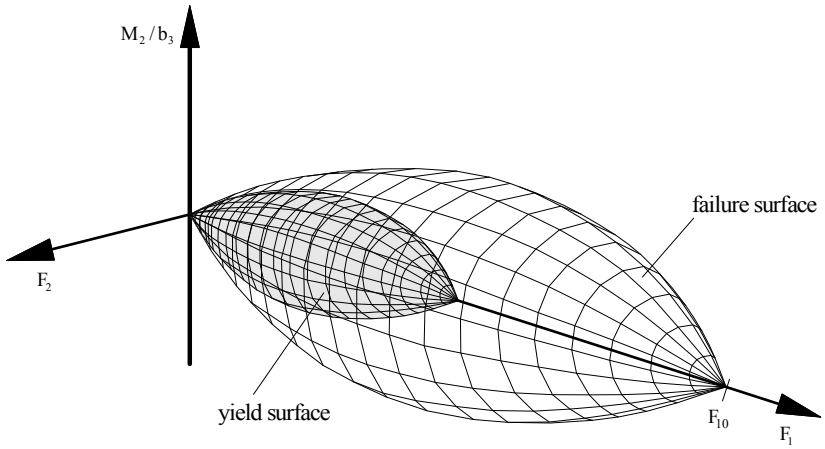

Figure 7. Isotropic expansion of the yield surface in the loading space.

5 CONCLUSION

A design method has been presented which describes the complex behavior of shallow foundations under loading up to failure. The model includes a failure condition defining the ultimate bearing capacity. Hence, the separate analysis of different failure modes is no longer necessary. Together with the methods proposed by Low and Phoon (2002) and Low (2005) a practical application for the determination of the Hasofer-Lind index β_{HL} is formulated. With this formulation it is possible to indicate the safety of the system not only for the mean values but also in dependence of scatter and correlations of the parameters. The ability of the method was presented using an example of a vertical breakwater.

REFERENCES

Burcharth, H.F. 1997. Reliability based design of Coastal Structures. Advances in Coastal and Ocean Engineering, Vol. 3 Ed.: Liu, P. L.-F., World Scientific Publishing.

Cornell, C. 1969. A Probabilistic Structural Code. ACI Journal Vol. 66, pp. 974-985.

De Groot, M. B., Andersen, K. H., Burcharth, H. F., Ibsen, L. B., Kortenhaus, A., Lundgren, H., et al. 1996. Foundation Design of Caisson Breakwaters. Publ. No. 198 (Vol. 1).Oslo, Norway: Norwegian Geotechnical Institute.

DIN EN 1997-1 2005. Eurocode 7: Entwurf, Berechnung und Bemessung in der Geotechnik – Teil1: Allgemeine Regeln. Normenausschuss Bauwesen im Deutschen Institut fuer Normung e. V., Berlin (German version).

Hasofer, A. M. & Lind, N. C. 1974. An exact and invariant first order reliability format. Journal of Engineering Mechanics Division, ASCE 100, pp. 111-121.

Kisse, A. 2008. Entwicklung eines Systemgesetzes zur Beschreibung der Boden- Bauwerk-Interaktion flachgegruendeter Fundamente auf Sand. Mitteilungen aus dem Fachgebiet Grundbau und Bodenmechanik der Universität Duisburg-Essen, Heft 34, VGE Verlag, Essen. (in German)

Lesny K. & Richwien W. A 2002. Consistent Failure Model for Single Footings embedded in Sand. Proceedings of the International Workshop on Foundation Design Codes and Soil Investigation in View of International Harmonization and Performance Based Design, Kamakura, April 2002. Balkema, Lisse.

Lesny, K. 2001. Entwicklung eines konsistenten Versagensmodells zum Nachweis der Standsicherheit flachgegruendeter Fundamente. Mitteilungen aus dem Fachgebiet Grundbau und Bodenmechanik der Universität Essen, Heft 27, Verlag Glückauf GmbH, Essen. (in German)

Lesny, K., Kisse, A. & Richwien, W. 2002. Proof of Foundation Stability Using a Consistent Failure Model. Proc. of the Int. Conf. on Probabilistics in Geotechnics -Technical and Economic Risk Estimation, Graz, Austria, pp. 95-103.

Lesny, K., Perau, E., Richwien W.; Wang, Z. 2000. Some Aspects on Subsoil Failure of Vertical Breakwaters. Forschungsbericht aus dem Fachbereich Bauwesen, Heft 83, Universitaet Essen.

Low, B. & Phoon, K. K. 2002. Practical first-order reliability computations using spreadsheet. Proc. of the Int. Conf. on Probabilistics in Geotechnics: Technical and Economic Risk Estimation, Graz, Austria, pp. 93-46.

Low, B. 2005. Reliability-based design applied to retaining walls. Geotechnique 55, No. 1: 63-75.

Nova R & Montrasio L. 1991. Settlements of Shallow Foundations on Sand. Géotechnique, Vol. 41, pp. 243-256.

Mayne P W & Poulos H G. 2001. Discussion: Approximate displacement influence factors for elastic shallow foundations. Journal of Geotechnical and Geoenvironmental Engineering, Vol. 127, pp. 100-102.

Oumeraci, H.; Kortenhaus, A.; Allsop, W.; de Groot, M.; Crouch, R.; Vrijling, H.; Voortman, H. 2001. Probabilistic Design Tools of Vertical Breakwaters, A. A. Balkema, Lisse.

Zhang, L. M. & Ng, A. M. Y. 2005. Probabilistic limiting tol-erable displacements for serviceability limit state design of foundations. Geotechnique 55, No. 2, pp. 151-161.

ISGSR 2011 - Vogt, Schuppener, Straub & Bräu (eds) - © 2011 Bundesanstalt für Wasserbau ISBN 978-3-939230-01-4

Reliability in geotechnical design – some fundamentals

B. Simpson
Arup Geotechnics, London, UK.

ABSTRACT: This paper is written from the point of view of practical geotechnical design. Five features of the designer's situation are noted: (a) his specific knowledge of the site, the ground conditions and their possible variability; (b) the importance of extreme variations in causing failures; (c) the large number of variables usually involved in a design situation; (d) the need for "robustness"; (e) the significance of human error. It is argued that a set of safety provisions in a code of practice should accommodate these items. The possibility of using reliability analysis rather than factors of safety is discussed in the light of these issues.

Keywords: Geotechnics; design; robustness; reliability; variability

1 INTRODUCTION

Severe failures of civil engineering structures are fairly rare, but when they occur they may have serious consequences, involving multiple deaths or injuries. Less severe failures, leading to inconvenience and some cost for repairs, are more common. Designers and code drafters aim to avoid failures of all types, across the full range of severity. This is generally achieved by demonstrating that a design would not fail, even if parameters and conditions were significantly worse than those it is thought most likely to prevail. The parameters considered may be either basic input to the design calculations (eg actions and material strengths) or values derived within the calculations (eg action effects and resistances).

As a shorthand in this paper, severe failures leading to danger or gross economic loss will be regarded as ultimate limit states (ULS). Less severe failures, leading to inconvenience, disappointment or relatively minor cost will be termed serviceability limit states (SLS). Strictly, the failure occurs when the limit state is exceeded. References to clauses or paragraphs of codes will be shown thus: {...}.

In order to ensure that severe failures (ULS) are very unlikely, recent drafting of codes has mainly used a partial factor approach in some form. The factors are applied to parameter values that are thought to be reasonably likely to occur, in order to derive parameters values that are very unlikely to occur for the calculations. This approach is widely used in structural design, and has been taken up by the geotechnical community partly to achieve compatibility in the analysis of ground and structures as they interact and rely on each other.

For serviceability (SLS), two broad approaches are in use: (a) direct calculations of displacements, crack widths and damage, and (b) limits on the mobilisation of strength allowed, with the intention that this will limit displacements and damage. In both cases, it is normal practice to base calculations on reasonably likely values of parameters. Approach (a) is ideal in principle, but may be very difficult to apply in practice. In approach (b) the proportion of strength mobilised can be limited by applying a factor to the strength which is sometimes termed a "mobilisation factor", but which in use is difficult to distinguish from a partial factor applied to material strength or resistance, as might be used for ULS calculations (Osman and Bolton 2006, BS8002).

The "reasonably likely" values may be deliberately slightly cautious ("characteristic" in Eurocodes, "conservatively assessed means" in some US publications, "moderately conservative" in some UK practice) or perhaps mean values – the most likely to occur. The writer would argue that good designers

would not, by instinct, use mean values (the most probable values) in situations of significant uncertainty, except in safety formats that allow the designer to vary the factors applied as a function of his perception of variability. This latter was explicitly the case, for example, in earlier Swedish practice (Boverket, 1995).

An alternative approach, allowed by Eurocode 7 (EC7), is "direct assessment of design values", in which the designer consciously assesses a value sufficiently severe that a worse value is extremely unlikely to occur. It is not easy to define this value, and EC7 resorts to comparisons with factored values by saying "If design values of geotechnical actions are assessed directly, the values of the partial factors recommended in [the code] should be used as a guide to the required level of safety" {2.4.6.1(5)}.

A further alternative, not yet adopted in codes of practice, might be to perform a reliability calculation, in which the probability of failure is calculated, or alternatively an index to it such as the "reliability index" β. This is generally achieved by considering a stochastic spread of parameter values, including some that are very severe. Here again, therefore, the intention is to allow for a reasonable range of severe values.

2 COLLECTION AND INTERPRETATION OF GEOTECHNICAL DATA

2.1 *Specific knowledge of the site*

In structural design, it is commonly the case that drafters of codes of practice have more knowledge about the parameters of strength and loads relevant to a particular design, and their variability, than does the designer. For example, code drafters may be more knowledgeable about wind loading, floor loading, variations in dimension of cast in situ concrete, or seismic loading than is the designer, and the same applies to the variability of steel and concrete. However, in geotechnical design, the designer knows the location of the site, something of its geology and ground water conditions and the results, or paucity of results, of the ground investigation, together with their likely reliability. This information varies considerably from one design to another and could not possibly be known by the code drafter.

It is suggested, therefore, that the designer's understanding of the uncertainty of the parameters of the site is of critical value and must be included in a rational safety format.

EC7 achieves this, to some extent, by asking the designer to assess not the most likely value for a strength parameter, but "a cautious estimate of the value affecting the occurrence of the limit state" {2.4.5.2(2)}. This is essentially similar to the American "conservatively assessed mean" or British "moderately conservative" value, both discussed further by Simpson et al (2009). It is doubtful, however, whether this makes full use of the site-specific knowledge of the designer.

2.2 *Large variety of data*

Suitable geotechnical information is usually scarce. Besides requiring information gained from the site itself, good geotechnical engineering requires study of published literature, collection of comparable case histories and the assimilation of sets of data that are very diverse in both quantity and quality. This is a conceptually difficult process because it requires the combination of data that are precise (from the site) and relatively vague (from literature about similar soils), data that have obvious interpretation (eg vane tests for undrained strength) with others of more doubtful interpretation (eg penetration tests or liquidity indices), data that are plentiful (eg quick undrained triaxial tests) with those that are few (eg plate tests or triaxial stress-path tests), and so on. These all require a careful review of their relative reliability, which depends on factors such as the skill of operators, the details of equipment used, the specification followed (which may be unknown, for older information), and so on.

Assimilation of all this information to obtain parameters useful in calculations is a skilful, if inconvenient, process, not readily reduced to a computer activity. Nevertheless, it is very important that the geotechnical process does not discard any information that is potentially useful, unless careful examination shows that it is worthless.

A safety format suitable for geotechnical design must encourage this process and use it to best advantage. EC7 attempts to do this by making the designer responsible for the selection of the characteristic values of materials, avoiding mathematical prescription of their derivation. Inevitably, such a process leads to values affected by the subjective experience, knowledge and judgement of the designer. The author would contest that it is better to accept such subjectivity than to discard the valuable information it

provides. An important issue for codes of practice is to encourage and facilitate communication of such subjective information, so that it can be understood and examined by others.

3 THE IMPORTANCE OF EXTREME VARIATIONS

3.1 *Reasons for geotechnical failures*

It is often observed that severe failures rarely occur as a result of the reasonably expected statistical variation of parameters. Perhaps this should not be surprising since most safety formats are designed to prevent such failures. Arguably, some earlier failures of that type led to the introduction of partial factor formats (Simpson 2007). Most often, geotechnical failures occur because (a) the ground conditions and geological features are significantly different from those expected, beyond the anticipated range of variation, (b) groundwater pressures are worse than had been expected (Simpson et al 2011), or (c) human error has led to mistakes in calculation or omission of an important factor, such as a likely extreme load or a failure mode.

3.2 *Three examples*

In their report on the public inquiry into the Nicoll Highway collapse in Singapore, Magnus et al (2005) place the main responsibility on human errors in design. The diaphragm wall was designed to extend 3m below the soft marine clay into much stronger Old Alluvium. However, Magnus et al note that at the location where the collapse started, the surface of the clay had been eroded by a buried channel. Figure 1, taken from Whittle and Davies (2006), shows that as a result, the diaphragm had far less penetration into the Old Alluvium than was intended. The Inquiry report concludes that this "inadequate appreciation of complex ground conditions" was a contributory factor in the collapse. There was also an element of human error or poor communication, since the designer's original intention was for 3m penetration, yet the construction team were content to accept much less than this.

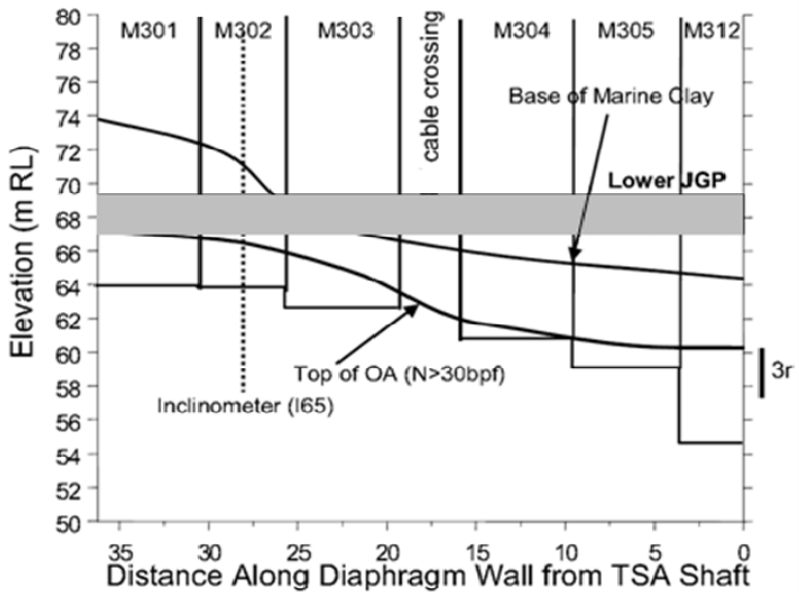

Figure 1. Lack of penetration at buried valley (after Whittle and Davies 2006)

Figure 2, taken from Potts et al (1990) shows a section through the Carsington dam embankment, which failed during construction. The cause was identified to be the presence of the "yellow clay", a layer that had not been identified in ground investigation and which behaved in a brittle manner, allowing the development of a progressive failure.

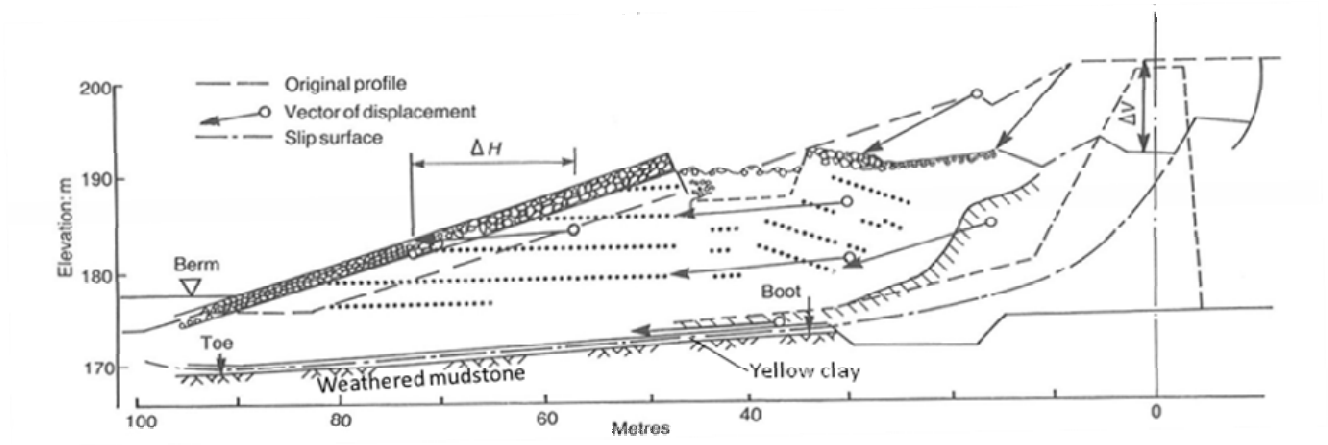

Figure 2. Cross section of Carsington dam (after Potts et al 1990)

Figure 3 shows an excavation for a small reservoir on sloping ground on Lias Clay in southern England. The "head" material was also stiff clay, but it had slipped down the slope and therefore contained pre-sheared surfaces, which also existed at the interface with the undisturbed material. The pre-sheared material exhibits a much lower angle of shearing resistance and, perhaps more important, does not dilate as it shears so its undrained strength is considerably lower. Failure to recognise these features led to the slip.

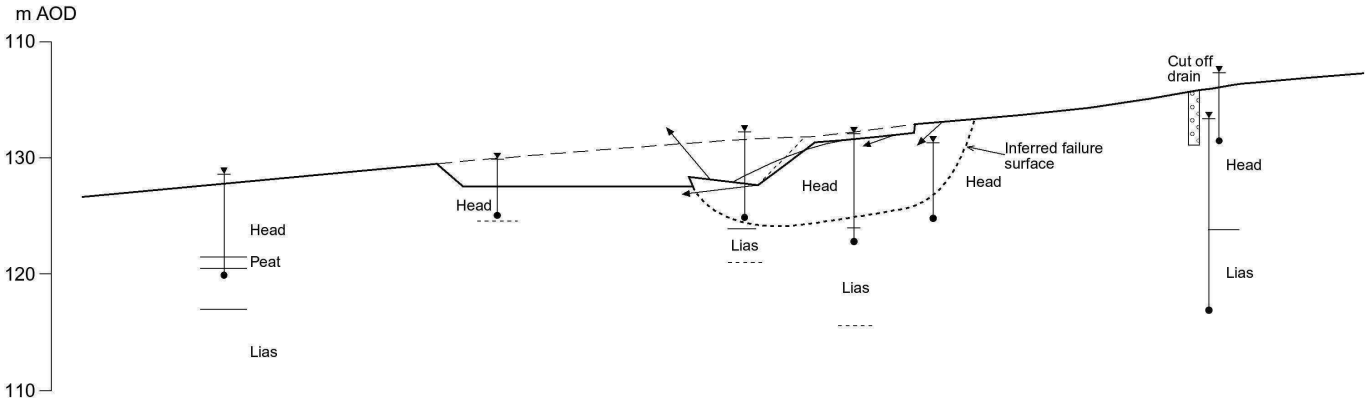

Figure 3. Slip at excavation for a small reservoir.

3.3 *Considering the "worst credible"*

In the writer's opinion, it is essential that engineering designers consciously consider the worst situations and parameter values that could be imagined on the basis of a reasonable and well informed engineering assessment. It is important that this involves and encourages "thinking outside the box", not merely extrapolating what is reasonably likely, but deliberately contemplating the effects of what is credible, even though unlikely. Simpson et al (1981) termed such a value the "worst credible" and suggested that it might be assumed to have a 1 in 1000 chance of occurrence, on the basis that designers would be unlikely to be able to believe that anything more remote might happen. The term "worst credible" will be used here with this meaning.

In contemplating the worst credible, designers need to give thorough consideration to the geological setting of the site, its history, geomorphology and hydrology. These have to be related to possible behaviour of the ground, including features such as buried channels, pre-sheared zones or slip surfaces, permeable bands within clays, etc., as illustrated by the three examples above.

None of these features are readily represented either by partial factors or in a reasonably simple reliability analysis. The danger of both these approaches is that applying prescribed factors or a more complex numerical calculation may give a false sense of security, attracting attention away from the essential tasks of geotechnical engineering discussed above.

EC7 attempts to tackle the problem of extreme conditions, to a degree, by providing extensive checklists of aspects of design and behaviour to be considered. In the writer's opinion, these are important, helping to outline the procedure to be undertaken in design, not just a numerical calculation. The writer

considers that one simple addition would improve EC7: to require that the designer checks that design values of ground parameters are, in his opinion, at least as severe as the "worst credible". In other words, it should not be possible that a ULS is caused by the occurrence (in a relevant body of soil) of a value for a ground parameter that the designer considered could credibly occur.

3.4 *Parametric variations*

It is often taught that calculations in which parametric variations of parameters are considered is a valuable feature of good engineering design. However, such calculations are rarely carried out, except in terms of load combinations, especially prevalent in bridge design. Parametric studies encourage checking a design for extreme values of parameters, usually considering one parameter at a time.

Conscious of these issues, Simpson et al (1981) proposed that designers should not enter calculations mainly on the basis of a "characteristic" or moderately "cautious" value, but that the starting point should be an assessment of the "worst credible" value of a parameter. A safety system was then devised, the "λ-method", in which this worst credible was taken as a pivot point, from which design values were derived. This was achieved by requiring the designer also to assess the "most probable" value, and using the difference between worst credible and most probable as a measure of uncertainty. The important point here, however, is that conscious thought about the worst credible was required.

Many safety formats used in codes of practice generate extreme values of parameters by applying partial factors. In most cases it becomes incredible that several variables could attain very extreme values simultaneously. This underlies the principles of load combinations following the principles developed by Turkstra and Madsen (1980), and much of seismic design, in both of which the effect of one dominant variable is considered while others are given less extreme values. When load combinations are used, it may be necessary to carry out several independent calculations, each treating a different action as the lead variable. This is also the underlying principle of "Design Approach 1" in EC7, in which two independent calculations are required, one with very severe loading, and the other with a very severe view of material strengths. In both cases, the "very severe" values are probably beyond the credible range, with the intention of ensuring that failure is incredible. The approach was discussed in more detail by Simpson (2007).

4 THE NEED FOR "ROBUSTNESS"

4.1 *Large number of secondary variables*

In conventional designs using factors of safety in some form, a small number of main variables is selected for factoring, effectively performing a parametric study. Similarly, in a reliability analysis a relatively small number of variables is usually considered. Real constructions in real ground are much more complex, and practical design has to accommodate a reasonable degree of unforeseen (and unforeseeable) variations in loading and geometry, including the precise disposition of materials and layers in the ground, and deterioration of structures. This is conventionally achieved, in part, by adopting additional margins or factors on the selected primary parameters.

For example, for situations dominated by water pressure, Simpson et al (2011) note that "secondary actions" could include sedimentation around a structure in water, excavation of the ground above a structure relying on the weight of ground, minor vehicle or ship impacts, considered too small to include in calculations, or vandalism of various kinds. If these "secondary" actions are large, failure could occur but the fault may be seen to rest with the owners or maintainers of the structure, or the vandals; alternatively, the designer should have foreseen them and was wrong to omit them from the primary actions for which the structure was designed. However, if the secondary actions are small, the owner would reasonably expect the structure to be sufficiently robust to withstand them. In this context, "large" and "small" effects have to be judged in relation to the magnitude of the primary actions.

It follows that the factors or margins applied to the primary parameters should accommodate the possible secondary parameters that are not otherwise included. These variations could be applied either to the actions themselves, in deriving design values, or to the action effects. Merely considering the variation of the primary parameters within the range the designer or code drafter considers credible may not provide sufficient safety.

4.2 *Human error*

In the writer's experience of investigating failures, errors in geotechnical engineering design are depressingly common. These include arithmetic errors, lack of expected basic knowledge, failures of communication, oversight or misunderstanding of important information, etc. Although such errors sometimes cause failures, it is fortunate for society and for the engineering profession that they often do not. In part, at least, this is because adequate factors or margins of safety have been incorporated in other aspects of the design.

A significant influence of human error in the results presented for trial calculations at the Eurocode 7 conference in Dublin was noted by Simpson (2005).

If an error is made involving a factor of 10, it is likely that the design will appear inadequate "by inspection" and it will be spotted during the process of design or construction. However, an error by a factor of 2 or less may be much more difficult to spot, except in cases of very repetitive design. Quality control and checking systems aim to catch such errors, but quite frequently fail. The agreed major cause of the Nicoll Highway collapse (Magnus et al 2005) was an error in steelwork design of this magnitude. Simpson et al (2008) argue that avoidance of other errors of similar or smaller magnitude could well have prevented the failure.

Errors also occur in construction, even when designs are sound. As with design errors, many of these do not cause failures because of the protection given by adequate margins or factors of safety.

The need for an adequate margin against human error is another important feature of robustness. It is essential that safety systems make provision for this. It is also important that codes and standards are both sufficiently comprehensive and sufficiently clear, and as simple as possible, in order to avoid misunderstandings that contribute to errors.

4.3 *Calibration – extrapolating from success*

A great deal of geotechnical design and construction leads to a successful outcome. This provides the biggest possible stochastic test of design approaches. It would be unwise, therefore to adopt a system that gave design results not comparable with conventional practice, especially if they were significantly less cautious.

In view of the difficulties of secondary variables and human errors, theoretical derivation of factors of safety has eluded most developers of codes of practice. Although reliability calculations are sometimes attempted, in reality almost all partial factors and margins used in codes have been derived by engineers considering what seems reasonable and, in particular, calibrating the factors to give results similar to previous, well tried practice.

Nevertheless, the need for both economy and sustainability motivate a gradual reduction in conservatism, until it becomes clear that this leads to failures, ULS or SLS. Hence it is appropriate to reduce factors of safety gradually as codes are evolved. A secondary issue for code drafters, in countries where designers have some freedom to choose between codes, is the fact that codes that give a more economic result will usually be adopted more readily.

Existing designs that have performed successfully have been adequate in terms of both ULS and SLS. Hence, in the calibration process it may be difficult to know whether the conventional factors or margins that were adopted were governed by the needs of ULS or SLS. This means that, inevitably, some of the partial factors used for ULS in codes, derived partly by calibration exercises, are influenced by the needs of SLS. It was noted above that it may be difficult to distinguish in practical design between mobilisation factors and partial factors of safety, and this difficulty also affects the calibration process.

5 RELIABILITY ANALYSIS

In the foregoing discussion, some basic requirements of a safety format to be used in geotechnical design have been considered. These have generally been expressed in terms of factors or margins of safety, which could be specified in codes and standards of the type currently available. The use of calculations based more directly on probability theory may have the potential to provide a more rational basis for design, if used directly by designers, or for the prescription of partial factors or safety margins in codes.

The analysis of the previous sections shows that an adequate safety format ought to include proper account of the following features:

- the designer's specific knowledge of the site, the ground conditions and their possible variability. This includes taking full account of the geology, history, geomorphology and hydrology of the site;
- an appropriate assimilation and compilation of data from all available sources, including published literature, collection of comparable case histories and test results, often form several types of test, of varying number, means of interpretation and reliability;
- a parametric study, to reveal the significance of variations of the lead variables;
- in particular, a careful assessment of the worst credible values of parameters. This will often not be obtained from a study of likely values and statistical variations around a mean;
- adequate robustness. This entails providing adequate margins for secondary actions and other variations that are not related to the primary parameters, including moderate human errors;
- adequate prescription for both ULS and SLS, noting that these may be difficult to separate.
- Reliability analyses have the advantage that they provide a comprehensive parametric study. In the author's view, it is possible that advanced reliability analysis may be able to take account of all the aspects listed here, including consideration of extreme values. However, simple reliability analysis, such as based on a study of means and standard deviations, will not achieve this. Indeed, such an analytical approach is more likely to distract attention from the main issues relating to geology, history, geomorphology and hydrology.

Although reliability analysis can provide an overall control on relative safety and economy, it is likely that use of partial factors can be targeted more precisely when using the outcome of calibration exercises.

6 CONCLUDING REMARKS

The purpose of the paper has been to consider what is needed in a safety format that reflects and encourages good geotechnical engineering. These basic requirements are listed in the previous section. It is very important that the attention of design engineers is concentrated on these aspects, and that they are distracted as little as possible by calculation. Hence, in the author's view, codes of practice should strive to provide for these requirements with as little complexity of calculation as possible.

The author submits that these principles should underlie the choice of safety format, whether partial factor, reliability calculations, or other approaches.

REFERENCES

Boverket. 1995. Design Regulations BKR 94 – Mandatory provisions and general recommendations. Swedish Board of Housing, Building and Planning.

BS8002. 1994. British Standards Institution Code of Practice for Earth Retaining Structures.

Magnus, R. Teh, C.I. & Lau, J.M. 2005. Report on the Incident at the MRT Circle Line worksite that led to the collapse of the Nicoll Highway on 20 April 2004. Subordinate Courts, Singapore.

Osman A.S. and Bolton M.D. 2006. Design of braced excavations to limit ground movements. Proceedings of Institution of Civil Engineers, Geotechnical Engineering 159 (3), 167-175.

Potts, D. M., Dounias, G. T. & Vaughan, P. R. 1990. Finite element analysis of progressive failure of Carsington embankment. Géotechnique 40, No. 1, 79-101.

Simpson, B. 2005. Eurocode 7 Workshop – Retaining wall examples 5-7. ISSMGE ETC23 workshop, Trinity College, Dublin.

Simpson, B. 2007. Approaches to ULS design – The merits of Design Approach 1 in Eurocode 7. ISGSR2007 First international symposium on geotechnical safety & risk. Tongji University, China.

Simpson, B, Morrison, P, Yasuda, S, Townsend, B, and Gazetas, G. 2009. State of the art report: Analysis and design. Proc 17th Int Conf SMGE, Alexandria, Vol 4, pp. 2873-2929.

Simpson, B. Nicholson, D.P. Banfi, M. Grose, W.G. & Davies, R.V. 2008. Collapse of the Nicoll Highway excavation, Singapore. Proc Fourth International Forensic Engineering Conference. Thomas Telford.

Simpson, B., Vogt, N. and van Seters, A.J. 2011. Geotechnical safety in relation to water pressures. Proc 3rd International Symposium on Geotechnical Safety and Risk (ISGSR2011), Munich, June 2011.

Turkstra C. J. & Madsen H. O. 1980. Load combinations in codified structural design. ASCE, ST12, 2527-2543.

ISGSR 2011 - Vogt, Schuppener, Straub & Bräu (eds) - © 2011 Bundesanstalt für Wasserbau ISBN 978-3-939230-01-4

The Effect of Model Uncertainty on the Reliability of Spread Foundations

W. S. Forrest & T. L. L. Orr
Trinity College, University of Dublin, Ireland

ABSTRACT: In reliability analyses of the ultimate limit state design of a spread foundation, the probabilistic modelling of the calculation model is often ignored. However, as part of any reliability analysis, it is important to consider the uncertainty in the calculation model as well as the uncertainties in the soil strength parameters and applied loads. This paper investigates the model uncertainty by applying a random variable model factor, *M*, to the calculation model and examining what level of variation this random variable would need to have to affect the reliability of a foundation design. This is carried out by increasing the coefficient of variation of *M* and observing the effect this has on the reliability index, β and on the sensitivity factors, α, which represent the relative sensitivities of the basic random variables. A spread foundation subjected to different loads is examined at the ultimate limit state for drained and undrained conditions. This paper shows that a model factor to account for the model uncertainty is not required in the ultimate limit state design of a spread foundation since the uncertainties in the soil strength parameters or the loads in the case of an eccentrically loaded foundation are found to control the reliability of the designs.

Keywords: Spread foundation, bearing resistance, model factor, reliability analyses

1 INTRODUCTION

In reliability analyses of the ultimate limit state design of a spread foundation, the probabilistic modelling of the calculation model is often ignored. As part of any reliability analyses, it is important to consider the uncertainty in the calculation model as well as the uncertainties in the soil strength parameters and applied loads. For example, in the bearing resistance equation for a spread foundation for drained conditions there is some uncertainty in the equation itself, in particular in the value of the N_γ factor. Phoon (2005) suggested the model factor be considered as a random variable in reliability analyses and that approach is adopted in this analysis.

This paper investigates the uncertainty in the calculation model by applying a model factor, *M*, as a random variable in the calculation model. The coefficient of variation of this model factor, CoV_M, represents the uncertainty in the calculation model and the value of CoV_M is increased to examine the effect this has on the reliability index, β and on the sensitivity factors, α, which represent the relative sensitivities of β to the different soil strength and load random variables in the calculation model.

2 RELIABILITY THEORY

2.1 *Limit state design concept*

In the last four decades there has been increased interest in the application of reliability theory in civil engineering. Part of this application of reliability theory has been in the design of structures to ensure their safety and their ability to fulfil their design requirements. Modern geotechnical design codes, such as Eurocode 7 (2004), are based on the limit state design concept, the fundamental concept of which is that all possible limit states for a structure must be considered and their occurrence shown to be suffi-

ciently unlikely to occur (Gulvanessian et al., 2002). In order to ensure that the occurrence of a limit state is sufficiently unlikely, a probabilistic or semi-probabilistic approach is adopted in the design process in order to achieve a certain target level of safety or β value.

2.2 *Bearing resistance calculation model*

Eurocode 7 gives in Annex D the following calculation model (equation) for the design drained bearing resistance, $R_{d,d}$, for a spread foundation:

$$R_{d,d} = A'(c'_d N_c s_c i_c + q' N_q s_q i_q + 0.5 B' \gamma' N_\gamma s_\gamma i_\gamma) \quad (1)$$

where:

$$N_q = e^{\pi \tan \phi'_d} \tan^2(45 + \phi'_d/2) \quad (2)$$

$$N_c = (N_q - 1)\cot \phi'_d \quad (3)$$

$$N_\gamma = 2(N_q - 1)\tan \phi'_d \quad (4)$$

$$s_q = 1 + (B'/L')\sin \phi'_d \quad (5)$$

$$s_\gamma = 1 - 0.3(B'/L') \quad (6)$$

$$s_c = (s_q N_q - 1)/(N_q - 1) \quad (7)$$

$$i_c = i_q - (1 - i_q)/(N_c \cot \phi'_d) \quad (8)$$

$$i_q = \left[1 - H_d/(V_d + A' \cot \phi_{d'})\right]^m \quad (9)$$

$$i_\gamma = \left[1 - H_d/(V_d + A' \cot \phi_{d'})\right]^{m+1} \quad (10)$$

$$m = [2 + (B'/L')]/[1 + B'/L'] \text{ when } H_d \text{ acts in the direction of B'} \quad (11)$$

where B' is the effective foundation breadth, L' is the effective foundation length, A' is the effective area (B' x L'), H_d is the design horizontal load and V_d is the design vertical load.

The design undrained bearing resistance, $R_{u,d}$, was determined using the calculation model in Annex D of Eurocode 7 consisting of the following equation:

$$R_{u,d} = A'((\pi + 2)c_{u,d} s_c i_c + q) \quad (12)$$

where A' is the effective foundation base area, s_c is a shape factor equal to 1.2 for a square foundation, q is the overburden pressure at the foundation base and i_c is an inclination factor given as follows, where H_d is the horizontal load:

$$i_c = 0.5(1 + \sqrt{1 - H_d/(A' c_{u,d})}) \quad (13)$$

2.3 *First-Order Reliability Method*

The first-order reliability method may be used to determine the β values for the designs and the sensitivity factors $\alpha_{tan\phi'}$, $\alpha_{c'}$, α_{cu}, α_γ, α_G, α_{Qv} and α_{Qh} for the random variables $tan\phi'$, c', c_u, G_v, Q_v and Q_h. This method was originally proposed by Hasofer and Lind (1974) for normally distributed variables and was later extended for non-normal distributions by Rackwitz and Fiessler (1978). In accordance with the reliability analysis program STRUREL (2004), all the basic variables are normalised as follows:

$$Z_i = (X_i - \mu_i)/\sigma_{X_i} \qquad \text{(for i = 1, ……N)} \quad (14)$$

The reliability analyses were carried out using the following equations as the performance or limit state functions that define the limit state surfaces for drained and undrained bearing resistance failure:

$$Z_1 = M_1 A'\left(c_d' N_c s_c i_c + q' N_q s_q i_q + 0.5 B' \gamma' N_\gamma s_\gamma i_\gamma\right) - \left(G_d + Q_{v,d}\right) \quad (15)$$

$$Z_2 = M_2 A'\left((\pi + 2) c_{u,d} s_c i_c + q\right) - \left(G_d + Q_{v,d}\right) \quad (16)$$

where M_1 and M_2 are the model factors for the drained and undrained equations respectively.

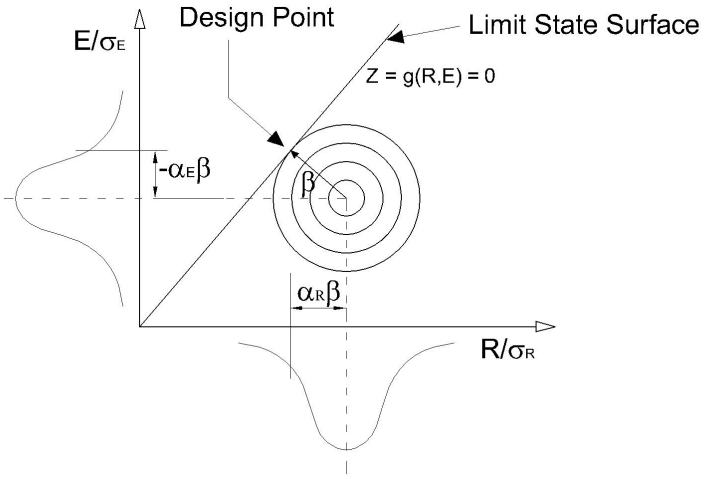

Figure 1. Reliability index and sensitivity factors in normalised space

The reliability index, β is defined as the minimal distance from the limit state surface to the origin in normalised space as shown in Figure 1. The sensitivity factors α_i, or cosine directors, are the components of the unit vector indicating the direction of the vector giving the minimal distance of the design point from the limit state surface (Honjo et al. , 2000). There is an α_i value for each random variable being considered in the reliability analysis and the α_i values are in the range -1 to +1. The closer a particular α_i value is to -1 or +1, the greater effect the random variable i has on the β value.

It was assumed that there is a positive correlation between the horizontal and vertical variable loads and a negative correlation between *tanϕ'* and *c' (Cherubini, 2000, Forrest and Orr, 2010b)*. All the other random variables were assumed to be independent. The assumed correlations between the random variables in this analysis are given in the correlation matrix in Table 1.

Table 1. Correlation matrix with correlation factors relating the random variables

	G	Q_v	Q_h	γ	$tan\phi'$	c'
G	1	0	0	0	0	0
Q_v	0	1	0.5	0	0	0
Q_h	0	0.5	1	0	0	0
γ	0	0	0	1	0	0
$tan\phi'$	0	0	0	0	1	-0.47
c'	0	0	0	0	-0.47	1

2.4 *Model factor*

A model factor to account for uncertainty in the bearing resistance equation is usually not included in the analysis of geotechnical design situations. However uncertainty in the calculation model may be significant and Rackwitz (2000) said it should be accounted for by including a quantity which captures the uncertainty in the calculation model. This is addressed in this study by applying a model factor, M, as a random variable with a mean value of unity to the calculation model, as shown in Equations 15 and 16, and examining what level of uncertainty in the calculation model, represented by the coefficient of variation of M (CoV_M), is necessary for this uncertainty to affect the reliability of the design. This is carried out by increasing the value of CoV_M and observing the effect this has on the β values and on the α_i values. The coefficients of variation (CoV) and probabilistic distributions for all the parameters are given in Table 2.

Table 2. CoVs and probability distributions for the parameters in the ULS sensitivity analyses

Parameter under analysis	Model factor		Other parameters	
	CoV range (%)	Distribution type	CoV range (%)	Distribution type
M	0 – 20	Normal	-	-
G	-	-	10	Normal
Q_v	-	-	20	Lognormal
Q_h	-	-	20	Lognormal
c_u	-	-	25	Normal
tanϕ'	-	-	10	Normal
c'	-	-	120	Gamma

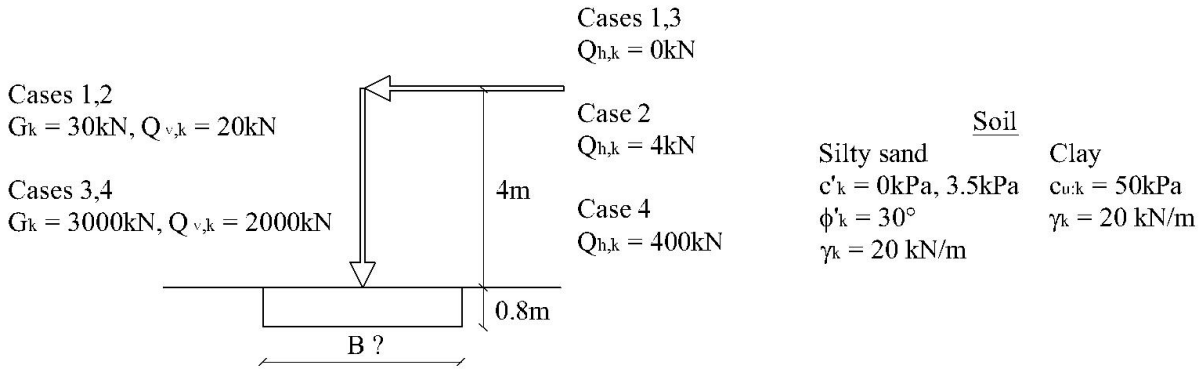

Figure 2. Square spread foundation

3 RELIABILITY ANALYSES

3.1 *Foundation design example*

To investigate the reliability of spread foundations designed to Eurocode 7, the following example shown in Figure 1 has been chosen, which is similar to an example for the International Workshop on the Evaluation of Eurocode 7 held in Dublin (Orr, 2005, Forrest and Orr, 2010a). This square pad foundation for a building is at 0.8m embedment depth, the groundwater at great depth, and two design situations, resting on a coarse-grained soil (silty sand) and on a fine-grained soil (clay), are considered. The first-order reliability method outlined above was used to design the foundation against ultimate limit state bearing resistance failure for the following four different load cases shown in Figure 1: Case 1 having small loads consisting of a characteristic vertical permanent load, G_k = 30kN, a characteristic vertical variable load, $Q_{v,k}$ = 20kN and no horizontal variable load, $Q_{h,k}$; Case 2 having the same small loads G_k = 30kN, $Q_{v,k}$ = 20kN but with $Q_{h,k}$ = 4kN; Case 3 having large loads consisting of G_k = 3000kN, $Q_{v,k}$ = 2000kN and $Q_{h,k}$ = 0; while Case 4 also having larger loads with G_k = 3000kN, $Q_{v,k}$ = 2000kN and $Q_{h,k}$ = 400kN.

Reliability analyses of the spread foundation were carried out assuming the dependencies between the random variables given in Table 2 for the four load cases listed above for drained conditions for the coarse-grained and fine-grained soils and for undrained conditions for the fine-grained soil. The results of these analyses are plotted in Figures 3 to 10 as graphs showing how the α values for the random variables in the analyses vary and the β values decreases as the value of CoV_M, increases. In the following discussion of the results of the analyses, a variable is only considered to have a significant influence on the β value if its α value exceeds 0.3.

3.2 *Results of drained reliability analyses*

The results of the drained reliability analyses of the vertically loaded foundation on coarse-grained soil plotted in Figures 3 and 4 show that, in both Case 1 and 3, tanϕ' is the only variable, apart from M, with an α value greater than ±0.3 and therefore this is the only variable which has a significant influence on the β value. When there is no model uncertainty (CoV_M = 0), $\alpha_{tan\phi'}$ is close to one and therefore tanϕ' dominates the entire reliability analysis. The sensitivity factors for all the other random variables, α_G, α_{Qv} and α_γ, are in the range -0.3 to 0.3 and therefore are not significant variables in these Cases. It can be seen that as CoV_M increases, α_M becomes the largest α value and M becomes the dominant variable when CoV_M >

17%. The magnitude of the loads has little effect on the reliability of foundation designs with vertical loads only since the α and β values in Figure 4 are similar to those in Figure 3.

For the vertically loaded foundations on fine-grained soil, the variations in the α values as CoV_M increases are more complex and are not the same as for Cases 1 and 3, as shown in Figures 5 and 6. In Case 1, $\alpha_{\tan\phi'}$ and $\alpha_{c'}$ are the leading random variables when $CoV_M = 0\%$. However, as CoV_M increases, α_M becomes dominant while $\alpha_{tan\phi'}$ reduces significantly and $\alpha_{c'}$ remains relatively unchanged. Interestingly, α_M has a larger value in Case 1 than in Case 3. Therefore the design on fine-grained soil is more sensitive to uncertainty in the calculation model when the loads are smaller and hence when the foundation breadth is smaller. When the load is larger, as in Case 3, Figures 5 and 6 show that the design is more sensitive to uncertainty in *c'* since the $\alpha_{c'}$ values are larger for Case 3 than for Case 1. The result is that, not only is $\alpha_{tan\phi'}$ reduced significantly in the case of the larger loads, but α_M is also reduced so that β is not greatly affected by uncertainty in the calculation model, even when the model factor has a large coefficient of variation (e.g. $CoV_M \approx 20\%$).

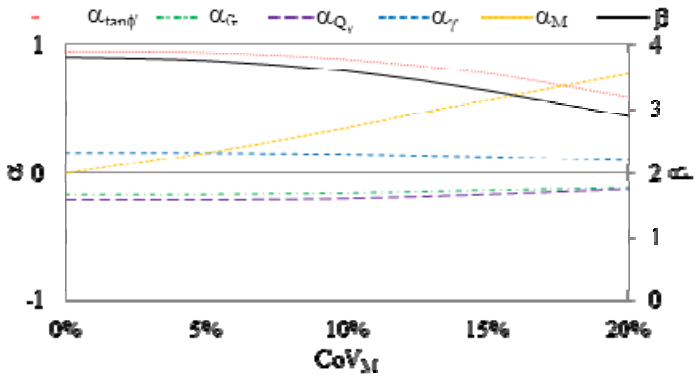

Figure 3. Sensitivity analysis of vertically loaded foundation with small loads on coarse-grained soil (Case 1)

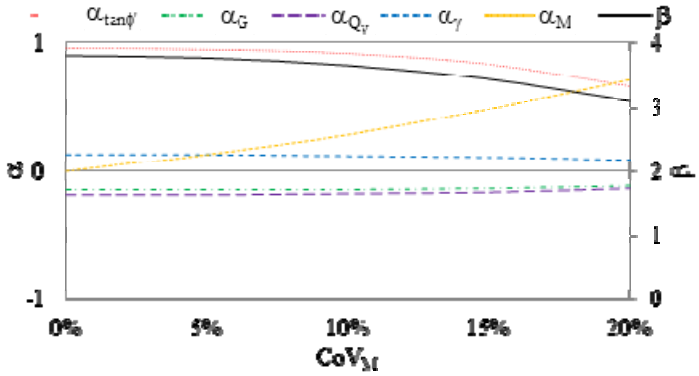

Figure 4. Sensitivity analysis of vertically loaded foundation with large loads on coarse-grained soil (Case 3)

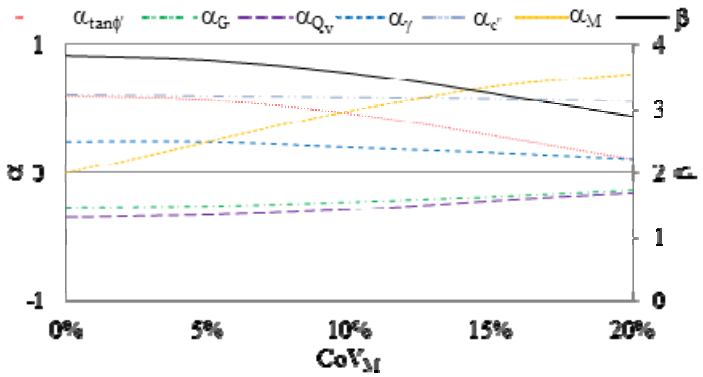

Figure 5. Sensitivity analysis of vertically loaded foundation with small loads on fine-grained soil (Case 1)

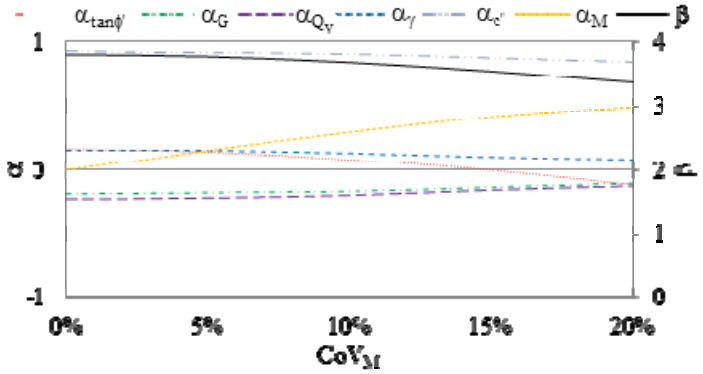

Figure 6. Sensitivity analysis of vertically loaded foundation with large loads on fine-grained soil (Case 3)

With regard to the two inclined-eccentrically vertically loaded foundations on coarse-grained soil, in Case 2, with the smaller vertical and horizontal loads, Q_h is the dominant variable and both G and tanϕ' (Figure 7) are significant as their α values exceed -0.3 and 0.3 respectively, whereas in Case 4, with the larger loads, tanϕ' is the dominant variable (Figure 8) since $\alpha_{tan\phi'} \geq 0.64$ while all the other α values are less than 0.3, This is due to the smaller loads in Case 2 requiring a smaller foundation width and hence the reliability of the designs is more sensitive to Q_h than to the soil strength parameters. In Case 2, the β values are only significantly affected by the model uncertainty, i.e. α_M is only > 0.3, when CoV_M > 17%. In Case 4, uncertainty in M has a greater effect since α_M becomes > 0.3 when CoV_M > 12%.

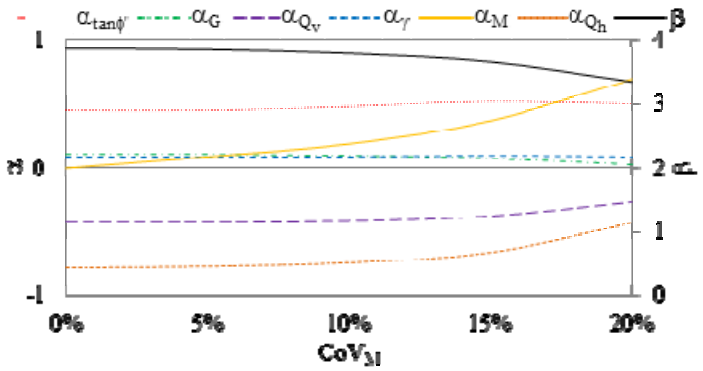

Figure 7. Sensitivity analysis of inclined-eccentrically loaded foundation with small loads on coarse-grained soil (Case 2)

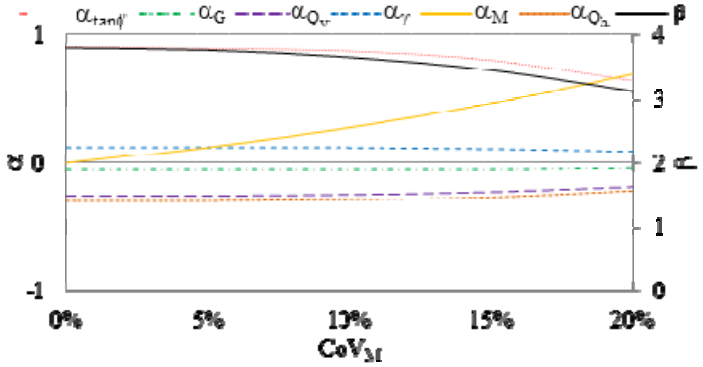

Figure 8. Sensitivity analysis of inclined-eccentrically loaded foundation with large loads in coarse-grained soil (Case 4)

For the two inclined-eccentrically loaded foundations on fine-grained soil, the graphs in Figures 9 for Case 2, the foundation with the small loads, show that α_M never exceeds 0.3 and therefore model uncertainty does not have a significant effect on the reliability, and, as for the inclined-eccentrically foundation on the coarse-grained soil, Q_h is the dominant variable. In Case 4, the foundation with the larger loads, the graphs in Figure 10 show that, while G is still significant with α_{Qv} > 0.3, c' dominates the reliability and uncertainty in the calculation model only becomes significant when CoV_M exceeds 15% and α_M exceeds 0.3.

3.3 *Results of undrained reliability analyses*

The reliability analyses of the foundations for undrained conditions were performed again for the CoVs and probabilistic distributions given in Table 2 and for the same four load cases. The results of these analyses showed that, for all the load cases, the α value for the undrained shear strength, c_u is close to 1.0 while the α values for the loads and the model factor are all close to zero and α_{c_u} remains close to 1.0 and the α values for the loads and α_M remain close to zero as CoV_M increases from 0% to 20% so that the β value is relatively unchanged. Therefore uncertainty in the calculation model has little effect on the β value for these four load cases and the variation c_u dominates the reliability of the designs.

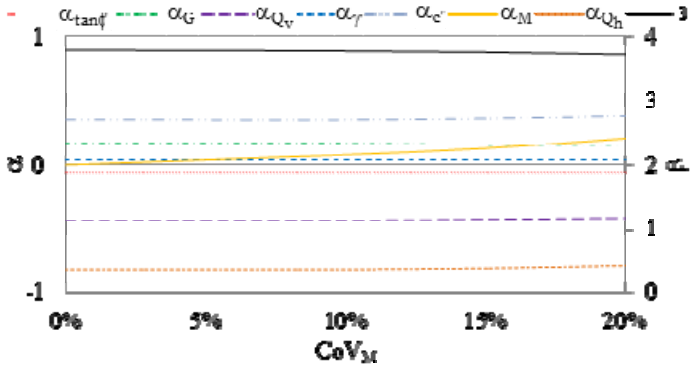

Figure 9. Sensitivity analysis of inclined-eccentrically loaded foundation with small loads on fine-grained soil (Case 2)

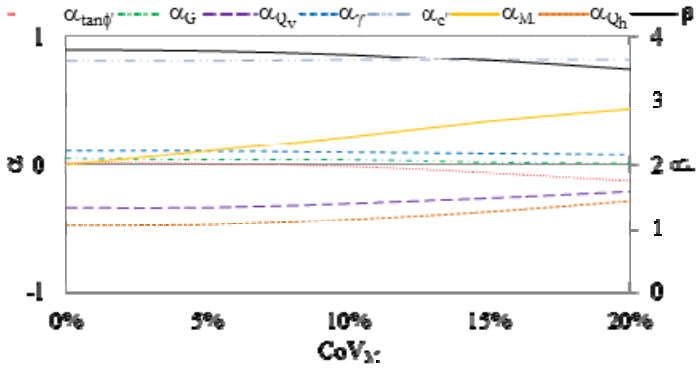

Figure 10. Sensitivity analysis of inclined-eccentrically loaded foundation with large loads on fine-grained soil (Case 4)

4 CONCLUSIONS

The effect of uncertainty in the calculation model for the bearing failure of a spread foundation has been investigated using reliability analyses for four load cases for both drained and undrained conditions. For all the cases examined, it has been found that the CoV_M needs to exceed about 15% before the uncertainty in the calculation model has any significant effect on the β value and hence on the reliability of a foundation design. Since in practice the CoV_M value will be very much less than 15% when using the bearing resistance equation for a spread foundation, the results of the analyses show that, for both drained and undrained conditions, it is not necessary to include a model factor in the design of a spread foundation subjected to either a vertical or an eccentric-inclined load because the uncertainties in the soil strength parameters or the loads will dominate the design. Uncertainty in the calculation model is more significant in the case of spread foundations for drained conditions than for undrained conditions due to the variation in the soil parameter values being less for the drained conditions. For undrained conditions, the uncertainty and variability of the undrained soil strength dominate the reliability of the design and the inclusion of a model factor has a negligible effect on the β values. Hence the inclusion of a model factor in the design of a spread foundation for undrained conditions will not significantly improve the reliability of the calculation. These findings justify the recommended value of 1.0 in Eurocode 7 for the partial model factor $\gamma_{R,d}$ to account for uncertainty in the calculation model for geotechnical designs.

REFERENCES

CEN 2004. EN1997-1:2004 Eurocode 7: Geotechnical design - Part 1: General rules. In: STANDARDIZATION, E. C. F. (ed.). Brussels.

CHERUBINI, C. 2000. Reliability evaluation of shallow foundation bearing capacity on c', f' soils. Canadian Geotechnical Journal, 37, 264-269.

FORREST, W. S. & ORR, T. L. L. 2010a. Reliability of Shallow Foundations Designed to Eurocode 7 Georisk: Assessment and Management of Risk for Engineered Systems and Geohazards, 4 Issue, 186-207.

FORREST, W. S. & ORR, T. L. L. 2010b. Reliability of spread foundations on clay designed using the Eurocode 7 Design Approaches. In: LI, J. C. C. & LIN, M.-L., eds. 17th South East Asian Geotechnical Conference, 2010b Taipei, Taiwan. Tiawan Geotechnical Society and South East Asian Geotechnical Society, 421-424.

GULVANESSIAN, H., CALARGO, J.-A. & HOLICKY, M. 2002. Designers' Guide to EN1990 - Eurocode: Basis of structural design, London, Thomas Telford.

HASOFER, A. M. & LIND, N. C. 1974. Exact and Invariant Second-Moment Code Format. Journal of the Engineering Mechanics Division, 100, 111-121.

HONJO, Y., SUZUKI, M. & MATSUO, M. 2000. Reliability analysis of shallow foundations in reference to design codes development. Computers and Geotechnics, 26, 331-346.

ORR, T. L. L. 2005. Proc. International Workshop on the Evaluation of Eurocode 7, Dublin, Kelly Comm. Print, Dublin 12.

PHOON, K. K. 2005. Reliability-Based design incorporating model uncertainties. 3rd International Conference on Geotechnical Engineering. Samarang, Indonesia.

RACKWITZ, R. 2000. Reviewing probabilistic soils modelling. Computers and Geotechnics, 26, 199-223.

RACKWITZ, R. & FIESSLER, B. 1978. Structural reliability under combined random load sequences. Computers and Structures, 9, 489-494.

STRUREL 2004. COMREL and SYSREL:Users Manual, Munich, RCP Consult GmbH.

ISGSR 2011 - Vogt, Schuppener, Straub & Bräu (eds) - © 2011 Bundesanstalt für Wasserbau ISBN 978-3-939230-01-4

Reliability analysis of tunnel final lining

P. Fortsakis, D. Litsas, M. Kavvadas & K. Trezos
National Technical University of Athens, Greece

ABSTRACT: Tunnel final linings are usually designed according to the methods and safety levels required by the Eurocodes. These codes are mainly applicable in conventional structures, where variability of the permanent loads is mainly due to the uncertainty of unit weights. On the contrary, the loads on the final lining of tunnels result from the interaction of the surrounding rock mass with the temporary support and the final lining. Therefore, they are subjected to much larger uncertainty as the geotechnical properties of the rock mass and the calculation model of the structural interaction both involve appreciable uncertainty. This paper investigates the variation of final lining loads using Monte Carlo simulation for the variability of the rock mass geotechnical parameters. The analyses show that the coefficient of variation of the loads is 20% - 50%, appreciably larger than the usually assumed typical value of 10% corresponding to the self weight and other permanent loads. As a result, reinforced concrete tunnel lining sections designed according to the partial factors of the Eurocodes have appreciably larger probability of failure than conventional reinforced concrete structures. The paper finally calculates the required modification of the partial factors for tunnel linings to achieve different reliability levels (e.g. the same reliability level with the conventional structures).

Keywords: Tunnel, final lining loads, Monte Carlo simulation, partial factors, reliability analysis

1 INTRODUCTION

Plain or reinforced concrete tunnel final linings are designed to undertake loads such as pressure from the surrounding geomaterials and groundwater, live loads, accidental loads (e.g. explosion, fire), temperature and seismic loads. Among them, the most important is the ground pressure applied directly (due to ground creep) or indirectly (due to long-term deactivation of the temporary support). The magnitude of this load depends on the interaction of the surrounding ground with the temporary support and the final lining and is influenced by the construction sequence and especially the time interval between the construction of temporary support and final lining in case of geomaterials with time dependent behaviour.

The final lining of tunnels is usually designed according to the methodologies and the partial factors proposed by the Eurocodes. These codes are mainly applicable in conventional structures, where variability of the permanent loads is mainly due to the uncertainty of unit weights. On the contrary, the loads on the final lining of tunnels result from the interaction of the surrounding rock mass with the temporary support and the final lining. Therefore, they are subjected to much larger uncertainty as the geotechnical properties of the rock mass and the calculation model of the structural interaction both involve appreciable uncertainty. The large uncertainty of the geotechnical parameters and the lack of a widely approved methodology for the design of the tunnel final lining have led to conservative designs with "hidden" safety factors, such as the empirical methods for the estimation of tunnel lining loads and the very conservative assumption of complete de-activation of all temporary support measures in the long-term. Consequently, failure incidents of tunnel final lining are rare, but the reason is an over-conservatism in the design rather than good understanding and modelling of the mechanisms involved.

This paper investigates the ground loads on the final lining of tunnels through probabilistic methods. In the first part the coefficient of variation of tunnel loads from the surrounding rock mass is estimated

using empirical and analytical methods through Monte Carlo simulation. The second part calculates the values of the partial factors of permanent loads to achieve different reliability levels. Analogous probabilistic approaches in tunnel excavation and loading are presented in the papers of Papaioannou et al. (2009), Mollon et al. (2009), Courage and Vervuurt (2009) and Fortsakis et al. (2010).

2 ESTIMATION OF FINAL LINING LOAD VARIATION

2.1 *Description of probabilistic analyses*

The factors controlling the uncertainty of tunnel final lining loads are the geometrical parameters (tunnel section, depth of overburden etc), the properties of the surrounding ground and construction materials (strength and deformability, including their long-term behaviour) and the empirical, analytical and numerical models used (e.g. constitutive models, failure criteria of the rock mass, etc). Since it is impossible to take into account all these factors, the present paper concentrates on the most important among them, which is the variability of the geotechnical properties of the rock mass surrounding the tunnel.

The rock mass properties are described using an elastic-perfectly plastic model following the Hoek-Brown failure criterion (Hoek et al., 2002). The model parameters are determined via empirical correlations with rock mass index properties such as the Geological Strength Index (GSI), the uniaxial compressive strength of the intact rock σ_{ci} and the rock-type constant m_i. The probabilistic characteristics of these parameters were originally quantified in the present paper taking into account suggestions from the literature (Hoek, 1998; Baecher, 1983; Park et al. 2005).

The coefficient of variation of GSI was determined from the density of the isolines in the GSI chart (Marinos and Hoek, 2000; Marinos et al., 2005). The range was assumed to be s=±5, for GSI values lower than 30, s=±7 for GSI between 30 and 40 and s=±10 for GSI values larger than 40. In the case where GSI distribution was assumed uniform the scatter defined the upper and lower limits and in the case where the distribution was assumed normal it defined the 90% confidence interval, leading to the calculation of the standard deviation. The coefficient of variation of σ_{ci} (assuming truncated normal distribution) was chosen in accordance with the values proposed for the cohesion (c), the undrained shear strength (S_u) and the unconfined compressive strength of soil formations in the literature (Harr, 1987; JCSS, 2001a; Kuhlway, 1992; Fredlund and Dahlman; 1971; Schultze 1971). The coefficient of variation of m_i (assuming truncated normal distribution) was calculated based on the values proposed by Marinos and Hoek (2001) assuming that the scatter corresponds to 90% confidence interval. The values of $V_{\sigma ci}$ and V_{mi} were decreased by 20% to take into account in an indirect way the spatial variation (El Ramly et al., 2002); whereas this decrease was not applied to GSI since it is a macroscopic parameter which corresponds to a large volume of rock mass. The rock mass deformation modulus was calculated according to the relationship proposed by Hoek et al. (2002) and the rock mass deconfinement due to tunnel face advance was determined based on the curves proposed by Chern et al. (1998).The values for all deterministic and probabilistic parameters used in the parametric analyses are presented in Table 1.

Final lining loads were estimated through widely used empirical and analytical methods: Terzaghi empirical method (Terzaghi, 1946), Unal (1983), Protodyakonov (1948), Terzaghi analytical method (Terzaghi, 1943) and convergence - confinement method (Duncan Fama, 1993). Although these methods are based on different assumptions and thus give a wide range of results (Fortsakis, 2009), they can provide a representative range for the coefficient of variation (V_p) of the final lining loads.

Table 1. Range of parameters for the final lining load probabilistic analyses.

Parameters	Range / Values
Overburden height	H = 20-300m
Tunnel section radius	R = 8, 10m
Geostatic stress ratio	K = 0.5-1.5
Rock mass unit weight	$\gamma = 0.025 MN/m^3$
GSI	Distribution: Normal, Uniform, m_{GSI} = 10-70 & σ_{GSI}: it depends on m_{GSI}
Intact rock uniaxial compressive strength	Distribution: Truncated normal, $m_{\sigma ci}$ = 4-30MPa & $V_{\sigma ci}$ = 25%
Material constant	Distribution: Truncated normal, m_{mi} = 6, 10 & V_{mi} = 10%, 16% (depends on m_{mi})
Disturbance factor	D = 0
Rock mass Poisson ratio	$\nu_m = 0.30$
Shotcrete thickness	$d_{shot} = 0.20m$
Shotcrete elastic modulus	$E_{shot} = 20GPa$
Shotcrete Poisson ratio	$\nu_{shot} = 0.20$

2.2 *Probabilistic analyses results*

The results of the stochastic analyses for all the empirical and analytical methods are presented in Fig. 1 as a function of GSI mean value or the mean geotechnical conditions quantified via the factor σ_c/p_o (σ_c=2ctan(45+φ/2), Mohr-Coulomb uniaxial compressive strength and p_o=γH, vertical geostatic stress). Terzaghi empirical method and Unal method lead to values of V_p from 5% to 25%. Protodyakonov method, due to the load mechanism adopted, results to a narrower range than the other two analytical methods (V_p=30%-45%) for most of the analyses. In the case of Terzaghi analytical method the distribution of V_p as a function of $m_{\sigma c}/p_o$ is "radial" since each "radius" corresponds to a different value of overburden height (V_p=10%-80%). Finally according to the results of the convergence - confinement method the coefficient of variation V_p lies between 10% and 80%.

Figure 2 illustrates the distribution of V_p as a function of the mean normalized load for the Terzaghi analytical method and the convergence – confinement method. It becomes evident that the large values of V_p correspond to low values of mean load, which is a result of the proportional large decrease of the denominator of V_p.

The very high values of variation (>60%) are not taken into account, since they correspond to favourable geotechnical conditions where the final lining loads are small and the values of V_p are much more sensitive to the computational procedure. For example in the Terzaghi analytical method, in case of high overburden, the silo mechanism leads to very low final lining load, resulting to unrealistically large values of V_p. Moreover the "weighting factor" of the analytical methods is larger than the one of the empirical methods, which are much simpler and take into account only one parameter. As far as the type of distribution of the load, it varies in respect with the method and the geotechnical conditions from symmetrical to highly non-symmetrical. Finally in the second part of the paper the distribution of the tunnel loads was assumed to be normal and the range for the load coefficient of variation is V_p=20%-50%.

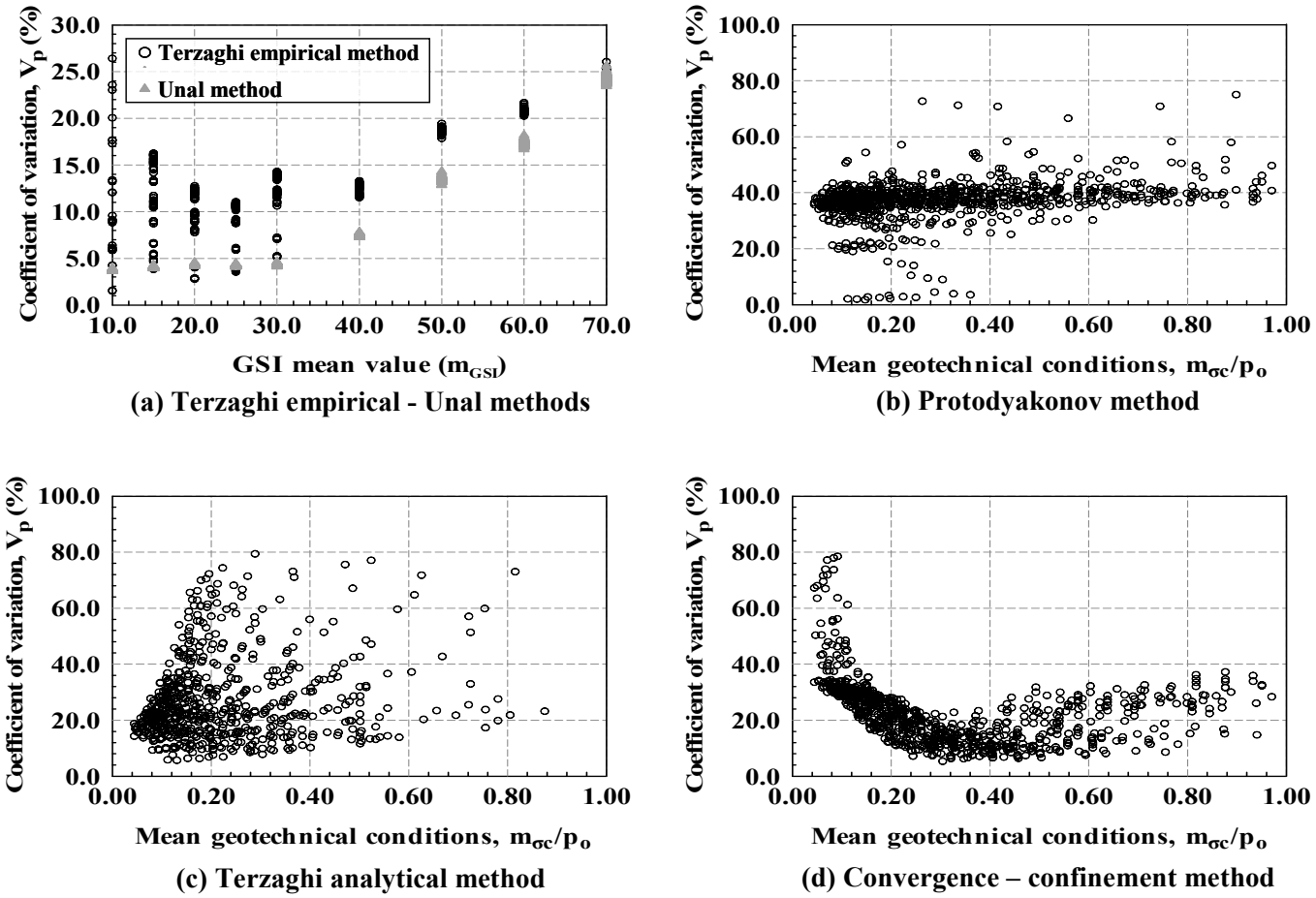

Figure 1. Calculation of coefficient of variation of tunnel final lining loads (V_p) through empirical and analytical methods and Monte Carlo simulation.

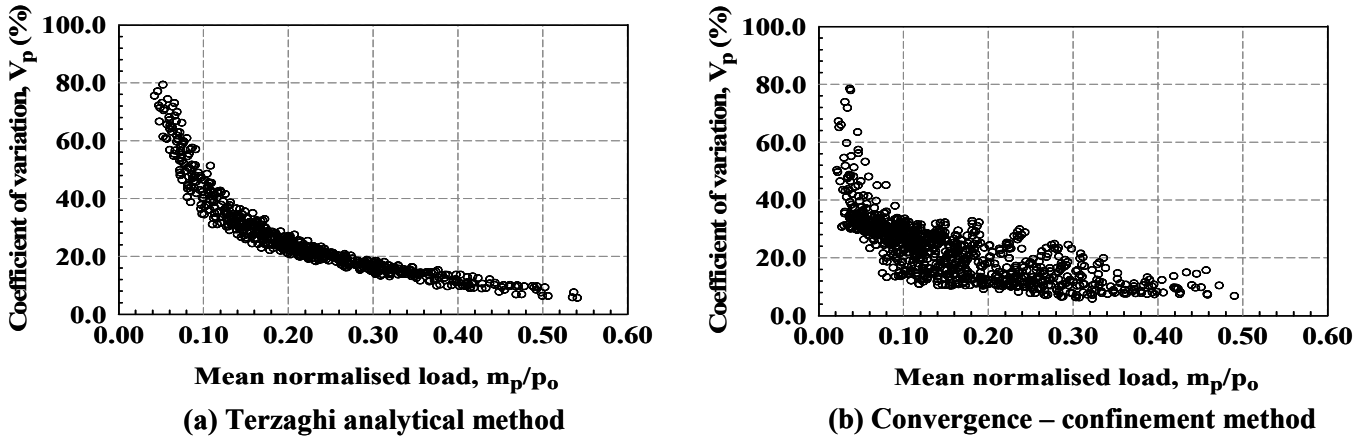

Figure 2. Coefficient of variation of tunnel final lining loads as a function of the mean normalized load.

3 RELIABILITY ANALYSIS OF FINAL LINING

3.1 *Description of probabilistic analyses*

According to Haar (1987) and JCSS (2001b) the coefficient of variation of the unit weight (main permanent load in conventional structures) can be assumed equal to 10%, significantly lower than the range calculated for the tunnel loads in the previous paragraph. The scope of the probabilistic analyses, in the second part, is to estimate the probability of failure (reliability index) of typical final lining sections constructed with reinforced concrete, subjected to loads with different coefficients of variation in terms of axial force and bending moment and consequently calculate the required partial factors, in order to achieve specific reliability levels.

The parameters used in the probabilistic analyses are presented in Table 2. The strength of concrete and steel were assumed to follow normal distribution and the coefficients of variations were set according to the suggestions of Araujo (2001) and Thomos and Trezos (2006). The variation of the axial force and moment has been assumed equal to the variation of the final lining load, since they are considered to be a result of this load only (the influence of live, accidental and other permanent loads is disregarded). Additionally this admission is reasonable as the design is based on elastic analyses. Bending moment has been expressed in terms of eccentricity $m_M = m_N \times e$.

Table 2. Parameters for the reinforced concrete probabilistic analyses.

Parameters	Range / Values
R/C section width	b_{RC} = 1.00m
R/C section height	h_{RC} = 0.30 – 1.00m
Concrete compressive strength	Distribution: Normal f_{ck} = 20, 25, 30MPa, V_c = 10%
Steel yield strength	Distribution: Normal f_{yk} = 400, 500MPa, V_s = 5%
Final lining load coefficient of variation (According to the results presented in the previous paragraph)	V_p = 10% – 50%
Mean value of axial force	m_N =0.10 – 8.00MN
Axial force eccentricity	e/h_{RC} = 0, 0.20, 0.40

Figure 3 illustrates the interaction diagram of a specific reinforced concrete section designed according to the partial factors proposed by Eurocodes. The range between the uniaxial strength in tension and compression has been divided into 1000 increments. For each one of the axial force values, the distribution of M_R is determined, through Monte-Carlo simulation (considering f_c and f_y as random variables). The probability of failure is equal to $p_f=p(M_R<M_{sd})$. It is evident that the breadth of the 90% confidence interval increases as the axial force increases since the participation of concrete, which has larger coefficient of variation than steel, is larger. Yet, in Figure 3-b it is shown that the reliability index β ($\beta=Erf^{-1}(1-p_f)$) is larger in the area of compression than the area of tension, due to the relatively large partial factor of concrete. The highest values of reliability index are calculated around the area of maximum moment (ν_d=0.40-0.60).

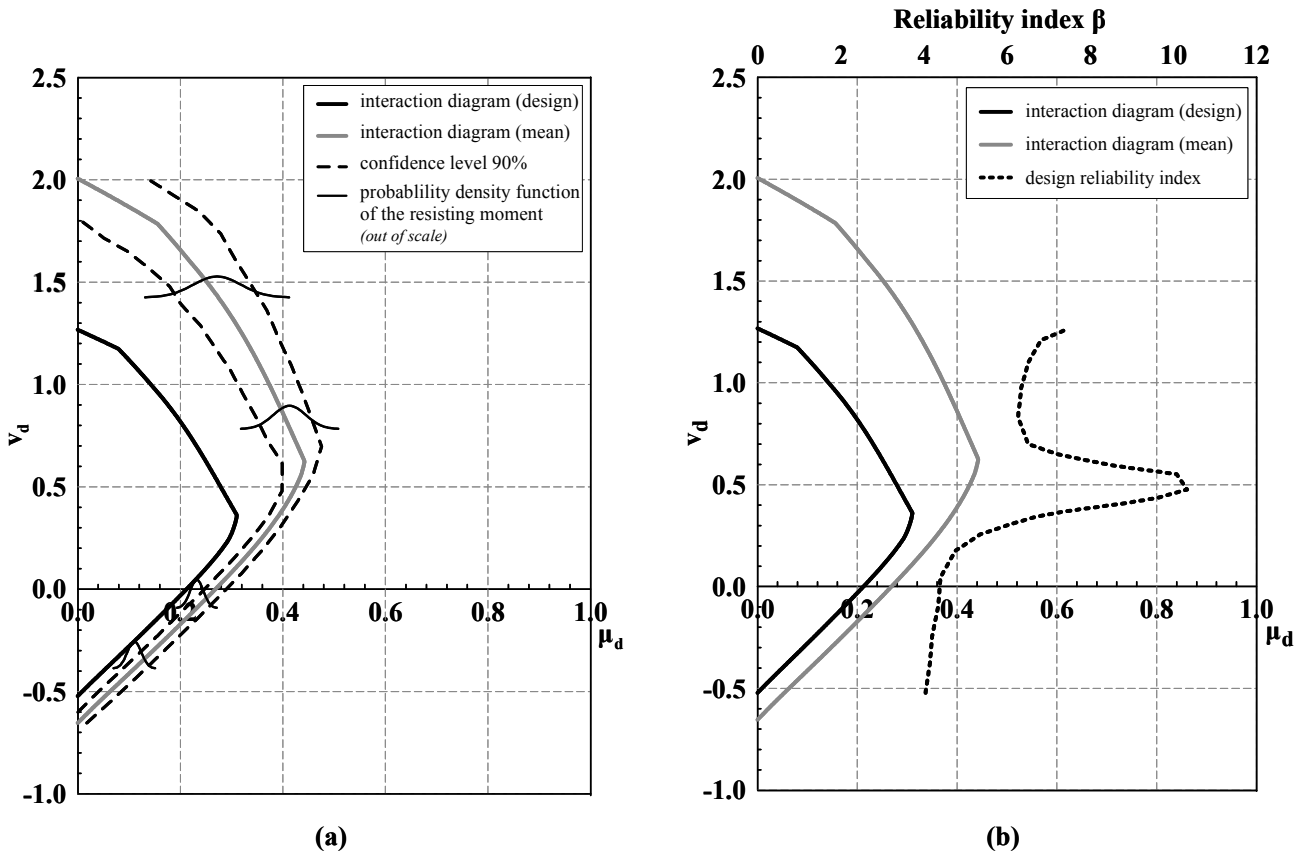

Figure 3. (a) Design and probabilistic interaction diagrams of a specific reinforced concrete section (b) Distribution of reliability index as a function of normalised axial force ν_d (b_{RC}=1.00m, h_{RC}=0.50m, A_S=40cm^2 per side, f_{ck}=25MPa, f_{yk}=500MPa, V_p=0.10).

3.2 *Probabilistic analyses with Eurocodes partial factor for permanent loads*

Initially the reliability level of the typical reinforced concrete sections for the different values of V_p is calculated. The value V_p=10% corresponds to the conventional structures and the values 20% to 50% to tunnel loads. It is noted that the value of V_p affects not only the probabilistic calculations but also the deterministic since it differentiates the characteristic values.

- Initial input parameters: b_{RC}, h_{RC}, m_N, e, V_N=V_M=V_p, f_{ck}, V_c, f_{yk}, V_s.
- Calculation of the mean value of concrete and steel strength (α corresponds to 95% percentile according to Eurocodes).

$$m_c = \frac{f_{ck}}{(1+aV_c)},\ m_s = \frac{f_{yk}}{(1+aV_s)} \qquad (1)$$

- Calculation of the mean value of bending moment: m_M=m_N×e.
- Calculation of the characteristic values of axial force and bending moment (α corresponds to 95% percentile).

$$N_k = m_N(1+aV_N),\ M_k = m_M(1+aV_M) \qquad (2)$$

- Calculation of the design values of all the parameters according to the partial factors proposed in Eurocodes.

$$N_d = \gamma_g N_k = 1.35N_k,\ M_d = \gamma_g M_k = 1.35M_k,\ f_{cd} = f_{ck}/\gamma_c = f_{ck}/1.50,\ f_{yd} = f_{yk}/\gamma_s = f_{yk}/1.15 \qquad (3)$$

- Calculation of the required reinforcement (A_s), which is considered symmetrically constructed. The minimum reinforcement is considered 0.008×b_{RC}×h_{RC}.
- Calculation of the probability of failure / reliability index of the reinforced concrete section considering the axial force, bending moment and strength parameters as stochastic variables following normal distribution through Monte Carlo simulation with 60000 iterations. The number of iterations leads to satisfactory convergence of the results.

The axial force and the bending moment are presented in terms of the normalised factors ν, μ. It is noted that the horizontal axis corresponds to the ν_d values calculated with $V_{p=}10\%$. Although values of ν_d larger than 1.00 are considered very high, they are plotted to illustrate the trend of the curves as axial force increases.

$$\nu = \frac{N}{bhf_{cd}},\ \mu = \frac{M}{bh^2 f_{cd}} \qquad (3)$$

According to the results of the parametric analyses (Figure 4) the reliability index decreases until a local minimum which corresponds to the maximum value of ν_d for which the minimum reinforcement is sufficient. This point depends on the values of V_p and e and it is not the same for all the curves because the horizontal axis corresponds to the ν_d of V_p=10%. Moreover in the case of e=0.20h_{RC} the distribution of β after the local minimum is qualitatively similar to the distribution of β in Figure 3-b. It must be noted that the reliability indexes are generally high especially compared to geotechnical problems.

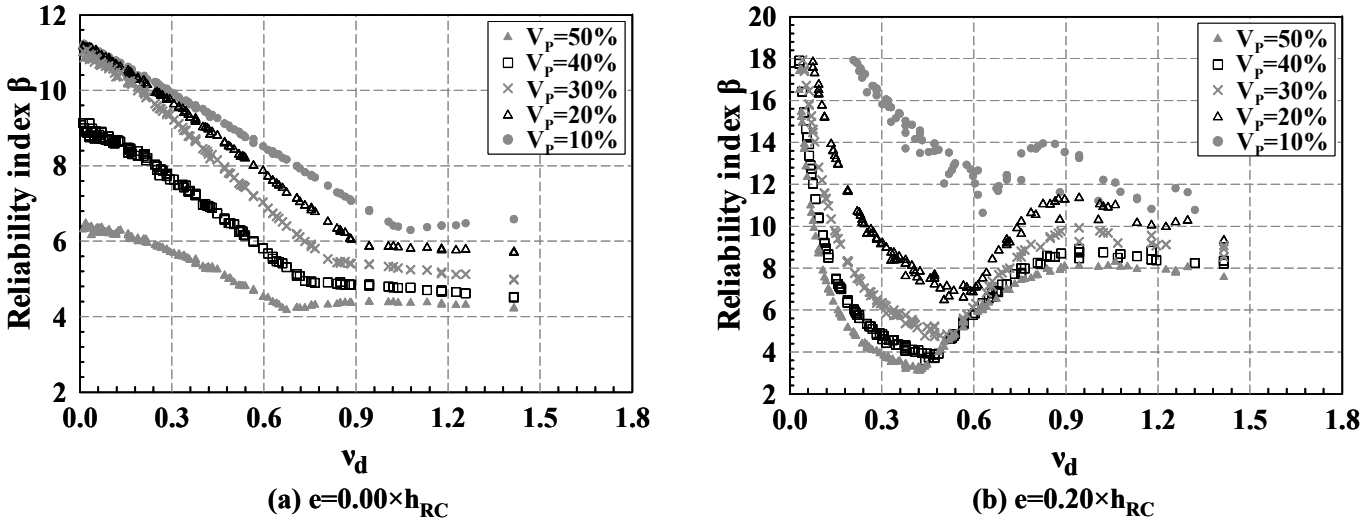

Figure 4. Distribution of reliability index as a function of design normalised axial force for two different values of eccentricity. (f_{ck}=25MPa, f_{yk}=500MPa). The horizontal axis (design value of the normalised axial force ν_d) corresponds to V_p=10% and γ_g=1.35.

3.3 *Calculation of permanent load partial factors for different reliability levels*

Based on the same methodology described for the probabilistic analysis in the previous paragraph, an iterative analysis is performed, in order to calculate the requisite partial factors of permanent loads for the following cases. During this procedure the dimension of each section studied remain constant and the additional strength required from the increased partial factor, that leads to the requisite reliability level is achieved through additional reinforcement. The results are presented in Figure 5 as a function of the normalised axial force ν_d for V_p=10%.

- Reliability index β = 4.26 – 5.61 (probability of failure (10^{-8} to 10^{-5}).
- Reliability index β equal to the reliability level of the same section which corresponds to loads with V_p=10%.

The values of the partial factors increase as the coefficient of variation and the reliability level increase. In the case that the requirement is the reliability level to be equal to the one corresponding to V_p=0.10, the resulting partial factors are very high, since the probability of failure was very low as it was discussed in the previous paragraph. Moreover the partial factors proposed by Eurocodes seem to be sufficient for the lower range of variation examined.

The distribution of the partial factors is similar to the reliability index distribution in Figure 4, whereas the local maximum of the partial factor diagram coincides with the local maximum of the reliability index one. This is presented in detail in Figure 6 where both variables have been plotted in the same diagram.

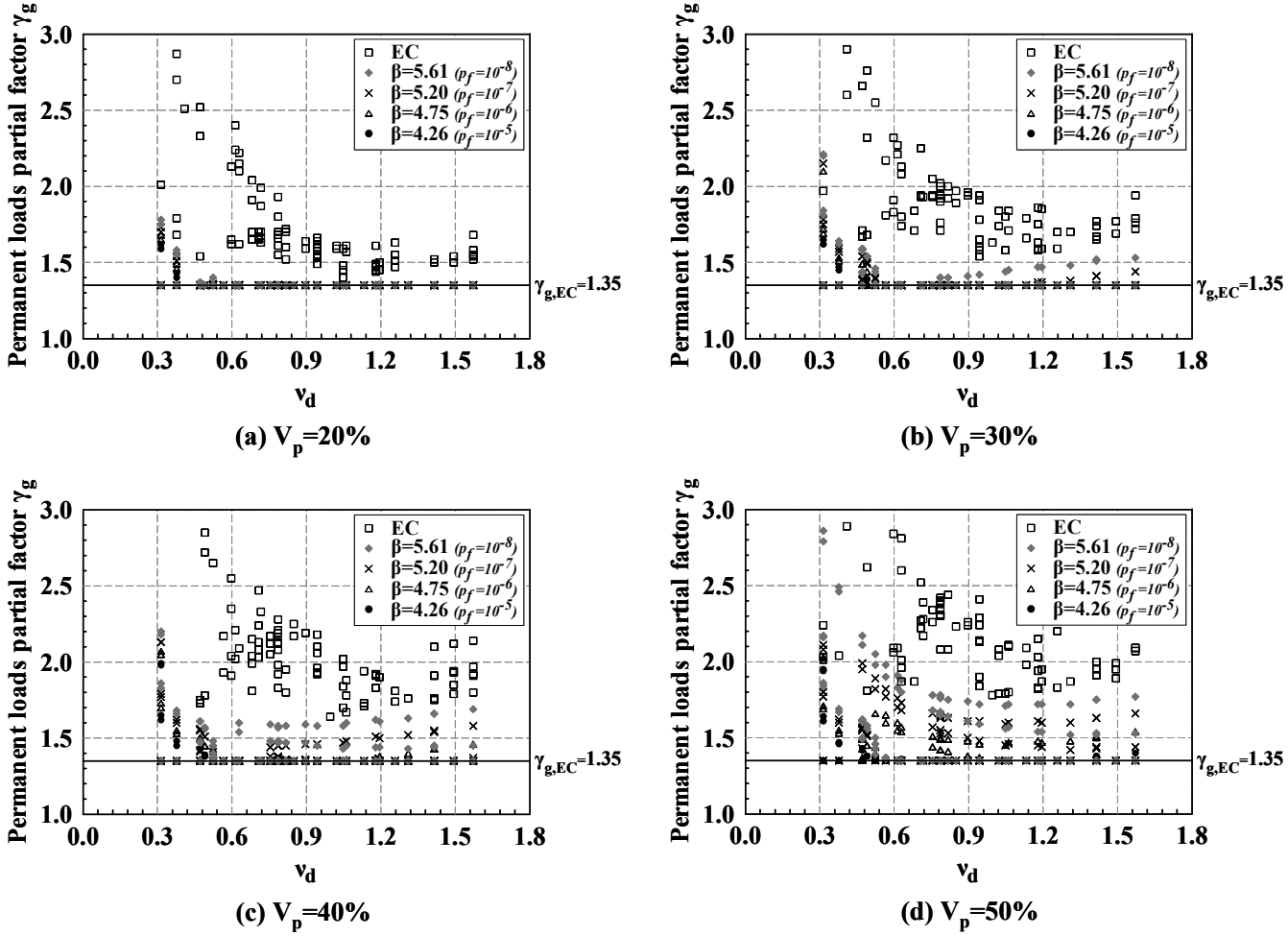

Figure 5. Requisite value of permanent load partial factor as a function of V_p and the reliability level. The symbol EC stands for the case where the demand is the reliability index to be equal with the corresponding of the case V_p=10% and γ_g=1.35. The horizontal axis (design value of the normalised axial force ν_d) corresponds to V_p=10% and γ_g=1.35.

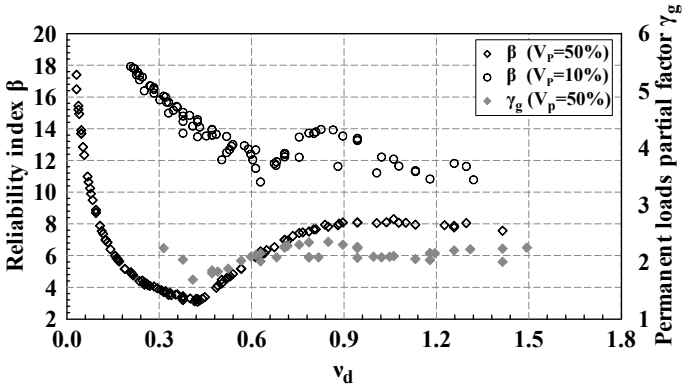

Figure 6. Distribution of reliability index β and calculated permanent loads partial factor γ_g as a function of ν_d (f_{ck}=25MPa, f_{yk}=500MPa). The horizontal axis (design value of the normalised axial force ν_d) corresponds to V_p=10% and γ_g=1.35.

4 CONCLUSIONS

The design of the final lining of tunnels has much larger uncertainties compared to conventional structures, because the applied loads result from the interaction between the surrounding ground, the temporary support and the final lining and, furthermore, the ground parameters include significant uncertainty. The paper performs probabilistic analyses using empirical and analytical methods for the estimation of the tunnel loads and concludes that the corresponding coefficient of variation V_p is in the range 20% - 50%. Actually, this range may be even larger, since not all the factors affecting the uncertainties of tunnel loading can be incorporated in probabilistic analyses. These values are much larger than the corresponding values for conventional structures.

Consequently, when the design of the final lining of tunnels is performed using the partial factors for conventional structural elements (e.g. those required by the Eurocodes), the design results in lower reliability level. Based on this conclusion, the required values of the partial factors for permanent load were determined for certain reliability levels. In the case of large coefficients of variation and high reliability level, the required partial factors increase significantly compared to the values proposed in the Eurocodes (1.35) and can range even between 2.0 - 2.5. The required increase of the partial factors leads to a corresponding increase in the steel reinforcement, which can be large in some cases. Because of that, and since ground variability cannot be reduced, there is a need to rationalise the design of final lining, establish more accurate design methods for the calculation of ground loads on tunnel linings and thus maintain a high reliability level combined with low cost.

REFERENCES

Araujo, J.M. 2001. Probabilistic analysis of reinforced concrete columns. Advances in Engineering Software, 32, pp. 871-879.

Baecher, G.B. 1983. Statistical analysis of rock mass fracturing. Mathematical Geology, 15 (2), pp. 329-348.

Chern, J.C., Shiao, F.Y., & Yu, C.W. 1998. An empirical safety criterion for tunnel construction. Proceedings of the Regional Symposium on Sedimendary Rock Engineering. Taipei, pp. 222-227.

Courage, W.G., & Vervuurt, H.M. 2009. Risk analysis software for underground constructions. Proceedings of EURO: TUN 2009, 2nd International Conference on Computational Methods in Tunnelling (Meschke, G., Beer, G., Eberhardsteiner, J. Hartmann, D. & Thewes, M. (eds)). Bochum, Germany, 9-11 September, 2, pp. 601-608. Freiburg: Aedificatio Publishers.

Duncan Fama, M.E. 1993. Numerical modeling of yield zones in weak rocks. In Comprehensive rock engineering (Hudson, J.A., Brown, E.T., Fairhurst, C. & Hoek, E. (eds)).

El Ramly, H., Morgenstern, N.R., & Cruden, D.M. 2002. Probabilistic slope stability analysis for practice. Canadian Geotechnical Journal, 39, pp. 665-683.

Fairbairn, E.M.R., Ebecken, N.F.F., Paz, C.N.M., & Ulm, F.J. 2000. Determination of probabilistic parameters of concrete: solving the inverse problem by using artificial neural networks. Computers and Structures, 78, pp. 497-503.

Fortsakis, P. 2009. Estimation of tunnel final lining loads. Proceedings of 4iYGEC (Baligh, F., Adbelmohsen, H., Abouseeda, H. & Abdelghani, K. (eds)). Alexandria, Egypt, 3-6 October, pp. 325-328.

Fortsakis, P. Arvaniti, D., & Kavvadas, M. 2010. Study of final lining loads via probabilistic methods. 6th Hellenic Conference on Geotechnical and Geoenvironmental Engineering. Volos, Greece 29 September – 1 October, pp. 587-594. Athens: Technical Chamber of Greece. (in Greek)

Fredlund, D.G., & Dahlman, A.E. 1972. Statistical geotechnical properties of glacial lake Edmonton sediments. In Statistics and Probability in Civil Engineering. London: Hong Kong University Press, distributed by Oxford University Press.

Harr, M.E. 1987. Reliability based design in civil engineering. New York: Dover Publications INC.

Hoek, E. 1998. Technical note, Reliability of Hoek Brown estimates of rock mass properties and their impact on design. International Journal of Rock Mechanics and Mining Sciences, 35, pp. 63-68.

Hoek, E., Carranza-Torres, C. & Corkum, B. 2002. Hoek-Brown failure criterion. Proceedings of 5th North American Rock Mechanics Symposium and 17th Tunnelling Association of Canada: NARMS-TAC, Toronto, Canada, 1, pp. 267-273.

JCSS (Joint Committee of Structural Safety). 2001a. Probabilistic model code, Part 3.7 – Soil properties.

JCSS (Joint Committee of Structural Safety). 2001b. Probabilistic model code, Part 2.01 - Unit weight.

Kulhawy, F.H. 1992. On the evaluation of soil properties. ASCE Geotechnical Specialty Publication, 31, pp. 55-115.

Marinos, P., & Hoek, E. 2000. GSI: a geologically friendly tool for rock mass strength estimation. Proceedings of GeoEng2000 at the International Conference on Geotechnical and Geological Engineering. Melbourne, Australia, pp. 1422-1446. Lancaster: Technomic publishers.

Marinos, P. & Hoek, E. 2001. Estimating the geotechnical properties of heterogeneous rock masses such as Flysch. Bulletin of Engineering Geology & the Environment, 60, pp. 85-92.

Marinos, V., Marinos, P., & Hoek, E. 2005. The geological strength index: applications and limitations. Bulletin of Engineering Geology and the Environment, 64, pp. 55-65.

Mollon, G., Dias, D., & Soubra, A.H. 2009. Reliability based approach for the stability analysis of shallow circular tunnel driven by pressurized shield. Proceedings of EURO: TUN 2009, 2nd International Conference on Computational Methods in Tunnelling (Meschke, G., Beer, G., Eberhardsteiner, J. Hartmann, D. & Thewes, M. (eds)). Bochum, Germany, 9-11 September, 2, pp. 593-600. Freiburg: Aedificatio Publishers.

Park, H.J., Terry, R.W., & Woo, I. 2005. Probabilistic analysis of rock slope stability and random properties of discontinuity parameters, Interstate Highway 40, Western North Carolina, USA. Engineering Geology, 79, pp. 230-250.

Papaioannou, I., Heidkamp, H., Duester, A., Rank, E. & Katz, C. 2009. Random field reliability analysis as a means for risk assessment in tunnelling. Proceedings of EURO: TUN 2009, 2nd International Conference on Computational Methods in Tunnelling (Meschke, G., Beer, G., Eberhardsteiner, J. Hartmann, D. & Thewes, M. (eds)). Bochum, Germany, 9-11 September, 2, pp. 585-592. Freiburg: Aedificatio Publishers.

Protodyakonov, M. 1960. Klassifikacija Gorotworu. In French T. at O.S. Paris, 1974.

Schultze, E. 1971. Frequency distributions and correlations of soil properties. Proceedings of 1st International Conference on applications of statistics and probability in soil and structural engineering. Hong Kong, pp. 371-387.

Terzaghi, K. Rock defects and loads on tunnel supports. 1946. In Rock tunnelling with steel supports (Proctor, R.V. & White, T.L. (eds)). pp. 17-99. Youngstown: Commercial Shearing and Stamping Company.

Terzaghi, K. 1943. Theoretical Soil Mechanics. 1943. New York: Wiley.

Thomos, G., & Trezos, C. 2006. Examination of the probabilistic response of reinforced concrete structures under static non-linear analysis. Engineering Structures, 28, pp. 120-133.
Unal, E. 1983. Design guidelines and roof control standards for coal mine roofs. PhD thesis. Pennsylvania State University.

ISGSR 2011 - Vogt, Schuppener, Straub & Bräu (eds) - © 2011 Bundesanstalt für Wasserbau ISBN 978-3-939230-01-4

A procedure for determining the characteristic value of a geotechnical parameter

A. J. Bond
Geocentrix Ltd, Banstead, Surrey, United Kingdom

ABSTRACT: Practising engineers are shown to be poor at predicting the appropriate degree of caution needed to select the 'characteristic' value of a geotechnical parameter, as defined by Eurocode 7. The paper presents a procedure for determining this characteristic value, based on simple statistical methods provided in readily available business software. The procedure is illustrated with data from two sites, obtained using cone penetration and standard penetration tests. Limitations of the procedure are discussed.

Keywords: characteristic value; statistics; Eurocode 7; worked examples

1 INTRODUCTION

Eurocode 7 defines the characteristic value of a geotechnical parameter as 'a cautious estimate of the value affecting the occurrence of the limit state'. For limit states that depend on the strength of the ground (typical of many ultimate limit states), it is the mean strength mobilized along the failure surface that is required – Eurocode 7 suggests that this should be selected with 95% confidence.

The author has conducted a series of experiments in which practising engineers have been asked to choose the characteristic value of various geotechnical parameters that vary with depth. The results reveal a very wide range of interpretations of the data – and that this variation increases as the data becomes more 'noisy'. The gap between the uppermost and lowermost interpretations is large enough to lead to significantly different design outcomes.

To help reduce this variation in interpretation, this paper proposes a simple procedure that engineers could follow to produce a repeatable characteristic value that is consistent with its definition in Eurocode 7. In outline, it involves the following steps:

1) Using readily-available statistical tools (such as those available in Microsoft Excel), determine the best-fit line through the data taking account of its variation with depth
2) Determine the residual (or fitting error) of each data point
3) Calculate the standard deviation of the residuals, s_X
4) Determine the appropriate degree of caution needed to establish a 95% confident mean value (using Student's statistical coefficient k_n, which takes account of the number of data points available)
5) Plot the resulting characteristic line parallel to the best fit line, using the expression $X_k = X_{mean} - k_n s_X$, where k_n is the statistical coefficient from Step 4 and s_X the standard deviation from Step 3

The paper illustrates this procedure with the results from a number of sites where the geotechnical parameter varies linearly with depth and compares the outcome with more rigorous statistical analysis. A variation on the procedure is outlined for situations where the geotechnical parameter does not vary linearly with depth.

2 DEFINITION OF THE CHARACTERISTIC VALUE

Eurocode 7 defines the *characteristic value* of a geotechnical parameter as:

a cautious estimate of the value affecting the occurrence of the limit state

Since the volume of ground that controls the occurrence of a limit state is usually much larger than a test sample, Eurocode 7 further states says that the characteristic value should be selected as:

a cautious estimate of ... the mean of a range of values covering a large surface or volume of the ground

In structural engineering, the resistance of the structure usually depends on the strength of an individual structural element. For example, the resistance of a concrete beam is limited by the strength of the concrete across its weakest section. The strength of the concrete across this section does not vary greatly, although it might differ across different sections. In the Eurocode system, the characteristic value in this case is selected as the 5% fractile, i.e. a value that will be exceeded in 95% of all tests.

A key aspect of geotechnical engineering, which is alluded to in thes second quote above, is that the resistance of a foundation usually depends on the strength of the continuum, not just an element of the ground. For example, the bearing resistance of a footing on clay is limited by the undrained strength of the soil along the external and internal boundaries of the failure mechanism. Any variation in strength of the clay along those boundaries is 'averaged out' over the whole mechanism. The characteristic value is a cautious estimate of that average value. In the Eurocode system, the characteristic value in this case is selected as the 50% fractile (i.e. the mean value) at the 95% confidence level.

3 ENGINEERS' ASSESSMENT OF CHARACTERISTIC VALUES

The task of assessing 'a cautious estimate' of a geotechnical parameter is not an easy one. This is most vividly demonstrated by comparing the estimates made by more than one hundred engineers who were asked to assess the characteristic value of various parameters from typical site investigation data.

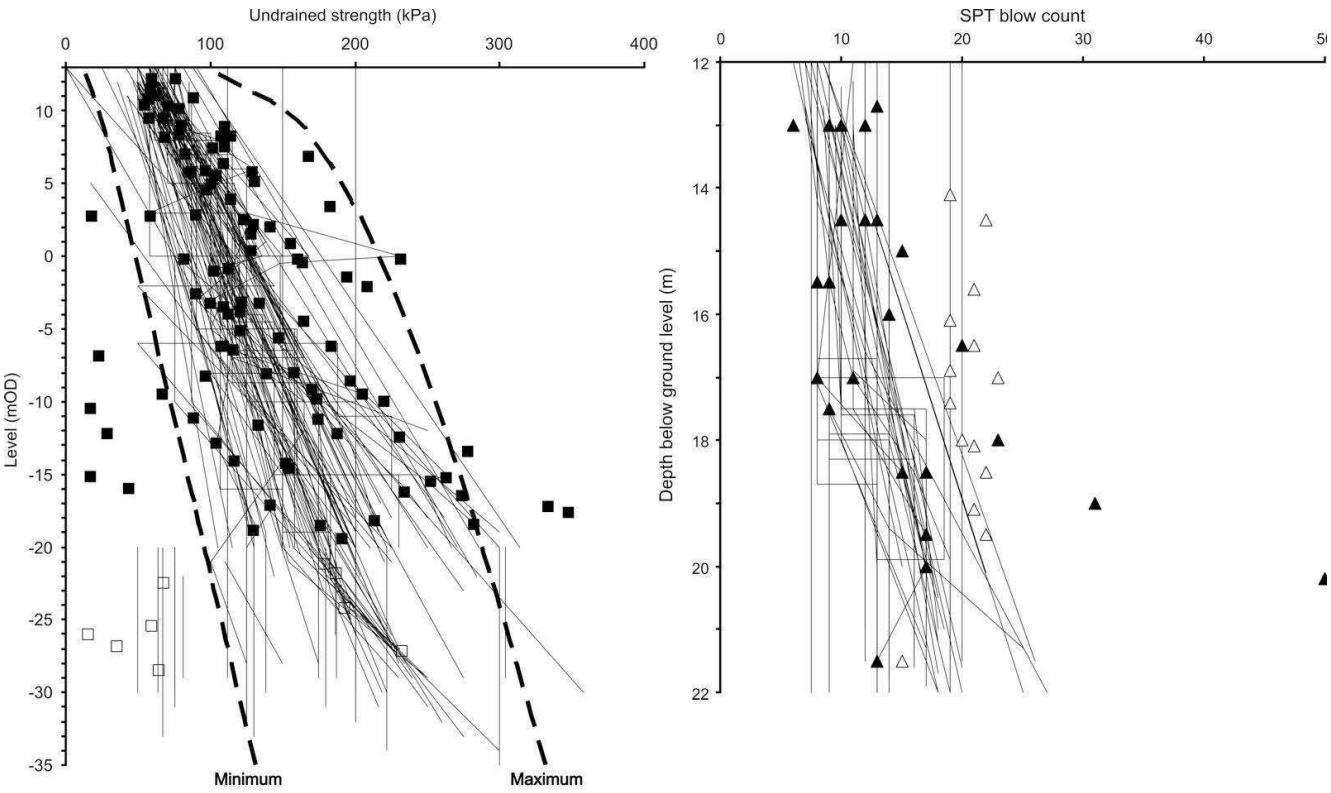

Figure 1. Engineers' interpretation of the characteristic value of (left) the undrained strength of London and Lambeth clays from results of triaxial compression tests; (right) SPT blow-count in Thames Gravels

Figure 1 (from Bond and Harris, 2008) shows, on the left, the results of triaxial compression tests on London and Lambeth clays and, on the right, blow-counts measured in standard penetration tests in Thames Gravels.

The symbols on these graphs represent individual data points and the superimposed lines are engineers' assessment of the characteristic value based on this data (alone). The scatter in the data is not at all unusual in these materials; the spread of the lines, however, is worrying, since it indicates little agreement between different engineers regarding the most appropriate value to select as 'characteristic'.

Bond and Harris concluded that "engineers are not particularly good at selecting a cautious estimate of the characteristic value, particularly when the available data is scattered. Statistical treatment of large data sets … may help to guide engineers in this task".

The remainder of this paper presents a simple procedure that can help in this task.

4 PROCEDURE FOR DETERMINING THE CHARACTERISTIC VALUE

4.1 *Step 1 – determine the best-fit line through the data*

The first step in the proposed procedure is to establish the best-fit line through the data, taking account any trend for the data values to increase or decrease with depth below ground surface.

For example, consider the results of four cone penetration tests (CPTs) conducted in dense sand, as shown in Figure 2 (left). The data is taken from ETC 10 Design Example 2.1 (ETC 10, 2009) and will be used in this paper to illustrate the procedure for establishing 'the' characteristic value.

As can be seen from Figure 2**,** there is a marked tendency for the measured cone resistance to increase with depth, as is commonly the case in dense sand. The water table at this site is located at 6 m below ground level.

A trend line through this data can be obtained using simple linear regression, using (for example) Microsoft Excel's 'Linear Trendline' feature. For one of the cone tests (CPT3), this produces the best-fit line shown in Figure 2 (right) given – with a coefficient of determination $R^2 = 0.7521$ – by the equation:

$$y = 0.487x - 4.66 \tag{1}$$

where y = depth below ground surface (z, in m) and x = measured cone resistance (q_c, in MPa). On rearranging the coefficients, we get the more useful expression:

$$q_c = 9.57 + 2.05z \tag{2}$$

which is illustrated by the dashed line on Figure 2 (right). Although this trend-line is a reasonable fit to the data down to about 7 m, it overestimates the cone resistance below that depth.

The 'coefficient of determination' R^2 is the square of Pearson's correlation coefficient R and is an imperfect measure of the trendline's 'goodness of fit'. See Wikipedia for a simple and easily-accessed explanation.

It is worth noting that Excel's 'Linear Trendline' feature (which one of its Chart Tools) does not always give reliable answers. In processing the results for CP4 for this paper, the predicted trendline was seriously in error and differed significantly from that produced by Excel's alternative Regression tool (in its Data Analysis pack) and other statistical software. This error became apparent when comparing the predicted trendline with the raw data. This reiterates the importance of *looking* at the data, not just processing the numbers!

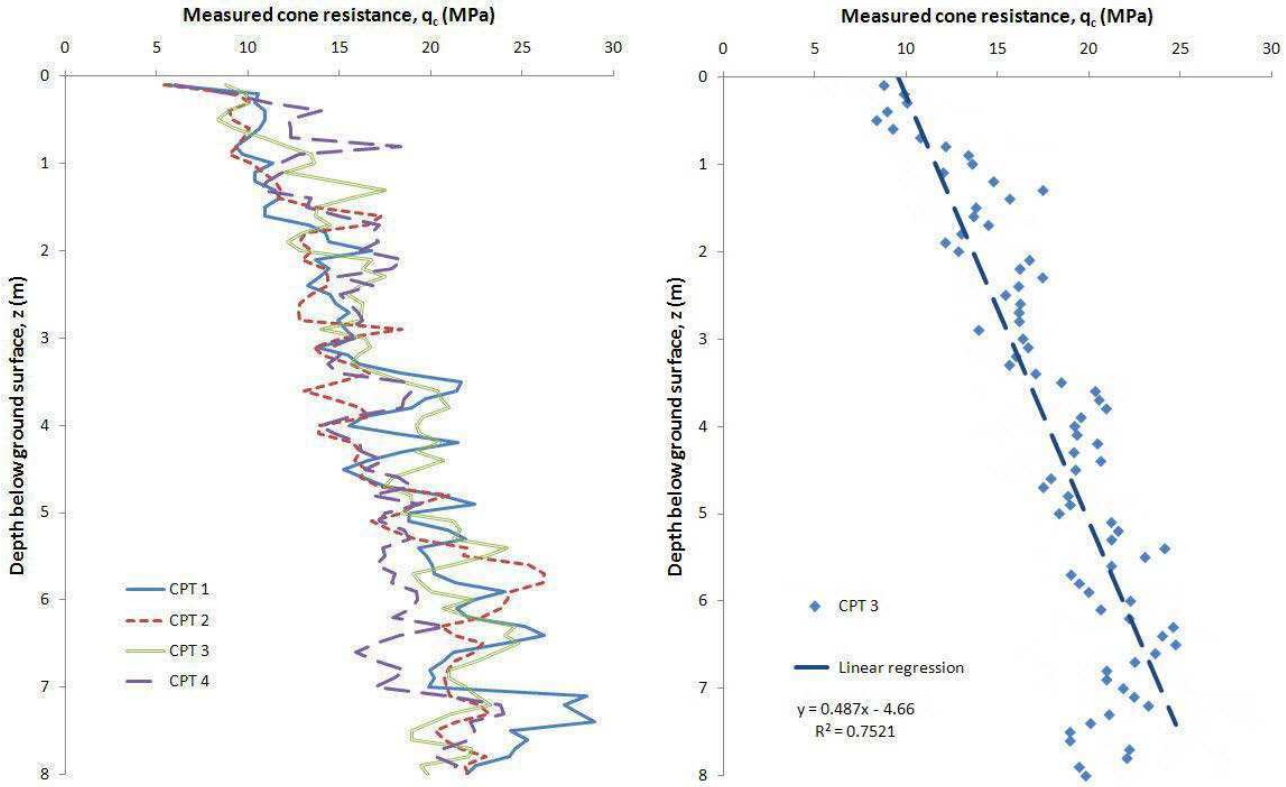

Figure 2. (left) measured cone resistance vs depth from four CPTs; (right) best-fit linear regression through data from CPT3

4.2 *Step 2 – determine the residual (or fitting error) of each data point*

The second step in the procedure is to determine the difference between each data value and that predicted by the best-fit line – in other words, the horizontal separation of each data point from the trend line shown in Figure 2 (right). These 'residuals' are plotted (to an enlarged scale) versus depth in Figure 3 (left) and as a histogram in Figure 3 (right).

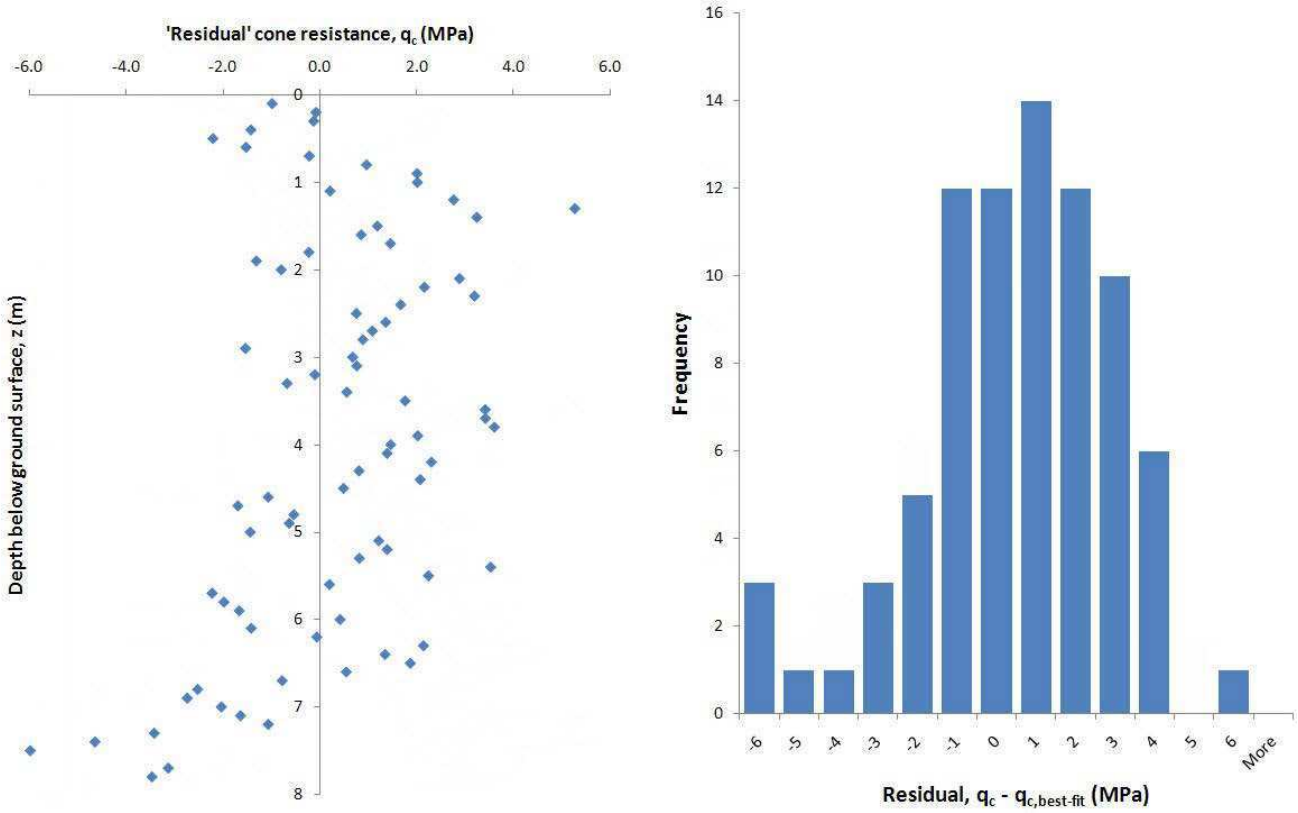

Figure 3. (left) residuals calculated for CPT3; (right) histogram of the same residuals

It is important to plot the residuals at this stage in the procedure, in order to detect any skew in the trend line. In this example, there is a marked tendency for the residuals to become negative below 7 m, suggesting that the trend line overestimates cone resistance below this depth (Figure 3, left). The histogram (Figure 3, right) makes this even more apparent, indicating that the data set as a whole, while broadly following a normal distribution (i.e. a bell-shaped curve) about a zero value, clearly is not homogenous.

Although not shown here, similar departures from a strictly linear trendline are obtained for CPTs 2 and 4. These results necessitate re-evaluation of the chosen trendline and – although there are several techniques that could be employed to obtain a better trend – for simplicity here I am going to ignore all data below the water table at 6 m. Hence the prediction made from now on will apply solely to the dry sand.

Repeating the procedure followed thus far, but on the reduced data set for CPT3, gives the revised residuals and corresponding histogram shown in Figure 4 and a trendline expressed by:

$$q_c = 9.05 + 2.47z \tag{3}$$

where z = depth below ground surface (in m) and q_c is cone resistance (in MPa).

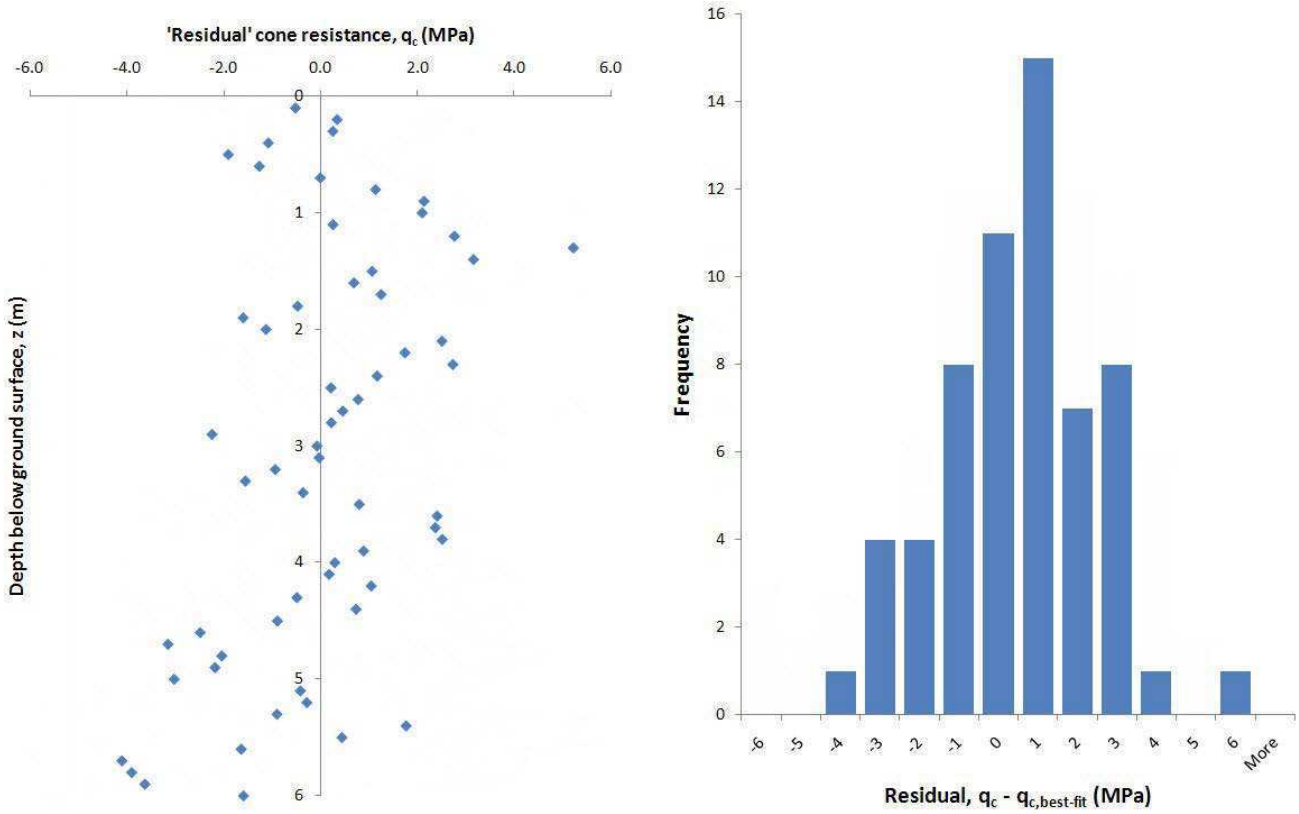

Figure 4. (left) revised residuals calculated for CPT3; (right) histogram of the same revised residuals

The residuals appear more evenly scattered about the zero line and the histogram – although not perfectly following the expected bell-shaped curve – nevertheless gives a much improved fit (cf Figure 3, right).

4.3 *Step 3 – calculate the standard deviation of the residuals*

The next step in the procedure is to calculate the standard deviation s_X of the residuals, assuming (in this case) a normal distribution about zero. This can once again be achieved readily using Microsoft Excel's STDEV() function applied to the residuals. For the data from CPT3, this gives s_X = 1.88 MPa.

4.4 *Step 4 – determine the appropriate degree of caution*

Eurocode 7 requires the characteristic value of a spatially-averaged parameter to be selected as a 95% confident mean value. As explained by Bond and Harris (2008, §5.5.2), the lower (or 'inferior') characteristic value $X_{k,inf}$ of a geotechnical parameter X is given by:

$$X_{k,\inf} = m_X - k_n s_X \tag{4}$$

where m_X is that parameter's mean value (i.e. as predicted by the trend line from Step 1); s_X is the standard deviation calculated in Step 3; and k_n is a statistical coefficient that depends on number of data points available, n. For cases where the standard deviation is not known *a priori*, this statistical coefficient is given by:

$$k_n = t_{n-1}^{95\%} \times \sqrt{1/n} \tag{5}$$

where $t_{n-1}^{95\%}$ is Student's t-value for $(n - 1)$ degrees of freedom at a confidence level of 95%, as shown in Figure 5 (from Bond and Harris, 2008).

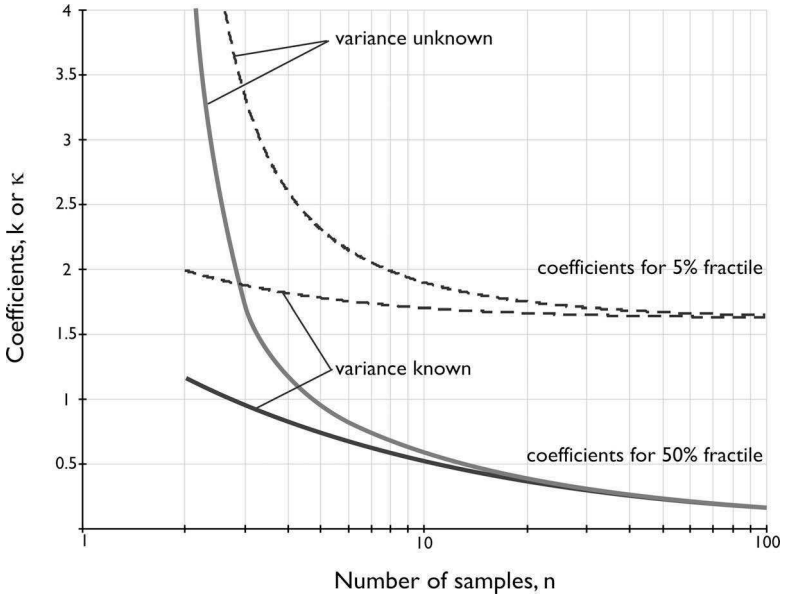

Figure 5. Statistical coefficients for determining the 5% and 50% fractiles with 95% confidence

Hence, to determine the appropriate degree of caution, we need to look up the value of k_n from Figure 5 for the 50% fractile, with variance unknown. The 50% fractile is chosen because we are seeking the *mean* value of cone resistance; the 'variance unknown' curve is chosen because we rarely know the degree of scatter our tests results are likely to have.

For the $n = 60$ data points shown in Figure 2 (right) above 6 m, $k_n = 0.216$. Hence the mean value of q_c predicted by the trend line given by Equ. (3) must be reduced by an amount Δq_c given by:

$$\Delta q_c = -k_n \times s_X = -0.216 \times 1.88 = -0.406 MPa \tag{6}$$

where $s_X = 1.88$ MPa was calculated in Step 3.

4.5 *Step 5 – plot the resulting characteristic line*

The final step in the procedure for determining the characteristic value is to adjust the best-fit line by the amount calculated in Step 4.

Figure 6 shows predictions of the characteristic values (solid lines) – and compares them with the corresponding best-fit lines for the reduced data set (dashed lines) – for all four cone tests.

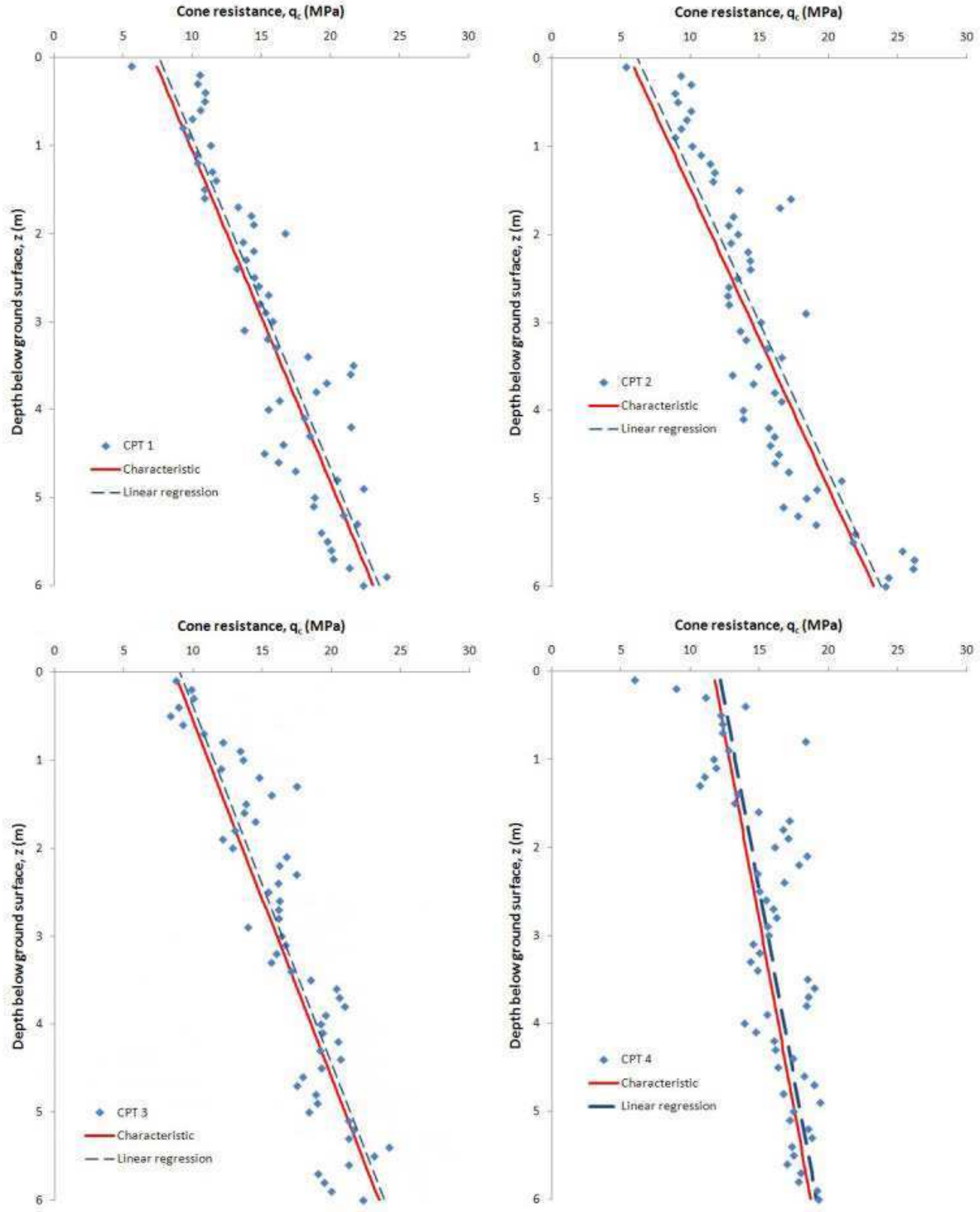

Figure 6. Characteristic mean lines through the data (solid lines) compared with actual mean (dashed lines) for (top-left) CPT1; (top-right) CPT2; (bottom-left) CPT3; and (bottom-right) CPT4

It is remarkable how small the separation between the solid and the dashed lines is, which is a consequence of the large number of data points available (60) and the reasonably small degree of scatter in the data (which was obvious from Figure 2, left). In other circumstances, the separation would be much greater.

5 SECOND EXAMPLE

The procedure described above has been applied the results of standard penetration tests performed at a site comprising highly variable Boulder Clay. The data is taken from ETC 10 Design Example 2.2 (ETC 10, 2009) and is shown in Figure 7 together with the best-fit linear regression line (dashed) and the predicted characteristic line (solid). The two very high blow counts (> 90) at 6 m have been ignored.

Figure 7, characteristic mean line (solid) compared with actual mean line (dashed) for standard penetration test results from ETC 10 Design Example 2.2

In this example, there are only 28 usable data points and so, from Figure 5, $k_n \approx 0.322$ (compared with 0.216 used previously for CPT3, i.e., 50% higher). With a larger deviation in data as well, this results in greater separation between the best-fit and characteristic lines.

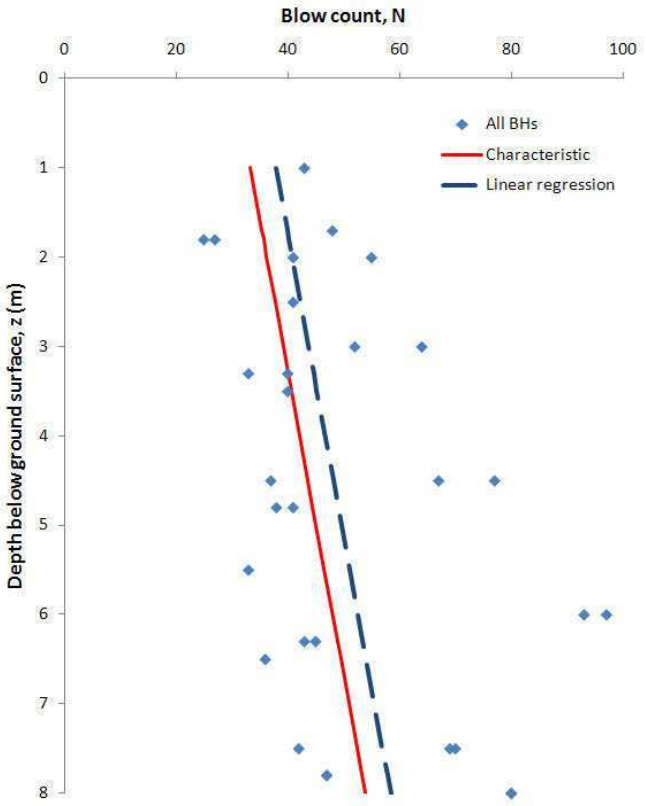

Figure 7.

6 LIMITATIONS OF THE PROCEDURE

The procedure described in this paper has a number of important limitations. First, it has been assumed that the data values increase linearly with depth; second, that the scatter in the data is random (i.e. there is no systematic influence affecting the data points); and third, that the differences between the data points and the trend-line (the residuals) fit a normal distribution.

The first limitation may be overcome by adopting a non-linear trendline, based perhaps on geological and geotechnical knowledge of the site. The second limitation is more difficult to overcome, since it is rare that we have sufficient knowledge to understand any systematic relationship between successive data points. In the absence of that knowledge, this is a limitation that we must live with. The third assumption can be checked during the procedure and data points omitted (as was done earlier) to rectify if possible.

7 CONCLUSION

Predictions of the characteristic value of a geotechnical parameter have been shown to vary greatly from one engineer to another, particularly when the data on which those predictions are made is highly scattered. Unfortunately, for many sites that is often the case. A procedure has been proposed to enable a consistent prediction of the characteristic value to be made using simple statistical techniques that follow the principles of the Eurocodes and are relatively easy to put into practice. The results of this procedure have been illustrated with data from two sites, one in sand and the other in clay.

REFERENCES

Bond, A. J. and Harris, A.J. (2008). Decoding Eurocode 7, Taylor and Francis, London, 608pp.

EN 1997-1, Eurocode 7: Geotehnical design – Part 1: General rules.

ETC 10 (2009). ISSMGE European Technical Committee 10, Evaluation of Eurocode 7. Design Examples 2 can be found at www.eurocode7.com/etc10.

Wikipedia, http://en.wikipedia.org/wiki/Pearson_product-moment_correlation_coefficient

ISGSR 2011 - Vogt, Schuppener, Straub & Bräu (eds) - © 2011 Bundesanstalt für Wasserbau ISBN 978-3-939230-01-4

Determination of characteristic soil values by statistical methods

C. Pohl
ELE – Consulting Engineers Ltd., Essen, Germany

ABSTRACT: According to new European standard, EC 7, characteristic values are the fundamental input data for geotechnical verifications using the concept of partial safety factors. Characteristic values have to be determined for impacts as well as for soil properties. Although, European standard, EC 7, and German supplementary rules, specified in DIN 1054, give a consistent definition of characteristic values of a soil property, first experiences with the concept of partial safety factors have shown some problems with the interpretation of these definitions.

Besides, the geotechnical expert has significant discretion in the determination of characteristic soil values and this influences the results of geotechnical verifications. If results of field- and laboratory tests are available in an adequate sample size, statistical methods are an effective tool to determine characteristic soil values in a verifiable way and to get best possible information from realized site investigations. The following paper points out simple statistical methods and gives recommendations for their practical application. All procedures are demonstrated with the help of examples.

Keywords: characteristic value, laboratory test, site investigation, standard, statistical analysis

1 INTRODUCTION

In general, geotechnical stability could be verified, as shown in figure 1, by deterministic or probabilistic procedures. Deterministic procedures involve comparisons of single values for design impacts (F) and design resistances (R); however, probabilistic procedures take the distributions of all parameters (soil values, forces, etc.) and results in the probability p_F of a certain occurrence. In geotechnical practice probabilistic procedure is still only applied in exceptional cases. Regarding to deterministic procedures, the determination of single appropriate values for parameters that are characterized by statistical spread influences the results of geotechnical analysis essentially.

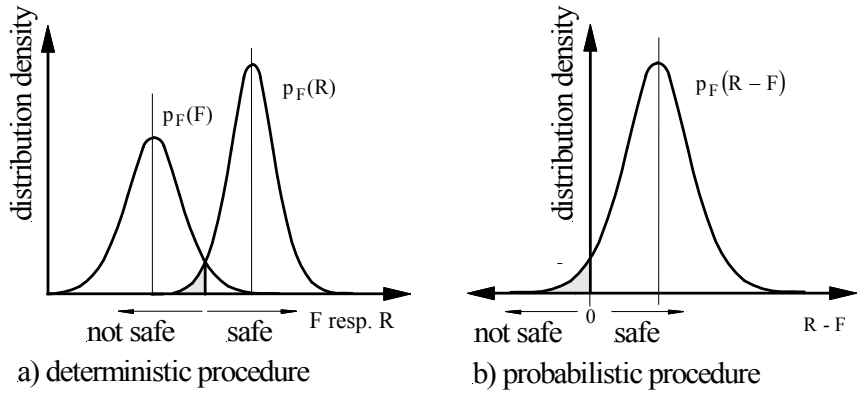

Figure 1. Deterministic vs. probabilistic procedure

Thus, with harmonization of European standards towards the concept of partial safety factors, as stipulated in EC 7 (DIN EN 1997), the phrase of characteristic soil values has been anchored in geotechnical verifications. Characteristic soil values should be representative values for soil properties of a homogeneous zone. Indeed, this approach is well known by geotechnical experts, but new European standards give much more precise definitions how to determine characteristic soil values than former national standards.

Finally, the determination of characteristic soil values is complex. As a consequence of its spatial variability and its local dispersion, there is much more uncertainty in soil properties than for other materials in civil engineering, like steel or concrete. Especially for spatial extensive projects or large depots, the soil is, as result of its history, often inhomogeneous and the properties – even of a homogeneous zone – spread widely. Furthermore, economic arguments may sometimes prevent an acceptable size of samplings.

As consequence to the restriction of DIN EN 1997 and DIN 1054 on qualitative definitions of characteristic soil values, geotechnical expert has a considerable discretion. Hence, it is hardly surprising, that characteristic soil values are still frequently determined by individual experience. Often, only the median values of test results are used. Nonetheless statistical methods can be an effective tool to determine characteristic soil values in a verifiable way, an adequate sample number presumed. Reasonably applied, statistical methods increase information content of site investigation and contribute to minimizing soil risk.

2 CHARACTERISTIC VALUES OF SOIL PROPERTIES

According to DIN 1055-100, the characteristic value is the fundamental representative value for actions. The analog intent must be taken for characteristic values of soil properties.

Nevertheless, no all-embracing definition of characteristic soil values is available up to now. Rules and specifications for determination of characteristic soil values have to be composed from several consistent standards. DIN EN 1997-1 gives within the general rules in section 2.4.3(5), the following basic definition:

"The characteristic value of a soil or rock parameter shall be selected as a cautious estimate of the value affecting the occurrence of the limit state."

This formulation has been chosen consciously. *Cautious estimate* should underline principle of caution. *Selection* is a hint to necessary geotechnical expertise. Reference to *limit state* emphasizes an obligatory regard to the respective construction and limit state. With this background, characteristic values of soil properties have to be determined in case of complex constructions in cooperation with the structural engineer. The basis of characteristic soil values must always be formed by field and laboratory tests, completed by local information and by experience if available.

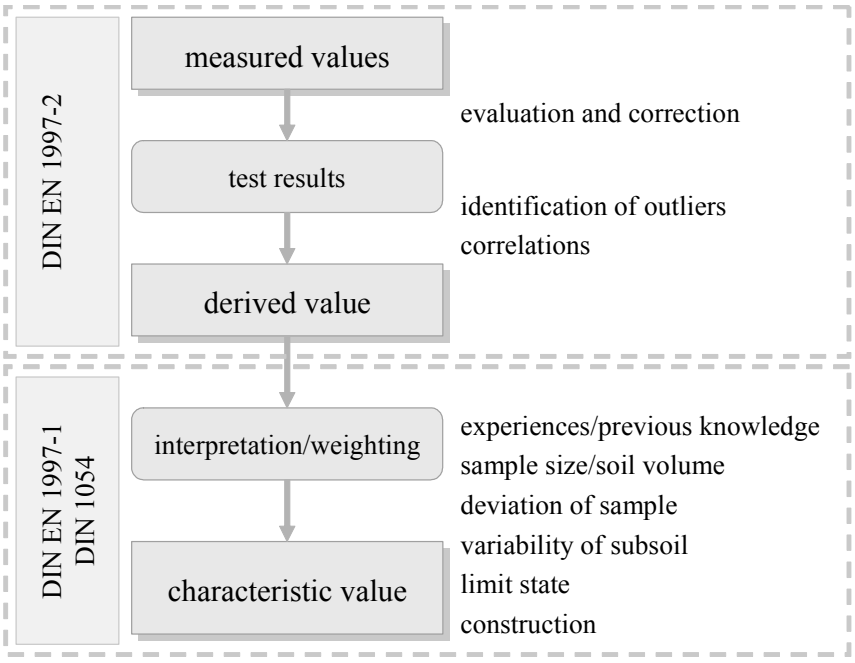

Figure 2. Characteristic value of a soil property

More practical advice for the deduction of characteristic soil values of a homogeneous soil layer from field and laboratory tests is given in DIN EN 1997-2. Principally, it is recommendable to proceed as shown in figure 2 in a simplified way in accordance to Bauduin (2001). First, tests results have to be ascertained by evaluation and correction of measurements, e.g. shear strength from a direct shear test. Afterwards, outliers have to be identified and correlated values from indirect tests, e.g. undrained shear parameters from penetration tests, have to be added to get so-called derived values.

Characteristic values of a soil property follow then by interpretation and weighting of these derived values. Useful experiences as well as previous knowledge of regional subsoil could be regarded, above all, sample size of tests, statistical spread of results and variability of subsoil have to be taken into consideration. Limit state and ability of the construction to rearrange impacts are furthermore important factors for interpretation.

This general procedure, which is shown in figure 2 in accordance with European standards and German supplementary rules, is analogously valid for site investigations everywhere in the world, because local spreading and regional variability of subsoil is naturally a common problem.

3 STATISTICAL METHODS

Site investigations are always just samples. The sample size controls information content and therefore representativeness of investigation. Statistical methods allow surveys of test results (descriptive statistic) as well as founded estimation from sample to population (deductive statistic).

With regard to DIN EN 1997-1 (sec. 2.4.5.2(11)), the arithmetic probability for a worse value should not exceed 5 % in the regarded limit state if statistical methods are applied. In this context a cautious estimation of the mean of a limited set of geotechnical parameters corresponds to a mean with a confidence level of 95 %. In cases when a local failure cannot be excluded, a cautious estimation of the low value corresponds to the 5 % fractile.

3.1 *Descriptive statistic*

The survey quality of samples with n single values x_i depends strongly on the distribution function that is chosen. In the case of soil properties, a normal distribution often already shows an adequate compliance. This distribution has the favorable attribute that every linear combination of normal distributed values is again normally distributed. Thus, if two or more normal distributed parameters are summarized within a linear relationship to a resultant resistance, the resistance still keeps the normal distribution.

Normal distribution is described by the arithmetical mean:

$$\bar{x} = \frac{\sum x_i}{n} \tag{1}$$

and by standard deviation:

$$s = \sqrt{\frac{1}{n-1} \sum_{i=1}^{n} (x_i - \bar{x})^2} \; . \tag{2}$$

For soil parameters, which show typically a large scattering, as for example the water permeability, the lognormal distribution is preferable, because it does not take any negative values.

Depending on the available data set, much more complex distributions, as e.g. the Weibull distribution or the beta distribution, could give a better compliance with derived values, but in fact, normal and lognormal distribution are well-known and their compliance is often already satisfying.

Hence, in geotechnical practice, statistical analysis is actually restricted most times on these two simple distributions. Compliance of the selected distribution should be verified by visual verification or by a test of goodness of fit.

3.2 *Deductive statistic*

Deductive statistic permits an estimation of the mean or the lower value of the population on the basis of available samples from a site investigation by definition of confidence intervals, as shown in figure 3. Width of the confidence interval is designated by the requested probability α.

For small sample sizes, as it is often unavoidable in the case of site investigations, the student-distribution (t-distribution) allows an estimation of the variance (deviation of the population). Characteristic values x_k as cautious estimation of the mean are then given by:

$$x_k = \bar{x} \pm t_{n-1}^{\alpha} \frac{s}{\sqrt{n}} . \qquad (3)$$

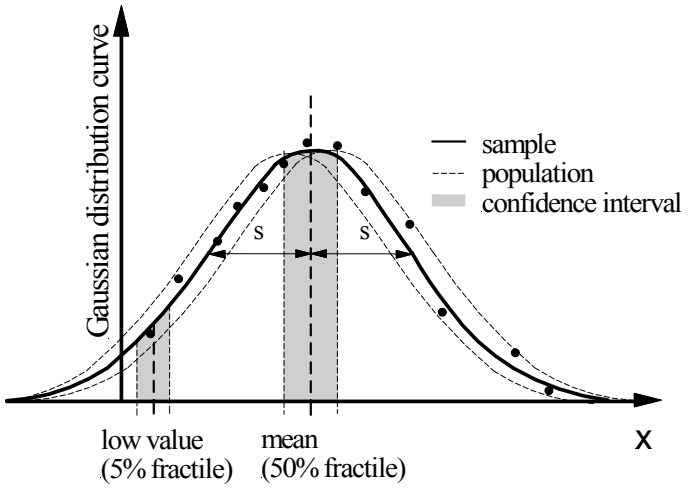

Figure 3. Gaussian normal distribution and confidence intervals for 5 % fractile and for 50 % fractile

Student-distribution is tabulated as a function of probability α and of degree of freedom, which is equal to the sample size n reduced by one.

For larger sample sizes the t-distribution decreases as a consequence of better information content of site investigation; the level of confidence becomes smaller. For endless sample sizes, the variance can be assumed to be known and the t-distribution tends to the 5 % fractile of the standard normal distribution ($t_{\infty}^{\alpha} \rightarrow 1{,}645$).

The necessary sample sizes for this assumption are regularly only available, if geotechnical expert have access to a regional database or to correlations with the results of indirect investigations, which could often be performed in much higher quantity than direct field or laboratory tests.

Characteristic values of soil properties as 50 % fractiles are only under the condition tolerable, that the construction shows an appropriate ductility. If for example a superstructure, which is founded on individual footings, could not compensate differences in soil strains, a low value (5 % fractile) of the stiffness has to be taken into account. Estimation of variance follows in this case by a Taylor series expansion.

Pre-factors K, which already summarize estimation function t and sample size n as well as probability α, have been established to disburden application of deductive statistic. Through this facilitation of eq. 3, characteristic values x_k could be determined by:

$$x_k = \bar{x} \pm K \cdot s . \qquad (4)$$

Values for K are documented in table 1.

Table 1. Values for K of a normal distributed attribute

n	$K_{50\,\%}$	$K_{5\,\%}$
10	0.580	2.911
20	0.387	2.369
40	0.266	2.126
100	0.166	1.927
∞	0	1.645

3.3 *Test of goodness of fit*

Authenticity of the selected (theoretical) distribution with the actual (empirical) distribution should be verified. First, a visual comparison of empirical and theoretical distribution is recommendable. If both distributions show a satisfying fitting visually, a hypothesis test should also check the theoretical distribution. In this context the Kolmogorow-Smirnow-Test according to Lilliefors has become popular, because of its very simple procedure (Hartung et al., 1989).

The hypothesis "The existing differences between empirical and theoretical distribution are not stochastic justified" has to be dismissed, if maximum discrepancy L_n^{norm} (Figure 4) of both distributions does not exceed a critical value $l_{n,1-\alpha}^{norm}$:

$$\sqrt{n} \cdot L_n^{norm} \leq l_{n;1-\alpha}^{norm} \qquad (5)$$

with

$$L_n^{norm} = \sup_x \left| \phi\left(\frac{x - \bar{x}}{s}\right) - F_n^0(x) \right| \tag{6}$$

and

$F_n^0(x)$ = value of empirical distribution at point x

$\phi\left(\frac{x - \bar{x}}{s}\right)$ = value of theoretical (normal) distribution at point x

$l_{n;1-\alpha}^{norm}$ = critical value for the test of unspecified normal distributrion according to tab. 2

$1 - \alpha$ = level of significance (usually 0.95).

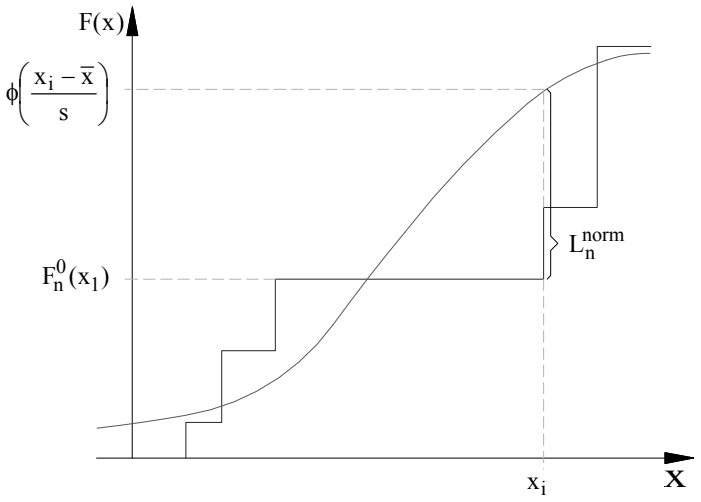

Figure 4. Kolmogorow-Smirnow-Test according to Lilliefors

Table 2. Values for $l_{n,1-\alpha}^{norm}$ of a normal distributed attribute (Hartung et al., 1989)

n	5	8	10	20	30	> 30
$l_{n;0.90}^{norm}$	0.72	0.74	0.76	0.79	0.80	0.81
$l_{n;0.95}^{norm}$	0.76	0.81	0.82	0.85	0.88	0.89
$l_{n;0.99}^{norm}$	0.91	0.94	0.94	1.03	1.03	1.04

3.4 *Characteristic values with regard to trend analysis*

Some soil mechanical properties follow a trend, e.g. drained shear resistance increases approximately linear with stress level resp. to depth.

Assuming, that no useful experience is available, the confidence level of a linear regression curve for the mean could be concluded by estimation of standard deviation s_1 (Bauduin, 2001):

$$s_1^2 = \frac{1}{n-2} \cdot \left[\frac{1}{n} + \frac{(z - \bar{z})^2}{\sum_{i=1}^{n} (z_i - \bar{z})^2} \right] \cdot \sum_{i=1}^{n} \left[(x_i - \bar{x}) - b\,(z_i - \bar{z}) \right]^2 \tag{7}$$

resp. for the 5 % fractile:

$$s_2^2 = \frac{1}{n-2} \cdot \left[1 + \frac{1}{n} + \frac{(z - \bar{z})^2}{\sum_{i=1}^{n} (z_i - \bar{z})^2} \right] \cdot \sum_{i=1}^{n} \left[(x_i - \bar{x}) - b\,(z_i - \bar{z}) \right]^2 . \tag{8}$$

Hence, characteristic value x_k at depth z could be written by:

$$x_k = \bar{x} + b(z - \bar{z}) \pm t_{n-2}^{\alpha}\, s_1 \tag{9}$$

resp.:

$$x_k = \bar{x} + b(z - \bar{z}) \pm t_{n-2}^{\alpha}\, s_2 , \tag{10}$$

where

$$b = \frac{\sum_{i=1}^{n} (x_i - \bar{x})^2 (z_i - \bar{z})^2}{\sum_{i=1}^{n} (z_i - \bar{z})^2}. \quad (11)$$

As a consequence of the additional variable z, the value of the t-distribution has to be metered with sample size n reduced by two (n – 2).

Figure 5 emphasizes estimation of the characteristic soil value with regard to a trend analysis with the help of a shear stress – normal stress diagram; the underlying data has been taken from Kruse (2003). Altogether 25 single direct shear tests of a marl have been performed at 5 stress levels, varying in a range from 100 kN/m² to 500 kN/m². The linear regression results in a medium friction angle of $\varphi'_{medium} = 33.8°$ and a cohesion of $c'_{medium} = 23.2$ kN/m².

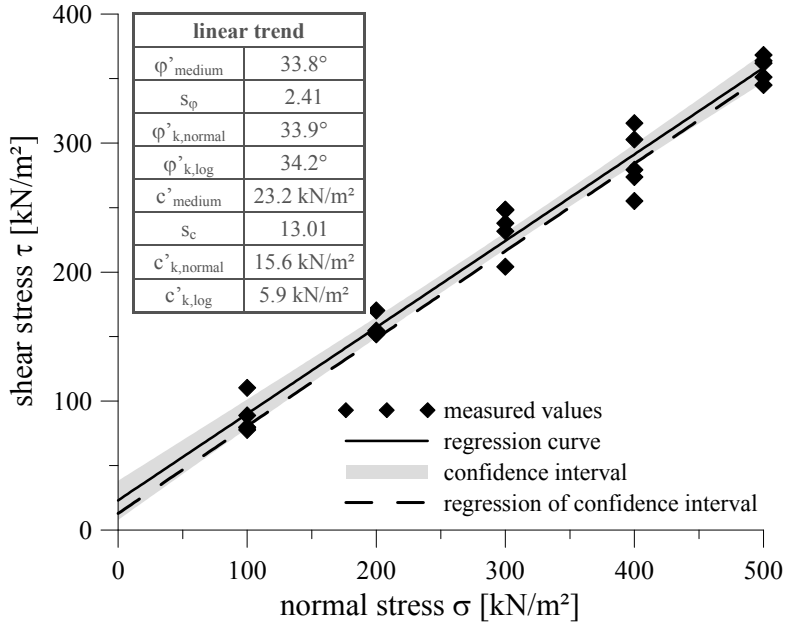

Figure 5. Characteristic values, taking a linear trend into consideration (values from Kruse (2003))

The confidence intervals of the linear regression curve are slightly hyperbolic functions due to standard deviation s_1 resp. s_2 (Fellin et al., 2008; Fellin 2005). The hyperbolic relationship could be linearized again, if absolutely necessary. Characteristic shear parameters are then conform to inclination and zero crossing of the regression of the confidence interval; due to the hyperbolic relationship is $\varphi'_{k,\,normal} = 33.9°$ close to the medium friction angle, but c_k' has decreased to $c'_{k,\,normal} = 15.6$ kN/m².

Assuming a lognormal distribution of derived values, c_k' decreases to $c'_{k,\,log} = 5.9$ kN/m², whereas φ_k' increases a little to $\varphi'_{k,\,log} = 34.2°$.

4 RECOMMENDATIONS

Statistical methods are always a great tool, if they are applied professionally and if circumstances are compatible. The procedures, which have been arranged in section 3, should give a little reminder, that simple statistical methods can increase the information content of site investigations significantly. Nevertheless, statistical methods cannot replace necessary expertise.

The indispensable condition for the implementation of statistical methods for the determination of characteristic values of soil properties is a sufficient sample size. Mathematical considerations provide a much larger size than established in site investigation practice.

For a given tolerable discrepancy of the upper value from the mean $\Delta\hat{x}_p = \hat{x}_p - \hat{x}_p^u$, the statistical sample size could be estimated by:

$$n \geq \left(\frac{2\, t_{n-1,\,1-\alpha/2} \cdot s}{\Delta\hat{x}_p} \right)^2 . \tag{12}$$

Eq. 12 demands knowledge of the standard deviation. Thus, the investigation size would have to be extended iteratively until eq. 12 is fulfilled, something that is in practice not compatible with activities in a building place and that is often contrary to tolerable costs and time effort.

In general, the estimation of 5 % fractiles requires larger samples than the estimation of 50 % fractiles. However, soil values, which are usually used as 5 % fractiles, frequently tend to result in extensive test procedures. Fischer (2001) stipulates sample sizes above 10. If on the one hand technical and economical aspects are passable and on the other hand the specific soil composition does not require larger sample sizes, 30 repetitions per type of soil seem to be adequate.

Although the t-distribution is an effective instrument for the estimation of variance, this estimation is still risky. Useful experience as well as results of indirect site investigations can help to reduce this uncertainty. Variance could be implemented from results of indirect tests, which are frequently performed in much higher quantity than direct tests. To consider useful experiences, a decision has to be made if this information is representative enough to assume a fully known variance. Otherwise useful experience could be implemented by a Bayesian analysis. Additionally, correlations could exceed the information content.

It has to be noticed, that using best possible information from available data is also in the interest of the client. Hence, he should be insistent that mean value, standard deviation and characteristic values as 50 % fractile and as 5 % fractile are declared.

5 EXAMPLE

Figure 6 illustrates the consequence of interpretation strategy (cf. Kisse et al. 2008). Drained shear parameters of Frankfurt clay have been taken from Moormann (2002). The database comprehends n = 56 resp. n = 57 values for the friction angle φ' and for the cohesion c'.

Applying the statistical methods according to sec. 3.1 to 3.3, the characteristic mean values (50 % fractile) of the normal distributed attributes exceed always the analogous values of the lognormal distributed attributes.

Characteristic lower values (5 % fractiles) behave contrarily. 5 % fractiles of the lognormal distributed attributes exceed most times the 5 % fractile of the normal distributed attributes. This tendency becomes very obvious in the case of the cohesion, because 5 % fractile of the normal distributed cohesion take a nonsensical negative value. In contrast to this, the 5 % fractile of the lognormal distributed cohesion is still conform to a positive value $c_k' = 9{,}3$ kN/m².

In figure 6, the available data of Frankfurt clay has been handled as results of a local site investigation, but in fact these data have only the character of a regional experience, which has to be supplemented in the practical case by local subsoil data. If previous knowledge does not suffice for conclusion on variance, characteristic values have to be determined by Bayesian estimation. The Bayesian theorem implicates probability of independent data of previous knowledge and local site investigation.

If for example 5 pairs of shear parameters of local subsoil have been ascertained, with $\bar{\varphi}' = 22{,}5°$, $s_\varphi = 4{,}0$ and $\bar{c}' = 35$ kN/m² and $s_c = 7{,}5$ kN/m², characteristic values are calculated to $\varphi_k' = 21{,}5°$ and $c_k' = 33{,}4$ kN/m².

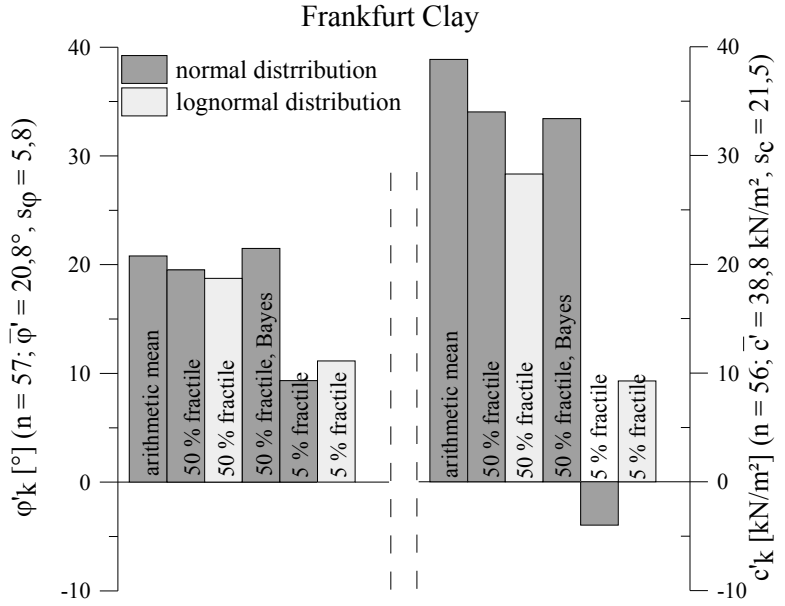

Figure 6. Example Frankfurt clay (values from Moormann (2002))

6 CONCLUSIONS

Current geotechnical design practice is mainly based on a deterministic procedure. Single (characteristic) values for impacts and resistances are the fundamental input data for geotechnical verifications (Schneider, 1993). Nevertheless, statistical methods are a reasonable instrument for determination of these characteristic values from the results of field and laboratory tests. Perhaps, application of statistical methods is the first step for a change to aspired probabilistic procedures in the future.

In the previous sections, well known and in other parts of engineering well-established statistical methods have been arranged. Examples have shown simplicity of their application. Unfortunately, due to the necessary sample sizes, statistical methods are rarely practiced in geotechnics up to now, even though DIN EN 1997 underlines their optional application explicitly.

Information content of site investigations is optimized by statistical methods and process of determination of characteristic soil values becomes verifiable.

REFERENCES

Bauduin, C. 2001. Determination of characteristic values. Geotechnical Handbook – Volume 1: Fundamentals. Smoltczyk (Ed.). Berlin: Ernst & Sohn.

Fellin, W., Berghamer, S., Renk, D. 2009. Konfidenzgrenzen der Scherfestigkeit als Grundlage zur Festlegung charakteristischer Scherparameter. Geotechnik 32/1. pp. 30-36. (in German)

Fellin, W. 2005. Assessment of characteristic shear strength parameters of soil and its implication in geotechnical design. In: Analyzing Uncertainty in Civil Engineering. Fellin, W., Lessmann, Oberguggenberger, M., H., Vieider, R. (Ed.). pp. 33-49.

Fischer, L. 2001. Das neue Sicherheitskonzept im Bauwesen. Bautechnik Spezial. Berlin: Ernst & Sohn. (in German)

Hartung, J., Elpelt, B., Klösener, K. H. 1989. Statistik – Lehr- und Handbuch der angewandten Statistik. 7. Auflage. R. Oldenbourg Verlag GmbH (in German)

Kisse, A., Pohl, C., Richwien, W. 2008. Konsequenzen der Festlegung von charakteristischen Bodekennwerten für geotechnische Nachweise. Baugrundtagung 2008. DGGT (Ed.). (in German)

Kruse, B. 2003. Status quo bei der Festlegung charakteristischer Werte von Bodenkenngrößen. In: Stochastische Prozesse in der Geotechnik. Ziegler, M. (Ed.). Schriftenreihe Geotechnik im Bauwesen. TU Aachen. pp. 43-53 (in German)

Moormann, Ch. 2002. Trag- und Verformungsverhalten tiefer Baugruben in bindigen Böden unter besonderer Berücksichtigung der Baugrund-Tragwerk- und der Baugrund-Grundwasser-Interaktion. Katzenbach (Ed.). Mitteilungen des Institutes und der Versuchsanstalt für Geotechnik der Technischen Universität Darmstadt. (in German)

Schneider, H. R. 1993. Defintion and determination of characteristic soil properties. Proceedings of the 14th International Conference on Soil Mechanics and Foundation Engineering. Hamburg, Balkema. pp. 2271-2274.

ISGSR 2011 - Vogt, Schuppener, Straub & Bräu (eds) - © 2011 Bundesanstalt für Wasserbau ISBN 978-3-939230-01-4

Resistance Factors for Design of Piles in Sand: Tools to Understand Design Reliability

K. C. Foye
CTI and Associates, Inc., Wixom, Michigan, United States

M. Prezzi, R. Salgado
Purdue University, West Lafayette, Indiana, United States

ABSTRACT: Load and resistance factor design (LRFD) of foundations is a popular design code format. Common methods used to establish resistance factors for geotechnical structures include calibration to assumed factors of safety and reliability analysis using field load test databases. Reliability analyses are the preferred tools for this work, but the needed probabilistic information regarding design method uncertainty is difficult to obtain. This paper illustrates an approach to uncertainty assessment that seeks to isolate the various sources of uncertainty. Using this approach, reliability analyses are used to develop resistance factors for the design of driven pipe piles in sand. The results illustrate how engineers with differing degrees of probability knowledge can use LRFD or the underlying reliability analyses to understand and manage risk. By attempting to isolate different sources of uncertainty, the paper suggests a methodology for quantitatively assessing the relative value of differing degrees and types of design knowledge.

Keywords: Deep Foundation, Cone Penetrometer Test, Reliability Analysis, Load and Resistance Factor Design

1 INTRODUCTION

Load and resistance factor design (LRFD), a specific format for limit states design (LSD), is a design framework that indirectly addresses the uncertainty in the methods of calculating a foundation's capacity (resistance) and estimating the demands (load) placed upon it. This indirect assessment affords the engineer a tool to manage risk in design decisions. LRFD factors for use in design practice can be determined through a number of methods, including calibration to customary factors of safety and probabilistic reliability analysis. Reliability analysis requires a probabilistic characterization of foundation analysis method uncertainty. For pile design, this characterization can include consideration of pile load test databases or studies of the individual contributing sources of uncertainty. This paper focuses on some interesting outcomes from applying a detailed analysis of the contributing sources of uncertainty.

1.1 *Basic LRFD Formulation for Piles*

In terms of LSD, pile foundations must be designed against any possible ultimate limit state (ULS). Axially loaded piles are often designed based exclusively on an ULS associated with either plunging or excessive settlement. The basic LRFD inequality for this ULS is

$$(RF)R_n \geq \sum (LF)_i Q_i \tag{1}$$

where RF is a resistance factor, R_n is the nominal design resistance, and $(LF)_i$ is a load factor for a particular load type Q_i. In pile design, both base and shaft resistance contribute to the overall load-carrying capacity of a pile. These two contributions suggest two possible LRFD inequalities:

$$(RF)(R_s + R_b) \geq \sum (LF)_i Q_i \tag{2}$$

or

$$(RF)_s R_s + (RF)_b R_b \geq \sum (LF)_i Q_i \tag{3}$$

where R_s and R_b are the shaft and base resistances, respectively, and $(RF)_s$ and $(RF)_b$ are the shaft and base resistance factors, respectively. Although shaft and base resistance depend on many of the same soil properties, they develop by different physical processes and are computed separately using equations with differing degrees of uncertainty. Therefore, it is more useful to apply $(RF)_s$ and $(RF)_b$ as separate resistance factors, as in Eq. (3).

1.2 *Probabilistic Framework to Develop LRFD Factors*

When using probability to develop LRFD factors, values of *RF* and *LF* are selected such that the resulting factored load $\Sigma(LF)_i Q_i$ and resistance $(RF)R_n$ satisfying Eq. (1) lead to designs with an acceptable probability of failure. The reliability index is a number that expresses the probability of failure (i.e., of achieving a limit state) relative to the uncertainty of the design variables. The simplest, first-order second-moment definition of reliability index β when the problem can be reduced to a single design variable X is

$$\beta = \frac{\mu_X - x_{LS}}{\sigma_X} \tag{4}$$

where μ_X is the mean (often, the design value) of X, x_{LS} is the limit state value of X, and σ_X is the standard deviation of X. For multi-variable equations, computing β involves an optimization process. In this paper, the spreadsheet solution method proposed by Low and Tang (1997) is used. Obtaining values of *RF* and *LF* for use in design therefore becomes a further process of optimization where β is fixed and *RF* and *LF* are computed for a range of design scenarios to obtain the most conservative values (lowest *RF* and highest *LF*). An assessment of the design method uncertainty (e.g., σ_X in the simple case exemplified by Eq. 4) is needed to perform this optimization.

One technique to quantify the uncertainty in design methods is to examine databases of predicted versus measured pile performance (e.g., Paikowsky 2004). An advantage of this technique is that a relatively large amount of data can be assembled on which to perform statistics. On the other hand, a disadvantage of this technique is that the method cannot discriminate between the various sources of uncertainty contributing to the observed scatter between predictions and measurements.

An alternative approach, adapted from Ellingwood (1980) in Foye et al. (2006a,b), is to identify the different sources of uncertainty separately, assign probabilistic models to each, then combine them in the final analysis. This approach is conceptually illustrated in Figure 1. Each contributing source of uncertainty results in increased overall uncertainty as their contributions are aggregated. Thus, this approach requires data quantifying each of the component uncertainties – for example, data that only contain error introduced by *in situ* testing. In Figure 1, we show that an *in situ* test measurement results from soil variables (soil state and soil intrinsic variables), and from this *in situ* test measurement a pile resistance can be calculated. In the component approach, the variability of these individual transformations would be assessed. The difference between the database approach and the component approach is that the database approach only allows an examination of the final, actual versus predicted data (lower-left graph), whereas the component approach allows an explicit quantification of the individual analysis steps (all graphs) and their impact on the final, aggregated uncertainty.

2 EXAMPLE RESISTANCE FACTORS FOR PIPE PILES IN SAND

Pile design methods are either direct or property-based (Salgado 2008). Direct design methods rely on direct correlations between *in situ* tests performed prior to pile installation and measured pile capacity following driving. Thus, direct design methods omit the uncertainty from soil property correlations (upper right in Figure 1). Property-based design methods compute pile capacity using various soil parameters as input. These parameters are computed from *in situ* and/or laboratory tests performed on the soil prior to pile installation.

Property-based design methods present a greater challenge to designers because the underlying analyses typically fail to capture the physics of the problem and, in addition, the design variables in these

methods are more difficult to obtain reliably in the field. This condition results in property-based design methods that are significantly less reliable than comparable direct design methods.

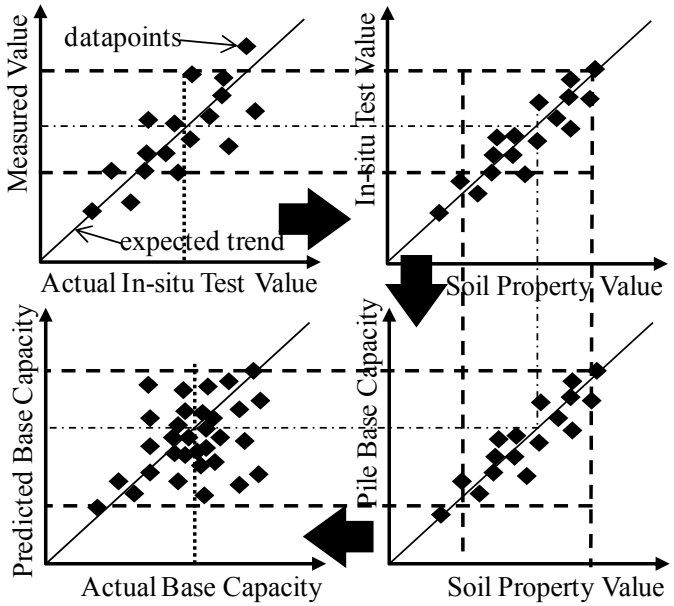

Figure 1. Conceptual representation of accounting for individual sources of uncertainty (clockwise from upper left): measurement, property correlation, capacity model, and final, aggregated uncertainty. The dashed line bounds qualitatively express the cumulative uncertainty at each step in pile capacity analysis. The alternating broken line represents the expected value.

2.1 *Direct Estimation of Pile Shaft Capacity*

The shaft capacity of a pile is computed by summing up the contributions of imaginary segments along the length of the pile. The total shaft capacity of a pile is expressed as

$$R_s = \sum_{i=1}^{n} q_{sLi} A_{si} \tag{5}$$

where q_{sLi} is the unit limit shaft resistance (force/unit area) for each segment i and A_{si} is the shaft area for that segment. Segment shaft area A_{si} is computed as $A_{si} = a_s \mathrm{d}L$, where a_s is the perimeter of the cross section and dL is the segment length. Based on results by Lee et al. (2003) for open-ended piles, q_{sL} from Eq. (5) is defined as

$$q_{sL} = \left(\frac{q_{sL}}{q_c} \right) q_c = 0.002 q_c \tag{6}$$

Design equation (6) represents the model relationship between pre-driving CPT measurements and post-driving pile shaft resistance for open-ended pipe piles. To assess the uncertainty in this model relationship, the calibration chamber data from Paik and Salgado (2003) for shaft resistance was considered. The probabilistic model of this uncertainty was also aggregated with the uncertainty introduced by the equations used to estimate q_c within the calibration chamber. The corresponding *RF* value, determined for reliability index $\beta = 3.0$, was computed as 0.41 when used in conjunction with ASCE-7 (ASCE 2000) load factors. This value is repeated in Table 1 for comparison with other results given below.

2.2 *Direct Estimation of Pile Base Capacity*

The base capacity of a pile is computed by

$$R_b = q_{b,10\%} A_b \tag{7}$$

where A_b is the gross pile base area,

$$A_b = \pi \left(\frac{d_0}{2} \right)^2 \tag{8}$$

and d_o is the outside diameter of the pipe pile base. For open-ended piles, $q_{b,10\%}$ from Eq. (7) is defined as

$$q_{b,10\%} = \left(\frac{q_{b,10\%}}{q_c} \right) q_c \tag{9}$$

where

$$\frac{q_{b,10\%}}{q_c} = -0.00443 IFR(\%) + 0.557 \tag{10}$$

IFR is the incremental filling ratio, a measure of the state of plugging of the pile at any point during driving (Paik et al. 2003). Lee et al. (2003) provide guidance on estimating values of *IFR* when field measurements are not available. The $q_{b,10\%}/q_c$ relationship (Eq. 10) was developed by Lee et al. (2003) based on calibration chamber test results of $q_{b,10\%}$. The uncertainty of this relationship was assessed similarly to the method discussed for shaft capacity.

Table 1. Summary of design of driven open-ended (OE) pipe piles in sand using results from CPT or SPT. Resistance Factors (*RF*) are given for use with ASCE-7 and AASHTO load factors. *FS* indicates an approximate value of safety factor corresponding to the resistance factors given.

Design Method	*RF* using ASCE-7 *LF*s	*RF* using AASHTO *LF*s	Representative *FS*
Direct Design – CPT			
OE pipe shaft (Eq. 6)	0.41	0.45	3.7
OE pipe base (Eq. 9)	0.54	0.59	2.8
Property-Based Design – CPT			
OE pipe shaft (Eq. 11)	0.47	0.50	3.7
OE pipe base (Eq. 14)	0.42	0.45	3.5
Property-Based Design – SPT			
OE pipe shaft (Eq. 11)	0.42	0.45	4.0
OE pipe base (Eq. 14)	0.40	0.42	3.7

2.3 *Property-Based Estimation of Shaft Capacity*

For open-ended piles q_{sL} from Eq. (5) is computed from

$$q_{sL} = \frac{K_s}{K_0} \tan\left(\frac{\delta_c}{\phi_c} \phi_c \right) \left(K_0 \sigma'_v \right) \tag{11}$$

where K_s/K_0 is the ratio of the coefficient of lateral earth pressure after pile installation to the coefficient of lateral earth pressure at rest K_0, δ_c/ϕ_c is the ratio of the interface friction angle δ_c to the critical-state friction angle ϕ_c, and $(K_0 \sigma'_v)$ represents the initial horizontal effective stress at the depth of the pile segment considered. Based on data presented by Paik and Salgado (2003), the ratio K_s/K_0 is computed as

$$\frac{K_s}{K_0} = \beta\left(7.2 - 4.8 PLR\right) \tag{12}$$

where

$$\beta = 0.00018 D_R^2(\%) - 0.0089 D_R(\%) + 0.329 \tag{13}$$

with $20\% < D_R < 90\%$. *PLR* is the plug length ratio ($0 \le PLR \le 1$), defined as the ratio of plug length to pile penetration length, and $D_R(\%)$ is the relative density, expressed as a percent.

The prediction of the unit limit shaft resistance, q_{sL}, represented by Eq. (12), contains uncertainties from three sources: 1) the increase in lateral earth pressure due to pile driving and pile loading expressed by K_s/K_0, 2) the coefficient of interface friction $\tan\delta_c$, and 3) the pre-driving lateral earth pressure ($\sigma'_h = K_0 \sigma'_v$).

The combined uncertainty in the ratio K_s/K_0, defined by Eq. (12), is due to the variable uncertainties of D_R and *PLR* and to the model uncertainty present in the results of Paik and Salgado (2003). Foye et al. (2006a) examined the uncertainty of relative density determined from the CPT. The uncertainty in the

K_s/K_0 model relationship was deduced directly from the scatter in the results of Paik and Salgado (2003) since D_R, σ'_h, and degree of plugging were closely controlled or measured.

The uncertainty of *PLR* predictions was assessed by considering the recommendations by Lee et al. (2003) and the data presented by Paik and Salgado (2003). Given that the sand around the pile can be described as loose, medium-dense, or dense, the designer will be able to estimate *PLR* to within ±0.15 of the actual value when aided by prototype pile driving results. The least biased probability density function to describe the uncertainty in this estimate is a uniform distribution with bounds ±0.15 of the expected value. Without the benefit of such results, *PLR* may be completely unknown. The most extreme expression of this uncertainty is a uniform distribution with bounds *PLR* = 0 and *PLR* = 1. The consequences of this difference in knowledge of *PLR* are explored below.

The uncertainty of δ_c was assessed by considering ϕ_c and the ratio δ_c/ϕ_c. Uncertainty in critical state friction angle ϕ_c was obtained from results reported by Bolton (1986). Uncertainty in the ratio δ_c/ϕ_c was assessed by considering the results of high-quality, direct-interface shear tests by Lehane et al. (1993), Jardine and Chow (1998), and Rao et al. (1998).

The uncertainty of σ'_h cannot be systematically assessed. Although σ'_v can be easily computed in practice, K_0 is not so easily assessed. Correlations have been found between K_0 and ϕ and between K_0 and void ratio e or D_R and overconsolidation ratio, which is often unknown. However, the determination of ϕ and D_R from *in situ* tests is dependent on K_0. Hence, in typical design practice, an assumption of K_0 is required.

2.4 *Property-Based Estimation of Base Capacity*

For open-ended piles $q_{b,10\%}$ was found by Paik and Salgado (2003) to be related to the relative density, D_R(%), and the effective lateral earth pressure, σ'_h, as

$$q_{b,10\%} = \alpha\left(326 - 295\frac{IFR(\%)}{100}\right)\sigma'_h \tag{14}$$

where

$$\alpha = 0.0112D_R(\%) - 0.0141 \tag{15}$$

with 20% < D_R < 90%. The prediction of unit base resistance q_b for open-ended pipe piles, represented by Eq. (13) contains uncertainties from two sources: 1) uncertainty in the $q_{b,10\%}/\sigma'_h$ relationship and 2) uncertainty in the initial lateral earth pressure σ'_h. As seen in Eq. (14), $q_{b,10\%}/\sigma'_h$ also depends on D_R. The uncertainty of these relationships was assessed using the same methodology discussed for pile shaft resistance.

3 RESISTANCE FACTORS AS INDICATORS OF UNCERTAINTY

Table 1 summarizes the resistance factors determined for each of the presented pile design methods when the reliability index $\beta = 3.0$. Resistance factors are presented for use in conjunction with both the ASCE-7 (ASCE 2000) load factors and the AASHTO (AASHTO 1998) load factors. Lower resistance factors are expected for design methods with greater uncertainty. Direct design methods are expected to have less uncertainty than property-based methods. This expectation is met by the *RF* results for open-ended pipe pile base resistance. Also, *in situ* test methods that introduce greater uncertainty are expected to produce lower *RF* values. This expectation is confirmed by the relative values of *RF* obtained for CPT- and SPT-based methods.

3.1 *Effect of IFR and PLR Estimate Confidence on Resistance Factor*

Table 2 illustrates the effect of different degrees of confidence in *IFR* estimates on the reliability of the direct design of open-ended pipe pile base resistance (Eq. 9). Since parallel analysis of the effect of estimates of *PLR* on shaft resistance has similar results, this discussion is limited to *IFR* and base resistance. Two cases are considered; 1) when *IFR* is unknown, it can assume any value between 0 and 100% with equal likelihood (uniform distribution) and 2) when *IFR* is estimated from prototype pile test results and is modeled as uniformly distributed within ±15% of the estimated value. For both cases, Table 2 includes

the calculated results for the *RF* value required to achieve a reliability index $\beta = 3.0$, the value of β for *RF* = 0.54 as obtained in Table 1, and the probability of failure P_f if *RF* = 0.54.

According to Table 2, if a pile is designed using *RF* = 0.54 without measuring *IFR* for a test pile (the completely unknown case), P_f = 7.44%. If a test pile is used and *IFR* measured, the same *RF* = 0.54 value will lead to P_f = 0.131%, a considerable difference in risk to the project. It is clearly unacceptable to have a 7.44% probability of failure. Also, designing piles twice as conservatively as may be necessary is a waste, as is indicated by the ratio of *RF* values for $\beta = 3.0$. Therefore, this example shows how the difference in *RF* values are an indirect indicator of relative risk. Also, the difference in *RF* values highlights the value of measuring *IFR* in this specific case and of obtaining information about other variables in other types of project at costs that are comparatively small.

The following sequence is suggested by these results: 1) design the piles following a conservative estimate of *IFR* (higher values), 2) measure *IFR* during the installation of test piles at the site, and 3) revise the design as needed to reflect the site conditions. This technique allows information to be introduced and used to improve the estimated reliability or economy of the project.

Table 2. Resistance factors *RF* for β = 3.0, reliability indices β for *RF* = 0.54, and probabilities of failure P_f for ULS design checks of OE pipe pile base resistance using the Paik et al. (2003) method (Eq 9).

IFR determination	*RF* for $\beta = 3.0$	β if *RF* = 0.54	P_f if *RF* = 0.54
completely unknown	0.26	1.44	7.44%
estimated from prototype	0.54	3.00	0.131%

3.2 *Effect of Design Method Uncertainty on Resistance Factor*

The ratio $q_{b,10\%}/q_c$ (Eq. 9) for closed-ended pipe piles can be assessed by considering the results of high-quality instrumented pile load test results by Vesic (1970), BCP Committee (1971), Gregersen et al. (1973), Beringen et al. (1979), Briaud et al. (1989), Altaee et al. (1992, 1993), and Paik et al. (2003) (Figure 1). Based on these results, a viable relationship for $q_{b,10\%}/q_c$ appears to be

$$\frac{q_{b,10\%}}{q_c} = 1.02 - 0.0051 D_R(\%) \tag{16}$$

where D_R(%) is the relative density, expressed as a percent. Figure 3 shows that the distribution of residual $q_{b,10\%}/q_c$ values (trend subtracted from data) with respect to Eq. (16) resembles a normal distribution with *COV* = 0.17. Since this field test database includes uncertainty due to inherent soil variability, CPT testing, and the relationship between measured values of q_c and $q_{b,10\%}$, this distribution was used directly to determine resistance factors for use with Eq. (9) and Eq. (16), without further consideration of additional probabilistic models for soil and CPT testing. Hence, these data most closely resemble the scenario presented in the lower left quadrant of Figure 1.

These results – both in terms of the suggested design value and the resulting resistance factors – compare favorably to the Paik and Salgado (2003) calibration chamber results, as expressed in Eq. (10). Regarding the suggested design value, an *IFR* = 0 indicates the plug length is not growing even as the pile penetration length is increasing, which suggests the pile is responding as a closed-ended pile. In the close-ended or fully plugged condition, Eq. (10) becomes

$$\frac{q_{b,10\%}}{q_c} = 0.557 \tag{17}$$

Since the fully plugged condition was approached in the Paik and Salgado (2003) study only for open-ended piles driven in dense sands (80-100%), Eq. (17) is in agreement with Eq. (16). The distribution of residual $q_{b,10\%}/q_c$ values by Paik and Salgado (2003) with respect to Eq. (10) resembles a normal distribution with *COV* = 0.10. Aggregation of this uncertainty with the uncertainty due to estimates of q_c in the calibration chamber results in a distribution of $q_{b,10\%}/q_c$ values best fit by a beta distribution with bounds 0.54*f*(IFR) and 5.92 *f*(IFR), and distribution parameters $\alpha = 3.5$ and $\beta = 40.2$.

Reliability analyses based on the load test database and on the Paik et al. (2003) results are used to develop resistance factors for use with Eqs. (16) and (17). These resistance factors are compared to examine the differences in the two sources of data and the effect of these differences on the results of the reliability analyses. First, the case of the probability distributions actually obtained during this study is presented. In this case, the value of *RF* obtained for use with Eq. (17) in conjunction with ASCE (2000)

load factors is $RF = 0.54$. This RF value is identical to the value obtained for use with Eq. (10) because the sources of the design method uncertainty, calibration chamber uncertainty, and CPT measurement uncertainty are also identical.

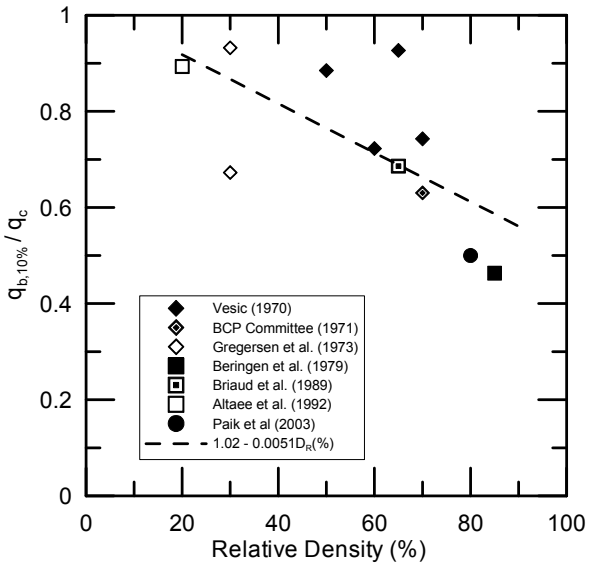

Figure 2. Plot of $q_{b,10\%}/q_c$ from database of high-quality instrumented pile load tests.

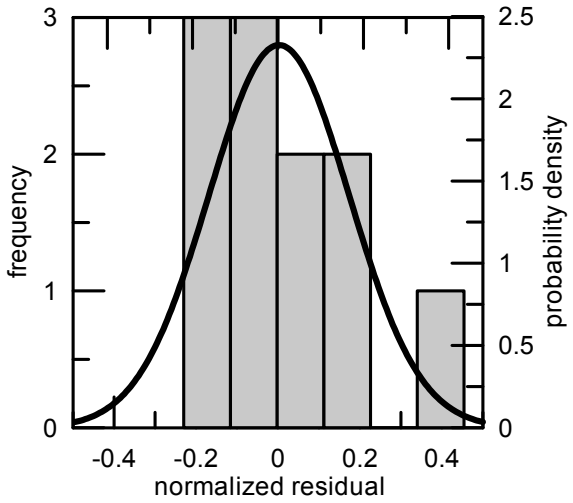

Figure 3. Histogram of data scatter about $q_{b,10\%}/q_c$ relationship for closed-ended pipe piles in sand based on field results (Figure 2). Line indicates a normal distribution with COV = 0.17.

The value of RF obtained for use with Eq. (16), calculated from the pile load test database, is also $RF = 0.54$. While this coincidence lends some credence to the analysis methods discussed in this paper, further investigation of the relationship between $q_{b,10\%}/q_c$, COV and RF is useful to understand the significance of the uncertainty aggregation technique.

Figure 4 plots the values of RF obtained for different input values of COV defining the normal distribution representing the uncertainty in design relationship $q_{b,10\%}/q_c$. Figure 4 shows that RF is significantly less sensitive to COV for Eq. (17) (Paik and Salgado 2003) than for Eq. (16) (pile test database). The reason is that other sources of uncertainty (e.g., q_c measurement) are separately evaluated in the

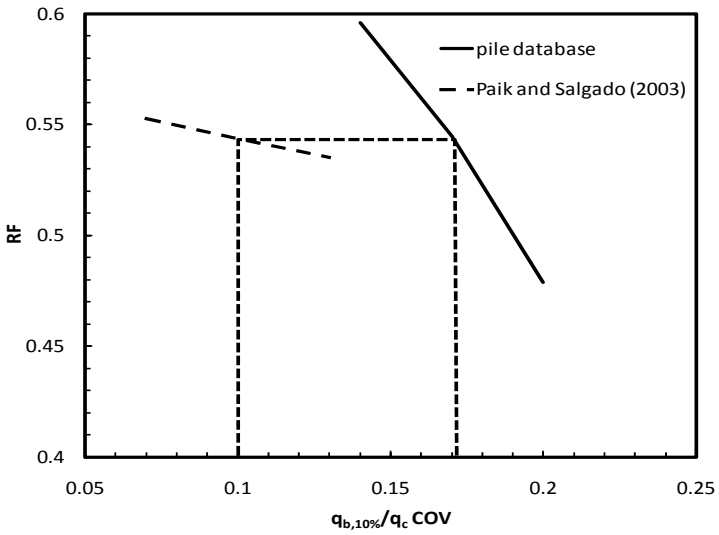

Figure 4. Plot of calculated resistance factors, varying the COV representing the uncertainty of the $q_{b,10\%}/q_c$ model relationship obtained from both the database of high-quality instrumented pile load tests and the Paik and Salgado (2003) calibration chamber data. Short dashed lines indicate the RF values obtained for the actual distributions found in the study.

analysis of Eq. (17) – as in the upper-left and lower-left quadrants of Figure 1 – that cannot be separately evaluated in the analysis of Eq. (16). Accordingly, the separate analysis of the various sources of uncertainty may allow more confident assessments of RF values since this approach is less sensitive to errors in the assessment of individual probability distributions. Conversely, small errors in the assessment of load test databases, or revisions of these databases, may result is significant changes in recommended RF values.

4 CONCLUSIONS

In this paper, we computed resistance factors appropriate for use in the direct and property-based design of driven pipe piles in sands. Resistance factors are a useful quantitative tool to express the relative uncertainty of load capacity of different pile types and pile design methods. Property-based design methods tend to have higher uncertainty (lower *RF*) but apply to general cases. Direct design methods tend to have lower uncertainty (higher *RF*) but apply only to cases resembling the specific piles and soils of the source direct design database.

By systematically disassembling the design equations and considering the uncertainty associated with each design variable or relationship separately, we quantified the various sources of uncertainty for each method. Using this technique, we identified where the sources of uncertainty are different between design methods. An example of *RF* calculations was given to illustrate the significance of this uncertainty aggregation technique. The example shows that separately accounting for each source of uncertainty can reduce the sensitivity of *RF* values to individual model or measurement distributions. Furthermore, as these distributions are researched and updated, this technique allows a modular approach to updating the relevant models and calculating new values of *RF*.

Finally, we presented an example showing the difference in resistance factors obtained when *IFR* is measured or unknown. This example illustrated the ability of resistance factors to convey the design value of this additional information. Conversely, the impact on the reliability or risk of the design by omitting this information can be similarly assessed.

5 REFERENCES

Altaee et al. (1992). "Axial load transfer for piles in sand: I. Tests on an instrumented precast pile." *Canadian Geotechnical Journal*, 29, 11-20.

Altaee et al. (1993). "Load transfer for piles in sand and the critical depth." *Canadian Geotechnical Journal*, 30, 455-463.

American Society of Civil Engineers (ASCE) (2000). *Minimum design loads for buildings and other structures*, ASCE 7-2000, ASCE, Reston, Virginia.

AASHTO (1998). *LRFD Bridge Design Specifications, 2nd ed*. American Association of State Highway and Transportation Officials, Washington D.C.

BCP Committee (1971). "Field tests on piles in sand." *Soils and Foundations*, 11(2), 29-49.

Beringen, F. L., Windle, D. and Van Hooydonk, W. R. (1979). "Results of loading tests on driven piles in sand." *Proc. Conference on Recent Developments in the Design and Construction of Piles*, ICE, London, 213-225.

Bolton, M. D. (1986). "The Strength and Dilatancy of Sands." *Geotechnique*, 36, 65-78.

Briaud, J.-L., Tucker, L. M., and E. Ng. (1989). "Axially Loaded 5 Pile Group and a Single Pile in Sand." *Proc. 12th Int. Conf. Soil Mechanics and Foundation Engineering*, Rio de Janeiro, 2, 1121-1124.

Ellingwood, B., Galambos, T. V., MacGregor, J. G., and Cornell, C. A. (1980). *Development of a probability based load criterion for American National Standard A58 - Building Code Requirements for Minimum Design Loads in Buildings and other Structures*, National Bureau of Standards, Washington, D.C.

Foye, K. C., Salgado, R., and Scott, B. (2006a). "Assessment of Variable Uncertainties for Reliability-Based Design of Foundations." *Journal of Geotechnical and Geoenvironmental Engineering*, ASCE, 132(9): 1197-1207.

Foye, K. C., Salgado, R., and Scott, B. (2006b). "Resistance Factors for Use in Shallow Foundation LRFD." *Journal of Geotechnical and Geoenvironmental Engineering*, ASCE, 132(9): 1208-1218.

Gregersen, O. S., Aas, G., and Dibiagio, E. (1973). "Load tests on friction piles in loose sand." *Proc. 8th Int. Conf. Soil Mechanics & Foundation Engineering*, Moscow, 2, 109-117.

Jardine, R. and Chow, F. C., (1998). *Research into the Behaviour of Displacement Piles for Offshore Foundations*, OTO 98 833, Health and Safety Executive.

Lee, J., Salgado, R., and Paik, K. (2003). "Estimation of Load Capacity of Pipe Piles in Sand Based on Cone Penetration Test Results." *Journal of Geotechnical and Geoenvironmental Engineering*, ASCE, 129(6), 391-403.

Lehane, B. M., Jardine, R. J., Bond, A. J., and Frank, R. (1993). "Mechanisms of Shaft Friction in Sand from Instrumented Pile Tests." *Journal of Geotechnical Engineering*, ASCE, 119(1), 19-35.

Low, B. K., and Tang, W. H. (1997). "Efficient Reliability Evaluation Using Spreadsheet." *Journal of Engineering Mechanics*, ASCE, 123(7), 749-752.

Paik, K. and Salgado, R. (2003). "Determination of Bearing Capacity of Open-Ended Piles in Sand." *Journal of Geotechnical and Geoenvironmental Engineering*, ASCE, 129(1), 46-57.

Paik, K., Salgado, R., Lee, J., and Kim, B. (2003). "Behavior of Open- and Closed-Ended Piles Driven Into Sands." *Journal of Geotechnical and Geoenvironmental Engineering*, ASCE, 129(4), 296-306.

Paikowsky, S. G. (2004). *Load and Resistance Factor Design for Deep Foundations*, NCHRP Report 507, Transportation Research Board, Washington, D.C.

Rao, K. S., Allam, M. M., and Robinson, R. G. (1998). "Interfacial Friction Between Sands and Solid Surfaces." *Proc. ICE, Geotechnical Engineering*, 131, 75-82.

Salgado, R. (2008). *The Engineering of Foundations*. McGraw-Hill.

Vesic, A. S. (1970). "Tests on Instrumented Piles, Ogeechee River Site." *J. Soil Mech. Found. Div.*, ASCE, 96(2), 561–504.

Withiam, J. L., Voytko, E. P., Barker, R. M., Duncan, J. M., Kelly, D. C., Musser, S. C., and Elias, V. (1997). *Load and resistance design (LRFD) for highway bridge substructures*. Federal Highway Administration, Washington, D.C.

ISGSR 2011 - Vogt, Schuppener, Straub & Bräu (eds) - © 2011 Bundesanstalt für Wasserbau ISBN 978-3-939230-01-4

Influence of Model Accuracy on Load and Resistance Factor Calibration of Multi-anchor Walls

Y. Miyata
National Defense Academy, Yokosuka, Japan

R.J. Bathurst
GeoEngineering Centre at Queen's-RMC, Kingston, Canada

T. Konami
Okasan Livic, Tokyo, Japan

ABSTRACT: Multi-anchor walls (MAWs) are now a well-established earth retaining wall technology in Japan. This paper examines the accuracy of MAW design models on load and resistance factor design calibration. Measured anchor loads and anchor plate capacities from full-scale tests reported in the literature are compared to predicted values using the analytical models recommended in Japan by PWRC. Modified load and resistance models are proposed that preserve the general form of the PWRC equations but introduce correction factors to improve accuracy. The correction factors are empirically-based and are selected by back-fitting to measured loads to achieve a load bias mean equal to one and a low coefficient of variation (COV) of bias values. In developing the pullout capacity model, a large number of small-scale anchor capacity tests carried out in pullout boxes were also used to guide the selection of back-fitted parameters. This research work represents the first attempt at rigorous reliability-based load and resistance factor calibration for MAW systems.

Keywords: reinforced soil walls, multi-anchor walls, load and resistance factor design, limit states design, load and resistance factors, reliability analysis

1 INTRODUCTION

Reinforced soil wall techniques are now well established and offer economical solutions to geotechnical soil retaining wall problems. Reinforced soil walls can be broadly classified into metallic, geosynthetic and multi-anchor categories. Since ISO 2394 was introduced, there has been increased interest in the development of rigorous reliability-based design approaches for reinforced soil wall systems in Japan, Europe and the USA.

Multi-anchor walls (MAWs) are constructed with steel plate anchors bolted to round bar sections that are attached at the opposite end to the wall facing. Fig. 1 shows details of the key components in the Japanese MAW system. The reinforced concrete panels are 1.5 m wide, 1 m high and 180 mm thick. Pinned connections at the back of the facing panels are used to attach the anchor rods on 0.75 m centers in the running length of the wall face. Each rod is attached to a plate using a threaded end, washer and nut. The standard steel anchor plates are 300 mm by 300 mm.

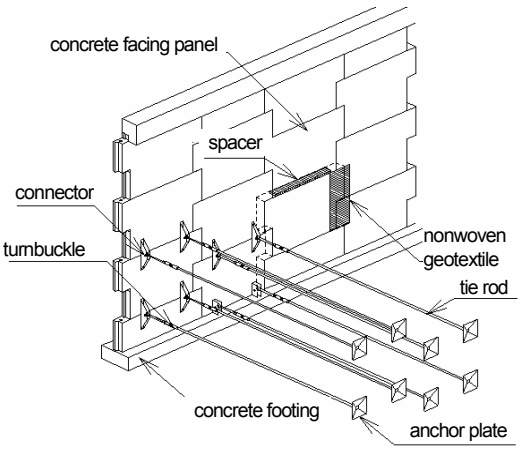

Figure 1. Multi-anchor walls

The current approach for external and internal stability design of reinforced soil wall systems in Japan is based on a classical factor of safety approach (PWRC 2002). Recently, the Public Works Research Center (PWRC) has expressed interest to move towards a more rigorous reliability-based design approach.

An important step to develop a reliability-based design method is calibration of load and resistance factors. A methodology to undertake calibration that explicitly includes underlying model error and variabil-

ity in model input parameters has been described in the work by Allen et al. (2005) and Bathurst et al. (2008a, 2011). This approach requires measured resistance and load values from a database of laboratory and full-scale tests reported in the literature, predicted values using design models for resistance and load side of limit state equations and, statistical analysis of the bias values computed from the ratio of measured to predicted values. The bias value statistics are used to calibrate load and resistance factors to be used in current PWRC models and new modified design models. The new models preserve the general form of the PWRC equations but introduce correction factors to improve accuracy. The relative accuracy of the models investigated in this paper can be quantified by comparing the magnitudes of the mean and coefficient of variation (COV) of the bias values. This research work represents the first attempt at rigorous reliability-based load and resistance factor calibration for MAW systems.

2 GENERAL APPROACH

The general approach used here to perform load and resistance factor calibration for the pullout ultimate limit state for MAW anchors follows that reported by Allen et al. (2005) and Bathurst et al. (2008a, 2011). They used a database of steel grid soil reinforced walls to demonstrate calculation steps for simple limit states.

The pullout limit state functions in this paper have the general form:

$$g = R_m - Q_m \geq 0 \tag{1}$$

where R_m = measured resistance (pullout capacity) and Q_m = measured (axial) load under operational conditions.

Bias is defined as the ratio of measured to predicted (calculated) value. In limit states design terminology the calculated value is often called the nominal value. Hence, a measured value can be expressed as the product of bias and nominal value; specifically:

$$R_m = X_R R_n \tag{2}$$

$$Q_m = X_Q Q_n \tag{3}$$

where X_R = resistance bias, X_Q = load bias, R_n = nominal resistance, and Q_n = nominal load. In limit states design the limit state function is expressed in terms of the nominal values of the resistance and load terms which are computed using deterministic equations; hence for design the limit state function can be expressed as:

$$g = X_R R_n - X_Q Q_n \geq 0 \tag{4}$$

The failure of a reinforcing anchor occurs when $g < 0$ and therefore the probability of failure must be related to actual (i.e. measured) load and resistance values. Bias statistics allow predicted values to be adjusted to measured values so that probability of failure is computed for the considered limit state conditions. If the equations for load and resistance give values that are equal to measured values then, $X_R = X_Q = 1$. This is unlikely in engineering practice since there are always errors in equation accuracy due to the combined effect of model error and other sources of variation in input parameter values (e.g. random variation in input parameter values, spatial variation in input values, quality of data and, consistency in interpretation of data when data are gathered from multiple sources). In this paper, the source of model accuracy is all of these contributions to error in load and resistance predictions.

In limit state design practice for the case of one resistance term and one load term, the limit states design equation can be expressed as:

$$\varphi R_n - \gamma_Q Q_n \geq 0 \tag{5}$$

Here, γ_Q = load factor and φ = resistance factor. Re-arrangement of Eq. (4) leads to:

$$g = (\gamma_Q/\varphi)\, X_R - X_Q \geq 0 \tag{6}$$

If load and resistance bias values are log-normally distributed and the limit state function is linear, the reliability index β can be calculated as:

$$\beta = \frac{\ln\left[(\gamma_Q/\varphi)(\mu_R/\mu_Q)\sqrt{\left(1+COV_Q^2\right)/\left(1+COV_R^2\right)}\right]}{\sqrt{\ln\left[\left(1+COV_Q^2\right)\left(1+COV_R^2\right)\right]}} \tag{7}$$

where μ_R and COV_R = mean and coefficient of variation of resistance bias values, and μ_Q and COV_Q = mean and coefficient of variation of load bias values. For a given load factor and set of bias mean and COV values, a resistance factor value can be found to satisfy a target reliability index value using Eq. (7).

3 DATABASE OF PHYSICAL TEST RESULTS

Anchor loads recorded from eight full-scale MAW wall sections were collected by the writers (Table 1). All of the walls performed well with facing deformations falling within serviceability criteria recommended by PWRC (2002). Details of these walls can be found in the paper by Miyata et al. (2009).

Anchor capacity data were taken from 28 full-scale in-situ anchor load tests (Table 2). Additional data from reduced-scale laboratory anchor load tests (Table 3) were also used to assist in the formulation of a new anchor pullout capacity design equation.

Table 1. Summary of multi-anchor wall case studies for load models.

Designation	Wall height, H (m)	Soil unit weight, γ (kN/m^3)	Peak friction angle, ϕ_{tx} (deg.)	Cohesion, c (kPa)	Fines content, F (%)	Rod length, L (m)	Reference
MAW-1	6.0	16.0	36	0	6	4.0	PWRC (1995)
MAW-2	6.0	15.4	30	2	19		
MAW-3	6.0	15.3	11	4	42		
MAW-4	4.0	15.0	38	2	8	4.0	
MAW-5	4.0	15.7				2.5	
MAW-6a	3.0	15.0	33	0	7	3.5	Aoyama et al. (2000), Futaki et al. (2000)
MAW-6b	4.0						
MAW-7	6.0	18.0	35	0	0.2	12.8	Kitamura et al. (2000)

Table 2. Summary of MAW full-scale in-situ anchor load tests for pullout (resistance) models.

No.	Soil unit weight, γ (kN/m^3)	Peak friction angle, ϕ_{tx} (deg.)	Cohesion, c (kPa)	Fines content, F (%)	Rod length, L (m)	Plate size, B (m)	Confining stress, σ_v (kPa)	Reference
1	16.0	36	0	6	4.0	0.3	32 – 80	PWRC (1995), Kondo et al. (1995), Nakamura et al. (1995)
2	15.4	30	2	19	4.0	0.3	31 – 77	
3	15.2	11	4	42	4.0	0.3	45 – 61	
4	15.0	34	0	8	4.0	0.3	15 – 45	PWRC (2002)
5	14.4	25	6	68	4.0	0.3	29 – 43	
6	18.9	5	16	52	2.0 – 5.0	0.4	19 – 57	Fukuoka et al. (1984b)
7	17.9	11	18	68	2.0, 4.0	0.3	36	
8	19.8	30	0	10	2.0, 4.0	0.3	40	

Table 3. Summary of MAW reduced-scale laboratory anchor load tests used to develop new pullout capacity model.

No.	Soil unit weight, γ (kN/m^3)	Peak friction angle, ϕ_{tx} (deg.)	Cohesion, c (kPa)	Fines content, F (%)	Rod length, L (m)	Plate size, B (m)	Confining stress σ_v (kPa)	Reference
1	13.8	38	0	n.a.	n.a.	0.051	0.4 – 3.2	Neely et al. (1973)
2	15.8	34	0	0	0.64	0.051	0.9 – 2.7	Das (1975)
3	14.8	31	0	0	0.61	0.032	0.4 – 3.2	Das et al. (1977)
	15.8	34	0	0				
	16.9	41	0	0				
4	14.0	35	0	3	0.3	0.021 – 0.035	2.4 – 12.0	Fukuoka et al. (1984a)
	13.1	22	12	87			9.8 – 39.2	
5	15.8	34	0	0	0.64	0.025 – 0.051	0.6 – 2.2	Hoshiya et al. (1984)
6	15.1	35	0	0	0.9 – 2.5	0.075 – 0.125	50 – 150	Takeoka et al. (2009), Watanabe et al. (2009)

4 CURRENT DESIGN MODELS

4.1 *Formulations*

In the current PWRC (2002) approach, the maximum anchor load (T_{max}) is computed in units of force as:

$$T_{max} = \left[K_a \sigma_v - 2c\sqrt{K_a} \right] S_v S_h \quad (8)$$

where K_a = coefficient of active earth pressure, $\sigma_v = \gamma z$ = maximum vertical (confining) stress acting at the elevation of the reinforcement (here γ is soil unit weight and z is the depth of anchor below the backfill surface), S_v = anchor vertical spacing, S_h = horizontal anchor spacing (S_h = 0.75 m for MAW anchors), and c = soil cohesion. K_a in Eq. (8) is computed as:

$$K_a = \frac{\cos^2 \phi}{\cos\delta \left\{ 1 + \sqrt{\frac{\sin(\phi+\delta)\sin\phi}{\cos\delta}} \right\}^2} \quad (9)$$

where $\delta = 2\phi/3$ is the interface friction angle between the soil and back of the panel facing.

In the current PWRC (2002) approach, the ultimate anchor plate capacity (resistance) (R_p) is computed in units of force as:

$$R_p = \left[cN_c + K_a \sigma_v (N_q - 1) \right] B^2 \quad (10)$$

where, N_c and N_q = non-dimensional capacity factors expressed as functions of soil peak friction angle (ϕ), c = cohesion, K_a = active earth pressure coefficient, σ_v = vertical (confining) stress at the anchor rod elevation and, B = height (width) of the square anchor plate. The non-dimensional capacity factors (solid lines) shown in Fig. 2 are calculated from a plasticity model proposed by Miura et al. (1994).

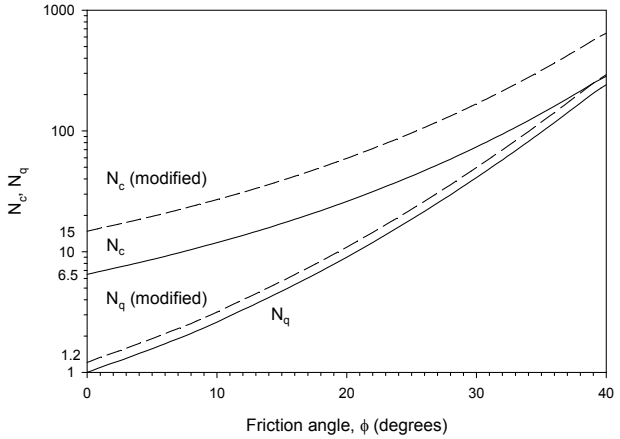

Figure 2. Non-dimensional anchor capacity factors. Note: solid curves are for current model (Miura et al. 1994) and dashed curves are for modified model.

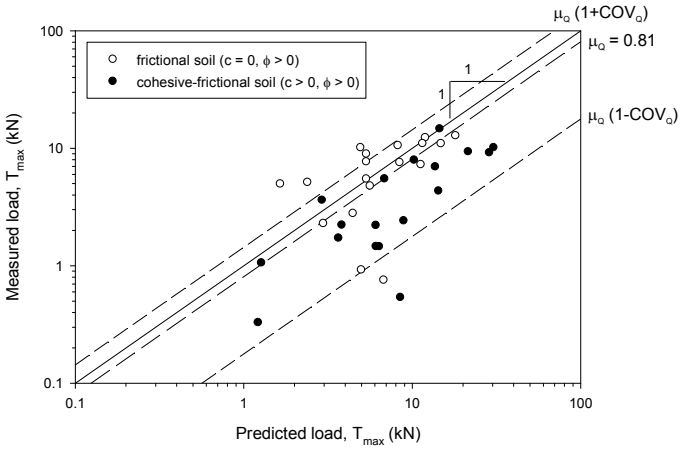

Figure 3. Measured versus predicted maximum anchor loads using current design model.

4.2 *Accuracy of current design models*

Measured versus predicted loads using the current load model are plotted in Fig. 3. The data are plotted using logarithmic axes to improve visibility for small load values. Values of μ_Q and COV_Q for all data and data subsets are shown in Table 4. These numbers show that for granular soil backfill wall cases the prediction of maximum anchor loads is reasonably accurate on average. However, for cohesive-frictional soil wall cases the bias statistics are much poorer. On average, measured anchorage loads are about 50% of the predicted values. However, the low mean bias value and large bias COV value demonstrate that the current load model is very inaccurate and if these values are used in load and resistance factor calibration they result in unrealistic load and resistance factors. A more accurate load model is desirable to improve calibration outcomes.

Measured versus predicted anchor capacities using the current design model are plotted in Fig. 4. Again, the data are plotted using logarithmic axes to improve visibility for small load values. The quantities μ_R and COV_R are the mean and coefficient of variation (COV) of anchor capacity bias values for all data points in each data set. Bias statistics are summarized in Table 5. These bias statistics show that the accuracy of the current anchor capacity model also depends on soil type. This dependency is smaller than that for the load model. However, improvement of the pullout capacity (resistance) model can be expected to lead to better bias statistics and therefore load and resistance factors that are closer to one.

5 MODIFICATION OF DESIGN MODELS

5.1 *Modification of load model*

A modified design equation to predict the maximum load in an anchor at end of construction has been proposed by Miyata et al. (2009) which can be written as:

$$T_{max} = \bar{\sigma} D_{tmax} \alpha \Phi_c S_v S_h \quad (11)$$

where $\bar{\sigma}$ = average active earth pressure computed as:

$$\bar{\sigma} = \frac{1}{H}\int_0^H K_a \gamma z \, dz = \frac{1}{2} K_a \gamma H \quad (12)$$

The other terms not defined earlier are D_{tmax} = load distribution factor, H = the height of the wall, and α = empirical factor applied to Φ_c. The latter is called the soil cohesion factor which reduces the anchor load due to the cohesive component of soil strength. The cohesion factor is computed as:

$$\Phi_c = 1 - \lambda \frac{c}{\gamma H} \quad (13)$$

These equations have been inspired by the structure of similar expressions to estimate loads in geosynthetic reinforced soil walls proposed by Miyata and Bathurst (2007) and Bathurst et al. (2008b).

Parameters α and λ have been estimated by back fitting to measured loads in the full-scale walls summarized in Table 1 as explained below. D_{tmax} is the ratio of measured T_{max} normalized with T_{mxmx} = maximum anchor load in the wall and is plotted against depth z normalized with H in Fig. 5. For design, D_{tmax} is taken as the dashed line shown in this figure. This is different from the generally monotonically increasing load distribution for anchor loads using the current PWRC design method (Eq. 8).

Both α and λ are estimated using an optimization technique with the objective function taken as the mean of the load bias value equal to one where load bias = T_{max} (measured) / T_{max} (predicted) = X_Q. This analysis gives α = 1.21 for frictional backfill soils, α = 1.02 for cohesive-frictional soils and λ = 15.2. A practical consequence of Eq. (13) with λ = 15.2 is that walls with $c/\gamma H \geq 0.06$ will not generate any anchor loads. However, the designer must decide if the cohesive soil strength component is available for the life of the structure.

Table 4. Summary of statistics for ratio (bias) of measured to predicted reinforcement loads using current design model.

	All	Granular soil backfill (c=0, ϕ>0)	Cohesive-frictional soil backfill (c>0, ϕ>0)
μ_Q	0.81	1.14	0.50
COV_Q (%)	79	65	62

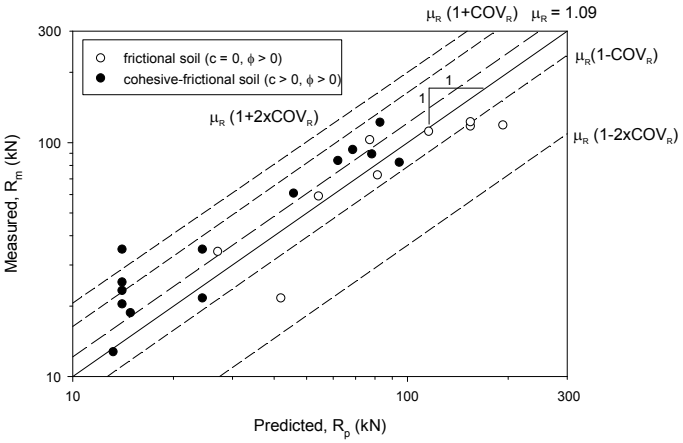

Figure 4. Measured versus predicted anchor pullout capacity using current design model.

Table 5. Summary of statistics for ratio (bias) of measured to predicted anchor pullout capacity using current design model.

	All	Granular soil backfill (c=0, ϕ>0)	Cohesive-frictional soil backfill (c>0, ϕ>0)
μ_R	1.21	0.96	1.39
COV_R (%)	35	31	30

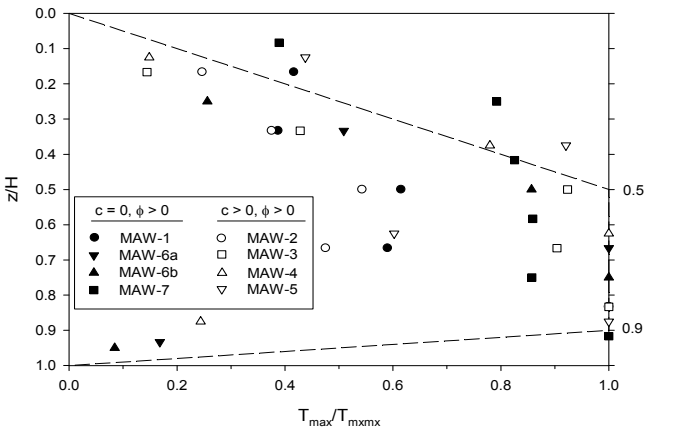

Figure 5. Distribution of D_{tmax} = ratio of maximum anchor load (T_{max}) to maximum anchor load in the wall (T_{mxmx}).

Measured versus predicted loads using the modified load model are plotted in Fig. 6. The visual impression is that there is better agreement between predicted and measured values since the data is more closely grouped around the 1:1 correspondence line compared to Fig. 3 using the current design approach. The summary of bias statistics using the new load model shown in Table 6 confirms that the proposed approach to compute reinforcement loads is better than the current Japanese model (PWRC 2002). The quantitative improvement is greatest for the cohesive-frictional backfill soil cases. In a related earlier

work the writers have demonstrated that the new load model is also accurate for MAW systems subjected to transient flooding conditions (Miyata et al. 2009).

5.2 *Modification of anchor pullout capacity model*

A modified design equation to predict anchor plate capacity is proposed to improve the accuracy of the current ultimate anchor pullout capacity equation (Eq. 10) for MAW systems:

$$R_p = S_L \left[cN'_c + K_a S_d \sigma_v (N'_q - 1) \right] S_B B^2 \quad (14)$$

Here, N'_c and N'_q = new bearing capacity factors modified from the original values (Fig. 2). The modified bearing capacity coefficients are computed using empirically determined constant correction factors m_c and m_q:

$$N'_c = m_c \, N_c \quad (15)$$

$$N'_q = m_q \, N_q \quad (16)$$

The other parameters are: S_L = correction factor for the influence of anchor rod length L; parameter S_d = correction factor for influence of anchor depth, and; parameter S_B = scale factor on anchor plate size. This is similar to the approach used to modify the classical bearing capacity equation for a strip footing to account for the effect of other footing shapes, load eccentricity and the like.

Correction factors were based on back-analysis and optimization using in-situ load test measurements for the case studies shown in Table 2. Measurements from the reduced-scale laboratory pullout tests are summarized in Table 3 and plotted against predicted values in Fig. 7. These data were used to examine the accuracy of the form of the correction terms but were not used quantitatively in the back-calculation process. The correction terms with constant coefficient terms ξ, ψ_1, ψ_2 and ζ are expressed as:

$$S_L = \xi \, L \quad (17)$$

$$S_d = \left(\psi_1 \frac{z}{B} \right)^{\psi_2} \quad (18)$$

$$S_B = \left(\frac{0.3}{B} \right)^{\zeta} \quad (19)$$

The new constant coefficients are taken as or calculated as: m_c = 2.27, m_q = 1.21, ξ = 0.25 [unit =1/m], ψ_1 = 1/6, ψ_2 = 1.0 for $1/3 \le z/6B \le 1$ or $\psi_2 = -0.5$ for $z/6B > 1$ and ζ = 0.5.

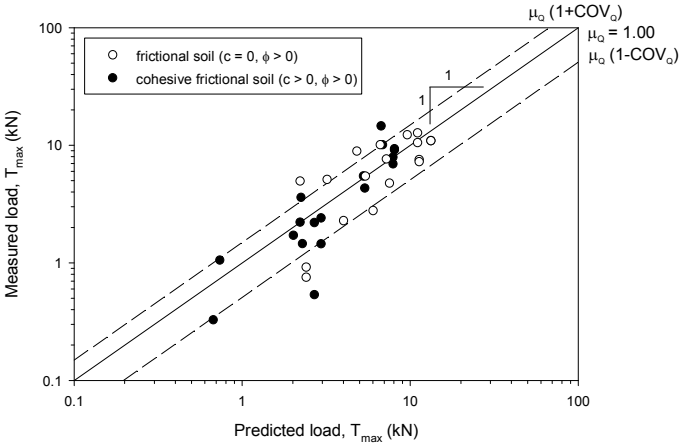

Figure 6. Measured versus predicted maximum anchor loads using modified design load model.

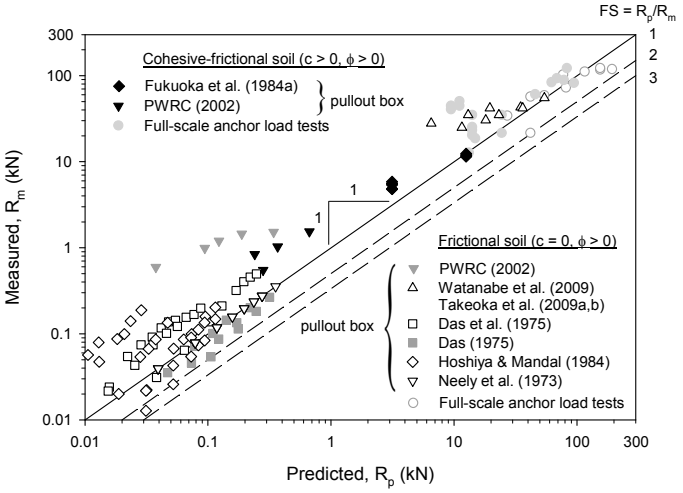

Figure 7. Measured versus predicted maximum anchor capacity using current design model and results of laboratory pullout tests and full-scale anchor pullout tests.

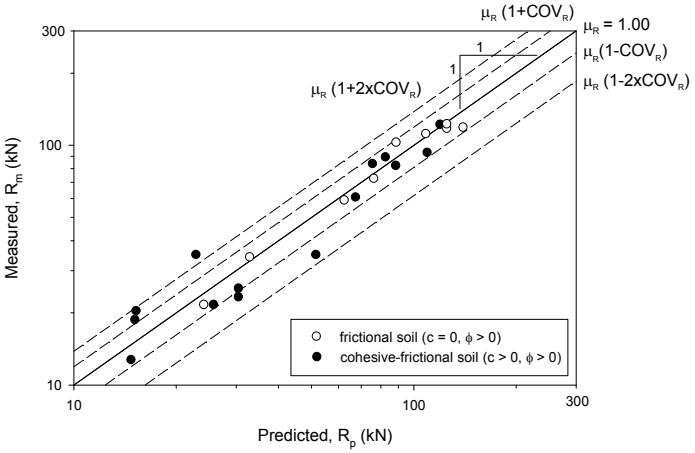

Figure 8. Measured versus predicted maximum anchor capacity using modified design model and full-scale anchor pullout tests.

The accuracy of the original ultimate anchor pullout capacity equation (Eq. 10) can be seen in Fig. 4 for all available data. The improvement in anchor capacity prediction for full-scale anchors is shown in Fig. 8 where measured versus predicted anchor capacities using the new modified anchor capacity model are plotted. The visual impression is that the data for both soil types is more closely distributed about the one-to-one correspondence line compared to the data in Fig. 4 (current model). Computed mean and

spread in bias statistics are shown in Table 7. These numbers show that the proposed approach to compute anchor pullout capacity is quantitatively better than the current Japanese (PWRC 2002) for frictional backfill cases. The quantitative prediction accuracy is even greater for c-ϕ backfill soil cases using the new anchor capacity method.

Table 6. Summary of statistics for ratio (bias) of measured to predicted reinforcement loads using modified design model.

	All	Granular soil backfill (c=0, ϕ>0)	Cohesive-frictional soil backfill (c>0, ϕ>0)
μ_Q	1.00	1.00	1.00
COV_Q (%)	50	53	46

Table 7. Summary of statistics for ratio (bias) of measured to predicted anchor pullout capacity using modified design model.

	All	Granular soil backfill (c=0, ϕ>0)	Cohesive-frictional soil backfill (c>0, ϕ>0)
μ_R	1.00	1.00	1.00
COV_R (%)	19	11	24

6 INFLUENCE OF MODEL ACCURACY ON LOAD AND RESISTANCE FACTORS

For a target reliability index β and prescribed load factor γ_Q a value of resistance factor φ can be computed using the limit state function (Eq. 6) and Monte Carlo simulation or the closed-form solution given by Eq. 7. The results of this calculation using the closed-form solution are shown in Fig. 9 using the bias statistics for current anchor load and anchor capacity equations (Tables 4 and 5) and the corresponding new equations (Tables 6 and 7). The plots show that the resistance factor is closer to one using the new approach which is a better outcome for load and resistance factor calibration and design.

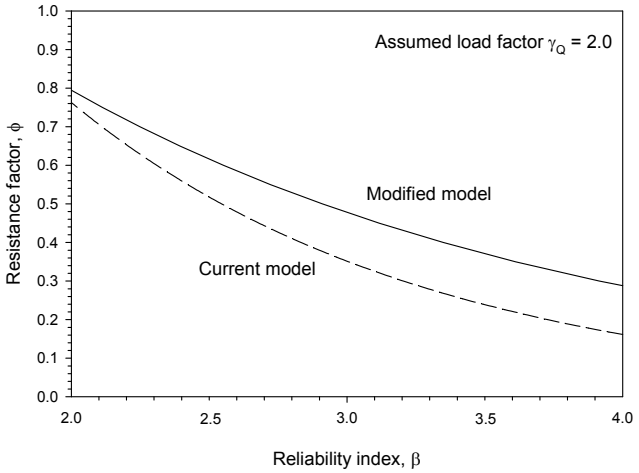

Figure 9. Estimated resistance factor with current or modified model.

7 CONCLUSIONS

This paper examines the accuracy of the MAW design models on load and resistance factor design calibration. Measured anchor loads and anchor plate capacities from full-scale tests reported in the literature are compared to predicted values using the analytical models recommended in Japan by PWRC.

Modified load and resistance models are proposed that preserve the general form of the PWRC equations but introduce correction factors to improve accuracy. The following conclusions can be made:

1) Accuracy of the current PWRC (2002) design model to calculate anchor loads was evaluated by using measurements from a series of eight full-scale wall sections. For purely frictional backfill soil cases, the current model was shown to slightly over-predict loads on average. For cohesive-frictional soil cases, accuracy of the current model was much poorer.
2) A new load model is proposed to improve prediction accuracy. The model with constant coefficients back-fitted to measured loads was shown to improve maximum anchor load predictions on average and to reduce the spread in bias values defined as the ratio of measured to predicted load values.
3) Accuracy of the current PWRC (2002) design model to calculate anchor plate pullout capacity was evaluated by using a total of 28 tests from multiple sources. The current resistance model is demonstrated to predict loads that vary widely from measured values in many cases.
4) A new resistance model is proposed that preserves the general form of the current PWRC (2002) model but includes correction factors to improve accuracy for the pullout ultimate limit state condition. Coefficients in the correction factor expressions were estimated from back-fitting analysis similar to the new load model development. The model gives improved predictions of anchor capacity for both frictional and cohesive frictional soil cases based on the mean and COV of resistance bias values where bias is the ratio of measured to predicted anchor load.
5) The results of load and resistance calibration assuming a simple linear limit state function leads to resistance factors that are closer to one which is a desirable outcome for load and resistance factor calibration and design.

ACKNOWLEDGEMENTS

The first author is grateful for funding awarded by the Japan Ministry of Education, Culture, Sports, Science and Technology (Grant-in-Aid for Scientific Research (B) No.21360229) and the Japan Ministry of Defense. The second author is grateful to the JSPS Invitation Fellowship Program for Research in Japan which provided support to work in Japan and complete the study described here.

REFERENCES

Allen, T.M., Nowak, A.S. and Bathurst, R.J. 2005. Calibration to determine load and resistance factors for geotechnical and structural design. Transportation Research Board Circular: E-C079, 93 p.

Bathurst, R.J., Allen, T.M. and Nowak, A.S. 2008a. Calibration concepts for load and resistance factor design (LRFD) of reinforced soil walls. Canadian Geotechnical Journal 45(10) 1377–1392.

Bathurst, R.J., Miyata, Y. Nernheim, A. and Allen, M.T. 2008b. Refinement of K-Stiffness method for geosynthetic reinforced soil walls. Geosynthetics International 15(4) 269-295.

Bathurst, R.J., Huang, B. and Allen, T.M. 2011. Load and resistance factor design (LRFD) calibration for steel grid reinforced soil walls. Georisk (in press)

Aoyama, K., Kikuchi, N., Konami, T. and Mikami, K. 2000. Full-scaled shaking table test for multi-anchored retaining wall with large shear box (Part I). In proceedings of the 35th Japanese Geotechnical Society annual meeting, Gifu, Japan, pp. 2213-2214 (in Japanese).

Das, B.M. 1975. Pullout resistance of vertical plate. ASCE Journal of Soil Mechanics and Foundations Division 100(GT1) 87-91.

Das, B.M, Seeley, G.R. and Das, S.C. 1977. Ultimate resistance of deep vertical anchor in sand. Soils and Foundations 17(2) 52-56.

Fukuoka, M., Imamura, Y., Sawada, S., Katada, M. and Watanabe, T. 1984a. Laboratory pullout tests on plate-anchors. In proceedings of the 19th Japanese Geotechnical Society Annual Meeting, Matsuyama, Japan, pp. 1179-1180 (in Japanese).

Fukuoka, M., Imamura, Y., Sawada, S., Nishimaki, S. and Ieda, T. 1984b. Field pullout tests on plate-anchors. In proceedings of the 19th Japanese Geotechnical Society Annual Meeting, Matsuyama, Japan, pp. 1181-1182 (in Japanese).

Futaki, M., Misawa, K. and Tatsumi, T. 2000. Full-scaled shaking table test for multi-anchored retaining wall with large shear box (Part II). In proceedings of 35th Japanese Geotechnical Society annual meeting, Gifu, Japan, pp. 2215-2216 (in Japanese).

Hoshiya, M. and Mandal, J.N. 1984. Some studies on anchor plates in sand. Soils and Foundations 24(1) 9-16.

ISO 2394. 1998. General principles on reliability for structures. International Organization for Standardization, Geneva, Switzerland.

Kitamura, Y., Misawa K. and Tatsumi, T. 2000. In CD proceedings of the 55th Japan Society of Civil Engineers annual meeting, Sendai, Japan, CD-ROM, III-B293, 2 p.

Kondo, K., Nakamura, S., Dobashi, K. and Miyatake, H. 1995. Full scale test of reinforced soil wall constructed on the shore – Multi-anchor wall (Part I), Anchor loads during water table rise. In proceedings of the 50th Japan Society of Civil Engineers Annual Meeting, Sapporo, Japan, Vol. III, pp. 1598-1599 (in Japanese).

Miyata, Y. and Bathurst, R.J. 2007. Development of K-Stiffness method for geosynthetic reinforced soil walls constructed with c-ϕ soils. Canadian Geotechnical Journal 44(11) 1391-1416.

Miyata, Y., Bathurst, R.J. and Konami, T. 2009. Measured and predicted loads in multi-anchor reinforced soil walls in Japan. Soils and Foundations 49(1) 1-10.

Miyata, Y., Bathurst, R.J., Konami, T. and Dobashi, K. 2010. Influence of transient flooding on multi-anchor walls. Soils and Foundations 50(3) 373-384.

Nakamura, S., Kondo, K., Dobashi, K. and Miyatake, H. 1995. Full scale test of reinforced soil wall constructed on the shore – Multi-anchor wall (Part II), Pullout resistance of anchor plate. In proceedings of the 50th Japan Society of Civil Engineers Annual Meeting, Sapporo, Japan, Vol. III, pp. 1600-1601 (in Japanese).

Neely, W.J., Stuart, J.G. and Graham, J. 1973. Failure loads in vertical anchor plates in sand. ASCE Journal of Soil Mechanics and Foundations Division 99(SM9) 669-685.

PWRC. 1995. Technical report on rational design method of reinforced soil walls. Public Works Research Center, Tsukuba, Ibaraki, Japan, 278 p. (in Japanese).

PWRC. 2002. Design method, construction manual and specifications for multi-anchored reinforced retaining wall. Public Works Research Center, Tsukuba, Ibaraki, Japan, 248 p. (in Japanese).

Takeoka, Y., Watanabe, Y., Kodaka, T., Nakano, M. and Noda, T. 2009a. Pullout test of reinforcement in sandy soil considering bearing resistance and friction resistance. In proceedings of the 44th Japanese Geotechnical Society Annual Meeting, Yokohama, Japan, pp. 465-466 (in Japanese).

Watanabe, Y., Takeoka, Y., Kodaka, T., Nakano, M. and Noda, T. 2009. Pullout test of reinforcement with anchor plates in sandy soil. In proceedings of the 44th Japanese Geotechnical Society Annual Meeting, Yokohama, Japan, pp. 463-464 (in Japanese).

4 Codes and Standards

ISGSR 2011 - Vogt, Schuppener, Straub & Bräu (eds) - © 2011 Bundesanstalt für Wasserbau ISBN 978-3-939230-01-4

Reliability Assessment of Eurocode 7 Retaining Structures Design Methodology

S. H. Marques & A. T. Gomes & A. A. Henriques
University of Porto, Faculty of Engineering, Department of Civil Engineering, Porto, Portugal

ABSTRACT: This paper is a contribution for the application of Eurocode 7 design methodology, based on the limit state design (LSD) approach. The design methodology of Eurocode 7 is applied to a concrete gravity retaining structure resting on a relatively homogeneous c-φ soil, and the different design approaches are compared to deterministic and semi-probabilistic solutions, considering the bearing resistance failure of the foundation. A reliability assessment is performed for different conditions, selecting different geotechnical parameters, particularly characteristic values and coefficients of variation of soil properties, and taking into account the effects of vertical fluctuation scale by using a simplified approach. Several uncorrelated and correlated random variables are considered, and probabilistic solutions are achieved and compared with a target ultimate limit state reliability index β for a medium risk structure and fifty years reference period, considered as 3.8. For this purpose, reliability techniques such as the first-order reliability method (FORM) and the Monte Carlo simulation (MCS) are applied and compared to other methodologies. Based on the obtained results, the Eurocode 7 design methodology is discussed, and the indispensable engineering judgment is outlined.

Keywords: Eurocode 7; limit state design; retaining structures; reliability; variability

1 INTRODUCTION

The Eurocodes are a set of European Standards for the design of buildings and other civil engineering works, based on the limit state design (LSD) approach, used in conjunction with a partial factor methodology. A wide range of types of structures and products is covered and moreover, the harmonization of safety levels in construction is a contribution to improve the competitiveness of the construction industry in the global markets. In this context, the adoption of Eurocodes may be attractive worldwide, also outside European Union, taking into account the flexibility provided by a system of nationally determined parameters.

Eurocode 7 is a geotechnical design code that shares common bases with the design methodology for structures, consisting of two parts: EC 7-1 (General rules) and EC 7-2 (Ground investigation and testing). The design approaches and the values of the partial factors are specified by each Member State in a National Annex, and extensive education and training is required in implementation towards harmonization. In the long term, matters relating to the development of new items will be examined, for example harmonization of calculation methods or evaluation of test results with respect to the selection of characteristic values of soil properties. According to this, research is strongly encouraged for further harmonization of geotechnical design in European Union: the values of recommended partial factors have been based largely on reproducing existing designs, with traditional levels of safety and sustainability, and further investigation about economic issues is therefore relevant; other practical interest is the application of numerical methods in addition to the classical calculation models (Schuppener, 2010).

It may be argued that comparative studies of the different design approaches and values of the partial factors are required for harmonization, thus further research about reliability assessment of Eurocode 7 design methodology is a promising and valuable contribution for the development of insight, allowing the acquirement of new skills. According to this, partial results of a study concerning Eurocode 7 design

methodology and reliability are introduced in this paper. Design concepts of Eurocode 7 with regard to retaining structures on a relatively homogeneous c-φ soil are presented, and a reliability-based design (RBD), level I and level II, is performed by selecting different geotechnical parameters, particularly characteristic values and coefficients of variation of soil properties. For this purpose, several uncorrelated and correlated random variables are considered. The effects of vertical fluctuation scale are accounted considering different vertical spatial correlation lengths, even as vertical characteristic lengths. Finally, different methodologies for reliability evaluation are compared, and the influence of probability distribution is also outlined.

2 CHARACTERISTIC VALUES

The estimation of characteristic values depends on risk tolerance, in other words, affects stability as well as economic feasibility, and shall be based on the results of field and laboratory tests. This means that a clear definition of characteristic values is essential. Characteristic values are representative values of parameters, evaluated by considering uncertainties, and considered as the most adequate values to estimate the occurrence of limit states. Due to genetic and anthropogenic processes, soil is nonhomogeneous regarding its geometrical and physical characteristics, wherefore soil properties are predicted through models. Even so, the spatial variability of soil properties in a relatively homogeneous layer may be broad and affect significantly the reliability of geotechnical systems. Therefore, the investigation concerning characteristic values provides very valuable insights into reliability-based design (RBD), and an important issue is the soil variability owing to insufficient test data (Yoon *et al*.,2010).

This paper presents results based on the definition of eight sets of characteristic values of soil properties X_k - pure mean values (considered as a superior reference) (1), Schneider's equation values (2), Ovesen's equation values (3), 95% reliable mean values (according to the number of test results and for unknown or known Cv_x, referenced as mean) (4), 5% fractile values (from a normal probability distribution) (5), and 5% fractile values (according to the number of test results and for unknown or known Cv_x, referenced as low) (6):

$X_k=X_m$ (1); $X_k=X_m-0.5\sigma_x$ (2); $X_k=X_m-1.645\sigma_x/\sqrt{N}$ (3);

$X_k=X_m(1-k_{n,mean}Cv_x)$ (4); $X_k=X_m-1.645\sigma_x$ (5); $X_k=X_m(1-k_{n,low}Cv_x)$ (6)

in which X_m is the mean value, σ_x is the standard deviation, Cv_x is the coefficient of variation, N is the number of test results, and $k_{n,mean}$ and $k_{n,low}$ are statistical coefficients taking into account the sampling (only local, when Cv_x is considered unknown, or local in conjunction with relevant experience, when Cv_x is considered known), the number of test results, the value affecting the occurrence of the limit state (the mean value, or the lowest value, respectively), and the statistical level of confidence required for the assessed characteristic value, expressed by a considered t factor of Student's distribution (Frank *et al*., 2004; Yoon *et al*., 2010). A relatively homogeneous soil and normal probability distributions for the values of soil properties were assumed, although this assumption is not always valid (for the considered example, all characteristic values of soil properties yield positive results). Characteristic load values were considered as 95% fractile values (from a normal probability distribution).

3 EXAMPLE

A concrete gravity retaining structure is shown in Figure 1. For bearing capacity predictions (inclined eccentric loading problem) the performance function can be described by the simplified equation (7):

$$M = f(B_1, B_2, H_1, H_2, \gamma_c, \varphi_w, \gamma_w, c_f, \varphi_f, \gamma_f, q) \quad (7)$$

where the sum of B_1 and B_2 is the foundation width B; H_1 is the wall height; H_2 is the foundation height; γ_c is the unit concrete weight; φ_w is the friction angle of the soil on the active and passive sides of the wall; γ_w is the unit soil weight on the active and passive sides of the wall; c_f is the cohesion of the foundation soil; φ_f is the friction angle of the foundation soil; γ_f is the unit weight of the foundation soil; and q is the variable surcharge at ground surface. Other considered parameters are: the soil-wall interface friction

angle on the active side of the wall $\delta_w a = 2/3\,\varphi_w$; and the soil-wall interface friction angle on the passive side of the wall $\delta_w p = 0$.

Table 1 summarizes the data based on the results of some tests on a c-φ soil or published values in the literature, where the coefficient of variation is both considered unknown or known (some references are Cherubini, 2000; Duncan, 2000; Forrest *et al*., 2010; Phoon *et al*., 1999a; Phoon *et al*., 1999b).

The effects of spatial variability are accounted by the approach described by equation (8):

$$\Gamma^2 = \left[\frac{\theta_v}{L_v}\left(1 - \frac{\theta_v}{4L_v}\right)\right] \text{ for } \frac{\theta_v}{L_v} \leq 2 \qquad (8)$$

where Γ is the variance reduction factor; θ_v is the vertical spatial correlation length; and L_v is the vertical characteristic length, related to the dimensions of the potential failure surface (VanMarcke, 1983).

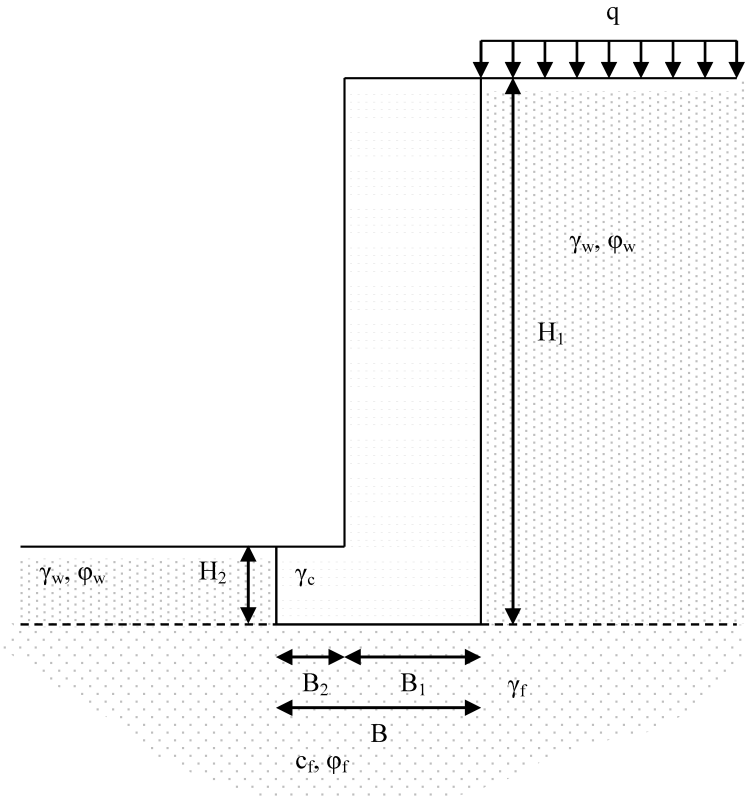

Figure 1.Concrete gravity retaining structure.

Table 1.Data based on the results of some tests on a c-φ soil or published values in the literature.

Basic random variables	Probability distribution	Number of test results	Mean value μ	Standard deviation σ	Coefficient of variation Cv
B_1 (m)	Normal	-	-	-	0.04
B_2 (m)	Normal	-	1.00	0.04	0.04
H_1 (m)	Normal	-	7.00	0.28	0.04
H_2 (m)	Normal	-	1.00	0.04	0.04
γ_c (kN/m³)	Normal	-	24.00	0.96	0.04
φ_w (°)	Normal	5	33.00	2.4495[a] μ*Cv[b]	0.0742[a] 0.10[b]
γ_w (kN/m³)	Normal	5	18.80	0.8367[a] μ*Cv[b]	0.0445[a] 0.05[b]
c_f (kN/m²)	Normal Lognormal	5	14.00	4.1833[a] μ*Cv[b]	0.2988[a] 0.20;0.40;0.60[b]
φ_f (°)	Normal	5	32.00[a,b] 25.00;30.00;35.00;40.00[b]	2.3452[a] μ*Cv[b]	0.0733[a] 0.05;0.10;0.15[b]
γ_f (kN/m³)	Normal	5	17.80	0.8367[a] μ*Cv[b]	0.0470[a] 0.05[b]
q (kN/m²)	Normal	-	10.00	2.50	0.25

[a]Coefficient of variation unknown, obtained from the results of some tests on a c-φ soil.
[b]Coefficient of variation known, obtained from published values in the literature; central values of Cv are recommended values and were generally used (exception for Figures 7 and 8); φ_f=32.00 (exception for Figure 9).

4 RESULTS

Based on the definition of eight sets of characteristic values of soil properties X_k, the minimum foundation width B was determined for the different Design Approaches of Eurocode 7: DA.1.1 (Design Approach 1 Combination 1, essentially a STR limit state approach), DA.1.2 (Design Approach 1 Combination 2, essentially a GEO limit state approach), DA.2 (Design Approach 2, an action and resistance factor approach, partial factors applied to the ground resistance and to the actions), DA.2* (Design Approach 2, an action and resistance factor approach, partial factors applied to the ground resistance and to the effects of actions), and DA.3 (Design Approach 3, an action and material factor approach); a similar foundation width B is derived for DA.1.2 and DA.3; the design for DA.1 is governed by DA.1.2; partial factors from Annex A of EC 7-1.

Figures 2 and 3 show respectively, the characteristic values of soil properties X_k based on the definition of eight sets, and the corresponding foundation width B, for the different Design Approaches DA.1.1, DA.1.2, DA.2, DA.2*, and DA.3. According to Table 1, the different foundation widths $B=B_1+B_2$ are derived from a variable B_1, considering a single B_2, and performing the vertical equilibrium for the inclined eccentric loading problem with regard to bearing capacity predictions.

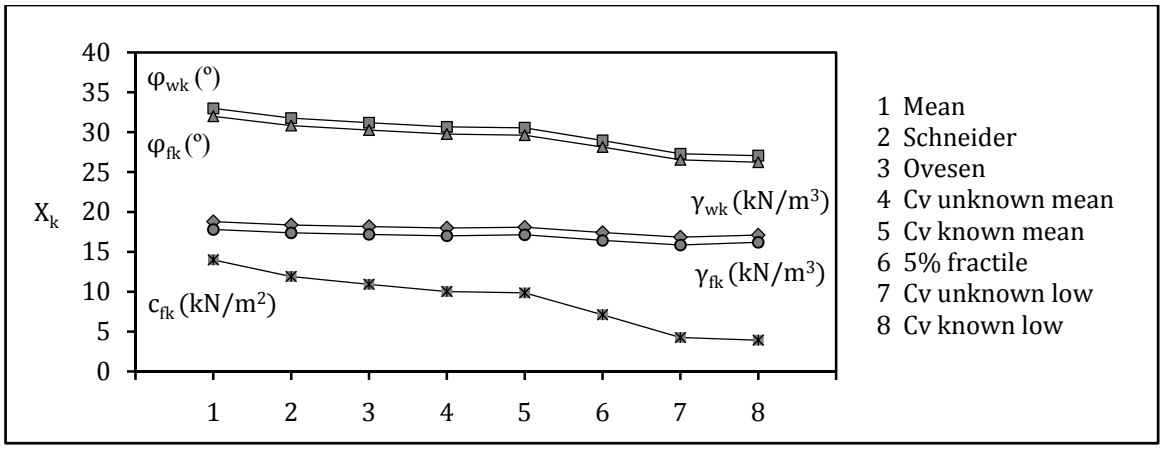

Figure 2.Characteristic values of soil properties X_k based on the definition of eight sets.

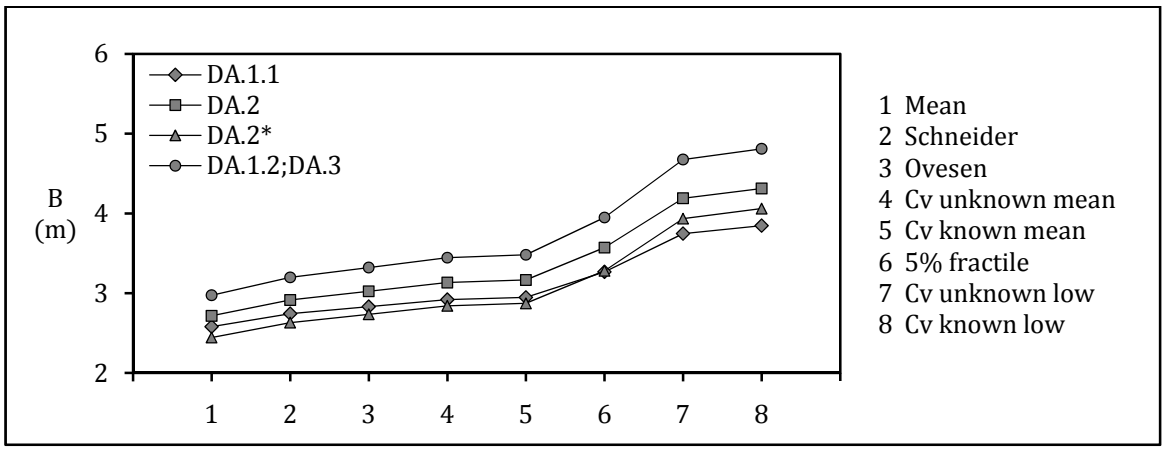

Figure 3.Foundation width $B=B_1+B_2$ based on the definition of eight sets of X_k for the different Design Approaches DA.1.1, DA.1.2, DA.2, DA.2* and DA.3.

Based on the definition of eight sets of X_k, the mean factor of safety Fs_m and the characteristic factor of safety Fs_k, described respectively by equations (9) and (10), are shown in Figures 4 and 5 for the different Design Approaches DA.1.1, DA.1.2, DA.2, DA.2* and DA.3. The characteristic resistance is computed by geotechnical formulas using conservative estimates of the soil properties, namely characteristic values, while the characteristic load is the sum of conservative unfactored estimates of characteristic load actions acting on the system; Fs_m is derived when the mean values are considered as characteristic values.

$$Fs_m = \frac{\text{mean resistance}}{\text{mean load}} \quad (9); \quad Fs_k = \frac{\text{characteristic resistance}}{\text{characteristic load}} \quad (10)$$

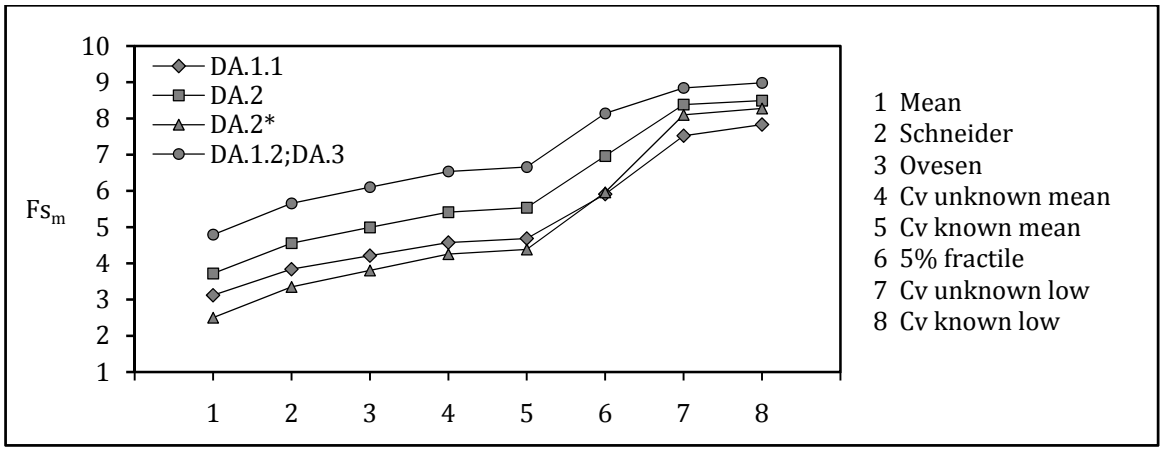

Figure 4.Factors of safety Fs_m based on the definition of eight sets of X_k for the different Design Approaches DA.1.1, DA.1.2, DA.2, DA.2* and DA.3.

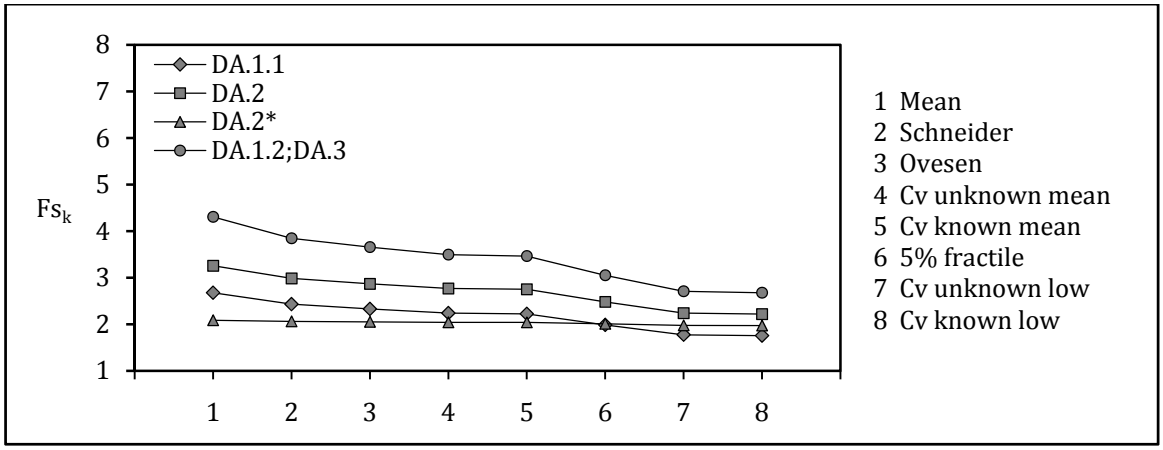

Figure 5.Factors of safety Fs_k based on the definition of eight sets of X_k for the different Design Approaches DA.1.1, DA.1.2, DA.2, DA.2* and DA.3.

Reliability assessment was performed considering normal and lognormal probability distributions, but according to the estimation of characteristic values, the results introduced in this paper are based essentially on normal probability distributions for all basic random variables, with exception to the parameter c_f, normal or lognormal, for comparative study. Therefore, based on the definition of eight sets of X_k, the reliability index β obtained by FORM method (minimizing), considering c_f normal or lognormal and uncorrelated random variables, is shown in Figure 6 for the different Design Approaches DA.1.1, DA.1.2, DA.2, DA.2* and DA.3 (target ultimate limit state reliability index β=3.8).

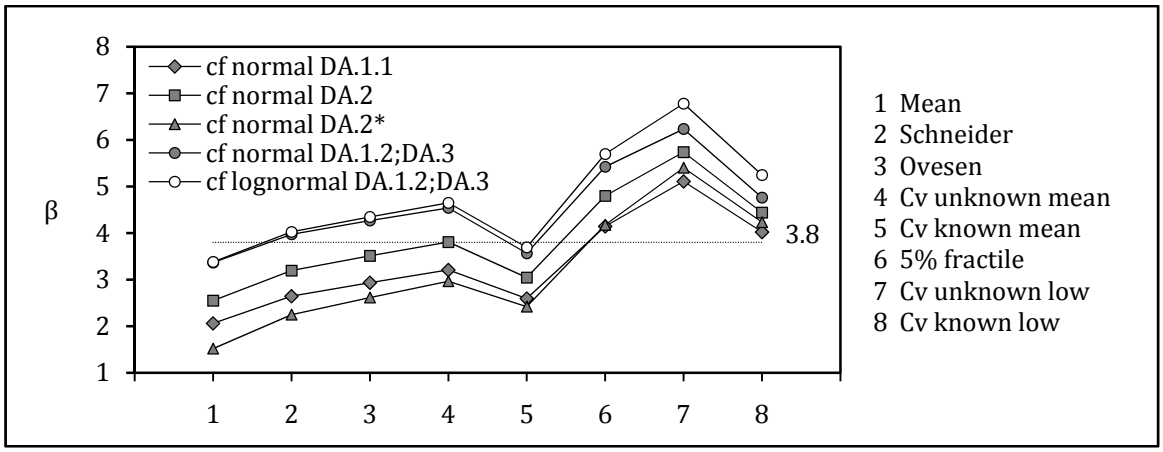

Figure 6.Reliability index β based on the definition of eight sets of X_k, obtained by FORM method (minimizing) considering c_f normal or lognormal and uncorrelated random variables, for the different Design Approaches DA.1.1, DA.1.2, DA.2, DA.2* and DA.3.

The reliability index β obtained by FORM method (minimizing), considering different coefficients of variation of c_f and φ_f or different friction angles of the foundation soil φ_f, is shown in Figures 7 and 8 or 9, respectively (target ultimate limit state reliability index β=3.8). The case Cv known mean was considered for the different Design Approaches DA.1.1, DA.1.2, DA.2, DA.2* and DA.3.

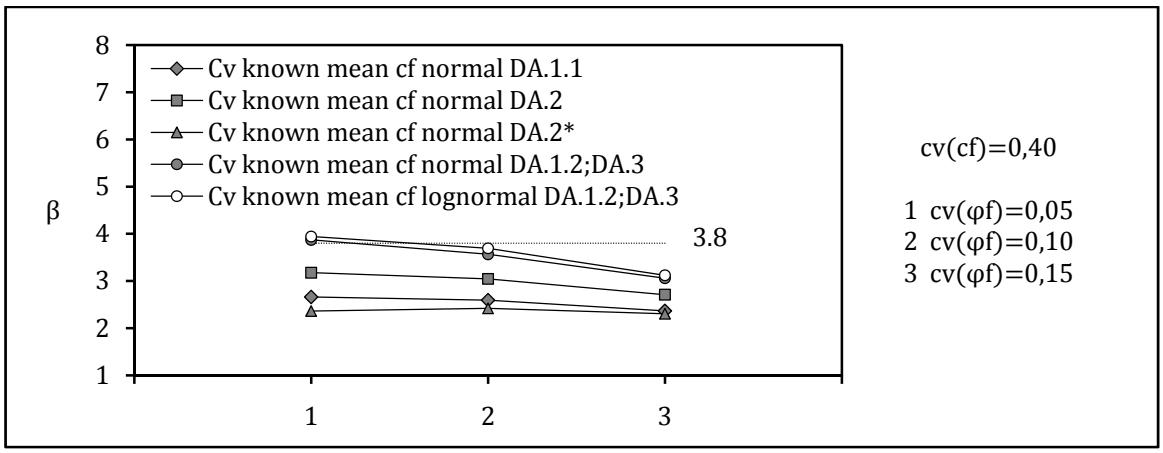

Figure 7.Reliability index β for the case Cv known mean, obtained by FORM method (minimizing) considering c_f normal or lognormal and different coefficients of variation of c_f and φ_f (uncorrelated random variables), for the different Design Approaches DA.1.1, DA.1.2, DA.2, DA.2* and DA.3.

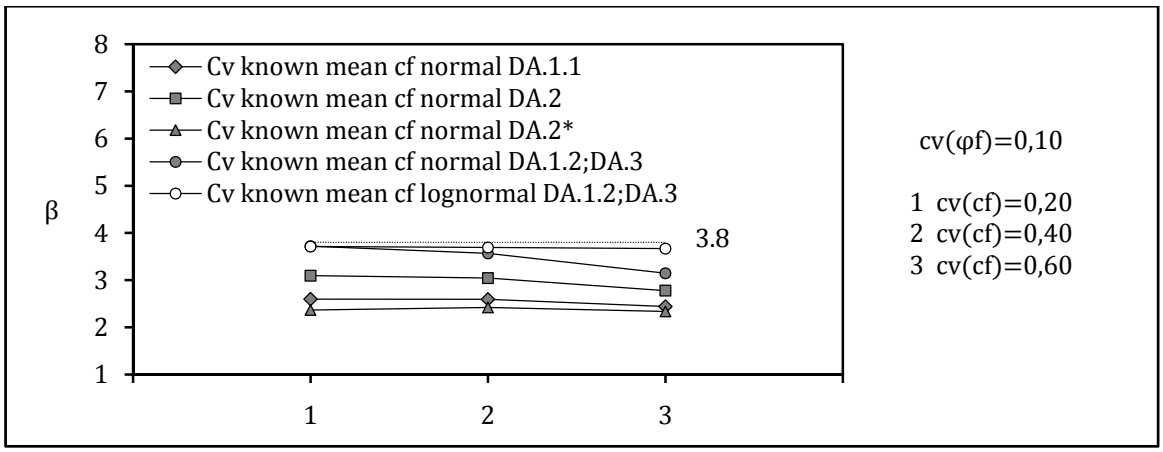

Figure 8.Reliability index β for the case Cv known mean, obtained by FORM method (minimizing) considering c_f normal or lognormal and different coefficients of variation of c_f and φ_f (uncorrelated random variables), for the different Design Approaches DA.1.1, DA.1.2, DA.2, DA.2* and DA.3.

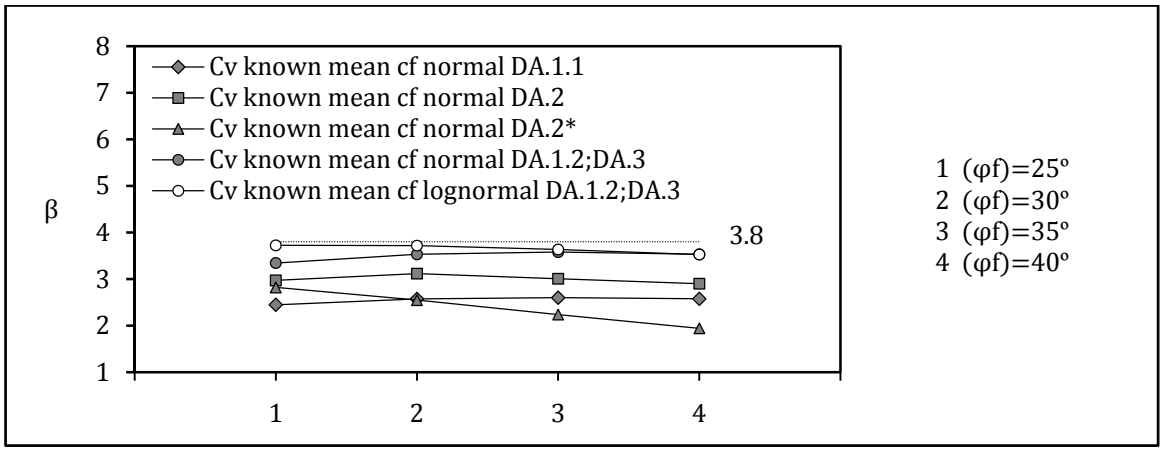

Figure 9.Reliability index β for the case Cv known mean, obtained by FORM method (minimizing) considering c_f normal or lognormal and different friction angles of the foundation soil φ_f (uncorrelated random variables), for the different Design Approaches DA.1.1, DA.1.2, DA.2, DA.2* and DA.3.

The influence of correlation between c_f and φ_f is illustrated in Figure 10 for the Design Approaches DA.1.2 and DA.3, considered the cases Schneider, Ovesen, Cv unknown mean and Cv unknown low.

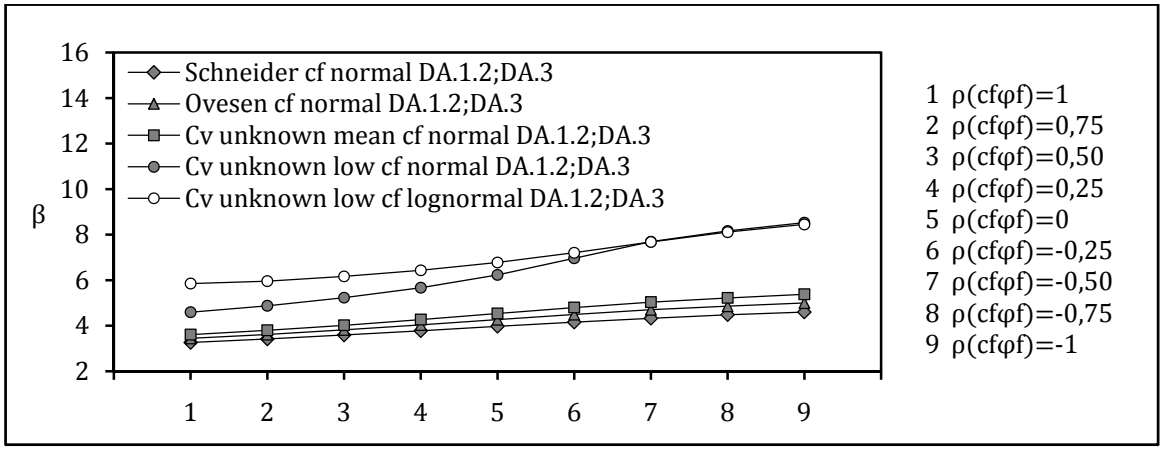

Figure 10.Reliability index β for the cases Schneider, Ovesen, Cv unknown mean and Cv unknown low, obtained by FORM method (minimizing) considering c_f normal or lognormal and different coefficients of correlation between c_f and φ_f, for the Design Approaches DA.1.2 and DA.3.

The influence of spatial variability of soil properties is illustrated in Figure 11 for the Design Approaches DA.1.2 and DA.3, considered the case Cv known mean, for different vertical spatial correlation lengths θ_v and vertical characteristic lengths $L_v=H_2+B$ or $L_v=H_2+1.8*B$ (target ultimate limit state reliability index $\beta=3.8$).

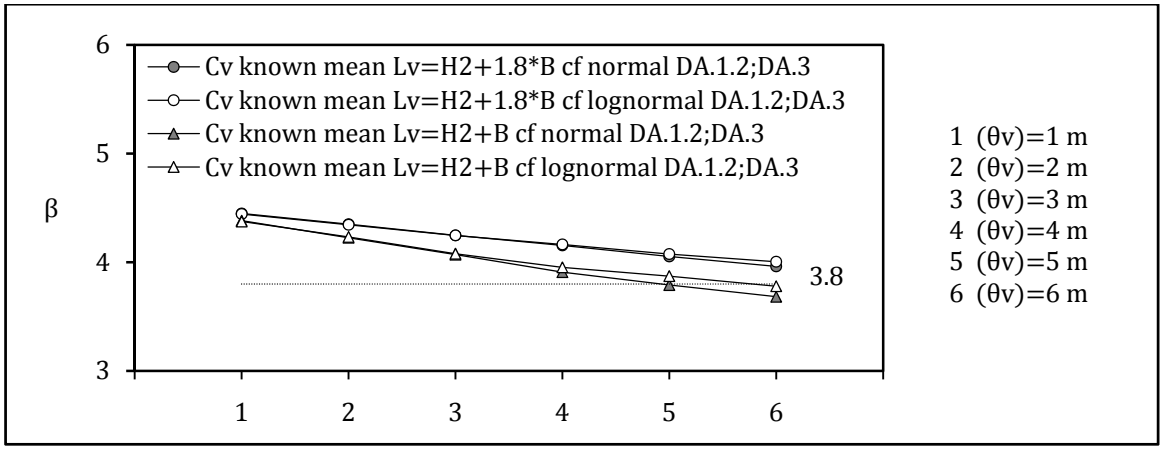

Figure 11.Reliability index β for the case Cv known mean, obtained by FORM method (minimizing) considering c_f normal or lognormal and different vertical spatial correlation lengths θ_v, even as vertical characteristic lengths $L_v=H_2+B$ or $L_v=H_2+1.8*B$ (uncorrelated random variables), for the Design Approaches DA.1.2 and DA.3.

The reliability index β obtained by different methodologies for the Design Approaches DA.1.2 and DA.3, considered the case Mean, for c_f normal and uncorrelated random variables, is shown in Figure 12.

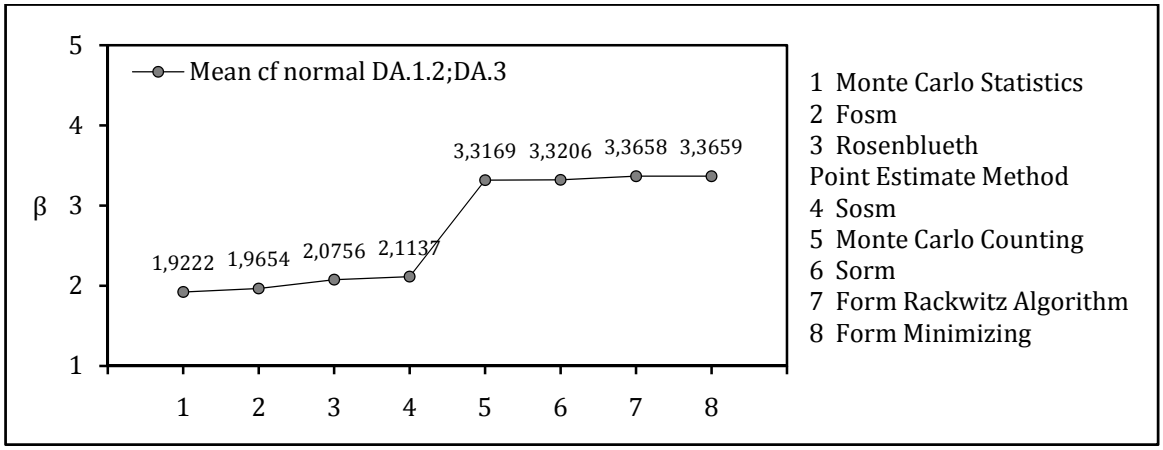

Figure 12.Reliability index β for the case Mean, obtained by different methodologies considering c_f normal and uncorrelated random variables, for the Design Approaches DA.1.2 and DA.3 (MCS results from 24 simulation runs, each one with 3000000 simulation steps; MCS failure probability percentage error 1.1%).

5 DISCUSSION

Based on the definition of eight sets of characteristic values of soil properties X_k, and for the partial factors recommended in Annex A of EC 7-1 for the three Design Approaches, the minimum foundation width B is variable from: 3.20 m to 4.81 m for the Design Approaches DA.1 and DA.3; 2.92 m to 4.31 m for the Design Approach DA.2; and 2.63 m to 4.06 m for the Design Approach DA.2* (case Mean excluded). According to this, the estimation of characteristic values is a determinant issue when analyzing considerable differences in geotechnical design, and moreover, the selected design approaches and values of the partial factors specified by each Member State may be somewhat variable. Therefore, it may be argued that a more formal basis for the exercise of engineering judgment is required, particularly, the value of analysis is considerably enhanced when a complementary reliability assessment is performed.

Considered an acceptable overall factor of safety between 2 and 3, Fs_m or Fs_k, the corresponding reliability index β for the considered design approaches is variable, sometimes lower or even much higher than 3.8, the target ultimate limit state reliability index β for a medium risk structure (reliability class RC2, according to NP EN 1990:2009) and fifty years reference period. Model parameters as dimensions derived from the choice of characteristic values, and coefficients of variation or correlation of soil properties are relevant when comparing solutions, as well as the wide range of geotechnical parameters. According to some results, the friction angle of the foundation soil, φ_f, was considered variable from 25º to 40º and sensitivity analysis point out φ_f as one of the most important parameters concerning reliability, as shown in Figure 7. The effects of spatial variability are favourable, but dependent on θ_v, the vertical spatial correlation length, and L_v, the vertical characteristic length, related to the dimensions of the potential failure surface and considered in the literature between H_2+B and H_2+2*B: according to Figure 11, for θ_v=6 m and L_v=H_2+B, the target ultimate limit state reliability index β is not achieved. The influence of probability distribution is another important item, and results from different methodologies for reliability evaluation may be quite differing, as illustrated in Figure 12 (Haldar *et al*., 2000).

6 CONCLUSION

Further harmonization of geotechnical design in European Union is required in the future to improve the competitiveness of the construction industry and promote sustainable development (Schuppener, 2010). More research about reliability assessment of Eurocode 7 design methodology, based on classical calculation models or application of numerical methods, can yield precious new insights into economic issues by considering the optimization of resources when comparing probabilistic solutions with a target limit state reliability index β: mainly for complex problems, the decision-making process is improved when analyzing considerable differences in geotechnical design. This paper still demonstrates that risk and reliability are complementary, depending on the considered analysis model, and that engineering judgment is essential for the selection of reliable characteristic values for geotechnical design.

REFERENCES

Cherubini,C. (2000). "Reliability evaluation of shallow foundation bearing capacity on c', φ' soils". Canadian Geotechnical Journal. Vol.37, N.º 1, p.264-269.

Duncan,J.M. (2000). "Factors of safety and reliability in geotechnical engineering". Journal of Geotechnical and Geoenvironmental Engineering. Vol.126, N.º 4, p.307-316.

Forrest,W.S.; Orr,T.L.L. (2010). "Reliability of shallow foundations designed to Eurocode 7". Georisk: Assessment and Management of Risk for Engineered Systems and Geohazards. Vol.4, N.º 4, p.186-207.

Frank,R.; Bauduin,C.; Driscoll,R.; Kavvadas,M.; Ovesen,N.K.; Orr,T.; Schuppener, B. (2004). "Designers' Guide to EN 1997-1 Eurocode 7: Geotechnical design-General rules". Thomas Telford.

Haldar,A.; Mahadevan,S. (2000). "Probability, Reliability and Statistical Methods in Engineering Design". John Wiley & Sons.

Phoon,K.K.; Kulhawy,F.H. (1999a). "Characterisation of geotechnical variability". Canadian Geotechnical Journal. Vol.36, N.º 4, p.612-624.

Phoon,K.K.; Kulhawy,F.H. (1999b). "Evaluation of geotechnical property variability". Canadian Geotechnical Journal. Vol.36, N.º 4, p.625-639.

Schuppener,B. (2010). "Eurocode 7 Geotechnical design. Part 1: General rules and its latest developments". Georisk: Assessment and Management of Risk for Engineered Systems and Geohazards. Vol.4, N.º 1, p.32-42.

VanMarcke,E. (1983). "Random Fields: Analysis and Synthesis". MIT Press.

Yoon,G.L.; Yoon,Y.W.; Kim,H.Y. (2010). "Determination of geotechnical characteristic values of marine clay". Georisk: Assessment and Management of Risk for Engineered Systems and Geohazards. Vol.4, N.º 1, p.51-61.

ISGSR 2011 - Vogt, Schuppener, Straub & Bräu (eds) - © 2011 Bundesanstalt für Wasserbau ISBN 978-3-939230-01-4

Reliability analysis of bearing capacity for shallow foundations based on Eurocode 7

C. Onisiphorou
Frederick University, Nicosia, Cyprus

ABSTRACT: In Eurocode 7, the application of statistical methods and reliability analyses is encouraged though not much guidance is clearly given for the practitioner. Reliability analyses can effectively model parameter uncertainty and provide more meaningful results in terms of a reliability index and probability of failure. The current work focuses on the development of a methodology for calculating bearing resistance using reliability analysis, in terms of Eurocode 7. Random fields of soil cohesion and friction angle are generated and converted to characteristic values for checking the GEO failure criterion in ULS. The analysis is performed for a simple example of a shallow foundation, comparing the methods of Monte Carlo simulation and First Order Reliability Methods. For both methods the reliability index and probability of failure were determined. It was found that both methods can be applied for an increasing uncertainty in friction angle though FORM results for low uncertainty are closer to the deterministic solution than Monte Carlo simulations.

Keywords: Bearing Capacity, Reliability Analysis, Eurocode 7, Shallow Foundations

1 INTRODUCTION

1.1 *General*

Conventional design methods in geotechnical engineering generally consider the calculation of a reasonable global factor of safety. This global safety factor is simply a comparison of actual to required strength and indicates whether the system is safe or not, in what is termed as a deterministic approach. However, due to the large uncertainty resulting from in-situ soil variability, even in homogeneous soils, it may not always represent a realistic situation. The effect of variability in soil properties cannot be efficiently modelled in such an analysis. For these cases, the use of probability theory can be implemented in terms of a probabilistic or a reliability analysis to model ground uncertainties.

The interest here is not in calculating simply a factor of safety but to investigate the probability of failure for an engineering system. A reliability analysis presents a more meaningful approach for geotechnical design, rather than the calculation of a factor of safety, as this can be used for risk-based decision making. It also indicates the performance and reliability for a geotechnical problem. To initiate a reliability analysis, random fields of soil properties are commonly generated to derive the required statistical parameters, e.g. mean and standard deviation. A method of reliability analysis is then selected for determining the probability of failure and the reliability index. Some commonly used techniques include the Monte Carlo simulation, First Order methods and Point Estimate method. A detailed description for each of these methods is presented in Baecher and Christian (2003). The present work deals with the reliability based analysis of bearing capacity for shallow foundations, in terms of Eurocode 7 requirements.

1.2 *Background to analysis*

Reliability analysis has extensively been used in geotechnical engineering, especially in recent years. The types of analyses can be either practical reliability based computations and applications as included in Phoon (2008), or stochastic analysis using finite elements or other numerical method aiming at risk as-

sessment, for example in Hicks (2007) and Fenton and Griffiths (2008). Applications covered may range from complex liquefaction analysis (Hicks and Onisiphorou 2005) to applications in retaining wall design Low (2005) and rock slope analysis (Onisiphorou 2010).

With regards to reliability analysis of bearing capacity, Cherubini (2000) evaluated the performance of c-φ' soils for varying correlation coefficients, while Fenton and Griffiths (2003) investigated effects of spatial variability for c-φ' soils using random finite element methods. Recently, reliability analyses published by Fenton et al (2007, 2008) state an aim of promoting the creation of reliability-based design codes for geotechnical engineering. The applications of Eurocode methodologies in combination with reliability analysis for modelling spatial variability provides a new area of research and a lot of ground still needs to be investigated (Simpson & Driscoll 1998), especially with implementation and experience gained with Eurocode 7 design. Orr & Breysse (2008) present some important issues on the EC7 partial factor approach in geotechnical design and include example reliability analyses for spread foundations. Furthermore, Hicks & Samy (2004) developed and presented a stochastic approach for determining characteristic values of soil properties for Eurocode 7, based on the confidence levels suggested by the code.

2 BEARING CAPACITY BASED ON EUROCODE 7

2.1 *General on Eurocode 7*

EN 1997 is based on limit state conditions defined as "the state beyond which the structure no longer fulfils the relevant design criteria". In general, Eurocode 7 considers two limit state design situations, the Ultimate Limit State (ULS), associated with collapse or failure, and the Serviceability Limit State (SLS), associated with unsatisfactory service requirements. These limit states are explained in detail in EN 1997 itself and specialised publications, e.g. by Frank et al (2004) and Orr and Farrell (1999). Furthermore, for the calculations at ULS, five different failure criteria exist, depending on possible cause of failure. These are Structural (STR), Geotechnical (GEO), Equilibrium (EQU), Uplift (UPL) and Hydraulic (HYD) and are defined in detail in EN 1990.

Eurocode 7 has considered the spatial variability and uncertainty of soil properties as significant for geotechnical design and suggests taking this uncertainty into account using statistical methods. One way of doing this is by applying the recommended partial factors to characteristic values of soil properties, which on their turn can be based on resulting statistics from extensive in-situ or laboratory data. These are considered as semi-probabilistic analyses, as referred to by Orr & Breysse (2008), as opposed to fully probabilistic or reliability analyses, though not much detail is included in the code on how to do this. It should be noted that currently a reliability analysis is mostly based on the experience and engineering judgement of the designer, rather than direct guidance from Eurocode 7.

The characteristic value of a soil property, X_k, is based on mean value but actually defined as a cautious estimate of the value affecting the occurrence of the limit state (EN1997-1). It maybe determined by

$$X_k = \mu_X (1 - kV_X) \qquad (1)$$

where μ_X = mean of property X, V_X = coefficient of variation of X ($=\sigma_X/\mu_X$), k = a statistical coefficient depending on type of characteristic value, available test results and level of reliability. For defining k, the confidence level of 95% maybe too high sometimes for soils (as discussed by Orr and Breysse (2008)) leading to conservative results. Therefore, for the purpose of the current work, the characteristic value mentioned above is based on the following practical relationship by Schneider (1997).

$$X_k = \mu_X - 0.5\sigma_X \qquad (2)$$

where X = the randomly varying soil property and σ_X = standard deviation of X. Taking Equation (2) into account, random fields are generated for the characteristic values of soil properties.

2.2 *Methodology for calculating bearing capacity*

According to Clause 2.4.7.3.1, when checking the bearing resistance of a shallow foundation, the GEO criterion must be checked, which is related to failure in the ground. Therefore, the following inequality must be satisfied:

$$E_d \leq R_d \qquad (3)$$

where E_d = the design value of the effect of actions, R_d = the design value of the bearing resistance of the ground. The effect of actions is represented in the analyses in the following sections solely by the design value of vertical forces V_d, which also includes the weight of foundation and overburden soil.

The bearing resistance for a shallow foundation can be calculated using the well known Terzaghi equation. A methodology based on the above equation is presented in Annex D of Eurocode 7 and is adopted here. For the present case only vertical load is considered and so the inclination factors i_c, i_q, i_γ are omitted in the equation. The equation to be used simplifies to the one given below:

$$\frac{R_k}{A} = cN_c s_c + \gamma_d D N_q s_q + \frac{1}{2} B \gamma_d N_\gamma s_\gamma \qquad (4)$$

where R_k = characteristic value of bearing resistance, c = soil cohesion, A = foundation area, N_c, N_q, N_γ = bearing capacity factors, s_c, s_q, s_γ = shape factors, q = overburden pressure at level of foundation base, B = foundation width, D = embedment depth, γ_d = design value of soil unit weight.

The bearing capacity factors, N, are given below:

$$N_c = (N_q - 1)\cot\phi' \qquad (5)$$

$$N_q = e^{\pi \tan\phi} \tan^2(45 + \phi'/2) \qquad (6)$$

$$N_\gamma = 2(N_q - 1)\tan\phi' \qquad (7)$$

The shape factors for a rectangular footing are as follows:

$$s_c = (S_q N_q - 1)/(N_q - 1) \qquad (8)$$

$$s_\gamma = (1 - 0.3)(B/L) \qquad (9)$$

$$s_q = 1 + (B/L)\sin\phi' \qquad (10)$$

Finally, the design value of bearing resistance is given by

$$R_d = \frac{R_k}{\gamma_R} \qquad (11)$$

where γ_R = the partial factor for bearing resistance = 1.4 for Design Approach 2, as taken from Table A.5, Annex A of EN 1997-1.

3 VARIABILITY OF SOIL PROPERTIES AND EXAMPLE APPLICATION

The randomly varying variables selected for the analysis are the shear strength parameters, the soil cohesion, c, and angle of internal friction, φ. It is assumed that the two random variables are uncorrelated for the purpose of the analysis, even though it is reasonable to assume a degree of cross-correlation. However, previous research work by Fenton and Griffiths (2003) has shown that the effect of correlation is not significant to the final result. Random fields are then generated from which sets of values are converted for each property. This is done by assuming a pre-described probability distribution for each property. It has been assumed that both variables follow a Normal distribution with statistical parameters as shown in Table 1 below.

Table 1. Statistical properties of random variables

Property	Point Statistics	
	μ	σ
c (kPa)	5	1.0
φ (°)	31	2-4

The assumptions for these distributions and the coefficient of variation for each parameter are based on previously published correlations and recommendations, such as Lacasse and Nadim (1996) and Phoon and Kulhawy (1999). The coefficient of variation for φ , V_φ , will be varied from 2-4 degrees in order to investigate the effects of increasing uncertainty in friction angle on system reliability. The random sets of properties, required for the Monte Carlo simulations are generated using the general equation

$$Y = F^{-1}(U)$$

where Y = random variable following a prescribed cumulative distribution $F(.)$, U = random variable uniformly distributed between 0 and 1.

The application problem considers a shallow foundation with dimensions L = 2.2m, B = 1.8m and embedment depth D = 2.0m. The soil is medium dense sand with unit weight assumed constant at γ = 19 kN/m^3. The permanent load is G_k = 650 kN and variable load is equal to Q_k = 400 kN. Using partial factors γ_G =1.35 and γ_Q = 1.5 for permanent and variable loads respectively (as taken from Tables A.3 and A.4 in Annex A of EN 1997-1), the value of V_d = 1478 kN (kept constant throught the analyses). Note that this value includes the weight of foundation and overburden soil.

4 RELIABILITY ANALYSIS USING MONTE CARLO SIMULATIONS (MCS)

4.1 *Methodology*

For the Monte Carlo simulations, 5000 realisations were performed. For each of these analyses a different characteristic value of cohesion and friction angle is used in the Equation (4) for calculating bearing capacity.

The performance function (or safety margin) for the foundation can be defined by

$$g(x_1, x_2, ..., x_i) = R_d - V_d \qquad (12)$$

where x the set of random variables. The reliability index, β, following a run of the realisations for the Monte Carlo simulations can be computed by

$$\beta = \frac{\mu_g}{\sigma_g} \qquad (13)$$

If a Normal distribution is assumed for the performance function $g(x_i)$, the resulting probability of failure, p_f, is given by

$$p_f = P(g < 0) = 1 - \Phi(\beta) = \Phi(-\beta) \qquad (14)$$

where $\Phi(\beta)$ is the value of the cumulative standard Normal distribution.

4.2 *Results*

Figure 1 below shows the distribution of an Over-design Safety Factor (*OFS*), equal to ratio R_d/V_d deducing from Equation (3), in an analogy to the safety factor. For varying coefficients of variation for friction angle, it can be seen that this distribution results in a slightly skewed distribution, approximating a log normal distribution.

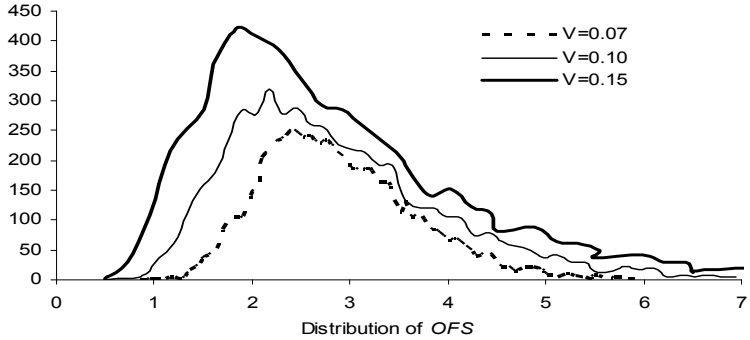

Figure 1. Distribution of Over-design Safety Factor (*OFS*) for varying *V* of friction angle

The mean *OFS* visibly decreases as uncertainty becomes larger in the characteristic value of friction angle (increased *V*). It should be noted that the deterministic solution gives a value of 3.1 well above the reliability based solution. The same skewed distribution has been observed for the safety margin $g(x_i)$, therefore it was decided to calculate the probability of failure, p_f, using the lognormal probability distribution instead of Equation (14), in order to avoid highly conservative results.

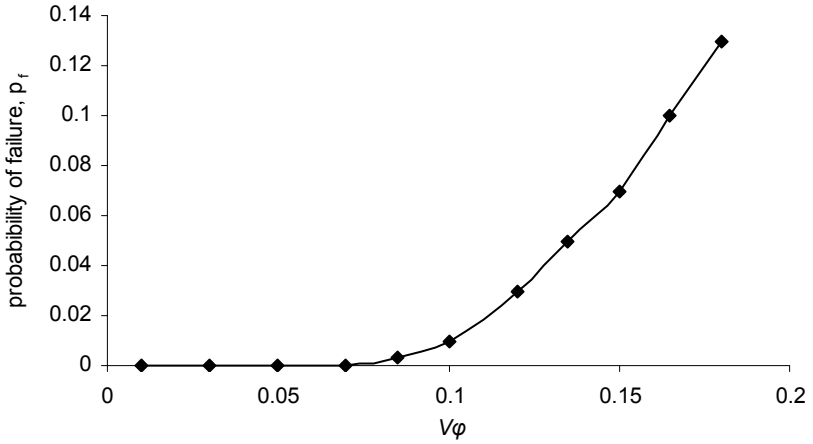

Figure 2. Probability of failure p_f for varying *V* of friction angle (Monte Carlo)

The results are summarised in Figure 2 below for varying *V* of friction angle. For cases of low variation such as V_φ = 0.05-0.08 (and less uncertainty), probability of failure is relatively low (less than 0.0002). As variation increases with $V_\varphi > 0.1$, a sudden increase is evidenced in probability of failure. This is reflected in low values of reliability index, β ranging from 1.0 to 3.0.

5 ANALYSIS USING FIRST ORDER RELIABILITY METHOD (FORM)

5.1 *Method of analysis*

The present analysis is based on the approach suggested by Hasofer and Lind (1974) for finding the minimum distance d (represented by the reliability index β) between the mean value and the failure surface for $g(x) = 0$, where *g* the safety margin as defined by Equation (12). For the present work, the analysis using FORM is performed using solver in spreadsheets, based on the matrix formulation by Low & Tang (2007). The starting trial values are equal to the characteristic values of the soil properties

This equation used for the reliability index is

$$\beta = \min_{x \in F} \sqrt{\left[\frac{x_i - \mu_i}{\sigma_i}\right]^T [R]^{-1} \left[\frac{x_i - \mu_i}{\sigma_i}\right]} \qquad (15)$$

where β = reliability index, x_i = random variables, μ_i = mean values of *ith* variable, σ_i = standard deviation of *ith* variable, *R* = correlation matrix, *F* = failure domain, i.e. $g(x)$=0. As discussed in Section 3 above, cohesion and friction angle are assumed uncorrelated. The point statistics used are tabulated in Table 1 of Section 3 and the probability of failure is calculated from Equation (14).

5.2 *Results*

Figure 3 shows summarised results for the FORM analysis. The variation of the reliability index with regards to an increase of uncertainty in friction angle is plotted. As can be seen the reliability index ranges from 3-5 for low variation while steadily droping to lower values of $\beta < 2$ for larger *V*. Figure 4 presents the values of probability of failure for various coefficients of variation for friction angle and is comparable to Figure 2 for the Monte Carlo simulations. The FORM method gives a lower probability of failure than Monte Carlo, especially as uncertainty becomes significant.

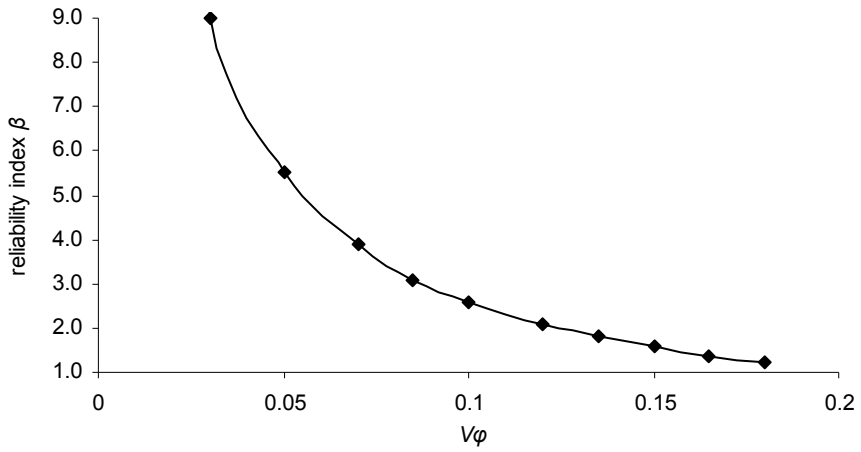

Figure 3. Reliability index β for varying V of friction angle

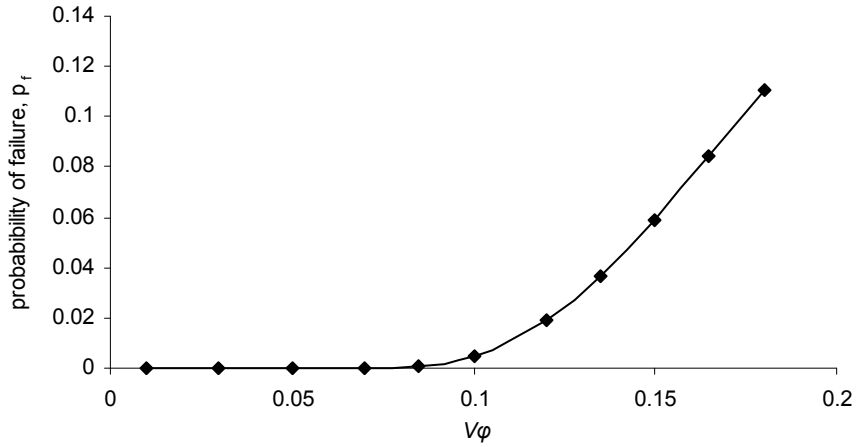

Figure 4. Probability of failure p_f for varying V of friction angle (FORM)

6 CONCLUSIONS

Conventional deterministic analyses may not always capture the soil variability and the uncertainty in soil properties. In these cases, a reliability analyses maybe more appropriate as statistical properties can be used to determine the probability of failure and reliability index. The importance of reliability analyses has been recognised by the recently implemented Eurocode 7 and is encouraged to use whenever suitable. However, experience needs to be gained among researchers and practitioners in various applications in geotechnical engineering.

The current research work presents a methodology for calculating the bearing resistance of the ground using reliability analysis. A recommended deterministic solution by Eurocode7 has been implemented while characteristic values were input as random variables for cohesion and friction angle. The application considered a shallow foundation with vertical loads and the system was analysed using two well known reliability techniques, the Monte Carlo simulations and the First Order Reliability Method (FORM).

The effect of varying the friction angle was investigated for the bearing capacity of a shallow foundation. It was found that the reliability index for Monte Carlo simulations was lower than the FORM solution, when variability is small. When uncertainty increases, the reliability indices for the two methods increase for both methods and are closer together. This is possibly due to an improved modelling of uncertainty using the Monte Carlo simulations. Overall, the two methods approach the deterministic solution as uncertainty increases, though FORM result gives a closer approximation as Monte Carlo is also dependent on the number of realisations.

REFERENCES

Baecher, G.B. & Christian, J.T. 2003. Reliability and Statistics in Geotechnical Engineering. Wiley, Chichester, UK.

Cherubini, C. 2000. Reliability evaluation of shallow foundation bearing capacity on c', φ' soils. Canadian Geotechnical journal, 37, 264-269.

EN 1990: 2004: Basis of structural design. CEN, European Committee for Standardization, Brussels.

EN 1997-1: 2004. Eurocode 7: Geotechnical Design. Part 1: General rules. CEN, European Committee for Standardization, Brussels.

Fenton, G.A. & Griffiths, D.V. 2001. Bearing capacity of spatially varying c-φ soils. Proc. 10th Intl. Conference on Computer Methods and Advances in Geomechanics (IACMAG01), Tucson, Arizona, 1411-1415.

Fenton, G.A. & Griffiths, D.V. 2003. Bearing capacity prediction of spatially random c-φ soils. Canadian Geotechnical Journal, 40(1), 54-65.

Fenton, G. A. & Griffiths, D.V. 2008. Risk Assessment in Geotechnical Engineering. Wiley, New Jersey.

Fenton, G.A., Zhang, X.Y., & Griffiths, D.V. 2007, Reliability of shallow foundations designed against bearing failure using LRFD, Georisk: Assessment and Management of Risk for Engineered Systems and Geohazards, 1(4), 202-215.

Fenton, G. A., Griffiths, D.V. & Zhang, X.Y. 2008, Load and resistance factor design of shallow foundations against bearing failure, Canadian Geotechnical Journal, 45(11), 1556-1571.

Frank, R., Bauduin, C., Driscoll, R., Kavvadas, M., Krebs Ovesen, N., Orr, T.L.L. & Schuppener, B. 2004. Designer's Guide to EN 1997-1 Eurocode 7: Geotechnical Design-General Rules. Thomas Telford, London.

Griffiths, D.V., Fenton, G.A. & Manoharan, N. 2002. Bearing capacity of rough rigid strip footing on cohesive soil: Probabilistic study. ASCE Journal of Geotechnical and Geoenvironmental Engineering, 128(9), 743-755.

Hasofer, A.M. & Lind, N.C. 1974. An exact and invariant first-order reliability format. ASCE Journal of the Engineering Mechanics Division, 100(EM1), 111-121.

Hicks, M.A. (ed.) 2007. Risk and variability in geotechnical engineering. Thomas Telford, London.

Hicks, M.A. & Onisiphorou, C. 2000. Stochastic evaluation of static liquefaction in a predominantly dilative sand fill. Geotechnique, 55(1): 123-133.

Hicks M.A. & Samy K. 2002. Reliability-based characteristic values: a stochastic approach to Eurocode 7, Ground Engineering, 35(12), pp30-34.

Lacasse, S. & Nadim, F. 1996. Uncertainties in characterizing soil properties. Uncertainty in the geologic environment. Madison, WI, USA, ASCE: 49-75.

Low, B.K. 2005. Reliability based design applied to retaining walls. Geotechnique, 55(1): 63-75.

Low, B.K. & Tang 1997. Efficient reliability evaluation using spreadsheets. ASCE Journal of Engineering Mechanics, 123(7), 749-752.

Onisiphorou, C. (2010), Reliability based assessment of rock slope stability. Proc. European Conference on Rock Mechanics in Civil and Environmental Engineering, Lausanne, Switzerland, 563-566.

Orr, T.L.L. & Farrell, E.R. 1999. Geotechnical Design to Eurocode 7, Springer, London.

Orr, T.L.L. & Breysse, D. 2008, Eurocode 7 and reliability based-design. Reliability-based design in geotechnical engineering: computations and applications (Chapter 8), 298-343, Phoon, K.K. (ed.), Taylor & Francis Group.

Phoon, K.K. & Kulhawy, F.H. (1999). Characterization of geotechnical variability. Canadian Geotechnical Journal, 36, 612-624.

Phoon, K.K. (ed.) 2008, Reliability-based design in geotechnical engineering: computations and applications, Taylor & Francis Group.

Schneider, H.R. 1997. Definition and determination of characteristic soil properties. Proc. 12th Intl. Conference on Soil Mechanics and Geotechnical Engineering, Hamburg, Germany, 4, 2271-2274.

Simpson, B. & Driscoll, R. 1998. Eurocode 7, A Commentary. ARUP/BRE, Construction Research Communications Ltd, London.

ISGSR 2011 - Vogt, Schuppener, Straub & Bräu (eds) - © 2011 Bundesanstalt für Wasserbau ISBN 978-3-939230-01-4

Risk Analysis and Observational Methods in practice: what do new codes improve?

W. Steiner, S. Irngartinger
B+S AG, Bern, Switzerland

ABSTRACT: The construction of cuts, embankments and dam in and on different ground require the analyses of slope stability, deformations and often the use of the observational method. New codes, such as Eurocode 7 or its sister code in Switzerland SIA 267, prescribe the use of partial factors on friction angle and cohesion for slope stability analyses. This methodology has many shortcomings, as experienced in practice, in particular with steep slopes and irregular ground conditions. Examples with substantial deviation between analyses with the partial factors of safety and the global factor of safety will be presented. The use of the factor of safety on shear strength will be proposed, as had been used before in the limiting equilibrium methods, which is also called global factor of safety. The factor of safety on shear strength integrates the effects of shear strength, whether undrained shear strength, effective strength described by cohesion intercept and friction angle or curved envelopes; the effect of geometry and seepage and porewater pressures. With this approach stability analyses, deformation prediction and the observational method can be integrated this ultimately leads to safer construction.

Keywords: Slope, Safety factor, Stability, Friction, Cohesion

1 INTRODUCTION

The authors are involved in many types of stability problems in practice involving field measurements and site investigations. For the analysis the authors have used different types of analyses and have experienced the appearance of new codes with the change to the use of partial factors. Also the Observational Method has appeared in these codes to be applied in geotechnical construction. The experience has shown that the Observational Method is often poorly applied in practice. Often a poor site investigation is carried out; followed by a similar insufficient analysis and some observations and then some measurements are planned, that usually lead to the reinforcement with tie-backs. For judging the relative risk of slopes the use of probabilistic methods has proven as practical tool (Steiner et al. 1992). These findings are supported by practical examples.

1.1 *Geotechnical code with partial factors*

The new geotechnical codes such as Eurocode 7 and national (SIA 267) codes prescribe the use of separate Partial Factors of Safety on cohesion and friction angle, this reduction has led to the fact that the analyses have to be carried out with a fictitious soil material, in several cases we have noted that the obtained critical siding surface for the analyses with partial factors on cohesion and frictional strength deviate substantially from the factor of safety on shear strength. Such deviations can only be detected by carrying out analyses in parallel.

1.2 *Application of probabilistic methods*

The use of probabilistic method has proven useful in practice (Steiner et al., 1992) to judge the relative risk and the influence of the dispersion of the significant parameters, like undrained shear strength of a

cohesive soil. The use of a factor of safety only would not have led to the same conclusions as with probabilistic methods.

2 BACKGROUND OF SLOPE STABILTY ANALYSES

There a many different types of analyses available, the slip circle method (Taylor, 1937), charts for estimating slopes with the consideration of cohesion, friction and pore pressure by Janbu (1954), and Bishop & Morgenstern (1960), these charts are also published in soil mechanics books (Lang et. Al 2008) . Similar charts are published in rock mechanics literature (Hoek and Bray, 1977; Wyllie and Ma, 2004). Such charts are limited to simple geometries with one type of soil or rock material. Complex ground conditions have to be simplified with respect to geometry and to geotechnical conditions. For practical cases the use of a method of slices with limit equilibrium methods has become standard practice since complicated geometric conditions and different geotechnical layers can be relatively easily analyzed (Wright,1969; Krahn, 2003; Duncan & Wright, 2005). More recently Finite element methods are used with the shear strength reduction method, SSR (Krahn,2007), which requires knowledge of deformation properties.

2.1 *Basics of Limit Equilibrium*

In the following the most important basic facts and assumptions in limit equilibrium are recalled. For a complete treatment reference is made to the literature (Duncan & Wright, 2005; Krahn, 2003 & 2004; Fredlund & Krahn, 1977). The available shear strength is defined as shown in Equation (1)

$$s = \frac{1}{F}\left[c' + \left(\sigma_n - u\right)\tan\Phi'\right] \quad (1)$$

where s = available shear strength, c'= cohesion intercept, Φ' = friction angle, σ_n = total normal stress on the base of the sliding surface, u = porewater pressure on the sliding surface, on the base of the slice.

This formulation goes back to Bishop (1955), since he had noted that the Ordinary method of slices or Fellenius' method did not fulfil equilibrium at the slices and gave substantial deviations. Krey (1936) had developed an essentially similar method as Bishop's without iteration. At that time only manual computations were feasible and the method had to be available for hand calculation. Janbu's (1957) simplified method is similar to Bishop's (1957), instead of fulfilling the moment equilibrium horizontal force equilibrium is fulfilled.

The next step for slope stability analyses came with the availability of computers and Morgenstern & Price (1963), who considered the complete equilibrium in the analysis. It is interesting to note the very limited computing power available in a major computer centre compared to today in a personal computer. Spencer (1967) developed a different formulation of the side forces inclined at a constant angle, which corresponds to a special case of Morgenstern-Price with constant function..

The problem of a sliding mass with the method of slices is highly statically indeterminate (Lambe & Whitman, 1969) and requires that assumptions on the internal stress distribution or in case of the method of slices on the lateral forces between the slices. The interslice forces involve normal and shear forces; these have also to fulfil the equilibrium conditions. The slices are assumed as rigid bodies and the static equilibrium equations have to be fulfilled (Fredlund & Krahn, 1977; Steiner, 1977).

2.2 *Fulfillment of equilibrium*

The different methods of slices fulfil the equilibrium conditions on the individual slice and the entire sliding bodies to different degrees (Table 1). The accuracy of different methods has been presented for different slopes by Whitman & Bailey, 1963; Wright, 1969; Wright et al., 1973, Krahn, 2003.

Many comparisons have been published and often Spencer's method has been recommended as the most practical to apply. One has to note that Spencer's method is a special case of the Morgenstern-Price method, namely with constant inter-slice function. Often there convergence problems of the solutions may arise, for this purpose Fredlund and Krahn, (1977) and Krahn (2004) have compared the development of the factor of safety with the inclination of the interslice forces for moment and force equilibrium and found that the differences between the methods can be attributed to the treatment of the interslice forces.

With the General Limit Equilibrium GLE (Krahn, 2004) convergence of force and moment equilibrium can be evaluated in the computer code Slope/W. Often only the simplified methods are treated in text books (Lang et al. 1990, 1996). From our experience simpler methods, such as Bishop's and Janbu's, originally developed for manual computations, may deviate in either direction from the result with complete consideration of the internal stresses for complex geometries and ground.

Table 1. Equilibrium conditions applied in method of slices

Method	Global Equilibrium			Equilibrium on slice			Inclination of inter-slice forces
	Moment	Vertical forces	Horizontal forces	Moment	Vertical forces	Horizontal forces	
Fellenius	Yes	No	No	No	No	No	None
Krey (3)	Yes	*(Yes)*	No	No	Yes	No	Horizontal
Bishop modified	Yes	*(Yes)* (1)	No	No	Yes	No	Horizontal
Janbu modified	No	*(Yes)*	*(Yes)*	No	Yes	Yes	Horizontal
Janbu general (GPS) (2)	*(Yes)*	*(Yes)*	*(Yes)*	Yes	Yes	Yes	According to line of thrust assumed
Morgenstern-Price	*(Yes)*	*(Yes)*	*(Yes)*	Yes	Yes	Yes	Variable, depends on assumed distribution
Spencer	*(Yes)*	*(Yes)*	*(Yes)*	Yes	Yes	Yes	constant

(1) Global equilibrium of vertical forces is fulfilled, because it is fulfilled for each slice.
(2) The general method of slices by Janbu implies the use of a computer.
(3) Krey's method is similar to Bishop's; the factor of safety is mostly not calculated with iteration.

2.3 *Importance of interslice forces or internal stress state on stability*

The practical important effect of the interslice forces became apparent to the senior author (Steiner, 1985) analyzing an avalanche deflection dam, similar to Figure 1.

There had been a 10 meter high dam without berms in operation for several decades, when it had to be raised to 16 m. The analysis was not straightforward, a standard analysis as retaining wall was not satisfactory and manual analysis, with Bishop's and Janbu's method then used in practice gave factors of safety around one, i.e. the dam should be unstable. The stability of the dam was analyzed with the Morgenstern-Price method, assuming a step function as illustrated on the right side of Figure 1 to simulate the internal forces closer to reality.

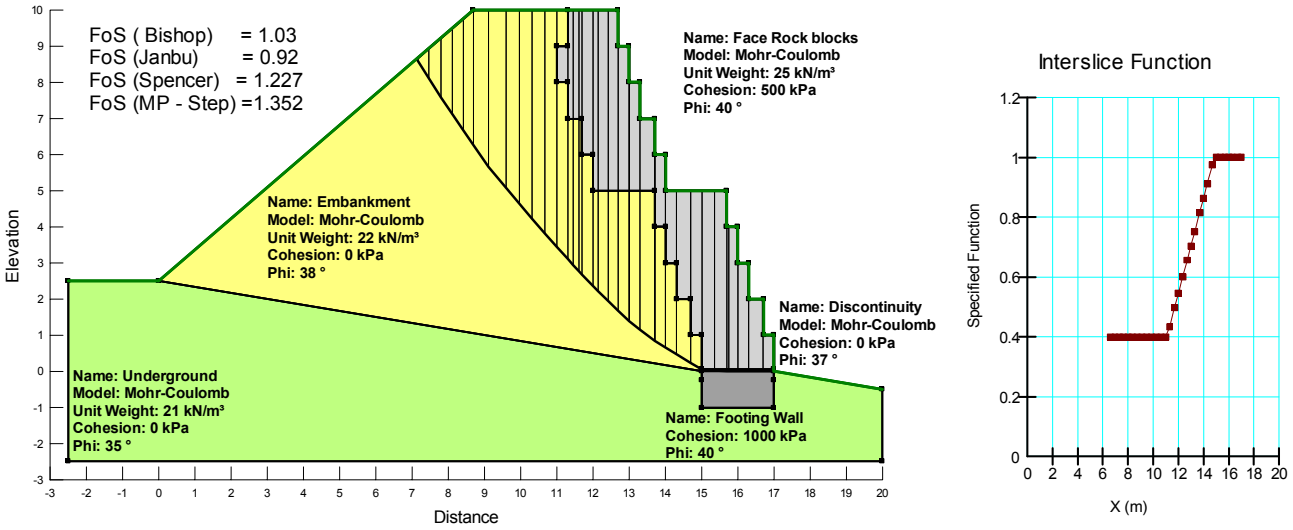

Figure 1. Analysis of a snow avalanche deflection dam with different method of slices: Section and results on left side; right side: interslice step function describing the inclination of the thrust line in Morgenstern Price method.

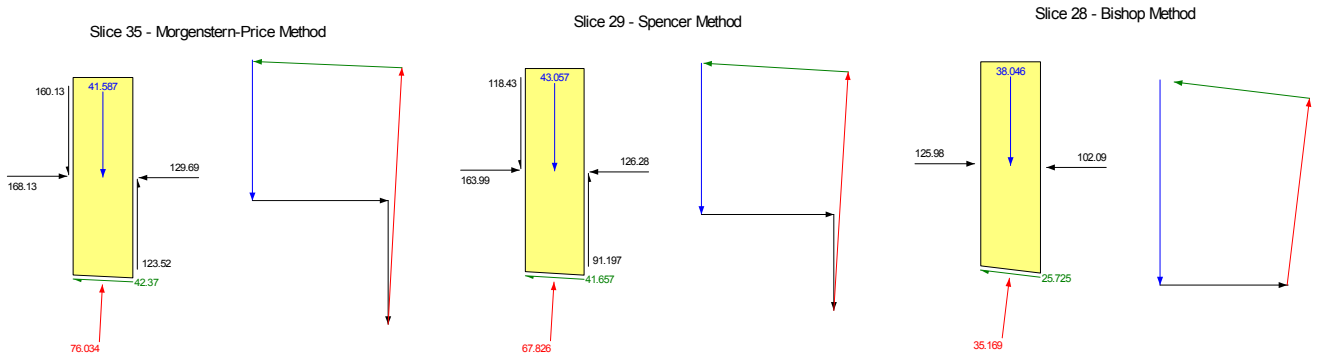

Figure 2. Comparison of force equilibrium in zone of transition of sliding surface from embankment into the block wall for Morgenstern-Price method with step function (left), Spencer's method (centre) and Bishop's method (right).

The value of the step function was assumed 1, as long as the slices cut through the block wall and 0.4 when the slices are completely located in the embankment fill and are linearly decreasing in between, with this the effect of the vertical component of earth pressure was simulated. The sliding surface must pass through the discontinuities between the horizontal rock blocks. The analysis with the Morgenstern-Price method yields a factor of safety FoS = 1.35, with Bishop's method FoS = 1.03 and with Janbu FoS= 0.92. With Spencer's method, equivalent to Morgenstern and Price with a constant function, gives a factor of safety FoS = 1.227. The forces acting o a slice at the transition of the sliding surface into the block wall are presented in Figure 2. The force polygons are very revealing: with Bishops method (right side of Figure 2) the normal force on the base of the slice is les than half of the force for the case with the step function and slightly more than half of Spencer' method. The force polygons show that more vertical and forces are considered in these analyses.

This example illustrates that the internal forces in a slope may play an important role in slope stability and must be considered. It is also evident that there is no unique solution for a safety factor as the internal stresses are influenced by the stress history of the ground. The deviation between the different assumptions of complete methods appears not as large, as between the simplified methods and complete methods.

2.4 *Estimation of the internal stresses*

The direct estimation of the internal stresses in the slope is empirical and requires some experience. In order to facilitate the estimate of the initial internal stresses Krahn (2007) proposed to run a Finite Element analysis of the slope first and then to introduce the obtained stresses in slope stability analyses and to run limit equilibrium analyses. This method is called the strength summation method (SSM) and has the advantage that there are less convergence problems as the factor of safety is directly determined.

2.5 *Application of the Finite Element method: Shear strength reduction method (SSR)*

With the finite element method deformations and the stress state in the ground can be modelled, depending on the accuracy of the constitutive models. The stability of slopes can be estimated by applying the Shear Strength Reduction method (SSR). With this method along slip surfaces the factor of safety is determined and the shear strength reduced (cohesion and friction angle) by the same factor. This procedure is carried out until a slip surface form; where the factor of safety with the reduced shear strength reaches one. The factor with which the shear strength is reduced is the factor of safety on shear strength. Problems may arise with convergence since the method approaches an instable condition in the analysis.

3 CASE STUDY OF A SLOPE WITH SIMPLE GEOMETRY

Considered is a slope of 5 m height and an inclination of $\beta = 40°$ without influence of water table (seepage) or external loads. The soil parameters are unit weight $\gamma = 20$ kN/m^3; friction angle: $\varphi_k' = 30°$ ($\varphi_d' = 25.7°$); cohesion intercept: $c_k' = 5$ kN/m^2 ($c_d' = 3.33$ kN/m^2). Stability calculations with the method of slices and limit equilibrium with the Morgenstern-Price method with constant inter-slice function for characteristic and design shear strength values. As a variant the strength summation method SSM, where the limit equilibrium method is combined with a stress distribution based on finite element stress-strain

analysis has been used. The third method is shear strength reduction (SSR) method with finite element with characteristic soil parameters.

The results are shown in Figure 3 for the limit equilibrium analysis with the Morgenstern-Price method and the constant function, actually equivalent to Spencer's method, on the left side the results obtained with characteristic values and the factor of safety on shear strength are shown, on the left side the sliding surface with design values, i.e. characteristic values reduced by partial factors. The results for the strength summation method are presented in Figure 4 and in Figure 5 the results for the analysis with the shear strength reduction and the finite element method. The obtained factors of safety on shear strength for calculations with characteristic shear strength and level of utilization μ are compiled in Table 2

Although for all cases the estimated FoS or μ are nearly equal, the detailed shape of the sliding surface deviates from one method of calculation to the other. From a general inspection one might conclude that the analysis with characteristic values and the determination of the factor of safety on shear strength does not deviate substantially from analyses carried out with design values, i.e characteristic values reduced by partial factors. Apparently for not to steep slopes with simple geometries or "text-book" slopes only small deviations between the different approaches are found.

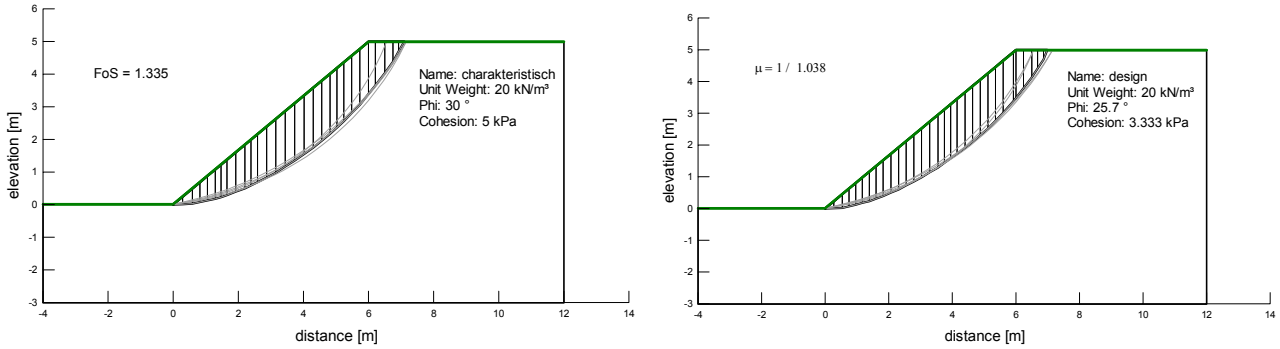

Figure 3. Sliding surfaces determined with limit equilibrium method (Morgenstern-Price with constant function) and factor of safety und shear strength and characteristic values (left) and with design values (partial factors).

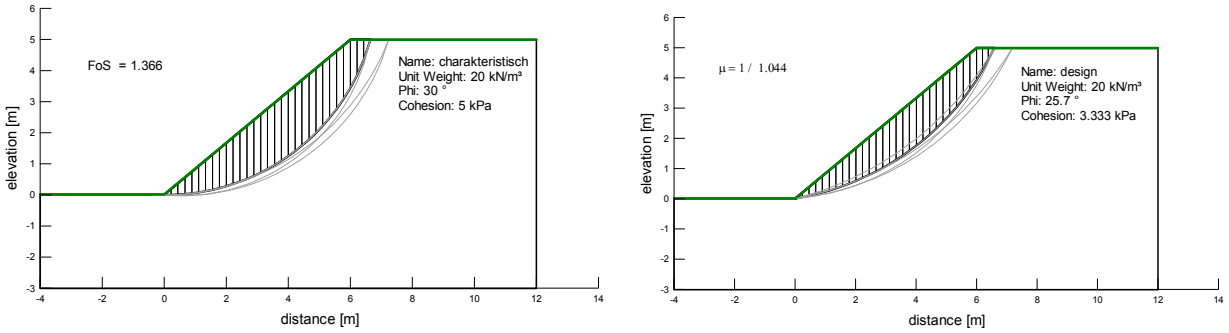

Figure 4. Comparison of sliding surfaces with strength summation method (SSM) and factor of safety on characteristic values (left side) and with design values and partial factors (right side)

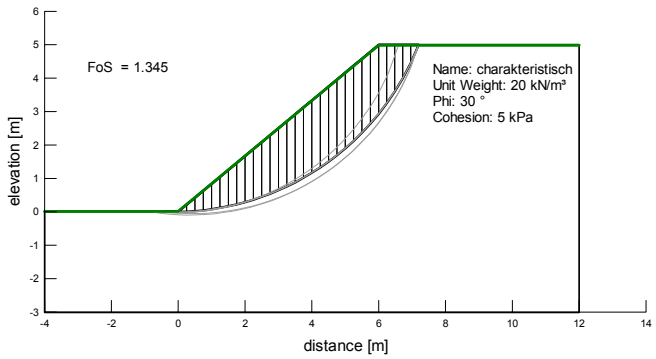

Figure 5. Critical slip surface determined with Finite Element method and shear strength reduction method (SSR) and characteristic values

Table 2. Results of stability calculation with different methods for the case study of a simple slope

Method	Parameter	Limit equilibrium (LE),	Strength summation (SSM)	Shear Strength reduction method (SSR)
Factor of safety on shear strength	Factor of safety on shear strength: FoS	1.335 Morgenstern-Price: constant 1.348 Bishop; 1.286 Janbu	1.366	1.345
Partial factors on strength	Level of utilization μ	0.964 Morgenstern-Price: constant 0.952 Bishop; 1.0163 Janbu	0.958	Not possible to determine

4 APPLICATION OF STABILITY ANALYSES IN PRACTICE

From their experience with real structures involving steeper slopes and heterogeneous foundations the authors have found that there are substantial differences between sliding surfaces determined with the factor of safety on shear strength and with design strength and level of utilization.

4.1 *Geogrid reinforced structure*

The 25 m high structure, reinforced with geo-grids shows substantially deviating critical sliding surfaces (Figure 6 left). The slip surface (Figure 1 right) obtained with design values does not appear plausible.

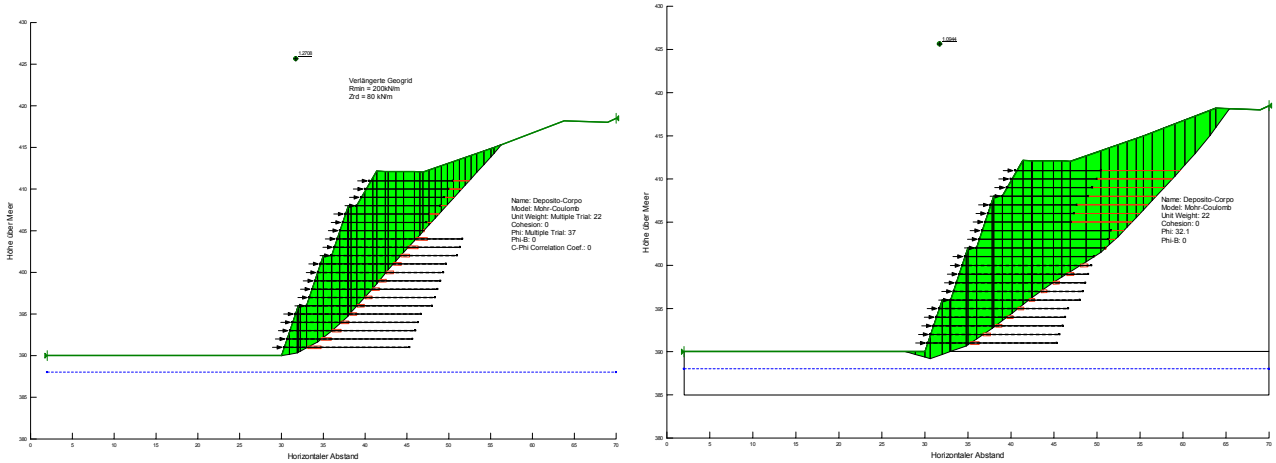

Figure 6. Comparison of Geo-grid reinforced wall in cohesionless soil (c'=o; Φ'= 37°) on left side designed with factor of safety on shear strength (former global factor of safety) F = 1.27 compared to design with partial factor of safety on right side (γ_Φ= 1.2) and Degree of Utilization μ = 0.91.

4.2 *Fill deposit on soft clay deposit*

The geogrid structure is founded on a 15 to 20 m thick glaciolacustrine deposits (pink layer) overlain by about 10 m of sand and gravel.

The design with characteristic values and factor of safety on shear strength (Figure 7) give a critical slip surface through the reinforced slope whereas with the design values a much deeper reaching critical sliding surface (Figure 8) is obtained.

The sliding surface obtained by the determination of the minimal factor of safety on shear strength is more plausible. In this particular case the soft clay layer was modeled by undrained strength, which was reduced by the partial factor γ_c =1.5. Since the stress distribution plays an important role and is determined with consideration of the activated shear strength, this led to this unlikely sliding mass. The resulting critical sliding surface is the result of fictitious material properties obtained by reducing the real properties by a partial factor of safety. In the above particular case the observational method is used and from the analyses the true sliding surfaces should be known, as one would expect the largest displacement to occur close to this zone. For the design also finite element analyses were carried out with characteristic values, since for the evaluation of the stability the deformation occurring during construction have to estimated and then compared to measured displacements.

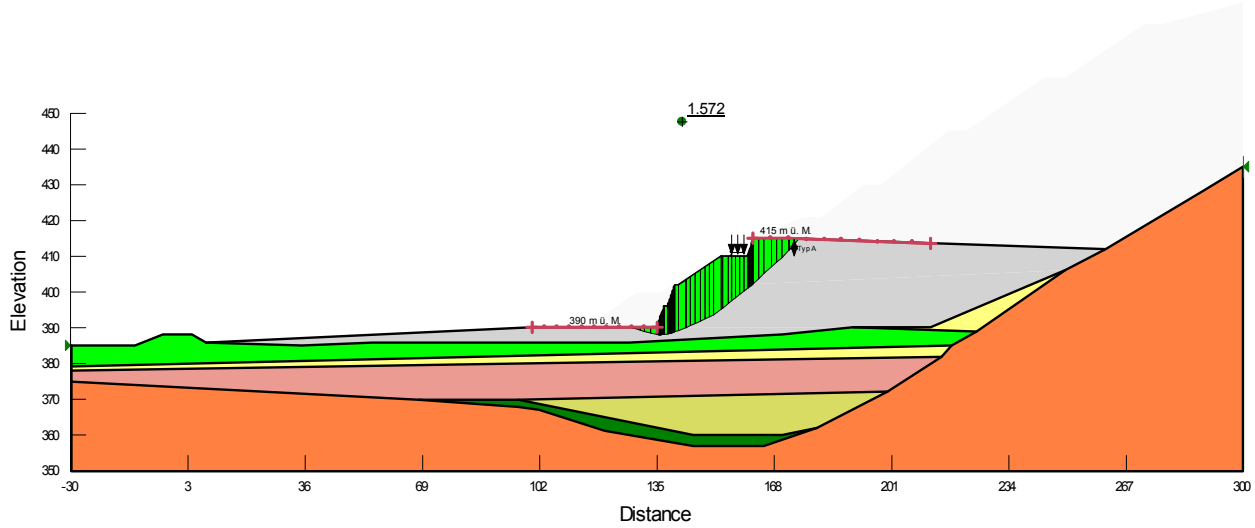

Figure 7. Stability Analysis of geogrid supported embankment on foundation with soft clay layer. FoS =1.572

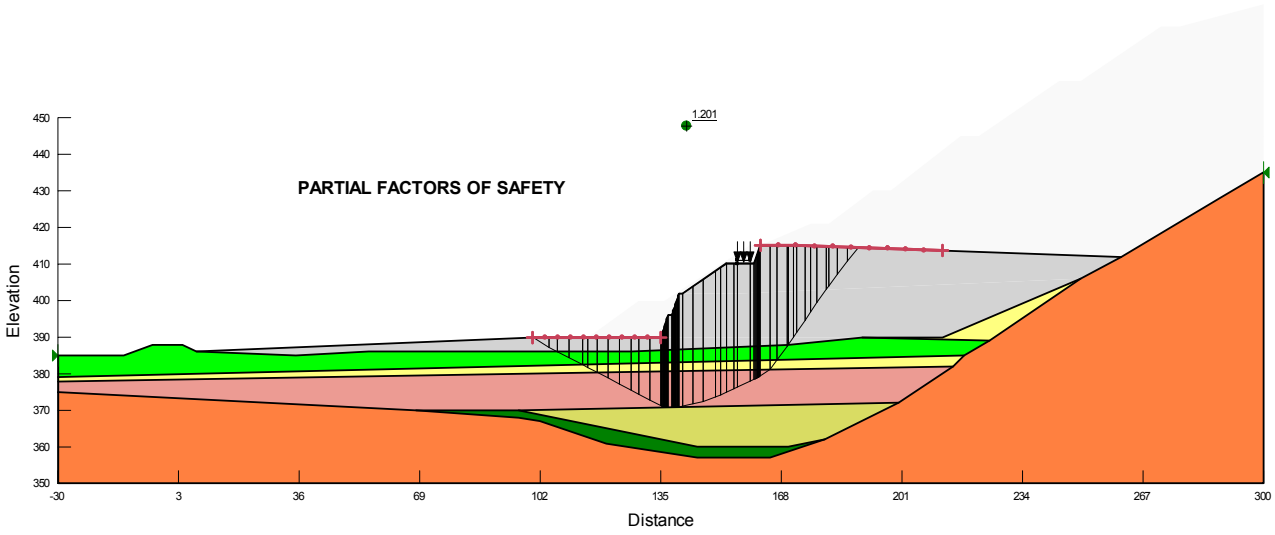

Figure 8. Critical slip surface determined with strength parameters reduced by partial factors for same geometry and geology as shown in Figure 3. Partial factor of on friction γ_{Φ}= 1.2 and cohesion γ_c =1.5. Degree of Utilization = 0.84.

4.3 *General shortcomings of the method with partial factors of safety*

For a method to be valid in practice it must work in all cases. One cannot proof with examples that the method is generally valid, however, one can proof with examples that the method has fundamental shortcomings. As shown earlier the stress state inside the sliding mass is important, as the initial state of stress depends on the geologic history of the ground. With partial factors of safety one assumes that strength parameters are independent and geometry (height) of the slope does not play a role. With partial factors an artificial material is created with little relation to reality and as consequence the analyses are performed with a fictitious equilibrium in the sliding mass.

5 PROBABILISTIC METHODS

The following practical example deals with a small slope that had to be excavated in a built-up area. The soil is a dense gravel and with an estimated friction angle (Φ'_k= 38°; Triangular distribution: 36; 38; 40°) and some difficult to estimate cohesion (c'_k = 15 kPa; Triangular distribution: 1, 15, 20 kPa). The corresponding design values are: Φ'_d= 32.8°; c'_d = 10 kPa. The analysis with Spencer's method (Figure 9) yields a factor of safety on shear strength FoS =1.535. With partial factors a level of utilization μ= 0.86 was obtained. One would judge with both methods that the excavation would be safe. The consideration of the distribution of the Factor of safety on shear strength (Figure 9right side) indicate a probability close to 2% that FoS < 1, i.e. there is a substantial risk that a failure could occur. For this reason we proposed to the owner to use a vertical wall supported with soil nail that eliminates this risk.

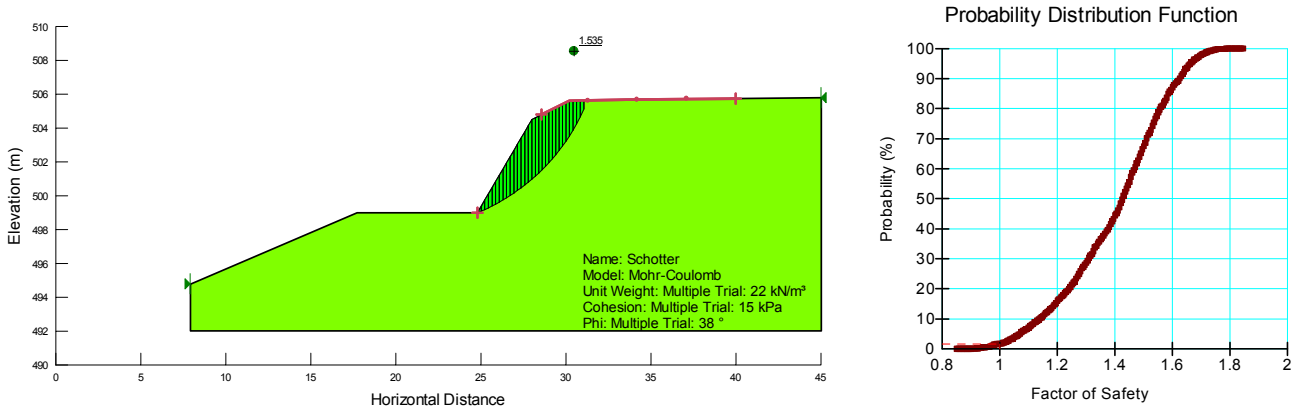

Figure 9. Analyses of slope in gravel with factor of safety on shear strength (FoS = 1.535), partial factors of safety (level of utilization μ= 0.86) and probabilistic method with $p_f \approx 2\%$

For this case an estimate of the strength parameters was used. Probabilistic methods allow one to judge the effects of measured dispersion of soil properties on safety (Steiner et al. 1992) and the risk and consequences of slope failures (Christian et al. 1994; Baecher & Christian, 2003). Probability and reliability approaches allow taking into consideration the spatial variability of the ground, although this may not be an easy task (El-Ramly et al., 2006). Slope stability programs (Krahn, 2004) can simulate the variation on a single slip surface; this may provide a better understanding of the effect of parameters involved. For evaluating the overall probability of failure the evaluation of many slip surfaces may be necessary (Cho, 2010). Silva et al. (2008) have proposed a framework for subjective assessment of slope stability.

6 CONCLUSIONS

Based on practical experience we conclude that the application of partial factors of safety as described in Eurocode 7 (EN 1997-1) and national codes (SIA 267) for slope stability do not provide a reliable tool for judging the safety of slopes. Our experience is from steeper slopes and embankment with heterogeneous conditions that are present in mountainous regions, like the Alps. In more complex cases slip surfaces obtained substantially deviate from the slip surfaces obtained with the factor of safety on shear strength. These slip surfaces appear not plausible.

The use of the Factor of safety on shear strength allows considering the effect of geometry, different materials and pore pressures in the ground (seepage) in stability analyses with a stress state in the ground corresponding to the real state. The effect of individual parameters or modification can more easily compared

With this approach also deformation computations necessary for comparing with measurements of displacements can be integrated. Predictions of displacements made with numerical methods can be compared to field measurements (observational method) and, if necessary, appropriate actions taken.

REFERENCES

Baecher, G.G. & Christian, J.T. (2003) Reliability and statistics in geotechnical engineering, Wiley, Chicester, UK

Bishop, A.W. (1955), "The Use of Slip Circle in the Stability Analysis of Slopes", Géotechnique, Vol. 5, pp 7-17.

Bishop, A.W.; Morgenstern, N.R. (1960);"Stability coefficients for earth slopes. Géotechnique, 10, 129-150.

Cho, S.E. (2010) "Probabilistic Assessment of Slope stability that considers the spatial variability of soil properties"; Journal of Geotechnical and Geoenvironmental Engineering, 136, (7), 975 - 984.

Christian, J.T.; Ladd, C.C.; Baecher, G.B. (1994) Reliability applied to slope stability analysis". J. Geotech. Engng 120 (12), 2180 - 2207

Duncan, J.M.; Wright, S.G. (2005) Soil Strength and Slope Stability. John Wiley & Sons, Hoboken, New Jersey, 297p.

El-Ramly, H., Morgenstern, N.R., Cruden, D.M. (2006) Lodalen slide: a probabilistic assessment, Canadian Geotechnical Journal, **43**, 956-968.

EN 1997-1 (2004) Eurocode 7: Geotechnical Design – Part 1: General rules

Fellenius, W. (1936), "Calculation of the Stability of Earth Dams", Trans. 2nd Congress on Large Dams, Vol. 4, pp 445-459.

Fredlund, D.G. & Krahn, J. (1977), Comparison of Slope Stability Methods of Analysis, Canadian Geot Jour., 14(3), 429-439.

Hoek and Bray (1977) "Rock Slope Engineering" 2nd edition, The Institution of Mining and Metallurgy, London.

Janbu, N. (1954) „Stability Analysis of Slopes with Dimensionless Parameters“, Harvard Soil Mechanics Series, No. 46, 81 pp.
Janbu, N. (1957) “Earth Pressure and Bearing Capacity by Generalized Procedure of Slices”, Proc. 4th International Conf. on Soil Mechanics, Vol. 2, pp 207-212.
Krahn, J. (2003) “The Limits of Limit equilibrium analysis, The 2001 R.M. Hardy Keynote Adress, Canadian Geotechnical Journal, Vol. 40, pp 643-660.
Krahn, J. (2004), “Stability Modelling with Slope/W, an Engineering Methodology. Geoslope Calgary, Alberta, Kanada.
Krahn, J. (2007) Limit Equilibrium, Strength Summation and Strength Reduction Methods for Assessing Slope Stability, Proc. 1st Canada-U.S. Rock Mechanics Symposium, *Vancouver, BC, Canada*
Krey (1936) Erddruck, Erdwiderstand und Tragfähigkeit des Baugrundes, 5th edition, Ernst & Sohn, Berlin
Lambe, T.W. and Whitman, R.V. (1969), “Soil Mechanics”, John Wiley and Sons, Inc., New York.
Lang, H.J. & Huder, J. (1990), „Bodenmechanik und Grundbau“, 4. Auflage, Springer Berlin.
Lang, H.J., Huder, J.; Amann, P. (1996), „Bodenmechanik und Grundbau“, 6. erweiterte Auflage, Springer Berlin
Lang, H.J.; Huder, J.; Amann, P.; Puzrin, A.M. (2007) „Bodenmechanik und Grundbau“, 8. ergänzte Auflage, Springer Berlin
Morgenstern, N.R. & Price, V.W. (1965), „The Analysis of the Stability of General Slip Surfaces, Geotechnique, (15), 79-93.
SIA 267 (2003) Geotechnik, Geotechnical Design, Swiss Standard
Silva, F., Lambe, T.W.; Marr, W.A. 2008: “Probability and Risk of slope Failure” ”. J. Geotech. Engng 134 (12) 1691 – 1699.
Spencer, E. (1967), “A Method of Analysis of the Stability of Embankments Assuming Parallel Inter-Slice Forces”, Geotechnique, Vol. 17, No. 1, pp 11-26.
Steiner, W. (1977) “Three-Dimensional Stability of Frictional Slopes” Master of Science Thesis, MIT, Cambridge, 111 p.
Steiner, W. (1985)”Stability Analysis of avalanche dam Sogn Placi with Morgenstern-Price method and step function”. Department of Public works, Canton of Grisons, unpublished report
Steiner, W.; Metzger, R., Marr, W.A (1992) "An Embankment on Soft Clay with an adjacent cut", *Proceedings ASCE Conference Stability and Performance of Slopes and Embankments II, Berkeley, 1992,* ASCE, New York, NY. pp. 705-720.
Taylor, D.W. (1937), “Stability of Earth Slopes”, Journal Boston Society of Civil Engineers, pp 337-386.
Whitman, R.V. and Bailey, W.A. (1966), “Use of Computers for Slope Stability Analysis”, Proc. Conf. on the Stability of Slopes and Embankments, ASCE, pp 519-532.
Wright, S.G. (1969), “A Study of Slope Stability and the Undrained Strength of Clay Shales”, Thesis submitted to the Univ. of California at Berkeley in partial fulfilment for the Degree of Doctor of Philosophy.
Wright, S.G., Kulhawy, F.H. and Duncan, J.M. (1973), “Accuracy of Equilibrium Slope Stability Analysis”, ASCE, JSMFD, Vo. 99, No. SM10, pp 783-791.
Wyllie, D.C.; Ma C.W. (2004) Rock Slope Engineering, Civil and Mining, 4th edition, Spon Press. Taylor and Francis Group, London and New York.

ISGSR 2011 - Vogt, Schuppener, Straub & Bräu (eds) - © 2011 Bundesanstalt für Wasserbau ISBN 978-3-939230-01-4

A Comparative Study of Pile Design Using Eurocode 7 and RBD^E

J. Wang, Y. Wang & Z. Cao
Department of Building and Construction, City University of Hong Kong, Hong Kong

ABSTRACT: A comparative study of pile design is presented using Eurocode 7 and an expanded reliability-based design (RBD^E) method that is recently developed by the authors. A design example that has been used in the literature to illustrate Eurocode 7 is re-designed using RBD^E. The RBD^E method gives designs that are consistent with the designs from Eurocode 7 or correspond to the target failure probability (p_T) adopted in EN 1990. The RBD^E method allows design engineers to adjust the design p_T easily to accommodate the needs of a particular project without additional computational efforts. In addition, design engineers have the flexibility to make assumptions and/or simplifications deemed appropriate in designs. Such flexibility is illustrated by exploring the effect of different probability distributions of soil effective friction angle on design.

Keywords: Pile, Eurocode 7, Reliability-Based Design, Monte Carlo Simulations

1 INTRODUCTION

Reliability-based design (RBD) of foundations has attracted increasing interest over the last two decades, and several RBD methodologies have emerged, such as the partial factor design method in Eurocode 7, the load and resistance factor design (LRFD) method for highway structure foundations (Barker et al. 1991, Paikowsky et al. 2004, Paikowsky et al. 2010), and the Multiple Resistance Factor Design (MRFD) method for transmission line structure foundations (Phoon et al. 2003a&b). These RBD methods aim to provide designs with appropriate degrees of reliability, which is usually expressed in probabilistic terms, such as the target probability of failure $p_T = 7.2 \times 10^{-5}$ or target reliability index $\beta_T = 3.8$ adopted in EN 1990 (European Committee for Standardization 2002). Through some calibration process, Eurocode 7 provides tabulated partial factors for actions (i.e., loads), material properties, and resistances. Design engineers select appropriate partial factors from the table and carry out design calculations using a trial-and-error approach. The calibration of partial factors in Eurocode 7 has been primarily based on deterministic methods that calibrate to the long experience of traditional design with the aid of historical and empirical methods (Orr and Breysse 2008). As the numerical values of the partial factors are obtained from deterministic methods, it is of great interest to use full probabilistic methods (e.g., Monte Carlo Simulations (MCS)) to investigate the performance of these partial factors in achieving the desired degrees of reliability. In addition, the partial factors in Eurocode 7 aim for $p_T = 7.2 \times 10^{-5}$ only, partial factors for other p_T values commonly are not available. This fact limits a designer's flexibility to adjust the p_T to accommodate specific needs of a particular project.

To address these limitations, an expanded reliability-based design (RBD^E) method was recently developed that formulates the foundation design as an expanded reliability problem (Wang et al. 2011, Wang 2011). In this paper, a comparative study of pile design using Eurocode 7 and RBD^E is described. After a brief introduction of Eurocode 7 and RBD^E, a pile foundation design example is described that has been used to evaluate Eurocode 7 in literature (Orr 2005a). Then, the design example is re-designed using RBD^E and compared with the designs from Eurocode 7. In addition, the effect of the probability distributions of soil effective friction angle on designs is explored using RBD^E.

2 PARTIAL FACTOR DESIGN METHOD IN EUROCODE 7

Eurocode 7 contains three Design Approaches (i.e., DA1 with Combination 1 (C1) or 2 (C2), DA2, and DA3), and it aims to achieve that the probability of exceeding some limit states during a specified service period of the structures is smaller than the p_T valued adopted. Consider, for example, the ultimate limit state (ULS), the $p_T = 7.2 \times 10^{-5}$ is adopted in EN 1990. For the ULS design of piles under axial compression, the design equation is given as (e.g., Orr 2005b):

$$F_{c,d} \le R_{c,d} \qquad (1)$$

where $F_{c,d}$ is the design action (load) and $R_{c,d}$ is the design resistance of the pile. The design vertical action, $F_{c,d}$ is given as (e.g., Orr 2005b):

$$F_{c,d} = \gamma_G G_k + \gamma_Q Q_k \qquad (2)$$

where G_k is the characteristic permanent load, Q_k is the characteristic variable load, γ_G and γ_Q are the relevant partial load factors. The values of γ_G and γ_Q are given in Eurocode 7 and depend on the Design Approach being used. The design compressive resistance of piles is given by (Orr 2005b):

$$R_{c,d} = R_{b,d} + R_{s,d} = R_{b,k}/\gamma_b + R_{s,k}/\gamma_s \qquad (3)$$

where $R_{b,d}$ and $R_{s,d}$ are the design base and shaft resistances, $R_{b,k}$ and $R_{s,k}$ are the characteristic base and shaft resistances, and γ_b and γ_s are the relevant partial resistance factors.

3 EXPANDED RELIABILITY-BASED DESIGN (RBD^E) METHOD

An expanded reliability problem herein refers to a reliability analysis of a system in which a set of system design parameters are artificially considered as uncertain with probability distributions specified by the user for design exploration purposes (Wang et al. 2011, Wang 2011). For example, consider the pile with the pile length L as the design parameter. The design process is one of finding an L value that satisfies both the ULS and SLS requirements and achieve the design target p_T or β_T. In the context of RBD^E, the L of the pile is considered as independent discrete random variables with uniformly distributed probability mass function p(L). The pile design process is re-formulated as a process of finding failure probabilities corresponding to designs with various L values [i.e., conditional probability p(Failure|L)] and comparing them with p_T. Failure refers to events in which the load exceeds resistance (i.e., F > R). Feasible designs are those with p(Failure|L) ≤ p_T. Note that the uniform probability mass function p(L) does not reflect the uncertainty in L, because L represents design decisions and no uncertainty is to be associated with it. Instead, it is used to yield desired information about p(Failure|L). Using Bayes' Theorem (e.g., Ang and Tang 2007), the conditional probability p(Failure|L) is given by:

$$p(\text{Failure}|L) = \frac{p(L|\text{Failure})}{p(L)} p(\text{Failure}) \qquad (4)$$

in which p(L|Failure) = conditional probability of L given failure. Since L is independent discrete uniform random variables, p(L) in Equation (4) is expressed as:

$$p(L) = \frac{1}{n_L} \qquad (5)$$

in which n_L = number of possible discrete values for L. Using a single run of MCS, p(Failure) and p(L|Failure) can be estimated. Details of the RBD^E and MCS are given by Wang et al. (2011) and Wang (2011).

RBD^E can result in a large number of feasible designs. The requirement of the economic optimization limit state (EOLS) then is adopted to finalize the design as the one with the minimum construction cost (Wang and Kulhawy 2008, Wang 2009). The construction cost of pile is estimated using published, annually-updated, unit cost data, such as Means Building Construction Cost Data (Means 2007). The construction costs for all feasible designs are calculated as the product of their unit costs and pile lengths, and the final design is determined accordingly by comparing their construction costs.

4 PILE FOUNDATION DESIGN EXAMPLE

Orr (2005a&b) illustrated Eurocode 7 using a bored pile design example shown in Figure 1. The bored pile with a diameter B = 0.6 m is installed in sand with a total unit weight γ = 21 kN/m^3, a characteristic effective friction angle ϕ'_k = 35° (effective cohesion c' = 0), and SPT-N = 25. Groundwater level is at a depth of 2 m below the ground surface. The pile is designed to support an axial compression load with a characteristic permanent load G_k = 1200 kN and a characteristic variable load Q_k = 200 kN. The unit weight of concrete is 24 kN/m^3. The only design parameter is pile length L.

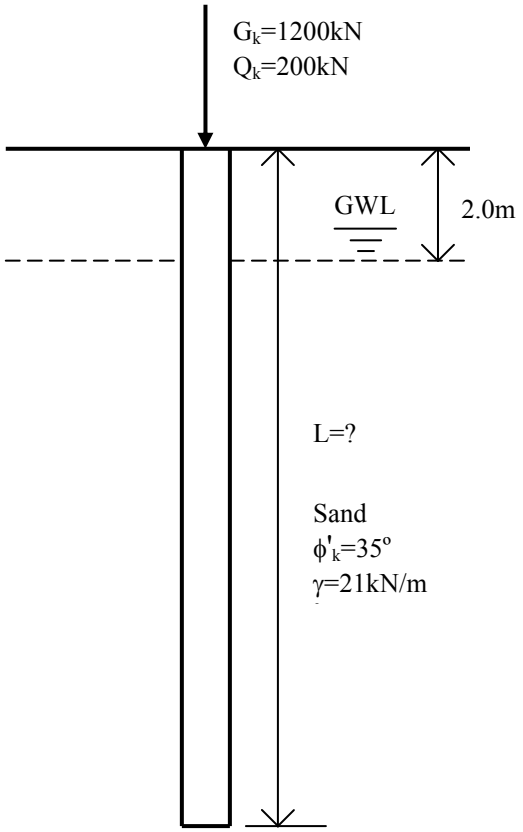

Figure 1. Pile foundation example (after Orr 2005a).

Table 1. Partial factors for the pile example

Design Approach	Permanent Load Factor, γ_G	Variable Load Factor, γ_Q	Base Resistance Factor, γ_b	Shaft Resistance Factor, γ_s	Model Factor, γ_R	Material Factor, γ_M
DA1, C1	1.35	1.5	1.25	1	1.5	—
DA1, C2	1	1.3	1.6	1.3	1.5	—
DA2	1.35	1.5	1.1	1.1	1.5	—
DA3	1.35	1.5	—	—	—	1.25

Table 2. Summary of pile designs using Eurocode 7

Design Approach	Pile Length, L (m)	Overall Factor of Safety, OFS	Probability of Failure, p(Failure)
DA1. C1	14.9	2.4	1.9×10^{-3}
DA1. C2	14.6	2.4	2.6×10^{-3}
DA2	14.0	2.3	4.4×10^{-3}
DA3	16.7	2.7	2.4×10^{-4}

Using three DAs of Eurocode 7, Orr (2005b) provided a set of model solutions to this design example. The characteristic resistances are obtained as $R_{b,k} = A_b q_{bk}$ and $R_{s,k} = A_s q_{sk}$, where q_{bk} and q_{sk} are the characteristic base resistance and shaft friction obtained from the soil parameters and A_b and A_s are the areas of the pile base and pile shaft. Table 1 summarizes the partial factors used for different DAs in this example. The values of the partial factors γ_b and γ_s are corrected by a model factor, γ_R = 1.5. The design resistance for DA3 is obtained by applying the partial material factor γ_M = 1.25 to $\tan\phi'_k$ to obtain ϕ'_d which is

used to obtain the design resistances. The base bearing resistance is given by $q_{bk} = \sigma_{v0}' N_q$, where σ_{v0}' is the vertical effective stress at the pile base and N_q is a bearing capacity factor estimated using N_q versus ϕ' relationship proposed by Berezantzev et al. (1961). The shaft resistance is given by $q_{sk} = 0.5 (1-\sin\phi') \sigma_{v0}' \tan\phi'$.

Table 2 summarizes the L values obtained from three DAs. The L values vary from 14.0 m to 16.7 m, and the overall factors of safety, OFS (defined as $R_{c,k}/F_k$), vary from 2.3 to 2.7. This design example is re-designed in the next section using the RBD^E method (Wang et al. 2011, Wang 2011).

5 RBD^E DESIGN

The RBD^E approach conceptually contains four basic steps: (1) establish deterministic calculation models, (2) model geotechnical-related uncertainties, (3) perform MCS and identify a pool of feasible designs, and (4) select the final design based on economic evaluation. To enable a consistent comparison with the design by Orr (2005b), the deterministic ULS calculation models in this section follow those adopted in the previous section. In addition, the permanent load G is treated as constant and equal to the characteristic permanent load G_k (i.e. G=1200kN). The total unit weight γ = 21 kN/m^3 of soil is also taken as deterministic.

5.1 *Uncertainty Modeling*

Uncertainties in design loads and material properties in Eurocode 7 are reflected through their respective characteristic values. The uncertain variables in this design example include the variable load, effective friction angle of soil, and length of pile, as shown in Table 3. The characteristic value for a design load in EN 1990 is defined as the load magnitude that corresponds to 5% or 2% probability of exceedance (i.e., an upper 95% or 98% fractile of its probability distribution) (European Committee for Standardization 2002). The variable load Q is considered as a lognormal random variable with a coefficient of variation COV_Q = 0.5, and its characteristic value Q_k is taken as the upper 95% fractile of the probability distribution. Then, the mean value (i.e., Q_m) of variable load is calculated as:

$$Q_m = \frac{Q_k}{\left(1 + 1.645 COV_Q\right)} \qquad (6)$$

Using Q_k = 200 kN (Orr 2005a&b) and COV_Q = 0.5, Q_m is estimated as 110 kN.

The effective friction angle ϕ' of soil is considered as a lognormal random variable with a coefficient of variation $COV_{\phi'}$ = 0.1. The mean value (i.e., ϕ'_m) of effective friction angle of soil is calculated as (Schneider 1997):

$$\phi'_m = \frac{\phi'_k}{\left(1 - 0.5 \mathrm{COV}_{\phi'}\right)} \qquad (7)$$

Using $\phi'_k = 35^o$ (Orr 2005a&b) and $COV_{\phi'}$ = 0.1, ϕ'_m is estimated as 36.84^o.

In addition, the pile design parameter L is treated as independent discrete uniform random variable. The possible L values vary from 12 m to 21 m with an increment of 0.3 m.

Table 3. Uncertain modeling in RBD^E design

Variables	Variable Load, Q		Effective friction angle of soil, ϕ'				Pile Length, L		
	Mean	COV*	Min*	Max*	Mean	COV*	Min*	Max*	Interval
Values	110 kN	0.5	24^o	40^o	36.84^o	0.1	12 m	21 m	0.3 m
Distribution Type	Lognormal Distribution		Lognormal Distribution				Discrete Uniform Distribution		

* COV = Coefficient of Variation, Min = Minimum, Max = Maximum

5.2 *Monte Carlo Simulation (MCS)*

MCS is performed using the software package Matlab (Mathworks 2010), which is equipped with random number generators for various probability distributions, such as "lognrnd" for lognormal variables, "normrnd" for normal variables, and "rand" for uniform variables. Random samples of the lognormally distributed variable load and effective friction angle of soil are generated by "lognrnd" with their respec-

tive means and standard deviations. Because the N_q versus ϕ' relationship proposed by Berezantzev et al. (1961) is only applicable for the ϕ' values between 24° and 40°, the ϕ' values are taken as 24° and 40°, respectively, when the ϕ' values generated from the random number generator are smaller than 24° or larger than 40°. Random samples of uniformly distributed L are generated by "rand". For each set of random samples, the loads and resistances of the pile are calculated. The pile is considered "failed" when the sum of the permanent and variable loads exceeds the bearing resistance. A single run of MCS with a sample size of 9,000,000 is performed for RBD^E, and the p(L|Failure), p(Failure), and conditional failure probability p(Failure|L) are estimated from MCS using Equation (4) accordingly.

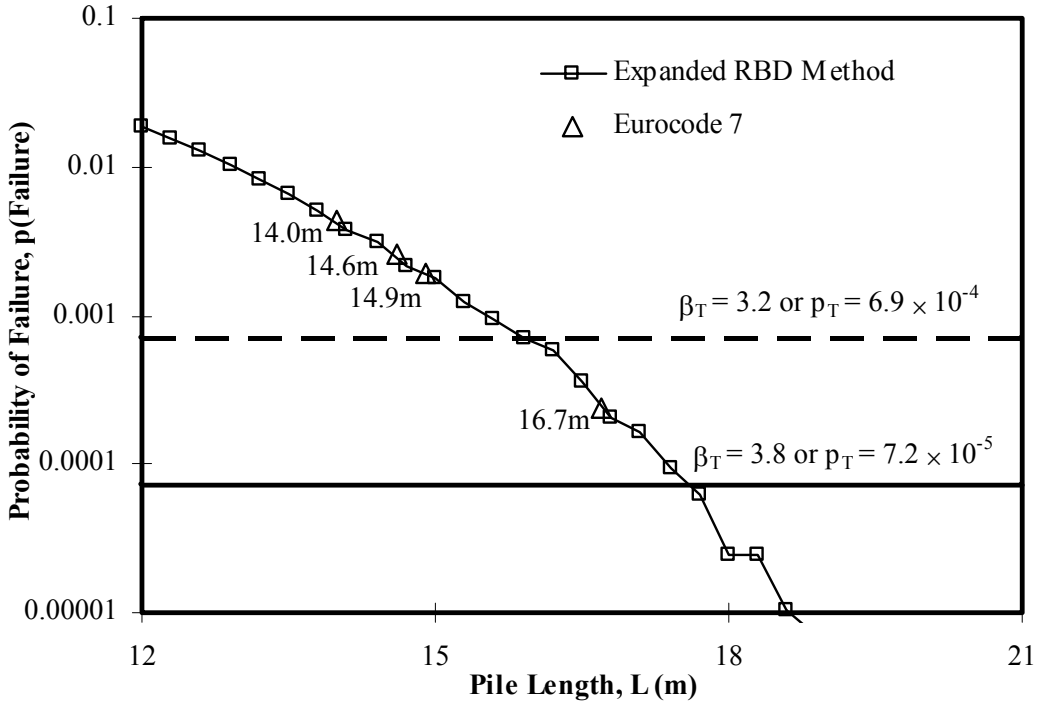

Figure 2. Conditional probability of failure from Monte Carlo Simulation.

5.3 *Results*

Figure 2 shows the conditional failure probability p(Failure|L) obtained from a single run of MCS. Note that p(Failure|L) is a variation of failure probability as a function of L. Failure probability p(Failure) decreases as L increases. Figure 2 also includes the $p_T = 7.2 \times 10^{-5}$ adopted in EN 1990, and feasible designs are those that fall below the p_T, as shown in the figure. In this example, the feasible designs are the piles with $L \geq 17.7$ m. The economic requirement then is adopted to determine the final design (Wang and Kulhawy 2008, Wang 2009). Since the construction cost is the product of pile depths and unit costs, the economic design for a given value of B is the one with the minimum L value. Therefore, among the pool of feasible designs obtained from RBD^E, the final design is a pile with L = 17.7 m.

6 RESULT COMPARISONS

Figure 2 also includes the failure probability p(Failure) for the design pile length obtained from Eurocode 7 (see Table 2). Each p(Failure) is obtained by performing a run of MCS with a sample size of 1,000,000, and the exact values of p(Failure) are summarized in Table 2.

These p(Failure) values vary from 4.4×10^{-3} to 2.4×10^{-4}, and they follow the p(Failure) versus L curve obtained from the RBD^E method. They are all however significantly larger than the $p_T = 7.2 \times 10^{-5}$ adopted in EN 1990. This implies that using the partial factors recommended in Eurocode 7 does not guarantee automatic fulfillment of its target reliability. It is interesting to note that, however, these p(Failure) values are consistent with the empirical foundation failure rates of about 10^{-2} to 10^{-3} (Baecher 1987).

In addition, it is worth noting that, in RBD^E, feasible designs for different p_T values are inferred directly from Figure 2 without additional computational efforts, which allows designers to adjust easily the

design p_T to accommodate the needs of a particular project. To illustrate such flexibility, Figure 2 also includes the $p_T = 6.9 \times 10^{-4}$ (i.e., $\beta_T = 3.2$) that have been adopted in the reliability – based designs of foundations for transmission line structures in North America (Phoon et al. 2003a&b). The corresponding design is a pile with L = 16.2 m, which falls among the range of pile length obtained from Eurocode 7.

7 EFFECT OF PROBABILITY DISTRIBUTIONS OF SOIL EFFECTIVE FRICTION ANGLE

The RBD^E method allows designers to make assumptions and/or simplifications deemed appropriate in designs. This section illustrates this flexibility by using different probability distributions of soil effective friction angle ϕ' in the design and exploring its effect. The ϕ' is considered as a normal random variable with the same mean value (i.e., $\phi'_m = 36.84^o$) and coefficient of variation (i.e., $COV_{\phi'} = 0.1$). Random samples of the normally distributed effective friction angle of soil are generated by the Matlab function "normrnd" with its mean and standard deviation. The ϕ' values are taken as 24° and 40°, respectively, when the ϕ' values generated from the random number generator are smaller than 24° or larger than 40°. A single run of MCS with a sample size of 9,000,000 is performed for RBD^E, and the results are shown in Figure 3.

Figure 3 compares the results for normal distribution with those for lognormal distribution. The p(failure) values both decreases significantly as the pile length increases. The p(failure) versus L relationship for the normal distribution moves towards the upper right corner of the plot, indicating a significant increase of failure probability for the same L value or a significant increase of design L value for the same p_T value. For the $p_T = 7.2 \times 10^{-5}$ adopted in EN 1990, the feasible designs are the pile with $L \geq 18.9$ m, and therefore, the final design is the pile with L = 18.9. For $p_T = 6.9 \times 10^{-4}$ (i.e. $\beta = 3.2$), the final design pile length is 17.4 m. These results indicate that probability distribution types have significant effect on the design.

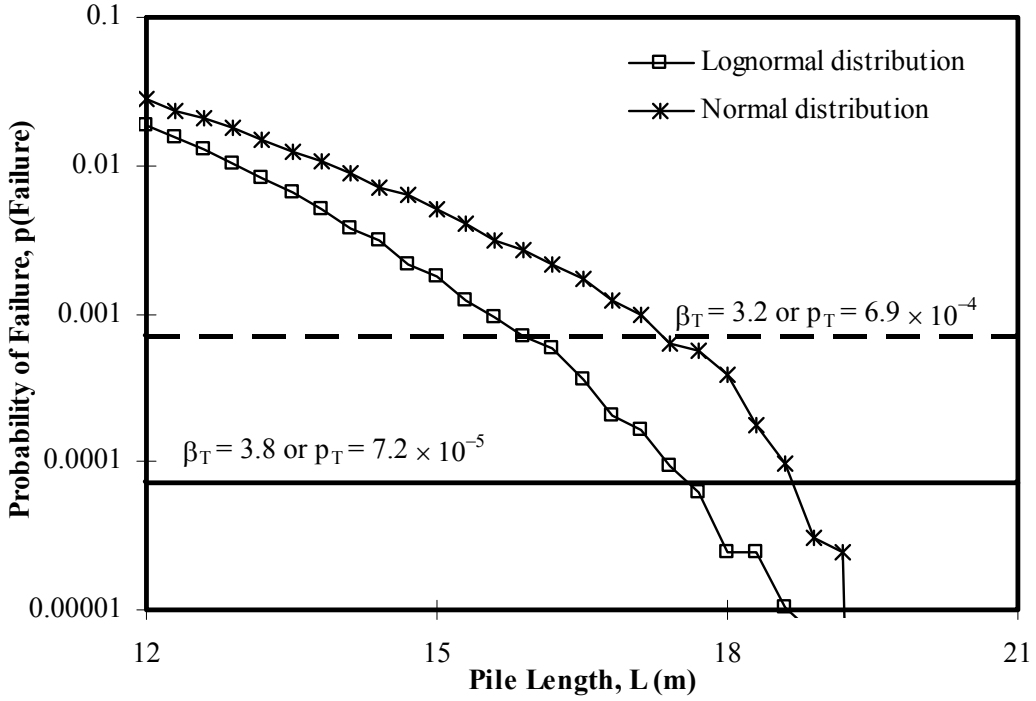

Figure 3. Effect of probability distributions of soil effective friction angle.

8 SUMMARY AND CONCLUSIONS

A comparative study was presented for pile design using Eurocode 7 and RBD^E. An example that was used to illustrate Eurocode 7 was re-designed using RBD^E. The RBD^E method gives designs that are consistent with the designs from Eurocode 7 or correspond to the target failure probability p_T adopted in EN 1990. It is also found that, using the partial factors recommended in Eurocode 7 does not guarantee automatic fulfillment of its target reliability, although the resulting failure probabilities are consistent with the

empirical rates of foundation failure. In addition, it is worth noting that, in RBD^E, feasible designs for different p_T values are inferred directly without additional computational efforts, which allows designers to adjust easily the design p_T to accommodate the needs of a particular project. The RBD^E method also gives designers the flexibility to make assumptions and/or simplifications deemed appropriate in designs. This flexibility was illustrated by using different probability distributions for soil effective friction angle in the design and exploring its effect. It was found that probability distribution types have significant effect on the design.

ACKNOWLEDGEMENTS

The work described herein was supported by a grant from the Research Grants Council of the Hong Kong Special Administrative Region, China [Project No. 9041484 (CityU 110109)] and a grant from City University of Hong Kong (Project No. 7002568). The financial supports are gratefully acknowledged.

REFERENCES

Ang, A. H.-S. and Tang, W. H. 2007. Probability concepts in engineering: Emphasis on applications to civil and environmental engineering. Wiley, New York.

Baecher, G. B. 1987. Geotechnical risk analysis user's guide. Report No. FHWA/RD-87-011, Federal Highway Administration, McLean, Va., USA.

Barker, R. M., Duncan, J. M., Rojiani, K. B., Ooi, P. S. K., Tan, C. K., and Kim, S. G. 1991. Manuals for the design of bridge foundations. NCHRP Report 343, Transportation Research Board, Washington, DC.

Berezanysev, V.G., kristoforov, V.S., and Golubkov, V.N. 1961. Load bearing capacity and deformation of piled foundations. Proceedings Ⅴ International Conference on Soil Mechanics and Foundation Engineering, Paris, France, 2, 11-15

European Committee for Standardization 2002. EN 1990: Eurocode – Basis of Structural Design, Brussels.

Mathworks, Inc. 2010. MATLAB – the language of technical computing, *<http://www.mathworks.com/products/matlab/>* (March 9, 2010).

Means. 2007. 2008 RS means building construction cost data. R.S. Means Co., Kingston, MA.

Orr, T. L. L. 2005a. Design examples for the Eurocode 7 Workshop. Proceedings of the International Workshop on the Evaluation of Eurocode 7, Trinity College, Dublin, 67-74.

Orr, T. L.L. 2005b. Model solution for example 3 - Pile foundation designed from soil parameter values. Proceedings of the International Workshop on the Evaluation of Eurocode 7, Trinity College, Dublin, 85-86.

Orr, T. L. and Breysse D. 2008. Eurocode 7 and reliability-based design. Reliability-Based Design in Geotechnical Engineering: Computations and Applications, Chapter 8: 298-343, Edited by Phoon, Taylor & Francis.

Paikowsky, S. G., Birgisson, B., McVay, M., Nguyen, T., Kuo, C., Baecher, G., Ayyub, B., Stenersen, K., O'Malley, K., Chernauskas, L., and O'Neill, M. 2004. Load and resistance factor design (LRFD) for deep foundations. NCHRP Report 507, Transportation Research Board, Washington, DC.

Paikowsky, S. G., Canniff, M. C., Lesny, K., Kisse, A., Amatya, S., and Muganga, R. 2010. LRFD design and construction of shallow foundations for highway bridge structures. NCHRP Report 651, Transportation Research Board, Washington, DC.

Phoon, K. K., Kulhawy, F. H., and Grigoriu, M. D. 2003a. Development of a reliability-based design framework for transmission line structure foundations. Journal of Geotechnical and Geoenvironmental Engineering, 129(9), 798-806.

Phoon, K. K., Kulhawy, F. H., and Grigoriu, M. D. 2003b. Multiple resistance factor design (MRFD) for shallow transmission line structure foundations. Journal of Geotechnical and Geoenvironmental Engineering, 129(9), 807-818.

Schneider, H. R. 1997. Definition and determination of characteristic soil properties. Proceedings of the XII International Conference on Soil Mechanics and Geotechnical Engineering, Hamburg, 2271-2274, Balkema, Rotterdam.

Wang, Y. 2009. Reliability-based economic design optimization of spread foundations. J. Geotech. and Geoenvir. Eng., 135(7), 954-959.

Wang, Y. 2011. Reliability-based design of spread foundations by Monte Carlo Simulations. Geotechnique, doi: 10.1680/geot.10.P.016.

Wang, Y., Au, S. K., and Kulhawy, F. H. 2011. Expanded reliability-based design approach for drilled shafts. J. Geotech. and Geoenvir. Eng., 137 (2), 140-149.

Wang, Y. and Kulhawy, F. H. 2008. Economic design optimization of foundations. J. Geotech. and Geoenvir. Eng.,134(8), 1097-1105.

ISGSR 2011 - Vogt, Schuppener, Straub & Bräu (eds) - © 2011 Bundesanstalt für Wasserbau ISBN 978-3-939230-01-4

Application of reliability based design (RBD) to Eurocode 7

T. Hara, Y. Honjo, Y. Otake & S. Moriguchi
Gifu University, Gifu, Japan

ABSTRACT: This study aims to discuss harmonization of Design Approaches in Eurocode 7 and National Annexes from the viewpoint of reliability. Relative reliability difference of the different design results, which are estimated from respective Eurocode 7 Design Approaches, DA1, DA2, DA3, and National Annexes, with respect to a design example is studied based on the results of level III reliability based design, and several issues concerning reliability are discussed in this paper.

Keywords: Eurocode 7, Partial factor, Reliability based design

1 INTRODUCTION

The developments of design codes grounded on the reliability based design (RBD) are actively taking place in various part of the world today. RBD is considered to become the central tool of the design code developments. We consider it desirable that Eurocode 7 (EC7), which is recognized as one of the most important geotechnical design codes in the world, would introduce this concept and stand on the same ground. The introduction of RBD would provide useful information for the development of Design Approaches (DAs) and National Annexes (NAs), which is one of the central tasks EC7 is now encountering. It would also facilitate the harmonization of EC7 to other structural Eurocodes as well as other geotechnical design codes in the world, because once reliability (i.e. a quantified measure of the structure performances) become a common language, we would obtain common ground for communication.

Recognizing these backgrounds, this study focused on the different design results depending on respective DAs and NAs, which were presented in the 2nd International workshop of ETC10 in Pavia in April 2010. In this paper, the relative reliability difference of the different design results with respect to a design example is studied from a comparison with results of a level III RBD, and several issues concerning reliability are discussed.

2 PRCEDURE FOR THIS STUDY

In this study, as shown in Figure 1, EC7 based design and a level III RBD on a design example are carried out at first, and the relative reliability level difference is studied from the relationship between reliability levels and foundation dimensions, which were obtained from the RBD. Finally, future issues on EC7 that is discussed based on the study done in the first part: determination of partial factors based on target reliability and code calibration of NAs are discussed.

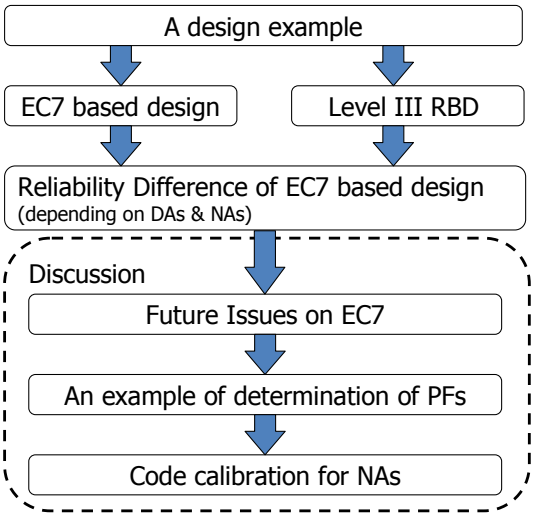

Figure 1. Procedure for this study

3 EC7 BASED DESIGN AND THE RELIABILITY

3.1 *Target Design Example*

The target design example is one to determine the width of a square pad foundation on a uniform and very dense fine glacial out wash sand layer of 8m thick on the underlying bedrock, as shown in Figure 2, which is one of the six examples set by ETC10 in Pavia in 2010 (ETC10 2010). In this example in the ETC10, both stability and serviceability, which the settlement should be less than 25mm, are required. In this section, mainly stability as Ultimate Limit State (ULS) is focused. Different design results of Serviceability limit State (SLS), which were estimated by respective NAs, are described in the ETC10. The necessity of partial factor for SLS design is also discussed in the subsequent section.

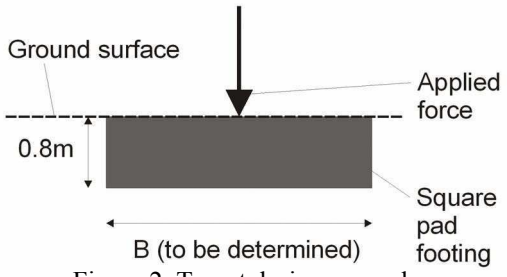

Figure 2. Target design example.

In the given condition of the design example, the pad foundation is to be built at embedded depth of 0.8m, and vertical permanent and variable loads of the characteristic values 1000kN (excluding weight of the foundation) and 750kN are respectively applied. Four CPT test results within 15m radius from the point, where the pad foundation is to be constructed, and digitized q_c and f_s values of 0.1m interval are given from the ground surface to 8m depth. The groundwater is at 6m depth from the ground surface and the unit weight of sand of 20kN/m^2 are also specified.

3.2 *EC7 Based Design*

The recommended characteristic values of the foundation ground presented in the ETC10 workshop by Sorensen et al. (2010), are shown in Table 1, which are based on the specifications of EC7. These values are adopted in the EC7 based design of this study. Design equations and partial factors, which are quoted from EN1997-1 Annex A, D and the 1st ETC10 report (Orr 2005), are presented in equation (1), (2) and Table 2, respectively.

$$V_d = \gamma_G \cdot \left(G_k + \gamma_c \cdot A \cdot d\right) + \gamma_Q \cdot Q_k \quad (1)$$

$$R_d = A' \cdot \left(q' \cdot N_q \cdot s_q + 0.5 \cdot \gamma' \cdot B' \cdot N_\gamma \cdot s_\gamma\right) / \gamma_R \quad (2)$$

$$N_q = e^{\pi \cdot (\tan\phi'/\gamma_M)} \cdot \tan^2\left[\pi/4 + \left\{\tan^{-1}\left(\tan\phi'/\gamma_M\right)\right\}/2\right], \quad N_\gamma = 2 \cdot \left(N_q - 1\right) \cdot \left(\tan\phi'/\gamma_M\right)$$

$$s_q = 1 + \sin\left\{\tan^{-1}\left(\tan\phi'/\gamma_M\right)\right\}, \quad s_\gamma = 0.7$$

where, A and A' are the total and effective area of the foundation (= B^2 in this case) respectively, γ_c is unit weight of RC, B' is effective width (B' = B in this case), s_q and s_γ are shape factors for N_q and N_γ, q' is effective overburden pressure at the level of the foundation base.

Table 1. Proposed characteristic design value (Sorensen et al. 2010)

Layer no.	Depth (m)	Mean depth (m)	$q_{c,m}$ (MPa)	$q_{c,k}$ (MPa)	E (MPa)	φ (degree)
1	[0.0; 0.5]	0.25	9.32	8.22	20.6	35.4
2	[0.5; 1.5]	1.00	11.60	10.52	26.3	36.8
3	[1.5; 2.5]	2.00	14.72	13.77	34.4	38.4
4	[2.5; 3.5]	3.00	15.32	14.67	36.7	38.7
5	[3.5; 4.5]	4.00	17.67	16.45	41.1	39.4
6	[4.5; 6.0]	5.25	19.60	18.33	15.8	40.1
7	[6.0; 8.0]	7.00	21.83	20.58	51.4	40.7

Table 2. Partial factors in EN1997-1 Annex A

Design Approach		γ_G	γ_Q	γ_M	γ_R
DA-1	Comb. 1	1.35	1.5	1.0	1.0
	Comb. 2	1.0	1.3	1.25	1.0
DA-2		1.35	1.5	1.0	1.4
DA-3		1.35	1.5	1.25	1.0

Table 3. Design results based on EC7 DAs.

	DA-1		DA-2	DA-3
	Comb. 1	Comb. 2		
B (m)	1.19	1.57	1.38	1.73
R_d (kN)	2510	2040	2540	2560
V_d (kN)	2510	2040	2530	2560

Table 3 shows the results of the EC7 based design by the different DAs. According to the results, the maximum difference between the results estimated by respective DAs was about 25%.

Furthermore, Figure 2 shows the design results based on NA of several European countries, which are reported by Bond (2010) at the time of the workshop. In this figure, vertical and horizontal axes present the design results of ULS and SLS respectively. Although the concrete contents of the respective NAs are not necessarily clear, the large differences of the results are observed. It is considered that the differences of the design results by different EC7 DAs and NAs based on the same ground information and design conditions indicate reliability difference.

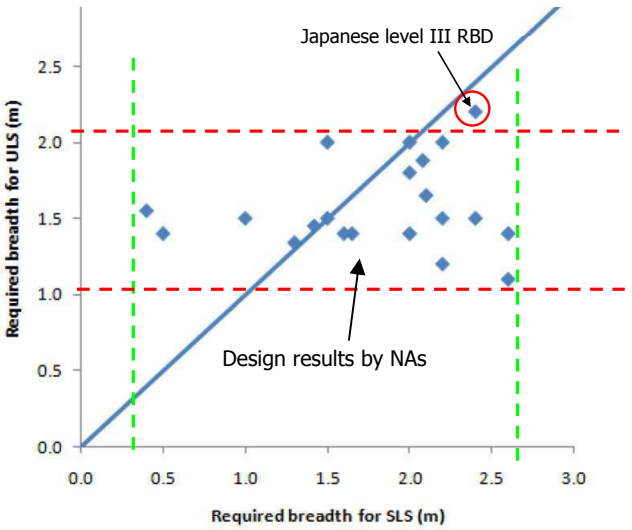

Figure 2. Variation of design results based on NAs

3.3 *A Level III RBD*

The reliability difference of the different design results based on different EC7 DAs and NAs is studied from a level III RBD (Honjo et al 2010). Only the relative reliability level, however, is considered in the study, because the uncertainties in the formulas to derive ϕ' from CPT q_c (EN1997-2 Annex D) and to estimate bearing capacity (EN1997-1 Annex E) are not clear. The different formulas, which uncertainties are analyzed, from EN1997 Annexes' ones are adopted in this design.

Although, designs for both ULS and SLS were carried out in this RBD, due to the limitation of the space, only ULS case is described in this paper.

3.3.1 *Procedure for Level III RBD*

Figure 3 shows the procedure for the level III RBD adopted in this study. This procedure consists of three parts, statistical analysis, geotechnical analysis and reliability analysis. In the statistical analysis, the uncertainties of the formulas to derive geotechnical parameters from subsurface exploration and the inherent vertical and horizontal spatial variations of the geotechnical parameters are quantified. In the geotechnical analysis, a response surface, as an approximate relationship between the structural response and the basic variables is estimated from a series of geotechnical calculations with respect to the vicinity of the limit state (*e.g.* g = R/S =1.0). In the reliability assessment, the reliability is estimated from Monte Carlo Simulation (MCS) based on the uncertainties (obtained from the statistical analysis) and the response surface (obtained from the geotechnical analysis).

Advantage of this procedure is the separation of the geotechnical analysis and the uncertainty analysis. MCS can be carried out without using geotechnical calculation method. Therefore, if the scheme is fitted to include sophisticated geotechnical analysis tools, such as FEM, to level III RBD.

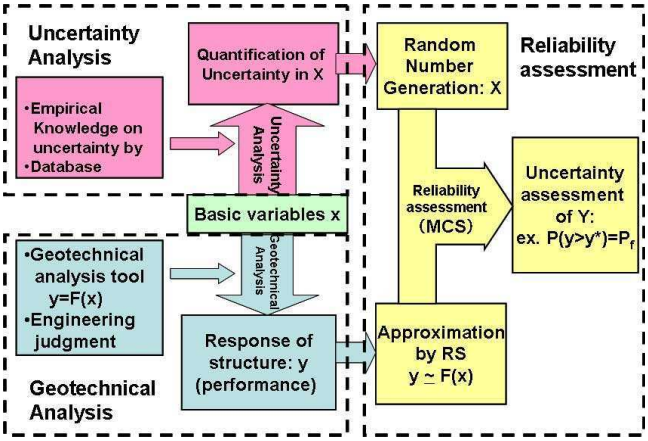

Figure 3. Procedure for a level III RBD

3.3.2 *Uncertainties*

(1) Inherent spatial variation of CPT q_c

The given q_c values (MPa) at 4 points from the example are plotted in Figure 4. A liner trend model with constant variance along the depth was fitted to this

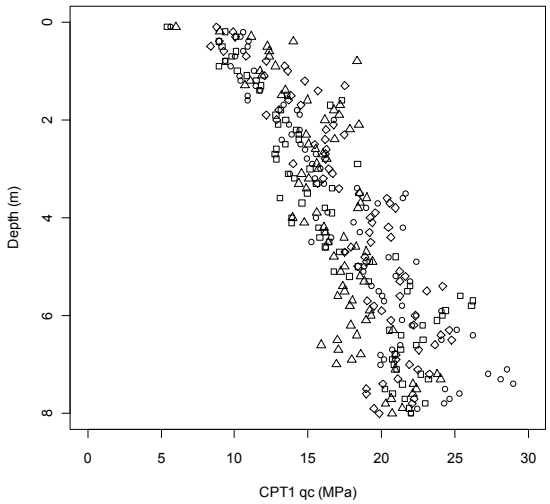

Figure 4. CPT q_c profiles

data whose results are presented in Table 4.

Table 4. Result of regression analysis on CPT q_c value.

Variable	Regression coefficient	t-statistics
(Intercept)	10.54	40.9
Depth z (m)	1.66	30.1

Residual standard error: 2.28, R^2=0.740, F-statistics: 906.9

Thus, the trend component of qc (MPa) is obtained for depth z (m):

$$q_c = 10.54 + 1.66 \cdot z \quad (3)$$

The coefficient of determination, R^2, is 0.74, which is fair, and t-values give significantly high values. The residual components of qc are plotted vs. depth in Figure 5. They are found to fit to the normal distribution well with mean value 0 and standard deviation (SD) 2.28 (MPa).

The autocorrelation function is estimated for the vertical direction for each CPT data by the standard moment estimation method, whose results are presented in Figure 6. There are small differences from a CPT to another, however, it is possible to say that autocorrelation distance may lie between 0.4 to0.5m if we fit an exponential type autocorrelation function. Thus we fix it to 0.4m. No correlation for the horizontal direction was found within the data given.

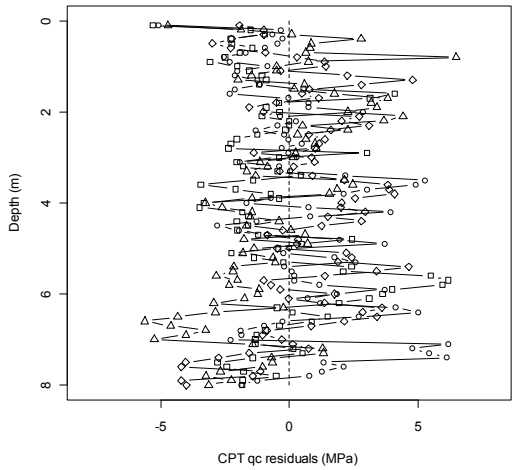

Figure 5. CPT q_c residuals from the trend.

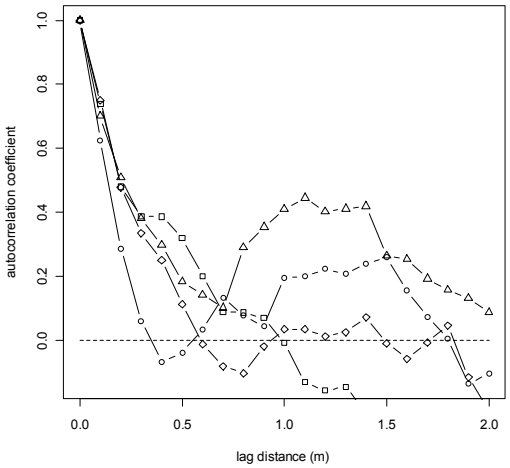

Figure 6. Vertical correlation of the residuals.

Based on these results, the characteristic value of CPT qc at the site is determined as follows;

Mean value: $q_c = 10.54 + 1.66 \cdot z$ (MPa) (4)

Standard deviation: $2.28 \cdot \Lambda_G = 2.28 \times 0.7 = 1.60$ (MPa) (5)

where, Λ_G is estimation variance function (Honjo et al. 2007), that is a function of number of samples (n), spatial averaging distance (L) and autocorrelation distance (θ), which gives the following result;

$$\Lambda_G(n, L, \theta) = \Lambda_G(10, 1.0, 0.4) = \sqrt{0.512} = 0.716 \approx 0.7 \quad (6)$$

(2) Transformation error: Friction angle from CPT

The internal friction angle of the sand layer is estimated from CPT qc values by the correlation, which is described in "Manual on Estimating Soil Properties for Foundation Design (Kulhawy et al. 1990)". In this correlation, the friction angle is related to the normalized cone tip resistance, which is give as equation (7);

$$\phi'_{tc} = 17.6 + 11.1 \cdot \log\left((q_c / q_a) / (\sigma'_{v0} / p_a)^{0.5} \right) \quad (7)$$

where, pa = atmospheric pressure , σ'_{vo} = effective overburden stress. SD of the correlation is estimated to be 2.8 degrees.

Eq. (7) is applied to the given data to convert q_c to ϕ'_{tc} whose results are presented in Figure 7. Due to the effect of the overburden effective stress, the transformed ϕ'_{tc} keeps constant along the depth to 8m ex-

cept the first 2m where σ'_{vo} is relatively small. It is hard to imagine that the geological origin of the first 2m sand is different from the below layer, thus it is judged that larger ϕ'_{tc} in the first 2m is result of smaller σ'_{vo} that makes the conversion inaccurate. For this reason, ϕ'_{tc} below 2m is statistically treated to obtain the characteristic value of ϕ'_{tc}. The mean and SD of ϕ'_{tc} are estimated to be 42.8degrees and 0.60degerees. since COV of ϕ'_{tc} is much less than 0.01, ϕ'_{tc} is assumed to be a deterministic variable in the further analysis.

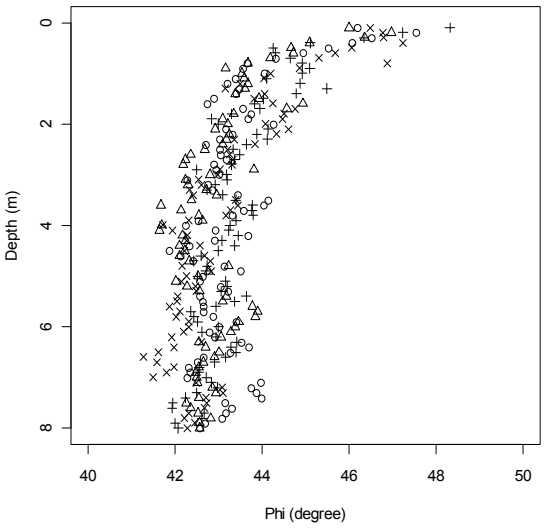

Figure 7. Distribution of converted φ'_{tc} vs. depth

(3) Model error: Evaluation of bearing capacity

The evaluation of bearing capacity, Eq. (8), which is employed in "Specifications of Highway Bridges (JRA 2002)", is adopted in evaluating the bearing capacity of the pad foundation in this design.

$$R_u = A_e\left\{\kappa \cdot q \cdot N_q \cdot S_q + \frac{1}{2}\cdot\gamma_1\cdot\beta\cdot B_e\cdot N_\gamma\cdot S_\gamma\right\} \qquad (8)$$

$$\kappa = 1+0.3\cdot\frac{D_f'}{B_e} = 1+0.3\cdot\frac{0.8}{B_e} = 1+\frac{0.24}{B_e},$$

$$q = \gamma_2\cdot D_f = 20\cdot 0.8 = 16\ (\mathrm{kN/m^2}),$$

$$N_q = \frac{1+\sin\phi}{1-\sin\phi}\cdot\exp(\pi\cdot\tan\phi),\ \ S_q = \left(\frac{q}{q_0}\right)^{\upsilon} = \left(\frac{16}{10}\right)^{-1/3} = 0.86,\ \ \gamma_1 = 20\ (\mathrm{kN/m^3}),\ \ \beta = 0.6$$

$$N_\gamma = \left(N_q - 1\right)\cdot\tan\left(1.4\cdot\phi\right),\ \ S_\gamma = \left(\frac{B_e}{B_0}\right)^{\mu} = \left(\frac{B_e}{1.0}\right)^{-1/3} = B_e^{-1/3}$$

where, A_e is the effective area of the foundation (= B^2 in this case), B_e is effective width (B_e = B in this case), κ and β are shape factors for N_q and N_γ, q is overburden pressure at the foundation bottom, D'_f is embedded depth, S_q and S_γ are scale factor for N_q and N_γ, B_0 and q_0 are reference width and load respectively. The bias of Eq. (8) has found as 0.894 with SD of 0.257 from the comparison with the calculated results and the plate loading tests (Kohno et al. 2009).

(4) Statistical properties for loads

The statistical properties assumed for the permanent and variable loads are taken from literatures widely accepted in EU (JCSS 2001 and Holicky et al. 2007) as presented in Table 5.

3.3.3 *Reliability analysis and results*

The performance function with employing the bearing capacity formula, Eq. (8), to be used in the reliability analysis is obtained as presented by Eq. (9).

$$M = R_u\cdot\left(B,\phi'_{tc}\right)\cdot\delta_{Ru} - G_k\cdot\delta_{Gk} - Q_k\cdot\delta_{Qk} \qquad (9)$$

where, M is safety margin, R_u is bearing capacity of the foundation, δ_{Ru} is uncertainty in bearing capacity evaluation, G_k is characteristic value of permanent load, Q_k is characteristic value of the variable load, δ_{Gk} is uncertainty in the permanent load, and δ_{Qk} is uncertainty in the variable load.

The properties of basic variables used in the reliability analysis are listed in Table 5.

Table 5. List of basic variables.

Basic variables	Nota-tion	Mean	SD	Distribution type
Spatial variability	ϕ'_{tc}	42.8 (degree)	0	Deterministic variable
Conversion error from q_c	ϕ'_{tc}	42.8 (degree)	2.8 (degree)	Normal
R_u estimation error	δ_{Ru}	0.894	0.257	Lognormal
Permanent action	δ_{Gk}	1.0	0.1	Normal(Note)
Variable action	δ_{Qk}	0.6	0.35x0.6 = 0.21	Gumbel distribution(Note)

(Note) Based on JCSS(2001) and Holicky, M, J. Markova and H. Gulvanessian (2007).

The result of the reliability analysis by Monte Carlo simulation (MCS) with 10,000 runs is presented in Figure 8. According to EN1990 annex B, the target reliability index, β, of 3.8 (i.e. 10^{-4} failure probability assuming a normal distribution for β) is required for an ultimate limit state considering 50 years design working life. Thus, the foundation width of more than 2.2 (m) is necessary.

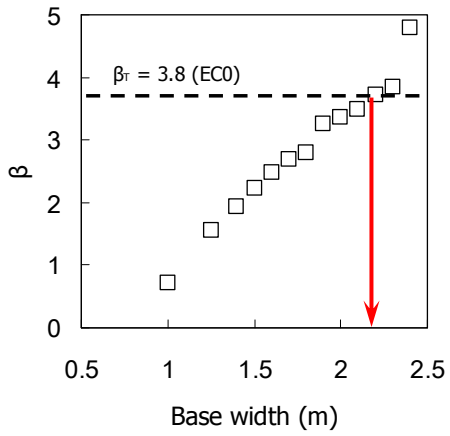

Figure 8. Design results of the RBD

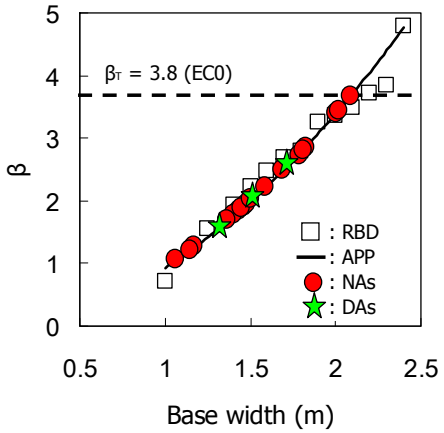

Figure 9. Reliability comparison (ULS)

3.4 *Reliability Difference on EC7 DAs and NAs*

In order to study the reliability differences on the different design results obtained from EC7 DAs and NAs, the results of base width are plotted on an approximate line based on the RBD results as shown in Figure 9. To make reflections on the reliability difference is the objective of this study. However, only relative reliability difference can be considered due to the particular formula to derive φ from CPT q_c and to evaluate the bearing capacity adopted in the RBD. According to the results, it is speculated that the different design results depending on different EC7 DAs and NAs have large relative reliability differences. The differences are as much as about 50% in the DAs' difference, and more than 3 times in the NAs' difference.

4 DISCUSSION

4.1 *Future Issues on EC7*

The authors would like to point out four issues that need to be resolved in EC7 development.

4.1.1 *Different Design Results depending on DAs*

The difference of the design results by the respective DAs under the same design condition, i.e. using the same characteristic values of geotechnical parameters and the same design formula, can be considered as the reliability difference on DAs. However, the ways of determining the characteristic values and design formula are different in various countries, it is not possible to compare the reliability level for each design result. That is to say the error in the transformation from soil investigation results and model error in the design formula are different for different design. If EC7 desires to specify the same reliability level to the different DAs, the RBD similar to the one done in the previous section should be carried out in each case to obtain the reliability level. Otherwise only ways to unify the reliability level would be either unification of DAs to one DA or adjustment of partial factors in the respective DAs so as to obtain the same design result.

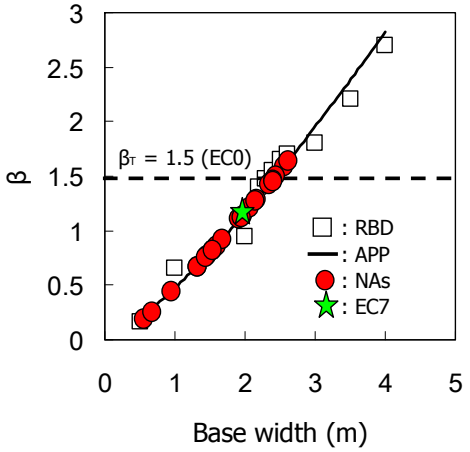

Figure 10. Reliability comparison (SLS)

4.1.2 *Model Error Consideration in Material factor*

According to Eurocode 0 – Basis of structural design –, material factor is to be constituted from uncertainties on both resistance model and material properties. However, it is not clear how EC7 is taking model uncertainty into the partial factors. It goes without saying that the experiences of engineers is important in determination of partial factors in geotechnical design. In spite of this fact, some sort of qualitative consideration concerning the model uncertainty would be necessary.

4.1.3 *Partial Factor depending on subsurface exploration*

Uncertainty of derived geotechnical parameters is different depending on the types of subsurface exploration, e.g. in-situ tests (SPT, CPT and so on) or laboratory tests.

Furthermore, design parameters are derived from the investigation results where transformation error would enter. Hence some quantification on uncertainty on the transformations from subsurface exploration to the geotechnical parameters would be unavoidable.

4.1.4 *Partial Factor for SLS Design*

Variation of the SLS design results obtained from respective NAs is large as shown in Figure 2. The SLS design results plotted on the line based on the SLS RBD are presented in Figure 10. According to the result, the relative reliability difference is extremely large, i.e. more than 10 times by the reliability index. It is speculated that the requirement for reliability level for SLS may be different for different countries. This background need to be disclosed and may be expressed in the form of a partial factor.

4.2 *An Example of Determination of Partial Factors*

Determination of Partial factors based on the target reliability is often employed in the recent development of design codes. The target reliability is determined from reliability level of the existing design practice in this paper, whose procedure is shown in Figure 11. Based on the reliability analysis on the structures designed by current practice, the target reliability level is determined. The partial factors are then determined by trial and error procedure until the structure with the target reliability level is designed. For example, if one set the target β (β_T) to 3.0 based on the fact that the reliability level of the pad footing designed by EC7 DA3 possesses reliability index (β) of about 3.0, the partial factors of the other DAs are calculated as presented in Table 6. Table 7 describes the design results with using determined partial factors. It should be noticed that there are many cases that the load factors are already given, and only the partial factors concerning resistance should be determined. This is also the case for this example, and only the partial factors on resistance are determined.

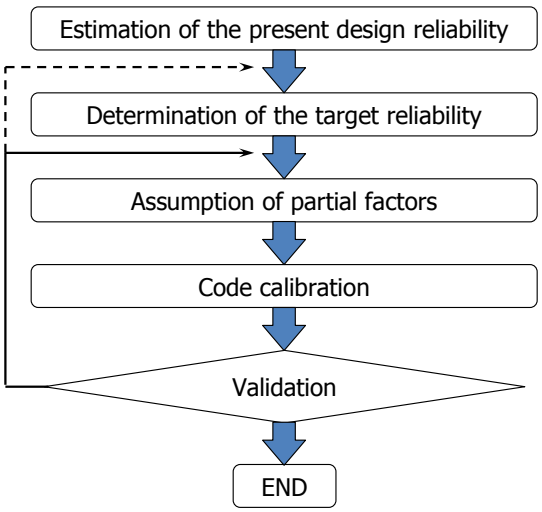

Figure 11. Determination of partial factors

Table 6. An Example of assumption of partial factors

Design Approach		γ_G	γ_Q	γ_M	γ_R
DA-1	Comb. 1	(1.35)	(1.5)	(1.0)	(1.0)
	Comb. 2	1.0	1.3	**1.35**	1.0
DA-2		1.35	1.5	1.0	**2.35**
DA-3		1.35	1.5	1.25	1.0

Table 7. Design results by the assumed partial factors.

	DA-1		DA-2	DA-3
	Comb. 1	Comb. 2		
B (m)	(1.19)	**1.76**	**1.72**	1.73
R_d (kN)	(2560)	2050	2560	2560
V_d (kN)	(2480)	2040	2550	2560

In code calibration, the applicability of the assumed partial factors to structures with different design conditions should be studied. Finally, it should be confirmed that the structures designed by the assumed partial factors preserves the reliability level similar to the target reliability, otherwise the procedure should be repeated until the appropriate partial factors are determined.

4.3 *Target Reliability, Partial Factors and Code Calibration for NAs*

There is a concern that because of the large variation of the results of the design as shown in Figure 2, the foundation design may considerably change in some countries once EC7 fixes a unified reliability level. The authors, however, consider there are some more issues to be investigated before we reach the conclu-

sion above. As discussed in the previous sections, the difference in resulting foundation size may not directly reflect the difference of the reliability level of the respective NAs.

We consider the first step of the flow chart in Figure 11, "Estimation of the present design reliability", is of vital importance. The transformation from soil investigation results to geotechnical parameters used in design may depend on the type of soil investigation method and soil types. The error involved in this transformation may be affected by many factors including local geological conditions. The inherent spatial variability of the ground may depend on the local geology. Each design formula has different model error. The expected skill for geotechnical engineers may be different for different countries in geotechnical design. After disclosing these factors, we can start to talk about the reliability level of each NA.

Even after these studies, one need to recognize the performance requirements for geotechnical structure may be different from one country to another, e.g. redundancy for the limit state depends on the structure, and/or room for allowable displacement may be different.

5 CONCLUSION

Under the condition that the developments of design codes based on reliability are actively taking place in various parts of the world, this study focused on the differences in the design results by EC7 DAs and NAs, which were reported in ETC10 workshop in Pavia. An example of level III RBD on the examples set by ETC10 are shown together with an example of determination of partial factors, and several important issues concerning the development of DAs and NAs of EC7 are discussed..

Certainly, RBD is not only correct method to evaluate of structural safety. The engineering judgments based on experiences are important to achieve the structural safety in geotechnical design practice. By saying so, it is considered that RBD can serve as an effective tool to solve the issues concerning the reliability level of the geotechnical structures.

REFERENCES

European Technical Committee 10 (ETC10), Design example 2 2010, http://www.eurocode7.com/etc10/index.html

Sorensen, C.S. & Cenor, J.B., Pad foundation with vertical central load on dense sand, 2nd Intl. Workshop on Evaluation of Eurocode 7., Pavia, Italy, http://www.eurocode7.com/etc10/index.html

Orr, T.L.L. 2005, Model solutions for example 1 – Pad foundation with a vertical central load, Proc. of the 1st Intl. Workshop on the Evaluation of Eurocode 7, Dublin Ireland, 77-80

Bond, A. 2010, Introduction to ETC10 design example 2, 2nd Intl. Workshop on Evaluation of Eurocode 7., Pavia, Italy, http://www.eurocode7.com/etc10/index.html

Honjo, Y., Hara, T., Otake, Y. & Kieu Le, T.C. 2010, Reliability based design of examples set by ETC10, Geothchnique, (submitted)

Honjo, Y. & Setiawan, B. 2007, General and local estimation of local average and their application in geotechnical parameter estimations, Georisk, 1(3), 167-176

Kulhawy, F.H. & Mayne, P.W. 1990, Manual on estimating soil properties for foundation design, Report EL-6800, Electric Power Research Inst., Palo Alto, 306 p.

Japan Road Association (JRA) 2002, Specification of highway bridges

Kohno, T., Nakaura, T., Shirato, M. & Nakatani, S. (2009). An evaluation of the reliability of vertically loaded shallow foundations and grouped-pile foundations, Proc. of The Second International Symposium on Geotechnical Risk and Safety (IS Gifu), Gifu, Japan, 177-184

Holicky, M., Markova, J. & Gulvanessian, H. (2007). Code calibration allowing for reliability differentiation and production quality. Applications of Statistics and Probability in Civil Engineering. Kanda, Takada & Furuat (eds)

ISGSR 2011 - Vogt, Schuppener, Straub & Bräu (eds) - © 2011 Bundesanstalt für Wasserbau ISBN 978-3-939230-01-4

Risk assessment through Romanian codes in geotechnical engineering

I. Manoliu
Technical University of Civil Engineering, Bucharest, Romania

R. Ciortan
University "Ovidius", Constantza, Romania

ABSTRACT: The paper presents matters related to risks in geotechnical works and structures in two Romanian technical regulations: Code NP 074-2007 regarding geotechnical documentations for constructions and Code NP 120-06 on the design and construction requirements for excavations in urban areas.

Keywords: code, risk, hazard, geotechnical category

1 INTRODUCTION

By its very mission, any code in the field of geotechnical engineering, be it for design or for execution, is aimed at reducing to acceptable levels risks associated with the construction of geotechnical works. In most situations, the notion of risk is not even mentioned as such.

There are, however, cases in which risks are explicitly present in the code. Two such cases, are found in the list of technical regulations currently in use in Romania. Matters related to risks in the two Codes will be presented in what follows.

2 THE CODE NP 074 REGARDING GEOTECHNICAL DOCUMENTATIONS FOR CONSTRUCTIONS

In 2007 started to be applied the Code NP 074 – 2007 regarding the geotechnical documentations for constructions [1]. This represented an improved version of GT 035 – 2002 "Guide for the elaboration and verification of geotechnical documentations for constructions", the first of this kind in Romania.

Both GT 035 - 2002 and NP 074 – 2007 stipulate that the nature and content of the geotechnical documentations are differentiated depending on the design stage and on the geotechnical category. Three geotechnical categories are introduced, as in the Eurocode 7 Part 1, in order to establish the geotechnical design requirements.

NP 074 – 2007 shows that the geotechnical category is associated with the geotechnical risk, which is low in the case of the geotechnical category 1, moderate in the case of the geotechnical category 2 and high in the case of the geotechnical category 3.

NP 074 - 2007 recommends a methodology for establishing the geotechnical category.

At first, four criteria are considered:

- ground conditions
- ground water conditions
- class of importance of the construction
- vicinities

For ground conditions, three groups are defined: good ground conditions, medium ground conditions and difficult ground conditions. As good ground conditions are considered, for instance, dense non-cohesive soils and fine soils having consistency index $I_c \geq 0.75$. As medium ground conditions are considered, for instance, medium dense non cohesive soils and fine soils having $0.5 < I_c \leq 0.75$. As difficult

soils are considered loose non-cohesive soils, fine soils of low consistency (Ic< 0.5), loesssial collapsible soils prone to large settlements when wetted, expansive clays a.o.

For the ground water conditions, three situations are considered:

a. excavation is above ground water level, no dewatering is required;
b. excavation descends below the ground water table, but routine dewatering works are anticipated, implying no damages to structures in the vicinity;
c. excavation descends below the ground water table under exceptional hydrogeological conditions, requiring exceptional dewatering works.

For the classification of constructions, the classification in four classes of importance, according to the governmental act 766/1997, is used:

- exceptional
- special
- normal
- low

The geotechnical category depends on the way in which excavations, dewatering and foundation works associated with the structure to be designed can affect structures and underground networks situated in the vicinity. From this stand point, the risk for the structures and underground networks can be considered:

a. non-existent or negligible
b. moderate
c. major

NP 074 – 2007 gives in the following table three examples of correlations between the four factors previously described:

Table 1.

Factors to be considered	Examples of corelation					
	Example 1	Points	Example 2	Points	Example 3	Points
Ground conditions	Good	2	Medium	3	Difficult	6
Ground water conditions	No dewatering	1	Normal dewatering	2	Exceptional dewatering	4
Class of importance of the construction	Low	2	Normal	3	Special exceptional	5
Vicinities	No risk	1	Moderate risk	3	Major risk	4
Geotechnical risk	Low	6	Moderate	11	High	19

The recommended methodology, in order to define the geotechnical category, implies the following steps:

- to each of the cases pertaining to the four factors specified in the table 1 is attributed a number of points, corresponding to the respective case;
- the sum of points corresponding to the four factors is made;
- to the points thus established are added points corresponding to the seismic zone in function of the design ground acceleration a_g defined in the Code P 100/1/2006, namely:
  - two points for zones having $a_g \geq 0.24$ g;
  - one point for zone having $a_g = (0.16 \ldots. 0.20)$g

The decision on the geotechnical category is made on the basis of the total number of points, according to the table 2.

Table2.

No	Geotechnical risk		Geotechnical category
	Type	Range of points	
1	Low	6 … 9	1
2	Moderate	10 … 14	2
3	High	15 … 21	3

3 THE CODE NP 120-06 ON THE DESIGN AND CONSTRUCTION REQUIREMENTS FOR EXCAVATIONS IN URBAN AREAS

NP 120-06 [2] was prepared by the authors following a number of incidents occurred during the execution of deep excavations in Bucharest, which revealed that the risks associated with such works were not properly assessed.

The list of potential users is large: investors, beneficiaries of the construction works, public authorities involved in the authorization process of constructions, designers, contractors, specialists undertaking inspection and quality control activities, specialists from insurance companies.

The scope of the Code is twofold:

- the use by the target public of the basic requirements concerning the design and construction of deep excavation;
- the definition of specific requirements for the monitoring of the new construction and of the neighbouring buildings during the execution and the exploitation.

A whole chapter in the Code is devoted to risk sources (hazards) associated with the construction of deep excavations in urban areas, which have to be considered in the design and execution of these type of works.

In what follows, risk sources mentioned in NP 120-06 are briefly presented:

1. risk sources generated by the position of the site in the urban plan
   Sites located in urban areas are distinguished by at least one of the following peculiarities:
   - the presence in the immediate vicinity of buildings and/or historical monuments;
   - existence on the site or in the immediate vicinity of underground networks (water, sewage, gas, electricity etc);
   - the proximity of public transport means;
   - various surcharges;
   - juridical aspects regarding the limits of the property and effects generated by the new construction beyond these limits.
2. risk sources generated by the geometrical characteristics of the deep excavations
   The shape and dimensions in plane, as well as the depth of the excavation, represent sources of risk.
3. risk sources generated by the ground conditions on the site
   A heterogeneous stratification, including layers with unfavorable mechanical properties, a groundwater level above the final level of the excavation or of a water layer under pressure below the final level of excavation, the lack of an impervious layer to allow the embedment of a trench wall or a sheet pile wall, are just some examples of sources of risk due to the geotechnical or hydrogeological peculiarities of the site.
   A second group of risks associated with ground conditions derives from the fact that ground investigation is based, inevitably, on a limited number of borings, open pits and field tests and on laboratory tests on a relatively small number of samples. Hence, the risk of not putting into evidence geological peculiarities with great relevance for the design and execution of the excavation or geotechnical parameters representatives for various layers.
4. risk sources occurring at the design of the deep excavation
   Even when ground conditions are well established and the design is entrusted to specialists using methods accepted in the current design practice, one should recognize that the accuracy of geotechnical computations is limited. This requires the use of a design strategy able to diminish or eliminate this source of risk, in first-place by adopting adequate safety factors.
5. risk sources occurring at the execution of the deep excavation
   Regardless the solution adopted, deep excavations should be considered as works with special character. Each component of such a work brings, through the technics and materials used, its own source of risk. To add those presented by a contractor without the experience of works in similar ground conditions or lacking adequate equipments.
6. risk sources generated by the seismic action
   Romania is a country of high seismicity. The Code NP 120-06 shows that the occurrence of an earthquake during the life of the work should be considered for both the work itself and for the buildings and installations in the vicinity. Check must be performed, to observe that stresses and deformations are within acceptable limits.

In other chapters of the Code, particularly those devoted to various solutions which can be selected for deep excavations, details of possible sources of risk are given.

For instance, in the case of diaphragm walls, a number of sources of risk are identified, such as:

- the use of a bentonite suspension with unfavorable characteristics resulting from preparation or produced by the seepage, which could lead to the collapse of the wall during excavation;
- a too high velocity in the circulation of the ground water, which could remove fine particles from the freshly poured concrete and affect the imperviousness of the wall;
- an insufficient difference between the level of the mud in the trench and the ground water level, with unfavorable consequences on the stability of the wall during excavations;
- lack of ensuring a non-interrupted development of execution phases (excavation of the panel, placing the reinforcement cage and joints formwork, concreting, removal of formworks) and lack of compliance with the minimum and maximum time intervals admitted between phases, with negative consequences on the capacity of the wall to retain water, both along the panels and at joints;
- the use of too long panels, reducing the number of joints but increasing the risk of a non-adequate concreting and the development in the concrete mass of mud inclusions, through which significant volumes of water can flow, particularly under high water pressures (when the high level of the groundwater is associated with a very deep excavation);
- a too high density of bars in the reinforcement cage (bars too close to each other), with unfavorable consequences on the quality and imperviousness of the concrete;
- the way in which are made the vertical joints between panels as well as horizontal joints between the wall and the slab;
- lack of the required verticality of the panel.

The Code enumerates also the sources of risk linked to the use of ground anchors with unfavorable consequences particularly in situations of superposition of factors such as the high level of the groundwater table, the influence of the variation of this level on layers of soils easily carried by the flow of water, the large depth of the excavation, the creep of clay soils, the great length of anchors, the presence in the immediate vicinity of buildings and utilities.

The responsibility of the Contractor to ensure a good sequence among the phases of the excavation works and a tight correlation between excavation works and construction works to follow, is underlined in the Code. Large time intervals between the correlation of the excavation and construction works such as placing the reinforcement bars and concreting the slab represent a major source risk both for the excavation itself and for the structures in the vicinity.

Reference is made in the Code to the Eurocode 7 Part 1 and to the series of European standards on the execution of special geotechnical works.

A distinct chapter is reserved in the Code to monitoring works, pertaining both to the excavation itself and to constructions in the vicinity. A monitoring project, as part of the project of the deep excavation is compulsory. The Code stipulates that the costs incurred by all monitoring works must be supported by the investor of the new structure the deep excavation is aimed for.

4 CONCLUSIONS

The two technical regulations in Romania to which reference was made in the paper are different in character. One is devoted to geotechnical documentations (NP 074-2007), developing the concept of geotechnical category of relevance for ground investigation and for method to be used in the design process. The second one (NP 120-06) refers to works which quite often cause much trouble: deep excavations in urban areas.

The two regulations have in common the objective of making aware the parties involved, including the owner/investor, of the risks inherent to geotechnical works and to help them to take appropriate measures.

Both technical regulations are under revision, based on the experience gained in the 5 – 6 years of use.

REFERENCES

"Normativ privind documentatiile geotehnice pentru constructii", Indicativ NP 074-2007, Monitorul Oficial al Romaniei, Partea I, Nr. 381/6.VI.2007. [1]

"Normativ privind cerintele de proiectare si executie a excavatiilor adanci in zone urbane", Indicativ NP 120-06, Monitorul Oficial al Romaniei, Partea I, Nr. 911/9.XI.2006.[2]

ISGSR 2011 - Vogt, Schuppener, Straub & Bräu (eds) - © 2011 Bundesanstalt für Wasserbau ISBN 978-3-939230-01-4

Geotechnical safety in relation to water pressures

B. Simpson
Arup Geotechnics, London, UK

N. Vogt
Technische Universität München, Zentrum Geotechnik, Munich, Germany

A. J. van Seters
Fugro GeoServices, The Netherlands

ABSTRACT: Provision of adequate safety in geotechnical designs dominated by water pressure has always been difficult and controversial. It is also of very great practical importance since a significant proportion of geotechnical failures is caused by the unforeseen effects of water pressure. To varying degrees, modern codes have attempted to guide rational judgments and also to provide precise formats in which safety can be prescribed. A recurrent difficulty lies in the fact that the density of water is known quite accurately, and many designers are therefore reluctant to apply factors that increase the design value of its density. Furthermore, changing the design density of water has complicated effects on the mechanics used in calculation, which may lead to unintended increases or decreases in safety.

The paper references case histories of failures caused by water pressure and reviews the safety provisions related to water pressure in some existing geotechnical codes. It discusses the provisions of Eurocode 7 and the way they are currently being interpreted and applied in individual countries. Seven examples that were discussed in the workshop on Eurocode 7 in Pavia, 2010, are considered in more detail in order to illustrate alternative approaches. The authors attempt to identify the common features of approaches to water pressure that provide a sound, rational basis for design in problems in which water pressures are a major concern.

Keywords: Geotechnical design; safety; water pressures

1 INTRODUCTION

The pressure of water in the ground and the forces exerted by free water are very important in geotechnical design. Because soil is a frictional material, its shear strength is greatly affected by pore water pressure, so increases in water pressure often reduce geotechnical resistance as well as increasing applied loads. Hence changes and uncertainties in water pressure may have large consequences that are not readily accommodated in a consistent manner by factors of safety.

Some codes of practice and design guides specify how the designer is to derive values for water pressures to be used in calculations, while others leave the question open. Advice may be qualitative, using terms such as “worst probable”, probabilistic, referring to return periods, or specified in terms of assumed margins such as tidal lags behind quay walls. Some of this guidance will be reviewed below, with particular reference to the text of Eurocode 7 (EC7). In a recent questionnaire on further development of EC7, respondents gave high priority to the need for further guidance on this topic.

Problems caused by groundwater pressures are frequently encountered in temporary states during construction. In the longer term, many cities are experiencing a rise in ground water levels, either at the water table due to leakage from supply pipes and sewers or at greater depth due to cessation of pumping from dewatered aquifers (eg Simpson et al 1987). Also water surrounding a building due to floods of adjacent rivers may cause unforeseen water pressures. The Dublin European Conference of ISSMGE in 1987 was concerned particularly with the importance of groundwater to geotechnical design. In a General Report, Stroud (1987) noted several situations in which unexpected groundwater problems have confronted engineers, in some cases leading to catastrophic failures. More recently, issues of safety in relation to water pressures have been discussed previously by Orr (2005), Simpson et al. (2009) and by Simpson (2011).

This paper is limited to considering conditions of hydrostatic water pressures or steady state seepage, in which water pressures are specified in calculations, independent of the loading and stress-strain behaviour of the ground. Situations involving the time-dependent response of the ground are not discussed.

Reference is made in this paper to "the designer". This is taken to mean the person or people responsible for taking decisions and carrying out calculations. It may represent one individual engineer, a company, or a combination of geotechnical and structural engineers, checkers and public authorities who have to be satisfied that the design is sound.

2 CASE HISTORIES OF FAILURES CAUSED BY WATER PRESSURE

2.1 *Basement excavation in Singapore*

An example from Singapore, discussed by Davies (1984), is shown in Figure 1. The site was in an area of decomposed granite away from adjacent buildings and no special problems were anticipated. The basement required an excavation 8m deep which was generally carried out in open cut except locally where an anchored sheet piled wall was used to support marine clays. Excavation in the clayey decomposed granite proceeded without problems up to a depth of about 6m and was more or less dry. However, when the excavation reached about 6.5m, the southern half of the base of the excavation suddenly 'heaved', accompanied by a rapid increase in groundwater flow. This resulted in the base of the excavation (which up to then had been quite firm) being reduced to a slurry. Construction traffic sank into the base of the excavation and it was only possible to walk across the site on planks.

Subsequent investigations showed that a highly permeable zone existed within the decomposed granite just above rock head and water had been trapped in this zone at more or less its pre-construction pressure. When the excavation reached a depth of 6.5m, the water pressure exceeded the weight of the overburden and the excavation based heaved, increasing the permeability of the clayey soils to create vertical flow and reduce the water pressures in the permeable zone. Fortunately, in this case the consequences of the problem were not serious. However, Davies noted that Ramaswamy (1979) reports a similar case in Singapore where damage to a raft occurred due to heave as a result of high uplift water pressures being trapped in permeable laminations within a stiff clay.

This case illustrates the need to consider carefully uplifting water pressures in the ground beneath excavations, and to make allowance in design for uncertainties in the balance between water pressure and weight of ground.

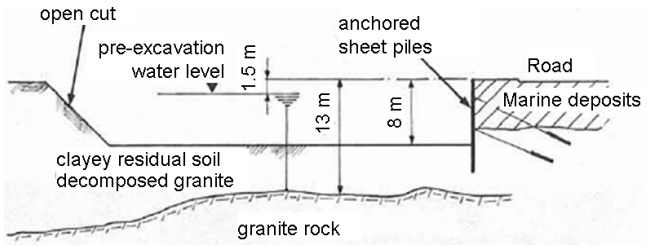

Figure 1. Section through an excavation in decomposed granite (after Davies 1984)

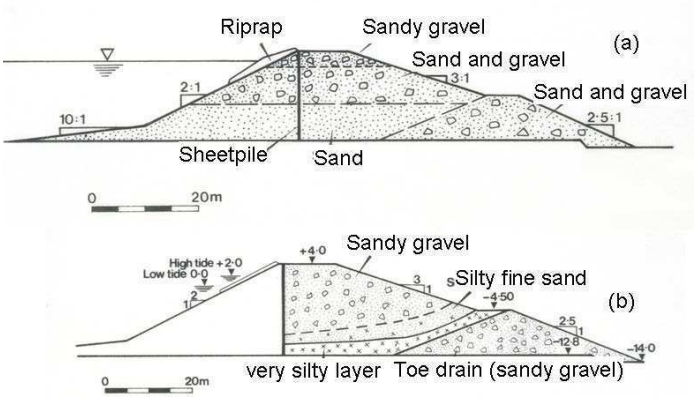

Figure 2. Cross section through cofferdam for Dubai Dry Dock: (a) as intended), (b) as built.

2.2 *Earth cofferdam in Dubai*

Figure 2a shows the intended cross section of a cofferdam used in the construction of the Dubai Dry Dock. The material used was the product of dredging sand and weak carbonate sandstone from the seabed. This was constructed by first forming the toe bund by dropping coarse material from bottom dump barges, then pumping hydraulic fill from cutter suction dredgers to form the rest of the bund. When the site was dewatered to allow construction of the dry dock, severe seepages were noted from the downstream slope, leading to erosion which it was feared could cause a catastrophic failure.

Small excavations were rapidly undertaken, which revealed that the as-built cross section was of the type shown in Figure 2b. Fine material deposited from the dredging had apparently proceeded ahead of

the main filling, forming a layer of low permeability over the more permeable toe bund. Trench drains were rapidly constructed, and fortunately they stabilised the situation.

This example illustrates how difficult it may be to predict water pressures in the ground in non-hydrostatic situations. It is important that designers consider a range of possibilities, dependent on the uncertain distribution of permeabilities.

2.3 *Water storage basin near Stuttgart*

Figure 3 shows a cross-section through a circular water basin. It was built by using pre-fabricated concrete elements connected to a cast in situ floor slab. During first filling the construction failed: several neighboured elements toppled over. The cause was seepage due to leaky gaskets leading to uplifting forces at the bottom side of the horizontal base of the L-shaped concrete elements.

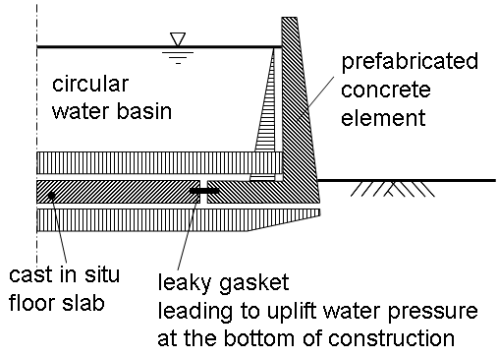

Figure 3. Water storage basin

3 EXISTING GEOTECHNICAL CODES AND GUIDANCE DOCUMENTS

3.1 *UK documents*

3.1.1 *General*

The UK documents noted here include British Standards and also guidance documents published by the Construction Industry Research and Information Organisation (CIRIA). The requirements of the UK National Annex to EC7 are considered later in the paper.

British codes specify the water pressures to be used in design calculations in a variety of ways. None of them require application of factors to water pressures.

3.1.2 *BS8002(1994) – Code of Practice for Earth Retaining Structures (now obsolete)*

In BS8002, partial factors (termed "mobilisation factors") are applied to soil strengths, and no load factors are applied. The use of structural action effects derived from this code is not fully clear, however, so some structural designers apply further factors to bending moments etc derived from BS8002. Following consultations among structural engineers, Beeby and Simpson (2001) proposed that no further factors on action effects are needed for design of embedded walls designed using the prescribed overdig allowances, but in other cases calculated bending moments etc should be multiplied by 1.2.

For water pressures, BS8002 requires that "The water pressure regime used in the design should be the most onerous that is considered to be reasonably possible."

3.1.3 *BS 6349 – Maritime structures*

BS6349-1 (2000) specifies (Clause 37) that "Maritime structures should be designed to withstand safely the effects of the extreme range of still water level from extreme low water ... to extreme high water ... expected during the design life of the structure. These extremes should be established in relation to the purpose of the structure and the accepted probability of occurrence ..., but should normally have a return period of not less than 50 years for permanent works." The same clause notes "Reduced safety factors are appropriate in relation to soil pressures, mooring and berthing forces, forces from other floating objects and wave forces, when considered in conjunction with extreme water levels."

The water levels to be assumed behind quay walls are given for specific circumstances (Clause 58). These may be related to tidal ranges, maximum changes of river levels in 24 hours, heights above flap drains, etc, as appropriate.

BS6349-3 (1988) requires a factor of safety not less than 1.2 against uplift (BS6349: Part 3: 1988, 2.5.21). Since it is not suggested that water pressures should be increased, this could be considered as a factor of 0.83 (=1/1.2) on favourable, stabilising weight.

3.1.4 *CIRIA Report C580 (2003) – Embedded retaining walls: guidance for economic design*

CIRIA Report C580 (Gaba et al 2003) uses a partial factor method similar to EC7 Design approach 1 Combination 2. It was written during the ENV period of EC7 and essentially supports its approach. For ULS calculations it requires that design calculations should use: "water pressure and seepage forces

which represent the most unfavourable values which could occur in extreme or accidental circumstances at each stage of the wall's construction sequence and throughout its design life. An example of an extreme or accidental event may be a burst water main in close proximity to the wall."

For SLS, CIRIA Report C580 requires that design calculations should use: "water pressures and seepage forces which represent the most unfavourable values which could occur in normal circumstances at each stage of the wall's construction sequence and throughout its design life. Extreme events such as a nearby burst water main may be excluded, unless the designer considers that such an event may reasonably occur in normal circumstances."

3.1.5 *PD6694-1(2011) – Recommendations for the design of structures subject to traffic loading to BS EN 1997-1:2004*

This BSI "Published Document" notes the alternative approaches available in EC7 (discussed below) and adds "because of the site-specific nature of uncertainty in water levels and the associated difficulties in calibration, no partial factor is given for ground-water pressure in the UK National Annex to BS EN 1990 for the design of bridges." Nevertheless, it notes: "if the hydrostatic effects are predominant and it is unrealistic to apply a significant safety margin to the water level (because, for example, the characteristic water level is close to the top of the retaining structure), it might be prudent to apply a model factor to the effect of hydrostatic pressure even when the level and density of water are known with a high degree of certainty. This model factor is required to take account of inaccurate assessment of the effects of loading, unforeseen stress distribution in the structure, construction tolerances and other secondary effects normally covered by the model factor incorporated in γ_F (see BS EN 1990:2002+A1, 6.3.2, and UK National Annex to BS EN 1990:2002+A1, Table NA.A2.4(B), Note 9, and Table NA.A2.4(C), Note 9)."

It is understood that this model factor is to be applied to structural bending moments, etc.

3.2 *German documents*

3.2.1 *DIN 1054 (2005) – Subsoil – Verification of the safety of earthworks and foundations*

This basic German standard requires that the highest and lowest water pressures that are expected during the design life of a structure have to be specified for every construction. These water pressures may be limited by the use of drainage systems or by allowing flooding of hollow constructions such as basements. Non-hydrostatic conditions and the effects of seepage have to be considered. Concerning safety factors it is possible to distinguish between persistent, transient and extremely improbable or accidental situations. As partial factors to be applied on pressures due to variable water tables those belonging to permanent actions and effects of actions may be used.

3.2.2 *DIN 4084 (draft 2002) – Subsoil – Calculation of embankment failure and overall stability of retaining structures*

In natural slopes the observational method is recommended to find water pressures. Therefore also back-analyses of critical observed situations are recommended. Water pressure in fissures in soils and rocks has to be considered.

3.2.3 *DIN 19700-10 (2004) – Dam Plants – General specifications*
DIN 19702 (1992) – Stability of Solid Structures in Water Engineering
DIN 19712 (2007) – River Dikes

According to these central standards to care for the protection against floods, economic, ecological, technical and aspects concerning urban developments should be considered when fixing the high-water-table for the design of dams, dikes and adjacent constructions in their design basis. Long term observations shall be analysed using statistical methods and in standard situations of urban areas a return period of 100 years shall be considered. In general multiple levels of water barriers and control systems are required. Different design situations are defined to consider also defects in one or even both of the prescribed two sealing elements. According to the probability of occurrence, different partial safety factors are defined.

3.3 *Dutch documents*

3.3.1 *NEN 6740/NEN 6702*

In the NEN–Standards for Geotechnics water pressures are mentioned. However, the value to be used for the ULS- and SLS-checks is not specified, apart from the general probability of failure.

3.3.2 *CUR 166 – Guidelines on Sheet pile walls*

In CUR 166, the water pressure values should preferably be determined by means of statistical analysis. Attention is given to correct distribution of the water pressures at both sides of the wall, which in case of permeable soils means that the water pressure at the tip of the wall is equal at both sides.

Based on probabilistic analyses, the water level at the active and passive sides for sheetpile design in ULS should respectively be increased by 0.05 m and lowered by 0.2 m.

3.4 *AASHTO LRFD Bridge Design Specifications (2008)*

The AASHTO code {10.6.3.1.1} requires that "bearing resistance shall be determined based on the highest anticipated position of groundwater level at the footing location", but it does not apply factors to water pressures for foundation or retaining wall design, despite factoring effective earth pressures. This appears to imply that in a situation where ground water pressure is dominant the design would rely almost entirely on the resistance factors in both the ground and the structure. This issue was discussed in relation to the AASHTO code by Simpson and Hocombe (2010).

4 REQUIREMENTS OF EC7

4.1 *Main text*

4.1.1 *Section 2 – Basis of geotechnical design*

In 2.4.2(9)P, EC7 says "Actions in which ground- and free-water forces predominate shall be identified for special consideration with regard to deformations, fissuring, variable permeability and erosion." An important note is added: "Unfavourable (or destabilising) and favourable (or stabilising) permanent actions may in some situations be considered as coming from a single source. If they are considered so, a single partial factor may be applied to the sum of these actions or to the sum of their effects." This note raises the important issue that the various water pressures involved in a design are often physically linked and so should not have different factors applied to them, giving physically unreasonable design values.

In Eurocodes, a "design value" is a value already incorporating safety elements, being derived in most cases by factoring characteristic or representative values of parameters. In 2.4.6.1(6)P, EC7 says "When dealing with ground-water pressures for limit states with severe consequences (generally ultimate limit states), design values shall represent the most unfavourable values that could occur during the design lifetime of the structure. For limit states with less severe consequences (generally serviceability limit states), design values shall be the most unfavourable values which could occur in normal circumstances." It is important to note that this paragraph refers directly to design values, not characteristic values, of water pressures, imposing requirements on their physical significance that may not be readily represented by processes of factoring. Despite this, paragraph 8 of the same sub-clause states "Design values of ground-water pressures may be derived either by applying partial factors to characteristic water pressures or by applying a safety margin to the characteristic water level ...". It is apparent, therefore, that various different approaches to derivation of design values of water pressure could be used with EC7.

In 2.4.7.3.2(2), EC7 says "In some design situations, the application of partial factors to actions coming from or through the soil (such as earth or water pressures) could lead to design values which are unreasonable or even physically impossible. In these situations, the factors may be applied directly to the effects of actions derived from representative values of the actions." This opens the possibility that allowance for the uncertainty in effects of water pressure could be made by factoring the effects, such as structural bending moments for example, rather than the water pressures themselves.

Some more detailed consideration of these requirements can be found in SC7 document N0471rev1 of June 2009.

4.1.2 *UPL and HYD*

Two particular situations can be identified in which water pressures are principally balanced by other loads (weight of structures or ground): uplift failure and hydraulic failure, termed UPL and HYD in EC7, as illustrated there in Figures 10.1a), 10.1e) and 10.2. EC7 provides factors of safety to be used in checking these limit states, but it is not clear about where in the calculation they should be applied. Orr (2005) noted a very large range of possible design results based on differing interpretations of the requirements for HYD.

4.1.3 *Design Approaches*

EC7 allows partial factors to be combined in three different ways, specified as "Design Approaches". In Europe, each nation can elect to use one (or more) of the Design Approaches for the design of projects to be constructed on its territory. Table 1 shows the factor combinations of the three design approaches, using the default values of partial factors specified in the common version of EC7. These values can also be varied nationally, and some of the values shown in Table 1 are not supported by the present authors. The weight or pressure of water is an action.

Table 1 Default values for the partial factors in EC7. Note: the values can be varied nationally, and the values shown are not necessarily supported by the present authors.

			DA1			**DA2**	**DA3**
			Comb 1	Comb 2	Piles		
Actions	Permanent	unfav	1,35			1,35	1,35
		fav					
	Variable	unfav	1,5	1,3	1,3	1,5	1,5/1,3*
Soil	tan ϕ'			1,25			1,25
	Effective cohesion			1,25			1,25
	Undrained strength			1,4			1,4
	Unconfined strength			1,4			1,4
	Weight density						
Spread	Bearing					1,4	
footings	Sliding					1,1	
Driven	Base				1,3	1,1	
piles	Shaft (compression)				1,3	1,1	
	Total/combined (compression)				1,3	1,1	
	Shaft in tension		1,25		1,6	1,15	1,1

Note: Values of all other factors are 1.0. Further resistance factors are provided for other types of piles, anchors etc.
* 1.5 for structural loads; 1.3 for loads derived from the ground.

Design Approach 1 requires two separate calculations using two "combinations" of factors. The design has to accommodate both combinations. The action factors in Combination 1 of DA1 are generally applied to the actions themselves, but in some cases EC7 2.4.7.3.2(2) is followed, applying the factors to action effects. In this paper, this latter approach will be referred to as DA1*. Combination 2 of DA1 is unaffected by this.

Design Approach 2 (DA2) includes factors to be applied to actions. Originally these were to be applied to actions themselves, meaning the basic pre-defined loads acting on a structure, at the start of the equilibrium calculations and this form of DA2 is furthermore used by some countries. However, some developments, particularly in Germany, have specified that equilibrium and compatibility calculations are carried out in terms of unfactored characteristic values, applying the factors to derived action effects (such as bending moments, bearing pressures or active earth forces). This approach, called DA2*, is considered to follow EC7 2.4.7.3.2(2).

In Design Approach 3, factors are generally applied to actions, not to action effects. The calculations are performed using design values for loads and material strengths rather than characteristic values.

4.2 *National annexes*

4.2.1 *Survey of partial factors*

Partial factor values adopted for water pressures by European countries are listed in document N0467rev1 of June 2008. This information is also available on the GeoSNet website at http://www.geoengineer.org/forum/viewtopic.php?p=11619#11619. These documents concentrate particularly on the distinction between permanent and variable water pressures, and the notes included place important qualifications on the table of factors.

4.2.2 *UK National Annex*

The UK National Annex for EC7 requires the use of DA1. It notes that the normal load factors of STR and GEO "might not be appropriate for self-weight of water, ground-water pressure and other actions de-

pendent on the level of water, see 2.4.7.3.2(2). The design value of such actions may be directly assessed in accordance with 2.4.6.1(2)P and 2.4.6.1(6)P ... Alternatively, a safety margin may be applied to the characteristic water level, see 2.4.6.1(8)". This reference to 2.4.7.3.2(2) indicates that the variant DA1* of DA1 may be applicable in the case of water pressures (see 4.1.3).

Thus, by allowing three alternative approaches, the UK National Annex leaves much of the responsibility for derivation of design water pressures with the designer. For particular situations, for example along the sides of rivers, local public authorities normally specify the design water levels to be used for flood barriers and other river-side constructions.

Similar wording is repeated for the uplift case, UPL. The default values for partial factors $\gamma_{G;dst}$=1.1, $\gamma_{G;stb}$=0.9 and $\gamma_{Q;dst}$=1.5 are retained, with an added note: "The partial factor specified for permanent unfavourable actions does not account for uncertainty in the level of ground water or free water. In cases where the verification of the UPL limit state is sensitive to the level of ground water or free water, the design value of uplift due to water pressure may be directly assessed in accordance with **2.4.6.1**(2)P and **2.4.6.1**(6)P of BS EN 1997-1:2004. Alternatively, a safety margin may be applied to the characteristic water level, see **2.4.6.1**(8) of BS EN 1997-1:2004."

For HYD, the default partial factors $\gamma_{G;dst}$=1.35, $\gamma_{G;stb}$=0.9 and $\gamma_{Q;dst}$=1.5 are retained, with an added note: "In applying the specified partial factors in Equation (2.9a) of BS EN 1997-1:2004, the hydrostatic component of the destabilizing total pore water pressure ($u_{dst;d}$) and the stabilizing total vertical stress ($\sigma_{stb;d}$) can be considered to arise from a single source …" This implies that the same factor is applied to both stabilising and destabilising water pressures.

4.2.3 *German National Annex*

The German National Annex for EC7 requires the use of DA2* (see 4.1.3). It refers to a new DIN 1054 which was published in 2010 and which mostly conserves the regulations of the former DIN 1054:2005 in connection with EC7. The national values for the partial factors differ according to three different design situations: persistent, transient and accidental. As for uplift verifications the dead loads of constructions and the water pressure are well known and so it is sufficiently conservative to use the partial factors $\gamma_{G,stb}$ and $\gamma_{G,dst}$ close to 1 (0.95 to 1.05). In cases when German standards are officially introduced by German building authorities they need to be very precise and should not leave large room for adjustment by owners, designers and constructors.

4.2.4 *Dutch National Annex and supplementary National Code NEN 9997-1*

The Dutch National Annex, adopting Design Approach 3, combines most of the Dutch regulations of NEN 6740:2006 with EC7. For ULS and SLS verifications, the characteristic low or high values (whichever is unfavourable) for the design life of the structure based on statistical analysis must be taken.

In most cases, however, a statistical approach is not feasible because of the poor quality and limited number of the data. In practice a geo-hydrologist examines the piezometer readings over a 5 to 10 year period from neighbouring locations together with readings at the site for some months (at most). Often the maximum or minimum measured value is then taken as a characteristic high or low value, sometimes the maximum characteristic value is taken at ground level. In the Dutch code there is no guideline/rule for determination of the characteristic value of the groundwater table. Normally the water table is taken as a constant corresponding with the highest/lowest value. Fluctuations of water levels are therefore not considered as a transient load.

For water pressures in STR/GEO-limit state a load factor of 1.2 is taken where a higher water level is physically not possible. In other, seldom used cases, a load factor of 1.35 is applied. Alternatively, in case of retaining structures the characteristic water table at the low, excavated side must be lowered by an offset of 0.25 m to derive at a design value.

For Uplift (UPL) and Hydraulic actions (HYD), partial factors for $\gamma_{G,stb}$ and $\gamma_{G,dst}$ of respectively 0.9 and 1.0 are prescribed. This means that the factors on water pressure are 1.0 in these cases. The Dutch standard must be followed by designers and constructors, but alternative methods are possible as long as the required safety level is proven!

5 SOME FUNDAMENTAL CONSIDERATIONS

5.1 *Primary and secondary actions*

Even in cases where the magnitudes of the primary actions are fixed with no possibility of unfavourable variations, designs should be sufficiently robust to accommodate unknown and unpredictable secondary actions. In the cases considered in this paper, the primary unfavourable actions are derived from water pressure, which in some cases may have very clear limits. Secondary actions could include, for example, sedimentation around a structure in water, excavation of the ground above a structure relying on the weight of ground, minor vehicle or ship impacts, considered too small to include in calculations, or vandalism of various kinds.

If these "secondary" actions are large, failure could occur but the fault may be seen to rest with the owners or maintainers of the structure, or the vandals; alternatively, the designer should have foreseen them and was wrong to omit them from the primary actions for which the structure was designed.

However, if the secondary actions are small, the owner would reasonably expect the structure to be sufficiently robust to withstand them. In this context, "large" and "small" effects have to be judged in relation to the magnitude of the primary actions. It follows that even where there is no real possibility of unfavourable variation of the primary actions, it may be necessary to include some variation of them in design in order to accommodate the possible secondary actions that are not otherwise included. The variations could be applied either to the actions themselves, in deriving design values, or to the action effects.

5.2 *Compatibility with structural codes*

It is very desirable that geotechnical and structural codes of practice can be used together in a compatible way. This is a basic principle of the Eurocodes and other sets of codes. Many structural codes include partial factors on actions that take the magnitudes of the actions to unrealistic levels. In part, this may be a way of accommodating secondary actions, and it creates no difficulties in most aspects of structural design.

In geotechnical design, two related features are very important: (a) water pressure may be a dominant action, determined by the density of water which is accurately known, and (b) because soil is a frictional material, its shear strength is greatly affected by water pressure. Unrealistic factoring of water pressure therefore raises concerns.

These issues underlie the discussions in this paper.

5.3 *Water retaining structures*

Some of the examples considered in this paper involve water retaining structures. The release of a large body of fluid may create an unusually dangerous situation, so structures retaining free water might have to be considered as high risk, requiring better standards of design checking, construction and maintenance. Higher factors of safety might also be considered, though they could give false confidence. This issue is not the subject of discussion in this paper.

6 EXAMPLES

6.1 *General*

SC7 document N0471rev1 provided six examples which had been developed to illustrate particular issues in relation to water pressures. Under the auspices of ISSMGE ETC10, a Workshop on EC7 was held in Pavia, Italy, in April 2010, three of these were briefly discussed among other design examples (Simpson 2011). Some of these design situations will be discussed in more detail in this section.

6.2 *Example 1 – Submerged anchor block*

Figure 4a shows an anchor block, for which the total weight W is a permanent stabilising (favourable) force and the anchor force F is a variable destabilising (unfavourable) force. The characteristic total density of the block is γ_c and that of the water γ_w. The water forces are taken to be permanent.

The strength of the ground or structure are not at issue, so the only ultimate limit state to be considered for the anchor block is uplift, UPL. For this, EC7 provides two factors for permanent actions, abbreviated

here as $\gamma_{G;dst}$ (generally > 1) for the destabilising force and $\gamma_{G;stb}$ (generally < 1) for the stabilising force; the factor for the variable destabilising force is $\gamma_{Q;dst}$ (> 1).

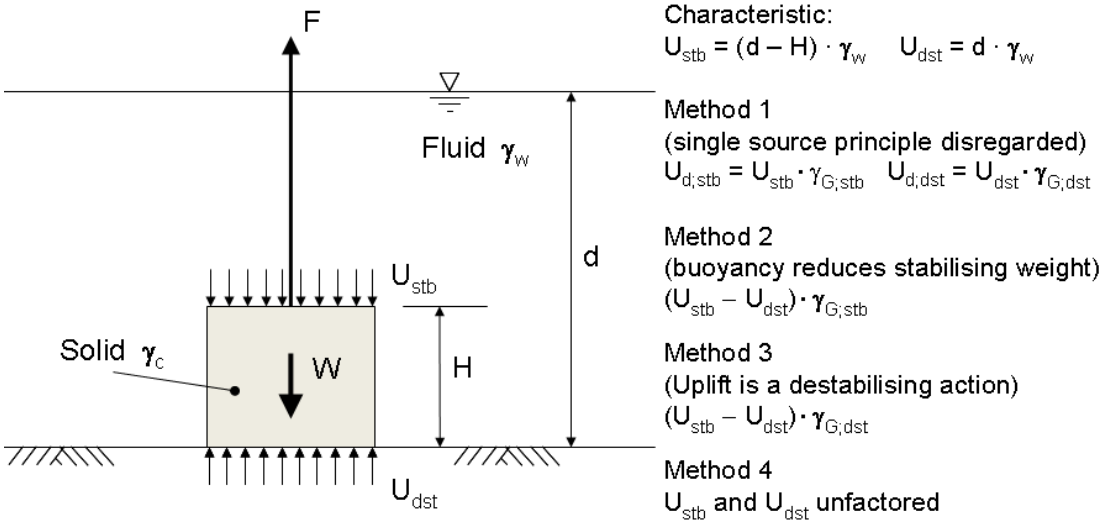

Figure 4. Submerged anchor block

It is clear that the characteristic weight of the block, W_k, will be multiplied by $\gamma_{G;stb}$ to derive the design value for UPL, and the characteristic anchor force, F_k, will be multiplied by $\gamma_{Q;dst}$. Four possible methods of applying partial factors to the water pressures could be considered.

In Method 1, the destabilising water pressure beneath the block is multiplied by $\gamma_{G;dst}$, and the stabilising water force above the block by $\gamma_{G;stb}$. Thus the limit state requirement is:

$$W_k \cdot\gamma_{G;stb} + U_{stb} \cdot\gamma_{G;stb} \geq U_{dst} \cdot\gamma_{G;dst} + F_k \cdot\gamma_{Q;dst} \quad (1)$$

In Method 2, the buoyant weight of the block is taken to be the stabilising force. The limit state requirement is:

$$(W_k - \Delta U) \cdot\gamma_{G;stb} = W_k \cdot\gamma_{G;stb} + (U_{stb} - U_{dst}) \cdot\gamma_{G;stb} \geq F_k \cdot\gamma_{Q;dst} \quad (2)$$

where $\Delta U = U_{dst} - U_{stb}$

In Method 3, the two water forces are recognised as coming from a "single source" which is considered to be destabilising. The limit state requirement is:

$$W \cdot\gamma_{G;stb} - \Delta U \cdot\gamma_{G;dst} = W_k \cdot\gamma_{G;stb} + (U_{stb} - U_{dst}) \cdot\gamma_{G;dst} \geq F_k \cdot\gamma_{Q;dst} \quad (3)$$

In Method 4, water pressures are not factored. The limit state requirement is:

$$W \cdot\gamma_{G;stb} - \Delta U = W_k \cdot\gamma_{G;stb} + (U_{stb} - U_{dst}) \geq F_k \cdot\gamma_{Q;dst} \quad (4)$$

Thus the factors applied to the water forces may be summarised as shown in Table 2, with the resulting equations. The design water pressures are shown in Figure 4b; the pressures for Method 1 coincide with those of Method 2 above the block and with those of Method 3 below the block. In Figure 5, the allowable characteristic anchor force, F_k, is plotted against the "Density ratio" γ_c/γ_w; F_k is normalised by dividing by W_k. For the purpose of this figure, the values of partial factors have been taken from the UK National Annex: $\gamma_{G;dst} = 1.1$, $\gamma_{G;stb} = 0.9$, $\gamma_{Q;dst} = 1.5$.

Table 2 Summary of factors applied to water forces in Example 1.

Method	Description	Factor applied to water forces		Maximum allowable value for F_k/W_k
		U_{dst}	U_{stb}	
1	Treat destabilising and stabilising water forces separately	dst	stb	$(W_k \cdot\gamma_{G;stb} + U_{stb} \cdot\gamma_{G;stb} - U_{dst} \cdot\gamma_{G;dst}) / W_k \cdot\gamma_{Q;dst}$ $= \gamma_{G;stb}/\gamma_{Q;dst} + (\gamma_w/\gamma_c)(d/H-1) \cdot\gamma_{G;stb}/\gamma_{Q;dst} -$ $(\gamma_w/\gamma_c)(d/H) \cdot\gamma_{G;dst}/\gamma_{Q;dst}$
2	Consider buoyant weight of block as the stabilising force	stb	stb	$(W_k \cdot\gamma_{G;stb} + (U_{stb} - U_{dst}) \cdot\gamma_{G;stb}) / W_k \cdot\gamma_{Q;dst}$ $= \gamma_{G;stb}/\gamma_{Q;dst} - (\gamma_w/\gamma_c)(\gamma_{G;stb}/\gamma_{Q;dst})$
3	Consider both water forces as coming from a single source, which is destabilising	dst	dst	$(W_k \cdot\gamma_{G;stb} + (U_{stb} - U_{dst}) \cdot\gamma_{G;dst}) / W_k \cdot\gamma_{Q;dst}$ $= \gamma_{G;stb}/\gamma_{Q;dst} - (\gamma_w/\gamma_c) \cdot(\gamma_{G;dst}/\gamma_{Q;dst})$
4	Unit factors on water	1	1	$(W_k \cdot\gamma_{G;stb} + (U_{stb} - U_{dst})) / W_k \cdot\gamma_{Q;dst}$ $= \gamma_{G;stb}/\gamma_{Q;dst} - (\gamma_w/\gamma_c) \cdot(1/\gamma_{Q;dst})$

Figure 5a shows that for Method 1 the allowable anchor force depends on the water depth (normalised by dividing by the height of the block). This occurs because different factors are applied to the destabilising and stabilising water forces. This is considered to be physically unreasonable, except, perhaps, in very rare circumstances for which the pressures above and below the block are independent because they are not from a "single source". As the water becomes deeper, the allowable anchor force reduces for the same block, and for d/H=5 no force can be taken unless the density of the block is more than twice that of water.

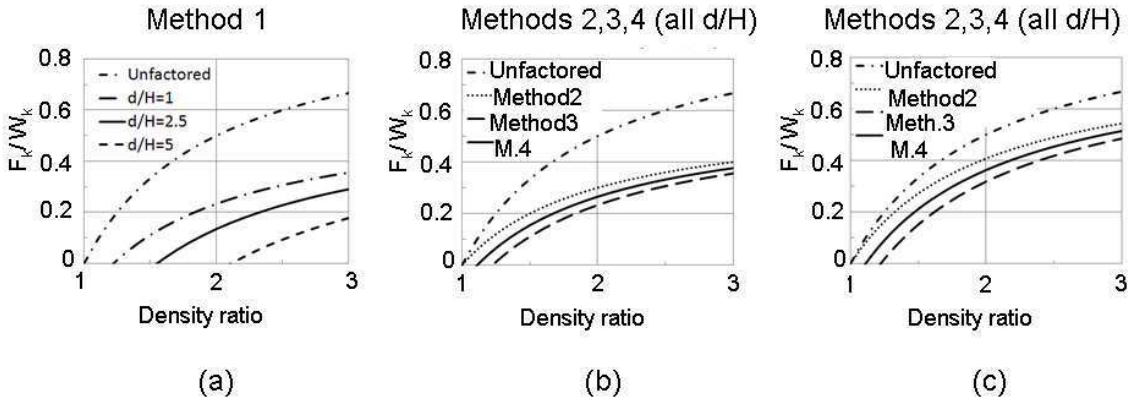

Figure 5. Submerged anchor block – allowable anchor force in relation to density of block.
(a) Method 1, (b) Methods 2 to 4, (c) Methods 2 to 4 assuming the anchor force is permanent.

The results for Methods 2 to 4, shown in Figure 5b, are independent of the water depth. For Method 2, the allowable F_k tends towards the unfactored value for low density ratios. Figure 5c is similar, except that it is assumed that the anchor force is permanent, rather than variable (ie $\gamma_{G;dst}$ has been applied to F in place of $\gamma_{Q;dst}$). In this case, Method 2 provides very little safety for low density ratios. A further important objection to Method 2 is that it applies a reduction factor ($\gamma_{G;stb}<1$) to the buoyancy effect of the water, which is clearly a destabilising effect.

Methods 3 and 4 both follow the single source principle, and so avoid the need to distinguish between stabilising and destabilising actions of water pressures. Method 3 provides apparently reasonable results, though in effect the density of water is factored, which could lead to difficulties in more complex situations where the strength of soil is affected by water pressures. This difficulty might be avoided if all actions of connected water are combined to find a resultant destabilizing uplift force, which is then factored by $\gamma_{G,dst}$. This method clearly shows where safety on water pressures is applied, by considering the block weight and water uplift separately.

Method 4, with no factors on the water forces, also provides reasonable results, indicating that for this problem it may not be necessary to apply factors to water pressure, either directly or indirectly. The resultant of water actions, which is destabilising, is not increased, so the overall factor of safety is lower than obtained with Method 3.

If the factors on water pressure are set to 1.0, all four methods become the same, in regards to their treatment of water.

6.3 *Example 2 – group of submerged tanks*

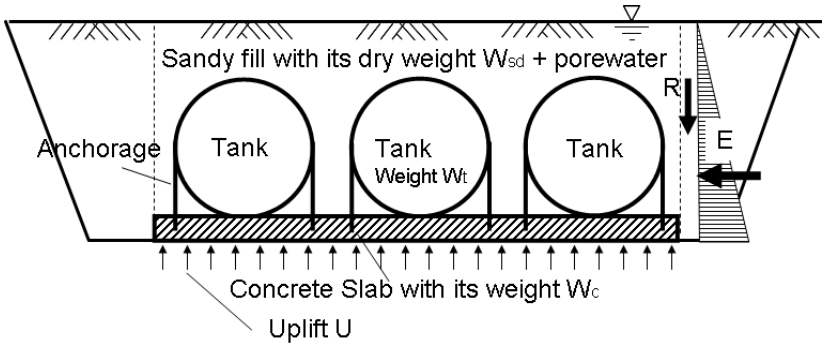

Figure 6. Group of submerged tanks on a concrete slab

The example in Figure 6 includes a sand fill with its pore volume filled with water. Again there are different methods to fulfil the ultimate limit state requirement. In the following considerations the influence of friction forces at the sides of the fill is omitted.

Prioritizing the single source principle, a resultant uplifting force, which is the difference between all water pressures acting upwards and downwards, has to be used as destabilizing force. This is mathematically the same as using the unit weight of water multiplied with the volume of the slab and of the tanks and of the grains of the soil as the destabilizing force. Physically and philosophically there might be a difference as the second way uses the weight of water that is absent, because of the presence of other solids, as a destabilizing force. The second way addresses the Archimedean effect of water rather than its direct actions, but it will be used in the following to work out the difference to the other applied methods. EC 7 allows for looking at the effects as well as for looking at the actions themselves.

Stabilizing forces are the weight of the concrete slab Wc + the weight of the tanks Wt + the weight of the dry sand Wsd. There is a danger of mistake with the effects of the sand fill: the volume of the fill must be multiplied with γ_d (dry density) to find the stabilizing weight and with $(1 - n) \cdot \gamma_w$ (n = porosity, γ_w = unit weight of water) to find the-uplift acting on the grains. The limit state requirement is:

$$\gamma_w \cdot \text{Volume(slab + tanks + soilgrains)} \cdot \gamma_{dst} \leq \text{Weight (slab + tanks + soilgrains)} \cdot \gamma_{stb} \quad (5)$$

The formulation shows that an increase of the density of the soil which increases the number of grains in the volume leads to increasing both destabilizing and stabilising forces and effects. The necessary weight of the slab may be expressed as

$$\text{Weight(slab)} \geq \gamma_w \cdot \text{Volume(slab + tanks + soilgrains)} \cdot \gamma_{dst}/\gamma_{stb} - \text{Weight (tanks)} - \text{Weight (soilgrains)}$$

With a second method it can also be looked at a horizontal cross section at the base of the concrete slab. Destabilising is the integral of uplifting water pressure U at this depth, stabilising are Wc, Wt, Wsd and the weight of the water in the pore-spaces of the sand Ww:

$$U \cdot \gamma_{dst} \leq (Wc + Wt + Wsd + Ww) \cdot \gamma_{stb} \quad \text{this is identical to}$$

$$\gamma_w \cdot \text{Total Volume} \cdot \gamma_{dst} \leq \text{Weight(slab + tanks + soilgrains + Water in pore-space)} \cdot \gamma_{stb} \quad (6)$$

The necessary weight of the slab comes from the requirement

$$\text{Weight(slab)} \geq \gamma_w \cdot \text{Volume(slab + tanks + soilgrains + pore-space)} \cdot \gamma_{dst}/\gamma_{stb} - \text{- Weight(tanks) - weight(soilgrains) - Weight(Water in pore-space)}$$

With this consideration the action of the water beneath and above the slab is factored with different partial factors, thus the single source principle is violated. This could be hidden by using the saturated unit weight of the sand instead of Wsd + Ww which mathematically would be the same. However there might be good reasons to apply a partial factor to the saturated weight including the weight of water in order to account for other secondary effects and to be very cautious about the stabilizing weight.

The difference between both requirements is to be found in the handling of the water in the pore-spaces of the sand. In (5) it is omitted on both sides of the requirement. In (6) its weight $\cdot \gamma_{dst}$ enlarges the left side and its weight $\cdot \gamma_{stb}$ enlarges the right side. Applying (6) leads to a concrete slab with higher weight than by applying (5). The difference in the weight of the slab is Volume (pore-spaces) $\cdot \gamma_w \cdot (\gamma_{dst}/\gamma_{stb} - 1)$.

In a 3rd method the actions of water can be taken as design actions without applying partial factors:

$$\gamma_w \cdot \text{Volume(slab + tanks + soilgrains)} \leq \text{Weight (slab + tanks + soilgrains)} \cdot \gamma_{stb} \quad (7)$$

or identically

$U \leq Ww + (Wc + Wt + Wsd) \cdot \gamma_{stb}$. This leads to a necessary weight of the slab of

$$\text{Weight(slab)} \geq (U_{\text{at the bottom of the slab}} - \text{Weight(Water in pore-space)})/\gamma_{stb} - \text{Weight(tanks) - weight(soilgrains)}$$

which leads to the most economical design and to the lowest total safety. By choosing this method and maintaining former total safety it is necessary to decrease the partial factor for stabilizing forces.

6.4 *Example 3 – Gravity construction on clay retaining free water*

The construction in Figure 7 has to be checked for its bearing capacity on the subsoil and not to fail by sliding or toppling. It is doubtful whether it could, in reality, topple without first having a bearing failure either in the ground or in the structure, which ever failed first.

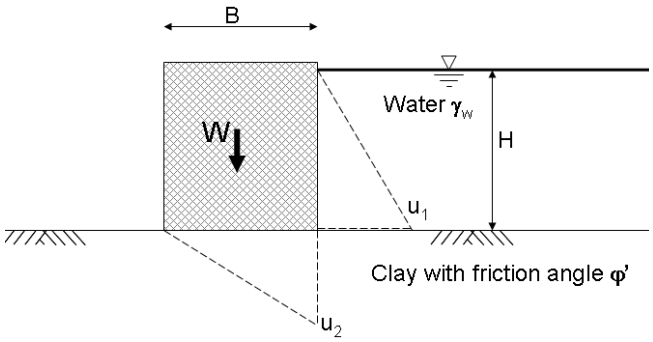

Figure 7. Gravity construction retaining free water

A further requirement often imposed is that the resultant force through the base should not approach too close to the edge. For example, a "middle third" rule might be imposed. Eurocode 7 has a "middle two-thirds" rule, but allows the resultant force to approach even closer to the edge of the base if the design has been reviewed with exceptional care. In practice, it might be unwise to allow the resultant force to lie outside the middle two-thirds. For this type of problem, the relevant resultant force will generally be the design effective force (i.e. excluding water pressure) between the structure and the ground. A further practical consideration is that it might be necessary to maintain total pressure greater than water pressure u_2 at the rear of the block, in order to stop separation that could allow water to penetrating, changing the pressures beneath the base. However, for simplicity, this is not considered here. Physically the water pressure u_1 cannot exceed $\gamma_w \cdot H$, as the water would flow over the construction. Nevertheless safety elements have to be introduced for the above mentioned checks. The water pressures u_1 and u_2 are from the same source, thus partial factors on the actions u_1 and u_2 should ideally be the same.

The effect of u_1 is a horizontal force $F_H = u_1 \cdot H/2$ at the base of the gravity construction. The resistance against sliding is $R_H = (W - B \cdot u_2/2) \cdot \tan\varphi$. Three possible approaches can be considered for this problem: (a) factoring water pressures; (b) factoring the effects of water pressures; (c) relying on use of "worst" water pressures or levels, without application of factors. The partial factor to be applied on the actions (γ_f) and effects (γ_e) of water pressure which are clearly defined and not subjected to large stochastic variations has a wide scatter in the different European countries.

As an example of approach (a), the Dutch National Annex to EC7 applies $\gamma_U = 1.2$ to the water pressures. The water pressure in the resistance term is also factored with the same partial factor γ_U of 1.2 (one source principle) in combination with a favourable partial load factor $\gamma_G = 0.9$ for the weight of the block and a partial material factor of 1.15 on tan φ.

One way to deal with the above mentioned constraints is to apply partial factors on the effects of actions (approach (b)) rather than on the actions themselves and to apply safety checks in which the increase of destabilizing effects accounts for any uncertainty – not only for uncertain unit weight or water table. This is done as an example for the check against sliding. Applying a partial factor γ_e on the effect F_H and a partial factor γ_R on the resistance R_H leads to the formal check: $F_H \cdot \gamma_e \leq R_H/\gamma_R$. The German NA requires $\gamma_e = \gamma_G = 1{,}35$ in geotechnical design and for groundwater influence.

Approach (c) using $\gamma_f = 1$ is preferred by the UK NA to EC7, though some discretion is left with the designer and use of approach (a) is allowed. The design will usually be governed by the analyses of sliding or bearing, for which the safety margin is given by the factors on soil strength. In some cases, the "middle two-thirds" rule will govern.

In connection with water tables within concrete structures such as locks (Figure 8) effects due to variable water tables as the bending moment in cross section a - a may also be factored by $\gamma_e = \gamma_Q = 0$ (favourable) or $\gamma_e = \gamma_Q = 1{,}5$ (unfavourable).

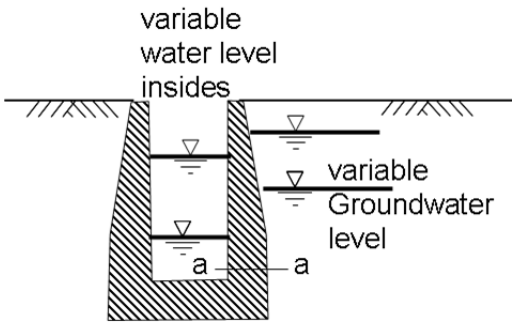

Figure 8. Lock with its water actions

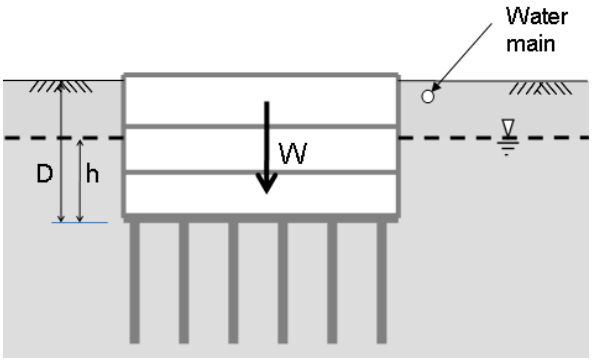

Figure 9. Deep basement subject to uplift

6.5 *Example 4 – Basement with tension piles*

Figure 9 shows a deep basement extending below the water table. No drainage is provided beneath the base slab, so hydrostatic water pressures are expected. Some unplanned variation in the water level is possible, for example due to leakage from a water main. The total weight of the structure, which could include superstructure built on the basement, is W and its area in plan is A. If needed, tension piles are to be provided to prevent uplift.

The uplift force beneath the basement is given by $U = \gamma_w Ah$.

If the characteristic uplift force U approaches or exceeds the characteristic weight W, the tension force T in the piles has to be derived. For ULS UPL we find

$$U_k \cdot \gamma_{G,dst} \leq W_k \cdot \gamma_{G,stb} + T_d \quad \text{which means } T_d = U_k \cdot \gamma_{G,dst} - W_k \cdot \gamma_{G,stb} \tag{8}$$

It is also possible to look at the problem as ULS STR/GEO. Then we get

$$U_k \cdot \gamma_G - W_k \cdot \gamma_{G,inf} = T_d \quad \text{and} \quad T_d \leq R_d = R_k/\gamma_{P,t} \tag{9}$$

As in most countries the partial factors $\gamma_{G,dst}$ and γ_G are different as well as $\gamma_{G,stb}$ and $\gamma_{G,inf}$ are different there is a need for guidance and clarity. The German NA to DIN EN 1990 gives a special set of partial factors $\gamma_{G,dst}$* and $\gamma_{G,stb}$* for cases where the resistance of building elements is necessary to fulfil ULS EQU and UPL requirements . Their values are $\gamma_{G,dst}$* = 1,35 and $\gamma_{G,stb}$* = 1,15 instead of $\gamma_{G,dst}$ = 1,05 and $\gamma_{G,stb}$ = 0,95 or γ_G=1,35 and $\gamma_{G,inf}$=1,0 leading to intermediate results. But this again means factoring of water pressure which is physically connected with the already discussed problems.

In situations where U greatly exceeds W, the precise sequence of calculation in which the factors are applied and the value of the partial factors may vary according to national practice, but the outcome is much the same. The case of W greatly exceeding U, which would require compression piles if the slab is suspended, is not considered here.

The problem is more debatable when the characteristic (unfactored) values of W and U are close, especially in formats that use $\gamma_{G;inf}$ = 1.0, which is common. If W_k=U_k and γ_G>1 is applied to water pressure, tension piles are needed, but if water pressure is not factored or adjusted in some other way no piles are needed, even if a factor is applied to the resultant (U_k–W_k), which in this case equals zero.

To illustrate this problem, suppose n piles are to be provided each with a characteristic resistance in tension R_k. For the purpose of plotting results of calculations, it is convenient to define $W_w=\gamma_w AD$; this is not the buoyancy force, which is $U_k=\gamma_w Ah$. When $U_k=W_k$, $h/D = W_k/W_w$. In Figure 10 the number of piles required, n, represented by nR_k/W_w, is plotted against h/D for a typical case in which W_k/W_w=0.25. The values of partial factors used here are adopted for illustration only, and may not represent any particular national practice. Some countries prefer to view tension piles as providing a favourable action, which would also lead to adoption of different factors. In Figure 10, the critical area of the graph is shown as an enlarged detail.

In the unfactored case, piles only become necessary when $h/D > W_k/W_w = 0.25$ in this example. If factors are applied to the unfactored resultant force in the piles, together with pile resistance factors, a line such as line (b) is obtained, for which γ_R=1.7 was used for the piles. The gradient of this line depends on the values of the factors, but when $h/D = W_k/W_w = 0.25$ no tension piles will be provided and there is no reserve of safety for deviation from the characteristic values of water pressure and weight. This is considered to represent an unacceptable situation.

If the water pressure beneath the base is multiplied by a partial factor γ_G=1.35, a line such as line (c) in Figure 10 is obtained; in plotting this line a lower value of pile resistance factor γ_R=1.3 has been adopted, in acknowledgement of the increased value of γ_G. In this case, a reserve of safety is provided when $h/D = W_k/W_w$, requiring some tension piles. However, the number of piles might be regarded as excessive for the case of a high water table, h/D approaching 1, where the water pressure beneath the base becomes physically unreasonable.

An alternative approach could be to avoid factoring water pressure but to require an increase in the water head h. For example, line (d) in Figure 10 shows the results when the free height above the water table (D–h) is reduced by 10%. This has an advantage in the case where h is large (eg h/D=1) that it does not enhance the water pressures unreasonably, requiring too many piles. The amount by which the water head should be raised is difficult to specify for general application in a code of practice, however. If this approach is preferred, it may be necessary to rely more heavily on the expertise of the designer to decide what margin is appropriate. This is consistent with the approach of EC7 {2.4.6.1(6)P} using direct assessment of design values: "When dealing with ground-water pressures for limit states with severe consequences (generally ultimate limit states), design values shall represent the most unfavourable values that could occur during the design lifetime of the structure."

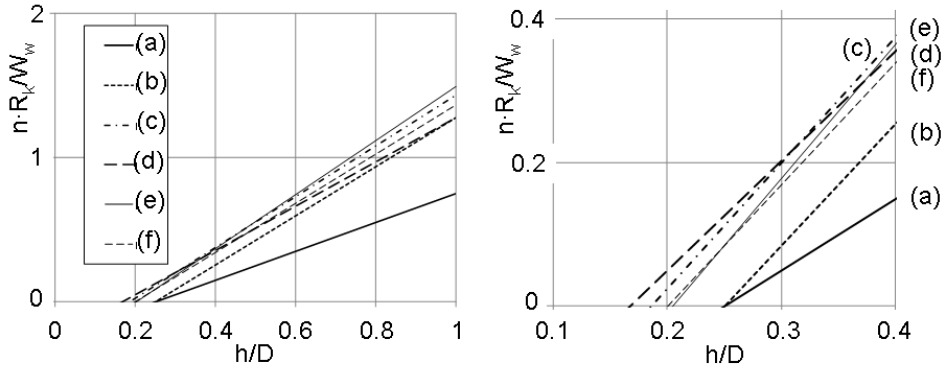

Figure 10. Number of piles required (normalised). (a) unfactored, (b) pile resistance factored, (c) $g_G = 1.35$ on water pressure, (d) water table adjusted, (e) UPL, (f) $g_{G;fav} = 0.8$ on weight.

In relation to EC7, the discussion above relates to the "STR/GEO" requirements normally used for finding the number and required resistances of piles. EC7 has another requirement for uplift cases, UPL, which is normally understood to require a factor $\gamma_{G;dst} > 1$ applied to uplifting water pressure and a factor $\gamma_{G;stb} < 1$ applied to stabilising total weight. Line (e) in Figure 10 is plotted for typical values $\gamma_{G;dst} = 1.1$, $\gamma_{G;stb} = 0.9$, with the resistance factor for the piles γ_R=1.7. This requirement can produce sensible results provided that (a) it is agreed that piles are to be designed using loading derived from UPL and (b) an appropriate system and values of factors is adopted in applying these loads to pile design. As with other schemes involving factors on water pressure, it becomes unreasonable when the water table approaches ground level (h/D=1) and may demand more piles than are really needed.

In this problem, it is necessary to change the water pressure or the building weight from their characteristic values in order to increase safety when U_k is close to W_k. A possible alternative, not considered by Eurocode 7 but recommended for further consideration, would be to apply a reduction factor to the weight of the building, say 0.8, while leaving the water pressure unfactored. This is shown as line (f) in Figure 10, plotted with γ_R=1.7. This provides safety when $h/D = W_k/W_w$, but it avoids factoring water pressure and has a smaller effect than some of the alternatives, such as UPL, when h/D=1. The results of the approach using $\gamma_{G,dst}$* = 1,35 and $\gamma_{G,stb}$* = 1,15, in which water pressure is factored, are almost identical with this.

6.6 *Example 5 – Anchored quay wall*

In Figure 11 an anchored sheetpile quay wall is shown. Water levels in the retained ground and in the excavation vary. The sheet pile is driven into the clay layer, therefore the water pressures inside and outside the building pit are different and do not represent a single source.

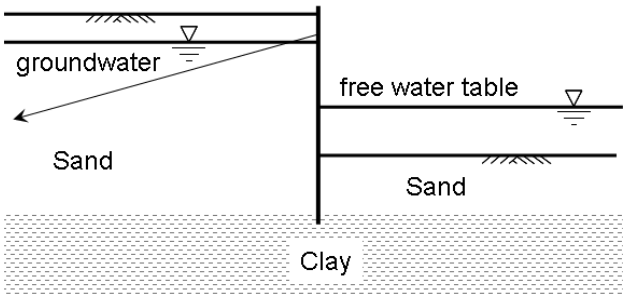

Figure 11. Anchored quay wall

It has to be clarified if the water levels are already considered "the most unfavourable values that could occur during the design lifetime of the structure" (EN1997-1, 2.4.6.1 (6)) or "the most unfavourable occurring in normal circumstances". In the first case the corresponding water pressures could directly be considered as design values. On the other hand German and Dutch requirements even look at water pressures due to water tables belonging to a flood occurring statistically only once in 50 to 100 years as characteristic values and their effects are factored with γ_G. In the second case ("the most unfavourable occurring in normal circumstances") it is doubtless that safety elements such as additional water heads or application of partial factors have to be applied. The water pressures in case 2 are considered as characteristic values.

In the UK two separate calculations are required for the two combinations of Design Approach 1. The way in which design water pressures are derived is not fully prescribed, leaving the designer to judge what is appropriate in particular circumstances, as described above in 4.2.2. One approach compatible with DA1 is to use (a) "the most unfavourable occurring in normal circumstances" in Combination 1, applying a partial factor of 1.35 to action effects, such as the resulting bending moment of the sheet pile, and (b) "the most unfavourable values that could occur during the design lifetime of the structure" in

Combination 2, with unit factors on all permanent actions and their effects. The application of the factors in (a) indicates that the approach used for water pressures is DA1*.

In Germany (DA2*) only the characteristic water pressures are used in the calculations and a partial load factor is applied at the end of the calculation to the loading effects for every critical part (anchor, sheet pile wall, reactive force to be held by passive earth pressure).

In the Netherlands (DA3), the design value of the water pressure is derived by application of an offset to the water levels, i.e. lowering water level by 0.20 m at the low side and increasing the water level by 0.05 m at the high side. The ULS-check to determine the sheet pile dimensions and anchor capacity, is then performed in combination with material factors on the soil friction properties.

All three approaches are probably adequate in most circumstances, and all three have advantages and disadvantages. The UK approach is the least prescribed, relying more heavily on engineering expertise, and so might be thought to have a greater risk of misjudgements and arguments between parties involved in the design. It has the potential, however, to cover a very wide range of circumstances and aims to avoid a need for designers to violate physical principles. The German approach could provide insufficient resistance if a small change in water pressures could lead to a change of more than 35% in action effects; similarly, if very little change of action effects is possible it could be unnecessarily conservative. It has the advantage, however, of relatively complete prescription leaving less room for argument or mistakes by designers. The Dutch approach using DA3 is similar in principle to DA1 Combination 2, but the water levels to be used are more strictly prescribed. This leaves less room for debate, but the values prescribed might not be suitable in all circumstances, or for a wider range of problem types.

6.7 *Example 6 – Gravity wall retaining free water – level slightly uncertain*

An L-shaped wall is retaining 3 m depth of water (Figure 12). In a very unlikely event of a blocked drain pipe at 3 m height, however, the water level may increase up to 4 m before the water flows over the wall. The soil below the wall consists of clay, with the concrete cast directly upon it. The downstream groundwater level is at ground level.

The water level increase up to 4 m height can be considered as an accidental situation, for which most codes and countries apply a partial factor of 1.0 to the actions. Therefore two load cases are considered with 4 m water height with a partial factor of 1.0 and 3 m water height with partial factors as discussed in 6.4 above. Discussions about the water pressure beneath the base, u_3 in Figure 12, are also similar to those in section 6.4.

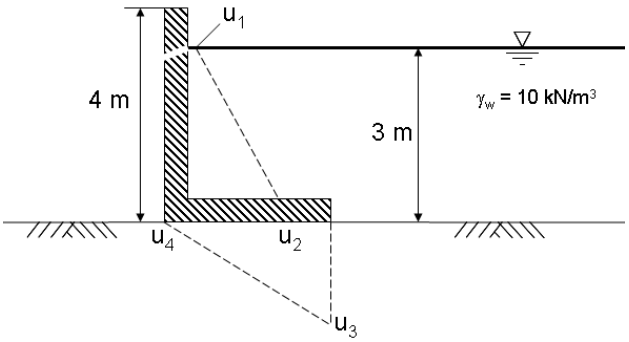

Figure 12. Gravity wall retaining free water

For EQU, the accidental case is always governing, as the ULS-state for the accidental water level results in a u_2-value of 40 kPa compared to a design water pressure u_2 of 33 kPa for the 3 m water level with a partial factor of 1.1. For sliding and bearing, both the 3 m and 4 m water levels should be considered, with the appropriate factors for normal and accidental conditions; which case is more critical depends on the factors used. For illustration purposes, a partial factor of 1.35 is used in this example. For structural design, the bending moment in the wall for 4 m depth is $\gamma_w 4^3/6 = 107$ kNm/m and for 3 m with a 1.35 partial factor it is $1.35\gamma_w 3^3/6 = 61$ kNm/m. So if the 4 m level has to be considered, a 1.35 factor on 3 m is not adequate.

In water constructions in Germany the effects of extreme water tables or of a damage or failure of sealing systems is regularly handled as an accidental design situation by using special partial factors equal or near to 1. There even exists a separate set of partial factors (factors on effect of actions as well as on resistance) assigned to transient design situations which is applied in connection of the occurrence of an exceptional large action or for an action that is planned to happen only once.

6.8 *Example 7 – Groundwater pressures below a basement*

In Figure 13 a basement is shown with floor levels at – 2.8 m and – 8.2 m. The floors are supported by tension piles to overcome uplift. The characteristic water level is at -1.0 m. For the evaluation of the tension capacity of the piles for STR/GEO, the water load must be multiplied by a load factor of 1.35 (or 1.2 in the Netherlands) or a partial factor γ_E should be applied to the load effects.

This would lead to a design water pressure of 1.35 * 18 = 24 kPa against the upper floor and 1.35 * 72 = 97 kPa at the lower floor. These pressures correspond with water levels of – 0.4 m and + 1.5 m for the upper and the lower floor respectively. These design levels are not equal for the same structure and the water level of + 1.5 m may be physically impossible!

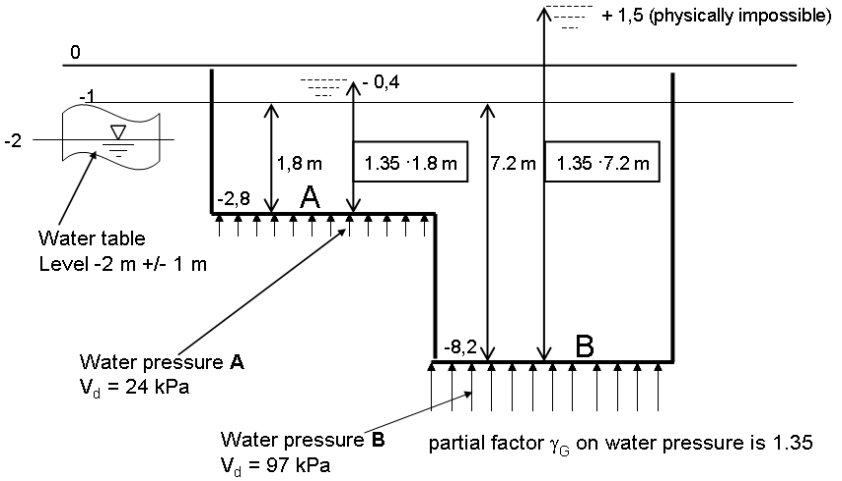

Figure 13. Groundwater pressures below a basement

Possibilities to deal with these apparent inconsistencies are:

1. Consider the water pressures as a load and apply a partial safely factor to the load. This safety factor is then considered part of the overall safety concept and does not reflect solely the uncertainty of the load.
2. Use a constant offset in the water level to incorporate the uncertainty in water level. However, an offset would result in a lower safety for the lower floor and a higher safety factor for the upper floor.
3. Apply a partial safety factor on the water pressures, but consider a maximum level for the water table, equal to ground level (as suggested in EC7 clause 2.4.6.1). The water pressures cannot exceed this limit value. Again, for the lower floor the factor of safety is below 1.35!

The Eurocode does not give a clear solution in these cases. When the water level at ground level can be considered as an absolute limit (like example 6), the corresponding water pressures can be considered as an accidental load and Option 3 would be applicable.

However, when the water pressures are caused by water in a confined deep aquifer, groundwater head above ground level is well possible. In this case Options 1 or 2 apply.

Both options 1 or 2 are possible. As described above, Option 1 would lead to maintaining the overall safety concept for the structure, but ignores the magnitude of variation in water table. Option 2 would consider the limited water table variation, but does not incorporate other uncertainties in the overall safety of the structure.

When adopting a partial factor γ_E to the load effects, the calculation is performed using characteristic values for the water pressures. This case agrees with Option 1.

7 RECOMMENDATIONS

Through intensive discussions, the authors have been able to reach agreement on the following points:

1. The effects of water pressures are very important in geotechnical design. Their actual values can have significant uncertainties, and values outside the range anticipated in design can cause major failures.
2. Partial factor design applies factors to a small number of leading, or "primary" actions. In real design situations, secondary actions of relatively small but unpredictable nature and magnitude should also be accommodated; that is, a degree of robustness it required. Often, these are accommodated by increasing the partial factors applied to primary actions or action effects.
3. Designers must explicitly accommodate the worst water pressures that could reasonably occur. Reliance on factors of safety together with less extreme water pressures or water levels may give a false sense of security.
4. Application of partial factors to the density of water should generally be avoided.
5. One useful way to maintain a prescribed degree of safety is to require an offset in water pressure, raising or lowering the water surface or piezometric level.
6. The single source concept should be applied whenever possible.
7. The "star" approach (DA2* or DA1*, introduced here) has advantages when dealing with problems dominated by water pressures because it avoids the application of partial factors to the density of water or to water pressures. This means that partial factors are applied to action effects rather than to actions themselves. The details of its use depends on the way other partial factors are applied, to resistances or to material strengths, and on their values. In situations where material strength is important (STR/GEO), if fairly low factors are applied to resistance (1.1) it might be necessary to enhance the

loads (or load effects such as an uplifting force), even when they are very certain. But if larger factors are applied to resistance (1.25 or 1.4), then it may not be necessary to enhance loads where they are well defined.

8. In uplift problems, it is necessary to vary either water pressures or the magnitudes of favourable, stabilising weight, in order to ensure safety in view of possible secondary actions. In order to avoid factoring water pressures, the possibility of a reduced factor on favourable weight, perhaps between 0.8 and 0.9 should be considered.
9. To prevent toppling failure of structures loaded laterally by water pressure, a "middle 2/3rds" rule could be considered, applied to unfactored actions, or to actions with unit factors.
10. Although there are obvious advantages in making codes of practice as precise and prescriptive as possible, the need for engineering expertise and careful evaluation of the full range of credible scenarios cannot be replaced. This is particularly true of situations in which water pressure has a dominating role.

The following points are not agreed among the authors and remain to be debated and researched further. In some cases, appropriate conclusions may depend on other features of the safety formats adopted, for example the differing Design Approaches of Eurocode 7.

11. Whether it is desirable to apply factors to water pressures. Several approaches that avoid this have been discussed, but in some approaches factors are applied to water pressures in some circumstances.
12. Whether it is reasonable to apply partial factors to forces (action effects) directly derived from water pressures. It is agreed that this may raise problems, which have been discussed, but the authors could not agree that it can always be avoided.
13. The use of the "star" approach, factoring action effects, in cases where it is directly equivalent to factoring water pressures, either complying with the "single source" principle or not compliant. The problem particularly relates to situations in which equilibrium is not maintained throughout the geotechnical calculations of stability, including sliding, bearing, toppling and uplift. An example is given by approach (b) in Example 3 above, where the design horizontal force transmitted to the ground is not in equilibrium with the water pressures. Less concern is felt about application of factors to action effects internal to structures, such as bending moments in walls and slabs or forces in piles.

REFERENCES

AASHTO (2008) LRFD Bridge Design Specifications, 4th edition, 2007 with 2008 Interim Revisions. American Association of State Highway and Transportation Officials.

Beeby, AW & Simpson, B (2001) A proposal for partial safety factors for soil pressures in BS8110. The Structural Engineer.

BS8002 (1994) Code of Practice for Earth Retaining Structures. BSI.

BS 6349-1 (2000) Maritime structures - Part 1: Code of practice for general criteria. BSI.

CUR 166 (2008), Damwandconstructies (Earth retaining structures), CUR Bouw&Infra, The Netherlands

Davies, RV (1984) Some geotechnical problems with foundations and basements in Singapore. Proc Int Conf on Tall Buildings, Singapore, pp643-650.

DIN 1054 (2005) – Subsoil – Verification of the safety of earthworks and foundations.

DIN 4084 (draft 2002) – Subsoil – Calculation of embankment failure and overall stability of retaining structures.

DIN 19700-10 (2004) – Dam Plants – General specifications.

DIN 19702 (1992) – Stability of Solid Structures in Water Engineering.

DIN 19712 (2007) – River Dikes.

Gaba, A.R, Simpson, B. Powrie, W. & Beadman, D.R. 2003. Embedded retaining walls: guidance for economic design. CIRIA Report C580.

Orr, T.L.L. (2005). Model Solutions for Eurocode 7 Workshop Examples. Trinity College, Dublin.

PD6694-1(2011) Recommendations for the design of structures subject to traffic loading to BS EN 1997-1:2004. BSI.

Ramaswamy, S.D. (1979) "Some Aspects of Practice and Problems of Foundations in Singapore" Proc. 6th Asian Regional Conf. on Soil Mech. and Found. Eng., Singapore, 1979.

Simpson, B. (2011) Water pressures. Proc. 2nd International Workshop on Evaluation of Eurocode7, Pavia, 12-14 April 2010.

Simpson, B and Hocombe, T (2010) Implications of modern design codes for earth retaining structures. Proc ER2010, ASCE Earth Retention Conference 3, Seattle, Aug 2010.

Simpson, B., Blower, T., Craig, R.N. and Wilkinson, W. B. (1989) The engineering implications of rising groundwater levels in the deep aquifer beneath London. CIRIA Special Publication 89, 1989.

Simpson, B, Morrison, P, Yasuda, S, Townsend, B, and Gazetas, G (2009) State of the art report: Analysis and design. Proc 17th Int Conf SMGE, Alexandria, Vol 4, pp. 2873-2929.

Stroud, M.A. (1987) The Control of Groundwater. General Report and State of the Art Review to Session 2 of IX ECSMFE Dublin

ISGSR 2011 - Vogt, Schuppener, Straub & Bräu (eds) - © 2011 Bundesanstalt für Wasserbau ISBN 978-3-939230-01-4

Performance Based Design and Eurocode

H. Heidkamp
SOFiSTiK AG, Oberschleißheim, Germany

I. Papaioannou
Chair for Computation in Engineering, Technische Universität München, Munich

ABSTRACT: Along with the introduction of the Eurocodes, an extensive and continuing discussion process regarding the implemented safety concept has been triggered in the engineering community. Typically, these discussions soon tend to focus on technical aspects of the suggested design *procedure* – and, unfortunately, obscure the view of underlying essentials of the Eurocode safety *concept*.

This paper advocates a holistic perception of the structural design process. By shortly reflecting the design process, it aims to identify common characteristics of 'good' structural design: A common postulate is always the definition of, or the agreement upon, specific structural requirements that conform to the intended function and life-time of the structure – *performance criteria.*

Then, what are suitable engineering tools, tools that support the development of a qualified design? At this point, the paper attempts to contribute to some demystification of reliability based design. Not least by practical geotechnical case studies, reliability based design is motivated as an engineering tool which adds value to engineering decision making and finally helps to contribute to a 'good' – performance based – structural design.

Finally, what is to say about the normative background? Are the Eurocode concept and the notion of performance based design extremes? To shed some light on these relevant, practically motivated questions, the EN 1990 is critically reviewed and discussed.

Keywords: Structural Design Process, Eurocode Design Concept, Reliability Analysis, Performance Based Design

1 STRUCTURAL DESIGN

1.1 *'Good' design*

What is the essence of 'good' structural design? To attempt a cautious answer to this question, an exemplary design case is considered.

The 'tree swing project' nicely illustrates possible pitfalls over the project planning phase by means of a rather simple structure, a tree swing (Figure 1). The accentuated representation reveals the problematic nature of non-integral thinking: The client orders a tree swing. The structural engineer then succeeds to come up with a design that provides for sufficient structural resistance. Good structural design? In this fictitious case, the assessment seems clear; in fact however, the question cannot be answered satisfactorily, without considering the envisioned service of the structure.

Scenario A) (unlikely): The tree swing is meant as an artwork, no specific use is assigned. In this case, the design might meet the requirements.

Scenario B) (more likely): The tree swing is meant as a gift for the client's little son. With this background the assessment differs. The design indeed ensures the required safety standards; however, it fails to meet the intended function of the structure. During the design process, a necessary constraint, sufficient structural resistance, has become an end in itself and finally the primary goal of the design.

The disappointment of scenario B) could have been avoided, if client and planners had agreed upon specific *performance criteria* a priori – structural requirements that conform to the intended function of the structure. Moreover, if client and planners had commonly tried to identify the desired performance,

there might have been opportunity to realize, that the solution that meets the client's needs best, is a tire swing – rather than a board swing.

a) What the client had in mind

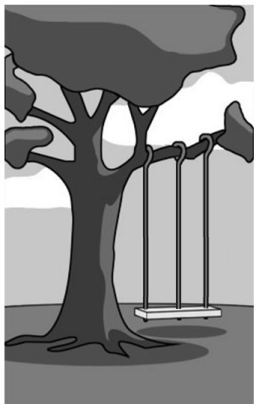
` b) How it was designed

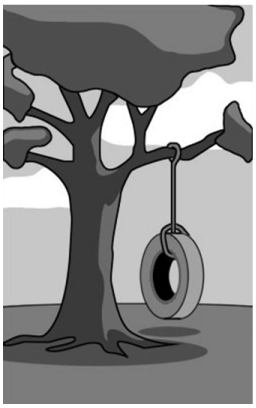
c) What the client really needed

Figure 1. Variants of a tree swing [http://www.projectcartoon.com/].

1.2 *Evolution of structural design concepts*

For a long time, the structural design process was almost entirely based on empirical knowledge which had primarily been gained by trial and error. As a consequence, structures were repetitive and increases in scale were incremental. Along with the evolution of the theory of structures, material science and computational possibilities, the first design concepts were established. In the beginning of this process, simple instructions and guidelines documented the state of knowledge. Successively, with origin in the early 20th century, a comprehensive system of technical directives and codes was developed. The underlying safety concept was and is continuously adapted to the attained practical and experimental experience, the increased theoretical knowledge and – not least – the computational possibilities.

Currently adopted design concepts can be classified into deterministic, semi-probabilistic and full-probabilistic approaches. Differences can readily be contrasted, when considering the design goal 'structural safety' (ultimate limit state). It is important to realize, that the common background of all approaches is the control of the vast amount of inherent uncertainties. These uncertainties, to name a few, are induced by variation of material properties, by the limited predictability of loading or by the construction process itself. Hence, the objective can be identified as limiting the probability of failure to an acceptable level.

The deterministic approach adopts the simplest safety definition

$$R/\gamma \geq S \qquad (1)$$

where R denotes the resistance, S is the effect of the action and γ is an empirically determined global safety factor that is meant to incorporate all uncertainties (Figure 2a).

A more refined version is represented by partial safety factors:

$$R_k/\gamma_R \geq S_k \cdot \gamma_S \qquad (2)$$

In this case, uncertainties on action and resistance side are accounted for, separately. They are reflected by the load factor γ_S and the resistance factor γ_R (Figure 2b). Computation remains purely deterministic but since the partial safety factors are calibrated to match a predefined probability of failure level P_d (=acceptable probability of failure), the approach is classified as semi-probabilistic [Marek et al. (1998), Honjo et al. (2009)].

The full probabilistic approach finally abandons the definition of (partial) safety factors; it simply imposes the constraint on the probability of failure P_f directly (Figures 2c-d):

$$P_f = P\{R - S \leq 0\} < P_d \qquad (3)$$

This most general approach ultimately leaves the domain of deterministic calculation; some background in reliability theory is required. In return, it is consistent and general-purpose. In particular, it does not rely on the differentiation between action and resistance – an important aspect, when considering, e.g., soil-structure interaction scenarios. As will be illustrated further, the concept can be employed for serviceability assessment in a straight-forward manner; in fact, *any criterion* that is considered relevant for

successful *performance* of the structure can be adopted. Last but not least, this direct approach inherently respects the design philosophy that *a designer should keep track of the most likely behavior of the structure throughout the design calculations as much as possible* [cf. Honjo et al. (2009)] – which is of particular relevance in nonlinear settings.

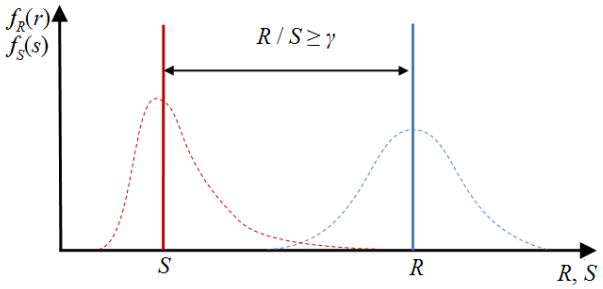

a) Deterministic safety concept

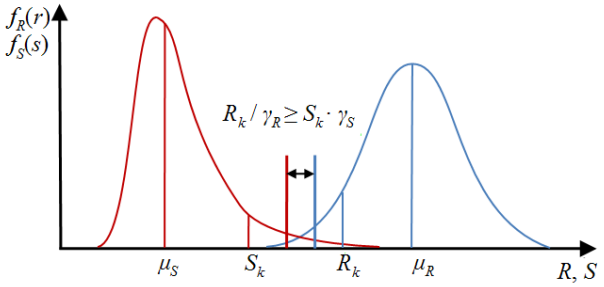

b) Partial safety factors

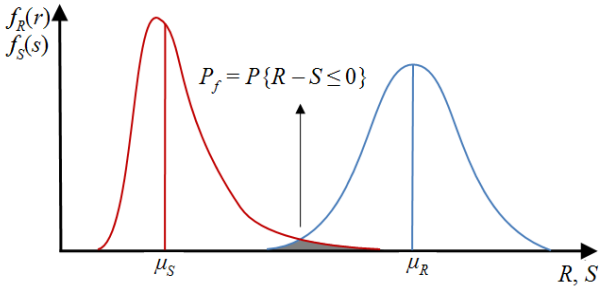

c) Probabilistic safety concept

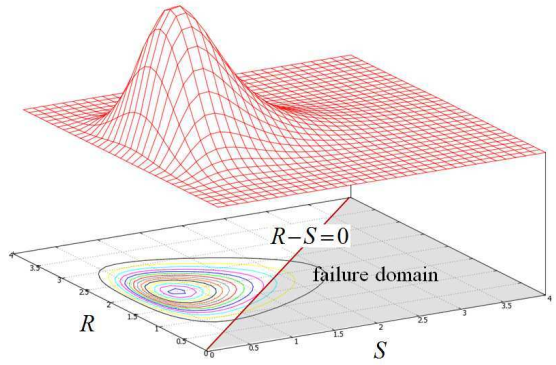

d) Probabilistic safety concept – alternative illustration

Figure 2. Illustration of safety concepts.

2 RELIABILITY ASSESSMENT

In many cases, the definition of the probability of failure given in Eq. (3) is not sufficient, since it may not be possible to reduce the design condition to a simple R versus S relation. In a more general context, there may be many different parameters that are expected to present an uncertain behavior. Typical examples are dimensions, loads, material properties as well as any other variable that is employed in structural analysis and design procedures.

The corresponding generalized reliability concept features two basic ingredients.

In a first step, the uncertain parameters are modeled by a vector of basic random variables $\mathbf{X} = [X_1, X_2, \ldots, X_n]^T$ with a joint probability density function (PDF) $f_{\mathbf{X}}(\mathbf{x})$. The joint PDF is usually approximated using marginal distributions and correlations [e.g. see Der Kiureghian and Liu (1986)], which are estimated based on observed data and engineering judgment. The joint PDF for the two variable-case $\mathbf{X} = [R, S]^T$ is shown in Figure 2d.

The second component is concerned with the intended function of the structure, i.e. the design goals. Criteria that are considered as relevant for a successful performance of the structure are expressed by means of a corresponding *performance function* $g(.)$, defined in terms of the vector $\mathbf{X}$. The performance function $g(\mathbf{X})$ is defined by convention, such that failure of successful performance occurs when $g(\mathbf{X}) \leq 0$. Note that a more general definition of the performance function can include several performance criteria, leading to the parallel- or series-system reliability problem. The probability of failure is computed by:

$$P_f = P\{g(\mathbf{X}) \leq 0\} = \int_{g(\mathbf{X}) \leq 0} f_{\mathbf{X}}(\mathbf{x})\, \mathrm{d}\,\mathbf{x} \qquad (4)$$

The notion of *performance criteria* overcomes the constrictive character of Eq. (3) and leads to a general definition of the probability of failure. The strength of this approach lies in the fact that the performance criteria can be tailored individually to the specific requirements of the structure to be designed. However, it is important to note the trivial result that, for the special case where $\mathbf{X} = [R, S]^T$ and $g(\mathbf{X}) = R - S$, Eq. (3) is recovered (Figure 2d).

A corresponding measure of safety may be chosen as any decreasing function of P_f. The standard reliability measure is the generalized reliability index [Ditlevsen and Madsen (1996)], defined as:

$$\beta = -\Phi^{-1}\left(P_f\right) \tag{5}$$

where $\Phi^{-1}(.)$ is the inverse of the standard normal cumulative distribution function.

The difficulty in the evaluation of the integral in Eq. (4) lies in the fact that the performance function is usually not known in an explicit form, but depends on the outcome of a structural analysis calculation for any given realization of the random variables. Since the computational time for the underlying structural analysis may be considerable, methods that aim at limiting the required number of structural computations have been developed. A series of reliability methods have been coupled to the SOFiSTiK structural finite element analysis and design program [Papaioannou et al. (2009)], in an attempt to achieve a balance between accuracy and efficiency for a variety of possible performance criteria. These include first order reliability methods as well as a number of simulation techniques. In addition, the methods may be combined with a response surface approximation of the performance function to further enhance the efficiency of the reliability assessment. In the following section, the SOFiSTiK reliability module is employed for the reliability-based design of a geotechnical application.

3 CASE STUDY

The considered design case study is a deep excavation with a vertical retaining wall and a horizontal supporting strut (Figure 3). The soil consists of two layers of clay. A conservative estimation of the soil strength parameters is given in intervals, as shown in Table 1. The design goal is the determination of the wall thickness against a serviceability requirement.

The soil is modeled in 2D with elasto-plastic plane strain finite elements and the soil's shear strength is described by the Mohr-Coulomb criterion. For the wall, beam finite elements are adopted, while the interface between wall and soil is resolved by special elements featuring a reduced shear capacity compared to the soil base material. A horizontal spring is used to model the supporting strut. The computational model is depicted in Figure 4a.

A displacement-based deterministic design for the wall thickness is first performed considering the lowest values of the strength parameters given in Table 1. For serviceability reasons, the design is targeted at a restriction of the maximum inward wall displacement at the bottom of the trench to a threshold value of $u_{\max}$ = 3.5cm. Apart from accounting for the lower bound soil strength only, no further safety margins are incorporated in this design. The design process yielded a wall thickness of 1.0m. Figure 4b shows the deformed configuration for the deterministic design of the wall thickness at the final excavation step.

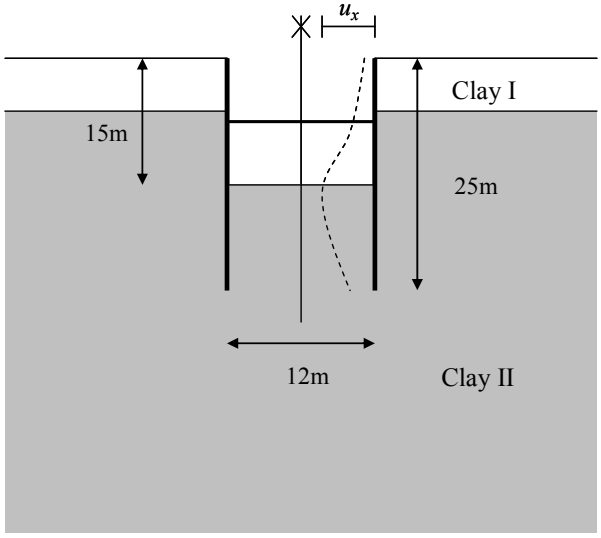

Figure 3. Deep excavation with retaining wall.

Table 1. Estimated strength parameters of the soil materials

Parameter	Clay I	Clay II
Friction angle φ [°]	12-22	18-28
Cohesion c [kPa]	5-10	15-25

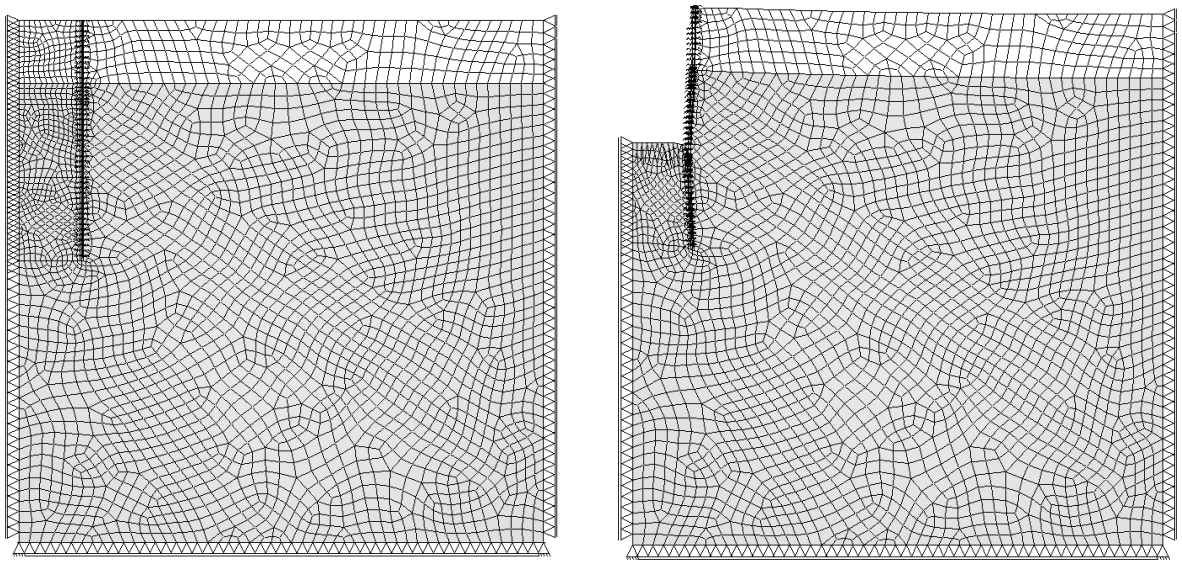

a) Finite element mesh b) Deformations at the final excavation step magnified by a factor of 20

Figure 4. Numerical model.

In a second step, a probabilistic design is performed, accounting for randomness in the strength parameters of the soil. Two cases are considered. In the first investigation (Case I), the conservative Uniform distribution is employed, assuming the same probability density for any value of the strength parameters in the given intervals (Table 2). For the second case (Case II), the Beta distribution is used, taking as mean values the middle points in the intervals and allowing for a 10% coefficient of variation (COV) inside the intervals (Table 3). The Beta distribution includes lower and upper bounds, but distributes the probability content according to the second order properties (mean and variance). This means that we assume additional information than the given estimation in Table 1, which reduces the uncertainty in the model. Therefore, Case II should lead to a less conservative estimation of the reliability. However, it should be noted that the Beta distribution is a much more realistic assumption for the description of physical quantities compared to the Uniform distribution. For both cases, the typical value of –0.3 is chosen for the correlation coefficient between the strength parameters of the same materials.

A displacement-based performance function is adopted, restricting the horizontal wall displacement at the bottom of the trench:

$$g(\mathbf{X}) = u_{\max} - u_x(\mathbf{X}) \qquad (6)$$

For this, $u_{\max}$ = 3.5cm is chosen again, which represents the maximum displacement of the deterministic design.

Table 2. Random variables of the soil strength properties (Case I)

Parameter	Distribution	Min	Max
Friction angle (Clay I) φ_{I} [°]	Uniform	12	22
Cohesion (Clay I) c_{I} [kPa]	Uniform	5	10
Friction angle (Clay II) φ_{II} [°]	Uniform	18	28
Cohesion (Clay II) c_{II} [kPa]	Uniform	15	25

Table 3. Random variables of the soil strength properties (Case II)

Parameter	Distribution	Mean	COV	Min	Max
Friction angle (Clay I) φ_I [°]	Beta	17	0.1	12	22
Cohesion (Clay I) c_I [kPa]	Beta	7.5	0.1	5	10
Friction angle (Clay II) φ_{II} [°]	Beta	23	0.1	18	28
Cohesion (Clay II) c_{II} [kPa]	Beta	20	0.1	15	25

A series of reliability analyses were carried out for different values of the wall thickness applying the first order reliability method (FORM) combined with a quadratic response surface. The FORM is an approximation method, which computes the probability of failure by performing a first order approximation of the failure domain at the most probable failure point (MPFP) of an independent standard normal space derived from an isoprobabilistic transformation of the basic random variables. The MPFP is computed by solving an equality-constrained quadratic optimization problem [Der Kiureghian (2005)]. The quadratic response surface is computed applying a central composite design at the basic random variable space [Faravelli (1989)]. The reliability indices computed for the different values of the wall thickness are shown in Figure 5.

For the assumed scenario of a serviceability-driven design, the EN 1990 directive quantifies the target serviceability failure probability to a value of 2×10^{-3} (Table 4), which corresponds to a reliability index of 2.9 [CEN (2002)]. Based on this condition, the probabilistic design is computed by interpolating between the combinations of wall thicknesses and calculated reliability indices (Figure 5). The design results in a wall thickness of 0.92m for the conservative probabilistic scenario (Case I), which considerably reduces the thickness compared to the deterministic design (1m). Moreover, in the case where more data is available to support the assumption of a more realistic probability distribution (Case II), the wall thickness design may further decrease to 0.88m.

With this result, a possible benefit of using a fully probabilistic design approach is imposingly highlighted. The findings illustrate the potential of a direct account of parameter uncertainties to realize a significantly more economical design; note that this can be achieved without eroding the targeted safety level.

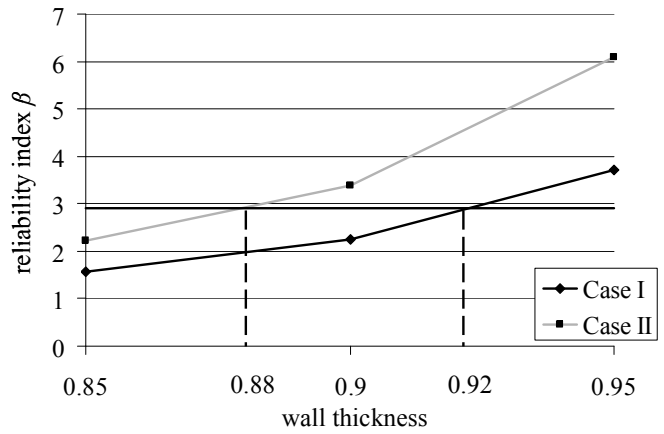

Figure 5. Reliability index vs. wall thickness.

Table 4. Target reliability index β and corresponding probability of failure P_f values (EN 1990)

Limit state	Target reliability index β		Target probability of failure P_f	
	1 year	50 years	1 year	50 years
ULS	4.7	3.8	1×10^{-6}	7.2×10^{-5}
SLS	2.9	1.5	2×10^{-3}	6.7×10^{-2}

4 PERFORMANCE BASED DESIGN AND EUROCODE

In the previous section, an application of reliability-based design based on a tailored performance criterion was presented; reliability levels were adopted in line with the Eurocode design directive. The applied design concept, termed here performance-based design, is defined as follows: *A structure shall be designed in such a way that it will with appropriate degrees of reliability and in an economical way attain the required performance*. In this definition, we attempt a generalization of different aspects included in the Eurocode design concept. The generalization is based on the central notion of *required performance.* This notion may include any subjective requirement that is considered critical for the successful performance of a specific structure. The following question arises: How does this definition compare to the Eurocode?

The Eurocode design concept is based on two fundamental requirements for the reliability of structures; structural safety and serviceability [CEN (2002)]. Appropriate design criteria and diversified reliability levels are reflected by the provision of corresponding limit states, the ultimate and serviceability limit states, respectively. The ultimate limit state includes failure conditions due to a number of reasons, such as loss of equilibrium, excessive deformations, loss of stability and fatigue. The serviceability limit state is concerned with the functioning of the structure under normal use as well as the comfort of people and the appearance of construction works. In addition, it is noted that *usually the serviceability requirements are agreed for each individual project* [cf. CEN (2002)]. These two categories of criteria require different minimum reliability levels (see Table 4). The reliability of the design should be verified against all relevant limit states, which will depend on the specific characteristics of each individual structure. We assert that a careful choice of these relevant criteria will lead to a successful *performance* of the structure. In fact, the above devised definition of performance based design is only a slight variation of the 'basic requirements', stated in EN 1990 [cf. CEN (2002)].

The Eurocode allows for two different approaches for the verification of structural reliability; the partial safety factor or semi-probabilistic method and the full probabilistic method (see Section 1.2). The application of the partial safety factor method is based on choosing the correct safety factor for each design parameter and targeted limit state. The provided partial safety factors are meant to be calibrated for each different limit state to match the corresponding required reliability level. On the other hand, the full probabilistic approach requires the direct evaluation of the structural reliability and probability of failure, respectively. Based on the general definition of the probability of failure (see Section 2), it seems that this approach, while being in perfect alignment with EN 1990, is appropriate for application to the generalized concept of performance-based design. As demonstrated in Section 3, this combined approach employs a reliability-based design technique.

Evidently, the notion of performance-based design and its direct link to probabilistic methods seem to be in good agreement with the Eurocode design concept. Nevertheless, the lack of a general directive for the application of full probabilistic procedures leads to apparent difficulties for the designer. These include the fact that he has to do an extensive literature review to acquire available data and models. Moreover, this will lead to subjective designs, depending on different amounts and types of information collected by different designers. A solution to these problems is suggested by the Joint Committee on Structural Safety (JCSS) that published a Probabilistic Model Code (PMC) [see Vrouwenvelder (2002)]. The suggestions given in the PMC may be applied in conjunction with the performance-based design concept leading to objective reliability-based designs.

5 CONCLUSION

This paper attempts to identify a general performance-based design concept, tailored to the needs of individual structures, that contributes to a 'good' structural design. Moreover, we argue that a consistent realization of this design concept requires the consideration of probabilistic approaches and ultimately leads to a reliability-based design. In light of a geotechnical design application, we demonstrate how this approach can add value to engineering decision making, compared to standard design approaches, and that its application can potentially lead to more economical designs. Nota bene, this approach conforms well to the basic design concept of the Eurocode directive.

The significant progress regarding advanced algorithms and increased computational power have made full probabilistic procedures feasible for practical engineering applications. Nevertheless, it must be admitted that to date there is an obvious lack of guidance regarding the application of these procedures. However, there are signs of an increasing awareness of the potential of performance based design in con-

junction with probabilistic reliability assessment. At the same time, promising developments – like the draft of the above mentioned Probabilistic Model Code – may well contribute to establish a best practice regarding the concept's application to practical engineering tasks.

REFERENCES

CEN European Committee for Standardization 2002. Eurocode: Basis of Structural Design. EN 1990:2002.

Der Kiureghian, A. 2005. First- and second- order reliability methods. Chapter 14 in Engineering Design Reliability Handbook, Nikolaidis, E., Ghiocel, D.M., Singhal, S. (eds.), CRC Press.

Der Kiureghian, A., Liu, P.-L. 1986. Structural reliability under incomplete probability information. Journal of Engineering Mechanics ASCE 112(1), 85-104.

Ditlevsen, O., Madsen, H.O. 1996. Structural reliability methods. John Wiley & Sons.

Faravelli, L. 1989. Response surface approach for reliability analysis. Journal of Engineering Mechanics ASCE 115(12), 2763-2781.

Honjo,Y., Chung, K.L.T., Hara, T., Shirato, M., Suzuki, M., Kikuchi, Y. 2009. Code calibration in reliability based design level I verification format for geotechnical structures. Geotechnical Risk and Safety, 435-452.

Marek, P., Gustar, M., Bathon , L. 1998. Tragwerksbemessung – Von deterministischen zu probabilistischen Verfahren. Academia Praha.

Papaioannou, I., Heidkamp, H., Düster, A., Rank, E., Katz, C. 2009. Integration of reliability methods into a commercial finite element software package. Proc. 10th Intl. Conference on Structural Safety and Reliability, Osaka, Japan.

Vrouwenvelder, A.C.W.M. 2002. Developments towards fully probabilistic design codes. Structural Safety 24, 417-432.

ISGSR 2011 - Vogt, Schuppener, Straub & Bräu (eds) - © 2011 Bundesanstalt für Wasserbau ISBN 978-3-939230-01-4

Reliability Theory and Safety in German Geotechnical Design

B. Schuppener
Federal Waterways Engineering and Research Institute, Karlsruhe, Germany

M. Heibaum
Federal Waterways Engineering and Research Institute, Karlsruhe, Germany

ABSTRACT: In Germany the reliability theory using a probabilistic approach in geotechnical design was officially introduced as the basic concept for geotechnical design at the German National Geotechnical Conference in 1978 as it had also been adopted as the common safety concept for the future Eurocodes. In the following years numerous research studies were published on the application of the reliability theory in the various geotechnical verifications. In the end, however, it was only the selection of characteristic values of ground properties where the application of the reliability theory was implemented in Eurocode 7 "Geotechnical design - Part 1: General rules" and the German geotechnical design standards. The paper describes the history of the discussion in the German geotechnical community and the results of those discussions.

Keywords: reliability, safety, safety factors, geotechnical design, standards

1 INTRODUCTION

At the first international symposia on geotechnical safety and risk, which were held in Shanghai in 2007 and in Gifu, Japan, in 2009, colleagues from Asia mainly reported on their scientific studies on Reliability Based Design (RBD) and its application in practice. By contrast, a large number of European papers focused on presenting the Eurocodes for structural design, in particular Eurocode 7 "Geotechnical design", in which the probabilistic approach now only plays a subordinate role. When work on writing the Eurocodes began in the 1970s, the probabilistic approach was still one of the basic components of the safety philosophy of the Model Codes. So why had its application disappeared almost entirely from European design standards? This issue needed to be clarified before we could enter into productive scientific discussions with the proponents of RBD on the usefulness of a probabilistic approach in geotechnical design standards.

The review presented in this paper is limited to the debate in Germany although several Swiss and Austrian publications are also considered. It describes the discussions that took place up until 2010 and may therefore reflect an intermediate stage and the problems of yesteryear. Perhaps the 3rd International Symposium on Geotechnical Safety and Risk will provide new ideas that can contribute to advancing standardization in Germany and Europe.

2 THE HISTORY

2.1 *The German National Geotechnical Conference of 1978*

The traditional safety factor concept has the serious disadvantage that the actual variability of the soil strength is not directly taken into account, and consequently a particular conventional safety factor does not necessarily have the same meaning for all soils. Comparison of different designs with different soil types, or even different designs with the same soil type, is not easy. A probabilistic approach instead of the traditional global concept is therefore a fascinating vision for geotechnical engineers as it not only provides a rational basis for the quantification of geotechnical safety but also a meaningful and consistent

basis for comparison (Lumb, 1970). By defining a probability of failure, direct comparison is possible while global safety factors are related to every single verification format that cannot be compared with each other.

The reliability theory had been adopted as the common safety concept for the future Eurocodes (Joint Committee on Structural Safety, 1976). As a consequence, a special committee was established in Germany which lay down the principles for the application of the reliability theory in future structural standards (Arbeitsausschuß "Sicherheit im Bauwesen" ("Safety in Structural Design" committee), 1981). For geotechnical design, the reliability theory using a probabilistic approach was officially introduced at the German National Geotechnical Conference in 1978. The concept was presented by G. Breitschaft (Breitschaft and Hanisch, 1978) who was president of the DIBt (Deutsches Institut für Bautechnik, an institute of the German Federal and *Laender* Governments for a uniform fulfilment of technical tasks in the field of public law) and later became chairman of the technical committee of CEN in charge of the structural Eurocodes (TC 250). The lecture intended to promote the ideas among German geotechnical engineers and to lay the basis for future standardization work in Europe and Germany.

Standards writers were fascinated by the reliability theory as it was a practice-related safety theory that promised to enable them

- to state the actions in a uniform way that was independent of the type of construction and construction materials and
- to specify the resistances of structures and members in a rational manner,
- thus permitting the introduction of a consistent safety level for different types of construction.

The application of the reliability theory is based on knowledge of the statistical data of those parameters that have a significant effect on safety (in geotechnical engineering, the shear parameters φ' and c' and the loads), i.e. the mean values, standard deviations and type of distribution as well as any distribution limits. The statistical distributions of the parameters are analysed by means of the statistical methods of the reliability theory in order to obtain a measure of the reliability of a structure. The result is based exclusively on verified technical data, is therefore rational and free from any subjective and qualitative experience. It is not intended to present the theoretical basis of the safety concept here but rather to draw attention to well-known papers and publications. For probability based design, the approximate method of Hasofer and Lind (1974), usually known as the "first order reliability method" (FORM), was favoured.

It does not need to be emphasized that the concept was expected to deliver new ideas for ways to optimize construction both technically and economically. Owing to these promising advantages, the probabilistic safety concept was welcomed, not only by those involved in developing European and German standards for structural engineering but also by well-known experts in the field (Joint Committee on Structural Safety, 1976, Arbeitsausschuß "Sicherheit im Bauwesen", 1981).

2.2 *The German National Geotechnical Conference of 1982*

In the following years numerous research studies on the application of the reliability theory were conducted and published for the various geotechnical verifications (e.g. Rackwitz, R. and Peintinger, B., 1981). Moreover, a revised guidance paper was drawn up by the "Safety in Structural Design" committee of DIN (NABau Arbeitsausschuß "Sicherheit im Bauwesen", 1981) which was intended to serve as a mandatory basis for all future structural design standards.

However, the subject of the probabilistic safety concept was not brought up again until a special session held during the National Geotechnical Conference in 1982. Pottharst (1982) presented his findings for the verification of the bearing capacity of shallow foundations. He evaluated a number of test results obtained with sand and demonstrated that the distribution of the single values of φ' could best be approximated by means of a logarithmic normal distribution with its lower boundary at 20°. In his model calculation, Pottharst also took into consideration that the standard deviation of the mean value of the angle of shearing resistance on the potential failure surface is lower than that of the single values obtained in the tests. He showed that it is possible to perform a verification of the bearing capacity of soil with partial safety factors derived on the basis of the statistical safety concept and to achieve a relatively consistent safety level. By contrast, verifications performed in accordance with DIN 4017, in which a global safety factor, η_p, of 2.0 is only applied to the loads, yield safety levels that are inconsistent and, above all, are also lower. In spite of this positive result for the probabilistic approach, Pottharst stressed the limitations of the method which he considered primarily to be the insufficient proof of the distribution of the distribution densities of very low and very high values and the fact that errors in planning and execution cannot be taken into account. Gässler (1982) applied the safety concept to anchored walls and nailed walls and arrived at a similar conclusion. He stressed that the new type of design did not involve more

work for designers but that, on the other contrary, the use of diagrams and equations would simplify their work instead. Three other papers dealt with the problem of how to evaluate test results with regard to their spread and their correlations (Peintinger, 1982; von Soos, 1982) and how prior knowledge can be used (Rackwitz, 1982).

The most interesting part of the special session was a panel discussion. Most of the arguments for and against the probabilistic safety concept, which have been repeated over and over again in discussions since then, were put forward there. They were as follows:

- The probabilistic approach does not take account of human error in design and execution although it is the main cause of damage (Blaut, 1982).
- The possibilities of collecting statistical data on soil are severely limited in practice (Vollenweider, 1982).
- The differences between geotechnical engineering and other areas of structural engineering are not only the higher coefficients of variation in the former – soil cannot be produced with clearly defined characteristics according to a set formula – but also that the geotechnical engineer only ever sees a limited part of the structure he is designing (Vollenweider, 1982).
- Damage is usually due to risks which are connected with the soil but which go undetected (Smoltczyk, 1982).
- Distributions of geotechnical basic variables that have no upper or lower limit are unsuitable as it is not possible to measure very high and very low values, nor are such values considered likely to occur for mechanical reasons (Kramer, 1982).
- Soil excavations and tests of the mechanical properties of soil never provide enough data to enable a probability calculation to be performed (Lackner, 1982).

All in all, the most prominent German geotechnical engineers took rather a critical view of the probabilistic approach (in favour: 3; undecided: 5, against: 4). However, it was generally agreed that greater effort was required during soil investigations, there was a definite need for databases for information on soil to be set up and that more extensive checks and inspections of geotechnical engineering work were necessary.

2.3 *Research and discussions in the following years*

In the following years the probabilistic approach was a research topic at nearly all university geotechnical engineering departments in Germany and nearly all analyses in geotechnical design were examined to establish whether they were suited to application of the probabilistic approach. Eder recalculated the failure of a rock slope (Eder, 1983), Heibaum examined the stability of anchored retaining walls at deep slip surfaces (Heibaum, 1987), Genske and Walz (Genske and Walz, 1987) as well as Smoltzcyk and Schad (Smoltczyk and Schad, 1990) considered the application of the probabilistic safety philosophy to calculations of the bearing capacity of soil, Reitmeier researched the possibility of applying a stochastic approach to quantifying differential settlements (Reitmeier, 1989) while Hanisch and Struck applied the method to evaluate pile loading tests (Hanisch and Struck, 1992).

In addition, there were a number of publications dealing with the evaluation of soil investigations in terms of how the results could be used in connection with the probabilistic approach (Hanisch and Struck, 1985, Soos, 1990, and Alber, 1992) as well as papers in which the new concept was clearly set out and explained to colleagues in the field with the intention of promoting it (Gudehus, 1987 and Franke, 1990).

Even though the future direction of standardization work in geotechnical engineering seemed to have been firmly established by a decision of the steering committee of the national committees in charge of drafting geotechnical engineering standards in 1982, the "Principles for the specification of safety requirements for structures" (Arbeitsausschuß " Sicherheit im Bauwesen", 1981) were repeatedly the subject of fundamental criticisms in the years that followed. Thus Franke (Franke, 1984) demonstrated the problems that occur when the probabilistic safety concept is applied to piles, commenting scathingly that the possibility (of applying the probabilistic approach) was viewed most optimistically by those colleagues who were least involved in conducting soil and rock investigations and describing soil and rock on a daily basis in practice. He went on to say that, in his view, the observation method was a far superior aid even though it is not mentioned in the "Principles for the specification of safety requirements for structures".

Furthermore, it was also shown that, for a constant safety level, the partial factors depend on the magnitude and number of parameters involved and in particular on the coefficient of variation (Heibaum, 1987). However, it is seldom possible to obtain more than only a rough estimate of the coefficient of variation of geotechnical parameters.

Fundamental criticism of the new safety concept was voiced above all by Swiss colleagues. After analysing 800 cases of structural damage that had been described by means of the same criteria and evaluated in different ways, Matousek and Schneider concluded that random deviations of the material properties, the resistances of structures or the loads on structures from the expected values are evidently well covered by the conventional safety concept and by specifying the appropriate safety factors in the structural calculations. The vast majority of cases of damage occur during execution. Matousek and Schneider went on to state that while every care is taken to consider the use of structures at the design stage the construction conditions are often viewed as of secondary importance although they require greater attention (Matousek and Schneider, 1976). Schneider considered the probability of serious errors generally to be far greater (ten- to a hundredfold) than the theoretical probabilities of failure (Schneider, 1994). Vollenweider expressed similar doubts about the safety goal of a very low probability of failure for which only values with a low probability of occurrence are relevant. He questioned whether the statistical data for this range of values, if available at all, was sound and whether the correct distribution laws were applied. Vollenweider spoke out in favour of applying the hazard scenario approach instead to enable the risk potential to be managed more reliably (Vollenweider, 1983 and 1988).

Summing up the scientific studies and the attendant debate up until around 1990 it can be seen that the probabilistic approach in geotechnical engineering yielded a great number of interesting scientific research results and findings in Germany but that it was not yet possible to develop a convincing standardization concept for application in everyday practice. Although the partial safety concept had won through, the probabilistic approach no longer had any part to play during discussions between standards writers on the issue of which parameters partial safety factors should be applied to and what the values of those factors should be. There were only a few isolated voices who continued to advocate taking the probabilistic approach into account in geotechnical engineering standards (Hanisch, 1998).

Although the probabilistic approach was finally abandoned in German geotechnical design standards the subject continued to be attractive in scientific research. Thus Hartmann and Nawari attempted to discover new ways of evaluating uncertainty and risk with the aid of fuzzy logic and the fuzzy set theory (Hartmann and Nawari, 1996), Pöttler et. al. examined the application of the probabilistic approach to tunnel construction (Pöttler et. al., 2001), Ziegler considered the possibilities of risk simulation calculations (Ziegler, 2002), Katzenbach and Moormann used the data collected for Frankfurt clay over many decades to examine the structural performance of piled raft foundations (Katzenbach and Moormann, 2003), Stahlmann et. al. employed probabilistic methods to simulate the inhomogeneities in the soil properties of a railway embankment (Stahlmann et. al., 2007) and Russelli compared various probabilistic methods as applied to investigations of the bearing capacity of soil, demonstrating the great influence of the combination of friction and cohesion (Russelli, 2008). So far, none of these studies has been taken into account in standards or recommendations.

2.4 *Eurocode 7*

Work on the Model Code for Eurocode 7 "Geotechnical design" started in 1981 and was headed by Krebs Ovesen (Orr, 2007) who chaired the committee in charge of the work for 18 years. One of the fundamental ideas was that the Eurocode should only contain qualifying rules, in other words, should require the bearing capacity to be verified but would not specify which method of calculation should be used. Naturally, this improved the likelihood of reaching a consensus on the rules. There were intense discussions on the applicability of the statistical safety concept in the European committee as the original enthusiasm for the probabilistic approach had vanished. It was agreed that, should the probabilistic safety concept be introduced in geotechnical engineering, a great number of difficulties would still need to be overcome and that the partial factors would initially have to be based on experience but would have to be confirmed by probabilistic analyses at a later date (Sadgorski, 1983). The drafts of the Eurocode differentiated between the core text and supplementary comments. Initially there was no intention of specifying numerical values for either the loads or the partial factors in the core text of the Eurocode (Sadgorski, 1983); the values were to be set in National Annexes instead.

In 1987 the "Draft Model for Eurocode 7 – Common unified rules for Geotechnics, Design" was published (Representatives of the Geotechnical Societies within the European Countries, 1987) as a report prepared for the European Communities. The annex of the draft model specified partial factors after all. Reference was made to the relevant loading codes for structures above ground level for variable actions while a partial factor, γ_g, of 1.0 was specified for permanent actions from the structure, ground and groundwater. The following partial factors were given for geotechnical parameters: $\gamma_\varphi = 1.2$ on the tangent of angle of internal friction, $\gamma_{c1} = 1.8$ on the cohesion when verifying the load-bearing capacity of

foundations and γ_{c2} on the cohesion when verifying the stability and earth pressure. Moreover, partial factors were stated for the load bearing resistance of piles and anchors and for structures under construction.

In 1989 "Eurocode 7 Geotechnics" was published as a Preliminary Draft for the European Communities on the basis of the December 1987 version of the Model Code produced by the ISSMFE (EC 7 Drafting Panel, 1989). A chapter 7 for piles and a chapter 8 for retaining structures had not yet been prepared. This version now gave numerical values for partial factors in the core text and it was emphasized in the preface that "they represented the best estimate of the drafting panel. In geotechnical engineering limited experience has been gained until now on a European basis on the use of limit state design and partial safety factors. Consequently there is a strong need for calibration of all safety elements introduced into the draft before it is issued for use". In Chapter 2 "Basis of Design" it was stated as a fundamental requirement that: "(1) A structure shall be designed and constructed in such a way that: - with acceptable probability, it will remain fit for the use …., and – with appropriate degrees of reliability, it will sustain all actions ....". However, neither principles nor application rules were given for the derivation of partial factors on actions and ground parameters by means of reliability theory.

A first complete version of Eurocode 7 was published in 1994 as prestandard ENV 1997-1:1994 "Geotechnical design - Part 1 General rules". For the verification of ultimate limit states in the ground two combinations of partial factors had to be investigated: Case B and Case C. Case B aimed to provide safe design against unfavourable deviations of the actions from their characteristic values. Thus, in Case B, partial factors greater than 1.0 were applied to the permanent and variable actions from the structure and the ground, the factors being the same as those used in other fields of structural engineering. By contrast, the calculations of the ground resistance were performed with characteristic values, i.e. the partial factors for the shear parameters, γ_φ, γ_c and γ_{cu}, were all set at 1.00. Case C in the prestandard aimed to provide safe design against unfavourable deviations of the ground strength properties from their characteristic values and against uncertainties in the calculation model. It was assumed that the permanent actions corresponded to their expected values and the variable actions deviated only slightly from their characteristic values. Thus, the partial factors for the characteristic values of the ground strength parameters were $\gamma_\varphi = \gamma_c = \gamma_{cu} = 1.25$ while the characteristic values of the permanent actions from the structure (with γ_G set at 1.00) were used in the verification.

This concept for the verification of two cases, A and B, was strongly opposed in Germany. The philosophy for Cases B and C was not convincing because it could not guarantee a sufficient safety level for the combination or superposition of the uncertainties of the material properties (soil and other material) and the actions. Furthermore, there were strong objections to the mandatory application of partial factors to the ground strength properties φ', c' and c_u in order to determine the design values of the resistances of the soil. Although this corresponded to German practice for the verification of slope stability, in which the Fellenius method was applied, it was not the case for the verification of the design of shallow foundations and retaining walls. The application of partial factors to the ground strength properties would have resulted in some cases in larger dimensions and in others in smaller dimensions than would have been obtained if the former global safety concept had been applied (Weißenbach, 1991). Moreover, with factored shear strength parameters, the relevant verification would be based on non-reliable failure geometries in the ground. A more detailed critical review and a proposal for an improvement of the prestandard of EC 7 can be found in Schuppener et. al. (1998) and Weißenbach (1998).

These fundamental criticisms were shared by many other European countries. As a compromise, the final version of EC 7 of 2004 (CEN 2004) gives three design approaches (DA) as options. Each Member States has to establish in its National Annex to EC 7 which of the three DA is mandatory for which limit state verification. Among these three approaches, only DA2 without factored shear strength parameters of the ground avoids the above-mentioned drawbacks.

2.5 *DIN 1054 "Safety in Earthworks and Foundation Engineering"*

The steering committee of the national committees in charge of drafting geotechnical engineering standards decided in 1982 to gradually incorporate the new safety concept into the standards for that field (Gudehus, 1987). It was even decided to prepare a Guidance Paper on Reliability in Geotechnical Design. A new standardizing committee "Safety in Earthworks and Foundation Engineering" was established. Its aim was to act as a mirror committee for the European subcommittee drafting Eurocode 7 "Geotechnical Design" (EC 7) and revise the German standard DIN 1054 with the new title "Safety in Earthworks and Foundation Engineering" to make it compatible with the principles and application rules of the future Eurocode 7.

The first draft of the revised DIN 1054 "Safety in Earthworks and Foundation Engineering" (Deutsche Gesellschaft für Erd- und Grundbau, 1990) was circulated as a draft for discussion at the German National Geotechnical Conference. It was stated in the foreword that: "In spite of a great deal of research work it has not been possible to find an indisputable scientific basis for specifying even a few of the partial factors. Although adapting the specifications to take account of tried-and-tested methods of verifying safety was seen as a way around the problem, it constituted a deviation from the aim of the 'Principles for the establishment of safety requirements for structures'". As in the 1989 version of the Eurocode, the design values of the actions and resistances of the soil were determined by applying partial factors to the geotechnical parameters, i.e. $\gamma_\varphi = \gamma_\delta = 1.20$ for friction and wall friction and $\gamma_c = 1.70$ for cohesion. Depending on the load case and application, the factors had to be increased or reduced by γ^μ, with $0{,}5 \geq \mu \leq 1{,}4$.

Weißenbach demonstrated in his study (Weißenbach, 1991) that, for retaining walls, there are numerous cases in which greater dimensions are required given the above conditions but that there are also instances in which smaller dimensions are obtained than with the former global safety concept. The reason for this is that it is not possible to maintain a constant safety level if a partial factor is applied to the coefficient of friction, tan φ. For example, there is a lower reduction in the coefficient of active earth pressure for small angles of shearing resistance than for large ones. Moreover, the introduction of a partial factor, γ_φ, on the angle of shearing resistance means that the failure pattern geometry is no longer realistic so that loads that were previously outside the soil mass under consideration are now inside it, with the result that different loads are determined than previously. In addition, it is not possible to determine an earth pressure load for slopes inclined at angles between $\beta = \varphi'_d$ and $\beta = \varphi'_k$. In order to eliminate such inconsistencies, Weißenbach proposed determining the characteristic actions and resistances from the characteristic values of the soil parameters first and then applying the partial factors to the resultant values. The values of the partial factors would then have to be specified in such a way that the former safety level was maintained. A further advantage of this method was that it enabled not only the ultimate limit state but also the serviceability limit state to be verified using the characteristic values (Weißenbach's concept).

The following version of DIN 1054-100 (1996) thus included partial factors on the characteristic forces for both the actions and resistances of the soil in analyses of the stability of retaining walls, shallow foundations, piles and anchors (Load and Resistance Factor Approach). Partial factors were only applied to the shear strength of the soil in the analysis of the stability of slopes (Material Factor Approach).

The idea behind revising DIN 1054 at the same time as Eurocode 7 was being drafted was to familiarize German geotechnical engineers with the new design concepts as early as possible and to enable them to make technically sound contributions to the discussions held during the process of writing the Eurocode. In doing so, it was quite clear that it would no longer be possible for Eurocode 7 and DIN 1054 to apply side-by-side in future. The current version of DIN 1054 (2010) therefore only contains specifically German rules, which are not given in Eurocode 7 (CEN, 2004). The title of the DIN standard has been amended accordingly to "Subsoil – Verification of safety of earthworks and foundations – Supplementary rules to DIN EN 1997-1".

3 CONCLUSIONS

3.1 *Reliability theory*

The objectives of the new probabilistic safety concept covering all areas of structural design in Europe were essentially as explained below:

1. The concept aimed primarily at achieving a consistent probability of failure for all structural members by means of a probabilistic safety concept in which designs are based on a known stochastic distribution of the magnitudes of the actions and the mechanical properties of construction materials. It was clear from the outset that a comprehensive "level II" probabilistic verification would only be feasible in exceptional cases, on account of the great deal of time and effort required, and in fundamental design analyses. Therefore, for the day-to-day work of structural engineers, it was planned to use "level I" design methods employing partial safety factors with values derived from comprehensive probabilistic analyses of each limit state.

2. For the application of the concept in practice and its implementation in European design standards it was also desirable for the same numerical values of the partial factors on the actions to be used in all fields of structural design. It was intended for the partial factors for the resistances of the various materials to be derived from the stochastic distribution of the mechanical properties.

3. Moreover, designs based on the new safety concept should only be permitted to result in greater dimensions than those achieved with the global safety concept of previous standards in well-founded exceptional cases. Any appreciable reduction in the safety level compared with the previous one would have met with objections by the building inspectorates.

The discussion very soon revealed that it would not be possible for all three of those demands to be incorporated into a geotechnical design concept suitable for inclusion in standards. The greatest problems lay in the consistent implementation of the probabilistic approach. The studies and discussions conducted by the standards committees over the years showed that the data required for a sufficiently reliable statistical description of the soil parameters in practice was only available in exceptional cases and that, even then, it was not always possible to achieve a sufficiently consistent safety level for the ground strength properties. The probabilistic approach was therefore no longer taken as a basis for specifying partial factors for geotechnical engineering in national and European standardization work. The original probabilistic approach has only been retained in EC 7 for the purpose of specifying the characteristic values of the ground properties (CEN, 2004) and as informative Annex C in "Eurocode - Basis of structural design" (CEN, 2002). The probabilistic approach may have been a psychological aid and provided the initial spark for the work of harmonizing the numerous national concepts during the drafting of the European construction standards but it became clear during the discussions that it was not a suitable means of describing the safety and reliability of structures in standards. In ISO 2394 (1998) "General principles on reliability for structures", however, the principles of probability-based design are still covered in the core text and in an informative annex.

3.2 *Partial factors*

Germany has a tradition of standards for geotechnical engineering that dates back more than 70 years. The first edition of DIN 1054, entitled *Guidelines for the permissible loads on ground in building construction,* was published in 1934. Since then, geotechnical standards have continuously been optimized and have reached an outstanding quality. The safety level of the former global safety concept proved successful and the specified safety factors made safe and economic geotechnical designs possible. The Advisory Board of the Standards Committee for Building and Civil Engineering of the German Standards Institute, DIN, therefore decided in 1998 that any increase in cost as a result of new standards had to be justified. As the existing standards were well tried and tested, it was decided that the safety level of the former global safety concept should be maintained when the geotechnical standards were adapted to accommodate the partial safety factor concept of the Eurocodes. This meant that the design approaches and the partial factors had to be selected in such a way that a foundation designed according to EC 7 would have roughly the same dimensions as a design in accordance with the previous standards. This was a prerequisite as serious problems regarding the acceptability of the Eurocodes would otherwise have arisen. For example, a structure undergoing modification might need strengthening or even underpinning according to the new safety concept, although this may not have been necessary under the previous one. As reliability theory was not considered to provide partial factors for ground resistance and ground properties, maintaining the safety level of the former global safety concept was also a necessary assumption for the determination of the partial factors for geotechnical actions and resistances. In order to maintain that safety level in the concept of partial factors the equation $\gamma_R \cdot \gamma_{G/Q} \approx \eta_{global}$ must be fulfilled, where γ_R is the partial factor for the resistance of the ground, $\gamma_{G/Q}$ is a weighted mean partial factor for the effects of permanent and variable actions and η_{global} is the global safety factor used hitherto. The values recommended in Annex A of "Eurocode - Basis of structural design" (CEN, 2002), which are $\gamma_G = 1.35$ and $\gamma_Q = 1.50$ for the permanent and variable effects of actions respectively, were adopted in EC 7 and in German geotechnical design standards as they had been in the other fields of structural engineering. As the permanent actions are generally greater than the variable actions in geotechnical engineering, a weighted mean value, $\gamma_{G/Q}$, of 1.40 was used to calculate the partial factor for the ground resistance, γ_R, for the various verifications. Thus the following partial factor, γ_R, for the resistance is obtained from $\gamma_R \approx \eta_{global} / \gamma_{G/Q}$. For the ground bearing resistance, where a global safety factor η_{global}, of 2.00, was used in Germany we then arrive at a partial factor of $\gamma_{R,v} = 2.00/1.40 \approx 1.40$. The partial factors for the ground resistance in each limit state were determined in this way.

The numerical values of the partial factors for actions have been specified by structural engineers and it is therefore certainly debatable whether they provide a realistic description of the uncertainties in geotechnical engineering. Yet SC 7 and the national German standards committee for geotechnical engineering considered it more important for common partial factors to be used in all fields of civil engineering in

future than for specific partial factors to be laid down for geotechnical design, especially as selecting the values would also have given rise to endless discussions.

However, several problems arose in geotechnical engineering. As is generally known, the global safety factors for geotechnical engineering differ from those used in the design of concrete, masonry and steel structures, some of the factors being lower (safety against sliding and overall slope stability) while others are higher (bearing capacity of the soil). If the partial factors for unfavourable permanent actions, γ_G = 1.35, and variable actions, γ_Q = 1.50, which were originally set for the design of concrete, masonry and steel structures, are applied to verifications of the safety against sliding, for which high variable horizontal loads frequently need to be analysed, most of the safety on the loads is already utilized if the mean partial factor γ_{G+Q} is greater than 1.40. A partial factor on the resistances, e.g. on the shear parameters, would result in greater dimensions for foundations than previously when the design was performed with a global safety factor, η, of 1.50. For the verification of the safety against sliding, a partial factor, γ_{Sl}, of 1.10 has therefore been applied to the resistances (base friction and the passive earth pressure in front of foundations, as appropriate) instead of the shear parameters and it has been taken into account that greater dimensions will be required for foundations than in the past if high levels of variable actions are expected to occur.

The verification of overall slope stability, for which a global safety, η, of 1.40 used to be required, is even more difficult. If, in this case, the partial factor γ_Q = 1.50 were applied to variable actions and γ_G = 1.50 to the loads from the self-weight of the ground, a partial factor, γ, greater than 1.0 on the shear parameters or the resistances of the ground would result in a considerably less economic design than was previously the case. It is for this reason that the partial factors γ_G = 1.0 for the permanent actions, γ_Q = 1.30 for the variable actions and, for the resistances, $\gamma_\varphi = \gamma_c = \gamma_{cu}$=1.25 for the shear parameters were recommended for the verification of overall slope stability in Eurocode 7.

3.3 *Critical remarks on the safety concept of the Eurocodes and Eurocode 7*

The introduction of the partial safety concept provided a common format for analyses in structural design for different types of construction and construction materials. However, a common safety level, in terms of a common probability of failure, has not been achieved, even if very similar partial factors have been introduced for the actions in all areas of structural design. As explained above, these partial factors have also been adopted in geotechnical engineering, with no attempt being made to develop separate partial factors for geotechnical actions. Thus they are not – as was originally planned – a measure of the reliability with which the magnitude of geotechnical actions can be determined. The same applies to the partial factors for the resistances as they were derived on the basis of the condition that approximately the same dimensions for foundations should be obtained for designs in accordance with the partial safety concept as for those performed with the former global safety concept. Thus, in actual fact, the partial safety concept is also a global safety concept. The incorporation of the new concept into all German geotechnical engineering standards and recommendations has meant that these have been harmonized and thus become more user-friendly. Any technical progress was only an indirect consequence owing to the fact that the German standards and recommendations were, of course, brought up to date and improved as they were being revised to include the partial safety concept.

Eurocodes do not take account of human error, nor are such errors mentioned in the definitions of the partial factors. Instead, all Eurocodes have a list of assumptions which define and make sure that everything is planned, executed, supervised and maintained according to the plans by personnel having the appropriate skill and experience. Although human error was never explicitly referred to in the standards based on the global safety concept it was implicitly assumed that it was covered, at least to a certain extent, by the safety factors. The objective was always to achieve a robust yet economic design that would not fail just because of a few minor errors. The adoption of the safety level of the previous standards has thus meant that “minor” human errors are now included in the partial factors.

4 SUMMARY AND OUTLOOK

The attempt to introduce a probabilistic approach into geotechnical design standards has failed as, in practice, the data required for a sufficiently reliable statistical description of the ground strength properties is only available in certain exceptional cases and, even then, the design calculations required are so time-consuming that they are not (yet) suitable for inclusion in standards. The approach has therefore only been retained for the specification of the characteristic values of the ground strength properties in

EC 7 and as the informative Annex C “Basis for partial factor design and reliability analyses” in “Eurocode - Basis of structural design”. The introduction of the ψ-factors to take account of variable actions that occur simultaneously can also be viewed as a pragmatic application of the probabilistic approach.

Reliability Based Design lacks a way of taking account of human error. The Eurocodes do not take account of human error either. However, the latter is covered, at least to a certain extent, by calibrating the partial factors to comply with the level of the former tried-and-tested global safety concept.

There is general agreement amongst experts that human error presents the greatest risk in building and civil engineering as a whole and that reducing it would be the most effective way of improving safety in this field. The authors therefore believe that, in future, the incorporation of the hazard scenario approach (Vollenweider, 1983, SIA 260:2003 and SIA 267:2003) or risk simulation calculations (Ziegler, 2002) into geotechnical engineering standards would be more appropriate, especially as the theories behind them are closer to engineering practice. However, in this context, the supervision of the execution of structures by building inspectorates or test engineers is particularly important. Unfortunately, the opposite path has been taken by the political powers that be and evidence of its adverse effects can already be seen.

REFERENCES

Alber, D. (1992): Überlegungen und Verfahren zur Schätzung statistischer Parameter von Bodenkennwerten, Bauingenieur 67 (1992), S 39 - 45.

Arbeitsausschuss „Sicherheit im Bauwesen“, (1981): Grundlagen für die Festlegung von Sicherheitsanforderungen für bauliche Anlagen (Principles for the establishment of safety requirements for structures), Beuth Verlag, Berlin

Blaut, H. (1982): Diskussionsbeitrag bei der Podiumsdiskussion zur Spezialsitzung „Sicherheit im Grundbau“ Vorträge der Baugrundtagung, Braunschweig

Breitschaft, G. and Hanisch, J. (1978): Neues Sicherheitskonzept im Bauwesen aufgrund wahrscheinlichkeitstheoretischer Überlegungen – Folgerungen für den Grundbau unter Einbeziehung der Probennahme und der Versuchsauswertung, Vorträge der Baugrundtagung in Berlin, Deutsche Gesellschaft für Erd- und Grundbau, Eigenverlag, [Reference text]

CEN (2002) Eurocode: Basis of structural design. European standard, EN 1990: 2002. European Committee for Standardization: Brussels.

CEN (2004) Eurocode 7 Geotechnical design - Part 1: General rules. Final Draft, EN 1997-1:2004 (E), (F) and (G), November 2004, European Committee for Standardization: Brussels, 168 pages (E).

Deutsche Gesellschaft für Erd- und Grundbau (DGEG) (1987): Final comments and suggestions on the Draft Model Code for Eurocode 7

Deutsche Gesellschaft für Erd- und Grundbau (DGEG), editor (1990): Normentwurf DIN 1054 „Sicherheitsnachweise im Erd- und Grundbau“, Diskussionsvorlage zur Baugrundtagung 1990. Spezialsitzung Normung

Deutsches Institut für Bautechnik (DIBt) (1984): Deutsche Übersetzung der Abschnitte 1 und 2 des EC 7, Geotechnik 1984/7, S 189-195

DIN 1054-100 (1996): Subsoil – Verification of the safety of earthworks and foundations – Analysis in accordance with the partial safety concept, Beuth Verlag, Berlin

DIN 1054 (2010): Subsoil – Verification of the safety of earthworks and foundations – Supplementary rules to DIN EN 1997-1, Beuth Verlag, Berlin

Representatives of the Geotechnical Societies within the European Countries (1987): Draft Model for Eurocode 7 – common unified rules for Geotechnics, Design.

EC 7 Drafting Panel (1989): Eurocode 7 Geotechnics, Preliminary Draft for the European Communities, Geotechnik 13 (1990), S 1-40

Eder, F. (1983): Erläuterung des Statistischen Sicherheitskonzepts am Beispiel einer Rutschung, Buchkapitel in: Mitteilungen des Instituts für Bodenmechanik, Felsmechanik und Grundbau, TU Graz, Nr.6

Franke, E. (1984), Einige Anmerkungen zur Anwendbarkeit des neuen Sicherheitskonzepts im Grundbau, geotechnik, Jg.7, Nr.3, S.144-149

Franke, E. (1990): Neue Regelung der Sicherheitsnachweise im Zuge der Europäischen Bau-Normung - Von der deterministischen zur probabilistischen Sicherheit auch im Grundbau? Bautechnik 7/1990

Gässler, G. (1982): Anwendung des statistischen Sicherheitskonzeptes auf verankerte Wände und vernagelte Wände, Vorträge der Baugrundtagung, Braunschweig, S 49 – 81

Genske, D.D. und Walz, B. (1987): Anwendung der probabilistischen Sicherheitsphilosophie auf Grundbruchberechnungen nach DIN 4017, geotechnik 10, S 53 – 66

Gudehus, G. (1987): Sicherheitsnachweise für Grundbauwerke , Geotechnik 10, S. 4-34

Hanisch, J. und Sadgorski, W. (1984): Die Sondersitzung zum Eurocode 7 Geotechnik 1984/7, S 182 - 189

Hanisch, J. und Struck, W. (1992): Betrachtungen zur Ermittlung der Sicherheitsbeiwerte für Pfahlbelastungen aus Stichprobenergebnissen und zusätzlichen Informationen, Geotechnik 1992, S 138 ff

Hanisch, J. und Struck, W. (1985): Charakteristischer Wert einer Boden- oder Materialeigenschaft aus Stichprobenergebnissen und zusätzlicher Information, Bautechnik 10/1985

Hanisch, J. (1998): Ist der EUROCODE 7 noch zu retten? - Wird der EC 7 zur Hilfe oder zur Bremse bei der Beurteilung der Zuverlässigkeit neuer Bauarten? Bautechnik 9/1998

Hartmann, R., Nawari, O. (1996): Ansatz der Fuzzy-Logik und –Set Theorie in der Geotechnik – neue Wege zur Unsicherheits- und Risikobewertung. Vorträge der Baugrundtagung in Berlin, Deutsche Gesellschaft für Erd- und Grundbau, Eigenverlag

Hasofer, A.M., Lind, N.C. (1974): An exact and invariant first order reliability format. Journal of Engineering Mechanics Division, ASCE, 100 (EM1), 1974, pp. 111-121

Heibaum, M. (1987): Zur Frage der Standsicherheit verankerter Stützwände auf der tiefen Gleitfuge, Darmstadt; Mitteilungen des Instituts für Grundbau, Boden- und Felsmechanik, Heft 27

ISO 2394 (1998): "General principles on reliability for structures", International Organization for Standardization, Case postale 56, CH-1211 Genève 20, Switzerland

Joint-Committee on Structural Safety (1976): Common unified Rules for Different Types of Construction and Material, Comité-Euro-International du Beton (CEB), Bulletin d´ínformation No 116 E

Katzenbach, R., Moormann, C. (2003): Überlegungen zu stochastischen Methoden in der Bodenmechanik am Beispiel des Frankfurter Tons, Heft 16 der Gruppe Geotechnik, Technische Universität Graz, pp 255-282

Kramer, H. (1982): Diskussionsbeitrag bei der zur Spezialsitzung „Sicherheit im Grundbau" Vorträge der Baugrundtagung 1982, Braunschweig

Lackner, E. (1982): Diskussionsbeitrag bei der zur Spezialsitzung „Sicherheit im Grundbau" Vorträge der Baugrundtagung 1982, Braunschweig

Lumb, P. (1970): Safety factors and the probabilistic distribution of soil strength, Canadian Geotechnical Journal, 7, 225-242

Matousek, M. und Schneider, J. (1976): Untersuchungen zur Struktur des Sicherheitsproblems bei Bauwerken, Bericht Nr. 59 aus dem Institut für Baustatik und Konstruktion ETH Zürich, Basel und Stuttgart: Birkhäuser Verlag

Orr, T. (2007): The Story of Eurocode 7, Spirit of Krebs Ovesen Session, European Conference on Soil Mechanics and Geotechnical Engineering, Madrid, 2007

Peintinger, B. (1982): Auswirkung der räumlichen Streuung von Bodenkennwerten, Vorträge der Baugrundtagung Braunschweig,1982, S 105 – 117

Pöttler, R.; Schweiger, H.F.; Thurner, R. (2001): Probabilistische Untersuchungen für den Tunnelbau – Grundlagen und Berechnungsbeispiel, Bauingenieur - Ausgabe 03-2001, S. 101

Pottharst, R. (1982): Erläuterung des statistischen Sicherheitskonzepts am Beispiel des Grundbruchs, Vorträge der Baugrundtagung, Braunschweig, S 9 – 47

Rackwitz, R. und Peintinger, B., (1981), Ein wirklichkeitsnahes stochastisches Bodenmodell mit unsicheren Parametern und Anwendung auf die Stabilitätsuntersuchung von Böschungen, Bauingenieur 56, 215 – 221

Rackwitz, R. (1982): Können Vorinformationen über den Baugrund quantifiziert werden? Vorträge der Baugrundtagung 1982, Braunschweig, S 83 – 104

Reitmeier, W. (1989): Quantifizierung von Setzungsdifferenzen mit Hilfe einer stochastischen Betrachtungsweise, Lehrstuhl und Prüfamt für Grundbau, Bodenmechanik und Felsmechanik der Technischen Universität München, Schriftenreihe Heft 13

Sadgorski, W. (1983): Neues vom Eurocode 7, Geotechnik 6, S 107 – 110

Schneider, J. (1994): Sicherheit und Zuverlässigkeit im Bauwesen, B. G. Teubner Verlag, Stuttgart

Schuppener, B., Walz, B., Weißenbach, A. and Hock-Berghaus K. (1998): EC7 – A critical review and a proposal for an improvement: a German perspective, Ground Engineering, Vol. 31, No. 10

SIA 260:2003 „Grundlagen der Projektierung von Tragwerken", Editor: Schweizerischer Ingenieur- und Architektenverein (2003) Postfach, CH-8039 Zürich

SIA 267:2003 „Geotechnik", Editor: Schweizerischer Ingenieur- und Architektenverein, Postfach, CH-8039 Zürich

Smoltczyk, U. (1982): Diskussionsbeitrag bei der zur Spezialsitzung „Sicherheit im Grundbau" Vorträge der Baugrundtagung, Braunschweig

Smoltzcyk, U. und Schad, H. (1990): Zur Diskussion der Teilsicherheitsbeiwerte für den Grundbruchnachweis, Geotechnik 13 (1990) S 41-43

Stahlmann, J.; Schmitt, J.; Fritsch, M. (2007): Anwendung probabilistischer Methoden zur Simulation der stofflichen Inhomogenitäten des Untergrunds in der Geotechnik, Bauingenieur - Ausgabe 5/2007, S. 214-223

Vollenweider, U. (1982): Diskussionsbeitrag bei der zur Spezialsitzung „Sicherheit im Grundbau" Vorträge der Baugrundtagung, Braunschweig

Vollenweider, U. (1983): Denkanstöße im Grundbau oder die Lösung grundbaulicher Probleme mittels Gefährdungsbildern, Schweizer Ingenieur und Architekt, 7/83

Vollenweider, U. (1988): Gedanken zur Sicherheit im Grundbau, Schweizer Ingenieur und Architekt Nr. 39, S 1069-1075

von Soos, P. (1982): Zur Ermittlung der Bodenkennwerte mit Berücksichtigung von Streuung und Korrelationen, Vorträge der Baugrundtagung 1982, Braunschweig, S 83 – 104

von Soos, P.: (1990), Die Rolle des Baugrunds bei der Anwendung der neuen Sicherheitstheorie im Grundbau, geotechnik 13 (1990), S, 82-91

Weißenbach, A. (1991): Diskussionsbeitrag zur Einführung des probabilistischen Sicherheitskonzepts im Erd- und Grundbau, Bautechnik 68, Heft 3 S 73-83 (1991)

Weißenbach, A. (1998): Umsetzung des Teilsicherheitskonzepts im Erd- und Grundbau, Bautechnik 9/1998

Ziegler, M. (2002): Risikosimulationsrechnung – eine Möglichkeit zur Quantifizierung von Sicherheit und Risiko in der Geotechnik, Vorträge der Baugrundtagung in Mainz, Deutsche Gesellschaft für Erd- und Grundbau, Eigenverlag

ISGSR 2011 - Vogt, Schuppener, Straub & Bräu (eds) - © 2011 Bundesanstalt für Wasserbau ISBN 978-3-939230-01-4

Findings from the 2nd Set of Eurocode 7 Design Examples

T. L. L. Orr
Trinity College Dublin, Ireland

A. J. Bond
Geocentrix Ltd, Banstead, UK

G. Scarpelli
University of Ancona, Italy, UK

ABSTRACT: In April 2010 the 2nd International Workshop on the Evaluation of Eurocode 7 was held in Pavia, Italy. This Workshop was organised by ETC 10 and the SC7 Maintenance Group. In preparation for the Workshop, a set of six design examples was prepared and published on a website together with online questionnaires for each example. These examples were completed by geotechnical engineers from different European countries using the partial factors in their own National Annexes and submitted online. Whereas the design examples for the 1st International Workshop held in Dublin in 2005 provided the characteristic parameter values, the design examples for the 2nd International Workshop held in Pavia did not but provided instead the results of the geotechnical investigations for each example. These included field and laboratory tests and required the characteristic values to be selected from this geotechnical information. Reviewers were appointed to evaluate the designs submitted for each example and to report to the Pavia Workshop on the designs received. This paper presents an overview of the findings from the second set of Eurocode 7 design examples. These findings are compared with the findings from the first set of design examples for the Dublin Workshop and assessed in the light of the implementation of Eurocode 7 in Europe in 2010.

Keywords: Eurocode 7, Pavia Workshop, design examples, limit states, confidence

1 INTRODUCTION

1.1 *Eurocode 7 Workshops*

The 1st International Workshop on the Evaluation of Eurocode 7, organised by European Technical Committee 10 (ETC 10) of the International Society for Soil Mechanics and Geotechnical Engineering and the European Geotechnical Thematic Network, Geotechnet, was held in Dublin in 2005 and a volume of Workshop Proceedings was published (Orr, 2005). Since in April 2010, the suite of Eurocodes, with Eurocode 7 for Geotechnical Design, superseded the existing national standards for structural and geotechnical design in the 26 CEN (European Standardization Committee) member countries it was appropriate that the 2nd International Workshop was held in the EUCENTRE in Pavia, Italy in April 2010. This Workshop was organized by ETC 10 together with the Maintenance Group of the CEN committee for Eurocode 7, TC 250/SC7 – Geotechnical Design. The main findings from the examples presented at this Workshop are reviewed in this paper based on the draft Proceedings (due to be published later).

1.2 *Dublin Workshop*

Prior to the Dublin Workshop in 2005, a set of 10 geotechnical design examples involving the design situations shown in Table 1 were circulated by email to engineers in Europe and worldwide. The characteristic values of the parameters were provided for the engineers to obtain solutions for the examples in accordance with Eurocode 7. A total of 90 solutions were received from engineers from 11 countries, including some solutions from Japanese engineers, who carried out the designs using Japanese codes and reliability analyses. The finding from the reliability analyses are not discussed in this paper but a paper on them will be included in the Workshop Proceedings.

Table 1. Details of Eurocode 7 design examples

Examples	Design situation	Required parameter	Reporter(s)
1st Set			
1	Spread foundation, vertical central load	*B* – foundation width	G. Scarpelli & V. Fruzzetti
2	Spread foundation, inclined eccentric load	*B* – foundation width	G. Scarpelli & V. Fruzzetti
3	Pile foundation from parameter values	*L* – pile length	R. Frank
4	Pile foundation from load test results	*N* – number of piles	R. Frank
5	Gravity retaining wall	*B* – wall base width	B. Simpson
6	Embedded retaining wall	*D* – embedment depth	B. Simpson
7	Anchored retaining wall	*D* – embedment depth	B. Simpson
8	Uplift of a deep basement below GWL	*T* – slab thickness	T. Orr
9	Heave of an excavation due to seepage	*H* – hydraulic head	T. Orr
10	Embankment on soft ground	*H* – embankment height	U. Bergdahl
2nd Set			
2.1	Spread foundation, vertical central load	*B* – foundation width	J. Brito & C.S. Sorensen
2.2	Spread foundation, inclined eccentric load	*B* – foundation width	N. Vogt
2.3	Pile in clay	*L* – pile length	A. van Seters
2.4	Earth and water pressures on basement wall	*d* – depth of groundwater behind wall	H.R. Schneider
2.5	Embankment on soft peat	*H* – embankment height (initial stage)	E.R. Farrell
2.6	Pile in sand (from parameter values)	*L* – pile length	B. Kłosiński

Reports on the solutions submitted to the first set of examples were prepared by the reporters listed in Table 1 and are included in the Proceedings of the Dublin Workshop (Orr, 2005). A large scatter was obtained for some of the examples, particularly for the eccentrically loaded foundation, the pile designed from soil parameters, and the uplift example. However, the reporters concluded that the scatter in the solutions when using Eurocode 7 was generally within the range of scatter obtained when using the different national standards and was more due to using different calculation models and design assumptions, which are not specified in Eurocode 7, than to different interpretations of Eurocode 7 or using the different Design Approaches.

1.3 *Pavia Workshop*

In geotechnical designs, there are three main components that affect the resulting design: the geotechnical parameter values, the calculation model, and the safety factors. In practice, these factors are often moderated by the designer's experience. In the first set of examples, the characteristic values were provided, so the variation in the designs received were due to the calculation models used and the partial factors chosen, which in the case of designs to Eurocode 7 means the particular Design Approach, and how it is applied. In the second set of design examples, the raw geotechnical data was provided rather than the characteristic values and hence the authors first had to determine the characteristic parameter values before calculating design values. This made these examples more realistic and also made it possible to investigate how much of the scatter in the designs received was due to the selection of characteristic values and how much was due to the choice of calculation model and adoption of a particular Design Approach and set of partial factors.

The second set of 6 geotechnical design examples, prepared for Pavia, are listed in Table 1. Besides providing raw data rather than characteristic parameter values, the second set of design examples differed from the first set in another way; the examples were placed on a website (www.eurocode7.com/etc10) and engineers were invited to submit their solutions via an online questionnaire comprising about 20 questions. The questions were circulated widely in Europe and also worldwide, and while almost 100 solutions were received, it was disappointing that 78% came from just four countries – Poland, UK, Germany and Italy – and the remaining 22% came from only six countries – Greece, Netherlands, France, Japan, Ireland, and Portugal. As in the case of the first set of examples, the solutions received for the second set were reviewed by the reporters listed in Table 1, who made presentations on their findings during the Pavia Workshop (these will be reported in the Workshop Proceedings).

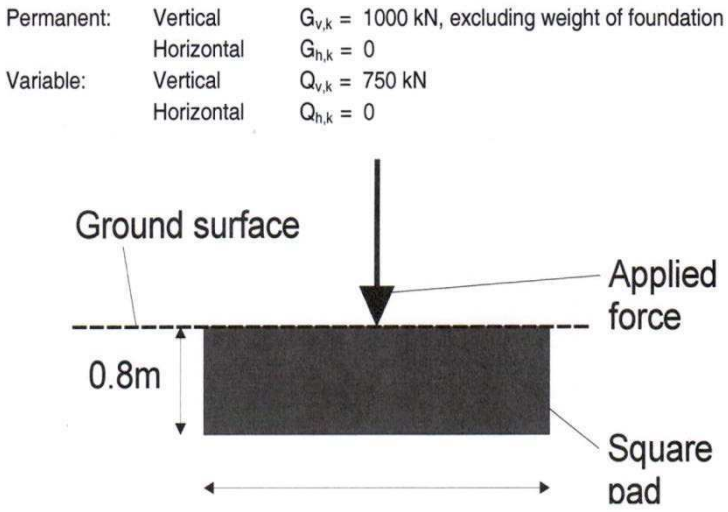

Figure 1. Example 2.1 Pad foundation on dense sand design situation

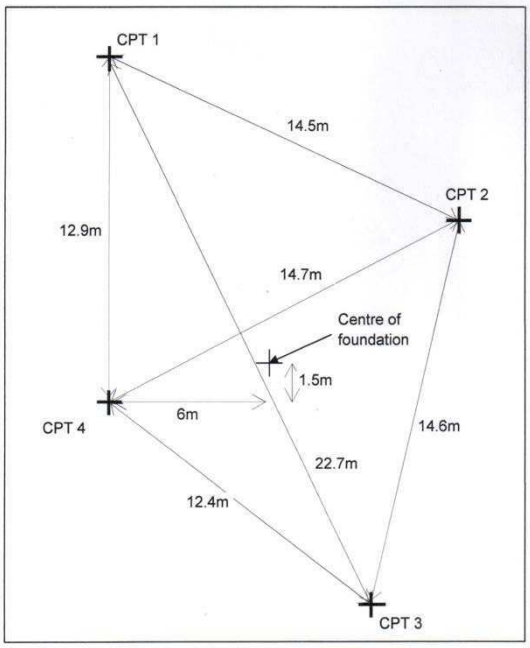

Figure 2. Example 2.1 site plan and borehole locations

2 SECOND SET OF DESIGN EXAMPLES

2.1 *Example 2.1 – Pad Foundation with Vertical Central Load on Dense Sand*

The first of the second set of examples was to determine the width of the square pad foundation shown in Figure 1 supporting a vertical central permanent load of 1000kN and a vertical variable load of 750kN, no horizontal load, and founded on a dense sand stratum. The geotechnical data provided were obtained from CPT tests carried out in four boreholes located on the site with respect to the centre of the foundation as shown in Figure 2. The q_c values measured in the CPT tests are plotted in Figure 3.

Brito and Sorensen (2010), in their presentation on this example, noted that the respondents gave no special weighing to any particular borehole or set of CPT results. They also noted that there two are main interdependent tasks to be considered in most geotechnical design problems when selecting geotechnical parameter values: one is to divide the soil into a few well defined homogeneous layers and the other is to select appropriate geotechnical parameter values for each layer, which for designs to Eurocode 7 are characteristic values. The characteristic values selected by the respondents are plotted in Figure 3, showing that the respondents selected a wide range of $q_{c,k}$ values from close to the mean of the test results down to below a lower bound value. When selecting the characteristic E values, the respondents selected an even greater range of values.

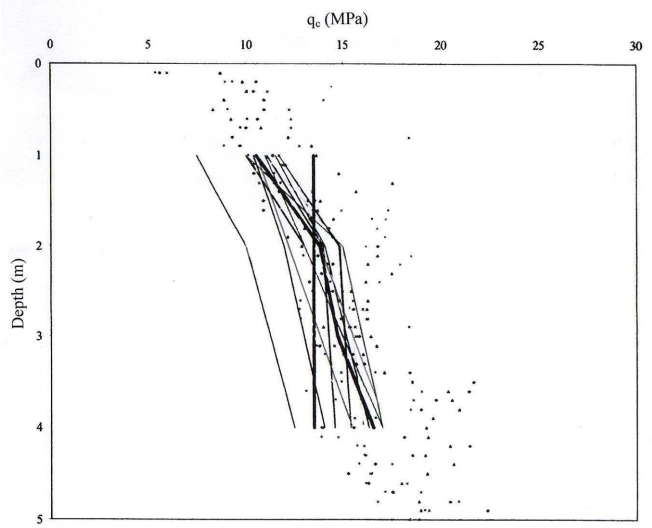

Figure 3. Example 2.1 measured q_c and selected $q_{c,k}$ v. depth

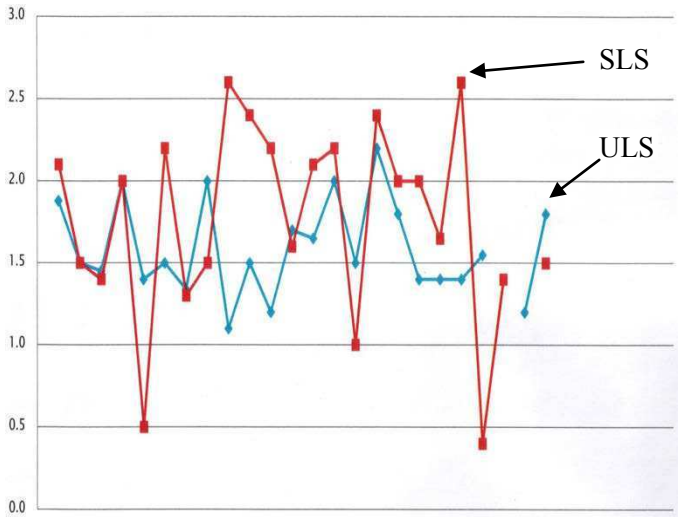

Figure 4. Example 2.1 ULS and SLS design foundation widths

With regard to the calculation model for ULS design, about half (48%) of the respondents used the bearing resistance equation in Annex D of EN 1997-1, a quarter (24%) used other equations from their National Annexes and the other quarter (28%) used other bearing resistance equations, such as Brinch Hansen's.

With regard to the method to estimate settlement, over half (59%) used either or Annex D.3 of EN 1997-2Annex F.1 of EN 1997-1. The Design Approach chosen by the respondents reflects the DA adopted in their National Annex with the result that those from Portugal, Italy and the UK chose DA1; those from Greece, France, Germany, and Poland chose DA2; those from Denmark and the Netherlands chose DA3; and of the two results from Ireland, one used DA1 and the other DA2.

The design foundation widths for ULS and SLS conditions obtained by the respondents are plotted in Figure 4. The ULS widths ranged from 1.1m to 2.3m with an average value of 1.6m, while the SLS widths ranged from 0.5 to 2.6m with an average value of 1.8m. Thus there was much more variability in the SLS design widths than in the ULS widths reflecting the greater number of calculation models used and the wide range of E_k values selected.

The variability in the ULS and SLS design widths is particularly significant in this example because, depending on the parameter values selected and calculation model and Design Approach adopted, the results in Figure 5 show that 56% of the respondents found that the design was controlled by the SLS while 35% found it was controlled by the ULS with the remainder finding that the ULS and SLS designs were the same.

This demonstrates the sensitivity of this particular design to the SLS requirement and the need for reliable methods to estimate the settlement of a foundation.

2.2 *Example 2.2 – Pad Foundation with Inclined Eccentric Load on Boulder Clay*

The second example was to determine the width of a square pad foundation shown in Figure 5 with a vertical central permanent load of 1000kN and a variable load of 750kN at a height of 2m and resting on stiff to very stiff boulder clay. The geotechnical data provided consisted of the results of SPT tests, carried out in four boreholes around the proposed location foundation, as shown in Figure 6, and water content and index tests. The SPT *N* values are plotted in Figure 7 and show considerable scatter.

Vogt (2010), in his presentation on this example, noted that, when selecting the data from the different boreholes for the design, the majority of the respondents (73%) either chose the average of the data from all the boreholes or did not consider the borehole location, while 20% considered the trend of the boreholes, biased towards the nearest.

One respondent, who was familiar with this particular soil, commented that experience of this soil has shown it can vary in an apparently random manner across the site.

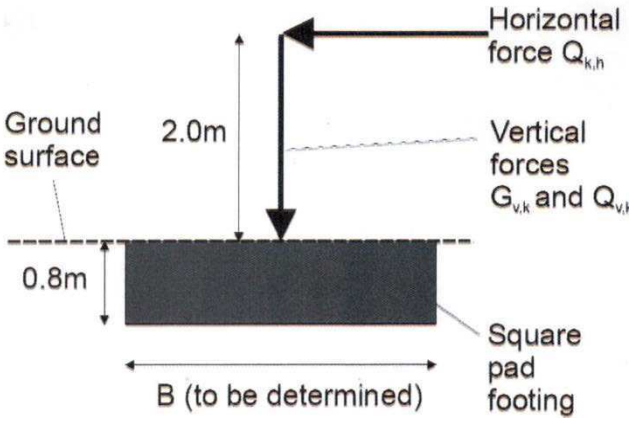

Figure 5. Example 2.2 – Pad foundation with inclined load design situation

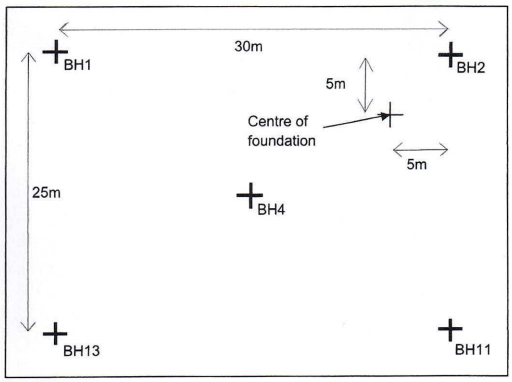

Figure 6. Location of boreholes and centre of foundation

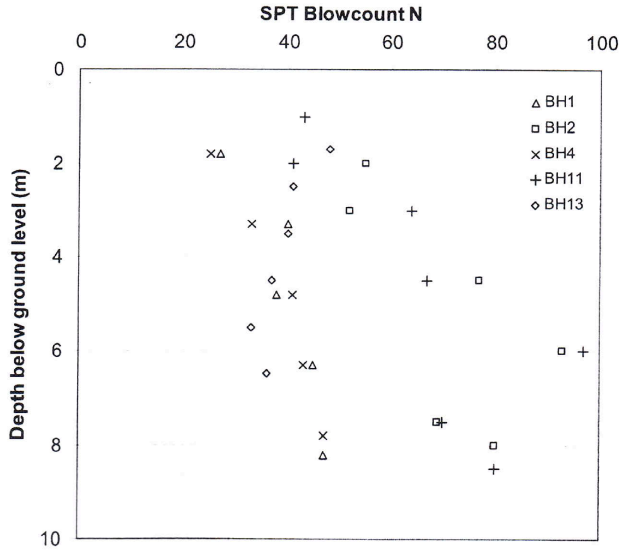

Figure 7. SPT N values v. depth

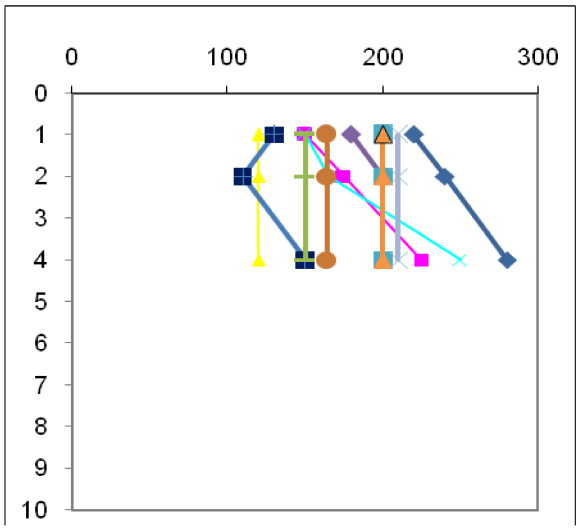

Figure 8. Selected characteristic $c_{u,k}$ values v. depth

Table 2. Design widths of foundation with an inclined and eccentric load

	Stage 1	
	ULS	SLS
Range of design widths (m)	3.1 – 4.66	1.2 – 4.5
Average (m)	4.08	3.46
Coefficient of variation (COV)	0.14	0.29
	Stage 2*	
	ULS using own selected $c_{u,k}$	ULS using given benchmark $c_{u,k}$
Range of design widths (m)	3.5 – 4.63	3.5 – 4.63
Average (m)	4.55	4.19
Coefficient of variation (COV)	0.03	0.12

* Only four respondents submitted Stage 2 design widths. Two were same as the original widths and two were much reduced

Regarding the parameters used to determine the ULS design foundation width, 93% used c_u, 67% used φ' and 33% used c'. Therefore, while almost all the respondents checked for undrained conditions, only two-thirds checked drained conditions as well and half of those assumed that $c' = 0$. With regard to SLS design, a variety of methods were used to calculate the foundation settlement with 33% using one of the methods in Annexes F1, F2 and F3 of EN 1997-1. One respondent noted that, in accordance with paragraph 6.6.2(16) of EN 1997-1, it was not necessary to calculate the settlement since the ratio of the bearing resistance of the ground at its initial undrained shear strength to the serviceability loading was less than 3, while another respondent noted that the tilt condition was more critical than settlement. Various parameters were used to calculate the settlement including E_u, E' and m_v.

A variety of correlations were used by the respondents to derive the c_u value; most involving correlations with the N value based on the index properties. In view of the considerable scatter in the N values, the respondents gave a large number of methods for how they selected the characteristic value, which included by eye (20%) and by statistical analysis (13%). The characteristic $c_{u,k}$ values selected by the respondents are plotted in Figure 8. As in Example 2.1, the respondents selected a wide range of characteristic values.

With regards to which calculation method was used to check against bearing failure, the majority (71%) of the respondents used the bearing resistance equation in Annex D of EN 1997-1. Others used alternative models given in their National Annexes or standards and one respondent used the Brinch Hansen bearing resistance equation. Regarding the Design Approach adopted, 64% used DA1 and 29% used DA2 or DA2*. No respondent used DA3.

The design widths to avoid a ULS calculated by the respondents are shown in Table 2 and ranged from 3.1 to 4.66m, with an average value of 4.08 and a coefficient of variation (COV) of 0.14. All the respondents found that the SLS design width of this foundation on stiff soil was less than the ULS design width so that the design was controlled by the ULS. The COV of the SLS widths at 0.29 was greater than the value of 0.14 for the ULS widths due to different calculations models used to estimate the settlement. While only four respondents submitted Stage 2 designs using benchmark $c_{u,k}$ values, two of these were

the same as the original values and two were smaller with the result that their average design width reduced but the COV of their design widths increased significantly from 0.03 to 0.12. This indicates that, in his example, the variation in the design widths is more due to how $c_{u,k}$ is selected than to the calculation model used or the Design Approach adopted.

2.3 *Example 2.3 – Pile in Clay*

Example 2.3 was the design of a 450mm diameter pile in clay to support a permanent load of 300kN and a variable load of 150kN as shown in Figure 9. The ground consisted of 0 - 3 to 4m of made ground over London Clay with sand at a depth of 34m. The geotechnical data provided consisted of the results of CPT, SPT and pressuremeter field tests and laboratory undrained triaxial (UU) tests. The results of the UU tests are shown in Figure 10.

Van Seters (2010), in his presentation on this example, noted that all the ULS designs were based on the c_u values. A number of different correlations were used to determine the c_u value from the field tests, some of which were taken from existing standards. When determining the c_u value, almost the same number (53%) used an average of the tests from all the boreholes as those who took the location of the boreholes into account and used the nearest borehole (47%).

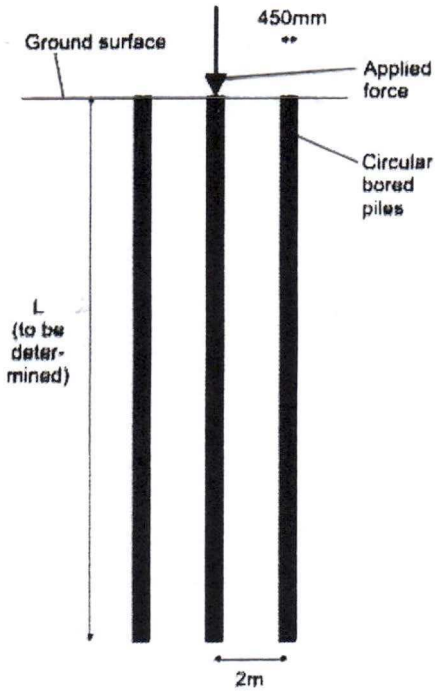

Figure 9. Example 2.3 - Pile in clay design situation

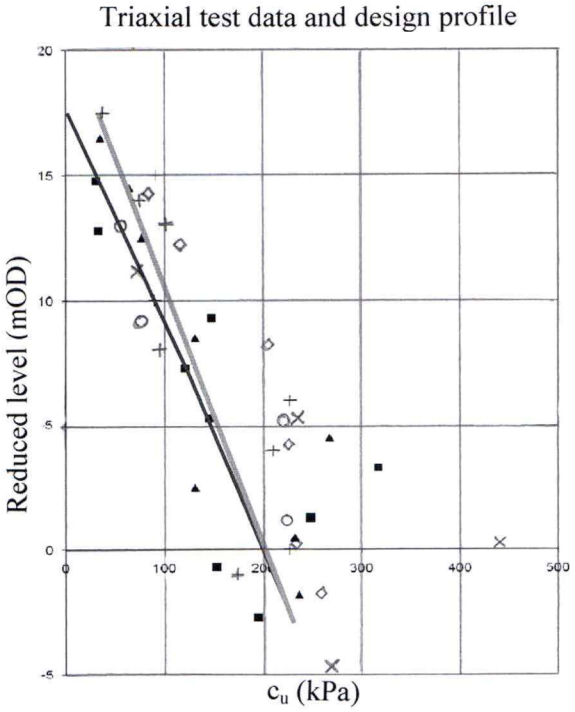

Figure 10. Laboratory c_u v. depth

The most popular method to select the characteristic $c_{u,k}$ value was "by eye", which was used by 53%; linear regression was used by 18% and other methods were used by the remainder. In spite of the different geotechnical data sources used and the different methods adopted to select the characteristic $c_{u,k}$ value, the COV of the $c_{u,k}$ values was less than 0.10 below a depth of 7m. The UK and Portuguese respondents used model factors of 1.4 and 1.5 respectively on c_u. The respondents from these countries also used the alternative design method based on the $c_{u,k}$ value with the model factor applied whereas the other respondents used the model pile method and a c_{uk} value selected from field test results. A majority, 69%, of the respondents used DA1 while the remainder, used DA2.

The average design pile length was found to be 15.1m for the ULS and 14.0m for the SLS so that the ULS controlled the design. The COV of the chosen pile lengths was 0.20 for SLS and 0.28 for ULS. The reporter makes the interesting observation that the average pile length chosen by the UK respondents was 12.5m, which is significantly less than the average for all the other respondents. This probably reflects the fact that the UK designers have used their "local experience" of the performance of piles in London Clay to obtain a more economic design.

2.4 *Example 2.4: Earth and Pore Water Pressures on a Basement Wall*

Example 2.4 differed from the other design examples in that it did not ask the respondent to determine the design dimensions of a particular structure; instead it asked them to address the realistic design situation of assessing design water levels behind and earth pressures acting on the retaining wall shown in Figure 11, which has fill directly behind the wall, with no drainage provided, and natural ground beyond the fill. Water depths measured in boreholes at three distances of 10, 25, and 50m from the wall were 2.2, 1.5, and 3.1m, so that the average water depth was 2.3m. The respondents were asked to give, for both ULS and SLS design situations, the characteristic and design water depths at the back of the wall for the following three design situations with different combinations of fill and soil types: A) Clay soil and clay fill, B) Clay soil and granular fill, and C) Gravel soil and granular fill; and to state how they would calculate the ULS earth pressures.

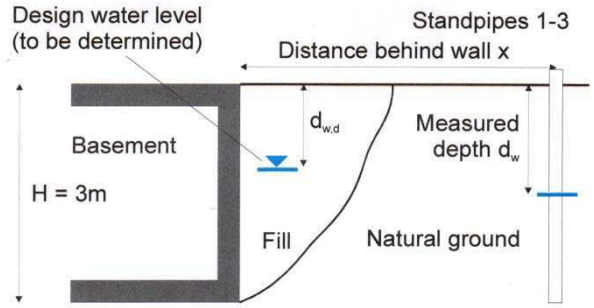

Figure 11: Example 2.4 - Basement wall design situation

Table 3. Water depths and thrusts on basement wall

Design Situation	Natural ground and Fill material	Average water depth (m)	Average characteristic water depth, d_k	SLS depth, d_{SLS}	Water thrust $P_{w,SLS}$ (kN/m)	ULS depth, d_{ULS}
A	Clay soil and clay fill	2.3	0.7	0.7	28	All situations
B	Clay soil and granular fill	2.3	0.7	0.7	28	56%: $d_{w,ULS} = d_k$
C	Gravel soil and granular fill	2.3	1.3	1.3	16	Others: $d_{w,ULS} = 0$

Schneider (2010), in his presentation on this example, gives the average of characteristic, SLS and ULS water depths chosen by the respondents and the average SLS water thrust on the wall for the three design situations, which are shown in Table 3.

Comparing the solutions received for all the examples, the greatest variability in the results, and hence the largest COV values, occurred in the case of this example, with COV = 0.57 for SLS and 0.40 for ULS. For SLS design of the basement wall, all the respondents except 2 stated that the design water depth was equal to the characteristic water depth. For Design Situation A, with clay soil and clay fill, the average of the given characteristic water depths was 0.7m. For Design Situation B, with clay soil and granular fill, the average of the given characteristic water depths was 0.66m, while for Design Situation C, with gravel soil and granular fill, the average of the given characteristic water depth was 1.3m. The thrust on the wall from the water pressure is non-linear and hence is very sensitive to the chosen design water depth. In summarising the responses to this example, Schneider (2010) noted that:

- The deepest average characteristic water depth of 1.3m, which is 1.0m higher than the average measured water depth, was obtained for Design Situation C with gravel soil and granular fill; while a shallower average characteristic water depth of 0.7m was obtained for both Design Situation A and B with the clay soil and granular fill and the clay soil and granular fill
- The SLS water depth was chosen as the characteristic water depth by all respondents
- The water thrust was calculated assuming a triangular water pressure distribution
- 56% of the respondents chose the characteristic water depth for the ULS water depth while, of the remaining respondents, most chose the characteristic ground water level at the surface, i.e. $d_{k,ULS} = 0$
- To calculate the earth pressure, 22% used K_a, 50% used K_0, 11% used $(K_a + K_0)/2$, 6% including compaction pressure and it was unclear how 6% calculated the earth pressure
- With regard to Design Approach, 24% used DA1 with both Combinations 1 and 2, 18% used DA1 and just Combination 1, while 58% used DA2
- With regard to factoring the characteristic water pressure, 50% factored it by 1.35 but when the characteristic water level was chosen at the ground surface, a factor of 1.0 was often applied.

In conclusion, Schneider noted that more guidance was needed in EN 1997-1 concerning the selection of the characteristic water depth and the selection of the depths for ULS and SLS design situations. He posed the following questions:

- Should a partial factor greater than 1.0 be applied when the characteristic water level is at the ground surface?
- Does a partial factor greater than 1.0 on the characteristic water force make sense on physical grounds or should a partial factor only be applied to the water depth?

2.5 *Example 2.5: Embankment on Soft Peat*

Example 2.5 was to determine the height for the initial stage of an embankment to be constructed on pseudo-fibrous to amorphous peat resting on sand at a depth of 7m. The geotechnical information provided consisted of 5 borehole logs spaced at 40m to 50m along the centreline of the embankment and 5 field vane tests giving the measured $c_{u,vane}$ values shown in Figure 12. It was stated that the topsoil in this example was not to be removed, there was to be no hydraulic fill behind the embankment, no construction traffic on the embankment and no serviceability requirements or accidental design situations.

Farrell (2010), in his presentation on this example, noted that to derive c_u for this example, a majority of the respondents, 83%, used the measured $c_{u,vane}$ values directly and only 17% applied a correction factor to account for the field test conditions including a factor of 0.5 to account for the fibrous nature of the peat. With regard to accounting for the location of the boreholes and field vane tests, since no allocation plan for the embankment was given, 50% of the respondents used the average of the results from all the boreholes and 17% made a pessimistic choice of borehole. The characteristic $c_{u,k}$ values selected by the respondents have been plotted in Figure 13 and are very different from each other: 58% selected the $c_{u,k}$ value by eye while the remainder used a statistical approach. Some of the selected $c_{u,k}$ values are constant with depth while others decrease at first and then increases.

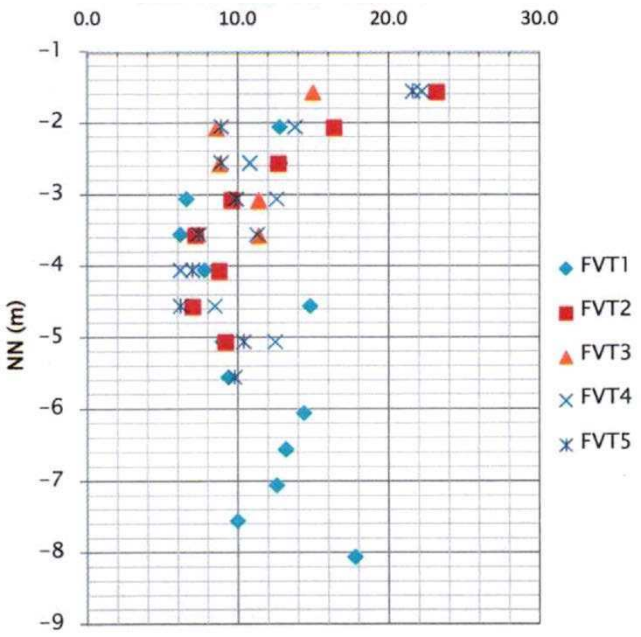

Figure 13. Example 2.5 measured $c_{u,vane}$ v. depth

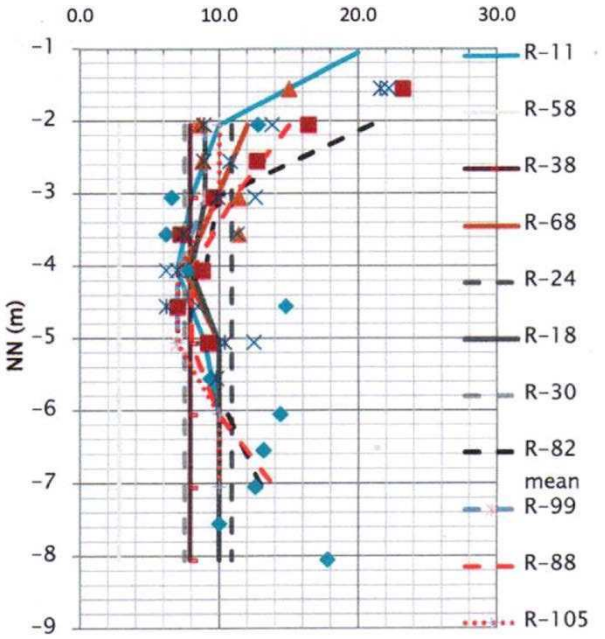

Figure 14. Example 2.5 characteristic $c_{u,k}$ values v. depth

Farrell (2010) noted that only two responses were obtained concerning the type of calculation model used to determine the maximum height of the embankment. However two models were mentioned: a slip circle analysis using Bishop's variable interslice forces, and a bearing resistance failure model. With regard to the Design Approach adopted, 58% used DA1, and 33% used DA2 and/or DA3 and 8% used a purely statistical method. The range of design heights obtained by the respondents was very large, ranging from 0.6m to 2.35m, with an average height of 1.67m and a COV of 0.32. This range was reduced in the second stage, when the respondents were given benchmark $c_{u,k}$ values to use. Only 4 respondents submitted designs based on the benchmark $c_{u,k}$ values. These design height values had very similar COV values to their designs based on the selected $c_{u,k}$ values, 0.28 compared to 0.30, but the embankments heights with the benchmark values ranged from 1.0m to 2.0m, with an average value of 1.53m compared to their original heights which ranged from 1.1m to 2.35m with an average value of 1.63m. This indicates that, unlike the spread foundation in Example 2.2, the differences between the designs is not principally due to how

$c_{u,k}$ was selected but due to the other choices made during the design process, such as the calculation model, Design Approach and partial factor values.

In his report on this example, Farrell (2010) listed the following issues, raised by the respondents, that either require consideration when designing an embankment to Eurocode 7 or should be taken into account when revising the current version of EN 1997-1:

- How to account for local experience and whether to use correction factors for c_u from field vane tests
- Whether it is appropriate to use the bearing resistance model in Eurocode 7 for design of embankments
- The effect of using different calculation models
- How to apply the partial factor on earth resistance in slope stability analyses using DA2
- The merging of DA1 and DA3 for the analysis of slopes
- The different way partial factors may be applied in slope stability analyses
- Whether to account for tension cracks in the analysis of an embankment.

2.6 *Example 2.6: Pile in Sand*

Example 2.6 was to determine the design length of 450mm diameter bored piles supporting a building on clay with peat seams over fine sand. The piles were required to support a vertical compressive permanent load of 300kN and variable load of 150kN. The geotechnical data provided were a borehole log and a CPT test result showing a cone resistance value varying around a mean value of about 3MPa in the clay, increasing to about 17MPa in the top of the sand at a depth of 18m and then slowly decreasing in the sand to about 11MPa at a depth of 28m. The piles were being used to transfer the loading from the building to the lower sand stratum. It was stated that settlements would not control the design and since it is a small project load, no load testing was to be carried out.

Table 4. Average characteristic cone, pile shaft and pile base resistances and average pile design length

Depth (m)	av. $q_{c,k}$ (MPa)	COV $q_{c,k}$	av. $q_{s,k}$ (MPa)	COV $q_{s,k}$	av. $q_{b,k}$ (MPa)	COV $q_{b,k}$	av. L	COV L
2.5	4.2	0.70	16.0	1.33				
7.5	3.0	0.46	20.4	0.79				
12.5	2.5	0.43	22.6	1.41			18.73	0.08
17.5	13.5	0.24	84.4	0.44	3564	0.60		
22.5	13.8	0.08	97.8	0.43	3846	0.68		

The questionnaire for this design example asked the respondents to select the characteristic cone resistance $q_{c,k}$, characteristic unit pile shaft resistance $q_{s,k}$ and characteristic unit base resistance $q_{b,k}$ at the selected depths of 2.5, 7.5, 12.5, 17.5 and 22.5m. The way the respondents selected their characteristic values was: by eye – 50%, by statistical analysis – 23% with the others using a variety of different methods including previous design experience. Annex D of EN 1997-2 provides two models for calculating the resistance of a pile from CPT tests results and, while 38% of the respondents used these models, the majority used alternative calculation models to obtain q_s and q_b.

The average of the characteristic values selected by the respondents and their COVs are given in Table 4 together with the average design pile length, L and the COV of the L values. As Kłosiński (2010) has noted in his report on this example, there was a large scatter in the $q_{c,k}$ values chosen by the respondents for the upper clay stratum, with many respondents selecting $q_{c,k} = 0$ while others selected high values of 4, 5 and even 8MPa. This large scatter is reflected in the high COV values for $q_{c,k}$, which range from 0.43 to 0.70. There was less scatter in the $q_{c,k}$ values chosen for the sand stratum, which had a COV of 0.24 at a depth of 17.5m and a COV of only 0.08 at a depth of 22.5m. The large scatter in the $q_{c,k}$ values in the clay resulted is the very large scatter in the $q_{s,k}$ values as shown by the COV values for $q_{s,k}$ in Table 2.4 which range from 0.79 to 1.41 in the clay stratum. This large COV value for the clay arises because many respondents chose $q_{s,k} = 0$ while others chose $q_{s,k}$ values of 74kPa at 2.5m, 52kPa at 7.5m and 111kPa at 12.5m. Although there was less scatter in the $q_{c,k}$ values selected for the sand stratum, there was still a great scatter in the respondents' $q_{b,k}$ values, which ranged from 56 (!) to 6600kPa at 17.5m depth, with a COV of 0.60.

With regard to the Design Approaches adopted and the partial factors chosen to calculate the design length of the pile, Kłosiński reported that 46% used DA1, 38% used DA2, 8% used DA3 and 8% used a reliability based design. However, when adopting these Design Approaches, Kłosiński noted that the partial factor values used by some of the respondents, which were taken from their National Annexes, are larger than the recommended values in EN 1997-1. The design pile lengths were found to range from 16.5 to 21.0m and had a COV value of only 0.08. Thus, in spite of the large scatter in both $q_{s,k}$ and $q_{b,k}$, there

was little scatter in the design pile lengths. Indeed, this COV value is the lowest for all the six design examples. The reason for this appears to be that, when carrying out their pile designs, the respondents have made use of their experience regarding the performance of a pile and the fact that it needs to be founded in the sand stratum, so that they have selected their characteristic pile resistances and chosen their calculation method and partial factor values, together with correlation and model factors, in such a way that, in this design example, the different decisions made during the design process tend to compensate and the pile designs tend to converge.

In reviewing this example, Kłosiński expressed disappointment with regard to the level of harmonisation that has taken place in the design of piles following the introduction of Eurocode 7. Indeed he states that it is difficult to say if a method of designing piles to Eurocode 7 exists since Eurocode 7 allows so much freedom with regard to the calculation methods for the design of piles. If the use of Eurocode 7 does not lead to uniformity in the calculation methods, he says it should at least achieve a comparable level of safety and economy for pile designs.

3 OVERVIEW OF SECOND SET OF DESIGN EXAMPLES

3.1 *Comparison between first and second set of examples*

Bond (2010), in his presentation at Pavia, compared the two sets of design examples by looking at the interquartile range (in which 50% of values lie) normalised by the mean. The results of the 1st and 2nd set of examples presented in Dublin and Pavia are presented in Figures 15 and 16. These figures show that, in spite of providing the raw data rather than the characteristic parameter values for design, the scatter in the results for the spread and pile foundations was generally less in the second set than in the first, particularly in the case of the piles; however the scatter for the earth/ water pressure and embankment exampleswas greater than for the first set. The reduction in scatter for the spread and pile foundations reflects, to some extent, the passage of five years and experience gained in the use of Eurocode 7 since the first set of examples. It also indicates that the selection of characteristic parameters from raw data does not significantly affect the scatter obtained in the designs. However, in the case of the earth/water pressure example, the selection of characteristic water level significantly affects the design and this is an aspect on which Eurocode 7 provides little guidance and which needs to be addressed.

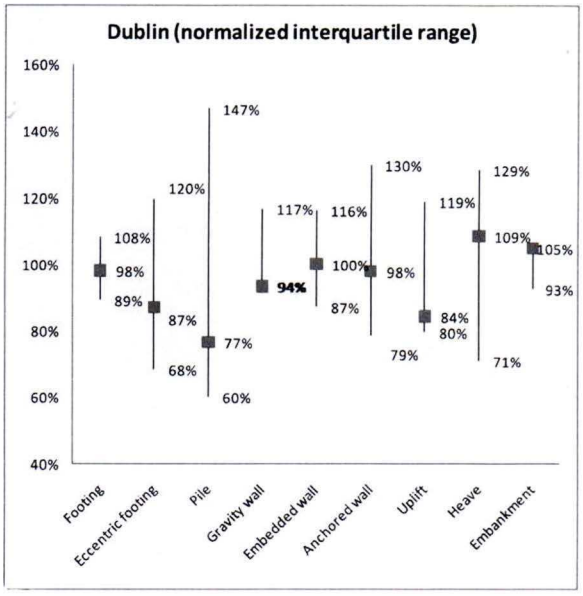

Figure 15. Normalised results for 1st Set of examples

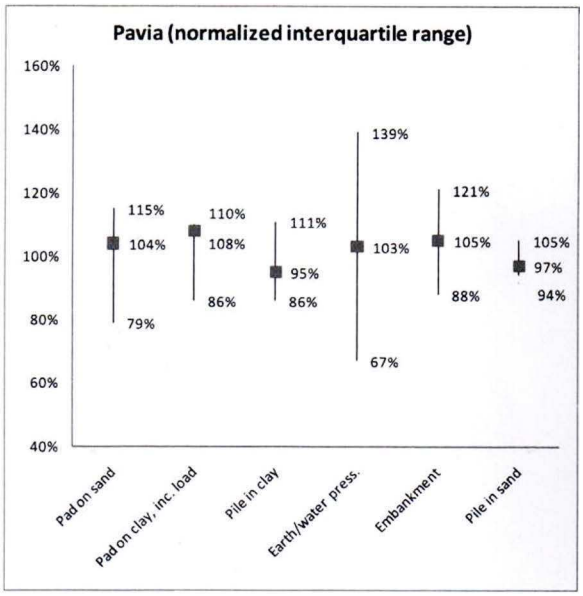

Figure 16. Normalised results for 2nd Set of examples

There was great variability in the embankment designs and a high COV value was obtained for the designs in the case of this example. When examining the designs for this example, particularly when comparing the initial designs based on the raw data with those based on the benchmark characteristic $c_{u,k}$ values, it was concluded that the variability was mainly due to the calculation model chosen and the Design Approach and partial factor values adopted rather than the how the $c_{u,k}$ value was selected.

3.2 *Confidence in the designs to Eurocode 7*

The questionnaires for the different examples asked the respondents to assess their designs to Eurocode 7, whether they thought designs to Eurocode 7 were sound, how conservative they thought their designs were and how they compared to their previous national practice. A summary of the responses to these questions for Example 2.2, 2.3, 2.5 and 2.6, expressed in terms of the percentage of the total number of respondents, is provided in Table 5. These results show that, for all these examples, which involving different design situations, the vast majority (82%) of the respondents were confident that their designs to Eurocode 7 were sound and, with regard to the conservatism of their designs to Eurocode 7, 60% on average considered to them be about right and 35% considered them to be conservative or very conservative.

Table 5. Assessment of Designs to Eurocode 7

Example	Confident / very confident Eurocode 7 designs are sound (%)	Conservatism of designs to Eurocode 7 (%)				Eurocode 7 conservatism compared to previous national practice (%)		
		Very cons.	Cons,	About right	Uncons,	More cons.	About Same	Less cons.
2.1	86	0	27	72	0	5	72	22
2.2	73	0	25	67	8	0	67	33
2.3	94	8	23	62	8	17	67	17
2.4	78	0	57	43	0	31	62	8
2.5	83	14	14	71	0	38	50	12
2.6	69	0	54	36	9	18	55	27
Averages	82	3	32	60	4	16	64	20

When comparing the Eurocode 7 designs with those to existing national practice, they were considered to about right by 64%, less conservative by 20% and more conservative by 16%. Hence the respondents' assessments of the designs to Eurocode 7 were favourable. They generally were confident in their designs to Eurocode 7 and the majority considering their designs to be about the same as previous designs and to be about right or conservative.

4 CONCLUSIONS

The 2nd set of Eurocode 7 design examples presented at the Pavia Workshop in 2010 have provided some interesting information about Eurocode 7 and its application in practice. They have shown that, since the 1st set of examples were presented at the Dublin Workshop in 2005, geotechnical engineers have developed confidence and consistency in the use of Eurocode 7 for the design of spread and pile foundations. However, there is still great variability in how characteristic values are chosen. This is particularly so in the case of water levels for basement wall and retaining structures and hence this is an area that requires to be addressed in a future revision of Eurocode 7.

REFERENCES

Bond A.J. 2010. Results of the NDP survey, presentation at 2nd Int. Workshop on the Evaluation of Eurocode 7, Pavia, Italy, www.eurocode7.com/etc10/Pavia/proceedings.html.

Brito J. and Sørensen C.S. 2010. Design Example 2.1 – Foundation with central vertical load, presentation at 2nd Int. Workshop on the Evaluation of Eurocode 7, Pavia, Italy, www.eurocode7.com/etc10/Pavia/proceedings.html.

Farrell E. 2010. Design Example 2.5 – Embankment of soft peat, presentation at 2nd Int. Workshop on the Evaluation of Eurocode 7, Pavia, Italy, www.eurocode7.com/etc10/Pavia/proceedings.html.

Orr T.L.L. 2005. Evaluation of Eurocode 7, Proceedings of 1st Int. Workshop on the Evaluation of Eurocode 7, Dublin, Department of Civil, Structural and Environmental Engineering, Trinity College Dublin

Schneider, H.R. 1997. Definition and determination of characteristic soil properties. 12th Int. Conference on Soil Mechanics and Foundation Engineering. Hamburg: Balkema

Schneider, H.R. 2010. Design Example 2.4 – Earth & pore water pressures on basement walls, presentation at 2nd Int. Workshop on the Evaluation of Eurocode 7, Pavia, Italy, www.eurocode7.com/etc10/Pavia/proceedings.html.

Van Seters A. 2010. Design Example 2.3 – Pile foundation in stiff clay, presentation at 2nd Int. Workshop on the Evaluation of Eurocode 7, Pavia, Italy, www.eurocode7.com/etc10/Pavia/proceedings.html.

Vogt N. 2010. Design Example 2.2 – Foundation with inclined load, presentation at 2nd Int. Workshop on the Evaluation of Eurocode 7, Pavia, Italy, www.eurocode7.com/etc10/Pavia/proceedings.html.

ISGSR 2011 - Vogt, Schuppener, Straub & Bräu (eds) - © 2011 Bundesanstalt für Wasserbau ISBN 978-3-939230-01-4

Determining design loads – comparative calculations between DIN 1054 and EC7-1

M. Ziegler & E. Tafur
Geotechnical Engineering, RWTH Aachen University, Germany

ABSTRACT: The current German standard for geotechnical design DIN 1054 (2005) will be withdrawn in a few years, being substituted by the German version of Eurocode 7-1, the German National Annex and complementary regulations in DIN 1054 (2010). The new standards allow a new design approach which takes into account that by determining the design value the temporary actions or their effects are reduced by multiplying them with combination factors ($\psi_i \leq 1{,}0$). This new approach leads to lower design values as a design with DIN 1054 (2005), where design values are calculated by adding all actions with their full amount.

In order to show the influence of the combination factors on the geotechnical design, comparative calculations for selected geotechnical structures have been carried out. For this purpose a sheet pile quay wall and a foundation of a production hall have been designed according to the new standards and to DIN 1054 (2005). The results presented in this paper show for various cases that the calculations with both design concepts lead to similar results.

Keywords: combination factors, design value, standard, foundation, sheet pile quay wall.

1 INTRODUCTION

Geotechnical structures in Germany are currently still designed according to the German standard DIN 1054 (2005). However, it will be substituted by DIN EN 1997-1 (German version of EC7-1), the German National Annex DIN EN 1997-1/NA and complementary regulations in the new DIN 1054 (2010). These new standards implement a new approach to determine the design values for temporary actions taking into account that not all independent actions occur simultaneously with the same probability. This is achieved by reducing the temporary actions or their effects by multiplying them with combination factors $\psi_i \leq 1{,}0$. On the contrary, the current German standard DIN 1054 (2005) does not consider any combination factors, calculating the design value by adding all actions with their full amount. Generally, lower design values are obtained with the new approach compared to DIN 1054 (2005) leading probably to lower levels of safety. Hence, it is necessary to investigate, if the geotechnical design with the new approach differs considerably from the design according to DIN 1054 (2005) and to what extent a lower level of safety is achieved.

In a research project, funded by DIBt (Deutsches Institut für Bautechnik), comparative calculations for selected geotechnical applications with various considerable independent temporary actions have been carried out. A sheet pile quay wall and a foundation of a production hall have been designed according to the new standards and to DIN 1054 (2005). For this purpose, the ratios Q_{Tot}/G_{Tot} and Q_A/Q_{Tot} have been determined. The first one indicates the ratio of temporary to permanent actions, the second one the ratio of accompanying actions to total temporary actions. Of major importance was to identify the critical ratios Q_{Tot}/G_{Tot} and Q_A/Q_{Tot} for which considerable differences in the structure's design were to be achieved. Furthermore, it was expected that the differences with increasing rate of reduced temporary actions would also increase.

2 GEOTECHNICAL DESIGN ACCORDING TO DIN 1054:2005-01 AND THE NEW DESIGN STANDARDS

2.1 *Design situations*

Different situations are defined for the geotechnical design, which consider the duration, combination and frequency of occurrence of actions. DIN 1054 (2005) specifies for the ultimate limit state (ULS) three load cases as design situations: load case LF1 (permanent situation), load case LF2 (temporary situation) and load case LF3 (accidental situation). In the new standards the load cases are replaced by the design situations BS-P (permanent situation), BS-T (temporary situation), BS-A (accidental situation) and BS-E (earthquake situation). Basically, the load cases of DIN 1054 (2005) correspond to the design situations of the new standards, with the only difference being the separation of load case LF3 into an accidental situation BS-A and an earthquake situation BS-E (see Table 1).

Table 1. Comparison between load cases (DIN 1054 (2005)) and design situations (new standards)

Load cases	Design situations
LF1	BS-P
LF2	BS-T
LF3	BS-A
	BS-E

2.2 *Design values*

The determination of the design value E_d using DIN 1054 (2005) is based on the partial safety concept. Hence, the actions or their effects are multiplied with partial safety factors, distinguishing between partial factors for permanent and for temporary effects of actions. Independent of the load case the design value results from the addition of the full amount of effects of actions multiplied with the corresponding partial factor (see Equation (1)).

$$E_d = \sum_{j\geq 1} \gamma_{G,j} \cdot E\left(G_{k,j}\right) + \sum_{j\geq 1} \gamma_{Q,j} \cdot E\left(Q_{k,j}\right) \tag{1}$$

where E_d = design value, $E(G_{k,j})$ = characteristic effect of a permanent action ($j \geq 1$), $E(Q_{k,j})$ = characteristic effect of a temporary action ($j \geq 1$), $\gamma_{G,j}$ = partial factor for permanent effects, $\gamma_{Q,j}$ = partial factor for temporary effects

The new standards are also based on the partial safety concept. They consider for the determination of the design value not only partial factors but also combination factors ($\psi_i \leq 1{,}0$). While the partial factors multiply the permanent and temporary effects of actions, the combination factors are only applied to the temporary ones. They reduce the accompanying actions, while the leading action remains unmodified. The new DIN 1054 (2010) specifies that each independent temporary action must be set as leading action in order to find out the dominant design value. Furthermore, the value of combination factors depends on the design situation, e. g. applying lower combination factors in the design situations BS-A and BS-E than in BS-P or BS-T. Thus, a lower probability of a simultaneous occurrence of independent temporary actions in BS-A or BS-E is considered.

The combination factors should be taken from Table A 1.1 of the National Annex DIN EN 1990/NA for structural design. Especially, for the geotechnical design the combinations factors for "other actions" ($\psi_0 = 0{,}8$, $\psi_1 = 0{,}7$, $\psi_2 = 0{,}5$) of the mentioned Table should be used.

Equation (2) shows the determination of the design values for the design situations BS-P and BS-T.

$$E_d = \sum_{j\geq 1} \gamma_{G,j} \cdot E\left(G_{k,j}\right) + \gamma_P \cdot E\left(P_k\right) + \gamma_{Q,1} \cdot E\left(Q_{k,1}\right) + \sum_{j>1} \gamma_{Q,j} \cdot \psi_{0,i} \cdot E\left(Q_{k,j}\right) \tag{2}$$

where E_d = design value, $E(G_{k,j})$ = effect of a permanent action ($j \geq 1$), $E(P_k)$ = effect of an action due to pre-stressing, $E(Q_{k,1})$ = effect of a leading action, $E(Q_{k,j})$ = effect of accompanying actions ($j > 1$), $\gamma_{G,j}$ = partial factor for permanent effects, γ_P = partial factor for effects due to pre-stressing, $\gamma_{Q,1}$ = partial factor for temporary effects of a leading action , $\gamma_{Q,j}$ = partial factor for temporary effects of accompanying actions, $\psi_{0,i}$ = combination factor for accompanying actions $Q_{k,j}$

Actions that are multiplied with combination factors are called representative values of actions, while those unmodified are named characteristic values of actions. A particular case occurs when a geotechnical design is carried out with geotechnical actions and foundation loads. Then, if the foundation loads are representative values of actions (containing already combination factors) and the geotechnical engineer considers them as characteristic values of actions, he would multiply them again with combination factors, reducing the temporary actions twice. This leads to lower design values and therefore probably to a lower level of safety.

3 DESIGN OF SELECTED GEOTECHNICAL STRUCTURES

In order to show the influence of the combination factors on the geotechnical design two selected geotechnical applications have been designed according to DIN 1054 (2005) and to the new standards, taking into account various independent temporary actions occurring simultaneously. The selected examples are a sheet pile quay wall for a container terminal and a foundation of a production hall. Furthermore, an incorrect design of the foundation with a double consideration of combination factors possibly caused by a misunderstanding between structural and geotechnical engineer has been analysed. For both examples the calculations have been carried out for four different types of soil, namely gravel, sand, silt and clay.

3.1 *Sheet pile quay wall*

The sheet pile quay wall has been designed without and with consideration of combination factors using the Recommendations of the Committee for Waterfront Structures Harbours and Waterways EAU 2004. The design has been carried out against loads caused by soil self weight ($E_{ah,g}$), container weight ($E_{ah,Cont}$), operating crane ($E_{ah,Cr}$), pore water pressure (W), and bollard pull (P_{Pull}) (see Figure 1). The earth pressure has been calculated considering a redistribution of the earth pressure according to EAU 2004.

The calculations have been carried out assuming a theoretical depth of 10 m, a groundwater level 4,4 m below ground surface, a variable channel water level depending on the load case and design situation respectively and a bollard positioned 3,0 m below ground level. Only one soil layer was considered. Friction angles between 30,0° and 37,5° for cohesionless soils and between 22,5° and 27,5° for cohesive soils were chosen. The cohesion was set between 5 kN/m² to 20 kN/m².

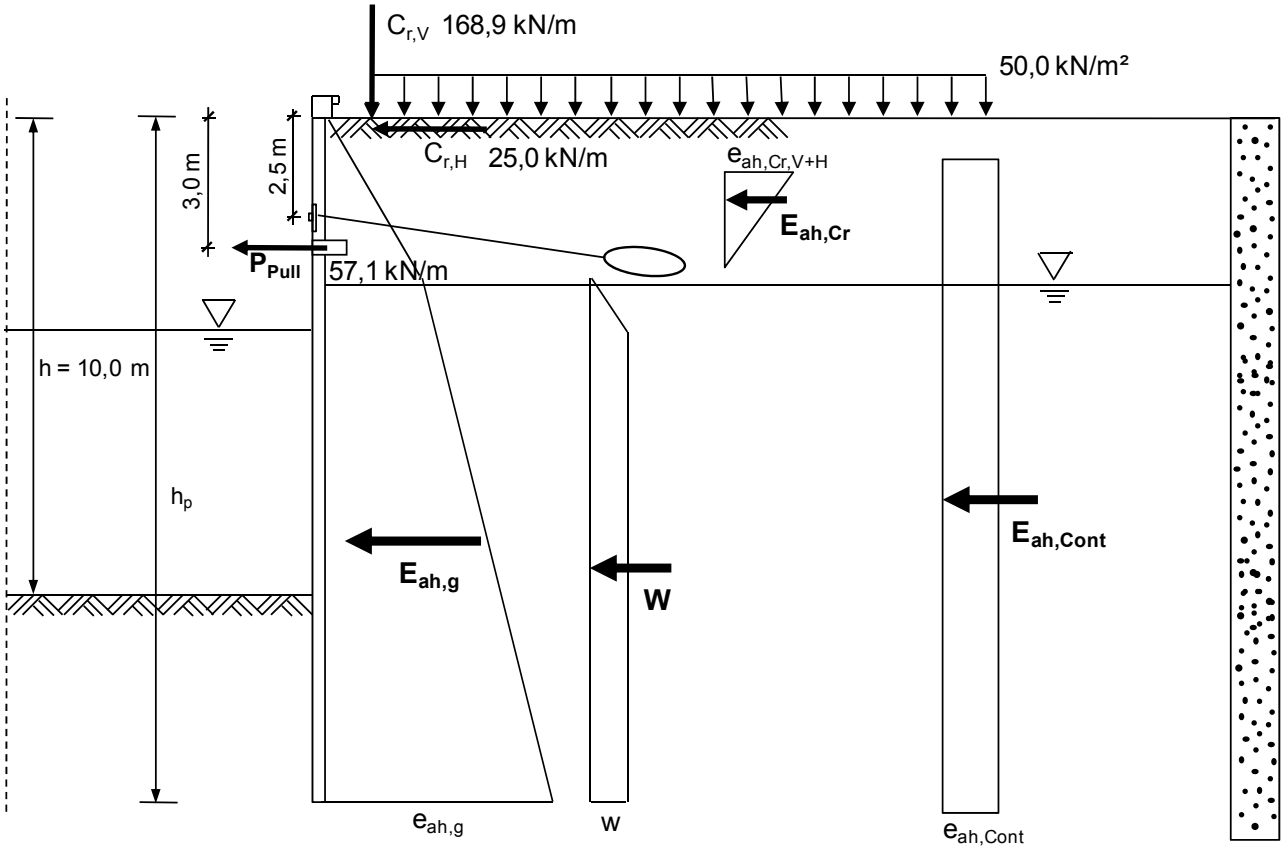

Figure 1. Loads and dimensions for the design of the sheet pile quay wall

The assumed structural system was a fully restrained, one-anchored sheet pile wall with a restraint degree of 100% in order to minimize deformations. The anchor was placed 2,5 m below ground surface (see Figure 1). Depending on the anchor position and the construction method, backfilling or excavation, an earth pressure redistribution according to EAU 2004 was assumed. It was chosen backfilling, redistributing the earth pressure near the anchor in accordance with EAU 2004, Figure E 77-4, case 6.

When calculating the permanent situation (load case LF1 or design situation BS-P) loads caused by soil self weight, container weight, operating crane and pore water pressure were taken into account. For the temporary situation (load case LF2 or BS-T) as well as for the accidental situation (load case LF3 or BS-A) additional loads caused by a bollard pull and a scouring have been considered.

For all design situations embedment depth, anchor length and sheet pile section have been calculated. The final design value was the maximum value of all cases. The sheet pile section has been determined carrying out a verification against structural failure depending on the bending moment and the section modulus. The anchor length has been calculated verifying the stability for anchoring at the lower failure plane. The required embedment depth has been determined by equilibrium calculations showing that the resistance on the passive side is sufficient to prevent a soil failure. Furthermore, the safety against vertical failure of the embedded wall has been verified.

When designing with the new standards, each independent temporary action was set as leading action, applying the combination factors ψ_i to the remaining accompanying actions.

In order to indicate the ratio between temporary and permanent actions the ratio Q_{Tot}/G_{Tot} has been determined taking into account the earth pressure from soil self weight ($E_{ah,g}$), container weight ($E_{ah,Cont}$) and operating crane ($E_{ah,Cr}$) as well as pore water pressure (W) and a load caused by a bollard pull (P_{Pull}). Equation (3) shows the calculation of the ratio Q_{Tot}/G_{Tot}.

$$\frac{Q_{Tot}}{G_{Tot}} = \frac{E_{ah,Cont} + E_{ah,Cr} + W + P_{Pull}}{E_{ah,g}} \tag{3}$$

The ratio Q_A/Q_{Tot} indicates the ratio of the amount of reduced temporary actions (accompanying actions) to the total temporary actions. Equation (4) shows the calculation of the ratio Q_A/Q_{Tot} for the load caused by container weight as leading action.

$$\frac{Q_A}{Q_{Tot}} = \frac{E_{ah,Cr} + W + P_{Pull}}{E_{ah,Cont} + E_{ah,Cr} + W + P_{Pull}} \tag{4}$$

3.2 *Foundation of a production hall*

The foundation of a production hall has been designed without and with consideration of combination factors. In addition, a design with a double consideration of combination factors has been carried out. In this manner, it was intended to analyse an incorrect design caused by a false interpretation of the foundation loads. If the structural engineer delivers foundation loads already reduced with combination factors but without any specifications, the geotechnical engineer would apply again combination factors to the foundation loads, reducing them twice.

In this geotechnical example a square foundation has been dimensioned to resist loads caused by self weight (G_D, G_S and G_F), wind (W_H), snow (S) and operating cranes ($C_{r,v}$ and $C_{r,h}$) with an assumed embedded depth of 0,8 m (see Figure 2). The calculations have been carried out for one soil layer, considering friction angles between 30° and 37,5° for cohesionless soils and between 22,5° and 27,5° for cohesive soils. The cohesion was varied between 5 kN/m² and 20 kN/m² for drained conditions and between 20 kN/m² and 60 kN/m² for undrained conditions.

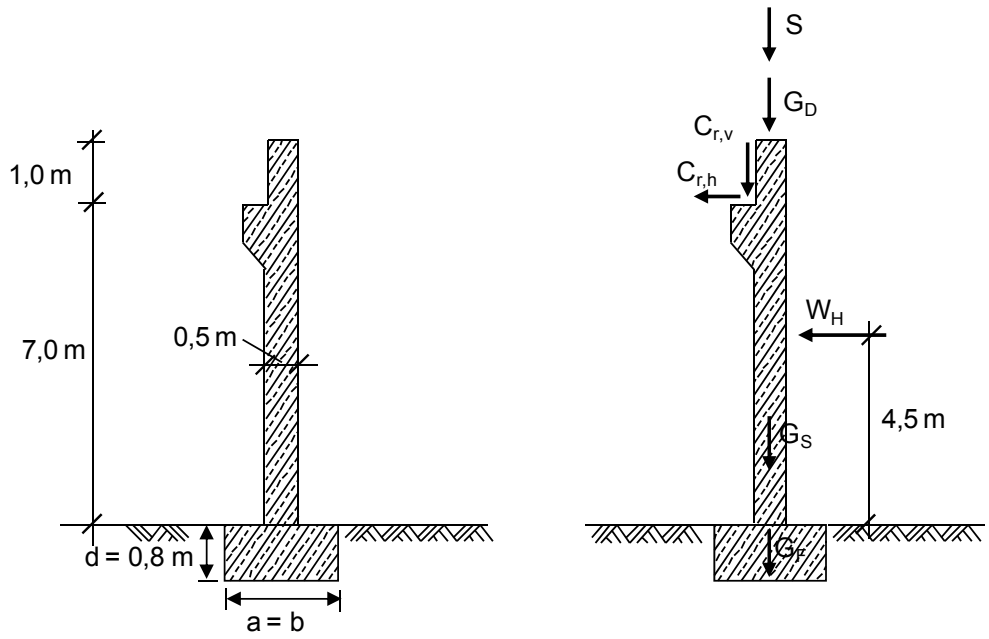

Figure 2. Loads and dimensions for the design of the production hall foundation.

The required foundation width has been determinated for each limit state, verifying the safety against ground bearing failure, the safety against failure by sliding on the base and the allowed eccentricity.

When determining the design value for the permanent and temporary situations, loads caused by self weight, wind, snow and operating cranes were taken into account. The temporary situation differed from the permanent situation considering an excavation on one side of the foundation, assumed for repair works. For the accidental situation, an extreme horizontal operating crane load caused by the impact of the trolley on the damping device additional to the loads in the permanent or temporary situation has been considered.

Moreover, three combinations of actions have been defined in order to find out the most unfavourable load case for each limit state and design situation. Combination of actions 1 considered loads caused by wind and self weight of the construction, resulting in the lowest normal forces in conjunction with the respective maximal tangential forces on the base. Combination of actions 2 considered loads caused by wind, operating crane and self weight of the construction. With this combination of actions the maximum bending moments have been obtained. Combination of actions 3 took into account loads caused by wind, snow, operating crane and self weight of the construction. This combination led to the highest normal forces.

Furthermore, the calculations have been carried out for four calculation cases in order to analyse the influence of combination factors and the design approach of the new standards on the geotechnical design. These are:

- Calculation case 1: foundation loads are characteristic values of actions, calculating without application of combination factors using DIN 1054 (2005).
- Calculation case 2: foundation loads are representative values of actions, calculating without application of combination factors using DIN 1054 (2005).
- Calculation case 3: foundation loads are characteristic values of actions, calculating with application of combination factors using the new DIN 1054 (2010).
- Calculation case 4: foundation loads are representative values of actions, calculating with application of combination factors using the new DIN 1054 (2010) (double consideration of combination factors).

In the framework of the research project the ratios Q_{Tot}/G_{Tot} and Q_A/Q_{Tot} have been determinated considering only the vertical foundation loads. The ratios Q_{Tot}/G_{Tot} and Q_A/Q_{Tot} have been calculated using Equations (5) and (6). Equation (6) shows the case when the load caused by operating crane is the leading action.

$$\frac{Q_{Tot}}{G_{Tot}} = \frac{C_{r,v} + S}{G_D + G_S + G_F} \tag{5}$$

$$\frac{Q_A}{Q_{Tot}} = \frac{S}{C_{r,v} + S} \tag{6}$$

4 RESULTS

In order to identify clearly the differences between a design according to DIN 1054 (2005) and one according to the new standards, the results have been represented in diagrams depending on the ratio Q_{Tot}/G_{Tot}.

The required embedment depth and the required anchor length for the sheet pile wall have been normalised both with the theoretical depth h and with the required sheet pile length h_p. The maximal calculated bending moment has been normalised by the product of the active earth pressure from soil self weight ($E_{ah,g}$) with h or h_p. Five different ratios Q_{Tot}/G_{Tot} have been calculated for each design value, one design value in accordance with DIN 1054 (2005) and up to four design values depending on the design situation and the amount of leading actions in accordance with the new standards.

Furthermore, the normalised bending moment calculated with the new DIN 1054 (2010) has been divided by the normalised bending moment calculated with DIN 1054 (2005), permitting to identify directly the differences between both design approaches. It could be observed that the differences increase with higher Q_A/Q_{Tot}. Figure 3 shows this bending moment ratio for gravel, relating the bending moments to the theoretical depth h. The legend contains the applied design standard, the design situation and the ratio Q_A/Q_{Tot} for each curve.

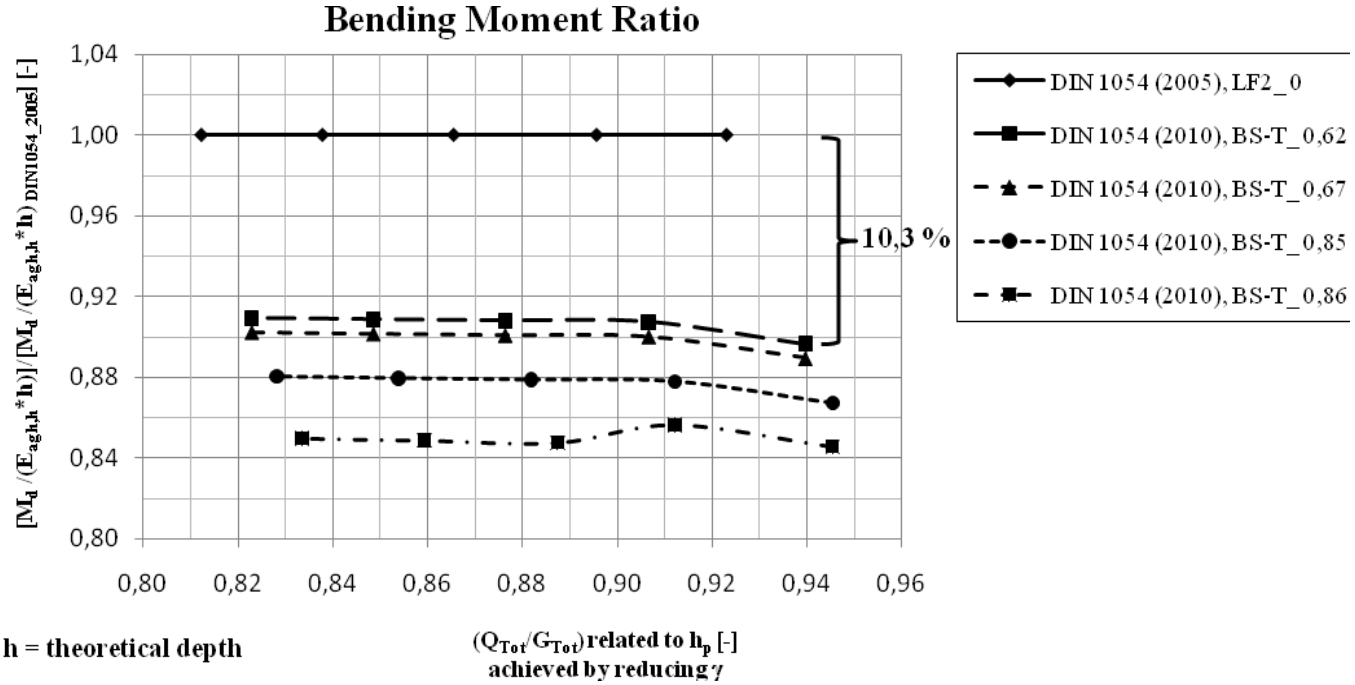

Figure 3. bending moment ratio for gravel with φ = 35°, related to the theoretical depth h.

The maximum difference of the bending moments was 10,3 % related to h and 6,8 % related to h_p. The influence of the combination factors on the design is not excessive for the selected sheet pile quay wall, but in unfavourable cases the value of the safety against structural failure (γ_M = 1,1) is achieved. The differences of the required embedment depth and anchor length were not considerable, being always lower than 4,0 %.

Moreover, it was intended to identify critical ratios Q_{Tot}/G_{Tot} and Q_A/Q_{Tot}, which describe the changeover from the required sheet pile section according to DIN 1054 (2005) to one required according to DIN 1054 (2010). The critical ratios could be determined for cohesive soils, but only for ratios with a high quota of temporary actions. For cohesionsless soils, the sheet pile sections calculated with DIN 1054 (2010) were either always another one or the same, not presenting a changeover like for cohesive soils. Figure 4 shows the critical ratios for clay.

It must be noted that the results have been obtained using the product range of one manufacturer. Considering the products of other manufacturers may therefore lead to different results.

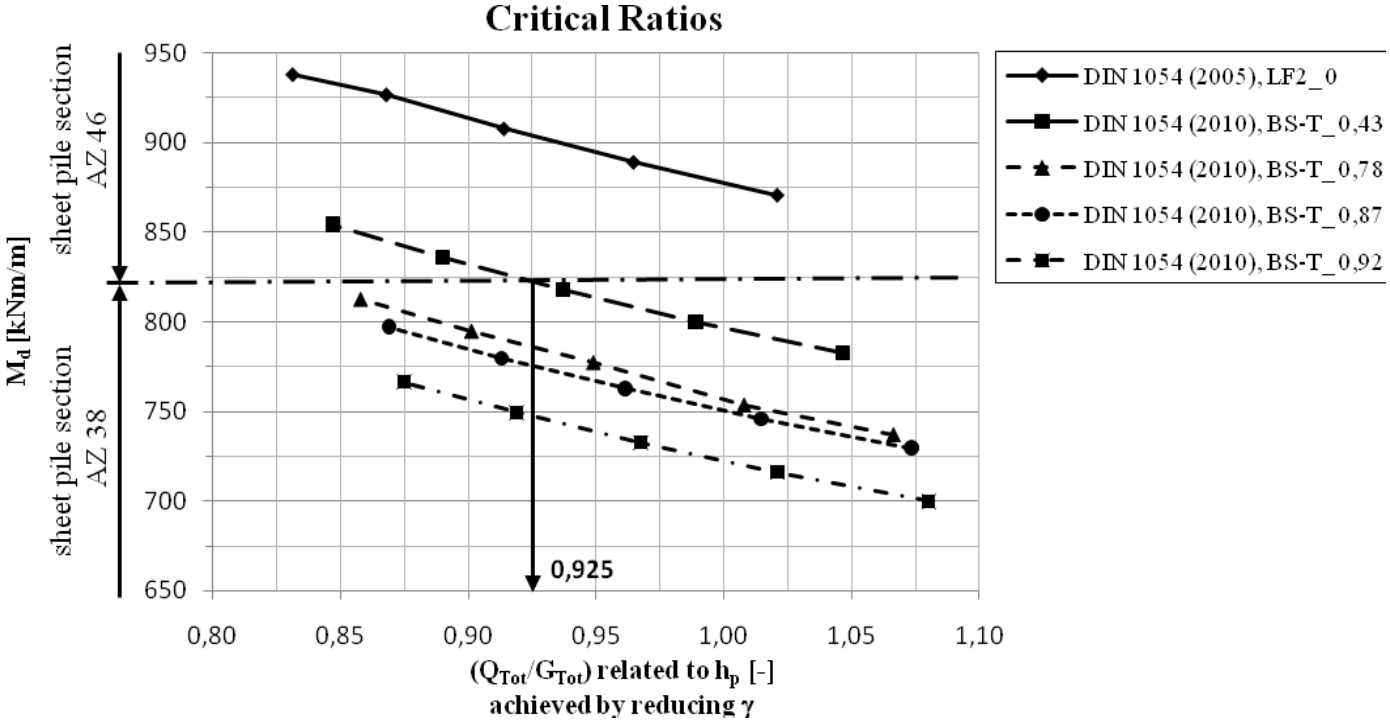

Figure 4. critical ratios Q_{Tot}/G_{Tot} and Q_A/Q_{Tot} for clay, $\varphi = 22{,}5°$ and $c = 20$ kN/m²

The results of the foundation of a production hall have been represented in diagrams depending on the ratio Q_{Tot}/G_{Tot} determined before the calculation ($(Q_{Tot}/G_{Tot})_{before}$), since the foundation width and therefore its weight was unknown before the calculation. Initially, the eccentricity e_x and the inclination of load H/V as well as the required foundation width have been calculated and represented for the combination of actions 3 (all actions considered).

Due to this last consideration an influence of the combination factors on the design can be identified more clearly. However, the combination of actions 3 was not always the most unfavourable load case, so that the foundation width has been also calculated using combination of actions 1 and 2. Furthermore, the required foundation width has been determined for the calculation cases described in chapter 3 and for each leading action.

In general a design without and with consideration of combination factors has shown the biggest effect for silty soil. However, none of the differences are significant. For silty soil the foundation width determined with calculation case 4 (with double consideration of combination factors) was only 8,0 cm smaller than determined with calculation case 1 (without consideration of combination factors). That implies only a difference of 2,0 %. In some cases a design according to calculation case 4 resulted in 1,0 up to 2,0 cm larger foundations. Figure 5 shows the calculated required foundation width for silt with wind as dominant leading action.

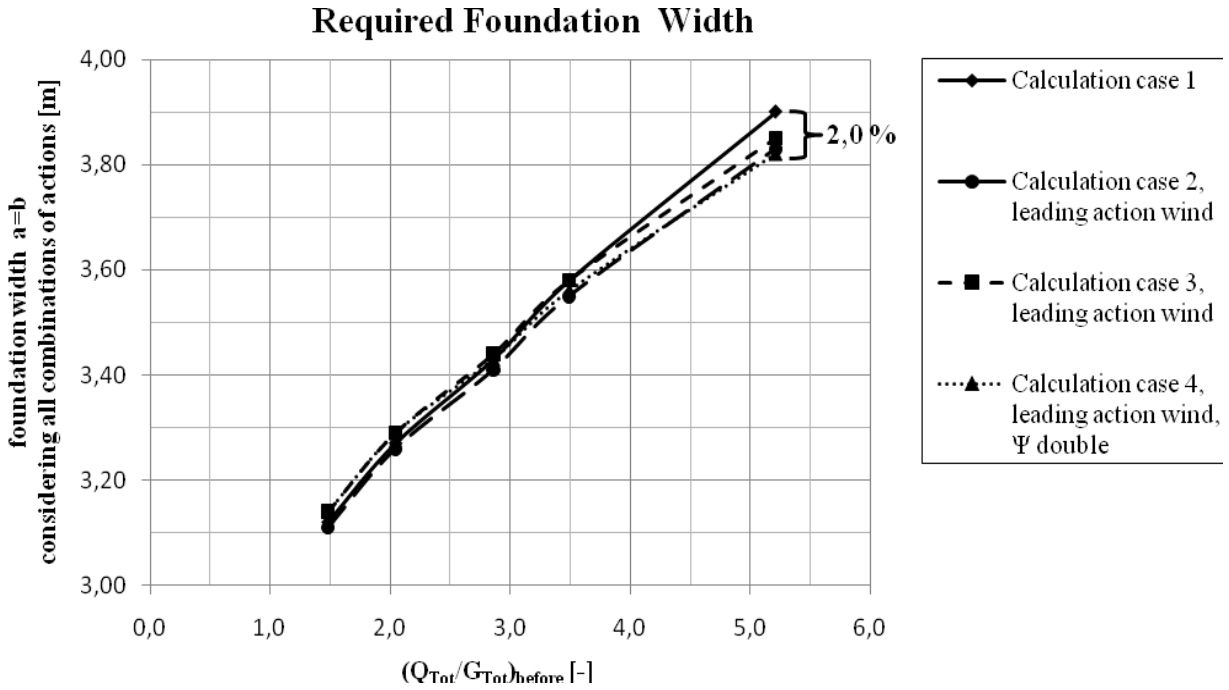

Figure 5. required foundation width considering all calculation cases, leading action wind, silt $\varphi = 27{,}5°$, $c_k = 5$ kN/m² or $c_{u,k} = 20$ kN/m².

5 CONCLUSIONS

The new standards DIN EN 1997-1, the German National Annex DIN EN 1997-1/NA and the new DIN 1054 (2010) allow to take into account that not all independent actions occur simultaneously with the same probability by applying combination factors ($\psi_i \leq 1{,}0$) to the temporary actions. This new approach leads mostly to lower design values than a determination of the design values according to DIN 1054 (2005).

Considering the design of the sheet pile quay wall, it has been shown that the required embedment depth and anchor length calculated according to DIN 1054 (2010) do not differ considerably from those determined according to DIN 1054 (2005). The resulting differences were lower than 4,0 %. However, only for the bending moment the differences were up to 10,3 %, leading in some cases to a lighter sheet pile section than the one determined according to DIN 1054 (2005).

The results of the foundation of a production hall have shown that the combination factors do not influence considerably the design, even by a double consideration of the combination factors reducing the temporary actions twice.

For the selected geotechnical applications it has been demonstrated that the reduction of the temporary actions, proposed by the new standards applying combination factors, do not lead to a significant lower safety level. Therefore, it is to consider if the effort is worth to invest extra calculation work by determining more than one design value depending on the amount of leading actions. It is suggested that the consideration of combination factors should rather be optional than obligatory.

REFERENCES

DIN 1054: 2005. Subsoil - Verification of the safety of earthworks and foundations

DIN 1054: 2010. Subsoil - Verification of the safety of earthworks and foundations - Supplementary rules to DIN EN 1997-1

DIN EN 1997-1: 2009. Eurocode 7- Geotechnical design - Part 1 - General rules; German version EN 1997-1:2004 + AC:2009

DIN EN 1997-1/NA: 2010. National Annex - Nationally determined parameters - Eurocode 7- Geotechnical design - Part 1- General rules

EAU 2004:2006. Grundbau, Recommendations of the Committee for Waterfront Structures Harbours and Waterways: EAU 2004. Ernst & Sohn.

5 Flood Defence

ISGSR 2011 - Vogt, Schuppener, Straub & Bräu (eds) - © 2011 Bundesanstalt für Wasserbau ISBN 978-3-939230-01-4

The Use of High Quality Data Sets in Flood Risk Management

M. T. (Martin) van der Meer
Fugro Ingenieursbureau B.V., The Netherlands

R. F. (Bob) Woldringh
Fugro Consultants Inc., United States of America

ABSTRACT: Time and time again, flood disasters show us that there are still many lessons to be learned from nature. For many generations, the Dutch, used to living below sea level and behind dikes, have actively shared their expertise and ideas to improve flood prevention and mitigation measures. Being a Dutch company, Fugro gladly participates in the Dutch Flood Control 2015 program, this gives us the opportunity to apply Dutch knowledge to dike and flood problems we encounter all over the world.A key issue is to find new ways to use state-of-the-art high quality area encompassing data and real-time data sets in assessing dike strength and its variations in space and time. In this paper, modern technologies to help manage Flood Risks and other Geo Hazards are presented, and some practical applications are demonstrated.

Keywords: mapping, laser, geological investigation, risk management, uplift, seepage

1 INTRODUCTION

1.1 *Flood Risk Management in the Netherlands*

The Netherlands is situated as a 'delta country' in Northwest Europe situated at the downstream end of the rivers Rhine, Meuse and Scheldt. The Netherlands has 16.4 million habitants, and with an area of 41,528 km^2 one of the most dense populated countries in the world (2007). The total length of the dike system is 17,500 km, of which 3600 km are primary dikes and 14,000 km are secondary dikes. The total length of the waterway system is ca. 5000 km. Table 1 shows an overview of some historic floods that have occurred in the Netherlands in the past 1200 years (Jonkman 2007).

Table 1. Historic Floods in the Netherlands

year	Coastal floods	Victims
838	Frisia coast	?
1228		100 000
1287	Wadden Sea st. Lucia flood	50 000
1404	Zeeland, 1st Elisabeth flood	?
1421	Southwest NL, Elisabeth flood	100 000
1530	Zeeland, st. Felix flood	>100 000
1570	Coast NL, Allerheiligen flood	20 000
1686	North NL st. Maartens flood	1558
1717	Western coast	11 000
1916	Southern sea	15
1953	Southwest NL watersnood	1836
	River floods	
1784	Betuwe area	?
1809		275
1855	Betuwe area, Maas, Waal	13
1861	Bommelerwaard, Maas, Waal	37
1880	Land van Heusden en Altena	2
1926	Meuse	?

Inevitably, water management became the core competence of the Dutch. Living in the Netherlands was, is and will also be in the future 'living with water':

- Flood Protection is vital for the Netherlands: 60% of the land – including the cities of Amsterdam and Rotterdam -and 70% of our Gross National Product (450 billion €) will be at risk during floods. The large 1953 flood was the 'wake up call' for the Dutch initiating their first 'Delta Plan'.
- The Dutch know that sea levels have been rising and the land has been subsiding for hundreds of years, and probably will continue to rise and respectively sink for the coming hundreds of years.
- Their river systems are part of bigger catchments (Rhine, Meuse, and Scheldt), so they established long term agreements with neighbouring countries.
- The water system is very fragile, coping with a very high groundwater level, subsidence problems of our very soft soils and oxidation of peat. The Dutch expect to have increasing salinity problems due to sea level rise and subsidence, which will affect fresh water supply and agriculture.

The backbone of the Dutch dike safety approach is the composition of the system to 53 dike-rings with each a safety standard by law (figure 1), controlled by 26 strong water boards responsible for the periodic safety assessments every 5 years. The water boards are responsible for water safety, quantity and quality management (included waste water treatment). The water boards collect their own taxes, ensuring dedicated money to be spent on water issues only. Per water board the maintenance budget is ca. 100 mln euro/year, of which 5% is spent on dike maintenance, ca. 45% on water quantity and ca. 50% on water quality.

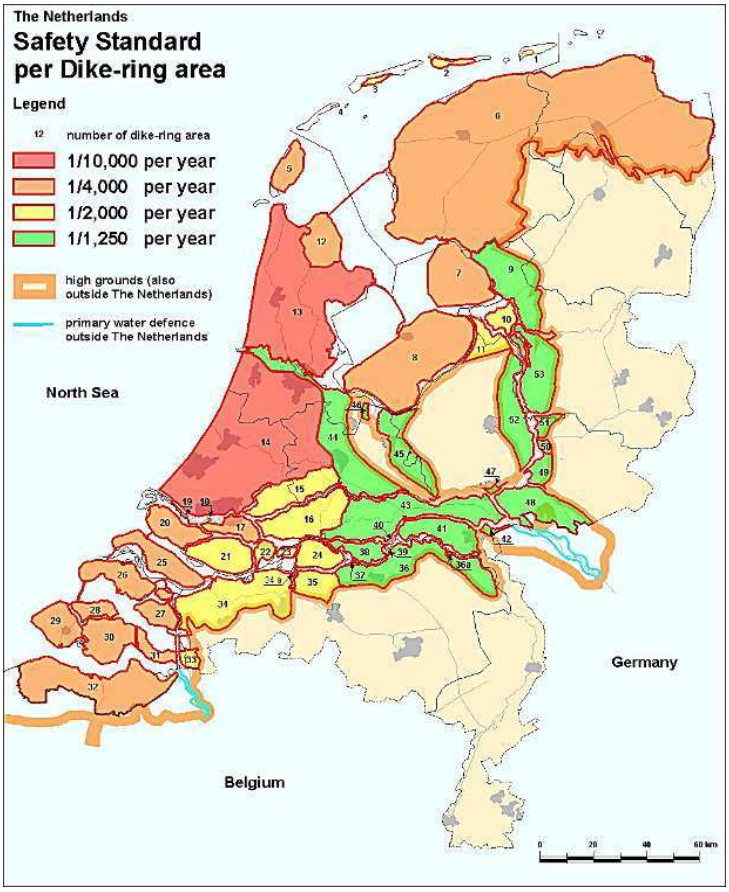

Figure 1. Dike rings and safety standards in the Netherlands

The Netherlands, being a small country at the end of the western European river system, have taken the initiative to set up some important European directives on Water Management: the EU Water Framework Directive (22 December 2000) and the EU Flood Directive (26 November 2007).

The EU Flood Directive 2007/60/EC regarding the assessment and management of flood risks became effective on 26 November 2007. This Directive requires that member countries map their flood plains, determine the potential flood consequences (loss of life and assets) and identify and execute flood risk reduction measures. The goal of this directive is not only to reduce flood risks, but also to manage them with an emphasis on human health, environment, cultural heritage and economy.

The Directive requires Member States to first carry out a preliminary assessment by 2011 to identify the river basins and associated coastal areas at risk of flooding. For such zones they would then need to draw up flood risk maps by 2013 and establish flood risk manage-ment plans focused on prevention, protection and preparedness by 2015. The Directive applies to inland waters as well as all coastal waters across the whole territory of the EU.

The Directive shall be carried out in coordination with the Water Framework Directive, notably by flood risk management plans and river basin management plans being coordinated, and through coordination of the public participation procedures in the preparation of these plans. All assessments, maps and plans prepared shall be made available to the public.

Member States shall furthermore coordinate their flood risk management practices in shared river basins, including with third counties, and shall in solidarity not undertake measures that would increase the flood risk in neighbouring countries. Member States shall take into consideration long term developments, including climate change, as well as sustainable land use practices in the flood risk management cycle addressed in the Flood Directive.

The EU Directives have been incorporated into Dutch legislation. E.g. detailed Flood Risk Maps are made available by internet for the public.

1.2 *Trends in Data Acquisition and Data Integration*

Modern airborne mapping technologies, using state-of-the-art remote sensing technology, serve a wide range of natural resources management, urban planning, economic development, emergency response, environmental, and engineering activities. This includes:

- Photogrammetric mapping: High resolution orthoimagery for base mapping and image classification, topographic contours, and planimetric mapping.
- Panoramic mapping: Simultaneous vertical and oblique orthoimagery combined with powerful 3D mapping and visualization software.
- LiDAR mapping: Fast and accurate elevation modeling for engineering-grade corridor mapping (FLI-MAP) and large-area topographic and bathymetric mapping.
- IFSAR and InSAR mapping (GeoSAR): Rapid production of regional and countrywide maps through clouds and dense foliage.

There are several methods for Light Detection And Ranging (LiDAR):

- Fixed wing Wide Area LiDAR, used to measure overall topography with fast aerial surveys, accuracy 10 cm, 4 points per m2. Often combined with area / region wide aerial photography.
- Helicopter LiDAR (FLI-MAP), originally developed for corridor mapping (for powerlines, railroads, pipelines, dikes etc.) but also used for very accurate overall topography mapping, accuracy 3 cm, 40 – 50 points per m2, combined with digital photo and video images.
- Terrestrial LiDAR (DRIVE-MAP), using a car mounted LiDAR data acquisition platform, used for detailed surface mapping (figure 2).

High quality continuous digital terrain models (DTM's) are a very useful tool for asset management, for both authorities and private parties. E.g. they allow detailed condition assessment, such as shallow gully detection by surface inversion, which is very important for dike safety assessments. For this and other reasons, most dike corridors in the Netherlands are mapped with very accurate FLI-MAP measurements, and subsequently the whole of the Netherlands is also flown in with helicopter LiDAR, to improve the height model from 1 point per 16 m2 to 10 points per m2. This enables the assessment of detailed flood risk maps.

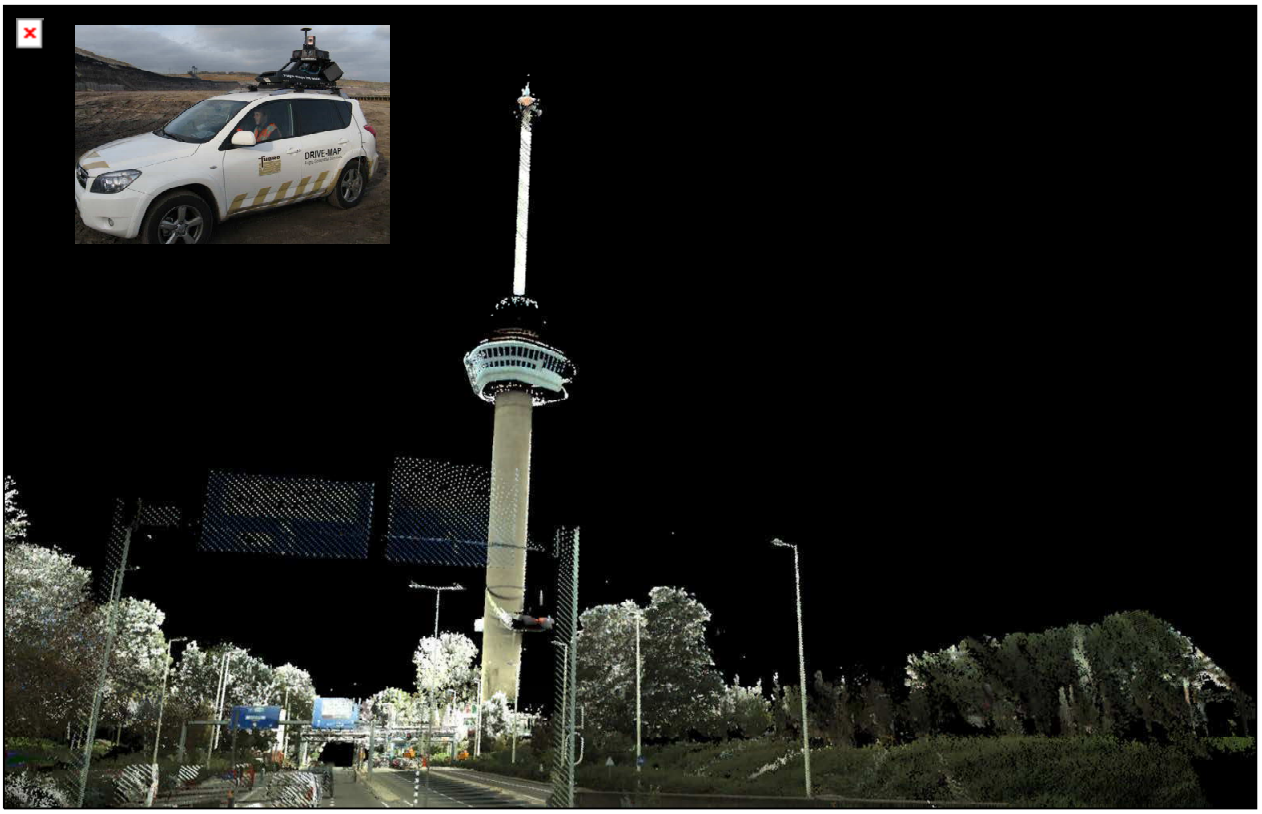

Figure 2. High quality terrestrial LiDAR data acquisition with DRIVE-MAP

1.3 *Dike strength as the backbone for Flood Risk Management*

In the Netherlands the safety levels of dikes are expressed as the required exceeding frequency of the water surface elevation WSE that the dike can withstand safely. Dutch secondary dikes are evaluated for WSE's having a return period of 10 to 1000 year. As shown in figure 1, Dutch primary dikes are evaluated for the 1,250 to 10,000 year event. In the USA most dike evaluations concern the 100 – 500 year event.

Dike strength analysis is all about first finding the weak(est) spots in the dike system, mostly hidden in the subsoil or the dike core. Knowing these weak(est) spots enables the responsible authorities to take appropriate action; this can be acquiring additional data, the installation of a monitoring system, a dike reinforcement program, the preperation of flood control plans (inspection, preparation of appropriate measures), or the elaboration of likely flood scenarions in calamity plans.

Fugro is partnering in the Dutch flood control research networks to develop and test new ways to tackle these problems. In the Flood Control 2015 program, amongst others the following dike strength topics are being studied:

- continuous dike strength mapping and automated engineering;
- real-time dike strength assessments;
- use of remote sensing in dike strength assessments.

2 REAL® CONCEPT

It has been observed that there is a need for a tool to perform dike analyses in long dike reaches, involving dense surface and subsurface data sets, and enabling large numbers of standard dike analyses in a GIS environment (Van der Meer 2007).

To make better use of the FLI-MAP and other state-of-the-art high quality data sets, Fugro developed the Rapid Engineering Assessment of Levees (REAL®) system. This tool allows cost- and time effective assessments of large numbers of dike km's and it enables cost and time effective re-assessments (physical and/or dike safety) if conditions or requirements change in time. The REAL® tool was first demonstrated in California (Van der Meer 2009).

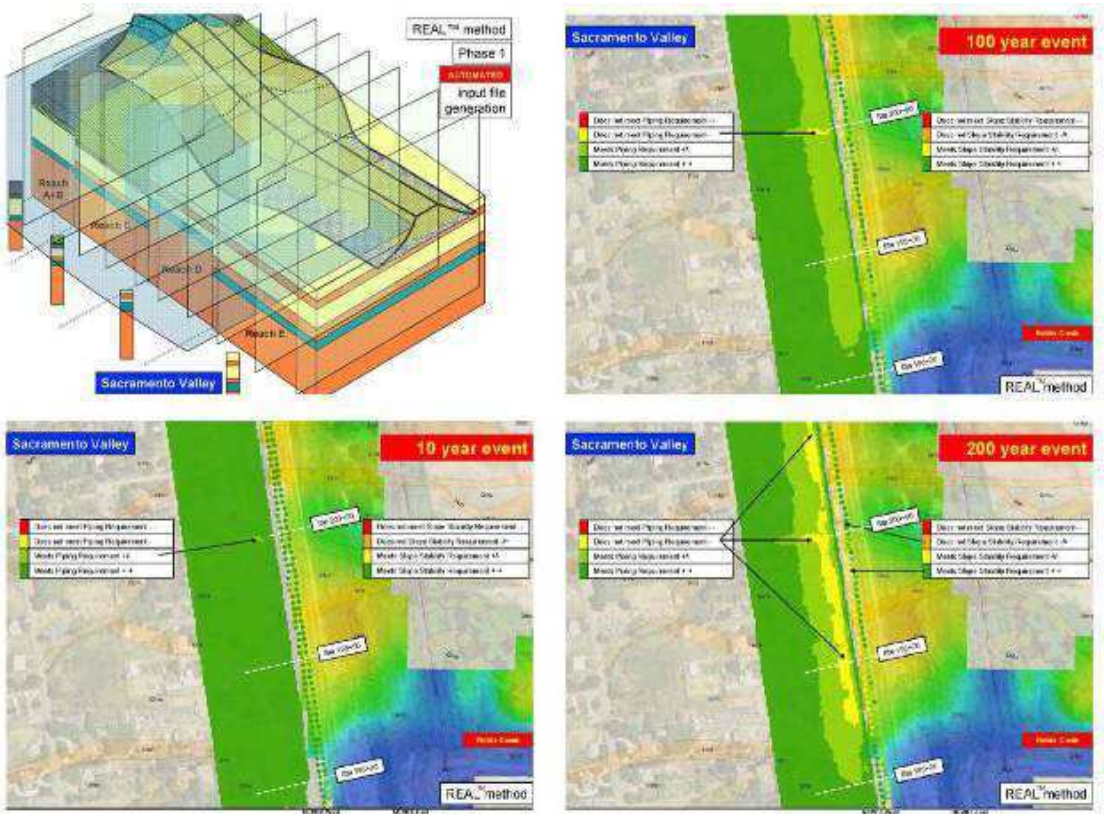

Figure 3. REAL® and multi WSE analyses presented in GIS

The REAL® concept enables us to make full use of the detailed Digital Elevation Model, acquired with the FLI-MAP system, to complete area covering dike strength analysis on all relevant failure mechanisms. E.g. the uplift and piping mechanisms can be checked with grid and vector analyses directly in GIS.

It's also possible to use off the shelve software to do cross section analysis for e.g. piping and/or slope stability analysis. Modules are made to perform automated cross section generation to perform automated engineering using off the shelve software, such as the GeoSlope suite, or the DAM platform and M-series developed by Deltares.

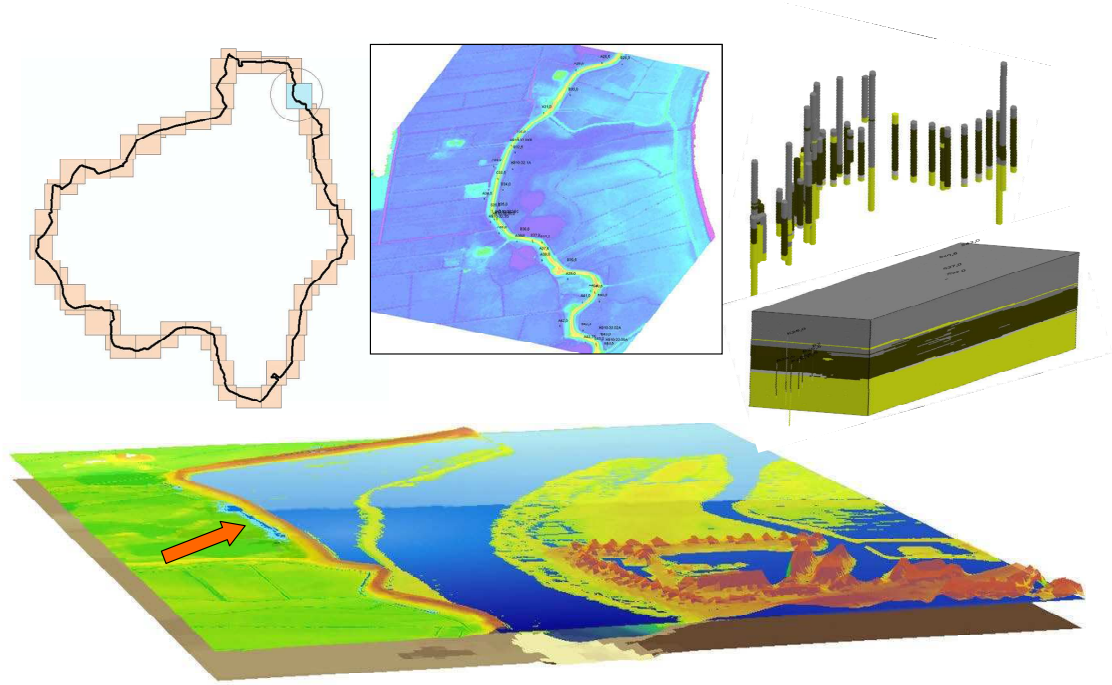

Figure 4. REAL® dike ring analysis, case 'Mastenbroek', the Netherlands

Figure 4 shows the modelling of an entire dike ring, in this case the ring 'Mastenbroek' of the water board 'Groot Salland', the Netherlands. The key of this project was to demonstrate the near real-time strength calculation of large dike sections in GIS. The figure shows the composition of the dike ring in sections allowing efficient GIS processing, the presentation of subsoil data and the generation of a subsoil model of the toplayers behind the dike, and a helicopter view on calculated uplift and piping safety during high water. The arrow points at a weak spot where the safety is below required standards.

Note that there are similarities between Flood Risk Management and the management of other Geo Hazards. E.g. modern technology developed for Landslide Risk Management or Earthquake Risk Management can be efficiently merged with Flood Risk Management technology and information systems.

3 TREE RISK MAPS

Trees can potentially reduce the safety of flood defences. The interaction between geotechnical failure mechanisms and tree physics is a key component in assessing the impact on dike safety. Tree parameters, derived from a database of the physical characteristics of several thousand trees, growing on or near by dikes, are integrated with geotechnical knowledge of embankment structures. The result is a tree risk zoning map, that represents a practical and useful tool to assess the influence of individual trees on dike integrity and safety.

Figure 5 shows an example of a tree risk map, which Fugro created for the Dutch water board Brabantse Delta. Of course this can easily be combined with the REAL® concept, allowing the creation of tree risk maps for any specific water level.

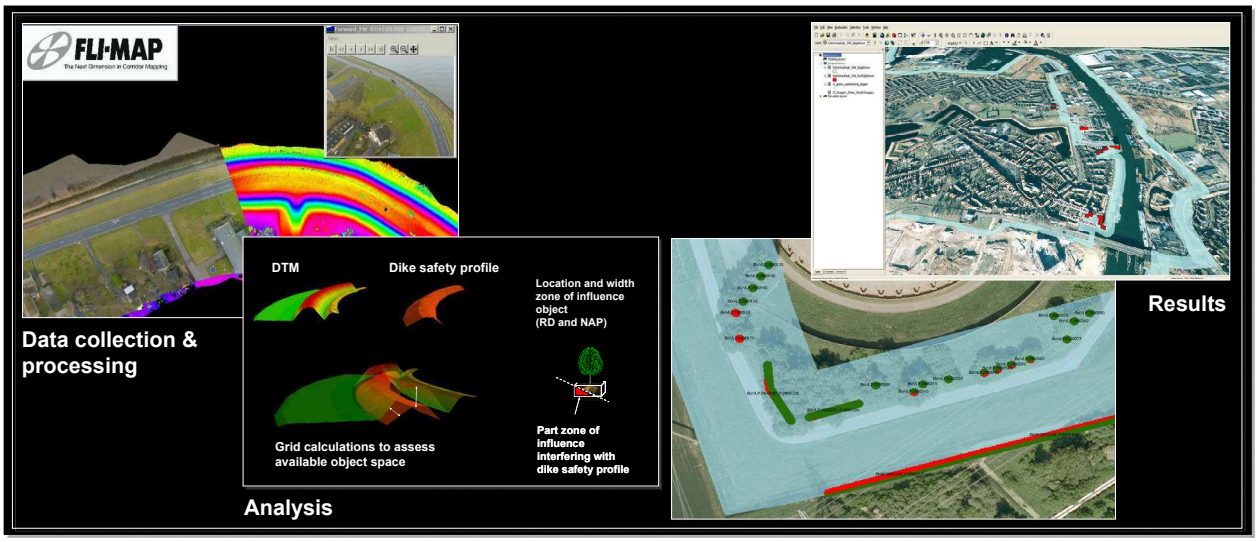

Figure 5. Tree risk map, results dike section Brabantse Delta, the Netherlands

4 CONTINUOUS DTMS AND 3D SUBSOIL MODELS

In all cases, the quality of data and the subsoil model is key for accurate failure predictions. So an important topic is the improvement of subsoil models, used for dike strength analyses, using airborne data acquisition techniques.

A known problem for geotechnical praticioneres is that important features are easy to miss when only using conventional ground investigation techniques. Also for the Californian dikes, we combined LiDAR data and Helicopter Electro Magnetics airborne data with more conventional data from cpt's, borings and geological knowledge (Pearce, 2009). In (Pearce, 2010) a detailed surficial geologic mapping for the northern Sacramento-San Joaquin Delta is presented, thus providing key data to document deposits, past processes, and geomorphic environments. An important first step is combining continuous surface and underwater DTMs to one continuous DTM (see figure 6).

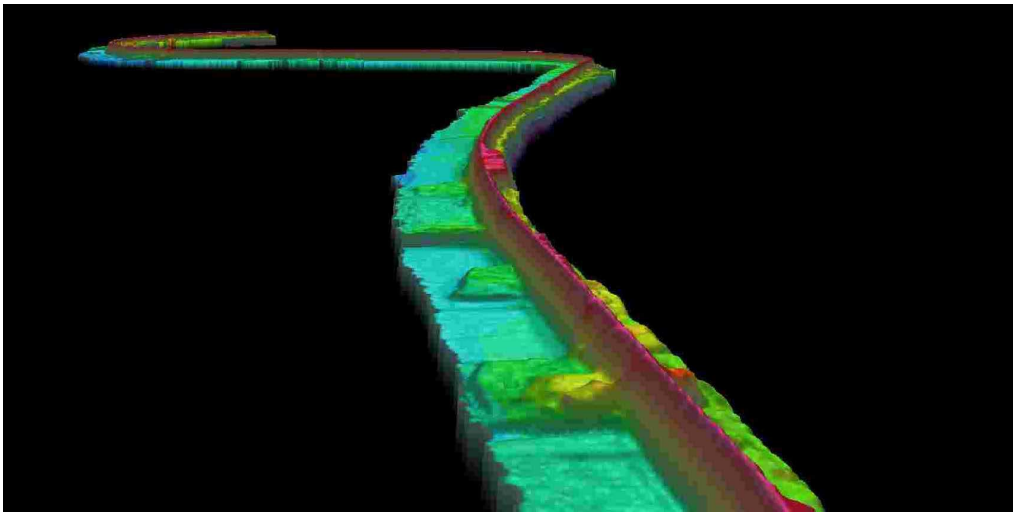

Figure 6. Continuous: bathymetrical and aerial elevation data model of a Californian dike section

5 DIGITAL CITY MODELS

Cities are becoming more and more important. Especially cities in delta regions are subjected to increasing flood risks, as a result of growing population and worse conditions due to climate change.

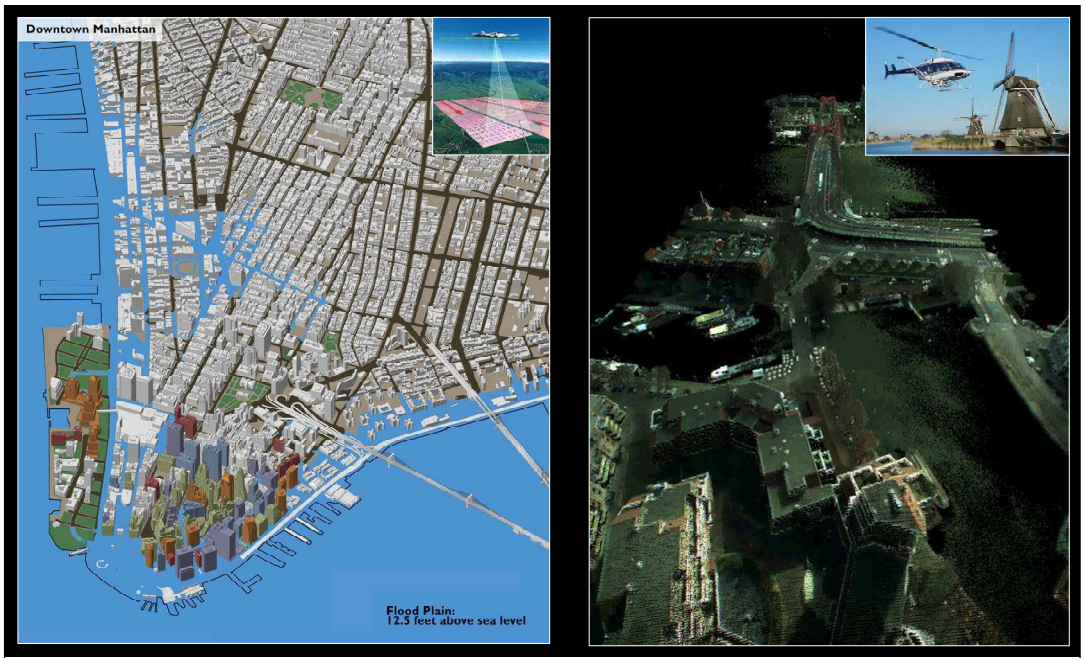

Figure 7. Digital city models, examples New York (Manhattan) and Rotterdam (detail of Willems bridge)

Figure 7 shows examples of digital city models for New York and Rotterdam. These models are used for urban flood risk planning, but also for various other purposes.

Another example is the use of comprehensive GIS-based mapping capabilities for the city of Norfolk (Virginia). This is being used to integrate tidal and other data into a flood prediction model that reacts to various environmental or design criteria input by the user.

These evaluations are being used to prioritise areas for flood defence improvements, to refine engineering design criteria and to analyse alternative flood mitiagion measures and emergency response plans within the city of Norfolk.

6 CONCLUSIONS

The following conclusions can be drawn, regarding the use of high quality data sets in flood risk management:

- Integrated Flood Risk Management (prevention, spatial planning and mitigation) needs accessable and visualized information systems, that should be based on solid reliable data.
- High quality data sets provide added 'users value' for both daily and extreme conditions when combined and used for REAL® solutions.
- REAL® accomodates Technology Transfer between several Geo Risk Management compartments (Flood Risks, Landslide Risks, Earthquake Risks etc.).

REFERENCES

Jonkman, S.N., 2007. Loss of life estimation in flood risk assessment - Theory and applications. Phd thesis Delft University, the Netherlands.

Meer, M.T., October 2010. The ongoing struggle to live safely in flood prone areas – the Dutch approach. Hong Kong Conference on Climate Change, Hong Kong.

Meer, M.T. van der, Lam, K.S and Knotter, H., June 2007. FAST4DMAP® Continuous GIS-based Strength Analysis of River Levees, Pilot Study Lek River Levee, The Netherlands. ASFPM Annual Conference in Norfolk, Virginia USA, June 2007.

Meer, M.T. van der, R.F. Woldringh and K. Knuuti, June 2009. Comparison of the Dutch and American Levee Safety Approach. ASFPM Annual Conference in Orlando, Florida USA.

NWP 2009. National Water Plan 2009 – 2015, 22 December 2009. (see: www.verkeerenwaterstaat.nl/english).

Pearce, J.T., Sowers, J.M., Brossy, C., and Kelson, K. October 2010. Surficial geology of the northern Sacramento – San Joquin Delta, recognizing deposits, landforms, and sedimentary environments and their relevance to science and engineering. San Francisco (California) Bay-Delta Science Conference, San Francisco.

Pearce, J.T., Marlow, D., Avila, C. and Selvamohan, S., June 2009. Use of Airborne Geophysical and Surficial Geologic Data for Analysis of Levees and Floodplain Processes. ASFPM Annual Conference, Orlando.

ISGSR 2011 - Vogt, Schuppener, Straub & Bräu (eds) - © 2011 Bundesanstalt für Wasserbau ISBN 978-3-939230-01-4

Estimating the probability of piping-induced breaching of flood embankments

M. Redaelli
Halcrow Group Limited, London, UK
previously University of Strathclyde, Glasgow, UK

ABSTRACT: A new tool for the rapid assessment of the structural performance of flood embankments during extreme hydrologic events was recently developed in the UK. This paper describes how the probability of failure due to piping through the manmade fill was included in the new methodology. Piping through the foundation (under-piping) and piping through the embankment (through-piping) are associated to different physical processes. While satisfactory mathematical models are available to study under-piping, through-piping is not currently amenable to satisfactory mathematical modelling. As a consequence it is not possible to define a performance function for reliability analyses. In this study, to overcome this obstacle, the probabilities of breaching by through-piping were estimated by elicitation of subjective judgement. In flood defence networks some characteristics of the structures are often unknown. To quantify the impact of this lack of knowledge on the performance prediction the probability of breaching was estimated in a finite, but extensive, number of scenarios, covering most cases of practical relevance.

Keywords: Erosion, Flood embankments, Piping, Reliability, River.

1 INTRODUCTION

1.1 *Reliability of flood embankments*

The probability of breaching of flood embankments (levees in American English) is an important component of flood risk modelling (Sayers *et al.* 2002). Its assessment, however, shows some problematic aspects. In particular quantifying the probability of failure due to piping through the manmade fill of the embankment's body is difficult (Figure 1). More generally the expected response to flooding events must be often assessed without knowing some key characteristics of the earth structure (epistemic uncertainty).

Through-piping is the most frequent failure mode for large embankment dams (Foster *et al.* 2000a&b, Richards & Reddy 2007). Although less data are available for fluvial embankments, also for this kind of earth structures various forms of piping seem to account for a non negligible percentage of breaches (Vorogushyn *et al.* 2009).

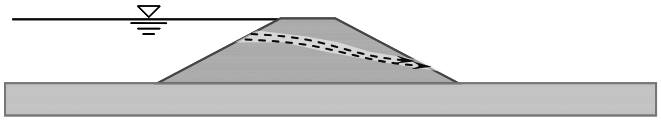

Figure 1. Schematic representation of through-piping.

1.2 *Problematic aspects in modelling through-piping*

Three main approaches are available to estimate the probability of failure of engineering systems: the statistical analysis of historical performance, the methods of reliability analysis (FORM, Monte Carlo simulation, etc.) and the elicitation of expert judgement. In the case of flood defence networks, which are extended systems with largely unrecorded and uncertain characteristics, there are not enough data on past breaches to confidently derive the probability of failure as a function of the water level. The methods of

reliability analysis require a mathematical model which separates safe states from failure states. Unfortunately, while credible models are available for other failure modes (CUR/TAW 1990), a satisfactory and complete model for trough-piping is not available to date (Fell & Fry 2007, Richards & Reddy 2007).

The availability of mathematical models for other failure modes and their successful use in the reliability analysis of flood defence networks (Vrijling 2001) has concealed this significant gap in the current methodologies. It is worth noting how the sea-dikes in the Netherlands, the first flood defences to be studied with reliability methods, are not subject to through piping due to their fill: a sand core completely surrounded by a compacted clay layer. This configuration effectively prevents an internal erosion process like the one depicted in Figure 1, even if other seepage-related adverse phenomena can still occur (Allsop *et al*. 2007).

An attempt to use mathematical models to estimate the probability of through-piping was made by USACE (1999) comparing the internal erosion model for macroscopically intact soil by Khilar *et al.* (1985) with an empirical criterion known as "Rock Island District procedure". For water levels approaching the levee crest the difference in the calculated probability of failure was of six orders of magnitude. USACE (1999) concludes that "there is no single widely accepted analytical technique or performance function in common use for predicting internal erosion".

A recent research project funded by the European Commission produced a catalogue of flood defences failure modes and associated mathematical models (Allsop *et al*. 2007); no model for the initiation of through-piping could be included. Fragility curves for through-piping produced by Bujis *et al* (2005, pp 9-11) are applied by Gouldby *et al.* (2008) to flood embankments in the UK; however the probability of failure was calculated with a criterion for the erosion of soil under impervious structures (Lane 1935), overstretching its use well beyond its range of applicability. There is no conceptual justification for the use of a model developed for a different physical process and its results should be regarded as misleading, as discussed by Redaelli & Dyer (2009) and Redaelli (2009, pp 28-30).

1.3 *Need for a new approach*

To overcome the current limitations a new methodology for the assessment of flood embankments reliability was developed. The new tool, named the Reliability Rating System, is based on a performance indicator which quantifies the probability of breaching only for a small number of water levels, above and immediately below the embankment crest. Although it does not produce a full reliability analysis, the methodology incorporates important, previously neglected geotechnical aspects and assists the final user in handling the remarkable lack of knowledge (epistemic uncertainty) typically associated with the safety assessment of flood defence networks.

One of the innovative aspects of the Reliability Rating System is the use of subjective probabilities to deal with through-piping, beside traditional reliability analyses for other failure modes like under-piping and breaching due to grass cover failure/fill erosion. This paper focuses on the determination of the probability of breaching due to through-piping. The general framework of the methodology and the other modes of failure are discussed in Redaelli (2009).

2 ESTIMATING THE PROBABILITIY OF PIPING-INDUCED BREACHING

2.1 *Lack of a satisfactory model for internal erosion*

Historically the term piping has been used in different contexts to indicate a variety of physical processes creating an often confusing terminology, particularly when disciplinary boundaries are crossed. For flood embankments the most relevant forms of piping are internal erosion – initiated along cracks or zones of concentrated leakage – and backward erosion – initiated at the exit point of seepage in a homogeneous granular material. Criteria to check safety against backward erosion in the foundation of water retaining structures can be found in the literature (Lane 1935, Weijers & Sellmeijer 1993).

Al least one theoretical formulation (Zaslavsky & Kassif 1965) and a mathematical model (Kilar *et al.* 1985) are available for piping through fine grained soils; however they refer to macroscopically homogeneous materials and do not consider erosion along cracks or zones of concentrated seepage. Several authors have studied the removal of grains due to water flowing in an opening (Worman & Olafsdottir 1992, Mohamed 2002, Bonelli *et al.* 2006). These models can correctly reproduce the process of pipe-growth and breach evolution. However the ability to capture accurately the presence or genesis of heterogeneities and anomalies which initiate the erosion still eludes the efforts of researchers. No mathematical model is

currently capable of describing the complete chain of events leading to breaching by through-piping (Richards & Reddy 2007, p 398) and even if some parts of the process are relatively well understood the associated quantitative tools are still being refined (Brown & Bridle 2008). For this reason, in embankment dam engineering, the probability of breaching by through-piping is not calculated with the methods of reliability analysis. Instead the statistical analysis of historical performance or the elicitation of subjective probabilities, often supported by the event tree approach, are regularly used (Fell *et al.* 2000, Fell & Fry 2007). Not enough data are currently available on the past performance of flood embankments to support a robust statistical analysis. The only remaining option is the elicitation of subjective judgement.

2.2 *Quantifying subjective judgement*

Subjective probabilities, in combination with the event tree technique, are extensively used by owners of large portfolios of dams (Beacher & Christian 2003). Published examples and guidance are available in the North American (Ladon-Jones *et al.* 1996), European (Johansen *et al*. 1997) and Australian literature (Fell *et al.* 2004).

In the event tree approach the failure is decomposed in chains of simpler events. These component events are organised in a graphical representation - the tree - which starts with an initiating event and then branches repeatedly, identifying some sequences leading to failure and some others leading to a safe state. The probability of some, or all, the component events along failure chains can be assessed, in absence of other solutions, by expert judgement. In order to produce credible results the judgement elicitation process must be rigorously structured and follow a precise procedure (Vick 1999 & 2002, Beacher & Christian 2003, USACE 2006). Techniques like the association with verbal descriptive statement (Lichtenstein & Newman 1967) and the "action approach to elicitation" (betting, reference lottery, wheel of fortune, etc.) are available to facilitate the assessment.

In most cases the opinions hold by experts are based on intuition, qualitative knowledge, personal experience and other ways of simplified reasoning. The mental processes behind the integration of information of various types into subjective probabilities are studied by cognitive psychology with the aim of achieving coherence and calibration. Subjective probabilities are coherent if they conform to probability theory; they are well calibrated if they reflect frequencies that are (or would be) observed in the real world. The informal methods used by people to estimate subjective probabilities are called heuristics. Several studies show that, in some circumstances, heuristics can lead to systematic errors called cognitive biases (Edwards & Tversky 1967, Kaneman *et al.* 1982, Taversky & Kahneman 1983). In the elicitation process presented here care was taken to minimise the anchoring bias, the representativeness bias, the conjunction fallacy, the availability bias. Overconfidence and misperception of extreme probabilities (Fischhoff *et al.* 1977, Vick 1997) were also considered. The interested reader can find a more detailed discussion of heuristics and biases, and their implication in geotechnical engineering practice in Beacher & Christian (2003).

2.3 *The elicitation process*

2.3.1 *Context*

In the Reliability Rating System (Redaelli 2009) the probabilities of breaching due to various failure modes are estimated for a small number of water levels. In particular the probability of breaching due to through-piping is evaluated only with the water level at the crest of the embankment. This paper describes results used in the Reliability Rating System; therefore all the probabilities of breaching mentioned in the following text do refer to this specific loading condition.

The Reliability Rating System is conceived for comparison among different embankments in a flood defence network, without any attempt to quantify the probability of network failure. Correlations in space are not included in the methodology and, similarly to other regional-scale tools (Gouldby *et al*. 2008), individual defences are identified splitting the network in sections not longer than 600m.

2.3.2 *Structured procedure*

In order to provide the end user with a tool for the quick quantification of reliability it was important to construct a methodology able to cover the wide range of scenarios possibly encountered in practice. This was done:

a) identifying the basic characteristics affecting the performance of embankments in flooding conditions;

b) establishing a realistic range of variation for each of these characteristics;

c) dividing the range in a tractable number of quantitative or qualitative classes;
d) estimating the probability of breaching for each relevant combination of classes.

As tables reporting the estimated probabilities of failures were complied, the final users have simply to locate the characteristics of an existing embankment in the appropriate classes to obtain an estimate of the probability of breaching by each failure mode and an overall index of expected performance.

The assessing panel which estimated the probability of failure by through-piping was composed by three persons: the author, then a PhD student at the University of Strathclyde (Glasgow), M. Dyer, then appointed to the Chair in Construction Innovation at Trinity College (Dublin), and S. Utili, at the time postdoctoral researcher at the University of Strathclyde (later Lecturer at the University of Oxford). All participants have a background in civil engineering with particular emphasis on geotechnics and experience in the geotechnical aspects of flood defences safety deriving form both professional practice and academic research.

The elicitation process was performed in a period of six months between March and September 2008 and was structured according to state-of-the-art recommendations (Vick 1999 & 2000, Beacher & Christian 2003, USACE 2006). With the aim of achieving coherence and good calibration the procedure was organised in five phases:

1. Motivating phase: developing an effecting working relationship among the assessors and clarifying the aims of the process.
2. Training phase: highlighting the biases potentially affecting the assessment in order to avoid, or at least mitigate, them.
3. Structuring phase: in which the problem was analysed and decomposed to an appropriate level of detail; this phase was introduced by an extensive literature review.
4. Assessing phase: consisting in the separate quantification of probabilities by each individual and by the subsequent discussion within the panel, finally leading to consensus on the final results.
5. Documenting phase: recording the process and the conclusions for verification and credibility.

2.3.3 *Initial formulation*

In principle the structural failure of a flood embankment could, and perhaps should, be studied with the event tree method. However the panel found that, while in embankment dam engineering, their use is supported by a reasonably detailed knowledge of the earth structure, for flood embankment a comparable level of knowledge is unimaginable. This makes the use of event tree still possible but more challenging and time consuming than affordable in the study presented here. For this reason, after an initial attempt, the assessors abandoned the event tree approach in favour of a different format.

This alternative approach builds on the formal structure of a historical performance method, known as University of New South Wales method (Foster *et al.* 2000a, b), which was modified to adapt it to the use of subjective probabilities. The adopted formula is:

$$P\left(B_{tp}\right) = \prod_i w_i \times P_{ref} \qquad (1)$$

where $P(B_{tp})$ = probability of breaching by through-piping, w_i = weights, i = characteristic affecting the performance, P_{ref} = probability of breaching by through-piping of a reference embankments with fixed characteristics.

Equation (1) reduces the task of the panel to the estimate of the probability of failure for a reference embankment and a system of weights to account for the different characteristics of individual structure. Hence the assessors went through the five phases described in the previous Section; in particular, during the structuring phase:

- the relevant characteristics influencing the probability of through-piping were identified;
- for each of these characteristics the level of information available in practice was discussed and an appropriate subdivision in classes chosen accordingly.

These activities have been guided by the literature on the condition assessment and performance estimation of flood embankments, with particular attention to the British reality (e.g. Environment Agency 2006, Morris *et al.* 2007). In the assessing phase:

- a reference embankment was chosen and a weight of 1.0 assigned the each one of its characteristics;
- the weights for each class of the various characteristics were established;
- the probability of failure for the reference embankment was estimated.

The last two steps had to be repeated iteratively: first to bring internal coherence to the system of weights devised by each individual; then to harmonise the different systems and achieve consensus through discussion. These activities were guided by the literature on the performance of embankment dams (e.g. Foster *et al*. 2000a&b, Fell *et al*. 2004, FEMA 2005a&b) combined with a significant dose of engineering judgement to adapt the indications to the case of flood embankments.

Achieving a well calibrated estimate of the probability of breaching for the reference embankment is problematic, partly because failure is the result of a complex process, partly because the probability is likely to be, in most cases, very low, thus falling in the field affected by the overconfidence bias. However the guidance offered by USACE (1999) in the form of verbal descriptors of the performance associated with probabilities of failure was used for this purpose.

Table 1. Weights estimated by the panel for the characteristics affecting the resistance to piping; the conditions of the reference embankment (optimal resistance) are in *italics*.

CHARACTERISTIC	CLASSES & WEIGHTS					
Animal burrowing w_{burr}	Yes, likely to completely cross the earthfill 200	Yes, unlikely to completely cross the earthfill 50	*No* 1			
Seepage w_{seep}	Muddy leakage 50	Clear leakage 30	Pooling water 10	*None* 1		
Differential settlement w_{sett}	Inducing recognisable cracking 30	Visible, no recognisable cracking 10	*Not visible* 1			
Compaction w_{com}	No compaction 25	Some compaction 10	*Good compaction** 1			
Culvetrt w_{cul}	Many poor details** 25	Few poor details 10	Optimal condition 15	*None* 1		
Fill type w_{soil}	Silt LL<50*** 21	Clean Sand 15	Clayey Sand Silty Sand 6	Silt LL>50 5	Clay LL<50 4	*Clay LL>50* 1
Plant roots w_{root}	Trees 15	Bushes 5	*Grass only* 1			
Fill origin w_{geo}	Alluvial 8	Aeolian, Colluvial 5	Residual, Lacustrine, Marine, Volcanic 4	*Glacial* 1		

* According to BS 6031:2009 or equivalent modern standard; ** list and discussion of relevant details can be found in Redaelli (2009); ***LL = liquid limit.

2.3.4 *Refined formulation*

During the structuring phase the panel identified eight main characteristics which affect the piping resistance; these characteristics are visible in the first column of Table 1. A convenient subdivision in classes for each of the characteristic was also identified. It was also decided to take as reference an embankment with optimal characteristics for piping-resistance and a length of 500m.

After some attempts the assessors found impossible, using Equation (1), to reflect a sufficient worsening of the performance when only one or few negative factors were present and simultaneously satisfy the basic condition $P(B_{tp}) \leq 1$ for combinations of several negative factors. The problem was overcome adopting a more complex formula, in which coefficients of influence are introduced:

$$P\left(B_{tp}\right) = \prod_{j} \max\left(w_j \times r_j , 1.0\right) \times P_{ref} \qquad (2)$$

where j = position of the weight in the list of characteristics, arranged form the most to the least influential.

To calculate the probability of failure a list of the eight key characteristics is made, ordering them from the most influential (highest weight) to the least influential (smallest weight). Then each weight is multiplied by a coefficient of influence reduction, which has unit value for the first characteristic, then progressively lower values for the following characteristics. Given that the reference embankment is the one with optimal resistance the individual weights w_i, also after multiplication with the coefficients of influence reduction r_i, cannot be less than 1. The panel has found convenient expressing the coefficients of influence reduction with the formula:

$$r_i = 1/a^{j-1} \qquad (3)$$

where a is a constant, which becomes part of the judgement elicitation process.

2.4 *Outcome of the elicitation process*

The weights estimated by the panel of assessors at the end of the elicitation process are reported in Table 1. The panel also proposed coefficients of influence reduction based on

$a = 3$ which leads to $r_1 = 1, \quad r_2 = 1/3, \quad r_3 = 1/9, \quad \cdots$

The probability of breaching for the reference embankment, with water at crest level, was estimated to be in the range of:

$$P_{ref} = 9.0 \times 10^{-5}$$

The probability of failure of the embankment with the highest proneness to piping, calculated using the ordered list of characteristics given in Table 2, is:

$$P(B_{tp}) = 9.0 \times 10^{-5} \times 1.1 \times 10^{4} = 0.99$$

Table 2. Weights and coefficients of influence reduction of the embankment with the most unfavourable characteristics for piping resistance; only the first three characteristics affect the probability of failure.

j	Characteristic	Class	w_i	r_i	Max[$w_i \times r_i$, 1]
1	Animal burrowing	Yes, likely to cross fill	200	1	200
2	Seepage observed	Muddy leakage	50	1/3	16.7
3	Differential settlement	Yes, inducing cracking	30	1/9	3.33
4	Compaction	Not compacted	25	1/27	1.0
5	Culvert	Many poor details	25	1/81	1.0
…	…	…	…	…	…

The interval covered by the presented approach is shown in Figure 2 against the performance descriptors by USACE (1999). The reference embankment is estimated to have a "good" performance also in the very severe loading condition assumed, while the "worst case" embankment, with 99% chance of failure, is almost certainly breaching.

3 DISCUSSION

3.1 *Handling epistemic uncertainty*

In many practical cases some of the characteristics affecting the piping-resistance are uncertain. The values provided here can quantify of the impact of this lack of knowledge on the performance prediction. For example Figure 3 shows how the interval of possible probabilities of breaching for an embankment with optimal characteristics, but unknown compaction and fill type/origin, becomes significantly narrower once the information on the fill is gathered.

3.2 *Use and limitations*

The subjective probabilities elicitation was conducted following a rigorously structured procedure according to state-of the-art recommendations. Nevertheless the small size of the panel and the relatively uniform background of the participants suggest that better results could be obtained by a larger panel which included a wider spectrum of competencies and covered more completely the different roles that individuals should play in the elicitation process (Baecher & Christian 2003, p 510).

The presented approach was dictated by the need to develop the elicitation process in a very parsimonious way, which made good use of limited time and resources. This work demonstrates how the appropriate use of subjective judgement can lead to sensible, if not extremely well calibrated, predictions. Hopefully more complete studies on this subject will be performed in the near future within the civil engineering community.

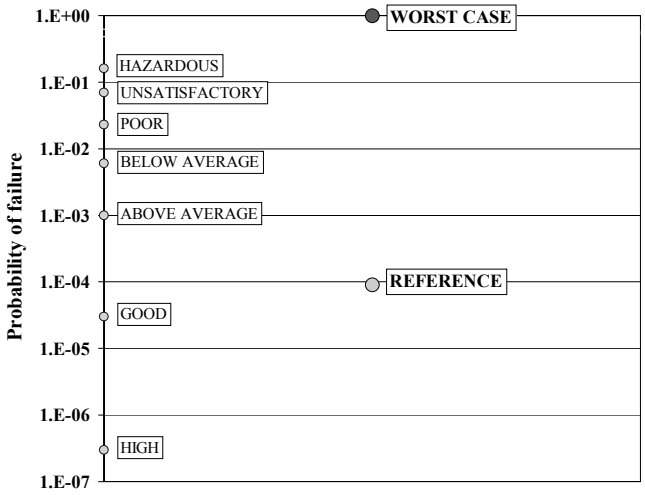

Figure 2. Expected performance, with water at crest level, for the reference embankment (optimal resistance to piping) and for the "worst possible" embankment; values are compared with verbal descriptors from USACE (1999).

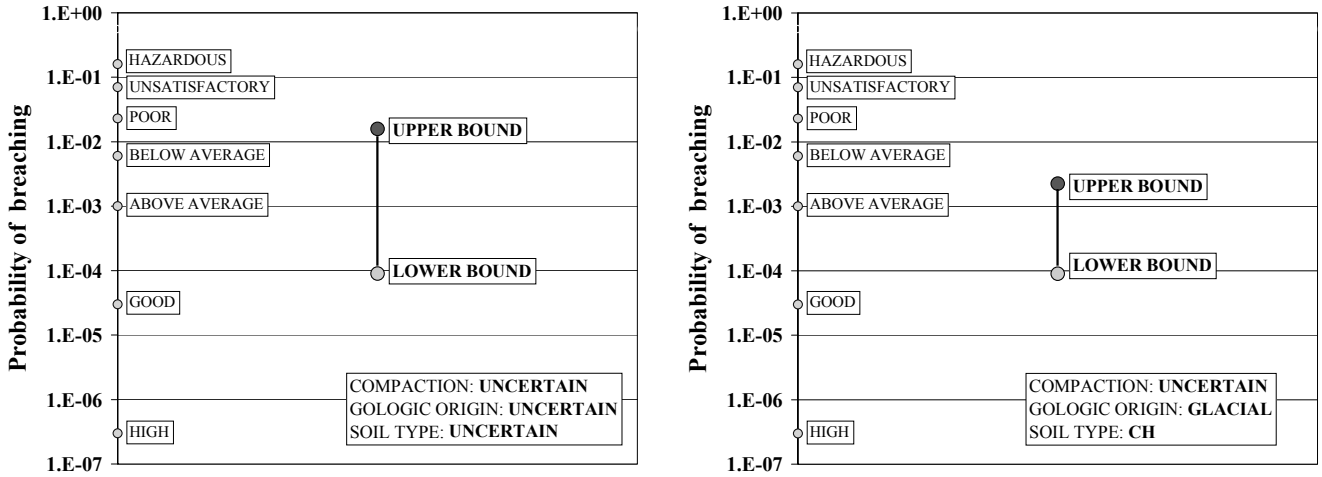

Figure 3. Bounds on the probability of breaching for an embankment with uncertainty about compaction, type of the soil in the earthfill and geologic origin of the earthfill (left). The interval narrows once the information on the fill becomes available (right); CH = high plasticity clay (liquid limit above 50), according to the Unified Soil Classification System.

3.3 *Future research: the need for through-piping fragility curves*

The probabilities of breaching presented here are all estimated for a specific loading condition. These vales have been derived to offer some guidance regarding the safety against through piping during extreme floods. They are also employed, with a large set of tabulated results on other failure modes, in a simplified reliability assessment methodology proposed by Redaelli (2009), which provides an index of overall performance.

To conduct a complete flood risk analysis, however, the knowledge of the probability of breaching in one loading condition is insufficient: fragility curves, defining the conditional probability of failure given the load for each relevant water level, are needed (Figure 4). While several works on fragility curves for under-piping are available and the underlying theory and assumption are widely accepted, to the author's knowledge no satisfactory fragility curves for piping through the fill of fluvial embankments has been developed to date. This is largely due to the absence of a credible mathematical model ant the consequential impossibility to adopt the traditional methods of structural reliability.

Considering that through-piping plays an important role in the safety of flood embankment the urgency of developing a satisfactory set of fragility curves for this failure mode should be perceived by all researchers active in this field. It is here suggested that an elicitation process, similar to the one presented here but involving a larger and more complete panel of experts, should be arranged to work at the definition of through-piping fragility curves. Working on a longer time scale and mobilising larger resources a more advanced approach could be adopted, possibly making use of event trees like the one shown in Figure 5.

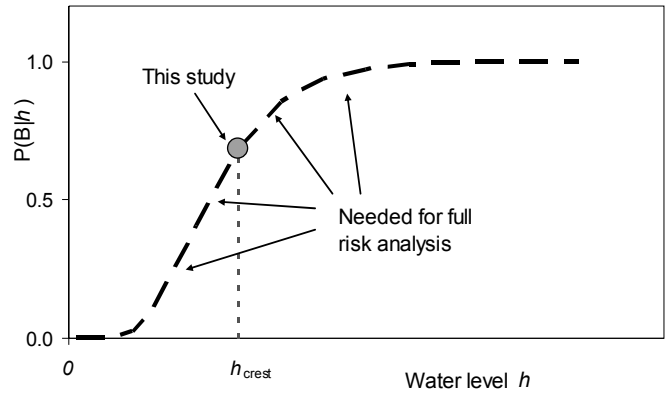

Figure 4. This study provides estimates of the probability of failure for one loading condition (water at the crest level); for a complete flood risk analysis fragility curves are needed.

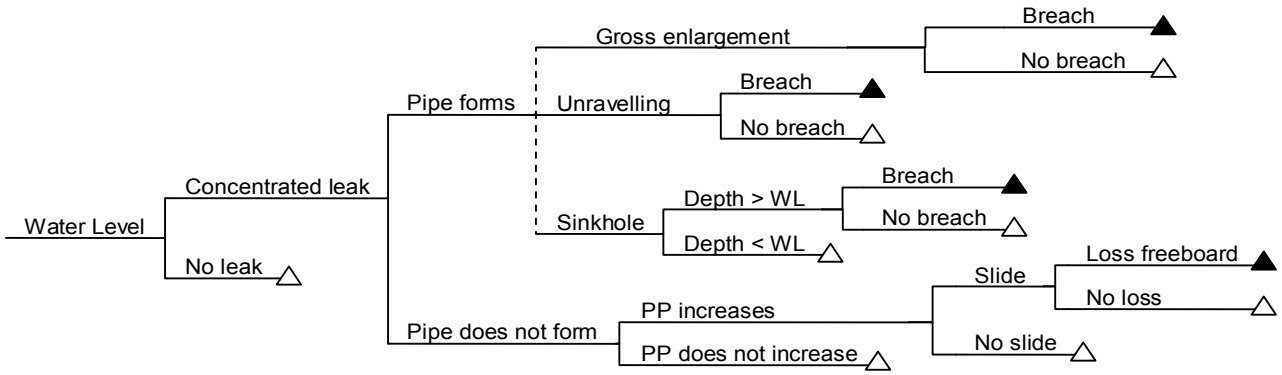

Figure 5. Event tree for breaching by piping through the earthfill of flood embankments proposed by Redaelli (2009). Dotted branches connect events that are not mutually exclusive; WL = water level, PP = pore pressure.

4 CONCLUSION

Through-piping is an important failure mode for flood embankments which cannot be studied with the methods of reliability analysis due to the lack of a satisfactory and complete mathematical model. This paper presents probabilities of piping-induced breaching which were estimated via a rigorously structured process of judgement elicitation. These probabilities of failure are linked to eight key characteristics of flood embankments and were assessed for a wide range of scenarios, covering most cases of practical relevance.

The presented results enable a first assessment of piping resistance of existing embankment and offer a way of quantifying the impact of epistemic uncertainty on the performance prediction. These results are part of a wider body of work on the development of an innovative methodology for the simplified reliability assessment of flood embankments, which combines the traditional methods of reliability analysis and the elicitation of subjective probabilities to incorporate various failure modes in a quantitative measure of the overall expected performance (Redaelli 2009).

The probabilities of breaching reported here were estimated for a single loading condition, which is water level at the crest of the embankment. To support full flood risk analyses it is necessary to produce fragility curves that provide the conditional probability of failure given each relevant value of the water level. It is urgent that the flood risk community addresses the current absence of adequate fragility curves for through-piping.

5 ACKNOWLEDGMENTS

The author is grateful to Prof. M. Dyer and Dr S. Utili for their participation in the judgement elicitation process. The work presented in this paper has been jointly funded by the Department of Civil Engineering and by the Faculty of Engineering of the University of Strathclyde (Glasgow). Comments by Prof M. Hicks and Prof. R. Lunn have contributed to improve the first version of this research project.

REFERENCES

Allsop W., Kortenhaus A. & Morris M., 2007. *Failure Mechanisms for Flood Defence Structures*. Technical Report T04-06-01, FLOODsite Consortium.

Baecher G.B. & Christian J.T., 2003. *Reliability and Statistics in Geotechnical Engineering.* John Wiley, New York.

Bonelli S., Brivois O., Borghi R. & Benahmed N, 2006. On the modelling of piping erosion. *Comptes Rendus Me´canique* 334, 555–559.

Buijs F., Simm J., Wallis M. & Sayers P., 2005. *Performance and Reliability of Flood and Coastal Defences.* Joint Defra/EA Flood and Coastal Erosion Risk Management R&D Programme, Technical Report FD2318/TR2.

CUR/TAW, 1990. *Probabilistic Design of Flood Defences*. Centre for Civil Engineering Research / Technical Advisory Committee on Flood Defences, Report 141, Gouda, The Netherlands.

Edwards W. & Tversky A., 1967. *Decision Making: Selected Readings*, Penguin Books.

Environment Agency, 2006. *Managing Flood Risk - Condition Assessment Manual*. Ref. 166_03_SD01.

Fell R. & Fry J.-J., 2007. *Internal Erosion of Dams and Their Foundations*, Taylor & Francis, London.

Fell R., Bowles D.S., Anderson L.R. & Bell G., 2000. The status of methods for estimation of the probability of failure of dams for use in quantitative risk assessment, *Proc. 20th ICOLD Congress*, Beijing, China.

Fell R., Wan C.F. & Foster M., 2004. *Methods for Assessing the Probability of Failure of Embankment Dams by Internal Erosion and Piping.* UniCiv Report No. R-428 May 2004, University of New South Wales, Sydney, Australia.

FEMA, 2005a. *Technical Manual for Dam Owners: Impacts of Animals on Earthen Dams*. Federal Emergency Management Agency, US Department of Homeland Security.

FEMA, 2005b. *Technical Manual for Dam Owners: Impacts of Plants on Earthen Dams.* Federal Emergency Management Agency, US Department of Homeland Security.

Fischhoff B., Slovic P. & Lichtenstein S., 1977. Knowing with certainty: the appropriateness of extreme confidence. *Journal of Experimental Psychology: Human Perception and Performance* 3(4), 552-564.

Foster M., Fell R. & Spannagle M., 2000a. The statistics of embankment dam failures and accidents. *Canadian Geotechnical Journal* 37(5), 1000-1024.

Foster M., Fell R. & Spannagle M., 2000b. A method for assessing the relative likelihood of failure of embankment dams by piping. *Canadian Geotechnical Journal* 37(5), 1025-1061.

Gouldby B., Sayers P., Mulet-Marti J., Hassan M.A.A.M. & Benwell D., 2008. A methodology for regional-scale flood risk assessment. *Proc. ICE, Water Management* 161(3), 169–182.

Johansen P.M., Vick S.G. & Rikartsen C., 1997. Risk analysis for three Norwegian dams. In Broch, Lysne, FlatbÆ, Helland-Hansen (Eds), *Hydropower 97*, Balkema, Rotterdam, 431-442.

Kahneman D., Slovic P. & Tversky A., 1982. *Judgment Under Uncertainty: Heuristics and Biases*, Cambridge University Press, Cambridge, UK.

Khilar K.C., Fogler H.S. & Gray D.H., 1985. Model for piping-plugging in earthen structures. *Journal of Geotechnical Engineering* 111(7), 833-846.

Landon-Jones I., Wellington N.B. & Bell G., 1995. Risk assessment of Prospect Dam. *ANCOLD Bulletin* 103, Australian National Committee on Large Dams, 16-31

Lane E.W., 1935. Security from under-seepage: masonry dams on earth foundation. *Transaction ASCE* 100, 1235-1272.

Lichtenstein, S. & Newman, J. R., 1967 Empirical scaling of common verbal phrases associated with numerical probabilities. *Psychonomic Science, 9* (10), 563-564

Mohamed M. *Embankment Breach Formation and Modelling Methods*. PhD thesis, The Open University, 2002.

Morris M., Dyer M. & Smith P., 2007. *Management of Flood Embankments - A Good Practice Review*. Defra/Environment Agency Flood and Coastal Defence R&D Programme, Technical Report FD2411/TR1.

Redaelli M. & Dyer M., 2009 Discussion: A methodology for regional-scale flood risk assessment by B. Gouldby et al. 2008, *Proc. ICE, Water Management* 162(WM5), 347-348.

Redaelli M., 2009. *A Reliability Rating System for Flood Embankments in the UK.* PhD Thesis, University of Strathclyde, UK.

Richards K.S. & Reddy K.R., 2007. Critical appraisal of piping phenomena in earth dams. *Bulletin of Engineering Geology and the Environment* 66(4), 381-402.

Sayers P.B., Hall J.W., Meadowcroft I.C., 2002. Toward a risk-based flood hazard management in the UK. *Proc. ICE*, *Civil Engineering* 150, 36-42.

Tversky A. & Kahneman D., 1983. Extension versus intuitive reasoning: the conjunction fallacy in probability judgment. *Psychological Review* 90, 293-315.

USACE, 1999. *Risk-Based Analysis in Geotechnical Engineering for Support of Planning Studies*. US Corps of Engineers Publication No. ETL 1110-2-556.

USACE, 2006. *Reliability Analysis and Risk Assessment for Seepage and Slope Stability Failure Modes for Embankment Dams*. US Corps of Engineers Publication No. ETL 1110-2-561.

Vick S.G., 1999. *Considerations for Estimating Structural Response Probabilities in Dam Safety Risk Analysis*. US Bureau of Reclamation Technical Report, Ref. No. 99D88313040, USBR Technical Service centre, Denver, CO, USA.

Vick S.G., 2002. *Degrees of Belief: Subjective Probability and Engineering Judgement*. ASCE, Reston, VA, USA

Vorogushyn S., Merz B.& Apel H., 2009. Development of dike fragility curves for piping and micro-instability breach mechanisms. *Nat. Hazards Earth Syst. Sci.* 9, 1383–1401.

Vrijling J.K., 2001. Probabilistic design of water defense systems in the Netherlands. *Reliability Engineering & System Safety* 74(3), 337-344.

Weijers J.B.A. & Sellmeijer J.B., 1993. A new model to deal with the piping mechanism. In Brauns J., Heibaum M., Schuler U., (Eds), *Filters in Geotechnical and Hydraulic Engineering*, Balkema, Rotterdam.

Worman A. & Olafsdottir R., 1992. Erosion in a granular medium interface. *Journal of Hydraulic Research* 30(55), 639-655.

Zaslavsky D. & Kassiff G., 1965. Theoretical formulation of piping mechanism in cohesive soils. *Geotechnique* 15, 305-316.

ISGSR 2011 - Vogt, Schuppener, Straub & Bräu (eds) - © 2011 Bundesanstalt für Wasserbau ISBN 978-3-939230-01-4

Reliability Analysis and Breach Modelling of Coastal and Estuarine Flood Defences

M. Naulin, A. Kortenhaus & H. Oumeraci
Leichtweiß-Institute for Hydraulic Engineering and Water Resources (LWI), Technische Universität Braunschweig, Germany

ABSTRACT: Failures of flood defences caused by extreme storm surges can result in severe flooding of the hinterland leading to loss of life and catastrophic damages. In order to quantify the risk of flooding, an integrated risk analysis is being performed within the German 'XtremRisK' project. Within one subproject of XtremRisK, reliability analyses and breach modelling of coastal and estuarine flood defences are performed. In this paper, the methods of the failure probability calculations of coastal and estuarine flood defence structures under the loading of extreme storm surges are discussed. Moreover, the analysis of dike breaches is introduced. Preliminary results of the failure probabilities and the breach modelling are presented exemplarily for estuarine dikes of the Elbe Estuary in the urban area of Hamburg, Germany. Furthermore, gaps in knowledge related to time-dependent failure mechanisms are addressed where an approach is introduced to consider the unsteady conditions of storm surges implemented exemplarily for the failure mechanisms of 'wave overtopping' and 'overflow'. These results are put in context of an integrated risk analysis approach used in XtremRisK.

Keywords: reliability analysis, dike, failure modes, time-dependent analysis, flood risk

1 INTRODUCTION

Impacts of extreme storm surges can cause failures of coastal flood defences and hence flooding of the hinterland resulting in human casualties and enormous economic damages. Especially low-lying coastal areas such as UK, The Netherlands, or Germany are at risk. Due to climate change it may be expected that the risk of flooding will still increase (IPCC, 2007). In order to quantify the present and future flood risk of extreme storm surges, an integrated risk analysis approach is being performed within the German 'XtremRisK' project (www.xtremrisk.de). For this purpose, the source-pathway-receptor model (Figure 1) is applied to an open coast using the example of the island of Sylt, North Sea, and to an estuarine urban area using the example of the Elbe Estuary in Hamburg, Germany. The source-pathway-receptor concept has already been used in flood risk analysis and systematically addresses (Oumeraci, 2004): (i) sources of the risk (storm surge), (ii) risk pathways (way the risk "travels", e.g. across coastal defences or other storm surge protection measures), and (iii) receptors of risk which can be assets such as houses, industry, farming area, etc., or people. The overall approach of XtremRisK comprises four subprojects which deal with risk sources, risk pathways, risk receptors, and their integration as summarized in Figure 1.

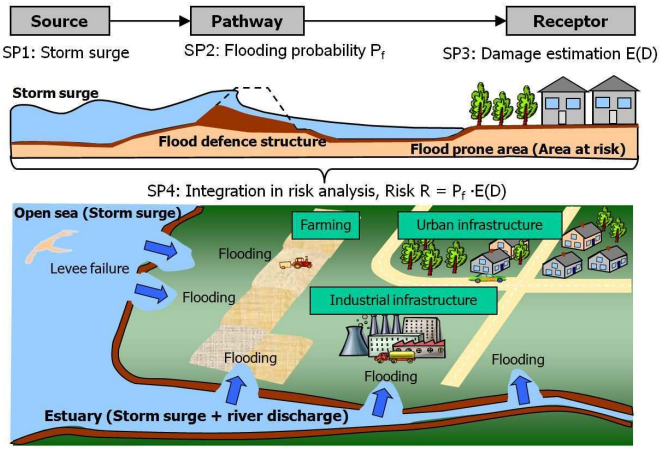

Figure 1. Source-pathway-receptor concept and associated subprojects (SP) in XtremRisK (Oumeraci et al., 2009).

In this project, flood risk is defined as the product of flooding probability Pf and related consequences E(D). Hence, one of the key tasks is to

predict the first component of the flood risk, i.e. the failure probability of the flood protection systems which is assumed equivalent to the probability of the hinterland being flooded. Within subproject 2 (SP 2) of XtremRisK, the failure probabilities of flood defences are determined. Moreover, initial flooding conditions at the breach locations (breach width, breach hydrograph, etc.) are modelled. The overall results will be delivered to subproject 3 (SP 3) of XtremRisK for inundation modelling and to subproject 4 (SP 4) for risk integration (Burzel et al., 2010).

This paper presents key elements of the research work of SP 2 aiming at the flooding probability Pf. First, the pilot site of Hamburg is introduced. Second, the applied methods of SP 2, i.e. reliability analysis and breach modelling, are presented. Third, preliminary results of the failure probabilities and the breach modelling using the example of estuarine dikes in Hamburg are presented. Furthermore, gaps in knowledge related to time-dependent failure mechanisms are addressed and an approach is introduced to consider the unsteady conditions of storm surges implemented exemplarily for the failure mechanisms of 'wave overtopping' and 'overflow'. These results are put in context of an integrated risk analysis approach used in XtremRisK. Finally, a summary is given, including a brief description of future prospects.

2 PILOT SITES

The pilot sites, Hamburg and Sylt, are located in the northern part of Germany (Figure 2a). As an example for an open coast, the island of Sylt in the North Sea is analysed whereas the Elbe Estuary of the city of Hamburg serves as an example for an estuarine urban area. Since the focus of this paper is set to exemplarily methods and results of estuarine dikes in Hamburg, only this study area is introduced in the following section.

Hamburg is a mega-city with 1.8 million inhabitants and represents the second largest city of Germany. As a centre for trade, transportation and services, the city is one of the most important industrial sites in Germany with the port of Hamburg being one of the world's leading seaports.

To a large extent, Hamburg's flood defence structures consist of flood defence walls and dikes with sand core, clay layer and grass cover. Moreover, a variety of structures to close openings of the flood defence line is found such as flood defence gates, tidal gates, flood barriers, etc. The area protected by flood defence structures comprises 270 km², i.e. 1/3 of Hamburg's territory, where 180,000 people live and 140,000 people work. Within this area goods amounting to a total value of 10 billion Euros are in stock (LSBG, 2007).

The main hydraulic conditions of the pilot sites for Hamburg are a mean high water level of 2.1 mNN (mNN = German datum for water level) and a mean river discharge of 708 m³/s. The highest recorded storm surge water level was measured at 6.45 mNN in 1976 and the highest river discharge at 3,620 m³/s in 1940, respectively. In the past, Hamburg has suffered severe damages caused by extreme storm surges, e.g. the 1962 storm surge led to several dike breaches where more than 300 people lost their lives.

Since a complete risk analysis of the total area of Hamburg would exceed the work capacity in the framework of XtremRisK, typical subareas with characteristic properties were selected. In Hamburg the subareas of Wilhelmsburg, Polder Hamburg Süd, and a part of the city centre were selected for the detailed study (Figure 2b).

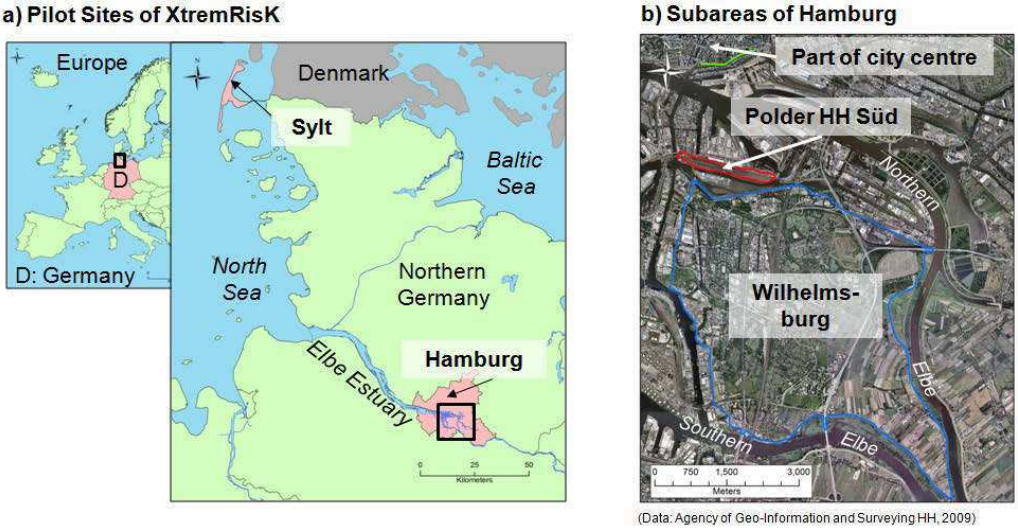

Figure 2. Location of pilot sites selected for this study in XtremRisK: a) Hamburg and Sylt b) Subareas of Hamburg.

3 METHODOLOGY OF SUBPROJECT 2 IN XTREMRISK

Within SP 2 the loading and stability of coastal defences under extreme storm surges were analysed. As input for the analysis, the water levels and wave parameters of an extreme storm surge event together with their occurrence probabilities were provided by SP 1.

As a first step within SP 2, the flood defence line was divided into characteristic sections and the characteristic properties of the flood defences were determined (see section 3.1). On this basis, a reliability analysis was performed in order to calculate the failure probabilities of the coastal flood defences (section 3.2). Moreover, in case of structural failure of sea dikes the breaching of these defences was analysed in order to describe the initial conditions of the flood wave at the breach for an inundation modelling of the hinterland (section 3.3).

The applied methods within SP 2 will be briefly introduced in the following subsections. A more detailed description has been provided by Naulin et al. (2010).

3.1 *Analysis of Flood Defence Line*

Input parameters describing the characteristics of the flood defences were needed in order to perform reliability analysis and breach modelling. For the selected characteristic subareas of the pilot sites, an overview and a detailed parameterisation of all flood defence structures were performed based on an intensive analysis of inventory data such as measurements of the coastal defences as well as geotechnical surveys and digital elevation models. The data collection was carried out in collaboration with the local flood defence authorities of Hamburg.

Using this data basis, which was managed in a geographical information system (GIS), the flood defence line of each subarea was then divided into homogeneous sections with similar characteristics such as type of structure, geometric and geotechnical parameters. Moreover, the hydraulic conditions such as water level and wave conditions were considered for the subdivision. For these sections, all input parameters and their uncertainties were investigated based on the results of the intensive data collection and analysis.

3.2 *Reliability Analysis*

Using a probabilistic approach by taking into account the uncertainties of input parameters and models, a reliability analysis for the flood defences of the subarea Wilhelmsburg was carried out. For this purpose, different failure modes described by limit state equations ($z = R - S$) were analysed (Figure 3a). Since the flood defence line consists of a number of different types of flood defence structures, all failure mechanisms of the documented flood defence structures were examined based on the results of previous projects such as FLOODsite (Allsop et al., 2007) and ProDeich (Kortenhaus, 2003).

For different extreme storm surge scenarios determined by SP 1 the conditional failure probabilities associated to all failure mechanisms were calculated using Monte-Carlo simulations. This procedure of calculating conditional failure probabilities for different extreme storm surge scenarios was chosen since it allowed for performing an event-based inundation modelling and damage estimation.

For each type of flood defence structure, failure mechanisms were organised in a fault tree. The structure of the fault tree represents the different chains of events leading to an overall failure of the flood defence structure (top event) which was defined in this study as flooding of the hinterland.

An overview of a general structure of a fault tree combing different limit state equations for dikes is presented in Figure 3b. From the failure probability of each flood defence section, the overall failure probability of the flood defence system of each subarea was calculated also using a fault tree approach.

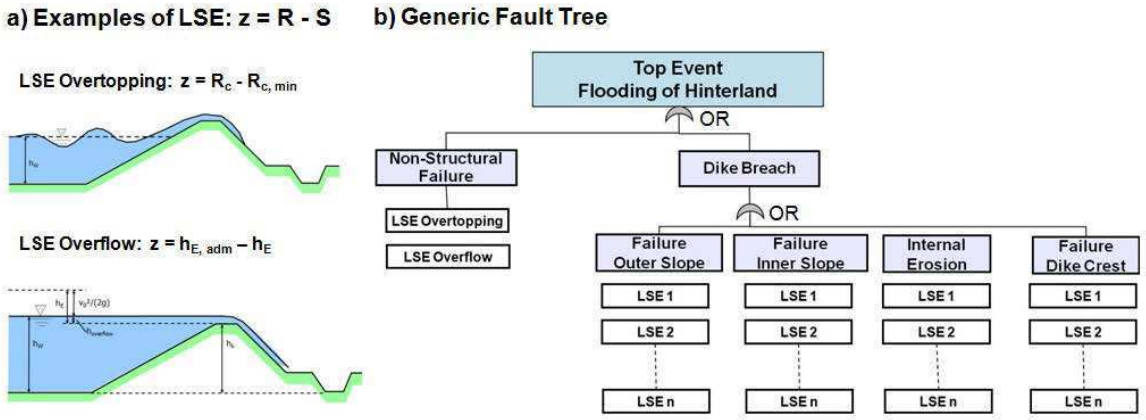

Figure 3. Limit state equations (LSE) of dikes: a) examples of LSE overtopping and overflow b) generic fault tree.

Reviewing failure mechanisms and fault trees of different flood defences based on a literature study, knowledge gaps were identified and an attempt was made to close them by including new or updated limit state equations and by developing missing fault trees for structures not yet considered, e.g. updating limit state equation for critical velocity of grass slopes of dikes according to an approach described by Tuan and Oumeraci (2010b), and including limit state equations for cross-shore profile response of dunes due to wave impact and overwash by applying analytical models developed by Larson et al. (2009).

For the failure probability calculations software tools such as the FLOODsite software tool RELIABLE (Van Gelder et al., 2008) or ProDeich (Kortenhaus, 2003) were applied. For this purpose, all relevant failure mechanisms and fault trees were implemented within the software tools.

The results of the probability of flooding were delivered to SP 4 for risk integration. Moreover, the fault tree analysis allowed determining the probability of breaching of dunes and dikes and gave an indication of the causes of breach initiation, e.g. wave impact on outer slope or overtopping on inner slope. Preliminary results of the failure probability calculations are presented in the next section. However, first the methodology of the breach modelling is introduced in the following subsection.

3.3 *Breach Modelling*

The total failure of the flood defences includes breaching of flood defence structures such as sea dikes. The results of the reliability analysis indicated if and where breaching might occur, i.e. sections with a high probability of breaching. Moreover, the identification of causes and failure modes that may induce an initial breach can be assessed by a fault tree analysis. In case of a high probability of breaching, the process was further analysed and modelled in order to specify the initial conditions of the flood wave for the inundation modelling of the hinterland.

The causes of breach initiation depend on the structure of the dike and on the hydraulic and morphological boundary conditions. In general, several causes for the initiation and formation of a breach can be distinguished, e.g. wave overtopping, overflow, wave impact and seepage. Breaching of sea and estuarine dikes are caused by the following main failure mechanisms (TAW, 1999): (i) erosion and sliding initiated on landside slope by wave overtopping and overflow, and (ii) erosion of seaward slope resulting from breaking wave impacts and the flow induced by wave run-up and run-down. While breaking wave impacts on the seaside slope act on a very limited area and during very short, intermittent periods, the shear stress related to wave overtopping acts on the entire landside slope and during longer time periods.

There are different breaching models for the different causes of breach initiation available, e.g. breaching initiated on the landside by wave overtopping and overflow is described by D'Eliso et al. (2006) and Tuan and Oumeraci (2010a,b) as well as breaching initiated on the seaside by breaking wave impacts is described by Stanczak et al. (2008). Depending on the loading conditions (wave overtopping/ overflow or breaking wave impacts) and thus depending on the breach initiation (landside or seaside) one of the above introduced breaching models was applied to the case study area.

As a result, the breach development could be described in time with specifications on breach initiation, breach duration, and the final breach width and depth. Furthermore, the outflow hydrograph of the breach could be estimated. The results of the initial condition of the flood wave were delivered to SP 3 where inundation modelling of the hinterland and damage estimation was performed.

4 PRELIMINARY RESULTS OF ESTUARINE DIKES IN HAMBURG

Preliminary results are exemplarily given for estuarine dikes of the subarea of Hamburg Wilhelmsburg (Figure 2b) analysing the first XtremRisK scenario of an extreme storm surge event in Hamburg under current climate conditions. In the following section, the hydraulic conditions of the extreme storm surge as well as the intermediate results of the analysis of the flood defence line, the reliability analysis, and the breach modelling are described.

4.1 *Hydraulic Condition of Extreme Storm Surge Scenario*

In SP 1, different extreme storm surge scenarios under current and future climate change conditions are determined. The first investigated storm surge event under current climate conditions has a peak water level of 8.0 mNN at the gauge Hamburg St. Pauli which is 5.9 m above the mean high tide level and 0.7 m above the design water level. The occurrence probability was determined to $1.0 \cdot 10^{-5}$ per year based on multivariate statistics (Wahl et al., 2010). The results of the wave modelling simulated wave heights H_S up to 0.8 m with peak periods of up to Tp = 6.0 s. For the reliability analysis, the duration of the peak water level was estimated to 7.0 hours considering the time of exceedance of a threshold water level of 5.6 mNN which is 3.5 m above mean high water level, i.e. equivalent to the definition of a 'very extreme storm surge' according to the The Bundesamt für Seeschifffahrt und Hydrographie (Federal Maritime and Hydrographic Agency). Hence, preliminary results of failure probabilities represent an overestimation of what might actually occur. However, for the breach modelling the unsteady conditions in terms of the time series of the water level were considered.

4.2 *Analysis of Flood Defence Line*

The main part of the flood defence line of Hamburg Wilhelmsburg, i.e. 19 km out of 23 km, consists of dikes. The dikes are built of a sand core, a clay layer with a thickness of up to 2.0 m and a grass cover on top. The crown heights of the dikes vary from 7.80 mNN to 8.35 mNN and in general the outer and inner slopes are 1 in 3.

The result of the division of Wilhelmsburg's flood defence line into "homogeneous" sections according to similar characteristics such as type of structure, geometric and geotechnical parameters as well as hydraulic conditions is shown in Figure 4. Overall the flood defence line is divided into 84 sections. Out of these sections a total number of 62 segments are dikes and 7 sections are walls. Furthermore, there are 15 so called "point structures" such as gates etc.

Based on an intensive data analysis, the 62 dike sections are parameterised and over 80 input parameters are determined. In case of a lack of data – especially in the case of geotechnical parameters – the data and their uncertainties were estimated by literature references.

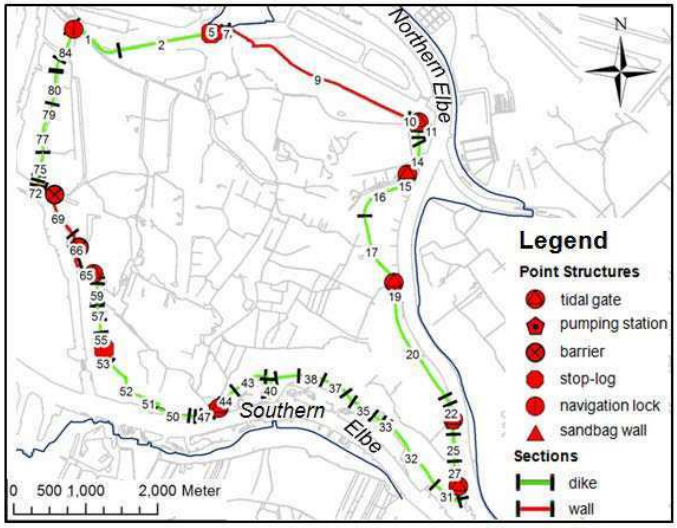

Figure 4. Sections of the flood defence line of the study subarea Wilhelmsburg, Hamburg.

4.3 *Failure Probabilities*

For the reliability analysis of dikes a total of 22 failure mechanisms are considered in this study. An overview of the applied limit state equations is given in Table 2. Two failure modes leading to non-structural failure, i.e. overflow and wave overtopping, as well as 20 failure mechanisms inducing dike breaching are analysed. For further details it is referred to Kortenhaus (2003) and Allsop et al. (2007).

Considering the uncertainties of input and model parameters, the conditional failure probabilities of the failure mechanisms for each of the 62 dike sections under the loading of the first extreme storm surge scenario were calculated by using Monte-Carlo-Simulations. The combination of all failure modes lead-

ing to the top event of inundation is performed by a fault tree approach whereas the general structure of the fault tree shown in Figure 3b is applied.

The overall results of the failure probabilities of the top event, i.e. flooding of the hinterland, reach very high values of almost Pf = 1.0 per year for 45 out of 62 dike sections of the flood defence line. The dominating failure mechanisms leading to the high probability of flooding are identified as non-structural failure in terms of wave overtopping and overflow due to the very high storm surge level as compared to the dike heights. In order to analyse the structural stability of the inner slope, the results of the failure probabilities of the failure of the inner dike slope are examined. For most dikes the failure probabilities of the failure of the inner dike slope are rather low ($1.0 \cdot 10^{-4}$ per year). Only in some areas higher values (between 1.0·10-2 and 1.0·10-3 per year) are calculated. These dike sections are identified as weak spots since they have less resistant inner slopes or are exposed to more severe hydraulic loading. Breach modelling will be applied to these "weaker" sections as described in the next subsection.

However, failures of dikes represent highly complex hydrodynamic and morphodynamic processes. The applied reliability analysis uses relatively simple limit state equations combined within a fault tree analysis. Although the approach represents an adequate tool in order to analyse the performance of the flood-defence system and its components, and in order to identify weaker areas with a higher probability of flooding, there are still gaps in knowledge like e.g. time dependent processes.

Table 1. Limit state equations (LSE) of failure mechanisms of dikes applied in this study with details on name, comparative parameters of LSE, units of LSE, and time dependence as function of storm surge parameters.

LSE No.	Name	Comparison of...	Unit	Time-Dependence as Function of Storm Surge*		
				t_S	h_W	H_S
Non-Structural Failure						
1	overflow (functional failure)	overflow rates (or energy heights)	m³/s/m or m/m		X	
2	wave overtopping (functional failure)	overtopping rates (or freeboards)	m³/s/m or m/m		X	X
Failure of Outer Slope						
3	velocity wave run-up	wave velocities	m/s	X		X
4	wave driven erosion	times	h	X	X	X
5	wave impact	cohesions	kPa			X
6	cliff erosion by wave impact	times	h	X	X	X
7	erosion of revetment armour (rock)	stone diameters	m			X
8	uplift of the revetment	forces of revetment elements	kN/m			X
9	deep slip (Bishop)	moments of single Bishop's slices	kNm			
Failure of Inner Slope						
10	overflow velocity	overflow velocities	m/s	X		X
11	wave overtopping velocity	wave overtopping velocities	m/s	X		X
12	erosion by overflow/ wave overtopping	times	h	X	X	X
13	sliding of clay layer**	times & forces	h & kN	X	X	X
14	clay uplift**	times & forces	h & kN	X	X	X
15	deep slip (Bishop)	moments of single Bishop's slices	kNm			
16	partial breach	times	h	X	X	X
Sliding and Internal Erosion						
17	sliding of dike with clay cover (functional failure)	forces	kN/m²		X	
18	piping**	times & pressure gradient	h & -	X	X	X
19	matrix erosion**	times & sediment diameter	h & mm	X	X	X
Failure of Dike Top						
20	erosion of inner slope & dike top failure**	times & moments of single Bishop's slices (sand)	h & kNm	X	X	X
21	sliding of inner slope & dike top failure**	times & forces & moments of single Bishop's slices (sand)	h & kN & KNm	X	X	X
22	clay uplift of inner slope & dike top failure**	times & forces & moments of single Bishop's slices (sand)	h & kN & KNm	X	X	X

* t_S = time of storm surge duration [h], h_W = water level [mNN], H_S = significant wave height [m]
** Combination of different LSE

In the following, the aspect of time-dependent processes as a function of the storm surge parameters is further discussed. Table 1 shows the dependencies of the failure mechanisms on storm surge parameters such as duration time, water level, and wave parameters. However, until now only single constant values of each parameter have been considered. In order to show the significance of the consideration of the unsteady state of the storm surge event, the failure mechanisms of overflow and wave overtopping are adopted and analysed in more detail.

For this purpose, at first the deterministic combined overtopping and overflow discharges are determined using two different ways to account for the storm surge parameters: (i) constant maximum water level and constant associated wave parameters with a storm surge duration of 7 h as applied in the reliability analysis (see section 4.1), (ii) unsteady conditions of water level and wave parameters using a time series of ca. 28 hours with time steps of 15 minutes.

The combined overtopping and overflow discharges are calculated according to an approach after Bleck et al. (2000) using existing weir formulae and wave overtopping formulae for all 84 sections of the flood defence line considering 62 dike sections as sloped structures and 22 sections as vertical structures.

The results of taking into account the unsteady conditions of water level and wave parameters show that within a time period of 2.5 hours water overtops and/or overflows the dikes and maximum values of mean discharges of up to 0.660 m³/s/m are determined. Considering the lengths of the flood defence sections and the time of the storm surge, the total overtopping volume of all 84 sections amounts to 10.5 million m³.

In contrast using the mean overtopping discharge under consideration of constant maximum water level and wave parameters over storm surge duration of 7 hours, the overtopping volume is estimated to 74.5 million m³. The time-dependent calculation of volumes instead of discharges with constant parameters over a storm surge event has considerable advantages since it represents a better approximation of the time-dependent process, i.e. no overestimation of overtopping volume. Furthermore, the storage capacity of the hinterland is taken into account, i.e. exceedance of critical overtopping discharge might occur for a short period at the peak of the storm surge; however this does not necessarily lead to flooding.

As a next step, it is intended to convert the present deterministic approach of comparing admissible overtopping volumes with actual overtopping volumes to a probabilistic procedure. Moreover, the realisation of taking into account the unsteady condition of storm surge level is further analysed and adopted for other main failure mechanisms.

4.4 *Breach Modelling*

The results of the reliability analysis illustrated that overflow and wave overtopping represent the major forcing of the first analysed storm surge scenario in Hamburg Wilhelmsburg. For this reason wave overtopping-induced erosion of the inner slope of grassed sea-dikes is simulated. The breach initiation is modelled using the BREID model which is a numerical model for simulating BREaching of Inhomogeneous sea Dikes (BREID) developed by Tuan and Oumeraci (2010a,b). The modelling of breach initiation is based on the approach of excess bed shear for grass erosion. For the determination of the bed shear stress, the flow structure of wave overtopping on the inner slope is refined according to turbulent wall jet formulations in order to account for the high turbulence with entrained air bubbles for the conditions of wave overtopping on grass slopes. The critical velocity for grass erosion is determined based on depth-dependent strength concept together with a mobilized shear strength coefficient (Tuan and Oumeraci, 2010b). The results of the modelling of breach initiation - which are described in detail in Naulin et al. (2010) - revealed that for moderate grass conditions, the erosion of the grass layer was initiated to a depth of only 7.0 cm; i.e. a breach would not develop.

Further studies will analyse the effects of different grass conditions. Therefore, the results of laboratory experiences analysing the root volume ratio of grass samples in Hamburg Wilhelmsburg will be implemented in the model. Moreover, the existence of possible weak spots in the grass layer such as holes or cracks will be analysed. In case of a breach initiation, the breach development will be further analysed. Finally, the breach width and the breach outflow hydrograph will be obtained in order to specify the initial conditions of the flood wave at the breach for inundation modelling of the hinterland.

However, regardless of whether a full breach would develop, the analysed extreme storm surge leads to a total overtopping volume of 10.5 million m³ and therefore to severe flooding of the hinterland. A detailed analysis of the inundation modelling and damage estimation of the hinterland will be carried out by SP 3 using the time series of the discharges of the flood defence sections as input parameters.

5 SUMMARY AND FUTURE PROSPECTS

The German research project XtremRisK (www.xtremrsik.de) performs an integrated flood risk analysis for extreme storm surges and consists of four subprojects. The city of Hamburg serves as a pilot site for an estuarine urban area, and the island of Sylt as an open coast. Subproject 2 (SP 2) of XtremRisK deals with a probabilistic reliability analysis and breach modelling of coastal and estuarine flood defences.

In this paper, the methods to determine failure probabilities of flood defence structures as well as the methods for breach modelling of sea dikes are outlined. Furthermore, preliminary results of failure probability calculations and breach modelling are given exemplarily for estuarine dikes in Hamburg with crest heights between 7.80 mNN and 8.35 mNN and for a first extreme storm surge scenario with water levels up to 8.2 mNN and duration of 28 h (7 h above 5.6 mNN), modification of wave height and period up to 0.8 m and 6.0 s, and a probability of occurrence of $1.0 \cdot 10^{-5}$ per year. The reliability analysis allowed identifying relevant failure mechanisms and "weaker" dike sections for the case investigated here leading to 45 dike sections which will either overflow or overtop (failure probability of $P_f \sim 1.0$). The total overtopping volume for all 84 flood defence sections was determined to 10.5 million m³. Hence, the analysed extreme storm surge directly leads to severe flooding. Since wave overtopping and overflow were identified as the major forcing in this scenario, a breach model simulating overtopping and grass erosion on the inner dike slope was applied. As the results showed, the erosion of the grass layer was initiated to a depth of only 7.0 cm; i.e. a breach would not develop for moderate grass conditions. Further studies will analyse the effects of different grass conditions and possible weak spots in the grass layer such as holes or cracks. The overall results of flooding probabilities and initial flooding conditions will be delivered to subproject 3 in order to model the inundation of the hinterland for damage estimation and to subproject 4 in order to combine the results in an integrated risk analysis.

Future prospects within subproject 2 include further applications of the introduced methods of reliability analysis and of breach modelling for both pilot sites. Moreover, it is intended to update and further develop limit state equations and fault trees. For example, methods are analysed in order to consider the time dependence of failure mechanisms in terms of the unsteady conditions of the storm surge, e.g. by changing the limit state equations for 'wave overtopping' and 'overflow' from discharges to volumes as introduced in this paper. Furthermore, missing limit state equations and fault trees for failure mechanisms and structures not yet considered should be included in the reliability analysis, e.g. updating limit state equation for critical velocity of grass slopes of dikes according to an approach described by Tuan and Oumeraci (2010b), and including limit state equations for overwash of coastal dunes using analytical models developed by Larson et al. (2009).

ACKNOWLEDGEMENTS

The project XtremRisK is funded by the German Federal Ministry of Education and Research BMBF (Project No. 03 F 0483 A). The funding is gratefully acknowledged by the authors. Furthermore, the collaboration and the provision of data by the Cooperative and Consulting Partners of the project such as LKN-SH, HPA and LSBG are also gratefully acknowledged.

REFERENCES

Allsop, N.W.H.; Buijs, F.; Morris, M.W.; Hassan, R.; Young, M.J.; Doorn, N.; Van der Meer, J.W.; Kortenhaus, A.; Van Gelder, P.H.A.J.M.; Dyer, M.; Redaelli, M.; Visser, P.J.; Bettess, R.; Lesniewska, D. (2007): Failure mechanisms for flood defence structures. FLOODsite - Integrated Flood Risk Assessment and Management Methodologies, T04-05-01, 150 p.

Bleck, M.; Oumeraci, H.; Schüttrumpf, H. (2000): Combined wave overtopping and overflow of dikes and seawalls. Proceedings International Conference Coastal Engineering, ASCE, no. 27, Poster paper, Sydney, Australia.

Burzel, A.; Dassanayake, D.; Naulin, M.; Kortenhaus, A.; Oumeraci, H.; Wahl, T.; Mudersbach, C.; Jensen, J.; Gönnert, G.; Sossidi, K.; Ujeyl, G.; Pasche, E. (2010): Integrated flood risk analysis for extreme storm surges (XtremRisK). 32nd International Conference on Coastal Engineering (ICCE 2010), ASCE, Shanghai, China, 13 p.

D'Eliso, C.; Oumeraci, H.; Kortenhaus, A. (2006): Breaching of coastal dikes induced by wave overtopping. Proc. 30th International Conference Coastal Engineering (ICCE), San Diego, USA, ASCE, vol. 3, pp. 2844-2856.

IPCC (2007): Climate change 2007: WG II: Impacts, Adaptation and Vulnerability, Chap. 6. Coastal systems and low lying areas. Intergovernmental Panel on Climate Change (IPCC), Cambridge.

Kortenhaus, A. (2003): Probabilistische Methoden für Nordseedeiche. Ph.D. thesis, Dissertation, Fachbereich Bauingenieurwesen, Leichtweiß-Institut für Wasserbau, Technische Universität Braunschweig (2003), Braunschweig, Germany, 154 p.

Larson, M.; Donnelly, C.; Jimenez, J.A.; Hanson, H. (2009): Analytical model of beach erosion and overwash during storms. ICE, Proceedings of the Institution of Civil Engineers, Maritime Engineering, vol. 162, no. 3, pp. 115-125.

LSBG (2007): Hochwasserschutz in Hamburg, Bauprogramm 2007, Hamburg, Germany, 18 p.

Naulin, M.; Kortenhaus, A.; Oumeraci, H. (2010): Failure probability of flood defence structures/systems in risk analysis for extreme storm surges. 32nd International Conference on Coastal Engineering (ICCE 2010), ASCE, Shanghai, China, 15 p.

Oumeraci, H. (2004): Sustainable coastal flood defences: scientific and modelling challenges towards an integrated risk-based design concept. Proc. First IMA International Conference on Flood Risk Assessment, IMA - Institute of Mathematics and its Applications, Session 1, Bath, UK, pp. 9-24.

Oumeraci, H.; Jensen, J.; Gönnert, G.; Pasche, E.; Kortenhaus, A.; Naulin, M.; Wahl, T.; Thumm, S.; Ujeyl, G.; Gershovich, I.; Burzel, A. (2009): Flood risk analysis for a megacity: The German XtremRisK project, Proc. Conference on Road Map towards a Flood Resilient Urban Environment, Paris France, 8 p.

Stanczak, G., Oumeraci, H.; Kortenhaus, A. (2008): Detailed computational model for the breaching of sea dikes initiated by breaking wave impacts. Proc. 31st International Conference Coastal Engineering (ICCE). Hamburg, Germany, vol. 2, pp. 1787-1799.

Tuan, T.Q.; Oumeraci, H. (2010a): A numerical model of wave overtopping on seadikes. Coastal Engineering, vol. 57, pp. 757-772.

Tuan, T.Q.; Oumeraci, H. (2010b): Numerical modelling of wave overtopping-induced erosion of grassed inner sea-dike slopes. Coastal Engineering, submitted.

TAW (1999): Water retaining earth structures. Technische Adviescommissie voor de Waterkeringen (TAW), Technical report, Delft, The Netherlands, 105 p.

Van Gelder, P.H.A.J.M.; Buijs, F.; Van, C.M.; ter Horst, W.L.A.; Kanning, W.; Nejad, M.; Gupta, S.; Shams, R.; Van Erp, N.; Gouldby, B.; Kingston, G.; Sayers, P.B.; Wills, M.; Kortenhaus, A.; Lambrecht, H.-J. (2008): Reliability analysis of flood sea defence structures and systems. FLOODsite Executive Summary T07-09-20, 21 p.

Wahl, T.; Jensen, J.; Mudersbach, C. (2010): A Multivariate Statistical Model for Advanced Storm Surge Analyses in the North Sea, Proc. 32nd International Conference Coastal Engineering (ICCE), Shanghai, China.

ISGSR 2011 - Vogt, Schuppener, Straub & Bräu (eds) - © 2011 Bundesanstalt für Wasserbau ISBN 978-3-939230-01-4

Calibration of Piping Assessment Models in the Netherlands

J. Lopez de la Cruz & E.O.F. Calle
Deltares, Unit Geo-engineering, Delft, Netherlands

T. Schweckendiek
Delft University of Technology, Department of Hydraulic Engineering, Delft, Netherlands
Deltares, Unit Geo-engineering, Delft, Netherlands

ABSTRACT: New insights into the failure mechanism piping (under-seepage) regarding the physical process as well as reliability aspects have led to a revision of the Dutch design and safety assessment rules for dikes. This paper describes how the required factor of safety for piping is derived from a top level requirements formulated in terms of an acceptable probability of flooding. The main steps herein are (a) to account for the length-effect to translate requirements on dike ring (system) level to admissible probabilities of failure on dike section (element) level and (b) the calibration of safety factors as a function of the (element) target reliability.

Keywords: code calibration, piping, under-seepage, target reliability, length-effects

Nomenclature

D [m] : thickness of sand layer
F_F [-] : force factor
F_G [-] : geometrical shape factor
F_R [-] : resistance factor
F_S [-] : scale factor
H [m] : hydraulic head difference (across structure)
H_c [m] : critical hydraulic head difference
L [m] : seepage length
RD [-] : relative density
RD_m [-] : mean relative density (small scale experiments -0.725)
c [-] : erosion coefficient
d_{70} [m] : 70-percentile value of grain size distribution of the piping-sensitive layer
d_{70m} [m] : mean value of d_{70} value in the experiments (small scale experiments -2.08e^{-4})
h [m+REF]: waterside water level
h_b [m+REF]: landside water level
γ_p [N/m^3]: unit weight of particles
γ_w [N/m^3]: unit weight of water
η [-] : Whites constant
ϑ [DEG]: Bedding angle of sand
κ [m^2] : intrinsic permeability
α_R [-] importance factor
V_R [-] coefficient of variation
γ_p [-] safety factor
h [m] the normative water level
d [m] Blanket layer thickness
h_b [m] decimal height

1 INTRODUCTION

Primary flood defenses in the Netherlands undergo a 5-yearly safety assessment. Based on economic as well as societal risk acceptance criteria, the current safety standards are defined in terms of exceedance probabilities of hydraulic load conditions (see Figure 1). For failure mechanisms other than overtopping these are commonly interpreted as admissible probabilities $P_{f,adm,dr}$ of (system) failure of a dike ring (polder). That implies that the criteria to be handled for individual dike sections and failure mechanisms need to be stricter: $P_{f,adm,ds,mech} < P_{f,adm,dr}$. That is for two reasons: (a) each mechanism can cause failure and (b) (b) failure of each individual section means system failure. We are dealing with a serial system. A third component is the length-effect. The probability of failure increases with increasing length of a dike section with statistically homogeneous properties (Vrouwenvelder, 2006).

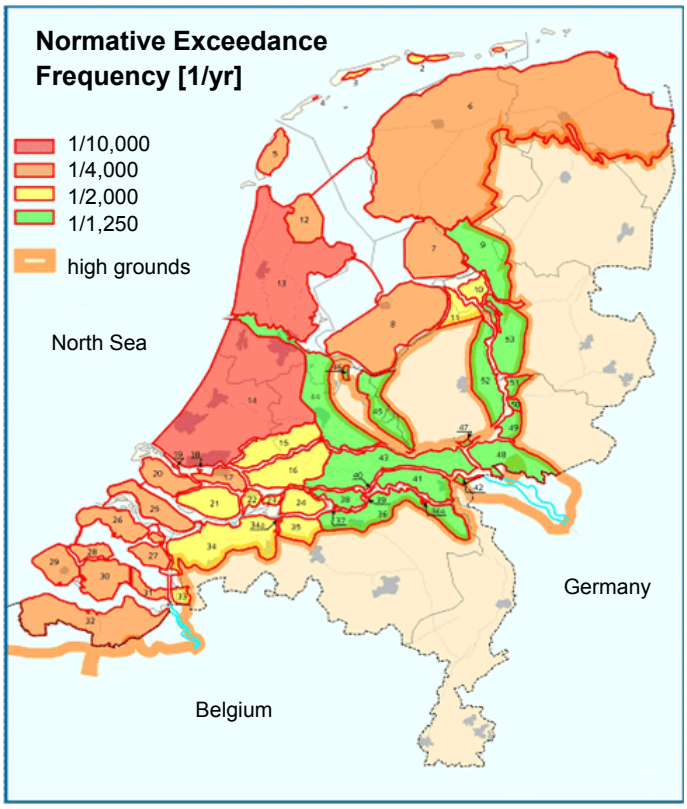

Figure 1. Normative exceedance probabilities of Hydraulic Load Conditions in the Netherlands

All these aspects illustrate the need to establish higher target reliabilities locally and for each failure mechanism in order to achieve a sufficiently reliable dike ring (system). In order to translate these requirements into practical terms, semi-probabilistic assessment and design rules need to be derived, using characteristic values and (partial) factors of safety instead of reliability analysis techniques.

This paper describes how a local assessment rule for piping (under-seepage) has been derived, the goal of which is to be consistent with the high level criteria in terms of probabilities of flooding. Before going into the details of the calibration code, the revised piping model is described, including a concise discussion of the model uncertainty. Subsequently, the format of the new safety assessment rules is presented and the derivation of the required factor of safety is discussed. The latter consists of two main steps: (a) derivation of the acceptable probability of (piping) failure of a dike section and (b) the calibration of the required factor of safety as function of the target reliability.

2 REVISED PIPING MODEL

2.1 *The Equilibrium Model by Sellmeijer (1988)*

Sellmeijer (1988) proposed a computational for piping with three main elements: groundwater flow, pipe flow through the erosion channel and limit equilibrium of soil particles in the channel. For safety assessment purposes, the following equilibrium condition was derived, which describes the critical gradient over the structure. In other words, for lower gradients (H/L) the erosion pipe development stops accord-

ing to the model, whereas for higher gradients the erosion may reach the upstream side and thereby endanger the integrity of the structure by "under-mining" it.

$$\frac{H}{L} = \frac{1}{c} = F_R F_S F_G \qquad F_R = \eta \frac{\gamma'_p}{\gamma_w} \tan\vartheta \qquad F_S = \frac{d_{70}}{\sqrt[3]{\kappa L}} \qquad F_G = \left\{ 0.68 - 0.1 \ln\left(0.25 F_S\right) \right\} \left(\frac{D}{L} \right)^{\frac{0.28}{\left(\frac{D}{L}\right)^{2.8} - 1}} \tag{1}$$

The geometry and soil parameters are specified in the section Nomenclature; coefficient c is composed of three factors:

- F_R: resistance factor, being the strength of the sand
- F_S: scale factor, relating pore size and seepage size
- F_G: geometrical shape factor

Notice that this criterion does not address the appearance of sand boils like exit gradient-based criteria do. Using this equilibrium criterion in safety assessment one implicitly allows sand boils to occur, while pipe development until the upstream side is avoided.

For more complex geometries than a simple aquifer covered by a blanket layer, both with constant thickness, the criterion (in a slightly simplified form) has been implemented in MSEEP, a numerical code for groundwater flow computations.

2.2 *Revision of the Sellmeijer Model*

Recently, a detailed experimental research of the piping mechanism in The Netherlands (Lopez de la Cruz et al., 2010) has provided better insights into the underlying physical phenomenon and led to a revision of the Sellmeijer model. A multivariate regression analysis enabled re-calibrating the coefficients in the model, by assessing the influence of each measured variable on the critical head simultaneously, resulting in

$$\frac{H_c}{L} = \frac{1}{c} = F_R F_S F_G$$
$$F_R = \eta \frac{\gamma'_p}{\gamma_w} \tan\vartheta \left(\frac{RD}{RD_m} \right)^{0.35}$$
$$F_S = \frac{d_{70}}{\sqrt[3]{\kappa L}} \left(\frac{d_{70m}}{d_{70}} \right)^{0.6} \tag{2}$$
$$F_G = 0.91 \left(\frac{D}{L} \right)^{\frac{0.28}{\left(\frac{D}{L}\right)^{2.8} - 1} + 0.04}$$

Besides new coefficients the revised model contains a dependency on the relative density (*RD*) of the piping sensitive sand layer (i.e. aquifer, usually the upper few decimeters). However, for safety assessment purposes, the influence of *RD* is not taken into account. It is hard to determine in the field and of little influence despite the large uncertainty. Therefore, it was preferred to include it in the model uncertainty. Notice that for "non-standard" geometries the piping module in MSeep is also available for the revised model and recommended for determining F_G.

2.3 *Model Uncertainty*

The model uncertainty is accounted for by a multiplicative model with factor m_c:

$$\frac{H_c}{L} = m_c \frac{1}{c} = m_c F_R F_S F_G \tag{3}$$

The experimental results from Beek et al. (2010) have been analyzed for determining the parameters of the model factor, which is chosen to be modeled by a lognormal distribution. Its standard deviation is determined by a weighted variance-analysis, in which more weight is given to the available data from prototype scale than to the small and medium scale laboratory experiments (Lopez de la Cruz et al., 2010). The resulting standard deviation of the model factor is σ_{mc}=0.12, the scatter of the comparison of predicted versus observed critical head difference is illustrated in Figure 2.

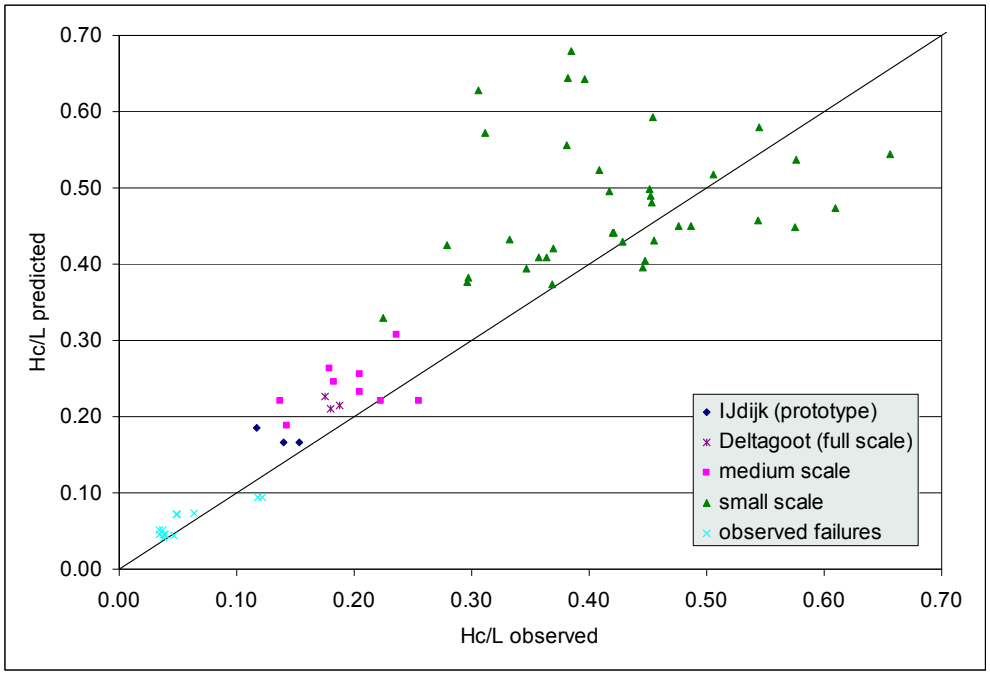

Figure 2. Observed vs. predicted (revised piping model) critical piping gradients

3 SAFETY ASSESSMENT RULE

The revised piping model can be used to assess the resistance against piping in terms of the critical head difference:

$$H_c = m_c F_R F_S F_G L \qquad (4)$$

For safety assessments this value can be compared to the head difference the structure experiences. For the Dutch safety assessment rules it was decided to handle the same reduction term as in the current guidelines:

$$H = h - h_b - 0.3d \qquad (5)$$

Consequently, the format of the new safety assessment rule is chosen such that the ratio of the critical head difference H_c (resistance) and the head difference including reduction term (load) using characteristic values (5% respectively 95% quantiles) is required to be larger than the safety factor γ_p:

$$\frac{R_k}{S_k} = \frac{H_{C,k}}{H_k} = \frac{m_{p,k} F_{R,k} F_{S,k} F_{G,k} L_k}{h_k - h_{b,k} - 0.3d_k} > \gamma_p \qquad (6)$$

Notice that the characteristic factors $F_{i,k}$ are determined by using 5%/95%-quantiles for their input parameters. Furthermore, the characteristic (or, in fact, design value) for the water level h_k is taken to be the normative water level (MHW) as defined in the Hydraulic Boundary Conditions (Rijkswaterstaat, 2007). The procedure to determine the characteristic values is beyond the scope of this study; reference is made to Eurocode 0.

4 TARGET RELIABILITY AND FACTOR OF SAFETY

The main goal of the calibration is to determine (partial) safety factors that, if consequently used in design or safety assessment, lead to a structure that is at least as safe as the predetermined target reliability.

Commonly, in codes and standards (e.g., Eurocode) the target reliability is chosen from safety classes that reflect the severity of the consequences - the more severe the consequences the higher the target reliability. For the Dutch flood defense system that basic concept is the same, except that the target reliability is defined by the exceedance probabilities[1] (Figure 1) as probabilities of flooding. In other words, these are admissible probabilities of (system) failure. The probability that any of the elements of a dike ring (i.e., dike or other flood defenses) fails is defined as: $P_{f,adm,dr}$ [1/yr]. That means that this probability cannot be used to define one target reliability for a particular structure in the system directly.

The first step is a apragmatic one: The probability of system failure is distributed over the failure mechanisms in the system that play a significant role. For piping the admissible probability of failure is 10% of the total: $P_{f,adm,dr,p} = 0.1\ P_{f,adm,dr}$. This distribution over failure mechanisms can be treated as economic optimization problem, however, these considerations are beyond the scope of this paper.

The second step is to translate dike ring requirements into dike section requirements. The latter beings the level at which designs and safety assessments are carried out. The key element in this step is the length-effect (Vrouwenvelder, 2006). The probabilities of failure of the flood defenses that form a dike ring are partially correlated. Usually, there is a large (spatial) correlation between the loads on different sections, where also the resistance properties are highly independent. That implies that the probability of failure somewhere in the dike ring is larger than the probability of failure of one (or the weakest) element (i.e., dike section): $P_{f,adm,dr,p} > P_{f,adm,ds,p.}$ This is accounted for by incorporating the length effect. The details are further discussed in section 5.

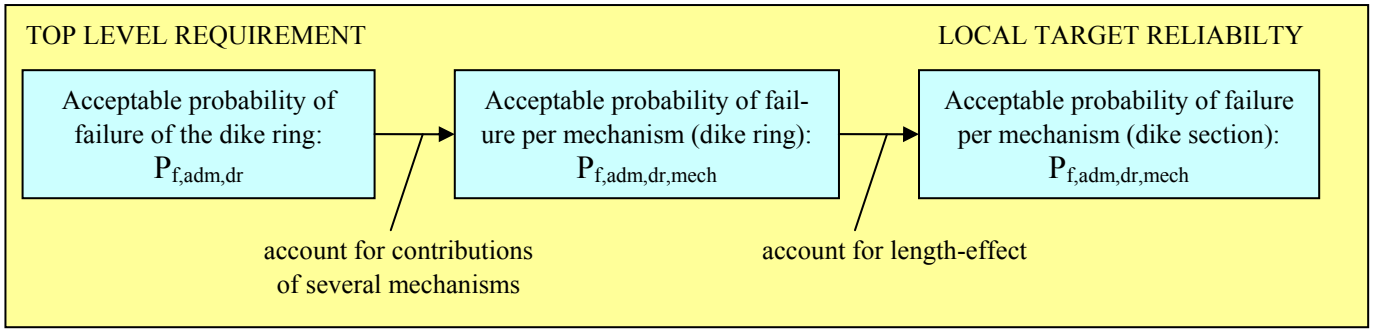

Figure 3. Steps to determine Target Reliability

Having determined the target reliability, the actual calibration code is applied. A convenient starting point is to pick standardized values for importance factors such as given in the Eurocode. For example, for a dominant load parameter: $\alpha_R = 0.8$ with the standard formulae for partial resistance factors. However, from the FLORIS project Rijkswaterstaat (2005) it is known that for piping the importance factors can vary significantly and even exceed $\alpha_R = 0.8$. Therefore, an appropriate value for γ_p for varying conditions is examined directly by the analysis described in Figure 4. Further details are discussed in section 6.

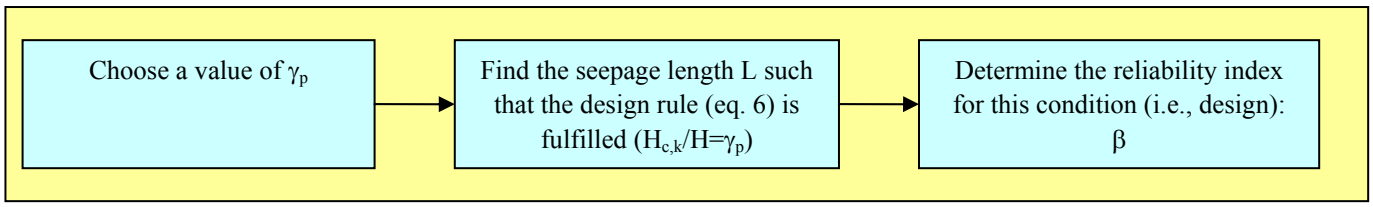

Figure 4. Steps to analyze the appropriateness of values for the required safety factor γ_p

5 LENGTH EFFECTS

Applying zero-level crossing theory for the input parameters to the piping model, a relationship between the admissible probability of failure for a dike section and the admissible probability of failure on dike ring together is established. This includes the influence of the dike sections lengths $L_{dr,s}$ that are sensitive to piping (i.e., potentially contribute to the probability of failure). A detailed description of this analysis is beyond the scope of this paper but more details can be found in Lopez de la Cruz (2010). The result is represented in Figure 5.

[1] The normative exceedance probabilities are not exactly the admissible probabilities of flooding, but in the context of code calibration for failure mechanisms other than overtopping are interpreted as such.

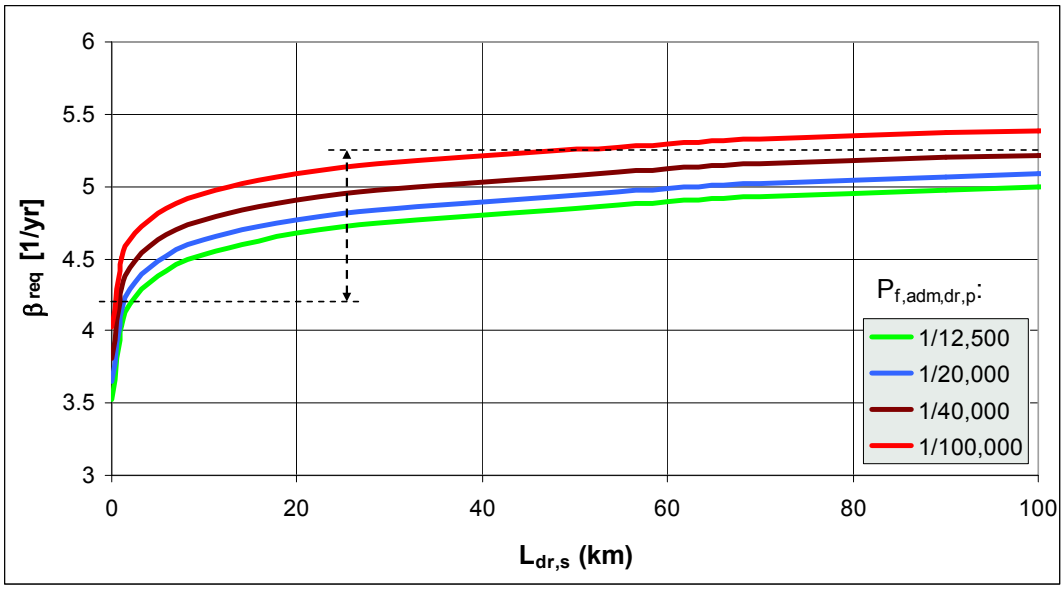

Figure 5. Relation between target reliability, (sensitive) dike ring length and acceptable probability of piping for a dike ring

The target reliability $\beta_{req}=-\Phi^{-1}(P_{f,adm,ds,p})$ increases with the (piping-sensitive) cumulative length of dike sections $L_{dr,s}$ forming the dike ring. For practical purposes, the following formula is proposed which fits the relations in Figure 5 very well:

$$P_{f,adm,ds,p} = \frac{0.1 P_{f,adm,dr}}{1+\alpha / l_{eq} \cdot L_{dr,s}} \qquad (8)$$

where

α Calibration factor

l_{eq} Correlation length of the limit estate function for piping

For characteristic Dutch conditions a value of α / l_{eq}=0.0028 is proposed.

6 UNCERTAINTIES AND CALIBRATION DATA SETS

In order to check the suitability of γ_p as described in Figure 4, a set of conditions to analyze (parameter sets) are needed as well as their probability distributions per parameter. For the latter, it is recurred to the probabilistic modeling in the FLORIS project. The distribution types and variation coefficients (or standard deviations) per parameter are given in Table 1.

Table 1. Probability distributions of piping load and resistance parameters

Parameters	Type	Mean	Spread (V=CoV, σ=Std)
D	Log-normal	nominal	V=5.0
k	Log-normal	nominal	V=1e-6
L	Log-normal	nominal	V=0.24
d70	Log-normal	nominal	V=6e-5
eta	Normal	0.25	V=0
theta	Normal	37	σ=0
m_p	Log-normal	0.12	σ=0.12
h_b	normal	nominal	σ=0.10
h	Gumbel	nominal	σ =0.39

The assessment rule should hold for the range of conditions that is expected to be encountered in practice. To establish these conditions, for each parameter with nominal mean value in the table a low, medium and high value (for typical Dutch conditions) have been chosen. The resistance parameters are summarized in Table 2.

Table 2. Nominal Values of Piping Resistance Parameters for Calibration Sets

Variable	Unfavourable	Average	Favourable
μ_D [m]	50	15	5
μ_k [m/s]	1E-04	1E-05	1E-06
μ_{d70} [m]	1,2E-04	2,0E-04	4,0E-04
μ_d [m]	0,1	2,5	6,0

For the load parameters (influencing the head difference H) three parameter sets are chosen to represent different hydraulic load regimes together with the according acceptable probability of flooding (see Table 3).

Table 3. Parameter Sets of Hydraulic Load Variables

	Coast	River	Estuary
P(h>MHW)	10000	1250	4000
h_k = MHW [m+NAP]	3,3	6,3	3,1
Δh_{10} (decimate height) [m]	0,75	0,7	0,35
μ_{hb} [m+NAP]	-2,5	4,2	-1,0

The first three parameters in the table above can be used to define a the Gumble distribution for the water level.

The“decimate height” is the water level difference that increases the exceedance probability of the water level by a factor 10 with respect to the normative water level with known exceedance probability:

$$P(h > MHW) = 10 \cdot P(h - \Delta h_{10}) \qquad (9)$$

Combining each load parameter set with each of the resistance variables, we obtain 243 (=3^5) calibration parameter sets.

7 CALIBRATION RESULTS

The calibration analysis has been carried out for each of the 243 parameter sets (previous section) and for six different values of the partial resistance factor γ_p: 1.0, 1.2, 1.4, 1.6, 1.8. This section presents a summary of the calibration results.

Each of the points in the figure 6 shows which value of the reliability index (horizontal axis) is found for the underlying parameter set and the γ_p (vertical axis).

The results present some clusters due to the hydraulic load regimes and the selected blanket layer thickness, which acts in this case as a load reduction term. In order to illustrate this, the data points are plotted with different colors and shapes (see legend).

From Figure 6, it can be seen that the load conditions together with the blanket layer thickness determine the performance of the safety factor.

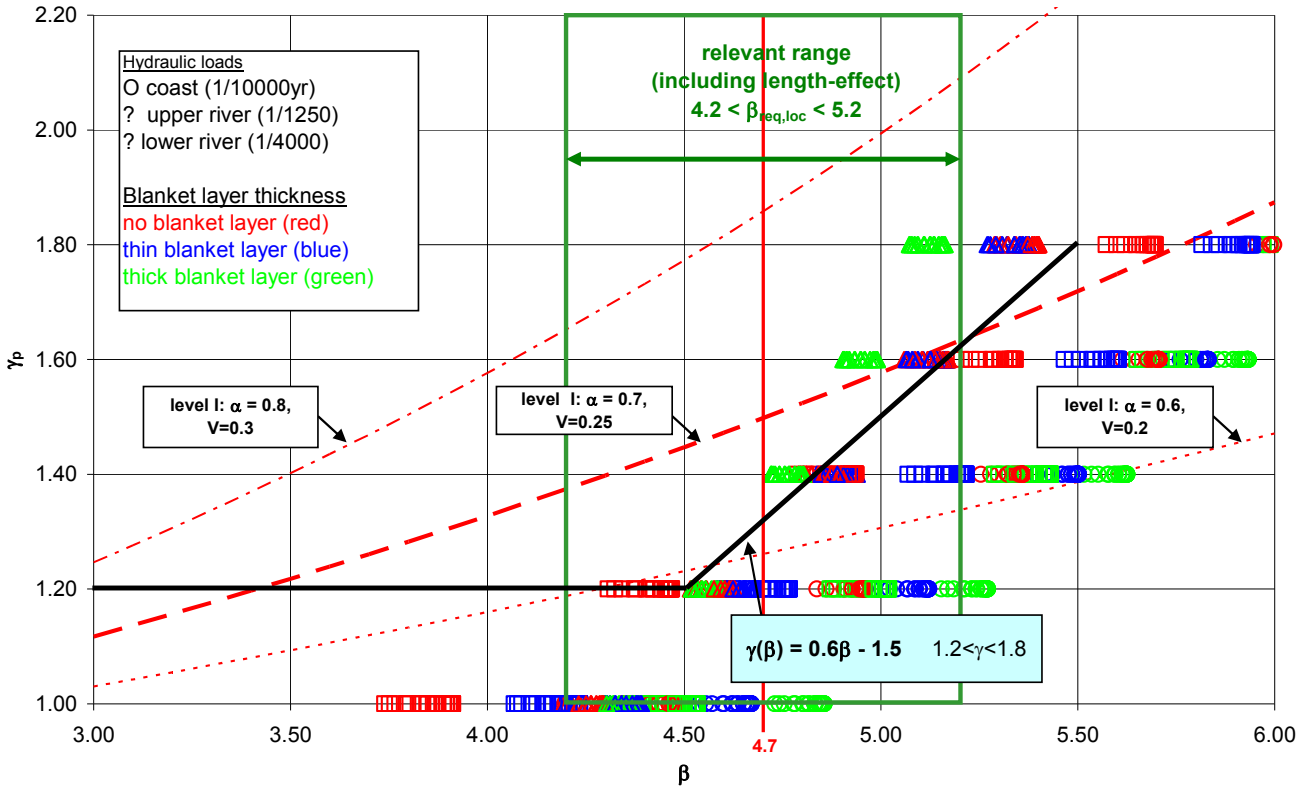

Figure 6: Overview Calibration Results: required safety factor γ_p vs. realized reliability index

The black line presents the proposed linear relationship between the required reliability and the partial resistance factor:

$$\gamma_p = 0.6\beta_{req} - 1.5 \qquad (1.2 < \gamma_p < 1.8) \qquad (10)$$

The line is chosen on the left of the scatter points, approximately through the 95%-quantiles per safety factor level. That means that for 95% of the (calibration) cases the reliability achieved by applying the safety factor is higher than the target reliability, while 5% of the (rather extreme) cases would result in a slightly unconservative design, which was supposed to be acceptable. The lower limit of γ_p was a political decision maintaining safety factor of 1.2 that is currently in use as a lower limit.

A point in the upper left region of the scatter implies a region with under-performance. However, all of these points are triangles, meaning that they represent river load conditions. In the Netherlands, those areas have safety requirements that do not exceed β_{req}=4.7 even for the longest dike rings. Therefore, these points are irrelevant.

The green in the figure 6, indicates the range of γ_p-values expected to be applied using the proposed assessment rule in the Netherlands, based on the relevant range of required reliability index including the length-effect. The resulting range is $\mathbf{1.2 < \gamma_p < 1.6}$ with the remark that values of 1.4 are expected to be exceeded only in rare cases such as long dike rings with low acceptable probability of flooding.

The red dashed and dotted lines indicate the resulting safety factor values after the standard level-I equations for lognormal distributed resistance is applied for different combinations of importance factor (α_R) and coefficient of variation (V_R).

8 DISCUSSION

A target reliability-dependent safety factor for piping is derived for design and safety assessment in the Netherlands. The incorporation of the presented results in the design guidelines is still pending. The target reliability is derived from specific flood protection norms in the Netherlands instead of consequence classes such as used in the Eurocode. In the derivation, it is accounted for system reliability aspects such as accounting for several mechanisms as well as for the length-effect.

Taking into account the scatter of the calibration points around the proposed relation between the safety factor and the target reliability shows a typical aspect of semi-probabilistic design and safety assessments. For a significant range of the chosen conditions, the approach leads to over-design. This can

be avoided by more differentiation. For example, by establishing different safety factors for different load regimes or by reliability-based design (reliability analysis in safety assessment).

REFERENCES

Beek, V. M. v., J. G. Knoeff, J. Rietdijk, J. B. Sellmeijer, and J. Lopez De La Cruz, 2010. Influence of sand and scale on the piping process - experiments and multivariate analysis, Physical Modelling in Geotechnics, Zürich, Taylor and Francis Group.

Eurocode 0. EN 1990 'Eurocode: Basis of structural design.

Lopez de la Cruz, J., Schweckendiek, T., Mai Van, C. & Kanning, W. 2010. Calibration of Partial Resistance Factors for Piping and Uplift. Deltares report no. 1202123-002-GEO-0005.

Rijkswaterstaat (2005). Main report of "Flood Risks and Safety in the Netherlands (Floris)".

Rijkswaterstaat (2007). Hydraulische Randvoorwaarden primaire waterkeringen (in Dutch). August 2007.

Vrouwenvelder, Ton (2006). Spatial effects in reliability analysis of flood protection systems. Proc. International Forum on Engineering Decision Making, Second IFED Forum, April 26-29, 2006, Lake Louise.

ISGSR 2011 - Vogt, Schuppener, Straub & Bräu (eds) - © 2011 Bundesanstalt für Wasserbau ISBN 978-3-939230-01-4

Overtopping and Overflow of Flood Protection Embankments – Risk Reduction of Embankment Dam Failure by the Use of Geosynthetics

K. Werth
BBG Bauberatung Geokunststoffe, Espelkamp, Germany

R. Haselsteiner
Enerjisa Enerji Üretim A.Ş., Ankara, Turkey

F. Steinbacher
Steinbacher Consult, Augsburg, Germany

ABSTRACT: In most cases common levee cross-section designs do not provide any safety against erosion of the slopes if crest overflow occurs. Recent floods highlighted again the vulnerability and risk of levee failure due to uncontrolled crest overflow, which results usually in the development of a breach and, consequently, in flooding of the downstream flood plains. The application of geosynthetics comprises many advantages such as the avoidance of damages, the deceleration of polder flooding and the stability increase of affected slopes. Particularly, the economic aspects are attractive for the investor since the design allows steeper slopes which saves earth works whilst providing overflow protection and avoiding long-term costs caused by flooding. The application of geosynthetics for overflow protection systems structures is still in research phase, although hydraulic and geotechnical institutes worldwide have carried out large scale model tests successfully. Further geosynthetic protection systems belong to the state of the art in coastal engineering where overtopping and surge loads are common design criteria. This fact confirms the general applicability of geosynthetics resisting strong dynamic hydraulic loads.

Keywords: geosynthetics, dams, dikes, crest overflow, overtopping

1 INTRODUCTION

In recent decades several major flood events have shown the vulnerability of flood protection structures. Frequently, the overtopping of flood protection dikes has caused total failure of the dike. Consequently, the polders were flooded and damaged not only real assets but also claimed human losses. Particularly, long lasting floods and locally concentrated extreme short lasting precipitation events were responsible for countless natural disasters (Heerten & Horlacher, 2002). Locally and regionally, the threats and risks may increase, as forecasted by several hydrological scientists and researchers (Hennegriff et al., 2006).

In Germany, the design of flood protection levees against overtopping and overflow loads is neither state of the art nor applied in practice (Haselsteiner et al., 2007b; DIN 19712, 1997; DWA M507, 2007). Only quite limited overflow sections have been constructed mostly using classical methods such as riprap and/or the application of binding materials (asphalt, cement, lime). For classical methods both long-term experience and design methods are available (LFU BW, 2004; Bosshard, 1991; CIRIA 116/1987; Powledge et al., 1989). Although, several German research institutes have carried out laboratory tests with geosynthetic protected overflow dikes successfully (Bieberstein, 2003; Haselsteiner, 2007a, b, c and others) the next step to develop a design method has not been carried out. LFU BW (2004) has already confirmed the applicability and economic efficiency of geosynthetic methods for overflow protection systems: *"In principle these [geosynthetic] construction methods allow considerable higher loads and steeper downstream slopes, hence, they can be also of importance in terms of economical aspects."*

Fundamental aspects of the application and effects of overflow protection measures using geosynthetics are discussed in Werth et al. (2007) (see also Haselsteiner et al., 2008). Overflow sections along rivers can be an effective means within flood protection concepts, in order to activate polders and to reduce peak discharges in downstream regions. The application of geosynthetics for this purpose combines both low construction costs and an extremely robust and durable structure if the corresponding, already available design principles are considered.

The proof and verification of new construction or design methods can be achieved by the application of accredited analysis or by full scale tests as already carried out by several hydraulic or geotechnical institutes worldwide. In spite of the successful full scale test results, and in spite of the unanimous agreement of researchers and engineers that the described methods can be favourable in comparison to classical methods under certain circumstances, the decision making parties such as authorities, owners and municipalities, etc. still hesitate to switch from the classical to geosynthetic methods. This is also true for the design of spillways of small dams since the corresponding design codes, regulations and recommendations based on theoretical studies and practical testing are missing or are do not belong to the state of the art which is defined in the corresponding codes, regulations, manuals, etc. The authors hold the opinion that the principles for the design of these structures are well-known and understood that only limited research work is required to develop mentioned design method and criteria which enables a standard application. Both the stress-deformation behaviour of corresponding structures and the hydrodynamic loads are still to be investigated in detail. For both of these research fields the fundamentals have been sufficiently developed and the physical basics are well described that the final step is "only" to be reflected by the superposition of the existing knowledge and experience of two basic subjects. Corresponding research works can be performed within the scope of applied science studies.

2 APPLICATION OF GEOSYNTHETICS FOR FLOOD PROTECTION DIKES

The application of geosynthetics in geotechnical and hydraulic engineering is described in Saathoff (2003) including also the field of flood protection dikes and embankment dams (see also Saathoff & Werth, 2003). The refurbishment of dikes has gained more importance in Western Europe since most of the flood protection dikes were built centuries ago. However, the modern techniques and methods of geotechnical and hydraulic engineering have only been applied approx. 50 – 75 years after the fundamentals of these fields were established. The application of geosynthetics for the refurbishment of dikes belongs to the state of the art regarding geosynthetic filters, reinforcement and sealings (Heerten & Werth, 2006; see Fig. 1).

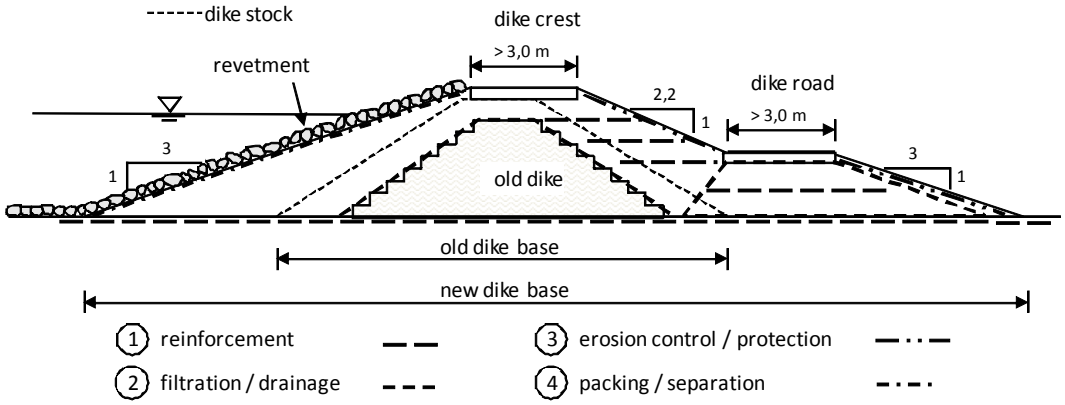

Figure 1. Application of geosynthetics within embankment dam and flood embankment structures (Haselsteiner, 2006)

Geosynthetic clay liners in particular (shown in Fig. 2) have been frequently applied in recent dike refurbishment measures in order to control seepage and to reduce water pressure in the dike body. The geosynthetic clay liner reflects an alternative to a natural clay surface sealing. Mostly, the persistent permeability of the geosynthetic clay liners were doubted, but it could be confirmed by long-term investigations and results (EAG-GTD, 2002; Egloffstein, 2001; Heerten et al., 2008). Geosynthetic filters are usually applied with a loading berm at the downstream slope of the dike. Thus, the original dike material shall be filtered in consideration of the usage of coarse, permeable fill material for the berm. Where soft, compressible soil such as turf is located beneath the dike base, geosynthetic grids may reduce settlement and deformation and also enable foundation on usually unsuitable soils. Of course, turf or other organic soils should not be exposed to harmful hydraulic gradients. If erosive, low cohesive soils are applied as sealing materials in small embankments, the application of geosynthetic filters is also favourable in terms of geometrical constraints in comparison to grain filters. Since this kind of soil exhibits negligible resistance to erosion or shows hydromorphic behaviour, both the underlying soil and the dike body itself have to be sealed. A combination of an underground sealing with a geosynthetic clay liner is shown in Fig. 2 as it can be used for correspondingly designed and loaded dikes.

Experience in applying geosynthetic products within geotechnical and hydraulic engineering has been gained over decades. In Germany, modern and accurate design standards and regulations for the application of geosynthetics were prepared in the eighties and nineties of the last century (EBGEO, 2010; DVWK 76, 1988). Since then, more and more experience and information has been gathered through the construction of many projects. Furthermore, the use of geosynthetics was also investigated for overflow protection issues at embankment dams including both coastal and river related structures.

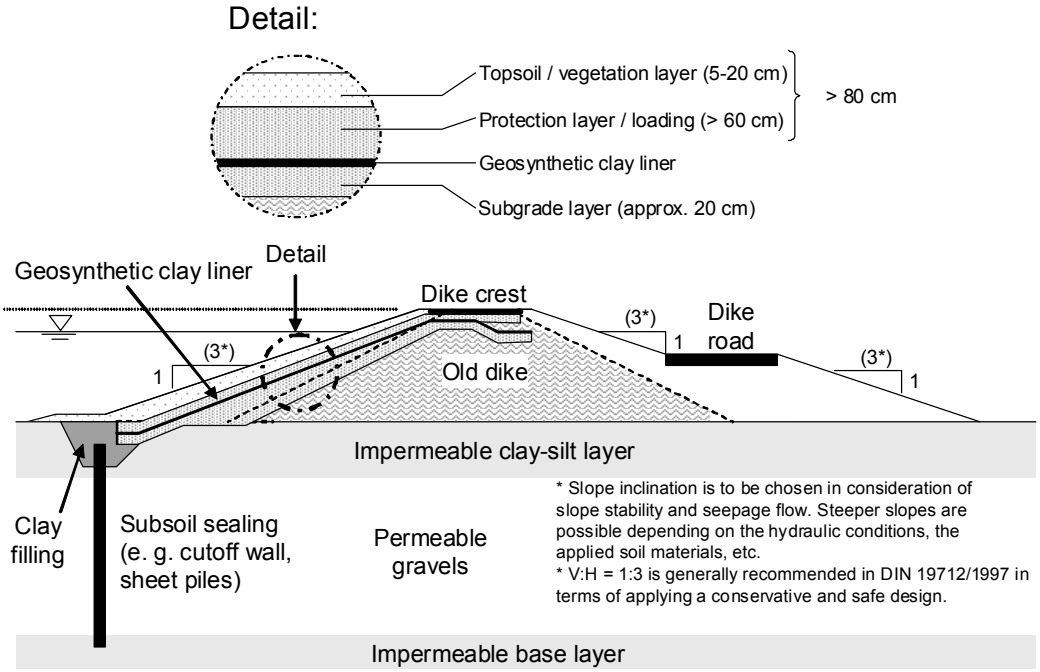

Figure 2. Application of a geosynthetic clay liner in the course of dike refurbishment works (Haselsteiner & Strobl, 2005)

Fig. 3 depicts an levee cross-section optimally reinforced and protected with geosynthetics. This cross-section of the levee was implemented in Poland after the 1997 Oder River flood. It offers optimal prerequisites for a long-term, protective, stable and overflow-secure levee. Its waterside has a surface seal of bentonite mats (preferably needle-punched GCL with powdered sodium bentonite and woven/nonwoven geotextile composite as carrier layer and nonwoven geotextile as cover layer). The levee's core has integrated erosion protection against overflow risks provided by encapsulating levee core material in nonwovens with the wrap-around method. A filter-effective configuration of air-side drainage is combined with a levee defence roadway. Breach behaviour, as would be exhibited by a levee with conventional cross-section consisting only of earthen materials, can be presumably eliminated.

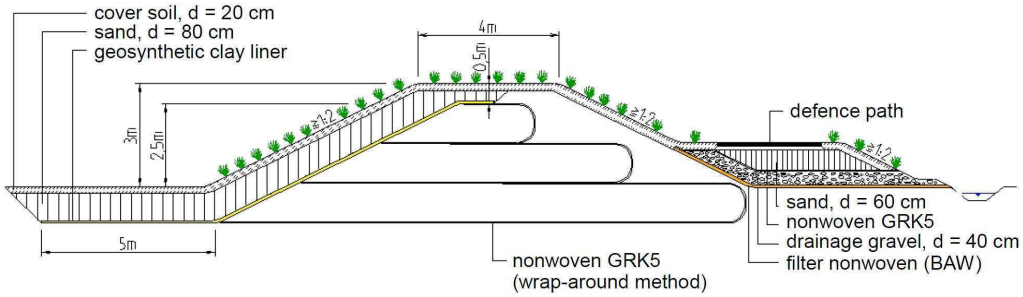

Figure 3. Cross-section of a reconstructed Oder River levee in Poland (Heerten, 1999)

3 BASIC DESIGN PRINCIPLES FOR OVERFLOW DIKES

Overflow protection systems are affected by many parameters and design considerations. For design, the following aspects should at least be taken into consideration and assessed in detail (Haselsteiner et al., 2008):

- Overflow hydraulics (tailwater conditions, specific discharge …)
- Function of overflow protection system (reactivation of retention volume, structural protection, retardation of flooding …)

- Choice of geosynthetic product (geotextile, geogrid, geonets …)
- Function of geosynthetic product (separation, filter, reinforcement …)
- Protection of geosynthetics against environmental impacts (animals, biochemistric fluids, UV radiation …)
- Definition of design overflow discharge and/or height (corresponding to flood protection principles and design criteria …)
- Energy dissipation (stepped spillway, stilling basin …)
- Protection of embankment shoulder, crest and bottom (layers, tubes, containers …)
- Definition of main design parameters (number of layers, layer distance, embedment length, embedment depth, number and length of earth anchors …)
- Soil material specifications (grain size, grain size distribution, shear parameters, permeability …) and subsoil treatment
- Seepage conditions and effects (loads, erosion, suffusion ...)
- Inspection, maintenance, rehabilitation/refurbishment, supervision

The legal framework for the application of geosynthetics in geotechnical and hydraulic engineering is well developed and sophisticated. In particular the quality management and the control of the suppliers are stressed within existing standards, engineering codes, guidelines and manuals. In Germany, the "Forschungsgesellschaft fur Straßen- und Verkehrswesen" which carries out research for roads and traffic engineering is the spearhead for the establishment of standards, specifications and requirements (FSGV, 2005a,b) along with the DIN institute (DIN: Deutsches Institut für Normung) and a few national engineering associations such as the DGGT (Deutsche Gesellschaft for Geotechnik), DVWK (Deutsche Vereinigung für Wasserwirtschaft, Abwasser und Abfall). Both in DVWK 221 (1992) and in DGGT EBGEO (1997) the general application fields are summarized and design recommendations and methods are presented (see also Saathoff, 2003). In FSGV (2005 a, b) the appropriate legal framework for the production, delivery, application, control and supervision is given. Geosynthetics are also affected by the work on Eurocode 7 (EC7) due to the European harmonization of the norms and standards and the transition of the German to European standards. Several papers describe the work progress and the effects on the application of geosynthetics (Ziegler, 2007). For reinforcement with geogrids DGGT EBGEO (1997) is helpful but is currently under revision (Bräu, 2007). The publication of the revised version was expected for mid 2010 and has already been published in an updated version in 2009. First experiences are already available and are discussed among researchers and industry (Herold, 2009; Vollmert & Schwerdt, 2010).

Depending on the different design options and situations, most of the research and development work resulted in the conclusion that geosynthetics for overflow protection systems (Fig. 4) can combine both robust design and economical efficiency. For design work, a separation of the specific dike parts is helpful. Thus, the crest, shoulder, slope and the downstream toe require special design considerations and structural solutions. The basic geotechnical and hydraulic aspects were investigated and summarized decades ago by e. g. Bosshard (1991) and Powledge et al. (1989). Also in Germany researchers studied the use of geosynthetics for overflow protection systems 30 years ago (Stalmann, 1980). Recently, overflow protection systems for flood protection dikes including geosynthetic methods were studied at several geotechnical or hydraulic institutes of the universities of Karlsruhe, Stuttgart, Darmstadt and Munich. Most of the research studies were focused on alternative concepts for overflow protection methods without the use of geosynthetics as the main component, except for the tests in Munich at the laboratory of the Institute of Hydraulic and Water Resources Engineering of the Technische Universität München.

This series of tests was carried out in the years 2006/07 at the hydraulic laboratory of the TU Muenchen in Obernach. The tests were focused on construction methods A and B as shown in Fig. 4. Both of the investigated methods revealed a highly robust and durable behaviour when subjected to hydraulic overtopping loads. The maximum load was 300 l/s*m resulting in an overtopping height of approx. 0.35 m. Within the test series downstream dike slopes of V:H = 1:1.5 to 1:2.5 were investigated. Pictures of tested designs A and B are shown in Fig. 5 for both the loaded and unloaded conditions.

In Fig. 6 and Fig. 7 the sections of the two mentioned test dikes are shown. The dike body was built of sand so that also a geosynthetic filter was applied between the gravel, which was used to form the superficial layer beneath the protection cover, and the sand body. A composite made of a geogrid and a nonwoven was installed for the test model as shown in Fig. 6. A needle-punched nonwoven geotextile was used for the model test with a wrap-around method as shown in Fig. 7. Both materials have different stress-strain-behaviour but due to the different application (wrap-around and slope parallel) both systems show high resistance against hydraulic loads.

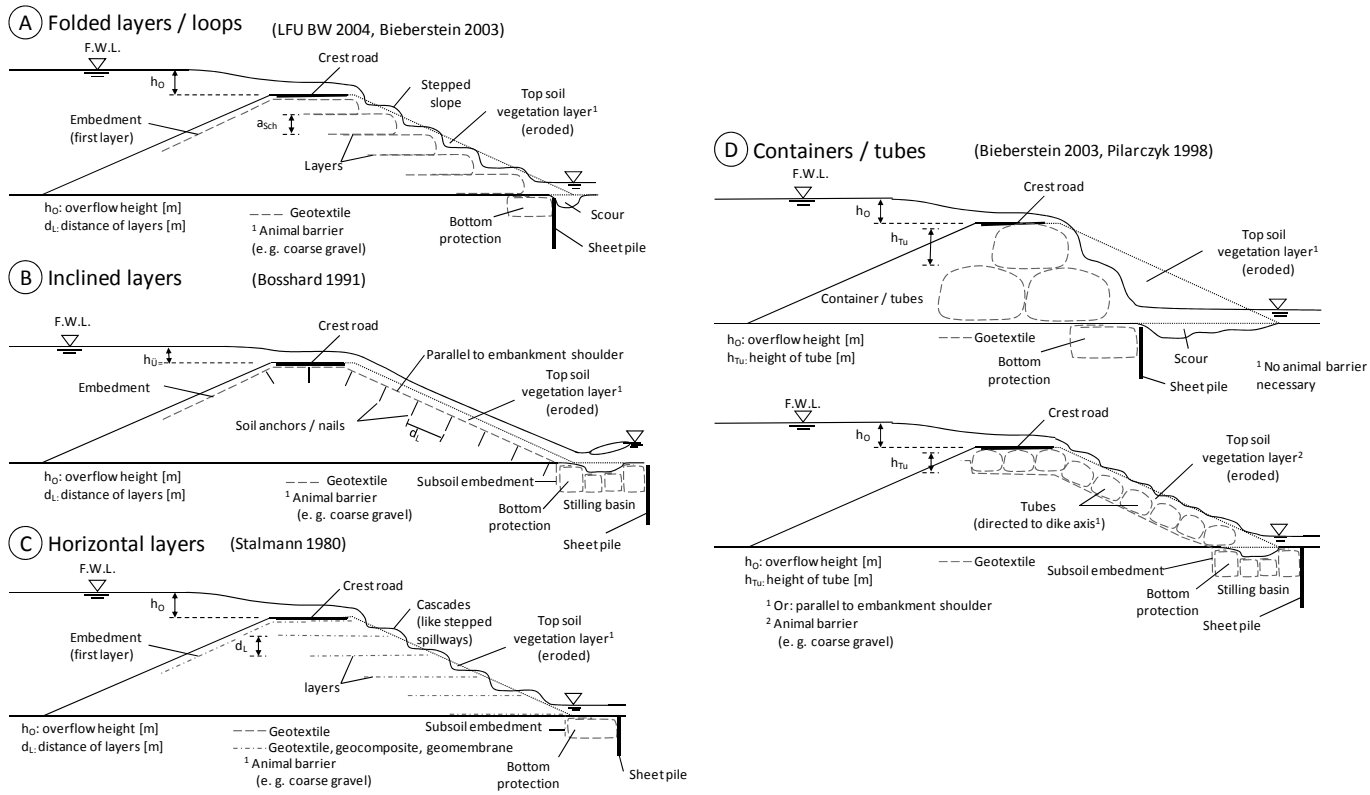

Figure 4. Typical overflow protection systems of flood embankments using geosynthetics (Haselsteiner et al., 2007a)

Figure 5. Loaded and unloaded dyke models with slope parallel geosynthetic layers using anchors for fixation (left) and wrap-around method (loops) (right) (Haselsteiner et al., 2008)

As mentioned in the list of design considerations above, the protection of the crest and toe area was guaranteed by the application of a tube at the toe and by bracing the applied geosynthetics. Both methods survived the tests without remarkable damage or deformation. For the fixed parallel geosynthetics method minor deformations occurred only after the applied soil nails/anchors were subsequently reduced.

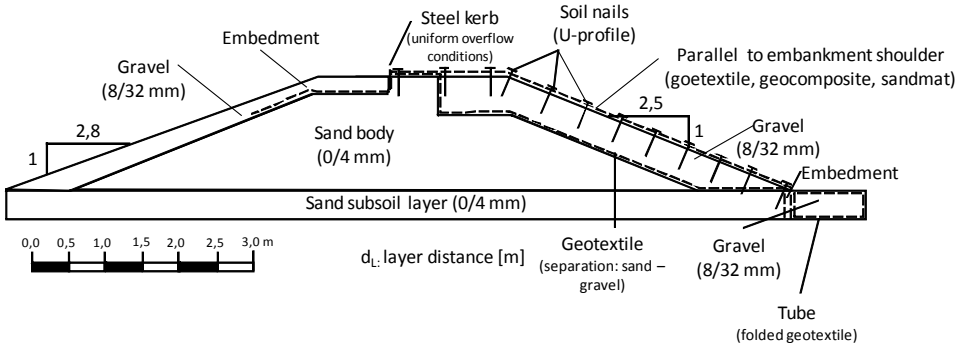

Figure 6. Dike model with layers parallel to embankment shoulder fixed by soil nails (Haselsteiner et al., 2008)

The advantages of the geosynthetic loops are the high robustness and the favourable energy dissipation provided by a stepped spillway. The fixed parallel geosynthetic layers can easily be applied to existing, stripped slopes without interference of the construction process. This method can also have some advantages if only isolated damaged spots are to be refurbished. Within the Munich tests a combination of a vegetation layer and a knitted geotextile was also investigated. For this purpose the downstream slope of

the test levee was covered with a topsoil where the knitted geotextiles were placed with different overburden heights of 5-10 cm. The final test series was dominated by a relatively fast failure of the protection system. But, the initiation of the failure began at the area which had not been reinforced by a knitted geotextile. The authors hold the opinion that the application of a knitted geotextile in combination with a topsoil/vegetation layer increases the resistance against erosion considerably. Currently, another test program is in preparation with the close collaboration of industry, engineering consultants and science.

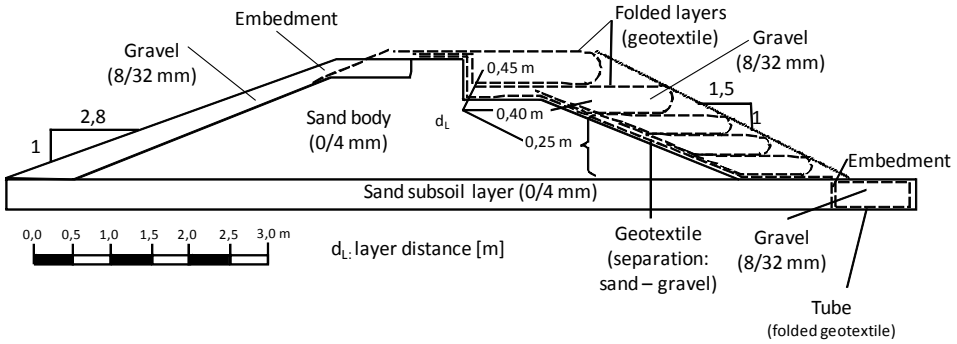

Figure 7. Dike model with wrap-around method (loops) (Haselsteiner et al., 2008)

4 NEEDS FOR RESEARCH

The geotechnical and (geo)hydraulic basics for flood protection embankments/levee overflow/overtopping are well-known as mentioned before. Depending on the preferred methods, (see Fig. 4) corresponding large or full scale laboratory or field tests should be applied in order to determine the hydrodynamic forces resulting from overtopping and the reaction of the geosynthetic protection system. For the described methods A and B (Fig. 4, Fig. 5, Fig. 6, Fig. 7) as well as for method D the stress-deformation behaviour of the applied geotextiles, geogrids and/or geocomposites dominate the embankment stability whereas method C exhibited unstable conditions due to the possibility of backward erosion caused by high hydraulic forces. Once, the stress-deformation behaviour of some of the mentioned design methods are determined, the application limits and required safety factors can be derived by analytical analysis and extrapolation. Future research work should still focus on small embankments where relatively limited deformations and hydrodynamic loads are to be expected. Also, particular attention has to be paid to the design of the crest, re-anchoring area and the downstream dam toe where high hydraulic forces can occur. A failure of the crest and/or the dam toe will inescapably lead to a total failure and, therefore, these parts should be designed conservatively. In terms of the necessity of energy dissipation and the avoidance of scouring downstream, the application of tubes is recommended since those design methods were tested successfully in Munich before.

Method A is a “State of the Art” application for reinforcement of embankments. For the application as overflow protection system, hydrodynamic loads on the stepped spillway and the stress-deformation behaviour of the geosynthetic loops need to be investigated in detail. For this measurement small piezometers and strain gauges can be used. The pore water pressures should be measured at the surface of the steps and in the dike body itself. Seepage uplift forces should be eliminated by using a high permeable fill material within the loops and by the application of an appropriate sealing system. Simultaneously, in order to obtain a better determination of the overflow velocities, an overflow kerb should be applied. Upstream and downstream water levels are important boundary condition parameters to monitor. For the loops, heavy geotextiles are as applicable as geocomposites consisting of a geogrid combined with a geotextile. The decisive research design parameters and aspects shall result in a recommendation of a standard design and they are as follows:

- Determination of specifications of the applied geosynthetic product (strength, permeability…)
- Determination of applicable layer distances and embedment lengths using the wrap-around method
- Determination and evaluation of the design of the steps in terms of energy dissipation and in terms of occurring loads
- Determination of the re-anchoring length / technique

To be competitive with classical overflow protection systems, hydraulic loads of more than 0.5 m³/s*m (500 litres/s*m) or even higher have to be envisaged. In this context, it has to be repeated that this solution is also a measure to stabilize the slope of the embankment so that the geostatic stability is also considerably increased depending on the applied materials and the actual slope inclination. Therefore, considerably steep slopes (V:H = 1:1.0-1.5) can most probably be applied. In Germany, similar investigations have already been carried out. But, the tests were made applying only limited monitoring and a small scale test dike so that a final design recommendation could not be prepared from the results (Bieberstein, 2003). The height of a test levee should be limited to 2-3 m also considering that most of the existing embankments along rivers have a considerably limited height. For example, the average height of over 1,000 km dikes in Bavaria (Germany) is approx. 2.5 m (Haselsteiner & Strobl, 2005).

Method B is a combination of a geosynthetic cover and soil nails for stabilization. The soil nails perform as anchors and the geosynthetic cover limits the deformation of the dam body and avoids erosion phenomena. Similar to Method A, a coarse grained soil material should be applied or already present within the old dike body. Otherwise a harmful migration / transport of the fines cannot be prevented and this can quickly lead to a total failure. Again, pore water pressures and deformations should be measured. Additionally to the previously mentioned instruments and measurements for Method A the forces on the soil nails should be measured since the arrangement of nails and the form and length of the nails are important aspects. In order to find a suitable standard design the following design parameters and aspects should be taken into consideration:

- Determination of specifications of the applied geosynthetic product (strength, permeability…)
- Determination of applicable soil nail arrangement and soil nail specifications (thickness, length, form, spacing …)
- Determination and evaluation of the energy dissipation and occurring hydrodynamic loads
- Determination of the re-anchoring length / technique

For Method B the applicable slopes are dominated by the natural slope stability of the embankment. Hydrodynamic forces and interflow (seepage) forces increase the loads on the downstream slope of method B (Fig. 4). Therefore, slopes with an inclination flatter than V:H = 1:2.0-2.5 should be used for the tests.

The previously mentioned method(s) D (Fig. 4) have been successfully applied in coastal engineering. For the use of geotextile containers/tubes, particularly for big-packs, the applicable size will be limited by the strength of the applied geosynthetic product. The application for small (H < 2 m) overflow flood protection dikes is also quite attractive and is worth to be discussed in the future.

REFERENCES

Bieberstein, A. (2003): Überströmbare Dämme – Landschaftsverträgliche Ausführungsvarianten für den dezentralen Hochwasserschutz in Baden-Württemberg. Zwischenbericht anlässlich des Staatsseminars von BWPLUS am 11./12.03.2003, Forschungszentrum Karlsruhe.

Bosshard, M. (1991): Überflutbarkeit kleiner Dämme. Versuchsanstalt für Wasserbau, Hydrologie und Glaziologie der Eidgenössischen Technischen Hochschule, Zürich.

Bräu, G. (2007): Bemessung von geokunststoffbewehrten Erdkörpern – EBGEO. 10. Informations- und Vortragsveranstaltung über „Kunststoffe in der Geotechnik“, Geotechnik Sonderheft 2007, S. 13 - 17, München.

CIRIA 116 1987. Design of reinforced grass waterways. Construction Industry Research and Information Association (CIRIA), Report 116, London.

DGGT EBGEO (2010): Empfehlungen zur Berechnung und Dimensionierung von Erdkörpern mit Bewehrungseinlagen aus Geokunststoffen. Deutsche Gesellschaft für Geotechnik e. V. (DGGT), Verlag Ernst und Sohn, Berlin.

DGGT EAG-GTD (2002): Empfehlungen zur Anwendung geosynthetischer Tondichtungsbahnen EAG-GTD. DGGT e.V., Ernst & Sohn, Berlin

DIN 19712 (1997): Flussdeiche. Deutsches Institut für Normung e.V. (DIN).

DVWK 76 (1986): Anwendung und Prüfung von Kunststoffen im Erdbau und Wasserbau. Schriften zur Wasserwirtschaft, Heft 76, Deutscher Verband für Wasserwirtschaft und Kulturbau, Verlag Paul Parey, Hamburg und Berlin.

DVWK 221 (1992): Anwendung von Geotextilien im Wasserbau. Merkblätter zur Wasserwirtschaft, Heft 221, Deutscher Verband für Wasserwirtschaft und Kulturbau, Verlag Paul Parey, Hamburg und Berlin.

DWA M507 (2007): Deiche an Fließgewässern. Gelbdruck des Merkblatts Nr. 507, Deutsche Vereinigung für Wasserwirtschaft, Abwasser und Abfall e. V. (DWA), Hennef

Egloffstein, T. (2001): Der Einfluss des Ionenaustausches auf die Dichtwirkung von Bentonitmatten in Oberflächendichtungen von Deponien. 2. Naue-Geokunststoffkolloquium, Geokunststoffe in der Geotechnik, Band III, 25./26.01.2001, Krefeld.

FGSV (2005a): Technische Lieferbedingungen für Geokunststoffe im Erdbau des Straßenbaues (TL Geok E-StB 05), FGSV-Nr. 549, Forschungsgesellschaft für Straßen- und Verkehrswesen, Köln.

FSGV (2005b) Merkblatt über die Anwendung von Geokunststoffe im Erdbau des Straßenbaues (M GeoK E). FGSV-Nr. 535, Forschungsgesellschaft für Straßen- und Verkehrswesen (FGSV), Köln.
Haselsteiner, R.; Strobl, T. (2005): Deichsanierung. Forschungs- und Entwicklungsvorhaben, Endbericht, im Auftrag vom Bayerischen Landesamt für Wasserwirtschaft (LfW), Lehrstuhl und Versuchsanstalt für Wasserbau und Wasserwirtschaft, Technische Universität München (not published).
Haselsteiner. R.; Strobl, T. (2006): Constraints and Methods of Refurbishment Measures of Dikes. 3rd International Symposium on Integrated Water Resources Management, 26 - 28 September 2006, Bochum.
Haselsteiner, R. (2006). Deichertüchtigung in Bayern - Eine Übersicht. Tagungsband zur Fachtagung "Deichertüchtigung und Deichverteidigung in Bayern", Berichte des Lehrstuhls und der Versuchsanstalt für Wasserbau und Wasserwirtschaft der Technischen Universität München, Band Nr. 107, S. 13 - 28, 13./14. Juli 2006, Wallgau.
Haselsteiner, R.; Mett, M.; Strobl, Th. (2007a): Überströmungssicherung von Deichen mit Geokunststoffen. 5. Naue-Geokunststoffkolloquium, 25./26.01.2007, Bad Lauterberg.
Haselsteiner, R.; Strobl, Th.; Heerten, G.; Werth, K. (2007b): Moderne Deichquerschnitte mit integrierten Sicherungsmaßnahmen aus Geokunststoffen – Ergebnisse aus Modellversuchen zur Überströmung. 10. Informations- und Vortragsveranstaltung über „Kunststoffe in der Geotechnik“, Geotechnik Sonderheft 2007, S. 39 – 48, München.
Haselsteiner, R., Strobl, Th.; Heerten, G.; Werth, K.; (2007c): Überströmungssicherung von Deichstrecken mit Geokunststoffen - Ein wirtschaftlicher Sicherheitsgewinn. Dresdner Wasserbaukolloquium 2007 "Fünf Jahre nach der Flut", 8.-9. Oktober 2007, Dresdner Wasserbauliche Mitteilungen, Heft 35, S. 145 – 156.
Haselsteiner, R.; Strobl, Th.; Heerten, G.; Werth, K. (2008): Overflow Protection of Flood Embankments with Geosynthetics. EuroGeo 4, Geosynthetics in Civil Engineering Applications, September 2008, Edinburgh, Scotland.
Heerten, G. (1999): Erhöhung der Deichsicherheit mit Geokunststoffen. 6. Informations- und Vortragstagung über Kunststoffe in der Geotechnik, Fachsektion Kunststoffe in der Geotechnik der Deutschen Gesellschaft für Geotechnik e. V. (DGGT), München, Germany.
Heerten, G., Horlacher, H.-B. (2002): Konsequenzen aus den Katastrophenhochwässern an Oder, Donau und Elbe. Geotechnik 25, Nr. 4, S. 231ff.
Heerten, G.; Werth, K. (2006): Anwendung von Geokunststoffen bei der Deichertüchtigung. Institut für Wasserbau und Wasserwirtschaft, TU München, Mitteilungsheft Nr. 107 zur Fachtagung Deichertüchtigung und Deichverteidigung in Bayern, am 13. und 14. Juli 2006 in Wallgau.
Heerten, G.; Heibaum, Haselsteiner, R.; Werth, K. (2008): Hochwasserbedrohungen - Neue Sicherheiten im Deichbau mit Geokunststoffen. DGGT, 30. Baugrundtagung, 24.-27. September 2008 in Dortmund.
Hennegriff, W., Kolokotronis, V., Weber, H. & Bartels, H. (2006). Klimawandel und Hochwasser, In KA – Abwasser, Abfall 53, No. 8. pp. 770 – 779.
Herold, A. (2009): Geokunststoffe und Böschungsvernagelung - Berechnung / Versuche / Beispiele. Vereinigung der Straßenbau- und Verkehrsingenieure (VSVI) Bayern, Fortbildungsseminar „Erdbau“, 05.03.2009, Nürnberg.
LFU BW (2004): Überströmbare Dämme und Dammscharten. Landesanstalt für Umweltschutz Baden-Württemberg (LfU BW), 1. Auflage, Karlsruhe.
Powledge, G. R., Clopper, P. E., Miller, P., Ralstone, D. C., Temple, D.M., Chen, Y. H. (1989): Mechanics of overflow erosion on embankments. Part I: Research activities. & Part II: Hydraulic and design considerations. Journal of Hydraulic Engineering (ASCE), Vol. 115, No. 8, 1989, Part I: pp. 1040 – 1055, Part II: pp. 1056 – 1075.
Saathoff, F. (2003): Geosynthetics in geotechnical and hydraulic engineering. Geotechnical Engineering Handbook, Volume 2, Procedures, Section 2.13, Publ. U. Smoltczyk, Ernst & Sohn Verlag, Berlin.
Saathoff, F., Werth, K. (2003): Geokunststoffe in Dämmen und Deichen. Sicherung von Dämmen und Deichen: Handbuch für Theorie und Praxis, S. 221 – 237, Hrsg. Hermann und Jensen, Universitätsverlag Siegen.
Stalmann, V. (1980). Überströmungssicherung von Deichen. Wasser und Boden 3, S. 109 – 112.
Vollmert, L.; Schwerdt, S. (2010): EBGEO 2010 – Erste Erfahrungen mit der Anwendung der neuen Bemessungsempfehlung und deren Umsetzung in der Praxis. 9. Sachsisches Bautextilien-Symposium (Bautex 2010), Bauen mit Geokunststoffen, Tagungsunterlagen, Chemnitz.
Werth, K.; Haselsteiner, R.; Heerten, G.; Strobl, Th. (2007): Deichquerschnitte mit integrierten Geokunststoffen. 37. Internationales Wasserbau-Symposium (IWASA), Lehrstuhl und Institut für Wasserbau und Wasserwirtschaft, Rheinisch-Westfälische Technische Hochschule Aachen (RWTH), 04./05. Jan. 2007, Aachen.
Ziegler, M. (2007): DIN 1054 und ihre Anwendung im Geokunststoffbereich. 10. Informations- und Vortragsveranstaltung über „Kunststoffe in der Geotechnik“, Geotechnik Sonderheft 2007, S. 3 -12, München.

ISGSR 2011 - Vogt, Schuppener, Straub & Bräu (eds) - © 2011 Bundesanstalt für Wasserbau ISBN 978-3-939230-01-4

Automated Engineering in Levee Risk Management

J.G. Knoeff & E.W. Vastenburg
Deltares, Delft, The Netherlands

ABSTRACT: The risk of flooding depends on the hydraulic load, strength of the levee and the estimation of flood consequences. To determine automatically the strength of levees, the Dike Analysis Module (DAM) has been developed. This platform is able to perform stability analysis for a large numbers of levees within a management area. In order to show the role of automated engineering in daily levee management, two study cases are presented here. The applicability of DAM is tested with real data. Spatial planning studies as an application of DAM are also discussed.

Keywords: Automated engineering, stability analysis, spatial planning, data management, study cases

1 INTRODUCTION

In many countries, levees play a major role in flood protection and flood risk management. Worldwide, hundreds of thousands of kilometers of levee exist. Often, these levees are old and little is known about their safety. Besides geometrical data, information on the subsoil conditions is of great importance for assessing the reliability of a levee system. In order to cope with this challenge, several programs on data management are currently being developed in the Netherlands.

Data acquired in the field or by geological analyses cannot be used directly in the models used to assess the safety of levees. This data needs to be first processed and filtered before it can serve as input for the models. Recently, the effectiveness and efficiency of data acquisition has advanced considerably. For example, laser scanning has enabled us to obtain topographical information (i.e., levee geometry) of large areas in a very short time. In order to advance at the same pace with the technology, it is necessary to improve also the data processing to enable effective and rapid safety assessments. The Levee Analysis Module (DAM) is a tool that automatically process and analyses the gathered data and can be used to support decision-making.

The required data depends on the goal of the assignment. The requirements during daily circumstances differ from the data necessary for flood control, policy management or levee assessment. The basic information (soil profiles, soil properties and geometries) remain the same for the different processes. The high degree of automation in DAM makes rapid analyses of levee systems on large geographical scale feasible. The degree of detail can vary depending on the goal of the analyses; from very strict in polices to very detailed in real-time assessments for decision support of flood control measures and emergency response.

This paper describes the application of DAM in two cases where the gained analysis capabilities by the automated engineering approach is described. The first case describes the use of REAL-DAM for a levee assessment. The suitability of DAM for spatial planning studies is discussed in the second case.

2 FRAMEWORK

2.1 *Dike Analysis Module*

DAM is a platform for automatically determining probability of levee failure. Based on a given hydraulic load, DAM calculates the strength of a levee automatically. It is a semi 3-dimensional determination of the levee strength. This means that cross sections are schematized from a three-dimensional terrain model complemented with point observations of soil structure. From these cross sections, the stability can be determined.

DAM features a highly modular design. For different applications, a configuration of relevant modules can be composed. The applied modules are dependent on the availability of data and purpose of the stability analysis.

The workflow structure of DAM is based on the four steps of a geotechnical analysis (see Figure 1). The first step is collecting processed data from subsoil models, digital terrain models (DTM) and hydrology models. The data has to be stored in standardized databases. Requirements for data quality and quantity depend on the purpose of the analysis. For example, a design calculation requires more detailed information than policy analysis estimations. In the second step, generic algorithms schematize representative cross sections. Different algorithms can be used. The algorithm selection depends on available data, purpose of the analysis and calculation models. In the Netherlands, for the regular safety assessment, conservative assumptions for schematizations are prescribed in guidelines.

To perform the correct actions during critical water levels, information about the actual levee strength is necessary. The third step is executing the actual stability calculation to determine the levee stability. Due to the modular structure of DAM, different models can be used to calculate the stability. The final step in the process involves the analysis, visualization and reporting of the geotechnical analysis.

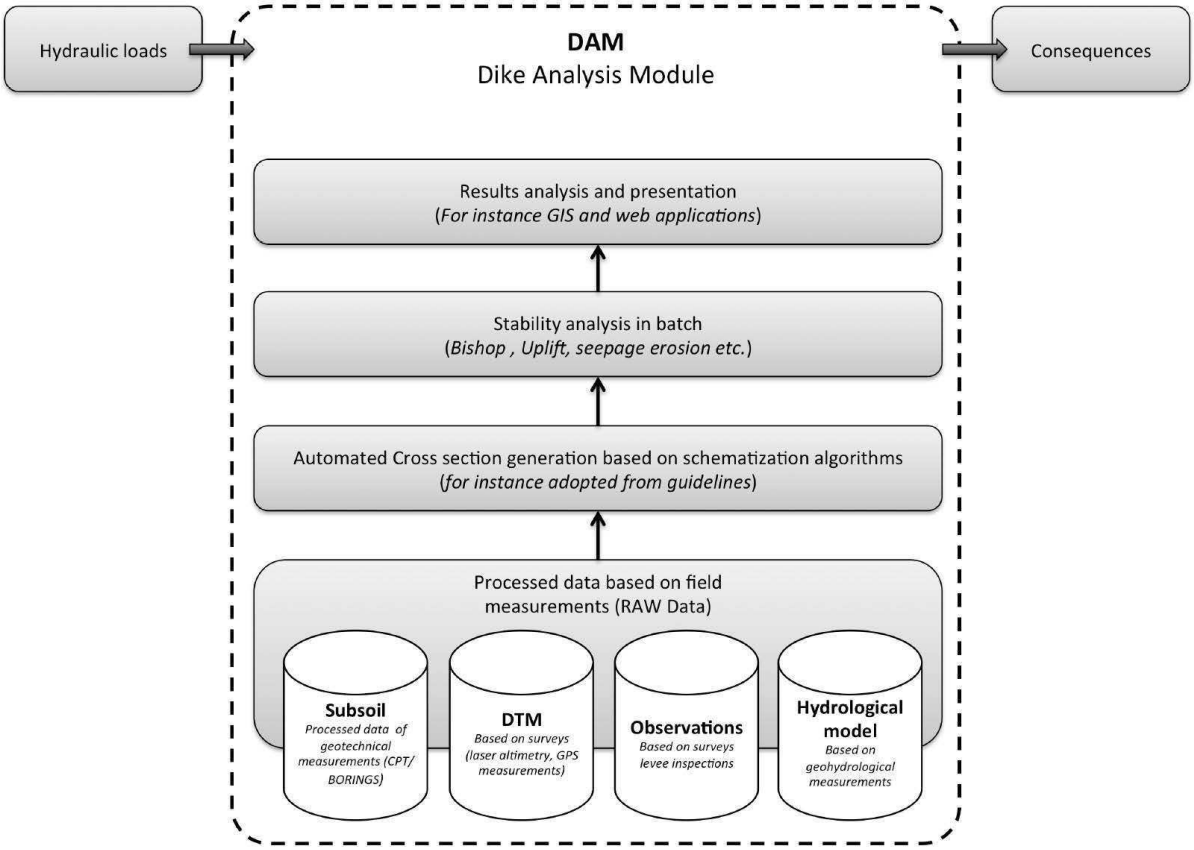

Figure 1. Structure of DAM

Normally, for every analysis the four steps are performed where the emphasis lies on the analysis of a representative cross section of a levee trajectory. For such an analysis, one or more cross sections are measured and several borings and cone penetration tests are performed. If necessary, pore pressures and soil properties are measured. From this data, a representative cross section is schematized and this labor takes a great deal of engineering judgment. Finally, the result of the geotechnical analysis is analogous reported and archived.

DAM assumes that in 21st century data of geometry and subsoil will be stored in digital databases. With clever codes and algorithms, relevant data can be extracted form these databases and automatically schematized for stability and strength analyses. The use of codes and standards reduces the engineering judgment. The schematizations are the input of geotechnical analysis of a levee. Results of the analysis are presented for further analysis in a GIS environment or in the web. In this way, with inbuilt intelligence, the four steps in DAM can be performed automatically in a short time. Real time analysis is even possible in case of a flood risk control.

When new data becomes available, it is simple to replace that particular module in DAM. The same holds for codes and standards. Due to its modular structure, it is not necessary to schematize the cross sections from scratch again, since the algorithms in the software do this automatically.

While using DAM as a platform to perform risk assessments for levee management, distinction is made between risk assessments for normal levee management and assessments for flood risk control. In case of flood risk control, the platform is used to show real-time information of levee strength, possible emergency measures and basic assumptions of the analysis. This article focuses on the risk assessments as part of the normal levee management.

In addition, the central data management promoted by DAM (see Figure 2) maximizes the efficiency of the assessments of the levee manager. Until recently, a levee operator depended on data from colleagues within or outside their organization to perform tests. Central data management allows the levee manager to access actual up to date data at any time.

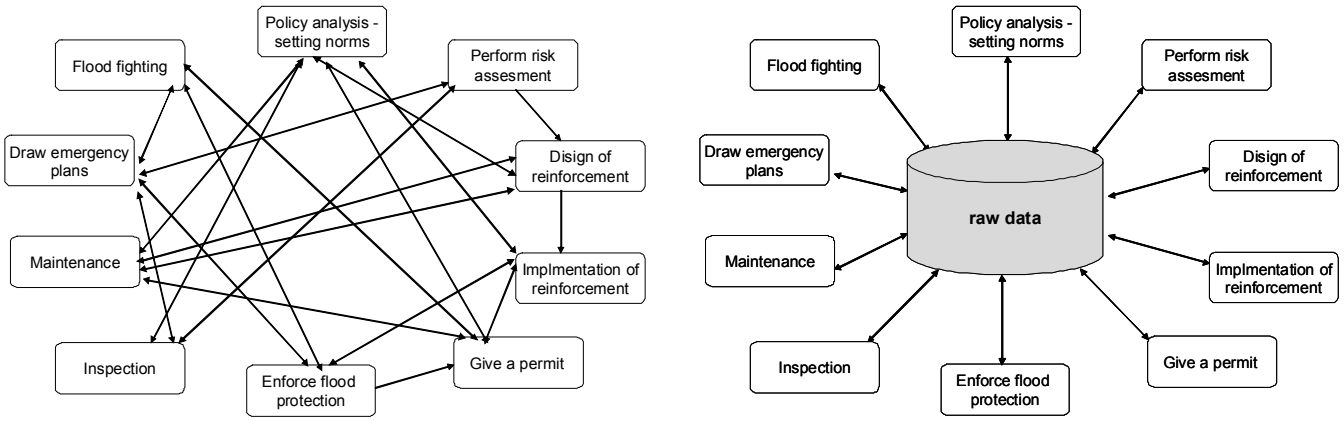

Figure 2. Current data management (left) and central data management structure offered by DAM (right)

2.2 *Levee management*

Figure 3 shows an overview of the processes for normal levee management in the Netherlands. In the figure, various cyclic processes are visible. The outer circle consists of the following processes:

- Setting standards and norms, this process involves determining the conditions that must withstand the levee and the procedures to be followed to show that the levee meets these requirements;
- Risk assessment every 6 years (stated in the law). The risk assessment shows which levees do not meet the requirements;
- Design of levee reinforcements. If levees do not meet the requirements, the levee must be strengthened;
- Implementation of reinforcements.

The inner circles relates to the daily processes with respect to levee management. These processes are related to daily maintenance and space planning.

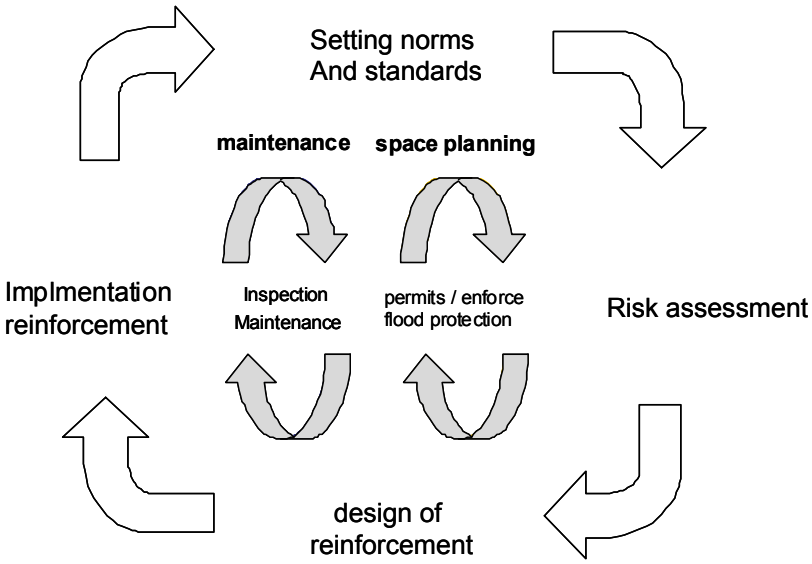

Figure 3. Normal levee management in the Netherlands

Table 2.1 shows an overview of the relation between levee management and the applicability of DAM. For every process, the table describes a purpose and the applicability of DAM.

Table 2.1 Applicability of DAM for different processes around a levee

Process	**Example of application of DAM**
Setting standards and norms for levees	Decision Support System for policy analysis. Quick-scan of possible consequences by changes in the standards and norms. An example is described in case 1
Risk assessment every 6 years	Risk assessment according to obligatory schematization procedures. This procedures are programmed within DAM. Example is described in Knoeff e.a. (2008)
Design of levee reinforcement	Support the choice of preferred alternative of reinforcement. Determines size and cost of levee reinforcement for a 3D-space with different alternatives.
Implementation of Reinforcement	Increase efficiency levee reinforcement. Determination of activities based on real-time levee strength (based on measured pore pressures).
Daily levee maintenance	Feasible maintenance plan. Prioritize maintenance based on available budget and actual risks.
Space planning around a levee	Determine limits of authorization. An example is described in case 2

3 CASE STUDIES

This section describes the application of DAM in three different cases. In the first case, setting of standards and norms in California is studied. The second case, analyses a spatial reservation Waterboard Groot Salland. In the third case, a levee reinforcement is designed.

3.1 *Case 1: Setting standards and norms in California*

Since 1995, a Dutch law enforced a six-year periodic assessment of the water retaining structures in the country. Very recent programs for systematic levee evaluations have been also introduced in the United States. The program FEMA's RiskMAP and the California Urban and Non Urban Levee Evaluation Programs are examples of this.

For the California Urban Evaluation Program, the California Department of Water Resources is facing a major challenge to conduct an appropriate and rapid geotechnical assessment to determine the safety of the levees. To face these challenges, Fugro and Deltares, combined contineous dike strength modelling in

GIS, according the REAL® method[1] with automated engineering provided by the DAM platform . Based on data of the evaluation program, almost 1.000 different levee cross sections are evaluated for three water levels and three failure mechanisms. Using the DAM platform, the speed in calculation is about two orders of magnitude faster than conventional evaluation techniques (Woldringh ea, 2009).

In this project, REAL protocols are used for data collection which is the first step in the analysis as described in section 2. REAL uses available information from a GIS, such as surface levels (digital terrain models), data acquisition with FLI-MAP system; CPT's; borings; water pressure measurements; geotechnical parameters (weight, cohesion, friction angle; geological maps). Information must be provided in digital form, with spatial XYZ coordinates, and preferably in a Geographic Information System (GIS). Using this data (step 2 of the analysis), a most-likely subsoil model is made with the geological knowledge and local experience for a levee compartment. A standardized grid of data is generated on each soil layer. Consequently, the reliability of the subsoil model can be checked and improved in each point, by comparing the layers with underlying (additional) information.

For the computations, the digital terrain model and 3D subsoil model is composed of cross sections every 25 feet. Using the DAM platform, calculations are made (step 3 of the analysis) for 3 different potential failure mechanisms: macro stability landside slope, macro stability waterside slope and internal erosion (piping) for all the cross sections. The results (step 4 of the analysis) of these calculations are then presented in the GIS.

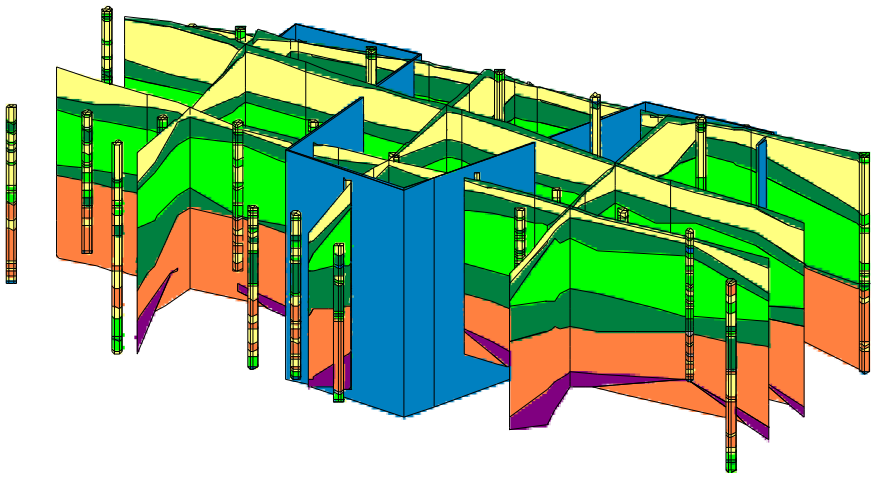

Figure 4. 3-dimensional subsoil model derived from REAL®

The stability of landside and waterside slopes are calculated according to the model of Bishop and Lift-Van with the MStab software. MStab is developed according Dutch standards. In the US, stability is in most cases checked with the method of Spencer.

In addition, there are some important differences between the US and Dutch standards for schematization and analysis of cross sections. For example, in the Netherlands a conventional effective stress analysis is used for the stability assessment of levees. The Californian standards prescribe undrained stress analysis with the SlopeW software. Another example is the estimation of pore pressures. On one hand, when there is no information available on pore pressures, a pre-described method for the schematization of the pore pressures is used in the Netherlands, where expert knowledge is allowed to be used to make a better schematization. For that reason, DAM supports this technique. On the other hand, in California pore pressures are calculated by different software called SEEP/W.

However, the objective of this project is not to assess the levees but to demonstrate automated engineering. Therefore, the MStab software and Dutch schematization of pore pressures is used where SlopeW can be easily linked to DAM due to its modularity.

[1] Rapid Engineering Assessment of Levees

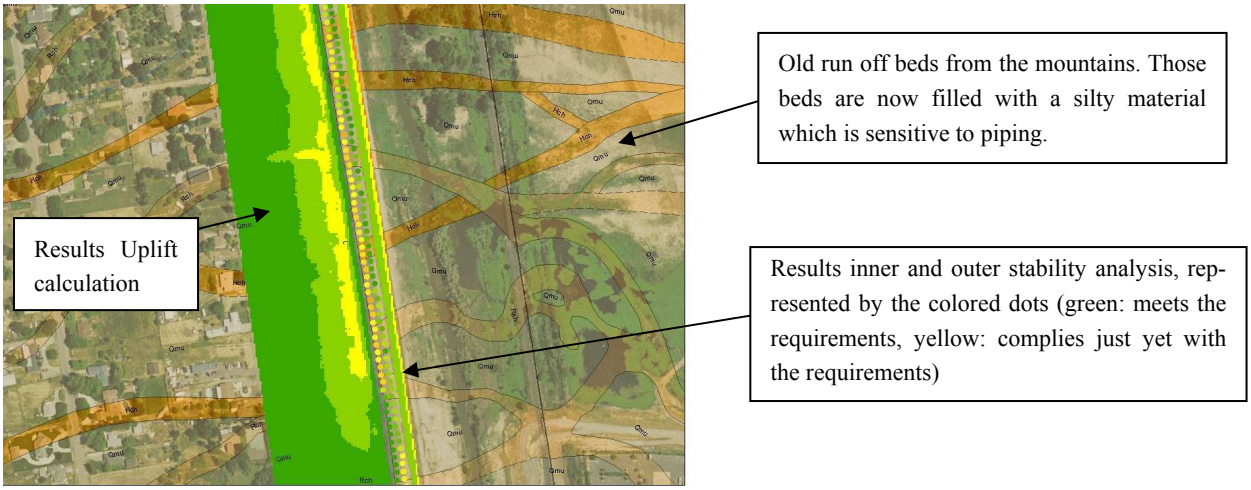

Figure 5. Results of REAL^{TM} analysis

Despite the differences between the US and Dutch standards, a comparison is made between the stability analyses for the 'official' levee program and the results DAM calculations by Deltares. Calculations of three cross sections (approximately every 750 feet) are made. The slip circles of the selected locations are compared with the DAM slip circles. In general, the position of the slip circle is comparable but the computed the safety factors are different. However, the difference decreases when the DAM calculations are made with estimated drained strength parameters for clay layers. From these results, it is possible to observe that in California many raw data is used in analyses. On this respect, DAM with little effort could translates this raw data into the information needed (levee strength).

3.2 *Case 2: Spatial reservation Waterboard Groot Salland*

Around a levee in The Netherlands different zones are defined; core zone, protection zone and outer protection zone. Within these zones, different rules are applied to protect the levee. For instance, it is prohibited to build within a zone without a permit. As described by Koelewijn & Hounjet (2007), there are three main reasons for the preservation of sometimes-precious space on both sides of a levee: maintaining the flood protection function now and in the future, avoiding damage to other functions arising from rehabilitation works necessary in the future an creating opportunities to avoid casualties in case of failure of the embankment under extreme conditions. The spatial reservation is divided in different zones and administratively determined in the so-called "Legger".

In the Netherlands, normally the zones are defined based on a "rule of thumb". For instance, for the landward side of the levee a reservation of 30 meters is made from the ditch behind the levee or 60 meters from the inner crest line in cases where no ditch exists (Koelewijn & Hounjet, 2007).

The pressure on the available space around a levee increases every day due to lack of space and building plans. In addition, in urban areas often constructions like houses, are present in the vicinity of levees. To achieve an optimum definition of the zones and thus the spatial use, the use of a rule of thumb to define conservative spatial reservations is not applicable anymore.

To optimize the zones, and get a better legal basis to the issue of space reservation around the levee, detailed stability analyses should be performed. By using the traditional calculation methods, the costs would be extremely high. DAM, however, is a valuable tool that can be used in this case to execute the calculations.

As described before, the zones are determined based on slope stability and seepage erosion calculations for the current situation. Information such as the situation for the year 2100, with changing hydraulic conditions (due to climate change) and settlement of the subsoil is also include for the analysis.

The analysis is performed in the following step: stability analysis of the current profile (see 3.2.1), assessment of the minimal required geometry for current situation (see 3.2.2) and assessment of the minimal required geometry for the year 2100 (see 3.2.2). After performing the calculations, the results are reported in a visual way in subsection 3.2.3.

3.2.1 *Stability analysis current profile*

The first step is to determine the actual stability of the levee as it is. In this case study, this is done with DAM. DAM uses the data from the databases of the water board, as described in section 2. Based on this

data and schematization algorithms, DAM is capable of automatically generate cross sections and perform stability analyses. As mentioned, the data scenarios are equal for all steps.

3.2.2 *Determining minimal required geometry for current situation*

To determine the minimum required levee geometry for the hydraulic loads of the year 2011, first an initial profile is defined. The next step is to determine the minimal required levee profile with respect to levee safety, based on the hydraulic loads for the year 2011. In normal engineering practice, this is done by setting up a model in a computer program. This is followed by a change in the geometry by hand, until the results of the stability analysis match the required safety factor. This is an intensive process and consumes a lot of time. In addition, in case of changing parameters, the process must be done allover again. Setting up the schematization and changing the geometry is automated in DAM and consists out of different steps.

The first step is checking if the height of the levee matches the required height, based on the hydraulic loads. For the case that the crest height is to low, the levee is heightened automatically. Here, algorithms are used to define the height of the phreatic plane based on guide lines, as well as expert knowledge and measurements. After completing the schematization, a stability analysis is performed. In case the derived safety factor meets the required safety factor, the batch process is stopped. The generated geometry is equal to the minimal required geometry. If the assessed safety factor is to low, DAM changes the geometry. Depending on the exit point of the slip circle, DAM changes the angle of the inner slope or creates a berm. If the exit point of the slip circle lies on the inner slope of the Levee, DAM changes the slope steepness to avoid not normative slip circles. To achieve this, DAM increases the slope width in steps until sufficient safety is found, or until the added width reaches a certain maximum (default 15 m.).

In case of adding a berm, the used algorithm is based on shifting the starting point along a straight line with a predefined slope (see Figure 6). The slope has a default ratio 1:3 (vertical:horizontal). The ratio can be altered in the configuration file. The starting point could be the inner toe of the levee or the outer crest of an already existing berm. The shifting process is performed in steps. The horizontal component of the shift and the maximum number of steps are configurable. The shifting process is repeated until a safe geometry is found which meets the required safety factor. This is an iterative process. This profile is exported to the database for further reporting.

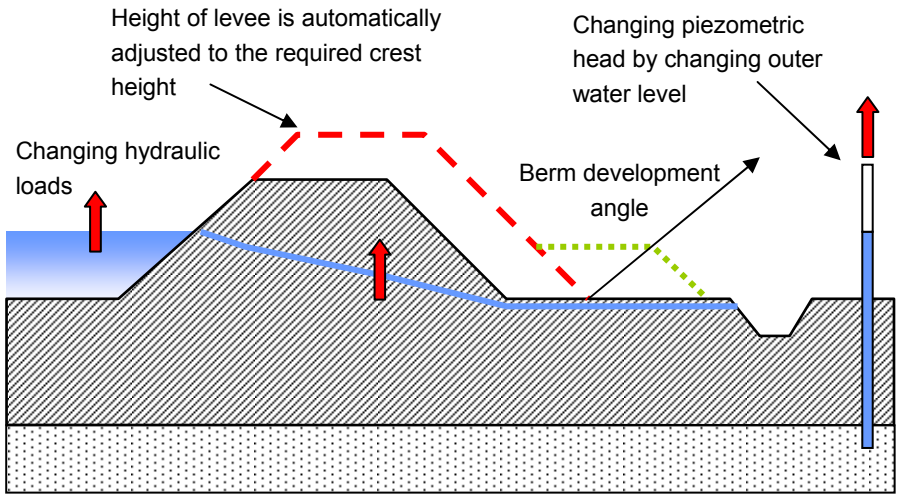

Figure 6. Automated geometry adjustments within DAM

3.2.3 *Determining minimal required geometry for the year 2100*

This calculation procedure is alike to the one described in subsection 3.2.2, only the values of the hydraulic loads and required levee height are different. This means that only some minor changes are made to perform the analysis for the year 2100. Other necessary data for performing the calculations is equal to the data used for the previous calculations. This means that the same database, for instance the subsoil model, can be used by DAM to generate the cross sections.

3.2.4 *Results*

After performing the calculations and optimizing the geometry to match the required safety factor, the adjusted profiles are exported and combined per cross section. In this way, it is possible to visualize the required minimum profiles for the space reservation (see Figure 7). In addition, characteristic points like the crest lines and toes of the levee can be plotted in a aerial map.

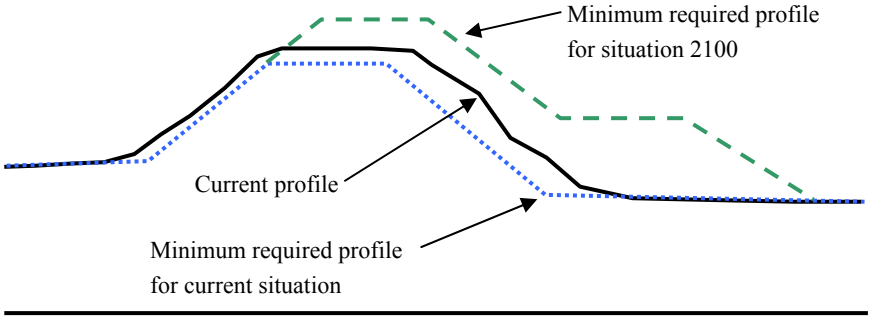

Figure 7. Example where the diffent determinde profiles with DAM are combined in one drawing

Based on the applicability of DAM, the Waterboard[2] considers to use DAM for their risk assessments. Due to the detail level of the employed databases, it is expected that the data used for defining the "Legger" can be used as well for the 6 yearly assessment of regional levees.

4 CONCLUSION

Based on the case studies here presented, it can be concluded that automated engineering can be used to optimize and automate different processes around levee management. Main advantages of automated engineering are:

- Legal management to the issue of space reservation around the levee by performing detailed stability analyses to define the different protection zones on a higher detail level.
- Transparent decisions based on comparable results and a transparent workflow and processes. It is easy to follow the different schematization steps (in the basic no engineering judgments).
- Efficient use of the feasible data (more calculations are performed). Different processes use the same databases. This prevents the use of outdated data.
- Due to the modular configuration of DAM it is quite easy to hook up other models to DAM or other guidelines. This makes the system suitable to use in different countries with different models and procedures.

REFERENCES

Knoeff, J. G., E.W. Vastenburg and E. Tromp, 2008. Rational Risk assessment of Dikes by using a stochastic subsurface model.
14th International Symposium on Flood Defence, Toronto, Ontario, Canada.
Koelewijn, A.R. & W.A. Hounjet, 2007. Space reservation required for flood embankments in urban areas. Proc. 14th European Conference on Soil Mechanics and Geotechnical Engineering Madrid, September, pp. 845-849. Rotterdam, Millpress.
Delta commissie, 2008. Samen werken met water – Een land dat leeft, bouwt aan zijn toekomst. Hollandia Printing, The Netherlands.
Woldringh, B; Knoeff, J.G., 2009. American and Dutch levee evaluations, Deep Foundation instistute Journal volume 3, 2009.

[2] The Waterboard is a public organization in The Netherlands responsible for levee management.

ISGSR 2011 - Vogt, Schuppener, Straub & Bräu (eds) - © 2011 Bundesanstalt für Wasserbau ISBN 978-3-939230-01-4

Assessment of Levee Breaching Risks to the Pearl River Delta

L. Zhang
Hong Kong University of Science and Technology, Clear Water Bay, Hong Kong, China

Y. Xu
China Institute of Water Resources and Hydropower Research, Beijing, China; Hong Kong University of Science and Technology, Clear Water Bay, Hong Kong, China

Y. Liu
Hong Kong University of Science and Technology, Clear Water Bay, Hong Kong, China

ABSTRACT: A levee system poses enormous risks to the safety of people protected by the system. Levee risk analysis is at the heart of levee risk mitigation and engineering decision making. An explicit methodology of levee risk analysis is desirable. In this paper, a case study on the risks of the North Pearl River Levee System (NPRLS) in Guangdong Province, China, is conducted to illustrate an explicit procedure of levee risk analysis. Data required for risk analysis is first collected and analyzed. The performance of the levee upon a 100-year flood at milestone 7+330 is evaluated. The failure probabilities are evaluated for three failure modes: overtopping, piping and slope sliding. The flood scenario resulted from a levee breach at water level 15.53m (100-year flood) is simulated. The loss of life is estimated following the risk analysis procedure and based on fatality rates suggested by the authors. Possible measures to mitigate the risks of the levee are also proposed in the paper.

Keywords: risk analysis, North Pearl River Levee System, levee breach

1 INTRODUCTION

Originating from the Damaokeng Mountain in Xinfeng County, Jiangxi Province, the North Pearl River is one of the main tributaries of the Pearl River. The North Pearl River enters the Pearl Delta after merging with the West Pearl River at Sixianjiao. The entire North Pearl River is 468 km long with a catchment area of 46,700 km^2.

The North Pearl River Levee System (NPRLS) starts from Shijiao Town and ends at Shishan Town. The location of the levee system is shown in Fig. 1(a). NPRLS is the main flood control system for the Pearl Delta, protecting three large cities with a population of over 10 million. One of them is Guangzhou, the capital city of Guangdong Province. Topographically the protected area is higher in the northwest and lower in the southeast. As shown in Fig. 1(b), there are essentially no natural barriers in the area so the consequence of any levee breach can be catastrophic. Although there are some dikes inside the flood plain, they are for controlling floods generated within the flood plain rather for guarding against possible levee-breaching floods.

Some levees along the North Pearl River were constructed 1600 years ago. In 1954, an embryo levee system was constructed. This system was heightened and strengthened from 1983 to 1987, which significantly raised the flood control standard. As of this time, the levee system is 63.34 km in length. It has been experiencing another comprehensive improvement since 2005. As the construction work is still going on, the data used in this paper refers to that before the improvement work.

The Pearl River Delta was threatened several times by floods from the North Pearl River. In 1915, the region bounded by the North Pearl River was subjected to an extraordinary flood of 200-year frequency as a result of levee breaches. During that disastrous event, most parts of Guangzhou, Qingyuan, and Foshan were inundated; over 100 thousand people lost their lives or were injured. Levee breaches also took place in 1931, 1949 and 1982. Dangerous situations caused by extreme river floods occurred from time to time: in 1968, 1976, 1994, 2005 and 2006. A well-known case was the June 1994 flood, which was slightly smaller than a 100-year flood. Although the NPRLS survived the flood, dangerous conditions occurred in over forty places.

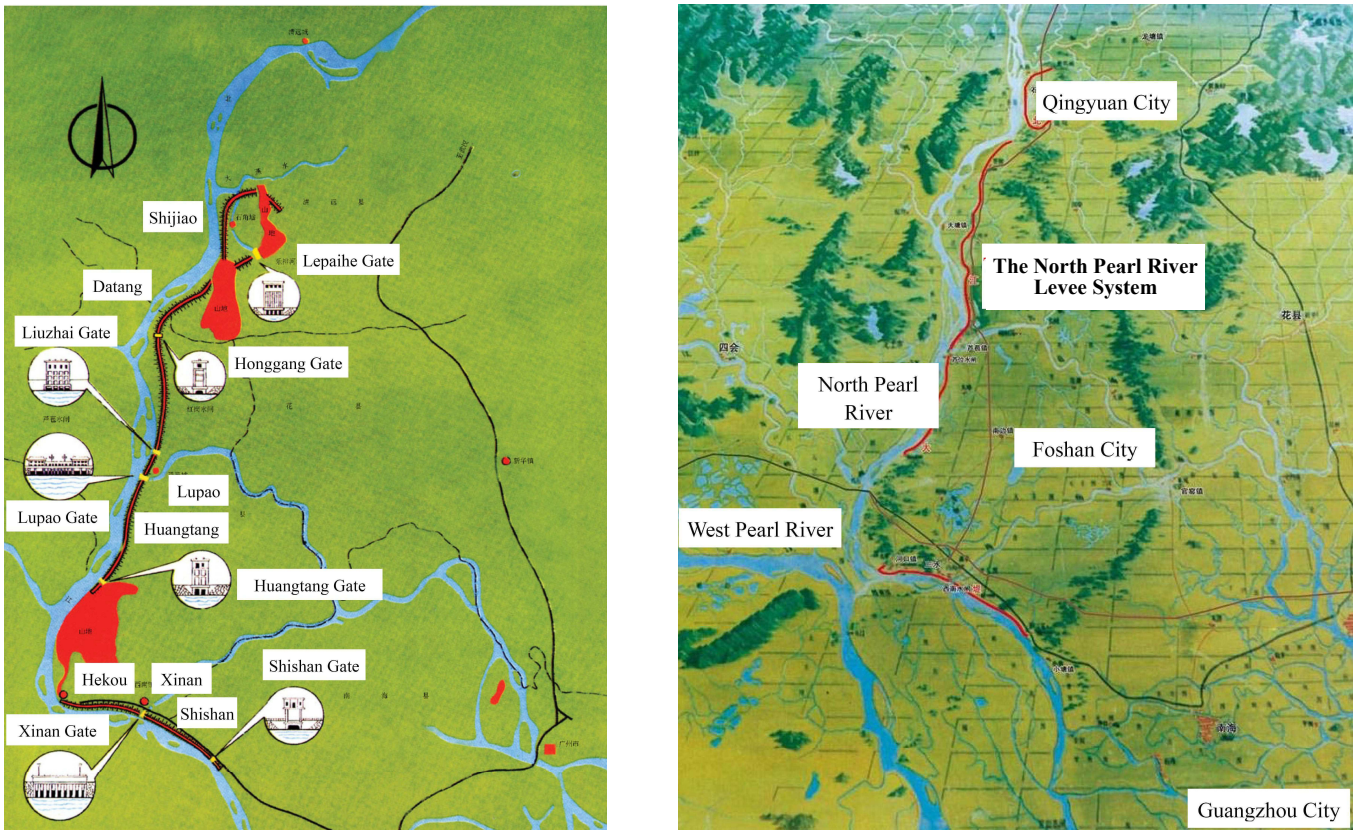

Figure 1. (a) Location of the North Pearl River Levee system; (b) Topographic condition of the flood plain.

Is the NPRLS safe enough to withstand a 100-year flood? What will be the consequence if the levee breaks? This paper attempts to answer these questions through an explicit risk analysis. In this paper, a detailed case study on the risks of the NPRLS upon a 100-year flood is conducted. Based on the risk analysis, possible measures to mitigate the risks of the levee are also proposed.

2 LEVEE FAILURE ANALYSIS

2.1 Hazards Identification and Failure Modes

Located at the beginning of the NPRLS, the Shijiao segment is investigated in this case study. Part of the segment is located on high permeability sand and is one of the most dangerous parts of the levee system. A typical cross section at Milestone 7+330 is chosen to represent this part, as shown in Fig. 2. Most part of the foundation is quaternary alluvium. The thickness of the pervious foundation, which is comprised of fine sand, coarse sand and gravel, is over 30 m.

The study area has very low seismicity. River floods are considered as the main source of natural hazard. In this study, the 100-year flood is chosen as the initiation event for risk analysis. Chou et al. (1999) conducted hydrological calculations. A flood hydrograph was obtained by referring to the 1915 flood and magnifying the 1994 flood to designated design peak discharge and flood volume. The corresponding relations between water elevation and time are shown in Fig. 3. Since the warning water level for the Shijiao segment is 10 m, the input hydrograph in the quantitative risk analysis begins at water level 10 m and assumed to stay at 10 m after the flood fades (Fig. 3(b)).

Based on the geologic conditions and historical performance, it is found that the NPRLS may have three possible failure modes: overtopping, piping in the foundation, slope instability, and bank erosion. The pervious foundation makes piping the main failure mechanism. Dangerous situations induced by this mechanism occurred many times in the past. Except for piping induced in the highly permeable foundation materials, slope instability due to the presence of clay layers is also a problem. The safety of the levee will be threatened if excessive settlement occurs as a result of the lack of bearing capacity or slope failures at sections where the clay layers have low shear strength. In addition, high velocity flows will erode the material at the toe of the levee and induce bank collapses. For the Shijiao segment studied in this case, bank erosion was not serious in the history. Therefore, only failures from overtopping, piping and slope instability are considered in the quantitative risk analysis.

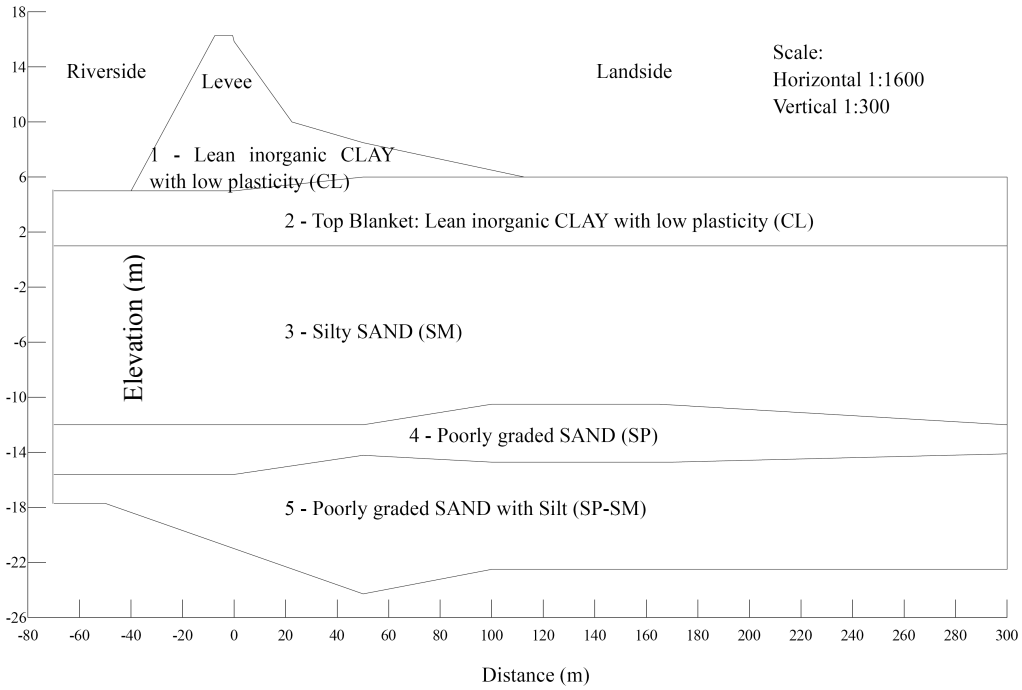

Figure 2. Typical cross section of the NPRLS at Shijiao.

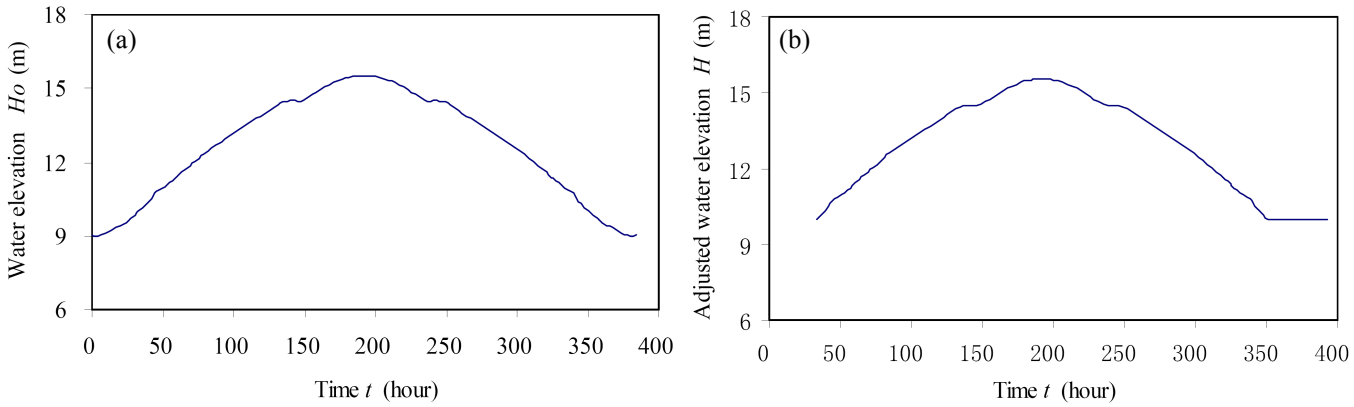

Figure 3. 100-year return flood for the North Pearl River: (a) Water level vs. time; (b) Adjusted water level vs. time.

2.2 Overtopping

Overtopping occurs when the water level exceeds the crest elevation of the levee. The elevation of the crest is 16.30 m and the peak water level of a 100-year flood is 15.53 m. The longitudinal flood wave and tide wave have already been taken into consideration. The 100-year return river flood level is lower than the elevation of the crest, hence overtopping is not a concern as long as the levee does not fail or settle excessively.

2.3 Piping in Foundation and Levee Body

Levee and subsoil profiles have been constructed based on borehole logs (Lin and Gu 2005). As shown in Fig. 2, the clayey levee is underlain by a layer of clay deposits, and these clay deposits sometimes contain sections of ancient levees. The top clay layer provides an impervious blanket at the top of the underlying sandy layers. The soil names in Fig. 2 are based on the soil classification system in ASTM D2488.

The soil properties are summarized in Table 1. Five random variables in Table 2 are defined for probabilistic analysis. The standard deviations of saturated permeability are given based on the original test data, with adjustments referring to reported data in the literature (e.g. Wolff 2008). In this study, the soils are assumed to be isotropic in terms of permeability.

Both steady-state and transient seepage analyses were conducted using SEEP/W. It is found that the maximum hydraulic gradient, i_{max}, from the transient analysis is larger than that from the steady-state analysis at the ending stage due to the slow dissipation of pore-water pressures in the levee. It also reveals

that a steady state of seepage cannot be reached within a 15-day flood period. Therefore, a transient analysis is considered more reasonable for simulating a real flood effect. Typical results of transient seepage analysis are shown in Fig. 4.

Table 1. Expected values of soil properties

Soil layer	Natural density (g/cm^3)	Water content	Specific gravity	Dry density (g/cm^3)	Void ratio	Cohesion (kPa)	Friction angle / angle of repose (°)	Saturated permeability (m/s)
1	1.89	0.227	2.69	1.54	0.747	13.2	23.6	2.0×10^{-6}
2	1.90	0.319	2.67	1.44	0.854	15.2	10.5	2.3×10^{-7}
3	1.86	0.265	2.66	1.47	0.872	5.0	35.0	1.7×10^{-5}
4	1.91	0.326	2.70	1.43	0.875	-	/30.5	2.2×10^{-3}
5	1.95	0.283	2.65	1.51	0.743	-	/33.7	3.25×10^{-4}

Table 2. Five random variables for seepage analysis

Parameter	Expected value	Standard deviation	C.O.V.
Thickness of the top blanket (Soil 2), z	5 m	1 m	0.2
Saturated permeability of levee clay (Soil 1), K_1	2.0×10^{-6} m/s	1.6×10^{-6} m/s	0.8
Saturated permeability of the top blanket (Soil 2), K_b	2.3×10^{-7} m/s	1.8×10^{-7} m/s	0.78
Saturated permeability of silty sand (Soil 3), K_{SM}	1.7×10^{-5} m/s	1.0×10^{-5} m/s	0.59
Saturated permeability of sand (Soil 4), K_{SP}	2.2×10^{-3} m/s	1.0×10^{-3} m/s	0.45

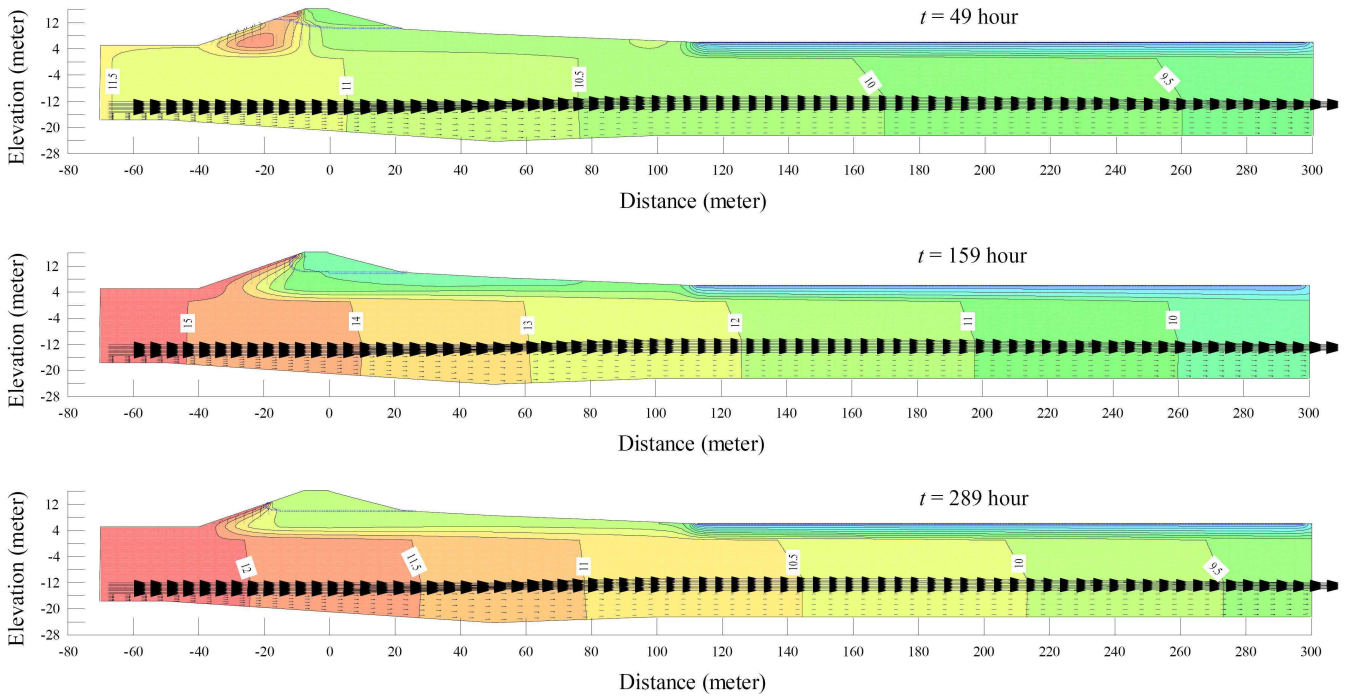

Figure 4. Typical results of transient seepage analysis.

Taylor's series finite-different method was used to calculate the probability of piping failure (Liu 2009). Eleven runs of SEEP/W were conducted. In addition to the first run using the expected values of the variables, ten more runs were conducted to determine the variance component of each random variable. For instance, the thickness of the top blanket is adjusted to the expected value plus or minus one standard deviation, while the other random variables remain at their expected values. A similar calculation is performed to determine the variance components contributed by the other four random variables. By comparing the magnitudes of the variance components (See Table 3), it is found that virtually most of the uncertainty is in the top blanket thickness. A similar result was found in under-seepage analysis of dikes along the Upper Mississippi River (Shannon Wilson Inc. 1994). This implies that when designing levees against under-seepage failure, effort must be made to obtain sufficient data to define the blanket.

When the variance components are summed, the total variance of the exit hydraulic gradient is obtained as 0.041. Taking the square root of the variance gives the standard deviation of 0.20. The exit gradient is assumed to be a lognormally distributed (Mean=1.19, Sta. Dev.=0.20). The critical exit gradient

is also assumed to be a random variable following a lognormal distribution (Mean=0.9, Sta. Dev.=0.18). Therefore, the conditional probability of piping failure in the foundation at water level 15.53 m is P_p (H =15.53m) = P(lni - lni_c > 0) = 0.86. Repeating this procedure for a range of flood water levels, the conditional probability of piping failure in the foundation is plotted in Fig. 5. As expected, the maximum probability of failure is at the peak water level. It means the levee is in the most dangerous situation against piping failure when the flood water elevation is the highest.

Table 3. Variance components of five random variables

	z	K_1	K_b	K_{SM}	K_{SP}	Total
Variance component	0.04	0	0.0009	0.00016	0.00031	0.04137

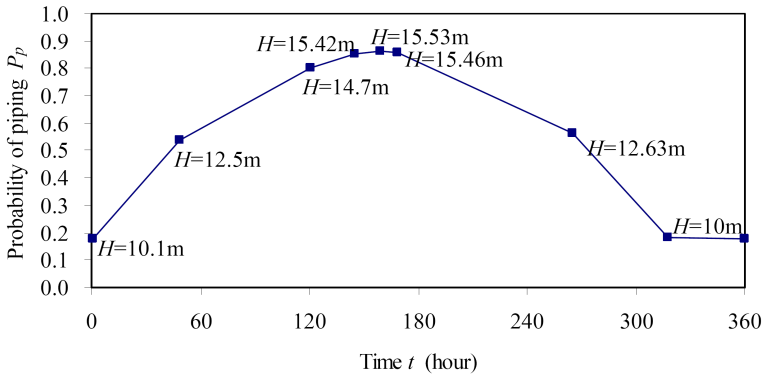

Figure 5. Conditional probability of piping failure in the foundation.

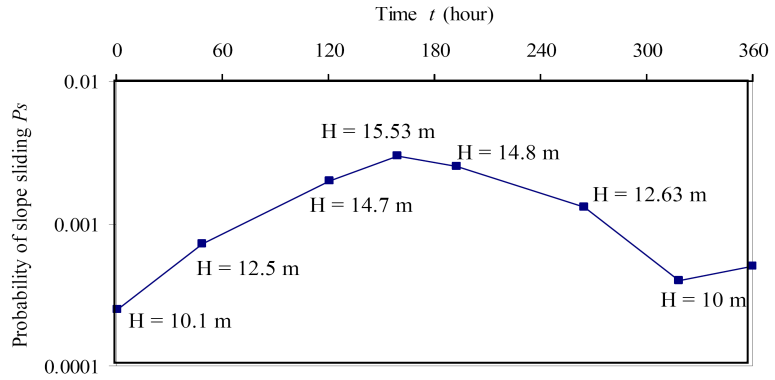

Figure 6. Conditional probability of slope failure.

2.4 Slope Instability

Slope stability analyses were conducted using SLOPE/W. The profile of the cross-section is shown in Fig. 2 and the shear strength properties are listed in Table 4. Besides the five random variables in seepage analysis, four additional random variables are involved in instability analysis, with their first and second moment values defined based on field exploration data. The coefficients of variation for the variables are comparable to those summarized by Wolff (2008). In preliminary analysis, the possible slope movement from right to left (Fig. 2) has been analyzed when the water level draws down. With the support of the static water pressure provided by the river water, the factor of safety (Fs) for the left-to-right movement is very high. Thus only the sliding failure mode from left to right is considered in detail.

Table 4. Four additional random variables for instability analysis

Parameter	Expected value	Standard deviation	C.O.V.
Cohesion of levee clay (Soil 1), C_1	13.2 kPa	8.5 kPa	0.640
Friction angle for levee clay (Soil 1), Φ_1	23.6°	2°	0.085
Cohesion of top blanket clay (Soil 2), C_b	15.2 kPa	6.5 kPa	0.428
Friction angle for top blanket clay (Soil 2), Φ_b	10.5°	3°	0.286

Again Taylor's series finite-difference method was adopted to calculate the probability of slope instability with the aid of SLOPE/W. It is found that most of the uncertainty is in the shear strength parameters; and the total variance of Fs is 0.128. The factor of safety is assumed to be a lognormally distributed ran-

dom variable (Mean = 1.768, Sta. Dev.=0.357). Thus the conditional probability of slope failure at water level 15.53 m is P_s (H =15.53m) = P(lnFs < 0) = 0.003. The variation of probability of slope failure with river water level is shown in Fig. 6. The probability of slope failure is also the highest when the water level is at its maximum. The probability of slope failure is the lowest when the water level just retreats to the lowest level.

2.5 Summary of Failure Modes

Piping in the foundation is found to be the dominant failure mode (P_p=0.86), which agrees with the historical records. Compared with piping, slope sliding is less likely (P_s=0.003). It should be pointed out that the failure modes only represent the initiating event. How the failure process evolves from the initial event to the final breaching is not the focus of this study.

3 FLOOD ROUTING ANALYSIS

A levee breach is assumed to occur at Milestone 7+330. Levee overtopping and breaching is analyzed in HEC-RAS (USACE 2008) by modeling the levee as a lateral structure. Levees can be connected to storage areas or another river reach. If the water going over or through the levee will pond, then a storage area is appropriate for modeling the area behind the levee. Here flood routing in the area behind the levee is concerned, thus it is appropriate to model the area as a separate river reach. An integrated flood routing analysis of a levee breach consists of three steps: one-dimensional unsteady flow analysis in the main river (i.e., the North Pearl River), levee breaching analysis, and one-dimensional unsteady flow analysis in the flood plain that is also assumed to be a river.

The inundation map and flood severity caused by the levee breach at water level 15.53 m are illustrated in Fig. 7. Details of the flooding routing analysis are available in Liu (2009).

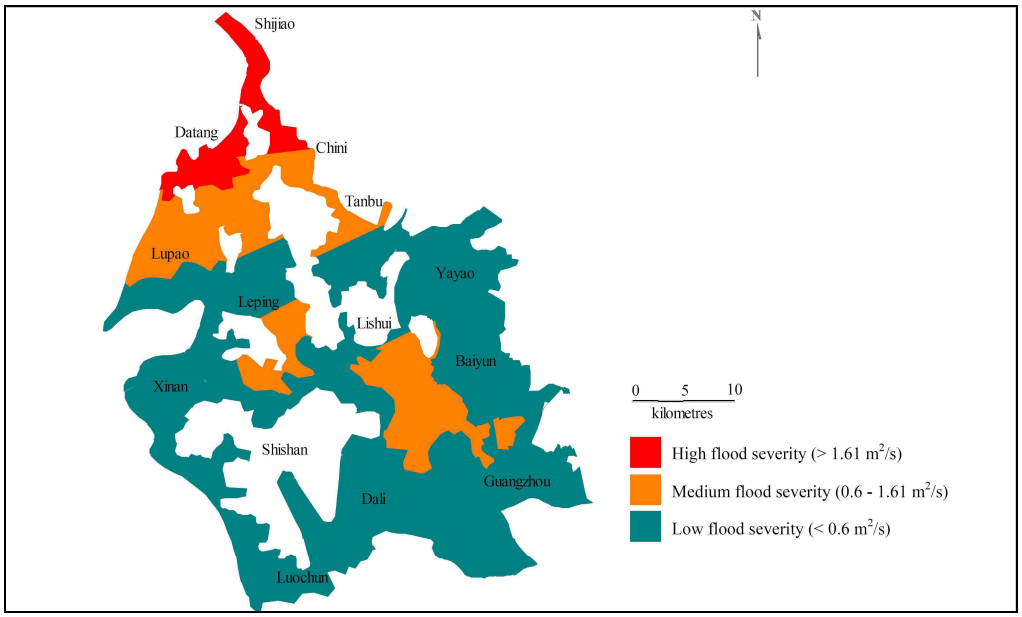

Figure 7. Flood severities of inundation, breach at water level 15.53 m.

4 ESTIMATION OF LOSS OF LIFE

The potential loss of life is often expressed as:

$$\text{Potential loss of life} = \text{Fatality rate} \times \text{Population at risk} \quad (1)$$

The population at risk (PAR) is estimated based on the inundation map generated by the flood routing analysis reported earlier and the statistics of registered population in 2006 (Yang et al. 2006). The administrative regions are divided into sub-regions, as small as possible whenever data is available. The population is assumed to be evenly distributed in each sub-region. The information of population distribution and inundation is well combined and displayed in MapInfo. Figure 8 shows a typical view of inundated

population distribution resulted by a levee breach at water level 15.53 m. During this flood, 23 sub-regions are influenced. The PAR of each sub-region is equal to the product of the population density and the inundation area. Finally, the exposed population for each flood scenario is summed up. All the people in the inundation zone are taken as the population at risk.

To estimate the vulnerability, four influence factors are investigated: warning time, flood severity understanding, flood severity and evacuation efficiency. Graham's model (1999) is applied to each sub-region to estimate the potential loss of lives. The model is refined with flood severity degree defined by Abt et al. (1989) and an evacuation model by van Zuilekom et al. (2005). Recommended fatality rates are presented in Table 5.

Based on the PAR values and fatality rates, the total losses of life are estimated for the case when no warning is issued (Loss of life = 4267) and the case when warning is issued (Loss of life = 3029) before the levee breaks. It is found that 29% of loss can be avoided if a warning is issued before the breach so a warning system is essential for the zones near the breach.

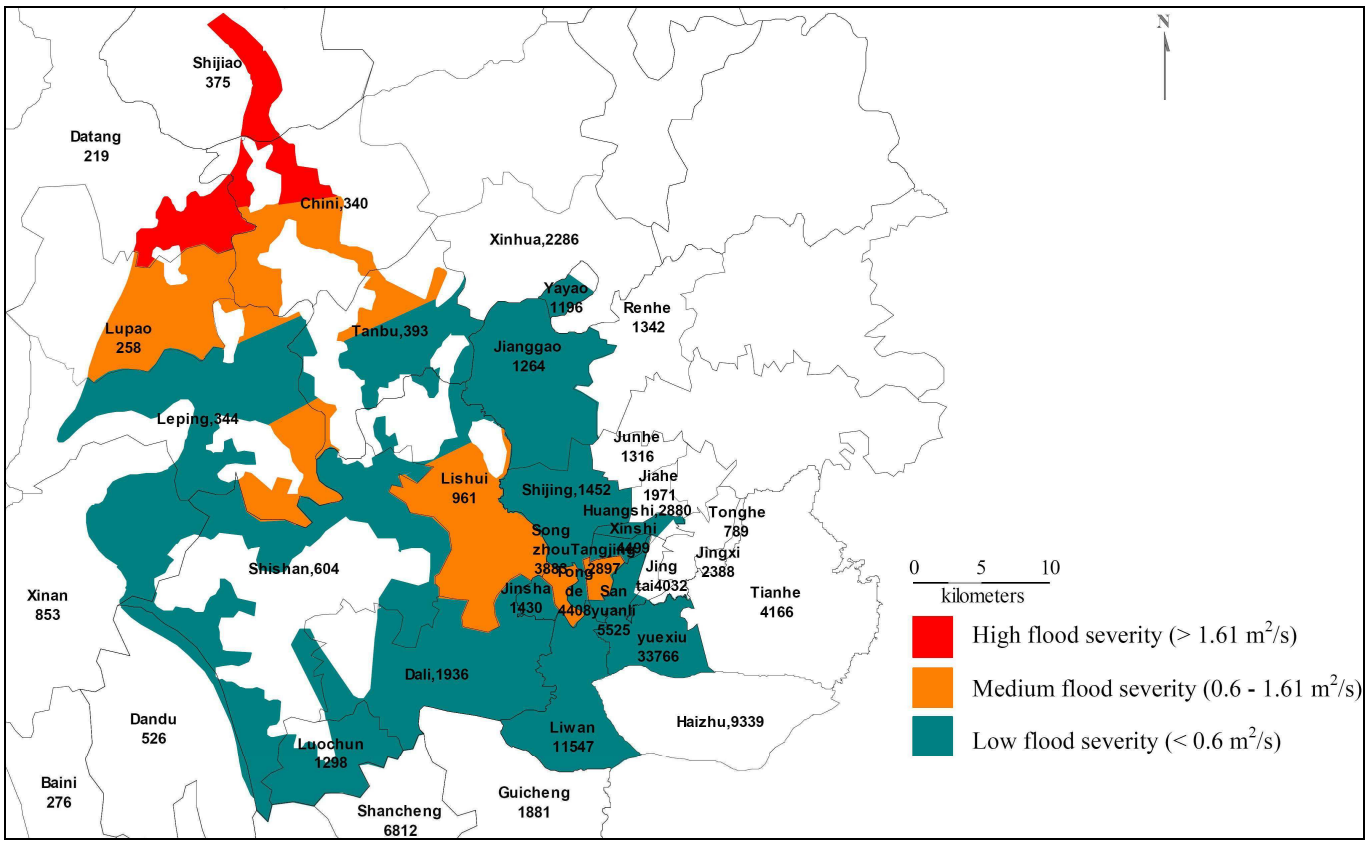

Figure 8. Population density in the inundation zone, breach at water level 15.53 m.

Table 5. Recommended fatality rates for levee failure in this study

Flood severity	Warning (minutes)	Flood severity understanding	Fatality rate
High	No warning	Not applicable	0.3
	15-60	Vague	0.27
		Precise	0.12
	>60	Vague	0.24
		Precise	0.06
Medium	No warning	Not applicable	0.03
	15-60	Vague	0.01
		Precise	0.005
	>60	Vague	0.005
		Precise	0.002
Low	No warning	Not applicable	0.005
	15-60	Vague	0.0007
		Precise	0.0004
	>60	Vague	0.0003
		Precise	0.0001

5 RISK EVALUATION

Risk is defined as

$$\text{Risk} = \text{hazard probability} \times \text{fatality rate} \times \text{population at risk} \quad (2)$$

Risk can be integrated into a systematic layout through a scenario tree. The effect of emergency actions and measures can be efficiently analyzed using the scenario tree. Figure 9 shows a flood scenario tree for the NPRLS at water level 15.53 m. Three failure mechanisms, i.e. overtopping, piping and slope sliding, are assumed to be mutually exclusive. The risk of the NPRLS against a 100-year flood is quantified in terms of total fatality, which is 270.

As indicated in the scenario tree, three aspects of measures can be taken to mitigate the risk: stabilizing the levee system, improving the emergency actions and decreasing the loss of life. In this case study, the levee is rather stable against sliding. Improving the slope stability will not effectively mitigate the risk. Instead, engineering measures should focus on decreasing the probability of foundation piping, such as installing relief wells and constructing a continuous concrete cutoff wall. Non-engineering measures such as developing an effective warning system is also highly recommended.

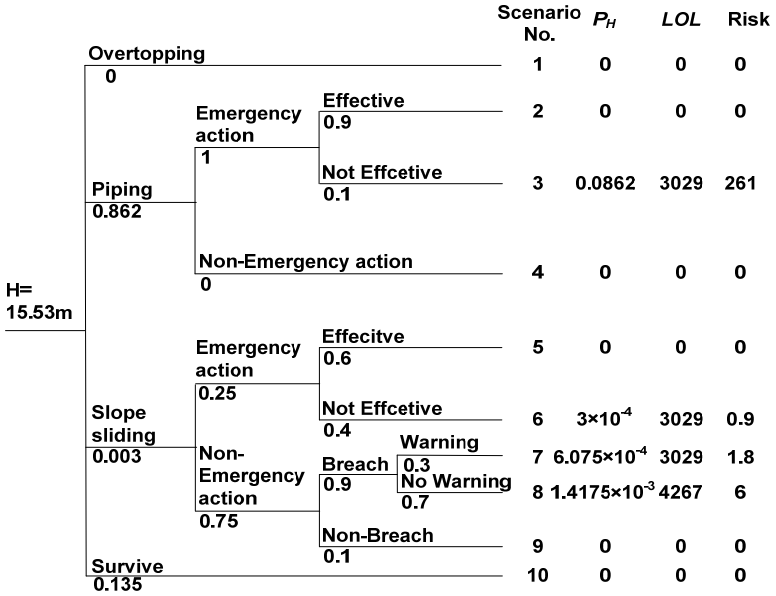

Figure 9. Scenario tree for risk assessment of the NPRLS upon water level 15.53 m.

6 SUMMARY

In this paper, a case study on the risk of the North Pearl River Levee System upon a 100-year flood is conducted following an explicit risk analysis procedure. In the Shijiao segment, piping in the foundation is found to be the dominant failure mode. Based on the estimates of probabilities of failure of piping and sliding, and loss of life, the risk of the levee is finally quantified in terms of fatality and presented in a scenario tree. Both engineering and non-engineering measures are suggested to mitigate the hazard and reduce the loss of life.

ACKNOWLEDGEMENT

The work reported was substantially supported by the Research Grants Council of the Hong Kong SAR (No. 622207).

REFERENCES

Abt S. R., Wittler R. J., Taylor A., & Love D. J. 1989. Human stability in a high flood hazard zone. Water Resources Bulletin, 25(4), 881-890.

Chou, J. W., Lu, J. K., Li, N. & Chen, H. 1999. The development of flood simulation model in flood risk information management system in Beijiang area. Journal of Catastrophology, 14(4), 17-21 (in Chinese).

Graham, W. J. 1999. A procedure for estimating loss of life caused by dam failure. Publication No. DSO-99-06, U.S. Bureau of Reclamation, Denver.
Lin. Z. & Gu, X. M. 2005. Comments on the piping problem in Shijiao segment of the North River levee system. Guangdong Water Resources and Hydropower, 5, 17-21 (in Chinese).
Liu, Y. 2009. An explicit risk-based approach for large-levee safety decisions. MPhil thesis, The Hong Kong University of Science and Technology, Hong Kong.
Shannon Wilson, Inc. & Wolff, T. F. 1994. Probability models for geotechnical aspects of navigation structures. Report to the St. Louis District, U.S. Army Corps of Engineers.
USACE 2008. Hydraulic reference manual of HEC-RAS. Hydrologic Engineering Center, U.S. Army Corps of Engineers.
Van Zuilekom, K., van Maarseveen, M., & van der Doef, M. 2005. A decision support system for preventive evacuation of people. Geo-information for Disaster Management, 229-253, Spring Berlin Heidelberg, Germany.
Wolff, T. F. 2008. Reliability of levee systems. In Kok-Kwang Phoon: Reliability-based design in geotechnical engineering, Chapter 12, 448-496. Taylor & Francis, London and New York.
Yang, H. W., Luo, Z. Q. & Tang, G. Z. 2006. Administration map of Guangdong Province. Cartographic Publishing House of Guangdong, Guangzhou, China.

6 Practical Applications and Case Studies

ISGSR 2011 - Vogt, Schuppener, Straub & Bräu (eds) - © 2011 Bundesanstalt für Wasserbau ISBN 978-3-939230-01-4

Dewatering Design for the Excavation of a Ship Lock Under Uncertainty from Karst-Conduit Dominated Groundwater Flow

H. Montenegro
BAW Federal Waterways Engineering and Research Institute, Karlsruhe, Germany

U. Hekel
HPC HARRESS PICKEL CONSULT AG Rottenburg am Neckar, Germany

ABSTRACT: The presence of Karst-conduits at the ship lock excavation site in Bolzum led to highly uncertain predictions of the groundwater inflows and drawdown evolution during dewatering of the pit. To asses the impact of the Karst-conduit-system on the dewatering operations at the relevant scale pumping test was carried out. These conditions demanded for the Observational Method Approach in which the drawdown is constantly recorded during dewatering and continuously interpreted by a transient groundwater model. Injection-schemes outside the pit were developed which allowed limiting a critical drawdown beneath a near by built-up area. The integrated approach of dewatering, iterative updating of the groundwater model according to observed drawdown and inflow along with previously established contingency actions led to a robust excavation pit without compromising safety.

Keywords: Excavation, groundwater lowering, dewatering, draw down, risk management, Karst

1 INTRODUCTION

The ship lock at Bolzum, located at the entrance of the Hildesheim Canal, covers a difference in height of 8 m between the Mittelland Canal and the adjoined Hildesheim Canal. To allow more economic freight traffic, a new lock (length/width/maximum loaded draught: 139 m, 12.50 m, 2.80 m) has been planned in the area southwest of the original lock (Figure 1).

Figure 1. Construction site of the new ship lock in Bolzum

2 HYDROGEOLOGICAL SETTINGS

The Bolzum lock lies at the eastern edge of the salt structure Lehrte – Sehnde – Sarstedt where a diapir has formed close to Bolzum. The rising of the salt dome has tilted the originally horizontal Mesozoic strata (Buntsandstein to Cretaceous strata), exerted tectonic stress on the bedrock strata and generated numerous fractures. Perpendicular to these fractures, faults have developed as well. Figure 2 depicts the geological structure below the sediments that has been influenced by the rising salt dome. Groundwater observation points, installed during the ground exploration campaign, as well as the location of sink-holes are depicted, too. The construction site of the new lock is located in an area of outcropping Middle Muschelkalk (mm) and Lower Muschelkalk (mu). Sinkholes are a common phenomenon in the area. They develop through dissolution processes in the gypsum layers of the Middle Muschelkalk stratum. The location of the mapped sinkholes in the strike of these strata is remarkable.

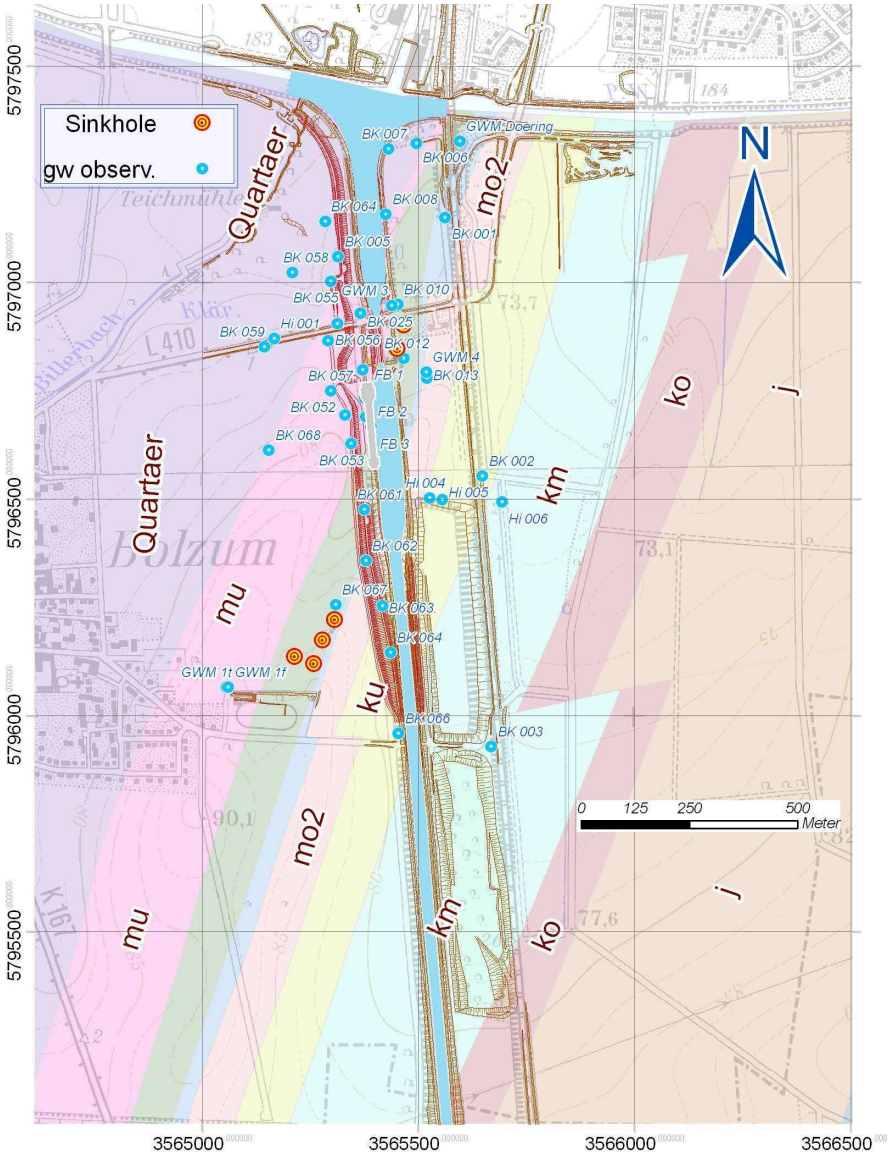

Figure 2. Location of geological units (mu: Lower Muschelkalk (Shell Limestone), mo: Upper Muschelkalk (Shell Limestone), ku: Lower Keuper, ko: Upper Keuper), of the excavation site (gray), of the groundwater monitoring (GWM) system and of known sinkholes.

2.1 *Local Karstification and Preferential Flow Paths*

The majority of the Middle Muschelkalk layers contain gypsum are carbonates. Due to their structure and chemical properties, their joint permeability is high and can be even increased through local karstification. The gypsum-containing layers of the Röt (uppermost Buntsandstein; below the Middle Muschelkalk layer, not depicted in Figure 2) consist mostly of weak fine sandy clay/silt and can be classified as having a very low hydraulic conductivity. However, depending on their degree of jointing, their conductivity can

also be moderate to low. Due to its high content of clay mineral, the conductivity of Keuper, similarly to Buntsandstein, is to be estimated as very low.

In the course the ground exploration water pressure tests were conducted in different geological units. The measured water injection rate depended on whether there was a conduit in the section of the boring where a packer had been placed. As expected, significantly varying rates of water injection were measured indicating large spatial variability of the hydraulic permeability. As illustrated above, it could be assumed that due to tectonic stress and dissolution processes, preferential flow paths had developed as Karst conduits in the bedrock which are significantly more permeable than the surrounding rock matrix.

3 GROUNDWATER MONITORING SYSTEM

Most groundwater observation points (see Figure 2) are equipped with data loggers that transmit the measured groundwater levels which then can be accessed online. Several groundwater hydrographs could only be interpreted through the existence of a Karst conduit system. If such permeable conduits/fractures are cut across during excavation, it can be expected that they will function as drainage. Thus, water will flow to the cut and the water pressure within the Karst conduit can be released at a large scale. It could be assumed that the system would be oriented in concordance with the NE – SW orientation of the Triassic strata however ground exploration did not reveal any direction. If there was an orientation in the conduits system directional dependence in their permeability properties (anisotropy) can be expected at a large scale. Most probable, this will influence the shape of the drawdown which will develop due to dewatering the pit. It soon became clear that even a more dense net of exploration borings would give no better clues on the orientation of the Karst conduit system. These hydraulic effects were therefore examined through large-scale aquifer testing.

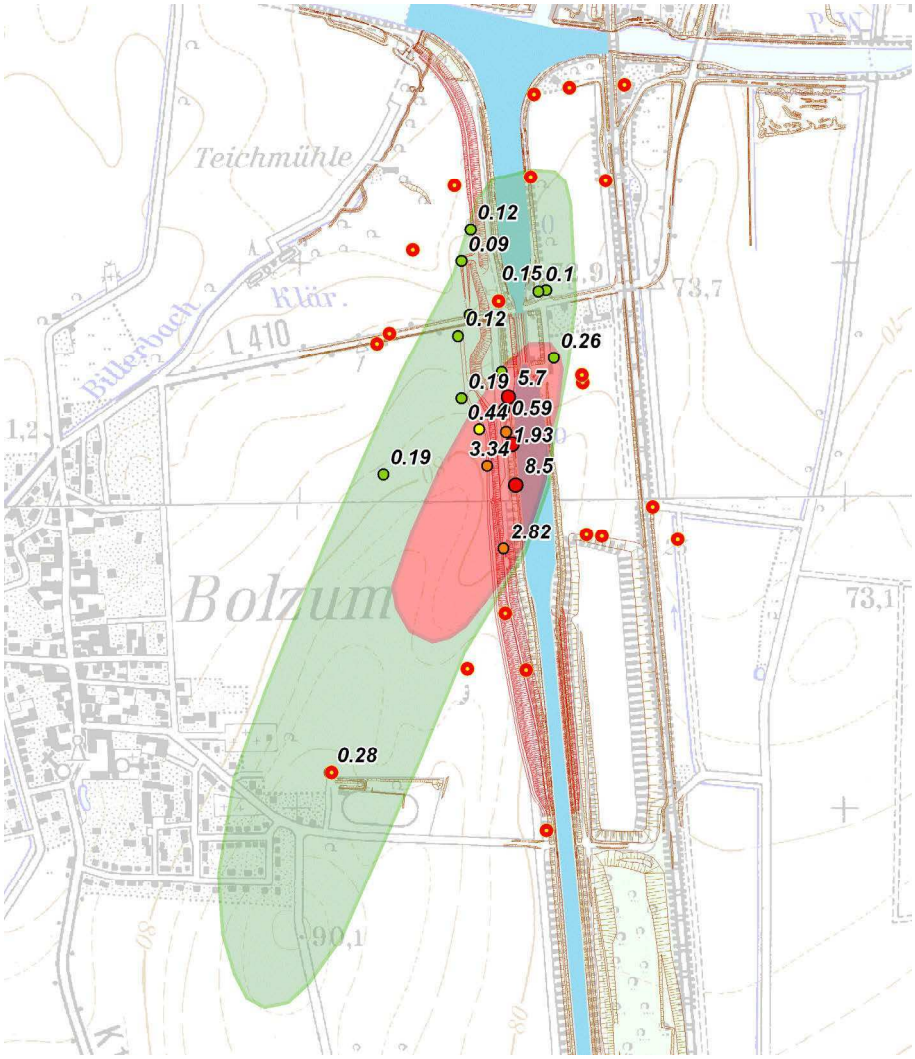

Figure 3. Observed drawdown [m] 7 days of pumping. Circles without label: insignificant lowering.

4 DETERMINING ACTIVE AQUIFER PROPERTIES THROUGH HYDRAULIC TESTS

Considering the complexity of the ground, the extent of the groundwater inflows to the pit and the range of groundwater drawdown can only be examined on a spatial and temporal scale relevant to the preferential flow paths. A pumping test was therefore conducted on the planned excavation site. Three extraction wells were installed to help lower the groundwater level up to 17 m (target level during the excavation 56 m a.s.l.) for a longer period of time. Three extraction wells with a bore diameter of 500 mm and a DN 300 delivery pipe of were installed in the area of the excavation site at intervals of 80 m. The well filter was placed in a section of approx. 16 m – 28 m below the ground surface. The actual aquifer test was conducted from January to February 2007. To allow the matching of the individual observation wells with the individual extraction wells, the latter were put into operation with time lags one after the other. Figure 3 shows the observed drawdown as a reaction to the pumping after 7 days.

The observed drawdown can be classified by ellipsis-shaped areas with a certain lowering range each (inner ellipsis: lowering rate larger than 0.25 m; outer ellipsis: lowering rate larger than 0.10 m). Comparing the orientation of the ellipses with the geological overview illustrated in Figure 2, an agreement in the spatial structure of the geological features and the drawdown induced by the pumping test is evident. The proximity of the observation wells which showed hardly any reaction to the pumping (symbols without labels) to the extraction wells is remarkable. The aquifer test displayed a system of conduits with relatively high permeability along the Muschelkalk layer that is surrounded at the sides by layers of low permeability. In such a system, dewatering of the pit will lead to a distorted ellipsis-shaped drawdown cone similar to that observed during the pumping test. The degree of distortion depends on the permeability contrast between the conduit and the surrounding sealing structures.

Later, the drawdown and recovery observed in individual observation points during the aquifer test were evaluated according to the type curve method, which yielded estimates for transmissivity and storage properties. It could be concluded that the aquifer conditions in the examined area are generally unconfined. Furthermore, hydraulic boundaries (Dirichlet boundaries) and impermeable boundaries could be identified. The determined storage and permeability properties allowed a first estimation of the expected inflow to the excavation pit (>200 m^3/h). They also gave hints on the hydrogeological structure to be represented in a groundwater model.

5 GROUNDWATER MODEL

To predict the spatial and temporal drawdown patterns a transient groundwater model is required. As the details of the geological structures could not be considered in all its complexity, the modeling of the geological structure was limited to a horizontal plane representation disregarding the tilted strata. As the aquifer test determined a radius of influence of around 30 m, a corresponding aquifer thickness was assumed. The aquifer basis was therefore significantly below the planned lowering level. The model features approx. 18,000 elements with a discretisation width ranging from 300 m to 3 m. Figure 4 depicts a detail of the FE mesh as well as the zones for which hydraulic parameters had been estimated from the aquifer test.

The most relevant boundary conditions were determined, besides groundwater recharge, based on the head of the Mittelland Canal (receiving water), the leakage boundary conditions of the Hildesheim Canal and the Billerbach that cuts across the quaternary aquifer. To estimate smaller flux boundaries, the surface catchment areas were taken as a reference (area of the Innerste and Leine rivers). The hydrogeological array of a preferential flow zone (Muschelkalk) bounded by slices of lesser permeability was an essential characteristic. The latter consist of the gypsum-containing Middle Muschelkalk layers in the east, and of a hydraulic barrier in the west which is probably the result of the infilling of the subrosion depression.

At first, a steady groundwater model was calibrated based on the median of the hydrographs in each of the numerous observation points. The pumping test, which revealed the reaction of the aquifer to pumping at a large scale, allowed a transient model calibration. Despite a substantial simplification the geological structures in the course of model validation the aquifer reactions to the pumping test could be reproduced in quite a fair fashion in 2/3 of the observation points and with plausible quality in the remainder.

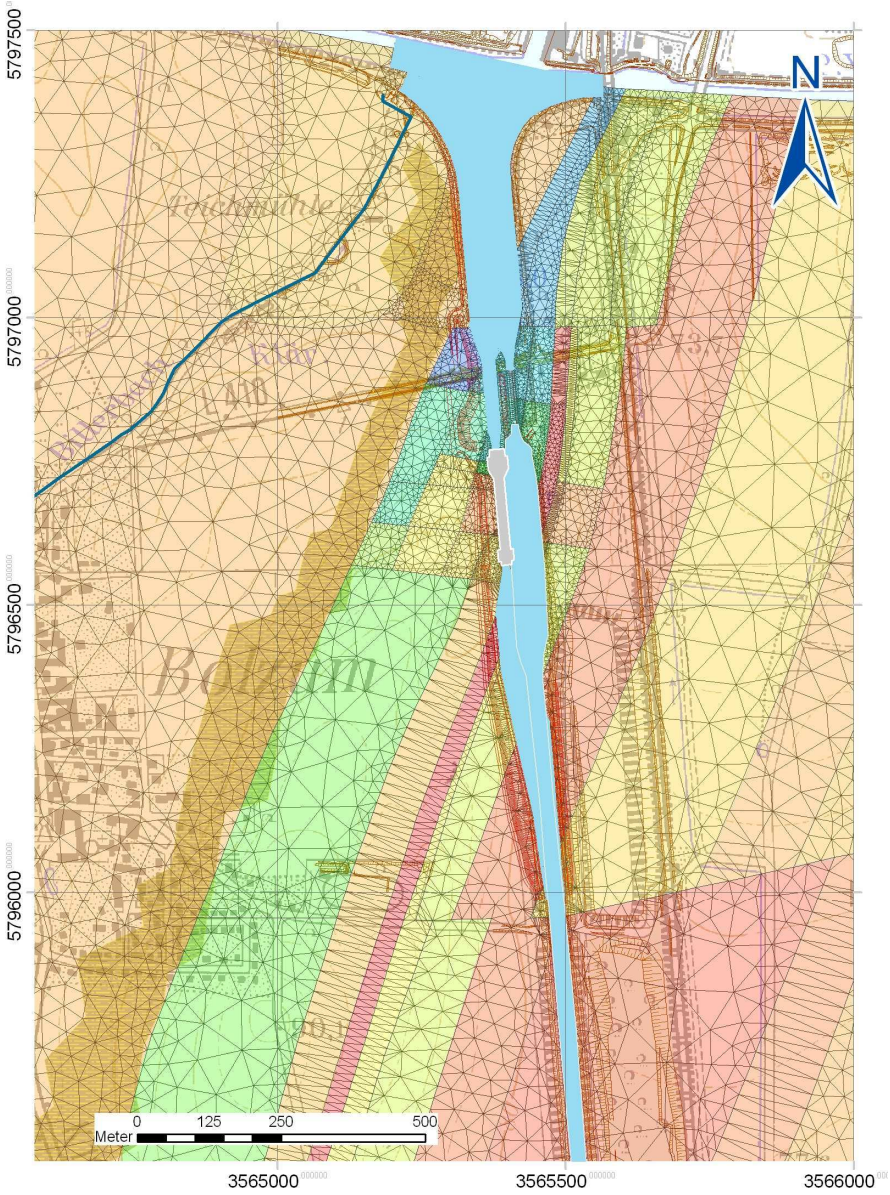

Figure 4. Extract of the FE mesh of the groundwater model and distribution of the model parameters

6 GEOHYDRAULIC DESIGN CONSIDERATIONS

Geotechnical and hydrogeological aspects as well as technical and economic parameters were considered in the design of the pit wall. The construction site covered an area of approx. 4,450 m². To avoid the forming of further sinkholes below the structure, the construction site was located at a reasonable distance from the Karst conduits. Due to the subsoil conditions, the excavation pits was planned as overlapped bored pile walls, serving to a large extent as a permanent wall. A slurry wall was discarded due to the risk of suspension losses in conduits and caverns.

6.1 *Inflow to the Excavation Pit and Propagation of the Groundwater Drawdown*

Based on the groundwater model described above, different scenarios were examined dealing with the hydraulic connection between the Hildesheim Canal and the groundwater. A good hydraulic connection between groundwater and surface water leads to high extraction rates and, at the same time, to a relatively flat drawdown. In contrast, complete clogging of the canal bed would have the opposite effect. During the examination inflow rates ranging from 100 – 270 m³/h were estimated. These inflow rates were much larger than the predictions before detection of the conduit system. During the excavation actual extraction rates of 200 – 280 m³/h were measured indicating an accurate characterisation of the hydrogeological system in the numerical model.

6.2 *Dewatering During Excavation*

To allow excavation works under dry conditions, it was necessary to dewater the aquifer in advance. During the excavation, an open dewatering was performed by longitudinal and complementary transverse ditches along the bored pile wall. The groundwater inflows and water from precipitation was collected in sump pits and then pumped out of the pit. As it could not be predicted during the excavation works whether new preferential conduits would be dug, additional preventive wells were installed in case of very high water inflow. In fact, single conduits were cut across during the excavation works. The excess water was conducted to the pumps by additional ditches.

6.3 *Groundwater Relief During Excavation*

At a depth of 10 m below mean groundwater level (63 m a.s.l.), provisions had to be made against the risk of hydraulic base failures. It was assumed that even a slight displacement of the pit wall could cause a joint through which the outer hydraulic potential could expand all the way down to the wall base. Relief wells were considered as an accurate preventive measure. A detailed 3D model helped to dimension the relief wells array. The wells were finally installed with a filter at a depth of 10 m (46 m a.s.l.) below the excavation bottom at intervals of 5 m as close as possible to the bored pile wall. If water can be released at the upper edge of the well pipe, in the vicinity of the relief wells a hydrostatic pressure distribution from the base of the excavation to the bottom of the well will be established. Without such relief measures, upward gradients at the excavation bottom would be significantly higher. Figure 5 illustrates how the water from the relief wells is conducted away by a vacuum system.

Figure 5. Relief wells installed to prevent hydraulic base failures at the bored pile wall

6.4 *Uplift Restraint During Excavation*

To prevent uplift of the bottom of the lock structure, the groundwater potential underneath may only be slightly higher than the upper edge of the most recent concrete layer. When the final depth of the excavation was reached, 1.5 m deep and 0.5 m wide ditches for pressure relief were installed perpendicular to the lock axis and in-filled with filter gravel. Longitudinal ditches were deliberately not dug to avoid hydraulic short circuits between upstream and downstream groundwater underneath the construction.These ditches, permanently installed below the construction, drain the inflow form the Karst-conduit system and are drained themselves by a well each. The filters of these wells reach, starting at the bottom of the excavation site, approx. 5 m into the rock layer. There is a hydraulic connection between the upper section of the filters and the gravel-filled ditch. The well pipes, leading through the concreted base of the structure, were originally intended to reach only the upper edge of the concrete layer so that an uplift of the structure could be avoided by the pressure release owing to groundwater outflow. However, due to operational

reasons, the wells were equipped with pumping rods and the water level was lowered so it would not overflow the structure's surface (as depicted in Figure 6). After uplift restraint was obtained by weight of the structure, the relief wells were properly sealed by grouting the well pipes.

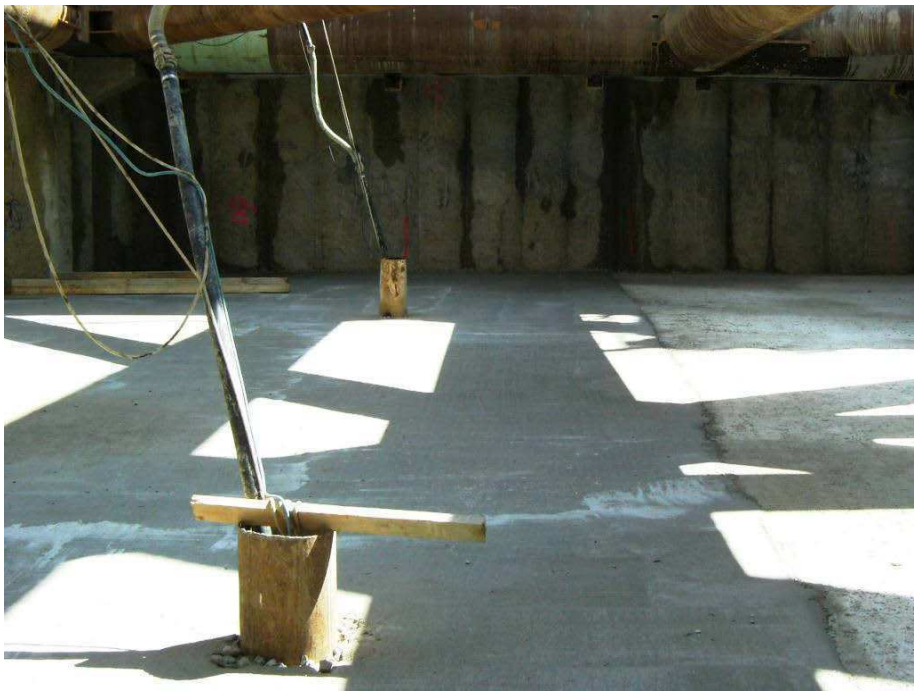

Figure 6. Relief well to prevent the bottom of the construction from uplift

7 INTERPRETATION OF THE MONITORING DURING THE EXCAVATION PHASE

Since cutting across Karst-conduit during the excavation works would lead to a significant change of groundwater flow, a remote data transmission groundwater monitoring program was indispensable. It was intended to record the dewatering-induced groundwater lowering and predict any further near-term development of the drawdown. However, as shown in Figure 2, interpretation individual hydrographs with varying decline rates was not a straight forward procedure. The recorded drawdown was ultimately analyzed within its hydrogeological context based on the groundwater model. The model parameters were continuously adapted to the observed drawdown, extraction rates measured in situ and/or to the groundwater recharge and near-term drawdown was calculated. This practice permitted to recognize critical groundwater lowering in time and to develop adequate countermeasures.

8 INFILTRATION FACILITY

Due to the preferential flow along the Karst-conduit-dominated Muschelkalk layer, lowering in the bedrock was observed in the area of the Bolzum sports field in September 2009. The Quaternary aquifer on top of the bedrock was at first not affected. However a prospective drainage of the Quaternary strata through the Karst conduits in the Muschelkalk could not be ruled out and an infiltration facility consisting of 5 injection wells was installed. Infiltration schemes should prevent further groundwater discharge through the Karst-conduits from the south to the pit. Figure 7 shows the location of the infiltration facility in the inflow area in the southwest of the excavation site. The infiltration facility allowed responding to varying pumping in the excavation site. The downside of this option is, however, that water has to be pumped in a circular manner since the infiltrated water of the conduit system also flows to the excavation site. As for the excavation site at Bolzum, the share of the circular pumping was less than 20 % compared to the total pumping. Since the injection wells in the conduit area were filtered an immediate response could be observed. This reaction as can be seen in Figure 8; results from December 2009 are particularly distinct.

Figure 7. Location of infiltration wells which are to prevent inflow from a southern direction

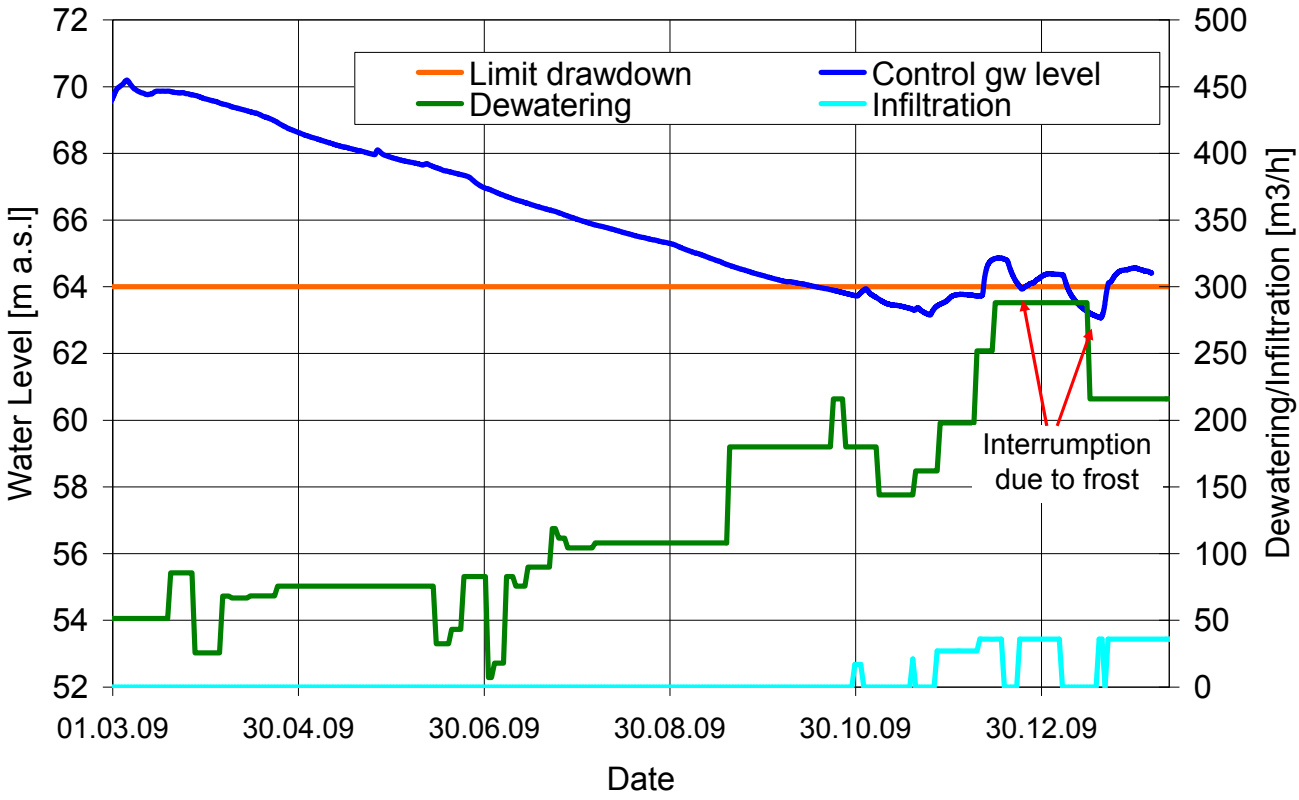

Figure 8. Temporal evolution of extraction rate, groundwater drawdown and infiltration rate

9 CONCLUSION AND OUTLOOK

It was concluded that conventional hydrogeological examination would not suffice to assess such a complex geological situation as found in Bolzum. The large spatial variability of the hydraulic conductivity, which is the result of conduit systems in the ground, can hardly be determined by means of exploration borings. Aquifer testing finally allowed determining the reaction of the hydrogeological system on a relevant spatiotemporal scale. The necessary storage and permeability parameters could also be estimated. Despite substantial simplification, crucial geological structures could be illustrated in a groundwater model. Since the lowering produced by the aquifer test led to water levels similar to those of the later dewatering, enough data was generated to make an unsteady calibration of the groundwater model possible.

A groundwater monitoring program, which was developed in the course of the exploration campaign, allowed recording geographic and temporal data of the lowering events. An infiltration facility in the inflow area of the excavation site was installed to prevent unwanted lowering events. The monitoring program, the permanently updated groundwater model and the infiltration facility were the preconditions to realize a dewatering campaign under such complex ground conditions.

REFERENCES

Christian, J. T. 2004. Geotechnical Engineering Reliability: How Well Do We Know What We Are Doing?. J. Geotech. and Geoenvir. Engrg. 130.

Finno, R., Calvello, M. 2005. Supported Excavations: Observational Method and Inverse Modeling. J. Geotech. and Geoenvir. Engrg. 131.

Griffiths D., Fenton, G. 2009. Probabilistic Settlement Analysis by Stochastic and Random Finite-Element Methods. J. Geotech. and Geoenvir. Engrg. 135.

Hachich W., Vanmarcke, E. 1983 Probabilistic Updating of Pore Pressure Fields J. Geotech. Engrg. 109.

Seitz, O. 1923: Stratigraphie und Tektonik der durch den Bau des Mittellandkanals zwischen Hannover, Peine und Hildesheim aufgeschlossenen Schichten.- 28 S., Berlin.

ISGSR 2011 - Vogt, Schuppener, Straub & Bräu (eds) - © 2011 Bundesanstalt für Wasserbau ISBN 978-3-939230-01-4

Case Study On The Assessment Of Sinkhole Risk For The Development Of Infrastructure Over Karstic Ground

N. Sartain
Arup, Solihull, United Kingdom

J. Mian
Arup, Solihull, United Kingdom

N. O'Riordan
Arup, San Francisco, USA

R. Storry
Bouygues Travaux Publics, Hong Kong

ABSTRACT: Karstic dolomite in the Centurion area of South Africa presents significant challenges to the geotechnical engineer. It has been recognised for many decades that sinkholes can occur in the residual soils overlying the Dolomite, but it is not possible to predict their occurrence or their size. Sinkholes present a significant hazard to infrastructure since they occur suddenly and result in a loss of ground support. In designing the Gautrain Rail Link, routed through the Centurion area, it was necessary to manage this hazard in a rational way. Adopting the maximum possible size of sinkhole that could occur and designing for this eventuality was considered unrealistic in terms of international practice. This paper presents a risk-based approach that was used as part of the design for the section of Gautrain running over the dolomites to demonstrate that sinkhole risks have been made as low as reasonably practicable. A quantitative risk assessment was undertaken to model numerically the consequence and likelihood of sinkhole occurrence. This approach enabled the risk from sinkholes to be quantified and was used to help define the design requirements for the infrastructure in respect of this hazard.

Keywords: Dolomite, Karst, Sinkhole, Risk management, Infrastructure

1 INTRODUCTION

The Gautrain Rail Link project connects the centre of Johannesburg with Pretoria (via Centurion), and the Oliver Tambo International Airport with Sandton. Civil construction works were substantially completed by the end of 2010 with the section between Johannesburg and Pretoria expected to be operational by mid-2011. Within the Centurion area of Pretoria the route crosses 15km of dolomitic ground, of which 5.8km are on viaduct. There are very significant geotechnical challenges associated with the design and construction of a high speed railway on the dolomite (such as extremely variable and often very deep rockhead, rock pinnacles and floaters, and residual soils that can be very strong and stiff close to the surface yet extremely weak and soft at great depth), but this paper considers only the particular hazard posed by sinkholes. The consequence of a large sinkhole occurring that may result in the failure of part of the railway infrastructure could be extremely serious, from both a safety and economic perspective.

The alignment could not avoid the dolomitic ground, so the designers had to consider for what size of sinkhole it was appropriate to design, balancing the requirements of capital cost, operational cost, passenger safety and uninterrupted railway operation. This paper describes the risk process undertaken to permit this decision to be made in an informed and robust manner.

2 THE SINKHOLE PROBLEM

The dolomite of the Centurion area of South Africa is 2500 million years old. It has been subjected to long periods of chemical weathering (dissolution by water) resulting in the formation of a thick, and highly variable 'residuum' over the rock. The residuum comprises 'wad' (a low density, weak material that is highly erodible and compressible), and very strong chert. The weathering of the dolomite has resulted in a highly pinnacled rockhead that in places is at the ground surface but elsewhere is at >100m be-

low ground level. The residuum (Wagener 1982) is often quasi-stable and sinkholes are a recognised ground hazard in the area. Significant efforts (Waltham *et al.* 2005) have been made to understand the conditions under which they occur, the processes that cause them and the influence of human factors on this (for example leaking wet services or lowering of groundwater). Nonetheless, neither the location of future sinkholes, nor their dimensions can be reliably predicted. It is, however, possible to estimate their maximum possible extent (Buttrick *et al*. 2001).

Sinkholes (defined as 'dropout' sinkholes, Waltham & Fookes 2003)[1] are hazardous because they open suddenly resulting in an immediate loss of support to foundation systems. Sinkholes have been responsible for a number of deaths and damage worth many millions of Rand in the study area.

Sinkholes in the Centurion area vary from the very small (1m diameter, 1m depth) to the very large (up to 45m diameter, 30m depth). The sinkhole size is a function of many factors including the depth to rockhead, the geometry of the rockhead, the properties of the overburden and the depth to groundwater (Buttrick *et al*. 2001). Their formation is the result of washing out of overburden into cavities in the dolomite rock, and for this reason they can be triggered anthropogenically, due to failures of 'wet' services (drainage, water supply, swimming pools etc.) or to groundwater drawdown resulting from pumping for agriculture use for example. Schöning (1990) found that 94% of sinkholes in wider Centurion area were in developed areas, and by implication were attributable to anthropogenic triggers. Other authors (Waltham *et al.* 2005) consider that this could be an underestimate. Additionally, and significantly for this study, large sinkholes (greater than 15m) have only been observed in areas where groundwater abstraction has resulted in significant drawdown of the water table.

3 EXISTING METHODS FOR MANAGING SINKHOLE HAZARD IN THE CENTURION AREA

Existing methods for controlling sinkhole risk around Centurion have focused on mitigating the consequence of sinkhole occurrence by stipulating the type of development permitted in areas classified by a risk rating after Buttrick *et al.* (2001). This approach was developed primarily in relation to planning for building development. However, when designing linear infrastructure such as rail routes, re-routing is rarely a feasible option for avoiding a specific hazard, given the multiple constraints on the route.

Initial design proposals for the Gautrain were to deterministically estimate the largest size sinkhole that could occur along the alignment and to design the infrastructure to cope. This was applied first to the design of at-grade infrastructure for which the appropriate sinkhole parameter is diameter. Using this deterministic approach, 30m was proposed as the design diameter and it was found that the impact on the construction cost due to a design having to cope for a 30m diameter sinkhole occurring beneath the alignment was extreme. Furthermore, after very long and detailed studies it appeared that for the elevated section founded on piles to rock no viable solution would be found.

A contractor's study for the Gautrain project estimated that the frequency of sinkhole occurrence with diameter >15m was 10^{-5}/km^2/annum. Designing for 30m diameter sinkholes, and incurring the associated costs, was therefore considered to be an excessively risk averse approach and outside normal international practice to risk management.

4 RISK-BASED APPROACH TO DESIGNING FOR SINKHOLE OCCURRENCE

A different approach was required, one which achieved a better balance between whole-of-life risk and capital cost. A number of expert groups were convened to review the sinkhole risk in order to determine realistic and robust design requirements.

The risk management of the Gautrain project was based on the approach of HSE (2001), which presents the concepts of intolerable risk, tolerable risk and broadly acceptable risk.

Intolerable risks must be addressed and are not permitted. Broadly acceptable risks are those which are sufficiently low so as not to be of concern. Tolerable risks lie between intolerable and broadly acceptable risks, and HSE (2001) requires that such risks are made 'as low as reasonably practicable', ALARP, Fig. 1.

[1] As well as 'dropout' sinkholes, there are also 'suffosion' sinkholes (Waltham & Fookes 2003) which are essentially subsidence events. They are also problematic for structures on dolomite, but are not considered in this paper. Only 'dropout' sinkholes have been considered since their sudden occurrence carries much greater likelihood of failure of infrastructure.

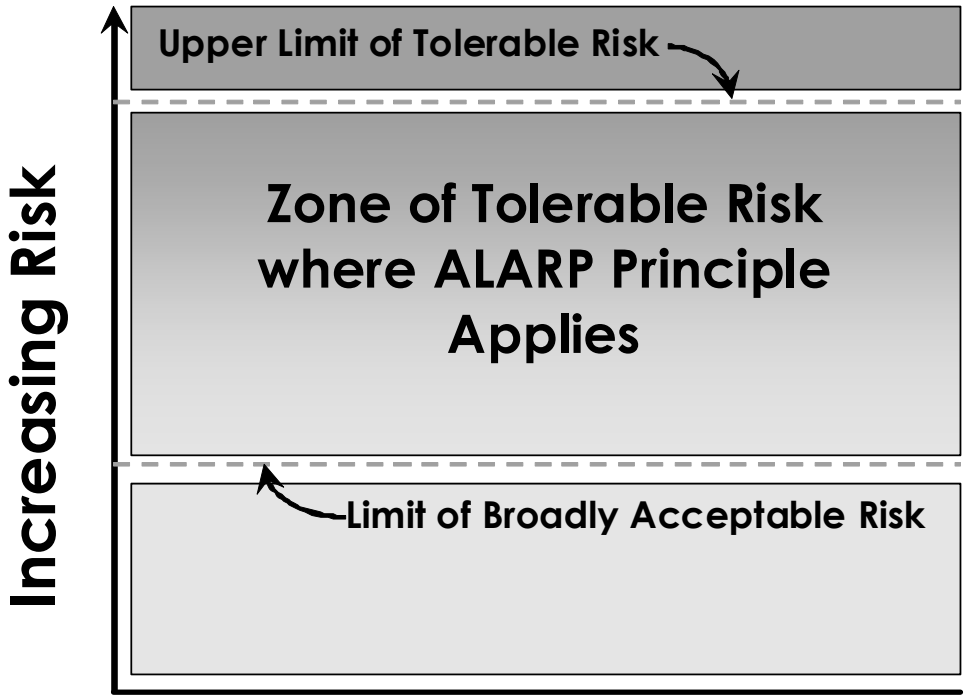

Figure 1. Tolerability of risk and the ALARP principle

The principle of this approach was to produce a design for which it could be demonstrated that the safety risk associated with sinkhole occurrence was tolerable. The threshold for intolerable risk (for all project risks) was defined quantitatively based on a review of literature (The Royal Society 1992; HSE 2001; Jonkman *et al.* 2003) as an annual frequency of passenger fatality of 10^{-5}. This paper presents one branch of the expert review in which a quantitative risk assessment (QRA) was undertaken to estimate the sinkhole risk and to identify the required performance of the mitigating measures using the ALARP principle. It uses the terminology presented in Free *et al.* (2006) when discussing hazard and risk.

4.1 *QRA*

The following paragraphs describe the QRA that was undertaken.

Initially it was necessary to define a model to describe how the occurrence of a sinkhole can lead to a negative consequence. Figure 2 presents a simplified model for the sinkhole problem, showing the stages of the analysis on the left, the steps that contribute to the outcome in the middle, and how each step was modelled on the right.

From the designer's point of view, it is important to note the effect the structural response has on the outcome. Sinkholes, just like earthquakes or landslides, do not have an inherent risk if they have no consequence. It is the interaction of the hazard with the population and its economic interests that gives rise to the risk, and it is the response of the infrastructure to the hazard that ultimately determines the level of risk.

Probability density functions were assigned to each uncertain variable, and then simulated using a Monte Carlo approach.

4.2 *Defining the sinkhole hazard*

The specific hazard under consideration is the sudden loss of support to foundations due to sinkhole formation. For shallow foundations this is be a loss of vertical support, whilst for piled foundations this could be primarily a loss of horizontal support accompanied by a lateral thrust into the newly-formed sinkhole. The level of risk is controlled by the size of the sinkhole, but the appropriate size metric adopted may change depending on the situation under consideration. Only the diameter is considered below, by way of example.

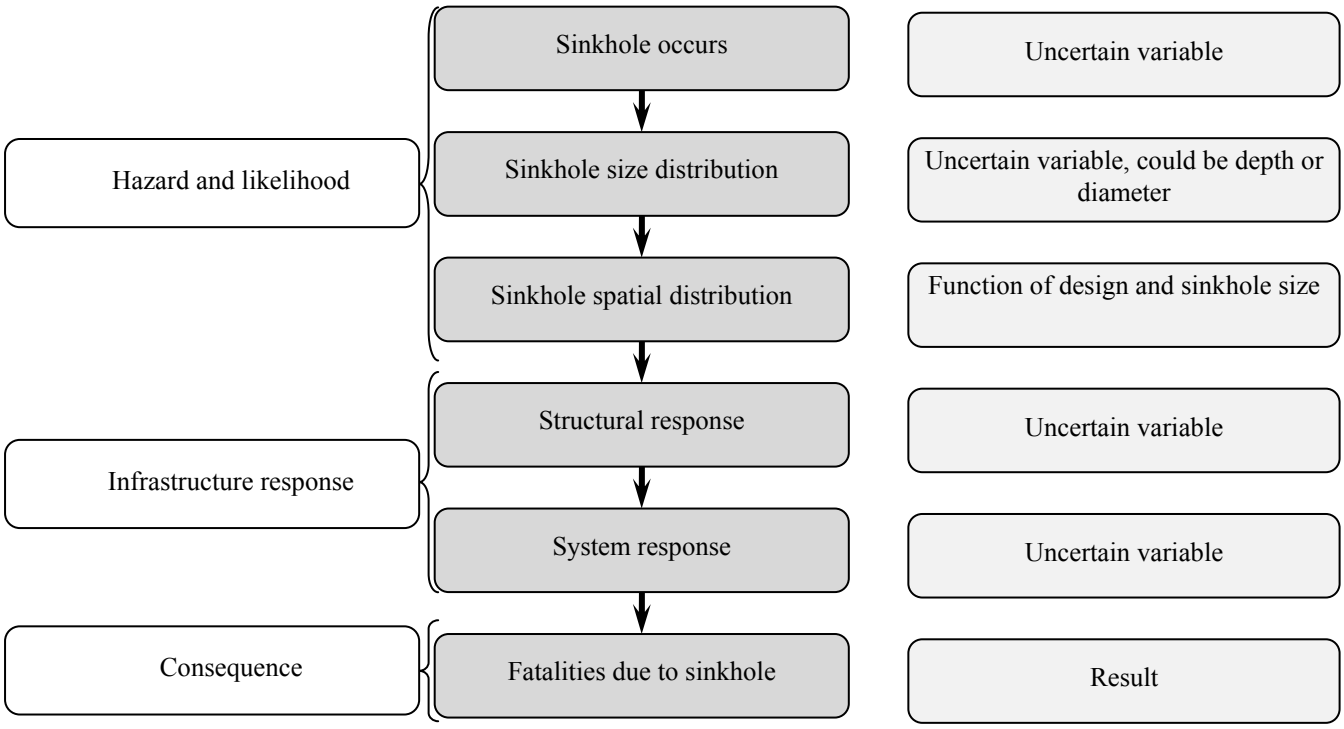

Figure 2. Example risk model for QRA for the sinkhole effect on infrastructure

A database detailing 287 sinkholes was acquired by the Gautrain project. The data were not complete, and careful interpretation was required to avoid misleading conclusions.

Figure 3 shows the sinkhole diameter distribution presented as a probability distribution for the sinkholes in the database. Note the peaks in the data at 5m, 10m, 15m etc. indicating that a significant amount of the data is estimated and rounded up or down, depending on the observer.

It appears that large sinkholes (>20m) are significantly over-represented in the database. The main reasons for this observation are thought to be:

- The dataset has been collected reasonably thoroughly in the past quarter-century (approximately), but includes larger sinkholes (that people would have remembered) from a greater time period. In this scenario the largest sinkholes will be over-represented and this is consistent with the data. This is analogous to the catalogue completeness in seismic hazard studies; the older the earthquake records, the higher the threshold of earthquake magnitude at which the catalogue is considered complete.
- Larger holes are more likely to suffer additional collapse of initially vertical walls which will tend to increase their size.

Figure 3 also presents the exponential probability density function (PDF) considered to best represent the available data and that was adopted for use in the QRA.

4.3 *Defining the sinkhole likelihood*

Having established a diameter distribution for sinkholes in the Centurion area thereby defining the hazard, it was necessary to determine the frequency of sinkhole occurrence, i.e. the likelihood of the hazard occurring. The rate of formation of new sinkholes (RNS) is measured in new sinkholes per area unit per time unit.

Sinkholes occur primarily as a result of failures in wet services or of groundwater drawdown (Waltham *et al.* 2005). RNS therefore depends not only on the natural geological and hydrogeological condition of the site, but also on factors such as the quality and density of wet services, regulation and control of wet services, the population density and groundwater abstraction. It is very difficult to estimate accurately the historical frequency of sinkhole occurrence because these factors have all changed over comparatively short timescales. Future RNS will depend on the existing and future wet infrastructure at the site under consideration. For major new projects, however, RNS can be expected to reduce significantly compared to recent years since the importance of these human influences is now understood and the budget for controlling them can be made available. For smaller projects, it is possible that RNS could increase as existing wet services age and degrade.

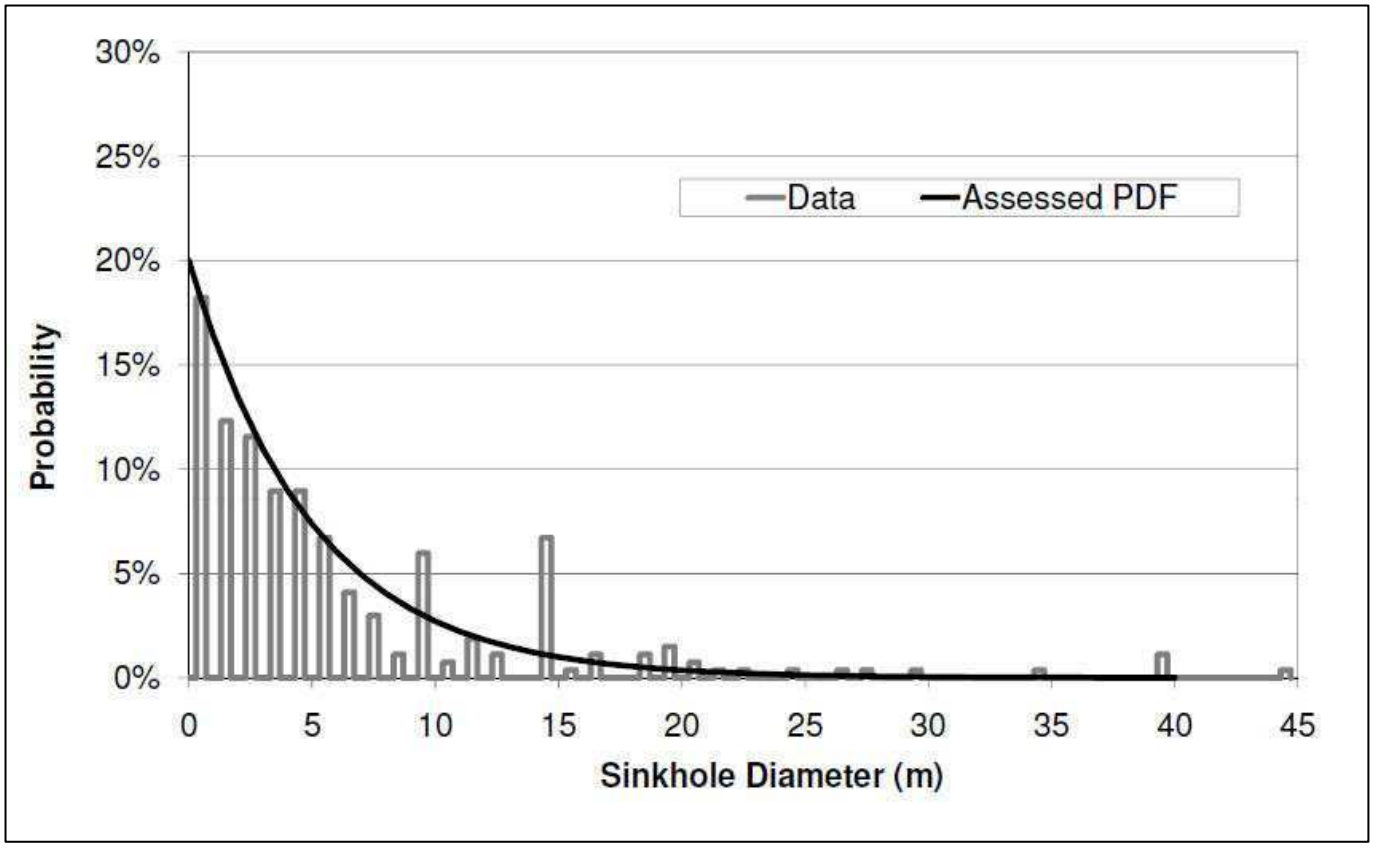

Figure 3. Sinkhole diameter distribution from sinkhole database in Centurion area

So, whilst it was not possible to calculate the future RNS, it was estimated from a review of the literature (Waltham *et al.* (2005), Waltham & Fookes (2003), The South African Department of Public Works (2004), Buttrick and van Shalkwyk (1998)) and by assessment of the available data.

A range of RNS was modelled in the QRA between the estimated upper and lower bounds of the RNS. The QRA therefore assessed the likely outcomes if existing conditions were observed. The effect on the risk of significantly improved management of 'wet' services within the railway corridor was left as a design decision to be taken later.

4.4 *Consequences of sinkholes*

The consequences of a sinkhole occurring adjacent to, or beneath, a structure are a function of the response of the structure to the sinkhole event. For the sections of the Gautrain at-grade and on embankment the engineering solution was to place the track in a reinforced concrete U-trough – effectively an at-grade bridge designed to span sinkholes up to the 'design' diameter.

The effects of the (assumed random) spatial distribution of sinkholes was included in the model. The relative likelihoods of small nearby sinkholes as well as large but further away sinkholes on the U-trough were modelled.

To simplify the QRA, the U-trough was assumed to have a binary response – for all sinkhole events below the 'design' diameter it did not 'fail', and for all events greater it did 'fail'. 'Failure' was defined as loss of performance sufficient that if a train passed over it, there would be sufficient movement that derailment of a train with consequent fatalities was possible.

Figure 4 presents sample results from the QRA for various confidence intervals. It shows the annual risk of a sinkhole occurring that could cause structural failure of the U-trough at various confidence intervals for increasing size of 'design' sinkhole diameter. The spread of confidence intervals is due to the use of PDFs as inputs within the logic tree.

4.5 *Design decisions and requirements for ALARP*

Having estimated the frequency of failure of the U-trough it was necessary to determine the diameter of sinkhole that the U-trough was designed to span, and what further mitigation measures would need to be implemented in order to achieve a tolerable risk at acceptable cost.

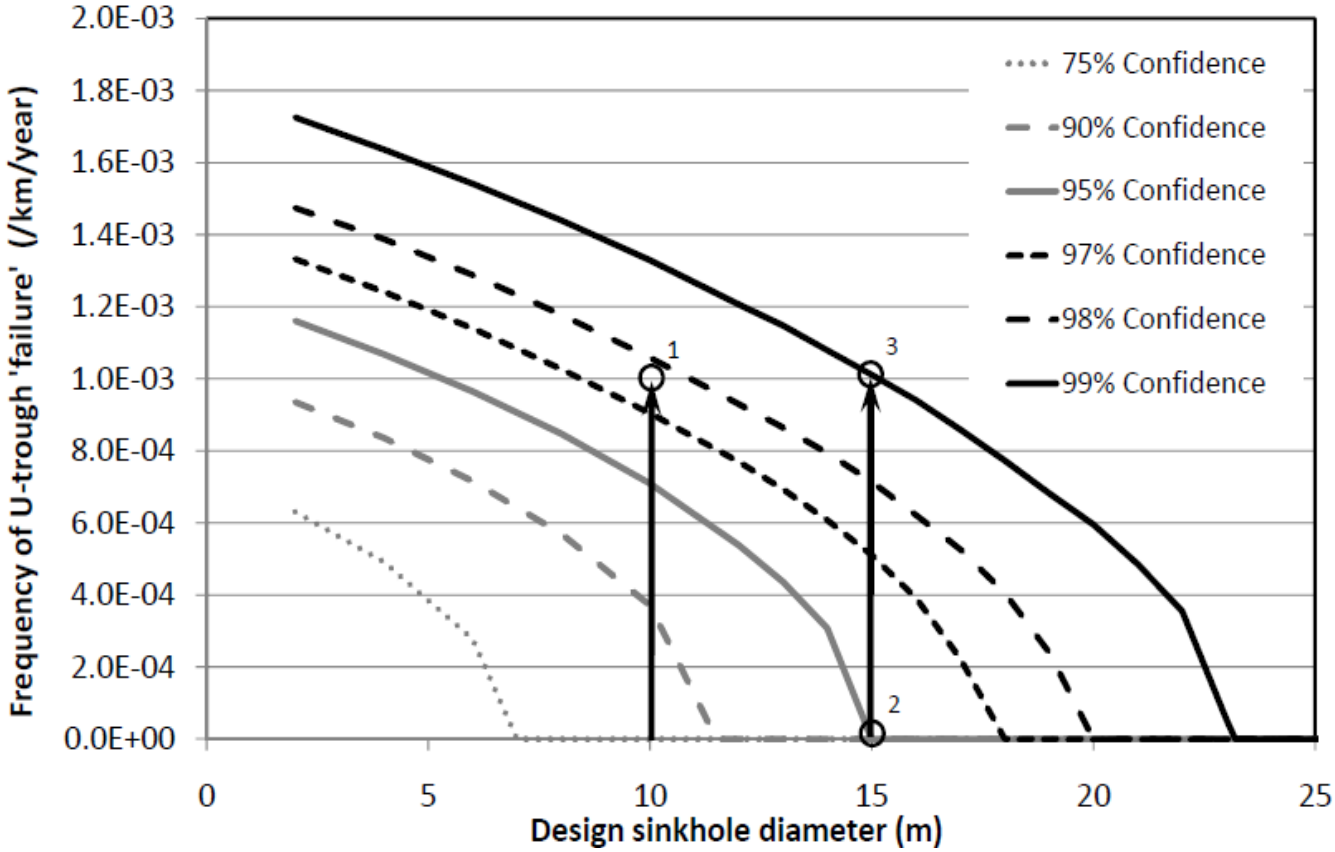

Figure 4. Result of QRA for U-trough showing relationship between frequency of 'failure' and 'design' sinkhole diameter, assuming existing 'wet' service conditions

Figure 4 shows that if the U-trough were to be designed to withstand a 10m diameter sinkhole, then the frequency of failure is around 10^{-3}/km/year with between 97% and 98% confidence (note 1 Figure 4), assuming similar RNS to observed in the recent past. Increasing the 'design' sinkhole diameter increases the confidence of a given frequency of failure, or for the same frequency of failure increases the confidence level.

So the study has established that for reasonable 'design' diameters, and for existing conditions, the frequency of failure is rare (approximately once in a thousand years) with a high degree of confidence, but not so rare that additional measures are not required to bring the risk down to tolerable levels (i.e. to levels where the annual frequency of passenger fatality is less than 10^{-5}.

Construction cost increases exponentially with increasing 'design' sinkhole size, but Figure 4 shows that designing for progressively larger sinkholes does not reduce the frequency of failure significantly, unless the confidence interval chosen for design is very close to the percentile of the 'design' diameter on the PDF in the QRA model. Therefore it was found to be cost effective to design for a smaller 'design' sinkhole diameter and to invest in robust sinkhole mitigation measures that would have a much greater impact on reducing the risk. For example, controlling the wet services could reduce the frequency of sinkhole occurrence from that adopted in the model by more than an order of magnitude. The benefit of the QRA was that it framed the risk in a way that enhanced the ability of the design team to make such decisions.

At this point the various expert groups that had been working on the problem were reconvened. It was determined that the most appropriate 'design' sinkhole diameter for the design of the U-troughs was 15m, for the following reasons:

- This study had shown that a 15m 'design' diameter gave a tolerable risk (actually zero risk) with 95% confidence (note 2 Figure 4), even assuming existing groundwater management, and a frequency of failure of approximately once in a thousand years with 99% confidence (note 3 Figure 4);
- The findings from other groups were that sinkholes of diameter >15m were only observed in areas of significant groundwater drawdown and therefore the actual RNS for these diameter holes was much lower (by up to two orders of magnitude) than predicted from the dataset studied. This difference appears very large, but note that the frequency used for the base QRA was estimated from data collected over recent decades at a time of relatively poor water management and that large sinkholes were over-represented in the dataset. These factors account for the bulk of this difference.

- There was a practical aspect of railway operation to consider. The 'design' sinkhole needed to be a rare event such that the robustness of the design to smaller and much more likely sinkholes was at a level where interruptions to the train operations were at an acceptable level.

To complement this choice of 'design' diameter the following measures were implemented following the principles of ALARP to ensure tolerable risk from sinkholes:

- Replacement (and sleeving) of utilities affected by the work within the rail reserve to minimise the chance of leakage
- Piezometers were installed along the route in the dolomite (and within the rail reserve) which will be monitored regularly and compared against predefined trigger levels to give an early warning of pumping/water drawdown
- Dynamic compaction was undertaken throughout the route as an investigation technique and full dynamic compaction treatment where the ground was considered to be collapsible in the top 10m or where soft areas were identified by the investigation work
- A monitoring system placed below the embankment was set up in the three highest risk zones (determined from investigations into the overburden) which acts as an early warning in the event that the ground settles/collapses beneath the embankment

The combined effect of these measures can be estimated to reduce the risk from sinkholes by three to four orders of magnitude. In this way the consequences of sinkhole occurrence on the Gautrain project were controlled by the engineering design and the risk from sinkholes was demonstrated to be tolerable, following the principles of ALARP, at lower cost than designing for sinkholes with diameter 30m.

The same approach was subsequently applied on the project when considering the design of viaduct foundations in the Dolomite. The detail of the analysis was different since for deep foundations the depth of sinkhole was found to be more significant than the diameter, and different mitigations were needed but the same principles were used.

5 CONCLUSIONS

It has become necessary in the case of Gautrain, and will become necessary for other infrastructure works, to develop the Dolomite land in the Centurion area. The Dolomite has a complex karst geology and sinkholes occur in the residuum materials above the rockhead.

Sinkhole hazard and likelihood were defined quantitatively using data of historic sinkhole events in the area and an understanding of the geology, hydrogeology and the significant role wet services play in determining sinkhole occurrence. The response of the infrastructure to sinkholes was determined quantitatively.

A risk model combined with Monte Carlo simulation was used to define the events leading to negative economic or safety consequences of sinkholes in a QRA. The outcome of the QRA was used to inform important design decisions on the Gautrain. By using the methodology presented in this paper, combined with the use of expert judgement, it has been possible to avoid designing for the worst-case sinkhole scenario through quantitative estimation of the risks and capital costs of the available engineering solutions. The design was undertaken to the ALARP principles set out in HSE (2001) and the risk from sinkholes to the Gautrain was reduced to tolerable levels.

6 ACKNOWLDEGEMENTS

The authors wish to acknowledge the kind permission given by the Gauteng Provincial Government and the Bombela Concession Company to publish this paper. The authors also wish to advise that the views and opinions expressed in the paper are solely those of the authors and not those of the Province or Bombela.

REFERENCES

Buttrick, D.B., & van Schalkwyk, A. 1998. Hazard and Risk Assessment for Sinkhole Formation on Dolomite Land in South Africa. Environmental Geology, 36 (1-2) November 1998.

Buttrick, D.B., van Shalkwyk, A., Kleywegt, R.J., & Watermeyer, R.B. 2001. Proposed Method For Dolomite Land Hazard And risk Assessment In South Africa. Journal of the South African Institution of Civil engineering, 43(2).

Free, M., Anderson, S., Milloy, C., & Mian, J. 2006. Geohazard Risk Management For Infrastructure Projects. Proc of the ICE, Civil Engineering 159, pp28-34.
HSE 2001. Reducing Risks, Protecting People. Report R2P2, ISBN 0 7176 2151 0.
Jonkman, S.N., van Gelder, P.H.A.J.M., & Vrijling, J.K. 2003. An Overview of Quantitative Risk Measures For Loss of Life and Economic Damage. Journal of Hazardous Materials A99, pp 1-30.
Schöning, W.L. 1990. Distribution of Sinkholes and Subsidences in the Dolomite Areas South of Pretoria. MSc Dissertation, University of Pretoria.
South African Department Of Public Works 2004. Appropriate Development Of Infrastructure On Dolomite: Guidelines For Consultants. PW344.
The Royal Society 1992. Risk: Analysis, Perception and Management. ISBN 0-85403-467-6.
Wagener, F von M. 1982. Engineering Construction on Dolomite. PhD Thesis, Dept. of Civil Engineering, University of Natal.
Waltham, T., Bell, F., & Culshaw, M. 2005. Sinkholes and Subsidence, Karst and Cavernous Rocks in Engineering and Construction. Praxis Publishing, UK, ISBN 3-540-20725-2.
Waltham, A.C., & Fookes, P.G. 2003. Engineering Classification of Karst Ground Conditions. Quarterly Journal of Engineering Geology and Hydrogeology, 36, pp101-118.

ISGSR 2011 - Vogt, Schuppener, Straub & Bräu (eds) - © 2011 Bundesanstalt für Wasserbau ISBN 978-3-939230-01-4

Risk management during the reconstruction of the underground metro station Rotterdam Central Station

R. Berkelaar
Rotterdam Public Works, Rotterdam, the Netherlands

ABSTRACT: At the moment the underground metro station at Rotterdam Central Station (CS) is being reconstructed from a two-track to a three-track station. The project is carried out under very complex circumstances. The most important one is the politically imposed demand that the underground station has to maintain its full functionality at all times. This demand together with the technical complexity of the project, the complicated project phasing and other circumstances lead to a very high risk profile requiring risk management during the design and construction phase of the project.

Different approaches to risk management were taken during the design and construction phase. During the design phase straightforward risk analyses were carried out. For the construction phase it was decided to switch to a fully integrated risk management system with a dedicated risk management team. This team was responsible for managing the so called 'soft' and 'hard' risks. Examples of soft risk management are account management with important licensing authorities and dealing with the project environment. Hard risk management deals with risks which are primarily controlled by monitoring the ground(water) and construction.

An example of risk defined monitoring deals with the requirement of the uninterrupted metro operation. To control the risk of metro traffic disruption caused by tunnel and track deformation, a set of parameters was defined which were monitored during construction. Furthermore, monitoring parameters were defined regarding legal obligations and standards, insurance and safety requirements and structural conditions imposed by the project environment.

For each monitoring parameter warning levels were defined. When the signal level is exceeded mitigating measures have to be implemented to avoid exceeding the intervention level. Exceeding an intervention level means that the risk of damage has become unacceptably large. The difference between signal- and intervention level is chosen in such a way that sufficient time to implement these measures is available.

Keywords: risk management, monitoring, warning levels, earth works, organisation

1 INTRODUCTION

The present Rotterdam Central Station (CS) was opened in 1957 in the period of rebuilding after World War II. The station and the public transport infrastructure in its vicinity has served its purpose well for many years. However, the increasing pressure on public transport has resulted in the development of several mega projects in and around Rotterdam CS, figure 1. Among these are the high speed railway line between Paris and Rotterdam and the recently opened RandstadRail metro line, van Zanten and Thumann (2008). These projects demanded an expansion and upgrading of the present underground metro station. The engineering department of Rotterdam Public Works provided the architect, performed the complete engineering, contract management and construction supervision.

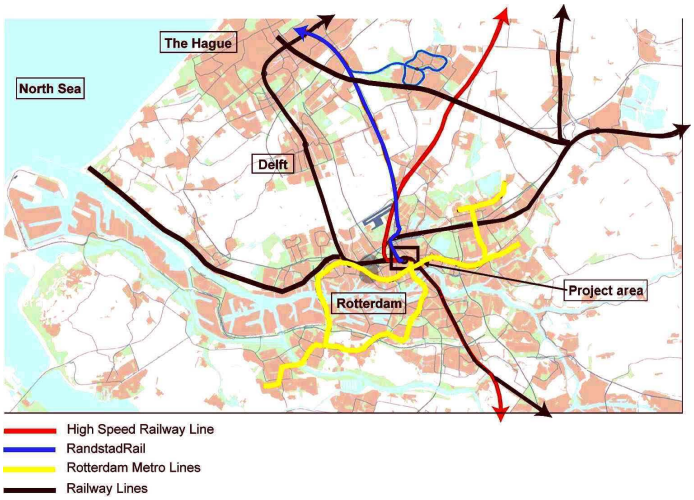

Figure 1. Heavy- and light-rail public transport in and around Rotterdam

The scope of the development of the new underground metro station is to upgrade the existing metro station from a two-track station with one platform into a three-track station with two platforms. The project is carried out under very complex circumstances. The most important one is the politically imposed demand that the underground station has to maintain its full functionality at all times. This means that a vast number of passengers use the metro station daily while construction under, next to and above the station continues. Other complicating circumstances are the deltaic soil conditions (soft soil with a high groundwater level), the fact that the location is right in the centre of Rotterdam, the technical complexity of the project and the complicated project phasing. These circumstances lead to a very high risk profile demanding explicit risk management during all project phases.

The excavation method of the building pit is based on isolating the Pleistocene sand aquifer inside the building pit by means of a diaphragm wall to a depth of NAP -38 m, figure 2. At this depth a continuous low permeable clay/loam layer is present. This method provides a water regime inside the building pit which can easily be maintained as only a very limited amount of water is expected to pass through the clay/loam layers and the diaphragm walls, Thumann and Haß (2007).

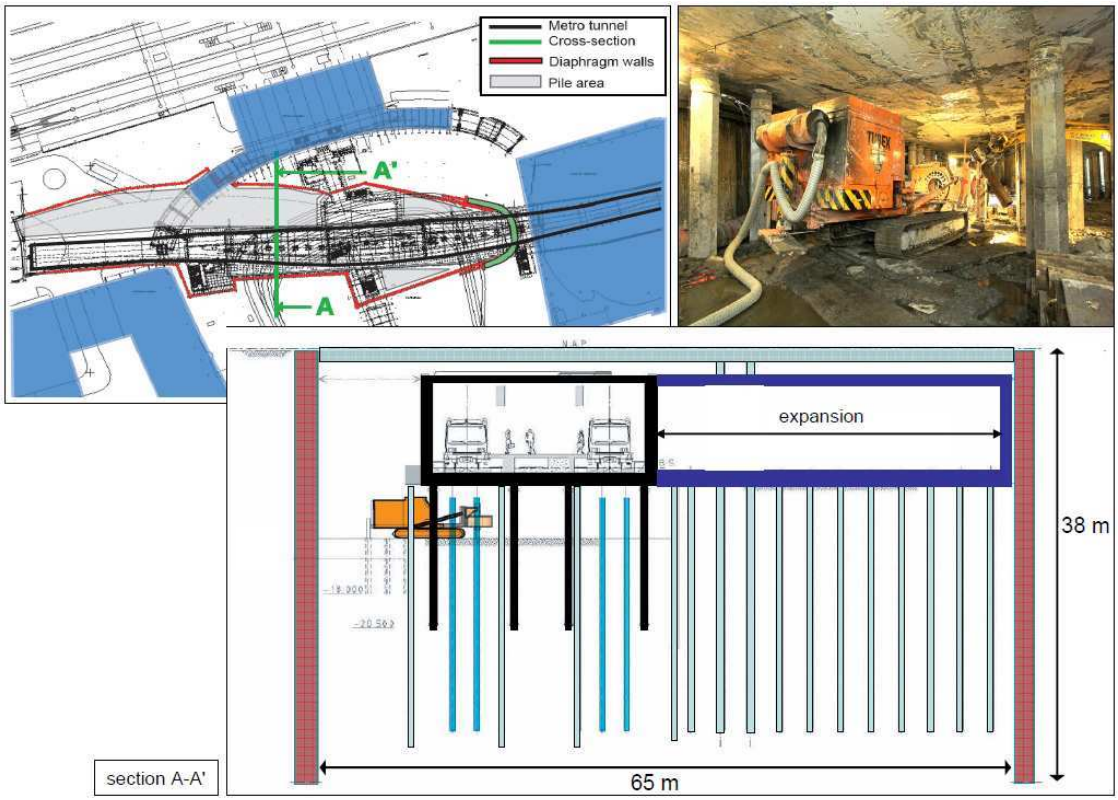

Figure 2. Plan view and cross section of the old metro station Rotterdam CS plus area of expansion and building pit contours, photograph of Tubex-grout injection pile installation under the old metro station

2 RISK MANAGEMENT DURING THE DESIGN PHASE

2.1 *Risk management approach and top risks*

The design phase can be entitled as a relatively 'static' phase concerning risk management. 'Relatively static' as there are no building activities yet and therefore the dynamics with the project surroundings are not as intense as during the construction phase. During the design phase risk management was primarily executed with straightforward risk analyses at set intervals and track was kept of the implementation of the remedial measures in the design and contract specifications. Because of the technical complexity of the project, focus was put on technical risks for: 1) risk remediation and 2) risk quantification. The results showed that the top risks are related with disturbance of metro operation and groundwater inflow in the building pit, table 1.

Table 1. Top risks

risk	cause	chance	consequence [M€]
leakage, water inflow in building pit	no water tight connection between diaphragm walls and metro tunnel	> 50 %	2
interrupting metro operations	deformation of metro tunnel due to multiple (interacting) causes such as: - strut failure - uncontrolled groundwater inflow - unexpected ground behavior	10 %	10

Emphasis was put on remediating the top risks. Therefore, a lot of effort was put in soil and obstacle investigation, implementation of design adjustments and the set up of a monitoring programme. Table 2 indicates the remedial measures belonging with the top risks.

Table 2. Top risks - remedial measures

risk	cause	remedial measure
leakage, water inflow in building pit	no water tight connection between diaphragm walls and metro tunnel	- historical and obstacle investigation - implement alternative design solutions
interrupting metro operations	deformation of metro tunnel due to multiple (interacting) causes such as: - strut failure - uncontrolled groundwater inflow - unexpected ground behavior	- soil investigation - set up of monitoring programme - struts with hydraulic jacks

Most remedial measures have been implemented during the design phase. In section 2.2 an example will be given of how the risk of ground water inflow in the building pit, at the point of entry of the metro tunnel, has been mitigated. Section 4 will illustrate how monitoring has been used as a remedial measure, or risk control tool, to mitigate the risk of interrupting metro traffic.

2.2 *Risk remediation by obstacle investigation and alternative design solutions, an example*

On the east-side of the project the existing metro tunnel enters the building pit, figure 3. The realization of a water tight connection between the diaphragm walls and the metro tunnel led to a very high risk of water inflow in the building pit. Obstacle investigation revealed the presence of a large number of obstacles at the same location: sheet piles walls, wooden piles, tie back anchors and the 'unknown' obstacles, figure 3. Several options on how to overcome these risks were considered. In this evaluation the alternatives were primarily compared on functionality, weighing on costs was secondary. Of the available design solutions ground freezing seemed most promising because of its water tightness, its variable (adaptable) geometry and the fact that obstacles do not interfere with the ground freezing process significantly, Thumann and Haß (2007).

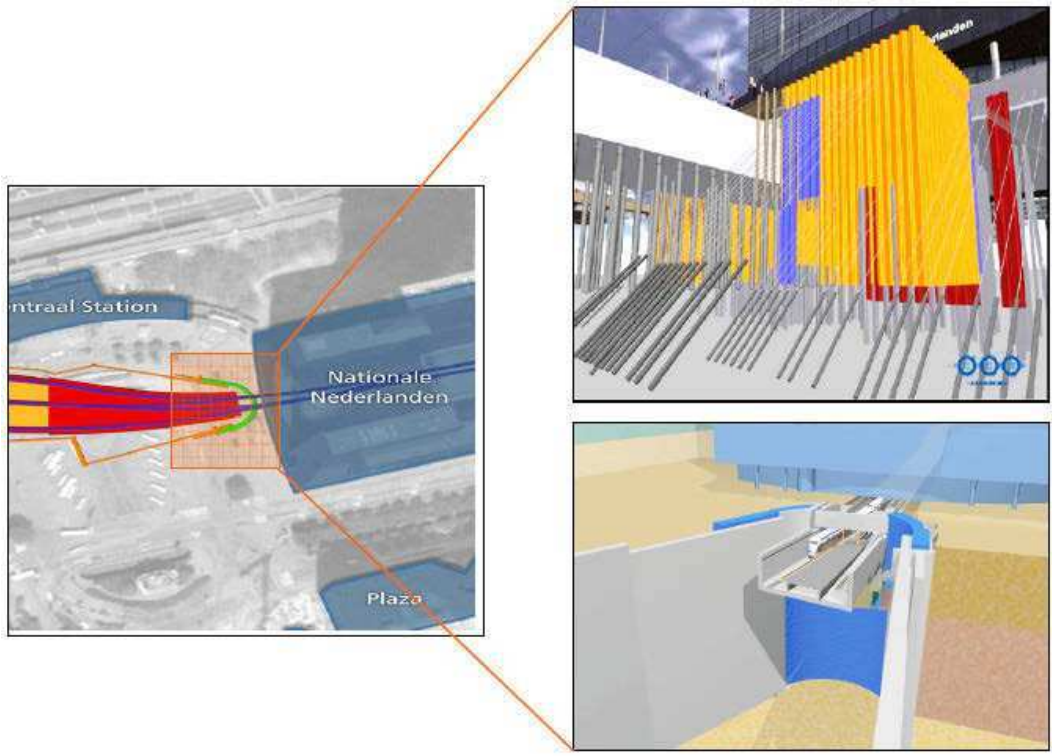

Figure 3. Results obstacle investigation and frozen ground body at the east-side of the building pit

The risk of groundwater inflow in the building pit has been mitigated by changing the design: introducing the frozen ground body. However, ground freezing has never been performed on this scale and context in the Netherlands before and in doing so new risks were introduced, such as unknown freezing pressures, frost heave and working with liquid nitrogen in confined spaces. These new risks were primary mitigated by making design adjustments such as making locally thicker diaphragm walls and reinforcing the existing metro tunnel. Secondary, a back up freezing system was implemented. Further, an extensive monitoring programme was set up to monitor the behavior of the metro tunnel and the frozen ground body.

3 RISK MANAGEMENT DURING THE CONSTRUCTION PHASE

In the construction phase the 'dynamics' of the project increase significantly. The interaction of the project with its surroundings becomes tangible and time pressure increases. Therefore, it was decided to make a switch in the risk management approach; from the straightforward risk analyses during the design phase to a fully integrated risk management system with a dedicated risk management team during the construction phase.

The risk management team is positioned as a staff department but has very close relations with (financial) control, engineering and construction supervision, figure 4. By giving the risk management team a clear position in the project organisation and by clearly delineating the responsibilities, it proved possible to act proactively. The team is managed by the risk manager and consist of specialists (geotechnical, hydrological, environment engineers etc.) but also of generalists (account manager to licensing authorities and a monitoring coordinator).

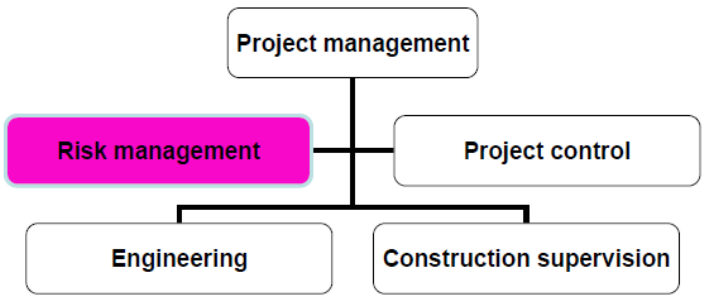

Figure 4. Position of risk management in the project organisation

This team was responsible for managing the so called ‘soft’ and ‘hard’ risks and the interaction of the two. The interaction is based on linking the ‘hard’ risk management, i.e. controlling risks by monitoring geotechnical and structural parameters, with the ‘soft’ risk management, figure 5. Examples of soft risk management are account management with important licensing authorities, dealing with the project environment and act as counter part of the insurance risk controller. Communication with these parties improved when it was demonstrated that risks and legal obligations were met using the monitoring results. In section 4 examples of ‘hard’ risk management will be given.

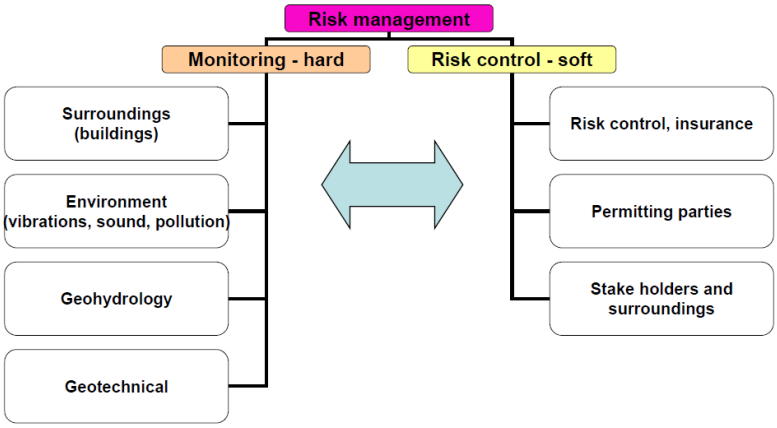

Figure 5. Organisation in risk management team

The main tasks of the risk management team are to ensure that remedial measures are actually implemented, to signal new risks and to make sure that all risks are allocated. This ‘risk monitoring’ is done in several ways. Firstly based on the actual monitoring results; unexpected behaviour of the ground or the structure may give indications of a risk about to occur. Secondly, risk based interviews and site visits, as well as communication with other team members on an almost daily basis, contributes to early risk detection.

4 MONITORING AS RISK CONTROL

4.1 *General*

The risk register at the end of the design phase gave significant input to the monitoring programme. Additional monitoring demands were based on legal obligations, insurance demands, safety requirements, demands from the project surroundings and research purposes. The monitoring programme has been made part of the contract specifications. The specifications gave detailed descriptions of how, what, where and when to monitor. Further the warning levels are defined as well as technical demands and reporting requirements.

Monitoring goes beyond just taking measurements. When using monitoring as a risk control tool the measurements should be compared with warning levels. For each monitoring parameter these levels are defined in advance. The warning levels consist of a signal level and an intervention level. When the signal level is exceeded, mitigating measures have to be implemented to avoid exceeding the intervention level. Exceeding an intervention level means that the risk of damage has become unacceptably high. The difference between signal- and intervention level is chosen in such a way that there is sufficient time to implement these mitigating measures.

A good example of risk defined monitoring deals with the requirement of the uninterrupted metro operation at all times during all construction works, see table 1 and 2. In this case monitoring serves to detect any changes in the deformational behaviour of the existing underground metro station. The main criteria for the warning levels were to assure the structural integrity of the existing metro station and safe operation of metro traffic, Berkelaar et al. (2007).

4.2 *Monitoring as risk control - example 1*

One of the first building activities was pile driving just north of station section A4. Within 4 weeks time a vertical deformation of 22 mm was detected, figure 6. Based on demands on the structural integrity of the

station the warning level was set at 35 mm and the intervention level at 50 mm absolute vertical displacement. The measured vertical deformation was directly related to the pile driving. Exceeding of the signal level could be expected shortly considering the development of the deformation. It was therefore decided to change the installation method of the piles by adding a pre-drilling phase. After this no significant additional settlement took place. The risk of disrupting metro traffic was therefore controlled effectively.

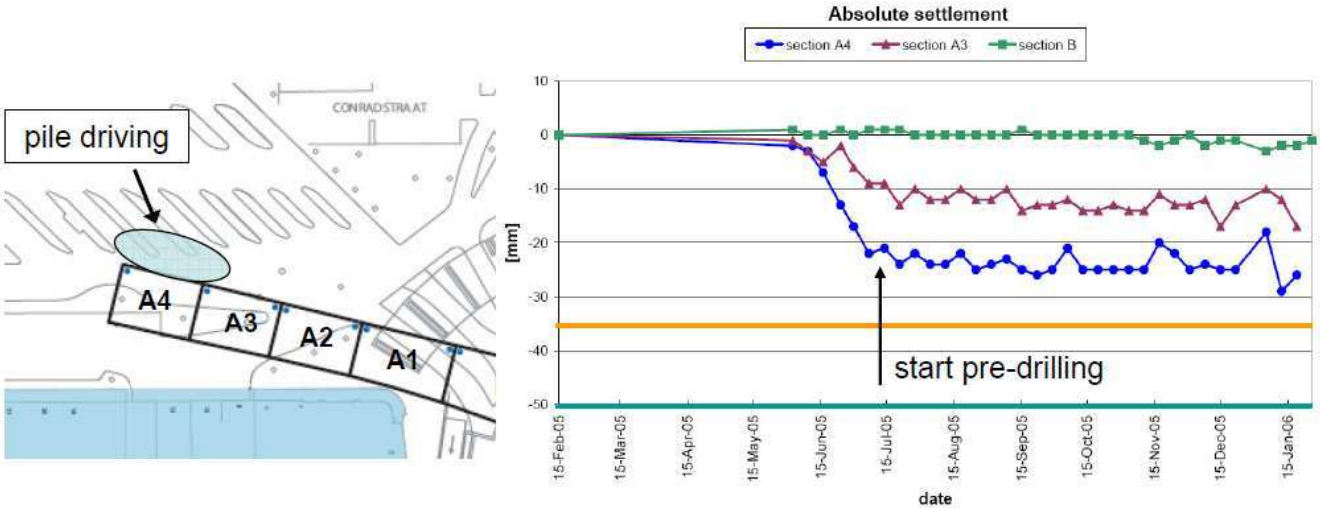

Figure 6. Example 1, Monitoring as risk control

4.3 *Monitoring as risk control - example 2*

An important warning value for safe metro operation was the differential settlement over station section joints. Figure 7 shows the development of the deformation over the joints. The warning levels were set at ±8 and ±10 mm. When the signal value was exceeded the operator of the station was informed. The operator decided to execute track corrections at the moment the intervention value was reached. After the track correction on joint W13-W14 the measurements were reset (not shown in figure 7). This case shows that monitoring proved to be very helpful in controlling the risk of disruption of metro traffic.

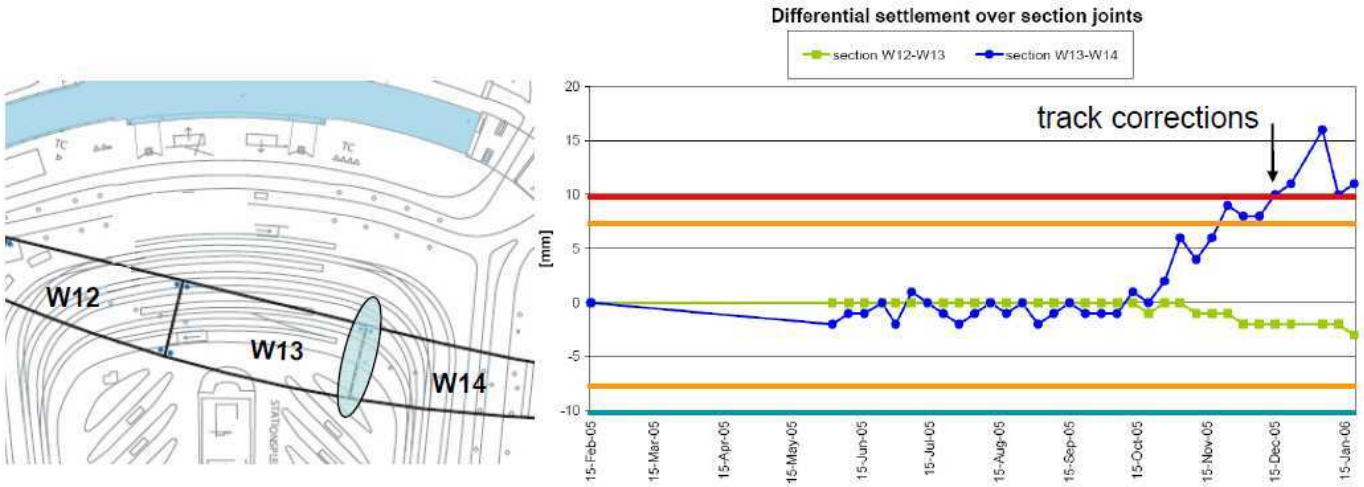

Figure 7. Example 2, Monitoring as risk control

4.4 *Monitoring as risk control - concluding remarks*

Full accessibility of all services in and around the underground metro station was maintained during all building activities so far. Monitoring proved to be very useful in controlling the risk of disruption of metro traffic caused by deformation of the station. However, not all risks can (completely) be controlled with monitoring. There is always the chance of the unexpected.

5 THE UNEXPECTED

Just before Christmas in 2007 a major leak occurred at a joint of the diaphragm wall at the time the maximum excavation depth of 14 m was reached. A huge amount, over 100 m^3/hour, of water and sand entered the building pit. Monitoring did not reveal any warnings before the leakage took place.

Immediately the four rigs for installation of Tubex-grout injection piles under the existing metro station were hoisted out of the building pit. Pumps to remove the water out of the building pit were installed and the public area was closed off because of the rapidly developing ground surface settlements. At the same time monitoring was intensified to check the possible deformations of nearby buildings. A poly urethane (PU) foam was injected to seal of the leakage, but it appeared that this could not solve the problem. The foam was washed away due to the enormous amount of water entering the building pit. After this it was decided to reduce the ground water flow by installing two drainage wells outside the building pit. Due to the reduction of the flow it was now possible to inject the PU-foam effectively. The final solution consisted of a sheet pile wall outside the building pit with jet grout piles, Thumann et al. (2009).

During the leakage an estimated 500 to 600 m^3 of sand entered the building pit. This resulted in an extensive ground surface settlement in an area of about 25 m by 25 m. Close to the leak the settlement was estimated to be over 2 m, figure 8.

Figure 8. Photographs of leakage and ground surface settlement

The above shows that, although monitoring can be very useful in risk control, one should always be prepared for the unexpected. When incidents as described occur, a fast switch from risk control to accident control has to be made. In these situations it is important to have good (alarm) procedures and have a good team (principal and contractor) to cope with the problem, resilience is essential. Risk management is a very useful tool to define the alarm procedures.

6 CONCLUDING REMARKS

From the risk management approach and case histories as described in this paper following concluding remarks can be made:

- It is important to make a difference in the approach in risk management during the design and the construction phase of a project. Straightforward risk analyses do not always meet the required level of risk management.
- Risk management should be given an explicit place in the project organisation. Risk management has to be visible. Depending on the contract type you have assign risk managing responsibilities.
- The most prominent risk, interference of operation of the metro station, did not occur. Full accessibility of all services was maintained during all building activities.
- Determine warning levels for each monitoring parameter and mitigation measures before construction works starts which can be taken when the warning levels are exceeded.
- Technical monitoring can be very useful in controlling risks, but be aware of the unexpected.

REFERENCES

Berkelaar, R., Huisman, L. & Luijten, C.J.L.M., 2007, Monitoring the underground metro station Rotterdam CS, a case study, Proceedings 7th FMGM, Boston, USA, 2007.

Thumann, V.M. & Haβ, H., 2007, Application of ground freezing technology for a retaining wall at a large excavation in the centre of Rotterdam, the Netherlands, Proceedings 14th ECSMGE, Madrid, Spain, 2007.

Thumann, V.M., Hannink, G., & de Doelder, B.R., 2009, Ground freezing and ground water control at underground station CS in Rotterdam, Proceedings 17th ICSMGE, Alexandria, Egypt, 2009.

Van Zanten, D.C. & Thumann, V.M., 2008, Engineering highlights of RandstadRail in Rotterdam, the Netherlands, Geotechniek, April 2008.

ISGSR 2011 - Vogt, Schuppener, Straub & Bräu (eds) - © 2011 Bundesanstalt für Wasserbau ISBN 978-3-939230-01-4

Probabilistic risk assessment of excavation performance in tunnel projects using Bayesian networks: a case study

O. Špačková
Czech Technical University in Prague, Czech Republic
D. Straub
Engineering Risk Analysis Group, TU Munich, Germany

ABSTRACT: A model for probabilistic assessment of excavation performance of tunnel projects is presented. The model is based on Dynamic Bayesian Networks (DBN) and enables to consider the quality of the design and construction process. It is applied on a case study, the excavation of a road tunnel by means of the New Austrian Tunnelling Method. The influence of main model parameters and assumptions (e.g. quality, distribution of unit time) is assessed through a sensitivity analysis.

Keywords: Tunnel, Risk, Excavation, Bayesian networks.

1 INTRODUCTION

Tunnel projects are prone to escalations of construction costs and duration. On average, final construction costs of tunnel and bridge construction projects are 34% above original estimates, and there has been no improvement over the past seventy years (Flyvbjerg et al. 2004). New techniques, which would improve the accuracy of these estimates and which would enable a systematic learning from past projects, are therefore needed.

Construction costs and duration are usually estimated by means of expert judgements. While these are irreplaceable, they should be underpinned by objective models, which enable a better quantification of the uncertainties associated with these predictions. Existing probabilistic models for tunnel projects are mostly based on Monte Carlo (MC) simulation of the construction process (Min et al. 2008, Chung et al. 2006, Ruwanpura & Ariaratnam 2007). Other models use Bayesian networks (Sousa 2010), artificial neural networks (Benardos & Kaliampakos 2004) or analytical solutions (Isaksson & Stille 2005). The models are mostly able to describe in detail the uncertainties in the prediction of geotechnical conditions and common variations of performance rates or unit costs, but in general they fail to consider the impact of other factors. These include extraordinary events (e.g. cave-in collapse, fires, flooding) as well as human and organizational factors. In particular the latter lead to a significant increase in the uncertainty of the final project cost and duration and should be included in a realistic model.

The proposed probabilistic model of tunnel projects aims to overcome the above-mentioned gaps. It utilizes dynamic Bayesian networks (DBNs) to model the process of tunnel construction, particularly the time needed to execute the excavation with regard to uncertain geotechnical conditions, varying unit time and quality of design and construction. In contrast to the DBNs models presented in Sousa (2010), the proposed model includes the full probability distributions of random variables such as unit time and cumulative (total) time even if it discretizes them.

The suggested model is applied to a case study which was taken from Min (2003). In the original work, the Decision Aids for Tunnelling (DAT) tool based on MC simulation was used for probabilistic assessment of construction time and costs. The DAT model has been developed since the 80s, and has been applied to a number of projects. In the case study described in this paper, the same assumptions as in the original model are first utilized in order to verify the results of the DBN model. In the second step, additional aspects (such as the influence of the human factor, adjustments of the unit time distributions, variable length of excavation cycles) are included in the DBN model and their effect on the final estimate is described within a sensitivity analysis.

2 BRIEF INTRODUCTION TO BAYESIAN NETWORKS

Bayesian networks (BNs) are directed acyclic graphical models that represent the joint probability distribution of a set of random variables. The nodes of the BN are random variables, while the directed links between them characterize their dependencies. Because of their graphical nature, BNs can be highly efficient for modelling and communicating complex models involving large numbers of random variables. BN have recently found a number of applications in engineering (Faber et al. 2002, Friis-Hansen 2004, Grêt-Regamey & Straub 2006, Langseth & Portinale 2007, Straub 2009). Detailed introductions to BN can be found in (Jensen & Nielsen 2007).

An example of a BN is depicted in Figure 1a. Here, the random variables are geology (G), construction time (T) and cost (C) and the causal dependence between them is represented by the links in the BN. In BN terminology, G is called a *parent* of T and C, whereas C is called a *child* of G and T. Each node is described by its probability distribution conditional on its parents. As an example, the distribution of construction time T is described conditional on the geology G; this conditional distribution is denoted as $p(t|g)$. Applying the chain rule, the joint probability distribution of this BN is obtained as

$$p(g,t,c) = p(g)p(t|g)p(c|t,g)\ . \tag{1}$$

In general, for any BN it holds that the joint probability distribution of the whole network is defined as the product of the conditional probabilities of all the nodes given their parents. In this way, the BN efficiently decomposes the joint probability distribution into local (conditional) probability distributions.

Stochastic processes describing the development of a system in time or space can be modelled by Dynamic Bayesian Networks (DBNs), an example of which is shown in Figure 1b. The ith slice of the DBN represents the state of the system in time/position i, here consisting of the two random variables G_i and T_i. The joint probability of G_i and T_i is obtained as

$$p(g_i,t_i) = \sum_{g_{i-1}} p(g_{i-1})p(g_i|g_{i-1})p(t_i|g_i), \tag{2}$$

where $p(g_{i-1})$ is the marginal probability distribution of random variable G_{i-1} describing the geology in slice $(i-1)$, $p(g_i|g_{i-1})$ is conditional probability describing changes of geology between neighbouring slices of the DBN and $p(t_i|g_i)$ is the conditional probability describing the construction time for given geological conditions.

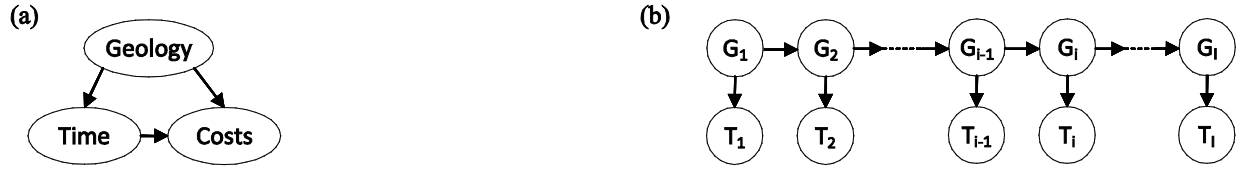

Figure 1. Example of (a) Bayesian network (BN), (b) dynamic Bayesian Network (DBN)

The graphical structure of the BN contains information on conditional independence of random variables in the network. In particular, once the state of variable G_i in the DBN of Figure 1b is known, the left and the right part of the network become statistically independent. More generally, if a DBN includes only links between neighbouring slices, it represents a Markov process. The basic feature of the Markov process is its single-step memory: once the state of the system at position or time i is known, the history of the process before position/time i can be neglected for making predictions about the future. The Markov assumption is commonly made in modelling tunnel excavation processes.

The goal of the DBN model is the computation of marginal probability distributions of selected random variables. In the context of the tunnel excavation, the interest is e.g. in computing the distribution of the total excavation time. A variety of algorithms exist for such computations. In the application presented in this paper, we use exact algorithms that require all random variables to be discrete. Details on exact algorithms for evaluating DBN can be found in (Murphy 2002).

3 MODELLING TUNNEL EXCAVATION PROCESS USING BAYESIAN NETWORKS

In the following, we present a BN model of the tunnel excavation process for a specific tunnel that was previously investigated by other researchers. This application facilitates the validation of the BN model, while it is sufficiently general to draw conclusions on the applicability of the model and to investigate the influence of the model assumptions.

3.1 *Tunnel specifics*

The Suncheon-Dolsan road tunnel is located in the south of South Korea between the towns Suncheon and Dolsan. The project and its modelling were described in Min (2003), Min et al. (2003), Min et al. (2005) and Min et al. (2008). The tunnel consists of two tubes with length of 1.9 km, of which we consider only one tube. The tunnel was constructed from both tunnel ends, the respective sections are denoted as section A (of length 610m) and section B (of length 1290m). In this paper, only results for section A are presented. The geometry and geotechnical zones as taken from Min (2003) are shown in Figure 2. The NATM with drill and blast technology was applied for excavation. Geological conditions in the area are good, consisting mostly of Micrographic Granite and Diorite. Based on the available investigations (borehole drilling, electrical resistivity survey and seismic exploration), five rock classes were defined by means of three parameters (RMR, Resistivity and Q-value) for modelling purposes.

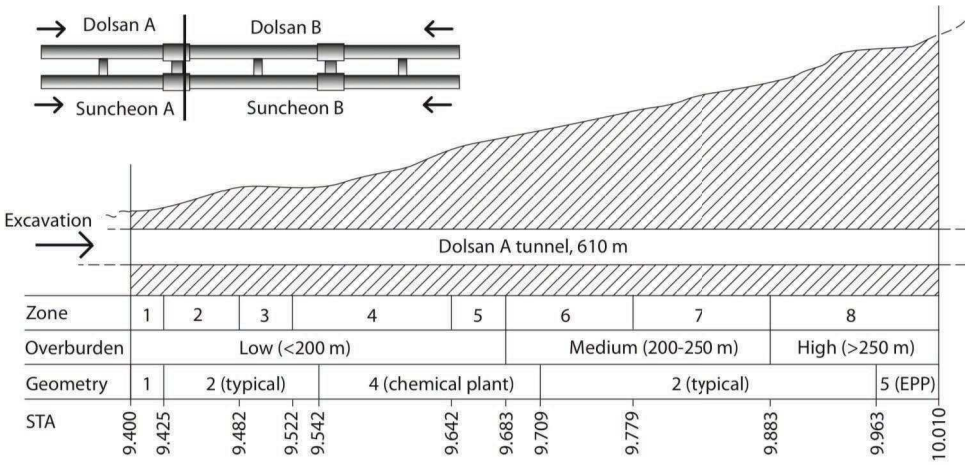

Figure 2. Scheme of the modelled tunnel

3.2 *Bayesian network model of tunnel excavation process*

A DBN model is developed to represent the various uncertain factors influencing the tunnel excavation process. Each slice in the DBN consists of random variables describing the uncertain geotechnical conditions and construction process variables in a tunnel segment of length Δl. The ith slice represents a tunnel segment from position $(i-1)\Delta l$ to position $i\Delta l$ along the tunnel axis. Within one slice, all random variables are modelled as constant, i.e. the states of the variables are fixed over the interval Δl. For this reason, Δl must be chosen in order to best represent the real excavation process, as discussed in Section 3.6.

Two alternative DBN models are shown in Figure 3. The variables of the models are described in Table 1. DBN (a) corresponds to the DAT model originally used in Min (2003). It should be remembered that the DAT does not use BN, yet every probabilistic model can be interpreted as a BN. DBN (b) displays an enhanced model, including additional variables and dependences in the construction process. Both DBN models are discrete-space Markov chain models. They are inhomogeneous, i.e. the conditional probability distributions of the variables are varying along the tunnel axis. Both DBN models are introduced in detail in the following sections.

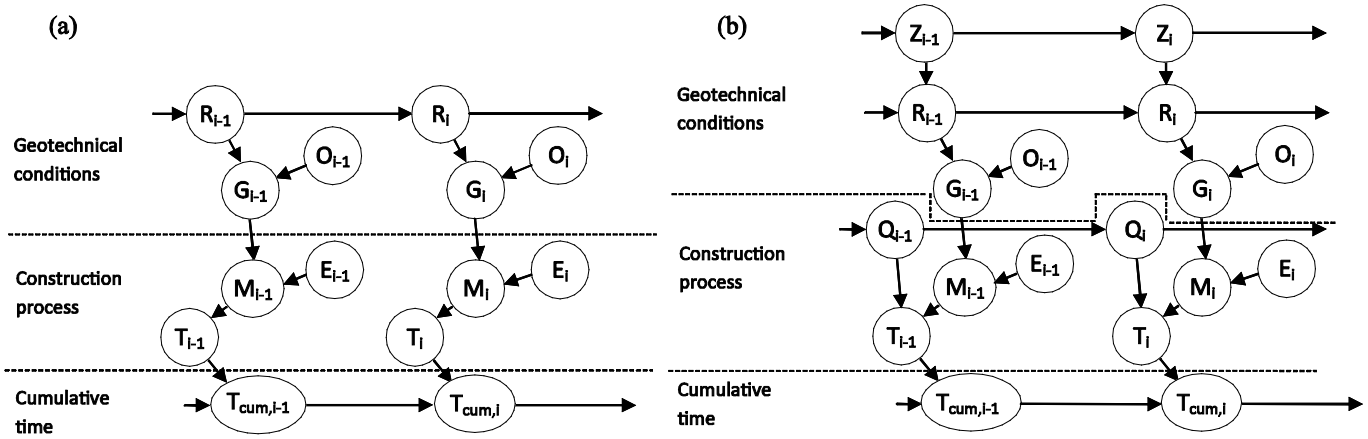

Figure 3. DBN for tunnel excavation: (a) Model with original assumptions. (b) Extended model. (The variables are explained in Table 1.)

Table 1. Overview of DBN model variables

Id.	Variable	Type	States of discrete/ type of continuous distribution
R	Rock class	Random/Discrete	I, II, III, IV, V
O	Overburden	Determ./Discrete	Low, Medium, High
G	Ground class	Random/Discrete	L-I, L-II, L-III, L-IV, L-V, M-I, M-II, M-III, M-IV, M-V, H-I, H-II, H-III, H-IV, H-V
E	Geometry	Determ./Discrete	1 (begin/end), 2 (typical), 4 (chem.plant) , 5 (EPP)
M	Construction method	Random/Discrete	P.1, P.2, P.3, P.4, P.5, P.6,P.2-1,P.2-2,P.2-3,P.EPP
T	Unit time	Random/Cont.	Triangular
Q	Quality	Random/Discrete	Poor, good, excellent
Z	Zone	Random/ Discrete	1,2,…,17

3.3 *DBN model of geotechnical conditions*

The geotechnical conditions within a slice i of the tunnel are described by the random variables rock class R_i, height of the overburden O_i, ground class G_i and, in the extended model, zone Z_i. For modelling the rock class R_i, the tunnel is first divided into zones within which the rock class can be modelled by the same conditional probability distribution. (In statistical terminology, rock class is a homogenous process within a zone.)

As evident from Figure 3, the spatial variability of rock class along the tunnel axis is modelled as a Markov process in both DBN models. The suitability of Markov processes for modelling of geotechnical parameters (including rock class, degree of jointing) along the tunnel axis was shown already in Chan (1981). Since then, the DAT model is based on continuous Markov process models. In the DBN model, the Markov process is discretized into a Markov chain (i.e. transformed to a discrete space represented by slices of the DBN). The rock class of each slice is described by a conditional probability table (transition probabilities), an example of which is given in Table 2. These conditional probabilities are derived from the parameters of the continuous Markov process reported in Min (2003), assuming that changes in rock class occur as a Poisson process, in accordance with Chan (1981).

Table 2. Conditional probability table for Markov model of rock classes in zone 1, for a DBN slice with length of $\Delta l = 4$m.

	R_{i-1}				
R_i	I	II	III	IV	V
I	0.1353	0.2149	0.2149	1	1
II	0.5707	0.3679	0.4172	0	0
III	0.2940	0.4172	0.3679	0	0
IV	0	0	0	0	0
V	0	0	0	0	0

In the enhanced DBN, the locations of borders of zones with statistically homogeneous rock class conditions are modelled as random by introducing the random variable Z_i. Let $\Pr(Z_i = k)$ denote the probability that the *i*th slice of the DBN is part of zone *k* and $\Pr(Z_{i-1} = k)$ the probability that the (*i*-1)th slice lies in zone *k*. Furthermore, let $F_{Bk}(x)$ be the known cumulative probability distribution function (CDF) of the location of the border between zones *k* and *k*+1. Assuming that probability distributions of zone borders are non-overlapping, the probability of the *i*th slice being in zone *k* can be determined as

$$\Pr(Z_i = k) = 1 - F_{Bk}\left(i\Delta l - \frac{\Delta \mathrm{l}}{2}\right) \tag{3}$$

The corresponding conditional probabilities are

$$\Pr(Z_i = k | Z_{i-1} = k) = \frac{\Pr(Z_i = k)}{\Pr(Z_{i-1} = k)} \tag{4}$$

$$\Pr(Z_i = k+1 | Z_{i-1} = k) = 1 - \frac{\Pr(Z_i = k)}{\Pr(Z_{i-1} = k)} \tag{5}$$

$$\Pr(Z_i = k+1 | Z_{i-1} = k+1) = 1 \tag{6}$$

The height of overburden O_i is modelled deterministically. The ground class G_i is defined deterministically for given R_i and O_i. As evident from Table 1, each G_i corresponds to a specific combination of R_i and O_i.

3.4 *DBN model of construction performance*

Construction performance in a slice i of the tunnel is described by the variables cross section geometry E_i, construction method M_i, excavation time T_i, and, in the extended model, design/construction quality Q_i.

The deterministic variable geometry E_i enables the variations of the cross section to be distinguished along the tunnel (e.g. typical cross section vs. extended cross section for emergency parking places EPP). It is also used to consider the special requirements for the construction process at the beginning/end of the tunnel and in the area where the tunnel passes underneath an existing chemical plant.

The applied construction method M_i describes the excavation type and the related support pattern and is determined conditional on the ground class G_i and tunnel geometry E_i. The modelling of M_i is taken from Min (2003), where the details of the different construction methods are described.

For every construction method M_i, the excavation time T_i is defined by a probability distribution $F(t_i|m_i)$. For representation in the DBN, the continuous distribution is discretized as described in Straub (2009). By not including a direct link between M_{i-1} and M_i, the model assumes full flexibility in changing construction methods from one slice to the next. In addition, it is assumed that changes of construction patterns are not connected with additional switch-over time. This neglects the fact that changes in the

excavation technology and the support structure can be demanding with respect to both time and costs (Sousa 2010).

In the extended model, the excavation time T_i is furthermore dependent on the design/construction quality Q_i. This additional variable represents the uncertain quality of design and construction works, which introduces dependence among the performance in each slice of the tunnel. The quality Q_i is in one of the three states "poor", "good" or "excellent" throughout the entire tunnel construction, i.e. the variable is fully dependent from one slice to the next and the conditional probability matrix $p(q_i|q_{i-1})$ in each slice is thus the 3x3 identity matrix. This simple model reflects the fact that the quality of a tunnel project cannot be directly measured and can only be deduced from the average performance over long sections of the tunnel project (Špačková et al. 2010). The quality influences the conditional distribution of the excavation time T_i: the better the construction quality, the lower the variability of T_i. For each state of Q_i and construction method M_i , a different distribution $F(t_i|m_i, q_i)$ is defined for the excavation time T_i.

3.5 *Calculation of the distribution of the total excavation time in the DBN*

In the application presented in this paper, the main output is the estimate of the total excavation time. In the DBN model, this is obtained by introducing the cumulative time $T_{cum,i}$ in each slice, defined as $T_{cum,i} = T_{cum,i-1} + T_i$. $T_{cum,i}$ represents the time needed for excavation of the tunnel from the beginning to location $i\Delta l$. Because exact inference algorithms are used for evaluating the DBN, in particular the Frontier Algorithm (Murphy 2002), both T_i and $T_{cum,i}$ must be discretized. Due to the required fine discretization of $T_{cum,i}$, and associated large number of states, the definition of the conditional probability table of $T_{cum,i}$ becomes impracticable. For this reason, the frontier algorithm was modified using a convolution function that allows defining the conditional probability table to be avoided. The new algorithm is computationally efficient (computations shown here take in the order of 20 - 180 seconds on a standard computer).

3.6 *Influence of slice length in the DBN model*

By choosing a slice length Δl in the DBN model, we make implicit assumptions about dependences among the variables along the tunnel. In the model, changes of conditions can only occur between slices. Therefore, Δl must be sufficiently small to capture the variability of geotechnical conditions along the tunnel axis, in particular the rock class R_i. This can be assessed by the probability that a change of R_i occurs within one slice. Using the Poisson assumption, this probability is $\Pr(Change) = 1 - \exp(-\Delta l / l_R)$ where l_R is the mean length of a particular rock class along the tunnel axis. For the Dolsan tunnel, l_R is in the range 1.5m – 43m. As a rule of thumb, a value of $\Delta l \leq l_R$ provides reasonable accuracy for modelling changes in the geotechnical conditions along the tunnel. This requirement must be considered along with other criteria.

Because the model assumes that the construction method in slice i is determined purely based on the geotechnical conditions (ground class G_i) and the cross section geometry E_i, it implies full flexibility in changing construction methods between slices. In reality, construction methods are only changed between excavation cycles. Therefore, for the model to be realistic, the slice length should not be shorter than the length of the excavation cycles. Unless otherwise specified, the calculations in this paper are based on $\Delta l = 4$m.

The conditional distribution used to specify the variables in the DBN must be adjusted for the slice length. In particular, the conditional probability table of R_i (as shown exemplarily in Table 2) must be calculated specifically for a given value of Δl using the Poisson assumption. Furthermore, the excavation time T_i depends directly on Δl. If the mean and variance of the time T_{ref} for a reference length Δl_{ref} are known, then the mean and variance of T_i are

$$\mathrm{E}[T_i] = \Delta l/\Delta l_{ref}\mathrm{E}\left[T_{ref}\right], \quad (7)$$

$$\mathrm{Var}[T_i] = \Delta l/\Delta l_{ref}\mathrm{Var}\left[T_{ref}\right]. \quad (8)$$

It is assumed that the probability distribution of T_{ref} is a triangular distribution. However, the choice of the distribution type has a little effect on the final results, due to the fact that the cumulative time is obtained as the sum of a larger number of T_{ref}'s.

4 NUMERICAL INVESTIGATIONS

4.1 *Original model - DBN in Figure 3a*

To validate the DBN model, the DBN in Figure 3a is constructed with the same assumptions as used in the DAT model presented in Min (2003). The resulting DBN is then applied to compute the total excavation time T_{tot} for the Dolsan A tunnel. Unlike in Min (2003), the delay between excavation of heading and bench was not considered in the DBN as it has little impact on total construction time and the excavation of the tunnel portal was not modelled because necessary data were not available. Even with these differences, the calculated mean value of T_{tot} is within 3% of the value given in Min (2003) and the standard deviation of T_{tot} is within 10% of the value given in Min (2003), as seen from Table 3.

The results presented in Min (2003) are based on an inconsistent definition of the probability distributions of the advance rates (it ignores the fact that the advance rate is defined as an average over certain lengths and that the variance of this average advance rate thus depends on the corresponding length of the tunnel). To overcome this inconsistency, the results presented in the following use the assumption that the variances of the advance rates given in Min (2003) are valid for 10m of tunnel excavation. With this assumption, the resulting T_{tot} is as given in Table 4. It can be observed that the variance of T_{tot} decreases compared to the results with the original definitions, where the given distributions of average advance rates are applied to sections that have lengths 10m – 120m.

Table 3**.** Comparison of results from DAT and DBN model (using the original assumptions of DAT)

	DOLSAN A	
Simulation type	Total constr. time (days)	
	Mean	St.dev.
DAT acc. to (Min 2003)	195	3.39
MC – discrete space	191	3.17
DBN	191	3.06

Table 4**.** Comparison of results from MC simulation and DBN model (using the modified assumptions of DAT)

	DOLSAN A	
Simulation type	Total excavation time (days)	
	Mean	St.dev.
MC – discrete space	190	1.66
DBN	190	1.64

4.2 *Extended model - DBN in Figure 3b*

In the extended DBN shown in Figure 3b, variables Q_i describing the design/construction quality and variables Z_i describing the uncertainty in the position of zone borders are introduced. The probability of different quality classes were assigned based on engineering judgement as $\Pr(Q = excellent) = 0.1$, $\Pr(Q = good) = 0.6$ and $\Pr(Q = poor) = 0.3$. The probability distributions of the excavation times T_i are now defined conditional on the quality; for projects with excellent quality, the distributions from the DAT model used above are applied. For projects with good and poor quality, distributions with higher variances are used. These models are based on data from a tunnel project in Czech Republic, which also used NATM, indicating that the variances of T_i are considerably higher than those given in Min (2003). (It is pointed out that the available data does not allow a representative statistic, but the observations cor-

respond with general experience on tunnel projects in the Czech Republic.) The conditional distributions of T_{Ref}, from which the distributions of T_i are calculated (see Par. 3.6), are shown exemplarily for a particular construction method in Figure 4. The calculations were performed under two different assumptions: (a) the mean value of the excavation times T_i is not dependent on the quality and is as in Min (2003) and (b) the mean value of the excavation times T_i is increased by a factor of 1.07 in the case of good quality and by a factor of 1.15 in the case of poor quality.

The comparison of the total excavation time T_{tot} for the Dolsan A tunnel with 610m length as calculated by means of the DBN model with the original assumptions and the extended DBN model is displayed in Figure 5. The variance of the T_{tot} is significantly higher with the extended model, in particular when including a dependence of the mean excavation time on the quality (case b), and is likely to more represent realistically the true uncertainties in the predictions of the tunnel construction process. The influence of the main assumptions in the extended DBN model is further studied in a sensitivity analysis.

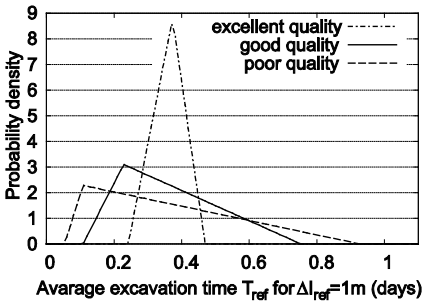

Figure 4. Excavation time distributions for construction method 4 under assumption (a) - same means for all qualities.

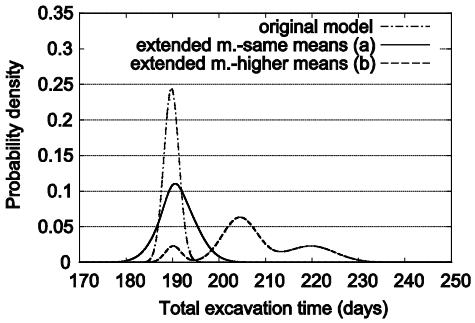

Figure 5. PDF of total time for excavation of Dolsan A tunnel – comparison of models.

4.3 *Sensitivity analysis*

Figure 6 displays the results of the sensitivity analysis performed with the extended DBN model (a). In Figure 6a, the influence of the spatial discretization is shown. With increasing slice length Δl, the variance of T_{tot} slightly increases. This is due to the assumption that the construction method can be freely selected for each slice. With the choice of a large Δl, a limited flexibility of the construction technology is assumed, which leads to a higher variance of T_{tot}. Figure 6b shows the influence of including the design/construction quality Q_i in the model. If Q_i is known to be excellent, the variance of T_{tot} is smaller than in the case of unknown Q_i. Finally, Figure 6c illustrates the effect of including the variables Z_i, which allow the position of the geotechnical zones to be modelled as random, in the DBN model. For this application, it is found that the consideration of this randomness has a negligible effect on the estimate of T_{tot}. However, this effect might be larger if the excavation times T_i would vary more strongly between different construction methods.

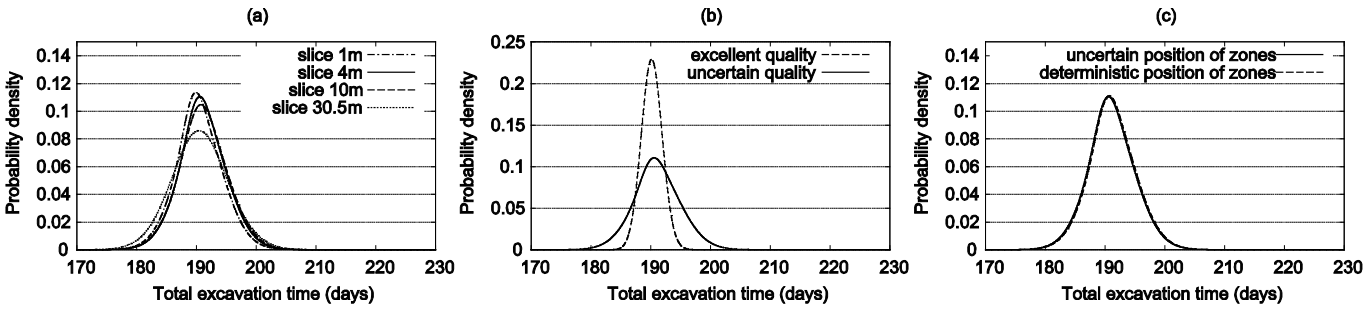

Figure 6. Results of the sensitivity analysis.

5 CONCLUDING REMARKS

A novel model for tunnel excavation processes based on Dynamic Bayesian Networks (DBN) was introduced in this paper. The main new feature of this model is that it explicitly includes the quality of the design and construction process. Because the quality is expected to be similar over the entire process, the uncertainty in the quality leads to an increased uncertainty (variance) of the estimate of the total construction time, which appears to reflect more realistically the actual uncertainties in tunnel projects. While it is not included in this paper, the modelling of the excavation cost can be performed analogically.

The main inputs to the DBN model, like to any other model of tunnel construction process, are the probability distributions of the excavation times (advance rates) for given construction methods and the geological conditions. When determining these probability distributions, due attention must be paid to the definition of these variables, since their variance is a direct function of the reference length (i.e. the length over which the advance rates are averaged). In our experience, estimates of the variances made by experts are not generally reliable (unlike estimates of the mean excavation times). Therefore, a next step will be to obtain more realistic estimates of these variances based on data from past tunnel projects.

The DBN model will be further developed along several lines. On the one hand, additional factors will be included in the model for assessing the full project risks. These include the switch-over time and cost as well as extraordinary events (e.g. cave-in collapses). On the other hand, the automatic updating of the model with observations made during the geological investigations and during the tunnel construction process will be facilitated. To this end, the algorithms for evaluating the DBN are currently further developed.

ACKNOWLEDGEMENTS

Funding by DAAD through the programme “Research grants for doctoral candidates” is gratefully acknowledged. Furthermore, this work has received financial support from the project SGS10/020/OHK1/1T/11 at the Czech Technical University in Prague and project No. TA01030245 of the Technology Agency of the Czech Republic.

REFERENCES

Benardos, A.G. & Kaliampakos, D.C. 2004. Modelling TBM performance with artificial neural networks. Tunnelling and Underground Space Technology 19, pp. 597-605.

Chan, M. H. C. 1981. A geological prediction and updating model in tunneling, M.Sc. thesis, Massachusetts Institute of Technology, Cambridge, USA.

Chung, T.H., Mohamed, Y. & AbouRizk, S. 2006. Bayesian updating application into simulation in the north Edmonton sanitary trunk project. J. of Construction Engineering and Management 8, pp. 882-894.

Faber, M. H., et al. 2002. Risk assessment of decommissioning options using Bayesian networks. J. Offshore Mech. Arct. Eng., 124(4), 231–238.

Flyvbjerg, B., Holm, M.K.S. & Buhl, S.L. 2004. What causes cost overrun in transport infrastructure projects? Transport Reviews, 24, pp. 3-18.

Friis-Hansen, P. 2004. Structuring of complex systems using Bayesian network. Proc., JCSS Workshop, DTU, Lyngby, Denmark.

Grêt-Regamey, A. & Straub, D. 2006. Spatially explicit avalanche risk assessment linking Bayesian networks to a GIS. Nat. Hazards Earth Syst. Sci., 6(6), 911–926.

Isaksson, T. & Stille, H. 2005. Model for estimation of time and cost for tunnel project based on risk. Rock Mechanics and Rock Engineering 23, pp. 373-398.

Jensen, F.V & Nielsen, T.D. 2007. Bayesian Networks and Decision graphs, 2nd edition. Springer, New York, USA.

Langseth, H. & Portinale, L. 2007. Bayesian networks in reliability. Reliab. Eng. Syst. Saf., 92(1), 92–108.

Min, S.Y. , Einstein, H.H., Lee, J.S. , Kim, T.K. 2003. Application of Decision Aids for Tunneling (DAT) to drill & blast tunnel. KSCE Journal of Civil Engineering, 7(5), pp. 619-628.

Min, S.Y. , Einstein, H.H., Lee, J.S. , Lee, H.S. 2005. Application of Decision Aids for Tunneling (DAT) to update excavation cost/time information. KSCE Journal of Civil Engineering, 9(4), pp. 335-346.

Min, S.Y. 2003. The application of decision Decision Aids for Tunneling (DAT) to the Sucheon tunnel in Korea. M.Sc. Thesis, Massachusetts Institute of Technology, Cambridge, USA.

Min, S.Y., Kim, T.K., Lee, J.S. & Einstein H.H. 2008. Design and construction of road tunnel in Korea including application of the Decision Aids for Tunneling - A case study. Tunnelling and Underground Space Technology 23, pp. 91-102.
Murphy, K. P. 2002. Dynamic Bayesian networks: Representation, inference and learning, Ph.D thesis, Univ. of California, Berkeley, Calif.
Ruwanpura, J. Y. & Ariaratnam, S. T. 2007. Simulation modeling techniques for underground infrastructure construction processes. Tunnelling and Underground Space Technology 22, pp. 553-567.
Sousa, R.L. 2010. Risk anpalysis of tunneling projects. Dissertation Thesis, Massachusetts Institute of Technology, Cambridge, USA.
Špačková, O. Ebermann, T., Kostohryz, O., Veselý, V., Šejnoha, J. 2010. Expert estimation of probability of failure during tunnel excavation. Tunel 19(4), pp. 15-23, Czech tunnelling association ITA-AITES.
Straub, D. 2009. Stochastic modeling of deterioration processes through dynamic Bayesian networks. J. of Engineering Mechanics 135 (10), 1089-1099.

ISGSR 2011 - Vogt, Schuppener, Straub & Bräu (eds) - © 2011 Bundesanstalt für Wasserbau ISBN 978-3-939230-01-4

Analysis of rock burst in critical section of second part of Karaj-Tehran Water Supply Tunnel

Khanlari. G. R
Bu_Ali Sina University, Hamedan, Iran.

Ghaderi-Meybodi, R.
Bu_Ali Sina University, Hamedan, *Iran*.

ABSTRACT: One of the geotechnical hazards in the tunnels under high overburden and high in situ stresses is the phenomenon of rock burst. Rock burst is a typical geologic phenomenon caused by excavation in rock masses. In this phenomenon, because of stress released and explosion in rock masses, they are broken as large and small pieces and are distributed, so that leads to damage of peoples or equipments. Therefore, familiar with this phenomenon and its mechanism of occurrence, is need to analyze this issue. The second part of water supply Karaj-Tehran tunnel with a length of 14 km and about 4.5 m diameter is located in Tehran province. Rock burst analysis has been carried out in the tunnel from kilometer 6 to 9.5 that is critical section because of high overburden (up to 800 m) and presence of faults and crushed zones. In this paper, for predicting rock burst in the critical section of second part of Karaj-Tehran tunnel, four criteria including, Strain energy, Rock brittleness, Seismic energy and Tangential stress criterion are used. Analysis results show that units with high overburden have high possibility of rock burst.

Keywords: Geotechnical Hazards; Tunnel; Rock burst; predict.

1 INTRODUCTION

When an excavation for a deep underground tunnel or chamber is undertaken in a strong and brittle rock, the change in stress results in dynamic damage to the adjacent rock, referred to as rockburst or break ways. Such rockbursts are a major hazard for the safety of engineers and engineering equipment as well as affecting the shape/size of the structure (Jiang et al., 2010).

The first recorded rockburst was in a British coal mine at Stafford in 1938(Jiang et al, 2010). Since that time there have been a number of reports of rock burst from all over the world. In recent years the importance of this geological hazard has become appreciated in infrastructure such as tunnelling and mining. Consequently rock burst has attracted a high degree of attention in engineering geology and rock mechanics. Cook et al. (1966), through experimental work, provided a theoretical method of predicting rockburst based on the opinion that violent damage of rock occurs when an excess of energy becomes available during the postpeak deformation stage. Brady and Leighton (1977) recorded a seismicity phenomenon before a moderate rock burst while Heunis (1980) introduced control strategies with regard to rockbursts in South African gold mines. At a seminar on 10 November 1983 E. T. Brown said, “It is difficult to reach an agreement on the definition of rock burst”.

Rock burst analysis has been carried out in critical section of second part of Karaj-Tehran tunnel because of high overburden and presence of brittle rock in tunnel route.

2 STUDY AREA

The second part of water supply Karaj-Tehran tunnel with a length of 14 km and about 4.5 m diameter is located in Tehran province which is located in the north of Iran (Fig. 1).

This tunnel is a part of water supply plan for the purpose of drinking water for Tehran. This tunnel is started from Amir Kabir Karaj dam and will continued to water softening (No: 6) of Tehran.

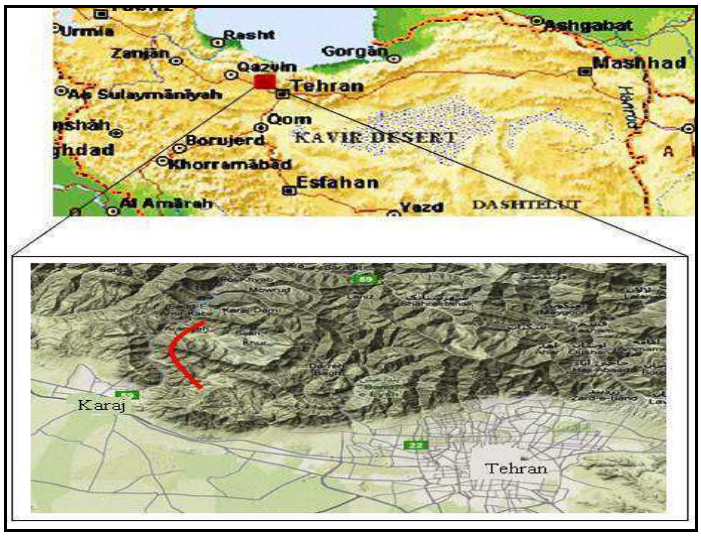

Figure 1. Location of study area in Iran (Alborz Mountain)

Rock burst analysis has been done in the tunnel from kilometer 6 to 9.5 as critical section because of high overburden (up to 800 m) and the presence of faults and crushed zones (Fig. 2). Engineering geological units in this section are formed with specific signs that are the initial letters of lithology of units.

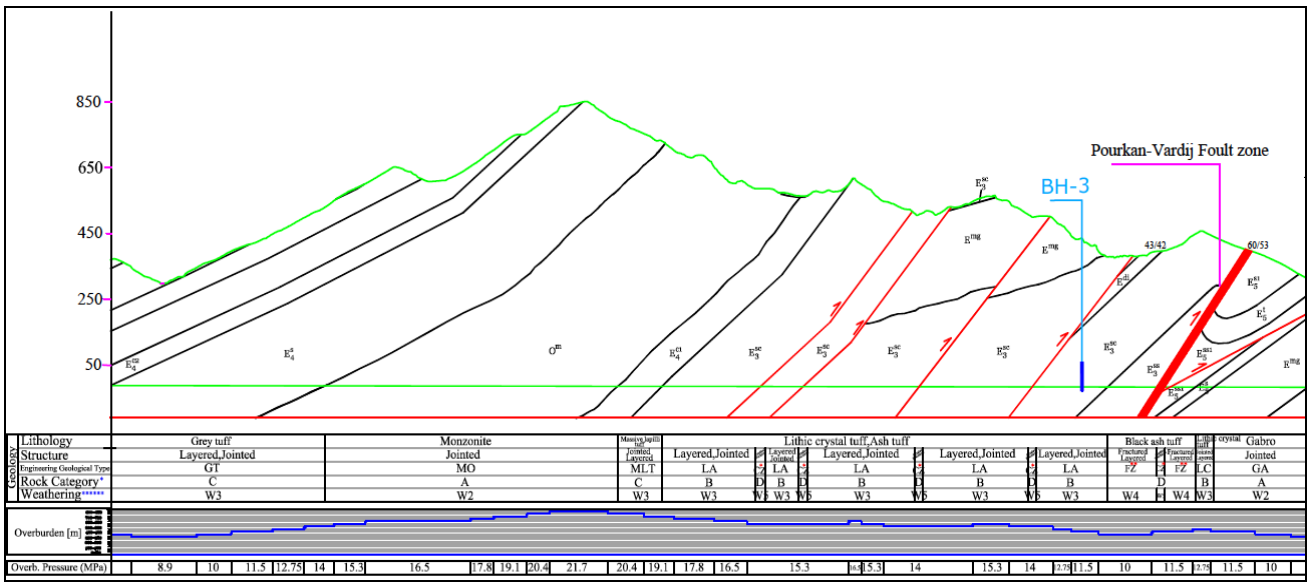

Figure 2. Critical section of Karaj-Tehran Tunnel route

3 ENGINEERING GEOLOGICAL STUDIES

Units of studied tunnel have been distinguished on the basis of some engineering geological characteristics such as lithology of layers, differences of structural features and geotechnical characteristics. In general, by considering the repeated units in different parts of the tunnel route, 20 engineering geological units were distiguished. Meanwhile, in the critical section, 8 units are located. Most units of critical sections have a pyroclastic source. This rock mass is including of many types of tuff such as MLT (Massive lapilli tuff), LA (Iithic crystal tuff, Ash tuff), LC (Lithic crystal tuff) and GT (Grey tuff). Igneous rocks of the studied section are Monzodiorite (MO) and Microgabro (GA).

There are several faults in the tunnel route. The main fault zone and crushed zone is Pourkan-Vardij fault zone that cuts the tunnel route in 6417 to 6442 meter from end of tunnel (Fig. 3). It should be noted, that CZ and FZ show crushed and fractured zone respectively due to fault activity.

Figure 3. A part of Pourkan-Vardij fault zone in tunnel route

For the study of strength and deformability properties of rock masses, a number of boreholes were drilled and needed core and block samples for laboratory studies have been selected. Some of geotechnical characteristics of intact rock that are essential for evaluation of rock burst problem are measured and are presented in Table 1.

Table 1. Some of geotechnical characteristic of intact rock of engineering geological units

Engineering geological units	saturated density (gr/cm^3)	Deformation modules (GPa)	Uniaxial compressive Strength (MPa)	Tensile strength (MPa)
GA	2.79-2.9	15-25	200-250	37.5
LC	2.3-2.7	20-40	100-150	4
LA	2.5-2.7	5-20	50-100	4
MLT	2.5-2.8	5-20	50-100	6
MO	2.55-2.8	15-25	100-200	32.5
GT	2.3-2.7	2.3-2.7	50-100	10
FZ	2.5-2.7	2.5-2.7	50-100	4
CZ	2.5-2.7	2.5-2.7	50-100	4

3.1 *Estimation of in situ stress*

The main origins of in situ stresses are geological conditions and geological history of the area. In general, estimating in situ stresses requires a detailed characterization of the site geology and considerable judgment (Amadei and Stephansson, 1997). Different expressions have been proposed in the literature for the coefficient K (ratio of horizontal to vertical stress).

Rummel (1986) presented an extensive literature review of stress variations with depth from deep hydraulic fracturing stress measurement conducted in various parts of the world and presented Eq. (2) for determining K_H and K_h at any depth. In this research, no field or laboratory test have been done for determination of stresses. Thus, they were calculated as:

$$\sigma_v = \gamma \times Z \qquad (1)$$

Where:

σ_v = vertical stress (MPa), γ = unit weight of rock mass (MN/m^3), Z = tunnel depth below surface in m. And for K_H and K_h (Amadei and Stephansson, 1997):

$$KH = 0.98 + 250/Z; Kh = 0.65 + 150/Z \qquad (2)$$

The results of equations are presented in Table 2. These empirical results are consistent with stress study at Amir Kabir dam site in the vicinity of Karaj-Tehran tunnel (Ahmadian et al.; 2007).

Table 2. Empirical results of stresses in Karaj-Tehran tunnel

Engineering units	Km from end of tunnel	Overburden (m)	σ_v (MPa)	K_H	K_h	σ_H (MPa)	σ_h (MPa)
GA	5971-6265	400	10.6	1.6	1.03	17.01	10.87
LC	6265-6322	500	13.25	1.4	0.95	19.61	12.59
FZ	6322-6417	450	11.925	1.5	0.98	18.31	11.73
CZ	6417-6442	450	11.925	1.5	0.98	18.31	11.73
FZ	6442-6559	400	10.6	1.6	1.03	17.01	10.87
LA	6595-6817	500	13.25	1.4	0.95	19.61	12.59
CZ	6818-6844	550	14.575	1.4	0.92	20.91	13.45
LA	6844-7171	550	14.575	1.4	0.92	20.91	13.45
CZ	7171-7197	550	14.575	1.4	0.92	20.91	13.45
LA	7197-7531	600	15.9	1.4	0.90	22.21	14.31
CZ	7531-7561	600	15.9	1.4	0.90	22.21	14.31
LA	7561-7663	600	15.9	1.4	0.90	22.21	14.31
CZ	7663-7693	600	15.9	1.4	0.90	22.21	14.31
LA	7693-7986	700	18.55	1.3	0.86	24.80	16.03
MLT	7985-8123	800	21.2	1.2	0.84	27.40	17.76
MO	8123-9037	700	18.55	1.3	0.86	24.80	16.03
GT	9037-9707	400	10.6	1.6	1	17	10.9

4 EVALUATION AND PREDICTION OF ROCKBURST

According to Zhang et al. (1994) rock burst is a type of brittle failure which occurs mainly in the rocks around tunnels and is associated with a sudden large release of latent pressures. Tao (1996) considered it occurs as a result of mechanical disturbance when the large quantity of strain energy accumulated within a rock mass is released suddenly, triggering a violent fracturing of the rock. Most authorities believe the main reason why rock bursts occur is related to the strain energy accumulated in a rock mass. However, the occurrence of rock burst depends not only on the accumulated strain energy but also on disturbance by external factors, e.g. Tao's "mechanical disturbance" (Tao, 1996). In tunnel constructions there are many such disturbances, e.g. explosion, vibration, stress impact from neighboring rock bursts, earthquakes, etc., all of which can be considered to involve dynamic loading (Blair, 1993).

Rockburst is one of the most complicated dynamic geological phenomena with intricate mechanism and numerous affecting factors, which accounts for the difficulty of predicting its characteristics. In the past few years, many methods of forecasting rockbursts, including rock mechanics assessment, stress detection and modern mathematical theories, have been proposed.

In this paper, for predicting rock burst in the critical section of second part of Karaj to Tehran tunnel, four criteria such as, Strain energy, Rock brittleness, Seismic energy and Tangential stress criterion have been used.

4.1 *Criterion of elastic strain energy*

Investigation (Kwasniewski et al., 1994) shows that the occurrence of shock and rockburst could be scaled by the so-called potential energy of elastic strain, PES i.e. the elastic strain energy in a unit volume of rock masses. Under uniaxial compression, the elastic strain energy stored in rock specimen prior to the peak strength is given by:

$$PES = \frac{\sigma_c^2}{2E_s} \tag{3}$$

Where, σ_c is the uniaxial compression strength (MPa), E_s is the unloading tangential modulus (MPa). In the opinion of Polish experts (Kwasniewski, 2000) if:

- PES<50 kJ/m^3, then the rockburst hazard is very low;
- 50<PES=100 kJ/m^3, then the rockburst hazard is low;
- 100<PES=150 kJ/m^3, then the rockburst hazard is moderate;
- 150<PES=200 kJ/m^3, then the rockburst hazard is high; and
- PES>200 kJ/m^3, then the rockburst hazard is very high.

4.2 *Criterion of rock brittleness*

Rock brittleness is defined by an index of the ratio of uniaxial compressive strength to tensile strength of rock, that is:

$$B = \frac{\sigma_C}{\sigma_T} \quad (4)$$

Where, σ_c is the uniaxial compression strength (MPa), σ_T is the tensile strength of the rock (MPa). Experimental study and in situ investigation of Qiao and Tian (1998) show that:

- B>40 then no rockburst;
- B=40-26.7, then weak rockburst;
- B=26.7-14.5, then strong rockburst; and
- B<14.5, then violent rockburst.

4.3 *Criterion of tangential stress*

This criterion considers both the state of in-situ stress in rockmass as well as the mechanical property of rock. The criterion of tangential stress is expressed by:

$$T_s = \frac{\sigma_\theta}{\sigma_c} \quad (5)$$

Where, σ_θ is the tangential stress in rockmass surrounding the openings or stopes (MPa) and σ_c is the uniaxial compressive strength of rock (MPa). The preliminary study (Wang et al., 1998) shows that:

- Ts<0.3, then no rockburst;
- Ts=0.3-0.5, then weak rockburst;
- Ts=0.5-0.7, then strong rockburst; and
- Ts>0.7, then violent rockburst.

To calculate the tangential stresses on the inner surface of the tunnel, Hook and Brown equations have been used (Palmstrom, 1996):

$$\sigma_{\theta r} = (A \times K - 1) P_v \quad (6)$$

Where, K is the ratio of horizontal to vertical stress, P_v is the vertical stress and K is 3 for circular tunnel. It should be noted that the tangential stress is calculated only on the roof of tunnel, because the amount of stress on roof is more and critical. The results of the three criteria described above with degree of rockburst are presented in Table 3.

Table 3. Determination of rockburst risk by using various criteria in the tunnel route

Engineering units	elastic strain energy criteria		rock brittleness criteria		tangential stress criteria		
	PES	Description	B	Description	tangential stress	Ts	Description
GA	1266.6	very high	6.0	violent	40.44	0.18	no
LC	260	very high	31.3	weak	45.58	0.36	weak
FZ	100	low	12.5	violent	43.01	0.86	violent
CZ	100	low	12.5	violent	43.01	0.86	violent
FZ	100	low	12.5	violent	40.44	0.81	violent
LA	225	very high	18.8	strong	45.58	0.61	strong
CZ	100	low	12.5	violent	48.15	0.96	violent
LA	225	very high	18.8	strong	48.15	0.64	strong
CZ	100	low	12.5	violent	48.15	0.96	violent
LA	225	very high	18.8	strong	50.72	0.68	strong
CZ	100	low	12.5	violent	50.72	1.01	violent
LA	225	very high	18.8	strong	50.72	0.68	strong
CZ	100	low	12.5	violent	50.72	1.01	violent
LA	225	very high	18.8	strong	55.86	0.74	violent
MLT	225	very high	12.5	violent	61.00	0.81	violent
MO	563	very high	4.6	violent	55.86	0.37	weak
GT	225	very high	7.5	violent	40.44	0.54	strong

4.4 *Criterion of seismic energy*

An event that sending a substantial kinetic energy about 104 joules has been introduced, as a seismic phenomenon. In all seismic phenomena, a kinetic energy released from a particular source. The actual seismic energy source that cause explosions in rock, include changes of induce stress resulting from drilling and sliding on the discontinuities e.g. geological faults.

Seismic energy values (E_S) is calculated by using Spoties and Gar equations (Bieniawski, 1987):

$$LogE_S = 1.5M_L - 1.2 \quad \text{(Mj)} \qquad (7)$$

$$M_L = LogM_S - 1.16 \quad \text{(Richter)} \qquad (8)$$

Where, M_S is the magnitude of shear wave, M_L is the magnitude of longitudinal wave. In this case, a classification scheme from Cook (1977) is presented in Table 4.

To determine the average of magnitude of possible earthquake on Richter scale, the engineering geological studies of second part of Karaj to Tehran tunnel has been used. According to studies conducted on studied area, the mean maximum of magnitude of possible earthquake, are in the ranges $6.5 \leq M_S \leq 7.7$.

By using equations (7) and (8), we get:

$$-3.5 \leq M_L \leq -0.27 \Rightarrow -1.72 \leq LogE_S \leq -1.6$$

$$19.05\times10^{-3} \leq E_S \leq 25.1\times10^{-3}(Mj)$$

$$19.05\times10^{3} \leq E_S \leq 25.1\times10^{3}(j)$$

Using Table (4), a level of damage has occurred by seismic energy is exfoliation of rocks. So by considering the situation, a serious threat for personals and equipments, will not be considered.

Table 4. Seismic event properties (Bieniawski, 1987)

Degree of damage	Monthly frequency	Richter scale	Seismic energy (j)	seismic event
Development of joints	2000	-3.5	0.4	Weak shake
	300	-2	63	
	80	-1	2×10^2	Weak earth-quake
Exfoliation	20	0	6.3×10^4	
	6	1	2×10^6	
Weak rockburst	1.5	2	6.3×10^7	
Strong rockburst	0.4	3	2×10^9	
Violent rockburst	0.02	4	6.3×10^{10}	

5 CONCLUSION

Critical section of second part of Karaj to Tehran tunnel, because of high overburden (up to 800 m) and the presence of faults and crushed zones, has been analyzed for rockburst risk. By using four criteria that including Strain energy, Rock brittleness, Seismic energy and Tangential stress, rockburst analysis has been carried out and results show, units with high overburden and weak rockmass because of high in situ stress and tangential stress have a high potential of rockburst. One of these areas can be found in Pour-kan-Vardij fault zone.

6 ACKNOWLEDGMENTS

Hereby, writers of this article have declared their appreciation to the Coast Institute of Consulting Engi-neers due to their cooperation and assistance in this study.

REFERENCES

Ahmadian, S., Eliassi, M., Zareinejad, M., 2007. The calculation of principal stress directions dominated on Amirkabir dam, 25 Gathering of Earth Sciences.

Amadei, B., Stephansson, O., 1997. Rock Stress and Its Measurement, Published by Chapman & Hall, First edition.

Bieniawski, Z.T., 1987. Strata control in mineral engineering, John wiley&sons, NewYork, Toronto, pp.135-146.

Blair, DP., 1993. Blast vibration control in the presence of delay scatter and random fluctuations between blast holes. Int J Numer Anal Methods Geomech 17: 3.
Brady, BT., Leighton, FW., 1977. Seismicity anomaly prior to anomaly prior to a moderate rock burst–case study. Int J Rock Mech Min Sci, Vol.14(3), pp.127–132.
Cook, N.G.W., Hoek, E., Pretorius, J.P.G, et al, 1966. Rock mechanics applied to the study of rockbursts. SAIMM Vol.66(10), pp.436–528.
Heunis, R., 1980. The development of rock-burst control strategies for South-African-gold mines. J S Afr Inst Min Metall Vol.80(4), pp.139–150.
Jiang, Q., Feng, X., Xiang, T., Su, G., 2010. Rockburst characteristics and numerical simulation based on a new energy index: a case study of a tunnel at 2,500 m depth. Engineering Geology Environment, Vol.69(3), pp. 353-363.
Kwasniewski, M., 2000, private communication.
Kwasniewski, M., Szutkowski, I., Wang, J. A., 1994. Study of ability of coal from seam 510 for storing elastic energy in the aspect of assessment of hazard in Porabka-Klimontow Colliery. Sci. Rept. Silesian Technical University, 1994.
Palmstrom , A., 1996, Some practical applications of the rock mass index (RMi), Tunneling and Underground Space Technology, VOL.11, NO.3, pp.287-303.
Qiao, C.S., Tian, Z.Y., 1998. Study of the possibility of rockburst in Dong-gua-shan Copper Mine. Chinese J. Rock Mech. Eng. Žexp. 17, 917_921.
Tao, ZY., 1996. Geology and geophysics – fundamentals of rock mechanics. The Publishing House of China Geoscience University, Wuhan.
Wang, Y.H., Li, W.D., Li, Q.G., 1998. Fuzzy estimation method of rockburst prediction. Chinese J. Rock Mech. Eng. 17 Ž5., 493_501.
Zhang, ZY., Wang, ST., Wang, N., 1994. Principles of analysis in engineering geology. Beijing Geological Publishing House, Beijing, pp 86–298.

ISGSR 2011 - Vogt, Schuppener, Straub & Bräu (eds) - © 2011 Bundesanstalt für Wasserbau ISBN 978-3-939230-01-4

The Optimization of the Design of a Concrete Faced Rockfill Dam by the Application of Sand-Gravel Fill Zones

R. Haselsteiner & V. Balat
EnerjiSA Enerji Üretim A.S., Ankara, Turkey

B. Ersoy
Fichtner GmbH & Co. KG, Istanbul, Turkey

ABSTRACT: The design of the dam case study presented was changed during different design and planning stages, switching from an ordinary CFRD type to a quite sophisticated CFSGD with deep foundations. Whilst obtaining more detailed information on the geological conditions and the available fill materials the engineers responsible decided to use the alluvial deposits close to the dam area for the fill. Originally, the dam was to have shallow foundations on the alluvial deposits present before clay layers with considerable thicknesses were encountered within the dam foundation. Therefore, the complete foundation concept had to be changed to a deep foundation in a highly permeable alluvium. Additionally, the left bank suffered from landslides during initial excavation works for the energy tunnel inlet so that the stability and design adjacent to the left bank has to be re-evaluated and re-designed. After agreeing on the detailed design principles and a general dam design material, investigations are ongoing and the optimization of the dam design is expected to be completed before starting dam fill works in mid of 2011.

Keywords: CFRD, CFSGD, Sand-Gravel Fill, Rockfill, Meta-Flysch

1 INTRODUCTION

In Turkey a huge number of hydropower projects are under construction. Frequently, these hydropower projects are for dams of considerable heights of more than 50 m (Haselsteiner et al., 2009a, b). Due to the threat of energy scarcity and thanks to the privatization of the energy sector at the beginning of this millennium, Turkish hydropower projects face a remarkable pressure in regard to project costs and realization periods exerted by the private sector. While previously, the projects were mainly financed and coordinated by governmental organizations the private investors and owners go for profit. One of the dominant newcomer private energy companies in Turkey is EnerjiSA, a joint venture of the Sabanci Group (Turkey) and Verbund (Austria). The goal is to reach an installed capacity of P = 5,000 MW by 2015 with a portfolio which increases by half the existing capacity of hydropower projects. Sabanci as newcomer to the energy sector grows tremendously, while relying on the support of Verbund with its long experience and considerable knowledge in construction and operation of hydropower plants in Austria. Both partners split the shares and the investment equally.

One main development area of EnerjiSA and also Turkey is South-East Anatolia where mountainous regions give rise to some of the large rivers of Turkey such as the Euphrates, Tigris, Seyhan and Ceyhan. On the latter rivers some well-known dam Turkish projects have already been constructed. Among them are the Aslantas, Sir, Berke and Menzelet dams (Figure 1). Berke Dam was the highest double arch curvature dam in Turkey with a height of 201 m before Ermenek Dam with a height of 210 m edged it out by only a few metres. Deriner Dam is now already underway and shall be the highest dam in Turkey when measured from foundation to crest, reaching H = 247 m (Wieland et al., 2007).

With these dam heights one should not forget that 100 m high dams reflect a considerable challenge and risk, particularly when geology does not act as anticipated and foundation as well as dam fill material create challenging engineering tasks. One of those projects is EnerjiSA's Sarigüzel Dam and HEPP which is located on the Ceyhan River approximately 1.5 h drive away from Kahramanmaras not far from Adana in South-East Anatolia. Sarigüzel is EnerjiSA's second project on the Ceyhan River, upstream of Hacin-

inoglu and downstream of Kandil (Figure 1) - another two projects owned by EnerjiSA. The cascade which belongs to EnerjiSA further consists of Dagdalen upstream of Kandil. At a contributory downstream of Hacininoglu, EnerjiSA overtook the Sucati project; a smaller project with 7 MW installed capacity which is also the first high RCC dam in Turkey. An overview of the development of the project of EnerjiSA is given by Kaya et al. (2010) for the reference years 2009/10.

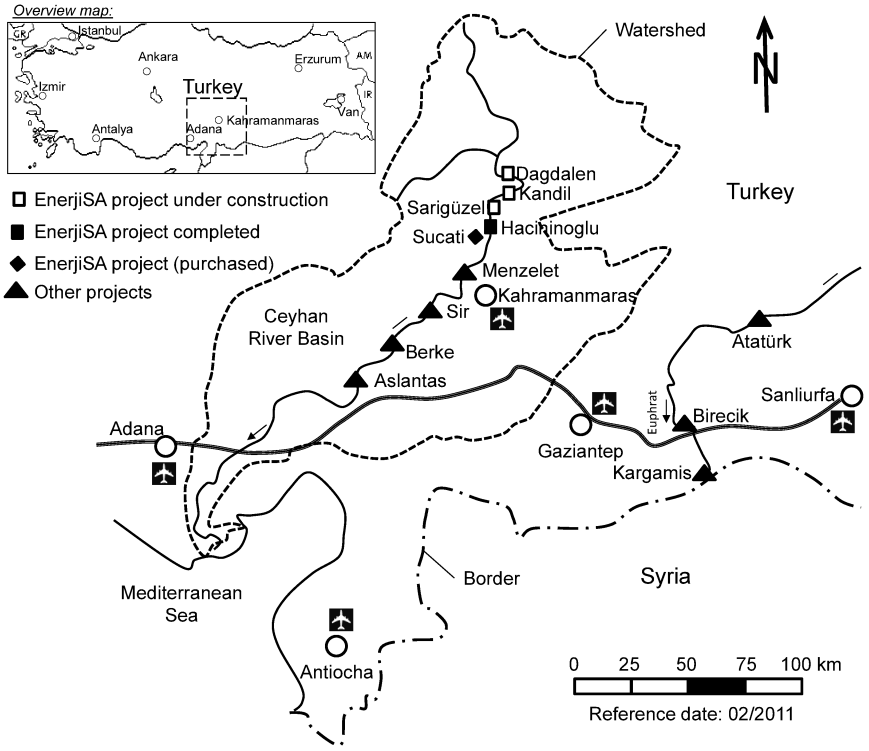

Figure 1. Ceyhan River Basin in South-East Turkey including EnerjiSA HEPPs and some large governmental projects

Although, the Turkish government initiated the "Güneydoğu Anadolu Projesi" (GAP) project consisting of over more than 19 large dams on the rivers Euphrates and Tigris decades ago, a number of large projects are still undeveloped in these regions, especially on the tributaries of these large rivers. One of the largest projects on a main stream which is part of the GAP project and is now under construction is the Ilisu project on the Tigris which has an installed capacity of P = 1,200 MW and a dam height of H = 130 m. This project faced much national and international resistance due to social and environmental impacts. Two of the most critical issues are the interference with important cultural heritage within the district town Hasankeyf and the large number of affected civilians. The project is being developed by the government.

Although, the Sarigüzel project is also a large dam the social and environmental impact assessment did not show serious impacts as the region does not have large settlements and/or cultural heritage within the project and reservoir area. Instead, the Seyhan and Ceyhan basins accommodate mountain torrents at high elevations. These are inhospitable conditions for big farms or settlements or for intensive agriculture. These conditions led only to small settlements which did not develop large cultural heritage and the people living there made their livings by extensive farming and livestock.

2 GENERAL CONDITIONS & DAM FILL MATERIALS

2.1 *General conditions*

The Sarigüzel Dam and HEPP has an installed capacity of approx. P = 104 MW including also an environmental powerhouse with an installed capacity of P = 3 MW. The total annual energy generation is assumed to reach A = 280-290 GWh/a (Haselsteiner & Ersoy; 2011a). The project consists of a dam and a headrace tunnel with a length of approximately six kilometres, two powerhouses and an ogee overflow spillway with six bays. Optimization measures may decrease the number of bays. The dam type and the general dam layout are discussed in the sections below.

In Table 1 the main data of the Sarigüzel project are summarized. Whereas some of the figures are taken from existing studies, some are still under discussion, particularly for the dam. These figures may be changed before detailed design is completed or even during the construction for optimization.

Table 1. Main basic data of the Sarigüzel project (see also Kaya et al., 2010; Haselsteiner & Ersoy, 2011a)

Item	Figure/data
Installed Capacity Main Plant P [MW]	101
Annual Generation Main Plant A [GWh/a]	257
Design Discharge Main Plant Q_D [m³/s]	111
Type of Units Main Plant	2 x Francis
Headrace Tunnel Main Plant L [km] / D [m]	5.5 – 6.0 / 6
Installed Capacity Env. Plant P_{Env} [MW]	3
Annual Generation Env. Plant A_{Env} [GWh/a]	25
Environmental Flow Q_{Env} [m³/s]	5.4
Catchment Area E_0 [km²]	6,500
Mean Annual Discharge Q_m [m³/s]	49
Maximum Probable Flood Q_{PMF} [m³/s]	4,863
Diversion Design Flood Q_{Div} [m³/s] / T [a]	546 / 25
Reservoir Volume $V_{R,tot}$ [Mio. m³]	≈ 50
Active Reservoir Volume $V_{R,act}$ [Mio. m³]	≈ 25-30
Normal Operation Reservoir Level [masl]	860
Minimum Reservoir Level [masl]	840
Dam type	CFSGD (former: CFRD)
Dam height H_D [m]*	≈ 80
Crest length L_C [m]	≈ 540
Dam Fill Volume V_D [Mio. m³]	≈ 3.1
Crest elevation [masl]	865
Upstream slope [1:V]	1.4 to 1.7
Downstream slope [1:V]	1.4 to 1.7

* Referring to thalweg elevation

2.2 *Geological and geotechnical conditions*

Special attention had to be paid to the occurrence of meta-flysch at the dam axis and along the headrace tunnel. The bedrock of both abutments consists of these metamorphic sedimentary rocks which show, particularly locally, poor rock properties and strengths. Additionally, the colluvium at the left bank suffered from a landslide caused by initial excavation works. Therefore, the left bank stability is being re-investigated and additional stability works will be executed. Fortunately, at the bottom of the left bank the quality of the meta-flysch is in better condition with regard to weathering, discontinuities and strength so that the occurrence of a global failure is unlikely to occur. Investigations are still ongoing for this subject.

Generally, two types of meta-flysch have been distinguished. Poor meta-flysch was characterized by an uniaxial compression strength of UCS = 10-15 MPa or smaller, whereas the stronger meta-flysch showed values of UCS > 15 MPa. Several specimens reached UCS > 30-50 MPa. Generally, the weaker meta-flysch is overlaying the stronger units at the left bank. Corresponding to the genesis of this formation some parts were classified as schist. The RMR values comprised a range of RMR = 30-40 on average (rough estimation) leading to values of GSI = 25-35. The stability of the left bank is still under investigation.

Before the construction works started, a drilling programme was undertaken that showed partly very poor TCR and RQD values. This led to a general underestimation of the geotechnical parameters of the rocks present. A second extensive drilling programme resulted in TCR values throughout of more than 90%, also comprising very weak, completely decomposed shear zones. This second drilling programme particularly contributed to a better understanding of the geology present. During the extensive drilling programmes the very weak shear zones were of major concern. Generally, these shear zones lead to decreasing shear strength between the potential shear surfaces which should not be affected by more than 10-20 % by the weak shear zones. The present metamorphic sedimentary rock types sand-, silt- and claystones are dominant.

The global orientation of the discontinuities, if valid for this kind of metamorphic rock formation, is considered to be favorable in terms of the global slope stability. Still, investigations and discussions are ongoing to determine the actual rock stress-strength and stress-shear behavior.

The local stability of the colluviums consisting of sandy-clay material with interbedded limestone blocks is dominated by an interface layer between the colluvium and the meta-flysch which showed very weak shear strength. After the landslide occurred at the left bank at the beginning of 2010, slickenside shear surfaces could be observed. Laboratory tests confirmed that the residual shear parameters correspond to typical slickenside surfaces showing φ_R = 12-15° and c_R = 0 kN/m². The colluvium itself shows peak strength parameters of approx. φ' = 25-30° and c' = 15-20 kN/m².

2.3 *Foundation conditions*

The Ceyhan River shows considerable alluvial deposits of more than 30-50 m thickness within the riverbed. Interbedded clay layers of several metres depth indicate large settlement if loaded. This was also the reason for the adjustment of the foundation design, since large settlements could not be excluded. The decision to change to deep excavation was taken reaching down to a depth of approximately 30 m corresponding to the depth that the clay layers were encountered.
Generally the alluvium shows permeable characteristics with $k \geq 10^{-4}$ m/s. Highly permeable coarse gravel layers are considered to be able to allow large seepage flow during the excavation of the foundation. This was the reason for applying cut-off walls up- and downstream of the excavated foundation area. Conversely, the abutments consisting of poor to medium classified meta-flysch show only very low permeability characteristics. The Lugeon values obtained do not exceed the value of approximately four Lugeon at an investigation depth down to 60 m below ground surface. The strength parameters are already described within the previous section.

2.4 *Available dam fill materials*

The availability of dam fill materials influenced the dam design considerably. Counter to initial expectations, when a rockfill dam design was favored, strong and decent rockfill material with an adequate volume was not encountered within a reasonable distance. Alternatively, the present alluvium was taken into consideration as dam fill material. In Figure 2 the site map is given of the Sarigüzel dam area. The alluvial deposits are close to the dam area mainly downstream of the dam. Still the volume of available materials is under investigation. Most of the areas are downstream of the dam axis. For materials in areas B, C and D field trial compaction tests were carried out.

During the first stages when no site testing had been performed and the borrow areas were not finally defined several sieve curves were prepared from some of the proposed borrow areas. In Figure 3 the sieve curve envelope for the main dam fill zone 3B is shown. Compared to benchmark curves the area 3B comprises sandy-gravels to gravelly cobbles/stones showing a maximum of over 50% of grains with block size. Benchmark data for sand-gravel fills are described in Cruz et al. (2009), Fell et al. (2005), Kutzner (1996) and Noguera et al. (1999). Generally, the dam fill material is considered to be very suitable as fill material if the technical specifications are defined appropriately.

The next step was to investigate all the borrow areas and test them in detail. The range of the sieve curves obtained is given in Figure 4 which more or less corresponds to the results of the first program. To be accurate, the material has to be classified as sandy gravel with low percentage of fines (< 10 %). Further processing cannot be excluded since some areas show very coarse material which may not give the predicted deformation requirements. The extraction and mixing process shall guarantee that no local alluviums with unfavorable gradations will be used.

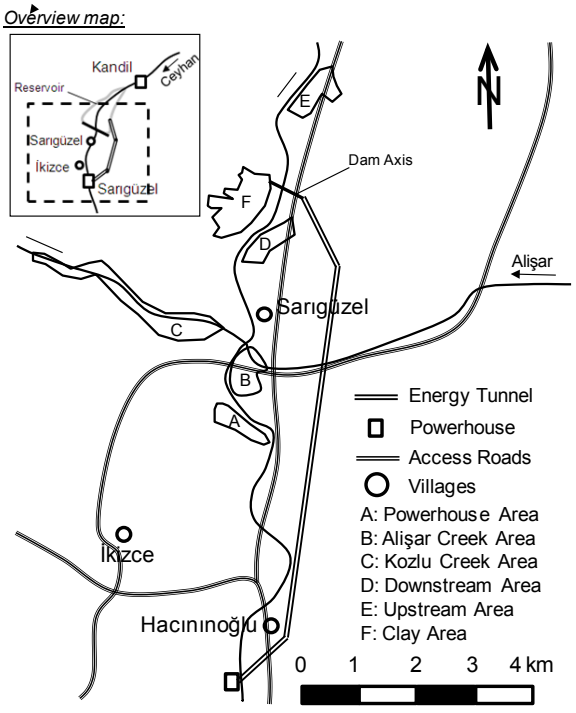

Figure 2. Sand-gravel fill (and clay) borrow areas A-E within the Sarigüzel project area

Laboratory and field trial compaction tests were carried out in order to determine the alluvium's parameters for construction conditions. Initial results are very promising, indicating a dry density of the compacted material of γ_d = 2.50 t/m³. For the time being, the layer height for zone 3B is most probably 60 cm applying four to eight passes, most probably six. Recent tests already indicate a deformation

modulus of E_{V2} = 200 MPa on average reaching peaks of 300 MPa for a 100 cm layer. Still higher values are expected which shall be confirmed by ongoing tests. Benchmark values (Fell et al., 2005; Cruz et al., 2009) confirm these high values for sand-gravel fill materials. The elasticity moduli of construction are approximately 3-4 times higher than for typical rockfill materials (Haselsteiner & Ersoy, 2011).

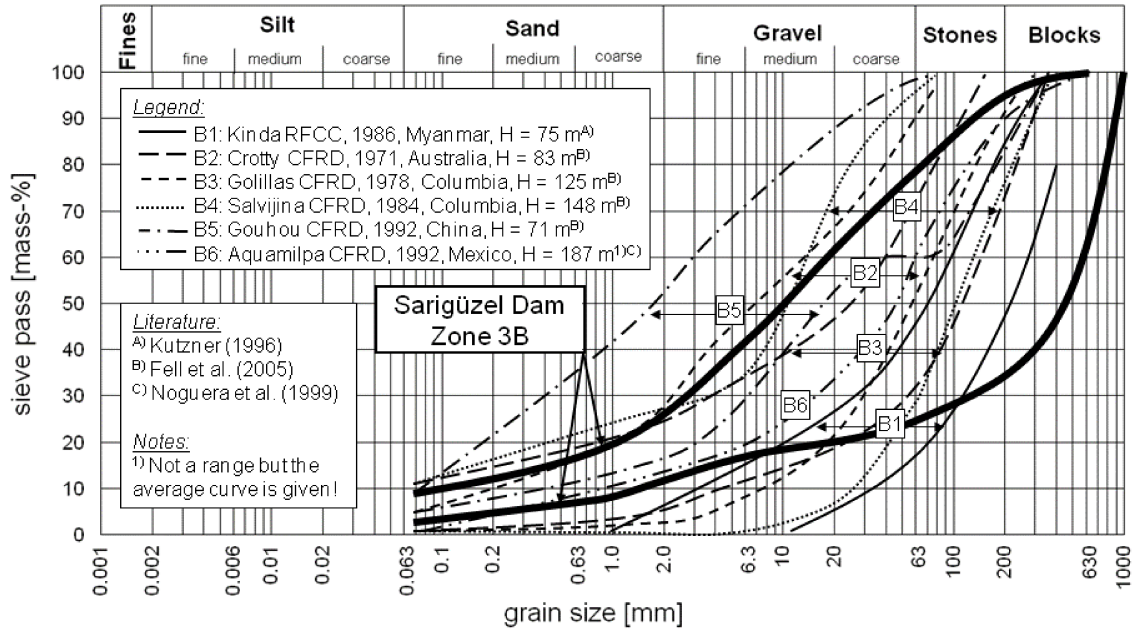

Figure 3. Sieve curve envelope for the sand-gravel fill material taken from several locations around the dam axis (1st stage investigation)

The resulting sieve curves during the 2nd investigation stage (Figure 4) do approximately correspond to the range of the sieve curves of the 1st investigation stage (Figure 3). Additionally, the field trial test embankments resulted in good material properties. Therefore, no concerns are directed to the applicability of the available material, particularly regarding the deformation characteristics.

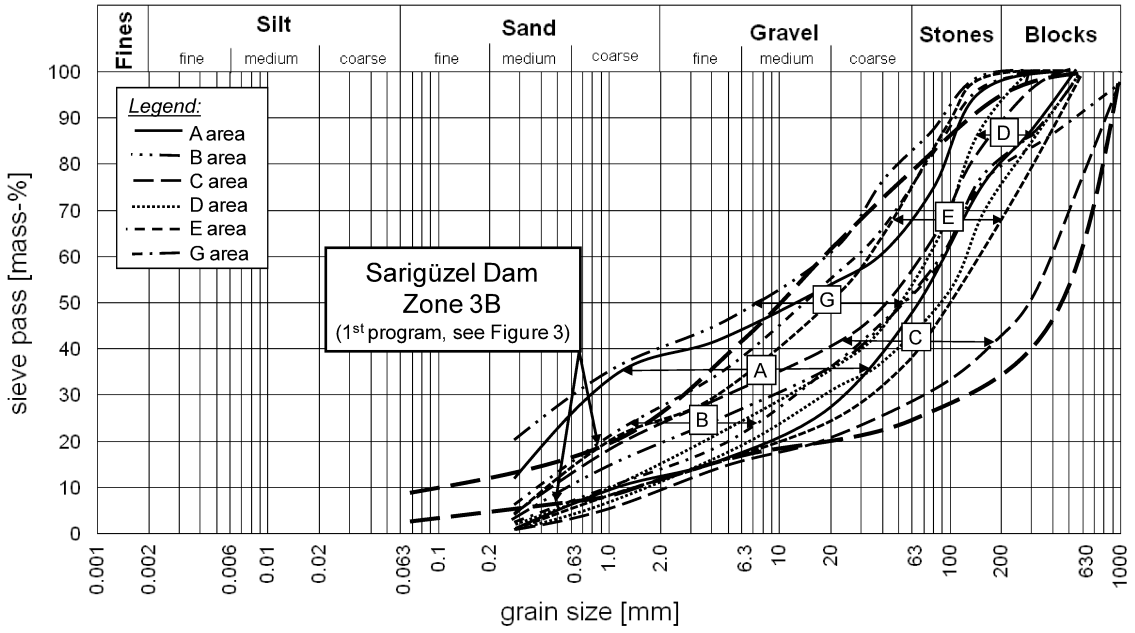

Figure 4. Sieve curve envelope for the sand-gravel fill taken from locations A, B, C, D, E and G (2nd stage investigations)

The optimum water content for compaction is still under investigation. Since the material will be extracted also underwater the natural moisture content maybe too high for immediate placement and compaction. The processing of the material will be adjusted for the results of the ongoing site trial tests which shall shed light on the range of applicable moisture content and on the deformation behavior. For the time being, the placement and compaction shall be done applying the natural moisture content of the material.

Currently, large scale triaxial tests have been agreed on and material was sent to Karlsruhe (Germany) which has a triaxial cell with a diameter of 80 cm (Bettzieche & Bieberstein, 2009). After receiving the test results the dam design will be revised again after consideration of stability and deformation aspects. Optimization is envisaged but is not guaranteed in advance, since sand-gravel fill materials show less favorable shear strength at low overburden pressures compared to rockfill materials.

Area G is not shown in Figure 2. Area F is not included in Figure 4 since its use for dam fill material is not decided.

3 DAM DESIGN DEVELOPMENT

3.1 *Clay Core Rockfill Dam*

During the different project phases, the dam type and design was changed several times and is still undergoing optimization. During the master plan the typical DSI (Turkish: Devlet Su Isleri; English: State Hydraulic Works) design for dams on moderate strong foundation was taken into consideration, which is a clay core rockfill dam (CCRF). These kind of dams are widespread in Turkey and are quite conservatively designed with slopes of V:H = 1:2.2-3.0. Since Turkey is a region prone to earthquakes this may be justified for single locations close to the Northern and Eastern Anatolia fault zone. With a conservative design the dam volumes show high values which is directly affecting costs and construction periods. For example, Akköprü Dam on the river Dalaman was finished recently after 15 years construction showing a volume of 13 Mio. m³ with a dam height of over 100 m and conservative flat slopes. This is not manageable for private companies which are dependent on profit. The second difficulty for a typical clay core rockfill dam is the availability of sufficient clay material. Since Sarigüzel is located in a mountainous region the clay borrow areas are limited.

3.2 *Concrete Face(d) Rockfill Dam*

Frequently, after private companies takeover a project from a governmental authority the feasibility studies are prepared, or if already available, are revised. The dam type is frequently changed to more efficient and economic dam type compared to CCRF, such as Concrete Faced Rockfill Dams (CFRD) and Roller Compacted Concrete Dams (RCC). Less frequently arch dams or other dam types are discussed or agreed on.

Sarigüzel Dam was also considered to be a CFRD dam assuming that enough rockfill material will be available within an economic distance of the dam axis. In this project phase, the possibility of using the large amount of alluvial deposits for the dam fill had still not been discussed. The CFRD should be partly founded on alluvial deposits. The plinth should be founded on bedrock after excavation of a limited depth of alluvium in the river bed.

3.3 *Concrete Face(d) Sand-Gravel Fill Dam*

Within a revision of the feasibility study the dam type was changed to a Concrete Face Sand-Gravel Fill Dam (CFSGD) due to the presence of a large volume of alluvium. The slopes were designed with H:V = 1.0:1.6-1.7 which is appropriate with regard to literature regarding stability and seepage control (Cruz et al., 2009). The dam volume increased compared to the former CFRD type. Seepage control was considered to be guaranteed by a L-shaped central drain layer (see Figure 5).

3.4 *Concrete Face(d) Sand-Gravel Fill Dam with Deep Excavation*

During the investigation in the course of the final design clay layers were detected within the river bed. The clay layers reach a thickness of several meters and are located deepest at 30 m depth below the river bed according to the available drilling data. This led to the decision for a deep excavation and backfilling with sand-gravel fill material as shown in Figure 6. In consideration of the expected seepage flow, upstream and downstream cut-off walls are to be used. Upstream, another cut-off wall shall connect the surface slab sealing to the underground sealing at the plinth.

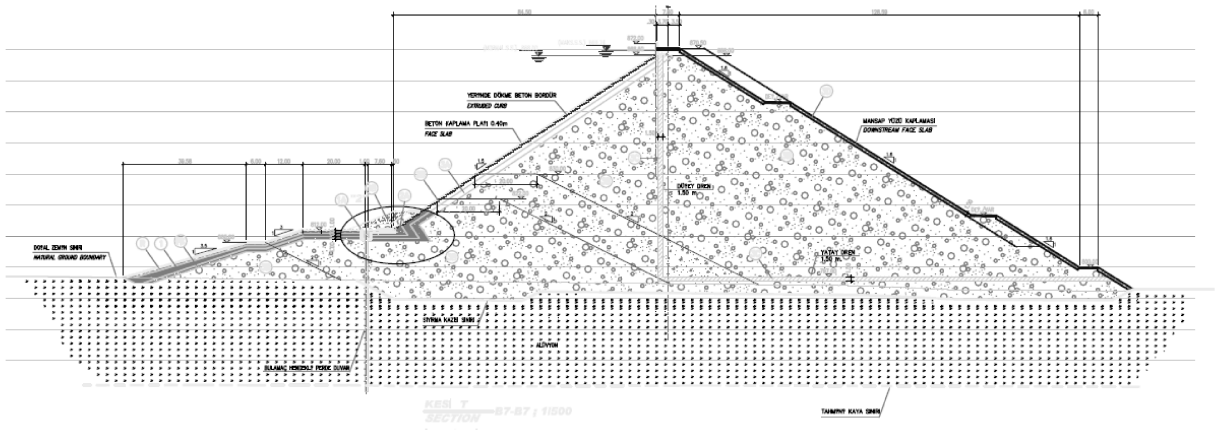

Figure 5. CFSGD with L-shaped drain founded on shallow alluvium

Since the design presented in Figure 6 still left a few critical questions open, such as the deformation of the concrete slab and the seepage control in case of cracks within the concrete face (see also Haselsteiner & Ersoy, 2011) the design is still under revision. The application of high friction rockfill at the upstream slope should have strengthened the slope in case of rapid drawdown, combining high friction at low stresses and high permeability. But, rockfill is, as mentioned above, more compressible than compacted sand-gravel fill and allows higher deformations and, therefore, is likely to lead to cracks in the slab.

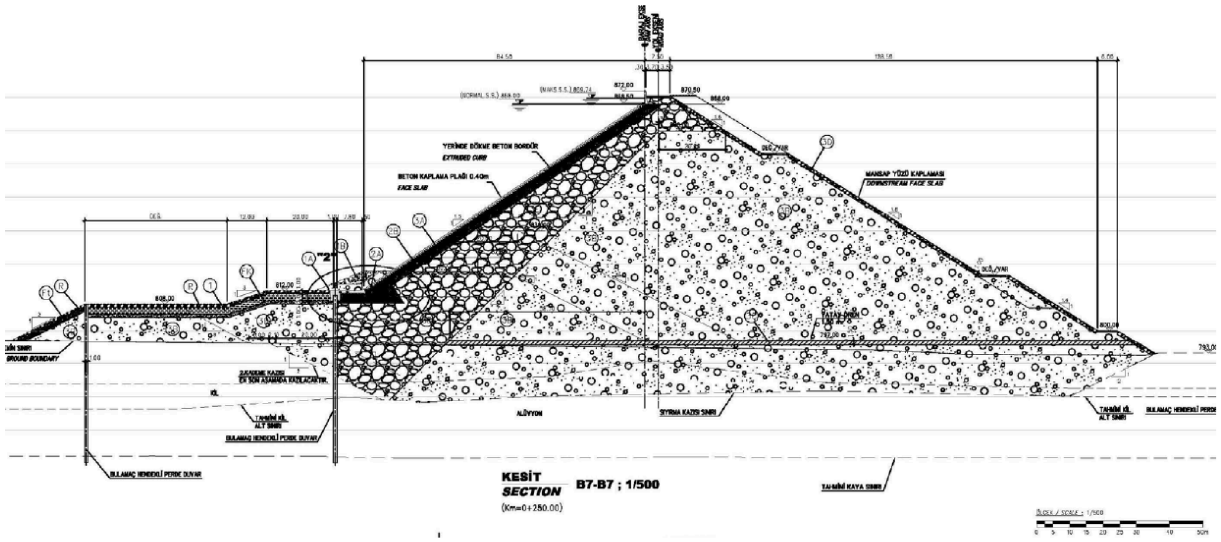

Figure 6. CFSGD with basement drain and rockfill beneath the surface slab and deep foundation

Due to the ongoing investigations and testing, a guideline dam design was prepared. This involves considering the typical dam design principles regarding stability, seepage and deformation (Figure 7). Under and close to the elements which are sensitive to deformations, low compressive and strongly compacted rockfill/sand-gravel fill shall be placed in consideration of the deformation requirements which are estimated by a 2D FEM deformation analysis.

After the field trial compaction tests are completed and the large scale triaxial test results are evaluated the design has to be reviewed and, most likely, revised. Other design options such as the application of a membrane on the surface slab are currently being discussed. The construction of the deep cut-off walls and the quality control are another issues within further discussions. Still the seepage behavior of the dam in case of cracks in the surface (Haselsteiner & Ersoy, 2011) is under investigation. For this purpose a drain toe consisting of selected rockfill material is considered to be valuable, improving both the seepage control function of the dam and the stability in terms of potential superficial sliding surfaces along the downstream slope.

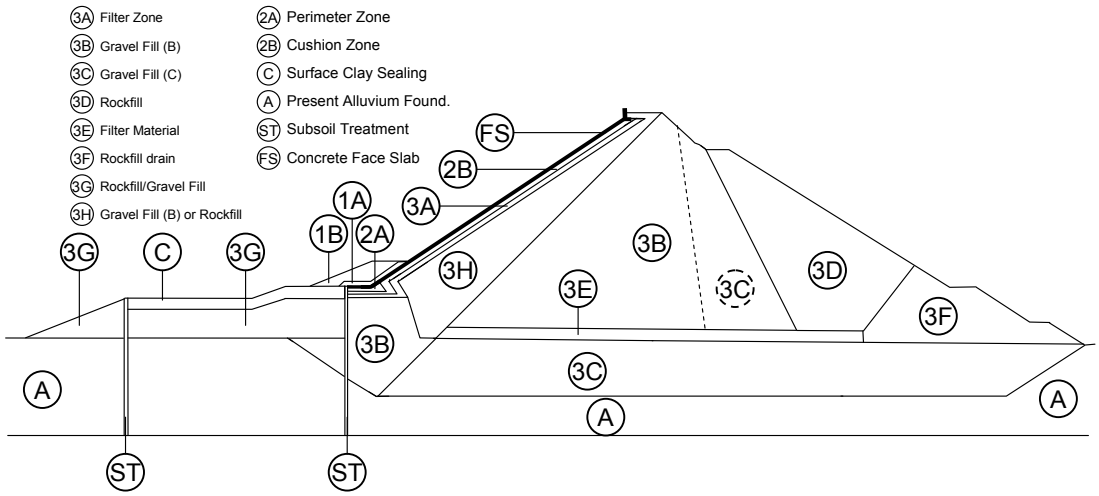

Figure 7. Guideline design for the CFSGD with basement drain, special zoning and deep foundation (adjusted after ANCOLD, 1991; ICOLD, 2005)

ACKNOWLEDGEMENT

The authors would like to thank the Design Engineer and the Consultants for their cooperation and their willingness to adapt new engineering ideas and approaches and adjust and optimize the dam design and the whole project persistently.

REFERENCES

ANCOLD 1991. ANCOLD Guidelines on Concrete-Faced Rockfill Dams. Australian National Committee on Large Dams (ANCOLD), Courtesy of the Hydro-Electric Commission (HEC) Tasmania.

Bettzieche, V., Bieberstein. A. 2009. Investigations of the Material of a 50 Years old Dam in the Course of the Deepened Examination. Long Term Behaviour of Dams (LTBD09), Technical University Graz, Austria, 12th –13th October 2009, Proceedings, pp. 743-748.

Cruz, P. T., Materon, B., Freitas, M. 2009. Concrete Face Rockfill dams. Dados Interncaionais de Catalogacao na Publicacao (CIP), Brazil.

Fell, R., MacGregor, P.; Stapledon, D.; Bell, G. 2005. Geotechnical Engineering of Dams. A. A. Balkema Publishers, Leiden London New York Philadelphia Singapore, 2005.

Haselsteiner, R., Ersoy, B. 2011. Seepage Control of Concrete Faced Dams with Respect to Surface Cracking. 6th International Conference on Dam Engineering, 15.-17.02.2011, Lisbon, pp. 611-628.

Haselsteiner, R., Ersoy, B. 2011a. Die Auslegung und Wirtschaftlichkeit von Restwasserkraftanlagen bei Großprojekten in der Türkei. 34. Dresdner Wasserbaukolloquium, Wasserkraft: mehr Wirkungsgrad + mehr Ökologie = mehr Zukunft", Institut für Wasserbau und technische Hydrodynamik (IWD), Dresden.

Haselsteiner, R.; Heimerl, S.; Arch, A.; Kohler, B.; Recla, R.; Bilmez, C.; Mesci, Ü. 2009a. Evaluation of small and medium hydropower in Turkey in consideration of economical aspects. Wasserkraftnutzung im Zeichen des Klimawandels - Waterpower and Climate Change. Dresdner Wasserbaukolloquium 2009, 12.-13. März 2009, Dresdner Wasserbauliche Mitteilungen, Heft 39, S. 335-358.

Haselsteiner, R.; Heimerl, S.; Arch, A.; Kohler, B.; Recla, R.; Bilmez, C.; Mesci, Ü. 2009b. Efficient Design, Construction and Maintenance of Hydropower Plants in Turkey. HYDRO 2009 - Progress, Potential, Plans, International Conference and Exhibition, Lyon, France, 26-28 October 2009.

ICOLD 2005. Concrete Face Rockfill Dams – Concepts for Design and Construction. International Committee on Large Dams – Committee on Materials for Fill Dams (Draft).

Kaya, S., Ücok, M, Evcimen, T. U. 2010. Case Studies of 6 Different Hydro Power Dams under Construction. 8th ICOLD European Club Symposium, "From research to design in European practice", 22th - 23th September 2010 in Innsbruck, Austria, Proceedings, pp. 105-110.

Kutzner, C. 1996. Erd- und Steinschüttdämme für Stauanlagen. Ferdinand Enke Verlag, Stuttgart.

Noguera, G.; Bellet, A.; Vidal, L. 1999. Design and Construction of Chile's Puclaro Dam. IWP & DC, September 1999, pp. 16-19.

Wieland, M., Aemmer, M., Ruoss, R. 2007. Die 249 m hohe Deriner Bogenmauer in der Türkei. Wasserwirtschaft 97/10, pp. 69-71.

ISGSR 2011 - Vogt, Schuppener, Straub & Bräu (eds) - © 2011 Bundesanstalt für Wasserbau ISBN 978-3-939230-01-4

Hydraulic Heave Safety at Excavations with Surcharge Filters

P. Schober & C. Boley
Bundeswehr University Munich, Neubiberg, Germany

B. Odenwald
Federal Waterways Engineering and Research Institute, Karlsruhe, Germany

ABSTRACT: When designing deep excavation pits next to waterways that are still being operated, verifying hydraulic heave safety is crucial to determine the necessary length of the pit walls. To reduce their embedment depth, a surcharge filter can be installed. However, studies based on numerical groundwater computations show that verification standards for hydraulic heave safety are not applicable for excavation pits with an installed surcharge filter. Standard approaches neglect significant vertical flow below the wall toe. A method which considers these flow forces was developed based on the numerical flow computations to determine reliably the necessary thickness of the surcharge filter. To examine this theoretical approach and the failure mechanism, several laboratory tests were performed which were evaluated with various methods.

Keywords: safety, groundwater, hydraulic heave, laboratory test, filter

1 INTRODUCTION

Installing deep excavation pits next to waterways which are still being operated has become a more and more frequent practice for construction measures to allow continued ship traffic. Verification of hydraulic heave safety is required to determine the length of the pit walls. To reduce the embedment depth of the walls, a surcharge filter can be installed at the pit bottom. Due to current construction measures on German waterways, the German Federal Waterways Engineering and Research Institute performed numerical groundwater flow computations. However, these brought up general questions on hydraulic heave safety in cases of a reduced embedment depth of the pit walls due to a surcharge filter installed inside the excavation pit. Odenwald and Herten (2008) already documented the results of the performed analyses in detail. Based on these, the Bundeswehr University Munich conducted comprehensive laboratory tests and evaluated these using various methods.

2 VERIFICATION OF HYDRAULIC HEAVE SAFETY

Lowering the groundwater level inside an excavation pit down to its bottom leads to groundwater flow to the excavation pit with an upward flow direction from the wall toe to the bottom of the excavation pit. If the thus caused flow force S suspends the buoyant weight of the soil G' as well as other possible stabilizing forces R, hydraulic heave results (Figure 1). This can lead quickly to the flooding of the excavation pit due to regressive erosion around the toe wall as well as to the collapse of the excavation pit.Based on the German geotechnical codes, hydraulic heave safety is verified according to approaches by Terzaghi-Peck (Terzaghi and Peck, 1948) or Baumgart-Davidenkoff (Davidenkoff, 1970). These use a simplified unstable block to determine the relevant forces. Both methods only compare the flow force S and the buoyant weight of the soil G'. Possible friction forces are neglected. Terzaghi-Peck's approach determines the forces with the help of a prismatic soil block whose height corresponds to the embedment depth t of the wall below the pit bottom and whose width corresponds to half of the embedment depth (b = t/2). Baumgart-Davidenkoff's approach uses a block whose width is negligible and whose height is

also the distance between the pit bottom and the wall toe. Since, in cases of undercurrent flow, the groundwater potential at the wall toe is always higher than the mean potential at the lower edge of the unstable block according to Terzaghi-Peck's approach, Baumgart-Davidenkoff's approach is always more conservative.

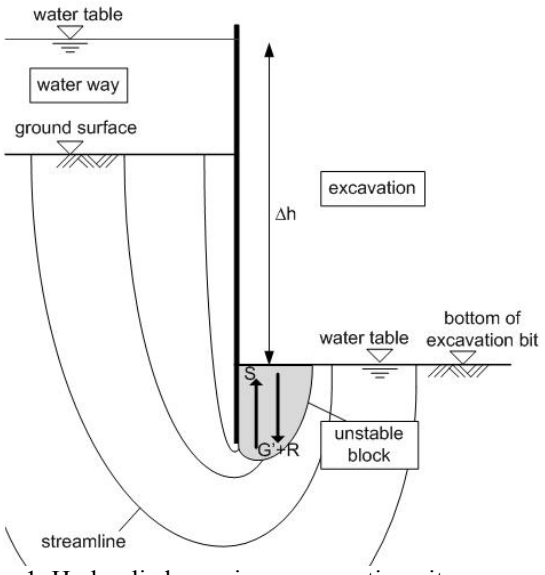

Figure 1. Hydraulic heave in an excavation pit

When using a surcharge filter, the height of the unstable block is the distance between the wall toe and the upper edge of the surcharge filter. The relevant width, however, according to Terzaghi and Peck (1948), corresponds only to a half of the embedment depth of the wall below the pit bottom. In this case, the weight of the surcharge filter needs to be considered as an additional stabilizing force. The installed surcharge filter needs to be filter stable against the soil below the pit bottom and may only cause a slight decrease of the groundwater potential. This means that the material used for the surcharge filter must be fine enough to prevent soil particles from being transported into the surcharge filter and coarse enough to allow the water penetrating the surcharge filter freely.

3 NUMERICAL GROUNDWATER FLOW COMPUTATIONS

3.1 *General*

The numerical groundwater flow computations were performed based on a steady state, vertical-plane groundwater model under simplified assumptions. This refers in particular to the assumptions of a groundwater potential at both sides of the pit wall at the height of the terrain or pit surface (below the surcharge filter) and of a homogeneous and isotropic ground. Thus, in cases of flow in direction of the pit, the groundwater potential can be described by only considering the quotient of the pit wall's embedment depth below the pit bottom and the groundwater potential difference Δh.

3.2 *Conventional approach*

According to Terzaghi-Peck's or Baumgart-Davidenkoff's approaches, the flow force results from the residual potential difference Δh_r between the lower edge of the unstable block at the wall toe and the pit bottom. Considering the applied simplified assumptions, the quotient of the residual potential difference and the total potential difference $\Delta h_r/\Delta h$ can be specified as a function of $t/\Delta h$ (Figure 2). As the length of the applied unstable block only corresponds to the distance from the pit bottom to the lower edge of the wall, the residual potential difference drops down to zero with decreasing embedment depth t. If an unstable block starting at the wall toe is used for the computations, vertical flow in the ground below the wall toe is not considered.

Applying the functional relation of $\Delta h_r/\Delta h$ and $t/\Delta h$ also allows determining the necessary thickness of the surcharge filter d_F depending on $t/\Delta h$. For the equilibrium state without any safety factors, a dimensionless variable including the quotients $d_F/\Delta h$ and γ_F/γ_W (γ_F: unit weight of the surcharge filter material; γ_W: unit weight of water) is specified for a ratio $\gamma_S'/\gamma_W = 1.0$ (γ_S' buoyant unit weight of the soil) depending on $t/\Delta h$ (Figure 3). As expected, according to the two approaches by Terzaghi-Peck and Baumgart-

Davidenkoff, the necessary filter thickness initially rises with constant potential difference and decreasing embedment depth. After reaching a maximum, however, the necessary filter thickness drops with constant potential difference and continuously decreasing embedment depth down to zero. Apparently, verifying hydraulic heave safety for a construction which involves a surcharge filter by using an unstable block that only reaches to the wall toe is inadequate to determine the necessary wall embedment in the ground.

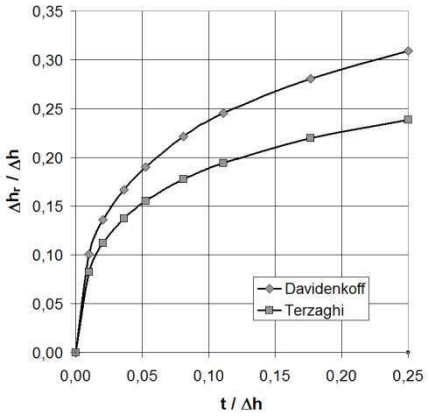

Figure 2. Residual potential difference Δh_r

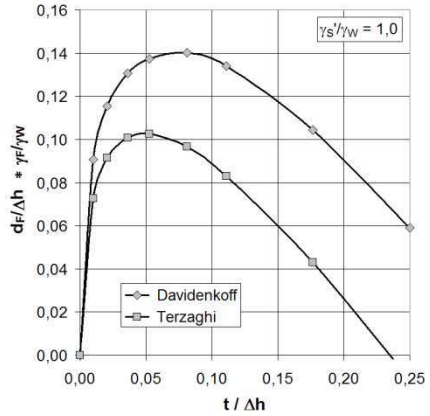

Figure 3. Required thickness of the surcharge filter d_F

3.3 *Approach with an extended unstable block*

The analyzed undercurrent flow below the walls of an excavation pit included flow in an upward direction below the wall toe. The performed numerical computations showed that in case of a surcharge filter installed on top of the pit bottom and pit walls with reduced embedment depth, significant vertical gradients may develop below the pit bottom, which partially lie significantly above the limiting gradient $i_{gr} = \gamma_S'/\gamma_W$.

To determine an unstable block which considers vertical flow in the ground in a sufficient manner, an area below the wall toe needs to be defined where the vertical component of the specific hydraulic gradient i_z is higher than the limiting gradient i_{gr}. Below this area, the specific soil weight is always higher than the specific flow force, so, for the verification of hydraulic heave safety, the equilibrium in this area is not exceeded. Hydraulic heave safety needs to be verified based on an unstable block that also covers the distance between the wall toe and the critical depth ($i_z = i_{gr}$). In the following, the new verification approach (based on Baumgart-Davidenkoff's approach) which involves the adapted unstable block is illustrated.

Using the extended unstable block, a corrected residual potential difference can be determined. This time, we did not consider the distance between the wall toe and the pit bottom but the distance between the critical depth ($i_z = i_{gr}$) below the wall toe and the pit bottom. The functional relation between the necessary thickness of the surcharge filter relating to the total potential difference $d_F/\Delta h$ and the quotient of embedment depth and potential difference $t/\Delta h$ can be determined in the same way as for the conventional unstable block. This is illustrated in Figure 4 for the equilibrium state and a quotient of the buoyant unit weight of the soil and the unit weight of water $\gamma_S'/\gamma_W = 1.0$. As opposed to the approach using an unstable block that starts at the wall toe, computations based on the new approach, using an extended unstable block, concluded that even if the embedment depth is reduced down to zero a surcharge filter is still needed. However, a maximum is also reached here, which means that at constant potential difference, a further reduction of the embedment depth requires a less thickness of the surcharge filter. To verify this apparently contradictory statement, laboratory tests were performed that are described in the following.

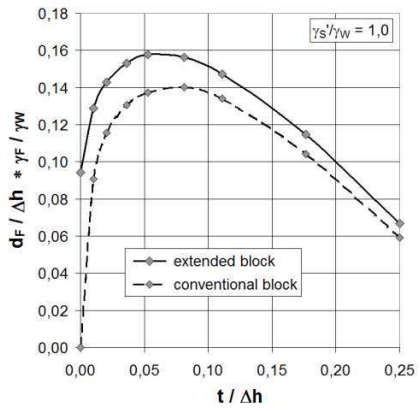

Figure 4. Required thickness of the surcharge layer d_F (conventional and extended unstable block)

The detailed computation basis for the verification of hydraulic heave safety using the method described above, also regarding relevant safety factors, as well as the determination of the necessary dimensions of the surcharge filter, with or without considering friction forces in the filter material, were described by Odenwald and Herten (2008).

4 VISUALIZATION OF FAILURE BY LABORATORY TESTS

To verify the theoretical approach, the Institute for Soil Mechanics and Geotechnical Engineering of the Bundeswehr University Munich carried out numerous laboratory tests in a specific box to simulate hydraulic heaves. During the experimental series, the embedment depth t of the wall and the thickness of the surcharge filter d_F were varied. Moreover, the elevations on the inside of the wall were detected by displacement transducers, the water pressure around the base of the partition panel was measured by water pressure sensors and the figure of failure was mapped by the Particle Image Velocimetry (PIV) method and video recording.

4.1 *Construction and design of experimental rig*

To visualize the fracture behavior and to verify the theoretical approach, we designed a specific apparatus to simulate hydraulic heaves (Figure 5). The test rig consists of two parts: the water supply, which is used to increase the potential difference continuously, and the test box. The water supply is delivered by a box with an installed overfall and a staff gauge to regulate the potential difference. The water supply and the test box were connected by a pipe (∅ 3 cm) and placed on a hand lift truck to change the potential difference continuously.

The rectangular test box has the following dimensions: length x width x height = 1.70 m x 0.40 m x 1.50 m. It consists mainly of 4 acrylic glass walls, a base plate and a vertically moveable partition acryl panel in the middle of the box. The partition wall simulates the retaining wall in the laboratory test. An inlet connects the test box with the water supply. On the feed stream side of the test box, 3 pipes, each with an internal diameter of 3 cm, allow free drain. To be able to distribute the sand homogeneously and in the default effective density, the test box can be split at a height of 90 cm, measured from the bottom. After filling in the sand, the test box can be sealed.

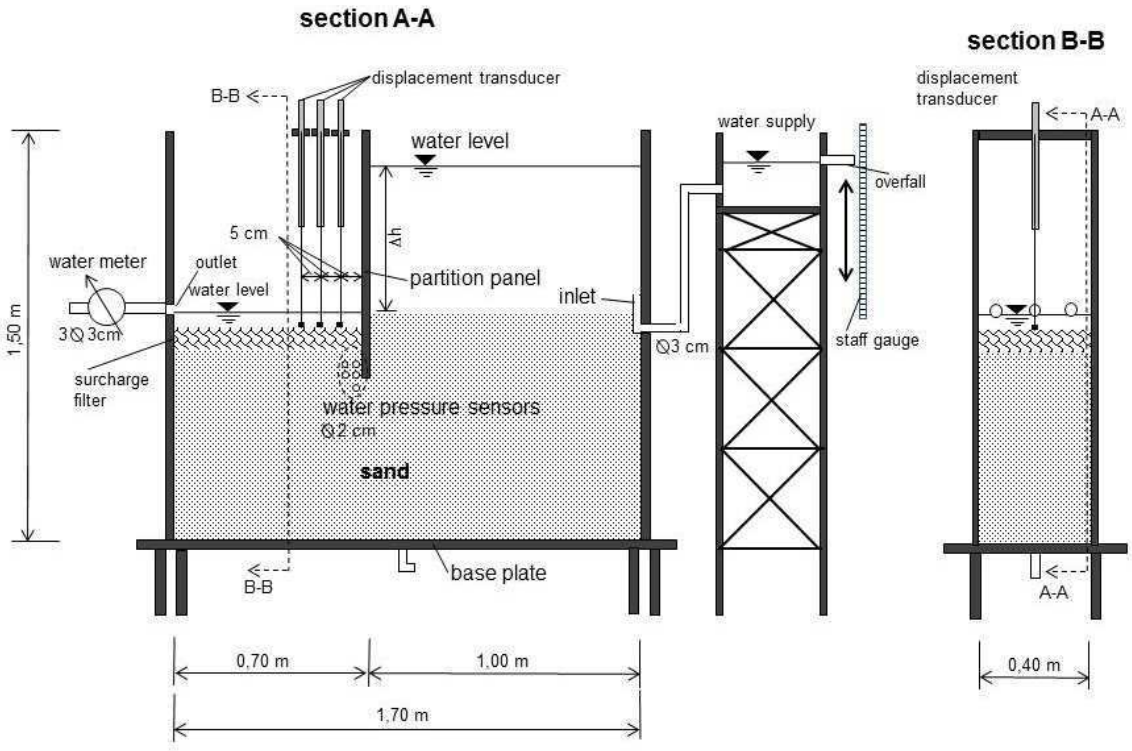

Figure 5. Construction of experimental rig

4.2 *Description of test material*

Sand (as basic material) and a mixture of coarse sand and fine gravel (as filter material) were used as test material for the simulations of hydraulic heave with filter layers at the excavation side of the wall.

As basic material, sand with a closeness of grain ρ_s = 2.72 g/cm³ and a grain size distribution of 0.1 mm to1 mm was used. The test sand can be classified as uniform fine- to medium-graded sand. The coefficient of permeability (k_f) was determined as $k_f = 5.83 \times 10^{-5}$ m/s.

The surcharge filter consists of coarse sand and fine gravel with a closeness of grain ρ_s = 2,70 g/cm³ and with a grain size distribution from 0.6 mm to 7 mm. For the selection of the filter material, the filter rule according to Terzaghi was chosen.

4.3 *Installation of test material and description of test procedure*

The sand was filled into the test box in 2 cm thick layers. To reach the default effective density D = 0.8, the dry mass per layer had to be determined. For one layer with an effective density D = 0.8, a dry mass m_d = 22.2 kg was required. The sand was filled into the box underwater and was compacted by a stemmer. The height of one layer of sand was checked with the help of marks placed on the walls of the test box.

The surcharge filter was filled into the test box similar to the sand, with a default effective density D = 0.8 and in 2 cm thick layers. The required dry mass m_d per layer (in front of the partition panel) was determined as m_d = 9.2 kg.

Altogether, we carried out 18 tests. The embedment depth t was varied between t = 0 and t = 8 cm in 1 cm steps. Moreover, the surcharge filter was installed in three different sizes, with a thickness d_F = 2, 4 and 6 cm. In the test series, the different embedment depths of the wall were combined with the three different sizes d_F of the surcharge filter.

At the beginning of each test, the water level on both sides of the partition panel was equal. Hence, there were no flow forces acting on the sand. The test was started by switching on all measuring instruments at the same time. This was necessary to permit a direct comparison of all measurement techniques. At first, the potential difference Δh was raised by 10 cm. In each of the following steps, it was further raised by 2 cm. This procedure was repeated until hydraulic heave occurred. The duration of one step was defined individually by using the measuring curves from the water pressure sensors. When the potential curves of the water pressure sensors were deflected after an increase of the potential difference Δh, it was assumed that a steady flow had occurred. At this point the next potential step was introduced.

4.4 *Experimental observations of failure mode*

We observed the failure mode of the hydraulic heave during the test series using several measurement techniques. The used measuring instruments and techniques were:

- 3 water pressure sensors around the base of the partition panel
- 3 displacement sensors in the middle of the test box
- fluid flow meter behind the outlet of the test box
- Particle Image Velocimetry (PIV) method

Two different temporal failure processes of hydraulic heave, depending on the thickness of the surcharge filter d_F, were observed. During the tests with a thickness of the surcharge filter d_F = 2 cm, relevant elevations were already detected some potential steps before the hydraulic heave occurred. As for the tests with the surcharge filter sizes d_F = 4 cm or d_F = 6 cm, the hydraulic heave occurred 1 to 3 minutes after the first elevation could be observed. Therefore, it can be assumed that the thickness of the surcharge filter d_F has a significant influence on the fracture behavior.

4.4.1 *Illustration of failure figure by Particle Image Velocimetry (PIV) method*

During these laboratory experiments, we observed fracture mechanics with the PIV method. Small displacements of the sand could be identified and their direction and amplitude could be determined. Figure 6 shows absolute displacements around the base of the partition panel for different potential differences with an embedment depth t of 4 cm and a thickness of the surcharge filter d_F of also 4 cm.

Figure 6 underlines that the displacements begin under the base of the partition panel at a potential difference Δh of 42 cm. Later on, the displacements spread to the downstream side of the partition panel (Δh = 46 - 50 cm). If the uplift on the upstream site of the panel has a certain value, the displacements spread

to the backside of the wall and the hydraulic heave is initiated (Δh = 50 cm - 54 cm). The same failure behavior was observed in almost all tests.

Furthermore, the yield line of the unstable block can be visualized by the PIV method for all potential differences. Hence, the geometry of the unstable block for several potential differences Δh can be determined. For further investigation, the results of the analysis can be used as a basis to develop the theoretical approach and adapt the unstable block.

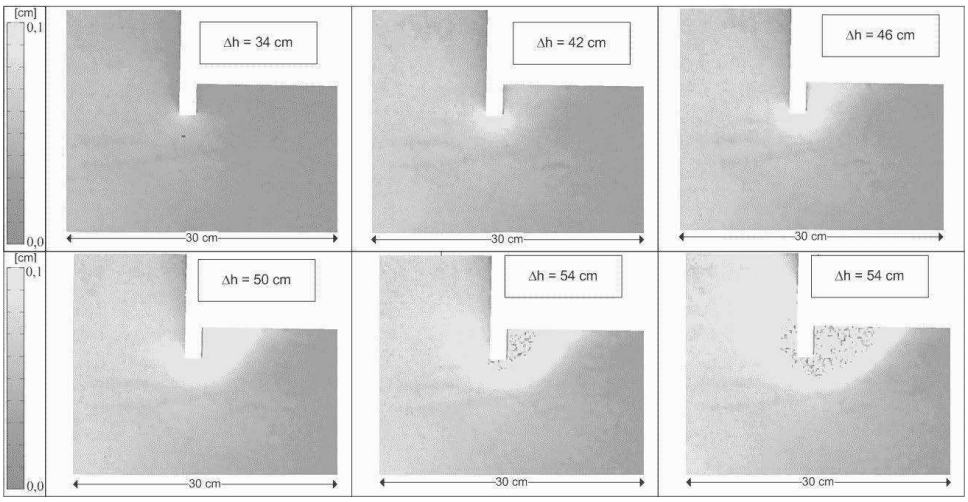

Figure 6. Absolute displacements around the base of the partition panel for different potential differences

4.4.2 *Vertical displacements in front of the partition wall*

Figure 7 shows vertical displacements on the surface of the sand in front of the partition panel measured by the PIV method. The diagram shows that the first significant vertical elevations happen at the potential difference of Δh = 50 cm. This corresponds to the results illustrated in Figure 6 which show that the significant displacements at the downstream of the partition panel start at the same potential difference. Furthermore, the diagram visualizes the shape and the length of the unstable block. In this test the maximum length of the unstable block, briefly before the hydraulic heave occurs, is about 13 cm.

Figure 8 shows vertical displacements on the surface of the surcharge filter in the middle of the test box. The displacements were detected by displacement transducers. Transducer 1, which is located at a distance from the partition panel of 5 cm, also shows the first significant elevations at the potential difference of Δh = 48 cm - 50 cm. This corresponds to the observations in Figure 7.

Transducer 2, at a distance of 10 cm from the partition panel, displays smaller elevations than transducer 1. However, the significant elevations begin at a potential difference of Δh = 52 cm. Transducer 3, at a distance of 15 cm from the partition panel, displays no significant elevations. This conforms to the results in Figure 7, where the displacements in a distance of 15 cm to the partition panel are also zero.

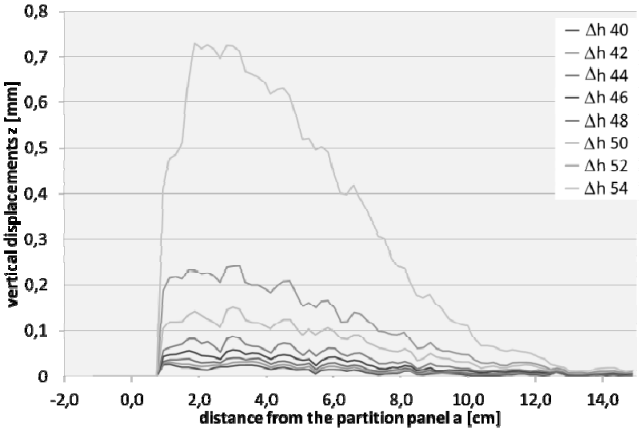

Figure 7. Vertical displacements z [mm] at the sand surface (PIV)

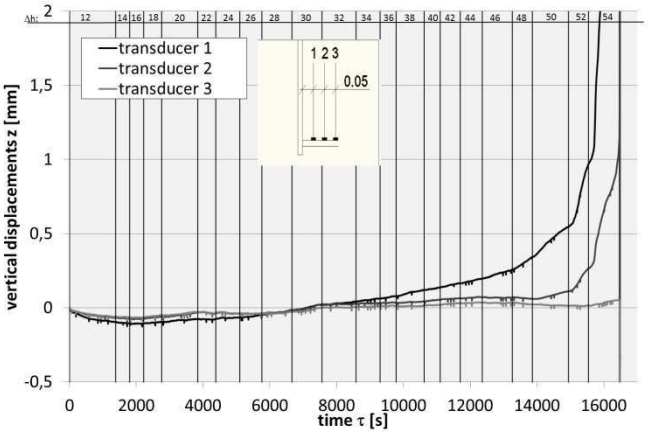

Figure 8. Vertical displacements z [mm] at the filter surface (transducer)

Additionally, the phenomenon of bulking could be observed during the test series. Figure 9 shows the bulking of the sand in front the partition panel for the test with an embedment depth t of 2 cm and a thickness of the surcharge filter d_F of 6 cm.

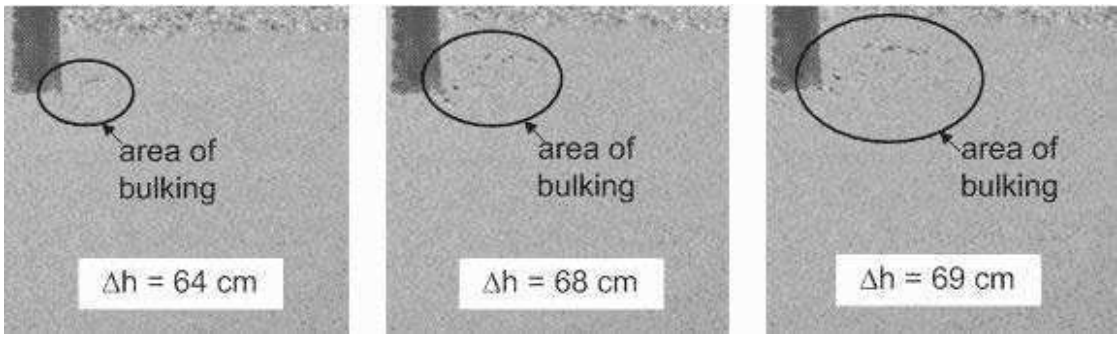

Figure 9. Bulking of sand in front of the partition panel

4.4.3 *Water pressure conditions around the base of the partition wall and flow rate*

The water pressure around the base of the partition wall was detected during each test by 3 water pressure sensors. The recorded pressure curves were used to control the duration of a potential step. Comparing the curves of the water pressure sensors with the illustration of the absolute displacements detected with the PIV method (Figure 6), it can be seen that the displacements at the base of the partition panel occur at the potential difference of $\Delta h = 42$ cm where the irregular run of the curves begins. Hence, relocations and/or displacements in the test sand can be detected by observing water pressure curves. Figure 10 shows the curves for the test with an embedment depth t of 4 cm and a thickness of the surcharge filter d_F of also 4 cm. The position of the water pressure sensors also is shown in Figure 10. At the beginning of the test, the hydraulic differences are relatively small. Hence, no relocations or displacements occur and the pressure curves run regularly ($\Delta h = 12$ cm – 38 cm in Figure 10). If the curves show jerky leaps or run irregularly, it can be assumed that relocations and/or displacements occur around the pressure sensor ($\Delta h = 38$ cm – 54 cm in Figure 10).

Figure 11 illustrates the flow rate in [l/min] for each potential step (with an embedment depth t of 4 cm and a thickness of the surcharge filter d_F of 4 cm). It can be seen that the rise of the flow rate is in a linear relation with the potential difference Δh. Hence, the permeability does not increase during the test even if relocation and/or displacements occur.

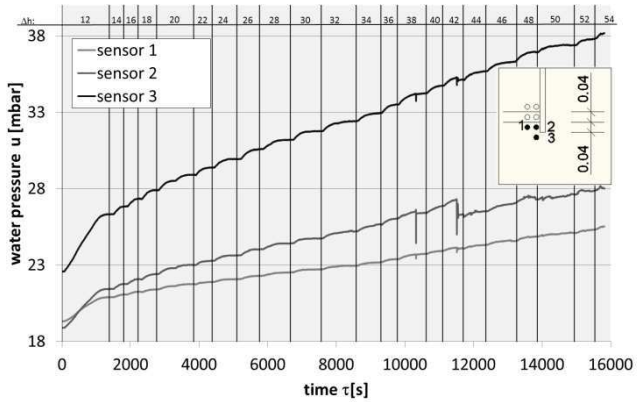

Figure 10. Water pressure u [mbar]

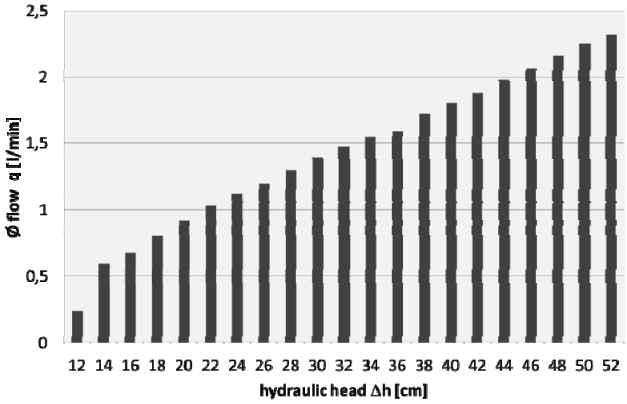

Figure 11. Flow rate for each potential step [l/min]

4.5 *Results of experiments*

Figure 12 shows the results of the experimental series and the theoretical approach as a function of $d_F/\Delta h$ and $t/\Delta h$. Similar to the results of the theoretical approach, the test results show that the required thickness of the surcharge filter d_F drops down from a defined ratio between the embedment depth of the wall and the potential difference $t/\Delta h$.

The results of the test series are clearly below the results of the theoretical approach. Hence, the theoretical approach can be assessed as being very conservative. In the theoretical approach, only the weight of the unstable block is considered. The assumption and the idealized unstable block in the theoretical approach cause the differences between the theoretical approach and the experimental tests.

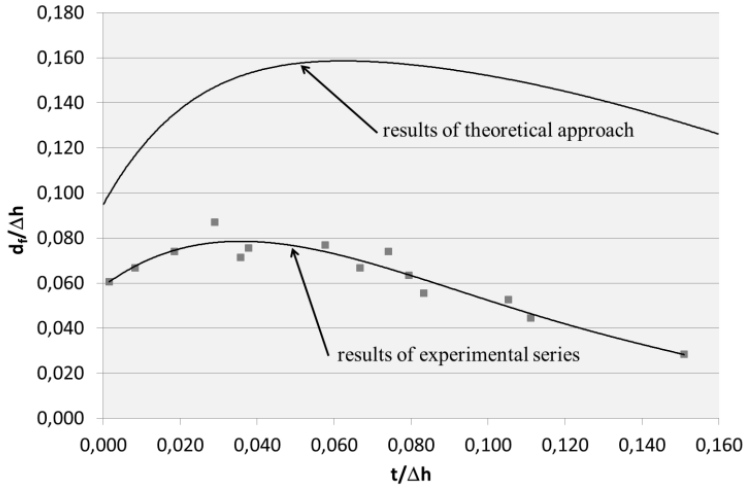

Figure 12. Results of experimental series as a function of $d_F/\Delta h$ and $t/\Delta h$

The theoretical and experimental series both prove that the hydraulic heave safety increases if the embedded depth of the wall is very small. Figure 13 illustrates this phenomenon clearly. For the test with an embedment depth t = 4 cm, a maximum potential difference Δh = 52 cm was reached. In comparison, for an embedment depth t = 0 cm, a maximum potential difference of Δh = 66 cm was reached. Although the embedment depth t was reduced 4 cm, the maximum potential difference Δh was 14 cm higher. The mechanical approach of this phenomenon will be object to further investigation.

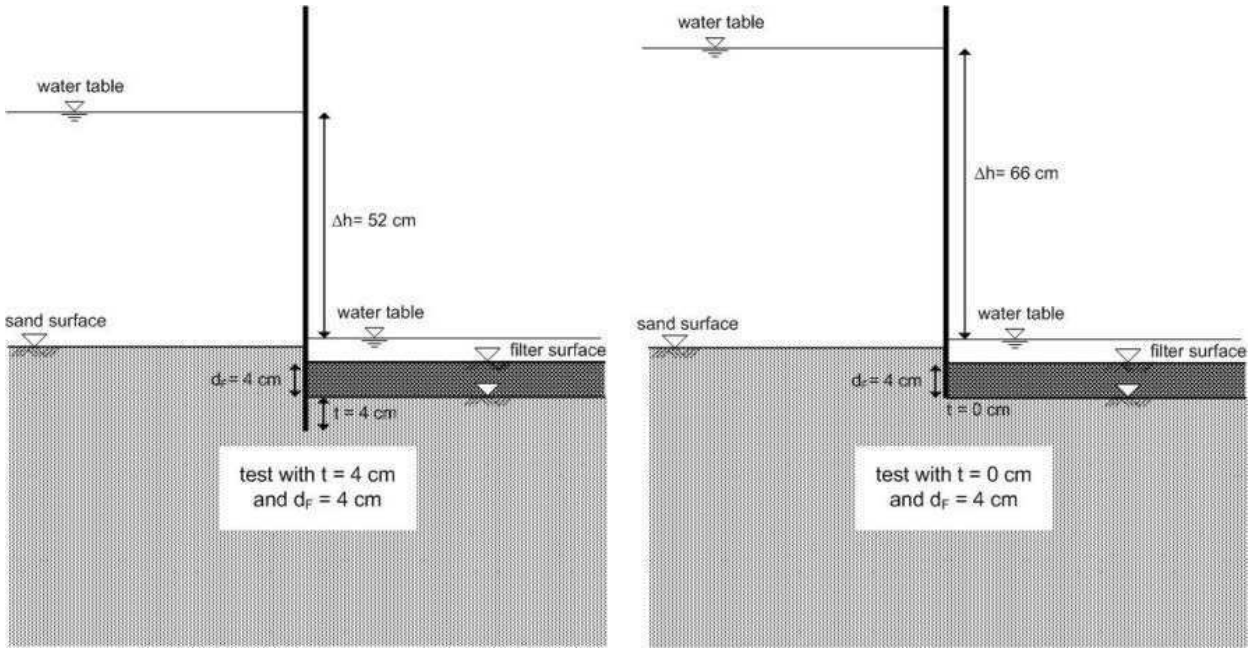

Figure 13. Illustration of the measured potential difference Δh for the tests with t = 4 cm and t = 0 cm (d_F = 4 cm)

5 CONCLUSION

The result of the numerical computation with an extended unstable block and the results of the experimental series show qualitatively similar results. If the ratio between the embedment depth of the wall and the potential difference $t/\Delta h$ falls below a defined value, the required thickness of the surcharge filter d_F drops. With the applied measurement techniques, the failure figure could be visualized and the failure mode was observed.

REFERENCES

Davidenkoff, R., 1970. Unterläufigkeit von Stauwerken, Wernerverlag, Düsseldorf
Odenwald, B., Herten, M., 2008. Hydraulischer Grundbruch: neue Erkenntnisse, Bautechnik 85, Heft 9, S. 585 -595
Terzaghi, K, Peck, R. B., 1948. Soil Mechanics in Engineering Practice, John Wiley and Sons, New York

ISGSR 2011 - Vogt, Schuppener, Straub & Bräu (eds) - © 2011 Bundesanstalt für Wasserbau ISBN 978-3-939230-01-4

Causes of Major Geotechnical Disasters

S. Van Baars
University of Luxembourg, Luxembourg

ABSTRACT: Many disasters are related to geotechnical failure. Both for risk management and for future research it is important to know what new knowledge is needed to prevent these disasters. Therefore eleven geotechnical disasters or failing projects of the last ten years in modern countries are studied and compared in this paper. All examples show that the disasters or failing projects had nothing to do with a large spread of the strength or load in a foreseen failing mechanism. There was also not an unknown failure mechanism or a lack of existing scientifical knowledge. All cases show a lack of available knowledge (or incompetence) of the designing part of the construction management. The mistakes which were made were often of a level not higher than a BSc or MSc teaching level. In none of these cases these mistakes were tackled by an internal project auditing and in none of these cases these mistakes were tackled by an external project design control, for example for a building permit.

The biggest risk parameter in geotechnical design is therefore not the spread of load or strength parameters, but by far the existence and quality of the internal project auditing and the external project design control.

Keywords: Analyses, Collapsing Soil, Consulting, Failure, Risk Management

1 INTRODUCTION

For optimisation of the academic research it is important to know what new knowledge is needed to prevent problems, failures and even disasters. There are several causes for geotechnical failure:

1. There can be an exceptional large load, an exceptional low strength, or a combination of these two, in a foreseen failing mechanism.
2. There can be an unknown or unforeseen failing mechanism or other lack of scientifical knowledge.
3. There can be a calculation error from a well-qualified engineer.
4. There can also be a lack of available knowledge or willingness (incompetence) at the designing part of the construction management, for example when a lack of time, money, qualified people or qualified material tempt or lead managers to take unacceptable known or unknown risks.

The first cause of failure is very often the core of a risk analysis. The second cause of failure is mostly difficult to quantify and is very often regarded as very small or zero and disregarded. Also the third and fourth causes are both difficult to quantify. Normally internal project auditing should tackle these two causes of failure. And if an internal project audit does not, an external project design control, for example for a building permit, should tackle these two causes of failure.

The question is which of those four causes show mostly up during failures of geotechnical structures. Therefore several geotechnical failures of the last ten years in modern countries will be discussed here. This might help to find the best way to improve risk analysis in geotechnical engineering.

2 CASE STUDIES GEOTECHNICAL FAILURES

2.1 *Collapse water defense system of New Orleans*

Figure 1. Destroyed housing area Lower Ninth Ward.

The biggest geotechnical failure of the last ten years in modern countries is probably the disaster of New Orleans on August 29th, 2003. The water levels provoked by hurricane Katrina were not higher than their local design level and also not extreme for Dutch standards, nevertheless the water defenses could not withstand it, due to many mistakes in the design. The water defense system was too long by not using a secondary water system. Some of the dikes or gates were missing. Some of the dikes or I-walls were too light and were whipped away. Very often the height of the dikes or walls was insufficient and also very often the effect of piping was not taken into account for in the design.

Figure 2. Washed-in sand by piping.

Figure 3. Thickness of the washed-in sand layer.

In the city center there are two examples of this. In just the short moment of the passage of the hurricane, large quantities of sand of the shallow sand layers were washed underneath the water defenses into the housing areas. It is even for Geotechnical Engineers interesting to see that a housing area can be washed under a layer of sand of more than a meter in just a few hours.

Figure 4. Creation of a new dike.

It is also interesting to see how the Unites States Army Corps of Engineers think they can make new impermeable dikes after the disaster. Some dikes become therefore far too permeable.

2.2 *Singapore metro tunnel collapse*

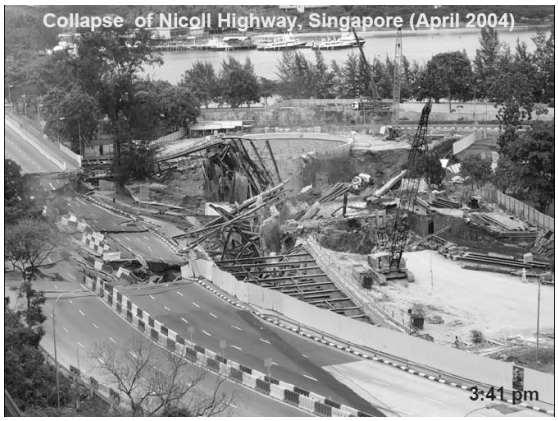

Figure 5. Collapse of the metro tunnel along Nicoll Highway, Singapore

In 2004 the building pit of a metro tunnel under construction in Singapore collapsed. Four people died. Many simple mistakes have been made in the design of the building pit and readings of instruments on site have indicated that things were not going as planned, but the warnings were not acted upon. The responsible manager was send to prison.

2.3 *Train station building pit collapse, Köln*

Figure 6. Collapse of a building pit of the North-South Line in Köln

The biggest construction disaster in Germany of the last few years is the collapse of a building pit of the North-South Line in Köln in 2009, leaving 2 people death and destroying one of the most important historical archives of the country. Workers had stolen up to 83% of the steel supports of the diaphragm walls and have sold this as old steel. And of course nobody, not even the inspectors, remember to have noticed anything.

2.4 *Subsidence along underground train station, Amsterdam*

During the construction of a building pit for a new underground station of the North-South Train Line in Amsterdam there were two identical incidents. Twice a diaphragm wall was leaking groundwater. This water washed sand particles away below the foundation piles of surrounding buildings, causing a subsidence of up to 23 cm of these old weaver houses. The only internal inspections of the diaphragm wall seemed to have been insufficient and there was no backup plan for this risk. There could have been a second line of defense for the most vulnerable areas like theses fragile houses. In the meantime the predicted costs have gone up from 1.5 to 3 billion euros and the project end shifted from 2011 to 2017.

Figure 7. Subsidence along an underground station of the North-South Train Line in Amsterdam

2.5 *Leaking tram tunnel, Den Hague*

In 1996 the city council in Den Hague, the Netherlands ordered to construct a Tram tunnel. In order to save some money, they had chosen not to use the common technique of a building pit with an underwater concrete floor retained by tension piles, but to use an experimental technique of deep arch-grouting. All contractors warned the municipality for the high risk of leakage with this technique, but that did not change the plans of the city council. Also the insurance companies warned the city council and decided not to ensure the project. The city council took the risk themselves.

Figure 8. Big Market tram tunnel in Den Hague

The predicted leaks appeared in 1998 causing the construction of the Tram tunnel to halt. The tunnel was for a long time under water, waiting for a new plan. This gave this tunnel its nick names: The Den Hague Swimtunnel and The Tramtanic. The tunnel was finished with a complex technique using high air pressure. In total 35.000 man-hours were worked under high air-pressure. The construction costs went up from 139 to 234 million euros and the opening was delayed from 1999 to 2004. In this way the construction of a 1250 m tunnel in Den Hague became more expensive than an 8 km long tunnel in Thüringen, built at the same time.

2.6 *Damage along garage building pit, Rotterdam*

Another example is the construction of the Museum Park Garage in Rotterdam, the Netherlands, which started in 2004. During construction the demolition of a large retention wall was needed, but the project organisation never thought of checking the effect of this on nearby buildings. Also excavating beyond a depth of NAP -4 m took place even though the geotechnical report had forbidden this. Therefore the construction of this so called “blunder-pit” caused damage to nearby buildings in 2005 and 2006. The municipality had to accept a delay of more than a year and an increase of the costs from 53 to 103 million euros.

Figure 9. Construction of the Museum Park Garage in Rotterdam

2.7 *Damage along garage building pit, Middelburg*

Figure 10. and Figure 11. Leakage and damage at the building pit of the new theater Middelburg

In 2004 in Middelburg, The Netherlands, the building of a new Theater with a large underground parking garage started. In 2005 a diaphragm wall started to leak and surrounding houses started to subside. To stop the disaster, the pit was filled with water and was nick-named the Biggest Swimming Pool. It remained this way until 2009 when new walls were placed in the pit and the pit was filled with 13,350 m^3 of concrete; a loss of almost half the volume of parking space. The remaining and very expensive parking is rather useless now, because the old theater has been renovated in the meantime.

2.8 *Peat dike failure, Wilnis*

Figure 12. Failure of a peat dike in Wilnis

Figure 13. Failure of a peat dike in Edenderry

In the summer of 2003 a peat dike in the Netherlands failed in the village Wilnis near Mijdrecht. The dike was shifted horizontally by the water pressure in the canal. This type of failure is not uncommon.In the summer of 1947 a peat dyke in Zoetermeer, the Netherlands, failed in an identical way. And also in January 1989 in Edenderry, Ireland, a peat dike failed in a similar way. The failure of the dike in Wilnis came not as a surprise, because this dike, only made out of peat, was for 28 years disapproved, but the responsible waterboard never improved the dike in all those years. Both in smaller hand calculations and in finite element calculations, the effect of the drying out of the crest of the dike above the groundwater table and the failure of the dike can be simulated. Not the failing of the dike is a mystery, but the reason why the Waterboards accepted for so many years to do nothing about the many dikes which were disapproved.

2.9 *Large vibration and noise nuisance at construction underground parking, Eindhoven*

In 2009 and 2010 in Eindhoven a new underground parking garage was build next to the PSV football stadium. A large number of big precast foundation piles have been driven through very dense sand layers in 2009. Therefore a production of very strong ground vibrations for many months was obvious, which would exceed the allowed maximum of the Dutch standards. The corresponding high level of environmental vibration nuisance for the people living around the building pit should not have been ignored by the project organisation and also by the controlling municipality.

Figure 14. and Figure 15. Vibration and noise nuisance at precast pile driving in Eindhoven

Also the arguments used by them in court against the citizens, that using a vibration-free bore pile would lead to identical problems as in Amsterdam (here were no pile installation problems but problems with leaking diaphragm walls in combination with a high groundwater table) and Köln (also no pile problems but stolen steal supports) were clearly incorrect and not good for the respect of our science and of the court system. In court the judge declared this project illegal, but did not halt the project unfortunately.

2.10 *Failing retaining wall of building pit, Differdange*

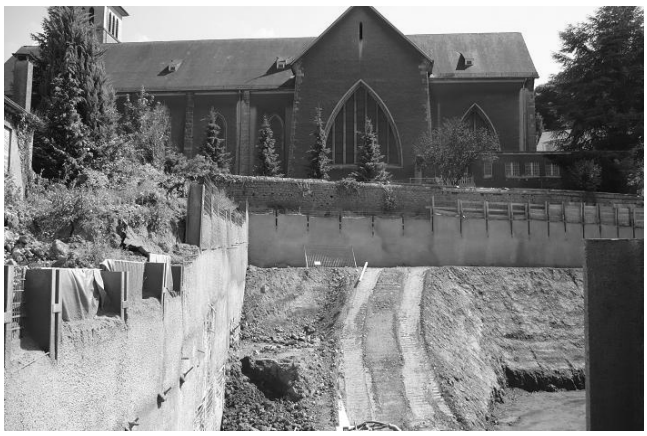

Figure 16. Failing retaining wall in Differdange

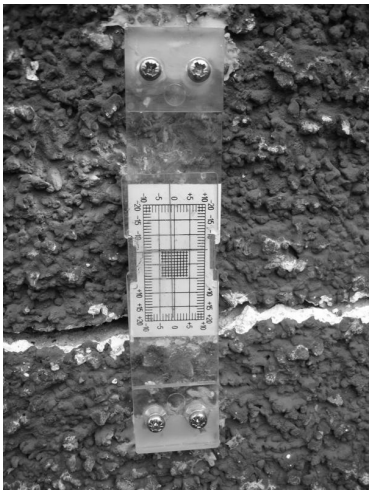

Figure 17. and Figure 18. Cracks in church Differdange

In 2010 in Differdange, Luxembourg, very close to the shallow foundation of the local church a building pit was made, in order to make a housing residence with a sub terrain parking garage. The project was halted when suddenly many cracks appeared in the church. Verification of the design calculations made

clear that several major mistakes were made. Only an active earth pressure was used in the calculations, while in order to prevent horizontal deformations, a more neutral earth pressure had to be used. Also the water pressure behind the Berlin-wall was forgotten. The anchoring was made very close to and just below the fundament of the church. And a very high drained cohesion was used in the calculations, only based on undrained phicometer borehole field tests.

2.11 *Unsafe rock face, Clervaux*

In Clervaux, Luxembourg, a vertically-layered rock-face was inspected by a geological and geotechnical engineer. He warned for the danger of rock parts breaking off. Nevertheless the owner never secured the rock-face. A few years later a large part broke loose and crushed a parked car; luckily nobody was in the car. First then the authorities intervened and secured the wall on the expanses of the owner.

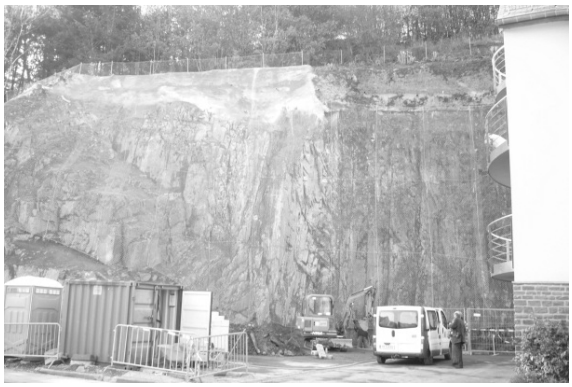

Figure 19. Rock face instability at Clervaux.

3 CONCLUSIONS

All examples show that the disasters or failing projects had nothing to do with the first three causes mentioned before: There were no exceptional large loads or low strengths in foreseen failing mechanisms. There was no lack of scientifical knowledge. There were also no calculation errors from well-qualified engineers. All cases show a lack of available knowledge (incompetence) at the designing part of the construction management. The mistakes which were made, were often of a level not higher than a BSc or MSc teaching level. In none of these cases the mistakes were tackled by an internal project auditing and in none of these cases these mistakes were tackled by an external project design control, for example for a building permit.

The biggest risk parameter in geotechnical design is therefore not the spread of load or strength parameters, but by far the existence and quality of the internal project auditing and the external project design control.

REFERENCES

Blom, C.B.M. & Heeres, O.M. July 2010, Case Museumgarage Rotterdam, Geotechniek., ISSN 1386-2758

Eindhovens Dagblad, B en W: heien mag doorgaan, Zondag 22 maart 2009

Kanning, W., Van Baars, S., Vrijling, J.K., August 2008, The Stability of Flood Defences on Permeable Soils: The London Avenue Canal Failures in New Orleans, Sixth International Conference on Case Histories in Geotechnical Engineering, Rolla, USA, ISBN 1-887009-13-2

Van Baars, S., June 2010, Keynote Lecture: Dike failures; Risks, Causes and Costs, The Northern Group of the ICE North East Annual Seminar, Newcastle

Van Baars, S., September 2008, Dutch peat dyke failure during the dry summer of 2003, International symposium Drougt and Construction SEC 2008, Marne-la-vallée, France, ISBN 978-2-72-8-2527-1

Van Baars, S. & Kanning, W. June 2007, Het waterkeringsysteem van New Orleans tijdens orkaan Katrina, Land+Water, ISSN: 0926-8456

Van Baars, S., May 2007, New Orleans tijdens orkaan Katrina, Land+Water, ISSN: 0926-8456

Van Baars, S, May 2005, The horizontal failure mechanism of the Wilnis peat dike, Géotechnique, Thomas Telford, London, ISSN 0016-8505

Van Baars, S., 2004, Peat dike failure in the Netherlands, European Water Management Online, European Water Association (EWA), Hennef, Germany, http://www.ewaonline.de/, ISSN 1954-8549

Van Tol, A.F., October 2010, Case study: Amsterdam Metro North-South Line – an update on the data obtained and lessons learned, GE & NCE Basements and Underground Structures Conference 2010, London
Van Tol, A.F. Koster, S., Ramler, J.P.G., Vrijling, J.K. & Verruijt, A., 2001, Imperfections in jetgrout layers, Proc. XV International Conference on Soil Mechanics and Foundation Engineering, Balkema, Rotterdam, pp. 1883-1886
Scharll, M. Der Schadenfall in Differdange durch eine Baugrube, BSc-thesis, University of Luxembourg

Author index